第十一届亚洲国际皮革科学技术会议

The 11th Asian International Conference of Leather Science and Technology

会议论文集

(Proceeding of Abstracts)

11th AICLST Oct.16th-19th,2018 XI'AN/CHINA

www.2018AICLST.org

Contents

O1 Improved Chrome & Salt Recovery System for Sustainable Effluent Treatment and Management In Leather Sector.... 1

O2 A New Two-stage Chrome Tanning Method under Variable Temperature.....5

O3 Consumer's Need for Sustainable Products In The Leather Industries.....17

O4 Pyrolysis Component Analysis of Different Leathers.....18

O5 An Eco-benign Organic Combination Tanning System for Manufacture of Garment Leathers.....19

O6 Study on theFunctionalizedGraphene Modified Waterborne Polyurethane Materials.....28

O7 The elimination of waste waters from unhairing/liming acid/salt pickle and chromium tanning processes in full scale wet blue manufacture.....35

O8 Property changes of Wet-blue influenced by bating with different acid protease.....36

O9 IUE 12 - Guidelines for Minimum Environmental Standards.....42

O10 A Novel Chrome-free Tanning Technology Based on the Complex of Zirconium and Highly-oxidized Starch 46

O11 Application and Preparation of A bio-polymer re-tanning agent based on Cattle hair hydrolysate..... 56

O12 Effect of Extraction and Coloring Condition on Chromium(VI) Determination.....63

O13 Study on the Effects of Glycosidases Specificity on Fiber Opening and Unhairing Processes.....67

O14. "Green" Technologies of Leather and Fur Raw Materials Processing on Basic of The Buryats and Mongols Peoples Traditions..... 78

O15 Reduction of Water Consumption in the Processing of Rawhide and Sheepskin Coat Materials.....84

O16 Microwave-Irradiated Tanning Reaction of Aluminum with Collagen..... 89

O17 Synthesis of rice husk modified graphene oxide for Cr (VI) removal in leather wastewater..... 101

O18 Circular economy: the green way for tanning.....107

O19 Preparation and Properties of Self-healing PolyacrylateFinishing Agent.....112

O20 Analyzing the Role of Industry/Trade Association or Business Society/Council in Sustainable Growth of Industry: evidence from Indian leather Industry..... 113

O21 Biological treatment of alkaline leather fleshing by a fleshing-enriched activated sludge reactor.....116

O22 A green retanning system with function of reducing free formaldehyde in leather.....121

O23 New insights into chrome tanning: When structure meets protein chemistry.....129

O24 Durable and Superhydrophobic Leather Based on Reactive Amphiphilic SiO_2 Janus Particles..... 130

O25 Consumer Complaint and Trend of Formaldehyde Content After Sales..... 133

O26.... Development of a Novel Biomass Wood Adhesive Basedon Gelatin and Oxidated Chitooligosaccharide Crosslinked Waterborne Polyurethane.....141

O27 NEW era for Leather mold-preventing is coming, are you touched?..... 151

O28 Tannery Waste Management in India – Towards Sustainability..... 155

O29 From Polyurethane Chemistry to Advanced Functional Leather.....162

O30 Control and optimization of the whole process of tannery wastewater treatment.....163

P1 Facile Preparation and Effect of Pu-Based Isocyanate on Collagen Fibre for Enhanced Elasticity of Leather.....168

P2 Some Factors on Synthesis of Nano-Encapsulated Phase Change Materials for Leather.....169

P3 Fabrication of "Silver Nanoparticle Sponge" Leather with Durable Antibacterial Property.....170

P4 Elimination of S^{2-} in tannery sludge by acclimated microorganisms.....171

P5 Study on the effluent treatment and circulation reuse technology of rex rabbit skin tanning process.....175

P6 Study on the Application of Cr (III) in Mordant Dyeing of Rabbit Skin.....176

P7 Effect of different organic ligandson Zr-Al tanning properties of rex rabbit.....177

P8 Study on Treatment of degreasing Waste Liquid of Rex Rabbit Skin with QZ-A01 and PAC Flocculant.....178

P9 A Novel Waterborne Polyurethane Coating Functionalized by Isobornyl Acrylate with Enhanced Antibacterial Adhesion and Hydrophobic Property.....179

P10 Reconstituted Leather Made Using Polyurethane Based on Star-Shaped Polyester Polyols.....180

P11 In-Situ Preparation of Silver Salts/Collagen Fiber Hybrid Composites and Their Photocatalytic and Antibacterial Activities.....181

P12 An Innovative Method to Produce Gymnastic Leather.....182

P13 183Study on preparation process and properties of UV-WPUA leather finishing agent.....183

P14 Determination of short chain chlorinated paraffins in leather based on hydro-dechlorination technique.....192

P15 Quantitative Study on Product Life Cycle of Female Sandals Based on Improved BASS Model.....193

P16 Research of Electrochemical Degradation and Product Characteristics on Wool.....198

P17 Industrial Production of Chrome-Tanned Leather Without Formation of Hexavalent Chromium by treating with a Combined Inhibitor.....205

P18 Discussing Again to Nowadays Chrome Tanning Agents.....206

P19 Preparation and Properties of Amino Acid Surfactants with Different Lipophilic Groups.....207

P20 Study on Modification of Collagen by Fluorescent Hyperbranched Polymer (HMEAP).....215

P21 The synthesis of self-colored waterborne polyurethane and its membrane performances.....222

P22 Preparation and characterizations of Gelatin-P(AA-AM) and GO-gelatin-P(AA-AM) super absorbent composite.....229

P23 Research on Determination of Isothiazolinone Fungicides in Leather*.....230

P24 The role of the source of raw hides in environmental impact for leather making by life cycle assessment.....239

P25 Fibering and Papermaking Technology of Finished Leather Cutting Waste.....249

P26 Controlling Translocation of Trivalent Chromium around Adsorbents with Light: One Step Closer to Sustainability.259

P27 Investigation on the influence factors of enzyme mass transfer in bating process.....260

P28 Modelling the kinetics of enzyme infusion in skin matrix.....267

P29 Effects of Enzymatic Unhairing by Combinations of Several Proteases.....268

P30 A Potentially Biodegradable and Biocompatible Tissue Scaffold Material: Composites of Dialdehyde Bacterial Cellulose and Gelatin..... 275

P31 Research on the fashion of leather products..... 284

P32 Fundamental studies using synchrotron SAXS highlighting pathways towards sustainable leather processing..... 285

P33 Establishment of Environmental Risk Assessment and Management System of Leather Chemicals..... 286

P34 Evaluation of the Biostability of Chrome Tanning Waste Liquid in Closed Recycling Process..... 287

P35 A Novel Approach for Lightfast Wet-white Leather Manufacture Based on Sulfone Syntan-aluminium Tanning Agent Combination Tannage..... 288

P36 Hydrolysis of Abandoned Cowhair and Preparation of Protein-Based Liquid Membrane..... 289

P37 Preparation of functionalized graphene nanosheet/waterborne organosilicon nanocomposites and their application in leather finishing..... 290

P38 Removal of acid dye from aqueous solution by using amphoteric polyvinylamine immobilized on ferroferric oxide.. 291

P39 The elimination of effluent fromthe unhairing-liming process by a novel recycling technology..... 299

P40 Preparation and application of a novel cationic fatliquoring agent 3.2 Surface tension of YW aqueous solution..... 310

P41 Research progress in gelatin-based biohydrogels..... 315

P42 Optimization of Hydrolysis Conditions of Chromium-containing Leather Shavings by Orthogonal Test..... 325

P43 Sunlight-activated color-tunable long persistent luminescent polyurethane leather coatings..... 331

P44 Optimization of the Process of Preparing Collagen Powder by Experimental Spray Dryer..... 332

P45 Preparation of mussel-like leather finishing materials and strong adhesion, self-healing ability..... 336

P46 Preparation of Chrome Tanning Liquor Using the Chrome Sludge from Chrome Shavings and its Application Performance..... 337

P47 Modification of Collagen Membrane with Sulphited Quebracho Extract..... 338

P48 Microwave irradiation：an effective and innovative routine to promote chrome tanning process..... 339

P49 Study on the influence of the crosslinkers on the properties of resin films..... 340

P50 Preparation and characterization of collagen fibers spun from liquid-crystalline collagen..... 347

P51 Synthesis and characterization of polyurethane-based polymeric surfactant with different length of fluorocarbon chain 352

P52 Smart Ag/TiO_2 and Ag/N- TiO_2 nanoparticles for leather surface coating and their cytoxicological impact..... 353

P53 The application of hyperbranched polymer modified buffing powder filler in PU film..... 354

P54 Application and prospect of microwave assisted technology in protein-related industry..... 355

P55 Self-matting waterborne polyurethane leather finishing agent..... 356

P56 Characteristics Analysis of Operating Liquid Properties in Liming Waste Liquid Recycling Process..... 365

P57 Study on hydrolysis of waste shavings by the system of calcium oxide/tetramethylammonium hydroxide..... 366

P58 Greener Dyestuff for Leather Industry..... 367

P59 Effects of pH on the Interaction between tannic acid and Collagen in Dilute Acidic Solution..... 368

P60 Preparation of ultrafine leather powder and its application in synthetic leather..... 369

P61 Preparation and properties of Superhydrophobic coating based on modified grapene oxide..... 378

P62 The Study of Preparation and Performance of Solvent-Free Polyurethane Synthetic Leather with Flame Retardant Properties..... 384

P63 Preparation and application of graphite based controllable adsorption material.....391

P64 Preparation of Amino Functionalized Carbon Quantum Dots and Its Application in Formaldehyde Detection..... 392

P65 A Novel Non-pickling Combination Tanning for Wet-white Leather Based on Granofin Easy F-90 and Tannic acid. 393

P66 Preparation and properties of protein plastics based on waste collagen.....394

P67 Preparation of Aminated Gelatin Nanoparticles Used to Stabilize Pickering Emulsion.....395

P68 Modification of collagen with a natural cross-linked agent oxidized chondroitin sulfate A.....396

P69 Study on adsorption of low concentration chromium (III) by porous organic polymer.....397

P70 Study on construction and properties of leather waterproof layer based on "lotus leaf effect"..... 398

P71 Preparation and Properties of Polyacrylate Coating Material Modified by Carbon Nanotubes.....399

P72 The Discussion on Design and Market Analysis of Affordable Luxury Leather Brands.....400

P73 Preparation of Cationic Polysiloxane Hybrid Emulsion and its Use as Superhydrophobic Leather Finishing Agent.... 409

P74 Preparation and application ofamphoteric polyurethane retanning agent with multi-aldehyde groups..... 416

P75 Poly(γ-glutamic acid)-NHS ester: a dual-functional modifier to prepare polyanionic collagen with superior thermal stability.....423

P76 Clean Tanning Technologies Based On Chrome Free Tanning Agent TWS..... 437

P77 Enhancement of Mass Transfer of Protease in Bating Process..... 438

P78 Study on Treatment of Leather WastewaterUsingChitosan Composite Flocculant..... 439

P79 Role of Zinc Ions in Enzymatic Unhairing of Bovine Hides.....445

P80 The Application of Interaction Design in the Field of Women's Shoes Design..... 446

P81 Proteolytic activity determination of protease with natural hide powder labeled with low temperature active dyestuff as substrate..... 447

P82 The Impact of Proteases on Elastin and Collagen Fibers in Wet Blue Bating..... 458

P83 Comparison of Protein Quantitation Assays in Active Protein Compositions of Typical Proteinase Preparations.....459

P84 Exploring the Innovative Methods of the Qiang's Yunyun Shoes Used in Modern Footwear Design.....460

P85 A surfactant-free degreasing method based on lipase multi-insertion in leather making process.....469

P86 Green Hybrid Nanocapsules for Leather Finishes: Fragrance-Controlled Release and Antibacterial Behaviors..... 477

P87 Insight into Accessibility of Clay Nanoparticles in the Transformation of Collagen Fibers to Wet-white Leather Matrix 478

P88 Determination of free formaldehyde in leather chemicals.....479

P89 Interaction of Al-Zr tanned leather with retanning agents.....480

P90 Study the Dyeing Effect of Myrica Extract on Rabbit Fur..... 481

P91 Fabrication of Polyacrylate/Nano-Ag Composites Toward Antibacterial and Antistatic Properties Enhancement of Leather..... 482

P92 Study on Physical-chemical Properties of Mink Shavings..... 483

P93 Effect of Hydrolytic Reagent on Amino Acid Composition of Mink..... 491

P94 Influence of Sodium Chromate Colorimetry Factors on Chromium Content in Chromium Wastewater..... 496

P95 Innovative design practice of local leather goods brands with “Chinese traditional culture gene”..... 497

P96 Research of Fluorine-containing Acrylate Leather Finishing Agent..... 498

P97 Synthesis and Application of Fluorine Silicon modified Polyacrylate Leather Finishing Agent..... 499

P98 Fabrication of MOFs and Their Application in Polyacrylate Leather Finishing Agents..... 500

P99 a Method of Generating Seamless Repeat Pattern Utilizing Adobe Illustrator for Simulating Litchi Grain Leather Surface..... 501

P100 Improve the Tanning Performance of Graphene Oxide by Thiol-ene Click Chemistry..... 502

P101 Research on the Design of Intelligent Shoes based on the Theory of Value Engineering..... 503

P102 Application of Chinese traditional Art in Shaped Design of Footwear..... 504

P103 Casein-based bifunctional antistatic flame retardant leather finishes..... 505

P104. Oxidized sodium alginate / layered double hydroxides Nanocomposite prepared by via exfoliation-reassembly: Application as a fatliquorting agent..... 506

P105 Preparation of Protein-based Liquid Agricultural Film with Hydrolyzate from Cowhair Waste..... 507

P106 Determination of short chain chlorinated paraffins in leather based on hydro-dechlorination technique..... 517

P107 Study on The Technology of Preparing Peptide Calcium Chelate from Leather Waste..... 518

P108 Study on hydrolysis of waste shavings by the system of calcium oxide/tetramethylammonium hydroxide..... 529

P109 Kinetic analysis of the thermal degradation of shorn sheep skin wastes..... 538

P110 Attapulgite Modified Polyacrylate Emulsion and its Flame Retardancy..... 539

P111 Research of Characteristics on Wool Electrochemical Degradation..... 540

P112 Degradation of Artificially Aged Vegetable-Tanned Leather using RP-HPLC and FTIR-ATR..... 541

P113 Chromium (Cr(III)) basic point - alkali (OH^-) capturing: the mechanism of high exhaustion chrome tanning..... 549

P114 Effects of Salt-enzyme Solution on the Opening of Collagen Fiber Bundles..... 550

P115 Proceedings of the 11th Asian leather conference-Xi’an, ChinaEffect of salt-lime solution on hide swelling and solution properties..... 558

P116 Fragrance Lasting/ Antibacterial Casein-based Microcapsule Leather Finishes via Interface Template Method..... 559

P117 Application of Soluble Soybean Polysaccharide in Leather Finishing..... 560

P118 Unhairing of Cowhides with KCl Assisted Neutral Protease for Leather Making..... 565

P119 Exploring Ionic liquids for Collagen Stabilization: A New Paradigm Aafiya Tarannum, J Raghava Rao, N Nishad Fathima*..... 574

P120 Application and Development of Interactive Design concept in Women's shoes.....575

P121 A cleaner chrome-free tanning process:tetrakis(hydroxymethyl)phosphonium sulfate and cage-likeocta(aminosilsesquioxane)..... 581

P122 Synthesis of an amphoteric polymer auxiliary agent and its application on the chrome-free leather.....582

P123.Effect of Food to Algal biomass ratio on the assimilation of ammonical nitrogen from the secondary tannery effluent coupled with bioenergy generation using grown algal biomass..... 591

P124 New hybrid nanocomposite applied to the leather finishing process, with favourable environmental impact.....599

P125 The Properties of Collagen Extracted from Pickled Skin..... 600

P126 Study on the RapidSoaking Clean Manufacturing Technique on Twinface Sheepskin.....602

O1

IMPROVED CHROME & SALT RECOVERY SYSTEM FOR SUSTAINABLE EFFLUENT TREATMENT AND MANAGEMENT IN LEATHER SECTOR

Dr. S. RAJAMANI

Chairman-Asian International Union of Environment (AIUE) Commission,

Old No. 18, New No. 45, First Street, South Beach Avenue, MRC Nagar,

Chennai-600028, India, Mobile : +91 9840063210

E-mail: dr.s.rajamani@gmail.com

1.INTRODUCTION

Annual leather process in Asian Countries is estimated at 8 to 10 million tons of hides and skins which is more than 50% of the world leather production of about 16 million tons per year.The tanneries in Asian countries including India, China, Vietnam, etc. discharge more than 350 million m^3 of wastewater per annum. In India there are 20 Common Effluent Treatment Plants (CETPs) mainly located in Tamilnadu, Uttarpradesh, Kolkata and Punjab.

Conventional physiochemical and biological treatment systems are designed and implemented only to reduce Biochemical Oxygen Demand (BOD), Chemical Oxygen Demand (COD), Suspended Solids (SS), Heavy metals etc. and not TDS and salinity which are mainly contributed by chlorides, hardness and sulphates. Due to inherent quality of wastewater from tanning industry, the treatment plants are unable to meet the prescribed standards in terms of TDS, chlorides in salinity in the treated effluent. The TDS limit is being enforced in India and other parts of the World depending upon the final mode of disposal. In addition to the removal of TDS in the treated effluent, it is necessary to recover water for reuse to meet the challenge of water shortage. In some of the states such as Tamilnadu in India, the pollution control authorities insist on water recovery integrated with Zero Liquid Discharge (ZLD) system. However, the Zero Liquid Discharge concept has got limitations in handling the composited stream from tanneries. The main technical and environmental challenge is the management of concentrated mixed saline stream reject with TDS more than 50000mg/l, COD more than 1500mg/l, etc. generated from Reverse Osmosis (RO) system and contaminated mixed salt from the Multiple Effect Evaporator (MEE), high operation and maintenance cost, etc.

With a view to address the technical challenges faced in the ZLD systemand to meet the environmental requirements, sustainable treatment technologies such as segregation of saline soak stream, separate physiochemical and biological trdatment, recovery of quality salt, development of improved centralized Centralized Chrome Recovery System and recovery of quality chromium cake for regeneration of Basic Chromium Sulphate (BCS). Due to this innovative technological development reduces the chromium level by 98% and TDS level by more than 60% and the overall effluent treatment cost is reduced by 50% compared to the operation maintenance cost of ZLD system.

2. CLEANER PRODUCTION AND SEGREGATION OF STREAMS FOR CONTROL OF CHROMIUM AND SALINITY

Due to inherent quality of industrial wastewater such as textile dyeing units, tanneries etc., the conventional treatment plants are unable to meet the prescribed TDS level of 2100 mg/l in the treated effluent. In addition to TDS management the control of volatile solids in hazardous category sludge is also becoming a necessity.

For control of salinity, chromium, sludge and viable management of TDS with recovery of quality water from wastewater, the required treatment steps are (i) Chrome recovery and other in process control including cleaner production, (ii) Segregation of saline streams such as soak and pickle and separate treatment for recovery of reusable quality salt, (iii) Application of advanced aerobic biological treatment systems with minimum use of chemicals and reduction of sludge

generation, (iv) Treatment of balance composite streams with low TDS and integration of treated tannery effluent with treated domestic sewage for sustainable TDS management.

The segregated soak liquor is collected from tanneries to the CETP through separate pipe line and after primary and secondary treatment units, membrane system is adopted for recovery of water and quality of saline stream for reuse in pickling. The balance treated saline stream is evaporated and quality salt (98% purity) is recovered for reuse without any difficulty. In addition to recovery and reuse of quality water by the industry, the additional benefits are savings in chemical usage in the tanning process and reduction in pollution load in the effluent.

The segregated chrome stream is taken for Centralized Chrome Recovery System (CCRS) for recovery of chromium in the form of chromium cake. The process flow diagram of the improved chrome recovery system is given below:

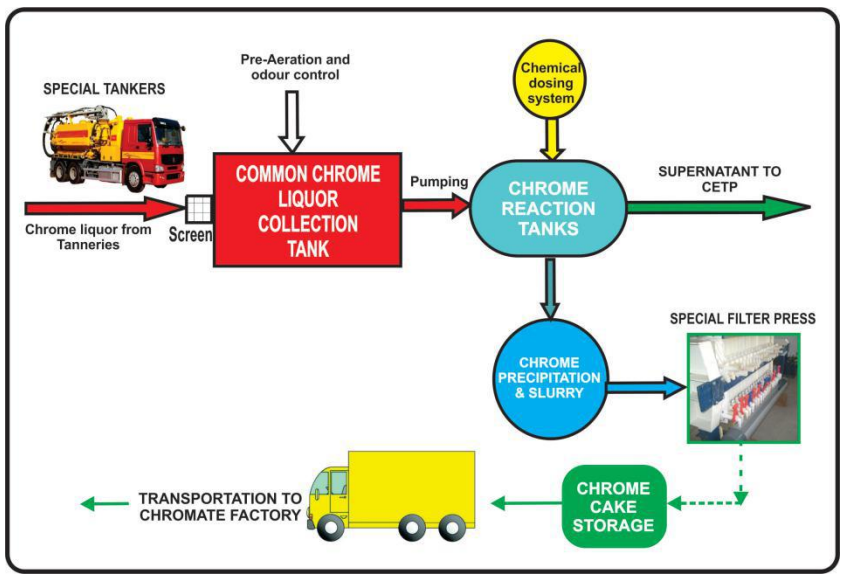

3.SUSTAINABLE INTEGRATED TREATMENT FOR TDS MANAGEMENT AND FINAL DISPOSAL

Due to the segregation of soak liquor and chrome stream for separate treatment and reuse, the TDS level in the main combined stream taken to the CETP is reduced from 18000mg/l to less than 9000mg/l. It has become viable to adopt total biological treatment system and enable the treated effluent mix with treated domestic sewage for achieving all discharge standards including TDS to the level of less than 2100mg/l.

The technological system developed and is being implemented for a capacity of 4.5million litres/day in accordance with the National Green Tribunal (NGT) and Pollution Control authorities is shown in the following process flow diagram.

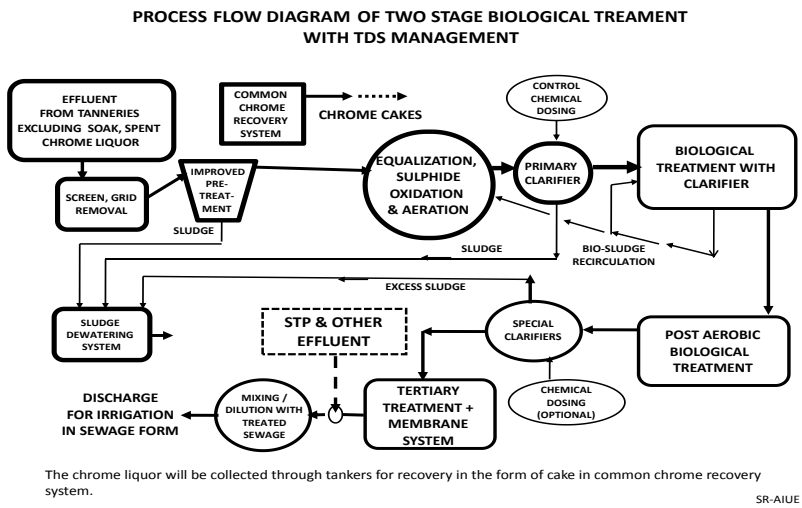

4.CONVERSION OF PHYSIOCHEMICAL TREATMENT IN TO TOTAL BIOLOGICAL TREATMENT

In conventional physiochemical treatment the effluent is collected in equalization cum mixing system, pumped to the primary clarifier, mixed with high dosing of chemicals such as lime alum, etc. The conventional system adopted in most of the CETPs in India could not reduce the sulphide level in the physiochemical treatment and the sludge accumulation in the equalization tank is one of the major problems. The COD reduction to the prescribed level of 250mg/l in the final treated effluent could not be met by the CETPs. The performances of the aerobic biological treatment system with limited detention time are not satisfactory and unable to produce required quality effluent.

The objectives of the advanced biological treatment are sulphide oxidation in the effluent, control the sludge settling in the equalization tank and to minimize the chemical usage in the physiochemical treatment. The equalization system has been upgraded with increased detention time, increased depth and usage of new type of jet aspirators integrated with compressor. The residual excess biosludge from secondary clarifier is pumped to the equalization tank which helps in biological oxidation process and reduces the chemical dosage in the first stage clarifier. The naval conversion of equalization cum mixing system in to aerobic biological oxidation using residual / excess biosludge is shown below:

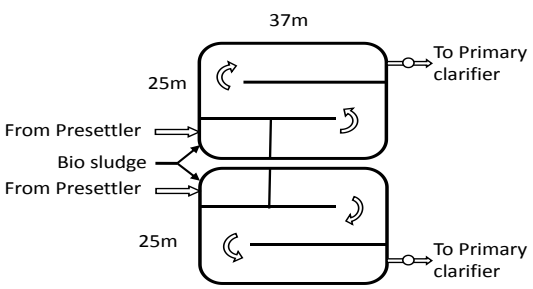

The primary clarifier units are also upgraded by providing elevated clarifiers with minimum required chemical dosing. This improved system is performing better in terms of sludge settling, withdrawal and dewatering. The elevated primary clarifier implemented in one of the CETPs is shown below :

Elevated Primary clarifier

The improved aeration system with jet aspirator has transferred oxygen at the rate 1.8kg/KWH and successfully adopted in many CETPs. The viable alternatives to ZLD have been developed and is being implemented in many CETPs. It is also estimated that nearly 80% capacity of the wastewater from Indian Leather Sector will be treated by adopting cleaner technologies, segregation of streams and separate treatment, integration with treated domestic sewage, etc. The long term sustainability of the CETPs which are forced to adopt ZLD by incorporating systems such as Multiple Stage Evaporator (MEE) may be reviewed considering the above detailed technological options.

5.CONCLUSION

The conventional physiochemical treatment systems are being upgraded and converted in to total biological treatment system to reduce sludge generation and to achieve the pollution control discharge parameters such as COD and clarity in the treated effluent. The Govt. of India organizations such as DIPP, NMCG, etc. extend financial support for upgradation of CETPs with Improved Cleaner Production Process, Centralized Chrome Recovery and Reuse systems, integrated treatment with treated domestic sewage for sustainable TDS management, etc. These technological developments and upgradation of CETPs are being implemented by many CETPs in India with financial outlay of more than 150 million US dollars.

ACKNOWLEDGEMENT

Contributions of Asian International Union Environment (AIUE) Commission and IUE Commission members from various countries, IUE Commission, IULTCS, UNIDO and European Union are acknowledged.

The contributions of Central Leather Research Institute (CLRI), China Leather Industry Association (CLIA), Taiwanese Leather Industry Association (TLIA), Indian Leather Technology Association (ILTA), National Green Tribunal (NGT), National Mission for Clean Ganga (NMCG), Department of Industry and Policy Promotion (DIPP), Central Pollution Control Board (CPCB), State Pollution Control Boards,Krishnapatnam International Leather Complex Private Ltd. (KPILC), Nellore, Andhra Pradesh, IL&FS, Leather Industry Associations and Common Effluent Treatment Plants (CETP) specifically Pallavaram CETP, Perundurai CETP, Jajmau CETP, Banthar CETP, Unnao CETP, etc. are acknowledged.

O2

A New Two-stage Chrome Tanning Method under Variable Temperature

Hui Zeng[1], Weixing Xu[1*], Jianfei Zhou[1], Bi Shi[1, 2]

1 Key Laboratory of Leather Chemistry and Engineering (Sichuan University), Ministry of Education, Chengdu 610065, China, Tel: +86 139 8084 5527, E-mail:xuwx@scu.edu.cn

2 National Engineering Laboratory for Clean Technology of Leather Manufacture, Sichuan University, Chengdu 610065, China

1. Introduction

Chrome tanning is the dominant tannage[i-ii] for leather manufacture due to that chrome tanned leather has good washing resistance, high shrinkage temperature (Ts) and supple handle[iii]. Nevertheless, chrome is a kind of limited resource[iv]. And enormous amount of chrome-containing wastewater will be generated during processing[v-vi]. As a result, chrome tanning has been regulated and limited in recent years[vii].

Many researchers were committed to achieving cleaner and more efficient technology of chrome tanning in recent decades. There are mainly two ways of doing so. One is the adjustment of leather making process. Some researchers tried to bring in a new section or restructure the existing sections to optimize the chrome tanning process, such as the inverse chrome tanning technology[viii-ix] , chrome tanning with ultrasonic wave[x-xii]. However, these methods were blocked in practice due to the large changes in equipment and processes. The other one is chrome-free tanning. A lot of new tanning agents were proposed, such as HOS-Zr[xiii], OSA [xiv] , d-lysine aldehyde[xv] and so on. But the property of leather prepared by these agents still could not catch up with that of chrome tanned leather.

In our opinion, the most feasible solution to solve the problem of chrome tanning is increasing the absorptivity of chrome tanning agent[xvi]. Only by increasing the absorptivity, the utilization of chromium can be increased and the content of chromium in tanning solution after tannage can be reduced, so as to realize the environmental benign chrome tannage. It was documented that the Cr_2O_3 content of wet-blue was increased by four times as the tanning temperature rose from 0°C to 50°C[xvii]. The fixation of chromium in collagen fiber network was also greatly affected by tanning temperature[xviii]. Hence, we speculated that the chrome tanning effect would be remarkably improved by adjusting the tanning temperature.

In this study, the molecular simulation software MinteqA2 (version 3.1) was used to simulate the hydrolysis and polymerization of Cr(Ⅲ) ions under different temperatures[xix]. Under the guidance of this simulation, pickled skin was tanned through a two-stage chrome tanning process under variable temperature. In stage Ⅰ, pickled skin was tanned with an amount of chrome tanning agent under room temperature to obtain basic hydrothermal stability. In stage Ⅱ, the tanned sample was tanned again under higher temperature. The Ts, mechanical properties and grain morphology of crust, and the comprehensive absorptivity of chrome tanning agent were characterized to evaluate the tanning effect. After all, a technology to achieve environment friendly chrome tanning with practical application can be established.

2. Experimental

2.1 Materials and equipment

Pickled skin with an average thickness of 1.0 mm and chrome tanning agent (25±1% Cr_2O_3, pH=2.0~3.0) were obtained from a local tannery in China. Sodium bicarbonate ($NaHCO_3$), sodium chloride (NaCl), sodium formate (HCOONa), formic acid (HCOOH), nitric acid (HNO_3) and hydrogen peroxide (H_2O_2) were all chemical pure and purchased from Kelong Chemical Reagent Factory, Sichuan, China. Degreasing agent was industrial grade and supplied by Sichuan Dowell Science & Technology Inc, Sichuan, China. Fatliquoring agent was industrial grade provided by Zschimmer & Schwarz, Shanghai, China. The drum (Ø 30 cm) commonly used in leather processing trials was employed to rotate the chemicals and pickled skin to aid penetration.

2.2Preparation of chrome tanned samples (wet-blue/crust)

To make the experimental results comparable, all the pickled skin samples (20 cm × 20 cm) were cut from butt area following back line. These selected samples were processed as Table 1 to obtain experimental wet-blue, and then were processed as in Table 2 to obtain experimental crust. Blank wet-blue / crust (tanned only through stage Ⅰ by 6 wt% chrome tanning agent) and control wet-blue / crust (tanning temperature in stage Ⅱ was 25 °C) were also prepared as Table 1 and Table 2 for comparison.

Table 1 Preparation process of experimental wet-blue

Step	Material	Dosage* (%)	Temperature (°C)	Time (min)	pH
Tanning Stage Ⅰ	H_2O	100	25	20	3.0
	NaCl	8			
	HCOOH (1:10)	0.2×n		10×n	
	Tanning agent	X%**		180	
Basification	$NaHCO_3$ (1:10)	0.2×n	25	15×n+60	3.8~4.0
	H_2O	100	38	180	
Overnight+60min, hanging for 24h					
Washing	H_2O	100	25	30	
	HCOOH (1:10)	0.2			
Tanning Stage Ⅱ	H_2O	100	25	10×n	3.0
	HCOOH (1:10)	0.2×n			
	Tanning agent	X%	X***	180	
Basification	$NaHCO_3$ (1:10)	0.2×n	25	15×n+60	3.8~4.0
	H_2O	100	38	180	
Overnight+60min, hanging for 24h					

*: The dosages were based on double weight of pickled skin;

**: X meant the dosage or the temperature was changed in different trails;

***: Tanning temperature was set to 15°C lower than Ts of wet-blue tanned after stage Ⅰ.

Table 2 Preparation process of experimental crust

Step	Material	Dosage* (%)	Temperature (°C)	Time (min)	pH
Rewetting	water	400	35	40	
	Degreasing agent	0.4			
Washing	water	400	35	10	
Neutralization	water	200	35	30	
	HCOONa	2			
	$NaHCO_3$(1:10)	0.6×n		10×n+90	6.5~7.0
Washing	water	200	35	10	
Fatliquoring	water	40	50	60	
	Fatliquoring agent	10			
Fixing	HCOOH(1:10)	0.5×n		10×n+30	3.8~4.0

Washing	water	100×3	25	15×3
Hanging to condition and milling				

*: All the dosages were based on the weight of wet-blue prepared by Table 1.

2.3 The main Cr(Ⅲ) species under different temperature

MinteqA2 (version 3.1) was used to simulate the distribution of main Cr(Ⅲ) species of 0.001mol/L $Cr_2(SO_4)_3$ solution with the temperature ranging from 25 °C to 100 °C at penetration stage of tanning (pH=3) and combination stage of tanning (pH=4).

2.4 Measurements and instruments

The thickness of all the crust was measured with a dial thickness gauge (MY-3130-A2, MingYu, Dongguan, China). The mechanical properties of all the crust were tested with a universal testing machine (AI-7000SN, GOTECH, Dongguan, China) according to international standards ISO 3376: 2002 and ISO 3377-2: 2002. The softness of all the crust was measured with a ball pressure softness tester (GT-303, GOTECH, Dongguan, China). The Ts of all the samples was determined according to International standards ISO 3380: 2002.

The grain morphology of crust was observed by stereo microscope (SZX12, Olympus, Japan). The Cr(Ⅲ) ions concentration in tanning solutions and digestion solution of all the wet-blue was tested by inductively coupled plasma optical emission spectrometer (ICP-OES, Optima 2100DV, PerkinElmer, American). The comprehensive absorptivity of chrome tanning agent was calculated as $1-(c_{1\text{-}2}+c_{2\text{-}2}) / (c_{1\text{-}1}+ c_{2\text{-}1}) \times 100\%$, where $c_{1\text{-}1}$and $c_{1\text{-}2}$ were Cr(Ⅲ) ions concentration (ppm) in tanning solutions before and after tanning stage Ⅰ, respectively, $c_{2\text{-}1}$and $c_{2\text{-}2}$ were Cr(Ⅲ) ions concentration (ppm) in tanning solutions before and after tanning stage Ⅱ, respectively. The Cr_2O_3 content of wet-blue was calculated as $1.52\times x\times V\times 10^{-6}/m\times 100\%$, where x, V and m represented the Cr(Ⅲ) ions concentration (ppm) in solution after digestion, the volume of digestion solution (mL) and the weight of wet-blue (g), respectively.

In order to semi-quantitatively characterize the distribution of chrome in all the wet-blue, wet-blue was split evenly into two layers. The chromium content in grain surface, split surface (either one) and flesh surface was detected by X-Ray Fluorescence (XRF, Epsilon 1, Parnaco, Netherlands).

The total organic carbon content in fatliquoring solutions was tested by total organic carbon analyzer (TOC, vario TOC, Elementar, Germany). The absorptivity of fatliquoring agent was calculated as $(1-P_2/P_1) \times 100\%$, where $P_1$and P_2 were total organic carbon content in fatliquoring solutions (ppm) before and after fatliquoring, respectively.

3. Results and discussion

3.1 The states of $Cr_2(SO_4)_3$ at penetration stage and combination stage of chrome tanning

The molecular simulation result of the distributions of main Cr(Ⅲ) species of 0.001mol/L $Cr_2(SO_4)_3$ solution with the temperature ranging from 25 °C to 100 °C at penetrationstage of tanning (Figure 1A, pH=3) and combination stage of tanning (Figure 1B, pH=4) is showed in Figure 1. At penetration stage of conventional tanning (25 °C), most Cr(Ⅲ) ions are monomers and no dinuclear and trinuclear Cr(Ⅲ) ions appeared. With the tanning temperature increasing, the proportion of Cr(Ⅲ) monomers decreases, the proportion of dinuclear Cr(Ⅲ) ions shows non-linear growth, and no trinuclear Cr (III) ions appears yet. At combination stage of tanning, a small amount of dinuclear Cr(Ⅲ) ions appears at 25 °C, and the proportion of dinuclear Cr(Ⅲ) ions and trinuclear Cr(III) ions gradually increases with the tanning temperature increasing.

The results of molecular simulation show that whether in penetration stage or combination stage, the increase of tanning temperature is beneficial to the increase of molecular size of chromium complexes, leading to the increase of multi-point bonding between collagen fibers and chromium complexes[xx].

However, since pickled skin is not resistant to high temperature[xxi](>60 °C), it needs to be tanned in two stages during practical tanning process. In stage Ⅰ, pickled skin needs to be tanned with an amount of chrome tanning agent under room

temperature to obtain basic hydrothermal stability. In stage Ⅱ, the sample can be tanned again under higher temperature to achieve better tanning effect with more multi-point bonding between collagen fibers and chromium complexes.

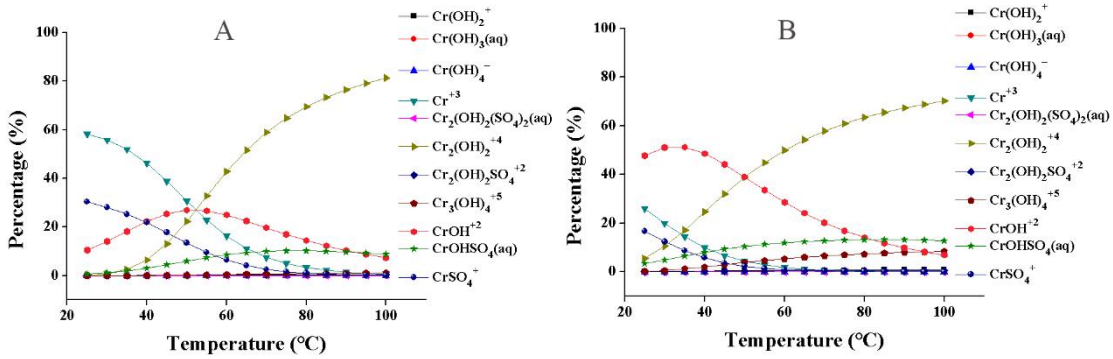

Figure 1 The distributions of Cr(Ⅲ) species in 0.001mol/L $Cr_2(SO_4)_3$

(A: penetration stage; B: combination stage)

3.2 Effect of the chrome tanning agent dosage in different stage on properties of wet-blue / crust

The code name of samples with different dosage of chrome tanning agent and the corresponding tanning temperature in stage Ⅱ are showed in Table 3.

Table 3 The code name of samples during different tanning progress

Code name	Dosage of chrome tanning agent in stage Ⅰ (%)	Dosage of chrome tanning agent in stage Ⅱ (%)	Tanning temperature in stage Ⅱ (°C)
Blank	6	—	—
N1	1	5	25
N2	2	4	25
N3	3	3	25
N4	4	2	25
N5	5	1	25
H1	1	5	55
H2	2	4	60
H3	3	3	82
H4	4	2	85
H5	5	1	92

3.2.1 Effect of the chrome tanning agent dosage in different stages on Ts of crust

Ts can reflect hydrothermal stability of leather and tanning effect. The Ts of crust prepared by different tanning processes is showed in Table 4. It shows that Ts of experimental crust were higher than that of blank crust and control crust. This result intuitively shows that the two-stage chrome tanning under variable temperature is conducive to the rise of Ts.

This phenomenon may be caused by two reasons. Firstly, collagen fiber network becomes looser under higher temperature, which is in favor of the penetration of chrome tanning agent. Secondly, the hydrolysis and polymerization of Cr(Ⅲ) ions will change when tanning temperature rises. More dinuclear Cr(Ⅲ) ions will produce when tanning temperature is higher than room temperature, especially at combination stage, which will lead to more multi-point bounding. In this case, Ts can be increased.

In addition, with the increase of dosage of chrome tanning agent in stage Ⅰ, Ts of experimental crust first increased then decreased. This is because the skin needed a tanning process to obtain basic hydrothermal stability in stage Ⅰ, and a

higher tanning temperature to achieve better tanning effects in stage Ⅱ. When the chrome tanning agent dosage used in stage Ⅰ was too little, the wet-blue failed to bear a higher tanning temperature in stage Ⅱ, which resulted in a relatively lower Ts, as H1. Correspondingly, when the chrome tanning agent dosage used in stage Ⅰ was too much, the agent used in stage Ⅱ would be limited, which would impede tanning effects and weaken the hydrothermal stability of crust, as H5.

Table 4 Ts of crust prepared by different tanning processes

Sample	Ts (°C)	Sample	Ts (°C)
Blank	107.2		
N5	100.8	H5	115.3
N4	102.2	H4	116.3
N3	110.2	H3	116.6
N2	105.7	H2	118.8
N1	107.0	H1	117.1

3.2.2 Effect of the chrome tanning agent dosage in different stages on comprehensive absorptivity of chrome tanning agent

The comprehensive absorptivity of chrome tanning agent prepared by different tanning processes was measured, as showed in Figure 2. The result shows the comprehensive absorptivity of chrome tanning agent of experimental wet-blue (>85%) is higher than that of control wet-blue (~80%) and blank wet-blue (~70%). With the decrease of dosage of chrome tanning agent in stage Ⅰ, the comprehensive absorptivity of chrome tanning agent of experimental wet-blue increases. Among all the samples, the comprehensive absorptivity of chrome tanning agent of H1 and H2 was up to 95.1% and 91.3%, respectively, which was very advantageous to achieving environment friendly chrome tanning. Taken together, the two-stage chrome tanning under variable temperature is beneficial to improving the comprehensive absorptivity of chrome tanning agent and reducing the waste of chromium.

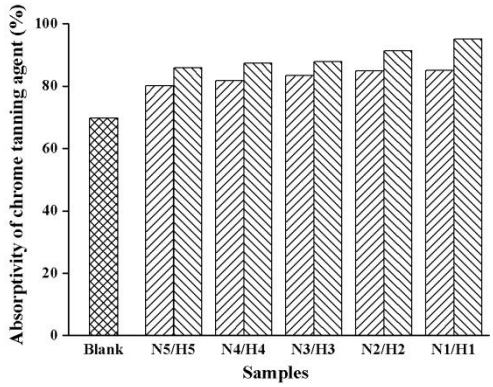

Figure 2 The comprehensive absorptivity of chrome tanning agent prepared by different tanning processes

3.2.3 Effect of the chrome tanning agent dosage in different stage on the Cr_2O_3contentof wet-blue

The Cr_2O_3 content of wet-blue was also measured as showed in Table 5. It can be seen that the Cr_2O_3 content of experimental wet-blue is higher than that of control wet-blue and much higher than that of blank wet-blue. Besides, the Cr_2O_3 content of experimental wet-blue increased with the dosage increase of chrome tanning agent in stage Ⅱ,which meet the increase of Ts as showed in 3.2.1.

Table 5 The Cr_2O_3 content of wet-blue prepared by different tanning processes

Sample	Cr_2O_3 content (mg/g)	Sample	Cr_2O_3 content (mg/g)
Blank	17.02	-	-
N5	19.19	H5	28.83
N4	23.17	H4	29.61
N3	23.17	H3	32.99
N2	23.32	H2	33.50
N1	28.68	H1	35.97

3.2.4 Effect of the chrome tanning agent dosage in different stage on mechanical properties of crust

The tensile strength, tear strength, elongation at break and softness index of crust were measured, as showed in Figure 3. It is observed that the mechanical properties of experimental crust are poorer than that of blank crust and control crust in most cases. This is because high temperature in stage Ⅱ may cause damage to the braided structure of collagen fiber network. When tanning temperature in stage Ⅱ was appropriate, the mechanical properties of crust wouldn't decline, as H2. The poor mechanical properties of H1 may be caused by the insufficient chromium penetration in stage Ⅰ.

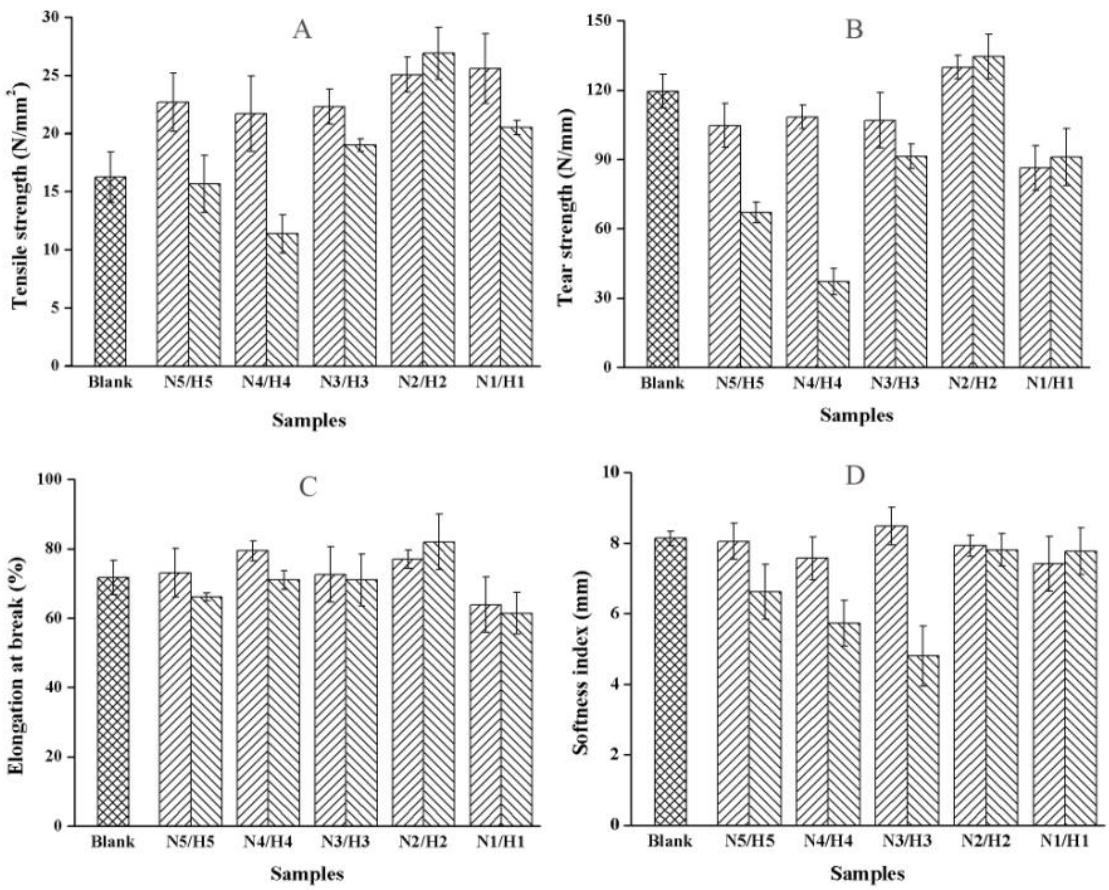

Figure 3 The mechanical properties of crust prepared by different tanning processes
(A: Tensile strength; B: Tear strength; C: Elongation at break; D: Softness index)

3.2.5 Effect of the chrome tanning agent dosage in different stage on the grain morphology of crust.

Figure 4 is the grain morphology of crust prepared by different tanning processes. It is observed that, comparing with blank crust and control crust, the grain of some experimental crust is rough, such as H5, H4 and H3. It may be caused by two reasons. A high tanning temperature in stage Ⅱ make the wet-blue shrank slightly. The reactivity of chrome tanning agent with collagen fiber increases at high temperature, resulting in a large part of chrome tanning agent reacting on the surface of wet-blue before penetration[xxii]. Further research is needed to determine the real reason.

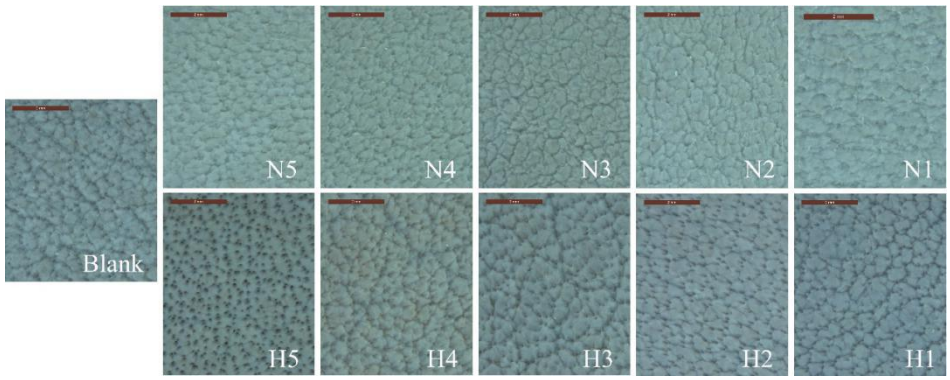

Figure 4 Grain morphology of crust prepared by different tanning processes

3.2.6 Effect of the chrome tanning agent dosage in different stage on the chromium penetration of experimental wet-blue

The chromium penetration of experimental wet-blue was conducted on XRF as showed in Figure 5. It shows that the chromium penetration of experimental wet-blue is relatively uniform. Hence, we infer that the rough grain of H5, H4 and H3 is not caused by the uneven penetration. The chromium penetration of H1 is uneven as we speculated before. This is because the chrome tanning agent dosage in stage Ⅰ is too little to fully infiltrate collagen fiber network, which will cause the sandwich layer of wet-blue untanned. In this case, the collagen fiber in the sandwich layer would denature in stage Ⅱ, which would affect the further penetration and fixation of chromium of stage Ⅱ and weaken the mechanical properties of H1. Among all the experimental wet-blue, the chromium permeability uniformity of H2 is the best.

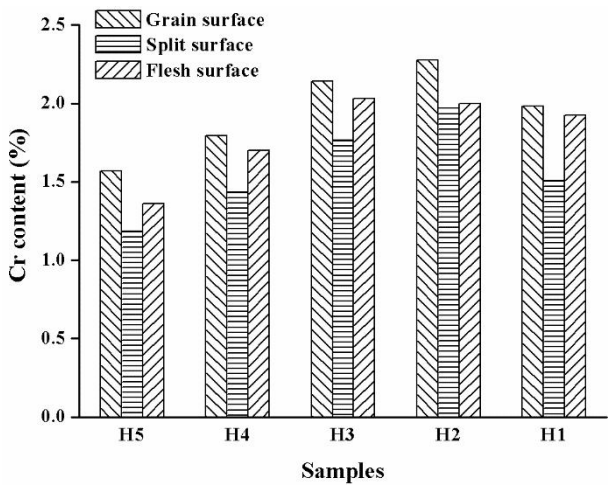

Figure 5 The chromium penetration of experimental wet-blue

3.3 Further optimization of the chrome tanning agent dosage of two-stage tanning under variable temperature

Former results proved the two-stage chrome tanning method under variable temperature can achieve a cleaner chrome tanning. Since the comprehensive absorptivity of chrome tanning agent and Cr_2O_3 content of experimental wet-blue were much higher than those of blank wet-blue, to achieve the efficient utilization of chrome, the chrome tanning agent dosage can be decreased. By comparing the properties of wet-blue/crust prepared by different tanning processes, H2 (the chrome tanning agent dosage in stage Ⅰ and stage Ⅱ was 2 wt% and 4 wt%, respectively) possessed better performance. Because chromium could infiltrate into H2 evenly, and 91.3% of chrome tanning agent could be absorbed by collagen fiber network. The Ts of H2 was 118.8 °C. The mechanical properties of H2 were not affected by tanning temperature (60 °C) in stage Ⅱ and its grain was fine. In this section, the dosage of the chrome tanning agent in stage Ⅰ was set to 2%, while the chrome tanning agent dosage in stage Ⅱ was gradually reduced from 4 wt% to 3wt%, 2 wt% and 1 wt%. These samples were named as H2-4, H2-3, H2-2 and H2-1, respectively. The tanning temperature in stage Ⅱ was set as 60 °C.

3.3.1 Effect of the chrome tanning agent dosage in stage Ⅱ on the tanning effects of experimental wet-blue/crust

Table 6 shows Ts, comprehensive absorptivity of chrome tanning agent and Cr_2O_3 content of H2-4, H2-3, H2-2 and H2-1. It shows that Ts of those crust all exceeded 100 °C which reached the basic industry requirement[xxiii]. Among these samples, H2-1 had the highest comprehensive absorptivity of chrome tanning agent with the least dosage of chrome tanning agent which achieved cleaner less-chrome tanning.

Table 6 The tanning effects of experimental wet-blue / crust with different chrome tanning agent dosage

Sample	Ts (°C)	Comprehensive absorptivity of chrome tanning agent (%)	Cr_2O_3 content (mg/g)
H2-4	118.8	91.3%	33.50
H2-3	115.3	93.3%	27.82
H2-2	111.1	95.7%	24.24
H2-1	104.6	96.3%	15.49

3.3.2 Effect of the chrome tanning agent dosage in stage Ⅱ on the properties of experimental crust

Figure 6 is the mechanical properties of experimental crust. Figure 7 is the absorptivity of fatliquoring agent. Figure 8 is the grain morphology of experimental crust. From these figures, it is found that the mechanical properties of these crust all meet the industryrequirement [xxiv], of which those of H2-1 are the best. Besides, the absorptivity of fatliquoring agent is around 90% and grain of these crust is fine.

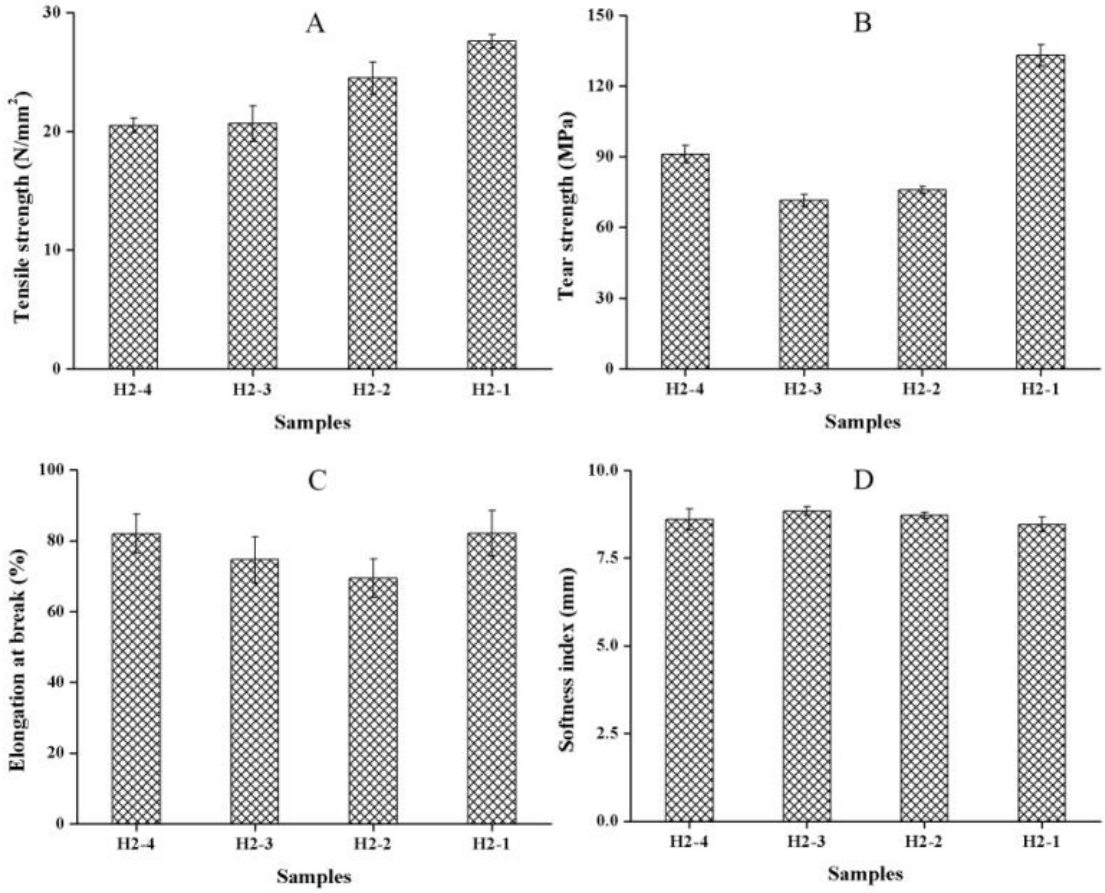

Figure 6 Mechanical properties of experimental crust with different chrome tanning agent dosage (A: Tensile strength; B: Tear strength; C: Elongation at break; D: Softness index)

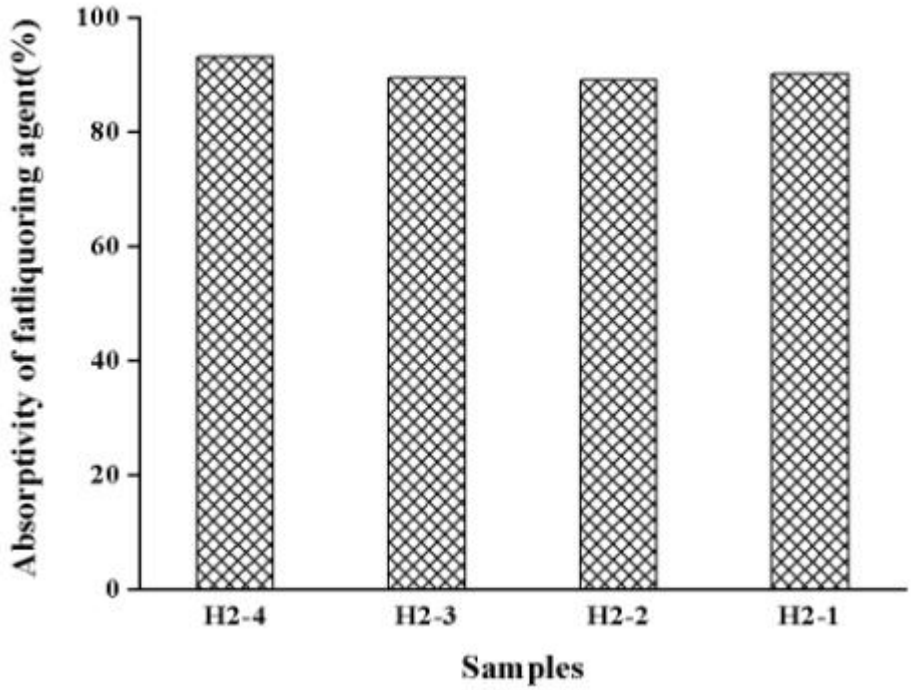

Figure 7 The absorptivity of fatliquoring agent of experimental crust with different chrome tanning agent dosage

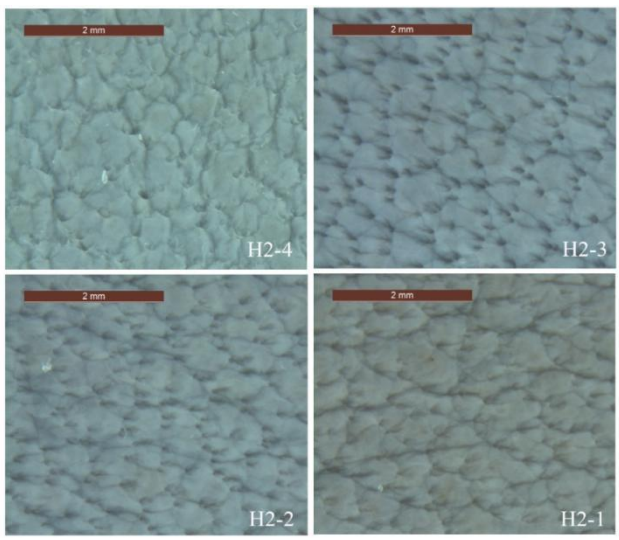

Figure 8 Grain morphology of wet-blue with different chrome tanning agent dosage

Hence, the optimal proportion of dosage of the two-stage chrome tanning under variable temperature is 2 wt% and 1 wt%, respectively.

4 Conclusion

A more environment friendly and more efficient method of chrome tanning can be achieved by a two-stage tanning under variable temperature. The technological processes are as follows: In stage Ⅰ, pickled skin was tanned with 2 wt% chrome tanning agent to obtain basic hydrothermal stability; In stage Ⅱ, wet-blue was tanned again with 1 wt% chrome tanning agent under 60 °C to improve the tanning effect. The wet-blue prepared by this method only need half of chrome

tanning agent (3 wt%) compared with the conventional tanning (6 wt%). The comprehensive absorptivity of chrome tanning agent can be as high as 96.3%, which is almost 40% higher than that of traditional technology (70%). With a Ts of 104.6 °C, satisfactory mechanical properties and smooth grain, the wet-blue prepared by this new method can be suitable for most leather types on the market. Since the changes of equipment and processes are quite little, this two-stage chrome tanning method under variable temperature has a prospect in practical application of leather making.

5 Acknowledge

The financial support of this study was from the Key R&D Program of Zhejiang Province (2017C03055).

Reference

[1] Seligsberger L. Leather research and technology in the age of chrome [J]. Journal of the American Leather Chemists Association, 1991, 86: 246-258.

[2] Sundar V J, Rao J R, Muralidharan C. Cleaner chrome tanning—emerging options [J]. Journal of Cleaner Production, 2002, 10(1): 69-74.

[3] Bieńkiewicz K. Physical chemistry of leather making [M]. Krieger Pub. Co, 1983.

[4] Zeng X T, Yuan C H, Hong X U, et al. Industrial situation and strategy of China's chrome resource [J]. Resources & Industries, 2015, 17(3): 39-44.

[5] Bacardit A, Morera J M, Ollé L, et al. High chrome exhaustion in a non-float tanning process using a sulphonic aromatic acid [J]. Chemosphere, 2008, 73(5):820-4.

[6] Cao S, Wang K, Zhou S, et al. Mechanism and effect of high-basicity chromium agent acting on Cr-wastewater-reuse system of leather industry [J]. ACS Sustainable Chemistry & Engineering, 2018, 6(3): 3957-3963.

[7] Nair B U, Thanikailevan P, Saravanabhavan S, et al. Integration of chrome tanning and wet finishing processes for making garment leathers [J]. Journal of the American Leather Chemists association, 2005, 100(6): 225-232.

[8] Chao W, Zhang W, Liao X, et al. Transposition of chrome tanning in leather making [J]. Journal of the American Leather Chemists association, 2014, 109(6): 176-183.

[9] Saravanabhavan S, Thanikaivelan P, Rao J R, et al. Reversing the conventional leather processing sequence for cleaner leather production [J]. Environmental Science & Technology, 2006, 40(3): 1069-1075.

[10] Sivakumar V, Rao P G. Application of power ultrasound in leather processing: an eco-friendly approach [J]. Journal of Cleaner Production, 2001, 9(1): 25-33.

[11] Zhang J, Wang Y, Bo T, et al. New chrome tanning method assisted by wringing and ultrasound [J]. Journal of the American Leather Chemists association, 2013, 108(12): 445-448.

[12] Sivakumar V, Swaminathan G, Rao P G, et al. Use of ultrasound in leather processing industry: effect of sonication on substrate and substances-new insights [J]. Ultrasonics Sonochemistry, 2010, 17(6): 1054-1059.

[13] Yu Y, Wang Y N, Ding W, et al. Preparation of highly-oxidized starch using hydrogen peroxide and its application as a novel ligand for zirconium tanning of leather [J]. Carbohydrate Polymers, 2017, 174: 823-829.

[14] Ding W, Zhou J, Zeng Y, et al. Preparation of oxidized sodium alginate with different molecular weights and its application for crosslinking collagen fiber [J]. Carbohydrate Polymers, 2017, 157: 1650-1656.

[15] Krishnamoorthy G, Sadulla S, Sehgal P K, et al. Greener approach to leather tanning process: d -Lysine aldehyde as novel tanning agent for chrome-free tanning [J]. Journal of Cleaner Production, 2015, 42(3):277-286.

[16] Ramasami T, Rajamani S, Rao J R. Pollution control in leather industry: emerging technological options [C]. Proceedings of the International Symposium on Surface and Colloidal Science and Its Relevance to Soil Pollution. 1994.

[17] RamonPalop. The effect of basification and temperature on chrome tanning [J]. Beijing leather: 2001(8): 45-48.

[18] Covington A D. Chrome tanning: exploding the perceived myths, preconceptions and received wisdom [J]. Journal of

the American Leather Chemists Association, 2001, 96(12): 467-480.

[19] Han W, Zeng Y, Zhang W. A further investigation on collagen-Cr(III) interaction at molecular level [J]. Journal-American Leather Chemists Association, 2016, 111(3): 101-106.

[20] Cheng J. The Effects of chromium-olation length on crosslinking effects investigated by molecular dynamics simulation [J]. Soft Materials, 2015, 13(1): 24-31.

[21] Onem E, Yorgancioglu A, Yilmaz O, et al. Evaluation of the analysis conditions for DSC instrument to realize the thermal behaviors of leathers [C]. IV International Leather Engineering Congress. 2017.

[22] Covington A D. Tanning chemistry: the science of leather [M]. Royal Society of Chemistry, 2009.

[23] Musa A E. Semi-chrome upper leather from rural goat vegetable tanned crust [J]. Journal of Applied and Industrial Sciences, 2013, 1(1):43-48.

[24] Xu W X. The reinforcement of leather split by in-situ polymerization and recombination [D]. Chengdu: Sichuan university. 2017.

O3

CONSUMER'S NEED FOR SUSTAINABLE PRODUCTS IN THE LEATHER INDUSTRIES

Yves MORIN - General Manager of "YVES MORIN CONSULTING"

Abstract:

From the beginning of "Globalization" until today, worldwide economy have change so much. Mass consumption and fast fashion are now driving the market trends.

Production have switched from western countries to developing countries and labor or environmental regulations did not follow this change in most of the producing countries. As a result some "unsustainable" situations appeared: workers in sweatshop factories, children at work, water and air pollution from textile mills and tanneries, forbidden chemicals in the products, etc

Since some years the consumers, as main stakeholders of the leather industries, are aware of this supply chain, thanks to the information coming from the NGO's and thanks to the social media which give a large audience to any abuse. In April 2013 the Rana Plaza drama was the start for a new era, most of the consumers now do not approve any more this organization and this kind of society.

So international sourcing companies, as well as local factories, are now ready for a move to protect their reputation and to keep on developing their business in a safer way.

We can see now a lot of private standards or international public rules which have been established, such as ISO 26000 about Corporate Social Responsibility, so that there are now solutions to correct the excess of "Globalization" and to give better future to the leather industries.

O4

Pyrolysis Component Analysis of Different Leathers

Keyong Tang[1*], Jie Liu[1],Yadi Hu[1], Pengyuan Yang[1], Eleni Tziamourani[2],S C Boyatyzis[2]

(1. School of Materials Science and Engineering ,Zhengzhou university ,Zhengzhou, Henan, 450001; 2.University of West Attica, Department of Conservation of Antiquities & Works of Art, Egaleo 12210, Greece)

**Corresponding author: kytang@126.com, Tel. +86 139 3852 6389*

Abstract：

Leathers have been being used by human for a long time, partly because of their good durability and flexibility. By now, however, little is know about the pyrolysis of leathers. Therefore, it is significant to study the pyrolysis of leathers. In this paper, TG-DSC, TG-MS and TG-FTIR techniques were employed to investigate the pyrolysis of pure collagen and collagen tanned with different agents, such as glutaraldehyde, formaldehyde and chrome. Results indicated that the pyrolysis of collagen in air may be divided in three stages, and that in argon only two. No matter in air or in argon, the first pyrolysis stage is dehydration of collagen. The second and third stages in air are the fast oxidation devolatilization and combustion of collagen respectively, while in argon correspond to the fast devolatilization and carbonization.

Polarized microscope analysis showed that there is crystal structure in collagen below 200 ^{o}C, which changes to a disordered structure when the temperature reaches 240 ^{o}C. The evolution of CH_4, SO_2, H_2O, CO and CO_2 were found during the pyrolysis process. Tanning does not affect the pyrolysis products of collagen. Whereas, the evolution temperature and content present a difference between the samples tanned with different tanning agents. By comparing the samples tanned with glutaraldehyde, formaldehyde and chrome, CH_4 evolution content of collagen tanned with glutaraldehyde is high and occurred through the whole pyrolysis process. Additionally, the SO_2 evolution temperature of formaldehyde tanned sample is higher than that of glutaraldehyde tanned sample, indicating formaldehyde interacted with the disulfide bond in collagen, thereby improving the stability of this bond. Further study on the sample tanned with different chrome tanning concentration showed that the evolved temperature of fragment ions such as m/z of 16, 17,18 44,45, 47, 48, 64 and 66 increased with the increase of chrome tanning solution concentration at the chrome tanning solution concentration below 10.0 g/L, no obvious change was found at 12.5g/L.

Key Words: collagen, hide powder, tanning, pyrolysis

O5

An Eco-benign Organic Combination Tanning System for Manufacture of Garment Leathers

A.E Musa[1*], G.A. Gasmelseed[2], E.F. Faki[3], H.E Ibrahim[2], O.A Haythem[4], M.A Manal[1], S.B Haythem[1]

1Department of Leather Technology, College of Applied and Industrial Sciences, University of Bahri, Khartoum – Sudan, P.O.Box 1660

2University of Science and Technology, Faculty of Engineering, Department of chemical engineering Khartoum – Sudan

3Department of Leather Engineering, School of Industrial Engineering and Technology, Sudan University of Science and Technology, Khartoum – Sudan,

4National Leather Technology Centre , , Khartoum – Sudan

Abstract

Tanners have been showing great interest in developing chrome-free tanning technologies in recent years and nowadays, the chrome-free leather is more favoured in the market. Oxazolidine is a tanning agent with a high affinity to the natural proteins. Mainly it used in combination with tanning material either vegetable or synthetic, gives more softness, fullness and lightweight leather compared to standard leather. Combination tanning using vegetable tannins and oxazolidine has been proved to be a preferred alternative to chrome tanning. In this study, organic combination tanning process based on garad powder (*Acacia nilotica sub. sp. nilotica*) and oxazolidine for the production of garment leathers is presented. Garad pods powder extract has been utilized in the combination tanning system with oxazolidine. Garad tanned leathers from sheep skins used as control leathers. It has been observed that garad - oxazolidine combination tanning which employs 20% garad pods powder extract and 5% oxazolidine provides a shrinkage temperature of 103°C, which is 19°C more than the control leathers. The characteristics of the leathers indicate that the garad -oxazolidine combination system provides leathers with good organoleptic properties and comparable strength properties. The experimental tanning system provides significant reduction in the discharge of total dissolved solids in the wastewater. The leathers have been further characterized for chemical analysis. The leathers obtained from the combination system are lighter in color compared to control leathers. The manufacture of garment leathers using combination of garad and oxazolidine suggest that this tannage is a promising alternative to traditional chrome tanning.

1. Introduction

Tanning is a multi-steps process whereby a perishable animal hide or skin is converted into leather, which resists microbial attack and may last indefinitely. Biologically, the skin is connective tissue, comprised mainly of the extracellular matrix, a fibrous collagen structure. Tanning stabilizes the collagen matrix, protecting it against heat, water, and microbes[1].

Chrome tanning has been used for more than 100 years and about 90% of all the tanneries in the world have adopted chrome tanning[2]. Though chromium is considered as the best mineral tanning agent which leads to high hydrothermal stability, i.e. shrinkage temperature (Ts) over 100°C,[2] it has a negative image. During tanning, the chromium may not be fully absorbed, and 20%-30% of chromium is discharged in the waste liquor so that it is wasted and the environment is polluted. In recent years, researchers have found that the Cr (III) is easy to oxidize to Cr(VI) by light, heat, sweat, chemical materials, etc and that it is a proven carcinogen[3-5]. So there is a requirement for an eco-friendly tanning process. Chrome-free tannage is an eco-friendly tannage. Nowadays, chrome-free leather is more and more favoured in the market and so it makes sense to study chrome -free tannages. Moreover, other tanning agents such as vegetable tannins, oxazolidine, aluminium, titanium, zirconium have associated disadvantages[6-8]. Combination tannages are thus considered as suitable alternatives for a chrome-free tanning system. Amongst the innumerable combination tannages that are currently exploited, vegetable tannins

and oxazolidine combination tannages; vegetable tannins and aluminium tanning agent combination tannages are the most promising options. They have different mechanisms in improving the stability of collagen. In the process, oxazolidine and aluminium act as crosslinkers so that it is possible to achieve a hydrothermal stability comparable that of chrome-tanned leather[9-11].

Oxazolidines, heterocyclic derivatives, are synthesized using amino-hydroxy compounds and aldehydes as raw materials[12]. In the 1970s, oxazolidines were developed and patented as a new class of tanning agent[7]. Among the oxazolidines, oxazolidine A and oxazolidine E (Fig. 1 and Fig. 2) have been produced and studied extensively for their use as tanning agents[3].

Oxazolidine will react with the amino groups of collagen to form cross-links to improve the shrinkage temperature of leather[7,14]. Under hydrolytic conditions, the rings open to form an N-hydroxymethyl compound, which can react with one or more amino groups to produce effective cross-linking (Fig. 3).[5]

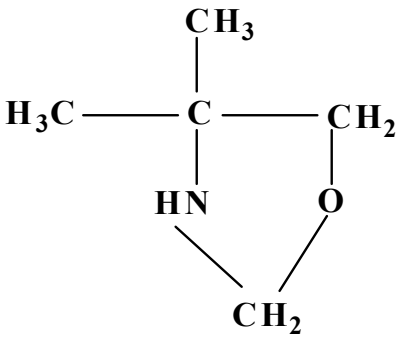

Figure 1: Oxazolidine A

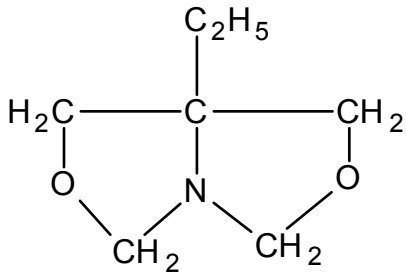

Figure 2: Oxazolidine E

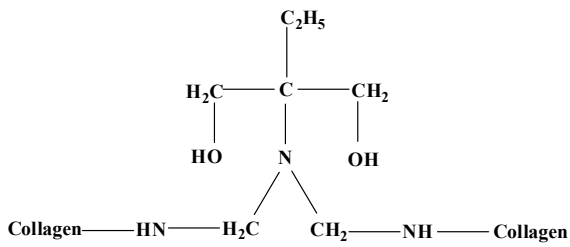

Figure 3: Ring opening of oxazolidine and cross-linking of collagen with oxazolidine

BIOTAN G100 (Heterocyclic synthetic tanning agent) is a concentrated oxazolidine product with excellent tanning properties. When used alone BIOTAN G100 produce leather with a good mellow full hand, fine grain, good tear resistance and of a light yellow colour. The more common use of BIOTAN G100 is in the pretanning of vegetable and chrome leather as well as retanning agent to improve mellowness, tear resistance and grain appearance. BIOTAN G100 used in pretanning of chrome leather improve fullness, softness of final article and the exhaustion of the tanning float. BIOTAN G100 is fully functioning in a range of pH from 3,5 to 9, therefore can be used without any adversity during retanning before or after neutralization[15].

Bio-active ingredients in the form of tannins are present in some of the plant materials capable of imparting tanning effect. Vegetable tanning is one of the traditional and eco-friendly processes in leather making involving plant materials[16].

The vegetable tannins are water-soluble polyphenolic compounds having molecular weight in the range of 500 –3000 Daltons[17,18]. Based on their chemical structure, the vegetable tannins are classified as Hydrolysable type (e.g. Myrobalan) and Condensed type (e.g. Wattle).

To the rural tanner of tropical and subtropical Africa and Asia, the acacias are one of the most important tannin-bearing trees. Several species, suc h as *Acacia Arabica*, *A. nilotica* and *A.adamsonia*, have supplied pods and bark since immemorial times.The leather produced by acacia pods is soft, plump, light colored and durable, and it can be readily dyed. The acacia pods and bark are known variously in the countries where they grow as babul (hindustan), babar (Sind) garad or sunt (Sudan), neb neb (*West Africa*) and gabarua (Nigeria).[19]

The pods used for tanning are from 10 to 15 centrimeters long and 1 centimeter broad, and they have 8 to 10 seeds. Contrary to common belief, the seeds do not contain tannin, which is present only in the pods. According to the conditions of the soil and the climate, their tannin-content varies from 20 to 30%. The material contains an undue proportion of nontans and a high proportion of sugary matter in the seeds. This results in a rapid fermentation of the liquor.

The bark of the *Acacia Arabica* does not contain more than 14% tannin and is mostly used in northern India under the name of babul bark. The bark from old trees yields a very dark colored tannin. It is best, therefore, to strip from trees which are from five to seven years old. When babul bark is used for tanning, it gives a leather which has a darker color and a tendency to crack and tear; but when it is suitably blended with myrobalan (3:1) or with a varam bark, it can be used with advantage, particularly in sole leather tannage[19]. *Acacia nilotica* (Sunt in Arabic) is a member family of subfamily *Mimosoidae* of leguminous trees. It is of multiple uses in the Sudan, Africa and many Arabic countries. The tree is readily distinguished by the long white spines, yellow head inflorescene and the grey necklace-like pods. Three subspecies are commonly found in the Sudan, namely *tomentosa* that characterized by the pubescent pods and grow throughout Sudan, *nilotica* that characterized by the glabrous pods and grow along the White Nile and *adansonii* that characterized by the broad pods and grow in western Sudan[20].The pods of ssp. nilotica have been used for tanning in Egypt for over 6 000 years. The inner bark contains 18-23% tannin, which is used for tanning and dyeing leather black. Young pods produce a very pale tint in leather, notably goat skins. Extracts from the bark, leaves and pods are used for dyeing cotton, silk and leather.

Since the garad extract contains natural products of relatively high molecular weight which have the ability to complex strongly with collagen, an attempt has been made in this study to utilize them in combination tannage with Oxazolidine.

2. Materials and Methods

2.1 Materials

Conventionally processed pickled sheep skins were taken for the combination tanning trials. Garad pods were sourced from Sudan and BIOTAN G100 (Oxazolidine) procured from Biokimica Group-Italy. Chemicals used for post tanning were of commercial grade. Chemicals used for the analysis of spent liquor were of analytical reagent.

2.2 Preparation of Aqueous Extraction of Tannins from Garad Pods

Dry garad pods obtained from Sudan were grounded into powder. Ground garad pods of known quantity have been soaked in water (1:10 w/v) at a temperature of 80±2°C in water bath for one hour, filtered through a piece of cotton cloth and concentrated and used in combination tanning. The total soluble content of the garad pods extract was determined to be 56±1%.

2.3Tanning Trials

The tanning experiments were carried out on pickled sheep skins. Experimental combination tanning trial oxazolidine followed by garad (Oxaz-garad) were carried out as per the process mentioned in Table I and combination tanning based on garad followed by oxazolidine (Garad -Oxaz) was carried out as per the process mentioned in Table II. Control garad tanning trial was carried out as per process given in TableIII. Both experimental and control leathers were processed into garment crusts following the post –tanning process mentioned in Table IV.

2.4Determination of shrinkage temperature

The shrinkage temperature of both control and experimental leathers were determined using the Theis shrinkage tester[21]. A 2 cm sample, cut out from the leather was clamped between the jaws of the clamp, which in turn was immersed in a

solution of glycerol: water mixture (3:1). The solution was stirred using mechanical stirrer attached with the shrinkage tester. The temperature of the solution was gradually increased and the temperature at which the sample shrinks was noted. Triplicates were carried out for each sample and the average values are reported.

2.5Visual assessment of the crust leather

Experimental and control crust leathers were assessed for softness, fullness, grain smoothness, grain tightness (break), general appearance and dye uniformity by hand and visual examination. Three experienced tanners rated the leathers on a scale of 0-10 points for each functional property, where higher points indicate better property.

Table I

Formulation of Oxaz-Garad Combination tanning process for Sheep pickled skin

Process	%	Product	Duration(min)	Remarks
Adjustment of the pH	50	Water		
	1	sodium bicarbonate	3 × 15	pH 6
Tanning	5	Oxazolidine-Biotan G100 (Biokimica)	90	
Garad tanning	2	Phenolic syntan	30	
	10	Garad extract	120	
	10	Garad extract	120	
Fixing	0.5	Formic acid	3 × 10 + 30	Check the pH to be 3.5.
Washing	300	Water	10	Drain the bath and pile overnight. Next day sammed and shaved to 0.8 mm. The shaved weight noted.

2.6 Physical testing

Samples for various physical tests from experimental and control crust leathers wereobtained as per IULTCS methods[22]. Specimens were conditioned at 20 ± 2 °C and 65 ± 2 % R.H over a period of 48 hrs. Physical properties such as tensile strength, percentage elongation at break,[23] grain crack strength[24] and tear strength[25]were measured as per standardprocedures. Each value reported is an average of four (2 along the backbone, 2 across the back bone) samples.

Table II

Formulation of Garad-Oxaz Combination tanning process for Sheep pickled skin

Process	%	Product	Duration (min)	Remarks
Adjustment of the pH	100	Water		
	0.75	Sodium bicarbonate	3 × 15	pH 4.5 -4.7
Tanning	2	Phenolic syntan	30	

	10	Garad extract	120	
	10	Garad extract	120	
	5	Oxazolidine - Biotan G100 (Biokimica)	90	
Fixing	0.25	Formic acid	3× 15	pH 4
Washing	300	Water	10	Check the pH to be 3.5. Drain the bath and pile overnight. Next day sammed and shaved to 0.8 mm. The shaved weight noted.

2.7 Analysis of spent liquor

The spent liquor from control and experimental tanning processing were collected, filtered and analyzed for chemical oxygen demand (COD), Biochemical oxygen demand (BOD_5), and total Dissolve solids (TDS) as per standard procedures[26].

2.8 Chemical Analysis of leathers

The chemical analysis was carried out for control and experimental leathers according to the standard procedures[27]. for total ash content, % moisture, % oils and fats, % water soluble, % hide substance, % insoluble ash and degree of tannage. Triplicates were carried out for each sample and the average values are reported.

Table III

Formulation of Garad tanning process (Control) for Sheep pickled skin

Process	%	Product	Duration(min)	Remarks
Adjustment of the pH	100	Water		
	0.75	Sodium bicarbonate	3× 15	pH 4.5 -4.7
Tanning		Phenolic syntan	30	
	10	Garad extract	120	
	10	Garad extract	120	
Fixing	0.25	Formic acid	3× 10 + 30	pH 3.5
Washing	300	Water	10	Check the pH to be 3.5. Drain the bath and pile overnight. Next day sammed and shaved to 0.8 mm. The shaved weight noted

3. Results and Discussion

Combination tanning trials using garad extract and oxazolidine (Biotan G100) were carried out with 5% offer of oxazolidine and 20% offer of garad powder. The shrinkage temperature data of leathers tanned with Garad - Oxaz and Oxaz-Garad combination along with garad control is given in Table V**.** From the table it is seen that both the combination resulted in leathers with good shrinkage temperature. The shrinkage temperature of leathers obtained from Garad -Oxaz combination tanning is slightly higher than Oxaz- Garad. However, both the combination tanning resulted in leathers with shrinkage temperature greater than **97°C**, which are better than control leathers from Garad of Ts 84°C.

Table IV

Formulation of Post-tanning process for making garment crusts

Process	%	Product	Duration (min)	Remarks
Washing	200	Water	10	
Neutralization	0.75	Sodium bicarbonate	3 × 15	pH 5-5.5
Retanning	100	Water		
	8	Syntan	90	
Fatliquoring	9	Synthetic fatliquor	40	
Dyeing	3	Acid dye brown	30	
Fixing	1	Formic acid	3 × 10 + 30	pH 3.5

Table V

Shrinkage temperature of crust leathers for experimental and control

Experiment	Shrinkage temperature, Ts (°C)
Oxaz- Garad	97±1
Garad -Oxaz	103±2
Garad (Control)	84±0.5

3.1 Ecological Impact - spent liquor analysis

The spent tan liquor contains highly organic matter in both control and experimental process liquor and it contributes to extremely high COD, dissolved and suspended solids. Hence, it is vital to assess the environmental impact from control and experimental tanning process. The COD, BOD_5, and TDS of the spent liquor for experimental and control trials have been determined and are given in Table VI. From the table, it is observed that the COD, BOD_5 and TDS of the spent liquor processed using both the experimental tanning system are lower than the spent liquor from Garad tanning (control). The BOD_5 and TDS of the spent liquor processed from Garad and Oxaz combination tanning trials have significantly reduced compared to the spent liquor of control Garad tanning trial.

Table VI: Characteristics of spent liquor for experimental and control

Experiment	COD (mg\l)	BOD_5(mg\l)	TDS(mg\l)
Garad (control)	124200±2550	26500±1100	102140±2000
Oxaz- Garad	109800±2000	17250±1300	50600±1250
Garad-Oxaz	108420±2650	14000±850	48450±1200

3.2 Tactile properties of crust leathers for experimental and control

The organoleptic properties (visual assessment) of garment crust leathers for experimental and control are given in Fig. 4**. (**Higher numbers indicate superior properties).From the figure, it is observed that crust leathers processed by experimental combination tanning system exhibited good softness, fullness, smoothness, general appearance and dye uniformity compared to control leathers from Garad tannage. The organoleptic properties of the Garad - Oxaz crust leathers are slightly better compared to Oxaz- Garad crust leathers.

3.3 Strength characteristics of experimental and control crust leathers

The physical strength measurements of experimental and control leathers are given in Table VII. The physical strength measurements viz., tensile strength, tear strength has been found to be better for experimental leathers. The experimental Garad - Oxaz tanning system resulted in leathers with good tensile and tear strength characteristics. The values for load at grain crack for both experimental and control leathers were comparable. All the physical strength parameters for both control and experimental leathers are found to exhibit the requirement of BIS norms. It is seen that the softness of experimental leathers are better than that of the garad control leathers.

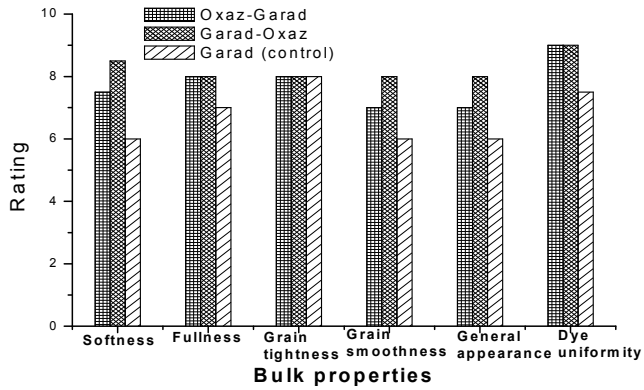

Figure 4: Graphical representation of organoleptic properties of the experimental and control leather

Table VII

Physical strength characteristics of experimental and control crust leathers

Parameter	**Oxaz- Garad**	**Garad -Oxaz**	**Garad (control)**
Tensile strength (Kg/cm^2)	186±2	198±2	174±3
Elongation at break (%)	67±2	75±4	58±2
Tear strength (Kg/cm)	53±3	66±2	49±1
Load at grain crack (kg)	24±0.7	26±0.5	21±0.5
Distention at grain crack (mm)	11±0.3	12±0.3	10±0.3

3.4 Chemical Analysis of the crust leather

The chemical analysis values of experimental crust leathers (Oxaz - Garad and Garad - Oxaz) and control (Garad) are given in Table VIII. The chemical analysis data for the experimental leathers is comparable to that of control leathers. However, the water soluble matter for the control leathers is more compared to the experimental leathers.

Table VIII

Chemical Analysis of experimental and control crust leathers

Parameter	Garad **(control)**	**Oxaz-** Garad	Garad **-Oxaz**
Moisture %	13.50	12.25	12.45
Total ash content %	2.65	2.20	2.60
Fats and oils %	3.45	3.30	3.15
Water soluble matter %	5.30	3.45	3.35
Hide substance %	53	52	51.50
Insoluble ash %	1.35	1.15	1.25
Degree of tannage %	44.15	53.56	54.95

4. Conclusion

Oxazolidine is a tanning agent with a high affinity to the natural proteins. Used in combination with tanning either vegetable or synthetic, gives more softness, fullness andLight weight leather compared to standard leather.

In the present study, an attempt has been made to produce garment leather using combination tanning process based on Garad and Oxazolidine. It is seen that combination tanning system with 20% Garad extract and 5% Oxazolidineresults in leathers with a maximum shrinkage temperature of 103^{o}C, which is 19^{o}C greater than the control leathers. The physical and chemical analysis indicates that the experimental leathers are comparable to control leathers in terms of all the properties. The Garad -Oxaz tanned leathers are softer than control. The bulk properties for the experimental leathers are better than control leathers. One of the main benefits of this work is the lower environmental impact. The spent tan liquor analysis shows significant reductions in COD and TDS loads compared to control. It is possible to manufacture lighter shade garment leathers from garad -Oxaz combination with a shrinkage temperature of 103^{o}C.

5. Acknowledgments

The authors would like to thank the Ministry of higher education and scientific research, Sudan for the financial support. Furthermore, the authors would like to thank Biokimica Group-Italy for the chemicals support.

6. References

1、Eleanor M. Brown,Maryann M. Taylor and Cheng-Kung Liu. (2016).Soluble Collagen App roach to a Combination Tannage Mechanism, *JALCA*, VOL. 111, 141-147.

2、Covington, A. D. (1997), Modern tanning chemistry. Chem. Soc. Rev., 26(2), 111-126.

3、Shrivastava, H. Y. and Nair, B. U. (2001), Chromium (III) mediated structural modifications of glycoprotein: Impact of ligand and the oxidants.Biochem. Biophys. Res. Commun., 285(4), 915-920.

4、Fathima, N. N., Rao, J. R. and Nair, B. U. (2001), Chromium (VI) formation:Thermal studies on chrome salt and chrome tanned hide powder.J. Amer. Leather Chem. Ass., 96(11), 444-450.

5、Balamurugan, K., Vasant, C., Rajaram, R. et al. (1999), Hydroxopentaammine chromium(III) promoted phosphorylation of bovine serum albumin: its potential implications in understanding biotoxicity of chromium. Biochim. Biophys. Acta, (3), 357-366, 1427.

6、Covington, A. D. and Sykes, R. L. (1984), Use of aluminium salts in tanning. J. Amer. Leather Chem. Ass., 79(3), 72-93.

7、Dasgupta, S. (1977), Oxazolidines – A new class of tanning agent. J. Soc. Leather. Technol. Chem., 61(5), 97-105.

8、Covington, A. D.(1987), Tannages based on aluminium(III) and titanium(IV) complexes. J.Amer. Leather Chem. Ass., 82(1), 1-14.

9、Covington, A. D. and Shi, B. (1998), High stability organic tanning using plant polyphenols. Part 1: The interactions between vegetable tannins and aldehydic crosslinkers. J. Soc. Leather. Technol. Chem., 82(2), 64-71.

10、Slabert, N. P. (1981), Mimosa – Al tannages – an alternative to chrome tanning. J. Amer. Leather Chem. Ass., 76(7), 231-234.

11、D'Aquino, A., Barbani, N, D'Elia, G. et al.(2004), Combined organic tanning based on mimosa and Oxazolidine development of a semi-industrial scale process for high-quality bovine upper leather. J. Soc. Leather. Technol. Chem., 88(2), 47-55.

12、Senkus, K. (1945), Some new derivatives of amino hydroxyl compounds. J. Am. Chem. Soc., 67, 1515.

13、 Choudhury, S. D., DasGupta, S. and Norris, G. E. (2007), Unravelling the mechanism of the interactions of oxazolidine A and E with collagens in ovine skin. Int. J. Bio. Macromol., 40, 351.

14、Gunasekaran, A. and Balasubramanian, K. (1988). Studies on 1,3-oxazolidine and 3 hydroxyethyl-1,3-oxazolidinea s tanning agents. J Soc. Leather Technol. Chem.,72(l), 25-26.

15、Biokemica technical data sheet: BIOTAN G100 Heterocyclic synthetic tanning agent.

16、Sivakumar, V., Gopi, K., Harikrishnan, M.V., Senthilkumar, M., Swaminathan, G., Rao, P.G. (2008); Ultrasound assisted diffusion in vegetable tanning in leather processing. JALCA 103, 330-337.

17、Balfe, M.P. (1948), Progress in leather science. British LeatherManufacturer Association.

18、Sundara Rao, V.S. and Santappa, M. (1982); Vegetable Tannins – A Review. J. Sci. Ind. Res. 41, 705-718.

19、FAO, (1960). Vegetable tannins for rural tanners, In rural tanning techniques, 55-56.

20、Elkhalifa, K.F., (1996). Forest Botany. Khartoum University Press.

21、McLaughlin, G.D. and Thesis, E.R. (1945); The chemistry of leather manufacture, Reinhold Publishing Corp., New York, p. 133.

22、IUP 2. (2000); Sampling. *JSLTC*84, 303.

23、IUP 6. (2000); Measurement of tensile strength and percentage elongation. *JSLTC*84, 317.

24、SLP 9 (IUP 9). (1996) Measurement of distension and strength of grain by the ball burst, Official methods of analysis. The Society of Leather Technologist andChemists, Northampton.

25、IUP 8. (2000); Measurement of tear load – double edge tear. *JSLTC*84, 327-329.

26、 Clesceri. LS, Greenberg AE, Trussel RR.Eds. (1989) In standard methods forthe examination of water and wastewater, 17th ed, American public health association Washington DC.

27、Official Methods of Analysis ,Soc.Leather Tech. Chem., U.K. 1965

O6

Study on theFunctionalizedGraphene Modified Waterborne Polyurethane Materials

GUO Song[1,2], DING Zhiwen[1,2], PANG Xiaoyan[*1,3], WANG Wenqi[2], YIN Yuetao[2], YOU Guanqun[2]

1. China Leather and Footwear Research Institute Co. Ltd., Beijing100015, China;

2. China Leather and Footwear Industry Research Institute（Jinjiang）Co.，Ltd，Jinjiang 362200, China;

3. National Engineering Laboratory for Clean Technology of Leather Manufacture, Sichuan University, Chengdu 610065, China

Abstract：

A new type of waterbornpolyurethane (WPG) is fabricated using the functionalized graphene. The mechanical properties, wear resistance, and heat aging resistance of the modified polyurethane materials were tested. It is confirmed that the grapheme oxide was introduced into the polyurethane chain as a hard segment by the infrared spectra. The results show that the initial thermal decomposition temperature (Td5) of polyurethane films increased from 217°C to 244 °C, the water absorption rate and the mechanical property of modified polyurethane film firstly decreases and then increases with the increase of functionalized grapheme. In addition, the wear resistance of modified polyurethane film decreases following the increase of functionalized grapheme. Furthermore, the heat aging resistance is best when the content of functionalized grapheme is 0.02% (wt). The centrifugal stability test shows when the content is less than 0.04%, the products are stable.

Key words： Waterborne polyurethane; Functionalized graphene; Heat resistance, Mechanical property; Wear resistance; Heat aging

*Corresponding author: pang_xiaoyan@126.com

1 Introduction

Graphene is a new carbon material, which was discovered by Novoselov and AndreGeim. It has outstanding physical and chemical characteristics, for instance, ultra-high specific surface area, superior thermal conductivity, mechanical characteristics, extremely high conductivity and water repellency. It is expected to become a high-grade filler for polymer-based carbon nanocomposites, providing the polymers based composites with outstanding performance, together with expanding their applications. Nevertheless, owing to the robust van der Waals force between the graphene layers, the dispersibility of graphene in typical organic solvents is quite poor that, as a response, exerts impact on both the compatibility and dispersibility of graphene in the composite substrate, accordingly impacting the performance of the composite film. That is why graphene is functionally modified for the enhancement of its compatibility with the polymers and reduction of its own agglomeration[1].

Graphene oxide is a functionalized graphene attained through the oxidation of graphite. The functional group just replaces few carbon atoms, meanwhile not destroying the crystalline cells of the whole graphene. Accordingly, graphene oxide still retains the crystalline characteristics of graphene. In the meantime, graphene oxide sheets contain extensive amounts of oxygen (hydroxyl, epoxy, glycol, ketone and carboxyl functional groups), which are capable of changing the van der Waals forces of their interaction, bringing to them enhanced compatibility with the organic polymers. At the edge of the sheet, there are also some carbonyl and carboxyl groups, making the graphene oxide sheets more hydrophilic, which make them more convenient to disperse in some solvents[2].

In the current paper, functionalized graphene modified polyurethane is employed for the preparation of high physical materials, which are capable of enhancing not only the heat resistance, but also the water resistance and aging resistance of waterborne polyurethane, in addition to improving the overall performance of materials. It is considered as quite helpful for developing the environment-friendly and high-performance composite materials.

2 Material and Methods

2.1 Materials

Graphene oxide (GO), prepared in the laboratory with the use of the Hummers method; Isophorone diisocyanate (IPDI),

industrial grade, Bayer China Ltd.; Stannous octoate catalyst (T-9), industrial grade, Jining Huakai Resin Co., Ltd.; Polypropylene glycol (PPG-2000), industrial grade (110 °C vacuum dewatering 2h), Jiangsu Hai'an Petrochemical Plant; 2,2-Dimethylolpropionic acid (DMPA), industrial grade, Jiangxi Southwest City Hongdu Chemical Technology Development Co., Ltd.; 1,4-butanediol (BDO), analytically pure, Komio reagent; Triethylamine (TEA), analytical grade, Tianjin Hengxing Chemical Reagent Manufacturing Co., Ltd.; Acetone, analytical grade, Beijing Chemical Plant; Universal Rally Machine, GT-AI-7000S, High Speed Rail Testing Instrument Co., Ltd.; Thermogravimetric Analyzer, Mettler TGA1100SF, METTLER TOLEDO Instrument Co., Ltd., Switzerland; Taber wear testing machine, GT-7012-T, High Speed Rail Testing Instrument Co., Ltd.; Tensor27 type Fourier infrared spectrometer, Bruker, Germany; DHG-9140A electric heating constant temperature blast drying oven, Beijing Yashilin Experimental Equipment Co., Ltd..

2.2 Experimental Methods

2.2.1 Preparation of Polyurethane Emulsion

In a 500-ml flask equipped with a stirrer, a thermometer, together with a condenser, IPDI 27 g, PPG-2000 30 g, DMPA 3.3 g was added; the temperature was raised to 85 °C, followed by reaction under a N_2 atmosphere for a period of two 2 hours, and 8 g of GO/DMF solution was added. Subsequently, BDO 4.1g was added, followed by adding an appropriate amount of acetone in order to lower the viscosity, and the reaction was performed at a temperature of 75 °C to react to a predetermined NCO value. Following cooling down to the room temperature, 2.5 g of neutralizer TEA was added. Subsequent to reacting for a period of 5 min, the reaction product was poured into an emulsified bucket, followed by addition of deionized water; moreover, the emulsion was attained with the help of high-speed stirring and shearing. The NCO value of the system during the reaction was determined by the di-n-butylamine titration. Eventually, acetone in the emulsion was distilled off subjected to the lowered pressure.

Configure GO/DMF solution: add a specific amount of dried graphene oxide to 8g DMF, together with dispersing it on a 600w power ultrasonic disperser for a period of 1h. The amount of GO is termed as the total weight of the material: 0% (G-0); 0.01% (G-1); 0.02% (G-2); 0.04% (G-3); 0.06% (G-4); and 0.08% (G-5).

2.2.2 Preparation of cured film

The prepared polyurethane emulsion was placed horizontally at the Teflon plate following 48h at the room temperature and placed in a vacuum drying oven. The sample was dried to a constant weight at a temperature of 60℃ and, eventually, a film with the thickness of almost 100μm was obtained.

2.2.3 Characteristic Method

(1) Fourier transforms infrared spectroscopy

Testing of the cured film was carried out by the Fourier transforms infrared spectroscopy, with the scanning range falling in the spectrum of 600~4000cm^{-1}.

(2) The test of TGA

Mettler TGA1100SF thermogravimetric analyzer was employed for the purpose of testing TGA with a heating rate of 20℃/minute in nitrogen atmosphere. The sample weight is between 7~8mg and the temperature falls in the range between 25℃ and 800℃.

(3) Water absorption rate of the cured film

Cut the cured film 2cm × 2cm, followed by soaking it in the deionized water for 24h, and finally using the filter paper for absorbing the surface moisture.

Water absorption rate=(m(after soaking)-m(before soaking))/ m(before soaking) × 100% (formula 1)

(4) Tensile strength and elongation at break of the cured film

In accordance with GB/T 1040-2006 and GB/T 2918-1998, the cured film is made into a dumbbell shape, and air-conditioned for 48 hours under the standard environment of 25 ° C as well as relative humidity of 50%; subsequent to

that, the tensile strength and elongation at break of the cured film were measured on the universal tensile machine, followed by averaging three times.

(5) Determination of cured film hardness [3]

In accordance with GB/T 6739-2006 paint and varnish pencil method, determine the hardness of the cured film.

(6) Cured film wear resistance test [4]

Refer to GB/T 1768-2006 standard, use Taber instrument and rubber grinding wheel, load 500g, rotate 1000 rpm, measure sample quality prior to and subsequent to rotation, followed by calculating wear in accordance with the formula (2).

Wear △m=sample quality before test (m1)-sample quality after test (m2) (formula 2)

(7) Heat aging resistance [5]

In accordance with GB/T9349-2002B method (oven method), the sample was placed in an oven for heat aging for a period of 48 hours, followed by measuring the mechanical strength of the test piece.

2.3 Results and Discussion

2.3.1 FTIR Analysis

Fig. 1 sheds light on the infrared spectrums of graphene oxide modified waterborne polyurethane as well as graphene oxide. In the spectrum of polyurethane and graphene oxide, the absorption peak of a hydroxyl group makes appearances at about 3300 cm^{-1}; the absorption peak of carbonyl in COOH makes appearance at about 1700 cm^{-1}, the absorption peak of C-O bond takes place at 1243 cm^{-1}, the stretching vibration absorption peak of C═C can be observed at almost 1600 cm^{-1}, which suggest that an extensive amount of functional groups was existent in both the polyurethane and graphene oxide.

The absorption peak at 3300 cm^{-1} in the polyurethane line emerges as not just small but also narrow, implying that the hydroxyl group of graphene oxide shows participation in the reaction. Owing to the fact that there is an extensive amount of carbamate, the C═O absorption peak at 1716 cm^{-1} is stronger. The -NCO absorption peak near 2300 cm^{-1} disappeared, and the absorption peak of the N-H bond on the carbamate made appearance at 1533 cm^{-1}, implying that the graphene oxide was integrated into the polyurethane. [8,9]

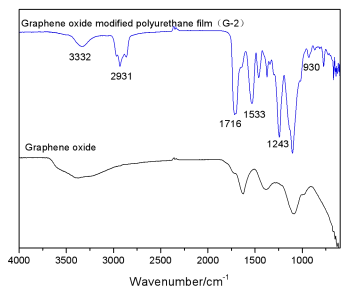

Fig. 1 FTIR spectrum of the polyurethane

2.3.2 Polyurethane film heat resistance

Fig.2 is the TGA curve of the polyurethane film.

The hard segment was thermally decomposed at a temperature of 250 ° C, accordingly, the mass retention of each sample was as hereunder: G-0 was 92.5%; G-1 was 92.9%; G-2 was 93.1%; G-3 was 93.3%; G-4 was 93.5%; and G-5 is 94.5%. It suggests that, following the addition of GO, the thermal decomposition of the hard segment is delayed, and GO, as a modified material, is able to act as a partial hard segment.

In the thermogravimetric analysis, the thermal weight loss 5% (Td5) is utilized as the initial thermal degradation temperature. As evident from Fig. 2, by increasing the amount of graphene oxide, the Td5 of the modified polyurethane

manifests an increasing law; moreover, as the graphene oxide mass fraction is 0.08%, the initial decomposition temperature manifests an increase by 27 ° C. This is likely to be owing to the fact that graphene oxide is capable of providing additional heat capacity, requiring more heat in order to break the urethane bond; the urethane bond developed by graphene oxide and isocyanate groups hampers the thermal decomposition of polyurethane [9].

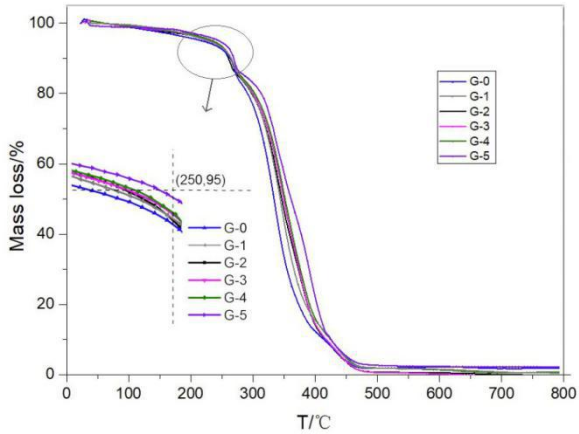

Fig. 2 TGA curves of the polyurethane film

2.3.3 Water Absorption Rate

Fig. 3 presents the water absorption rate of the polyurethane film. As the water enters the polyurethane, it produces the hydrogen bonds with the polar carbamate groups in the molecule, which immensely lower the hydrogen bonding between the original polymer backbones, leading to a substantial decline in the physical characteristics of the polyurethane [9].

With the increase in the amount of graphene oxide, the water absorption of the polyurethane film decreases first. On the one hand, since the graphene segment introduced on the polyurethane molecular chain has hydrophobicity, the hydrophobicity of the polyurethane film is increased. Conversely, by introducing graphene oxide, the level of crosslinking of the polyurethane film manifests an increase, and the cross-network structure of the polyurethane prevents the water molecules from making an entry to the inside of the film, lowering the contact area between the polyurethane film and water, accordingly minimizing the water absorption of the polyurethane film.

As the amount of graphene oxide continues to increase, the water absorption of the polyurethane film manifests an increase, which is owing to the fact that the hydrophilic group, not participating in the reaction in the graphene oxide increases, results into an increase in the hydrophilicity of the polyurethane film.

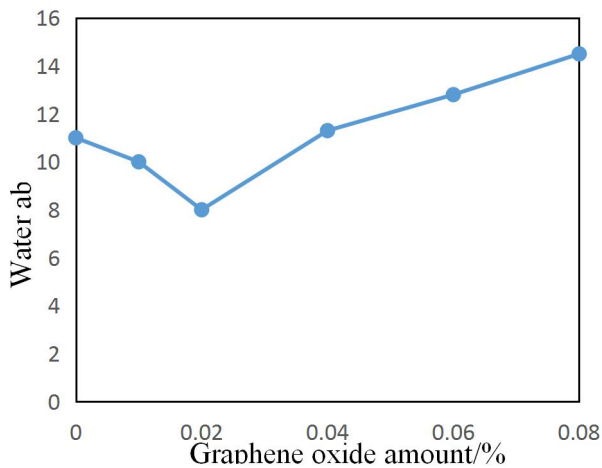

Fig. 3 Water absorption of graphene oxide modified waterborne polyurethane film

2.3.4 Mechanical Properties

Tab. 1 presents the mechanical characteristics of the polyurethane film. The tensile strength and elongation at break of the polyurethane film increase first, followed by decreasing, which is due to the fact that by using graphene oxide for the modification of the polyurethane, the level of crosslinking of the polyurethane film is increased, and the tensile strength and elongation at break of the polyurethane film are increased as well.

Since the tensile characteristics of graphene are weak, accordingly, with the increase in the amount of graphene oxide, the tensile and tensile characteristics of the entire polyurethane chain decline.

Table 1 Mechanical characteristics of polyurethane film

NO.	G-0	G-1	G-2	G-3	G-4	G-5
Tensile strength /Mpa	20.1	23.9	19.6	16.5	16.5	14.4
Elongation at break /%	420	550	550	420	280	260
Hardness	2B	2B	B	B	B	H B

2.3.5 Polyurethane Film Wear Resistance

Fig. 4 presents the test results of the wear resistance of polyurethane film. With the increase in the amount of graphene oxide, the wear of the polyurethane film manifests a gradual decline, which is owing to the robust interaction between graphene oxide and polyurethane molecular chains. In the meantime, the increase in the amount of graphene oxide gives rise to an increase in the hardness of the polyurethane film, lowering the deformation ability of the friction surface, and minimizing the area where the abrasion takes place. Besides, graphene oxide is a layered nanomaterial that has extremely high strength; moreover, the bonding force between carbon atoms in layers is below the bonding force between adjacent carbon atoms in the same layer, making the graphene oxide layer have a lower coefficient of friction, accordingly enhancing the wear resistance of the modified polyurethane composite[10,11].

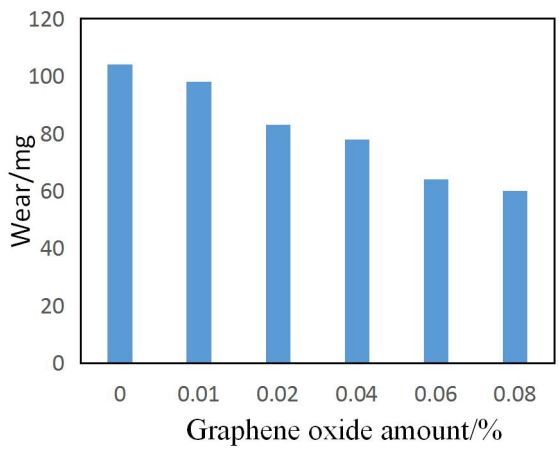

Fig. 4 The test results of wear resistance of polyurethane film

2.3.6 Polyurethane film heat aging resistance

Fig. 5 presents the tensile strength of polyurethane film both before and after the heat aging. The greater the amount of graphene oxide, the smaller the performance of the polyurethane film before and after aging. Graphene oxide manifests outstanding thermal conductivity and heat resistance, which are capable of enhancing the heat aging resistance of polyurethane. As revealed by the experiments, when the amount of graphene oxide is 0.02%, the mechanical characteristics of the polyurethane film are less affected, and better heat aging resistance can be attained.

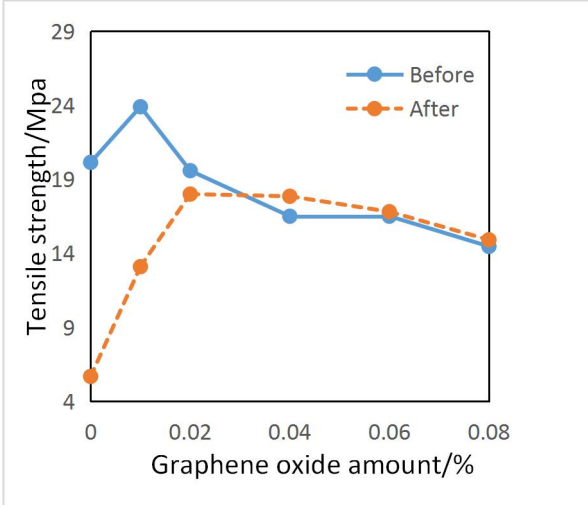

Fig. 5 The tensile strength of polyurethane film before and after heat aging

3 Conclusions

In the current research work, graphene oxide was put to use for the modification of the polyurethane materials, together with investigating the effects of different amounts of graphene oxide on the water resistance, mechanical characteristics, wear resistance and heat aging resistance of polyurethane.

As revealed by the results:

（1）The introduction of graphene oxide has the potential of improving the heat resistance, heat aging resistance and wear resistance of the polyurethane. Graphene oxide, being a hard segment in polyurethane, is able to enhance the hardness of the polyurethane film; moreover, when the amount of graphene oxide is small, the mechanical characteristics of the modified polyurethane film can be enhanced. However, with the increase in the amount, the mechanical characteristics of the polyurethane film are degraded.

(2) In this research work, the overall performance of polyurethane was optimized when the amount of graphene oxide was 0.02%.

4 Acknowledgments

The authors are grateful to the Science and Technology Support Plan Project in "Thirteenth Five-year" Period (2017YFB0308603) and Jinjiang City Science and Technology Plan Project (2017C007) for financial support.

5 References

[1] HOU Yanmin, WU Minghua, YU Deyou, et al. Preparation and properties of functionalized graphene modified waterborne polyurethane[J], Journal of Textile Research. 2015, 36(10): 80-85.

[2] YANG Hongjun, JIANG Zhenqi, BO Tao, et al. Synthesis and Characterization of Graphene/Polyurethane Composites[J], POLYMER MATERILS SCIENCE AND ENGINEERING. 2016, 32(5): 28-32.

[3] GB/T 6739-2006 Paints and varnishes - Determination of film hardness by pencil test.

[4] GB/T 1768-2006 Paints and varnishes - Determination of resistance to abrasion - Rotating abrasive rubber wheel method.

[5] HUANG Wanli. Study on improving the aging resistance of polyurethane materials[J], ANHUI CHEMICAL INDUSTRY. 2010,36(03): 44-46.

[6] GAO Xurui, YAO Bolong, WANG Likui, et al. Preparation of polyurethane/graphene composite coating and study on its properties[J], Electroplating & Finishing. 2017, 36(02): 61-68.

[7] Guo Song, Pang Xiaoyan, Ding Zhiwen. Preparation and Properties of R ed Polyurethane High Molecular Leather

Dye[J], FINE CHEMICALS. 2016, 33(11): 1249-1253.

[8] HU Ling, JIANG Pingping, ZHANG Pingbo， et al. Single layer graphene oxide modified waterborne polyurethane[J], POLYMER MATERIALS SCIENCE AND ENGINEERING. 2016,32(09): 147-152.

[9] Khatua B B, Das C K. Interchain crosslinkable polymer blends of polyurethane and polyacrylic elastomer (sulfur cure)[J]. Journal of Applied Polymer Science. 2004, 93(2): 845-853.

[10] LIU Shuan, JIANG Xin, ZHAO Haichao, et al. Corrosion Resistance and Wear Property of Graphene-Epoxy Coatings[J], Tribology. 2015, 35(05): 598-605.

[11] SUN Zhe, HE Yazhou, FAN Haojun, et al. The Preparation and Properties of Graphene/Polyurethane Composites for Leather Finishing[J], LEATHER SCIENCE AND ENGINEERING. 2016, 26(05): 10-15.

O7

The elimination of waste waters from unhairing/liming , acid/salt pickle and chromium tanning processes in full scale wet blue manufacture

Richard Daniels(1), Jiasheng Su(2), Falei Zhang(2), Zhuangdou Zhang(2)

(1)Greentech + Associates, Moulton Lane, Boughton, Northampton, NN2 8RF, UK, Phone +44 (0) 1604 843260, E-mail r.daniels@greentech.plus.com

(2)BIOSK, No.6, East Chang Jiang Rd, Development Zone, Shangqui City, Henan Prov, China, Phone +86 370 3861600, E-mail support@biosk.cn

Abstract

Within the chemical processing of hides into wet blue leather, the unhairing/liming and acid pickle/chromium tanning processes are the major contributors of pollutants.

Many attempts have been made to lessen this waste at source without jeopardising leather quality, but technologies in common use have basically remained unchanged for decades. Solutions to these problems are far reaching, and the details given in this presentation describe a technology that addresses and resolves these matters.

This new approach involves the complete retention and reuse of floats that are recovered from unhairing/liming, and pickle/chromium tanning in self-contained loops. In practice, this means no discharge of waste waters from both the unhairing/liming and the pickle/chrome tanning processes. This includes all the unused chemicals that normally wasted and discharged due to the poor efficiencies of conventional processing.

In addition to these chemical savings, there is a significant reduction in water use, suspended solids, COD/BOD, nitrogen, reduced salinity and reduced sludge for licenced disposal. There is no need for the removal/treatment of residual sulfide – hence no TDS generated by this oxidation – and no need for the collection/recovery and regeneration of chromium compounds.

This new approach also means the wet blue processing can focus on technology that has always been associated with high quality – that is: moderate pH, floats, mechanical action and processing conditions – techniques that best suit a sensitive and valuable raw material. And in practice, tanneries find that when compared to conventional technology, this new technology provides the advantages of a finer grain, more uniformity across each hide, and less quality variations due to seasonal changes.

This information was compiled through detailed on-site studies within four major tanneries. Here, approximately 70,000 wet salted US, European and Australian hides per week are being processed as high quality wet blue leather for direct sales, contact tanning, and further processing on site for footwear leather production. The technology commenced in full scale manufacture 2011, and the fourth tannery adopted the technology in 2016.

This paper describes and illustrates in full this radical new approach to leather manufacture. It provides key working information, supported by analytical findings from two independent Universities.

O8

Property changes of Wet-blue influenced by bating with different acid protease

Hao Li[1]，Deyi Zhu[1]，Jie Liu[1]，Feifei Zhang[1]，Tianping Yu[2], Yanchun Li[1]*，Shan Cao[1]*

1College of Leather Chemistry and Engineering, Qilu University of Technology(Shandong Academy of Sciences) 250353, Shandong, China, qlulyc@126.com;cs1988@foxmail.com.

2Shandong Leather Industry Research Institute,Jinan 250021,China

Abstract

Wet-blue bating with acid protease has attracted more and more attentions in recent years. Therefore, how the acid protease influence the physical and chemical properties of wet-blue needs to be investigated. In this paper, several acid proteases produced by different bacteria were applied for wet-blue bating, and the bating effect were evaluated as well as the mechanism was explained.

The wet-blue samples were collected for characteristic evaluation before and after bating process. Afterwards, the porosity and the dispersion of collagen fibers of wet blue leather were observed by Micro-CT and scanning electron microscopy (SEM). The results showed that appropriate acid protease usage increased the wet-blue properties including air permeability, softness and tensile strength. From Micro-CT analysis, it was seen that the collagen fibers of wet-blue were successfully dispersed by acid protease treatment, and theinter-space of collagen fibers increased, which significantly improved the properties of Wet-blue. Meantime, by SEM analysis, the cleavage of acid protease to collagen fibers was observed, and the bating pathway was analyzed. Based on these results, the acid protease could disperse the collagen fibers of wet-blue by moderate degradation, which was the main result to make the properties of wet-blue increase. This study could serve as a foundation for the choice and application of acid protease for wet-blue bating.

Key words: Acid protease; wet-blue bating; wet-blue properties; air permeability; degradation pathway.

Introduction

During the long time transportation and preservation, the leather collagenous fibre are glued to each other and make the leather becomes stiffness, which not only increases the defects of the leather grain but also affects the infiltration of the subsequent dyes and fatliquors, and lead to a decline in finished leather quality. Therefore, many tanneries will bating the wet blue in advance.On the one hand, it can make up for the inconsistencies in the processing of the previous processes. On the other hand, it will further disperse the collagen fibers and weaken the bond between the collagen fibers and create conditions for the subsequent treatment[1]. The bating process is the only process that can not be replaced by chemical action in the process of tannery. In this process, the enzyme can be used to degrade the residual non collagen in the raw skin very well, and to increase the flexibility and softness of the leather. The enzymes commonly used in the process of tannery include alkaline protease, neutral protease and acid protease[2-4]. The acid protease has many better characteristics, such as small molecular weight, good permeability and relaxation and uniform of action force. So it has been widely used in the bating process[5].

Air permeability is one of the most valuable physical properties of natural leather, and is an important indicator of hygienic properties of leather. In the process of tannery, there are some operations, such as acid treatment, alkali treatment, enzyme treatment and mechanical action and others which can enough to increase the degree of dispersion and porosity of collagen fibres, can increase the air permeability of leather[6]. At the moment, there are few reports about the effect of acid protease on air permeability of wet blue leather in bating process. In this study, the effect of acid protease on the air permeability of wet blue was investigated in order to apply the acid protease to get high quality leather products.

Experiments

Materials

Wet-blue leather（ShanDong DEXIN Leather Industry）, Powder of Wet blue(made by oneself) and Four acidic protease produced from different bacteria

Methods

Bating process of wet blue

A circular specimen with a diameter of 5cm is taken along the cowhide dorsal line. The samples were divided into 4 groups (group A, group B, group C and D). Under the same experimental conditions, each sample was placed in a 250mL conical bottle. In the incubator of constant temperature concussion, the conventional acid protease bating process of cowhide wet blue was used in different protease dosage (0%, 0.4%, 0.8%, 1%, 2%, 4%). The leather samples were bating. Group A was treated with B.subtilis-1 acidic protease, group B with B.subtilis-2 acidic protease, group C with Aspergillus acidic protease, and group D with A.niger acidic protease.

Determination of softness of crust leather

The softness of crust leather was determined by following the procedure described by literature[6].

Determination of change rate of air permeability

According to the literature[6] that the method of measuring and calculated the air permeability of leather, the air permeability of leather was measured by GT-7007-Q Leather Permeability Tester (High-iron Testing Instrument). Before bating process, the samples were dried properly and then air conditioned in a constant temperature and humidity box for 24 hours. The air permeability of sample was measured and calculated. After bating process, the sample were dried properly and then air conditioned in a constant temperature and humidity box for 24 hours. The air permeability of the sample was measured and calculated. The change rate of air permeability is calculated according to the following formula:

$$K\% = \frac{K_2 - K_1}{K_1} \times 100\%$$

K% ---------- Change rate of air permeability；

K_1---------- Air permeability before bating pocess，mL/（$cm^2 \cdot h$）；

K_2---------- Air permeability after bating pocess，mL/（$cm^2 \cdot h$）；

Observation on the gap of collagen fibre bundle by Micro-CT

Two samples of A group were selected, and the gap of collagen fiber bundles was observed by Micro-CT. At the same parts of the two samples to take a specimen with a size of 15mm x 5mm, and named A (without acid protease softening) and B (softened by acid protease) respectively. The gap between the collagenous fiber bundles in the corresponding region of the sample was observed and the scanning resolution was 1um

Observation on the dispersion of collagen fiber by SEM

The appropriate amount of wet blue is cut into small pieces and then grind 24 h with a ball mill to get wet blue shavings. Take appropriate amount of wet blue shavings and then freeze dry with freeze-drying machine. According to the bating process, the acid protease was uesd in bating process,After treatment of acid protease,the samples was treated in freeze-drying machine for 24 h. The dispersion of collagen fibers of wet blue shavings before and after treatment were observation by SEM.

Results and Disscusion

Change of grain surface state of crust leather

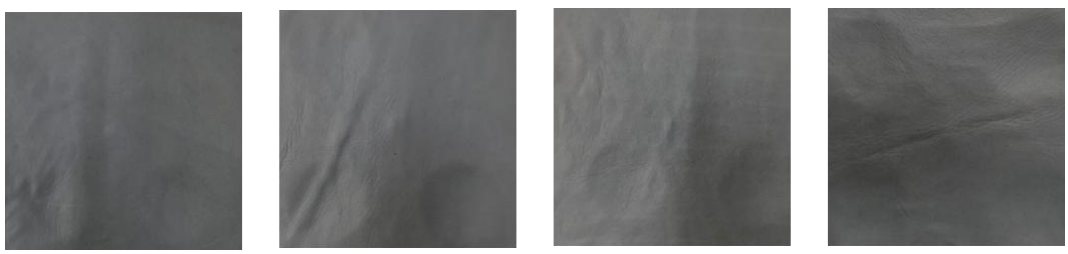

Fig 1 the grain surface condition of crust leather before bating process

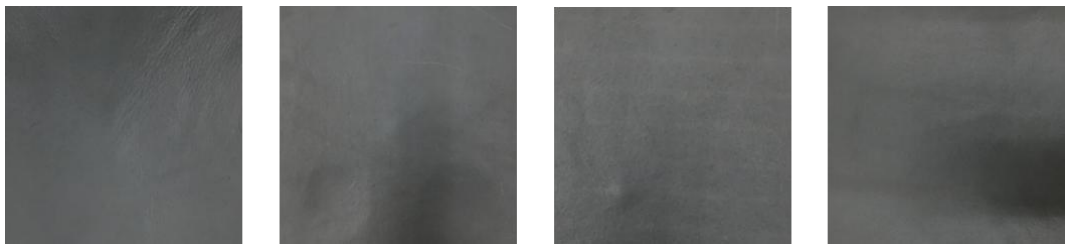

Fig 2 the grain surface condition of crust leather after bating process

In Figure 1, there are several sharp crease in the surface of the leather. But in Figure 2, the leather was treated with different acid proteases, the grain creases disappeared and the grain surface became more smooth.This suggests that acid protease plays an important role in fully dispersing collagen fibers and alleviating grain surface defects.

Change rate of air Permeability

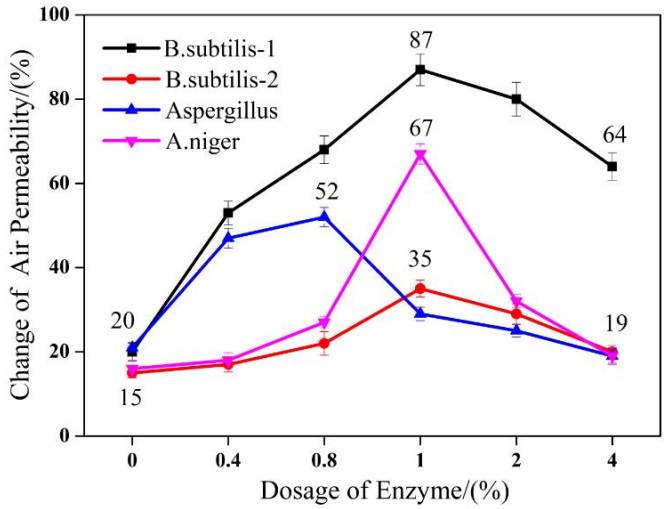

Fig 3 The rate of change of air permeability with different dosage of four acid protease. X-axis represents Dosage of acid protease, and Y-axis represents the rate of change.

Fig. 3 is a curve for the change rate of air permeability of the wet blue after bating process with 4 kinds acid proteases. The results showed that the air permeability of sample was all increased by 15%-85% with different dosage of acid proteases, which showed that the air permeability property of wet blue was obviously increased after the bating process. It's remarkable that although different acid proteases are used in bating process, the air permeability change rate of the wet blue is always increased firstly and then decrease with the increase of the amount of acid protease. The results showed that the bating effect of acid protease has a nonlinear relationship with the amount of acid protease in the bating process. On the one hand, collagen is not a specific substrate for acid protease, so acid protease does not have a greater destructive force on collagen and can not changes the triple helix structure of collagen to makes the collagen fiber moderately dispersed by acting on the non spiral region of collagen molecules. On the other hand, the rsistance to enzyme get enhanced after tanning. This makes the dispersion of collagen fibers only moderately increased under the action of acid protease, but does not increase linearly with the increase of enzyme activity.

The softness of crust leather

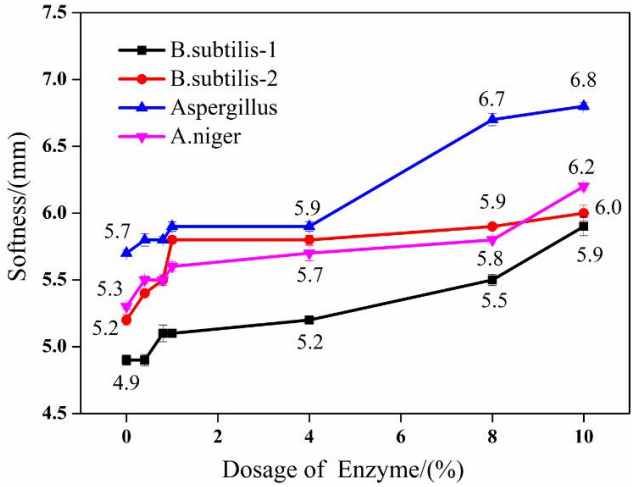

Fig 4 the softness of crust learher after bating process

Figure 4 shows that the softness of the crust leather has been significantly improved after enzyme treatment. Among them, the softness of the crust leather after Aspergillus acidic protease treatment is the best.

Gap of collagen fibre bundle by Micro-CT

Micro CT (Micro-CT) is a technology of high resolution three-dimensional imaging which using the principle of X ray imaging.It is an imaging means with high resolution to display the three-dimensional spatial distribution of the internal structure of the material. It can be used to perform high resolution three-dimensional imaging of various biological materials in vitro without destroying the sample. In this study, the micro-CT technique was applied to the three-dimensional reconstruction of collagen bundles in wet blue leather, which could reflect the softening effect intuitively and accurately in a large scanning range[7-8].

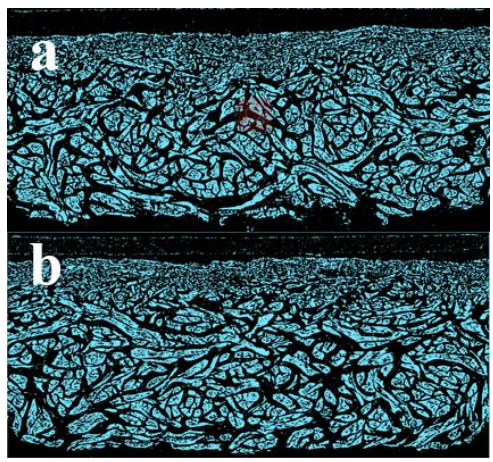

Fig 5 The Micro-CT image is the sample which treated by nothing,b is the sample whicn treated by protease.

Fig 5 is a Micro-CT image of the leather sample. The thin and dense part of each picture is a leather surface layer, and the thick and loose part in the lower part is a reticular layer. The blue and green in the reticular layer is collagenous fiber bundles, and the black background area between the collagen fiber bundles is the gap. Comparing with the Micro-CT images of the three parts of the leather sample, it can be seen that the gap degree of collagen fiber bundles in Figure B is higher than that in figure A, and the gap between fiber bundles is larger. So the leather has more excellent air permeability.

Dispersion of collagen fiber by SEM

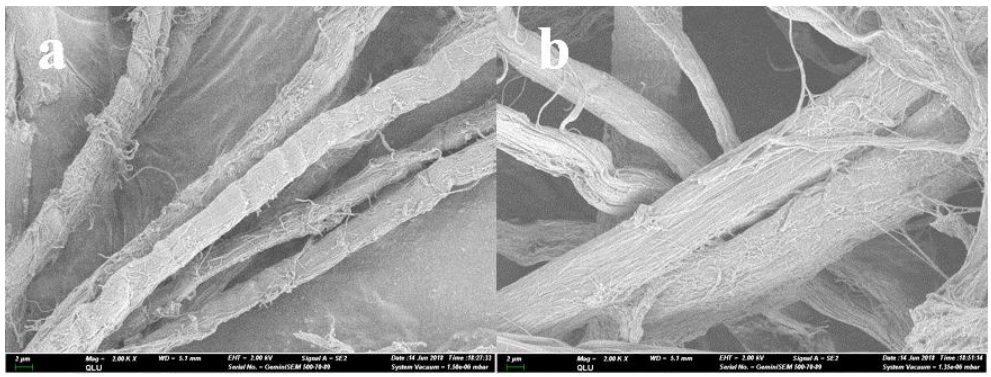

Fig 6The SEM image of sample (x 2000)

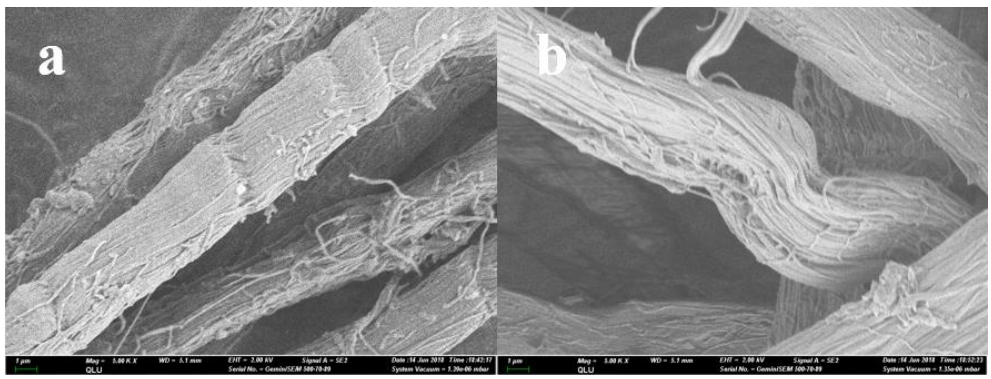

Fig 7The SEM image of sample (x 5000)

Fig 6 and 7 are the SEM images and magnification 2000 times and 5000 times respectively.a is the sample which treated by nothing,b is the sample whicn treated by protease.

Figure 6 and 7 are magnify2000 times and 5000 times of collagen fiber SEM images and the a and b in the two images are untreated and treated with acid protease,respectively. It can be clearly seen from a diagram and b diagram that in group A, the collagen fibers are tightly woven together and form a rod structure. In the b diagram, there was a clear separation between the collagen fibers and the rod like structure was destroyed. It showed that after the acid protease treated, the collagen fibers of the wet blue get disperse and the gap between the collagen fibers increased, so the air permeability of the wet blue increased.

Conclusion

Acid protease has a great influence on the air permeability of wet blue. After the bating process, the degree of dispersion of collagen fibers get increased, so the porosity of wet blue also rise and it cause the air permeability of the leather is increased obviously, so the hygienic properties of the leather are better. It is worth noting that in the bating process of wet blue, the more effective the more acid protease is used in bating process, this study clears the action law of acid protease, which have great significance for the better application of acid protease to the bating process of wet blue.

Acknowledgements

This study was financially supported by the National Key Research and Development Program of China under contract No. 2017YFB0308402.

Reference

[1] 李彦春，程宝箴，张铭让. 酸性酶软化蓝湿皮的研究[J]. 中国皮革. 2001, 30(21): 5-8.

[2] Wilson J A, Merrill H B. Another Important Role Played by Enzymes in Bating[J]. Industrial & Engineering Chemistry. 1926, 18(2): 185-188.

[3] Choudhary R B, Jana A K, Jha M K. Enzyme technology applications in leather processing[J]. Indian Journal of

Chemical Technology. 2004(11): 659-671.

[4] Hameed A, Natt M A, Evans C S. Short Communication: Production of alkaline protease by a new Bacillus subfilis isolate for use as a bating enzyme in leather treatment[J]. World Journal of Microbiology & Biotechnology. 1996(12): 289-291.

[5] 刘正华，魏世林，许雯等. 酸性蛋白酶软化处理铬鞣坯革有关作用探析[J]. 皮革科学与工程. 1991, 1(3): 11-15.

[6] 罗晓民，丁绍兰，周庆芳. 皮革理化分析[Z]. 北京: 中国轻工业出版社, 2013,306-307.

[7] 桂建保，胡战利，周颖等. 高分辨显微CT技术进展[J]. CT理论与应用研究. 2009, 18(02): 106-116.

[8] 仇晓慧，徐海，张光东. 显微 CT 在牙体牙髓病学研究中的应用[J]. 口腔医学. 2017(11): 1049-1052.

O9

IUE 12 - Guidelines for Minimum Environmental Standards

Introduction

In view of ever increasing social pressures, no tanner can afford to be unfamiliar with the main issues and principles of environmental protection pertaining to tannery operations. Among these, preventing pollution and promoting cleaner leather processing remain a priority. Yet, despite all preventive measures, there is still an amount of the pollution load to be dealt with by the end-of- pipe methods. The purpose of this document is to give tanners or tannery managers guidelines for the Minimum Acceptable Environmental Standards (MAES).

This IUE document is based on the environmental performances, not on the means required to achieve these performances. Therefore, tanners retain the freedom to choose which options they implement among prevention, clean technologies, end-of-pipe treatment, new and innovative solutions.

The objective is to protect the environment and nearby residents on a short term approach, so the guidelines include both on-site and off-site (waste and waste water) treatments.

This document does not refer to any national regulations and therefore the guidelines can be used in any country. Obviously this means that for some points the guidelines are less restrictive than some national regulations.

Scope

Greenhouse Effect Emissions are excluded from this reference document because policies around the globe are widely different from one country to another. Furthermore, Leather Carbon Footprint methodologies are still to reach an agreed consensus, so Carbon Footprint of the tannery is outside the scope of this guideline. However, there are basic good housekeeping practices improving energy efficiency that can be adopted showing commitment to good environmental practices with a knock- on effect for carbon emissions.

Guidelines for Minimum Environmental Standards

The basic environmental parameters to be checked are listed in the tables hereafter.

1. General requirements

General Parameters	Guidelines for Minimum Environmental Standards
Environmental Management	
Environmental Policy	The tannery should have a documented company environmental policy available for any stakeholder.
Supply Chain	
Visibility throughout the supply chain from raw to finish	A tanner should be able to provide identification of the source of the material supplied - especially for intermediate steps such as pickled hides and skins, wet-blue and crust leather. For example, documented identification of materials received at the tannery.
Water Consumption	
Water consumption	Water consumption has to be monitored and reported relative to the quantity of hides and skins processed. Data required: volume (m^3) per year, tons of hides and/or area (m^2) of leather. No threshold required for this parameter. It is a monitoring requirement.

2.Waste water

ParametersforWasteWater	MinimumforMinimum EnvironmentalStandards	
WasteWaterManagementandMonitoring	**Release intoaCommonorMunicipal EffluentTreatmentPlant(Sewer)**	**ReleaseintoSurfaceWater(fromaCETPorETP)**

Drainagesystems	Requirement isto haveapipingandInstrumentationdiagram(PID)that describesthedrainagesystemsofthetanneryspecifyingtheexisting segregationsystems(i.e., sulfides,chromium,processing(float)water,rinsing waterandotherwastewater).	
Wastewaterdischargemonitoring	Yes	Yes (Watervolume, Cr, sulfides,COD, suspendedsolids, nitrogenor
Totalchromium	Thequantityofchromiumusedinthe processshould beoptimized. Removal ofexcess chromiumat thesourceis preferredtotreatment viaaCETP. (SeeIUE-1)	2mg/l
Sludge	Sludgecontainingmorethan2500mg/kgdrymattershouldbemanagedina waynot toreleaseanychromiuminto the environment.	
Sulphides (SeeIUE8)	Whenunhairingwithsodiumsulphide, atreatment systembased onoxidation isrequired,preferablyinstalled adjacent tothebeamhousearea.It might also beanywhereinthetannery siteorwithintheCETP.It ishowever betterwhenminimisedat thesource. (SeeIUE8)	1mg/l
SuspendSolidsmanagement	1500mg/l	100mg/l
ChemicalOxygenDemand(COD)	-	300mg/l
Nitrogen(TKNorAmmonia)	-	50mg/lforTKN or 35mg/lforammonia
pH	5.5to9.5 (Except forsomemunicipalwaste watertreatment plantsthat welcome tanneryeffluentsto balancethepHof	6to 9
TotalDissolvedSolids(TDS) (SeeIUE1 andIUE3)	TDSshouldbeminimisedatsource.	Dependingonlocalconditions.

3. Solid waste

ParametersforSolidWaste	GuidelinesforMinimumEnvironmentalStandards
Wastesorting/separation (SeeIUE2)	Chromiumcontainingwasteandwastefreeofchromiumshouldbesortedand managedseparately.
Tannedwaste(shavings,wet-bluesplits,etc) (SeeIUE2)	Chromiumcontainingwasteshouldbemanagedinawaythat chromiumisnot releasedintotheenvironment.

Non-hazardousemptybarrelsandcontainers (SeeIUE2)	Thetanneryshouldfollowanon-hazardouswasteprocedurefornon-hazardous emptybarrelsandcontainers.
Hazardouswastemanagement	Thetanneryshouldfollowahazardouswasteprocedure.Hazardouswaste shouldbetreated/disposedofinadedicatedplant forhazardouswaste.

4. Chemical storage

ParametersforChemicalStorage	GuidelinesforMinimumEnvironmentalStandards
Flammablechemicalstorage	Flammablechemicalsshouldbestoredinadedicatedventilatedzone, retained inasecuredandisolatedarea,labeledandprotectedfrompossiblesourcesof
Non-flammablechemicalstorage	Hazardouschemicals(and hazardouswaste) shallberetainedina secure, isolatedareaandlabeled.
SafetyDataSheets(SDS)andlabeling (SeeIUE11)	AllSafetyDataSheets(SDS)shouldbeavailablewherethechemicalisstored. Chemicals shouldbehandledandusedaccordingto theSDS. Compatibityof chemicalshave to betakeninto account whenstoredinthesamearea.

5. VOC emissions

ParametersforVOCemissions	GuidelinesforMinimumEnvironmentalStandards
Solvent inventory (SeeIUE8)	VOCconsumptionshouldbemonitored(andregularlyupdated)usingdata provided bychemicalsuppliers(whensolventsareused).
Extractionforequipmentusingsolvents	Allequipementsusingsolvents, suchasfinishingspraybooths,haveto be equippedwithadequateextraction.
VOCratio	VOCemissions shouldbequantifiedandreportedrelativeto thesurfacearea ofleatherproduced(gramsofVOCspersquaremetreofleatherproduced). No thresholdrequiredforthisparameter.It isamonitoringrequirement.

6. Energy

ParametersforEnergy	GuidelinesforMinimumEnvironmentalStandards
Non-renewable energymonitoring	Non-renewableenergyshouldbemonitoredandreportedrelativeto the quantityofhides,skinsorleather. No thresholdrequiredforthisparameter.It isamonitoringrequirement.

7. Soil and ground water protection

ParametersforSoilandGroundWaterProtection	GuidelinesforMinimumEnvironmentalStandards
Seepage	Measurementsshouldbetakento checkthat no seepageofprocesswatersor chemical contaminatesthesoil.

8. Odour

ParametersforOdour	GuidelinesforMinimumEnvironmentalStandards
H_2Sgas (SeeIUE8)	H_2Sintheworkplace:amaximumof10ppmisnot tobe exceeded.
Odours	Allmeasuresshouldbetakentoavoidodoursfromputrefaction,sulphides, VOCs andthewastewater treatment plant.

O10

A Novel Chrome-free Tanning Technology Based on the Complex of Zirconium and Highly-oxidized Starch

Yue Yu[1], Zhen Wang[1], Min Zhu[1], Jianfei Zhou[1], Ya-nan Wang[1,2*], Bi Shi[1,2*]

1National Engineering Laboratory for Clean Technology of Leather Manufacture, Sichuan University, Chengdu 610065, China, Tel: +86-28-85405508, Email: wangyanan@scu.edu.cn, shibi@scu.edu.cn

2Key Laboratory of Leather Chemistry and Engineering (Sichuan University), Ministry of Education, Chengdu 610065, China

Abstract

Conventional chrome tanning process is facing rigorous environmental and social pressure due to the discharge of chrome-containing wastewater and solid waste. Therefore, the development of sustainable chrome-free tanning technology has become the focus of global leather industry. In this study, a complex tanning agent (Zr-HOS) composed of zirconium salt and highly-oxidized starch (HOS) was used for chrome-free tanning. The tanning performance and environmental impacts of Zr-HOS were evaluated. HOS with moderate oxidation degree (76.2%) and molecular weight (M_n 3500 g/mol) was able to coordinate with zirconium and improve the tanning effect, thus the leather tanned by Zr-HOS exhibited considerably better physical and organoleptic properties than traditional Zr-tanned leather. In comparison with conventional chrome tanning system, the surface charge, physical and morphological properties of this chrome-free tanned leather was comparable to chrome tanned one. In addition, TOC and metal emission loads in the wastewater from tanning and post-tanning processes of this cleaner system were reduced by 40% and 96%, respectively, and the biodegradability of wastewater was remarkably better. This novel chrome-free tanning technology provides an effective approach to eliminate the chrome pollution in leather manufacture.

Keywords: Chrome-free tanning, Zirconium tanning, Highly-oxidized starch, Coordination, Environmental impact

1. Introduction

Leather industry is facing with increasing environmental and social pressure due to the chrome-containing wastewater and solid waste resulted from the use of chrome tanning agent.[1] Therefore, chrome-free tanning agents has received much attention in recent years. Zirconium salt is regarded as a potential alternative to chrome tanning agent due to its relatively high tanning ability and low environmental risk.[2] However, traditional Zr-tanned leather has poor organoleptic properties, such as stiff handle and coarse surface, because zirconium salt usually precipitate on the leather surface without uniform distribution in leather.[3] Although small molecular ligands with hydroxyl, carbonyl and carboxyl, such as lactic acid, citric acid and tartaric acid, have been used as masking agents to coordinate with Zr ion and reduce its reactivity with collagen fibers,[4] the improvement of organoleptic properties of leather is still limited. The possible reason is that the functional groups in these ligands are not enough to coordinate and stabilize the Zr complexes. In addition, Zr complexes may be too small to form macromolecular cooperating unit, resulting in insufficient crosslinking reaction between collagen fibers.[5] Of course, ligands with too strong coordination ability probably hinder the reaction between Zr complexes and skin collagen, and ligands with too large molecular size may be difficult to penetrate and evenly distribute in leather. Hence, it is essential to design a ligand with more appropriate coordination effect and molecular size for zirconium tanning.

Starch, one of the most abundant polysaccharides in nature, is a glucose polymer composed of two polymeric units, amylose and amylopectin.[6] Abundant hydroxyl groups in starch molecular can be transformed into carbonyl and carboxyl groups by oxidation. Meanwhile, the molecular weight of oxidized starch can be regulated through controlling the rupture degree of α-(1-4) glycosidic bond.[7] Based on these facts, we have developed an environment-friendly multi-functional groups polymer ligand, viz. highly oxidized starch (HOS), using H_2O_2 and a copper-iron catalyst at high temperature. This ligand with appropriate coordinating group content and molecular size could improve the tanning performance of zirconium in laboratory scale trials.[8]

In the present work, the HOS was prepared according to our previous method and characterized by nuclear magnetic resonance (NMR), gel permeation chromatography (GPC), laser particle size and ultraviolet-visible (UV-Vis) analyses. Then pickled cattle pelts were tanned with zirconium sulfate and HOS for evaluation of the tanning performance and environmental impacts of Zr-HOS tanning agent.

2. Experimental

2.1 Materials

Corn starch (amylose content 28.3%), H_2O_2 (30%), $CuSO_4·5H_2O$, $FeSO_4·7H_2O$ and $Zr(SO_4)_2·4H_2O$ were of analytical grade and purchased from Chengdu Kelong Chemical Co., Ltd (Chengdu, China). The reagents used for analysis were of analytical grade, and the chemicals used for leather processing were commercial products.

2.2 Preparation of HOS

Corn starch (40.0 g) and a certain amount of distilled water were gelatinized at 90°C for 20 min in a 1000 mL three-neck flask. Then a combination of two metal salts ($CuSO_4·5H_2O$ and $FeSO_4·7H_2O$ in a mass ratio of 2:8) with a dosage of 0.015 wt% (based on the weight of starch, the same below) were introduced into the blend. After intensive stirring for 3 min, 60 wt% of H_2O_2 and a certain amount of distilled water were added to form a blend of 400 mL. Then oxidation reaction was conducted at 98°C for 2 h, and the products (HOS) were sampled from the reactor for NMR, molecular weight, particle size and UV-Vis analyses as described in our previous paper.[8]

2.3 Zirconium tanning trials

Pickled cattle pelt (3.5 kg) was cut along the back bone into matched pieces. One piece of the pelt was tanned with $Zr(SO_4)_2·4H_2O$ (6 wt% ZrO_2, based on the weight of pickled pelt) and 4.8 wt% HOS ligand. One piece was tanned with $Zr(SO_4)_2·4H_2O$ (6 wt% ZrO_2) and 4.8 wt% citric acid (CA, a commonly used ligand in zirconium tanning[9]). Another piece was tanned without ligand as control. After tanning, the leathers were sampled, split into three uniform layers and dried to constant weight at 102 °C. ZrO_2 content (based on the weight of dry leather) of each layer was determined using inductively coupled plasma atomic emission spectroscopy (ICP-AES, Optima 2100DV, PerkinElmer, USA). The Zr-tanned leathers were piled overnight, wrung and shaved to uniform thickness of 1.0 mm, and then the shaved leathers were rewetted, neutralized, retanned and fatliquored according to conventional processes. The grain surfaces of the crust leathers were observed using stereo microscope (SZX12, Olympus, Japan). The curst leathers were conditioned for 24 h at 20°C and 65% RH, and then their softness was measured.

2.4 Comparison of conventional chrome tanning and Zr-HOS tanning

Two pickled cattle hides (approx. 8 kg for each one) were used in the tanning experiments. One hide was tanned by Zr-HOS as shown in Table I, while the other hide was tanned by conventional chrome tanning method as shown in Table II. After tanning, the shrinkage temperatures (Ts) of wet white and wet blue were determined. The isoelectric points (pI) of both leathers were determined using zeta potential analyzer (MütekTM SZP-10, BTG, Germany). The leathers were sampled and split into three uniform layers, and each layer was dried to constant weight at 102°C. ZrO_2/Cr_2O_3 content (based on the weight of dry leather) of each layer was determined using ICP-AES after digesting with H_2O_2 and HNO_3.The grain surfaces and the cross sections of both leathers were observed using stereo microscope and scanning electron microscope (SEM, Pro X, Phenom, Netherlands), respectively.

The wet white and the wet blue were wrung and shaved to uniform thickness of 1.0 mm), and then typical post-tanning processes (Table III) were conducted to obtain crust leathers. The Ts of the crust leathers was measured. The grain surfaces and the cross sections of the crust leathers were observed as described above. Additionally, the curst leathers were conditioned for 24 h at 20°C and 65% RH, and then their physical properties such as softness, tensile strength, tear strength, bursting strength and elongation at break were measured.

The wastewater samples were collected at the end of each tanning and post-tanning processes. At the same time, the

volumes of the wastewaters were measured. The concentrations of Cr/Zr in wastewaters were analyzed by ICP-AES after digesting by H_2O_2 and HNO_3. TOC concentrations were determined using total organic carbon analyzer (TOC, Vario TOC, Elementar, Germany). Cr/Zr and TOC loads were calculated according the volume of wastewater per ton of pickled cattle pelt and expressed as kg/ton of pickled cattle pelt. In addition, biochemical oxygen demand (BOD_5) and chemical oxygen demand (COD_{Cr}) of wastewaters were determined using standard methods.

Table II Zr-HOS tanning

Process	Material	Content (%)[a]	Temperature (°C)	Time (min)	Remarks
Pickling	Water	100	25		
	Sodium chloride	14			
	Sulfuric acid	0.2		60	pH < 3.0
Tanning	ZrO_2	6	25		
	HOS	4.8		180	
Basifying	Magnesium oxide	2.4	25	30×4	
	$NaHCO_3$	4.8		5×20	pH 3.8-4.0
	Water	400	40	120	Next day run for 30 min and drain

[a] The content of material was based on the weight of pickled cattle hide.

Table II Conventional chrome tanning

Process	Material	Content (%)[a]	Temperature (°C)	Time (min)	Remarks
Pickling	Water	100	25		
	Sodium chloride	14			
	Sulfuric acid	0.2		60	pH < 3.0
Tanning	Chrome powder	14	25	240	
Basifying	Sodium formate	2	25	30	
	$NaHCO_3$	4		6×20	pH 3.8-4.0
	Water	400	40	120	Next day run for 30 min and drain.

[a] The content of material was based on the weight of pickled cattle hide.

Table III Post-tanning processes

Process	Material	Content (%)[a]	Temperature (°C)	Time (min)	Remarks
Rewetting	Water	400	35		
	Degreasing agent	0.5		40	Drain
Washing	Water	400×2	35	10×2	Drawn
Neutralizing	Water	200	35		
	Sodium formate	1		30	
	$NaHCO_3$	0.6×2		15+60	Drain, pH 6.0
Washing	Water	400×2	35	10×2	Drain

Retanning	Water	100	35		
	Acrylic resin	3			
	Dispersing syntan	1		30	
	Melamine resin	1			
	Dicyandiamide resin	2			
	Dyestuff	2		30	
	Dispersing syntan	1			
	Mimosa	5		60	
	Formic acid	0.4×2		10+30	Drain, pH 4.0
Fatliquoring	Water	150	50		
	Phospholipid	5			
	Sulfonated fatliquor	1			
	Synthetic fatliquor	9			
	Dyestuff	0.3		60	
	Formic acid	0.5×2		15×2	Drain, pH 3.8
Washing	Water	200	25	15	Drain

[a] The content of material was based on shaved wet blue and wet white weight.

3. Results and discussion

3.1 Characteristics of HOS

The HOS was characterized by NMR, GPC, laser particle size and UV-Vis analyses. The ^{13}C NMR spectra of native starch and HOS are demonstrated in Figure 1. The chemical shift of carbon for native starch has been identified in 100 ppm for C-1, in 77 ppm for C-4, in 74, 72, 70 ppm for C-3, C-2 and C-5, and in 61 ppm for C-6.[10] After oxidation, the signals of C-2, C-3 and C-6 were decreased and the new signals of carbonyl (actually aldehyde groups) and carboxyl groups appeared at 165 ppm and 178 ppm, respectively. These results indicated that the oxidation reaction primarily occurred on the hydroxyl groups at C-2, C-3 and C-6 positions.[11]

Molecular weights (M_w and M_n), polydispersity indexes (M_w/M_n) and average particle sizes of native starch and HOS are shown in Table IV. The M_w, M_n and average particle size of the native starch decreased dramatically after oxidation. This should be attributed to the degradation of starch during the oxidation process.[12] The polydispersity index (M_w/M_n) is generally used to evaluate the molecular weight distribution of polymers.[13] The polydispersity index of HOS was lower than that of native starch, indicating that the distribution of HOS components was concentrated.

Figure 2 shows that zirconium sulfate had no absorption peak in the wavelength range from 200 to 500 nm. The absorption peak of HOS at 273 nm underwent a red-shift to 330 nm after mixing with zirconium sulfate, indicating a formation of new complexes through coordination of HOS rich in functional groups (hydroxyl, carbonyl and carboxyl) with Zr ion.

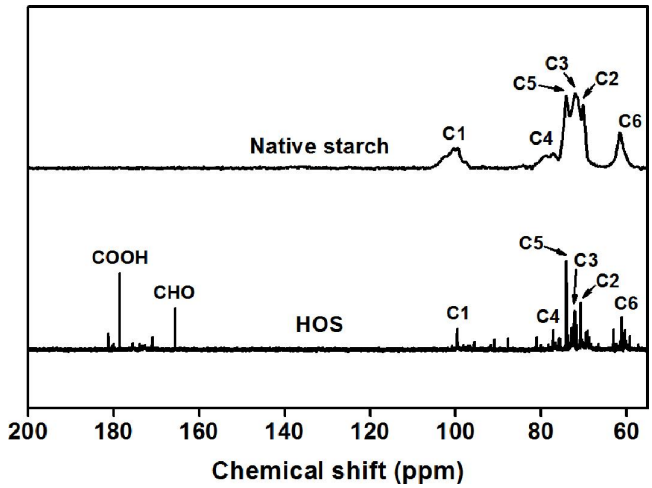

Figure 1. ^{13}C-NMR spectra of native starch and HOS.

Table IV Molecular weights and particle sizes of native starch and HOS.

Sample	M_w/(g/mol)	M_n/(g/mol)	M_w/M_n	Average particle size/nm
Native starch	3.736×10^6	647371	5.771	997.4
HOS	6833	3516	1.943	179.8

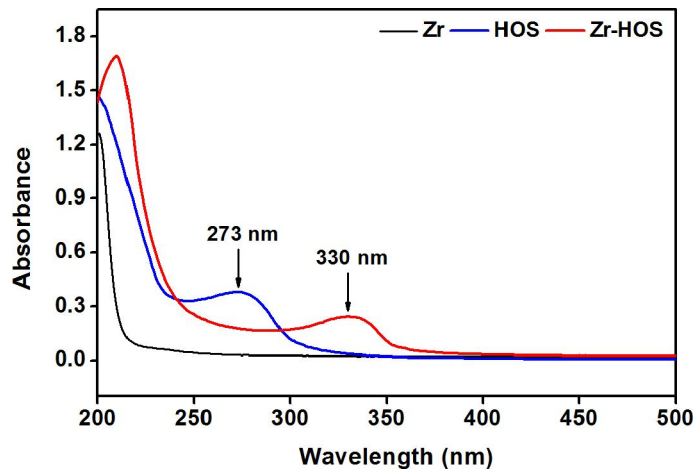

Figure 2. UV-Vis spectra of zirconium sulphate, HOS and Zr-HOS complex.

3.2 Zirconium tanning performance

As shown in Figure 3, HOS used as a ligand improved the uniform distribution and fixation of Zr in leather as well as the softness of crust leather compared with CA and the control (no ligand). It can also be observed from the stereo microscope images (Figure 4) that the traditional Zr-tanned crust leather (control) has a rather coarse grain surface because of the strong reaction of Zr on the surface, while the crust leather tanned with Zr and HOS has finer and smoother grain.The results can be explained by the fact that HOS can strongly complex with Zr ion and reduce the binding ability of Zr complexes to leather collagen fibers at the beginning of tanning, thus leading to a sufficient tanning and good organoleptic properties. Therefore, HOS is expected to be a desirable ligand used for zirconium tanning.

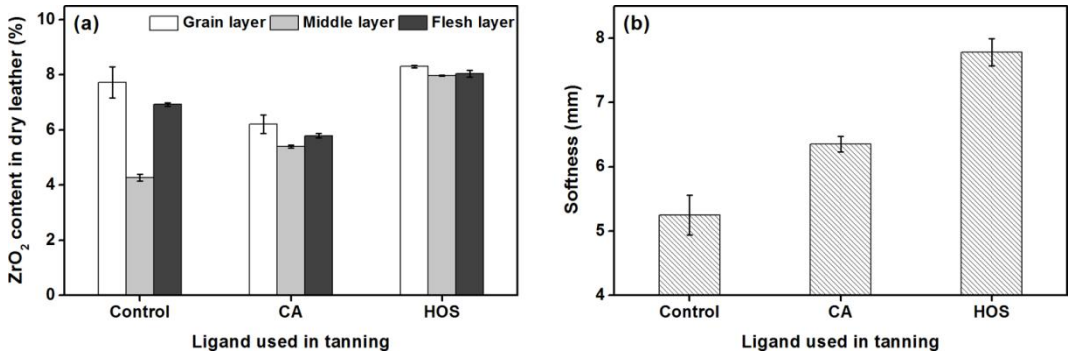

Figure 3. Effect of ligand on ZrO_2 distribution (a) and softness (b) of leather.

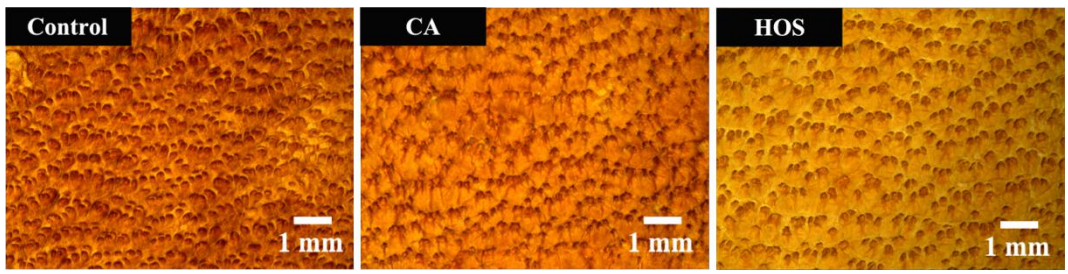

Figure 4. Stereo microscope images of grain surfaces of crust leathers.

3.3 Comparison of conventional chrome tanning and Zr-HOS tanning

3.3.1 Properties of wet white and wet blue

The wet white and the wet blue were split into three uniform layers, and the ZrO_2 and Cr_2O_3 content of each layer was determined, respectively. The uniform distribution of Zr in each layer of the wet white (see Table V) showed that Zr-HOS complexes can penetrate and fix on the leather matrix uniformly. This should be attributed to the use of HOS, which can strongly complex with Zr ion and thus reduce the binding ability of Zr complexes to leather collagen fibers at the beginning of tanning. Furthermore, comparing the Ts of the wet white and that of the wet blue (Table V), it can be seen that the hydrothermal stability of the wet white was lower than that of the wet blue, but already met the common requirement of leather goods (Ts around 90°C). The pI and the surface charge of leather play an important role in leather processing as they influence the penetration and the fixation of chemicals in leather matrix.[14] Table V shows that the pI of the wet white (7.03) was close to that of the wet blue (7.13), implying an excellent absorption capacity of the wet white to post-tanning chemicals. In addition, the grain surfaces of the wet white and the wet blue were observed by stereo microscope. It was found that the grain surfaces of both leathers were clear and fine (Figure 5(a) and 5(b)) due to the mild binding at surface during the tanning process as well as the uniform distribution of Zr/Cr in the leather matrix. Comparing Figure 5(c) and 5(d) shows that the wet white had a loose weave of collagen fibers and large porosity, which was very similar to the wet bule. This indicated that Zr-HOS possessed an excellent crosslinking performance for collagen fibers. In general, it can be inferred that the wet white had good tanning performance and should be suitable for the following post-tanning processes.

Table V Metal content, Ts and pI of leathers.

Sample	% ZrO_2/ Cr_2O_3 (based on dry weight of leather)			Ts (°C)	pI
	Grain	Middle	Flesh		
Wet white	8.99 ± 0.06	8.67 ± 0.08	8.81 ± 0.03	91.0 ± 0.6	7.03
Wet blue	4.91 ± 0.04	4.68 ± 0.03	4.71 ± 0.04	109.9 ± 1.3	7.13

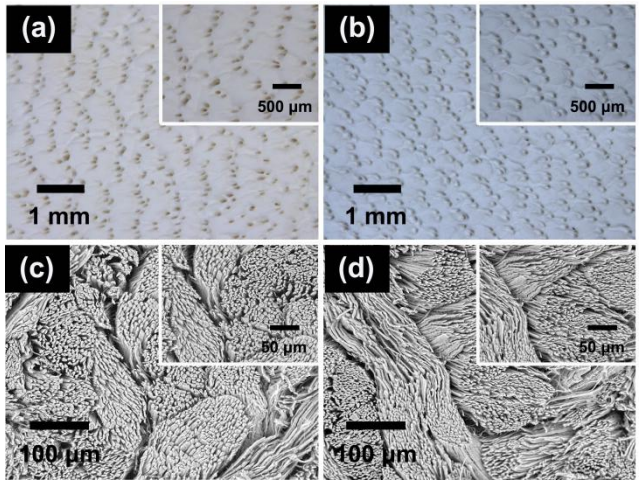

Figure 5. Stereo microscope images of leathers: (a) grain surface from wet white; (b) grain surface from wet blue. Scanning electron micrographs of leathers: (c) cross section from wet white; (d) cross section from wet blue.

3.3.2 Properties of crust leathers

Softness, tensile strength, tear strength, bursting strength and elongation at break are important physical properties of leather. Table VI presents physical properties of the Zr-HOS and the chrome crust leathers tested with the official methods. It can be found that the Zr-HOS crust leather had higher tensile, tear and bursting strength, but lower softness and elongation than the chrome crust leather, probably due to the strong filling ability of Zr. In addition, Figure 6 shows the microstructures of the two crust leathers observed by stereo microscope and SEM. It was found that the grain of the Zr-HOS crust leather showed better tightness but slightly worse fineness compared with that of the chrome crust leather (Figures 6(a) and 6(b)). Moreover, the Zr-HOS crust leather exhibited well-dispersed fibers similar to the chrome one. All the results above indicated that the Zr-HOS tanning agent can be applied in leather manufacture due to its reliable physical and organoleptic properties.

Table VI Physical properties of crust leathers.

Sample	Softness(mm)	Tensile strength (N/mm^2)	Tear strength (N/mm)	Bursting strength (N/mm)	Elongation at break (%)
Zr-HOScrust leather	8.32 ± 0.07	14.9 ± 1.02	49.8 ± 1.84	342.5 ± 9.67	46.1 ± 4.92
Chrome crust leather	8.42 ± 0.11	13.7 ± 0.94	44.8 ± 3.25	289.7 ± 15.23	55.9 ± 6.53

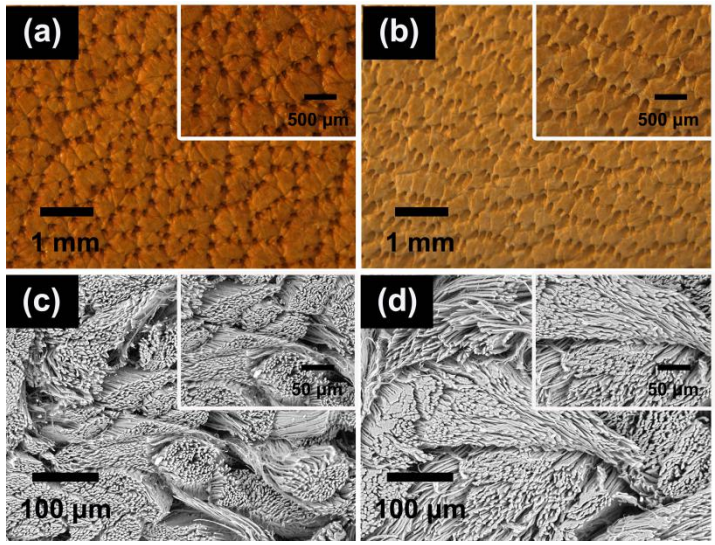

Figure 6.Stereo microscope images of crust leathers: (a) grain surface from Zr-HOS; (b) grain surface from chrome. Scanning electron micrographs of crust leathers: (c) cross section from Zr-HOS; (d) cross section from chrome.

3.3.3 Environmental benefits

The wastewaters from Zr-HOS and Cr tanning and post-tanning processes were collected, and their metal and TOC emission loads were determined as shown in Table VII. The results showed that the residual metal ion in tanning wastewater was the main origin of metal emission loads, and there was a sustained release of metal in almost all the post-tanning operations because of the existence of free and unstably combined metal ions in leather.[15] It is worth noting that the total metal emission load in the Zr-HOS processing wastewater (0.29 kg/ton of pickled pelt) was much lower than that in the chrome processing (7.73 kg/ton of pickled pelt), implying that the Zr-HOS was stably fixed on collagen fibers. As for the discharge of organics, the total TOC load in Zr-HOS post-tanning wastewaters was significantly lower than that in chrome post-tanning wastewaters. These results indicated that the Zr-HOS tanned leather possessed better affinity for post-tanning chemicals than the Cr tanned leather. In terms of the whole processes, the total metal and TOC emission loads were reduced by 96% and 40% using Zr-HOS processing, respectively, compared to chrome processing.

The ratio of BOD_5/COD_{Cr} is usually used for evaluating the biodegradability of wastewater. A higher ratio means a better biodegradability.[16] The biodegradability of Zr-HOS and Cr tanning and post-tanning wastewaters is shown in Table VIII. Apparently, the Zr-HOS tanning wastewater was more biodegradable than the chrome tanning wastewater due to the use of polysaccharide-based organic ligand. Additionally, the BOD_5/COD_{Cr} ratio of Zr-HOS post-tanning wastewaters (0.37) was also higher than that of Cr post-tanning wastewaters (0.24). The reason should be that the lower metal and organic contents in Zr-HOS post-tanning wastewaters were more conducive to microorganism growth. These facts demonstrated that the biodegradability of Zr-HOS processing wastewaters was better. Hence, it turned out that the Zr-HOS tanning system would be cleaner for leather processing.

Table VII Pollution loads in tanning and post-tanning wastewaters (unit: kg/ton of pickled pelt).

Process	Zr output	Cr output	TOC output	
	Zr-HOS	Cr	Zr-HOS	Cr
Tanning	0.15 ± 0.00	7.34 ± 0.01	8.49 ± 0.05	6.10 ± 0.11
Rewetting	0.07 ± 0.00	0.28 ± 0.01	3.02 ± 0.05	1.87 ± 0.01
Neutralizing	0.04 ± 0.00	0.02 ± 0.00	3.21 ± 0.18	2.74 ± 0.05
Retanning	0.01 ± 0.00	0.01 ± 0.00	5.36 ± 0.08	9.49 ± 0.08
Fatliquoring	0.02 ± 0.00	0.08 ± 0.00	16.38 ± 0.42	40.55 ± 0.47

Total	0.29 ± 0.01	7.73 ± 0.03	36.46 ± 0.78	60.75 ±0.71

Table VIII Biodegradability of tanning and post-tanning wastewaters.

Wastewater sample	COD_{Cr} (g/L)		BOD_5 (g/L)		BOD_5/COD_{Cr}	
	Tanning	Post-tanning	Tanning	Post-tanning	Tanning	Post-tanning
Zr-HOS	2.62 ± 0.05	4.10 ± 0.06	0.85 ± 0.07	1.50 ± 0.14	0.32	0.37
Chrome	1.96 ± 0.04	7.17 ± 0.08	0.25 ± 0.07	1.70 ± 0.14	0.13	0.24

4. Conclusions

Zr-HOS complex shows an excellent tanning effect in terms of their uniform distribution and effective crosslinking in leather matrix. The coordinating effect of HOS with Zr ion remarkably overcomes the drawbacks of the traditional Zr-tanned leather, and the physical and organoleptic properties of the Zr-HOS tanned leather are comparable to those of the chrome tanned leather. Besides, both the metal and TOC emission loads in the wastewater of the Zr-HOS tanning system are much lower than those of the conventional chrome tanning system. In summary, this novel chrome-free tanning process is a sustainable alternative to conventional chrome tanning due to the reliable leather quality and the environmental benefit.

Acknowledgements

This work was financially supported by the National Natural Science Foundation of China (21506129) and the National Key Research and Development Program of China (2017YFB0308500).

References

1. Chaudhary, R., Pati, A.Purification of protein hydrolyzate recovered from chrome tanned leather shavings waste. Journal of the American Leather Chemists Association, 2016, 111: 10-16.
2. Sizeland, K. H., Wells, H. C., Edmonds, R. L., et al. Effect of tanning agents on collagen structure and response to strain in leather. Journal of the American Leather Chemists Association, 2016, 111: 391-397.
3. Ramasami, T., Sreeram, J., Rao, J., Nair, B. U. Approaches towards elucidating the mechanism of tanning using an organo-zirconium complex. Journal of the American Leather Chemists Association, 2000, 95: 359-367.
4. Madhan, B., Sundarrajan, A., Rao, J. R., et al. Studies on tanning with zirconium oxychloride: Part II: Development of a versatile tanning system. Journal of the American Leather Chemists Association, 2003, 98: 107-114.
5. Covington, A. D., Lampard, G. S., Hancock, R. A., et al. Studies on the origin of hydrothermal stability: a new theory of tanning. Journal of the American Leather Chemists Association, 1998, 93: 107-120.
6. Li, H., Prakash, S., Nicholson, T. M., et al. The importance of amylose and amylopectin fine structure for textural properties of cooked rice grains. Food Chemistry, 2016, 196: 702-711.
7. Zhang, S. D., Liu, F., Peng, H. Q., et al. Preparation of novel c-6 position carboxyl corn starch by a green method and its application in flame retardance of epoxy resin. Industrial & Engineering Chemistry Research, 2015, 54: 11944-11952.
8. Yu, Y., Wang, Y. N., Ding, W., et al. Preparation of highly-oxidized starch using hydrogen peroxide and its application as a novel ligand for zirconium tanning of leather. Carbohydrate Polymer, 2017, 174: 823-829.
9. Sundarrajan, A., Madhan, B., Rao, J. R., et al. Studies on tanning with zirconium oxychloride: Part I: Standardization of tanning process. Journal of the American Leather Chemists Association, 2003, 98: 101-106.
10. Guo, J., Lian, X., Kang, H., et al. Effects of glutenin in wheat gluten on retrogradation of wheat starch. European Food Research and Technology, 2016: 1-10.
11. Zhang, S. D., Zhang, Y. R., Wang, X. L., et al. High carbonyl content oxidized starch prepared by hydrogen peroxide and its thermoplastic application. Starch-Stärke, 2009, 61: 646-655.
12. Chong, W. T., Uthumporn, U., Karim, A. A., et al. The influence of ultrasound on the degree of oxidation of

hypochlorite-oxidized corn starch. LWT-Food Science and Technology, 2013, 50: 439-443.

13. Chan, H. T., Leh, C. P., Bhat, R., Senan, C., et al. Molecular structure, rheological and thermal characteristics of ozone-oxidized starch. Food Chemistry, 2011, 126: 1019-1024.
14. Wang, Y. N., Huang, W. L., Zhang, H. S., et al. Surface charge and isoelectric point of leather: a novel determination method and its application in leather making. Journal of the American Leather Chemists Association. 2017, 112: 224-231.
15. Zhou, J., Hu, S. X., Wang, Y. N., et al. Release of chrome in chrome tanning and post tanning processes. Journal of the Society of Leather Technologists and Chemists, 2012, 96: 157-162.
16. Shi, B., Li, J., Wang, Y. N. et al. A novel wet white technology based on an amphoteric organic tanning agent. 2012, In: 9th AICLST Congress, Taipei

O11

Application and Preparation of A bio-polymer re-tanning agent based on Cattle hair hydrolysate

Luo Jianxun, Ma Hewei

Materials & Textile Engineering College, Jiaxing University, Jiaxing 314000,P.R.China

ABSTRACT

In order to promote the development of Clean production of Leather-making and recycle the cattle hair from hair-saving process, the cattle hair is hydrolyzed and applied in some fields. But because the cattle hair hydrolysate has the small molecular weight and poor re-tanning properties during the process of re-tanning of the leather, it was modified with vinyl monomers by radical co-polymerization using ammonium persulfate at 80°C for 3 hours to obtain a bio-polymer re-tanning agent. Compared with the viscosity, re-tanning properties of the bio-polymer re-tanning agent, the mol ratio of acrylic acid, acrylamide was confirmed to be 4.0, 1.0 and the consumption of acrylic acid, acrylamide is 80% based on the content of the hydrolysate. The structure of the bio-polymer re-tanning agent was characterized by FTIR. Applied result of the bio-polymer re-tanning agent on the re-tanning of the shaving sheepskin wet blue shows that it has good re-tanning and filling properties. When the optimal consumption of the bio-polymer re-tanning agent is in the range of 6% and 8%, the re-tanned leather is full , more uniform than before and no plastic feeling.

Keywords: Cattle hair hydrolysate; A bio-polymer re-tanning agent; Acrylic acid; Acrylamide; Re-tanning properties

INTRODUCTION

Leather industry is one of old & young industries in the world, which is also the most important way of making use of animal skins or hides. Because Leather goods have natural hand, beautiful appearances and high-grade characteristics, they are always favored. But during the process of Leather-making adopted by traditional technology, some pollutants are produced to pollute the environment[1]. So ecological technologies and clean production of leather-making can promote the sustainable development of Leather industry.

Now ecological technologies and clean production of leather-making include soaking with enzyme, de-furring without damage, de-liming without ammonia, pickle without salt, Chrome-less or Chrome-free tanning, etc[2-8]. The traditional process of de-furring can be easily processed, good de-furring effect and serious pollution. Therefore in order to decrease the pollution and reduce the cost of treating the waste water, the technology of de-furring without damage is studied and promoted which not only reduce the amount of pollutants, but also save the natural resources. But how to deal with the fur originated from the hair-saving process will be an important topic.

The fur contains lots of keratin which can be extracted and hydrolyzed by many methods such as enzyme, alkali solution, etc and be used in many fields[9]. Therefore the methods of hydrolysis of fur (cattle hair) were studied. Now the methods mainly include mechanical means, chemical process, biological methods, etc. Chemical processes often are adopted which cover hydrolysis with acid or alkali, oxidation or reduction approaches, etc[10]. However, the degree of hydrolysis can't be easy to be controlled so that the molecular weight of the hydrolysate is small.

The present work focus on the hydrolysis of cattle hair and preparing a bio-polymer re-tanning agent based on the hydrolysate by the copolymerization of acrylic acid, acrylamide, which has larger molecular weight and good filling properties during the re-tanning process of shaving sheepskin wet blue. The synthesis, co-monomer ratio, the molecular weight and the application properties are discussed.

EXPERIMENTAL

Materials

Acrylic acid (AAc), Acrylamide (Am), ammonium persulfate (APS), sodium hydroxide were of chemical pure grade. TRUPON SWS was provided from TRUMPLER Ltd. Cattle hair hydrolysate (the content of hydrolysate is 40-45% and the

molecular weight is 3000) was made by ourselves. The shaving chrome-tanned sheepskin leathers were purchased from Haining brother tannery, Zhejiang Province,China .

Preparation of the bio-polymer re-tanning agents

Based on the cattle hair hydrolysate, the bio-polymer was prepared by radical co-polymerization under the conditions listed in TABLE I and TABLE II.

TABLE I

Parameters of orthogonal experiment

Factor	Level 1	Level 2	Level 3
A/APS/wt%	1.5	2.0	2.5
B/[m(two moners)/m(Content of hydrolysate)]	0.6	0.8	1
C/n(AAc)/n(Am)	1:1	1:0.5	1:0.25

TABLE II

Formulation of copolymer reaction among cattle hair hydrolysate, acrylic acid and acrylamide

No	A/APS/wt%	B/[m(two moners)/m(Content of hydrolysate)]	C/n(AAc)/n(Am)
1	1.5	0.6	1:1
2	1.5	0.8	1:0.5
3	1.5	1.0	1:0.25
4	2.0	0.6	1:0.25
5	2.0	0.8	1:0.5
6	2.0	1.0	1:1
7	2.5	0.6	1:0.25
8	2.5	0.8	1:1
9	2.5	1.0	1:0.5

Firstly, the relevant Acrylic acid, Acrylamide and water were weighted and the mixture solution was neutralized with 30wt% sodium hydroxide solution to form mixed monomers solution. Secondly, the relevant ammonium persulfate solution was prepared. Thirdly, the co-polymerization was performed in a stirred 500mL four mouth flask with two feed funnels and a thermometer. At the beginning, the relevant cattle hair hydrolysate, water were added into the flask and heated to 80°C, then part of ammonium persulfate solution was added into the flask and stirred for 30min. The monomer mixture and the surplus ammonium persulfate solution were drip fed in. The rate of addition was controlled in order to be complete within 90min. Then the temperature was regulated to 82-85°C and was kept constant for 120min. At last the flask was cooled to 50°C and form the bio-polymer re-tanning agent. The scheme of the reaction is described in Fig.1.

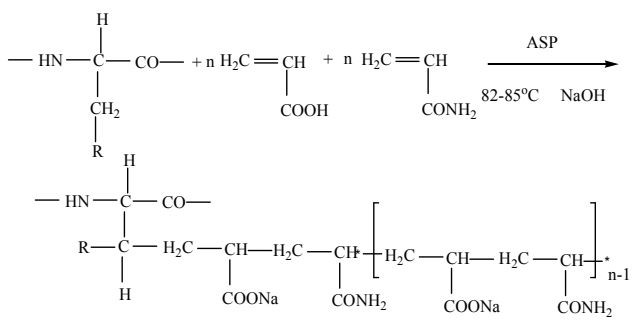

Fig.1. The preparation of the bio-polymer re-tanning agent

Application of series of the bio-polymers and the selection of the best synthetic recipe

Series of these bio-polymers were applied respectively in the re-tanning process of the shaving sheepskin wet blue. The re-tanning process is shown as TABLE III, and the thickening rates were examined. The thickening rate of the leather was investigated using a thickness gauge to measure the thickness of the Part A, Part B and Part C of the leather in the pre-re-tanning and the post- re-tanning stage. The part of the leather measured and the formula is separately described in Fig.2, Fig.3. Then the average thickening rate was calculated among Part A, Part B and Part C. Then according to data-processing method of the orthogonal experiment, the optimized synthetic recipe was confirmed. According to the best synthetic recipe, the bio- polymer re-tanning agent (BRA) was obtained.

TABLE III

There-tanning, fat-liquoring process of the shaving sheepskin wet blue

Process	Chemicals	%	T/°C	Time/min	Remarks
Re-wet	water	200	35		
	Degreasing agent	0.3			
	Formic acid	0.3		60	pH 3.8
Washing	Water	200	18-22		drain
Re-chrome	Water	200	30		
	Chrome B	4		60	
	Tannesco HN	2		30	pH 4.0
	Sodium bicarbonate	0.6			
Neutralization	water	150-200	30		
	Tanigan PAK-N-c	2			
	sodium formate	1		90	pH 5.8-6.0
	Sodium bicarbonate	1.5			
Washing	water	200			drain
Re-tanning	water	200	45		
	BRA	6		60	
	Fromic acid	0.2		15	pH 5.0 drain
Fat-liquoring	water	200	50	90	
	TRUPON SWS	15			
Fixation	Fromic acid	0.6		15	
	Fromic acid	0.6		15	pH3.6-3.7
Washing	water	200		20	drain, horse up, dry and milling

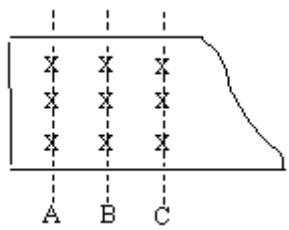

Fig. 2 Location plan of leather thickness measuring

$$Thickening\ rate = \frac{Thinckness\ of\ the\ leather\ in\ post\text{-}re\text{-}tanning - Thinckness\ of\ the\ leather\ in\ pre\text{-}re\text{-}tanning}{Thinckness\ of\ the\ leather\ in\ pre\text{-}re\text{-}tanning} \times 100\%$$

Fig. 3 Formula of the thickness rate of the leather

Molecular Weight of the bio-polymer re-tanning agent and its Structure determination

The molecular weight of the bio-polymer retanning agent (BRA)was investigated by gel permeation chromatograph (Sephadex G-25, using tetrahydrofuran as mobile phase, the flowing speed 1.0mL/min, using Polyethylene Glycol as Reference Standard). Then the bio-polymer re-tanning agent was precipitated with acetone and dried for 6hrs at 80°C in vacuo. The infrared (IR) spectrum was determined with Nicolet Nexus 470 FTIR spectrophotometer.

Application and the optimum amount of the bio-polymer re-tanning agent on the shaving sheepskin wet blue

The bio-polymer re-tanning agent (BRA)was respectively applied in the re-tanning process of the shaving sheepskin wet blue. The process is the same as TABLE III. The amount of the bio-polymer re-tanning agent (BRA) is 0, 2%, 4%,6%,8% respectively. The method of the thickening rate of the leather is consistent with the former. Compared with the thickening rate of the leather under the condition of different amount of the bio-polymer re-tanning agent (BRA), the optimal amount of BRA is determined.

RESULTS AND DISCUSSION

Analysis of the optimized formulation of the bio-polymer

TABLE IV shows the thickening rate in the re-tanning process of the shaving sheepskin wet blue with the different bio-polymer synthesized by the relevant recipe. Different bio-polymer may have different viscosity and molecular weight so as to show different results.

Based on the thickening rate and the viscosity, the mol ratio of monomers and the amount of total monoers have been optimized. The optimized mole ratio is $A_1B_{2\text{-}3}C_3$. That is, APS 1.5wt%, [m(two moners)/m(Content of hydrolysate)] 0.8-1.0, n(AAc)/n(Am) 1:0.25.

TABLE IV

Results of the synthesis of the bio-polymer among cattle hair hydrolysate, acrylic acid and acrylamide and its application

No	A/APS/wt%	B/[m(two moners)/m(Content of hydrolysate)]	C/n(AAc)/n(Am)	Thickening rate/%
1	1.5	0.6	1:1	9.6
2	1.5	0.8	1:0.5	9.8
3	1.5	1.0	1:0.25	11
4	2.0	0.6	1:0.25	7.2
5	2.0	0.8	1:0.5	6.8
6	2.0	1.0	1:1	6.7
7	2.5	0.6	1:0.25	9.2
8	2.5	0.8	1:1	9.7
9	2.5	1.0	1:0.5	10

Analysis of the molecular weight and the structure optimized formulation of the bio-polymer and its characteristics

As shown in Figure 4, the molecular weight and the distribution index (M_w/M_n) of the bio-polymer re-tanning agent (BRA) are 24634 and 3.19 respectively, which indicates that the BRA has larger molecular weight, suitable distribution of molecular weight and may be good re-tanning and filling properties.

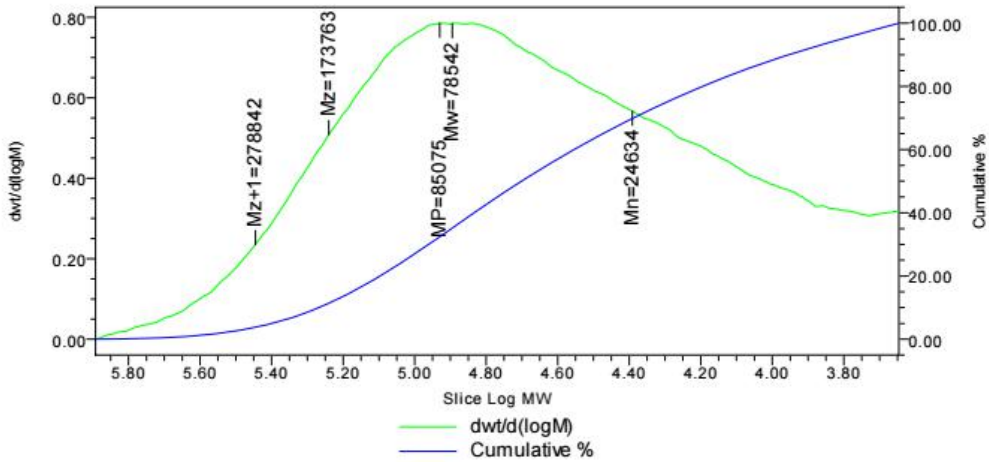

Fig. 4 Curve of GPC of BRA

Fig.5 shows the FTIR spectra of the bio-polymer re-tanning agent (BRA). The relation between the bands and its relevant groups was shown as Table V. So the chemical structure can be elementarily confirmed by FTIR.

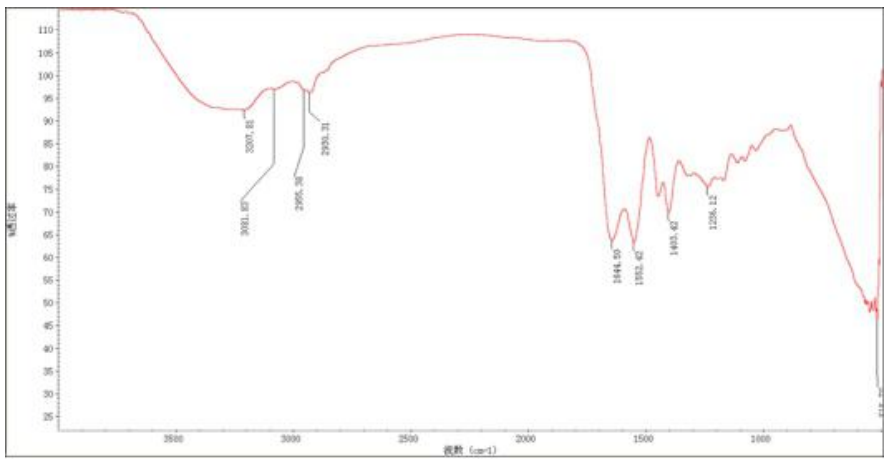

Fig.5. IR Spectrum of BRA

TABLE V Relation between the band and the relevant group of BRA

No	Band/cm^{-1}	Group
1	3207.81,3081.83	O-H (-COOH)
2	1644.5,1552.42	-COO^{-}
3	1403.42	C-O

Results of application on the shaving sheepskin wet blue

Fig.6 shows individually the relation between the consumption of the bio-polymer re-tanning agent (BRA) and the thickening rate of the leather during the re-tanning of the shaving sheepskin wet blue. With the consumption of the BRA increasing, the thickening rate of the leather rises, which show that the bio-polymer re-tanning agent has good re-tanning and filling properties. when the dosage of the BRA bio-polymer is 6%, the thickening rate of the leather is over 9%. So the best dosage of the APAA is between 6% and 8%. The leather re-tanned is full and uniform and have good hand without plastic feeling.

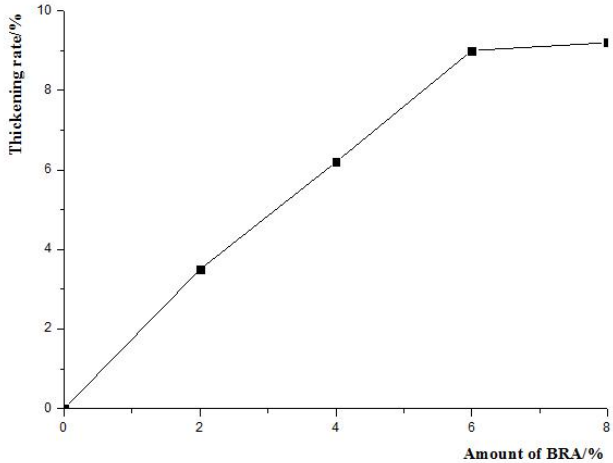

Fig.6. Relationship of the thickening rate of the leather re-tanned and the dosage of BRA

CONCLUSION

Clean production of Leather-making greatly induces the pollution from the traditional technology. Hair-saving process not only decreases the content of COD_{Cr} in the effluent, but also saves the hair. The hydrolysis is one of most important methods of resource utilization for the hair. Because the cattle hair hydrolysate has the small molecular weight and poor re-tanning properties during the process of re-tanning of the leather, then it was modified with vinyl monomers by radical co-polymerization using ammonium persulfate at 80°C for 3 hours to obtain a bio-polymer re-tanning agent. Compared with the viscosity, re-tanning properties of the bio-polymer re-tanning agent, the mol ratio of acrylic acid, acrylamide was confirmed to be 4.0, 1.0(1:0.25) and the consumption of acrylic acid, acrylamide is 80% based on the content of the hydrolysate. The structure of the bio-polymer re-tanning agent was elementarily characterized by FTIR. Applied results of the bio-polymer re-tanning agent on the re-tanning of sheepskin wet blue show that it has good re-tanning and filling properties. When the optimal consumption of the bio-polymer re-tanning agent is in the range of 6% and 8%, the re-tanned leather is full, uniform and no plastic feeling.

ACKNOWLEDGMENT

The author would like to acknowledge the support of Science and Technology Bureau, jiaxing City, Zhejiang Province and Haining Peace Chemical group, Zhejiang Province.

REFERENCES

1.Hu jing, Sun genxing. Pollution from the process of Manufacturing leather and pollution prevention.West Leather., 2011,33(22),17-21.

2.Yu zhimiao. Application of different enzyme is helpful for getting better leather quality and higher area yield: The application of soaking Enzymes. China Leather., 2006,35(9), 1-3.

3.JIN Liqiang,LIU Jie,ZHANG Feifei,etal.A close recycling technique of liming wastewater based on hair－saving unhairing process. China Leather., 2018,47(5), 33-38.

4.WANG Yanan,SHI Bi.Progress of key clean technologies in leather industry.CHEMICAL INDUSTRY AND ENGINEERING PROGRESS, 2016, 35(6), 1865-1874.

5.Luo Jianxun, Feng Yanjuan. CLEANER PROCESSING OF BOVINE WET WHITE: SYNTHESIS AND APPLICATION OF A NOVEL CHROME-FREE TANNING AGENT BASED ON AN AMPHOTERIC ORGANIC COMPOUND. *J.* Soc.*Leather. Technol. Chem.,* 2015, 99(4), 190-196.

6.Luo Jianxun, Feng Yanjuan, Shan Zhihua. Complex Combination Tannage among Phosphonium compounds, Vegetable tannins and Aluminium tanning agent. Journal of the Society of Leather Technologists and Chemists 95, 215-220.

7.Hernandez J.F., Kallenberger W.E., Combination tannage with vegetable tanning and aluminium,*J. Amer. Leather Chem. Ass*., 1984, 79(2), 182-206.

8.D·Aquino, A., Barbani, N, D·Elia, G., et al., Combined organic tanning based on mimosa and Oxazolidine development of a semi-industrial scale process for high-quality bovine upper leather. *J.* Soc.*Leather. Technol. Chem.,* 2004, 88(2), 47-55.

9.Hill P, Branthy H, DyKe M V. some properties of keratin biomaterials: Kerateines. Biomaterials, 2010,31:585-593.

10.Liu Meng，Cheng Haiming.Cattle Hair Hydrolysis and Properties of Hydrolytes. China Leather., 2012,41(17), 27-31.

O12

Effect of Extraction and Coloring Condition on Chromium(VI) Determination

Kazuya Takase[1], Mariko Terashima [1], and Keiji Yoshimura [2]

1 Tokyo Metropolitan Leather Technology Center, 3-3-14, Higashisumida, Sumida-ku, Tokyo, 131-0042, Japan,+81-3-3616-1671,takase.kazuya@hikaku.metro.tokyo.jp,terashima.mariko@hikaku.metro.tokyo.jp,

2 Japan Leather and Leather Goods Industries Association, 1-12-13, Komagata, Taito-ku, Tokyo, 111-0043, Japan, +81-3-3847-1451, yoshimurak@leather.onmicrosoft.com

Abstract

The test method for analyzing chromium (VI) content is specified in ISO 17075-1 (IUC 18-1) and ISO 17075-2 (IUC 18-2). In these methods, chromium (VI) content is not determined directly, but it is defined as the soluble chromium (VI) extracted from leather with phosphate salt solution at pH 7.0 to 8.0. Therefore chromium (VI) content varies in terms of the extraction condition such as temperature, shaking condition, leaving time after extraction, and so on. However it is not defined the extraction temperature and the leaving time after extraction in the documents. In addition, it is often carried out extraction using linear shaker instead of orbital shaker in Japanese laboratories. Therefore the objective of this study was to clarify the effect of extraction temperature, the leaving time after extraction, and the difference of shaker on chromium (VI) content.

Our results indicated that the chromium (VI) content increased in proportion to temperature rise. On the other hand, the chromium (VI) content was not almost affected by the leaving time after extraction in case of the preservation at a low temperature. In addition, it was not affected by the type of shaker. Therefore, from these results it can be concluded that it is necessary to define the extraction temperature in the documents.

Key words: chromium (VI), ISO 17075, extraction temperature, shaker, leaving time

1. Introduction

Chrome tanning is a relatively new technology in the history of leather making. However, it is accounts for approximately 80 % of the leather production in the world, and it has been used for more than a century.

Chromium is a heavy metal element and their compounds have mainly trivalent state or hexavalent state. The former is stable and harmless and the latter is classified as CMR substance (carcinogenic substance, mutagenic substance, reproductive toxic substance). Especially, chromium (VI) is known to cause severe allergic contact dermatitis in humans. Trivalent chromium salt, usually a basic chromium sulfate is used as a tanning agent in leather making. However, in the case of leather, it is known that chromium (III) can transform to chromium (VI) due to the oxidation of oil and fat, ultraviolet irradiation, heat, low moisture content, and so on. Nowadays, there are some practical methods preventing the chromium (VI) formation developed in the leather industry in the world.

With regard to chromium (VI) in leather, the risk of causing allergic dermatitis has been pointed out. The European Commission concluded that an unacceptable risk to human health arose where chromium (VI) compounds were present in leather articles and articles containing leather parts, coming into contact with the skin. Therefore, in 2014, EU issued regulation No 301/2014, whichleather articles coming into contact with the skin shall not be placed on the market where they contain chromium (VI) in concentrations equal to or greater than 3 mg/kg (0,0003 % by weight) of the total dry weight of the leather). Also in Japan, Japanese Association of Leather Technology established the Japanese Eco Leather Standard. One of the criteria for certification is that chromium (VI) is not detected (detection limit 3mg/kg).

Therefore, it is necessary for laboratories to measure chromium (VI) in leather with the same condition. The test method for chromium (VI) content in leather is specified in ISO 17075-1 (IUC 18-1) and ISO 17075-2 (IUC 18-2). The former is colorimetric method and the latter is chromatographic method. In these methods, chromium (VI) content in leather is not determined directly, but it is defined as the soluble chromium (VI) extracted from leather. Therefore, it is believed that the extraction conditions affect the chromium (VI) content.In the both ISO documents, it is defined the size of the leather piece, extraction solution, extraction time, and so on. On the other hand, extraction temperature is not specified in ISO 17075-1,

and it is defined as a room temperature in ISO 17075-2 which is unclear expression. Also the leaving time after extraction are not specified in the both documents. Furthermore, linear shaker instead of orbital shaker defined in the ISO is generally used in Japanese laboratories due to the difficulty in setting the temperature.

Therefore, in the present study, we investigated the effect of the extraction temperature, the leaving time after extraction, and the difference of shaker on the extractable chromium (VI) from leather.

2. Materials and Methods

2.1 Materials

Fifteen samples of chrome-tanned leather were used for the experiments. Some were the commercial leather and others were prepared susceptible to generate chromium (VI). Some samples were thermally aged at 80 °C for 24 hours so that chromium (VI) was intentionally detected. The sample was allowed to stand for 48 hours or more under conditions of a temperature of 20 °C ± 2 ° C and a RH 65% ± 5%. Then, according to ISO 4044, the leather samples are cut into small pieces of 3 mm to 5 mm side length using the scissors.

2.2 Determination of chromium (VI)

Test conditions prescribed in ISO, that is, cutting size of sample, extraction time, reagents, etc., were performed according to ISO 17075-1. In ISO, extraction flask is specified as 250 mL conical flask with stopper. However, it is difficult to obtain it in Japan, so we replaced it with a 300 mL stoppered Erlenmeyer flask. The temperature of the chromium (VI) extraction from leather was carried out at 20 ° C, 25 °C, and 30 °C. Two kinds of shakers, orbital type and linear type, were used. If the extraction solution was colored, the colored substances were removed by solid phase extraction with OASIS HLB (Waters Co. Ltd.). Color development of the extraction solution was carried out from just after filtration to after 19 days. In that case, the extract was stored at 4 °C until colorimetry.

3. Results and Discussions

3. Results and Discussions

3.1 Effect of shaker type on the extractability of chromium (VI)

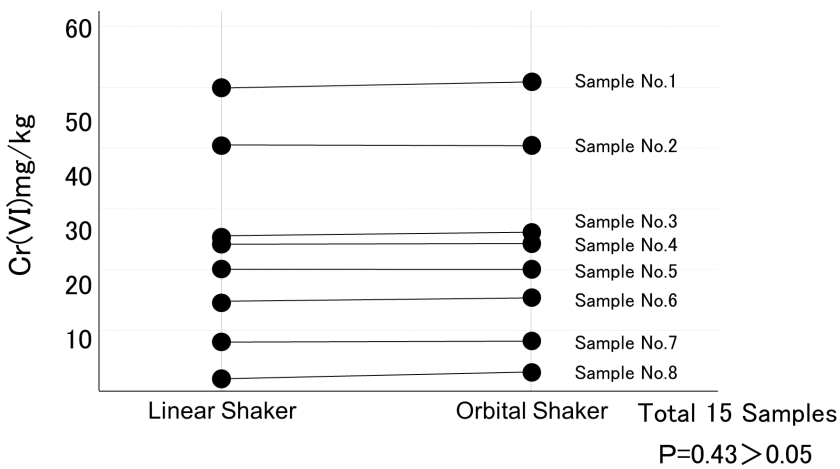

The results obtained by using two types of shakers are shown in Fig. 1. At any temperature, there was no difference in chromium (VI) content between orbital shaker and linear one. Therefore, there is no problem to use a linear shaker instead of an orbital shaker as specified in ISO.

Fig.1. The results obtained by using two types of shakers.

3.2 Effect of extraction temperature on the extractability of chromium (VI)

Analytical solution samples were extracted with the phosphate solution at an extraction temperature of 20 °C, 25 °C, and 30 °C. Figure 2 shows the results obtained three different extraction temperatures. The amount of chromium (VI) increased

with the increase of the extraction temperature. Possible reasons for this result are considered as follows. One reason is the extracted amount of chromium (VI) from the leather sample itself increased with the increase in the extraction temperature, and the other reason is some part of the chromium (III) in the extracted solution after filtration is converted to chromium (VI) affected by the temperature rise.

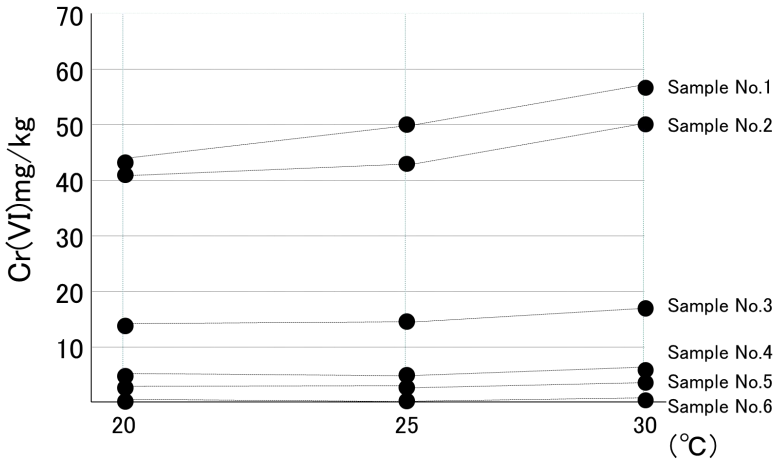

Fig.2. The amount of Chromium (VI) extracted at three different extraction temperature

If the direct oxidation of chromium (III) to the hexavalent form would be occurred in the extracted solution, chromium (VI) was supposed to increase by keeping at high temperature after extraction. Therefore, the extracted solution at 20 °C was kept at 30 °C for 3 hours after filtration. We compared the amount of chromium (VI) with or without keeping at 30 °C for 3 hours. No significant difference was observed between the amount of chromium (VI) extracted at 20 °C and those of keeping at 30 °C after extraction at 20 °C (Table 1). This result suggests that increase of chromium (VI) was resulted not because chromium (III) was converted to chromium (VI) by keeping at 30 °C, but because extracted chromium (VI) from leather increased with increasing the extraction temperature. From these results it was noted that the amount of extracted chromium (VI) depends on the extraction temperature.

Table 1. Temperature condition and extracted amount of Chromium(VI)

Temperature condition	Cr(VI) mg/kg (Ave.)
Extraction at 20℃	38.4
After extraction at 20 ° C, keeping at 30 ° C	38.8
Extraction at 30℃	49.2

3.3 The leaving time after extraction

To investigate the effect of time course change of the chromium (VI) content in the extracted solution, the solution was stored at 4 °C up to 19 days before developing color. Figure 3 shows that the effect of the leaving time after filtration on the amount of the extracted chromium (VI). In spite of the slight increase of the chromium (VI) was observed after one week, it eventually indicated to almost the same value as immediately after filtration over time. As for the chromium (VI) content in the extracted solution, there was no significant difference in the leaving time.

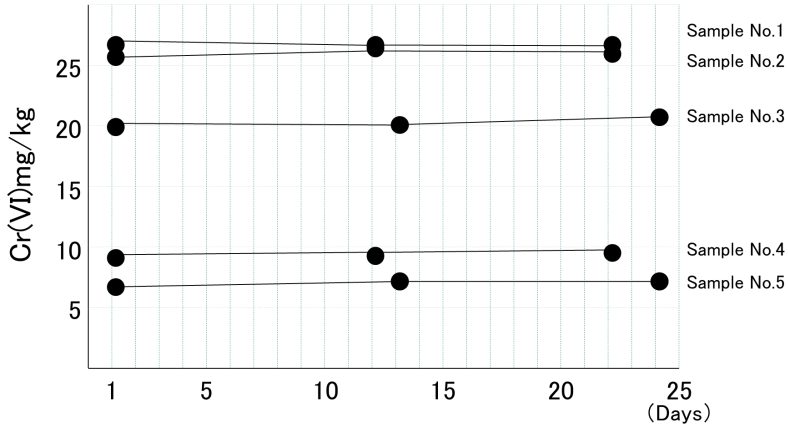

These results indicate that the extracted chromium (VI) is very stable at 4 °C in this method.

Fig. 3. Changes in detection amount due to leaving time

4. Conclusion

Chromium (VI) content in leather is not determined directly, but it is defined as the chromium (VI) extracted from leather. ISO 17075-1 (IUC-18-1) and ISO 17075-2 (IUC-18-2) specified that results obtained by using other extraction procedures are not comparable with the results produced by the procedure described in this document. It is not defined the extraction temperature and the leaving time after extraction in the documents. In addition, it is often carried out extraction using linear shaker instead of orbital shaker in Japanese laboratories. Therefore, we investigated the experimental conditions, including the extraction temperature, the leaving time until discovering color and the difference of shaker, for analyzing chromium (VI) content in ISO 17075 series.

The results obtained by using two types of shakers, there was no difference in chromium (VI) content between orbital shaker and linear one at any temperature. It is concluded that the both a linear shaker and an orbital shaker are available.

From the results obtained three different extraction temperatures, the amount of chromium (VI) increased with the increase of the extraction temperature. Considering these results, we strongly encourage to defining the extraction temperature in the ISO series.

Examining the effect of time course change of the chromium (VI) content in the extracted solution before developing color, we concluded that the extracted chromium (VI) is very stable at 4 °C in this method. It was found that developing color to the extracted solution can be performed at an appropriate time and it is not necessary to specified strictly.

O13

Study on the Effects of Glycosidases Specificity on Fiber Opening and Unhairing Processes

FengxiangLuo[2,3],ChunxiaoZhang[1,3],Yanhong Li[1,2], Jinming Liu[3],Rui Yao[3],BiyuPeng[1,2,3,*]

1. National Engineering Laboratory for Clean Technology of Leather Manufacture, SichuanUniversity, Chengdu 610065, China;

2. Key Laboratory of Leather Chemistry and Engineering of Ministry of Education, SichuanUniversity, Chengdu 610065, China;

3.College of Light Industry, Textile & Food Engineering, Sichuan University, Chengdu, China,

**E-mail of corresponding author:pengbiyu@scu.edu.cn*

Abstract

Glycosidase has been prepared in leather making process to assist fiber opening and control the pollution discharged from the conventional technology based on the lime and sodium sulphide, for it can remove the proteoglycan by its enzymatic catalysis. The effectiveness of a series of glycosidases which are specific to different glucosidic bonds on fiber opening and unhairing were evaluated, including xylanase, cellulase,β-glucanase, amylase, α-galactosidase and β-galactosidase. The results showed that, on different degree, all of the selected glycosidases can remove the proteoglycan from the hide and help to open up the collagen fiber. Cellulase and β-glucanase which both are selective to the site of β-glucoside have good collagen fiber bundles seperation and hair loosing or removal effect. Xylanase, being specific to bond of β-xyloside, has the best assistance to remove the proteoglycan while the fiber dispersing effectiveness is weaker than that of cellulase and β-glucanase. β-galactosidase specific to β-galactoside can also cut the link bridge of polysaccharide chain and core protein chain the same as xylanase has a less fiber open and hair removing effect as its high moleculor weight. Amylase and α-galactosidase, of which selective bond is α-glucoside and α-galactoside correspondingly, make collange fiber be loose to the lowest degree. What's more, the application of xylanase, cellulose,β-glucanase in the pretreating operation of enzymatic unhairing technology can accelerate dehairing effectively. Scanning electron scanning (SEM) results showed that the dispersed collagen fiber is comparison with that of the conventional process and the hair pores are undamaged, without causing into loose grain. And the physical and organoleptic properties of crust leather are improved. In addition, the dosage of lime and sulfide has been reduced significantly.

Key words: glycosidases; opening-up; dehairing; proteoglycan

1. Introduction

A large amount of waste water containing high BOD, COD and TS and solid waste in beamhouse hinder the sustainable development of leather industry, especially the tradition liming process used excessive lime and high concentration of sodium sulfide. Some cleaner measures such as sodium hydroxide or sodium metasilicate were used to open fiber, however, their fiber dispersion degree is excessive or insufficient. Application of enzymes with specificity, high activity in neutral pH, reduction in pollution is a promising clean method. Some glycosidases such as amylase, pectinase, hyaluronidase, galactosidase used with protease were thought to assist unhairing and fiber openning(Durga et al. 2017, Durga et al. 2016, Melville and Deasy 1977, Zeng et al. 2013, MadhanRao and Nair 2010). Among these, α-amylase specific to α-glucoside bond was thought to hydrolyze the interfibrillar substances which adhere to and wrap the collagen. But there are still controversial as these enzymes are commercial grade with concomitant proteases. Furthermore, the substrate and specific hydrolytic bond of glycosidases in skin and the relationship of glycosidase treatment and fiber separation or unhairing were unclear.

In order to solve these problems, the information of main substances related to fiber open was collected. There are two principal gel-like cement substances in skin to woven with the collagen fiber, one of which is hyaluron, a long chain glycoaminoglycan twined around but not bounded to collagen, so it is removed easily in soaking process(Alexander KTW

1986); the other is proteoglycan. Decorin is the most common proteoglycan in skin, which is a kind of dermatan sulfate-proteoglycan (DS-PG)(Uldbjerg and Danielsen 1988), covalently formed by one or two long chain glycosaminoglycans and core protein through O-glucosidic bond composed by galactosyl-β-l,3-galactosyl-β-1,4-xylosyl-serine, regularly distributed on the surface of the collagen fibrils. The core protein of the decorin are horseshoe-shaped structures arranged perpendicularly to longer axis of the collagen fibrils and nested with the protrusions on the fibrils, The core protein between the two proteoglycans is linked by the polysaccharide chain(Keene et al. 2000); The polysaccharide chain dermatan affects the polymerization process of collagen molecule and the existing collagen fibrils, thus affecting the collagen maturation and lateral growth of collagen. Therefore, removal of decorin and other glycosaminoglycan(GAG) is one of the most important step for fiber opening. Then according to the structure of cementing substance, the property and actitivity of six different glycosidases with specfic hydrolytic bond were chosen and studied. And then the fiber separation and unhairing effect of enzymes for application in soaking and unhairing process were evaluated. The property of crust was tested to find the effect of different specific glycosidases on fiber opening and unhairing. At last some carbohydrases with specificity were chosen for opening up and unhairing with clean production process and high quality of leather was developed.

2. Materials and methods

2.1. Materials and methods

Six kinds of glycosidases viz. xylanase, cellulose, β-glucanase, α-galactase, β-galactase and α-amylase were of commercial grade and procured from different corporration including Shandong Lonct Enzymes Co.,Ltd. Novozymes Biotechnology Co.,Ltd. Kunming Aikete Biological Technology Co.,Ltd. Wet-salted cattle hides from Sichuan, China, were purchased from a local tannery (Leshan Zhenjing Leather Industry CO., Ltd.). Unhairing protease was supplied by LANXESS Chemical(China)Co.,Ltd. (activity 60000u/mL at 30 ^{o}C, pH7). All chemicals used for conventional dehairing and tanning operations were of commercial grade. All other chemicals used were of analytical grade.

2.2 Assay of glycosidases activity and properties

Glycosidases hydrolytic activity was assayed based on the natural skin powder that contains relative high content of polysaccharide. Two grams of skin powder were incubated by 50mL distilled water at 30 ^{o}C for 60 min twice to remove soluble carbohydates. Then the water was removed by filtered, and remaining skin powder was mixed with suitable dilluted enzyme solution, 20 mL of 0.1 mol/L Briton-Robinson buffer (pH 6.0) incubated at 30°C for 120 min and stopped by adding 1 mL of 2 mol/L H_2SO_4 solution. Then the concentrations of total sugar(TS), protein and Glycosiaminoglycan(GAG) in waste were determinated according to phenol sulphuric acid method of Dubois using D-glucose as standard(Dubois et al. 1956), Lowry method using bovine serum albumin as standard(Lowry et al. 1951) and dimethylmethylene blue method using dermatan as standard(Farndale et al. 1986).

2.3 Soaking and dehairing process

Wet-salted cattle was cut into 8 parts(30cm×35cm), numbered from 1 to 8, separately. Glycosidases including xylanase, cellulase, β-glucanase, α-galactase, β-galactase and cool amylase were applied in soaking process to the 6 parts, respectively; meanwhile, two parts soaked without glycosidase as control group. The enzymatic soaking process was performed in drum with 200% buffer(0.1M, pH6.0), 0.5% glycosidase and 0.1% bactericide with 10 min running per hour for 6 times. The control soaking process was performed the same as the enzymatic soaking process except for glycosidase. Then the enzymatic dehairing process was carried out on number 1-7 skin by 120u/mL protease running for 5h after changing the pH value to 7.0 by adding 10% KOH solution. Then 0.6% sodium sulfide, 0.5% lime and 0.2% KOH were added to remove the remainent fine hair. The control dehairing process was performed by using a mixture of 1.2% sodium bisulfide and 0.8% liming auxiliaries SP running for 2h follwed by adding 1.5% sodium sulfide and 0.5% lime. At last 1.5% lime and 150% water were used for liming. The remaining pre-tanning, tanning and post-tanning processes were performed under the same

conditions for all the skins.

2.4 Carbohydrates and proteins content in soaking and dehairing wastewater

Soaking and unhairing liquor was sampled and centrifuged at 3000 rpm for 30 min. The supernatant liquors were taken for analysis of total sugar(TS), protein and Glycosiaminoglycan(GAG) concentrations.

2.5 Histological staining

Soaked and unhaired pelts samples were cut from the adjacent part and fixed in 10% neutral formalin for 48 h. Then, the samples were cut into sections of 10-20μm thicknesses using a freezing microtome(CM1950, Leica, Germany). Sections were stained with Weigert's iron hematoxylin Van Gieson's stain to differentiate collagen fibers, muscle fibers, hair roots and epidermis. Furthermore, Sections were stained with alcine blue to differentiate GAG. After staining, the histological sections were observed using a biological microscope.

2.6 Scanning electron microscopy (SEM)

The chrome-tanned leathers of each tanning group were sampled and freeze dried, then samples were viewed microscopically Scanning Electron Microscope.

2.7 Pore diameters of crust leather by an automatic surface area and porosimeter system

The specific pore diameter was measured by N_2-sorption by the BET and BJH model using an automatic surface area and porosimeter system (Micromeritics Tristar3000, U.S.A).

2.8 Compararionng of perfomance of different glycosidases soaking and unhairing process

In order to analyze the extent of fiber open, hair, epidermis and pigment removal, the grain of enzymatic soaked and unhaired pelts were captured using a digital camera, respectively.

2.9 Physical and bulk propertities of crust leathers

Samples from crust leathers along the parallel and perpendicular directions to the backbone of the leathers were obtained following standard methods(IUP 2 2000) for various physical tests. Specimens were conditioned at 20±2 ^{o}C and 65±2% relative humidity over a period of 48 h. The physical properties of the samples, such as tensile strength, elongation at break and bursting strength were examined following standard procedures(IUP 6 2000). Softness was evaluated following standard procedures(IUP 36 2000).

2.10 Chromium content of crust leathers

The chrome-tanned leather samples of each tanning group was taken out in the adjacent parts, and washed thoroughly to remove uncombined chromium salt. Then the samples were freeze-dried at -55 ^{o}C and 20 Pa vacuum for 24 h. The dried leathers were split into two layers using Precision Slice Machine. Properly dried leather sample was completely digested with the mixture of nitric acid and chloride acid at 100^{o}C for 120 min. The digestion solutions were appropriately diluted and filtered. The chromium content in each layer of the leather were determinated with AES-ICP and then calculated, which is an indirect measure of fiber opening in the skin matrix.

3 Results and discussion

In order to study the effect of glycosidases specificity on fiber opening and unhairing process, different kinds of glycosidases were chosen and used in soaking and unhairing process.

3.1 Glycosidases activity

Six kinds of glycosidases with specific hydrolytic bond were chosen and their propertities and enzyme activities were estimated. The result was showed in table 1. The glycosidases with different molecular weight and isoelectric point assisting the TS, protein and GAG release from animal skin powder. The total sugar means that the mucoid substance such as heparin and dermatan or their peptide complexes decorin or biglycan were romoved from animal skin into soluble which need to break the peptide chain or carbohydrate chain of complexes into short and unsoluble chain. GAG was the long acidic polysaccharide chain which was produced by breaking the linkage of peptide chain and polysaccharide chain or two bond in

saccharide chain far away from each other. Cellulose being specific to β-glucanase release highest TS and GAG followed by xylanase and β-glucanase as cellulose and β-glucanase cut β-glucoside linkages composed the disaccharide unit in polysaccharide chain into different chain molecules. β-glucanase was a constituent of cellulase, so it is more specifity than the latter which leading to less hydrolytic effect. Xylanase or β-galactosidase hydrolyzing the linking bridge of peptide chain and polysaccharide chain produced some GAG. While α-galactosidase specific to α-galactoside linkage and amylase which was specific to α-glucoside bond all promote TS release but did not produced GAG which may caused by hydrolysis of a little heparin sulfate and glycogen in skin which contain α-galactoside linkage and α-glucoside bond, respectively. The three latter release much less proteins than the former. In conclusion, the glycosidase activity based on skin powder was coninsistant to their specificity, but the protein release from skin powder was related to the proteolytic activity.

Table 1. Property and activity of glycosidases used in leather manufacture

Name	Mw/kD	Proteolytic	pI	Concentration in waste treat skin powder/ug		
				TS	Protein	GAG
Xylanase	72/60/19	388	4.7/8.5	175.76	5654	5.24
Cellulase	50	681	4.9/6.2	256.82	6917	92.77
β-glucanase	53	436	4.7	107.61	2860	0.00
α-galactosidase	99	0	4.6	86.09	264	0
β-galactosidase	103/66	0	4.3/8.2	68.87	66	15.71
Amylase	162/58	0	7.7	66.36	396	0

All glycosidases were used 0.5% of skin powder, exception of 2.5% of β-galactosidase.

3.2 Carbohydrates and proteins release by enzyme treatment

The literature show that during leather-making process, the release of proteoglycans is considered as a marker for fibre opening(Alexander KTW 1986, Song Jian etal. 2011). The concentrations of TS, protein and GAG in enzymatic soaked and unhaired liquors are shown in Table 2 and Table 3. Soluble TS in waste concentration was consistent with the glycosidase activity based on the natural skin powder. Cellulase assisting produced most of total sugar and GAG. β-galactosidase produced many GAG but a few TS. Xylanase hydrolyzing the second most TS and GAG. Cellulase , β-glucanase and xylanase with a few proteolytic activity produced most of protein. The produced carbohydrates treated by α-glycosidase including α-galactosidase and α-amylase was less than the three former glycosidase, except amylase produce lots of proteins.

Table 2. Concentrations of carbohydrates and proteins in soaking liquors

Enzyme	Concentration of carbohydrates and proteins(ug/mL)		
	TS	Protein	GAG
1#Control	27.88	242.19	14.29
2#Xylanase	36.85	334.38	19.05
3#Cellulase	57.84	446.88	19.53
4#β-glucanase	32.08	942.19	17.62
5#α-galactosidase	15.59	317.19	16.20
6#β-galactosidase	17.61	178.13	20.00
7#Amylase	26.42	915.63	16.67
8#Control	19.33	218.75	15.24

Table 3 showed that after adding protease, carbohydrates removal were not completely consistent to the glycosidase

activity based on skin powder partly because the hydrolysis of core protein of proteoglycan(Shakilanishi and Shanthi 2017). The skin treated by α-galactosidase and α-amylase release the highest TS and GAG may be related to the most remanent proteoglycan after soaking was hydrolyzed by protease and then long chain GAG was released. While xylanase and β-galactosidase release the least carbohydrates might because their product long chain GAG was similar to the protease and after soaking the remained proteoglycan in skin was less. Cellulase and β-glucanase produced medium TS and GAG may related to the hydrolysis of proteoglycan and produced long chain and short chain of polysaccharide. The liming process released most of protein and GAG because in strong alkali condition, the carbohydrate chains were easy to departure monosaccharide one by one and the proteins were sensitive to alkali which was one of the main reasons the tradition liming process has good unhairing and fiber open effect(Alexander KTW 1986).

Table 3. Concentrations of carbohydrates and proteins in unhairing liquors

Enzyme	Concentration of carbohydrates and proteins(ug/mL)		
	TS	Protein	GAG
1#Control	97.1	660.2	54.5
2#Xylanase	90.3	260.5	35.7
3#Cellulase	175.1	494.9	65.7
4#β-glucanase	131.1	416.8	41.7
5#α-galactosidase	272.9	439.5	61.9
6#β-galactosidase	121.0	394.9	37.6
7#Amylase	150.3	655.9	52.2
8#Lime	-	774.6	98.6

3.3 Histology of collagen and GAG

The histological micrographs of soaked and unhaired skin was in accordance with the quantities of carbohydrates release (Figure 1 and Figure 2). GAG in skin was removed after soaked by glycosidases. The remaining of GAG was according with the glycosidase activity and GAG removal in waste water except for β-galactosidase. According to the glycosidase activity based on natural skin powder in table 1, we know that the β-galactosidase produced most GAG but least TS and protein which means it is hardly to hydrolyze long chain GAG to short chain polysaccharide polysaccharide. Furthermore, the moleculor weight of β-galactosidase was about as twice as cellulase, xylanase and glucanase. The pelt treated by cellulase remained the least of GAG, followed by xylanase and glucananse. Control skin treated by non-glycosidase remained most of GAG, and remained GAG in the pelts treated by a-galactosidase and α-amylase were medium.

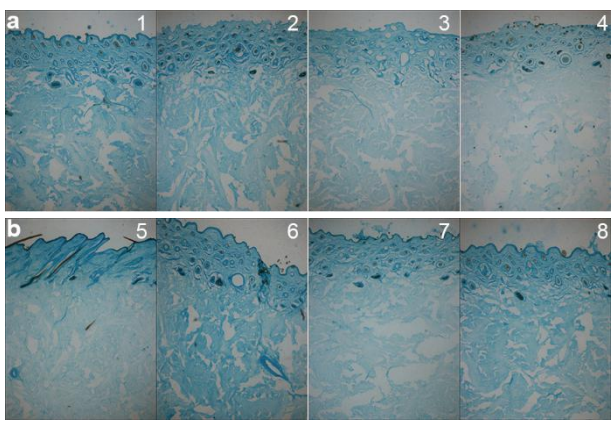

Figure 1. Photomicrographs of alcine blue stained sections of soaked pelts

1 from control soaked pelt, 2 from xylanase soaked pelt, 3 from cellulase soaked pelt, 4 fromβ-glucanase soaked pelt, 5

from α-galactosidase soaked pelt, 6 from β-galactosidase soaked pelt, 7 from amylase, 8 from control soaked pelt, 40X.

As figure 2 showed that most of GAG in the skin were removed when treated by glycosidases and proteases. The cellulase, xylanase and glucananse which are of high glycosidase activity remained the least GAG. The skin treated by lime still remained most of GAG even if it released lots of GAG from skin.

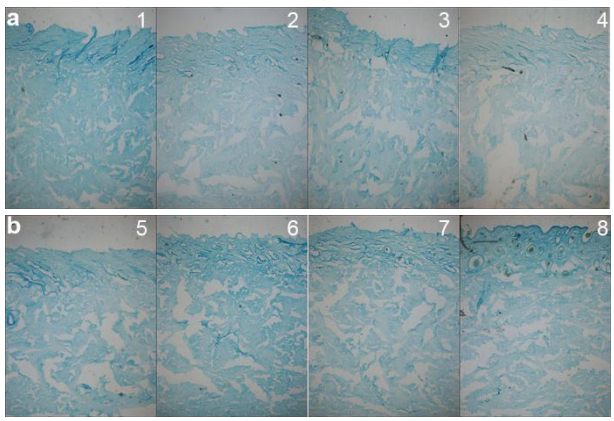

Figure 2. Photomicrographs of alcine blue stained sections of unhaired pelts

1-7 from protease unhaired pelt, 8 from lime unhaired pelt, 40X

Hematoxylin stained sections were analysed for the fiber open effect(Figure 3 and Figure 4). After soaking, collagen in papillary layer treated by xylanase, cellulose and glucanase opened, part of epidermis and hair follicle were removed as much TS, protein and GAG between collagen and around haif follicle was removed. The control skin showed the thickest fiber while the pelt treated by cellulose showed the smallest fiber.

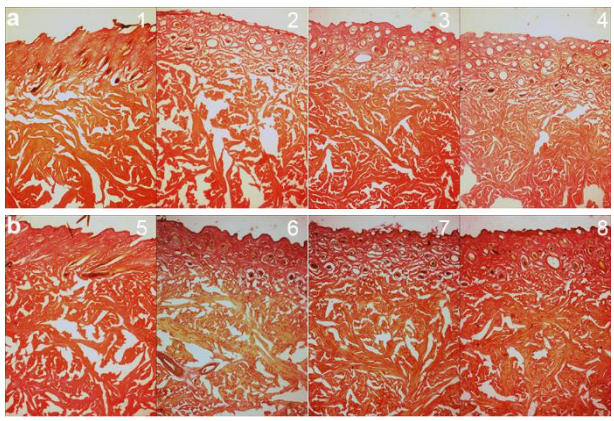

Figure 3. Hematoxylin stained sections of soaked pelts

1 from control soaked pelt, 2 from xylanase soaked pelt, 3 from cellulose soaked pelt, 4 fromβ-glucanase soaked pelt, 5 from α-galactosidase soaked pelt, 6 from β-galactosidase soaked pelt, 7 from amylase, 8 from control soaked pelt, 40X

As figure 4 showed that all the hair and epidermis were removed after unhairing except for the skin treated by lime and sulfide which remained scurf and pigment.

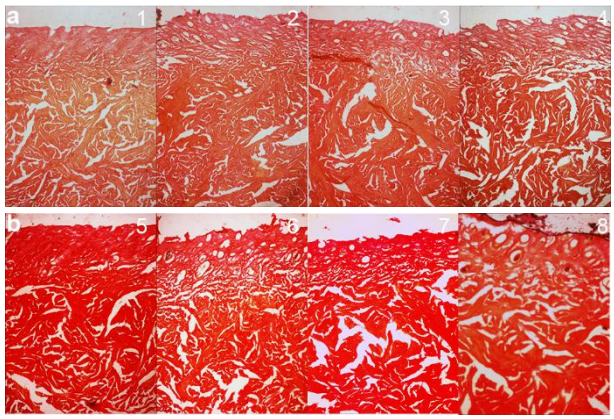

Figure 4. Hematoxylin stained sections of unhaired pelts

(1-7 from protease unhaired pelt, 8 from lime unhaired pelt, 40X)

3.4 Fiber opening measurement by scanning electron microscopy

Further information on effect of glycosidases soaked and proteases or lime unhaired crust were obtained by scanning electron microscopic (SEM) (Figure 5).

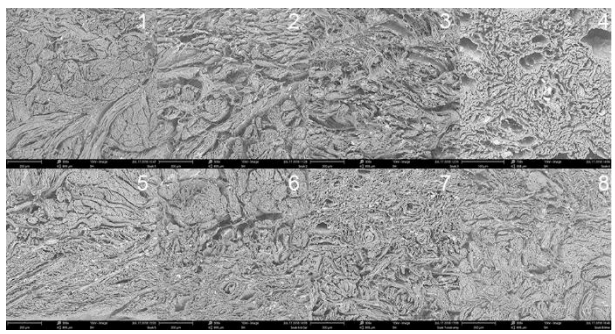

Figure 5. Scanning electron micrographs of crust leathers

Cross section of wet-blue soaked with glycosidases and unharing by protease or lime 500X(1 protease, 2 xylanase+protease, 3 cellulose +protease, 4 β-glucanase +protease, 5 α-galactosidase +protease, 6β-galactosidase +protease, 7 amylase+protease, 8 lime)

As Figure 5 showed that the fiber open effect of glucanase, cellulose had the best fiber open effect followed by xylanase. β-galactosidase produced most of GAG but few TS has a comparable separation effect with amylase which has high TS and protein hydrolysis effect. The fiber open effect of pelt treated by protease without glycosidase was lowest followed by treated by lime and sulfide. So, SEM pictures of crust indicated that the glycosidase assist in grain clean grain and collagen fiber bundles separation.

3.5 Pore size evaluation of crust leather

Barrett-Joyner-Halenda (BJH) average pore-size according to nitrogen adsorption-desorption isotherms of crust was showed in table 4. The results of pore size evaluation was according to the SEM pictures.The pore diameter of crust treated by xylanase, cellulose and glucanase showed greatly increased than control, followed by the crust treated by galactosidase and amylase which were comparable to the skin unhairing by lime. The pore diameter of skin unhairing by protease without glycosidases was the smallest of all which indicated that the glycosidases promoted the fiber bundles separating and showed wider space to help chemicals penetrate into the skin.

Table 4. BJH desorption average pore diameter of crust leather

Name	control	xyl	cel	β-glu	α-gal	β-gal	amy	Lime
Pore diameter(nm)	3.7851	22.8041	19.4141	17.2731	7.0621	7.3319	7.2168	7.2113

3.6 Depilation and grain surface

The digital photos of grain of soaked and unhaired pelts were shown in Figure 6. It can be observed that no hair was removed before enzymatic soaking in all parts(Figure 1(a)). Part of hair was removed when the pelts soaked by cellulose, xylanase and β-glucanase from the experiment hide (Figure 1(b)), which suggested that these kinds of glycosidases on hides can cause unhair after soaking for 6h at 30 °C, while no hair was removed but part of hair was loose of skin soaked by α-galactosidase and amylase. The skin treated by β-galactosidase with high molecular weight but produced lots GAG was slightly better than the α-galactosidase and amylase. The traditional soaked skin showed very tight hair.

During unhairing, the skin treated by xylanase, cellulose and β-glucanase then treated by protease unhairing much faster than the control. And the skin treated by α-galactosidase, β-galactosidase and amylase is analogous to the control. Xylanase and β-galactosidase both specific to link bridge of peptide chain and polysaccharide chain showed different hair loose and removal effect might as their different molecular weight. The traditional unhairing method removed hair clearly but remained a layer of scurf and pigment.

Carbohydrates and protein concentration in waste water were consistent with the hair loose degree in the soaking process. The highest degree of hair loose and removal was the skin treated by xylanase, cellulose and glucanase released lots of TS, proteins and GAGs, while the liquor treated α-galactosidase released higher proteins but little TS, and GAGs whose hair loose degree do not increase. This means that the hair loose was related to the release of carbohydrates including TS, and GAG but not the proteins. And β-galactosidase released most of GAG but little TS and protein don't help a lot to hair loose and removal. It can concluded that hair loose effect need lots of muciod substance hydrolyze into short polysaccharide chain not only long acidic GAG chain.

Extent of removal of epidermis, glandular structures, hair shaft and hair root are consistent to hematoxylin stained pictures(Figure 3 and Figure 4). After soaking, collagen in papillary layer treated by xylanase, cellulose and glucanase opened, part of epidermis and hair follicle were removed as much TS, protein and GAG was removed.

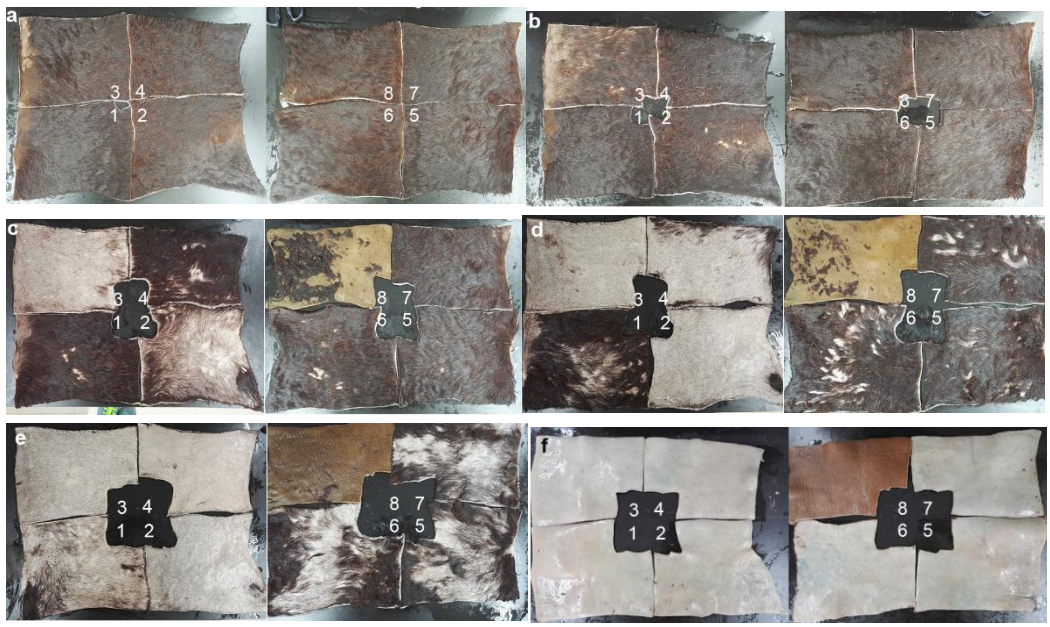

Figure 6. Grain of soaked and unhaired pelts treated differently and captured by digital camera

a pre-soaked, b soaked with glycosidase(1#Control; 2#LKT Xylanase; 3#LKT Cellulase; 4#Novo uL β-glucanase; 5AKT α-galactosidase; 6 β-galactosidase;7Cool amylase;8 Control), c unhairing (1-7#protease;8 Lime), d increasing pH value by adding KOH, e adding lime, f unhaired.

Grain damage information on effect of glycosidases soaked and proteases or lime unhaired crust were obtained by

scanning electron microscopic (SEM) (Figure 7). The grain of crusts treated by glycosidases except xlyanase and control were clean and smooth, while the grain of skin treated by lime was covered by a layer of scurf and wrinked.

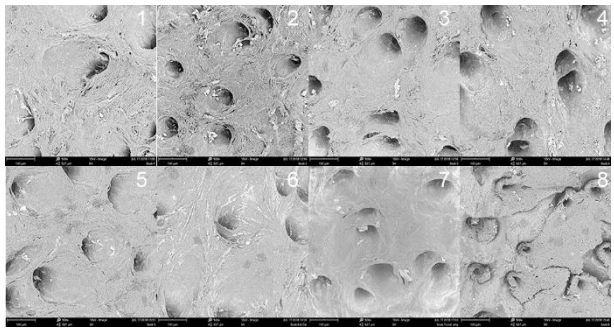

Figure 7. Scanning electron micrographs of crust leathers

Grain surface of wet-blue soaked with glycosidases and unharing by protease or lime 300X(1 protease, 2 xylanase+protease, 3 cellulose+protease, 4 β-glucanase+protease, 5 α-galactosidase+protease, 6 β-galactosidase+protease, 7 amylase+protease, 8 lime)

3.7 Physical properties and sense performance of crust

Physical properties and sense performances of leather were fundamental. So the results of physical propertities and softness were shown in table 5 and figure 8, respectively. Xylanase, cellulose and glucanase decreased the tensile strengh but increased the bursting strength which may because these glycosidases help to removed more interfibrillar substance. Cool amylase decreased the tensile strenth may caused by lots protein removal. Crust treated by galactosidase showed the best tensile strength and bursting strength.

Table 5. Physical properties of crust leather

Enzyme	tensile strength(N/mm^2)	elongation at break/%	Bursting strength N/mm
1#Control	10.1	135.9	211.6
2#Xylanase	7.3	153.8	223.9
3#Cellulase	7.7	93.6	249.4
4#β-glucanase	8.8	104.5	245.4
5#α-galactosidase	11.2	118.1	287.3
6# β-galactosidase	10.1	154.4	237.2
7#Amylase	8.8	122.0	273.1
8#Lime	5.9	208.1	135.1

Figure 8 showed that all crust treated by glycosidases were softer than control. Comparing with the release of TS, GAG and protein these interfibrillar substances and pore size, glycosidase help fiber open and get larger pore size in leather manufacturing process by removing more TS and GAG.

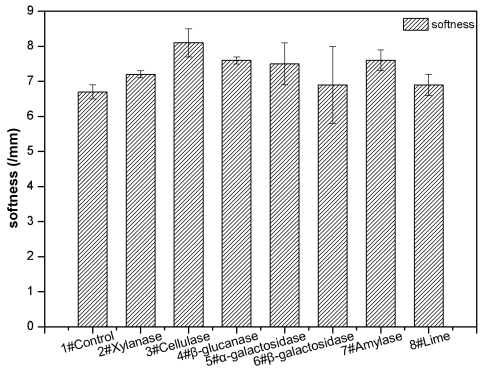

Figure 8. Softness of crust leather

3.8 Chromium content of crust

The main purpose of beamhouse was to removing substance unnecessary and opening fiber to prepare for tanning, fatliquoring and dying. Proper fiber open expose more reaction bond with chromium of collagen, so the content of chorium in crust suggested the fiber open effect. The result was showed in Figure 9. The best fiber open effect by glycosidase had the highest chromium content after retanning, average 3.98%, other are slightly higher than or comparable to the control.

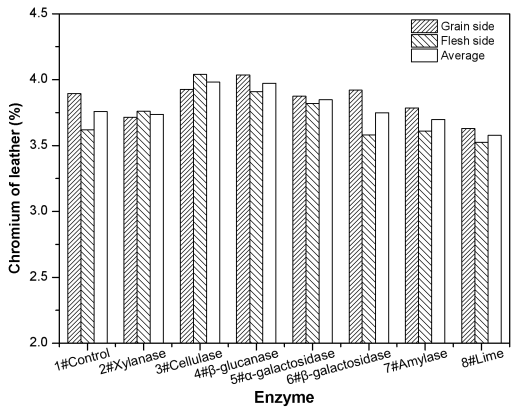

Figure 9. Choromium content of crust leather

4. Conclusions

To develop more glycosidase used in leather marking process, researchers can using the natural skin powder with high carbohydrates as substrate. Different glycosidases specific to different glycosidic bond of cementing substance used in soaking and unhairing help fiber opening and hair loosing or removing by releasing GAG and TS in skin, and won't influence much of the physical properties, especially increasing the bursting strength and softness and chromium content. The cellulase and β-glucanase specific to β-glucoside bond have the best fiber open effect as β-glucoside bond was the linkage between the backbone disaccharide unit consisting of polysaccharide and proteoglycan. But β-glucanase was one constituent of cellulase, so the fiber open and hair removing effect of β-glucanase was inferior to cellulase. Xylanase of hydrolysis β-xyloside bond and β-galactosidase of hydrolysis β-galactoside bond can break the unit of β-xylose-O-serine/threonine and galactosyl-β-galactosyl-β-xyloside which was the link bridge of polysaccharide chains and core protein peptide. But the former has a better fiber opening and hair removing effect as their specific linkages are more common. The α-galactase and α-amylase which hydrolyze the linkage of α-galacoside or α-glucoside have a little of fiber

open because α-glycosidic linkage was very little. So a new enzymatic open up and unhairing method which reduced the dosage of lime and sulfide was developed by using glycosidase specific to β-glucoside or β-galactoside or β-xyloside bond in soaking and before protease unhairing ang get high quality of crust by improving the hair removal speed and separation of collagen fiber bundles.

Acknowledgments

This work was financially supported by the National Key R&D Plan of the Ministry of Science and Technology(2017YFB0308402).

References

Jayanthi Durga, Ramakrishnan Ramesh, Chellan Rose & Chellappa Muralidharan,2017. Role of carbohydrases in minimizing use of harmful substances: leather as a case study. Clean Technologies and Environmental Policy, 5**,** 1567–1575.

Jayanthi Durga, Ammasi Ranjithkumar, Ramakrishnan Ramesh, Kozhikottu Thodu Puthan Veedu Girivasan, Chellan Rose & Chellappa Muralidharan,2016. Replacement of lime with carbohydrases-a successful cleaner process for leather making. Journal of Cleaner Production, 112**,** 1122-1127.

Warren Melville & Clara Deasy,1977. Effect of alpha amylase treatment on the tensile properties of steerhide and leather. Journal of the American Leather Chemists Association, 72**,** 216-229.

Y. H. Zeng, X. Kong, Y. N. Wang, X. P. Liao & W. H. Zhang,2013. Effective component in α-amylase preparation for unhairing. Journal of American Leather Chemists Association, 108**,** 86-92.

B. Madhan, J. Raghava Rao & Balachandran Unni Nair,2010. Studies on the removal of inter-fibrillary materials part Ⅱ:removal of protein ,proteoglycan ,glycosoaminoglycans from biobased pre-tanning process. Journal of American Leather Chemists Association, 105**,** 181-188.

Haines BM Walker M. Alexander KTW. 1986. Inflence of proteoglycan removal on opening-up in beamhouse. In Journal of American Leather Chemists Association, 85-100..

N. Uldbjerg & C. C. Danielsen,1988. A study of the interaction in vitro between type I collagen and a small dermatan sulphate proteoglycan. Biochem J, 251**,** 643-8.

D. R. Keene, J. D. San Antonio, R. Mayne, D. J. McQuillan, G. Sarris, S. A. Santoro & R. V. Iozzo,2000. Decorin Binds Near the C Terminus of Type I Collagen. Journal of Biological Chemistry, 275**,** 21801-21804.

Michel Dubois, K. A. Gilles, J. K. Hamilton, P. A. Rebers & Smith Fred. 1956. Colorimetric Method for Determination of Sugars and Related Substances. In Analytical Chemistry, 350-356..

R. W. Farndale, D. J. Buttle & A. J. Barrett,1986. Improved quantitation and discrimination of sulphated glycosaminoglycans by use of dimethylmethylene blue. Biochim Biophys Acta, 883**,** 173-7.

IUP 2,2000. Sampling. JSLTC, 84**,** 303.

IUP 6,2000. Measurement of tensile strength and percentage elongation. JSLTC, 84**,** 317.

IUP 36,2000. Measurement of softness. JSLTC, 84**,** 377.

Song Jian, Tao Wenyi & Chen Wuyong,2011. Kinetics of enzymatic unhairing by protease in leather industry. Journal of Cleaner Production, 19**,** 325-331.

S. Shakilanishi & C. Shanthi,2017. Specificity studies on proteases for dehairing in leather processing using decorin as model conjugated protein. International Journal of Biological Macromolecules, 103**,** 1069-1076.

O14

"GREEN" TECHNOLOGIES OF LEATHER AND FUR RAW MATERIALS PROCESSING ON BASIC OF THE BURYATS AND MONGOLS PEOPLES TRADITIONS

Dmitry Shalbuev

1Department "Leather and Fur Technology. Water Resources and Commodity Research" East-Siberia State University of Technology and Management, 670013, Russian Federation, Ulan-Ude, Kluchevskaya str., 40v, building 8, +79146311809, shalbuevd@mail.ru

The purpose of this work is to present ecological clean technology for leather and fur treatment, recycling of collagen-waste which allow reducing the anthropogenic influence on environment. It is a very important problem because more than 250 different chemicals are used today in modern technologies of leather and fur processing.

In 19th and 20th Centuries the Buryats used dairy products containing milk acid, lactic acid bacteria and enzymes for leather and fur processing. Traditional ways of processing were characterized by ecological compatibility, i.e. they had minimally harmful environmental impact. The Buryats not only used milk products but also pine and cedar cones, bark, manure and bergenia for leather and fur processing. Today we try to recover those lost technologies.

In order to develop a new technology, the following issues were studied: wastewater quality after leather and fur processing, traditional technologies of Buryat people, and the isolated microorganisms of effluents from the soaking and degreasing processes. The result of this research is an innovative, ethnic and green biotechnology that has application not only in leather and fur processing but also in the treatment of collagen-containing waste.

Keywords: green technologies, microorganisms, environmental protection, collagen, ferment milk composition

The availability of environmentally sound technologies is still the central aspect of the global transition to a resource-efficient "green" economy. In many cases, replacing obsolete technologies with modern sustainable alternatives can save money, improve human health and at the same time have a favorable impact on the state of the environment.

Modern or typical technologies used in the processing of sheepskin-fur and fur raw materials cause the formation of strongly acidic waste water after the process of pickling while the pH of sewage entering the reservoirs of the fishery should be between 6,5-8,5. It should also be noted that there is a high level of mineralization of effluents after pickling. In addition, the technologies currently used for the processing of fur raw materials and, in particular, sheepskins cause significant water consumption and, accordingly, water disposal.

Application of new methods of processing fur raw materials allows to reduce considerably the inflow of polluting substances into native water objects. Analyzing the current trends in improving the methods for conducting preparatory processing of sheepskin raw materials, several main areas can be identified: the development of new ways of introducing processing compounds into the skin tissue of collagen-containing raw materials; the development of new drugs, primarily synthetic surfactants (SS) and enzymes; designing new equipment. However, the use of the previously mentioned methods for the most part does not significantly reduce the level of toxic pollution of wastewater under the existing methods for its purification. The most promising methods, which allow initially to reduce the degree of contaminated waste water while maintaining the quality characteristics of the finished product are eco-biotechnological and / or drainless. The eco-biotechnological method consists in treating the raw material with a bacterial suspension and / or fermented milk compositions containing prokaryotic organisms and a complex of exoenzymes produced by these cultures under certain external parameters. The drainless method is based on the use of a unique composition that makes it possible to combine the processes of tanning and fattening the skin tissue of fur sheepskin with a significant minimization of the intake of trivalent chromium into sewage, the increase of the output of finished products by 5-10%, the decrease in consumption of chemical

materials 3-5 times and electricity as well, and also allows to regulate the degree of dilution of the sheepskin semi-finished product [1].

The purpose of this publication is to present the results of the development of a fundamentally new eco-biotechnological method for processing collagen-containing raw materials based on the use of waste products from the dairy industry, the products of vital activity of microorganisms and the method of spreading of chrome tanning and fattening.

The developed technology will optimally remove fatty substances from the surface of the hair and skin tissue, split the microstructure of the dermis into smaller structural elements and combine the processes of tanning and fattening which will significantly shorten their duration, the consumption of chemicals, reduce the level of negative impact and enable to get products that meet the requirements of GOST (State Standard) [2].

The eco-biotechnological method proposed for processing sheepskin raw materials has a number of advantages over the technologies that are currently applied at industrial enterprises. Carrying out soaking-degreasing with the help of a bac-suspension significantly minimizes the level of anthropogenic impact on the environment by eliminating formaldehyde, sodium carbonate from the working bath and significantly reducing the consumption of surfactants from 6,0-8,0 to 1,0-1,5 g/dm^3 while the closest methods do not reduce the level of toxic contamination or cause hair loss.

The use of dairy industry waste, in particular, fermented whey, pickling, will allow the collagen fibers to be split under milder conditions. Modern pickling technologies are based on the use of sodium chloride (40 g/dm^3), acetic acid and sulfuric acid (up to 3,0 and 1,5 g/dm^3, respectively) [3]. The disadvantage of this method using the already known composition is that acids impact on the hair of a fur semi-finished product, which leads to changes in hydrogen and salt bonds in keratin and weakens the hair structure.

The problem being solved in the proposed technology is to develop the method of pickling using fermented milk compositions while excluding sodium chloride and aggressive acids, in particular, sulfuric from the working composition.

The use of the original composition for the combined tanning-fatting process will allow to develop a drain less technology at this stage of processing sheepskin raw materials. The proposed composition has the ability to spontaneously penetrate into the structure of the dermis and evenly distribute through the skin tissue within a few minutes. The composition is absorbed by the skin tissue, binds with it and is practically not removed during subsequent treatments.

As a result of the development of the eco-biotechnological method of preparatory and pickling-tanning processes there has been achieved the following : the reduction in the consumption of chemical materials by 3-5 times; the possibility of regulating the degree of dilution of the sheepskin semi-finished product; the increase in the output of semi-finished products by 5-10%; the exclusion of sewage contamination with chromium salts and fats; the reduction of the consumption of synthetic surfactants from 8,0-6,0 to 0,5-1,0 g/dm^3; the exclusion of the use of formaldehyde, carbonate and sodium chloride in working baths; the decrease in the level of sewage pollution; the improvement of the quality of the skin tissue and the finished product hair; the possibility of carrying out certain stages of processing sheepskin raw materials at small enterprises without the use of special equipment.

Modern technological maps of the soaking I, II include the following chemical materials: sodium fluorosilicate, sodium sulfite and nonionic surfactant; and for the degreasing process such ones as formaldehyde, sodium carbonate and anionic surfactants. Conducting technological processes using the eco-biotechnological method allows to eliminate all these reagents completely reducing the consumption of surfactants to 0,5-1,0 g/dm^3 which is sufficient for emulsifying natural fat contained in hair and sheepskin tissue.

The influence of the consumption both of the detergent itself and the consistency of the bac-suspension on the degree of watering of the skin tissue, the destruction of the fatty substances contained in it and the hair covering of the fur sheep hair is of interest. In this connection, in the process of soaking and degreasing by the eco-biotechnological method two

variants of working baths were chosen: the first one was with a concentrated suspension in the presence of surfactants in the amount of 1,0 g/dm^3, the second one was with the bacterial suspension and tap water in a ratio of 1:1 and nonionic surfactant in the amount of 1,0 g/dm^3.

Technological processes were carried out using the bacterial suspension containing the culture *Bacillus licheniformis*. To carry out eco-biotechnological processing, samples of fur sheepskin after fresh-dry canning were used. They were selected by the method of symmetrical halves. One-half of the skins were treated with a concentrated solution of bacterial suspension (option 1), and the second one with the solution of a bac-suspension diluted with tap water in the ratio of 1:1 (option 2).

While soaking, the mass fraction of moisture was determined which for sheepskins after fresh-dry canning was 55%. This indicator was measured both at the end of soaking I and during the experimental soaking II after 1, 4, 16 and 24 hours of rehydration.

It was established that the degree of watering of the samples after the experimental soaking performed in two variants corresponded to the regulatory requirements. At the same time, sodium chloride which is traditionally used as an aggravating agent has not been added to the test formulations.

Degreasing the sheepskin hair is one of the main processes of its manufacture. It determines the shine and friability of the hair, the uniformity of the color. This process was carried out in two ways: the sheepskins were treated with a concentrated bacterial suspension (variant 1), the sheepskins were treated with a concentrated bacterial suspension and water ratio of 1:1 (variant 2).

The mass fraction of unbound fatty substances was determined before and after the degreasing process [4], the results are presented in Table 1.

Table 1 - Effect of the composition of the degreasing bath on the intensity of removal of fatty substances from the skin tissue and hair coat of fur sheepskin, %

Composition of working bath for experimental degreasing	Before degreasing		After degreasing	
	Skin tissue	Hair	Skin tissue	Hair
Bac-suspension (concentrated)	24,38	5,07	19,08	2,87
Bac-suspension - tap water (1: 1)	22,52	4,89	15,11	2,56

Analyzing the data obtained (Table 1), it can be stated that the dilution of the bac-suspension with tap water in the ratio of 1:1 allows to ensure optimal removal of fatty substances both from the surface of the hair and from the structure of the skin tissue of the fur sheepskin.

After eco-biotechnological degreasing washing, pressing and plating of fur sheepskin were carried out and then sheepskins were subjected to eco-biotechnological pickling with fermented milk compositions without adding sodium chloride into the pickling composition. Experimental treatment made by the spreading method was carried out using the fermented milk composition (FMC), since its microbiocenosis included not only mesophilic streptococci, thermophilic lactobacilli, lactose-fermenting yeast but also acetic acid bacteria, which make it possible to obtain FMC with high titrated acidity [5]. FMC was spread on the surface of the skin tissue of fur sheepskin with a brush with natural hair. Pickling by spreading is promising for the hair is not exposed to acids. The use of the fermented milk composition provided a "milder" effect of the pickle on the fur sheepskin. The composition expense was 10 cm^3/dm^2. After eco-biotechnological pickling, the samples of sheepskin were folded with skin tissue facing another skin tissue and left for 24 hours aging before covering

them with a polyethylene film. Hereafter the welding temperature was measured, being 44-45°C. Then the sheepskin samples were slicked on the fleshing machine with blunt knives.

The tanning-fattening process was carried out by the spreading method using the Baikal 11-10 emulsion prepared on the basis of Small Innovative Enterprise ECOM with a consumption of the emulsion 200 cm^3 per coat.

Before and after pickling and tanning, the welding temperature was determined [6], the results are shown in Table 2.

Table 2 - Change in the temperature of welding of leather fabric of fur sheepskin in eco-biotechnological pickling and tanning-fattening by spreading method, °C

Working bath composition for experimental degreasing	Pickling by spreading(FMC)		Tanning-greasing by spreading	
	Before	In 24 h	Before	In 24 h
Bac-suspension (concentrated)	63±1	45±1	45±1	81±1
Bac-suspension – tapwater (1:1)	60±1	44±1	44±1	87±1

The change in the thermodynamic characteristics of the skin tissue of the fur sheepskin in peeling and tanning-fattening by spreading method (Table 2) indicates that as a result of acid treatment (pickling) of the fur sheepskin the microstructure of the dermis is disintegrated at maximum with the destruction of some hydrogen and electrovalent collagen bonds the consequently reduces the welding temperature.

In tanning-fattening by spreading additional bonds were formed as a result of the interaction of chromium compounds with the functional groups of the protein, which ultimately led to an increase in the welding temperature of the investigated samples of fur sheep up to 81-87°C.

Further processing of the tanned semi-finished fur sheepskin was carried out according to the standard procedure. After fur sheepskin being treated, the semi-finished product was subjected to physical-mechanical testing and chemical analysis. The results are shown in Table 3.

Table 3 - Chemical and physical-mechanical characteristics of fur sheepskin fur skinned

Index	Treatment options		GOST (SS) STANDARD 4661-76
	1	2	
Welding temperature, °C, not lower than	87	96	70
Mass fraction of moisture,%, not more than	12,14	12,46	14
Mass fraction of ash,%, not more than	7,5	6,9	10
Mass fraction of chromium oxide,%	1,63	1,71	0,8-1,8
Mass fraction of unbound fatty substances,% in the skin tissue in the hair, not more than	 18,42 2,01	 18,76 2,13	 10-20 2,0
pH of aqueous extract	4,15	4,63	4,0-7,5
Tensile strength, H, not less than	138	140	120
Full lengthening at voltage of 9.8 MPa,%, not less than	28	36	30
Air permeability, $cm^3/cm^2 \times h$	10,5	10,7	-
Sheepskins size after pickling, dm^2 Sheepskins size after finishing, dm^2	215 225	184 190	-

Sheepskin yield, area,%	104,7	103,3	

According to the analysis of the effect of the eco-biotechnological method on the properties of sheared sheepskin the latter meets the requirements of GOST(State Standard) 4661-76 for physical, mechanical and chemical parameters. "Sheared sheepskin. Specifications »[2].

The increased temperature of welding in the samples of sheared sheepskins using the eco-biotechnological method is probably connected with better diffusion and an increase in the strength of the chromium bond with the functional groups of protein, a more even distribution of chromium over the layers of the skin. When treating sheepskins with FMC, the production cycle is reduced both due to the acceleration of tanning itself and by eliminating neutralization. The pH values of the aqueous extract in these cases correspond to the established standards and the chemical indices of the prototypes - to the requirements of GOST (State Standard) 4661-76.

Analyzing the output data of the fur sheepskin yield, all experimental compositions can be recommended. The use of spread pickling as well as tanning-fatting can increase the yield by 3-5%.

It is shown that the proposed eco-biotechnological method of sheepskin-degreasing makes it possible not only to obtain high-quality products but also to significantly reduce the level of negative impact on the environment by involving fatty substances in constructive and energy exchanges at the stage of their processing (Table 4).

Table 4 - Characteristics of waste water after degreasing

Quality indicators of waste water	Concentration of substances	
	Experimentalmethod	Standard method
Suspended solids concentration, mg/dm^3	4340	4750
Chemical consumption of oxygen, mgO_2/dm^3	954	1982
Biological consumption of oxygen, mgO_2/dm^3	155	244
pH	6,9	8,8
Synthetic surfactants concentration of, g/dm^3	0,36	4,8
Formaldehyde concentration , g/dm^3	0,0	0,45
Fatty substances concentration , mg/dm^3	95	2200

The analysis of the qualitative characteristics of wastewater generated after the standard and experimental procedures showed that the investigated parameters of the waste water after the experimental soaking-degreasing are a certain degree lower than the ones after the typical sheepskin method. Particular attention should be paid to the indicator "suspended matter". As can be seen from Table 4, the value of this indicator is almost the same and does not depend on the method of sheepskin treatment, which indicates that the amount of surfactants and bio-surfactants in working baths for soaking and degreasing with an eco-biotechnological method is sufficient and ensures optimal removal of the mineral impurity from the surface of the sheepskins hair.

The eco-biotechnological method of pickling based on the application of fermented milk compositions, wastes of the dairy industry was proposed while excluding sodium chloride and acids of various chemical nature from the pickling composition and carrying out pickling and tanning-fatigue using the method of spreading.

The introduction of the eco-biotechnological method will reduce the consumption of chemical substances 3-5 times and the consumption of surfactants from 8,0-6,0 to 0,5-1,0 g/dm^3, exclude the use of formaldehyde and sodium carbonate in working baths, improve the quality of the skin tissue and the hair of finished products. Tanning-fatting using the spreading method will make it possible to regulate the degree of dilution of the sheepskin-fur coat and fur semi-finished product, increase the output of the semi-finished product by 5-10%, exclude the contamination of sewage with chromium salts, fats, and thereby reduce the toxic pollution of sewage water.

Thus, based on the studies carried out, a fundamentally new method for the production of sheepskin and fur coat raw materials was developed. It is based on the application of both biotechnological methods and traditional methods of processing collagen-containing raw materials used by indigenous peoples living on the territory of the Republic of Buryatia.

REFERENCES

1. Shalbuev Dm.V., Sovetkin N.V., Radnaeva V.D. Ecologically clean and resource-saving ways of processing hides and fur raw materials // Collection of articles, IIId Intern. scientific-practical. conf. "Modern ecologically safe technologies for the production of leather and fur." Kiev: KNUTD, 2010. P.104-106.

2. GOST (SS) 4661-76. Sheepskin sheared. Technical conditions. M., 1976. 9 p. (System of standards for information, bibliography and publishing).

3. Grigoriev B.S, Vasilyeva A.I. Technology of wool skin processing , Moscow: Central Research Institute of Information and Technical and Economic Research of Light Industry, 1988. 200 p.

4. GOST (SS) 26129-84. Fur skins and sheepskins sheared. Method for determining the content of unbound fatty matter. Intr. 07/01/1985. Moscow: Publish.of standards, 1984. 6 p.

5. Shalbuev Dm.V. Eco-biotechnological way of pickling skin and fur coat raw materials / / Leather and footwear industry. 2009. № 1. P. 36-39.

6. GOST (SS) R 52959-2008. Fur skins and sheepskin sheared. Method for determining the welding temperature. M., 2008. 4 p. (System of standards for information, bibliography and publishing).

O15

Reduction of Water Consumption in the Processing of Rawhide and Sheepskin Coat Materials

Vera Radnaeva[1], Nicholai Sovetkin[2]

1 Department of Leather, Fur Technology. Water Recourses and Commodity Research, East Siberia University of Technology and Management, 670013 Kluchevskaya street, 40V, building 1, Ulan-Ude, Buryatia, Russia, tel: +7924584656, radnaevav@mail.ru

2 Department of Leather, Fur Technology. Water Recourses and Commodity Research, East Siberia University of Technology and Management, 670013, Kluchevskaya street, 40V, building 1, Ulan-Ude, Buryatia, Russia, tel: +79146306060, nsovetkin@mail.ru

Abstract

In recent years, water consumption in the world has grown substantially, which can lead to its shortage. Increasingly, scientists in describing problems related to water consumption use the term "strategic" resource in relation to water. One of the ways to solve the problem of water supply is to reduce the water intensity of production. A distinctive feature of tannery and fur production is large water consumption - for the processing of 1 ton of tanning raw material, 65 m^3 of water is needed. To return the used water to natural reservoirs, leather and fur producers spend a lot of money on cleaning it.

Processing of raw materials and sheepskin on innovative technologies was executed. The possibility of a significant reduction in water consumption and sewage using innovative technologies is shown. The analysis of water consumption on new technologies of leather processing for the top of footwear and fur coat is carried out. It is shown that introduction of new technologies will allow to reduce water consumption by 2 times per 1000 kg of tanning raw material and to exclude water consumption for tanning and fattening when making fur coat. The advantage of the technologies is not only in the reduction of water consumption, but also in the absence of waste solutions after the processes of tanning, dyeing, fattening in the production of leather, after tanning and fattening in the production of fur coats.

Key words: water consumption, wastewater disposal, leather, fur

Introduction

Water, along with energy and food has become one of the global problems of mankind. Water is used for different purposes, among which big industrial water consumption [1], in particular, for processing leather and fur.

Manufacturers spend a lot of effort to clean the used water to return it into natural bodies of water [2]. If we consider that the world's water reserves are approximately 13.5 million m^3, reserves fresh water of them is amount to 2,5%, it is easy to understand the seriousness of the environmental problems on tannery enterprises.

Liquid processes occupy 30-40% of the production cycle for the processing of leather and fur raw materials. The water consumption in each liquid process is from 70 to 400% by weight of the raw materials or semi-finished product. A particularly large amount of water is used in the fur processing, due to the presence of hair, which must be processed by repeated washing, degreasing, soaking. Water consumption for each process is amount to 1000-2500% by weight of the dryed skins.

The paper shows the possibility of a significant reduction of water consumption in the production processes in the leather and fur industries through the use of innovative technologies.

Materials and Methods

The main objects of the research were the raw materials of cattle (extreme light steers), wet-salted woolskin. Raw cattle was treated according to the method [3] including pickling. Woolskin was treated by the method [4] including pickling.

Pickled skins were treated on the new "Barguzin" technology [5]. A distinctive feature of the technology is the combined processes and low water consumption - 20 and 30% by weight of the semi-finished product. Finishing operations were processed with the help of the known technology. Quality of leather was assessed by following data (Table 1).

Table 1 – Methods for determining the properties of the finished leather

Data	State standard
Moisture content,%	938.1-67
Chromic oxide content,%, at least	938.3-77
Mass fraction of substances extractable by organic solvents, %	938.5-68
Tensile strength, 10 МПа, at least	ISO 3376-76
Elongation at a voltage 10 MPa,%	ISO 3376-76
Rigidity, Newton	RF Patent № 1395983 [2]
Leather cure temperature,^{0}C	ISO 3376-76

Pickling woolskins were covered by special consumption on the special device. Finishing operations were treated by the technology [4]. Quality of woolskins were evaluated by the indicators (Table 2).

Table 2 – Methods for determining the properties of the finished woolskin

Data	State standard
Moisture content,%	938.1 - 67
Chromic oxide content,%	53013 - 2008
Ash content,%	17631 - 72
Mass fraction of substances extractable by organic solvents, %	53018 - 2008
Rip load, N	52957 - 2008
Elongation at a voltage 10 MPa,%	52957 - 2008
pH water extract	53017 - 2008
Leather cure temperature,^{0}C	52959 - 2008
Color fastness to dry friction	53015 - 2008

The water consumption on the technological operations of the new technologies was determined. Water consumption on the pickling was determined by the weight from lime hide. Water consumption on tanning, fatliquoring, dyeing, filling, retanning were determined from the shaved weight . Water consumption for processing woolskins were determined by the weight of non-fat feedstock. Calculation of wastewater was performed according [6]:

$$WD = WC – WC \times \frac{P}{100} \quad (1)$$

WD – Volume of wastewater disposal, м^3;

WC – Volume of water consumption, м^3;

P– Lost production,%;

Production losses are on average 6-7% of total water consumption.

Results and Discussion

New leather processing uses the tan drum, water consumption is 20-30% by weight the pelts. The new technology processes are performed by a combined method of treatment in complex systems. Before doing the combined processes the

liquor left of the previous operation is drained. Then chemical compositions are added into drum during the rotating through a hollow axis of drum, which are fully absorbed by semi-finished product for 30-60 minutes. Thus, there is no waste water, and so there is need for their purification. Table 3 presents the data on water consumption and wastewater in the production of leather shoe uppers based on new technology in comparison with the known one.

Table 3 – Water consumption and water removal in production of upper leather on 1000 kg of hides

Process	Water consumption, m^3		Water removal, m^3	
	Variant			
	Experimental	Control	Experimental	Control
Pickling process, Pretanning	0,70	-	0,65	-
Pickling process	-	0,70	-	0,65
Tanning process	0,12	-	0,0	0,65
Retanning chrome salt	0,00	0,80	0,0	0,74
Washing	0,00	1,60	0,0	1,49
Neutralization	0,80	0,80	0,74	0,74
Washing	1,60	1,60	1,49	1,49
Dyeing	0,08	0,80	0,0	0,74
Fat-liquoring	0,00	0,48	0,0	0
Retanning organic tanning agents	0,00	0,80	0,0	0,74
Washing	1,60	1,60	1,50	0,74
Total:	4,90	9,18	4,60	7,98

As can be seen from Table 3, the water consumption can be reduced by a factor of 2 by using the new technology. Water removal reduced by 1.9 times, there are no dyes, chrome salt and retanning materials in waste water. Consequently, the degree of contamination of waste water tanneries could be reduced significantly. The quality of the finished leather meets the requirements of State Standard 938.3-88 (Table 4).

Table 4 – Comparative analysis

Data	State Standard 938.3-88	Variant	
		Experimental	Control
Moisture content,%	10-16	14,4	14,5
Chromic oxide content,%, at least	At least 4,3	5,3	5,6
Mass fraction of substances extractable by organic solvents, %	3,7-10,0	8,8	7,0
Tensile strength, 10 MPa, at least	At least 16	23	18
Elongation at a voltage 10 MPa,%	15-35	33,6	30,1
Rigidity, Newton	–	0,82	1,14

Yield of leather, %	–	110	100

The properties of finished leather treated with the new technology, not inferior to the control leather. The strength of leather is above 1,3 times, the area of yield of leather is larger on 10%. Woolskins were processed including the pickling. After pickling woolpskins were conducted processes: water removal, slicking and tanning – fatliquoring by using the device special design. Finishing processes and operations are conducted in accordance with [2]. Table 5 shows presents data on water consumption and wastewater for tanning – fatliquoring.

Table 5 – Water consumption and water removal on 1000 woolskins

Process	Water consumption, m^3		Water removal, m^3	
	Variant			
	Experimental	Control	Experimental	Control
Tanning – fatliquoring	0,00	22,05	0,00	21,00

Table 5 shows that the implementation of the process of tanning – fatliquoring on special device allows to eliminate water consumption completely for these operations, respectively, avoiding the formation of waste water.

Table 6 – Comparative analysis

Data	State Standard 1821-76	Variant	
		Experimental	Control
Moisture content,%	At most 14,0	11,8	12,3
Chromic oxide content,%, at least	1,5-3,5	2,9	2,0
Ash content,%	At most 9,0	3,8	4,1
Mass fraction of substances extractable by organicsolvents, %	At most 12,0	11,8	7,8
pH water extract	At least 4,0	6,0	7,8
Rip load, N	At least 250	570	440
Elongation at a voltage 10 MPa,%	At most 30	23	25
Leather cure temperature,^{0}C	At least 80	84	80
Raw material consumption by 1000 m^2 of finished woolskin, m^2	–	1106,7	1154,9
Color fastness to dry friction, point	At least 2	4	4

Table 6 shows that treatment with the new technology allows not only to reduce water consumption, but improve the properties of the finished product - increase in strength by 1.3 times, reduce the raw material consumption to 1.04-fold (4.2%). Quality parameters of finished woolskin meet the requirements of State Standard of Russia 1821-76.

Conclusion

In the research the comparative analysis of water use on new technologies for processing shoe uppers leather and woolskin was carried out. It is shown that the introduction of new technologies will reduce water consumption in 2 times on 1000 kg of raw materials and reduce water consumption for tanning and fatliquoring of woolskin. The advantage of the technology is not only in the reduction of water removal, but also in the lack of wastewater after tanning, dyeing, fatliquoring in the production of leather, after tanning and fatliquoring in the production of woolskins. The introduction of these technologies will reduce the costs on chemicals and improve the quality of the finished product.

Acknowledgements

We would like to express our gratitude to all who participated in the experimental part of our work.

References

1. Gulpenko K.V., Tsoy E.V. Classification of water resources for check and ordering payments. Problems of Modern Economics, N 2 (42), 2012, P. 473.

2.Radjamani S. Recent development on the cleaner production and environment protection in world leather sector. Proceeding of the IX International Scientific-Practical Conference "Leather and Fur in XXI Century: Technology, Quality, Environmental Management, Education", 2013, Ulan-Ude, Russia, PP. 301-311.

3.Balberova N.A. and others. Tanner Guide (Technology), Moscow, Legprombitizdat, 1986, 272 p.

4.Grigorjev B.S. Chemical and Fur Technology. Moscow, Ltd «Research Institute», 2005, PP. 57 – 59.

5. Radnaeva V. New Technology of Leather Processing "Barguzin", Book of Abstracts, 29-31 May, 2013, Istanbul, Turkey, P. 190.

6. Shalbuev D.V. Environmental Management in the Leather and Fur Enterprises. Ulan-Ude, ESSTU, 2004, 121 p.

O16

Microwave-Irradiated Tanning Reaction of Aluminum with Collagen

Yue Liu[1,2], Jinwei Zhang[1,2], Guirong Qiu[1], Li Zhang[1,2], Xiong Liu[1,2], Fangfei Liu[1,2], Wuyong Chen[1,2], Haibin Gu[1,2,*]

1Key Laboratory of Leather Chemistry and Engineering of Ministry of Education, Sichuan University, Chengdu 610065, China.

2National Engineering Laboratory for Clean Technology of Leather Manufacture, Sichuan University, Chengdu 610065, China.

**Corresponding author: Haibin Gu, E-mail address: guhaibinkong@126.com*

Abstract

Microwave irradiation is attracting considerable attention as a fast, uniform and energy-savingheating resource in the academic and commercial communities of leather industry. The present work was conducted to investigate the effect of microwave irradiation on the crosslinking process between aluminum sulfate and collagen, and the properties of the obtained crosslinked products. To achieve these goals, the collagen samples treated by aluminum sulfate under microwave irradiation were compared with the corresponding water bath ones, and the blank controls of collagen without heating treatment. The dynamic light scatter and very-positive differential scanning calorimetry (VP-DSC) were used to monitor these crosslinking reaction processes, and the obtained products were well characterized by circular dichroism, DSC, thermogravimetry, atomic force microscope and Flourier transformation infrared spectroscopy. Results show that both heating methods can accelerate the crosslinking reaction rate of aluminum with collagen and increase the crosslinking degrees, and the crosslinked products exhibited improved thermal stability, but no change was observed for the binding mode of aluminum with collagen. More importantly, microwave irradiation has more evident effects on these processes, and it is positive for the improvement of collagen crosslinking processes and product performances, which is caused probably by both thermal and non-thermal effect of microwave irradiation. This study will be potential in the theoretical guidance and practical reference for the application of microwave irradiation in the aluminum-based tanning and collagen modification.

Keywords: microwave irradiation, collagen, aluminum tanning, crosslinking, non-thermal effect

1. Introduction

The research and application of new technologies in leather industry, such as nano-technology, electronic information, ultrasonic wave, microwave, vacuum, high pressure and CO_2 supercritical technology, have attracted considerable attention because they could not only eliminate the pollution of leather industry, but also increase the productivity and realize the scientific management and operation of leather industry, which transform the traditional leather industry into automation and scientific modern industry[1]. Especially, Microwave is an electromagnetic wave with wavelength from 300 MHz to 300 GHz, it can inspire molecular rotational level transition, and cause dipole steering and interface polarization to heat material[2]. Microwave as a heat source can accelerate the speed of chemical reaction, reduce the reaction activation energy, and also can change the reaction kinetics[3,4]. Microwave heats substance from the inner through the energy generated by molecules friction, and indicates advantages of rapidity, uniformity and energy saving. Thus, it has been widely used in radar, communication, electronic countermeasure, and industrial and agricultural production fields[5].

In leather industry, microwave is widely researched as a kind of new heat sources with high efficiency and clean characteristic[6], and could be applied in sludge treatment[7-9], leather analysis[10-12], chemical modification[13-15], drying[16-18], dyeing and fatliquoring[19-22], tanning[23-30] and collagen extraction[31]. Microwave irradiation could accelerate leather-making technology, and improve the physical and mechanical properties of leather products, thence microwave has become a promising direction of leather-making technology. Microwave provides not only the thermal effect, but also some non-thermal effect, which would have positive effect on the performance of the leather.

Collagen is a natural material with good biological compatibility and well-characterized low antigenicity. It decomposes into well-tolerated physiological compounds. It could also be processed on an aqueous base and has enhanced cellular penetration and wound repair. For this reason, collagen has attracted attention for its use as a biomaterial in the medical fields including drug delivery and tissue engineering.[32–35] Collagen is also a major leather-making protein. More than 90% of the global production of leather is currently done by a chrome-tanning process.[36–38] The conventional methods employed for tanning lead to significant material loss and are of serious environmental concern. In some countries, restrictions concerning environmental toxicity and a demand for safe disposal of industrial wastes apply to the use of chrome-tanned leathers for certain purposes.[39]

Tanning is the most important process of tanning process in which the cross-linkage take place between tanning agent molecules and collagen, and thus leads to the remarkably improvement in the water-swelling resistance, chemical and microbial degradation resistance of collagen. Chrome tanning is the most important tanning method in the tanning industry because of its excellent tanning performance. However, with the increasing awareness of environmental protection, the negative impact of chrome tanning on the environment cannot be ignored [40], which makes people focus on other methods. Aluminum tanning is one of the most important inorganic tanning methods in leather industry. Aluminum tanned leather is soft, white and fine grain. The aluminum tanning process is conducted at a certain temperature, especially at the end of the aluminum tanning. Temperature rising could promote the hydrolysis and olation of aluminum complex. Thus, on the one hand, the aluminum complex can be better combined with the side-chain carboxyl group of collagen. On the other hand, cross-linkage can take place between collagen molecules by increasing the size of the aluminum complex.

For the protein cross-linking process that needs to be carried out at a certain temperature, the thermal effect of microwave irradiation can increase the temperature, and its non-thermal effect may affect the reaction rate, degree and product properties. Zhou et al.[41] reported that during the microwave treatment, each molecule in the protein membrane undergoes rapid frictional heat generation, which can cause a certain degree of cross-linking of amino, carboxyl, cross-linking molecules and other crosslinkable groups in the protein membrane, so that the network structure of the membrane can be changed. In addition, konjac glucomannan has a more stretched conformation in the protein after microwave. In the gel prepared by microwave heating, there is strong interaction between the polysaccharide side chain and the protein, and the gel strength and water retention capacity can be improved[42]. These studies indicate that microwave irradiation can promote the reaction process of proteins with other substances, and is beneficial to improve the performance of the final products. Therefore, the temperature of the aluminum tanning system is increased by the microwave heat source, and its thermal effect can be utilized to reduce the energy consumption. In addition, its non-thermal effect may accelerate the tanning rate, reduce the tanning time, improve production efficiency and increase the degree of tanning reaction, and also may change the binding ability of aluminum with collagen.

2. Experiments and methods

2.1. Materials

The acid soluble collagen used in this study was extracted from the fresh fresh adult bovine Achilles tendon in 0.5 M acetic acid with 2 w/w% pepsin to ensure the structural integrity of the collagen triple helix. The details can be found in previous work[43]. $Al_2(S0_4)_3 \cdot 18H_20$ were purchased from the Aladdin Reagent Company (Shanghai, China). All the other chemicals used were analytic grade, commercially purchased and used as received.

2.2. Sample preparation

$Al_2(S0_4)_3$ and collagen solutions were prepared with acetate buffer (12.4 mM sodium acetate, pH 4.0). Collagen solutions (0.5 mg ml^{-1}) were mixed with $Al_2(S0_4)_3$ (3g L^{-1}) and then heated at 30 ^oC for 30, 60 and 120 min, respectively, to prepare microwave samples I. The DLS and VP-DSC were used to characterize the effect of microwave irradiation on the crosslinking process between $Al_2(S0_4)_3$ and collagen. Collagen solutions (2.5 mg mL^{-1}) were mixed with $Al_2(S0_4)_3$ (3g L^{-1})

and then heated at 30 °C for 3 h to prepare microwave samples II. The 2.4. circular dichroism (CD), atomic force microscopy (AFM), FT-IR, DSC and TG were used to characterize the effect of microwave irradiation on the properties of the obtained crosslinked products. The water bath at the same temperature was used as a water bath control, and the unheated collagen-aluminum mixed solution was used as a blank control.

2.3. VP-DSC Measurements

Samples heated by microwave irradiation and water-bath were immediately measured on a VP-DSC microcalorimeter from Microcal Inc. (Northampton, MA) with a heating rate of 1.5 °C/min under the protection of nitrogen. The solvent acetic acid was used as the reference. The enthalpy change (ΔH) during the transition was calculated from the area under each peak. The experimental plot was obtained from averages of all the samples.

2.4. CD Measurements

Once the samples were treated by microwave irradiation or water bath heating to set temperatures, the CD spectra from 190 to 240 nm were recorded immediately on a JASCO J-810 CD spectropolarimeter (Tokyo, Japan), with an average of three scans at a speed of 20 nm/min for each sample. The molar ellipticity (Em) at 223 nm for nonirradiated collagen solution was obtained at a heating rate of 1 °C/min in the range 25-50 °C. The experimental plot was obtained from averages of samples with the solvent acetic acid as the reference.

2.5. Atomic force microscopy(AFM) observations

Mixture solutions **II** were dried at room temperature (25 °C or so) for 24 h. The microstructure of the dried samples was observed by atomic force microscopy (SHIMADZU SPM 9600, Japan) in dynamic mode at room temperature. Each sample was scanned with a scanning rate of 1 Hz.

2.6. Thermal analysis

TG analysis was performed with a TGA/DSC Mettler Toledo (Switzerland) under nitrogen flow (99.99%; 50 mL min^{-1}) at 40-800 °C with a heating rate of 10 °C min^{-1}. The samples (4-9 mg) were performed in a cylinder shape a-Al_2O_3 sample holder.

DSC measurements of the samples (1–3 mg) were performed in a sealed aluminum pan under nitrogen flow (99.99%; 50 mL min^{-1}), at 40–200 °C with a heating rate of 5 °C min^{-1} using a DSC 1/700 Mettler Toledo (Switzerland).

3. Results and discussion

3.1. The effect of microwave irradiation on the crosslinking process

3.1.1. DLS analysis

DLS was used to measure the change in particle size of the reaction solutions. As shown in Table 1, with the increase of the reaction time, the particle size of the reaction solutions containing collagen and aluminum sulfate gradually increased. Under the same conditions, the particle sizes of the microwave irradiation samples were larger than that of the water bath control. When the reaction reached 120 min, the particle size of the microwave irradiation sample is increased by 1993 nm, and the water bath control only is increased by 1336 nm. Under the pH condition of this experiment, most of the carboxyl group of collagen has been dissociated, and the carboxyl group (RCOO-) dissociated by collagen enters the inner boundary of aluminum complex, at the same time, aluminum forms a multinuclear aluminum complex by hydrolysis and olation, and leads to cross-linkage between different collagen molecules. The coordination effect is continuously enhanced with the extension of time, which increases the particle size of the micelle in the system[44]. Since the reaction of aluminum and collagen on microwave irradiation has an acceleration effect on the reaction rate, it has a promoting effect on the degree of reaction. Therefore, the particle size of the microwave test sample is always larger than that of the water bath control sample under the same reaction time.

Tab.1 Size change with time during the reaction

Time (min)	microwave irradiation (nm)	water bath heating (nm)
0	2752	2752
30	3109	2814
60	3696	3279
120	4745	4088

3.1.2. VP-DSC analysis

The VP-DSC results can reflect the thermal stability of the collagen solution. The curve is characterized by two endothermic peaks with pre-transformation T_{m1} and main denaturing transitions T_{m2}, corresponding to two transition temperatures of collagen, where T_{m2} is an indicator of the thermal stability of collagen. T_{m2} is the temperature at which collagen molecules change from a stretched fiber state to a random coil shape. A larger T_{m2} value indicates a higher thermodynamic stability[45]. The change of heat denaturation temperature T_{m2} after different heating treatments is shown in Table 2. Compared with the blank control sample, the T_{m2} of the microwave irradiation samples and the water bath control increased with the time, under the same conditions, the T_{m2} of the microwave irradiation samples was always larger than that of water bath control. From the initial stage of this reaction to 120 min, the T_{m2} is increased by 0.62 ^{o}C after microwave irradiation, and the water bath control is only increased by 0.40 ^{o}C.

Tab.2 The change of thermal denaturation temperature T_{m2} during the reaction

Time (min)	T_{m2}(^{o}C)	
	microwave irradiation	water bath heating
0	37.28	37.28
3	37.40	37.36
60	37.82	37.65
120	37.90	37.68

The results of VP-DSC indicated that the structural stability of collagen increased with the prolongation of reaction time, and the structure of microwave irradiation samples was more stable. During the reaction between aluminum sulfate and collagen, the collagen carboxyl group forms a coordination bond with aluminum ions, which forms a stable structure and improves the stability of the collagen triple helix structure. Therefore whether microwave irradiation or water bath heating, T_{m2} is rising. In the microwave irradiation samples, their values of T_{m2} are higher than those of the water bath control, indicating that the microwave irradiation can promote the complexation reaction of the aluminum complex and has a positive effect on the cross-linking reaction between collagen and aluminum.

3.2. The effect of microwave irradiation on the properties of the crosslinked products

3.2.1. Circular Dichroism analysis

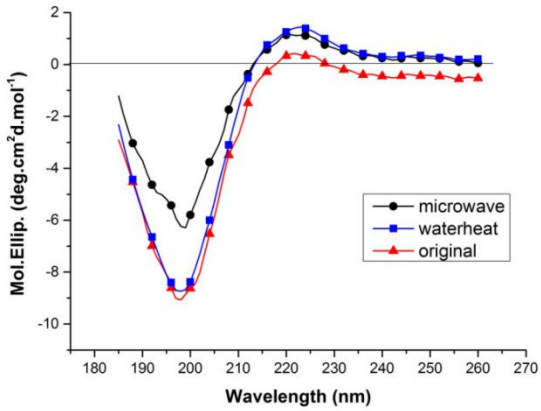

Fig.1 The CD images of collagen reacted with aluminum sulfate under different heating methods

Tab.3 The Rpn value of collagen reacted with aluminum sulfate under different heating methods

Samples	Negative peak intensity	Positive peak intensity	Rpn value
Blank control	9.1	0.5	0.055
Water bath heating	8.7	1.4	0.161
Microwave irradiation	6.3	1.1	0.175

Circular Dichroism (CD) is one of the simple and quick methods to obtain the conformation of biological macromolecules (α helix, β-sheet, β-turn, etc.). It is often used to detect the changes of collagen triple helix structure[46]. The Rpn value is the ratio of the positive peak intensity to the negative peak intensity and can be used to determine the conformation of the collagen solution. Generally, when the collagen is totally denatured or the triple helix structure is completely destroyed, the positive peak will completely disappear and the negative peak will be significantly red-shifted. For the partially denatured protein, the positive peak will be red-shifted, and the positive peak intensity and the Rpn value will decrease significantly[47]. Fig. 1 is the CD images of collagen reacted with aluminum sulfate under different heating methods. It is known from Fig.1 that the blank control has a negative peak absorption at 199 nm and a positive peak absorption at 222 nm. After microwave irradiation and water bath heating treatment, respectively, the positive peak did not disappear, and the negative peak did not red-shift, indicating that when the environmental temperature is lower than the collagen denaturation temperature, neither the microwave irradiation nor the water bath heating would denature the collagen.

The Rpn values of collagen treated by aluminum sulfate under different heating methods are shown in Table 3. Notably, both microwave irradiation and water bath heating can improve the Rpn values of collagen, and the Rpn value of the microwave sample under the same conditions was higher than that of the water bath control. Compared with the blank control, the Rpn value of the microwave irradiation sample is increased by 0.12, while the water bath control is increased by 0.106. After the cross-linking of collagen, the Rpn value will also be changed, and a higher Rpn value indicates a better cross-linking effect[48]. It can be seen from Table 3 that the Rpn value of the microwave irradiation sample is significantly larger than that of the water bath control sample, indicating that the microwave irradiation has more obvious promoting effects on the aluminum cross-linking with collagen.

In a word, the CD results indicate that the use of microwave irradiation during the reaction can promote the cross-linking process of aluminum with collagen and has no destroying effect on the triple helix structure of collagen.

3.2.2. FT-IR analysis

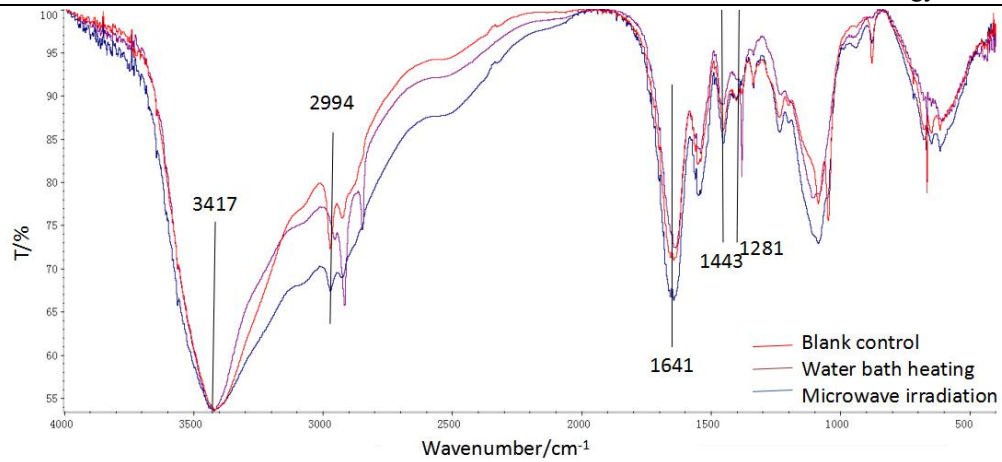

Fig.2 The FT-IR spectra of collagen reacted with aluminum sulfate under different heating methods

Infrared spectroscopy is an analytical method for determining the molecular structure of a substance and identifying compounds based on information such as relative vibrations and molecular rotations within the molecule. The absorption peak on the IR spectrum represents a specific vibration of a functional group. The FT-IR spectra of the protein can reflect the characteristic absorption peak position of the protein backbone, the side chain group and the vibration mode of the group, and thus the conformation of the protein could be inferred[49]. The IR spectra of collagen reacted with aluminum sulfate under different heating methods is shown in Fig. 2. The major feature of the IR spectra of collagen film is the band for the amide A at 3417 cm^{-1} for the N–H stretching vibration of the amide group in the protein. The weak absorption band at 2994 cm^{-1} is due to the amide B mode and can be assigned to the C–N stretching vibration of the collagen amide groups. Another feature of the IR spectra of collagen is the amide I band at 1641cm^{-1}, which arises from the C=O stretching vibration of the amide group in the protein. The strong absorption around 1550 cm^{-1} for the amide II mode is observed at 1443 cm^{-1} for a N–H stretching vibration strongly coupled to the C–N stretching vibration of collagen amide groups. Collagen has a high proportion of glycine and proline, which makes it unique compared with other proteins[39]. These two amino acids could be responsible for some of the spectral characteristics between 1200 and 1400 cm^{-1}. Signals in the spectra region of 1200–1400 cm^{-1} are generally attributed to the amide III for the C–N stretching and N–H in plane bending from amide linkages. The absorption at 1281 cm^{-1} can be attributed to amide III vibration.

It can be seen from Fig. 2 that compared with the blank control, the changes of the amide A band and the amide B band after microwave irradiation and water bath heating are more obvious, and the changes of the amide I, II and III bands are smaller. Among them, the amide A band was significantly broadened and the peak position has no change significantly, besides, the amide A band of the microwave irradiation sample was the widest. The amide I band also slightly shifts to the low wave number, wherein the microwave irradiation sample changes slightly in the water bath sample; the amide II band and III band show insignificant changes from the Fig. 2. As we know, when a functional group of collagen is combined with a metal complex, it will lead to charge transfer and the electron density between the bonding nuclei changes too, so that the bond force constant also changes and causes a phenomenon of frequency shift[50]. When the density of the electrons in the cores increases, the vibration frequency will increase; and if the electron density decreases, the vibration frequency will become smaller[50]. Therefore, the change of the amide A band indicates that the N-H bond is associated with the hydrogen bond and the hydrogen bond increases will result in a decrease in the bond constant of the N-H bond and a decrease in the stretching vibration frequency. Microwave irradiation samples of amide A bands move more toward low wavenumbers, indicating that microwave irradiation enhances the hydrogen bonding between collagen molecular chains. This is because microwave irradiation further promotes the process of aluminum cross-linking with collagen. The decrease in the frequency of the amide I band is probably due to the coordination of the oxygen atom on the C=O bond in the collagen with the central

metal ion Al^{3+}, which leads to a decrease in the electron cloud density of the C=O bond, and the telescopic vibration frequency is reduced. Under the same conditions, the frequency of the amide I band in the microwave irradiation sample decrease more, it indicates that the coordination of the carboxyl group of the collagen with aluminum is stronger, which lead to the decrease of the electron cloud density of the C=O bond. At the same time, due to the oxygen atom participating in the coordination, the cloud density of C-N electrons decreases, and the wave number of amide II and III decreases slightly. The decrease of microwave irradiation sample also indicate its stronger coordination effect.

3.2.3. Thermal analysis

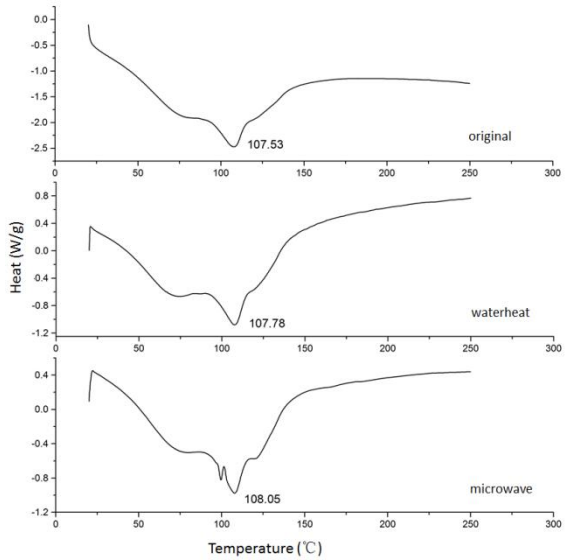

Fig.3 DSC curves of collagen reacted with aluminum sulfate under different heating methods

In order to study the effect of microwave irradiation on the thermal stability of collagen tanned by aluminum sulfate, the DSC curves of blank control samples, microwave irradiation samples and water bath control samples were determined in this experiment. As shown in Fig.3 that the thermal denaturation temperature of the blank control sample is 107.53 °C, the thermal denaturation temperature of the water bath heating sample is increased from to 107.78 °C, and the heat stable temperature is increased by 0.25 °C; the thermal denaturation temperature of the microwave irradiation sample is increased to 108.05 °C, an increase of 0.52 °C. The results of DSC show that both microwave irradiation and water bath heating can improve the thermal stability of collagen, and the former has more obvious effect, indicating that the thermal stability of collagen under microwave irradiation is higher. The temperature rise is beneficial to the cross-linking reaction between aluminum and collagen, so whether it is water bath heating or microwave irradiation, the thermal denaturation temperature of collagen is obviously improved. The thermal denaturation temperature of microwave experimental samples was higher than that of the water bath control, indicating that the microwave irradiation promotes more obviously the cross-linking reaction between aluminum and collagen.

Tab.4 The thermal decomposition temperature of collagen treated with aluminum sulfate using different heating methods

Samples	Thermal decomposition temperature (°C)		
	The first stage	The second stage	The third stage
Blank control	60.70	316.25	613.24
Water bath heating	61.52	318.12	597.75
Microwave irradiation	53.00	318.96	576.28

Tab.5 The weightlessness rate of collagen treated with aluminum sulfate by different heating methods

Samples	The first order	The second order	The third order	Carbon residue

	weightlessness rate	weightlessness rate	weightlessness rate	
Blank control	13.91%	58.94%	6.93%	20.22%
Water bath heating	11.36%	61.32%	6.38%	20.52%
Microwave irradiation	7.71%	50.86%	17.50%	23.93%

The change of mass loss of the product with temperature can be observed by thermogravimetric (TG) analysis, which could reflect the thermal stability of the reaction product, too. For collagen, there are mainly three thermal decomposition stages in the range of 50-700 °C. The first stage is below 100 °C, mainly the weight loss of water and other small molecular volatile substances. The second stage is the decomposition at 100-600 °C, mainly attributed to the fracture of the collagen peptide chain at high temperature and the weight loss of the carbonization process. The third stage is the decomposition after 600 °C, mainly corresponding to the continued weightlessness of a small amount of organic matter in the residual carbon.

When the cross-linking reaction between aluminum and collagen was promoted by microwave irradiation and water bath heating at about 300 °C, the corresponding temperature at the maximum weight loss rate was significantly increased. At the same time, microwave irradiation samples was 1.8 °C higher than that of the water bath control, indicating that the degree of crosslinking of aluminum and collagen was greater after microwave irradiation, and the thermal decomposition resistance of the product was better. As shown in Table 5, the weightlessness rate of the blank control, the water bath control and the microwave irradiation sample is decreased at first two stages, and the residual carbon amount is increased conversely. The weightlessness rate decreasing sequentially, especially at the second-order weight loss rate, is due to the increase of the degree of cross-linking between aluminum and collagen under different reaction conditions, the conformational stability of the product and the heat-resistant decomposition ability are enhanced. Since the amount of aluminum in the three samples is the same and aluminum is a non-volatile element, the difference in residual carbon ratio is due to the decomposition of organic matter in the product. The microwave sample has the largest residual carbon ratio, indicating that during the TG test, the organic matter has the least weight loss, that is, the heat resistance stability is the best. These experimental phenomena have shown that both water bath heating and microwave irradiation can promote the cross-linking reaction between aluminum and collagen, and improve the thermal decomposition resistance of the product. However, the effect of microwave irradiation on the process is more obvious.

3.2.4. AFM images

Fig. 4 shows the AFM images of samples including the blank control, water bath control and microwave irradiation, which could visually display the effect of different heating methods on the morphology of collagen molecules. For the blank control, collagen fibers are disordered and broken; for water bath control, collagen fibers is arranged in order and slender. While, in the case of microwave irradiation, the collagen fibers become thicker than water bath control, which indicates that more crosslinks are formed. Over all, these changes in morphology observed by AFM well are coincided that microwave irradiation can further promote the cross-linking reaction between aluminum and collagen, and improve the degree of crosslinked products.

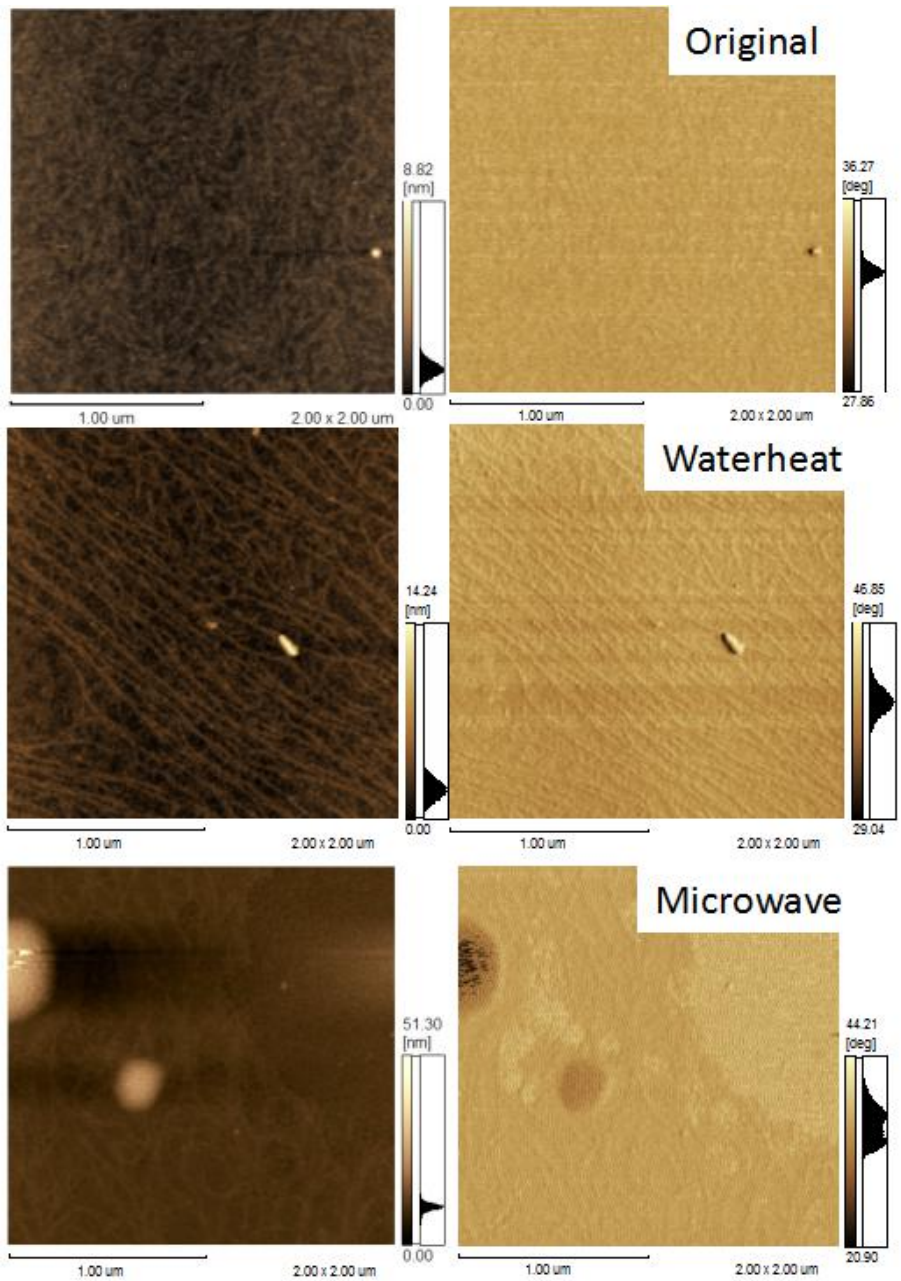

Fig.4 AFM images of collagen treated with aluminum sulfate using different heating methods

4. Conclusions

In the present work, the collagen samples treated by aluminum sulfate under microwave irradiation were compared with the corresponding water bath ones, and the blank controls of collagen without heating treatment to investigate the effect of microwave irradiation on the crosslinking process between aluminum sulfate and collagen, and the properties of the obtained crosslinked products. The results show that both microwave irradiation and water bath heating can promote the cross-linking reaction between collagen and aluminum without destroying the structure of collagen. However, under the same conditions, the microwave irradiation samples had a faster reaction rate during the crosslinking process, besides, the crosslinked products had higher thermal stability, which indicates microwave irradiation as better crosslinking effect. All of the above

results indicate that microwave irradiation can preferably promote the cross-linking process of aluminum sulfate and collagen and improve the properties of cross-linked products. The promoting effect may be the result of the combined effect of thermal and non-thermal effects of microwave irradiation.

Acknowledgement

Financial support from the National Natural Science Foundation (No. 21576171) is gratefully acknowledged.

References

[1] Ma J Z, Zhang Z J, Chu Y. High-tech in the future tannery industry[J]. Journal of Shanxi University of Science and Technology, 2004, 22(3): 50-55.

[2] Jin Q H, Dai S S, Huang K M. Microwave chemistry[M]. Beijing: Science Press, 1999. 1-38.

[3] Zhu Y J, Chen F. Microwave-assisted preparation of inorganic nanostructures in liquid phase[J]. Chemical Reviews, 2014, 114(12): 6462-6555.

[4] Gawande M B, Shelke S N, Zboril R. Microwave-assisted chemistry: synthetic applications for rapid assembly of nanomaterials and organics[J]. Accounts of Chemical Research, 2014, 47(4): 1338-1348.

[5] Leonelli C, Mason T J. Microwave and ultrasonic processing: now a realistic option for industry [J]. Chemical Engineering and Processing, 2010, 49(9): 885-900.

[6] Zhang J W, Wu J C, Chen W Y. Applications of microwave in leather field: further research for leather chemists and technologists [J]. Journal of the American Leather Chemists Association, 2017, 112 (9): 311-318.

[7] Liu Z Y, Huo Y J, Cheng G. Research progress of microwave treatment of excess sludge[J]. Guangdong Chemical Industry, 2017, 44(13): 167-168.

[8] Luo H J, Fu C L, Ning X A. Influence of microwave pretreatment on tannery sludge flocculating and dewatering performances[J]. Chinese Journal of Environmental Engineering, 2013, 7(5): 1933-1938.

[9] Puchana-Rosero M J, Adebayo M A, Lima E C. Microwave-assisted activated carbon obtained from the sludge of tannery-treatment effluent plant for removal of leather dyes[J]. Colloids and Surfaces A: Physicochemical and Engineering Aspects, 2016, 504: 105-115.

[10] Wang C Y, Zhang Q F, Lin J F. Simultaneous determination of the residual contents of 15 glycol ethers in leather and leather products by gas chromatography/tandem mass spectrometry coupled with microwave-assisted extaction[J]. Leather and Chemicals, 2014(6):11-17.

[11] Bo L F, Tian Y G, Lan Y J. Study on contents and distributions of tanning metal elements inleather by digestion-ICP-AES[J]. Chinese Journal of Spectroscopy Laboratory, 2010, 27(1): 173-176.

[12] Scheffler G L, Pozebon D. Trace element determination in leather samples using on-line internal standardization, ultrasonic nebulization and axial view-ICP OES [J]. Analytical Methods, 2015, 7(12): 5180-5185.

[13] Wang J G, Yang Z S, Zhao Z Q. Study on microwave-induced the modification of volanea tannin[J]. China Leather, 2006, 35(17): 30-33.

[14] Lai S L, Li Q J, Du J W. Preparation of anion organic silicon leather smoothing agent under microwave radialization[J]. China Leather, 2010, 39(7): 38-40.

[15] Hu Z Y, Yi S H, Hu W. Synthesis and urea-loading of a novel biosuperabsorbent polymer based on leather waste [J]. Journal of the Society of Leather Technologist and Chemists, 2015, 99(2): 51-57.

[16] Zhang, J W, Zhang, C L, Wu, J C, et al. The influence of microwave non-thermal effect on leather properties in drying [J]. Journal of the American Leather Chemists Association, 2017, 112(4): 135-139.

[17] Zhang J W, Zhang C L, Chen W Y. Influence of microwave drying on leather finishing film forming agent[J]. Leather Science and Engineering, 2016, 26(3):5-8.

[18] Pedreno-Molina J L, Monzo-Cabrerea J, Toledo-Moreo A, et al. Estimation of microwave-assisted drying parameters

using adaptive optimization inverse techniques [J]. International Communications in Heat and Mass Transfer, 2005, 32(3-4): 323-331.

[19] Gong Y, Cheng K, Zhang T. Automated clear leather dyeing assisted by wringing, ultrasound and microwave[J]. Journal- American Leather Chemists Association, 2011, 106(4):127-132.

[20] Xue Z. Study of dyeing properties of wool fabrics treated with microwave [J]. Journal of the textile institute, 2016, 107(2): 258-263.

[21] Gong Y, Zhang T, Chen W. Behavior of Fatliquored Leathers in a Microwave Field[J]. Journal of the American Leather Chemists Association, 2012, 107(2): 60-67.

[22] Abou El-Kheir A, Haggag K, Mowafi S I. Microwave-assisted bleaching of wool fabrics [J]. Journal of Natural Fibers, 2015, 12(2): 97-107.

[23] Wu J C, Liao W, Zhang J W. Thermal behavior of collagen crosslinked with tannic acid under microwave heating[J]. Journal of Thermal Analysis & Calorimetry, 2018(4):1-7.

[24] Cao N, Zhang J W, Chen W Y. Behaviors of chromium nitrate hydrolysis and olation under microwave irradiation[J]. Leather Science and Engineering, 2016, 26(4): 5-9.

[25] Zhang J W, Cao N, Zhou N, et al. Hydrolysis and olation of chromium sulphate under microwave irradiation [J]. Journal of the Society of Leather technologists and Chemists, 2017, 101(1):1-5.

[26] Chen J, Zhang J W, Zhou N. Influence of microwave irradiation on the stability of chromium(Ⅲ) complexes[J]. Leather Science and Engineering, 2017, 27(4): 5-9.

[27] Wu J C, Fan Z W, Zhang J W, et al. Impact of microwave irradiation on vegetable tanning [J]. Journal of Society of Leather Technologists and Chemists, 2018, 120 (1): 7-11.

[28] Wu J C, Zhang L, Zhang J W, et al. Electrochemical behavior of tannin solutions under microwave irradiation [J]. Leather & Footwear Journal, 2017, 17(2): 91-96.

[29] Fang Y T, Zhang J W, Ning G Q. Effects of microwave irradiation on hydrolysis of zirconium sulfate and thermal stability of zirconium tanned powder[J]. Leather Science and Engineering, 2017, 27(3): 12-16.

[30] Ruijgrok J M, De Wijn J R, Boon M E. A model to determine microwave‐stimulated cross‐linking of collagen using diluted glutaraldehyde solutions[J]. Scanning, 1993, 15(2):110-114.

[31] Zeng C H, Ma Y, Qi L. Preparation of wool keratin and application as formaldehyde scavenger for leather products [J]. Journal of the Society of Leather Technologist and Chemists, 2017, 101(4): 202-207.

[32] Friess W. Collagen-biomaterial for drug delivery[J]. European Journal of Pharmaceutics & Biopharmaceutics Official Journal of Arbeitsgemeinschaft Für Pharmazeutische Verfahrenstechnik E V, 1998, 45(2):113.

[33] Willoughby C E, Batterbury M, Kaye S B. Collagen corneal shields[J]. Indian Journal of Ophthalmology, 2002, 47(2):174-182.

[34] Sano A, Hojo T, Maeda M. Protein release from collagen matrices.[J]. Advanced Drug Delivery Reviews, 1998, 31(3):247.

[35] Shanmugasundaram N, Ravichandran P, Reddy P N. Collagen-chitosan polymeric scaffolds for the in vitro culture of human epidermoid carcinoma cells[J]. Biomaterials, 2001, 22(14):1943-1951.

[36] Wu B, Mu C, Zhang G. Effects of Cr^{3+} on the structure of collagen fiber[J]. Langmuir the Acs Journal of Surfaces & Colloids, 2009, 25(19):11905-10.

[37] He L, Mu C, Shi J, et al. Modification of collagen with a natural cross-linker, procyanidin.[J]. International Journal of Biological Macromolecules, 2011, 48(2):354-359.

[38] Gustavson K H. chemistry and reactivity of collagen[J]. Journal of Chemical Education, 1956, 33(3-4):270-270.

[39] Li H, Chen H L, Luo R. The interaction between collagen and an aluminum tanning agent[J]. Macromolecular

Bioscience, 2003, 3(7):344–346.

[40] Dasgupta S. Chrome free tannages. Part 1: preliminary studies[J]. Journal of the Society of Leather Technologists & Chemists, 2002, 86(5):188-194.

[41] Zhou H F, Zhang Z Y, Ou S Y. Preparation of an edible film composed of soy protein isolation and microwave processing effect on property[J]. Packaging Engineering, 2006, 27(2):28-30.

[42] Ji L, Xue Y, Zhang T, et al. The effects of microwave processing on the structure and various quality parameters of Alaska pollock surimi protein-polysaccharide gels[J]. Food Hydrocolloids, 2017, 63:77-84.

[43] Li D F, Mu C D, Zhang Q, et al. Effects of microwave irradiation on collagen denaturation.[J]. Journal of Food Biochemistry, 2010, 34(6):1319-1331.

[44] Ding K Y, Liu J, Zhang T Y. Study on the reactivity of organic acid masked aluminum(Ⅲ) complexes with collagen[J]. China Leather, 2002, 31(23):10-13.

[45] Ding C, Zhang M, Wu K, et al. The response of collagen molecules in acid solution to temperature[J]. Polymer, 2014, 55(22): 5751-5759.

[46] Chen X C, Liang H, He X W. Recent trends and spectroscopic methods for analysis of the protein conformation with circular dichroism[J]. Chinese Journal of Analytical Chemistry, 2004, 32(3):388-394.

[47] Usha R, Ramasami T. Structure and conformation of intramolecularly cross-linked collagen[J].Colloids Surf B Biointerfaces, 2005,41:21–24.

[48] Madhan B, Subramanian V, Rao J R, et al. Stabilization of collagen using plant polyphenol: role of catechin[J]. International Journal of Biological Macromolecules, 2005, 37(1–2):47-53.

[49] Zhu X X, An R, Li C P. Study on structures of collagen and gelatin: methods, results and analysis[J]. Leather Science and Engineering, 2012(5):9-14.

[50] Jin D M, Zhu W X. Coordination chemistry research method[M]. Beijing: Science Press, 1996.

O17

Synthesis of rice husk modified graphene oxide for Cr (VI) removal in leather wastewater

Jidan Tang[a], Tong Ouyang[a], Chang-tang Chang[b,*]

[a] *Key Laboratory of the Ministry of Education for Coastal and Wetland Ecosystems, College of the Environment & Ecology, Xiamen University, Xiamen 361102, China*

[b] *Department of Environmental Engineering, National I-Lan University, I-Lan City, Taiwan,*

**Corresponding authors: ctchang@niu.edu.tw, No.1, Sec.1, Shen-Lung Road, I-Lan City, 26015,Taiwan. (C.T. Chang)*

Abstract

This study mainly aims to remove Cr(VI) from an aqueous solution by using a novel graphene oxide-coated rice husk biochar composite(GO-RHB). GO-RHB is a synthetic material that has a porous structure with a high surface area and oxygen-containing functional groups that provide effective adsorption sites. $HCrO_4^-$ is the predominant form of Cr(VI) in aqueous solutions at low pH. The adsorption capacity of GO-RHB under acidic conditions is better than that under alkaline conditions. The maximum adsorption capacity (46.7 mg g^{-1}) of GO-RHB is obtained at pH 2.With a unique structure, low cost, and simple adsorption, GO-RHB is a promising material for the removal of Cr(VI) from wastewater.

Key words: chromium; graphene oxide; adsorption; carbon materials; composite materials

1. Introduction

In recent years, the pollution of heavy metals in wastewater has received great attention. High concentrations of heavy metals in wastewater can cause great harm to the environment and human health [1]. Hexavalent chromium is one of the most hazardous heavy metals in wastewater because of its high toxicity and mobility [2]. Chromium ions exist in the environment as Cr(VI) and Cr(III). Compared with Cr(III), Cr(VI) is 100 times greater than Cr(III) in toxicity[3]. Cr(VI) has been widely used in many industrial manufacturing, such as wood preservation, metal polishing leather tanning, electroplating[4, 5]. The concentration of Cr(VI) in wastewater produced by industries ranges from 0.1 to 200 mgL^{-1}[6]. Therefore, finding an effective and economical method to remove Cr(VI) from wastewater is of great significance. Until now, conventional Cr(VI) removal methods, including electro-chemical precipitation[7], biological process[8], reverse osmosis[9], ion exchange[10] and adsorption[11],have been developed. Among these methods, adsorption is one of the most widely used methods because of its cost-effectiveness and simple operation [12].

Biochar has become an important adsorbent for Cr(VI) removal in aqueous solutions because of its unique surface physicochemical properties and pore structure[13]. Rice husk(RH), an agricultural waste, will cause the waste of resources and environmental pollution if it is directly discarded or incinerated. Naiya et al[14] have studied the removal of Pb (II) using rice husk ash as an adsorbent. Graphene oxide(GO) is a new functional material, with many oxygen-containing functional groups, such as hydroxyl, carbonyl, carboxyl groups, etc., on the surfaces that can adsorb heavy metals[15]. Therefore, in this study, a new adsorbent composite was synthesized by taking advantage of structural features of graphene oxide and rice husk biochar to removal Cr(VI) in aqueous solutions.

2. Experimental

2.1 Materials

All chemicals used in this work were of analytical grade, including HCl(hydrochloric acid), NaOH(sodium hydroxide), H_2SO_4(concentrated sulfuric acid), $KMnO_4$(potassium permanganate), $NaNO_3$(sodium nitrate), H_2O_2(hydrogen peroxide), K_2CrO_7(potassium dichromate). Synthetic graphite powder was purchased from company. Rice husk was collected from a farm of Taiwan. The materials were dried at 110 °C for 24h prior to using.

A stock solution of 1000 mg L^{-1}Cr(VI) was prepared with dissolving 2.829 g of K_2CrO_7 in ultrapure water. The required concentration of Cr(VI) for experiments was obtained by diluting the stock solution with ultrapure water.

2.2 Preparation of graphene oxide

GO was synthesized by the modified Hummer's method. Briefly, 46 mL H_2SO_4 was mixed with 1 g $NaNO_3$ in a conical flask in an ice-bath that the temperature was maintained below 15 °C. After that, 2 g graphite powder was added into the mixture under stirring. 8 g of $KMnO_4$ was added into the mixture slowly and stirred evenly. The low temperature process lasted 2-3 h. Then, the mixture solution was placed into a constant temperature water bath at temperature of 35 °C for 2 h. Ultrapure water was added into the mixture.Then, the temperature increased to about 95 °C and the mixture turned tawny. The mixture was stirred for 20 min and then 30% H_2O_2 was added to the mixture until no bubbles emerge, and the color of the mixture turned to bright yellow. Finally the products were washed with HCl(10%) and ultrapure water for three times. The obtained materials were dried in a vacuum oven at 60 °C.

2.3 Preparation of graphene oxide coated rice husk biochar composite (GO-RHB)

GO-RHB composites were prepared by solid dispersion method [1].Firstly, 10 g rice husk biomass was mixed with 0.5 g graphene oxide and stirred for 2 h using a magnetic stirrer at 450 rpm to promote mix well. After that, the GO-RHB mixed materials were sonicated for 3 h, which can make GO suspension fully adsorbed to the RHB surface. Then, the mixed suspension was transferred to an oven and dried at 100 °C for 12 h. Finally, the obtained materials were placed in tube furnace under N_2 at temperature of 300 °C for 2h. The RHB was prepared with the same method described above.

2.4 Characterization

The surface morphology of GO-RHB was carried out with using a scanning electron microscope(SEM, Hitachi S-4800).The functional groups of GO-RHB were measured by a fourier transform infrared spectroscopy(FTIR, Nicolet iS 10).The surface states of the GO-RHB were characterized byX-ray photoelectron spectroscopy (XPS, Thermo Sigma Probe).

2.5 Adsorption experiments

A stock solution of 1000 mg L^{-1}Cr(VI) was prepared with dissolving 2.829 g of K_2CrO_7 in ultrapure water. The required concentration of Cr(VI) for experiments was obtained by diluting the stock solution with ultrapure water. Batch adsorption experiments of Cr(VI) were conducted using 80 mL serum bottles that contained GO-RHB with dosage ranged from 1.0 to 16 g L^{-1}. 50 mL of a Cr(VI) solution in an appropriate concentration was placed in a water bath shaker with a shaking speed of 150 rpm. For all adsorption tests, the initial pH values of the Cr(VI) solutions were adjusted with 0.1 M HCl and 0.1 M NaOH solutions, and the pH values were measured by a pH meter. After the adsorption processes, the mixture was filtered and the residual Cr(VI) concentrations were analyzed using the 1,5-diphenylcarbazide method by the double beam UV-visible spectrophotometer((Hitachi, U-3900)) at a wavelength of 540 nm.

The influence of initial pH on the adsorption of Cr(VI) was studied with an initial Cr(VI) concentration of 160 mg L^{-1} in a pH range of 2 to 9(2, 3, 4, 5, 6, 7, 8 and 9) at 25 °C. The zeta potentials of GO-RHB were measured in aqueous at pH 1 to 10 by a nano particle analyzer(Horiba SZ-100). For the kinetic study, the different initial Cr(VI) concentration of 80, 160, 240, 320 and 400 mg L^{-1} were measured at different time intervals from 10 to 240 min(10, 20, 30, 40, 50, 60, 90, 120, 180, 240 min). To investigate the maximum adsorption capacity and thermodynamic properties, adsorption isotherms of different initial Cr(VI) concentration of 80, 160, 240, 320 and 400 mg L^{-1} on GO-RHB were performed at pH 2 at 15, 25, 35 and 45 °C, respectively. Furthermore, RHB as adsorbent was also studied to better highlight the superiority of GO-RHB adsorption performance. The adsorption capacity, named as q_e(mg g^{-1}), and removal efficiency of Cr(VI) at equilibrium was calculated by the following equation (1) and (2) :

$$q_e = \frac{(C_0 - C_e)v}{w} \qquad (1)$$

$$\text{Removal efficiency} = \frac{C_0 - C_e}{C_0} \times 100\% \qquad (2)$$

Where,v (L) is the volume of solution;w (g) is the amount of adsorbent dosage;C_0 and C_e (mg L^{-1}) are the initial and equilibrium concentrations of Cr(VI), respectively.

3. Results and discussion

3.1 Characterization of GO-RHB

As shown in Fig.1(a, b), RHB presents round-hole structure with the flat surface and large thickness. GO-RHB displays sheet-like structure with uneven, irregular surface and wrinkled edges, which can provide more effective adsorption sites with higher surface area. As shown in Fig.1(c), the composite becomes much more smooth and well-knit, and the EDS shows that Cr(VI) ions are adsorbed on the surface of GO-RHB after the adsorption, named as GO-RHB-Cr, as shown in Fig.1(d).

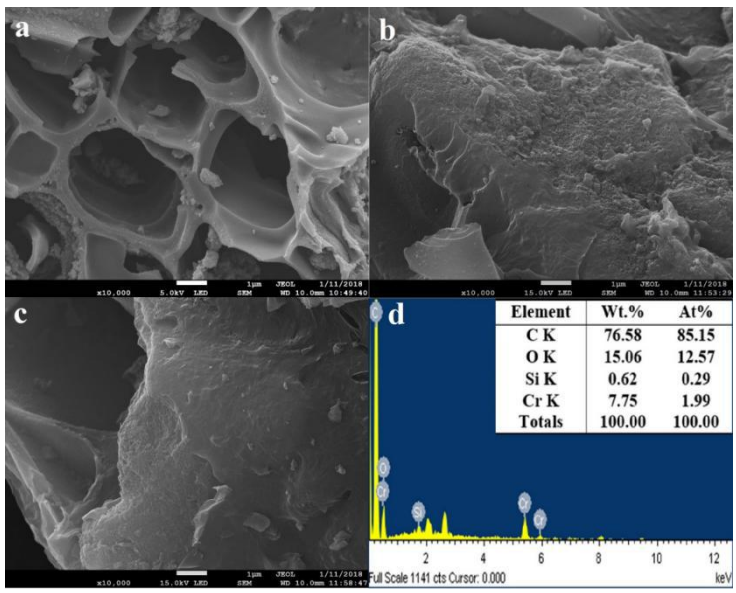

Fig.1 SEM images of (a) RHB, (b) GO-RHB, (c) GO-RHB-Cr after adsorption (d) EDS of GO-RHB-Crafter adsorption

3.2 Effect of initial pH and dosage on Cr(VI) removal

As shown in Fig. 2, the adsorption capacity of Cr(VI) decreases sharply with increasing pH values from 2 to 9. Thus, it is suitable for the Cr(VI) removal under acidic condition with GO-RHB.The hexavalent chromium exists in different forms, such as H_2CrO_4, $HCrO_4^-$, CrO_4^{2-} and $Cr_2O_7^{2-}$, in aqueous solution at various pH values[7]. The reactions of Cr(VI) in aqueous solution areshown in Equations (3), (4) and (5).

$$H_2CrO_4 \rightarrow H^+ + HCrO_4^- \qquad (3)$$

$$HCrO_4^- \rightarrow H^+ + CrO_4^{2-} \qquad (4)$$

$$2HCrO_4^- \rightarrow Cr_2O_7^{2-} + H_2O \qquad (5)$$

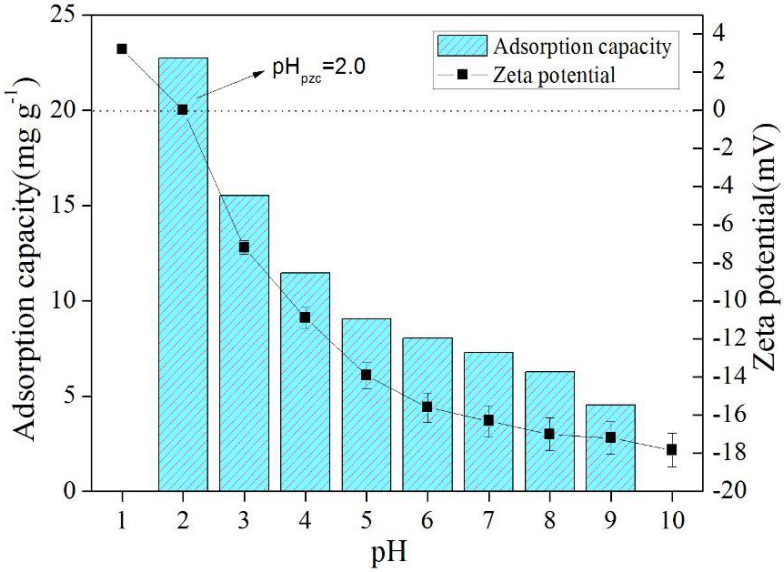

Fig.2 Effect of pH on Cr(VI) removal by GO-RHB and zeta potential of GO-RHB at different pH.

3.3 Effect of adsorbent dosage on Cr(VI) removal

As shown in Fig. 3, the removal efficiencyof Cr(VI) increases with the increase of dosage while the adsorption capacity of Cr(VI) decreases. The removal efficiency of Cr(VI) increases from 29.1% to 99% when the dosage of GO-RHB increases from 1 to 16 g L^{-1}.However, the adsorption capacity of Cr(VI) decreases from 46.7 mg g^{-1} to 10.0 mg g^{-1}. In addition, the removal efficiency would not increase significantly when the dosage of GO-RHB is above 8 g L^{-1}. When compared to the RHB, GO-RHB shows much higher removal efficiency, and the adsorption capacity of Cr(VI) is more than four times that of RHB at absorbent dosage of 8 g L^{-1}, optimal adsorbent dosage.

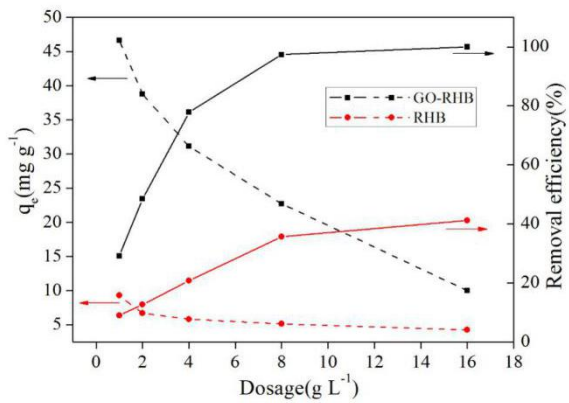

Fig. 3 Effect of adsorbent dosage on the adsorption of Cr(VI) by RHB and GO-RHB.(pH: 2.0; adsorbent dosage: 8 gL^{-1}; temperature: 25°C)

4. Conclusion

In this work, a new low-cost adsorbent was successfully synthesized and applied to remove Cr(VI) from aqueous solutions. The results show that GO-RHB has a porous structure with a high surface area and oxygen-containing functional groups on its surface. The adsorption capacity of GO-RHB is significantly affected by pH, and the maximum Cr(VI) adsorption capacityof 48.78 mg $g^{-1}$is obtained at pH 2. In addition, the removal mechanism of Cr(VI) presumably involves four steps, including core adsorption of GO-RHB, binding of Cr(VI) to GO-RHB via electrostatic interactions between

negatively charged Cr(VI), reduction of Cr(VI) to Cr(III) with the assistance of electrons on GO-RHB and complexation of oxygen-containing functional groups.

Acknowledgments

The authors would like to thank the National Natural Science Foundation of China (21077086) and the Ministry of Science and Technology of Taiwan for providing financial support for project MOST 106-2622-E-197-003 -CC3.

Reference

[1] Alemayehu E. Adsorption behaviour of Cr(VI) onto macro and micro-vesicular volcanic rocks from water[J]. Separation & Purification Technology, 2011, 78(1):55-61.

[2] Zhu J, Wei S, Gu H, et al. One-pot synthesis of magnetic graphene nanocomposites decorated withcore@double-shell nanoparticles for fast chromium removal[J]. Environmental Science & Technology, 2012, 46(2):977-985.

[3] Shang M, Liu Y, Liu S, et al. A novel graphene oxide coated biochar composite: synthesis, characterization and application for Cr(VI) removal[J]. Rsc Advances, 2016, 6(88).

[4] Ma Y, Liu W J, Zhang N, et al. Polyethylenimine modified biochar adsorbent for hexavalent chromium removal from the aqueous solution[J]. Bioresource Technology, 2014, 169(5):403-408.

[5] Dong X, Ma L Q, Li Y. Characteristics and mechanisms of hexavalent chromium removal by biochar from sugar beet tailing[J]. Journal of Hazardous Materials, 2011, 190(1–3):909-915.

[6] Owlad M, Aroua M K, Ashri W D W, et al. Removal of hexavalent chromium-contaminated water and wastewater: a review.[J]. Water Air & Soil Pollution, 2009, 200(1-4):59-77.

[7] Kongsricharoern N, Polprasert C. Chromium removal by a bipolar electro-chemical precipitation process[J]. Water Science & Technology, 1996, 34(9):109-116.

[8] Park D, Yun Y S, Jo J H, et al. Mechanism of hexavalent chromium removal by dead fungal biomass of Aspergillus niger[J]. Water Research, 2005, 39(4):533-40.

[9] Hafez A, El-Mariharawy S. Design and performance of the two-stage/two-pass RO membrane system for chromium removal from tannery wastewater. Part 3[J]. Desalination, 2004, 165(1-3):141-151.

[10] Rengaraj S, Joo C K, Kim Y, et al. Kinetics of removal of chromium from water and electronic process wastewater by ion exchange resins: 1200H, 1500H and IRN97H.[J]. Journal of Hazardous Materials, 2003, 102(2–3):257-275.

[11] Wu Y, Luo H, Wang H, et al. Adsorption of hexavalent chromium from aqueous solutions by graphene modified with cetyltrimethylammonium bromide[J]. J Colloid Interface Sci, 2013, 394(1):183-191.

[12] Monser L, Adhoum N. Modified activated carbon for the removal of copper, zinc, chromium and cyanide from wastewater[J]. Separation & Purification Technology, 2002, 26(2–3):137-146.

[13] Ding D, Ma X, Shi W, et al. Insights into mechanisms of hexavalent chromium removal from aqueous solution by using rice husk pretreated using hydrothermal carbonization technology[J]. Rsc Advances, 2016, 6(78).

[14] Naiya T K, Bhattacharya A K, Mandal S, et al. The sorption of lead(II) ions on rice husk ash.[J]. Journal of Hazardous Materials, 2009, 163(2-3):1254.

[15] Wang H, Yuan X, Wu Y, et al. Graphene-based materials: Fabrication, characterization and application for the decontamination of wastewater and wastegas and hydrogen storage/generation[J]. Advances in Colloid & Interface Science, 2013, s 195–196(7):19-40.

[16]Duan S, Ma W, Pan Y, et al. Synthesis of magnetic biochar from iron sludge for the enhancement of Cr (VI) removal from solution[J]. Journal of the Taiwan Institute of Chemical Engineers, 2017.

[17] Li R, An Q D, Mao B Q, et al. PDA-meditated green synthesis of amino-modified, multifunctional magnetic hollow composites for Cr(VI) efficient removal[J]. Journal of the Taiwan Institute of Chemical Engineers, 2017.

[18] Tan K L, Hameed B H. Insight into the adsorption kinetics models for the removal of contaminants from aqueous

solutions[J]. Journal of the Taiwan Institute of Chemical Engineers, 2017, 74:25-48.

[19] Boyd G E, Schubert J, Adamson A W. The Exchange Adsorption of Ions from Aqueous Solutions by Organic Zeolites. I. Ion-exchange Equilibria1[J]. Journal of the American Chemical Society, 1947, 69(11):2849.

[20] Mohan D, Singh K P. Single- and multi-component adsorption of cadmium and zinc using activated carbon derived from bagasse--an agricultural waste[J]. Water Research, 2002, 36(9):2304-2318.

[21] Debnath S, Maity A, Pillay K. Magnetic chitosan–GO nanocomposite: Synthesis, characterization and batch adsorber design for Cr(VI) removal[J]. Journal of Environmental Chemical Engineering, 2014, 2(2):963-973.

O18

Circular economy: the green way for tanning

Franca Nuti[1], Massimo Rinaldi[1], Nicola Culeddu[2], Maurizio Solinas[2], Mauro Marchetti[2]

[1]*FGL INTERNATIONAL, Via Francesca Nord, 73, 56022 Castelfranco di Sotto - Pisa – Italy, Tel. +39 0571 478851, e-mail: info@fglinternational.com*

[2]*Institue of Biomolecular Chemistry, National Research Council of Italy, trav. La Crucca 3, Sassari, Italy, Tel. +390792841203, e-mail: mauro@ss.cnr.it*

ABSTRACT

As a response to the growing concerns about a variety of environmental issues expressed by public opinion and political bodies, the leather industry needs to support its market by environmental criteria as a guarantee of quality.

Conventional methods of preparatory and tanning processes discharge enormous amounts of pollutants. Nowadays there is a high demand to obtain quality leather without the use of the standard mineral-tanning agents based on Zirconium, Chromium and Aluminium salts or on synthetic aldehydic organic compounds such as glutaraldehyde. These concerns are driving research industry to find practical solution and innovation toward a greener way for tanning applications.

For these reasons it is crucial to realize different formulates devote to leather tanning using environmental friendly substances. In this view and in respect with European indications about circular economy, we choose to apply some specific waste products arising from dairy industry after proper chemical modification.

Some tanning and other leather treatment experiments were carried out in our laboratories using new formulates obtained after oxidation by oxygen peroxide, in different experimental conditions. Encouraging results were obtained and spectroscopic evidences of interaction between the new substances and leather were recorded.

KEYWORDS

Circular economy, metal-free tanning, dairy whey, natural aldehyde tanning.

INTRODUCTION

Circular economy in Europe is going to be the major driving force able to increase jobs all over the Old Continent. This market has been evaluated to be worth of 2.2 trillion of euro and could provide 19 million of new employments. At the end of 2015, the European Commission adopted an ambitious circular economy package with measures aimed to cover the entire product lifecycle: from design, procurement, production and consumption to waste management and the secondary raw materials market. The rules aim to have a practicaleffect on the lives of European citizens. The provision obliges member countries to recycle at least 70% of municipal waste and 80% of packaging waste, and prohibit the disposal of biodegradable and recyclable waste. The rules should enter into force from 2030. The actual situation in Europe is rather inhomogeneous being countries such as Germany quite virtuous in the recycling procedures (up to 66%) and other, such as Czech Republic, that barely reaches 30%. Circular economy is something more than waste recycling, is about the attempt to replace the old linear economy by which something is produced and at the end of its lifecycle it become merely waste. In the circular economy there are two kinds of materials: bio-compounds that can be reintegrated in the biosphere and technical compounds that need to be re-valued and not reintegrated in the biosphere. Theoretically by circular economy we can manage to have a production without creating any waste: a product is made, used and disposed of without leaving a trace.

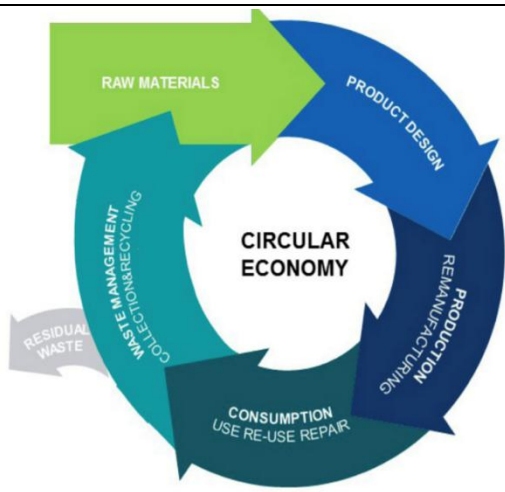

In this view conventional methods for tanning processes which produce an enormous amount of pollutants are subjected to regulations and restrictions.[1] Moreover, the market asks for metal free leather and not intentionally treated with substances classified as dangerous for health and the environment,[2,3] with the aim to achieve eco-friendly products.[4]

For these reasons it is crucial to realize different formulates devote to leather tanning using environmental friendly substances. In this view and in respect with European indications about circular economy, we hypothesized the use of whey from dairy waste production as potential ingredient for new formulated useful in the leather manufactory industry. Some tanning experiments were carried out in our laboratories using these formulates at different pH and after oxidation by oxygen peroxide.

THE INNOVATIVE IDEA

One of the major problems arising from dairy industry is related to the disposal of large amount of waste. It has been estimated that 2.5 million tons/year of milk serum originates from the processing of cheese. Only a minimal part of the waste produced is used while the rest must be disposed as it represents a pollutant for the soil. The serum, the main by-product obtained from cheese processing, it can be used, in most cases, for the production of ricotta and sometimes skimmed for the production of cream and butter. In case the dairy does not produce ricotta, the whey can be partially used for animal feeding, representing however a burden for the company. In this view the application of the so-called blue economy: “using the resources available in cascading systems where the waste of one product becomes the input to create a new cash flow” it may contribute to solve environmentally concerns related to the dairy industry and to the leather manufactory at the same time.

In particular, the use of the serum produced after cheese manufactory for industrial purpose would be attractive. The residues after cheese production may have different composition and it is obviously manly composed by water. By removing the water the chemical composition of the powdery residue may varies depending on the process of cheese production. The general chemical composition of the whey powder is listed in the following table.

Tab. 1. General chemical composition of dehydrated serum obtained after cheese production.

	Protein (%)	**Lactose (%)**	**Fat (%)**	**Ash (%)**	**Moisture (%)**
Whey powder	11.0-14.5	63.0-75.0	1.0-1.5	8.2-8.8	3.5-5.0

Ideally the lactose present in high percentage in this product could be oxidised and used as chemical in formulates for treatment in leather tanning processes. It isto note that carbohydrates are indeed known as potential tanning reagents, particularly if oxidised under the appropriate reaction conditions to get aldehydic derivatives. One example is the

well-known starch dialdehyde, obtained by oxidation of starch with periodic acid.[5]

Fig. 1. Ring opening of carbohydrate by periodic acid, to form a dialdehyde derivatives.

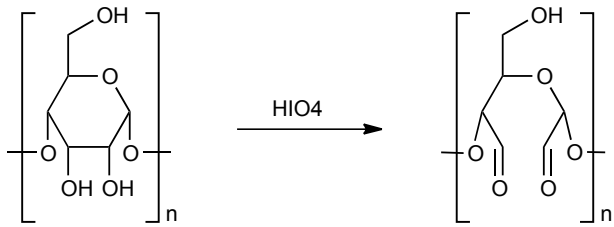

Starch is a large polymer and the final length of the dialdehyde compound can be controlled by the degree of oxidation; ultimately the oxidation can achieve 100%, when every glucose unit is opened up to create the shortest chain.[5] In principle other carbohydrates can undergo this reaction leading to aldehydic compounds depending on the oxidation conditions. Harsh oxidation reaction can lead to acidic derivatives while by mild condition it is likely to get oxidation of the primary alcohol into the corresponding aldehyde. Ideally, the product of the oxidation process can be applied in the tanning process of leather. We believe that lactose derived from serum produced after cheese manufactory could be, after proper chemical modification, used in the leather manufactory industry.

EXPERIMENTAL ACTIVITY

Chemical modification of whey powder.

The sample of whey powder in our hand has been obtained by a local cheese manufactory company and it has a lactose content >70%. Lactose is a disaccharide derived from the condensation of galactose and glucose, which form a β-1→4 glycosidic linkage. The glucose can be in either the α-pyranose form or the β-pyranose form, whereas the galactose can only have the β-pyranose form. Due to this equilibrium at the glucose moiety, lactose may undergo to reaction with amine to form imines that may eventually be reduced to form amines. This characteristic can be further exploited when, after chemical modification, we convert at least one of the primary hydroxyl groups (see the arrow in Fig. 2) of the molecule into an aldehyde. We speculated that oxidised lactose may potentially function as cross-linker by reacting with the NH_2 groups present in the collagen.

Fig. 2.α/β-D-galactopyranosyl-(1→4)-D-glucose

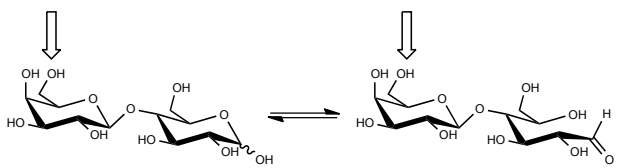

Fig. 2 shows highlighted the two primary hydroxyl groups that can potentially be oxidised to aldehyde. Moreover, the anomeric carbon of the glucose moiety is in equilibrium with its aldohexose formula. All these aldehydic groups can potentially react with the amino groups of the collagen leading to tanned leather. In this way the oxidised lactose may work as protein cross-linker.[6] In view of these considerations we have performed a series of oxidation reactions with the whey in our hands in order to modify the lactose molecule present in the mixture and to apply the obtained compound in experimental tannery. Table 2 shows some preliminary results by using as catalyst $FeSO_4$ and hydrogen peroxide as the oxidant.

Table 2. Oxidation of whey powder: preliminary results.

Entry	Whey powder (g)	Metal catalyst	Oxidant	Conditions
1	30	$FeSO_4 \cdot H_2O$	H_2O_2	30°/24 h
2	30	$FeSO_4 \cdot H_2O$	H_2O_2	30°/48 h
3	30	$FeSO_4 \cdot H_2O$	H_2O_2	50°/24 h
4	300	$FeSO_4 \cdot H_2O$	H_2O_2	50°/24 h

Reaction conditions: 300 g whey powder containing >70% lactose where dissolved in 210 mL H_2O. To this suspension 35 mg of $FeSO_4 \cdot 7H_2O$where added. 100 mL of H_2O_2 30% where carefully added. The reaction was allowed to proceed with mechanical stirring (150 rpm) at 50 °C for 24/48 hours.

At the end of the reaction ^{1}H-NMR analysis of the reaction mixture shows signals that are likely ascribable to aldehydic compounds. Reaction up scaling was necessary to collect enough material needed in experimental tannery trials.

Experimental tannery tests.

The tests were carried out in appropriate testing drums available in the experimental tannery department at the FGL International. The new formulate obtained was tested, initially, by performing tanning tests on pickled sheepskin to exploit the low thickness of the hides and to better evaluate the tanning effect. The tests were conducted starting from pH values <3 and reaching up pH 4.5-4.6 basifying with sodium bicarbonate. Tanningtests were also carried out after deliming/maceration processes with un-pickeled skin samples. In this case the tests were conducted in a pH range of 7.5-8.5. The tests were repeated also on cowhide at the two different pH ranges. After the tanning test, the skins were subjected to a re-tanning, fattening and dyeing process and dried to evaluate technical and chemical-physical aspects compared to sample tanned by organic and mineral tanning agents commonly used.

Other experimental tests

The whey powder has been also used in multi-purpose formulates for retanning experiments showing a satisfactory filling and leveling effects.

Evaluation of the tanned leather and other applications

The treated hides have been tested in the chemical laboratory at the R&D division. The evidence of the tanning effect was assessed by measuring the Tg (contraction temperature) before and after the treatment. Chemical-physical tests were also carried out to estimate the performance characteristics in terms of tensile strength, elasticity and elongation of the structure and of the grain. Further product considerations have been made to evaluate the effect of tanning on the grain and the effect in terms of softness, fullness and uniformity of dyeing. The stabilization of collagen after treatment with the new formulate was considered positive since the measured Tg values increased compared to the initial values of over 20 units, reaching about 70 ° C. The chemical-physical tests have shown data which are comparable to what is usually obtained with other organic aldehydic tanning agents and are in compliance with the technical standards of the most commonly produced articles.

The use of whey powder, as a component for formulates in retanning experiments, has shown interesting results in terms of fullness, surface uniformity and brightness, especially with nubuck leather samples.

Further insight on the leather obtained after experimental tannery tests was assessed by NMR analysis. A sample of sheepskin after treatment with oxidised whey powder has been analysed by high resolution HR-MAS NMR technique. Fig. 3 shows the HR-MAS spectra before (blue) and after treatment (red). The signal between 0.5 and 2 ppm (CH_2 aliphatic hydrogen) shows a strong decrease in intensity after treatment with oxidised whey (green arrow) that may be related with a lower fatty compounds content of the pickled leather. The signal highlighted by the orange arrow is related to the lactose

present in the whey and it may indicate that this compound is penetrated through the full substance of the hide. Finally, the signal specified by violet arrow (ca. 8.0-8.5 ppm) it is likely to be related to an imine functional group derived from the crosslinking betweenthe aldehydic group of the lactose and with the amine groups of collagen.

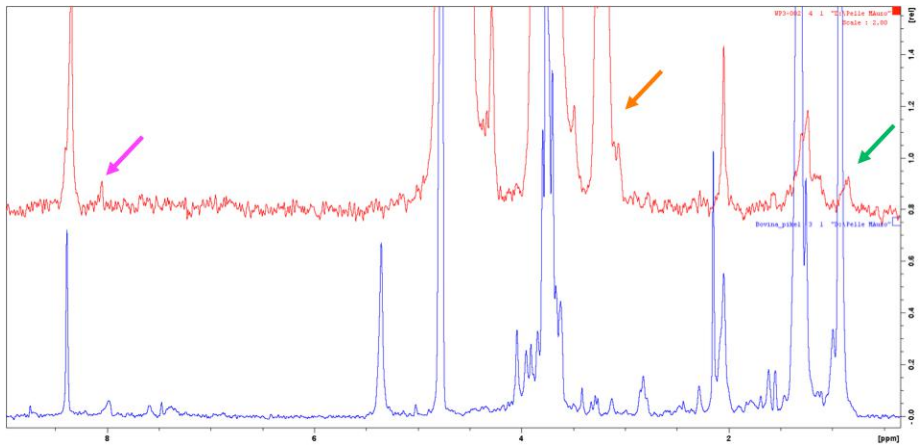

Fig. 3. HR-MAS ^{1}H-NMR spectra of ovine leather treated with oxidised whey powder.

CONCLUSION

The results obtained indicate that the use of chemicals deriving from food industry waste in particular whey powder can be used in the tannery industry. To be successful in this application it is necessary a proper chemical modification of the substrate aimed to create the functional groups needed for binding to the collagen. The use of whey powder in multi-purpose formulates fortanning and retanning processes can be an answer to the most restrictive needs of the leather industry, being an organic substance, metal free, with an irrelevant ecotoxicological impact and with the opportunity to put back into circulation a waste compound that is usually a significant problem in the food industry from which it derives. Further studies to understand the mechanism of the tannery process as well as optimisation and understanding of the oxidation process of the whey powder are currently underway.

BIBLIOGRAPHY

1. M. Aloy, A. Folachier and B. Vulliermet, *Tannery and pollution*, *Centre Technique Du Cuir*, Lyon, France, **1976**.

2. J. Gauglhofer, *J. Soc. Leather Technol. Chem.*, **1986**, 70, 11.

3. J. R. Rao, R. Venba, B. U. Nair, R. Suthantharajan, S. Rajamani, T. Ramasami and J. S. A. Langerwerf, *Proc. 30th LERIG*,

4. J. Buljan, *World Leather*, **1996**, *Nov.*, 65.

5. E. M. Filachione et al., *J. Arner. Leather Chern. Assoc.*, **1958**, *53*, 77.

6. A. Wijk, A. Siebum, R. Schoevaart and T. Kieboom, *Carbohydr. Res.*,**2006**, 341, 2921.

O19

Preparation and Properties of Self-healing PolyacrylateFinishing Agent

Dangge Gao[1,2], Jiahao Zhang[1,2], Bin Lyu[1,2], Jianzhong Ma[1,2], Zezhao Yang[1,2]

[1]*College of Bioresources Chemical and Materials Engineering, Shaanxi University of Science & Technology, Xi'an 710021, China.*

[2]*National Demonstration Center for Experimental Light Chemistry Engineering Education (Shaanxi University of Science & Technology), Xi'an 710021, China.*

Abstract

Leather is easy to suffer various scratches and easy discard of it results in a great waste of resources and economics.The appearance of self-healing materials couldefficiently solve this problem. We used methyl methacrylate (MMA), butyl acrylate (BA), furfuryl alcohol (FA) and bismaleimide (BMI) as raw materials to prepare self-healing polyacrylate emulsions (PA/(FA-BMI)) and applied it in leather finishing process. Fourier transform infrared spectroscopy (FT-IR), dynamic light scattering analyzer (DLS) and super deep scene microscope (SDSM) were used to characterize the emulsion and its film. The results showed that FA and BMI were dispersed uniformly in polyacrylate emulsions. With the increasing amount of FA and BMI,the DLS results showed that the size distribution of emulsion was more uniform and the dispersion was good. The emulsion filming results showed that the PA/(FA-BMI) couldbe self-healing completely when it was damaged. When the amount of FA and BMI was 5%, the self-healing property, physical and mechanical properties of the emulsion film were optimal. Dynamic observation through SDSM showed that PA/(FA-BMI) film and the leather after finishing with PA/(FA-BMI) could be fully self-healing in 5 hours at 50 °C. PA/(FA-BMI) endowed finishing leather good self-healing performance towards scratches on surfaces. Meanwhile, physical and mechanical properties ofleather, such astensile strength, tear strength, wet and dry rub resistance, had improved obviously.

Keywords: polyacrylate, self-healing, emulsion, leather finishing

O20

Analyzing the Role of Industry/Trade Association or Business Society/Council in Sustainable Growth of Industry: evidence from Indian leather Industry

Abstract

Sanjeev Gupta and Sandeep Kumar

In this competitive era, industries are under tremendous pressure to manage and perform under rising expectations and increasing regulatory business environment. It has become a business imperative to churn out strategies to efficiently utilize the available resources, and to develop a network of business support service providers. The Industry/Trade Association or Business Society/Council isone such institutional set-up which acts on behalf of either government or industry or both in order to support sustainable growth of associated or attached business organizations.Role of these institutions is not only limited to safeguard the interest of business enterprises keeping short-term advantages into consideration, but they may play the role of a responsible actor in guiding long-term sustainable growth of the industry according to stakeholder and institution theory. In this study, we made an attempt to analyze the role of various Industry/Trade Association or Business Society/Council in facilitating the development of leather industry in India. We found that these institutions have been designed to serve one or a combination of following purposes: export promotion, technical up-gradation, raw material sourcing, social linkage, environmental reporting, and skill development. However, we observed that there potential to lead the drive of sustainability promotion was either not noticed or underutilized due to absence of relevant policy measures. Hence, it is recommended that government should pursue these institutions to disseminate eco-friendly practices either through installing pilot or demonstration unit, which is supported by evidence-based decision making theory, or passing direct incentives to organizations considering Herzberg motivation hygiene theory. In future research, an extensive research should be conducted to design a framework for selection and delegation of responsibilities to Industry/Trade Association or Business Society/Council for sustainable industrial eco-system design.

Keywords: Industry/Trade Association; Business Society/Council; Leather; India

Introduction

According to conventional wisdom, ‘associations that are closely linked with and penetratedby an authoritarian state are significant chiefly as symbols of state dominationof society. Yet a review of empirical evidence suggests that the nature and significanceof incorporated or co-opted associations varies much more widely than the conventionalperspective suggests. Not only are close association-state linkages sometimeslooked upon favorably by societal participants, but some independent societal associationsactually seek to be co-opted by an authoritarian state. Moreover, incorporatedassociations often have more to do with strategies by state agencies and officials toaccomplish parochial goals than with state efforts to control society’ (Foster, 2001).This elucidatesa new analytical perspective to understand the dynamics and functioning ofincorporated associations, citing a wide range of empirical cases to show how this perspectivefacilitates a better understanding of the kinds of state-society engagement thatoccur within and through incorporated associations.

Self-regulation at the industry level is defined as "aregulatory process whereby an industry-level organization(such as a trade association) sets and enforcesrules and standards relating to the conduct of firmsin the industry" (Gupta and Lad, 1983). Self-regulation exists at the firm-level, theindustry-level, and the business-level of economic organization.Industry self-regulation has faced economic ("freerider") and legal (antitrust) impediments m widespreadimplementation, although there exist examples of effectiveindustry self-regulation, e.g., securities industry and the SEC,advertising and the FTC. By instituting industry codes ofconduct, national trade associations have shown to be naturalvehicles for self-regulation (Hemphill, 1992). Moreover, Lyytinen(2001) recognized that the role of institutionalinvolvement is imperative for the diffusion of innovations. Such institutions contain governmentalagencies, national and global standardization organizations,

localgovernment, and nonprofit private organizations like industry associations.The last type of organizations is also known as intermediatinginstitutions.

Recenlty, Barnett (2013) suggest that 'trade associationspending increases when the profitability of the four largest firms in anindustry decreases, but spending is unrelated to the profitability of the industryoverall. This implies that large firms exert control over trade associationagendas and may use these communal organizations to advance their owninterests rather than the shared interests of the entire industry. Moreover, itpoints to the need for further development of the currently anemic managementliterature on the activities of trade associations'.

In this competitive era, industries are under tremendous pressure to manage and perform under rising expectations and increasing regulatory business environment. It has become a business imperative to churn out strategies to efficiently utilize the available resources, and to develop a network of business support service providers. The Industry/Trade Association or Business Society/Council is one such institutional set-up which acts on behalf of either government or industry or both in order to support sustainable growth of associated or attached business organizations. Role of these institutions is not only limited to safeguard the interest of business enterprises keeping short-term advantages into consideration, but they may play the role of a responsible actor in guiding long-term sustainable growth of the industry according to stakeholder and institution theory. In this study, we made an attempt to analyze the role of various Industry/Trade Association or Business Society/Council in facilitating the development of leather industry in India.

Method

In this study, we conducted a survey to conduct qualitative analysis of issue related to role of association/councils in sustainability of leather business in India. In our research project, we ask following questions from Heads of few associations/councils/societies. The questions are:

1. Do you think that (name of association) is a stakeholder for Indian Leather Industry?
2. If Yes, what ways performance of Indian Leather Industry influence the performance of (name of association)?
3. What ways performance of (name of association) influence performance of Indian Leather Industry?
4. What role the (name of association) plays in sustainable growth of the leather industry in India?
5. How the (name of association) has evolved over the years in terms of associated members, functions, and contributions?

Findings

In our study, we first analyzed the different function performed by various existing association or councils or societies etc. we found that most of association are having inclination towards export promotion and skill development (please refer table 1). The crucial function like Environmental reporting and Social linkage have been almost neglected due uncontrolled constituting of these institutions.

Table 1 Check list for different function of the association

S. No.	Association	Export promotion	Technical up gradation	Raw material sourcing	Social linkage	Environmental reporting	Skill development
1	Council forLeatherExports (CLE)	√					
2	IndianLeatherTechnologists'Association		√				
3	Indian Leather Products Association						√

4	CentralLeatherResearchInstitute		√			√	√
5	AgraFootwearManufacturers andExportersChamber						√
6	All India Skinand HideTanners &MerchantsAssociation			√		√	
7	All India SmallScale Tannersand ExportersAssociation						√
8	IndianLeatherGarmentsAssociation	√					
9	IndianFinishedLeatherManufacturers & ExportersAssociation	√					
10	The TannersFederation ofIndia						√
11	IndianFootwearComponentsManufacturers Association(IFCOMA)	√					√
12	Confederation of Indian Footwear Industries				√		
13	Indian Shoe Federation	√					

We found that these institutions have been designed to serve one or a combination of following purposes: export promotion, technical up-gradation, raw material sourcing, social linkage, environmental reporting, and skill development. However, we observed that there potential to lead the drive of sustainability promotion was either not noticed or underutilized due to absence of relevant policy measures. Hence, it is recommended that government should pursue these institutions to disseminate eco-friendly practices either through installing pilot or demonstration unit, which is supported by evidence-based decision making theory, or passing direct incentives to organizations considering Herzberg motivation hygiene theory. In future research, an extensive research should be conducted to design a framework for selection and delegation of responsibilities to Industry/Trade Association or Business Society/Council for sustainable industrial eco-system design.

References

Foster, K. W. (2001). Associations in the embrace of an authoritarian state: state domination of society?. Studies in Comparative International Development, 35(4), 84-109.

Hemphill, T. A. (1992). Self-regulating industry behavior: Antitrust limitations and trade association codes of conduct. Journal of Business Ethics, 11(12), 915-920.

Gupta, A. K. and L. J. Lad: 1983, 'Industry Self-Regulation:An Economic, Organizational, and Political Analysis',Academy of Management Review 8 (3), 416-425.

Lyytinen, J. D. K. (2001). The role of intermediating institutions in Lyytinen the diffusion of electronic data interchange (EDI): How industry associations intervened in Denmark, Finland, and Hong Kong. The Information Society, 17(3), 195-210.

Barnett, M. L. (2013). One voice, but whose voice? Exploring what drives trade association activity. Business & Society, 52(2), 213-244.

O21

Biological treatment of alkaline leather fleshing by a fleshing-enriched activated sludge reactor

Jung-Jeng Su[1*], Shun-Ming Huang[1,2], Richard Pai[2], Rong-Shinn Lin[3]

[1*]*Dept. of Animal Science and Technology, National Taiwan University, Taipei, Taiwan; * Corresponding author; Email: jjsu@ntu.edu.tw.*

[2]*Tehchang Leather Products Co., LTD. Taoyuan City, Taiwan.*

[3]*Dept. of Biotechnology and Animal Science, National Ilan University, Yilan, Taiwan.*

ABSTRACT

After un-haring and liming processes, the raw hides will be fleshed to separate the hides and fleshing with alkaline moisture (pH = 12−13) in tannery industry. The objective of this study was to develop a biological fleshing treatment approach instead of fleshing incineration. All microorganisms for this study were isolated in the liming wastewater by nutrient agar (pH = 12) for selecting the alkaline-tolerant bacteria. The fleshing was cut into appropriated size in petri dishes and then inoculated with culture suspension of the isolates. The inoculated petri dishes containing fleshing were then incubated at 30°C. The isolate, strain P, capable of degrading fleshing efficiently was selected as the sole inoculum for this study. The biodegraded fleshing liquid was initially treated in a dairy activated sludge reactor (DASR) for investigating the feasibility of activated sludge system. The removal rate of the biochemical oxygen demand (BOD), chemical oxygen demand (COD), and suspended solids (SS) was 81±4, 60±8, and 55±6%, respectively. Therefore, the pre-biodegraded fleshing liquid can be treated by a DASR. When smashed fleshing (fleshing: water = 1:1) was ground and mixed with the strain P suspension, it was used for fleshing activated sludge enrichment in the reactor. For a 15-day time course experiment of smashed fleshing treatment by the fleshing-enriched activated sludge reactor (FASR), the removal efficiency of BOD, COD, and SS was 95.4±1.4, 75.5±4.8, and 83.5±11.2%, respectively. In coordinating with a fleshing-enriched sequencing batch reactor (SBR) (hydraulic retention time = 5 d), the removal efficiency of BOD and COD was 93.3 and 65.9%, respectively. Experimental results showed that the pre-biodegraded fleshing liquid can be efficiently treated by a fleshing-enriched activated sludge reactor.

Keywords:Leather fleshing, Alkaline-tolerant bacteria, Activated sludge reactor

1. INTRODUCTION

In leather processing, from every 1000 kg raw hide/skin only 150 kg of the raw material is converted into leather and nearly 850 kg is generated as solid wastes (Kanagarajet al. 2006). Most of the solid wastes are generated in beamhouse operations, especially in fleshing operation. In beamhouse, solid waste is generated during fleshing operation termed as ‘fleshings’ (Hashem et al., 2015) . The operation involves cutting or removing the offal from the flesh side of hide/skin. In the conventional leather processing, fleshing is done just after liming. In this stage hide/skin is easier to handle due to swollen condition. The fleshing operation produces a huge amount of inevitable solid waste (Hashem et al., 2015). It is clear that average 0.31±0.02 kg fleshings were generated from every kg of wet salted cow hide in fleshing operation. Similarly, 0.39±0.02 kg fleshings were generated from every kg of wet salted goat skin (Hashem et al., 2015). Fleshings contain sub-cutaneous tissue, fat and flesh. It contains protein 5−7%, fat 4−18%, lime 2−6%, sulphide 2−4% etc. (Lupo, 2006).

There are two tannery wastewater treatment approaches available including: (1) chemical approaches and Microbial approaches. The chemical approaches include: rotating disc electro-chemical system (Abdul Jameel, 2016), chemical coagulation system (Song et al., 2004), and Chemical oxidation (Dargo and Ayalew, 2014). The microbial approaches include: biological Wastewater treatment system (Durai and Rajasimman, 2011).

There are two processes for treating fleshings include: (1) physical/steam process and (2) biotechnological process. The centrifuge facility is applied for treating fleshing by a physical/steam process

(https://www.flottweg.com/applications/edible-fats-and-oils-biofuels/limed-fleshing-treatment). The by-products from the physical/steam process include: (i) solid: collagen hydrolysate and residues as fertilizer in farming; (ii) Fat: reused as a sulfated fatliquor in leather processing to instead of fish oil-based fatliquor for leather process (Nasr, 2017); (iii) Effluent: effluent treatment [i.e. activated sludge process (ACP), sequencing batch reactor (SBR), wetland and ponds, upflow anaerobic sludge blanket (UASB), hybrid biological process](Goswami and Mazumder, 2013). Some study had been isolated proteolytic bacteria from tannery sludge of a CETP for biogas production using liquefied fleshing, sludge, and cow dung as the feedstock (Vasudevan and Ravindran, 2007). The objective of this study was to develop a biological fleshing treatment approach instead of fleshing incineration.

2. MATERIALS AND METHODS

2.1. Inocula for isolation of alkaline-tolerant bacteria from tannery wastewater

The alkaline-tolerant bacteria were isolated from the tannery wastewater of Tehchang Leather Products Co., LTD, Taoyuan, Taiwan. Characteristics of the tannery wastewater (pH = 11) for isolation are shown in Table 1. The average biochemical oxygen demand (BOD) and chemical oxygen demand (COD) were1343±439 and 11531±1049 mg/L, respectively. The average BOD/COD ratio was 0.12±0.04%.

2.2. Isolation of alkaline-tolerant bacteria from tannery wastewater

The tannery wastewater was diluted and spreading into alkaline nutrient agar plates (pH = 11) for colony formation. The mixed bacterial colonies were sequentially purified with alkaline nutrient agar plates. All purified alkaline-tolerant bacteria were gram-stained and then enriched in separate alkaline nutrient broth for further studies. Also, all isolates were qualitatively tested for lipase activity by using a Spirit Blue Agar assay (http://himedialabs.com/TD/M445.pdf).

2.3. Preliminary test for pork biodegradation by the isolates

Cooked pork was cut to small strip and rinsed with clean water. Pork strips were then sterilized through spraying 75% alcohol followed by UV radiation for 30 min. The sterile pork strips were placed in autoclaved test tubes with either 3 mL of pure water or nutrient broth (NB) (pH = 7.5) and then inoculated with suspension of the isolates individually. All test tubes containing pork strip and water/NB were incubated at 30°C for periodical observation.

2.4. Biodegradation of limed fleshing by the isolates

2.4.1. Biodegradation of non-sterile limed fleshing

Cut non-sterile limed fleshing to a proper size (5cm × 5cm) and place fleshing pieces in sterile petri dishes. Pour 10 mL of sterile NB into each petri dish with 1 mL bacterial suspension of each isolates, the strains S4, S6, and P. All inoculated petri dishes containing fleshing pieces and NB were then incubated at 30°C for periodical observation. The fleshing pieces were turned over every two days and sterile de-ionized water was added periodically to avoid fleshing pieces dehydrated.

2.4.2. Biodegradation of UV irradiation sterile limed fleshing

Cut limed fleshing to a proper size (5cm × 5cm) and place fleshing pieces in sterile petri dishes. All fleshing pieces of the sterile sets were sterilized by UV irradiation for 30 min. Pour 10 mL of sterile NB into each petri dish with 1 mL bacterial suspension of each isolates, the strains S4, S6, and P. All inoculated petri dishes containing fleshing pieces and NB were then incubated at 30°C for periodical observation. The fleshing pieces were turned over every two days and sterile de-ionized water was added periodically to avoid fleshing pieces dehydrated.

2.5. Treatment of biodegraded fleshing liquid by a sequencing batch reactor (SBR)

2.5.1. Preparation of liquefied fleshing

Limed fleshing was cut into small pieces and inoculated 1-L of bacterial suspension of the strain P in 2-L Erlenmeyer flasks and incubated at 35°C for 5 days with continuous aeration.

2.5.2. The sequencing batch reactor (SBR)

The SBR reactor was an acrylic cylinder (17.4 cm i.d. × 111 cm height). The activated sludge for the SBR was enriched

by liquefied fleshing. One liter of liquefied fleshing was mixed with 200 mL strain P suspension and the final volume was brought to 15L by adding tap water. And then the SBR was aerated continuously until formation of activated sludge.

2.5.3. Treatment of biodegraded fleshing liquid

The time course experiments were operated under the hydraulic retention time (HRT) was 5 days. Daily influent volume was 250 mL of fleshing liquid. Samples of untreated fleshing liquid, influent, and effluent were taken and analyzed periodically. All water samples were analyzed for BOD, COD, SS, and so on (APHA, 1998).

3. RESULTS AND DISCUSSION

3.1. Isolation of alkaline-tolerant bacteria from tannery wastewater

There were about 8 alkaline-tolerant bacteria isolated from the tannery wastewater (pH = 11). All isolates were Gram-negative bacteria and rod-shape. Among these isolates, only the strain P, S4, and S6 with higher lipase activity using a Spirit Blue Agar assay (Table 2). Thus, the strains P, S4, and S6 were used for further experiments in this study.

3.2. Preliminary test for pork biodegradation by the isolates

During the 7-day time course experiments, the results showed that all isolates grew faster in Tryptic soy broth (TSB) than in distilled water (DW). However, only the strain P showed significant biodegradation of pork strips in 7 days in both TSB and DW medium (Table 3).

3.3. Biodegradation of limed fleshing by the isolates

The non-sterile limed fleshing was liquefied in 17 days by either the strains S4 or S6. However, the non-sterile limed fleshing was liquefied in 8 days by the strain P. For the UV irradiation sterilized limed fleshing, the surface sterile limed fleshing was liquefied in 12 days by either the strains S4 or P. However, the surface sterile limed fleshing was not liquefied in 12 days by the strain S6. Some alkaline-tolerant bacteria on the surface of limed fleshing might contribute some biodegradation of limed fleshing.

3.4. Treatment of biodegraded fleshing liquid by a sequencing batch reactor (SBR)

Time course experiments were performed under the ambient temperature between 15.0±0.8 and 20.6±2.1^{o}C (Table 4). Lower ambient temperature can affect bacterial metabolism and activity for treating fleshing liquid. The results showed that the COD in the untreated fleshing wastewater and effluent was from347.6 ± 27.7 to 521.2 ± 281.8 mg/L and from 132.2 ± 31.0 to 306 ± 174.6 mg/L, respectively. Removal efficiency of COD was 41−70%. Moreover, BOD in the untreated fleshing wastewater and effluent was from 144.0±18.8 to 252.1±179.4 mg/L and from 16.6±11.8 to 108.1± 87.8 mg/L, respectively. Removal efficiency of BOD was 57−93%. The lower the ambient temperature, the lower the removal efficiency of COD and BOD. Thus, thermostat should be applied for outdoor biological treatment of limed fleshing wastewater.

4. CONCLUSION

Limed fleshing can be biodegraded when proper conditions are provided under aerobic conditions. The strain *P* isolated from tannery wastewater can accelerate biodegradation of limed fleshing under ambient conditions. Biodegraded fleshing liquid can be completely treated by means of an activated sludge reactor, sequencing batch reactor (SBR). Biological treatment of fleshing wastewater can be affected by atmospheric temperature. Mesophilic conditions should be the optimal conditions for biological treatment of fleshing wastewater.

REFERENCES

[1] Abdul Jameel AG (2016) Treatment of tannery wastewater. LAP LAMBERT Academic Publishing. ISBN-10: 3659851663.

[2] APHA (1998) Standard Methods for the Examination of Water and Wastewater, 19th edn. American Public Health Association/American Water Works Association/Water Environment Federation, Washington, DC, USA.

[3] Dargo H and Ayalew A (2014) Tannery Waste Water Treatment: A Review. International Journal of Emerging Trends

in Science and Technology 1488−1494.

[4] Durai G and Rajasimman M (2011) Biological Treatment of Tannery Wastewater - A Review. Journal of Environmental Science and Technology 4: 1−17.

[5] Goswami, S., Mazumder, D., 2013. Treatment of chrome tannery wastewater by biological process - a mini review. World Academy of Science, Engineering and Technology, International Journal of Environmental and Ecological Engineering 7: 798−804.

[6] Hashem MA, Nur-A-Tomal MS, and Mondal BK (2015) Generation of fleshings at beamhouse in tannery and its environmental impact assessment: Bangladesh perspective. Bangladesh Journal of Scientific and Industrial Research 50: 227−232.

[7] Kanagaraj J, Velappan KC, Chandra Babu NK, and Sadulla S (2006) Solid wastes generation in the leather industry and its utilization for cleaner environment-A review. Journal of Scientific & Industrial Research 65: 541−548.

[8] Lupo R (2006) Fleshing treatment and compacting, Proc. II. Eurocongress, pp. 24−27 May 2006, IULTCS, Istanbul, Turkey.

[9] Nasr AI (2017) Reusing limed fleshing wastes as a fatliquor in leather processing. Egyptian Journal of Chemistry 60: 919−928.

[10] Song Z, Williams CJ, and Edyvean RGJ (2004) Treatment of tannery wastewater by chemical coagulation. Desalination 164: 249−259.

[11] Vasudevan N and Ravindran AD (2007) Biotechnological process for the treatment of fleshing from tannery industries for methane generation. Current Science 93(11): 1492−1494.

Table 1. Characteristics of the tannery wastewater for isolation (pH =11)

Samples	BOD (mg/L)	COD (mg/L)	BOD/COD*
1	1283	10445	0.123
2	654	11713	0.056
3	1470	11804	0.125
4	1487	11151	0.133
5	2246	12657	0.177
6	1113	9741	0.114
7	1344	12114	0.111
8	983	13066	0.075
9	1505	11085	0.136
Mean±S.D.	1343±439	11531±1049	0.12±0.04

Table 2. Qualitative analysis of the isolates for lipase activity

Isolates	Gram-staining	Shapes	Lipase activity*
P	negative	long rods	++++
C	negative	long rods	−
S1	negative	rods	−

S2	negative	rods	+
S3	negative	long rods w/ endospore	++
S4	negative	long rods	++++
S5	negative	rods	++
S6	negative	long rods	++++

*Lipase activity: positive (+), negative (−)

Table 3. Biodegradation of cooked pork strips by the isolates comparing with lipase activity

Isolates	Liquid in test tubes	Biodegradation of pork strip	Lipase activity (Spirit Blue Agar Test)
P	TSB	++++++	++++
	Water	++++	
S4	TSB	++++	++++
	Water	+++	
S6	TSB	++++	++++
	Water	+++	

Table 4. Treatment of fleshing wastewater by a SBR reactor

Water Quality Index	Treatment	Hydraulic Retention Time (HRT) = 5d		
		Run#1	Run#2	Run#3
COD (mg/L)	Before	478.4 ± 60.9	347.6 ± 27.7	521.2 ± 281.8
	After	144.6 ± 18.8	132.2 ± 31.0	306 ± 174.6
	Removal (%)	70	62	41
BOD (mg/L)	Before	248±60.6	144.0±18.8	252.1±179.4
	After	16.6±11.8	19.4±6.1	108.1± 87.8
	Removal (%)	93	87	57
Daily Average Temp. (°C)		18.3±3.1	20.6±2.1	15.0±0.8
Highest Temp. (°C)		21.3±4.5	23.9±3.5	17.3±1.7
Lowest Temp. (°C)		15.6±2.8	18.8±1.8	13.5±0.6

O22

A green retanning system with function of reducing free formaldehyde in leather

Wang Xuechuan[1] , Yan Zhuan[2], Liu Xinhua[3]

[1]*College of Bioresources Chemical and Materials Engineering, Shaanxi University of Science & Technology, Xi'an 710021, Shaanxi, China. Phone: 15802958501 Email: wangxc@sust.edu.cn*

[2]*College of Bioresources Chemical and Materials Engineering, Shaanxi University of Science & Technology, Xi'an 710021, Shaanxi, China. Phone: 15291878253 Email:18396813874@163.com*

[3]*College of Bioresources Chemical and Materials Engineering, Shaanxi University of Science & Technology, Xi'an 710021, Shaanxi, China. Phone: 18710981268 Email:liuxinhua@sust.edu.cn*

Abstract

Chromotropic Acid Grafted Amphoteric Polyurethane (CAGAPU) was synthesised with Chromotropic Acid (CA) as a modifier for Polyurethane (PU). It was followed by the test of FT-IR, ^{1}H-NMR of the structure. The retanning process and the experiments of CAGAPU with formaldehyde indicate the following: (1)The leather retanned by CAGAPU retanned system can be comparable or surpassed to the market retanned system in terms of shrinkage temperature and sensory performance. (2) The leather collagen fibers are more smooth and orderly which provides a potential value for the appearance of the leather and fur industry. (3) The CAGAPU retanned system can bring down the free formaldehyde content in aldehyde tanned leather to 56.08 ug/kg and the remove rate of free formaldehyde reached 80.95%. (4) The optimum dosage of CAGAPU is 20g and the best retanning time is 6 hours. Therefore, this paper provides the possibility for the sustainable development of leather. The work has changed the traditional way of "terminal treatment" and realized the " initial treatment" and may also offer a new idea of solving the problem of formaldehyde in the newly decorated houses or in the air.

Keywords: amphoteric polyurethane, chromotropic acid, leather, retanning, reducing free formaldehyde

1 Introduction

China is known as a country of leather manufacturing with an annual output value of 1 trillion and 350 billion.[1]With excellent performance, chrome tanning used to be taken as the primary method in the traditional tannery process. However, with the increasing awareness of environmental protection, people come to realize that the traditional chrome tanning method can bring pollution.[2-7]Therefore, researchers at home and abroad are considering completely replacing or partially replacing chrome tanning agents with aldehyde tanning agents.[8-10]But the problem is that aldehyde tanning agents will bring relatively high content of free formaldehyde which can induce carcinoma and promote cancer process, so there are strict regulations on the content of free formaldehyde in leather products in different countries[11]. Thus, it is of great necessity to explore methods to reduce free formaldehyde in the aldehyde tanned leather.

Currently, the extensively used formaldehyde capture agents for reducing free formaldehyde in leather are ammonia or amino derivatives, strong oxidizing substances, porous inorganic filler and tannin, starch, casein. [12-16]Rita Kakkar[17] studied the absorption of free formaldehyde on Nano Magnesium Oxide and found that Nano Magnesium Oxide had a certain absorption effect on free formaldehyde. Lam[18] realized decreasing formaldehyde via oxidation under visible light by doping Cr on thin film based on TiO_2. However, the above research methods have the disadvantages of high cost, complicated operation process and low removal rate of free formaldehyde, so they are not applicable in leather factories. Zhou Yongxiang[19-20] found that the combination of polymer with small monomer which can react with free formaldehyde can increase the removal rate of free formaldehyde. So if we can find a small monomer that can react with formaldehyde and then use the small monomer to modify a large polymer, then the modified polymer will be a combination of small molecules and large polymer, and the removal rate of free formaldehyde will increase. Young-Sihn Sihn[21], Bo-Long Poh[22], E. Fagnani[23] found that the chromotropic acid can react with formaldehyde so the chromotropic acid can be used as the small monomers. That is to say, if we want to achieve the idea of combining small monomer and polymer to improve the removal rate of free

formaldehyde, the key now is to choose a polymer. But which material could serve as the polymer?

At present, the amphoteric polyurethane retanning agent is widely used in leather retanning process because it can effectively solve the problem of loose grainand make leather plump, flexible, elastic. It can also increase the binding rate of subsequent anionic materials.[24-28] Different modifiers can give special properties and functions to polyurethane, such as amphoteric polyurethane with function of postpolymerization crosslinking, amphoteric polyurethane with self assembly properties and amphoteric polyurethane with temperature sensitive properties. [29-30] Therefore, it is assumed that amphoteric polyurethane (APU) will have the function of reducing free formaldehyde when polyurethane is used as polymer and the chromotropic acid was introduced onto the main chain of the polyurethane as the small monomers. When such APU is applied in the retanning process of the aldehyde tanned leather, leather can be retanned with low content of free formaldehyde.

In our work, Chromotropic Acid Grafted Amphoteric Polyurethane (CAGAPU) was synthesised with Chromotropic Acid (CA) as a modifier for Polyurethane (PU). The CAGAPU was then used in the retanning process of aldehyde tanned leather, which not only can avoid the problem of Cr (Ⅵ) pollution brought from traditional chrome tanning agent, but also can effectively reduce the free formaldehyde plagued by market aldehyde tanned system. What's more, the BOD, TDS, TSS have been reduced to a certain extent in the waste liquid of tannery. This paper may provides the possibility for the sustainable development of aldehyde tanned leather. Last but not least, the work may also offer a new idea for solving the problem of formaldehyde in the newly decorated houses or in the air.

2 Materials and methods

2.1 Materials

Pickled sheepskin was supplied by Hebei Dongming leather Co., Ltd.Isophorone Diisocyanate (IPDI, AR) were provided by Shanghai Dibo Chemical Technology Co., Ltd. Poly (Propylene Glycol 400) (PPG 400, ≥ 99.0%) and N-Methyldiethanolamine (MDEA, ≥ 99.0%) were purchased from Aladdin Industrial Corporation. Chromotropic Acid (CA, AR) was obtained from Shanghai Macklin Biochemical Co., Ltd. Triethylamine (TEA, ≥ 98.0%) was produced by Guangdong Chemical Reagent Engineering-technological Research and Development Center. Sodium bicarbonate (Na_2CO_3, ≥ 98.0%) was supplied by Tianjin Hongyan Chemical Reagent Factory. Dibutyltin dilaurate (DBTDL, ≥ 98.0%) was purchased from Chengdu Kelong Chemical Reagent Co., Ltd.

2.2 Preparation of CAGAPU

CAGAPU was synthesized by PU with CA as a modifier. 5g CA was dissolved with a small amount of acetone in a beaker. Then, the dissolved CA was poured into the 100ml PU solutions and the temperature was raised to 80℃. Then, the solution was stirred quickly for 3 h. Then, 20 mmol of TEA, a proper amount of distilled water were added to the three-necked flask and with the addition of sodium bicarbonate to adjust the pH to 5.0. Then CAGAPU, an ivory liquid with blue light, was obtained by removing the unreacted monomers and solvent through dialysis bag whose MWCO (Molecular Weight Cut Off) is 1000.

2.3 Fourier Transform-Infrared Spectroscopy (FT-IR)

Before characterization, the unreacted monomers and solvent were removed by dialysis bag whose MWCO is 1000. Then, the samples of CA, PU and CAGAPU were carried out using compressed pellets of KBr and the wave number ranged from 400 to 4000cm^{-1}.

2.4 Nuclear Magnetic Resonance Spectrum (NMR)

Before testing, the unreacted monomers and solvents were removed. Then the solid samples of CA, PU and CAGAPU were confected into a solution whose mass concentration was about 10% with DMSO-d6as the solvent and then the samples was scanned 32 times.

2.5 Measurement of Shrinkage Temperature (Ts)

The leather was hung on the hook of the test rack of the systolic temperature meter, the rack was then dropped into an electric cup equipped with water. While the spring in the device was stretched with the contraction of the leather, the systolic temperature meter would record the temperature simultaneously, which is the shrinkage temperature of the leather.[31]

2.6 Determination of Physical Properties

Horizontal and vertical samples from different parts of the leather were fixed on the XL-100A tensile testing machine. The tensile strength and tearing strength were tested and the average value was calculated.

2.7 Estimation of Free Formaldehyde Content In The Leather.

(1) In the light of standard appendix QB/T 19941-2005,[32]steam distillation rather than direct distillation was used for determining the content of formaldehyde in leather.

(2)The effect of the dosage of CAGAPU and different retanning time on the removal rate of formaldehyde

The aldehyde tanned leather was retanned with diverse dosages of CAGAPU and different retanning time, then the removal rate of formaldehyde is calculated by measuring the content of formaldehyde in the leather before and after retanning.

3 Results and discussion

3.1 FT-IR Analysis

Curve (a), (b) and (c) in Fig.1. show the FT-IR spectrum of CA monomer, CAGAPU and PU. The absorption peak at 3345 cm^{-1} of curve (b) indicates the stretching vibration of N-H. The absorption peak at 1739 cm^{-1} and 1546 cm^{-1} corresponds to the amide C=O bond stretching in the peptide bond (amide I, amide Ⅱ, respectively).[34] These characteristic peaks indicate that the CAGAPU(curve (b)) contain -CONH- functional groups. [35] The peak at 672 cm^{-1} and 632 cm^{-1} can be attributed to the out-of-plane bending vibration of C-H in the benzene ring. Compared with the curve (c), the characteristic absorption peak of the benzene ring appears in the curve (b) and the wide peak of the hydroxyl group in the curve (a) disappears, revealing that the CA was successfully grafted onto the polyurethane.

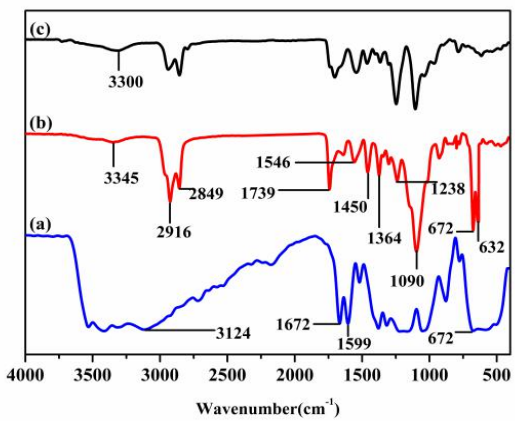

Fig.1. FT-IR spectrum of the CA(a) , CAGAPU(b) and PU(c)

3.2 ^{1}H-NMR Analysis

The ^{1}H-NMR spectrum of CA monomer, PU and CAGAPU were shown in Fig. 2. (A), (B), (C), respectively.From Fig.2. (C), it can be seen that δ: 7.68 shows the double peaks of hydrogen in the benzene ring, which is larger than the absorption peaks in Fig.2. (A) (δ: 6.95 and δ: 7.52). This is due to the induction effect of the benzene ring in CA and the isocyanate group in polyurethane.[33]And we can see that the peak at 2.50 in Fig.2. (A) did not appear in Fig.2. (B) and Fig.2. (C), indicating that all hydroxyl groups in CA were all involved in the reaction and turned into the -CONH-. It also confirmed

that CA was grafted onto the main chain of polyurethane.

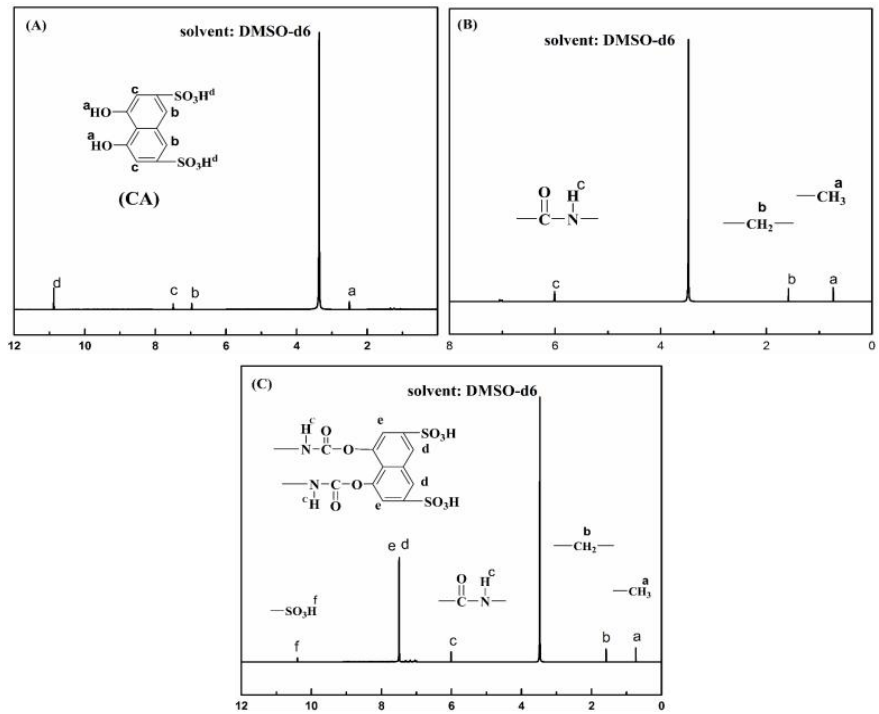

Fig.2. ^{1}H-NMR of the CA(A), PU(B) and CAGAPU(C)

3.3 Shrinkage Temperature (Ts, ℃).

The shrinkage temperature (Ts) of leather treated with different systems were measured which is shown in Table 1. It can be seen from Table 1 that the Ts by PU retanned system, CAGAPU retanned system and market retanned system were increased compared with that by the the market aldehyde tanned system. The results indicate that PU, CAGAPU and market retanning agents all permeated into the interval of the leather collagen fibers and produced transmission-quality from the drum bath to the leather collagen fibers. The Ts from CAGAPU retanned system and market retanned system all reach above 79℃ indicating that CAGAPU retanning agent can match the market retanning agent in improving the Ts.

Table 1. The shrinkage temperature of leather by multifarious systems (℃)

leather	along		across		average
	1	2	3	4	
acid hide	45.2	44.6	46.0	45.8	45.4±0.3
market tanned system	71.5	73.4	70.6	71.9	71.8±1.0
PU retanned system	74.3	74.7	76.2	75.5	75.2±0.5
CAGAPU retanned system	79.5	79.1	78.6	79.2	79.1±0.1
market retanned system	79.3	78.6	80.5	79.0	79.4±0.5

3.4 Physical Properties

The physical properties of leather disposed by varioussystems were shown in Fig.3. As Fig.3. shows, the tensile strength and tearing strength by the CAGAPU retanned system was higher than that by the PU system. The mechanical strength CAGAPU retanned system was lower than that of market retanned system, but what deserves our attention is that the

difference is not obvious. This was due to the large number of amide bonds in the CAGAPU can formed more hydrogen crosslinking with carboxyl group, amino group and hydroxyl group of leather collagen.[36] Due to the crosslinking between retanning agents and leather collagen fibers, the deformation of fibers can be effectively suppressed.[3] In addition, the cation in CAGAPU can form electrovalence bond with the carboxyl group in the leather collagen fibers (as shown in Fig 4.) Therefore, the tensile strength and tearing strength by the CAGAPU retanned system was good.

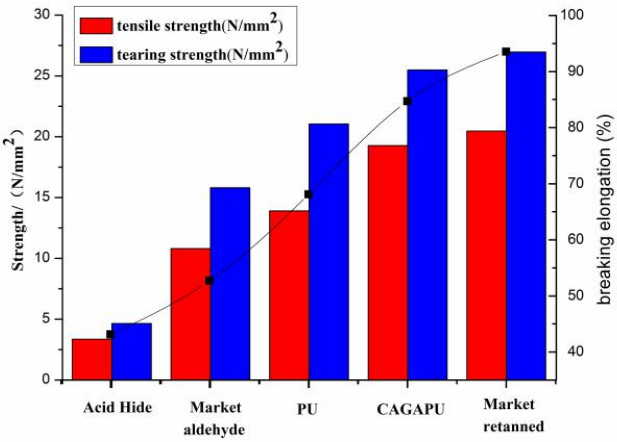

Fig.3. The physical properties of leather

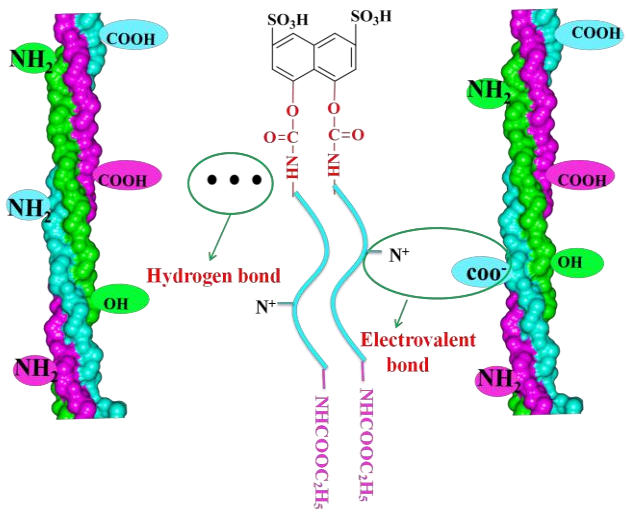

Fig. 4. Retanned mechanism of CAGAPU

3.5 Calculation the content of free formaldehyde

It was known from Table 2 that the free formaldehyde content in the leather retanned by CAGAPU retanned system was reduced to 56.08mg/kg, which conforms to EU countries' standards on leather products directly contact by humanbeings (75mg/kg). What is more, the value reduced greatly compared with that of the market aldehyde tanned system which indicates that the CAGAPU retanning agent can effectively reduce the free foemaldehyde in aldehyde tanned leather and the removal rate of free formaldehyde has reached 80.95%. The reason is that the CA monomer can react with free formaldehyde and endow the performance of CAGAPU whose modifier is a CA monomer with reducing the content of free

formaldehyde.[12-13]While, the PU retanned system and market retanned system did not have the function of reducing free formaldehyde in leather. The reason is that there is no monomer which can react with the free formaldehyde in the molecular structure of the PU and the market retanning agents.

Table 2. Free formaldehyde content of different systems

leather	absorbance	formaldehyde concentration	removal rate
market tanned system	1.38	294.38 (X_1)	0 (starting standard)
PU retanned system	1.39	296.50	-0.72
CAGAPU retanned system	0.26	56.08 (X_2)	80.95
market retanned system	1.37	290.25	1.40

3.6 The effect of the dosage of CAGAPU and retanning time on the removal rate of formaldehyde

The influence of CAGAPU's dosage and retanning time on the removal rate of formaldehyde was shown in the Fig.5. It can be seen from the Fig.5. that with the extension of CAGAPU's dosage and retanning time, formaldehyde-removal rate increased first and then remained unchanged. This is probably caused by the reaction between CAGAPU with formaldehyde in the leather which reached saturation point with 20g CAGAPU after 6 hours. For cost savings and efficiency consideration, the optimum dosage of CAGAPU is 20g and the best retanning time is 6 hours.

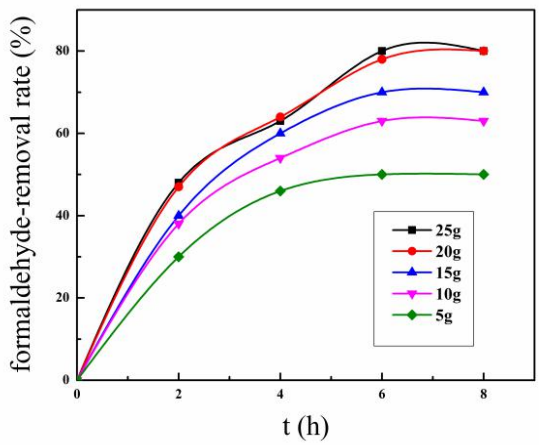

Fig.5. The influence of CAGAPU's dosage and retanning time on the removal rate of formaldehyde

4 Conclusions

In conclusion, an environmental polyurethane (CAGAPU) retanning with function of reducing free formaldehyde in leather has been synthesized and applicated. Through the comparison of multifarious systems, it was found that the shrinkage temperature of leather after CAGAPU retanned system is comparable with that after the market retanning agents. The leather collagen fibers become more orderly which provides a potential value for the appearance of the leather and fur industry. In addition, the CAGAPU system can make the content of free formaldehyde in aldehyde tanned leather reduced to EU standards. Therefore, the experiment may be of great significance to the cleaner production of the tannery industry. Last but not least, the work may also provide a new idea of solving the problem of formaldehyde in the newly decorated houses or in the air.

References

(1)Jiang, N. The Chinese leather industry under the numbers. J. Chinese leather. **2016,** (2), 74-79.

(2)Wang, L.; Han, W. M.; Yu, Y.; Zhou, J. F.; Zhang, W. H.; Shi, B. Thermodynamic investigations on chrome and aluminum tanning. J. Am. Leather Chem. Assoc. **2017,** 112 (11), 360-366.

(3) Qiang, T. T.; Gao, X.; Ren, J.; Chen , X. K.; Wang, X. C. A chrome-free and chrome-less tanning system based on the hyperbranched polymer. J. ACS Sustainable Chem. Eng. **2016,** 4 (3), 701-707.

(4) Tahiri, S.; Hassoune, J.; Alami, Younssi, S.; EI Krati, M.; Albizane, A.; Luisa, Cervera, M.; de la Guardia, M. Management of tannery wastewaters: treatment of spent chrome tanning bath and vegetable tanning effluents. J. Desalination and water treatment. **2013,** 51, 4467-4477.

(5) Ogata, K.; Kumazawa, Y.; Koyama, Y.; Yoshimura, K.; Takahashi, K. Measurement of hexavalent chromium in chrome-tanned leather: comparative study of acidic condition extraction with alkaline extraction. J. Soc. Leather Technol. Chem. **2015,** 99 (6), 293-296.

(6)Cui, L.; Qiang, X. H.; Yu, L.; Wei, X.; Li, C. T. A cleaner method for low-chrome tanning with no-salt pickling. J. Soc. Leather Technol. Chem. **2017,** 101 (5), 219-226.

(7) Wang, Z. H.; Bush, R. T.; Sullivan, L. A. Simultaneous redox conversion of chromium(VI) and arsenic(III) under acidic conditions. J. Environ. Sci. Technol. **2013,** 47, 6486−6492.

(8) Krishnamoorthy, G.; Sadulla, S.; Sehgal, P. K.; Mandal, A. B. Greener approach to leather tanning process: D-Lysine aldehyde as novel tanning agent for chrome-free tanning. J. Cleaner Prod. 2013, 42, 277−286.

(9)Luo, J. X.; Li, J.; Liao, X. P.; Zhang, W. H. Shi, B. Cleaner chrome tanning- a non-pickling process using an aliphatic aldehyde as pre-tanning agent. J. Soc. Leather Technol. Chem. **2012,** 96 (1), 21-26.

(10)Lai, S. Q.; Jin, Y.; Li, HP. Zhang, L.; Jin, X. Application of Y-shaped Polyurethane and Polyacrylic Acid as a Complex Retanning Agent in Aldehyde-tanned Goat Leather. J. Am. Leather Chem. Assoc. **2017,** 112 (11), 367-376.

(11)QB/T 2955-2008. People's Republic of China light industry standard, **2008.**

(12)Jennifer, Cowan.; Malyuba, Abu-Daabes.; Sujit Banerjee. Controlling formaldehyde emissions with boiler ash. J. Environ. Sci. Technol. **2005,** 39 (13), 5101-5104.

(13)Mohammad, Tasooji.; Guigui, Wan.; George, Lewis.; Heather, Wise.; Charles, E. Frazier. Biogenic Formaldehyde: Content and Heat Generation in the Wood of Three Tree Species. J. ACS Sustainable Chem. Eng. **2017,** 5(5), 4243-4248.

(14)Wang, X. C.; Zhang, T.; Ren, L. F. A active methylene hyperbranched formaldehyde catcher and its preparation method. P. 201610149881.2.

(15)Wang, X. C.; Ren, L. F.; Luo, Y.Y. An extract of aloe vera and its preparation method as a formaldehyde catcher. P. 201010140610.3.

(16)Ren, L. F.; Wang, X. C. Study on the preparation and capture behavior of formaldehyde catcher based on collagen from leather wastes. Ph.D. Dissertation, Shaanxi University of Science and Technology, Tempe, AZ, 2009.

(17)Kakkar, R.; Kapoor, N. P.; Klabunde, J. K. Theoretical study of the adsorption of formaldehyde on magnesium oxide nanosurface: size effects and the role of low coordinated and defect sites. J. Phys Chem B, **2004**, 108, 18140 -18148.

(18)Lam, R. C. W.; Leung, M. K. H.; Leung, D. Y. C. Visible -light assisted photocatalytic degradation of gaseous formaldehyde by paralled -plate reactor coated with Cr ion-implanted TiO_2 thin film. J. Sol. Energy Mater. Sol.Cells, **2007**, 91 (1), 54-61.

(19)Zhou, Y. X.; Chen, F. X.; Chen, J. Synthesis free formaldehyde catcher with amino. J. China leather. **2006,** 35 (11), 27-33.

(20)Zhou, Y. X.; Chen, F. X.; Fan, T. Retanning and dyeing properties of free formaldehyde catcher with amino. J. China leather. **2008,** (13), 8-11.

(21) Young-Sihn. Sihn.; J. K. Guillory.; Lee E. Kirsch. Quantitation of taurolidine decomposition in polymer solutions by chromotropic acid formaldehyde assay method. J. Journal of pharmaceutical and biomedical analysis. **1997,** 16(4), 643-650.

(22) Bo-Long Poh.; Chooi Seng Lim.; Kong Soo Khoo. A water-soluble cyclic tetramer form reacting chromotropic acid with formaldehyde. J. Tetraahedron letters. **1989**, 30(8), 1005-1008.

(23) E. Fagnani.; C. B. Melios.; L. Pezza.; H.R. Pezza. Chromotropic acid-formaldehyde reaction in strongly acidic media. The role of dissolved oxygen and replacement of concentrated sulphuric acid. J. Talanta. **2003,** 60(1), 171-176.

(24) Wei shilin. Modern chinese-english dictionary of leather and fur industry; Chinese Light Industry Press: Beijing, **2010.**

(25) He, X. W.; Zhou, J. F.; Wang, Y. N. Application method and principle exploration of amphoteric polyurethane retanning agent. J. Leather science and Engineering. **2017,** 27(1), 5-12.

(26) Chen, W. Y.; Li, G. Y. Tanning Chemistry; Chinese Light Industry Press: BeiJing, 2011.

(27)He, X. W.; Zhou, J. F.; Wang, Y. N.; Shi, B. Application method and principle exploration of amphoteric polyurethane retanning agent. J. Leather Science and Engineering. **2017,** (1), 5-12.

(28)Li, H. P.; Jiang, W. L.; Fan, B. Z.; Jin, Y. Research progress and development trend of waterborne polyurethane retanning agent. J. China leather. **2016,** (6), 62-69.

(29)Ren, Z. Y.; Liu, L.; Wang, H. F.; Fu, Y.; Jiang, L.; Ren, B. X. Novel amphoteric polyurethane dispersions with postpolymerization crosslinking function derived from hydroxylated tung oil: synthesis and properties. J. RSC advances. **2015,** 5 (35), 27717-27721.

(30)Qiao, Y.; Zhang, S. F.; Lin, O.Stabilized micelles of amphoteric polyurethane formed by thermoresponsive micellization in HCl aqueous solution. J. Langmuir. **2008,** 24 (7), 3122-3126.

(31) IUP 2. Sampling. J. Soc. Leather Technol. Chem. **2000,** 84, 303−309.

(32) QB/T 19941-2005. Leather−Chemical tests-Deetmrination of formadehude in leather. The light industry standards of the People's Republic of China, **2005.**

(33) Liu, Y. Q. Modern Instrumental Analysis; China Higher Education Press: Beijing, 2006.

(34)Wang, X. C.; Shang, Y. M.; Ren, L. F.; Zhang, S. F.; Guo, P. Y. Preparation and surface sizing application of sizing agent based on collagen from leather waste. J. Bioresources. **2015,** 10 (4), 7220-7231.

(35)Ma, J. Z.; Gao, J. J.; Wang, H. D.; Lyu, B.; Gao, D. G. Dissymmetry gemini sulfosuccinate surfactant from vegetable oil: a kind of environmentally friendly fatliquoring agent in the leather industry. J. ACS Sustainable Chem. Eng. **2017,** 5, 10693-10701.

(36) Hannah, C.; Wells, R. L.; Edmonds, N, K.; Adrian, H.; Stephen T. M.; Richard G. H. Collagen fibril diameter and leather strength. J. Agric. Food Chem. **2013,** 61 (47), 11524–11531.

O23

New insights into chrome tanning: When structure meets protein chemistry

Sujay Prabakar

Leather and Shoe Research Association of New Zealand, P.O. Box 8094, Palmerston North 4472, New Zealand (Phone: +64212386743, Email: sujay.prabakar@lasra.co.nz)

Abstract

Chrome tanning in its classical sense is the formation of covalent complexes between carboxyl groups of the collagen with the chromium (III) ions. However, many factors contribute to the stabilization of the collagen matrix in hides and skins during leather making. Using molecular level indicators from techniques such as SAXS (X-ray scattering), SANS (neutron scattering) and proteomics we have studied the interactions of chrome with collagen. Aspects such as hydrothermal stability, role of solvents, natural cross-links, masking and the importance of bound water will be discussed.

Keywords: SAXS, Collagen Structure, Leather Tanning, Sustainability

O24

Durable and Superhydrophobic Leather Based on Reactive Amphiphilic SiO_2 Janus Particles

Yan Bao[a,b]*, Yuanxia Zhang[a,c], JianzhongMa[a,b]*

[a] *College of Bioresources Chemical and Materials Engineering, Shaanxi University of Science and Technology, Xi'an, 710021, PR, China.*

[b] *Shaanxi Research Institute of Agricultural Products Processing Technology, Xi'an, 710021, PR, China.*

[c] *National Demonstration Center for Experimental Light Chemistry Engineering Education, Shaanxi University of Science and Technology, Xi'an, 710021, PR, China.*

**Corresponding author: Yan Bao, E-mail: baoyan@sust.edu.cn;*

Jianzhong Ma, E-mail: majz@sust.edu.cn.

ABSTRACT

The ideal superhydrophobic coatings on leather are of interest for high water contact angle, low contact angle hysteresis, high wear resistance and antismudge properties. However, they are suffering from two problems. On the one hand, the existing superhydrophobic coatings are poor robustness for application. On the other hand, fabrication of superhydrophobic coatings on leather surface is not easy due to current methods including some harsh environment such as strong acid and base, high temperature and the like, which is unacceptable to leather. In this paper, we propose an alternative approach for durable and superhydrophobic leather based on an reactive amphiphilic SiO_2 Janus particles. First, we developed the reactive amphiphilic SiO_2 Janus particles by thiol−ene click reaction, on which one face functionalized with hydrophobic 1-dodecanethioland the other face functionalized with hydrophilic β-mercaptoethylamine. Further, superhydrophobic leather were obtained by spraying the reactive amphiphilic SiO_2 Janus particles on the leather treated with polyurethane prepolymer. The durability and superhydrophobicity of the as-prepared leather were characterized by contact angle and wear resistant test. High contact angle of 179° revealed the formation of superhydrophobic leather. Furthermore, wear test demonstrated the as-prepared leather still retained excellent hydrophobicity with contact angle of 168° after cycling 300 times. This work provides a simple and feasible way for the fabrication of durable and superhydrophobic leather.

Keywords: Superhydrophobic; robustness; leather; amphiphilic SiO_2 Janus; reactive

1. INTRODUCTION

Inspired by nature, researchers have attracted extensive attention for engineer superhydrophobic surfaces due to their special wettability[1]. This special wettability not only endows the solid surface with excellent water resistance, but also makes it of great application value in the fields of self-cleaning[2], anti-icing[3], oil-water separation[4] and pipeline transportation resistance reduction[5]. To satisfy the practical applications of superhydrophobic surfaces in various fields, many methods for fabricating durable and superhydrophobic surface have been developed[6-8]. However, few studies on superhydrophobic leather have been done due to current methods including some harsh environment such as strong acid and base, high temperature and the like, which is unacceptable to leather. In our earlier studies[9], we put forward a facile spraying method to fabricate superhydrophobic leather coating via spraying polyacrylate emulsion and spraying ethanol dispersion of hydrophobic silica nanoparticles separately. The water contact angle of leather was as large as 170.3°. Unfortunately, as-obtained leather coating possesses poor wear resistance and unabiding hydrophobicity, which is attributing to weak physical combination between silica nanoparticles and polyacrylate emulsion. Hence, it is necessary to develop versatile approaches to prepare durable and superhydrophobic leather

In recent years, Janus colloidal particles with anisotropy have been widely investigated both theoretically and technologically due to excellent properties of mechanical[10], magnetic[11], optical[12], electrical[13] and special wettability[14], etc. Nevertheless, few studies have been done to fabricate a superhydrophobic coating using amphiphilic Janus particles. Synytska[15] et al. proposed an alternative approach for the modification of textiles with water contact angle

of about 140°, which is based on the use of amphiphilic Janus particles. It arouses us awareness of developing a amphiphilic Janus particles to fabricate superhydrophobic leather.

Inspired by the above works, reactive amphiphilic hollow SiO_2 Janus particles have been first fabricated successively in combination with click chemistry and Pickering emulsion methods, on which one face functionalized with hydrophobic 1-dodecanethiol and the other face functionalized with hydrophilic β-mercaptoethylamine. Further, durable and superhydrophobic leather was constructed by layer-by layer spraying, which is based on the use of amphiphilic Janus particles. We speculated that chemistry crosslinking will happened between reactive hydrophilic segments of amphiphilic Janus particles and hydrophilic base material by hydrophilic and hydrophobic interactions, and durable and superhydrophobic leather will be obtained.

2. RESULTS AND DISCUSSION

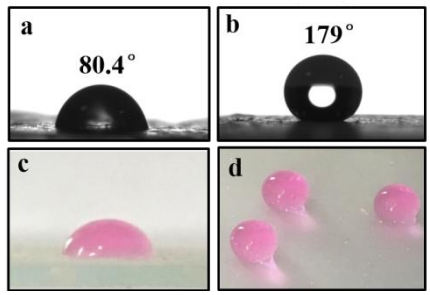

Figure 1. (a) Water droplet contour on the leather coating prepared by polyurethane prepolymer; (b) Water droplet contour on the leather coating prepared by polyurethane prepolymer and Janus NPs; (c) Photograph of water droplet (dyed with rhodamine B) on the leather coating prepared by polyurethane prepolymer; (d) Photograph of water droplet (dyed with rhodamine B) on the leather coating prepared by polyurethane prepolymer and Janus NPs.

As seen from Fig 1, the leather coating prepared by polyurethane prepolymer with a contact angle 80.4° is hydrophilic. Nevertheless, the leather coating prepared by polyurethane prepolymer and Janus NPs with a contact angle 179° is superhydrophobic. The physical photographs have been shown in Fig 1c and 1d, respectively. It reveals that amphiphilic SiO_2 Janus NPs is a candidate to fabricate superhydrophobic coating.

Wear durability is the main issue for limiting the widespread practical applications of superhydrophobic surfaces. Sandpaper abrasion tests were employed to evaluate the wear durability of the leather coating. After 50 cycles of abrasion in the sandpaper abrasion test in Fig 2, the coating shows a water contact angle of 168.6°. It still remains superhydrophobicity and its water contact angle is at 168° after 300 cycles, which indicates that the superhydrophobic behavior is resistant to mechanical forces.

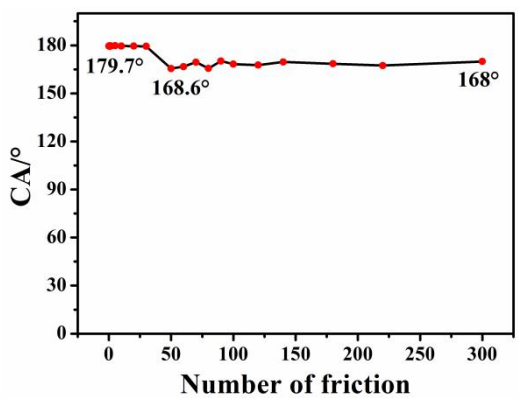

Figure 2. Contact angle of the leather coatings with the number of abrasion cycles.

In summary, on the basis of a spraying technique, superhydrophobic leather coating could be easily achieved by amphiphilic SiO_2 Janus NPs. As a result, as-obtained leather coating is superhydrophobic and the mechanical durability of the coating is well improved with asymmetric structure of amphiphilic Janus NPs. This study provides a facile method for the structure design of amphiphilic SiO_2 Janus NPs to meet its application requirements on superhydrophobic leather coating.

REFERENCES

[1] Jiang C, Liu W. Q, Yang M. P, Liu C. H, He S, Xie Y.K, Wang Z.F. Robust multifunctional superhydrophobic fabric with UV induced reversible wettability, photocatalytic self-cleaning property, and oil-water separation via thiol-ene click chemistry[J]. Applied Surface Science, 2019, 463: 34-44.

[2] Xue X, Yang Z, Li Y.Y, Sun P.C, Feng Y, He Z.Y, Qu T.J, Dai J.G, Zhang T, Qin J, Xu, L.J, Zhang W.D. Superhydrophobic self-cleaning solar reflective orange-gray paint coating[J]. Solar Energy Materials and Solar Cells, 2018, 174: 292-299.

[3] Wang N, Xiong D.S, Deng Y.L, Shi Y, Wang K. Mechanically robust superhydrophobic steel surface with anti-icing, UV-durability, and corrosion resistance properties[J]. ACS Applied Materials & Interfaces, 2015, 7(11): 6260-6272.

[4] Qiang F, Hu L. L, Gong L.X, Zhao L, Li S.N, Tang L.C. Facile synthesis of super-hydrophobic, electrically conductive and mechanically flexible functionalized graphene nanoribbon/polyurethane sponge for efficient oil/water separation at static and dynamic states[J]. Chemical Engineering Journal, 2018, 334: 2154-2166.

[5] Wu Y, Zhao M, Guo Z. Multifunctional superamphiphobic SiO_2 coating for crude oil transportation[J]. Chemical Engineering Journal, 2018, 334: 1584-1593.

[6] Li C.L, Sun Y.C, Cheng M, Sun S.Q, Hu S.Q. Fabrication and characterization of a TiO_2/polysiloxane resin composite coating with full-thickness super-hydrophobicity[J]. Chemical Engineering Journal, 2018, 333: 361-369.

[7] Qu J, Yu C.Q, Cui R.J, Qin J, Wang H.R, Cao Z.Y. Preparation of super-hydrophobic and corrosion resistant colored films on chemically etched 304 stainless steel substrate[J]. Surface and Coatings Technology, 2018, 354: 236-245.

[8] Bellanger H, Darmanin T, Taffin de Givenchy E, Guittard F. Chemical and physical pathways for the preparation of superoleophobic surfaces and related wetting theories[J]. Chemical Reviews, 2014, 114(5): 2694-2716.

[9] Ma J.Z, Zhang X.Y, Bao Y, Liu J.L. A facile spraying method for fabricating superhydrophobic leather coating[J]. Colloids and Surfaces A: Physicochemical and Engineering Aspects, 2015, 472: 21-25.

[10] Shi W, Wang Z. Mechanical and electronic properties of Janus monolayer transition metal dichalcogenides[J]. Journal of Physics: Condensed Matter, 2018, 30(21): 0953-8984.

[11] Song Y, Zhou, J, Fan J.B, Zhai W, Meng J, Wang S. Hydrophilic/Oleophilic magnetic Janus particles for the rapid and efficient oil–water separation[J]. Advanced Functional Materials, 2018: 1802493-1802496.

[12] Wang J, Shu H.B, Zhao T.F, Liang P, Wang N, Cao D, Chen X.S. Intriguing electronic and optical properties of two-dimensional Janus transition metal dichalcogenides[J]. Physical Chemistry Chemical Physics, 2018, 20(27): 18571–18578.

[13] Yang J, Zhang J.X, Li X.L, Zhou J.W, Li Y.P, Wang Z.P, Cheng J.L. Guan Q, Wang B. Single Janus iodine-doped rGO/rGO film with multi-responsive actuation and high capacitance for smart integrated electronics[J]. Nano Energy, 2018, 53: 916-925.

[14] Miller K, Tsyrenova A, Anthony S.M, Qin S.y, Yong X, Jiang S. Drying mediated orientation and assembly structure of amphiphilic Janus particles[J]. Soft matter, 2018, 14(33): 6793-6798.

[15] Synytska A, Khanum R, Ionov L, Cherif C, Bellmann C. Water-repellent textile via decorating fibers with amphiphilic Janus particles[J]. Acs Applied Materials & Interfaces. 2011, 3: 1216-1220.

O25

Consumer Complaint and Trend of Formaldehyde Content After Sales

DAISUKE MURAI

Consumer Product End-use Research Institute Co.,Ltd. Edobori 2-1-1-20F, Nishi-ku, Osaka, 550-0002, JAPAN, +81-6-6445-4674, csyh499@dnt.daimaru.co.jp

Abstract

Today, 'Japan Eco Leather' is gradually taking root since 2009. It is establishment that the definition of safety leather in JAPAN. Leather products are generally checked only in manufacturing. For safety, is it enough? We think, especially safety measures should be implemented at all stage, from manufacturing, sales, using to trash. Especially, anxiety is remained in sales and consumption stage, for example, migration from other clothes in stock at closet. This is the essential factor, when we consider the safety of leather products.

Then, we have two approaches to this problem, some simple experiments and survey our exclusive database on the customer's opinions of a major department store chain in Japan. Firstly, we tried to clear the characteristics of HCHO, on increasing and decreasing from leather, as time passes. For example, the leather many HCHO content left at outdoors, and measured the change of HCHO content, periodically. Secondary, we have the exclusive customer's opinion database. The database records more than 20000 for leather goods alone, and since 1998. Each record has offer details, and some records have scientific test results and views of engineers. We performed the database survey, and computed the incidence of skin disorders, by time series and products groups.

By above two items, we have a conclusion that the risk of skin disorders is highest at first time wearing, and the skin disorder will disappear with the passage of time from first time wearing. And, over time, the risk of skin disorders by HCHO gradually decreases. After all, in leather products, it seems that HCHO check may be enough at the time of manufacturing.

Keywords: HCHO skin disorder leather product safety

1. Introduction

Over the past several years, we have reported the basic characteristics of leather formaldehyde, transfer characteristics, practical tests at dealerships and general households separately for each theme, but this time we will compile them collectively. Also, by analyzing our own exclusive customer database, the actual situation on skin disorders became clear, so we will also report this. Through these investigations, we would like to discuss whether quality control on formaldehyde of leather products is sufficient at the manufacturing stage or whether the risk of skin disorders remain in sale or consumption stage.

We hope these studies will be utilized in a way that contributes to the development of the leather industry.

2. Material and methods

2-1. Air Concentrations at Stores

At the sales area in operation, we collected the air near the aisle for 30 minutes at 200 mL/min using the following sampling pump.

GL Science Sampling Pump SP208 1000 Dual

Also, the following two types of detection tubes were installed at 1.2m height from floor.

GASTEC detection tube 91P and 91PL

2-2. Storage at Sales Store Condition

2-2-1. Method

At the sales area in operation, we installed five polypropylene racks (width 14 cm x depth 34 cm x height 6 cm) in layers. And we kept leaving the samples for 1 month while setting the samples in each rack.

Meanwhile, every week, the samples were taken from store to our laboratory and the HCHO content was measured. We use the Acetylacetone colorimetric method based on Japanese law “Act on household products containing hazardous substance”.

2-2-2. Materials

Leather A: Black leather tanned by glutaraldehyde and vegetable tannin

Leather B: White leather tanned by formaldehyde

2-3. Storage at Home Condition

2-3-1. Method

We selected two site to investigate from dwellings actually living. Both are places where clothing items actually being used are stored. In the wardrobe case, the family is home during the day. And closet case, the family is absent during day while it is indoor environment closed.

We installed five polypropylene racks (width 14 cm x depth 34 cm x height 6 cm) in layers. And we kept leaving the samples for 1 month while setting the samples in each rack.

Meanwhile, every week, the samples were taken from store to our laboratory and the HCHO content was measured. We use the Acetylacetone colorimetric method based on Japanese law “Act on household products containing hazardous substance”.

2-3-2. Materials

Leather A: Black leather tanned by glutaraldehyde and vegetable tannin

Wool: ISO 105-F01:2001， Textiles−Tests for colour fastness−Part F01: Specification for wool adjacentfabric

2-4. Storage for long time

2-4-1. Storage Separately

To prevent the sample leathers from contacting with or overlapping with each other, it was placed in a wide room controlled at 20°C 65%RH for 3 months.

2-4-2. Storage Mixed

To mix the sample leathers in contact with each other, we randomly throw them into a corrugated cardboard box and stir them. After that, it was left in a room controlled at 20°C 65%RH for 3 months.

2-4-3. Measuring HCHO Content

We use the Acetylacetone colorimetric method based on Japanese law “Act on household products containing hazardous substance”.

2-4-4. Material

Sample leather is the cowhide wet-blue re-tanned with synthetic tannin and fatliquored. By changing the type of synthetic tannins, leather with different amount of formaldehyde is adjusted.

2-4-5. Left Outdoor

The sample leathers are hung at eaves of apartment house’s balcony in Japan and left for a certain period in winter.

To measure HCHO content, we use the Acetylacetone colorimetric method based on Japanese law “Act on household products containing hazardous substance”.

2-5. Effect of Storage Conditions

Leaving the sample leathers on the mesh rack in temperature and humidity testing chamber for a certain period. To prevent concentration of formaldehyde released from the sample leather, a simple device is installed to guide the air in chamber to water tank. This device is electric controlled and adjust to process the entire volume of the chamber.

To measure HCHO content, we use the Acetylacetone colorimetric method based on Japanese law “Act on household products containing hazardous substance”.

2-6. Effect of contact with other leather

In the room kept at 20°C 65%RH, the sample leather is placed on the white leather tanned by formaldehyde so that the respective surface are in contact with each other, and it is left for a certain period.

To measure HCHO content, we use the Acetylacetone colorimetric method based on Japanese law "Act on household products containing hazardous substance".

The sample leathers are following:

Baseball Glove Leather is tanned by chromium agent and thickness is 2.6 mm.

Vegetable Tannin Leather is commercial leather and thickness is 1.5 mm

Enamel Finished Leather is cut from commercial bag and thickness is 1.4 mm.

White Leather is tanned by formaldehyde for baseball ball and thickness is 1.8 mm.

2-7. Actual Condition of Product Complaints

Our customer's complaint received at the customer service center is collected to our exclusive database. From the database, we extract statistical analyzes.

The scope is 10 department stores in Japan, and it is a product complaint received in recent 10 years from 2008 to 2017. Furthermore, the total 14,707 cases including textiles, leather goods, living goods are analyzed.

But physical skin disorders and chemical skin disorders are all the same and are not distinguished. The record is based on the customer's declaration, and in all cases the cause of skin disorder and the problem of products have not been elucidated. It is not limited only to skin damage caused by formaldehyde. Also, the item discontinued and already improved item, now corresponding offers are included.

3. Results and Discussion

3-1. Air Concentrations at Stores

We measured the air concentrations of HCHO at various places in several Japanese department stores. The stores are 6 branches, located in Tokyo, Nagoya, Osaka, Kobe areas. See the table.1, every measured points are under 0.08 ppm at 23°C (WHO guideline and Japanese law regulation). Temperature and humidity are also measured and ranged from 23°C to 27°C, and 34%RH to 51%RH. Temperature and humidity had little change in business hours and closed time.

These results indicate, the concentration of formaldehyde in room air of sales floors are very low.

Table.1 The Air Concentrations of HCHO in department stores

Measured Floors	Results	Number of measurement points
Women's Clothing	0.04ppm	2
Women's Underwear	0.02ppm	1
Women's Shoe	0.03ppm	3
Men's Underwear	0.03ppm	5
Men's Shoe	0.02ppm	1
Children's Clothing	0.03ppm	5
In-store Wearhouse	0.04ppm	2

3-2. Storage at Sales Store Condition

Furtherly, we conducted small experiments at sales spaces in department stores. Two kinds of leather were left for long time. We had cut the samples and measured HCHO content as soon as possible. The results show that the HCHO content in the sample leathers does not increase in the sales stores. These results are consistent with the actual air concentrations described above. As far as the experimental environment is concerned, we could not confirm the actual condition of formaldehyde migration from other clothing to leather.

Table.2 The Change of HCHO content (Sales Store Storage)

Sales Floor	Samples	Initial	7 Days	14 Days	21 Days	28 Days
Children's Clothing	Leather A	>16	>16	>16	>16	>16
Men's Underwear	Leather B	316	240	212	191	173

Leather A: Black leather tanned by glutaraldehyde and vegetable tannin

Leather B: White leather tanned by formaldehyde

3-3. Storage at Home Condition

Next, we measured, the changes of HCHO content in the leathers were investigated at storage places in general homes. We investigated the change of HCHO content in leather by leaving the sample leathers in wardrobe and closet in actual use. The results show that the contents of sample leathers did not increase during storage at home. As far as the experimental environment is concerned, we could not confirm the actual condition of formaldehyde migration from other clothing to leather.

Table.3 Change of HCHO content (Home Storage)

Storage	Samples	Initial	7 Days	14 Days	21 Days	28Days
Wardrobe	Leather A	>16	>16	>16	>16	>16
	Wool	>16	>16	18	20	24
Closet	Leather A	>16	>16	>16	>16	>16
	Wool	>16	18	25	34	38

3-4. Storage for long time

In search of the possibility of HCHO migration from other leather during storage and using, we continued the experiments in other ways. As I will be described in details later, as far as the experimental results are concerned, the HCHO content in the sample leathers has almost decreased for long time, regardless of the storage conditions. From long-term perspective, these results indicate that the effect of HCHO migration from other garments is small.

3-4-1. Storage Separately

We investigated the changes of HCHO content in the leathers, when the random 23 types of leathers were left one by one. Storage conditions were wide room with 20°C, 65%RH, constantly. Three months later, HCHO emitted from most the sample leathers, and HCHO content was decreased.

Table.4 Change of HCHO content (Storage Separately)

Samples	Increased after 3 months	Decreased after 3 months
>16 at initial	1	9
16 to 75 at initial	2	2
75 to 300 at initial	0	7
300 over at initial	0	2

3-4-2. Storage Mixed

The next experiments are, when the random 51 types of leathers (using other leathers above mentioned, 4-4-1) were mixed in a box and were left. Storage conditions were wide room with 20°C, 65%RH, constantly. Three months later, despite the different types of the sample leathers, HCHO emitted from most the sample leathers, and HCHO content was decreased, similar trends were seen.

Table.5 Change of HCHO content (Storage Mixed)

Samples	Increased after 3 months	Decreased after 3 months
>16 at initial	3	28
16 to 75 at initial	1	7
75 to 300 at initial	0	8
300 over at initial	0	4

3-4-3. Left Outdoor

Subsequently, changes in HCHO content when the sample leather was left outdoor were examined. In the result for 21 days, it is found that formaldehyde emit from leather and HCHO content decreases. Even in winter in Japan that was actually cold and dry, it was confirmed that HCHO content in leather decreased as time passed, similar to our indoor experiment results.

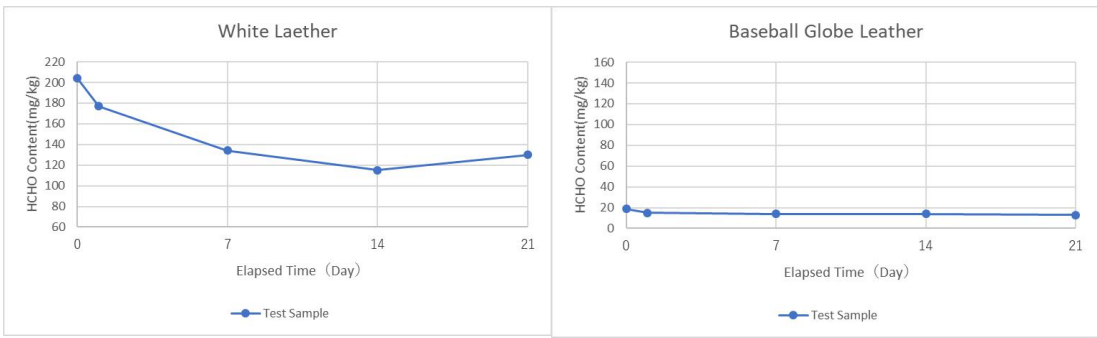

Fig.1 Change of HCHO content (Left Outdoor)

3-5. Effect of Storage Conditions

Furthermore, we investigated about the effect of the storage environments, for example temperature and humidity. We measured how HCHO content of the same leather changed during storage, in case of several temperature and humidity. The results were that, if the temperature and humidity are greater, the formaldehyde is emitted easier. It indicates that formaldehyde trends to be easier to emit in hot and humid summers than in winter.

Table.6 Change of HCHO content after 72H (Effect of temperature and humidity)

	20%RH	50%RH	80%RH
Initial	114		
10°C	91	71	74
20°C	71	-	38
30°C	87	91	34

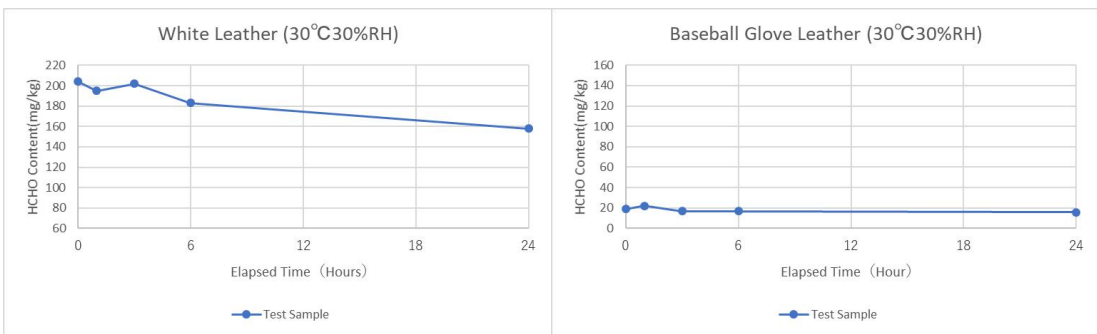

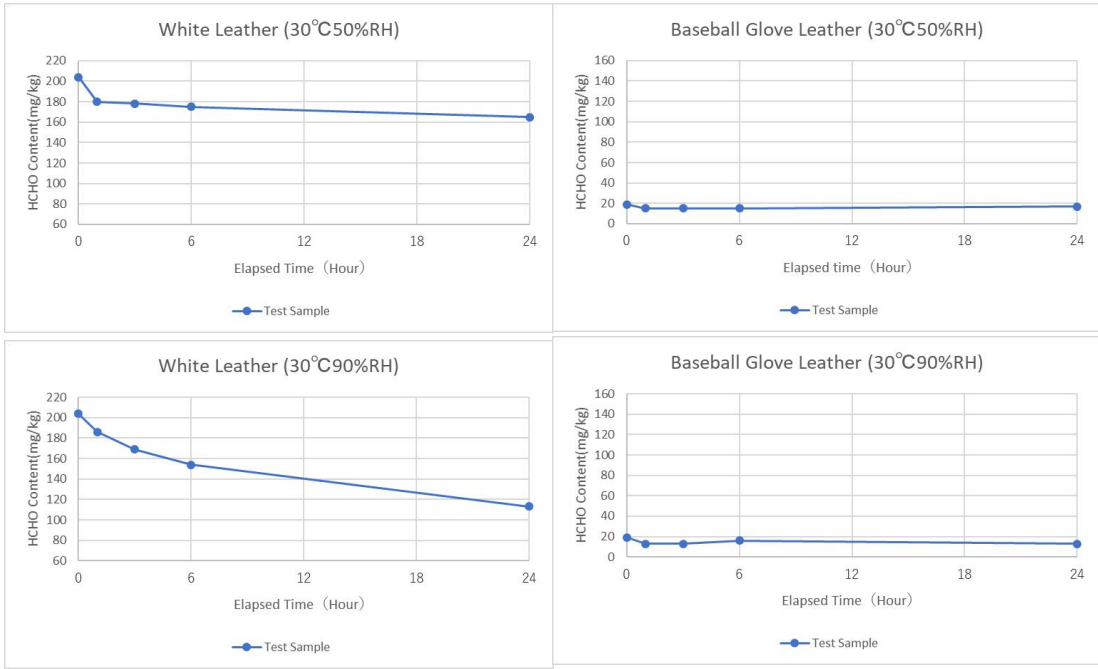

Fig.2 Change of HCHO content (Effect of humidity)

3-6. Effect of contact with other leather

Assuming a case of contact with other leather garments during storage, we investigated the change in HCHO content before and after contact. As our results,, it was found that formaldehyde increased up to a certain limit (about 30 mg/kg) due to the influence of transfer by contact. And, from the result of enamel finished leather, the finish coating seemed to block formaldehyde. From these results, it seems that the influence of migration caused by contact during storage is not so serious.

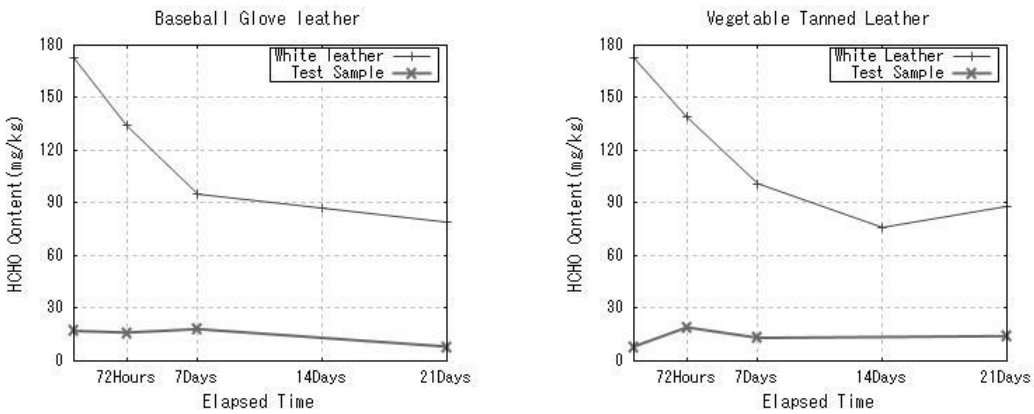

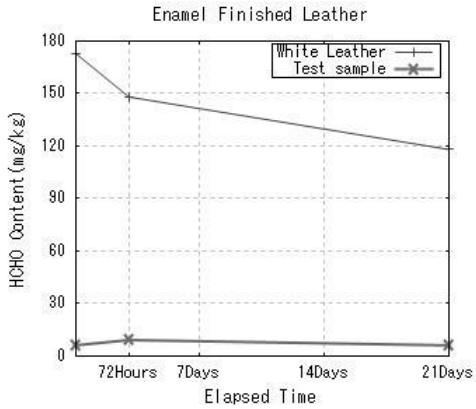

Fig.3 Change of HCHO content (Migration by contact with White leather)

3-7. Actual Condition of Product Complaints

Finally, we show actual our customer's complaints received at Japanese department stores in the last 10 years. The number of skin disorders is small, and the composition ratio is roughly 1% or less. Compared to products using other materials such as textile products, there is no feature seen only in leather products, and similarly the number of skin disorder is small.

In case of leather products, complaint for skin disorders were confirmed in women's shoes (with lots of sales and lots of product complaints) and watch bands (in direct contact with the human skin at wearing).

Table.7 Offered number of skin disorders in the past 10 years

Product Classifications	01: Leather		Textile and Other	
	Skin Disorder	Other	Skin Disorder	Other
01: Women's Coat	0	12	3	827
02: Women's Cloth（Outer）	0	4	11	735
03: Women's Skirt and Pants	0	1	6	659
11: Men's Coat	0	2	1	181
12: Men's Cloth（Outer）	0	4	4	586
31: Leather Garment	0	68	0	71
35: Leather Goods	0	39	1	33
50: Women's Shoes	15	808	17	1098
51: Men's Shoes	2	206	2	168
55: Bags	0	483	5	882
57: Belts	0	104	0	63
58: Leather and Synthetic Accessories	0	157	0	89
63: Watch and Watch Band	4	14	3	111
70: Furniture	0	5	4	61
Total	21	1907	57	5564

The analysis results on the time when we received a offer for skin disorder are shown in Fig.4 and Fig.5. Although the

population is small, the composition within one year is large. And the composition in a short period such as one month after sales tend to be largest.

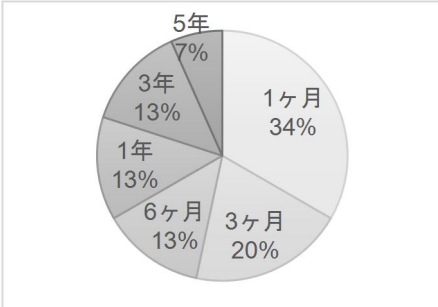

Fig.4 Period of offering skin disorder (Women's Shoes)

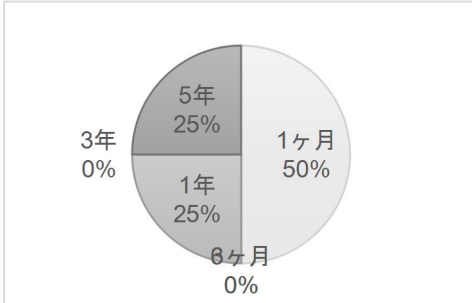

Fig.5 Period of offering skin disorder (Watch and Watch Band)

4. Conclusion

We confirmed the safety of leather products throughout the entire life cycle from manufacture to distribution and consumption and found the following conclusion.

1) Formaldehyde in the leather has become clear that it tends to decrease naturally with the passage of time basically.
2) As a result of analyzing declarations from our customers, we found that product complaints concerning skin disorders are as small as 1% or less of the total.
3) Furthermore, there are not many skin disorders related to leather products compared to other fields such as textile products.
4) The declaration of skin disorders related to leather goods was mostly in the early stage of use as soon as they were purchased. Compared with the time of purchase, products used for years, apparently seemed to be at a lower risk of skin disorders.
5) Formaldehyde in the leather may increase once due to external migration, but the amount of increase is small, not so large as to change the level of safety.
6) Because it does not wear leather apparel in summer, it is not related to general consumers much, but formaldehyde in leather was found to be more easily emitted as temperature and relative humidity are higher.
7) Furthermore, a thick finish coating like enamel finished leather is likely to block migration of formaldehyde from the outside.

From the above, at the beginning of the project, leather is porous and thick, and could not be washed with water, so we are concerned that formaldehyde would migrate from the outside at the consumption stage, but the risk seemed to be low enough although it is not zero.

Furthermore, the risk of skin disorder of leather products is the highest at the time of purchase, and it is found that the risk gradually declined with the passage of time. Therefore, it is sufficient to control the amount of formaldehyde at the manufacturing stage and it is considered efficient. We regard this as the conclusion of this survey.

5. Acknowledgement

We gratefully acknowledge the work of past and present member of our company, and Daimaru Matsuzakaya Department Stores Corp., Japan Association of Leather Technology (JALT).

6. References

1. JALT : Development and Practical Application Report for Japanese eco-leather (2008-2017)

O26

Development of a Novel Biomass Wood Adhesive Basedon Gelatin and Oxidated Chitooligosaccharide Crosslinked Waterborne Polyurethane

Xuechuan Wang[1,2*], Sixiao Zhang[1,2], Xinhua Liu[1,2], Xiaomei Lan[1,2]

[1]*College of Bioresources Chemical and Materials Engineering, Shaanxi University of Science &Technology, Xi'an 710021,China, TEL: 15802958501, E-mail: 15802958501@163.com*

[2]*National Demonstration Center for Experimental Light Chemistry Engineering Education ,Shaanxi University of Science & Technology, Xi'an 710021, China, TEL: 15802958501, E-mail: 15802958501@163.com*

Abstract:

Biomass-based adhesives are the focus of research and development in the future wood adhesive industry. In this study, the oxidated chitooligosaccharide(OCOS) with chemical-active aldehyde groups was obtained after the oxidation process of safe and non-toxic chitooligosaccharide(COS) by sodium periodate, and then OCOS was used as crosslinker to prepare oxidated chitooligosaccharide crosslinked waterborne polyurethane(OCOS-WPU). The adhesive was prepared through bridging the active aldehyde group and amino group of OCOS-WPU and industrial gelatin(INGE), which was called INGE/OCOS-WPU, and the application of INGE/OCOS-WPU on wood was further studied. Fourier transform infrared spectroscopy(FT-IR) and Ultraviolet-visible spectroscopy(UV-vis) analysis showed that the OCOS was successfully prepared and its aldehyde group content was determined to be 70% by hydroxylamine hydrochloride method. The effect of OCOS-WPU on INGE/OCOS-WPU adhesive was characterized by FT-IR, X-raydiffraction(XRD), thermogravimetric analysis(TG), and shear strength. The results indicate that OCOS has been successfully crosslinked with waterborne polyurethane to prepare OCOS-WPU, and the aldehyde group of OCOS-WPU could further react with the amino groups of INGE through Schiff's base. Compared with pure gelatin, the crystallinity of INGE/OCOS-WPU was reduced. Meanwhile, the wet shear strength increased to 1.05MPa(the wet shear strength of pure gelatin was 0MPa). The increase of wet shear strength indicates that the addition of OCOS-WPU can improve the adhesion and water resistance of INGE adhesive on wood. The TG results show that the thermal stability of the INGE/OCOS-WPU adhesive in the range of use was greatly enhanced.

Key words: oxidized chitooligosaccharide, waterborne polyurethane, industry gelatin, adhesive

1. Introduction

Collagen is a widely used natural polymer material, which is widely found in the extracellular matrix such as skin, Achilles tendon and blood vessels[1]. The leather industry produces a large amount of leather corner waste, which can be directly used to produce gelatin, feed, etc. Gelatin is a water-soluble protein produced by partial hydrolysis or denaturation of collagen, and its triple helix structure is partly destroyed[2]. As a natural polymer material with excellent compatibility and degradability, high quality bio-grade gelatin is widely used in biomedicine[3], tissue engineering scaffolds[4] and other fields. The tannery industry produces large amounts of leather corner waste (including chromium-containing and chromium-free waste) that can be used directly to produce gelatin. Gelatin produced from chromium-containing waste was used in the illegal production of "poison capsules" and "leather milk". The trivalent chromium is oxidized to hexavalent chromium, which can cause cancer and greatly endanger human health. Therefore, the use of industrial gelatin as a raw material to prepare wood adhesive with great demand, it not only realizes the reuse of waste resources and turns waste into treasure; but also avoids the occurrence of "toxic capsules" and "leather milk" incidents to a certain extent. What is more noteworthy is that gelatin itself has a certain degree of stickiness, which has a certain advantages in the preparation of adhesives. However, the defects such as low water resistance and poor mechanical properties limit its wide applications [5-6]. Therefore, gelatin must be modified to meet the needs of the human social production and living. Gelatin molecular chain contains a great deal of $-NH_2$, -OH, -COOH et.al, which can provide active sites for its modification.

Chemical modification is an effective way to improve the water resistance and mechanical properties of natural

protein materials by introducing stable covalent bonds between protein fragments [7]. The chemical modification of gelatin is generally to introduce other polymer chain segments on the molecular backbone to improve the water resistance and adhesive strength of gelatin adhesives. Polyurethane (PU) is a excellent performance polymer material formed by the polymerization of isocyanate and active hydrogen compounds. PU has a certain degree of softness. The use of polyurethane or polyurethane prepolymers to modify gelatin can improve the shortcomings of the hard and brittle of gelatin film. SE Kim used electrospinning to prepare a gelatin/PU hybrid nanofiber scaffold for wound dressings.With increasing of the amount of PU, the elasticity of the material will be inscreased. Meanwhile, when the amount of gelatin increases, the cell proliferation will be inscreased with the increase of culture time [8]. It shows that the introduction of PU can improve the shortcomings of hard and brittle of gelatin film, and the gelatin material has biocompatibility and does not produce toxicity. PU itself also has a certain stickiness. Waterborne polyurethane (WPU) uses water as a dispersant, which reduces the solvent to the environmental pollution to a certain extent. It has great advantages in terms of environmental protection, energy conservation, and mechanical properties. In order to successfully introduce the high molecular polyurethane into the gelatin molecular chain, a multifunctional cross-linking agent is required, which can be used as a "molecular bridge" to combine polyurethane with gelatin. Yabin used surface modification technology to graft bioactive macromolecule gelatin onto the polyurethane skeleton using glutaraldehyde as a coupling agent, which is conducive to enhancing cell-material interaction [9]. The chitooligosaccharide (COS) is a degradation product of chitosan chemistry and enzymatic hydrolysis. It is also the only large number of alkaline aminooligosaccharides in natural sugars. It has the advantages of good water solubility, safety and non-toxic [10]. The COS could be oxidized with sodium periodate, and the carbon at the 2,3-position of the COS is partially or completely oxidized to aldehyde groups. The oxidation product is called oxidized chitooligosaccharide (OCOS) [11]. Water-borne polyurethane with active aldehyde groups was prepared through the cross-link reaction between Part of hydroxyl groups and amino groups on the OCOS molecular chain and isocyanate groups of polyurethane prepolymers, the active aldehyde groups can react with amino groups on the gelatin molecular chain. Therefore, OCOS can be used as a crosslinking agent for bridging waterborne polyurethanes and industrial gelatin to make adhesives, and the adhesive itself and its glue products with will not release free formaldehyde in the process of use, and safe and nontoxic.

Based on the above, the subject uses the industrial gelatin (INGE) extracted from waste leather as raw material, and OCOS was used as a molecular bridge. Further, OCOS cross-linked waterborne polyurethane (OCOS-WPU) was used as a crosslinker to modified INGE for preparing adhesives. Meanwhile, the structural characterization and performance detection of the adhesives were carried out.

2. Materials and methods

2.1. Materials

Industrial gelatin (INGE) was extracted from leather solid wastes. chitooligosaccharide (COS) with the molecular weight of <1 kD was purchased from Sinopharm Chemical Reagent Co., Ltd. Sodium periodate($NaIO_4$), was supplied by Tianjin Kemiou Chemical Reagent Co., Ltd. Hydroxylamine hydrochloride was purchased from Tianjin Tianli Chenmical reagents Ltd. Polytetrahydrofuran (PTMG) of the molecular weight of 1 kD and Dime thylol propionic acid (DMPA) were purchased from Shanghai Macklin biochemical science and Technology Co., Ltd. Isophorone diisocyanate (IPDI) were obtained from Shanghai Dibo Chemical Technology Co., Ltd. dibutyltion dilautate was purchased from Shanghai Qingfang Chemical Technology Co., Ltd. Poplar veneer (moisture content, 5%~8%) used for the wood test were provided by Daming Palace construction material market in Xi'an, Shannxi Province, China. All reagents except INGE used in this study were analytical grade

2.2. Preparation of OCOS, OCOS-WPU and INGE/OCOS-WPU

2.2.1. OCOS

17g of sodium periodate was placed in light-resistant container, and dissolved in 400 g of deionized water to obtain a

sodium periodate solution. 8 g of COS was stirred for 2 d in the above solution, and the whole reaction process was far away from the light environment. After the reaction completed, the product was dialyzed by using dialysis membranes of 500 MWCO for 48 h to remove excess sodium periodate, then freeze-dry, collect remaining white solid, grind and crush, and finally get OCOS. The reaction mechanism is shown in Scheme 1. The aldehyde group content of OCOS was determined by hydroxylamine hydrochloride method and calculated according to the Eq.1, and the aldehyde groups content of the OCOS was 70%.

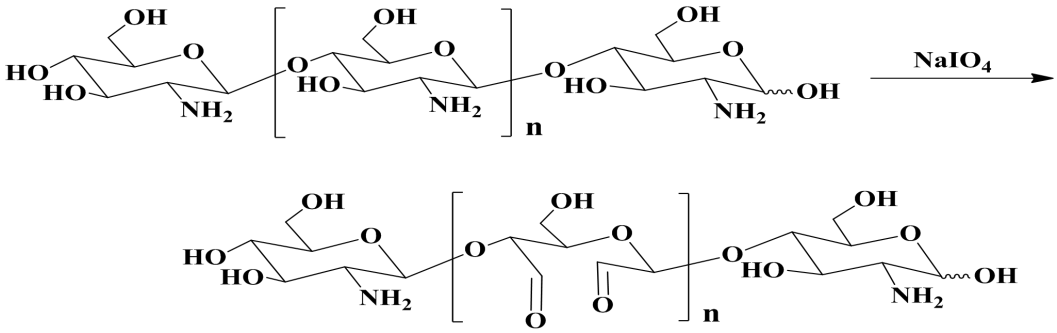

Scheme 1. Schematic diagram of OCOS by sodium periodate

2.2.2. OCOS-WPU

PTMG, IPDI and DBTDL were mixed in three-necked flask equipped with a thermometer, stirrer and condenser tube (ratio of NCO/OH was 3.5.). First, the reaction was set at 50 ℃for 20 min, then the temperature was raised to 70 ℃ for 1 h. After the reaction was completed, the temperature was raised to 80 ℃. DMPA was added to the mixed after 2.5 h, and then the measured oxidized chitooligosaccharide was introduced to continue the reaction for 1 h. The above system was cooled to 40 ℃, and then the TEA was added to neutralizethe DMPA for 30min, the viscosity was constantly adjusted with acetone throughout the experiment. Then, the temperature was cooled to room temperature. Finally, distilled water was slowly added to emulsified for 30 min under the stirring rate of 5000 r/min, and the OCOS-WPU emulsion with solid content of 25% was obtained after removal of acetone by vacuum distillation. The reaction mechanism is shown in Scheme 2.

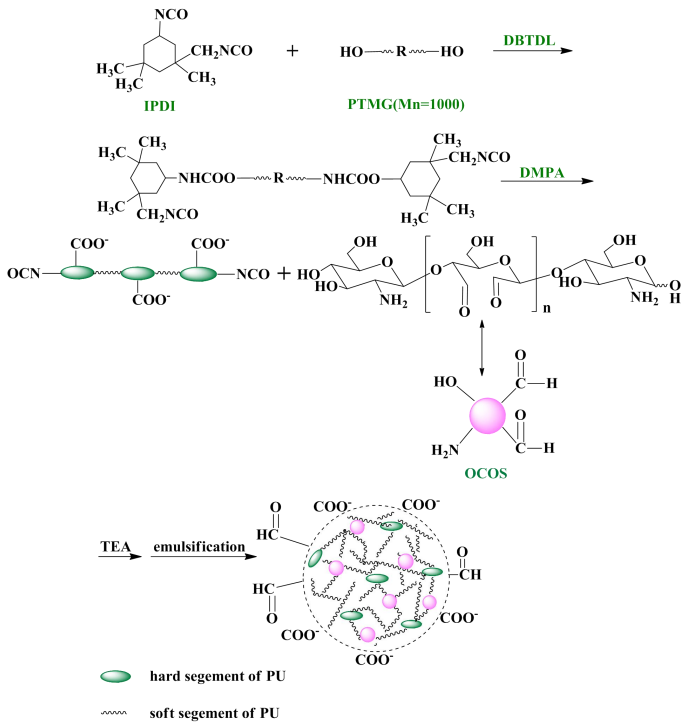

Scheme 2. Schematic representation of OCOS grafting to PU

2.2.3. INGE/OCOS-WPU

Weigh 10 g of INGE in a beaker, and add 90ml of deionized water to swell for 30min, then dissolve at 40 ℃ to obtain a gelatin aqueous solution with 10% solid content. 0%, 10%, 20%, 30%, 40%, and 50% amount of OCOS-WPU emulsion (Based on the mass of gelatin aqueous solution)was added drop by drop to the above system, which all can reacted at room temperature to obtain INGE/OCOS-WPU adhesive. The reaction mechanism is shown in Scheme 3.

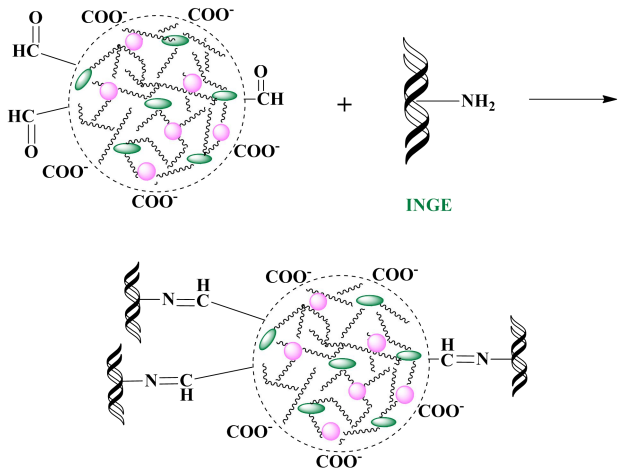

Scheme 3. Schematic representation of INGE react with OCOS-WPU

2.3. Characterization

2.3.1. Determination of OCOS oxidation degree[12]

Aldehyde group content of OCOS were obtained using hydroxylamine hydrochloride method. Weight 0.4 g of OCOS was added to the reactor equipped with a stirrer and a thermometer, added to 25 mL distilled water, adjusted pH to 5, and accurately added hydroxylamine hydrochloride reagent (0.05 g/mL, pH=5.0) at 40 ℃. After stirring for 4 h, it was then titrated to pH = 5.0 with a 1 mol/L sodium hydroxide standard solution, and a blank test that the same quality of COS was performed. The aldehyde group content was calculated by Eq.1.

$$\text{Aldehyde Group Content\%} = \frac{C(V_1 - V_2)}{m/M} \times 100 \quad (1)$$

Where C is the concentration of sodium hydroxide standard solution, V_1 represents the volume of the consumed sodium hydroxide, V_2 represents the volume of sodium hydroxide consumed by the blank test, m represents the mass of OCOS, M represents the relative molecular mass of the dialdehyde Chitooligosaccharide repeat unit.

2.3.2. Fourier transform infrared spectroscopy (FT-IR)

The purified adhesives were dried until constant weight in an oven at 60 ℃ and then the samples were tested by universal attenuated total reflectance (ATR) sampling device mode and KBr pressing method respectively. FT-IR spectra of the sample in the 4000-500 cm^{-1} range were recorded by VERTEX 70 spectrometer (BRUKER Company, Germany) Each sample was scanned by accumulating 32 scans at a resolution of 4 cm^{-1}.

2.3.3 X-ray diffraction (XRD)

The D/max2200PC XRD instrument(Ricoh, Japan) was used to test the film with a uniform thickness. The crystallinity of the film was measured by the intensity of the diffraction peak at the 2θ angle position of the spectrum. The film was measured in the 5 to 60° range of 2θ angle at the scanning speed of 4 ℃/min.

2.3.4 Thermogravimetric analysis (TG)

The purified adhesives were dried until constant weight in an oven at 60 ℃. About 3~5 mg of the samples were heated at 10 ℃/min over a temperature range of 50 ～600 ℃ under a nitrogen atmosphere. In roder to illustrate the weight loss rate as a function of temperature, the derivative thermogravimetric (DTG) curve of the TG data was obtained.

2.3.5 Preparation of wood samples

Poplar veneer was cut into 50 mm × 117 mm × 5 mm (width×length×thickness, width direction parallel with grain of poplar veneer). The synthetic adhesive was brushed onto the one surface side of the poplar veneer. The usage of the adhesive was 300 g/m^2 and glue area was 30 mm×117 mm. The adhesive-coated veneer was stacked under uncoated veneer with the grain directions of two stack veneers parallel to each other and stacked the head and the tail. The stacked veneers were put on a table at room temperature for 10 min, hot-pressed at 1.0MPa and the pressing temperature of 120 ℃ for 6 min. Then the stacked veneers were put on a table at room temperature again for 10 min, and cured at 23 ℃ and 50% relative humidity for 24 h. Each stacked veneers was cut into three pieces with dimensions of 50 mm×30 mm (length×width).

2.3.6 Adhesive strength measurements

For dry strength tests, the tensile test was performed at a speed of 1 min/mm under an electronic universal test tensile machine(UTM2102), and the maximum tensile force was recorded. The calculation of the dry strength was regarded as reference the Eq.2. The wet shear strength of the adhesive can be used to measure the water resistance. For wet strength tests, the wood samples were placed in hot water at 63 ± 2 °C for 3 h and then cooled at room temperature for 10 min. The calculation of wet adhesive strength was also reference the Eq.2.

$$\text{Bonding Strength(MPa)} = \frac{\text{Tension Force(N)}}{\text{Gluing Area(m}^2\text{)}} \quad (2)$$

3 Results and discussion

3.1 FT-IR analysis of OCOS

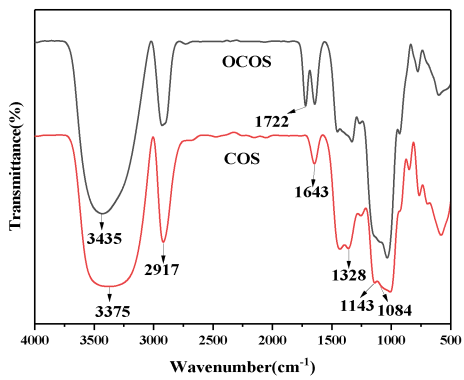

Fig.1. FT-IR spectrum of COS and OCOS

The Fourier infrared spectroscopy of COS and OCOS is shown in Fig. 1. The broad peak at 3375 cm^{-1} in the FT-IR spectra of COS is the stretching vibration absorption peak of -NH_2 and -OH [13], the absorption peak blue shifts to 3435 cm^{-1} and the shape of the peak becomes sharp after COS is oxidized by sodium periodate. The peaks of 2917 cm^{-1} attributed to asymmetric or symmetric stretching vibration peak of -CH_2 in COS [14]. The stretching vibration of C-O and asymmetric stretching vibration of C-O-C were located at 1084 cm^{-1} and 1328 cm^{-1} [15]. The stretching vibration absorption peak corresponding to C-O of secondary hydroxyl group was assigned to 1084 cm^{-1}[16]. OCOS has a new absorption peak at 1722 cm^{-1} compared with COS, which is the vibration absorption peak of the aldehyde group. It was confirmed that COS was oxidized by sodium periodate, and a certain amount of reactive aldehyde groups appeared on the molecular chain [17]. Therefore, the active group -CHO on OCOS can react with -NH_2 of gelatin to copolymerize to synthesize

INGE/OCOS-WPU adhesive.

3.2 FT-IR analysis of OCOS-WPU

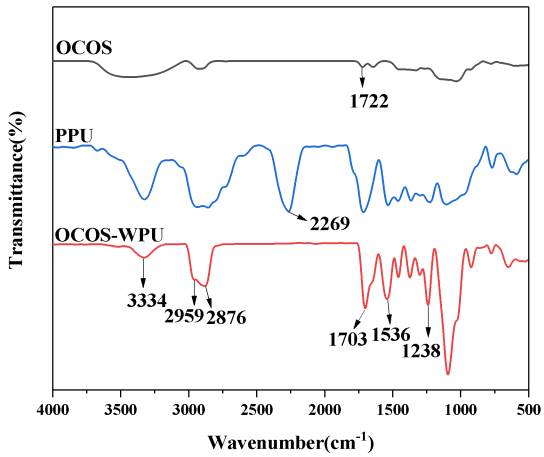

Fig. 2. FT-IR spectrum of OCOS, WPU and OCOS-WPU

Fig. 2 is an infrared spectrum of OCOS, WPU and OCOS-WPU. It can be seen from the above analysis that OCOS has an absorption peak at 1722 cm^{-1}, which is an absorption peak of the active aldehyde group of the group. There are a number of $-NH_2$ and -OH groups in the OCOS molecular chain, while $-NH_2$ has a higher reactivity with -NCO. Therefore, it can be considered that the first reaction between OCOS and polyurethane is the formation of urea group (-NHCONH-) [18], but because some of the amino groups of OCOS were oxidized during the preparation process, which may result in the decrease of amino groups in the system. As the reaction proceeds, the reaction between a hydroxyl group and -NCO took main place. In the OCOS-WPU spectrum, the peaks at 3334cm^{-1}, belongs to the N-H stretching vibration absorption peak of the carbamate group, and the stretching vibration of $-CH_3$ and $-CH_2$ contributed to peaks at 2935 cm^{-1} and 2858 cm^{-1}. The stretching vibration absorption peak of C=O in the carbamate of polyurethane was 1703 cm^{-1}. The absorption peak at 1238 cm^{-1} corresponds mainly to stretching vibration peak of C-O-C of polyether polyol in polyurethane, and the absorption peak at 1536 cm^{-1} arises from bending vibration absorption peak of N-H. It's worth noting that compared with PPU, OCOS-WPU has a peak disappearance at 2269cm^{-1}, corresponding to the stretching vibration absorption peak of -NCO, which indicats that OCOS-WPU has been successfully prepared, and the aldehyde group in OCOS has been successfully introduced after the synthesis of OCOS-WPU.

3.3 FT-IR analysis of INGE/OCOS-WPU

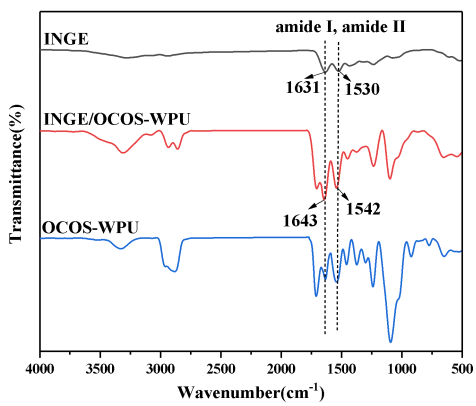

Fig. 3. FT-IR spectrum of INGE, OCOS-WPU and INGE/OCOS-WPU

Fig. 3 shows the FT-IR spectrum of INGE, OCOS-WPU and INGE/OCOS-WPU. The FT-IR spectrum of INGE mainly

exhibits to the characteristic absorption peak of amide band of protein. The characteristic absorption peaks for INGE are as follows: the amide I band corresponds to the peak of C=O stretching vibration at about 1673 cm^{-1}, the N-H bending and C-N stretching vibration contribute to amide Ⅱ of 1524 cm^{-1}, and amide Ⅲ at 1238 cm^{-1}, arises from the stretching vibration of C-N and N-H [19-21]. The symmetric and asymmetric stretching vibration absorption peaks of N-H bond and O-H were located at 3292 cm^{-1}, and 2935 cm^{-1} was assigned to symmetric and asymmetric stretching vibration of C-H. There are different changes in the absorption peaks of the functional groups within the range of 500~4000 cm^{-1},which may suggest that a certain chemical reaction might occurs between INGE and OCOS-WPU. From the infrared spectra of INGE/OCOS-WPU, it can be seen that the associated hydroxyl vibration peak at 3292 cm^{-1} has undergone certain changes, which may be produce hydrogen bonding. After the addition of OCOS-WPU, the peak intensity of the amide I band and the amide II band of INGE was significantly enhanced and shifted to the high wavenumber direction, indicating that OCOS-WPU may react with amino group of gelatin[22].

3.4 XRD

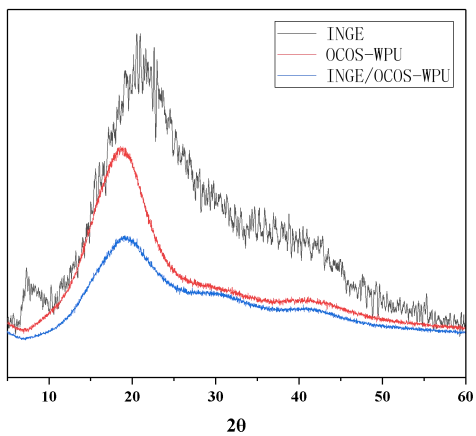

Fig. 4. the XRD pattern of INGE、OCOS-WPU and INGE-OCOS/WPU

Table 1 Crystallinity of INGE、OCOS-WPU and INGE-OCOS/WPU

sample	INGE	OCOS-WPU	INGE/OCOS-WPU
crystallinity/%	6.90	1.06	0.94

The XRD diagrams of INGE, OCOS-WPU and INGE/OCOS-WPU are shown in Fig. 4. The sharp peaks on the XRD diffraction pattern of INGE indicate that the crystal phase content is high and the grain size is large. In other words, the aggregate structure of INGE is dominated by crystalline structure. The wide peaks of OCOS-WPU in the XRD diffraction pattern demonstrate that the aggregate structure of OCOS-WPU is dominated by amorphous state structure. The diffraction peak of INGE/OCOS-WPU is wider than OCOS-WPU, indicating that the aggregation state is mainly amorphous. This is mainly because that the introduction of OCOS/WPU destroys the action among the gelatin chain segments and reduces the regularity of the gelatin structure, which leads to the decreased crystallinity of the INGE/OCOS-WPU[23]. The XRD spectrum of INGE showed a characteristic diffraction peak of gelatin at 2θ=7.5°. After interaction with OCOS-WPU, the characteristic diffraction peak of gelatin disappeared. According to the table 1, the crystallinity of the INGE/OCOS-WPU was 0.94%, which is lower than the unmodified INGE. It may be that the crosslinking between INGE and OCOS-WPU increases the crosslink density of the adhesive. At the same time, it reduces the regularity of the INGE segment.

3.5 TG

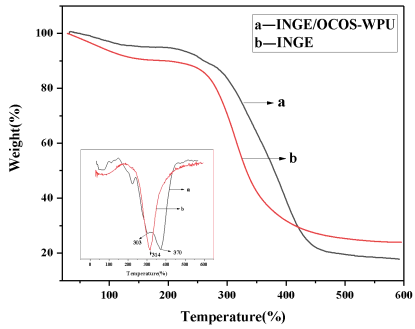

Fig. 5 TG and DTG curve of INGE and INGE/OCOS-WPU

Thermogravimetry is a means of characterizing the thermal stability of a material while providing decomposition information for the sample as determined by the weight loss ratio. The TG and DTG curves of INGE and INGE/OCOS-WPU were shown in Fig.5. It can be clearly seen that there are two weight loss areas in each sample. The first stage is the process of thermal decomposition of free water and bound water under 150 ℃, its weight loss was about 9 ± 1%. The second stage has a large weight loss ratio at 250~450 ℃, which is the thermal weight loss stage of INGE itself [24-25]. At the second stage beginning of the decomposition, the non-covalent bonds including hydrogen bond, electrostatic interaction and hydrophobic interaction in gelatin molecules were destroyed. As the temperature rises, the covalent bonds between the amino acid residues and the peptide backbone is disrupte, and the protein was vaporized to release gases such as CO_2 and NH_3 [26-27]. The decomposition of INGE/OCOS-WPU at this stage is mainly the decomposition of hard segments and soft segments [28]. The maximum decomposition temperature of INGE and INGE/OCOS-WPU were 325 ℃ and 370 ℃, respectively. The decomposition temperature of the modified film was remarkably increased, indicating that its thermal stability was improved in the range of use temperature.

3.6 Wet strength of wood samples

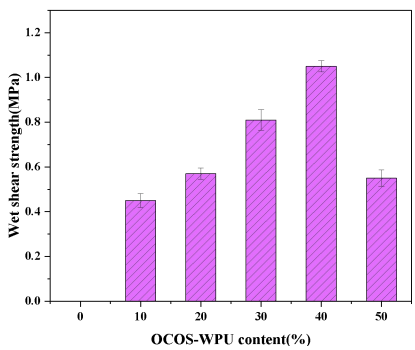

Fig. 6 Wet strength of INGE/OCOS-WPU adhesives

The wet strength of INGE and INGE/OCOS-WPU is shown in Fig. 6. The natural INGE has a wet strength of 0 MPa, which demonstrated that the poor water resistance of INGE adhesive before the introduction of the OCOS-WPU modifier. With the OCOS-WPU modifier was added, the shear strength of the adhesive was greatly improved, that is, the water resistance of the adhesive was improved. It was proved that the addition of OCOS-WPU promoted the application performances of the adhesive. The maximum wet shear strength of the adhesive was obtained when the amount of OCOS-WPU reached 40%. It may be bacause that the aldehyde groups of the OCOS-WPU could react with the amino groups of the INGE molecular chains to form a macromolecular network structure, which could increas the cohesive force of adhesive and reduce the the hydrophilic groups in the adhesive system. The hydrophilic INGE is wrapped by hydrophobicity

of OCOS-WPU, which reduces the possibility of water entering the adhesive and wood interface to a greater extent, thereby improving the wet shear strength of the adhesive. In addition, the exposure of hydrophobic amino acids and good distribution of hydrophobic groups in the INGE molecule also help to improve the water resistance of the adhesive [29]. When the amount of OCOS-WPU increased up to 50 %, the wet shear strength of the adhesive began to decrease, which may be that Reduction of adhesive groups on the molecular chain of gelatin, resulting in a lower adhesion between the wood and adhesive. Meanwhile, adding too much OCOS-WPU will reduce the interaction between OCOS-WPU and INGE. After the sample was immersed in water at 60 ℃ for 3 h, more water penetrated into the film, resulting in a decrease in wet shear strength. When the OCOS-WPU is added with 30% and 40%, its wet adhesive strength was 0.81 MPa and 1.05 MPa, respectively, which all meets the interior use panel requirement (≥0.7 MPa) according to the China National Standard (GB/T 9846.7-2004)

4 Conclusions

In this paper, OCOS was prepared after the oxidation of COS by $NaIO_4$, which was used as a crosslinking agent to obtain OCOS-WPU. Finally, INGE/OCOS-WPU adhesive was successfully prepared by OCOS-WPU reacting with gelatin. The wet strength of the adhesive up to 1.05 MPa. After cross-linking, the characteristic diffraction peak of INGE disappeared in XRD pattern and the crystallinity of INGE/OCOS-WPU decreased to 0.7%. The TG results indicate that the addition of OCOS-WPU contributes to the improvement of the stability of the adhesive in the range of use temperature. In general, the adhesive prepared in this study can meet the application requirements of industrial plywood and has certain application prospects.

Acknowledgments

The authors are grateful for the financial support from the National Natural Science Foundation of China(No.21476134) and the National Science and Technology Major Project(2017YFB0308500). All the authors declare that they have no conflicts of interest.

References

[1] Hu Y., Liu L., Gu Z. P., et al. Modification of collagen with a natural derived cross-linker, alginate dialdehyde. Carbohydrate Polymers, 2014, 102: 324-332.

[2] Samal S K, Goranov V, Dash M, et al. Multilayered Magnetic Gelatin Membrane Scaffolds. Acs Applied Materials & Interfaces, 2015, 7(41):23098.

[3] Zheng Junping, Shan Jiahui, Fan Zhaoming, et a1. Preparation and Properties of Gelatin-Chitosan/Montmorillonite Drug-loaded Microspheres. Journal of Wuhan Un iversity of Technology(Materials Science Edition), 2011, 26(4):628-633.

[4] Dashnyam K, Perez R A, Singh R K, et al. Hybrid magnetic scaffolds of gelatin–siloxane incorporated with magnetite nanoparticles effective for bone tissue engineering. Rsc Advances, 2014, 4(77): 40841-40851.

[5] Gomez-Guillen M C. Functional and bioactive properties of collagen and gelatin from alternative sources: A review. Food Hydrocolloids, 2011, 5(25): 1813–1827.

[6] Karim A A .Fish gelatin: properties, challenges, and prospects as an alternative to mammalian gelatins.Food Hydrocolloids,2009, 5(23): 563–576.

[7] Gerrard, J. A. Protein-protein crosslinking in food: methods, consequences, applications. Trends Food Sci. Technol. 2002, 13, 389–397.

[8] Kim S E, Heo D N, Lee J B, et al. Electrospun gelatin/polyurethane blended nanofibers for wound healing. Biomedical Materials, 2009, 4(4):3-11.

[9] Zhu Y, Gao C, He T, et al. Endothelium regeneration on luminal surface of polyurethane vascular scaffold modified with diamine and covalently grafted with gelatin. Biomaterials, 2004, 25(3):423-430.

[10] Zhou Q, Cui L, Ren L, et al. Preparation of a multifunctional fibroin-based biomaterial via laccase-assisted grafting of chitooligosaccharide. International Journal of Biological Macromolecules, 2018.

[11] Nianhua Dan, Weihua Dan, Xinhua Liu, et al. Oxidized chitooligosaccharide and its preparation method, CN 104004112 A. 2014.

[12] Changdao, Mu, Wei Lin, Hongli Li, et al. Preparation of dialdehyde carboxymethyl cellulose and determination of its aldehyde content, CN101250827. 2008.

[13] Kamari A, Aljafree N F, Yusoff S N. N,N-dimethylhexadecyl carboxymethyl chitosan as a potential carrier agent for rotenone. International Journal of Biological Macromolecules, 2016, 88:263-272.

[14] Liu H, Liu X, Lin Y, et al. Synthesis, characterization and bioactivities of N, O -carbonylated chitosan. International Journal of Biological Macromolecules, 2016, 91:220-226.

[15] Tian Jinhua,Yang Hua,Chi Guangwei, et al. Synthesis and Characterization of Chitooligosaccharides-Zinc Complex. Chinese Polymer Bulletin, 2011 (1): 71-74.

[16] Appunni S, Rajesh M P, Prabhakar S. Nitrate decontamination through functionalized chitosan in brackish water. Carbohydrate Polymers, 2016, 147:525-532.

[17] Liu X, Dan N, Dan W, et al. Feasibility study of the natural derived chitosan dialdehyde for chemical modification of collagen. Int J Biol Macromol, 2016, 83: 989-997.

[18] Silva S S, Menezes S M C, Garcia R B. Synthesis and characterization of polyurethane-g-chitosan. European Polymer Journal, 2003, 39(7):1515-1519.

[19] Pereda M, Ponce A. G, Marcovich N. E, et al. Chitosan-gelatin composites and bilayer films with potential antimicrobial activity, Food Hydrocolloids, 2011, 25(5): 1372.

[20] Staroszczyk H, Pielichowska J, Sztuka K, et al. Molecular and structural characteristics of cod gelatin films modified with EDC and TGase[J]. Food Chemistry, 2012, 130(2): 335-343.

[21] Farris S, Song J H, Huang Q R. Alternative reaction mechanism for the cross-linking of gelatin with glutaraldeHYde[J]. Journal of Agricultural and Food Chemistry, 2010, 58(2): 998-1003.

[22] Dandan Zhang. Study on the method of modification and the performance of gelatin modified by glutaraldehyde and transglutaminase[D]. Beijing Technology and Business University, 2016.

[23] Yuanmin Jin. Preparation and characterization of polyurethane/gelatin copolymers and its filming performance[D]. Shaanxi University of Science and Technology, 2012.

[24] Ullah A, Vasanthan T, Bressler D, et al. Bioplastics from feather quill[J]. Biomacromolecules, 2011, 12(10):3826.

[25] Rujitanaroj P O, Pimpha N, Supaphol P. Wound-dressing materials with antibacterial activity from electrospun gelatin fiber mats containing silver nanoparticles[J]. Polymer, 2008, 49(21): 4723-4732.

[26] Liu H, Li C, Sun X S. Soy-oil-based waterborne polyurethane improved wet strength of soy protein adhesives on wood. International Journal of Adhesion & Adhesives, 2017, 66-74.

[27] Das S N, Routray M, Nayak P L. Spectral, Thermal, and Mechanical Properties of Furfural and Formaldehyde Cross-Linked Soy Protein Concentrate: A Comparative Study. Journal of Macromolecular Science: Part D - Reviews in Polymer Processing, 2008, 47(6):576-582.

[28] Schmidt V, Giacomelli C, Soldi V. Thermal stability of films formed by soy protein isolate–sodium dodecyl sulfate. Polymer Degradation & Stability, 2005, 87(1):25-31.

[29] Wang C, Wu J, Bernard G M. Preparation and characterization of canola protein isolate–poly(glycidyl methacrylate) conjugates: A bio-based adhesive[J]. Industrial Crops & Products, 2014, 57(2):124-131.

O27

NEW era for Leather mold-preventing is coming, are you touched?

Fengming Shin, Hsinhui Chiu*
YCM Products Co Ltd. ycm@asiaycm.com

Abstract

In order to make sure that manufacturers could keep leather products stable during production and storage and lower the risk of mold spoiled naturally, YCM use a new way to analyze each factory's environment data called "Data Science". So far, the mold genus such as *Aspergillus*, *Penicillium*, *Paecilomyces*, *Trichoderma* and *Rhizopus*are founded to grow on leather usually. According to the systematic and environmental research of YCM, there are at least 20 kinds of molds species which can be found in factories and up to 40-50% of them are belonging to leather-based molds as previously mentioned. YCM can realize the characteristic of mold and define spores blow out index, source of nutrients for mold and space suspending mold index to use as systematic mold prevention planning by researching mildewed timing and speed of mold species that cause leather spoiled. In order to make sure the relationship between each index accurately, Pearson correlation was used to proof the highly correlated relationship among spores blow out index and source of nutrients for space suspending mold index (correlation coefficient: -0.83 and 0.8). It can be indicated that environmental mold concentration could be lower efficiently by controlling spores blow out index and the source of nutrients for mold to restrain the factories from moldy problem. Under a year of environmental investigation and anti-mold mechanism counselling, paired t-test was used for comparing the index of spores blow out, source of nutrients for mold and space suspending mold between before and after the improvement of factories. The result of the improvement was statistically significant difference ($p = 0.001$, $p = 0.0001$, $p = 0.001$). Moreover, the proportion of mold genus related to molded leather in the factory was decreased from 50% to 26% and there is no mold issue from leather goods for 396 days till now. This innovation method from YCM can not only avoid the mold issue from leather goods even for long-term storage but reduce the cost and chemical pollution during the production via focusing on non-overpackaging, choosing appropriated anti-mold products, reducing the usage of chemical anti-mold agent, systematic mold prevention planning, and mold growth factor controlling. The era of leather mold protection is here, DO YOU BE TOUCHED?

Introduction

The procedure of leather-manufacturing is a time-consuming process which takes approximately one month. This is due to the below-identified steps taking place, for example, if ten thousand feet of leather was manufactured the following process would need to take place: (1) Tanning takes fifteen days from salted hides to blue hides (2) There are ten days for mechanical, dyeing and stuffing, drying, lacquering -the hides are packaged as finished leather. As leather factories work with tanneries, if the goods are moldy when they are shipped to the customers, they charge both, which is a costly process as they have to pay compensation plus the high costs associated with the tanneries. More recently this has resulted in increasing costs as well as decreasing profit. Lowering risks of leather molding is an extremely challenging process which factories battle with. One solution is the use of mold inhibitors as a way of preventing leather from molding, but this raises the question about whose responsibility it is for molding after using mold inhibitor?

To address these issues it is important to understand the characteristics of mold. According to the difference between storage environmental conditions and the mold spora in the air, the amount and species will be different in the leather (Rathore, 2015). In common, high relative humidity may help mold production and also help molds to produce and develop during storage period. We know that the species of molds which will harm the leather are *Aspergillus, Penicillium, Paecilomyces, Trichoderma* and *Rhizopus* (Orlita, 2004). The environments they prefer are from 25°C to 35°C and the humidity is above 70%. Nowadays, most leather factories are located in tropical areas such as Vietnam, Indonesia,

Cambodia and China. These environments lend themselves to mold developing at any time. How can we solve these problems?

Based on the experience of thousands of factories' consulting, the data of spores blow out index, source of nutrients for mold and space suspending mold index were established for the database using for systematic mold prevention planning. The plan could assist factory to make overall improvement, create the environment which mold cannot grow and decrease the usage of chemical anti-mold products to get a health and eco-friendly environment for leather production and storage. In the research, mold was isolated and purified from molded leather to identify the species of mold. Based on the identification, the relationship between the mold from different colors of leather and its mildewed speed was researched. Furthermore, according to the actual improved situation of factories, the statistical analysis is used to confirm the effect of the difference between before and after the improvement.

Material and methods

Investigate mold species on molded leathers

Isolate and identify molds from twenty pieces of moldy leathers. First of all, observing moldy leathers' colonies by microscopy and selecting the more complete and fresher colonies. Picking spores or hypha by needles or scalpels and moving them on low water activity DG-18 plate medium for culturing 5-7 days in 25°C. Molds will be identified according to morphology and DNA sequencing. The PCR primers were using ITS 5 (5'-GGA AGT AAA AGT CGT AAC AAG G-3') and ITS 4 (5'-TCC TCC GCT TAT TGA TAT GC-3') to amplify rDNA sequence to compare nucleic acid sequence database in GenBank in using BLAST provided by NCBI to acquire information of close species sequence.

Effect on the growth rate of mold in different colors leathers

There were four groups in the test, the environment was the same relative humidity for 80% and different temperature 25°C, 30°C, 35°C, 40°C. The leathers chosen were suedes which had the roughest surface and were easy to let spores attached. There were thirteen colors suedes we collected as testing samples. We prepared three suedes samples in each color and cut into 5*5 cm^2. Before testing, all suedes were used UV light to sterilization for 30-50 minutes in laminar flow. After sterilization, we sprayed six mold species spore suspension (including 4 kinds of *Aspergillus*, 1 kind of *Trichoderma* and 1 kind of *Rhizopus*) on the suedes surface and put them in sterile petri plates individually, totally had 39 samples in each group. The groups were separately placed into Mold Growth Simulating Chamber (MGSC) with different temperature conditions 25°C, 30°C, 35°C, 40°C and observed the mold growth for 7 days.

Evaluate improvements of production factory

Analyze the relation among space suspending mold index, spores blow out index and source of nutrients for mold by Pearson correlation than used as improvements base. Take a factory that YCM counselling in Cambodia as an example, Paired t-test was used to prove the effects of improvement as the change of the three indexes which compares before-tutoring and after- counselling.

Results

Investigate mold species on leathers

Molds were isolated from twenty pieces of leathers including cow upper leather and suede by DG-18 medium. According to morphology and DNA sequence, we identified four mold genus including *Aspergillus*, *Curvularia*, *Fusarium* and *Trichoderma* and there amounted to nine kinds of molds. A large proportion of the molds is *Aspergillus*, approximately 66%.

Effect on the growth rate of mold in different colors leathers

The testing results of four groups under different temperatures show that the rate of molding in different color and different temperatures was the same and it started to grow molds on the third day. The suede in the same colors grew molds

in different temperatures, exception for 25°C. The result shows temperatures don't have much effect on suede in molds growing. Among the moldy suede, sky blue, red rose and black accounts for the most proportion.

Evaluate improvements of production factory

According to YCM's experience on counselling thousands of factories, there are 11 anti-mold indicators being formulated. In the research, we discussed three of them: spores blow out index, source of nutrients for mold and space suspending mold index. We analyzed above three indexes' relationship by Pearson correlation. The result indicates that the relation between space suspending mold index and spores blow out index is -0.83, the relation between space suspending mold index and source of nutrients for mold is 0.8. Which means spores blow out index and source of nutrients for mold are related to control space suspending mold index. Based on the relationship and the actual record of the before-after figures undergoing Paired t test, spores blow out index, source of nutrients for mold and space suspending mold index the improvement were statistically significant difference ($p = 0.001$, $p = 0.0001$, $p = 0.001$).

Discussion

Some mold on the leather may die during processing or storage, which cannot be isolated for mold. After microscopic examination for mold sample on leather, we chose the samples with more intact and clear colonies and hyphae. There were 9 species of mold isolated from 20 sample of moldy leather. Thorough morphology and DNA identification, there were 6 species belong to *Aspergillus*, accounting for 66%. Rest of them were *Curvularia*, *Fusarium* and *Trichoderma*. This result matches to previous studies about common mold on leather. According to ourresearch, most species grow on leather were *Aspergillus*. Thus, it was very important to pay attention to this genus of mold for leather storage.

We examined 13 different color of suedes and found that color had little effect on mold's growing speed on leather. However, we found more groups of molds on sky blue, rose red and black suede. Currently, the studies indicate that will affect mold's growth are 1. Optical signal, which prompts timing system of fungus like *Neurospora*, *Cercospora* and *Aspergillus*. They detect predictable daily environmental fluctuations
to regulate spore germinating or growth timing (Baker et al., 2012; Bluhm et al., 2010; Greene et al., 2003; Lombardi et al., 2005) 2. Carbon-Nitrogen ratio: Carbon and nitrogen are key elements for mold's growth . Thus, the Carbon-Nitrogen ratio in objects affects the speed and size of mold grow to certain degree. (Gunasekaran and Poorniammal, 2008). To understand why only 3 of these 13 colors are easier to get moldy, we still need more research to ensure if leather in specific colors is easier to get mold. Such as leathers in different colors may absorb light differently so that affect spore's germination, different carbon-nitrogen ratio in different color of leather or dyeing leather with whether natural or chemical dyes.

By using Pearson correlation to analyze the relevance of spacesuspending mold index, spores blow out index and source of nutrients for mold, we can conclude that increasing spores blow out index and reducing source of nutrients for mold may lower space suspending mold index. Regarding to practical implementation, take one of factories under YCMs' counseling for example, there are significant differences between the values of the three indexes before and after the improvement of the factory with paired sample t-test analyzation. It means that the improvement increased spores blow out index and reduced source of nutrients for mold and lower space suspending mold index. For the genus relate to moldy leather, like *Aspergillus*, *Penicillium*, *Paecilomyces*, *Trichoderma* and *Rhizopus*, the ratio reduces from 50% to 26%. This also reduce the chance leather get moldy to certain degree. Additionally, there has been no record of any mold issue for 396 days since the improving project completed till now.

Conclusion

Mold has been surviving on the earth over 700 million years. When the times that human civilization development, the influence and the problems of mold also come one after another. We always keep using all kinds of different chemicals try to eliminate, reduce the problems thatcomes from mold. The mold problem in the production supply chain always be a big issue. There are many new anti-mold products appearing on the market, but the moldy problem still exists. The main point to

solve the problem is to find where the problem comes out and use the right method to solve the problem, not just use anti-mold products endlessly and cause environmental pollution and protection problems.

For all these reasons, by doing the research YCM can realize the characteristic of molds and the growth condition than doing the test to set up mold growth control factors, like spores blow out index, source of nutrients for mold and space suspending mold index. In the same time, we will provide a suitable anti-mold planning for factories in different climate zone. By using environmental control to produce an environment that molds can not be grow easily to achieve the anti-mold effect. This method can both achieve anti-mold efficiency and focus on the environmental protection to reduce the destruction of the environment. The core of this new method is to peaceful coexistence with molds. The new era has new method, do you be touched?

Reference

Baker, C. L., Loros, J. J., & Dunlap, J. C. (2011). The circadian clock of Neurospora crassa. FEMS microbiology reviews, 36(1), 95-110.

Bluhm, B. H., Burnham, A. M., & Dunkle, L. D. (2010). A circadian rhythm regulating hyphal melanization in Cercospora kikuchii. Mycologia, 102(6), 1221-1228.

Greene, A. V., Keller, N., Haas, H., & Bell-Pedersen, D. (2003). A circadian oscillator in Aspergillus spp. regulates daily development and gene expression. Eukaryotic Cell, 2(2), 231-237.

Gunasekaran S. and Poorniammal R. (2008). Optimization of fermentation conditions for red pigment production from Penicillium sp. under submerged cultivation. African Journal of Biotechnology, 7(12), 1894-1898.

Lombardi, L. M., & Brody, S. (2005). Circadian rhythms in Neurospora crassa: clock gene homologues in fungi. Fungal genetics and biology, 42(11), 887-892.

Orlita, A. (2004). Microbial biodeterioration of leather and its control: a review. International biodeterioration & biodegradation, 53(3), 157-163.

Rathore, D. S. (2015). Study of fungal diversity on different types of finished leather and leather articles. Research journal of recent sciences, 4, 228-234.

O28

Tannery Waste Management in India – Towards Sustainability

S.V. Srinivasan*, G. Sathish, R. Nishanthi, K. Thirumaran, R. Suthanthararajan

Environmental Science and Engineering Division, CSIR-Central Leather Research Institute, Chennai – 600 020, India

**Corresponding author: srinivasansv@yahoo.com*

Abstract

Leather is one of important by-product industry in developing countries due to its employment, foreign exchange and export potentials. However, leather processing results in generation of wastewater and solidwaste which would affect the environment if it is not properly collected, treated and disposed-off. In order to control the pollution, initially individual Effluent Treatment Plants (ETPs) or Common Effluent Treatment Plants (CETPs) were installed with physico-chemical treatment followed by biological treatment to meet the discharge norms of SS, BOD, COD and Chromium during earlier 90's in India. In addition, chrome liquor generated from tannery is segregated and treated in the chrome recovery plant for reuse. Subsequently, in order to tackle the issue of Total Dissolved Solids (TDS) and to address the water scarcity in India (Tamil Nadu State), the Zero Liquid Discharge (ZLD) i.e., water recovery from secondary treated effluent through membrane system and evaporation of rejects has been implemented in ETPs/CETPs. However, the implementation of these systems required higher investment and O&M cost. This higher capital cost in ETPs/CETPs by tanneries was subsidized by the Central and State governments in 2010. Successful implementation of ZLD in CETPs has resulted in recovery and reuse of water and meets the compliance with local regulatory conditions. However, ZLD resulted in higher specific energy consumption and O&M cost which becomes burden to the tanneries and makes this option unviable and not sustainable. In order to reduce the O&M cost, CLRI has proposed Technology Mission to reduce the pollution load in process and upgradation of CETPs. The major upgradation includes technology upgradation in primary and secondary treatment, increase in percentage of water recovery in membrane system and implementation of solar photovoltaic energy system for electrical power in CETPs. The Upgradation measures aims to reduce the O&M cost and also carbon footprint from leather sector towards sustainable operation of ZLD in leather sector.

Key words: Tannery wastewater, ZLD, Capital cost, O&M cost, pollution

1.0Introduction

Indian tanning industry is one of the oldest and potential sector which has major role in Indian economy. There are about 1700 tanneries located in different parts of India with a total processing capacity of about 700,000 tons of raw hides and skins per year. More than 80% of tanneries in small and medium scale sector have processing capacity less than 2 tons of hides / skins per day. In India, there are 21 Common Effluent Treatment Plants (CETPs) and about 100 individual Effluent Treatment Plants (ETPs) are in operation to treat wastewater generated from these tanneries.

Conventional treatment process has been adopted in most of CETPs/ETPs which comprises of physico-chemical treatment followed by biological treatment in early 90's. Biological treatment inlcudes anaerobic treatment using Upflow Anaerobic Sludge Blanket (UASB) followed by extended aeration process or two stage extended aeration process or single stage extended aeration process. The conventional treatment system is able to remove pollutants such as Suspended Solids (SS), Biochemical Oxygen Demand (BOD) and Chemical Oxygen Demand (COD) and treated effluent is able to meet discharge standards of SS - 100 mg/L, BOD - 30 mg/L and COD - 250 mg/L except for Total Dissolved Solid (TDS), Sulphates and Chlorides (Discharge standard for TDS - 2100 mg/L; Sulphates -1000 mg/L; Chloride – 1000 mg/L). The TDS concentrations in the secondary treated effluent from tanneries processing semi-finished to finished leather and tanneries processing fromraw skin/hide to finished leather were in the range of 5000 – 7000 mg/L and 12000 to 20000 mg/L respectively. The major constituents that contribute towards TDS are chlorides and sulphates of sodium, calcium, magnesium etc.

Typical characteristics of compositewastewater from tanneries processing raw hide to finished leather and corresponding discharge standards (MoEF, 2016)

S. No	Parameter	Values	Discharge standards	
			Inland surface water	On land for irrigation
1	pH	7.0 - 9.0	6.0 - 9.0	6.0 - 9.0
2	Suspended Solids	3500 - 4000	100	100
3	Biochemical Oxygen Demand (BOD)	1500 - 2300	30	100
4	Chemical Oxygen Demand (COD)	3500 - 5000	250	250
5	Ammonical Nitrogen	320 - 430	50	NS
6	Total Dissolved Solids	12000 - 20000	2100	2100
7	Chloride as Cl^-	5000 - 7500	1000	1000
8	Sulphate as SO_4^{2-}	2000 - 3000	1000	1000
9	Sulfide as S^{2-}	300 - 350	2	2
10	Chromium as Cr	25 - 40	2	2

Note: *All values are in mg/L except pH.*

NS - Not specified.

Earlier discharge of effluent after conventional tretament with high TDS leads to increase in TDS concentrations of the ground and surface water in the adjoining area making it unpalatable. Also, treated effluent from the treatment plants is not suitable for reuse becuase of high TDS content. Moreover, due to inadequate water source and poor quality of available ground water in leather clusters, many tanneries in South India, transport water through tankers, for processing, at a higher cost. In this context, recovery and reuse of water in the process becomes beneficial for the tanneries. In addition, to meet United Nations New Millennium Development Goal i.e., ensure environmental sustainability by providing safe drinking water and basic sanitation for people, regulatory authorities have directed the CETPs in water scarce and land locked regions to implement Zero Liquid Discharge (ZLD) i.e., recovery of water from wastewater for reuse and there shall not be any discharge of effluent outside their premises. Operation of Zero Liquid Discharge system cannot be sucessful until the entire spectrum of treatment, starting from design, operation and monitoring of pre-treatment, primary, secondary and tertiary treatment, membranes system and evaporation process are properly carriedout.

In some of the CETPs located in urban areas where adequate treated sewage is available, the option of dilution of conventionally treated tannery effluent with treated sewage to meet TDS norms of 2100 mg/L has been permitted by the reguatory authorities with strigent monitoring mechanisms.

2 Treatment schemes adopted for tannery wastewater in India

2.1 Conventional method of treatment

The conventional tannery wastewater treatment schemeincludes physico-chemical treatment followed by secondary biological systems. The physico-chemical treatment includes screen, equilisation tank and primary settling tanks which removes the total suspended solids, chromium and some percentages of organics. In biological treatment process, the organics will be removed. The different treatment schemes adopted in CETPs in India are given below.

norms of 2100 mg/L has been permitted by the reguatory authorities with strigent monitoring mechanisms.

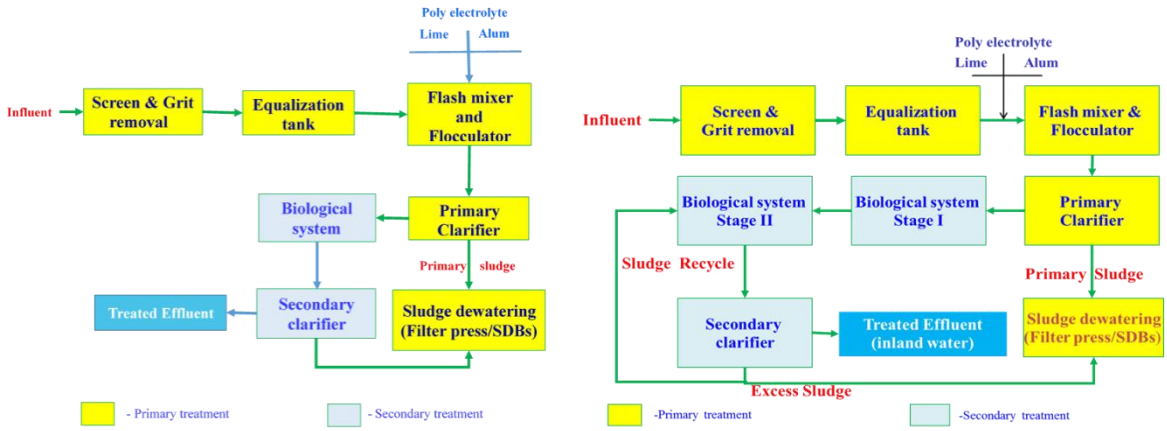

(a) CETPs adopting Single stage extended aeration system (b) CETPs adopting Two stage extended aeration system

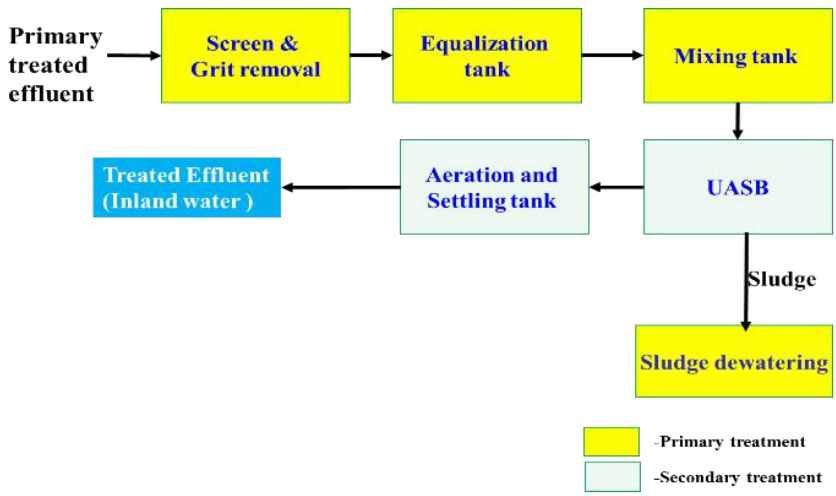

(c) CETPs adopting Two stage biological treatment (UASB andextended aeration system)

2 Treatment schemes adopted for tannery wastewater in India

2.1 Conventional method of treatment

The conventional tannery wastewater treatment schemeincludes physico-chemical treatment followed by secondary biological systems. The physico-chemical treatment includes screen, equilisation tank and primary settling tanks which removes the total suspended solids, chromium and some percentages of organics. In biological treatment process, the organics will be removed. The different treatment schemes adopted in CETPs in India are given below.

2.2 Zero Liquid Discharge

The Zero Liquid Discharge is a concept of recycle, recover and reuse of the treated wastewater by means of advanced wastewater treatment technologies to ensure that the wastewater does not enters the environment. Some CETPs in Landlocked and water scarce regions have implemented ZLD system which consists of pretreatment system with conventional physico-chemical treatment, secondary bilogical treatment, tertiary treatment and softening of the treated effluent, two stages Reverse Osmosis (RO) treatment for desalination of effluent and thermal evaporation of saline reject from RO to separate the salts in 2010. The RO rejects are evaporated in solar evaporation pans in the small ZLD plants with capacity less than 100 m^3/d and in the larger ZLDplants the RO rejects are thermally evaporated. But the operation of ZLD system requires high O&M cost which is big challenge both technically and financially.

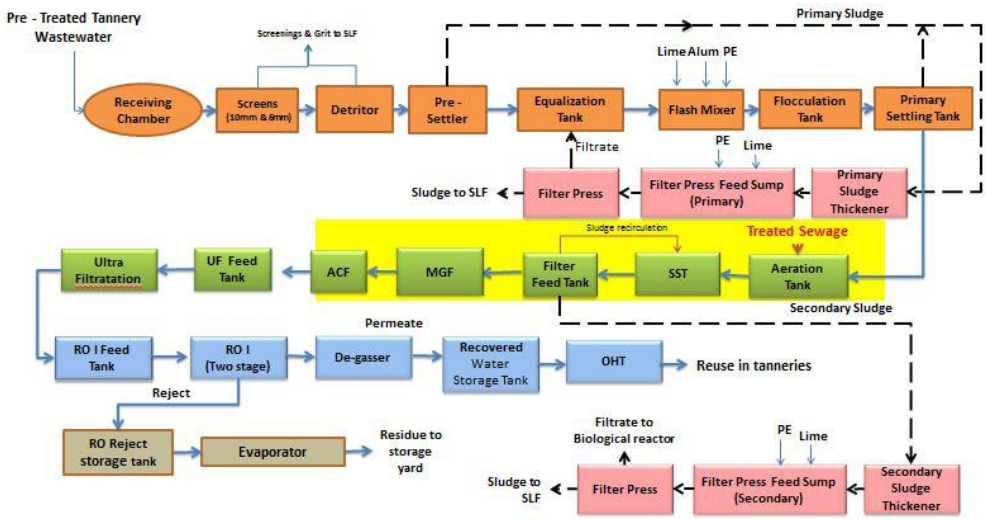

Process flow diagram of Zero liquid discharge (ZLD)

2.3 Current Issues of the ZLD system

The implementation of ZLD system needs very high investment and high operation & maintenance cost. The operation & maintenance cost of the ZLD system varies from Rs.400 – 600 /m^3 (5-7 Euros/m^3) of wastewater treated. In O&M cost, 25-35% is spent towards the electrical energy which is consumed in aeration tank and membrane system. ZLD requires trained manpower also for the operation of this system.

There are certain issues remain unsolved which has become an uphill task for the CETPs. In present ZLD system, even after secondary and tertiary treatment, residual organics (COD) with colour pose major challenge which also affects the performance of RO system. In addition, the residual mixed salt obtained after evaporation with non-degradable organics cannot be utilized. Similarly, in current treatment schemes, the ammonia present in the wastewater remains untreated, get concentrated in RO reject and reflects in the evaporator condensate causing odour nuisance and also pose a challenge for use of condensate in leather processing.

In ZLD system, about 65% to 70% of the water is recovered and remaining 30% to 35% of highly concentrated saline reject needs to be evaporated requiring additional cost of treatment. Steam generated from boiler, using fuel such as wood, briquettes and coal, is used for evaporation of the reject. The fuel cost contributes to high O&M cost and also the emission of the carbon-dioxide (CO_2) increasing the carbon foot print.

The concentrated reject from the Multiple Effect Evaporator (MEE) is crystallized and the mixed salt contains non-degradable organics is the end product. Currently, there is no potential utilization of this residual mixed salt and hence the CETPs have been storing this residual salt in the storage yard at their premises over the years. This requires large area

and shed with protective measures also contribute towards the capital cost.

In totality, implementation and operation of ZLD pose constraints in design, implementation and operation due to variations in quality and quantity of wastewater, high capital investment and operation & maintenance cost, high power requirements, difficulties in meeting feed water requirements for membrane systems and disposal of evaporated residual mixed salt.

3.0 Proposed Measures for improvement of ZLD systems

3.1 In-Process Control Measures at Sources

Prevention or reduction of pollution at source through in-process control measures assumes greater significance now in leather industry, because it is seen in practice that with end-of-pipe treatment alone could not meet the norms. In tanneries, processing chrome tanned leather, cleaner technologies such as (a) low-sulfide enzyme-assisted un-hairing (b) recycling of re-liming wastewater after partial treatment (c) waterless / dry chrome tanning are demonstrated. These measures reduces the usage of fresh water and chemical in the process. It reduced the pollution load especially Chromium, Sulfide and TDS.

3.2 Measures at CETP

(i) Sulfide Oxidation

In the process of Raw to finished leather, the sulfide level in the raw effluent is about 320 mg/L to 430 mg/L. Hence, before feeding the primary treated effluent to aeration tank, it is necessary to remove the sulfides. Sulfide oxidation can be done either by adding liquid oxygen or using oxidizing agents like MnO_2 with aeration in the pre-aeration tank. This improves the efficiency of biological treatment and also reduces the odour in the CETP.

(ii) Nitrification and De-Nitrification

The ammonia present in the wastewater remains untreated and it is necessary to remove the ammonia before membrane system as the residual ammonia is carried over to evaporator condensate. Therefore, proposed implementation of Nitrification and De-Nitrification system will remove ammonia. This increases the efficiency of membrane system and also reduces the ammonia concentration in the evaporator condensate making the condensate suitable for reuse in the leather processing in tanneries.

(iii) Improvements in aeration system of biological treatment

Currently, in aeration tanks, diffusers are used to have lesser life span and also requires regular maintenance. The oxygen transfer efficiency is also get reduced due to damage of diffusers. The Original Hydrodynamic Reaction (OHR) technology based Aerators areproposed which expected to have long life, less maintenance and non-clogging. It also ensures high oxygen transfer efficiency and complete mixing which increases the performance of biological treatment.

(iv) Advanced Oxidation Process

The advanced oxidation processes such as Ozone, Chlorination, Hydrogen Peroxide etc., are proposed to remove the residual organics and colour from secondary treated effluent. Reduction of residual organics will ensure control of scaling and bio-fouling in the membrane systems. As AOPs remove the color effectively, colourless mixed residual salt recovered from the evaporators can find potential applications. This system will not generate any sludge and there will not be increase in the TDS, Hardness, and Chlorides like in the conventional chemical treatment which increases the TDS load to the RO Plant and the Evaporator.

(v) Nano Filtration (NF) before RO system

NF membranes reject divalent ions and organics. Hence, Nano filtration allows water and monovalent salts to pass through the membrane while retaining multivalent ions, low molecular weight molecules, sugars, proteins and other organic compounds. The NF membranes separate the feed stream into a product (permeate) stream which contains mainly sodium chloride and a concentrate (reject) stream with high amount of sulphate, calcium etc. Polyamide seawater NF membranes with spiral membrane/PT Module configuration with high rejection of sulphate and multivalent ions is proposed to separate

chlorides and sulphates to find suitable applications.

(vi) High Pressure RO System (HPRO)

In two stage RO system, only 65% to 70% of water is recovered leaving 30% to 35% of saline water as reject. The HPRO system has been proposed to increase the water recovery in membrane system upto about 85% of wastewater. This reduces the volume of reject and reduces the capital investment cost required for evaporator. Further, increase in the salt concentration of reject (feed to evaporator) results in lesser fuel consumption in the evaporator which in turn reduces the operational and maintenance cost of the system (fuel to the boiler).

(vii) Multiple Effect Evaporator (MEE) – Agitated Thin Film Dryer (ATFD):

The reject from the membrane system is being evaporated in the Multiple Effect Evaporator. The evaporator with improved material of construction i.e., SS316L and titanium tubes are proposed to increase the life span of the system. During evaporation, the concentrated saline liquor is crystallized leaving the mother liquor which contains high amount of organic impurities. Earlier, this mother liquor was evaporated using solar evaporation pans which is not effective during winter and rainy seasons. However, Agitated Thin Film Dryer specially designed film type dryer for evaporation of this mother liquor is proposed which will ensure complete evaporation of the reject leaving solid residues.

(viii) Energy Conservation Measures

a. Solar Photovoltaic Energy System for power generation

In CETPs, about 25% to 35 % of the operation and maintenance cost is towards the electrical power cost. Hence, the solar photo voltaic system are proposed which reduces the O&M cost. Photovoltaic solar energy system of 1 MW is proposed for 1 MLD of feed wastewater to CETP. Utilization of green energy reduces the carbon footprint of the treatment plant and carbon foot print of leather production as a whole.

b. Energy efficient blowers and pumps

Major upgradation in primary and secondary treatment system is towards use of energy efficient pumps and the turbo blowers in aeration tank and other pumping systems. This is expected to reduce the O&M cost of the treatment system.

4.0 Conclusion

The ZLD system ensures near total recovery of water from wastewater for reuse in the leather manufacturing process which eliminates ground water usage. It also prevents discharge of wastewater from the treatment system to the environment. Moreover the upgradation by various technologies increase the quality of treated effluent which improves the water recovery rate and membrane life. Separation of salt through membrane process increases the scope for reuse of the recovered salt and minimize the salt disposal issue.

Use of Solar photovoltaic energy for the operation of CETP in place of conventional power reduce the O&M cost in addition to lesser carbon foot print and make the industry competitive and sustainable.

However in ZLD system, the residual salt from evaporator has no disposal method, but the research work on the purification of existing salt is under progress by CSIR labs. Further research on concentration of reject from HPRO system using membrane distillation with waste heat from boiler is also proposed to increase the salt concentration in evaporator and also to reduce fuel requirements in evaporator system which can further reduce the O&M cost and carbon foot print of ZLD system.

In-Process control measures in individual tanneries and improvements in existing ZLD system will make the CETP more efficient with lesser O&M cost. Hence, the implementation of these state of art technologies and upgradation measures make the ZLD system and leather industry sustainable as a whole by enhancing the leather production and providing more employment, proving that leather industry is no more a polluting industry.

References

W. Scholz and M. Lucas, Techno-economic evaluation of membrane filtration for the recovery and re-use of tanning chemicals, *Wat. Res.* **37,** (2003), pp 1859-1867.

R. Suthantharajan, E. Ravindranath, K. Chitra, B. Umamaheswari, T. Ramesh, S. Rajamani, Membrane application for recovery and reuse of water from treated tannery wastewater, *Desalination,* **164** (2004), pp 151-156.

Ali Altaee and Nidal Hilal (2015). High recovery rate NF-FO-RO hybrid system for inland brackish water treatment, Desalination 363, pp 19-25.

Kuppusamy Ranganathan, Shreedevi D Kabadgi (2011). Studies on feasibility of Reverse Osmosis (membrane) technology for treatment of Tannery wastewater, Journal of Environmental Protection, 2, pp 37-46.

O30

From Polyurethane Chemistry to Advanced Functional Leather

Yi Chen[1], Jinming Chang[1], Peikun Zhang[1], Saiqi Tian[1], Haojun Fan*[2]

[1] *Key Laboratory of Leather Chemistry and Engineering of Ministry ofEducation, Sichuan University, Chengdu 610065, P.R. China*

[2] *National Engineering Laboratory for Clean Technology of Leather Manufacture, Sichuan University, Chengdu 610065, P.R. China*

Abstract

Crust leather must be finished to hide any defect or irregular appearance, improve its physical properties, and in particular, impart important functionalities for specific applications. Here, we report how advanced polyurethane finishing agents with self-adaptive water vapor permeability, flame retardancy, antimicrobial activity, or thermochromic/photochromic properties can be designed and synthesized by exploiting polyurethane chemistry, and briefly touch upon their potential applications in making value-added leather. We expect the progress herein motivate continuous interest of materials scientists, leather chemists and engineers in rational design of advanced polyurethane finishing agents such that leather products exhibiting improved performance or unprecedented functions will be accessible soon.

Keywords: Leather; Finishing agent; Polyurethane; Chemistry; Functionality

O31

Control and optimization of the whole process of tannery wastewater treatment

Jianjun Zhou, Kai Du, Hexiang Dong

(Xi'an Eureka Environmental Technology Co., Ltd., Shaanxi Xi'an 710016)

Abstract

At present, there are many problems in the treatment process of tannery wastewater in China, such as low efficiency, unstable operation, high operation cost and large sludge production, etc.. Therefore, it is imperative to explore the technology of tannery wastewater treatment with high efficiency, stability and low operation cost. In this study, the technology of fine screening, pre-biological treatment, high-efficiency anaerobic, biological enhancement, sludge reduction, Fenton with novel Fe catalyst and other core technologies were used to control and optimize the whole process of tannery wastewater treatment, the synergistic removal of COD and TN during biochemical treatment was realized. Meanwhile, the processing efficiency and stability of the system was significantly improved, the sludge production of the system was reduced. The new process made up for the shortcomings of the traditional treatment process. Besides, the problems of the traditional Fenton process such as complicated process flow, narrow pH range and large amount of sludge production were solved during the improved Fenton reaction with novel Fe catalyst. This process did not produce iron-containing sludge, which can also help enterprises achieve the goal of tannery wastewater standardized discharge. This technology has broad market and application prospects.

Key words: tannery wastewater; treatment process; optimization; Fenton reaction

Tannery wastewater produced from the leather industry is a potential pollution source due to its high concentration of organic matters, nitrogen, suspended solids (SS) and specific pollutants, e.g., sulphides and chromium (Wiemann et al., 1998; Song et al., 2000; Suthanthararajan et al., 2004). An effective treatment process was required to reduce the effects of water pollution from the tannery industry on the environment (Song et al., 2001; Cotman et al., 2004; Calheiros et al., 2007). Sulphides in tannery wastewater were toxic substances for the methanogenic bacteria in anaerobic systems. For wastewater with high organics concentration, aerobic systems had difficulty in achieving the discharge standard, independently. Furthermore, temperature, pH, COD and SS concentration of the tannery wastewater varied significantly with the tanning procedure. Therefore, in order to meet discharge standards, an appropriate treatment system with anti-shock loading capability, high efficiency and low cost was necessary to study.

Wastewater treatment methods are broadly classified into physical, chemical and biological processes. Various treatment for tannery wastewater like physico-chemical methods such as sedimentation (Song et al., 2000), filtration (Cassano et al., 1999; Tiglyene et al., 2008) , precipitation (Esmaeili et al., 2005), coagulation (Zhi et al., 2009; Sengil et al., 2009), adsorption (Santosa et al., 2008), ion exchange (Kabir and Ogbeide, 2008) and biological methods such as anaerobic and aerobic process(Munz et al., 2008 Zupancic and Jemec, 2010). However, the conventional biological treatment does not always achieve satisfactory performance due to the toxicity of the tannery wastewater that affects the development of the bacteria. In addition, traditional physical-chemical processes are comparatively expensive because it needs additional chemicals, and may lead to secondary pollution. The drawbacks mentioned above have forced various industries to seek for effective alternative treatment technologies for pollutants removal.

Xi'an Eureka Environmental Technology Co., Ltd. is located in Xi'an Economic and Technological Development Zone, which is a high-new technology enterprise that focus on environmental technology and product development, environmental engineering design, construction, operation, environmental project investment, environmental new technology integration and promotion. The company focus on the whole process optimization of chemical wastewater treatment, like tannery, paper making, printing and dyeing, to improve the efficiency of the process and maximize the reuse of reclaimed water. At the same time, the company is committed to the resource, reduction and harmless treatment of industrial solid wastes, and strive

to achieve low consumption, low emissions, high efficiency, so as to promote the development of circular economy.

The aim of this study hosted by the Eureka company was to optimize the process of tannery wastewater treatment, improve the efficiency of treatment system and decrease its operation cost. During the tannery wastewater treatment optimization process, the technology of fine screening, pre-biological treatment, high-efficiency anaerobic, biological enhancement, sludge reduction, Fenton with novel Fe catalyst and other core technologies were used to control and optimize the whole process of tannery wastewater treatment.

1. Pretreatment process optimization

Grille, sedimentation, regulation are usually used for pretreatment of tannery wastewater treatment to reduce suspended solids (SS) and regulate water quality, but the conventional pretreatment process has some shortcomings: long water residence time, low processing power per unit area, large area reactor and so on. In addition, the coagulation/flocculation of tannery wastewater process has been investigated using inorganic coagulants such as aluminium sulphate, ferric chloride, ferrous sulphate to reduce organic load (COD) and SS as well as to remove toxic substances, e.g. chromium before biological treatment, and industries also must spend a lot of manpower and time to deal with the resulting sludge from coagulation/flocculation process.

The SFL hydraulic sieve produced by the company is a non-power separation equipment with a filtration range of 0.3 mm~1.0 mm, which can effectively reduce the concentration of suspended solids in wastewater and reduce the processing load of subsequent processes. It is suitable for filtering suspended solids such as floats, sediments in wastewater and used to recycle useful materials from waste liquids in production. Besides, the SFL hydraulic sieve can replace the pre-sedimentation tank and delay the reduction of wastewater temperature, and ensure that wastewater enters the biological system and has a higher temperature.

The main function of the traditional adjusting tank is to balance the quality and quantity of wastewater by aeration. The biological adjusting tank can also reduce the partial pollutant by adding activated sludge and make the most of the tank capacity and aeration.

2. Biological process optimization

Hydrolysis acidification (HA) has been a widely used bioprocess prior to the anaerobic system. The HA process as a biological pre-treatment could not only reduce the organic concentration and improve the biodegradability but also avoid the inhibiting issue of the sulphides on the methanogenic process. Moreover, this process was a low-cost process and did not require aeration or temperature control. Nowadays, the HA process has become a potential pre-treatment approach for the tannery wastewater prior to the aerobic system, the performance of the full-scale HA system on the tannery wastewater treatment has been reported. However, the effect of water quality variation and low temperature on the operational stability of the HA system was an important issue in actual operation.

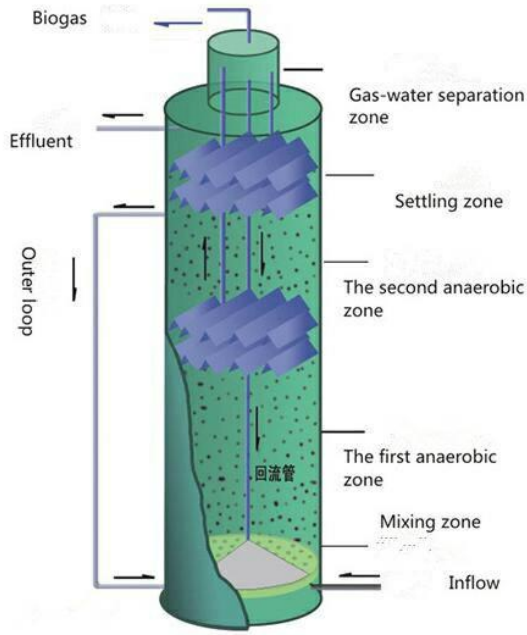

Fig. 1 Construction of IC Anaerobic Reactor

As shown in Fig. 1, internal circulation (IC) anaerobic reactors can effectively solve the problem of the contradiction between poor sludge retention and short hydraulic retention time (HRT) that occurs in a traditional anaerobic reactor. Hence, they have become an distinguished representative in the third generation of anaerobic reactors (Chen et al., 2017; Hu et al., 2017). In addition, the IC anaerobic reactor could offer a promising alternative for treating the tannery wastewater with high organic loading rate, powerful stress resistance, economic space utilization, excellent operation stability, and so on. This year, IC anaerobic reactor was successfully applied to the renovation project of Meihua Leather Industry Co., Ltd. sewage treatment plant to replace the HA process. Through the field test and operation, the system is proved to be reliable and stable.

Nowadays, integrated biological treatment using an anaerobic-aerobic system always works more efficiently in denitrification and organics removal of tannery wastewater. In particular, anoxic-oxic (A/O) or anaerobic-anoxic-oxic (A/A/O) process has been integrated with these anaerobic processes. Bioaugmentation, which use selected microbes to degrade organic compounds, can combine with different treating systems to remove some objective pollutant. The technology has advantages of high adaptability and efficiency, and shows a broad prospect in treatment of refractory wastewater. Studies were carried out on the bioremediation of tannery wastewater in A/O system, adding the acclimated activated sludge and biological agents for bioaugmentation. The results showed that the biological system after bioremediation treatment had a good removal effect on COD and ammonia nitrogen. Moreover, bioremediation can make the activated sludge take on better physiological activity and anti-shock loading capability. Therefore, it is pointed out that the development trend in the field of intensive biodegradation technique is to screen and apply dominant bacteria.

3. Advanced treatment optimization

The choice of wastewater treatment process depends on several factors like efficiency, cost and environmental capability.Moreover, the wastewater characteristics should also be considered when choosing the best process. Tannery wastewater are oxidized by four different reagents like ozone, hydrogen peroxide, Fenton oxygen and air. These procedures may also be combined with any one of oxidation process or agents are known as advanced oxidation process (AOP). The AOP procedure is particularly useful for cleaning biologically toxic or non-degradable materials such as aromatics,

pesticides, petroleum constituents, and volatile organic compounds in wastewater. Fenton is an effective method of AOPs to destroy recalcitrant and toxic organic pollutants in wastewater, based on the production of highly reactive hydroxyl radical by reaction between H_2O_2 and Fe^{2+}. However, there exist some drawbacks involving strongly acidic condition (effective pH: 2.0–4.0), generation of iron sludge, and high level of H_2O_2 dosage, a lot of attempts are still in process to address these problems, and nano-particles catalyzing Fenton seems to be a promising method. Though Fenton has been used to treat tannery wastewater, process optimization, especially focusing on COD removal, was still scarce.

The aim of this study was to investigate the performance of the improved Fenton reaction for COD removal in treatment of tannery wastewater. Compared to the traditional Fenton reaction, this process replaces ferrous sulfate with novel Fe catalyst, besides, when the Fenton reaction is over, it do not need to adjust the pH to alkalinity. The obtained results showed that the COD removal efficiency was 59.0% (from 220.50 mg/L to 90.41 mg/L) at pH 4.0 during the Fenton reaction with the addition of the Fe catalyst. The problems of the traditional Fenton process such as complicated process flow, narrow pH range and large amount of sludge production were solved during the improved Fenton reaction with zero solid waste. What's more, this process did not produce iron-containing sludge, which can also help enterprises achieve the goal of tannery wastewater standardized discharge.

4. Conclusions

In this study, the technology of fine screening, pre-biochemical treatment, high-efficiency anaerobic, biological enhancement, sludge reduction, Fenton with novel Fe catalyst and other core technologies were used to control and optimize the whole process of tannery wastewater treatment, the synergistic removal of COD and TN during biochemical treatment was realized. Meanwhile, the processing efficiency and stability of the system was significantly improved, the sludge production of the system was reduced. The performance of the Fenton reaction with novel Fe catalyst for COD removal in tannery wastewater treatment met our expectations, not only it did not produce iron-containing sludge, but also it can help enterprises achieve the goal of tannery wastewater standardized discharge.

Acknowledgement

We are very grateful that this work has been supported by Shaanxi University of Science and Technology, China.

References

Calheiros, C.S.C., Rangel, A.O.S.S., Castro, P.M.L. (2007). Constructed wetland systems vegetated with different plants applied to the treatment of tannery wastewater. Water Res. 41, 1790-1798.

Cassano, A., Criscuoli, A., Drioli, E. and Molinari, R. (1999). Clean operations in the tanning industry: aqueous degreasing coupled to ultra filtration, Clean Products and Processes, 1, 257–263.

Chen, C., Bin, L., Tang, B., Huang, S., Fu, F., Chen, Q., Wu, L., Wu, C. (2016). Cultivating granular sludge directly in a continuous-flow membrane bioreactor with internal circulation. Chem. Eng. J. 309 (2017) 108–117.

Cotman, M., Zagorc-Koncan, J., Zgajnar-Gotvajn, A. (2004). The relationship between composition and toxicity of tannery wastewater. Water Sci. Technol. 49, 39-46.

Esmaeili, A., Mesdaghi nia, A. and Vazirinejad, R. (2005). Chromium(III) Removal and Recovery from Tannery Wastewater by Precipitation Process, American J. Appl. Sci., 2 (10), 1471-1473.

Hu, Q., Fan, L., Gao, D. (2017). Pilot-scale investigation on the treatment of cellulosic ethanol biorefinery wastewater. Chem. Eng. J. 309 (2017) 409–416.

Justina, C., Elsa, M., Ana, P., Ana, L., Luis, S. and Maria, N. (2009). Membrane-based treatment for tanning wastewaters, Can. J. Civil Eng., 36 (2), 356-362.

Kabir, G. and Ogbeide, S. E. (2008). Removal of Chromate in Trace Concentration Using Ion Exchange From Tannery Wastewater. Int. J. Environ. Res., 2 (4), 377-384.

Munz, G., Gori, R., Cammilli, L. and Lubello, C. (2008). Characterization of tannery wastewater and biomass in a

membrane bioreactor using respirometric analysis. Bioresource Technol., 99, 8612-8618.

Santosa, S., Siswanta, D., Sudiono, S. and Utarianingrum, R. (2008). Chitin–humic acid hybrid as adsorbent for Cr(III) in effluent of tannery wastewater treatment. Appl. Surf. Sci., 254, 7846-7850.

Sengil, A., Kulac, S. and Ozacar, M. (2009). Treatment of tannery liming drum wastewater by electrocoagulation. J. Hazar. Mater., 167, 940-946.

Song, Z., Williams, C.J., Edyvean, R.G.J. (2001). Coagulation and anaerobic digestion of tannery wastewater. Process Saf. Environ. Prot. 79, 23-28.

Song, Z., Williams, C.J., Edyvean, R.G.J., (2000). Sedimentation of tannery wastewater. Water Res. 34, 2171-2176.

Song, Z., Williamsm, C. J. and Edyvean R. G. J. (2000). Sedimentation of Tannery Wastewater. Water Res., 34 (7), 2171-2176.

Suthanthararajan, R., Ravindranath, E., Chitra, K., Umamaheswari, B., Ramesh, T., Rajamani, S. (2004). Membrane application for recovery and reuse of water from treated tannery wastewater. Desalination 164, 151-156.

Tiglyene, S., Jaouad, A. and Mandi, L. (2008). Treatment of Tannery Wastewater by Infiltration Percolation: Chromium Removal and Speciation in Soil. Environ. Technol., 29 (6), 613 – 624.

Wiemann, M., Schenk, H., Hegemann, W. (1998). Anaerobic treatment of tannery wastewater with simultaneous sulphide elimination. Water Res. 32, 774-780.

Zhi, X., Qingzhi, F. and Weilei, Z. (2009). Research on orthogonal coagulated setting and coagulation-flotation test of tannery wastewater. J. Environ. Sci. Supp., S158-S161.

Zupancic, G. and Jemec, A. (2010). Anaerobic digestion of tannery waste: Semi-continuous and anaerobic sequencing batch reactor processes, Bioresource Technol., 101, 26-33.

P1

FACILE PREPARATION AND EFFECT OF PU-BASED ISOCYANATE ON COLLAGEN FIBRE FOR ENHANCED ELASTICITY OF LEATHER

[1]Yanting Han, [1,*]Jinlian Hu, [1]Xiao Hu, [1]Jianping Han

[1]*Institute of Textiles and Clothing, The Hong Kong Polytechnic University, Kowloon, Hong Kong*

[*]*Corresponding author: tchujl@polyu.edu.hk*

Abstract: A novel PU-based isocyanate (PUI) finishing agent based on hexamethylene diisocyanate and polypropylene triol was prepared by a facile method. PUI chains were insert between the collagen fibres by cross-linking of active terminal groups. The cross-linking effect of PUI reduced the hydrogen bonds between collagen fibre, resulting the improved rebound resilience of leather matrix without influence thermal stability of leather. When the usage amount of PUI was 6%, the stress at break of leather was improved to 21.1 MPa and strain at break increased to 67.8%. Moreover, the wrinkle recovery angle of leather was improved by 30%, indicating the enhanced elastic property of leather.

Keywords: polyurethane;finishing; collagen fibre; elasticity; leather

P2

Some Factors on Synthesis of Nano-Encapsulated Phase Change Materials for Leather

Xiaoxing Li[1], Haiteng Liu[2], Jie Chen*[3], Fangduo Sun[4]

[1]*China Leather and Footwear Research Institute Co. Ltd.,100016,China,+86-01064337830, ace660@sohu.com*

[2] *China Leather and Footwear Research Institute Co. Ltd.,100016,China,+86-01064337830, ace660@sohu.com*

[3]*Corresponding Author, China Leather and Footwear Research Institute Co. Ltd., 100016,China, +86-01064337830, chenjie73@163.com*

[4] *China Leather and Footwear Research Institute Co. Ltd.,100016,China,+86-01064337830, ace660@sohu.com*

Abstract

The fibers inside the leather are mesh structures, and there are more spaces between the fibers, which can be filled into some materials. Therefore, PCM can be introduced into leather to improve its temperature regulation and improve the comfort of leather products. Many phase change materials have poor compatibility and corrosiveness. One of the effective ways to solve these problems is to use microcapsule technology to prepare microcapsule phase change materials, and the preparation of nano-capsule phase change material for leather is more beneficial to its use in leather because of its small particle size. The nano-capsule phase change material for leather was synthesized by fine emulsion polymerization using the octadecane as the core material and the polymer of styrene and 3-trimethoxysilyl methacrylate as the wall material. The effects of emulsifier, initiator, co - stabilizer, and styrene - methacrylic acid - 3 - trimethoxysilyl methacrylate were studied. The particle size distribution and properties of the nano - capsule phase change materials were analyzed by means of laser particle size analyzer. The results showed that hexadecane co-stabilizer was beneficial to the formation of nanocapsules. The mass ratio of styrene to 3-trimethoxysilyl methacrylate was 3: 1, and the concentration of emulsifier sodium dodecyl sulfate was 2g/L, initiator azobisisobutyronitrile dosage of 0.2%, the resulting leather nano-capsule phase change material is better. The particle size is more concentrated, mostly around 450 nm.

Keywords: Nano-Encapsulated, Phase Change,Synthesis

P3

Fabrication of "Silver Nanoparticle Sponge" Leather with Durable Antibacterial Property

Gongyan Liu

National Engineering Laboratory for Clean Technology of Leather Manufacture, Sichuan University, Chengdu 610065, China (E-mail: lgy3506@scu.edu.cn)

Abstract

Leather product with durable antibacterial property is of great interest both from industry and consumer's point of view. To fabricate such functional leather, gallic acid modified silver nanoparticles (GA@AgNPs) were first *in situ* synthesized with a core-shell structure and an average size of 15.3 nm. Due to its hydrophilic gallic acid surface, the GA@AgNPs possessed excellent stability and dispersibility in wide pH range from 3 to 12 and also showed effective antibacterial activity with a minimum inhibitory concentration (MIC) of around 10μg·mL^{-1}. Then, such GA@AgNPs were used as retanning agent to be successfully filled into leather matrix during the leather manufacturing process. Moreover, taking the advantage of its high surface density of carboxyl groups, these GA@AgNPs could be further chemically cross-linked onto collagen fibers by chrome tanning agent. After retanning, the resultant leather was given a "AgNPs sponge" feature with high payload of silver nanoparticles against laundry, exhibiting high and durable antibacterial activity.

Keywords: Antibacterial, silver nanoparticles, leather, retanning

P4

Elimination of S^{2-} in tannery sludge by acclimated microorganisms

Zhi Wang[1], Jinghua Dong[2], Jie Chen[3*], Fangduo Sun[4]

1 China Leather & Footwear Institute Co. Ltd., No. 18, Jiangtai west road, Beijing 100015, China，+8615910949916, wangzhiv@live.com

2 China Leather & Footwear Institute Co. Ltd., No. 18, Jiangtai west road, Beijing 100015, China，+8613601160516, dongjinghuahao@sohu.com

3 China Leather & Footwear Institute Co. Ltd., No. 18, Jiangtai west road, Beijing 100015, China，+8613717913402, chenjie73@163.com

4 China Leather & Footwear Institute Co. Ltd., No. 18, Jiangtai west road, Beijing 100015, China，+8613051281669, 1031540380@qq.com

** Corresponding author*

Abstract

Sulfureted hydrogen is one of the main odor gases released from tannery wastewater treatment process. Properties like low odor threshold value, toxicity, corrosivity and explosive and flammability make it a serious air pollutant. Tannery sludge contains a lot of sulfur compounds and contributes a mass of sulfureted hydrogen during concentration and dehydration process. Effective solutions must be taken place to control the releasing of sulfureted hydrogen. In this study, we use microbiological method to restrict the releasing of sulfur hydrogen by elimination of S^{2-}. Acclimated microorganisms were collected and screened from tannery sludge, then they were inoculated directly back into the sludge. The high removal rate of S^{2-} and the improved dehydration property of the inoculated sludge indicated that the obtained microorganisms have good prospects for application in sulfured hydrogen control.

Key words: Tannery sludge; Sulfured hydrogen; Microorganism

Introduction

Tannery sludge in sludge thickener is a mixture of sludge from physical-chemical treatments and waste activated sludge from biological treatment units. The containing of organic matter and microorganisms make it one of the main odor spots in tannery waste water treatment plant.

Sulfureted hydrogen (H_2S) is a typical odor gas that generating from tannery sludge. It causes not only serious sensoric and toxic problems at certain concentrations, but also corrodes the concrete[1] and steel structures in waste water treatment plant[2]. Compared to biological methods, physical-chemical methods have inevitable drawbacks like needing complex treating process, easy to cause second pollution and hard to deal with the posttreatment[3]. Researches on biological leather malodorous treatment are focus on heterotopic control, most focus on biofilters[4]. Biofilters have great potentials in elimination of odor gases, but accessory equipment needs to be built to gather these gases. This will surely be a financial burden for tannery.

There are hardly any report on situ-control of the odor gases by microorganisms in wastewater treatment process. Our previous research indicated that no H_2S was detected after 4 hours' vibration and 19 hours under static condition. The pH of the sludge raised from 7.50 to 9.26. S^{2-} in the sludge can hydrolyze to HS^-, H_2S and OH^-. The reaction will be inhibited as the pH goes up, and H_2S then stop releasing. Based on these conclusions, S^{2-} must be eliminated as soon as possible before it turns to H_2S. In this study, we hope to use microorganisms to restrict the elimination of H_2S. The acclimation of the microorganisms and the effect of the microorganisms on the sludge was studied in this paper..

2 Materials and methods

2.1 Tannery sludge

Sludge simples in sludge thickener were collected from Xinji leather industry district, Hebei, China. The collected simples

were stored in refrigerator at 3°C to keep fresh.

2.2 Regent recipe

Copper regent was prepared by mix of HCl and $CuSO_4$, and resolved in distilled water to the final concentration of 50mM and 5mM respectively.

HCl was diluted to 50mM by distilled water and kept at 3°C.

2.3 Enrichment of S^{2-} removal microorganisms

The stored sludge samples were stirred at 30°C, 100rpm for 30 miniates and inoculated in enrichment medium (inoculate volume10%, v/v). Constituent of the medium was as follows: KH_2PO_4 2.0g/L, NH_4Cl 0.4g/L, Na_2CO_3 0.4g/L, $MgCl_2$ 0.2g/L, Na_2S 10g/L, pH 7.5.

The inoculated medium was cultured in a stable temperature horizontal shaking bath and shaking at 30°C, 100rpm for several days till it turns turbidity, which means the S^{2-} removal microorganisms were enriched successfully. The S^{2-} elimination ability was tested using Na_2S solution.

2.4 Acclimation of the microorganisms

The enriched microorganisms were transferred into a fresh medium (inoculate volume 10%, v/v) and shaking at 30°C, 100rpm for 3 days, then transferred to another fresh medium at same volume. Repeat 5 more times to make sure the flora was steady.

The steady flora was then inoculated into a sulfur strengthen medium (inoculate volume 10%, v/v), which contains 15g/L Na_2S, and shaking at 30°C, 100rpm for 3 days, then transferred to another fresh sulfur strengthen medium. Then increase the Na_2S to 20g/L, repeat the operation as described before to gain the acclimated flora.

2.5 Elimination of S^{2-}

The acclimated microorganisms were inoculated into tannery sludge (inoculate volume 10%, v/v) and cultured at 30°C, 100rpm for 1 hour. Tannery sludge inoculated with sterile water were used as contrast. Each experiment operates triplicates. The S^{2-} eliminating rate was tested after the experiment.

2.6 Effects of the microorganism on tannery sludge

Dry weight and filter property of the treated sludge were tested to evaluate the effects of the microorganism on the property of tannery sludge.

2.7 Determination of S^{2-}

S^{2-} react with Cu^{2+} to form CuS, which concentration can be represented by absorbance. So S^{2-} content can be characterized by turbidity of CuS[5]. Tannery sludge was centrifuged 10 minutes at 6000rpm. And then mixed the supernatant with the copper agent immediately at the volume ratio 1:2. The absorbance of the mixed solution was tested in a spectator at the wave length 480nm with the mixture of the supernatant and 50mM HCl as blank.

3 Results and discussion

3.1 The obtained microorganisms

After eleven days cultivation, all the enrich medium became turbidity. The enriched microorganism can clearly decline S^{2-} concentration of Na_2S without forming any apparent sediment (Fig.1).

The morphological characteristic of the obtained microorganisms was as shown in Fig.2. It's a mixed culture of chemoautotrophic bacteria and chemoheterotrophic bacteria and some fungus according to the microcosmic character. And some of them can swim in the medium.

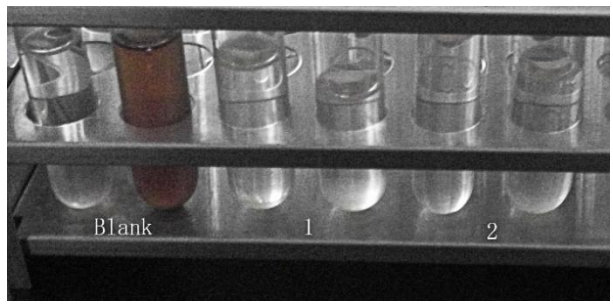

Fig.1 The S^{2-} elimination effect of enriched microorganisms (Blank is Na_2S solution without the microorganisms; 1 and 2 are Na_2S solution inoculated with the microorganisms. Test tube on the left side is Na_2S solution without copper regent and test tube on the right side is adding copper regent)

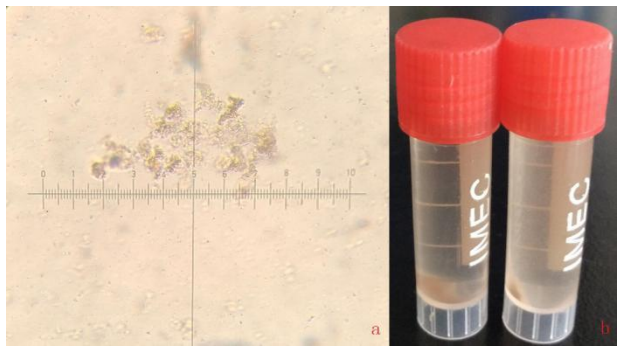

Fig.2 The morphological characteristic of the obtained microorganisms (a: Morphological characteristic of the obtained microorganisms under microscope, magnified 75 times; b: Macroscopic morphological characteristic of the obtained microorganisms)

3.2 S^{2-} elimination effect of the flora

The flora shown great S^{2-} elimination ability in 1 hour's cultivation. As is shown in table 1, the maximum elimination rate reached 72.02%. The pH of the experiment group and the blank group were similar, which indicate that S^{2-} was eliminated mainly through the flora transformation.

Table 1 S^{2-} elimination of the flora

	pH	Concentration of S^{2-} (Absorbency)	S^{2-} elimination rate
Blank	7.68	0.3617	72.02%
Experiment	7.55	0.1012	

S^{2-} oxidizing bacteria named Sulfur oxidizing bacteria (SOB). It is a kind of bacteria that reported can oxidize S^{2-} to S^0 and SO_4^{2-}[6, 7]. Chemolithotrophic SOB use S^{2-} as electronic donator to gain energy where oxygen (aerobic microbial species) or nitrates or nitrites (anoxic microbial species) serve as acceptor of electrons released during the oxidation of sulfides[6]. The reactions of the aerobic microbial species are as follows[8]:

$$H_2S + 0.5O_2 \rightarrow S^0 + H_2O, \Delta G^0 = -209.4KJ/reaction \quad (1)$$

$$S^0 + 1.5O_2 + H_2O \rightarrow SO_4 + 2H^+, \Delta G = -587.1KJ/reaction \quad (2)$$

$$H_2S + 2O_2 \rightarrow SO_4^{2-} + 2H^+, \Delta G = -798.2KJ/reaction \quad (3)$$

As is shown in the formula, H^+ is one of the products of the reaction. That can explain the slight pH change in the experiment group.

3.3 Effects of the microorganisms on tannery sludge

In order to investigate the side effects of the microorganisms on tannery sludge, the dry weight, filtration time and the volume of the sludge were investigated. After 5 days degradation, the dry weight of tannery sludge with the microorganisms declined 2.52% after constant weight, and the filtration time was halved, and the volume of the sludge was declined (Fig.3). The obtained microorganisms can degrade both organic matters and inorganic matters in the sludge, which will surely make component and structure change of the sludge. Meaning while, the microorganisms can pass through filter paper easily because their small size, so they did not add extra weight to sludge.

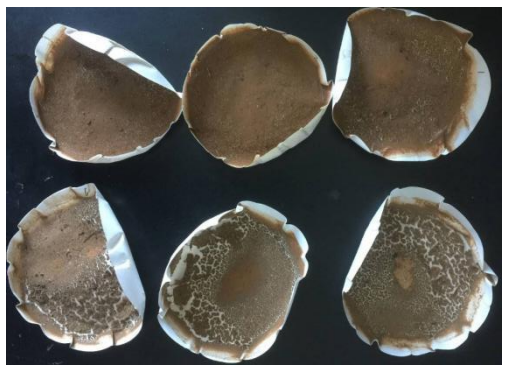

Fig.3 The morpha of the dried sludge after filtration (upper raw: tannery sludge without the microorganism; lower raw: tannery sludge with the microorganisms)

Conclusions

In this study, acclimated microorganisms were collected and screened from tannery sludge, and they can eliminate 72.02% S^{2-} in 1 hour. On the other hand, the obtained microorganisms can improve the filtration ability and reduce the volume of the sludge. All the results indicate that the acclimated microorganisms have good prospects for application in sulfured hydrogen control.

Acknowledgement

The authors want to thank the support of China leather & footwear research institute Co. Ltd. and all the help of their colleagues.

References

[1] S. Okabe, M. Odagiri, T. Ito and H. Satoh, Succession of sulfur-oxidizing bacteria in the microbial community on corroding concrete in sewer systems, *APPL ENVIRON MICROBIO*, **73** (2007), 971-980.

[2] L. Zhang, P. De Schryver, B. De Gusseme, W. De Muynck, N. Boon and W. Verstraete, Chemical and biological technologies for hydrogen sulfide emission control in sewer systems: a review, *WATER RES*, **42** (2008), 1-12.

[3] Y. Chung, C. Huang, C. Tseng and J.R. Pan, Biotreatment of H_2S- and NH_3-containing waste gases by co-immobilized cells bioflter, *CHEMOSPHERE*, **41** (2000), 329-336.

[4] L. Hua, R. Li and H. Ma, Operating Conditions for Removal of Leather Malodorous Gas by Trickling Biofilter, *CHINA LEATHER* (2012), 4-7.

[5] R. Cord-Ruwisch, A quick method for the determination of dissolved and precipitated sulfides in cultures of sulfate-reducing bacteria, *J MICROBIOL METH*, **4** (1985), 33-36.

[6] D. Pokorna and J. Zabranska, Sulfur-oxidizing bacteria in environmental technology, *BIOTECHNOL ADV*, **33** (2015), 1246-1259.

[7] K. Tang, V. Baskaran and M. Nemati, Bacteria of the sulphur cycle: An overview of microbiology, biokinetics and theirrole in petroleum and mining industries, *BIOCHEM ENG J*, **44** (2009), 73-94.

[8] M.T. Madigan and J.M. Martinko, *Brock Biology of Microorganisms*, Prentice Hall, Upper Saddle River,NJ, 2006.

P5

Study on the effluent treatment and circulation reuse technology of rex rabbit skin tanning process

Lingyun Li[1],Yao Tian[1],Guoyuan Han[1], Zongcai Zhang[1,2]

[1]*Key Laboratory of Leather Chemistry and Engineering of Ministry of Education, SiChuan University, 610065,China,15928998154,984748088@qq.com*

[2]*National Engineering Laboratory for Clean Technology of Leather Manufacture, SiChuan University, 610065,China,13320987123,zhang508@scu.edu.cn*

Abstract

The amount of chemical materials,water and neutral salt was used to the tanning process of the rex rabbit skin,which will inevitably lead to large amounts of effluent with complex component.From the perspective of environmental protection and cost,In order to reduce the effluent discharge and chemical materials inputs in rex rabbit skin processing,The effluent from rex rabbit skin tanning is properly treated and recycled again for the next batch processing.The amount of chemical materials added during recycling based on their content analysis,and the water quality was tested of the effluent circulation.When the COD value of the effluent up to a certain degree,etc.adding water treatment agent(QZ-A01) to reverse demulsification, Removing some organics and then back to the process. Finally, the physical and mechanical properties of skins were tested and make evaluation.This paper aims to improve the effluent reuse rate of tanning process, reduce the cost in production and effluent treatment and realize the sustainable development in processing industry of rabbit skins.

Key words: rex rabbit skin;effluent treatment; reverse demulsification; circulation technology

P6

Study on the Application of Cr (III) in Mordant Dyeing of Rabbit Skin

Yongguang WANG[1], Lingyun LI[1], Guoyuan HAN[1], Yao TIAN[1], Zongcai ZHANG[1,2]

[1]Key Laboratory of Leather Chemistry and Engineering of Ministry of Education, SiChuan University, (610065, China, 15198170362, 1309595647@qq.com)

[2]National Engineering Laboratory for Clean Technology of Leather Manufacture, SiChuan University , (610065, China, 13320987123, zhang508@scu.edu.cn)

Abstract

In order to reduce the environmental pollution and damage caused by the mordant of dichromate, this paper uses chromium trichloride [$CrCl_3 \cdot (H_2O)_6$] as mordant for fur dyeing.Comparing different dyeing methods and different mordant-dye ratio data,in terms of environmental pollution of chromium and dye uptake rate, it was concluded that post mordant dyeing is more feasible than the other two dyeing methods. Moreover, the mordant-dye amount is approximately 0.6 g/L,and the amount of dye is 0.8～1.0g/L . Among them, the residual amount of chromium in the dyeing bath is 0.6～0.92 mg/L, and the dye absorption rate is about 98.65%. Moreover, the mordant has no etching on the scaly layer of rabbit fiber, which will not have a great influence on the mechanical properties of rabbit skin.

Keywords: mordant; rabbit fur; dyeing; chromium chloride

P7

Effect of different organic ligandson Zr-Al tanning properties of rex rabbit

Guo-yuan HAN[1], Han LIU[1], Yao TIAN[1],Ling-yun LI[1],Zong-cai ZHANG[1,2*]

[1]*Key Laboratory of Leather Chemistry and Engineering of Ministry of Education, SiChuan University, 610065, China, 15198023193, 280005408@qq.com*

[2]*National Engineering Laboratory for Clean Technology of Leather Manufacture, SiChuan University, 610065, China, 13320987123, zhang508@scu.edu.cn*

Abstract

A rex rabbitskin's cleaner tanning technology based on Zr-Al tanning process was studied by different organic ligands with three kinds of materials which areformic acid,lactic acid, citric acid. The effects of different organic ligands on the shrinkage temperature, handle properties, physical property, the combination and distribution of the tanning agent within the skin, the dispersityof the fiber, and the water resistance were investigated. The result shows that when the n(metallic ion): n(organic ligands)=1:0.5, the turbid pH of the solutions in various methods of masking exceeds the basifying final pH. Masking with lactic acid has been improved greatly compared with the blank group in all aspects, and the comprehensive property of the three kinds of organic ligands is the best.

Key words: Zirconium-Aluminum complex tanning agent; organic ligands; tannage properties; rex rabbit skin; fur

P8

Study on Treatment of degreasing Waste Liquid of Rex Rabbit Skin with QZ-A01 and PAC Flocculant

Yao Tian[1],Yingying Chen[1],Lingyun Li[1],Guoyuan Han[1], Zongcai Zhang[1,2]

[1]Key Laboratory of Leather Chemistry and Engineering of Ministry of Education, SiChuan University;610065 China 13258368901,704549545@qq.com;

[2]National Engineering Laboratory for Clean Technology of Leather Manufacture, SiChuan University;610065 China,13320987123,zhang508@scu.edu.cn;

Abstract

In order to reduce the processing pressure of degreasing waste liquid during rabbit skin processing,In this experiment, COD, chromaticity and turbidity were used as indices to explore the optimal process of QZ-A01 reversed-phase demulsifier and PAC to treat degreasing waste liquid.At a temperature of 25°C, dosage of 2g/L, pH=6,QZ-A01 reversed demulsifier can reduce the COD value of degreasing waste liquid to about 650 mg/L, reduce the chromaticity to about 35, reduce the turbidity to below 30NTU, the removal rate of COD,chromaticity and turbidity can reach up to 71.97%, 95.05%, 98.77%;At a temperature of 30°C, dosage of 2ml, pH = 9,after PAC flocculants were used to treat degreasing waste liquid, the COD of the waste liquid was 357.4 mg/L, the chromaticity was 67, the turbidity was 20.8 NTU, and the removal rates were 83.57%, 35.58%, and 96.62%.

Key word:degreasing waste liquid;QZ-A01;PAC;COD;chromaticity;turbidity

P9

A Novel Waterborne Polyurethane Coating Functionalized by Isobornyl Acrylate with Enhanced Antibacterial Adhesion and Hydrophobic Property

1Jianhui Wu, 1Chunhua Wang, 2Wei Lin, 3Changdao MU

1Sichuan University, 2Sichuan university, 3Sichuan universty

ABSTRACT

We report a novel environmental friendly waterborne polyurethane (WPU) coating with good anti-bacterial adhesion property and hydrophobiciy. A key point of our approach is to functionize the polyurethane with isobornyl acrylate (IBA), a widely used natural material with unique chiral feature and good biocompatibility. The polyurethanes containing IBA have been synthesized by thiol-ene Michael addition reaction and poly-addition polymerization. The thiol mononer 3-mercapto-1, 2-propanediol (TPG) and vinyl monomer isobornyl acrylate (IBA) have been used to obtain dihydroxy-terminated IBA ($IBA(OH)_2$) with triethylamine as catalyst. The structure of $IBA(OH)_2$ have been identified by Fourier transform infrared spectrum (FTIR), proton nuclear magnetic resonance (^{1}H-NMR), and mass spectrometry (MS). $IBA(OH)_2$is then incorporated into polyurethane as a chain extender to yield a WPU with IBA side group (IWPU). The synthesized IWPU has been confirmed by FTIR, ^{1}H-NMR, X-ray photoelectron spectroscopy (XPS), and gel permeation chromatography (GPC). Thermogravimetric Analysis(TGA) measurements indicate that the thermal stability of IWPU is decreased slightly with the increasing content of $IBA(OH)_2$. The introduction of IBA side groups can improve the hydrophobicity of the polyurethane, which is favorable for wide application of the coatings . Additionally, the antibacterial adhesion performace of the polyurethanes has been evaluated by plate count method and optical density (*OD*) test. The results demonstrate that the polyurethane coatings with 25 wt% content of IBA side groups can exhibit effective resistance to bacterial adhesion, with the ihibition ratios of 89.3% and 80.4% for *E. coli* and *S. aureus*, respectively.

P10

Reconstituted Leather Made Using Polyurethane Based on Star-Shaped Polyester Polyols

Jie Yi, Shuqing Li, Jianxun Luo

(College of Material and Textile Engineering, Jiaxing College, Jiaxing 314001, China)

Abstract

The work described here concerns the synthesis of a special purpose adhesive and its use to bond chrome leather fibre in the preparation of reconstituted leather. The star-shaped polyester polyols based on initiators (trimethylolpropane or pentaerythritol) and ε-caprolactone were prepared by polycondensation reaction. The reconstituted leather were made using chrome-tanned leather fibre, star-shaped polyester polyols and crosslinker agent (hexamethylene diisocyanate trimer). The mechanical properties of reconstituted leather increased with decreasing the ratios of ε-caprolactone/trimethylolpropane and increasing the arm number of star-shaped polyester polyols. Leather wastes are a major solid waste and this research suggests that leather wastes can be used to produce reconstituted leather with polyurethane based on star-shaped polyester polyols.

Keywords: Reconstituted Leather, Star-shaped polyester polyols, Trimethylolpropane, Pentaerythritol, Polyurethane

P11

In-Situ Preparation of Silver Salts/Collagen Fiber Hybrid Composites and Their Photocatalytic and Antibacterial Activities

Hu Zhou(School of Chemistry and Chemical Engineering, Hunan University of Science and Technology, Xiangtan, 411201, China.) China zhouhu2006@163.com

Jie Zhou(School of Chemistry and Chemical Engineering, Hunan University of Science and Technology, Xiangtan, 411201, China.) China zhoujiehnust@163.com

Taofen Wang(School of Chemistry and Chemical Engineering, Hunan University of Science and Technology, Xiangtan, 411201, China.) China hnustchem@163.com

Jianxian Zeng(School of Chemistry and Chemical Engineering, Hunan University of Science and Technology, Xiangtan, 411201, China.) China 1763258894@qq.com

Lihua Liu(School of Chemistry and Chemical Engineering, Hunan University of Science and Technology, Xiangtan, 411201, China.) China 1415078612@qq.com

Jian Jian(School of Chemistry and Chemical Engineering, Hunan University of Science and Technology, Xiangtan, 411201, China.) China 759452147@qq.com

Abstract

To promote the utilization of collagen fiber, silver salts/collagen fiber hybrid composites with photocatalytic and antibacterial activities were successfully prepared in this study via the in-situ organic-inorganic process. The surface morphology, chemical composition and structure were discussed. Scanning electron microscopy (SEM) observation showed that the silver salts/collagen fiber hybrid composites were successfully prepared with silver salt particles (300-500 nm) distributing evenly on the surface of collagen fiber. X-ray diffraction (XRD) patterns and Fourier transform infrared spectroscopy (FTIR) analysis provided strong evidence for the successful coating of silver salts on the surface of collagen fiber and the hybrid mechanism was subsequently discussed. The photocatalytic activity was evaluated by degrading methyl orange (MO) under ultraviolet (UV) light and visible light, respectively. The results indicated that AgCl/Collagen Fiber showed the most efficient photocatalytic activity under UV and visible light irradiation. Furthermore, the introduction of Ag^+ endowed the photocatalysts with antibacterial performance, which was investigated by measuring the width of the bacteriostatic belts. The results indicated the antibacterial activity of the composites, proving that the photocatalysts were durable and reusable.

Keywords: Collagen Fiber; Hybrid Composites; Photocatalytic Activity; Antibacterial Activity

P12

An Innovative Method to Produce Gymnastic Leather

Ke Wang[2], Xiaoxiao Ma[3], Baozhen Cheng[1,2,3], Shan Cao[1,2,3*]

[1]*College of Leather Chemistry and Engineering, Qilu University of Technology (Shandong Academy of Sciences), Shandong, 250353, P. R. China*

[2]*College of Material Science and Chemical Engineering, Tianjin University of Science and Technology, Tianjin, 300457, P. R. China*

[3]*The Key Laboratory of Industrial Fermentation Microbiology of Ministry of Education,Tianjin University of Science & Technology, Tianjin 300457,China*

Abstract

In this paper, aldehyde tanning agent was considered for producing gymnastic leather owing to the requirement of white color of leather, while aldehyde tanning was considered to be environmentally friendly and inexpensive. It was expected to endow light color and high strength properties to the gymnastic leather. Glutaraldehyde (GT-X) was selected as the main tanning agent, while acrylic polymer and synthetic were used for retanning. The optimum usage of aldehyde agents in producing process were investigated through analyzing the shrinkage temperature and mechanical properties of tanned-leather. The results showed that tensile strength reached 27.06 Mpa as well as the elongation of the leather was 45.38% with the optimum usages of aldehyde agent. Therefore, it could successfully meet the strength requirements of gymnastic leather for actual application. Furthermore the present method had the potential application value for achieving high strength leather which had to be produced with non-chrome tanning.

Keywords: Gymnastics leather；High tensile strength；Low elongation rate; Aldehyde tanning; Clean production

P13

Study on preparation process and properties of UV-WPUA leather finishing agent

Chen Yongfang[1], Zhang Jianyong[2], Guo Song[1], Cheng Zhengping[1], Pang Xiaoyan[1]

(1.China Leather & Footwear Industry Research Institute Co., Ltd., Beijing, China;2. Institute of Wenzhou, China Leather and Footwear Industry Research Institute, Wenzhou, China)

Abstract:

UV curingpolyurethane acrylate (UV-PUA) resin was synthesized by polyetherlene glycol(PEG 1000), isophorone diisocyanate(IPDI), dimethylolpropionic acid(DMPA) and hydroxyethyl methacrylate(HEMA).The optimum technological conditions for the synthesis of PUA resin were as follows: prepolymerization reaction condition was 80℃, 1.5h; chain extension reaction condition was 80℃, 3.0h; end sealing reaction condition was 65℃, 6h. The optimum process conditions for emulsification of PUA resin were as follows: shear rate 3 000r/min, shear time 40min, neutralizing agent triethylamine(TEA), neutralization degree 80%~90%, and the leather finishing agent of ultraviolet curing waterborne polyurethane acrylate emulsion(UV-WPUA) was prepared with suitable particle size and good stable performance. The results show that the coating film of UV-WPUA leather finishing agent is changed from the linear structure before curing to the crosslinked network structure after curing for 25s, thus the film possesses good chemical resistance and physical and mechanical properties.

Key words: polyurethane acrylate; ultraviolet curing; leather finishing agent; film chemical resistance property; film mechanical property

Introduction

In recent years, with the increasing attention to environmental protection and gradual strengthening of environmental laws and regulations, the emission of volatile organic compounds (VOC) of traditional coatings have been more and more restricted. Therefore, the development of waterborne coatings, light-cured coatings, high-solid coatings and powder coatings with low or no pollution has become the main direction of research and development of coatings.

UV curing is the process of using medium and short wavelength ultraviolet light(300~800nm) radiation, in which the photoinitiator in liquid UV material is stimulated into free radicals or cations, and the polymerization of polymeric materials (resins) containing active functional groups is initiated, then the solid coatings is obtained. UV curing coatings are stable suspensions, and is prepared by dispersing pigment paste with monomers, oligomers, initiators and other auxiliaries. UV curing coatings possess fast curing speed, low operating cost, good performance of cured products, bright color and other advantages.

UV curable waterborne coatings combine the advantages of waterborne technology and UV curable technology, and have the advantages of fast curing speed, environmental friendliness and energy saving. It overcomes the shortcomings of skin irritability in traditional UV curing technology and poor film performance in water-based technology, which is incomparable to many traditional coatings[1-6]. More and more attention has been paid to UV-curable waterborne coatings, which has become one of the key research areas in recent years[7-10].

The advantage of UV curing technology in leather finishing is that it can make the coating film have excellent gloss and feel, improve the cross-linking degree of the film, improve the properties of coating, such as strength, water resistance, solvent resistance and adhesion [11].

A waterborne UV curable polyurethane acrylate (UV-WPUA) leather finishing agent was prepared by hydroxypropyl methacrylate grifted by urethane terminal group. The preparation and curing conditions were investigated and optimized. The curing behavior and the properties of the solidified coating film were studied by FTIR and ^{1}H-NMR. It has certain guiding significance for the application of high performance waterborne UV curable finishing agent in leather finishing.

1 Experiments

Main raw material

Isophorone diisocyanate(IPDI), dimethylolpropionic acid(DMPA), polycaprolactone diol (PCL1000), polyethylene glycol(PEG 1000), hydroxyethyl methacrylate(HEMA), dibutyltin dilaurate(DBTDL), triethylamine(TEA), industrial grade, Jining Huakai Resin Co., Ltd. ; acetone, hydroquinone, analytically pure, National Drug Group Chemical Reagents Co., Ltd.

1.2 Synthsis of ultraviolet curing waterborne polyurethane acrylate(UV-WPUA) leather finishing agent

(1)Prepolymerization of IPDI(-NCO) with PEG 1000(-OH): in 250mL four mouth flask with mixer, condensation tube and thermometer, the measured PEG 1000 and catalyst of DBTDL was added into, and stirred evenly, then IPDI was added, heating up to 80℃ for about 1.5h. The content of -NCO in the system was monitored by di-butylamine method, and when the content of -NCO reached the theoretical value, the prepolymer containing polyol segment and terminal group of -NCO was obtained.

(2)Introduction of hydrophilic groups: after the reaction system was cooled to 40℃, DMPA and small amount of acetone were added, heating up to 80℃ for about 3h. The content of -Nco in the system was monitored by di-butylamine method, and when the content of -NCO in the system reached the theoretical value, the prepolymer containing hydrophilic group of -COOH and terminal group of -NCO was obtained. If the viscosity of the reaction system is too large, add appropriate amount of acetone to control the viscosity. The long chain polyurethane prepolymer with side chain containing hydrophilic group of –COOH and terminal group of -NCO can be obtained by this reaction.

(3)End-seal reaction by introducing light curing double bond: the reaction system was cooled to 40℃, acetone solution of HEMA dissolved with polymerization inhibitor of hydroquinone was added. After the feeding was over, heating up to 65℃ for about 6h. After the full reaction of -NCO, the UV cured polyurethane acrylate(UV-PUA) resin was obtained.

(4)Neutralization, emulsification: cooling the reaction system to room temperature, TEA was added to neutralize the product under stirring until the pH of the system was between 7 and 8. The measured distilled water was added and stiring evenly, then the leather finishing agent of UV cured water-base polyurethane-acrylate (UV-WPUA) dispersion with a certain solid content was obtained by adding the measured distilled water to stir evenly.

2 Results and discussions

2.1 Optimization of the preparation conditions of UV-WPUA leather finishing agent

2.1.1 Reaction temperature and time

In the synthetic test, in order to determine the appropriate reaction temperature, the effect of reaction temperature on the reaction rate was studied. Prepolymerization reaction of isocyanate(-NCO) and PEG 1000(-OH), reaction of introduction of hydrophilic chain extender were carried out according to the conventional reaction, and the reaction temperature in these two stages was controlled at 80℃. The effect of reaction temperature on the synthesis reaction rate was focused on the temperature of end-seal reaction of introducing photocuring double bond in third stage. The reaction rate of the synthesis process was characterized by determining the content of the residual -NCO group in the system by using di-butylamine method. The result is shown in Figure 1.

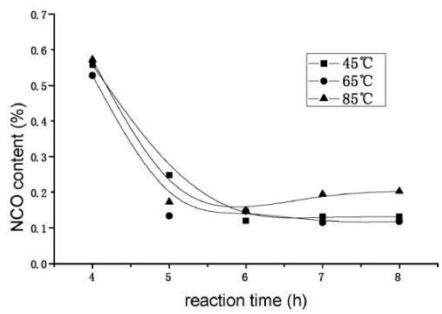

Fig. 1 -NCO content changes with time at different temperature of end-seal reaction of introducing

photocuring double bond in the third stage

Figure 1 shows that the higher the reaction temperature, the higher the reaction rate. When the reaction temperature was too low (45℃), the reaction rate was relatively slow, and the reaction time was 7~8h before the end point was reached, and when the reaction temperature was too high (85℃), the content of -NCO decreased rapidly, and a large amount of exothermic heat made the pre-polymerization reaction too violent to be controlled. It was easy to produce gel, even to made the reaction detonation phenomenon. Polymerization reaction was relatively mild at 65℃, and the reaction was easy to control, the reaction time was moderate. Therefore, the suitable reaction temperature of the third step was 65℃.

2.1.2 Reaction time

The specific reaction time of each stage of the synthesis reaction was studied, and the change of -NCO content in the reaction process was determined by di-butylamine method. Fgure 2 shows that the content of -NCO changes with reaction time at 80℃ in the first satge of prepolymerization. Figure 3 shows that the content of -NCO changes with reaction time at 80℃ in the second satge of hydrophilic group introduction. Figure 4 shows that the content of -NCO changes with reaction time of end-seal reaction by introducing photocuring double bond at 65℃ in the third stage.

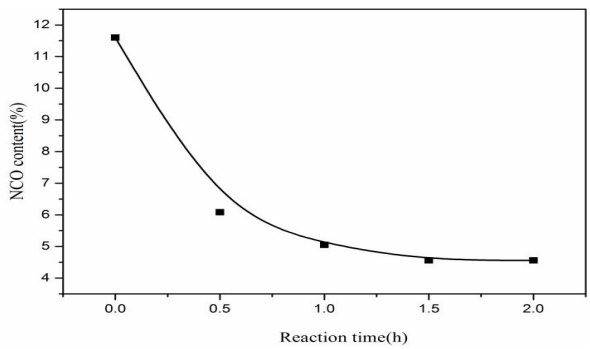

Fig. 2 Change of -NCO content with time of IPDI and PEG 1000 prepolymerization in the first stage

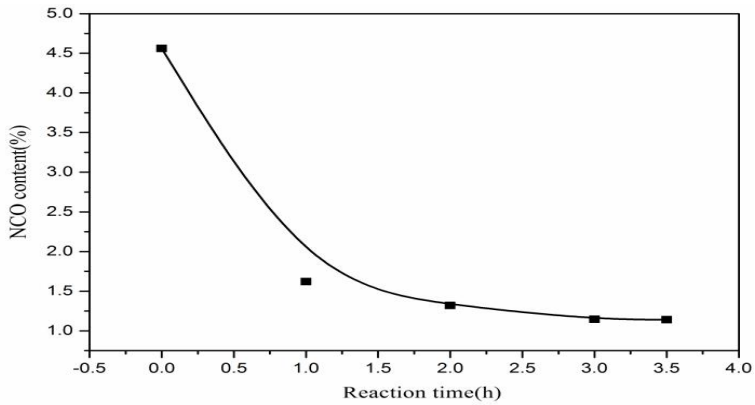

Fig. 3 Change of -NCO content with time of introduction of hydrophilic group in the second stage

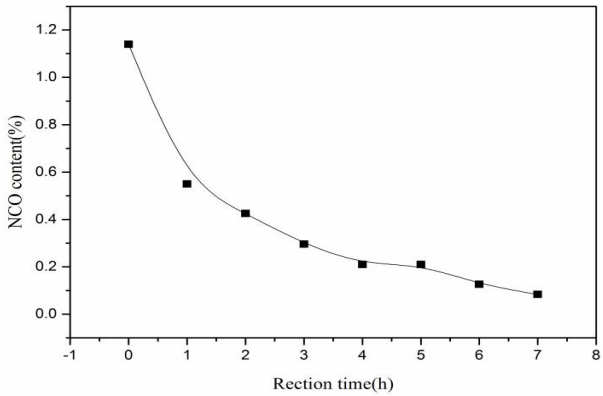

Fig. 4 Change of -NCO content with reaction time of end-seal reaction by introducing photocuring double bond in the third stage

It can be seen from figure 2 that the content of -NCO in the prepolymerization reaction is almost unchanged with the prolongation of reaction time after 1.5h, indicating that the reaction reaches the end point basically.

It can be seen from figure 3 that the content of -NCO in the second stage of hydrophilic group introducing reaction does not change much after 2.5h, which indicates that the reaction reaches the end point. Therefore, the first stage reaction time is 1.5h, the second stage reaction time is 3h.

It can be seen from figure 4 that in the third stage, the decreasing rate of the content of -NCO is slower than that of the first two stage. When the reaction reaches 6.0h, the content of -NCO in the system is 0.15%, which reaches the theoretical value. Therefore, the reaction time of the third stage is 6h.

At the end of the above three stages, the measured values of -NCO content are all lower than the theoretical values.

2.1.3 Infrared spectrum analysis of UV-PUA resin

Infrared spectrum of UV-PUA resin, as shown in figure 5.

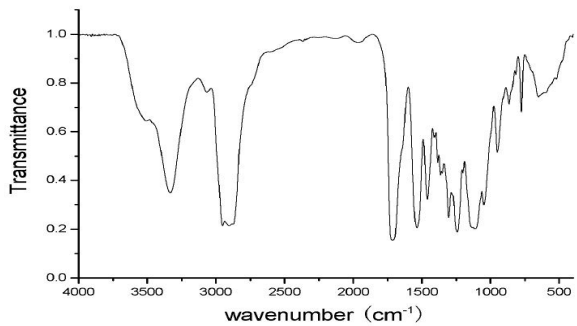

Fig. 5 Infrared spectrum analysis of UV-PUA resin

It can be seen from figure 5 that, the characteristic absorption peak of –NCO at 2270cm $^{-1}$ disappears after adding HEMA to the end of the reaction, which is obviously in the spectrum before sealing (ellipsis figure). So, in the system, the -NCO group of IPDI has reacted completely. The stretching vibration absorption peaks of the bonds of N-H at 3330cm^{-1} , -CH_2 at 2957cm^{-1}, C=O at1731cm $^{-1}$, C=C at1637cm $^{-1}$, meanwhile C-O at 1225cm $^{-1}$,1186cm $^{-1}$ and1068cm $^{-1}$. The peak of C-O at1637 cm^{-1} indicates that HEMA is connected to the main chain.

2.2 Optimization of emulsification conditions for UV-PUA resin

By adding neutralizer and ionic water into UV-PUA resin, stable leather finishing agent of UV-WPUA dispersion with certain particle size was obtained by high speed shear emulsification.

2.2.1 Effect of shear rate on UV-WPUA dispersion

The effect of shear rate on UV-WPUA dispersion was studied under the same conditions of neutralization, neutralization degree and shear time, as shown in figure 6 and table 1.

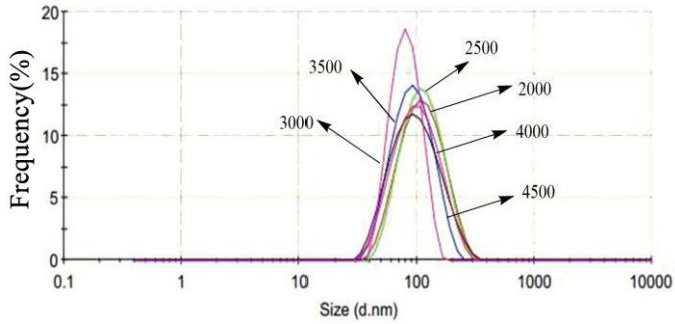

Fig. 6 Effect of shear rate on particle size of UV-WPUA dispersion

Table 1 Effect of shear rate on particle size of UV-WPUA dispersion

shear rate/ (r/min)	mean particle size/nm	particle size dispersion index	appearance of dispersion	mechanical stability
2000	96.48	0.236	milky white, transparent liquid	delamination
2500	83.64	0.224	milky white, transparent liquid	stable
3000	78.36	0.210	milky white, transparent liquid	stable
3500	82.31	0.219	milky white, transparent liquid	stable
4000	86.71	0.222	milky white, transparent liquid	stable
4500	89.10	0.224	milky white, transparent liquid	delamination

It can be seen from figure 6 and table 1 that the average particle size of the dispersion decreases first and then increases with the increase of shear rate. When the shear rate is 3000r/min, the average particle size of the dispersion is 78.36nm, the dispersion index of the particle size is 0.210, and the dispersion index of the particle size or the particle size of the dispersionis the best, which is beneficial to the preparation of UV-WPUA leather finishing agent. Therefore, the optimum shear rate is 3000r/ min.

2.2.2 Effect of shear time on UV-WPUA dispersion

The effect of shear time on UV-WPUA dispersion was studied under the same conditions of neutralization, neutralization degree and shear time, as shown in figure 7 and table 2.

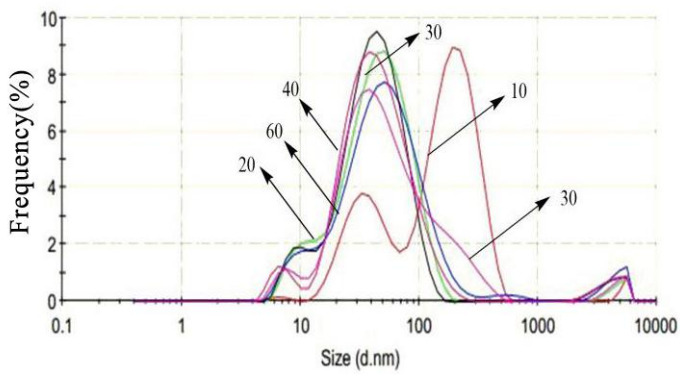

Fig. 7 Effect of shear time on particle size of uv-wpua dispersion

Table 2 Effect of shear time on particle size of UV-WPUA dispersion

shear time/ min	mean particle size/nm	particle size dispersion index	appearance of dispersion	mechanical stability
10	95.37	0.601	milky white, transparent liquid	delamination
20	42.30	0.432	milky white, transparent liquid	stable
30	39.31	0.417	milky white, transparent liquid	stable
40	33.08	0.383	milky white, transparent liquid	stable
50	36.39	0.399	milky white, transparent liquid	stable
60	38.67	0.433	milky white, transparent liquid	stable

It can be seen from figure 7 and table 2 that the average particle size of the dispersion decreases first and then increases with the increase of shear rate. When the shear rate is 3000r/min, the average particle size of the dispersion solution is 33.08 nm and the dispersion index of the dispersion size is 0.383, which is beneficial to the preparation of UV-WPUA leather finishing agent, regardless of the dispersion index of the particle size or the particle size of the dispersion solution. Therefore, the optimal dispersion time is 40min.

2.2.3 Effect of neutralization degree on UV-WPUA dispersion

The effect of neutralization on UV-WPUA dispersion was studied under the conditions of shear rate of 3000 r/min, shear time of 40min and neutralization agent of TEA, as shown in figure 8 and table 3.

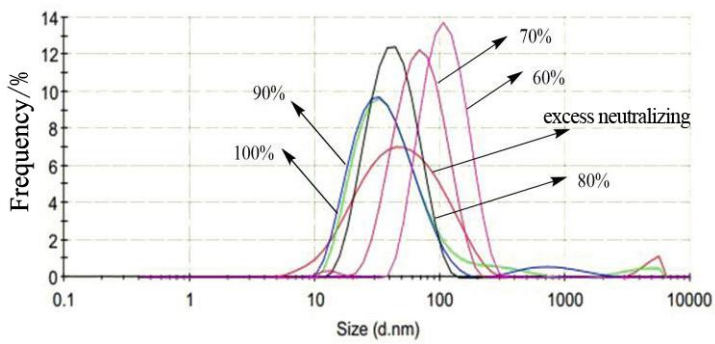

Fig. 8 Effect of neutralization degree on particle size of UV-WPUA dispersion

Table 3 Effect of neutralization degree on particle size of UV-WPUA dispersion

neutralization degree	mean particle size/nm	particle size dispersion index	appearance of dispersion	mechanical stability
overdose	40.15	0.434	milky white, transparent liquid	delamination
100%	36.08	0.315	milky white, transparent liquid	stable
90%	32.32	0.262	milky white, transparent liquid	stable
80%	35.89	0.170	milky white, transparent liquid	stable
70%	69.88	0.175	milky white, transparent liquid	delamination
60%	95.97	0.179	milky white liquid	delamination

From figure 8 and table 3, it can be seen that with neutralization degree from 60% to neutralization excess, the average particle size of dispersion decreases first and then increases. The average particle size of the dispersion is 35.89nm, the dispersion index is 0.170, the particle size distribution is the narrowest and the dispersion size is the most uniform, which is beneficial to the preparation of UV-WPUA leather finishing agent. Therefore, when neutralizer is used as TEA, the best neutralization degree is 80%~90%.

According to the average particle size and dispersion index of dispersion solution, the optimum conditions of emulsification are as follows: shear rate is 3000r/min, shear time is 40min, neutralizer is TEA, neutralization degree is 80%~90%. In this condition, the molecular chain of prepolymer is fully extended and shearing is sufficient, and the average particle size of the dispersion was 33.08nm.

2.3 Curing behavior and properties of UV-WPUA leather finishing agent

2.3.1 Curing behavior

The reactive groups in UV-WPUA leather finishing agent have an important influence on the curing process, curing time and curing film properties. The change of reactive groups is used as an important index to study the UV curing system. Absorption peaks of reactive acrylates C=C bond is detected by Infrared in UV-WPUA leather finishing agent (hereinafter referred to as "coating") at 810cm^{-1}.

The coating was prepared according to GB 1727-1992 General preparation method of paint film, and 5% (mass fraction) of photoinitiator PI 1173 was added into UV-WPUA leather finishing agent.

The coating film was placed in the oven at 60℃. After drying the 15min (to be completely volatilized), the film was taken out and solidified at room temperature under the UV lamp. The UV wavelength was 365nm.

The test results are shown in figure 9 and figure 10.

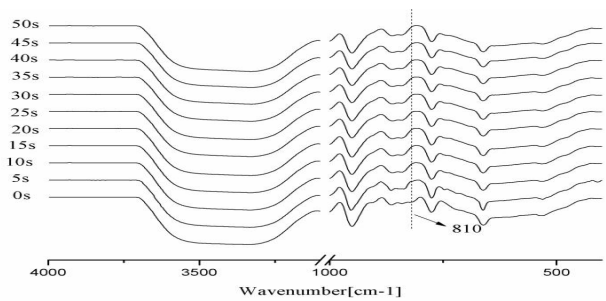

Fig. 9 Infrared spectrum of coatings with different curing time

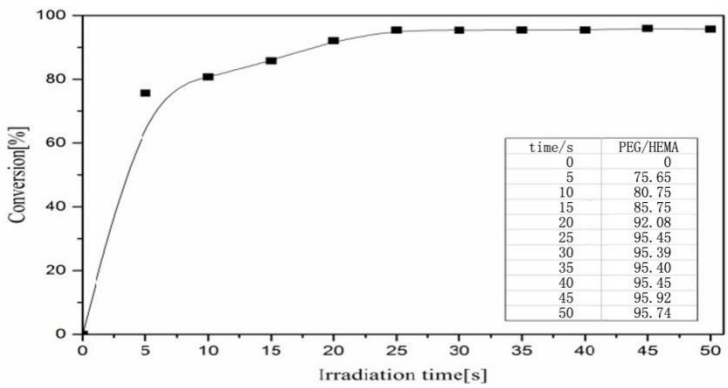

Fig. 10 C=C conversion rate with UV irradiation time curve in coating

From figure 9 and figure 10, it can be seen that the absorption peak of acrylate double bond at 810cm^{-1} decreases continuously with the prolongation of irradiation time. The results show that the curing behavior of the coating containing reactive acrylate C=C double bond polymer occurs continuously with the prolongation of UV irradiation time. The conversion rate of C=C double bond was 75.65$ at 5s of curing time, 95.45% at 25s, 95.74% at 50s. The conversion rate at 50s of curing time was not obviously different with one at 25s, indicating that the conversion of C=C double bond in the system reached equilibrium when the irradiation time(curing time) was 25s. Therefore, the curing time is determined to be 25s.

2.3.2 Chemical resistance of coating

The property of chemical resistance of the coatings before and after UV curing was tested, and the properties of resistance to acetone, deionized water, sodium hydroxide solution, sulfuric acid solution and sodium chloride solution were tested respectively.

Table 4 The swelling rate of the coating in various chemical medium **%**

sample	acetone	deionized wate	5%NaOH	5%H_2SO_4	5%NaCl
coating before UV curing	dissolve	17.2	42.6	13.7	12.5
coating after UV curing	swelling	9.3	27.1	7.6	8.7

From Table 4, it can be seen that the swelling rate of the coating in acetone before and after UV curing has changed from original dissolution to swelling, the swelling rate in deionized water has decreased from 17.2% to 9.3%, the swelling rate in 5% NaOH solution has decreased from 42.6% to 27.1%. The swelling rate in 5% sulfuric acid solution decreased from 13.7% to 7.6%, and in 5% sodium chloride solution the swelling rate decreased from 12.5% to 8.7%. The results showed that the property of chemical resistance of the coating was improved obviously after UV curing.

2.3.3 Mechanical properties of coating

The mechanical properties (tensile strength, elongation at break, brittleness temperature) of the film before and after UV curing were measured. The results are shown in Table 5.

Tabel 5 The mechanical properties of coating

sample	appearance	handle	Tensile strength/MPa	elongation at break /%	brittleness temperature/℃
coating before UV curing	transparent	sticky	13.6	534	-30
coating after UV curing	transparent	no sticky	17.1	496	-30

It can be seen from Table 5 that the tensile strength of the film after UV curing was obviously increased(by 25.7%), the elongation slightly decreased(by 7.1%), and the brittleness temperature of the coating after curing was not changed. The transparency of the film before and after curing did not change, and the handle was obviously improved. This is due to the transformation of the linear body into a network structure and the increase of the crosslinking density under UV radiation, which improved the mechanical properties of the coating.

(1)UV-WPUA leather finishing agent with different soft segments was successfully prepared, and the optimum synthetic process and emulsification process were explored.

(2)The optimum conditions for the synthesis of UV-WPUA leather finishing agent are as follows: prepolymerization of isocyanate and hydroxyl group at 80℃, reaction time 1.5h; chain extension reaction temperature 80℃, reaction time 3h; end sealing reaction temperature 65℃, reaction time 6.0h. The optimum emulsifying technology is as follows: shear rate is 3000r/min, shear time is 40min, neutralization agent is triethylamine (TEA), neutralization degree 80%~90%, ant then UV-WPUA leather finishing agent with suitable particle size and stable performance can be obtained by adding water to form salt.

(3)UV-WPUA leather finishing agent was made into the coating. After 25s of irradiation with ultraviolet light, the coating had transparent appearance, smooth handle, excellent chemical resistance and mechanical properties.

References

[1] Ma Wei, Lu Linong. Research progress of environment-friendly waterborne polyurethane [J]. Polyurethane Industry,2008,23(2):8-11.

[2] Kwak Y S, Kim E Y, Kim H D, et al. Comparison of the properties of waterborne polyurethane -ureas containing different triblock glycols for water vapor permeable coatings[J]. Colloid Polymer Science,2005,283(8):880-886.

[3] Yang Qingfeng, Qu Jinqing, Chen Huanqin. Progress in waterborne polyurethane coatings [J]. Chemical Science and

Technology Market,,2004(10):17-22.

[4] Zhao Hongzhen, Qi Shuhua, Zhou Wenying, et al. Research progress of UV curable coatings [J]. Chemistry and Bonding,2006,28(5):352-356.

[5] Maag K, Lenhard W, Loffles H. New UV curing systems for automotive applications[J]. Progress in Organic Coatings,2000,40(1-4):93-97.

[6] Nie Jun, Xiao Ming, He Yong. Progress in the study of UV-curable coatings [J]. Coating Industry 2009,39(12):13-16.

[7] Van den Berg K J, Van der Ven L G J, Van den Haak H J W. Development of waterborne UV-A curable clear coat for car refinishes[J]. Progress in Organic Coatings,2008,61(2-4):110-118.

[8] Yang Z L, Wicks D A, Hoyle C E, et al. Newly UV-curable polyurethane coatings prepared by multifunctionathioland ene-terminated polyurethane aqueous dispersionslmixtures: preparation and characterization[J]. Polymer,2009,50(7):1717-1722.

[9] Jin Yangzhi. Waterborne light-cured coatings[J]. Coating Industry,2006,36(6):54-58,61.

[10] Kim B K, Lee J C. Waterborne polyurethanes and their properties[J]. Journal of Polymer Science Part A: Polymer Chemistry,1996,34(6):1095-1104.

[11] Zhang Jing, Tu Weiping, Xia Zhengbin. Modification method of acrylic filled resin emulsion [J]. China Leather,2004,33(1):10-14.

P14

Determination of short chain chlorinated paraffins in leather based on hydro-dechlorination technique

Ma He-Wei* and Tu Xiao-Juan

(College of Material and Textile Engineering，Jiaxing University，Jiaxing 314001,China)

Abstract: Short Chain Chlorinated Paraffins (SCCPs) were analyzed based on the hydro- dechlorination technique combined with Gas Chromatography - Flame Ionization Detection (GC-FID). SCCPs were successfully dechlorinated and hydrogenated to the corresponding alkanes (C_{10}-C_{13}) in the GC injector which is filled with Pd catalyst. The relationship between the amounts of given SCCPs and the contents of yielded C_{10}-C_{13} could be well fitted by linear regression. The analytical procedure was applied for the determination of SCCPs in leather and presented 96-103% recovery and satisfactory precision (RSD＜8%) with detection limits 40 mg/kg. The real sample tests indicated the pollution significance of leather by SCCPs.

Keywords: Leather, Short chain chlorinated paraffins, Gas Chromatography, Determination

Correspondence author, Email: weimh88@163.com

P15

Quantitative Study on Product Life Cycle of Female Sandals Based on Improved BASS Model

HOU Keyu[1], WU Haozhen[1], ZHOU Jin[1,2]*

1.National Engineering Laboratory for Clean Technology of Leather Manufacture, Sichuan University, Chengdu 610065, China; 2.The Key Laboratory of Leather Chemistry and Engineering of Ministry of Education, Sichuan University, Chengdu 610065,China

Abstract

Sandals are fast-fashion products and their inventory supplement was usually predicted by the product sales record. Thereby, the purpose of this study was to apply sales data in the BASS modeling process and then to establish predict model for fast-fashion product. Sales data of casual sandals sourcing from Red Dragonfly smart store system within May to November 2017 which was the whole sale period were obtained. The improved BASS model was used to fitting the sales (individual and aggregate levels) records and the fitting curves were quantified in terms of amplitude, time to first peak curve and lasting days in peak. Our outcomes show that in terms of individual level, casual female sandals were sold 100 pairs at most and it occurred at the 51th day and lasted 11 days since it was promoted in the market; meanwhile, BASS model indicated that potential market was 11951.5, innovation factor was 0.005 and the imitation coefficient was 0.02. Further, in terms of aggregate levels. All those models were fitted good to excellent. Overall, according to improved BASS model, fast-fashion sandals' product life cycle could be accurately predicted and this protocol would provide a reliable result for enterprises.

Keywords: female sandals; product life cycle; BASS model

1 Introduction

The shoe industry has obvious seasonal and fashionable characteristics which can be classified as "fast fashion" products. “Fast fashion” refers to better meeting the needs of consumers by minimizing lead time, reducing the time required for fashion products from design development to finished product production, and finally to sales[1]. Fast fashion products are easy to face hidden dangers caused by inventory. The three main reasons are as follows: Firstly, the return of the new “slow fashion” concept leads to more inventory deviations. Secondly, fast fashion frequently causes quality problems and loses consumers’ trust.[2] Thirdly, the balance between fast fashion and sustainable development.[3]

Women's sandals are seasonal and have a short sales cycle. Compared with dress shoes, women's sandals are more typical of fast fashion products. The sales volume of sandals varies greatly in different time periods, and it is very prone to inventory backlog or shortage of stocks. Therefore, the shoe enterprises will determine the production volume of each sandal to ensure the stock of sandals by predicting the sales volume in advance. However, the predicted sales volume tends to deviate significantly from the actual results.

Based on the above situation, this paper took the sales data of Red Dragonfly casual style sandals as the research object, collected the data of sales volume of Red Dragonfly women's sandals, and used statistical analysis to study the life cycle model of women's sandals.

Theoretical Background

Nowadays, there are many researchers at home and abroad for the research of predicting the trend of sales volume and the method of establishing mathematical models[4,5,6]. Mathematical models such as Gompertz model, Logistic model and BASS model were built into the product life cycle model and then extended these to various industries. According to literature review, some scholars introduced growth models such as Gompertz model and Logistic model to describe the life cycle of products.[7,8] The Gompertz model and the Logistic model are symmetrical model curves, which are mainly used to describe the life cycle of durable goods.[9]

The improved BASS model is currently used to describe the life cycle of “fast fashion” products[10]. The conceptual basis of the BASS model to divide potential users into innovators and imitators is relatively reasonable; it uses relatively few

parameters to achieve a more accurate description of complex diffusion processes. Through the improved BASS model, it can be better combined with product features. Kurawarwala and Matsuo's research shows that the BASS model has a relatively good effect for predicting short-life products.[11]

The improved BASS model is more used in the "fast fashion" industry such as the apparel industry.[12] At present, there are few predictions on the life cycle of footwear, and there is no relevant literature to establish a life cycle model of footwear.

Methods

3.1 Subjects for Research

In this study, 19 store sales data with intelligent collection system installed from May 1th, 2017 to October 31th, 2017 was selected as a research sample to establish a corresponding life cycle. Sales figures only select casual style female sandals sales data as a sample to establish the corresponding life cycle.

The sales volume directly reflected the trend of the product life cycle, and the sales number of female sandals casual style was collected through the intelligent data collection system of Red Dragonfly offline. The data was exported through the intelligent store platform, and the corresponding mathematical model was established for analysis.

3.2 Impact Factor

The impact factor of this study was the time factor. The impact factor refers to the factors that will affect the product life cycle model. The sales of casual women's sandals products in this study were different at different times. The time factor refers to the time when the product was put into the market. The time when the product was put on the market was the start time, and the product stops production and exits the market as the termination time.

3.3 BASS Modeling

By referring to the relevant fast fashion product life cycle literature[13,14], we found the relevant models suitable for the footwear life cycle, and carried out experimental exploration methods to obtain improved BASS models.

Fitting and sales data are used in the BASS Modeling and the mathematical formulas of the non-cumulative BASS Model (Eq. 1) and cumulative BASS model (Eq. 2) are shown below:

(Eq. 1) $$N_{(t)} = m\frac{1-e^{-(p+q)t}}{1+\frac{p}{q}e^{-(p+q)t}}$$

(Eq. 2) $$n_{(t)} = m\frac{p(p+q)^2 e^{-(p+q)t}}{\left[p+qe^{-(p+q)t}\right]^2}$$

where, the $N_{(t)}$ is non-cumulative sales and the $n_{(t)}$ is cumulative sales. t determines the time; the parameters of m， p， and q indicate potential purchasers, innovation coefficient and imitation coefficient; p >0, q >0.

By bringing the sales of this study into the model, it was found that the improved BASS model is suitable for predicting the product life cycle of women's sandals.

Results

4.1 Improved BASS Model for Non-cumulative Data Fitting

Fitted BASS Model of non-accumulated data fitting was shown in Table 1. This indicate that the individual variable had moderate reliability (R2 is 0.515).The BASS model of curve quantitative analysis of non-cumulative data fitting was shown in Table 2,and its corresponding fitting result graph was Figure 1-A. These show that in terms of individual level, casual female sandals were sold 100 pairs at most and it occurred at the 51th day and lasted 11 days since it was promoted in the market. The sandals sold 65 pairs at the starting point and sold 15 pairs at the end point. And the curve has an overall fluctuation range of 85.

Table 1 The Non-accumulated Data Fitting by Improved BASS Model

Style	Parameter	m	p	q	$n_{(t)} = m\frac{p(p+q)^2 e^{-(p+q)t}}{\left[p+qe^{-(p+q)t}\right]^2}$ Improved BASS model	R^2
Casual	Sales	11916.2	0.005	0.02	$n_{(t)} = \frac{0.04e^{-0.025t}}{\left[0.005+0.02e^{-0.025t}\right]^2}$	0.515

Table 2 The Curve Quantitative Analysis of Non-cumulative Data Fitting by Improved BASS Model

Style	Parameter	Starting Point	Peak Point	End Point	Peak Time	Peak Duration	Curve Fluctuation Range
Casual	Sales	65	100	15	51	11	85

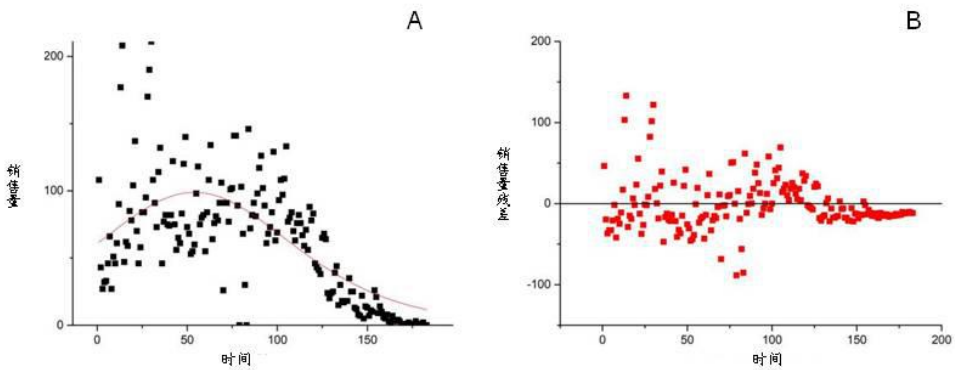

Fig.1 The Casual Style Fitting of Sales Volume by Improvement BASS Model

Fitting Result Graph(A), Fitting Residual Graph(B）

4.2 Improved BASS model for fitting cumulative data

BASS model of the cumulative data fitting indicated that potential market was 11951.5, innovation factor was 0.005 and the imitation coefficient was 0.02.

Table 3 The Cumulative Data Fitting by Improved BASS Model

Style	Parameter	m_1	p_1	q_1	Improved BASS model $N_{(t)} = m_1\frac{1-e^{-(p_1+q_1)t}}{1+\frac{p_1}{q_1}e^{-(p_1+q_1)t}}$	R^2
Casual	Cumulative Sales	11951.5	0.005	0.02	$N_{(t)} = 11951.5\frac{1-e^{-0.025t}}{1+4e^{-0.025t}}$	0.997

By fitting the experimental results, when the specified rate of change was less than 0.3%, the model no longer grows (ie, the last day of the rate of change equal to 0.3% is the peak time). Through this regulation, the quantitative analysis results of the

correlation curved in Table 4 can be obtained.

The applicable range of the prescribed cumulative sales data model was t=1 to the peak time (for example, the casual cumulative sales number: the applicable range was t=1 to t=153) was the effective interval. As shown in Figure 2-A, the cumulative sales of casual sandals was 10752 at peak time, and the curve fluctuation range was 10692. Meanwhile, the fitting residual graph was shown as Figure 2-B.

Table 4 The Curve Quantitative Analysis of Cumulative Data Fitting by Improved BASS model

Style	Parameter	Peak Time	Peak Duration	Curve Fluctuation Range
Casual	Cumulative Sales	10752	153	10692

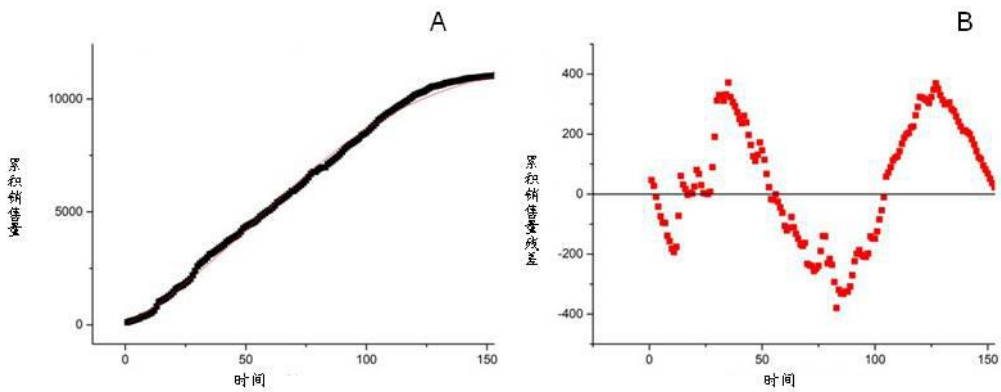

Fig.2 The Casual Style Fitting of Cumulative Sales Volume by Improvement BASS Model
Fitting Result Graph(A), Fitting Residual Graph(B）

Discussion

In this study, an improved BASS model (cumulative BASS model and non-cumulative BASS model) was developed after finding a suitable model for shoe life cycle. The model was used to predict the product life cycle trend of casual style sandals. The fitting analysis of sales volume and cumulative sales volume is not difficult to find that the life cycle of female sandals based on the improved BASS model can predict the cumulative sales volume of the product accurately. However, the non-cumulative sales data is low, because the low sample collection and the prediction accuracy was floating, but the correlation trend is found through the fitting results. Through fitting results, it was found that the relevant trend is more appropriate.

Therefore, our Bass Model is suitable for a group or a large company which has a series of retailers; however, those with a single shop or simple data could not benefit from our models.

Conclusion

This study predicted and analyzed the life cycle model of casual women's sandals by comparing the predictions of other short life cycle products, and found a BASS model that was more suitable for lifeline prediction of women's sandals. Through fitting, this study established the life cycle of the BASS model of casual style sandals, and introduced the sales data to put forward the relevant methods of the life cycle of footwear. It provided a basis for the sales forecast of footwear.

Through the study of the life cycle model of women's sandals, we can extend the analogy of the method to other shoes and

establish the life cycle model of all kinds of shoes.

References

[1] Christopher M, Lowson R, Peck H. Creating agile supply chains in the fashion industry[J]. International Journal of Retail & Distribution Management, 2004, volume 32(8):367-376(10).

[2] Xingqian Yuan, Jianwei Chen. Reasons for the production of fast fashion products and countermeasures [J]. Shandong Textile Technology, 2014(3).

[3] Joy A, Jr J F S, Venkatesh A, et al. Fast Fashion, Sustainability, and the Ethical Appeal of Luxury Brands[J]. Fashion Theory the Journal of Dress Body & Culture, 2012, 16(3):273-295.

[4] Yongfu Han, Fang Han, Song Han. Modern enterprise product life cycle curve prediction model and its application [J]. Journal of Zhengzhou University (Philosophy and Social Sciences Edition), 1999(1):44-50.

[5] Hui Xie Product Life Cycle Curve Prediction Model and Its Application in Marketing Decision [J]. Market Research, 2006(2):46-50.

[6] Yijie Xiong. Simulation study on the life cycle of commodity market [J] . Market Research, 1996(4):40-42.

[7] Cary A, Philip K. Ma rke ting:An Intro duetio n [M] .6, 2004: 48-50.

[8] Jueliang Hu, Qiuxia He, Shuguang Han. Life Cycle Research of Apparel Products Based on Improved BASS Model [J]. Journal of Zhejiang Sci-Tech University (Natural Science Edition), 2010, 27(1):69-73.

[9] Liben Mao, Qingwen Yu, Yuhua Jiang. Research on Demand Function and Demand Forecast of Several Durable Consumer Goods [J]. Economic Research,1981(10):72-77.

[10] Norton J A, BASS Frank M.A diffusion theory model of adoption and substitution for successive generations of high technology products [J]. Management Science,1987,33:1069 -1086.

[11] Kurawarwala A A, Matsuo H. Product Growth Models for Medium-Term Forecasting of Short Life Cycle Products[J]. Technological Forecasting & Social Change, 2002, 2(3):169-196.

[12] Qiuxia He. Empirical Study on the Life Cycle Model of Clothing Products [D]. Zhejiang Institute of Technology, 2009.

[13 Xianhao Xu, Qizhi Song. Improved BASS model for short life cycle product demand forecasting [J]. Industrial Engineering and Management, 2007, 12(5):27-31.

[14] Jianhua Zhang. Clothing product life cycle model and empirical research [D]. Beijing Institute of Fashion, 2004.

P16

Research of Electrochemical Degradation and Product Characteristics on Wool

Yuzeng Wang[1], Min Gu[1], Hui Chen[1], Jie Yi[2], Shuqing Li[2], Zhihua Shan[1*]

(1.National Engin. Lab. for Clean Tech. Leather Manuf., Sichuan University, Cheng Du, Sichuan, 610065, P.R.China; 2. College of Material and Textile Engineering, Jiaxing College, Jiaxing 314001, China)

Abstract

Wool is a valuable resource rich in keratin, but structural stability limits the use of wool resources. As an important resources of biochemical materials, the dissolution of wool is the basis for the utilization of wool keratin. The degradation of wool treated with electrochemical indirect oxidation method was explored in this paper. Through the optimization of experimental process and the analysis of the degradation product, it can be concluded that temperature, sodium chloride concentration and current density were important factors to affect the degradation of wool in electrochemical indirect oxidation. The optimal condition assembly of degrading wool into a solution was 150mA of current, 1.71mol/L of NaCl, 0.83mol/L of H_2O_2, 30°C. Degradation product features, such as amino acid composition, molecular weight and particle size in solution, were characterized. The results showed that electrochemical indirect oxidation can greatly increase efficiency to degrade wool keratin. Observed by scanning electron microscopy, it was shown that the scale layer of wool the degradation process was from the outside to the inside. Completely degraded product dispersed in solution in a translucence microemulsion form which showed the mean particle size was 458.8nm. According to the results of gel chromatography the largest molecular weight Mn was 388Da which belonged to low molecular electrochemical degradation. Elemental analysis of degradation product revealed that the S element content decreased to 1.12% and the N content dropped to 4.56%, which meant the structure of some amino acids were destroyed. Amino acid composition analysis also showed that some amino acids has been missing. It is the features that both advantages and disadvantages are simultaneous existence in the electrochemical indirect oxidation treatment of wool.

Keywords: Electrochemisty; Degradation; Wool; Keratin

1. Introduction

In the leather and shearing workshop, a large amount of wool by-products were produced, and there were also many waste wools or waste wool semi-finished products in the wool spinning industry[1]. These wools were often discarded because of forming hairball, resulting in a lot of waste of resources and environmental pollution. Wool is rich in keratin resources, the total amount of which accounts for about 95% of the dry mass of wool[2], and has been widely studied as a renewable keratin resource worthy of development. Wool keratin has good biocompatibility, biodegradability and can be used for treating wounds, delivering drugs, cosmetics and nutritional agents[3]. For example, the keratin solution is freeze-dried to obtain a stable keratin porous sponge-like substance, which is used as a matrix for cell growth, and mouse fibroblasts are cultured, and the number of cells cultured on the basis of collagen is 10 times greater than that under the same conditions. Wool keratin is rich in a variety of amino acids, which are beneficial to the selection for specialized application.

The wool structure contains large numbers of disulfide bonds, hydrogen bonds, salt bonds, and hydrophobic bonds[4], it is not easy to be hydrolyzed under normal conditions, so that the recycling of wool is limited. In order to maximise the use of wool resources, suitable methods must be used to dissolve wool according to different application purposes. The dissolving technology of keratin protein is the premise and basis of the recovery and reuse of wool isosceles protein resources, which directly affects the subsequent application realization, and it is also a difficult technology in the entire research. Keratin characterized by poor solubility attribute to the complex structure of α and β keratins including the presence of a high degree of disulfide-bond, numerous hydrogen bonds, and strong hydrophobic interactions[5]. The disulfide-bond which crosslink half-cysteine residues simultaneously stabilize the secondary structure of protein. Some extractions of wool keratin have

been conducted in various ways[6], which included acid, alkali, oxidizing or reducing agents and enzymes. Under the severe acid-base treatment, part of essential amino acids would be destroyed. Oxidizing or reducing agents convert the –S–S– to $–SO^{3-}$ or –SH to acquire soluble keratin solution. Enzymes have a property of specificity and high efficiency. The industrial enzymes regularly contain peptide hydrolysis enzymes besides disulfide bond reductase, those specificity and accessibility make the the polypeptide composition characterized obvious. However, the hydrolytic mixtures are not easy to purify. Actually various methods to extract keratin have a common principle, on which the wool can be dissolved only by cleaving the inter-molecular disulfide bonds[7]. As a new dissolution method the wool was catalyzedoxidation by electrochemical treatment in this experiment, which is non chemical dissolution and clean, purified, decolored. It was found that electrochemical degradation of wool is fast and efficient when the degradation product analyzed and represented. Meanwhile, a special degradable components can be obtained.

2. Experimental section

2.1 Materials

sodiumchloride, hydrogenperoxide, sodium carbonate, methanol, hydrochloricacid, glycerol, non-ionic degreasing agent, all were from Chengdu Kelong Ltd., China, and were of analytical grade. Tris, acrylamide, sodium dodecyl sulfate, methylene diacrylamide, TEMED, ammonium persulfate, mercaptoethanol, CoomassieR-250, all above used for the experimental work were from Chengdu Tiantai Science and Technology Ltd., China, and were of electrophoresis-grade reagents. 36mm dialysis bag(innerdiameter 1.3 nm, MW3500) was from spectrum company of USA.

2.2 Preparation of electrolytic samples

2.2.1 Preparation method

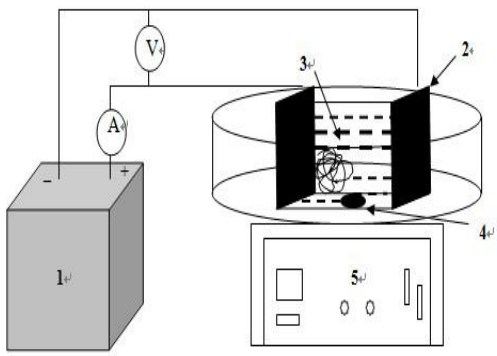

Fig.1 Apparatus in non-membrane electrolysis

Experimental wool sample was ground to 1~2 mm sizes, placed in a 500 mL triangularflask and degreased with 0.1 g non-ionic degreasing agent and 0.1g sodium carbonate at 25℃ for 2 hours. Put 10g dried preprocessed wool into electrolytic cell with graphite as the cathode and anode materials. the no membrane electrolytic device was shown in Figure.1 and 200 mL solution of sodium chloride and peroxide were added into the cell. The temperature was set at test value and stirring rate was set at 60r/min. Ensure that the current is stable during the electrolysis process and stoped electrolysis till the electro-catalytic treatment solution became nearly turbid liquid. During all electrochemical degradation process the pH of cell solution was adjusted to 4.5±0.2 with HCl. The wool keratin degraded solution was centrifuged at 4000g for 10min to separate the undissolved fragments. The centrifugate was dialyzed with diameter 1.3nm dialysis bag at 4℃ for 48 h to remove sodium chloride and small molecular organic, and then freezed drying, weighed, sealed store in refrigerator under 0℃ reserving as keratin solid powder samples(KSP).

2.2.2 Optimization group

In this experiment, wool solubility was mainly affected by temperature, sodium chloride, peroxide, and current size so we designed a $L_9(3^4)$orthogonalexperiment accordingly. Took a set of optimal conditions as the preparation of samples to repeat the electrolysis experiment.

Tab.1 Orthogonal experiment $L_9(3^4)$ electrolyzing of the wool

levels	I/mA	*w* (NaCl)/%	*w*(H_2O_2)/%	T/℃
1	100	6	2	20
2	150	4	4	30
3	200	2	6	40

2.3 Characterization of KSP

1) Preliminary observation of degradation: The treated wool was taken out from cell after 30 min or 60 min of electrolysis and observed by JSM-7500F Scanning Electron Microscope, JEOL.

2) Amino acids analysis: 100 mg preprocessed wool (degreased and dried) and 100 mg KSP were hydrolyzed in HCl 6N at 110℃ for 22 h in a nitrogen atmosphere, then eliminated acid and mixed with sample buffer. Amino acids were analyzed by A300 Automatic Amino Acid Analyzer, Mannheim, Germany.

3) The particulate size distribution: 10% KSP solution was dispersed in deionized water and mean diameter of degradation product was measured by Malvern laser particle size analyzer.

4) IR absorption: The infrared absorption of KSP was observed with KBr compression method by 670FT-IR Infrared Spectrometer, NEXUS, USA.

5) Elemental analysis: The characteristic elements of KSP were analyzed by Euro EA 3000 Elemental Analyzer, Liman-Lamberts Inc.

6) Molecular weight: KSP was dissolved in 5% triethanolamine water solution and determined molecular weight by means of GPC.

3. Results and discussion

3.1 orthogonal experiment analysis

NaCl was taken as supporting electrolyte and indirect electrooxidation materials, and the oxidation-reductants in electrode reaction were generated as follows.

$$2NaCl+2H_2O \rightarrow 2NaOH+H_2+Cl_2$$

$$Cl_2+H_2O \rightarrow HClO+HCl$$

The keratin was sensitive to oxidant and reductant. The disulfide bond of wool keratin was easily broken under the action of hypochlorite[8]. H_2 produced on the cathode can alsoturn the disulfide bond to sulfhydryl group when it contact with the keratin, but H_2 of small solubility was a weak reductant. The main degradation process of keratin was shown in the following equation.

$$P\text{-}S\text{-}S\text{-}P_1+HClO \rightarrow P\text{-}SH+ P_1\text{-}SOH+ P_2\text{-}SO_2H+ P_2\text{-}SO_3H+Cl^-$$

$$P\text{-}S\text{-}S\text{-}P_1+ H_2 \rightarrow P\text{-}SH+ P_1\text{-}SH$$

The HClO from electrolysis of NaCl has highest oxidation potential ($HClO^-/Cl_2 \approx 1.61V$) and highest the concentration of HClOin acidic solution. Oxide components distribution is in figure.2 and it means that the cysteine oxidized can be adjusted by system pH value easily[9].

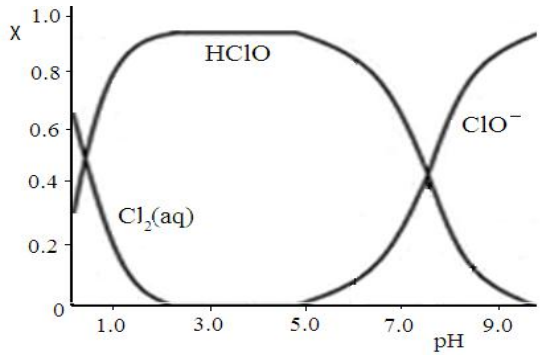

Fig.2 Solution pHand each component scores

When the pH value of solutions was 4.5±0.2, the electrochemical oxidation should have best efficient. Through analyzing the influence ofvarious factors on the solubility of the wool come to a conclusion that temperature, sodium chloride concentration and current density are the important factors of all. An result of the optimum composition conditions in the $L_9(3^4)$ orthogonalexperimentrange can be obtianed: current magnitude 150 mA, sodium chloride 6%, peroxide concentration 0.83 mol/L, temperature 30℃. Under the conditions the wool was completely dissolved within 3.5 h.

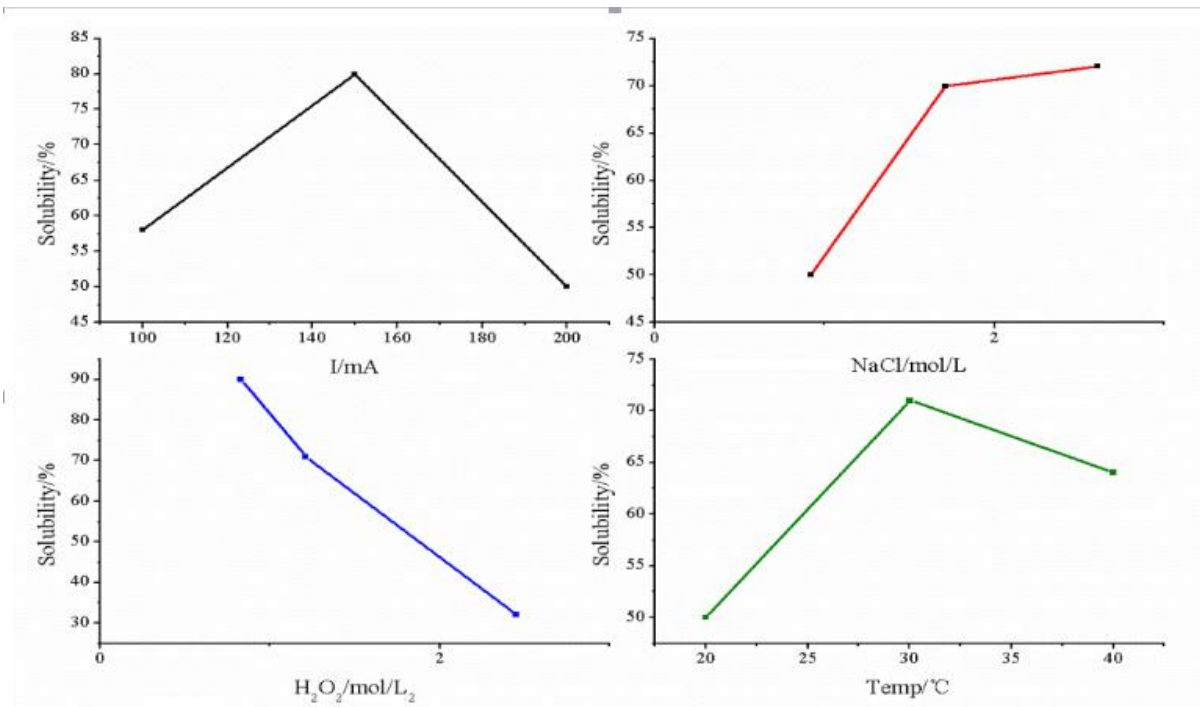

Fig.3 Wool solubility changes in electrochemical dissolution

As the peroxide concentration increases, the dissolution rate of wool gradually decreases because hypochlorite was consumed by peroxide, oxidation was weakened. From sodium chloride-solubility curve, the solubility increase with sodium chloride addition, until the curve become flat. It could be illustrated with the increase or extremity of hypochlorite oxidation. As can be seen from temperature-solubility curve, rising temperature accelerate the reaction rate, but the solubility decrease when temperature exceed 30℃, the reason maybe high temperature decomposed peroxide consequently make oxidization diminished. In the current magnitude-solubility curve, hypochlorite was generated as current density increase, hypochlorite oxidation was enhanced. Nevertheless, excessive current passivate electrode and make the solubility dropped.

3.2 KSP feature analysis results

degradation product. The strong absorption fall at 677 cm-1 of wool treated by Na2S belong to the -S- stretching vibration and not in KSP treated by electro-catalytic oxidation.

3)Amino acid analysis:

By analyzing the amino acid composition of raw wool and KSP, it can be known that raw wool contains 17 amino acids while KSP contains only 10 amino acids[11]. Total Amino acids content decline from 90.84% to 11.53%, cystine content decline by 13.95% which indicated that the disulfide bond has been cleaved by electro-catalytic oxidation. Besides, some new amino acids yield, such as taurine amino acid, tryptophan amino acid, hydroxylysine amino acid and ammonium ion. These new amino acids could come from modification of primary amino acids, or electrochemical synthesis of degradation products in process.

1) The hair observing: The apparent structure of electrolyzed wool samples at 30 min, 60 min was oserved with SEM. At the beginning of the experiment, we can obviously see that the scale layer of raw wool was complete and arranged orderly. After 30min of electro-catalytic treatment, the layer cracked and begun to fall off, surface of the wool became rough. The layer of 60 min treated samples was destroyed and exposed the corticallayer. The apparent structure change affirmed the increase of solubility over time at some point. It can be concluded from these SEM pictures that the wool was degraded from the outside to the inside, first the surface of scales and next the raised edge. The uneven effect of electro-catalytic treatment could refer to resistant to oxidation in chemical structure.

2) IR analysis of KSP: The infrared absorption spectrum of KSP treated by Na_2S reduction and electro-catalytic oxidation was shown in Fig.5. The N-H stretching vibration, fall at about 3500 cm^{-1}, Amide I known as sensitive to the secondary structure of proteins (between 1650 cm^{-1} and 1690 cm^{-1}) is mainly associated with the C=O stretching, Amide Ⅱ occurs in the range of 1650~1590 cm^{-1} due to the -N-H bending vibration and C-H stretching vibration. The absorption between 1400~1420 cm^{-1} belong to Amide Ⅲ result from C-N stretching vibration and -N-H bending vibration[10], which doesn't show N-H bending vibration of KSP treated by electro-catalytic oxidation, or the amino had been damaged in the

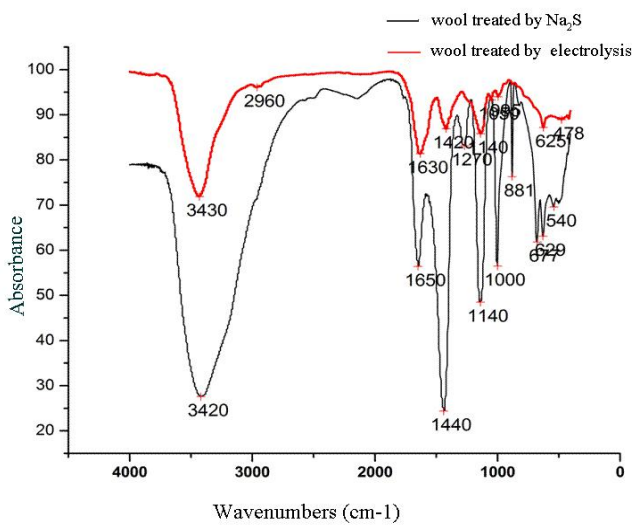

Fig .5 Infrared spectrogram of the wool treated by Na_2S and electrolysis

degradation product. The strong absorption fall at 677 cm^{-1} of wool treated by Na_2S belong to the -S- stretching vibration and not in KSP treated by electro-catalytic oxidation.

3)Amino acid analysis:

By analyzing the amino acid composition of raw wool and KSP, it can be known that raw wool contains 17 amino acids while KSP contains only 10 amino acids[11]. Total Amino acids content decline from 90.84% to 11.53%, cystine content decline by 13.95% which indicated that the disulfide bond has been cleaved by electro-catalytic oxidation. Besides, some new amino acids yield, such as taurine amino acid, tryptophan amino acid, hydroxylysine amino acid and ammonium ion. These new amino acids could come from modification of primary amino acids, or electrochemical synthesis of degradation products in process.

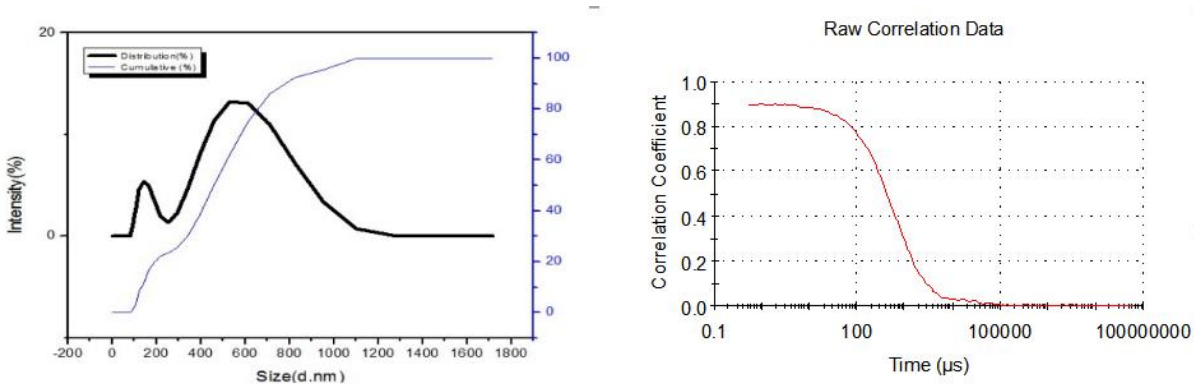

Fig 6 Particle Size Distribution

4) Particles size analysis:The particle size distribution diagram (see Fig.6) of 10% KSP solution appears two peaks in 141.8nm and 531.2nm. Calculated from the cumulative distribution curve the mean size of the particles is 458.8nm, which describes the relative width or non-uniformity degree of particle size distribution. On the basis of formula (D90-D10)/D50, the dispersion of the keratin solution is1.39.

Tab.2 N and S content of the raw and KSP

samples	*w*(N)/%	*w*(S)/%
Raw wool	16.71	4.66
KSP	4.56	1.12

5)N and S elemental analysis:N and S content determination of the raw wool and KSP, see Tab.2, aims to estimate amino acid and disulfide bonds contents. The amino acid content of raw wool is 93.44%, but very few N content in KSP can not countamino acid content if removing the ammonium nitrogen. It can be found in table 2 that many amino acids disappeared or broken. Total quantity of amino acid decrease 71.94% after electro-catalytic oxidation.

6)Molecular weight:

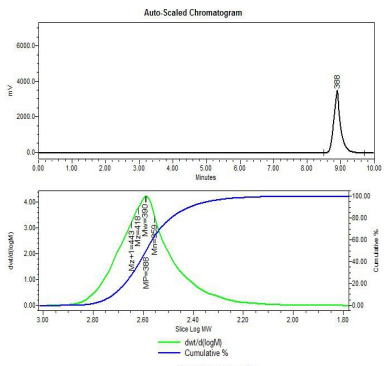

GPC Results

	MP (Daltons)	Mw	Mn	Polydispersity
1	3.88e+002	3.90e+002	3.59e+002	1.09

Fig 7 Gel chromatography

Fig.7 shows the molecular weight of KSP solution, the results Mn is 359, M_W is 390, M_p is 388 and the polydispersity is 1.09. No macromolecule exist in KSP. The KSP particals in water are in the form of aggregation, so that these particals can not thought the dialysis bag (innerdiameter 1.3nm, M_w3500).

4. Conclusions

In this paper, electrolytic method was applied to dissolve the wool fibers. There is a set of the optimum combination conditions: current magnitude 150mA, sodium chloride 6%, temperature30℃. The chemical and structural characteristics of KSP were investigated. KSP is an aggregation in water with a mean particle size 458.8nm. GPC determined the number-average molecular mass(Mn) was 359. As the chemical construction of KSP was concerned N-H bending vibration absorption disappearing, contents of N and amino acid type much decreasing all proved that electrochemical degradation damage initial amino acid structures during the process of degrading wool. But it also was found that there were some new amino acids generated, such as taurine amino acid, tryptophan amino acid and hydroxylysine amino acid, which may be significant for new ways to explore recycling of waste wool.

Acknowledgements:

The authors would like to thank the key item of Hunan Leather engineering technology center Xiangxiang (No.09H0746) for the financial support.

References

M.zoccola ,A.Aluigi,C.Tonin Macromol.938(2009)35-40.

[2]KELLYR. Application of Wool Keratins Ranging from Industrial Materials to Medical Devices[M].England:Woodhead Publishing Limited,2009: 323-331.

[3]ROUSEJG, DYKE MEV. A review of keratin-based biomaterials for biomedical application[J]. Materials, 2010, 3(2):999-1014.

[4] R.D.B. Fraser, T.P. MacRae, Linn Soc. Symp. Ser. 9 (1980) 67.

[5]Riessen, S., Antranikian, G., 2001. Isolation of Thermoanaerobacter keratinophilus sp.nov., a novel thermophilic, anaerobic bacterium with keratinolytic activity.Extremophiles 5, 399e408.

[6] K. Yamauchi, A. Yamauchi, T. Kusunoki, A. Kohda, Y. Konishi, J.Biomed. Mater. Res. 31 (1996) 439.

[7] J.A. Maclaren, B. Milligan, Wool Science, vol. 1, Science Press, 1981, pp.1–18.

[8] Roche CG,Michelle RM,Jillian R,et al.Mechanical and biological properties of keratose biomaterials[J]. Biomaterials,,2011,32:8205-8217.

[9]Moll F J.The oxidation of gelatin[J]. Journal of the photography science,1989,vol.37,14-18.

[10] E.Wojciechowska,A,Wlochowicz. Journal of molecular structure.614(2002)355-363.

[11] K. Yamauchi, H. Hojo, Y. Yamamoto, T. Tanabe, Mater. Sci. Eng. C1043 (2003) 1.

P17

Industrial Production of Chrome-Tanned Leather Without Formation of Hexavalent Chromium by treating with a Combined Inhibitor

KOKI OGATA[1*], TOSHITAKA INATSUGI[1], SHUNJI HATTORI[1], KEIJI YOSHIMURA[2] and KOJI TAKAHASHI[3]

[1]*Japan Institute of Leather Research, Kuwabara 520-11, Toride, Ibaraki 302-0017 Japan*

[2]*Japan Leather and Leather Goods Industries Association, Komagata 1-12-13, Taito, Tokyo 111-0043 Japan*

[3]*Scleroprotein and Leather Research Institute, Faculty of Agriculture, Tokyo University of Agriculture and Technology, Saiwai-cho 3-5-8, Fuchu, Tokyo 183-8509 Japan*

Abstract

The particular effect of a three-component inhibitor containing of 1.0 mmol of 3(2)-*t*-butyl-4-hydroxyanisole, 0.01 mmol of ascorbic acid, and 0.001 mmol of collagen peptide on the inhibition of C^{6+} formation from Cr-tanned leather industrially produced was analyzed from the results evaluated by determining the C^{6+} content of the heat-aged leather sample. the inhibitor was used by spraying on the dyed and fat-liquored Cr-tanned before pigment-finishing process. As a result, C^{6+} formation could be completely inhibited. In addition, physical strength was higher by treatment with inhibitor. In particular, the strength of surface (Ball burst) was twice as much as that of the untreated one. These results indicate that the three component inhibitor could be effectively applied industrially produce Cr-tanned leather not only without C^{6+} formation but also with an improved physical strength.

Keywords: Hexavalent chromium, Inhibitor combination, Leather production

P18

Discussing Again to Nowadays Chrome Tanning Agents

*DING Xiaoliang，SHAN Zhihua**

（The key Lab. of Leather Chem. and Engin. of Ministry of Education，

Sichuan University，Chengdu 610065，China）

Fu Xianbing, Sun Hu, Ying Xiaoyan

(Brother Scientific and Technical Co., Ltd., Haining 314407，China)

Abstract: So far chrome tanning agent is always an important material for leather manufacture because its tanning power cannot be achieved by other tanning agent. It is much beneficial again to understand the function of nowadays chrome tanning agents. The application characteristics of three kinds of chrome tanning agents, such as the glucose reduced chrome seriflux(GCr-L), the glucose reduced chrome(GCr-S) and the sulfur dioxide reduced chrome powder(SCr-S), were explored by modern tanning methods. By the contrast studies three chrome tanning agents were evaluated, including the hydrolysis and spectral absorption characteristics of three kinds of chrome tanning agents; the penetration and absorption of chrome tanning agents in pickled hides, physical mechanical properties of chrome tanned leather and the effects of retanning, dyeing and fatliquoring on wet blues. The result is that the pH of GCr-L and GCr-S are lower in the initial hydrolysis, closing the to the equilibrium pH. The entire absorption spectrum of GCr-L is violet-shifted, which testified have complex compositions and more organic complexes, show not as good as SCr-S whether the penetration speed or the absorption rate during tanning process. The crust leather tanned alone with SCr-S is superior in physical and mechanical properties. However, there are no obvious differences in the effect of dyeing, fatliquoring to three kinds of crust leathers. The finished leathers tanned with each chrome tanning agent turn out to be the same quality of leathers.

Keyword: glucose reduction; sulfur dioxide reduction; chrome tanning agent; application

P19

Preparation and Properties of Amino Acid Surfactants with Different Lipophilic Groups

Jiang Chenhui , Li Yun *,Huang Fenglin, Wang Quanjie

(School of Chemistry and Chemical Engineering, Yantai University, Yantai 264005, China)

Abstract

The collagen hydrolysate was prepared by waste leather shavings via alkali hydrolysis. According to Schotten-Baumann reaction, series collagen hydrolysate-based amino acid surfactants were prepared with collagen hydrolysate and different kind of acyl chloride with different carbon chain length (C10, C12, C14, C16). The optimal reaction conditions were determined by the free amino content in surfactant solution. The structures of amino acid surfactants were evaluated by Fourier transform infrared spectroscopy analyses (FT-IR). Their physicochemical properties, such as surface tension, foaming and foam stability were investigated. The results showed that, The optimal conditions for the synthesis of surfactants are as follows: the reaction pH value was 9, the volume ratio of ethyl acetate to lauroyl chloride was 2:1, the reaction temperature was 60℃ and the highest conversion rate was 77.9%. As carbon chain length of acyl chloride increasing, the free amino content in surfactants declined, and their foam stability increased. Lauroyl surfactant with C12 have the lowest surface tension and highest foaming stability.

Keywords: Amino acid surfactant; Abandoned chrome shavings; Schotten-Baumann reaction; Lauroyl chloride

Introduction

Statistically the capacity of world leather is about 1.5×10^{10} kg hides and skins per year. The average wastewater discharge is more than 1.5×10^{10} kg per day. Solid waste generation from tannery process is estimated as 6×10^{9} kg per year[1].The traditional leather industry characterized with high input and consumption increases the prominent economic efficiency, but it also leads to the tremendous environment pollution, biological chains destruction and the huge waste of resource. Thus, the recycling of leather waste is of great significance to the sustainable development of the tanning industry.

Leather wastes are mainly composed of collagen and chromium (III), in which collagen accounts for more than 90 % , and chromium (III) is about 3 % ~ 4 % of leather quality[2]. Treated by physical, chemical, or biological methods, collagen can be hydrolyzed into soluble compounds with relatively low molecular weight, known as collagen hydrolysates (CH)[3,4]. However, these collagen hydrolysates often exhibit a limited surface activity since the surface activity of collagen depends on the characteristics of molecular structure and the amount of the hydrophobic groups together with the polar moiety. Therefore, chemical modification of collagen might serve as a tool for improving their surface activity[5].

Surfactant made by waste chrome shavings not only provided a way to effectively synthesize surfactants but also effectively alleviated the pressure on the environment and resources of leather waste. Surfactant can be reused in the leather manufacturing process, which can effectively reduce the dependence on traditional surfactants and conform to the circular economy mode[6]. Meanwhile, Surfactant might broaden the application of cosmetics[7], drug delivery[8] and food industury[7].

Chi et al.[9-12] extracted collagen hydrolysates from the leather wastes and subsequently prepared collagen hydrolysate-based surfactant. Sripriya et al.[13] prepared water-soluble polyanionic collagens via importing a large amount of carboxyl groups of acylation of collagen with succinic anhydride. However, obtained water-soluble polyanionic collagens exhibited weak surface activity as a result of the strong hydrophilicity brought by the high acylation ratios. Li et al.[5,14-16] prepared acylated collagen based on reaction of ε-NH_2 in lysine groups of native collagen molecules with lauroyl chloride and succinic anhydride. The structural properties, thermostability, and surface morphology for acylated collagen were investigated.

However, the effect of surfactants made from different acid chlorides on the physicochemical properties and the surface activity of CLS was not investigated. Obviously, the understanding of these details is significant for the application of CLS

in diverse fields. In this study, collagen hydrolysate（CH） were first extracted from waste chrome shavings, and a series of different carbon chain length acyl surfactants (CLS) with different carbon chain length group were prepared. Then, the relationship between the free amino conversion and surface activities, such as surface tension, foaming capacity and foam stability was studied.

1 Materials and Methods

1.1 Materials

Chrome shavings was were provided by Shandong Wendeng Leather Factory. L-leucine, O-Phthalaldehyde (OPA) were provided by Shanghai yuanye Bio-Technology Co., Ltd. Decanoyl chloride(C10), Lauroyl chloride(C12), Myristyl chloride(C14), Palmitoyl chloride(C16), Sodium dodecyl sulfate（SDS） and other chemicals were of analytical grade.

1.2. Preparation of Collagen Hydrolysate (CH) and Different Carbon Chain Length Acyl Surfactants (CLS)

A certain amount of dry chrome shavings was weighed and added CaO（4wt%）, NaOH（4wt%）and water (500wt%) in turn. Hydrolysis reaction was conducted at 80℃ for 6 h under stirring. After being cooled, the pH of solution was adjusted to 7. The sample solution was then filtered,and then, the CH solution was obtained.

As for the graft modification reaction, the obtained CH solution was transferred to a 250 mL five-necked flask. The CH was stirred in a water bath of 30 °C for 4 h, while a certain amount of lauroyl chloride filled with ethyl acetate as solvent and 10% Na_2CO_3 solution were added drop by drop to make pH 8.0. The mixture was then heated to 80 °C, and the ethyl acetate in it was recovered. According to conversion rate of free amino groups. Influences of pH, the volume ratio of ethyl acetate and lauroyl chloride, temperature and different carbon chain length of acid chloride on free amino conversion were studied.

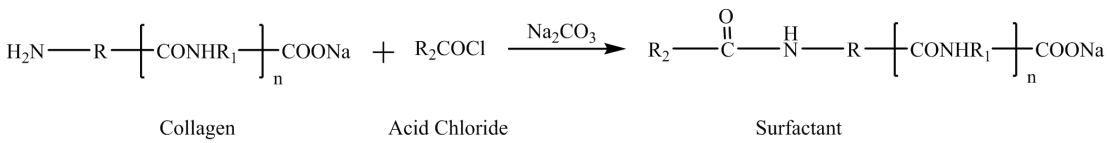

Figure 1. Synthesis of surfactant

1.3 Free Amino Group Content

Free amino group content of CH and CLSs was determined using OPA method [17,18]. The absorbance of L-leucine, CH, and CLB at 340 nm was measured using an ultraviolet-visible spectrophotometer (Shanghai Jinghua Technology Instrument Co., Ltd., China). A standard curve for free amino groups were plotted by changes in the concentration of L-leucine, and calculate the concentration of free amino groups in CH and CLB based on it. The conversion rate (R) was calculated as below：

$$R = \frac{C_0 - C_1}{C_0} \times 100\%$$

Free amino group content of CH was recorded as C_0 (mol/ml), Free amino group content of CLB was recorded as C_1 (mol/ml).

1.5 Characterization

1.5.1 Fourier Transform-Infrared (FT-IR) Spectroscopy

FT-IR spectra of CH and CLSs were measured using IRAFFINIT FT-IR spectrometer (Bruke, Germany) with potassium bromide disc technique.

1.5.2 Surface Tension

Surface tension measurements of CH and CHBSs were performed in triplicate at 25 °C by a JYW-200A automatic surface tension meter（Chengde Jinhe Instrument Factory, China）. A series of CH or CLS solutions with different concentrations were obtained by dilution of distilled water. Surface tension of CH or CLS was determined by different concentrations using automatic surface tension meter[19].

1.5.3 Foaming Capacity (FC) and Foam Stability (FS)

FC and FS of CH and CLSs were evaluated by Wei et al. [20]. It was prepared that 10 gL^{-1} of CH or CLS solution. Sample solution (10 mL) was added into a 50 mL plug gauge, and kept at SHZ-88 Thermostatic oscillator (Jiangsu Province of Jintan Medical Instrument Factory, China) of 40 °C for 5 min. The foam volume was recorded as V_0 (t = 0 min, mL) and V_{30} (t = 30 min, mL) after removal.

2. Results and Discussion

2.1 Effect of pH on Free Amino Conversion Rate

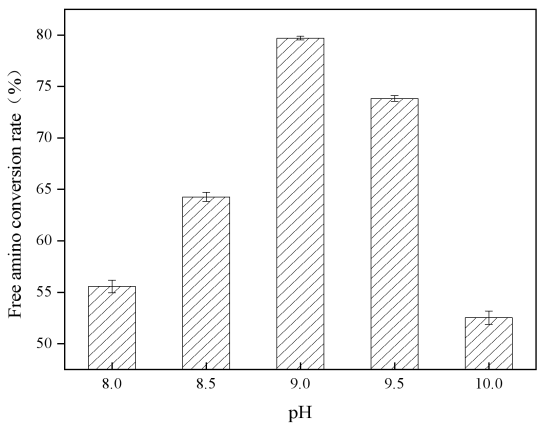

Figure 2. Effect of pH on free amino conversion rate

The graph about free amino conversion rate of C12LS against the pH of solution were plotted in Figure 2. The free amino conversion rate of CLSs first rise as pH value increased, and then decreased. The free amino conversion rate increased gradually from the value of pH 8.0 to pH 9.0, indicating that the molecules of collagen was not reacted completely. When the value of pH reached 9.0, the maximal free amino conversion rate was detected, suggesting that the reactivity between lauroyl chloride and CH might reach a maximum. When the pH was more than 9.0, the decomposition reaction of CH might become a dominant reaction, so that the content of free amino groups in the solution increased, resulting in a decreasd in the conversion rate of free amino groups. Therefore, the optimal pH value was 9.0.

2.2. Effect of Volume Ratio of Ethyl Acetate and Lauroyl chloride on Free Amino Conversion Rate

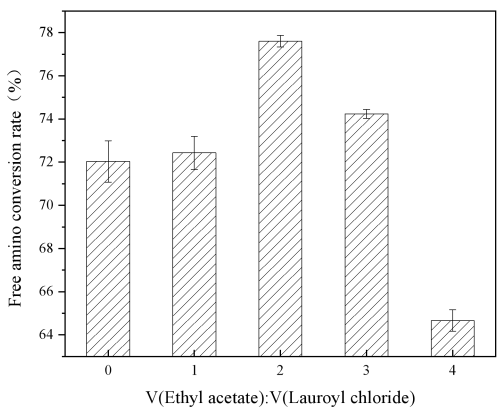

Figure 3. Effect of volume ratio of ethyl acetate and lauroyl chloride on free amino conversion rate

As shown in Figure 3, Free amino content changed quickly as the offer of the volume ratio of ethyl acetate and lauroyl chloride from 0:1 to 2:1, and then increased as further increase of the ratio. When volume ratio of ethyl acetate and lauroyl chloride reached 2:1, the maximal free amino conversion rate was detected. When volume ratio of ethyl acetate and lauroyl chloride exceeds 2:1, the reactivity between collagen and acyl chloride decreases, possibly due to the excessive content of ethyl acetate, resulting in a reduction in effective collision between reactant molecules. The experimental result indicated that the volume ratio of ethyl acetate and lauroyl chloride of 2:1 reached the maximum of 77.6%.

2.3. Effect of Temperature on Free Amino Conversion Rate

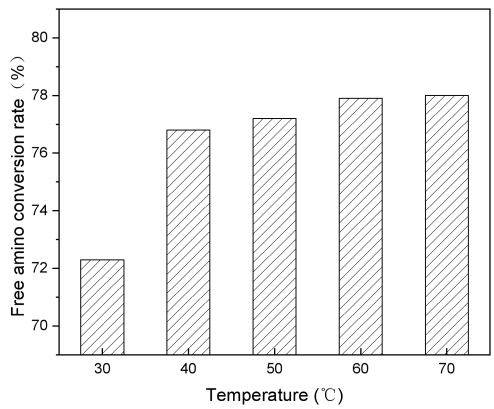

Figure 4. Effect of temperature on free amino conversion rate

The effect of temperature on free amino conversion rate were shown in Figure 3.As the temperature increased, CLSs exhibited an increasing trend in free amino conversion, which was presumably due to the increasing in chemical reaction rate. The temperature reaching 70℃ exhibited the strongest conversion rate. However, the conversion rate of free amino group at 60 ℃ was not much different from 70 ℃. However, the increase of temperature will cause waste of energy and economy. It implies that when the temperature was 60 ° C, the conversion rate of free amino groups approached a maximum of 77.9%.

2.4. Effect of Different Carbon Chain Length of Acid Chloride on Free Amino Conversion Rate

Figure 5 displayed the free amino conversion under different type of acid chloride. As the carbon chain length of acyl chloride increased from C10 to C12, the free amino conversion rate a slight declined, When the carbon chain length increased from C12 to C16, the conversion rate of free amino groups shown a sharp decrease. It might be due to the fact that the steric hindrance of the surfactant-forming reaction increased. Therefore, the conversion rate of the free amino group corresponding to C10LS reached a maximum of 78.1%.

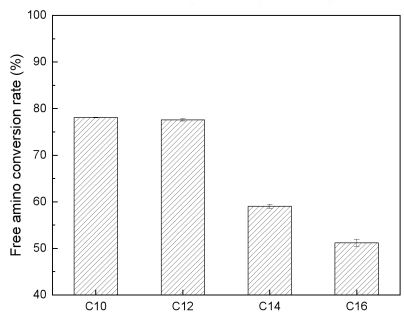

Figure 5. Effect of different carbon chain length of acid chloride on free amino conversion rate

2.5. Fourier Transform-Infrared (FT-IR) Spectroscopy

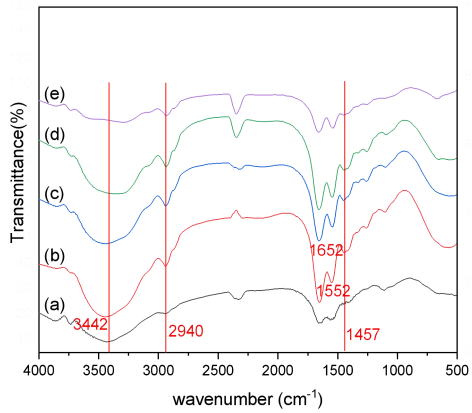

Figure 6. FTIR of CH(a), C10LS(b), C12LS(c), C14LS(d), C16LS(e)

In order to evaluate whether the acyl group has been successfully grafted onto CH, The FT-IR spectra of CH and CHBSs were measured and shown in Figure 6. CLSs displayed strong absorptions at 1652 and 1552 cm^{-1}, due to the stretching vibrations of amide C=O (amide I) and the bending vibrations of amide N−H (amide II), respectively[21]. These two absorption bands of CLSs were stronger in intensity than those of CH, mainly arose from the newly synthetic amide (NH−CO) through reaction between the amino groups of CH and the acyl chloride. Additionally, CLSs presented three stronger absorption peaks at 2940 cm^{-1} and 1457 cm^{-1} compared with CH. These two peaks were attributed to the asymmetric stretching vibrations and the bending vibrations of methylene, respectively[22], which proved the introduction of aliphatic chain in the products. CLSs displayed strong absorptions peak at 3442cm^{-1}, due to stretching vibrations. All these observations suggest that CLSs were successfully prepared by grafting the acyl group onto CH.

2.6. Surface Tension Analysis of CLS

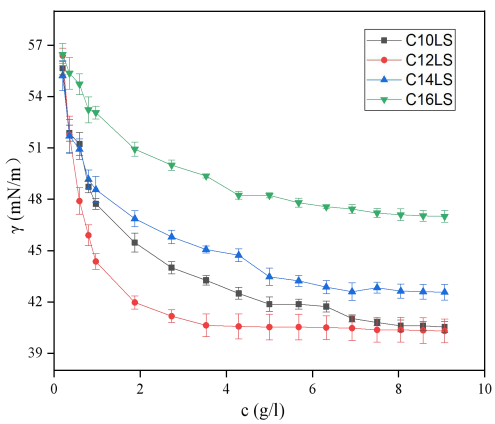

Figure 7. Surface tension of different CLSs

Surface tension (γ) of solution against the concentration of CLSs was plotted in Figure 7. A surfactant in aqueous solution will tend to be adsorbed at the air−water interface, thus resulting in a sharp decline of surface tension of solution. So, the surface adsorption characteristics of a surfactant are generally used as an index for assessing its surface activity. The area

occupied per molecule (A) provides the evaluation indicators regarding the surface adsorption at air−water interface. In addition, the A depends principally on the size of hydrophilic head. The smaller hydrophilic head is, the smaller the A is[11].The γ of CLSs first declined rapidly as the concentration increased, and then decreased slowly until a defined concentration was reached. It was also discovered that, as the carbon chain length increased from C12 to C16, the ability of CLS in reducing surface tension of solution was reduced. It coincides with the conclusion of Wang[23] in the research of the surfactants derived from amino acids. The phenomenon suggested that the carbon chain length increased gradually from C12 to C16, with longer hydrophilic groups,the area occupied per moleculebecame bigger, the molecules of CLS were packed more loose at the interface, and thus effectively increased the surface tension of solution[24].

2.7. Analysis of CLS Foaming Capacity and Foam Stability

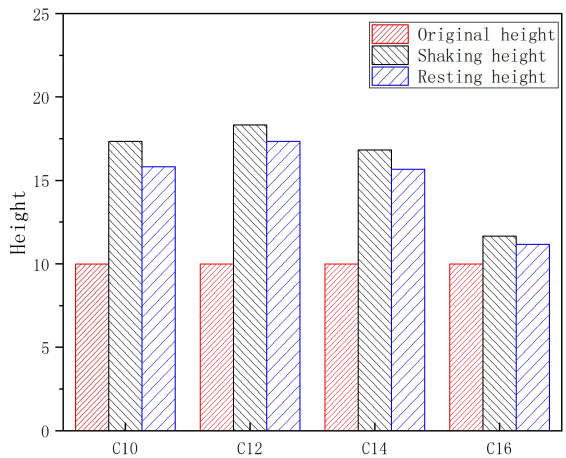

Figure 8. CLS foaming capacity and foam stability

Effect of different carbon chain length of acid chloride on the foaming properties is shown in Figure 8. The lower the surface tension of CLS, the tighter the arrangement of monomer molecules at the gas-liquid interface, the smaller the cross-sectional area occupied by molecules, and the better the foaming property[25]. It was found that the foaming capacities of C12LB was obviously better than other surfactants. Presumably because the surfactant with stronger capacity to reduce surface tension generally possesses better foaming activities. Addition, the foaming capacity of C10LS was slightly lower than C12LS, which might be associated with the relatively lower surface tension of C10LS. The foam stability of C16LB is better than the other, because of lower surface tension. Considering from foaming capacity and foam stability, C12LS got a better choice.

3. Conclusions

Acyl surfactant (CLS) with different carbon chain lengths was prepared by using leather waste, and its preparation conditions, physicochemical properties and surface activity were discussed in the present work. The results show that the optimum pH was 9.0, the volume ratio of ethyl acetate and lauroyl chloride was 2:1, the optimum reaction temperature was 60℃, the optimum carbon chain length was C12. As the carbon chain length of acyl chloride increased, the foam stability of CLS rose, while its free amino conversion decreased. The lauroyl surfactant (C12LS) possessed satisfactory foaming capacity. As the length of the carbon chain increases, the surface tension and foaming property of CLS increase first and then decrease. Therefore, the surface tension and foaming capacity of CLS can be well controlled by changing the type of acyl chloride. Meanwhile, the present work may have displayed a potential value of leather wastes, which was of great significance for the rational use of resources and the protection of the environment.

Acknowledgements

This work was supported by natural fund joint project of Shandong (ZR2015BL026) and key research and development project of Shandong (2016GSF117034).

References

[1] J. Hu,Z. B. Xiao,R. J. Zhou,et al. Ecological utilization of leather tannery waste with circular economy model[J]. Journal of Cleaner Production, 2011, 19(2-3): 221-228.

[2] X. P. Wang. Comprehensive utilization and prospect of tannery solid waste[J]. Western Leather, 2017, 39(17): 38-42.

[3] Robert H. Bogue. Conditions affecting the hydrolysis of collagen to gelatin[J]. Industrial and Engineering Chemistry, 2002, 15(11): 1154-1159.

[4] Marcos R. Bet,And Gilberto Goissis,Cristina A. Lacerda. Characterization of Polyanionic Collagen Prepared by Selective Hydrolysis of Asparagine and Glutamine Carboxyamide Side Chains[J]. Biomacromolecules, 2001, 2(4): 1074.

[5] C. H. Li,W. T. Liu,L. Duan,et al. Surface activity of pepsin-solubilized collagen acylated by lauroyl chloride along with succinic anhydride[J]. Journal of Applied Polymer Science, 2014, 131(14): 8.

[6] P. Foley,A. K. Pour,E. S. Beach,et al. Derivation and synthesis of renewable surfactants[J]. Chemical Society Reviews, 2012, 41(4): 1499-1518.

[7] R. Marchant,I. Banat. Biosurfactants: a sustainable replacement for chemical surfactants?[J]. Biotechnology Letters, 2012, 34(9): 1597-1605.

[8] T. Muthukumar,G. Sreekumar,T. P. Sastry,et al. Collagen as a potential biomaterial in biomedical applications[J]. Reviews on Advanced Materials Science, 2018, 53(1): 29-39.

[9] Y. L. Chi,M. Cui,X. P. Liao,et al. Optimization of Synthesis Process of Collagen Peptide-Based Surfactant[J]. China Leather, 2011, 40(23): 8-11.

[10] Y. L. Chi,M. Cui,Q. Yang,et al. Surface properties and biodegradability of collagen peptide-based surfactants[J]. China Leather, 2012, 41(11): 37-41+46.

[11] Y. L. Chi,Q. X. Zhang,X. P. Liao,et al. Physicochemical Properties and Surface Activities of Collagen Hydrolysate-Based Surfactants with Varied Oleoyl Group Grafting Degree[J]. Industrial & Engineering Chemistry Research, 2014, 53(20): 8501-8508.

[12] Y. L. Chi,R. J. Fu,W. M. Han,et al. Theoretical and experimental study on the synthetic route of five collagen peptide-based surfactants[J]. Chinese Scientific Papers, 2016, 11(18): 2115-2118.

[13] R. Sripriya,Ramadhar Kumar,S. Balaji,et al. Characterizations of polyanionic collagen prepared by linking additional carboxylic groups[J]. Reactive and Functional Polymers, 2011, 71(1): 62-69.

[14] C. H. Li,H. L. Tian,L. Duan,et al. Characterization of acylated pepsin-solubilized collagen with better surface activity[J]. International Journal of Biological Macromolecules, 2013, 57(6): 92-98.

[15] C. H. Li,Z. H. Tian,W. T. Liu,et al. Structural properties of pepsin-solubilized collagen acylated by lauroyl chloride along with succinic anhydride[J]. Materials Science and Engineering C-Materials For Biological Applications, 2015, 55(14): 327-334.

[16] C. H. Li,W. T. Liu,Z. H. Tian,et al. Surface tension of undenatured collagen biosurfactant and its surface adsorption[J]. Functional Materials, 2014, 45(23): 23075-23079.

[17] Q. Lin,W. Huang,Y. K. Song,et al. Comparison of three methods for determination of hydrolysis degree of cottonseed protein hydrolysate[J]. Fujian Journal of Agricultural Sciences, 2011, 26(06): 1076-1080.

[18] Y. H. Luo. Preparation and properties of different peptide chain length protein-based surfactants [D]. Shaanxi University of Science and Technology, 2017.

[19] Ricardo Lucas,Francisco Comelles,David Alcantara. Surface-active properties of lipophilic antioxidants tyrosol and hydroxytyrosol fatty acid esters: a potential explanation for the nonlinear hypothesis of the antioxidant activity in

oil-in-water emulsions[J]. Journal of Agricultural and Food Chemistry, 2010, 58(13): 8021-8026.

[20] X. X. Wei,Q. J. Wang,W. B. Zhang,et al. Synthesis and properties of collagen peptide-based surfactants[J]. China Leather, 2015, 44(14): 60-64.

[21] Nancy P Camacho,Paul West,Peter A Torzilli,et al. FTIR microscopic imaging of collagen and proteoglycan in bovine cartilage[J]. Biopolymers, 2015, 62(1): 1-8.

[22] K. J. Payne,A. Veis. Fourier transform IR spectroscopy of collagen and gelatin solutions: deconvolution of the amide I band for conformational studies[J]. Biopolymers, 1988, 27(11): 1749.

[23] L. L. Wang. Synthesis and surface activity of N-medium chain fatty acyl amino acid salt [D]. Nanchang University, 2013.

[24] C. M. Faustino,A. R. Calado,L Garcia-Rio. Dimeric and monomeric surfactants derived from sulfur-containing amino acids[J]. Journal of Colloid and Interface Science, 2010, 351(2): 472-477.

[25] J. Luan. Preparation of N-acyl polypeptide surfactants with different carbon chain lengths using waste shavings and their properties [D]. Yantai University, 2016.

P20

Study on Modification of Collagen by Fluorescent Hyperbranched Polymer (HMEAP)

Hou Ruiting*, Ding Haiyan, Sun Miao, Li Yun***

(School of Chemistry and Chemical Engineering, Yantai University, Yantai 264005, China)

Abstract

Recently, a new kind of unconventional fluorescent material has been a hot topic. The unconventional fluorescent hyperbranched polymers (HMEAP) were synthesized successfully, and were characterized by ^{1}H NMR, fluorescence spectral measurement and so on. The optimum modification conditions were obtained by measuring the shrinkage temperature and thickness rate of leather after tannage, after the hyperbranched polymers being added into tanned pickling goat skin. The results showed the shrinkage temperature was increased by 22.1℃, and the thickness rate of leather reached to 35.6%. The modified collagen has broad application prospects in area of bio-medicine.

Keywords: fluorescence; hyperbranched polymer; modification of collagen; tanning

Introduce

In recent years, hyperbranched polymers have received great attention due to their unique structural properties[1-5]. The study of biocompatible fluorescent hyperbranched polymers containing non-traditional chromophores has now become a hot research topic, and they have been well applied to many fields such as tissue engineering and bioimaging[6-9].

At present, leather industry has become the second largest source of pollution in China's light industry. Reducing the use of chrome tanning agents or developing chrome-free tanning agents has become an urgent problem. The hyperbranched polymer has a highly branched three-dimensional spherical structure and a large number of terminal functional groups, no entanglement with molecules, low viscosity, good solubility and so on. It has more reactive functional groups than ordinary leather tanning agents. If the terminal functional groups are chemically bonded with the terminal reactive group of the collagen fiber of the leather, the purpose of modifying the collagen fiber is achieved[7].

At present, the study of fluorescent polymers of non-traditional chromophores is mostly concerned with the study of dendritic or hyperbranched polymers with chromophores as amines, especially the hyperbranched and dendritic polyamidoamine PAMAM[10-11]. The Michael addition reaction is carried out from 1-(2-aminoethyl) piperazine AEPZ and acrylate. And the hyperbranched polymer PAMAMs containing different proportions of primary and tertiary amine groups can be synthesized by adjusting the feed ratio and reaction conditions. The polymer has good fluorescent properties. According to the quenching experiment of the HPAMAM functional group[12-13], it is found that the chromophore of the amine-based polymer is a tertiary amine in the branched structure. There are few studies on hyperbranched polymeric materials containing only tertiary amine chromophores.

In previous study, we had successfully prepared a series of tertiary amine hyperbranched polymers with different molecular weights by using the most common AB_2 type monomer polymerization method of polycondensation of polyfunctional monomers. The polycondensation reaction was carried out under the catalysis of tetrabutyl titanate $Ti(OBu)_4$ from N,N-dihydroxyethyl-3-aminemethylpropionate of AB_2 type, and the super branched polymer with good water solubility was obtained.

The hyperbranched polymer enters the pretreated skin, and a large number of active groups are combined with active groups of the side chain of the skin collagen, or accumulate between the leather collagen fibers and cover the surface of the leather fibers. The mesh can be formed by cross-linking, entanglement or adsorption, thereby exerting a tanning effect on the leather[14-16]. Therefore, the synthetic water-soluble tertiary amine-based hyperbranched polymer is used to modify the collagen to improve its comprehensive performance. Because the tertiary amine-based hyperbranched polymer has strong affinity and low toxicity, the modified collagen will have broad prospects of biomedical applications.

1 Materials and Methods

1.1 Materials

Diethanolamine (≥98%), tetrabutyl titanate (≥98%), methanol (≥99.5%) and ethyl ether (≥99.5%) were of analytical grade and purchased from Sinopharm Chemical Reagent Co., Ltd. Ethyl hydroxyethylamine (≥98%, Tahiti Chemical Industry), self-made goat acid skin.

1.2 Instrument and characterization

The ^{1}H NMR (300 MHz) was measured at room temperature by Bruker DRX-300, with tetramethylsilicon as internal standard and $CDCl_3$ or D_2O as solvent. Fluorescence excitation spectroscopy was measured at room temperature and the instrument model was Perkin-Elmer LS55. Leather thickness gauges, Weihai Gauge Factory Limited; HG shrinkage temperature recorder (HG-1).

1.3 Hyperbranched polymer polycondensation monomer MBAP syntheses

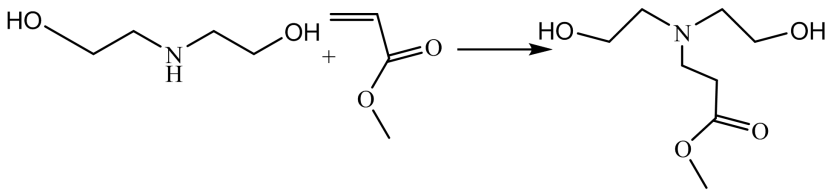

Fig.1 Synthesis of hyperbranched polymer polycondensation monomer MBAP

Diethanolamine (10.5 g, 0.1 mol) and methyl acrylate (9.1 g, 0.102 mol) were dissolved in 10 mL methanol and added into a 50 mL round-necked flask. Under room temperature and nitrogen conditions, the solution was stirred for 30 minutes, then the temperature of the solution was raised to 35 ℃, and the reaction continued for 4 hours. After the reaction was finished, the impurities at low boiling point were removed by vacuum and cooled to room temperature. The colorless oily product MBAP was obtained with a yield of 98.5%.

^{1}H NMR ($CDCl_3$): 3.67 (2H，CH_2OH)，3.55 (3H，CH_3)，3.45 (4H，$-CH_2OH$)；2.73 (2H, $-N-CH_2-CH_2-COO-$), 2.50 (4H, $-N-CH_2-CH_2OH$); 2.37 (2H, $-CH_2-COO-$)。

1.4 Synthesis of TERT amine hyperbranched polymer HMEAP

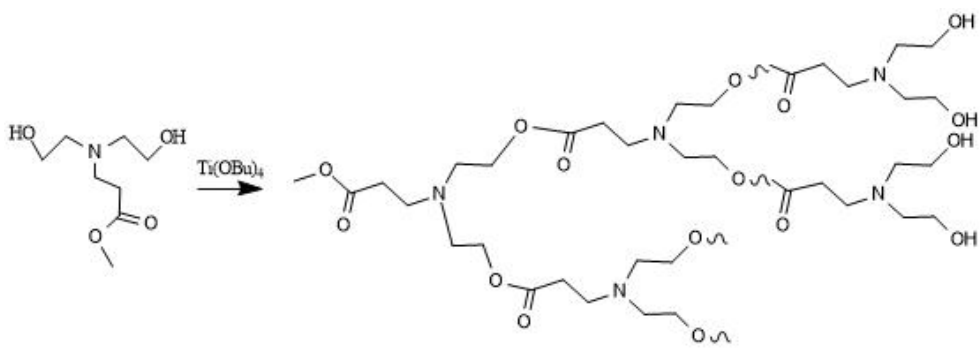

Fig 2 Synthesis of water-soluble hyperbranched polymer HMEAP

N, N- two hydroxyethyl -3- amine propionate MBAP (4.8g, 25mmol) and four butyl titanate Ti $(OBu)_4$ (0.17g, 0.5mmol) were added to the three neck round bottom flask of the 25mL nitrogen inlet and reflux condenser. Under the conditions of 130 ℃ and nitrogen, the reaction was stirred vigorously for 3 hours, then vacuum (250 mm Hg column) for 0.5 hours. Cool, then adding butyl tetracycline (0.085 g, 0.25 mmol), continued stirring reaction to 1, 3, 5 and 10 hours at high vacuum (10 mm Hg columns) and 130 ℃. The product was dissolved in 10mL methanol, filtrated solid, precipitated in the ether, and removed low boiling point impurity in a vacuum. The hyperbranched polyester HMBAP1, HMBAP3, HMBAP5 and HMBAP10 were obtained.

1.5 The modification of collagen by HMBAP

The acid skin was weighed and the liquid ratio were 200%, with a certain pH buffer solution, soaking 30min, adding a certain quality hyperbranched polymer HMBAP, tanning a certain time of a certain temperature, and taking out the skin to measure its thickness and shrinkage temperature. The effects of pH, amount to hyperbranched polymer HMBAP, tanning time and tanning temperature on HMBAP modified collagen were investigated.

2 Results and discussion

2.1 Study on fluorescence properties of tertiary amino hyperbranched polymer HMBAP

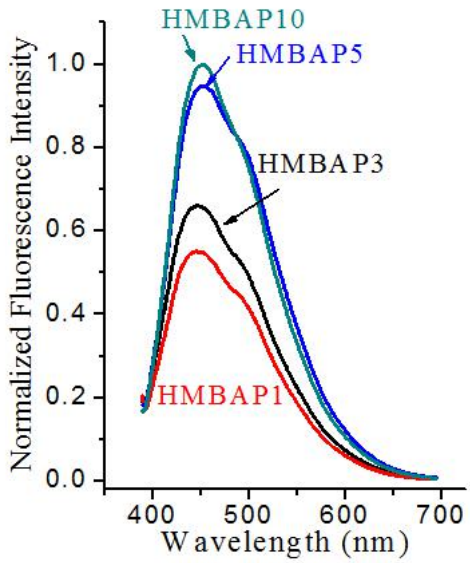

Fig 3 Fluorescence spectra of tertiary amine hyperbranched polymers HMBAP1, HMBAP3, HMBAP5 and HMBAP10 Polycondensation of MBAP catalyzed by $Ti(OBu)_4$. Test conditions: 1mg/mL aqueous solution λ_{ex} = 375 nm, room temperature test

Fig. 3 shows the fluorescence spectra of HMBAPs, a tertiary amine hyperbranched polymer, which was obtained by MBAP Polycondensation catalyzed by $Ti(OBu)_4$. It could be seen from the diagram that the relative intensity of fluorescence increased to the increase in molecular weight, which was similar to the results of PAMAM dendritic and PAMAM hyperbranched polymers[17]. Fluorescence was closely related to the collision relaxation rate and quenching of fluorescent groups[18], the higher chain activity and the collision relaxation rate, the weaker the fluorescence. The activity of hyperbranched polymer chains decreased with the increase in molecular weight[19], so the fluorescence of HMBAPs increased with the increase of molecular weight.

2.2 Effect of different pH on tanning properties

Figure 4 shows the effect of pH on the shrinkage temperature and thickening rate of HMBAP5 after tanning. As shown in the figure that the shrinkage temperature initially decreased to the increase in pH. When the pH was 5-6, the shrinkage temperature increased and the thickening rate reaches the maximum value, and then decreases. This was because the size of the hyperbranched polymer in the solution was affected by the pH of the solution. Studies have shown that after the pH of the solution changes, the size of the dendritic of the hyperbranched polymer could be increased or decreased by 50% in the solution[20]. Under weak acidic conditions, HMBAP5 penetrates into the skin, but too low pH affected the structural strength of skin collagen fibers and the modification of collagen. However, if the pH was too high, complex molecules of the tanning liquor were too large to facilitate the penetration and binding. Therefore, consider the optimal pH to choose 5~6.

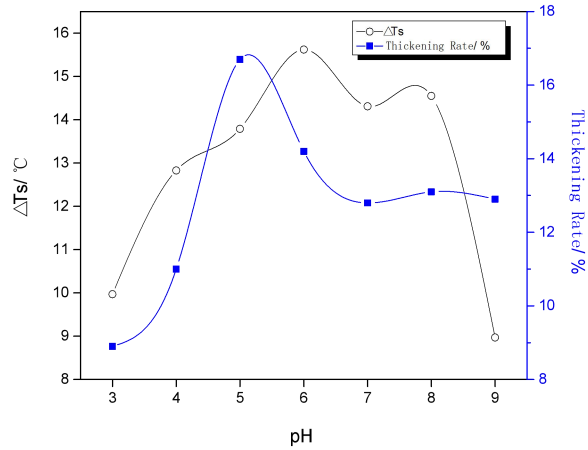

Fig. 4 Effect of pH on leather shrinkage temperature and thickening rate after HMBAP5 tanning

2.3 Effect of polymer dosage on tanning properties

Fig. 5 shows the effect of different polymer dosage on the shrinkage temperature and thickening rate of the modified collagen. It could be seen from the figure that when the amount of HMBAP5 was 6%, the increase in the thickening rate and the shrinkage temperature reaches a maximum, and there was no significant increase in the further increase in the amount. When the amount of hyperbranched polymer was too small, the tanning effect was not obvious, but when the amount of hyperbranched polymer was more than 6%, the cost was increased. Therefore, considering the shrinkage temperature, thickening rate and economic benefits, the optimum polymer dosage was 6%.

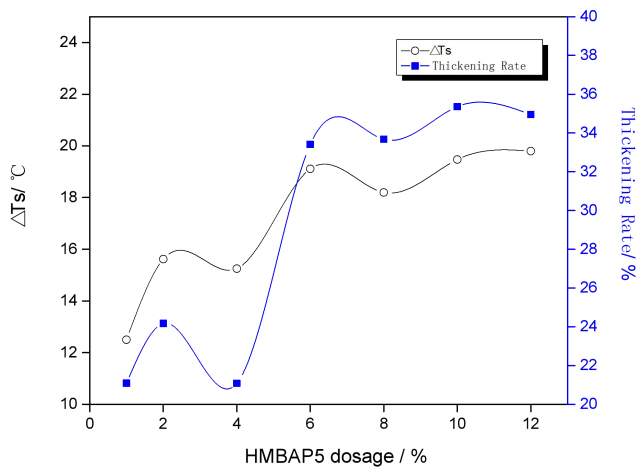

Fig. 5 Effect of HMBAP5 dosage on leather shrinkage temperature and thickening rate after tanning

2.4 Effect of tanning time on tanning properties

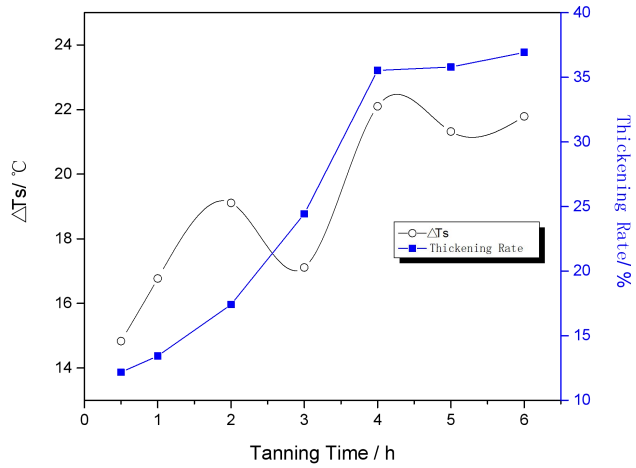

Fig 6 Effect of tanning time on leather shrinkage temperature and thickening rate after HMBAP5 tanning

Figure 6 is the results of the effect of tanning time of the shrinkage temperature and the thickening rate of collagen. As shown in the figure, the shrinkage temperature and the thickening rate increased in the increase in the reaction times at the beginning of the tanning, and the thickening rate and the shrinkage temperature did not increase significantly after the reaction time reaches 4 h. The reason was that as time passes, the molecules of the hyperbranched polymer penetrated into the hide. The more the molecular end groups of the hyperbranched polymer bound to the active groups on the side chain of the collagen, the more obvious the effect of modifying the collagen, and the shrinkage temperature and the thickening rate was gradually increased. When the reaction time reached 4h, the bindings with collagen were basically completed, and the extension time was no longer meaningful. The optimal reaction time was 4h.

2.5 Effect of reaction temperature on tanning properties

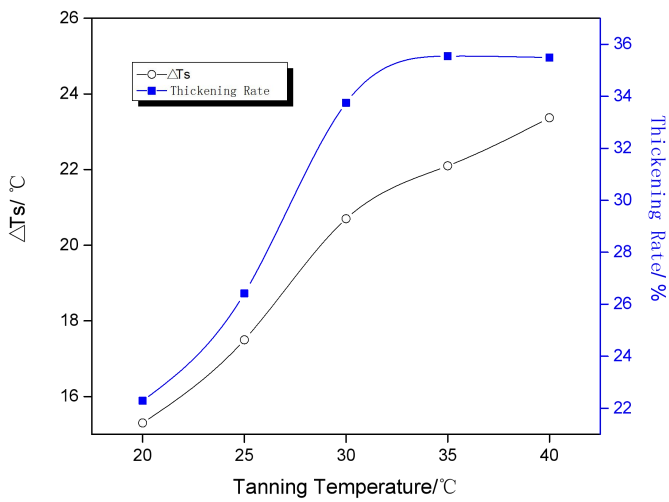

Fig.7 Effect of tanning temperature on shrinkage temperature and thickening rate of leather after HMBAP5 tanning

Figure 7 shows the effect of different reaction temperatures on the shrinkage temperature and thickening rate of modified collagen. By the graph, you could see that the initial shrinkage temperature increased with the increase of reaction temperature, the shrinkage temperature did not increase significantly with the increase of reaction temperature after 30 ℃,

and the thickening rate increased with the increase of reaction time, but did not increase significantly afterwards. When the temperature increased, the penetration rate of the polymer into the skin increased, and the binding rate and binding amount of the polymer would increase. However, when the temperature was too high, it would affect the leather grain surfaces and made the grain surface rough. Considering the overall consideration, choose the best reaction temperature was 25~30 °C.

3 Conclusion

The new non-conventional fluorescent hyperbranched polymer (HMEAP) was doped with the skin collagen to enhance the function of the modified collagen. The modification conditions of the skin collagen by fluorescent hyperbranched polymer (HMEAP) were optimized. The optimum pH was 5-6, the polymer dosage was 6%, the optimum reaction temperature was 25-30 °C, and the reaction time was 4 h. The experimental results show that the shrinkage temperature of leather after HMEAP was increased by 22.1 °C, and the thickening rate could reach 35.6%. Because of the low toxicity and excellent biocompatibility of HMEAP, modified collagen has a broad application prospect in biomedicine.

Acknowledgements: The authors acknowledge the financial support of the National Youth Nature Fund(21404088), Natural Fund Joint Project of Shandong (ZR2015BL026), Key Research and Development Project of Shandong (2016GSF117034), Shandong Province Outstanding Young and Middle-aged Scientists Research Award Fund（BS2014CL017）.

References

[1] Jikei M, Kakimoto M A. Hyperbranched polymers: a promising new class of materials[J]. Progress in Polymer Science, 2001, 26(8): 1233-1285.

[2] Inoue K. Functional dendrimers, hyperbranched and star polymers[J]. Progress in Polymer Science, 2000, 25(4): 453-571.

[3] Voit B. New developments in hyperbranched polymers[J]. Journal of Polymer Science part A: Polymer Chemistry, 2015,38(14): 2505-2525.

[4] Yang J, Zhang Y, Gautam S, et al. Development of aliphatic biodegradable photoluminescent polymers[J]. Proceedings of the National Academy of Sciences of the United States of America, 2009, 106(25): 10086-10091.

[5] Yang W, Pan C Y, Luo M D, et al. Fluorescent mannose-functionalized hyperbranched poly(amido amine)s: synthesis and interaction with E. coli[J]. Biomacromolecules, 2010, 11(7): 1840-1846.

[6] Matthews O. A, Shipway A N, Stoddart J F. Dendrimers-Branching out from curiosities into new technologies[J]. Progress in Polymer Science, 1998, 23(1): 1-56.

[7] Qiang X H, Liu A J, Guan J J, et al. Synthesis and application of hydroxy terminated hyperbranched polymer chrome-tanning assistant[J]. Fine Chemicals, 2008, 25(9):900-889.

[8] Domaille D W, Que E L, Chang C J. Synthetic fluorescent sensors for studying the cell biology of metals[J]. Nature Chemical Biology, 2008, 4(3): 168-175.

[9] Mrinmoy D E, Rana S, Akpinar H, et al.Sensing of proteins in human serum using conjugates of nanoparticles and green fluorescent proteinconjugates[J]. Nature Chemistry, 2009, 1(6), 461-465.

[10] Wang D, Imae T. Fluorescence emission from dendrimers and its pH dependence[J]. Journal of the Americian Chemical Society, 2004, 126: 13204-13205.

[11] Wang D, Imae T, Miki M.Fluorescence emission from PAMAM and PPI dendrimers[J]. Journal of Colloid & Interface Science, 2007, 306(2): 222-227.

[12] Yang W, Pan C Y.Synthesis and fluorescent properties of biodegradable hyperbranched poly(amido amine)s[J].Die Unterrichtspraxis/teaching German, 2009, 30(24): 2096-2101.

[13] Wu D C, Liu Y, He C B, et al. Blue photoluminescence from hyperbranched poly(amino ester)s[J]. Macromolecules, 2005, 38(24): 9906-9909.

[14] Qiang T T, Study on synthesis of hyperbranched polymer with terminal carboxyl and its effect as chrome-tanning assistant[D]. Shaanxi: Shaanxi University, 2007.

[15] Qiang T T, Gao X, Chen X K, et al. The application of a new tanning agent of hyperbranched polymer with terminal carboxyl groups-aluminum[J]. Leather Science and Engineering, 2015.

[16] Pallab Banerjee, Wilfried Reichardt, Ralph Weissleder, et al. Novel hyperbranched dendron for gene transfer in vitro and in vitro[J]. Bioconjugate Chemistry, 2004, 1(15-18): 960-968.

[17] Larson C L, Tucker S A. Intrinsic fluorescence of carboxylate-terminated polyamido amine dendrimers[J]. Applied Spectroscopy, 2001, 55(6): 679-683.

[18] Zhu L, Wu W, Zhu M Q, et al. Reversibly photoswitchable dual-color fluorescent nanoparticles as new tools for live-cell imaging[J]. Journal of the American Chemical Society, 2007, 129(12): 3524-3524.

[19] Meltzer A D, Tirrell D A, Jones A A, et al.Chain dynamics in poly(amidoamine) dendrimers: a study of carbon-13 NMR relaxation parameters[J]. Macromolecules, 1992, 25(18): 4541-4548.

[20]Ding K, Taylor M M, Brown E. Combination tanning based on tara: An attempt to make chrome-free garment leathers[J], Journal of the American Leather Chemistsassociation, 2007, 102(6): 198-204.

P21

The synthesis of self-colored waterborne polyurethane and its membrane performances

Yu-lu Wang*, Tianqi Yang, Hao Lan, Liqiang Jin, Hong Yang, Shaodi Xiu, Jinxu Xu

School of Leather Chemistry and Engineering, Qilu University of Technology (Shandong Academy of Sciences), 250353, China

** Correspondence: wangyulu@qlu.edu.cn; Tel.: +86-0531-8963-1786*

Abstract

A prepolymer of waterborne polyurethane prefabricated by isophorone diisocyanate, polytetramethylene-oxide glycol 1000, dimethylolpropionic acid and 1,4-butanediol was modified with the first generation hyperbranched poly(amine-ester) to prepare a novel waterborne polyurethane (WPU-H). Successively, a self-colored waterborne polyurethane (WPU-SC) was synthesized by the reaction of WPU-H with reactive brilliant red K-2G. Compared with WPU-H, new adsorption bands at 1635, 1413 and 1118cm^{-1} appeared in FTIR spectrum of WPU-SC and its particle size distribution increased. According to DSC and TG analysis, the glass-transition temperatures had no obvious change while thermal degradation performances above 200^{o}C became complex as the introduction of dye molecules.

Key words: waterborne polyurethane; reactive dye; membrane; thermal stability

1. Introduction

Recently, the design and manufacture of leather substitutes or artificial leather are spring up in Southeast Asia in order to meet the escalating demand for insufficient output of genuine leather, as well as are out of the ethical concern over animal rights [1-3]. Among various leather substitutes, microfiber synthetic leather is becoming increasingly popular on account of its highly realistic leather-like appearance and touch. Even more, its mechanical strength, chemical and thermal stability, quality homogeneity and material utilization are superior to genuine leather [4, 5]. The microfiber synthetic leather has found wide applications in the manufacture of shoes, garments, bags, upholsteries in aircrafts and automobiles and so on [3, 6].

Microfiber synthetic leather composes of a three-dimensional reticulated nonwoven fabric skeleton and a porous polyurethane matrix [3, 6]. The nonwoven fabric comprises numerous polyamide fibers with a fineness of less than 0.01 denier. In manufacturing, ordinary solvent-based polyurethane solution is impregnated into the fiber bundles firstly and successively coagulated *in situ* via a wet phase inversion process to achieve favorable elasticity and touch. However, some technical difficulties in coloration of microfiber synthetic leather are brought in naturally, which was due to different affinities between polyamide fibers and polyurethane matrix to anionic dye. Generally, acid dye is one of the most suitable dyes for polyamide as ionic bonds can form between protonated amino terminals in the polyamide component and dye molecules. Unfortunately, ordinary polyurethane cannot be dyed easily by acid dyes due to the absence of binding strongly sites with to acid dyes. Furthermore, both the soft segment and hard segment of polyurethane crystallize at room temperature, which prevents diffusion of dye molecules into the polyurethane matrix. This consequently leads to some technological problems, on one hand the final products have uneven coloration and poor color fastness, on the other hand high dye discharge in effluents are posing serious environmental threats [7-11].Recently, researchers had synthesized types of polyurethane chain extended with compounds containing trialkylamine groups in order to resolve the problems above [3, 12-13].

In the present article, we try to synthesize polyurethanes with covalent bonded dye molecules as filler for the manufacture of microfiber synthetic leather with good color fastness. More specifically, the microfiber synthetic leather should not be dyed further and it would significantly decrease environmental pollution caused by dye discharge. Based on this concept, a given amount of hyperbranched poly(amine-ester) with terminal hydroxyl groups was used as chain extender to prepare waterborne polyurethane with hydroxyl groups, and then it reacted with reactive dye to obtain self-colored waterborne polyurethane as the filler of microfiber synthetic leather. The particle sizes, chemical structure and thermal properties of intermediate and final products were systematically characterized.

2. Experimental

2.1 Materials

Polyoxytetramethylene glycol with number molecular weight of 1000 (PTMG 1000) was purchased from Wanhua Chemical (Yantai, China). It was dehydrated for 24h at 110°C under vacuum prior to use. Isophorone diisocyanate (IPDI), 1,4-butanediol (BDO) and acetone of analytical pure grade were purchased from Sigma Alderich (Shanghai, China) and used after dehydration with 4Å molecular sieves for 1 week. Dimethylolpropionic acid (DMPA), triethylamine, sodium hydroxide and dibutyltin dilaurate (DBTDL) were purchased from Sinopharm Chemical Reagent Co. Ltd. (Shanghai, China) and used as received. The reactive brilliant red K-2G (λ_{max}=510nm，CAS:12228-01-6) was supplied by Zhongcheng Chemical Co. Ltd. (Taizhou, China).

The first generation hyperbranched poly(amine-ester) (HPAE-1) with hydroxyl value of 563 was synthesized in our lab according to the method of reference [14], and all materials used were analytical pure grade and purchased from Aladdin Industrial Corporation (Shanghai, China).

2.2 Preparation of polyurethane samples

2.2.1 Synthesis of waterborne polyurethane (WPU)

50g PTMG was introduced into a flask equipped with a mechanical stirrer, nitrogen inlet, thermometer, and condenser with a drying tube, then 22.2g IPDI was dropped guttatim into the reactor at 80°C, followed with 0.05 wt.% DBTDL as catalyst. 2h later, 4 wt.% DMPA was added into the system and reacted for 1h. Subsequently, the temperature was decreased to 60°C and 1.91g BDO was introduced into the mixture for extension for 30min. After that, the mixture was neutralized by 2.32g TEA and acetone was used to reduce the viscosity of the mixture. A given amount of deionized water was added into the flask to emulsify the product and the acetone was removed under reduced pressure. The resulting product WPU was emulsion with blue light and polymer content was 30%.

2.2.2 Preparation of waterborne polyurethane modified by HPAE-1 (WPU-H)

The synthesis of waterborne polyurethane modified by HPAE-1 (WPU-H) was similar to the preparation of WPU, except that the chain extenders were 0.95g BDO and 3.66g HPAE-1.

2.2.3 Preparation of self-colored waterborne polyurethane (WPU-SC)

A given amount of WPU-H was added into a flask with a stirrer, thermometer and reflux condenser, its pH was adjusted to 9 by using 10 wt.% sodium hydroxide solution. 3 wt.% of reactive brilliant red K-2G (with respect to polymer of WPU-H) was dissolved in deionized water and introduced into the mixture at 60°C for 3h. Finally, self-colored waterborne polyurethane (WPU-SC) containing 20 wt.% polymer was gotten. The preparation procedures of waterborne polyurethane synthesized here were illustrated in Fig. 1.

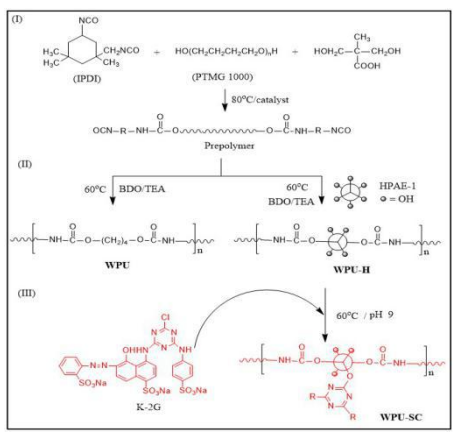

Figure 1 Synthesis procedures of WPU, WPU-H and WPU-SC

2.2.4 Preparation of polyurethane films

The polyurethane solution of WPU, WPU-H and WPU-SC were cast on plastic culture dishes and dried at room temperature for 72h. Then they were heated at 80°C under vacuum conditions to a constant mass. Finally, the resulting films were peeled off from the plates and stored in vacuum desiccators before analysis.

2.3 Characterization

2.3.1 Infrared spectra analysis

WPU, WPU-H and WPU-SC were dissolved into acetone and the concentrations of polymers were all 1 wt.%. A little of the sample above was dropped onto a piece of KBr preformed beforehand and dried completely under an infrared light. Infrared spectra of WPU, WPU-H and WPU-SC films were obtained by TENSOR-27 (Bruker, Germany) over a range of 1000-4000cm^{-1}.

2.3.2 Particle size analysis

Samples of WPU, WPU-H and WPU-SC were diluted by deionized water to a given concentration, and their particle sizes were measured by Zetasizer Nano ZS90 (Malvern, England) at room temperature.

2.3.3 Differential scanning calorimetry analysis

Differential scanning calorimetry (DSC) analysis of WPU, WPU-H and WPU-SC films obtained above were conducted on a DSC 200PC analyzer (Netzsch, Germany). Nitrogen gas was used for purging and liquid nitrogen was used for quenching. The samples were sealed in aluminum pans with lids, and heated from -100°C to 150°C at a heating rate of 10°C/min under a 60 mL/min nitrogen atmosphere. The DSC analysis was based on the second heating run to erase thermo-history.

2.3.4 Thermogravimetric analysis

The thermogravimetric (TG) characteristics of polyurethane films prepared above were investigated by Q500 thermogravimetric analyzer (TA, USA). The samples were put in ceramic pans and heated from room temperature to 600°C at a heating rate of 10°C/min.

3. Results and discussion

3.1 FTIR analysis

As shown in Figure 2, the chain structures of WPU, WPU-H and WPU-SC were confirmed by the FTIR spectrophotometer. The FTIR spectrum of WPU showed the typical absorption peaks of polyurethane at 3346cm^{-1} [ν(NH)], 2854cm^{-1} [ν(CH$_2$)], 1631cm^{-1} [ν(C=O)], 1465cm^{-1} [δ(N-H)] and 1110cm^{-1} [ν(C-O-C)] [15,16]. The NCO absorption peak at about 2270cm^{-1} disappeared in the spectrum, showing that NCO groups had completely reacted during the reaction.

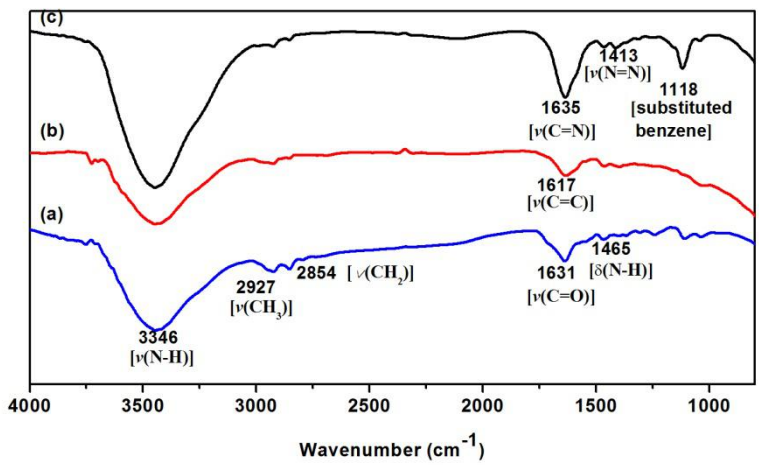

Figure 2 FTIR spectrum of waterborne polyurethane: (a) WPU, (b) WPU-H and (c) WPU-SC

The FTIR spectrum of WPU-H was very similar to it of WPU, despite that the absorption peaks at 1631cm^{-1} [ν(C=O)]

shifted to 1617cm^{-1}. This was probably because that unreacted hydroxyl groups in HPAE-1 would strengthen hydrogen-bond interaction of hard segments of polyurethane [17] and move the absorption peak of C=O from high wavenumber to low wavenumber. The typical absorption band of OH at 3400cm^{-1} was not obvious and might overlap with the absorption band of N-H [18], which was proved by the strength of the peak intensity. It was manifested that waterborne polyurethane containing free hydroxyl groups (WPU-H) was synthesized.

Generally, the FTIR absorption bands of WPU-SC were similar to those of WPU and WPU-H. However, the absorption peaks of 1635cm^{-1} [ν(C=N)], 1413cm^{-1} [ν(N=N)] and 1118cm^{-1} [1,4- substituted benzene] appeared [19], which was attributed to the introduction of dye molecule onto polyurethane. Based on the results above, the self-colored waterborne polyurethane was successfully prepared.

3.2 Particle size distribution

The particle sizes and the distribution of WPU, WPU-H and WPU-SC were shown in Figure 3. The particle sizes of WPU were in the range of 68-255nm and averaged of 116nm. The content of particles in the range of 90-140nm was more than 70%, which was proved that the WPU prepared above was nano-scale emulsion. Compared with WPU, the particle size distribution of waterborne polyurethane modified with HPAE-1 (WPU-H) increased. The range of WPU-H particle sizes was 43-295nm, and its average particle size decreased to 100nm due to the modification of HPAE-1. This was because that, on one hand, hydroxyl groups of HPAE-1 reacted incompletely with prepolymer of polyurethane and the free hydroxyl groups on polyurethane molecule increased its hydrophilic property. On the other hand, the chain extension of polyurethane used HPAE-1 together with BDO was more complex than that used BDO only and side chains on polyurethane backbone might appear.

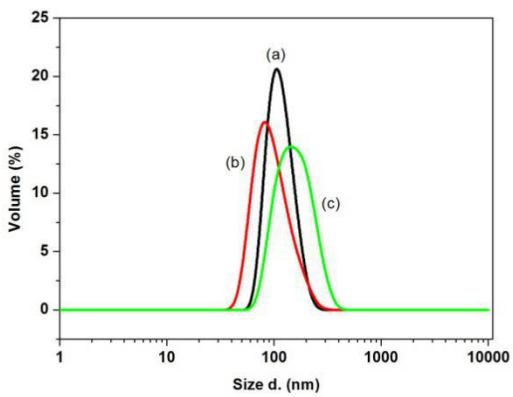

Figure 3 Particle size distribution of waterborne polyurethane: (a) WPU, (b) WPU-H and (c) WPU-SC

Compared with WPU-H, the particle size range and average size value of WPU-SC increased to 68-396nm and 162nm respectively. This was because that the hydroxyl group of WPU-H reacted with the active chlorine on reactive brilliant red K-2G, and the dye molecule was grafted onto the polyurethane and self-colored waterborne polyurethane was gotten.

3.4 Thermal properties

The thermal properties of all types of polyurethane measured by DSC were shown in Figure 4. It was shown that the glass-transition temperature (T_g) of soft segment of WPU was -75.8^{o}C, while the glass-transition temperature of WHU-H increased to -74.5^{o}C. It indicated that the HPAE-1 had little effect on the T_g of polyurethane under a small dosage of HPAE-1, moreover HPAE-1 was distributed in the hard segments of polyurethane molecule and the unreacted hydroxyl groups would form hydrogen bond interaction with urethane bond of polyurethane. After reacting with active brilliant red K-2G, the T_g of WPU-SC was also -74.5^{o}C. In one word, the grafting of dye molecule could not influence the thermal properties of soft segment of polyurethane.

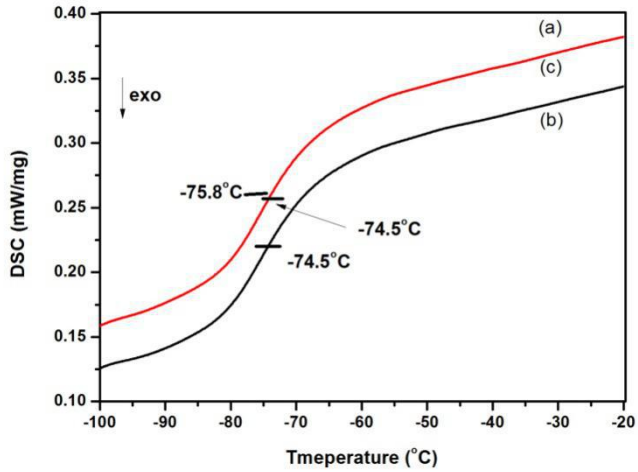

Figure 4 DSC curves of waterborne polyurethane: (a) WPU, (b) WPU-H and (c) WPU-SC

Thermogravimetric (TG) analyzer was applied to evaluate the thermal stability of prepared all types of polyurethane. TG curves of cured films of WPU, WPU-H and WPU-SC were shown in Figure 7. The 5% weight loss for WPU was at 266ºC, the 50% and 80% weight loss were at 372ºC and 396ºC respectively, while the WPU decomposed completely at 418ºC. In the case of WPU-H, 5%, 50% and 80% weight loss occurred at 270ºC, 383ºC and 406ºC, respectively. It indicated that the thermal stability of polyurethane increased after being modified by HPAE-1. Generally, the thermal decomposition of polyurethane presented two stages. The first step was the degradation of hard segment of polyurethane, whilst the second step was the decomposition of its soft segment [16, 20]. Thus, the thermal stability of the hard segment of WPU-H was higher than that of WPU due to the strengthening of hydrogen bond interaction via the free hydroxyl groups on HPAE-1. The results of TG agreed well with the records of particle size distribution and FTIR spectra analysis above.

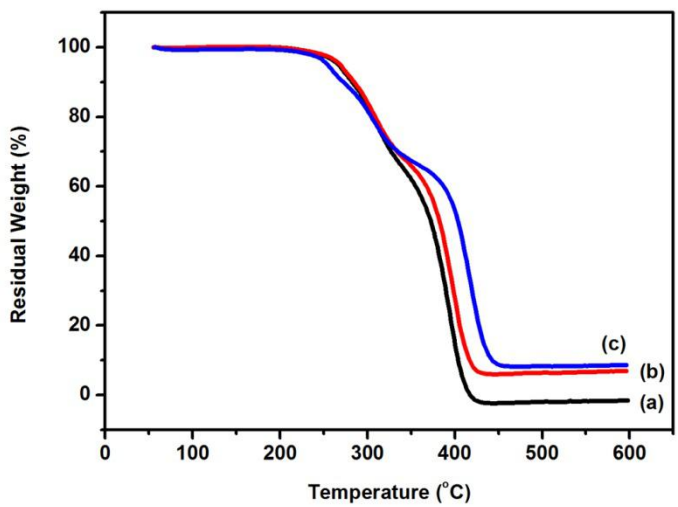

Figure 4 TG curves of waterborne polyurethane: (a) WPU, (b) WPU-H and (c) WPU-SC

The thermal stability at 200-280ºC of WPU-SC was inferior to WPU-H according to the TG curves shown in Figure 4 (b) and (c). This was because that as the grafting of dye molecule on polyurethane its bulkiness caused higher steric hindrance and consequently decreased the hydrogen bond interaction of the hard segments. However, the thermal stability of WPU-SC

was higher than WPU-H when the temperature was above 360°C, which was due to the influence of some unreacted dye molecules distributed and hydrogen bonded in hard segment of polyurethane[16, 20].

4. Conclusion

Waterborne polyurethane modified with the first generation of hyperbranched poly(amine-ester) was synthesized and reacted with reactive brilliant red K-2G to prepare the self-colored waterborne polyurethane. The FTIR spectra and particle size distribution analysis confirmed WPU-SC was successfully manufactured. DSC results revealed that the introduction of dye molecule would not affect the T_g of soft segment of polyurethane. Furthermore, the grafting of dye molecule on polyurethane decreased the stability of hard segment as the steric hindrance to hydrogen bonding, while the unreacted dye mainly distributed in hard segments increased its thermal stability as the intensifying action to hydrogen bonding of hard segments.

Acknowledgment

This paper was supported by the Shandong Provincial Key Research and Development Program, China (2017GGX80103), National Undergraduate Training Program for Innovation and Entrepreneurship, China (201810431025) and the National Key Research and Development Program of China (2017YFB0308503).

References

SM Burkinshaw, AD Hewitt, RS Blackburn, et al. The dyeing of nonwoven fabrics part 1: Initial studies. ***Dyes and Pigments***, 2012, 94:592-598.

N Mao, SJ Russell, B Poudeyhimi. Characterisation, testing and modelling of nonwoven fabrics. In: Russell SJ, editor. Handbook of nonwovens. Cambridge: Woodhead Publishing Limited; 2007.

R Liu, Y Chen, H Fan. Design, Characterization, dyeing properties, and application of acid-dyeable polyurethane in the manufacture of microfiber synthetic leather. ***Fibers and Polymers***, 2015, 16(9):1970-1980.

X Xu, Z Wang. Environmental cost analysis and upgrading research of synthetic leather industry. ***Energy Procedia***, 2011, 5:1341-1347.

SM Burkinshaw. Chemical principles of synthetic fiber dyeing. Glasgow: Chapman and Hall, 1995.

J Qu, C Zhang, J Feng, F Gao. Natural and synthetic Leather: A microstructural comparison. ***Journal of the Society of Leather Technologists and Chemists***, 2008, 92(1):8-13.

GA Baig. A study on the exhaust dyeing of various synthetic fibres with indigo. ***Coloration Technology***, 2012, 128(2):114-120.

SM Burkinshaw, YA Son. The dyeing of supermicrofibre nylon with acid and vat dyes. ***Dyes and Pigments***, 2010, 87(2):132-138.

L Ren, G Zhao, X Wang, et al. Study on dyeing improvements on microfiber synthetic leathers using amino-terminated hyperbranched polymers. ***Journal of Chemical Engineering of Chinese Universities***, 2014, 28(5):1138-1146.

T Qiang, X Wang, X Wang, et al. Study on the effect of dyeing properties of microfiber synthetic leather base by hydrolyzed collagen. ***Journal of functional materials***, 2014, 45 (14):14066-14071.

SK Lee, HY Lee, SD Kim. Dyeing properties of mixture of ultrafine nylon and polyurethane with different types of dye. ***Fibers and Polymers***, 2013, 14(12):2020-2026.

MS Yen, PY Chen, HC Tsai. Synthesis, properties, and dyeing application of nonionic waterborne polyurethanes with different chain length of ethyldiamines as the chain extender. ***Journal of Applied Polymer Science***, 2003, 90:2824-2833.

HH Wang, Li-En Lin. Modified polyurethane with improvement of acid dye dyeability. ***Journal of Applied Polymer Science***, 2003, 89:1397-1404.

X Wang, X Yuan, T Qiang, X Chen. Hyperbranched poly(amine-ester) polyol: Synthesis, characterization, thermal stability, solubility and surface activity. ***E-Polymers***, 2009, 9(1):1363-1377.

S Oprea. Molecular dynamcis, thermo-mechanical and optical studies on benzidine chain extended polyurethane-urea. ***Journal of Polymer Research***, 2011, 18:1777-1785.

HH Wang, IS Tzun. Modified polyurethane with a covalent bond of dye molecule. ***Journal of Applied Polymer Science***, 1999, 73:245-253.

S Wang, H Shi, H Fan, B Shi. Influence of hard segment content on properties of waterborne polyurethane. ***China Leather***, 2011, 40(11):18-22.

X Wang, Y Fu, L Ren, T Qiang, J Ren. Synthesis and characterization of PTMG aliphatic hyperbranched polyurethane. ***Journal of Functional Materials***, 2013, 44(2):289-293.

Z Sun, J Du, H Chen, W Gong. FTIR Study of nano-iron oxyhydroxides' decoloration on the azo dye. ***Spectroscopy and Spectral Analysis***, 2006, 26(7):1226-1229.

Z Jiang, K Yuan, S Li, Y Zhou. Study of FTIR spectra and thermal analysis of polyurethane. ***Spectroscopy and Spectral Analysis***, 2006, 26(4): 624-628.

P22

Preparation and characterizations of Gelatin-P(AA-AM) and GO-gelatin-P(AA-AM) super absorbent composite

Ma Haichuan[1], He Shengsheng[2], Chen Mianhong[3], Chen Min[4], Cheng Haiming[5]*

1. Key Laboratory of Leather Chemistry and Engineering of Ministry of Education, Sichuan University, CHENGDU, 610065, CHINA, +86-28-85405839, 2017223080025@stu.scu.edu.cn

2. Key Laboratory of Leather Chemistry and Engineering of Ministry of Education, Sichuan University, CHENGDU, 610065, CHINA, +86-28-85405839, 2015223085064@stu.scu.edu.cn

3. Key Laboratory of Leather Chemistry and Engineering of Ministry of Education, Sichuan University, CHENGDU, 610065, CHINA, +86-28-85405839, 2017226080001@stu.scu.edu.cn

4. Key Laboratory of Leather Chemistry and Engineering of Ministry of Education, Sichuan University, CHENGDU, 610065, CHINA; National Engineering Laboratory for Clean Technology of Leather Manufacture, Sichuan University, CHENGDU, 610065, CHINA, +86-28-85405839, chenmin_zhou@163.com

5. Key Laboratory of Leather Chemistry and Engineering of Ministry of Education, Sichuan University, CHENGDU, 610065, CHINA; National Engineering Laboratory for Clean Technology of Leather Manufacture, Sichuan University, CHENGDU, 610065, CHINA, +86-28-85405839, ChengHaiming@scu.edu.cn

Abstract

Super-absorbent resin is characterized with excellent water absorption and retaining water properties. It has been paid more and more attention due to it could be applied in various industries and civil areas. In this study, gelatin-(poly(acrylic acid-acrylamide) composite (G-P(AA-AM) was prepared by initiatation of the redox system through aqueous solution ploymerization as super-absorbent resin. The properties such as water absorption, salt resistance as well as biodegradability of the prepared G-P(AA-AM) was determined. The results showed that the absorption capacity of G-P(AA-AM) is at 1473.6 g/g in distilled water, while in 0.9 wt% NaCl solution is at 124.7 g/g. The addition of gelation into resin could promote its biodegradability. Moreover, Graphene oxide was introduced into G-P(AA-AM) to further enhance its absorption and mechanical properties.

Keywords: gelatin, Poly(acrylic acid-acrylamide), graphene oxide, super-absorbent resin, biodegradability.

P23

Research on Determination of Isothiazolinone Fungicides in Leather*

Li Shuqing**, Yi Jie, Wang Yaping

(College of Material and Textile Engineering, Jiaxing College, Jiaxing 314001, China)

Abstract

In order to tackle the update international regulation, the contents of major isothiazolinone fungicides widely used in leather making process, namely, 2-methyl-3-isothiazolinone(MI), 5-chloro-2-methyl-3-isothiazolinone (CMI) and 1,2-benzisothiazolinone (BI), were studied with methanol as selected solvent. The results indicate that the detection of aim chemicals by HPLC-DAD could get better results compared with that by GC-MS, with lower detection limit and high response. The optimized HPLC-DAD analyzing procedure to aim isothiazolinone is: fluent phase *V*(water):*V*(methanol) 65:35, column temperature 30℃, flow velocity 0.6 mL/min, and sample volume 15 μL. The peak area and the concentration of MI, CMI and BI show excellent linearity when the their concentration is 0.625~10 mg/L, with the related coefficient of above 0.9998. The detection limits of MI, CMI and BI are 0.026 mg/L、0.054 mg/L and 0.122 mg/L, respectively. Target objects in leather samples could be extracted by ultrasonic at the frequency of 40 kHz at 30℃ for 10 mins, with 30 mL methanol as solvent. In order to ensure the precision and accuracy of the detection experiment, recoveries of the standard working solution with various concentrations in blank samples of leather were researched and the results are between 91.7% and 98.6%. The stabilities of the standard stock solution at -18℃ and the standard working solution at -4℃ under the dark conditions were determined and both of them would be preserved for at least 60 days.

Key words: leather; isothiazolinone; determination; HPLC-DAD; ultrasonic extraction

Introduction

Since hide and skin are always put in the moist environment for a period of time before the following leather making process, antimicrobial agents are used to inhibit the growth of microbial, especially mold. Isothiazolinone (Often, combinations of methylisothiazolinone and chloromethylisothiazolinone, known as Kathon CG, or methylisothiazolinone and benzisothiazolinone are used) can greatly inhibit the growth of microbial, such as bacterial, fungi,

*Funded by "Jiaxing city leather and textile dyeing and finishing cleaner production innovation team ";

**Corresponding author, E-mail:576531210@qq.com

and mold. Consequently, it can be widely used in mildew proofing in the fields of industry and agriculture, besides leather making process.

Together with their wanted function, controlling or killing microorganisms, isothiazolinones also have undesirable effects: They have a high aquatic toxicity and some derivatives (namely chloromethylisothiazolinone or CMI) can cause hypersensitivity by direct contact or via the air. Some studies have shown MI to be allergenic and cytotoxic[1,2]. The toxic actions of methylisothiazolinone (namely MI) on developing neurons occur at much lower concentrations than those inducing lethal injury (1~3 micromolar). CMI is even more potent, working at concentrations as low as 0.1 micromolar. All those have led to some concern over its use.

Some types of the leather and its products, especially glove leather, directly contact with skin. Consequently, it is necessary to detect isothiazolinone derivatives widely used in leather, but there is few reports on this [3~10]. Therefore, it is necessary to study the detection method of MI, CMI and BI in leather.

Experimental

2.1 Main chemicals

MI with a purity of 99.5%, and BI with a purity of ≥98.0% were purchased from Sigma Inc; CMI was obtained as a 100 mg/L aqueous (water) solution from Accu Standard Inc. Methanol and acetone were of chromatographically pure.

For MI and BI, 200 mg/L standard stock solutions in methanol were prepared in a refrigerator at -18℃ in dark place. 10

mg/L standard working solution with the mixture of MI, BI and CMI in methanol were prepared and were stored at -4℃ in dark place.

2.2 Main equipment

Agilent 1100 equipped with C18 reversion phase chromatographic column (4.6 mm×250 mm×5 μm, Agilent Technologies) was used to carry out HPLC-DAD analysis. GC-MS analysis was carried out with an DB-5MS (30 m×0.32 mm×0.25 μm, Agilent Technologies) column.

Syringe filters (L=13 mm, d = 0.45 μm) were made of MCE.

2.3 Analysis of standard working solution

2.3.1 Optimization of HPLC-DAD analysis

To optimize isothiazolinones analyzing conditions, orthogonal test was adopted. Main controllable variables, viz. mobile phase, column temperature, and injection volume were selected. For each selected factor, three levels were investigated and listed in Table 1. Further studies of the flowing rate of mobile phase on the analyzing result see Table 2.

2.3.2 Optimization of GC-MS analysis

According to the reference 10, the analysis condition of the standard working solution was: the partial pressure of nitrogen was 0.6 Pa, injection volume 1 μL, injector temperature 270℃. The column oven temperature programme started at 50℃ (hold for 2 mins), set at 20℃/min to 80 ℃ (held for 6 mins), set at 15℃/min to 280℃ and held isothermally at 280℃ for 10 mins. Transfer line was also set at 280℃, quadrupole temperature was set at 150℃, and source temperature at 230℃. Optimized analysis condition of isothiazolinones was adjusted according to the peak intensity and responds time.

2.3.3 Optimization of pretreatment of positive sample

Effects of extraction methods (ultrasonic extraction and agitation extraction), extraction time, extraction temperature, and extraction frequency were studied in this experiment. Unless otherwise statement, all positive samples were fully washed with extraction solvent after the extraction. The extract liquor was diluted or condensed to suitable concentration before HPLC-DAD analysis.

2.3.4 Recovery and precision experiment

1 mL stepwise diluted liquid of standard working solution was added to the blank leather sample. Based on the optimized extraction method, sample was extracted and the extract liquor was condensed to 1 mL, and then analyzed by optimized analyzing method.

2.3.5 Stability of isothiazolinones

Stabilities of standard stocking solution and standard working solution were tested by periodic injection of the corresponding solution by optimized analyzing method.

Result and discussion

3.1 Optimization of analyzing method by HPLC-DAD

3.1.1 Optimization of analyzing condition of HPLC-DAD

Peaks and responds times of MI, CMI and BI were ascertained by comparing the chromatograms of standard working solution and the solutions of MI, CMI and BI, respectively. Based on the responds of DAD detector, the best detection wavelengths of MI, CMI and BI are determined and are 275.8 nm, 275.8 nm, and 318.8 nm, respectively.

Results of orthogonal experiment are listed in Table 1.

Table 1 Results of the orthogonal experiment of HPLC-DAD determination[1)]

Serial	*V*(methanol): *V*(water)	Column temp./℃	injection volume/μL	Peak area[2)]
1	25:75	20	10	808
2	25:75	30	15	1240

3	25:75	40	20	1632
4	35:65	20	15	1198
5	35:65	30	20	1682
6	35:65	40	10	820
7	50:50	20	20	1602
8	50:50	30	10	815
9	50:50	40	15	1237
K1	1227	1203	814	
K2	1233	1246	1225	
K3	1218	1230	1639	
R	15	43	824	

1） mean value of three analyzing results;

2） addition value of MI, CMI and BI.

Table 2 Optimization to the flow rate of mobile phase[1)]

Velocity/mL·min^{-1}	0.6	0.8	1.0
Peak area[2)]	2092	1541	1230

In Table 1, “R” is the variance of “Ki”, which demonstrates that factors could be arranged in the following order according to their decreasing ability of the effect on the analyzing result in the experimental range: injection value ＞ column temperature ＞ mobile phase. Peak area increases with the increase of the injection volume. In the experimental range, peak area increases with the increase of temperature and shows a peak at 30℃, and when the temperature is further increased, peak area is decreased. Mobile phase has a similar influence on the peak area with temperature, and gives the maximal area at V(methanol):V(water)=35:65. Data in Table 2 shows that peak area decreases with the increase of the flow rate, which might be explained by the increase of the detection time at the DAD detector and consequently the increase in the absorption time. To maintain the precision and the accuracy of the analyzing result, the optimum level of each variable is column temperature 30℃, V(methanol):V(water)=35:65, injection volumn 15 μL, flow rate 0.6 mL/min. Fig.1 is the HPLC-DAD chromatogram of standard working solution.

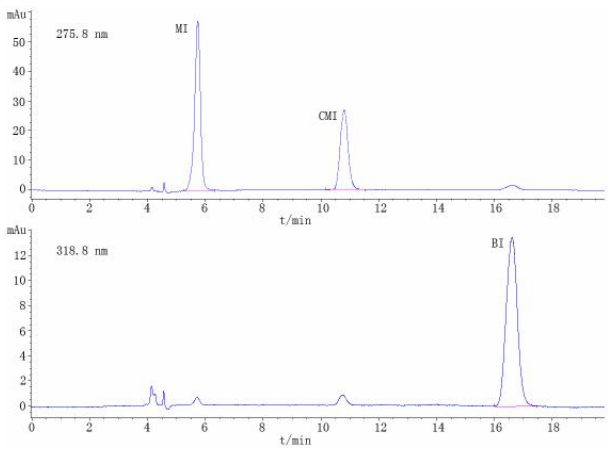

Fig. 1 HPLC-DAD chromatogram of standard working solution

3.1.2 Specification curve of isothiazolinone by HPLC-DAD analysis

Specification curve of MI, CMI and BI are prepared according to the results of HPLC-DAD analyses of the stepwise diluted standard working solution, and corresponding equations of linear regression of peak area to concentration are calculated (See Table 3). Fixing the signal-to-noise value at 3:1, detection limitations of MI, CMI and BI were determined by instrument and

are 0.026 mg/L, 0.054 mg/L and 0.122 mg/L, respectively.

Table 3 Effect of isothiazolinone concentration to peak area by HPLC-DAD analysis[1)]

Peak area	Concentration					Equation of linear regression[2)]	Regression coefficient
	A	B	C	D	E		
MI	61.18	117.3	238.4	419.8	1036	y=73.32x-2.04	0.99998
CMI	28.67	56.60	116.4	239.8	483.8	y=47.82x-0.24	0.99995
BI	19.73	45.97	87.74	175.4	363.7	y=37.65x-4.46	0.99981

mean value of three analyzing results, corresponding concentrations (mg/L) of A～E
are MI (0.537, 1.075, 2.149, 4.298, 10.746), CMI (0.625, 1.250, 2.500, 5.000, 10.000),
BI (0.613, 1.225, 2.450, 4.900, 9.800) ,respectively;

2） y is peak area; x is concentration (mg/L).

3.2 Optimization of GC-MS analysis

Primary GC-MS analyzing result of standard working solution indicates that target objects have tailed peaks. Through the adjusting of the heating program, acceptable analyzing result could be obtained. The optimized column oven temperature programme startes at 50℃ (held for 2 mins), set at 25℃/min to 150℃ (held for 1 min), set at 25℃/min to 190℃ (held for 1 min), and set at 25℃/min to 230℃ and held isothermally at 230℃ for 1 min.

3.2.1 Determination of target peak in GC chromatogram

Peaks of MI, CMI and BI were determined according to the corresponding mass fragments (See Fig. 2). Peaks of MI, CMI and BI are appeared at 6.4 mins, 6.8 mins and 9.4 mins in GC graph, respectively.

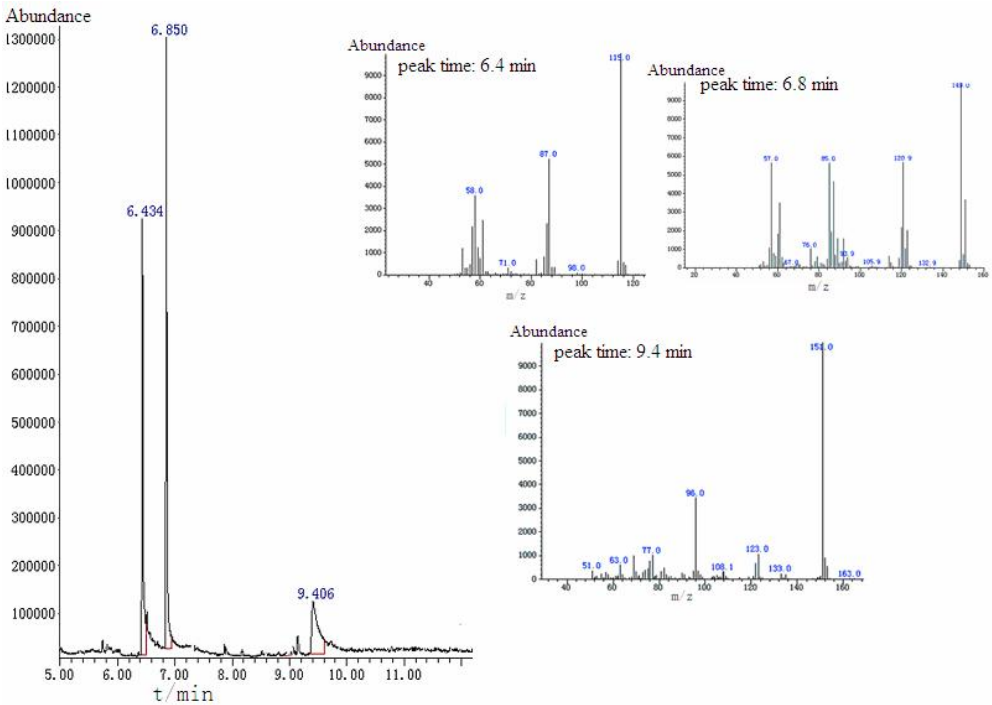

Fig. 2 GC chromatogram and mass fragments of standard working solution

3.2.2 Specification curve of isothiazolinone by GC-MS analysis

Fig. 3 is the GC chromatogram of stepwise diluted standard working solutions, which indicates that GC-MS equipped with DB-5 column is not an ideal instrument for the analysis of isothazolinone. When the concentration of BI is ≤ 2 mg/L, peak of BI is undistinguishable. This might be explained by the differences between polarities of DB-5 column and the target

objects. Considering the application popularity of the column DB-5 and other weak polarity columns in the inspection field [11~13], we think it is unsuitable for the detection of sothazolinone by GC-MS.

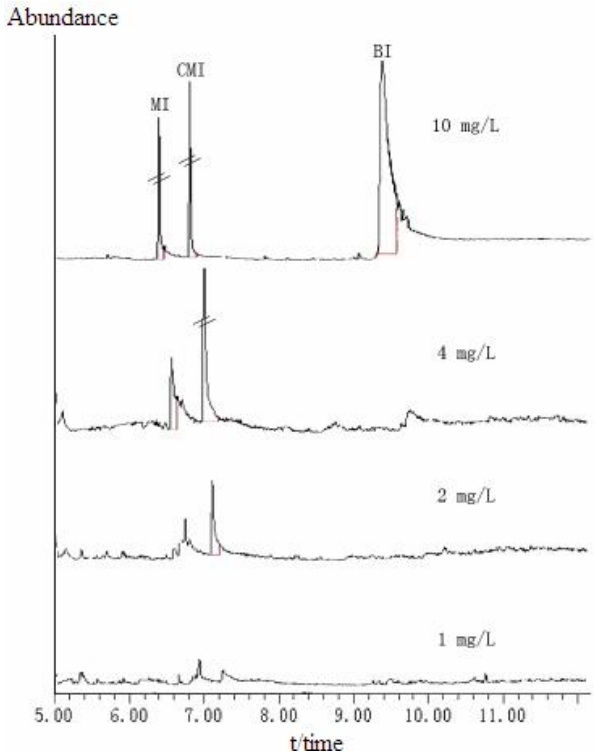

Fig. 3 GC graphs of standard working solution by stepwise dilution

Comparing the analyzing results of HPLC-DAD and GC-MS chromatographs, HPLC-DAD analyzing method outweighs GC-MS in detection limits and response in the analysis of isothazolinone.

3.3 Optimization of extraction process of positive leather sample

3.3.1 Optimization of extraction time

Table 4 is the effect of time on the extraction of isothazolinone. In the beginning of the first 30 mins of agitation extraction, peak area increases with the increase of the extraction time, and then maintains constantly on the whole, which illustrates that best extraction time is 30 mins; similarly, best extraction time for ultrasonic extraction is 15 mins.

Table 4 Effect of time on extraction result 1)

time/min	Peak area of agitation extraction			Peak area of ultrasonic extraction		
	MI	CMI	BI	MI	CMI	BI
15	308.6	470.0	0	349.8	528.7	0
30	343.6	506.3	0	340.6	524.4	0
60	344.8	507.4	0	343.6	519.2	0

1) mean value of three analyzing results; extraction temperature is 30℃.

3.3.2 Optimization of extraction temperature

Generally speaking, temperature is one of the main factors affecting the extraction effect. But the analyzing result in Table 5 indicates that little differences could be perceived when the extraction temperature is 20℃~40℃ regardless of extraction method. When the extraction temperature is increased from 30℃ to 40℃ by agitation extraction, peak area of MI is decreased slightly, which might be explained by the structure destroy of MI at comparatively high temperature for 30 mins.

As a result, both of the agitation and ultrasonic extraction could be carried out at 30℃.

Table 5 Effect of temperature on extraction result[1)]

Temp./℃	Peak area of agitation extraction(30 mins)			Peak area of ultrasonic extraction(15 mins)		
	MI	CMI	BI	MI	CMI	BI
20	350.7	539.0	0	358.8	541.7	0
30	348.0	523.4	0	360.5	544.7	0
40	339.0	524.7	0	365.5	544.1	0

1） mean value of three analyzing results.

3.3.3 Optimization of extraction frequency

Table 6 is the result of extraction frequency on the effect of extract. According to the standard curve y=Kx+b, percentages of the first extraction and the second extraction on the total amount of target objects could be calculated. Detail formulas are listed below:

First extraction $$W_1 = \frac{\frac{A_1 - b}{K} \times 125}{\frac{A - b}{K} \times 125} \times 100\% = \frac{A_1 - b}{A - b} \times 100\%$$

Second extraction $$W_2 = \frac{\frac{A_2 - b}{K} \times 10}{\frac{A - b}{K} \times 125} \times 100\% = \frac{(A_2 - b) \times 2}{(A - b) \times 25} \times 100\%$$

Where:

W_1——weight percentage of the first extraction to the total weight of two extractions;

W_2——weight percentage of the second extraction to the total weight of two extractions;

A_1——peak area of the first extraction to the total peak area of two extractions;

A_2——peak area of the second extraction to the total peak area of two extractions;

A——Peak area of the single extraction under optimized conditions;

K——coefficient between peak area and the concentration of target object;

b——constant for the equation of standard curve.

Constants 125 and 10 are the dilution multiple of aim objects in positive sample.

Table 6 Effect of re-extraction on extraction result[1)]

Frequency		Agitation extraction (30 min)			Ultrasonic extraction (15 min)		
		MI	CMI	BI	MI	CMI	BI
First extraction[2)]	peak area	344.4	509.3	0	339.8	522.5	0
	Percentage[4)]	99.0	97.3	0	94.2	95.9	0
Second Extraction[3)]	peak area	189.9	224.5	0	120.5	138.6	0
	percentage[4)]	4.3	3.4	0	2.6	2.0	0

1） mean value of three analyzing results;

2） methanol volume in the first extraction is 20 mL; extraction times are 20 mins by agitation extraction, and 15 mins by ultrasonic extraction;

3） methanol volume in the second extraction is 10 mL; extraction times are 10 mins by agitation extraction, and 5 mins by ultrasonic extraction;

4） weight percentage to the single extraction under optimized conditions.

Data in Table 6 indicates that in the frequency extraction experiment, aim objects extracted in first extraction could be weighed up to 96.8%~103.3% by single extraction, and single extraction has the advantage of feasibility. Resultantly, single extraction method is selected in this experiment. According to the peak areas in Table 6 and the formula in Table 3, amount of MI, CMI and BI in positive sample would be calculated and are 1.24×103 mg/kg, 2.85×103 mg/kg and 0, respectively.

3.4 Recovery and precision experiment

Recovery and precision experiment of blank leather sample are listed in Table 7.

Data in Table 7 indicates that recovery rates of aim products in blank sample are between 91.7%～98.6%.

Table 7 Result of recovery test[1)]

Aim product	amount/μg	Peak area		Recovery rate/%
		Standard solution	Extraction solution	
MI	2.49	189.92	179.75	94.64
	4.98	388.00	382.80	98.66
	9.95	765.94	719.44	93.93
CMI	1.25	64.12	60.22	93.92
	2.50	125.34	120.75	96.34
	5.00	248.69	228.00	91.68
BI	1.23	47.42	44.86	94.60
	2.45	94.13	92.73	98.51
	4.90	181.77	168.39	92.64

1) mean value of three analyzing results.

3.5 Stability of MI, CMI and BI

To maintain the accuracy of the analyses, it is necessary to analyze the stabilities of standard stocking solution and standard working solution (see Table 8 and Table 9).

Table 8 Result of stability of standard working solution

Table 9 Result of stability of standard stocking solution

Stocking day	1	4	7	10	13	16	19
MI/%	100.00	100.50	101.13	101.04	102.80	105.58	101.41
CMI/%	100.00	99.94	99.35	100.22	99.49	102.51	100.94
BI/%	100.00	97.86	101.51	100.41	100.00	105.85	99.96
Stocking day	22	25	28	31	34	37	40
MI/%	102.57	101.48	102.73	102.71	104.74	101.22	103.18
CMI/%	100.68	102.36	99.59	100.10	104.60	102.55	101.30
BI/%	101.73	100.85	100.32	100.88	101.37	100.69	101.59
Stocking day	43	46	49	52	55	58	60
MI/%	103.32	100.27	101.40	104.10	101.57	101.91	102.07
CMI/%	102.46	100.28	100.83	102.74	104.33	102.24	104.02
BI/%	100.29	101.02	100.12	104.70	103.40	102.91	103.69

Stocking day	1	3	6	11	14	17
MI/%	100.00	100.00	99.85	100.09	99.08	98.75
BI/%	100.00	100.00	98.08	96.35	96.73	96.73
Stocking day	20	27	30	33	36	39

MI/%	99.19	98.77	98.44	100.11	100.00	101.62
BI/%	97.12	97.37	96.22	100.71	100.00	99.73
Stocking day	42	45	51	54	57	60
MI/%	99.81	98.42	96.26	95.02	95.15	95.99
BI/%	98.57	98.69	98.58	98.18	96.93	95.97

Data in Table 8 and Table 9 demonstrate that both of the standard stocking solution and standard working solution could be kept in corresponding conditions for 60 days. Since CMI product is the 100 mg/L solution in water, it is no necessary to study its stability. According to the product certificate, CMI could be storage in -4℃ for 1 year.

4. Conclusions

To analyze main isothiazolinone (namely MI, CMI and BI) content in leather, HPLC-DAD was selected with methanol as solvent. The optimized HPLC-DAD analyzing procedure to aim isothiazolinone is: fluent phase V(water):V(methanol) 65:35, column temperature 30℃, flow velocity 0.6 mL/min, and sample volume 15 μL. Wavelength 275.8 nm for MI and CMI, and wavelength 318.8 nm for BI are chosen for the detection by DAD detector. When the concentration of MI, CMI and BI is between 0.625 to 10 mg/L, with the related coefficient of above 0.9998. The detection limits of MI, CMI and BI are 0.026 mg/L、0.054 mg/L and 0.122 mg/L, respectively.

Aim objects in leather samples could be extracted by ultrasonic machines, with 30 Ml methanol as solvent, extracting for 10 mins, and supersonic frequency of 40 kHz at 30℃.

Recoveries of the standard working solution with various concentrations in blank samples were researched and the results are 91.7%~98.6%.

The stabilities of the standard stock solution at -18℃ and standard working solution at -4℃ under the dark conditions were determined and both of them would be preserved for at least 60 days.

References

[1] A. Schnuch, J. Geier, W. Utur, P. J. Frosch. Patch testing with preservatives, antimicrobials and industrial biocides. Results from a multicentre study[J]. British Journal of Dermatology, 1998, 137(3): 467-476.

[2] A. C. De Groot, A. Herxheimer. Isothiazolinone preservative: Cause of a continuing epidemic of cosmetic dermatitis[J]. The Lancet, 1989, 333(8633): 314-316.

[3] HENG Shi-fang, LIU Xia, YANG Yue, et al. Synthesis of isothiazoles antibacterial agent and evaluation of its property[J]. Journal of Textile Research, 2007, 30(9): 87-92.

[4] ZOU Bing-guo, ZHANG De-hong. Application and prospect of isothiazolinone derivative and downstream product[J]. Technology & Development of Chemical Industry,2007,36(11):49-50.

[5] LIU Fen, DAI Jing-Jing, LIANG Wei, et al. Determination of IPBC in cosmetic. Practical Preventive Medicine[J], 2004, 31(6): 872-874.

[6] LIU Wen-guang, LI Yun-zhi, SHI Rui-chang, et al. Determination on isothiazolone solution content for silkworm by RP-HPLC[J]. Journal of Anhui Agricultural Science, 2009, 37(32): 15667-15668.

[7] LI Jie, ZHAO Shan, WU Da-nan. A HPLC method for determination of Kathon and 4p-hydroxybenzoates in cosmetic products[J]. Journal of Environment and Health, 2000, 17(4): 238-239.

[8] GE Bao-kun, GAO Jian-hui, WANG Wei, et al. Rapid determination of antifungal residues in grape wine by HPLC[J]. Chinese Journal of Food Hygiene, 2005, 17(2): 160-163.

[9] WANG Chao, ZHANG Qin, WANG Xin. Determination of methylisothiazolinone and chloro-methylisotldazolinone in cosmetics by high performance liquid chromatography[J]. Journal of Environment and Health, 2007, 06(24): 449-450.

[10] Astrid R, Sabine G, Frank S. Analysis of isothiazolinones in environmental waters by gas chromatography – mass spectrometry[J]. Journal of Chromatography: A,2007,1164(1-2):74-81.

[11] SN/T 1654-2005. Determination of 2 3 5 6-tetrachlorophenol residues in leather and leather products for import and export — Acetylation gas chromatography.

[12] GB/T 19942-2005. Leather and fur — Chemical tests — Determination of banned azo colourants.

[13] GB 19601-2004. Limit and determination of 23 harmful aromatic amines in dye products

P24

The role of the source of raw hides in environmental impact for leather making by life cycle assessment

Chen Mianhong[1], Duan Youdan[2], Chen Min[3], Cheng Haiming[4]*

[1] Key Laboratory of Leather Chemistry and Engineering of Ministry of Education, Sichuan University, Chengdu, 610065, +86-28-85405839, 2017226080001@stu.scu.edu.cn

2 Key Laboratory of Leather Chemistry and Engineering of Ministry of Education, Sichuan University, Chengdu, 610065, +86-28-85405839, 932443652@qq.com

3. Key Laboratory of Leather Chemistry and Engineering of Ministry of Education, Sichuan University, Chengdu, 610065, National Engineering Laboratory for Clean Technology of Leather Manufacture, Sichuan University, Chengdu, 610065, +86-28-85405839, chenmin_zhou@163.com

4. Key Laboratory of Leather Chemistry and Engineering of Ministry of Education, Sichuan University, Chengdu, 610065, National Engineering Laboratory for Clean Technology of Leather Manufacture, Sichuan University, Chengdu, 610065, +86-28-85405839, chenghaiming@scu.edu.cn

Abstract

Impact assessment methods help to explain LCA studies by converting emissions and resource extraction from the production process into a limited number of environmental impact scores. In this study, we collected inventory analysis data in leather-making process of two tanneries in China dealt with different sources of raw hides, and adopted two latest impact assessment methods ReCiPe2016 (midpoint level, hierarchist perspective) and CML-IA (baseline, 3.05 version) to quantify the impact of the consumption of materials and emissions on the environment during leather-making process. When 1,000 kg of raw hides was used as functional unit, B (fromVietnam) with highest leather yield has greater burden on all impact categories except marine eutrophication than A (from Uganda) and C (from China) due to the excessive consumption of materials in its production process. Results show that crush leather A and B have roughly the same production process, but B has a higher leather yield than A, resulting in 1 kg B was less environmentally burdened than A, among all impact categories. The production of crust leather C was more in line with the domestic production level, and its damage to global warming, ionizing radiation, terrestrial acidification and freshwater eutrophication are bigger than A, but A consumed more chromium powder in leather-making process so that the toxicity category such as freshwater and marine ecotoxicity are greater than C. All-round and more accurate data are needed to support the LCA research on leather in the future.

Keywords: life cycle assessment, impact assessment, ReCiPe2016, CML-IA, crush leather

1. Introduction

Life cycle assessment (LCA) is a widely accepted methodology for quantifying the environmental performance of products taking into account the complete part of or complete life cycle, which mainly include the production of raw materials, manufacture, use, and post-processing of the products. It has proven its efficiency as a good decision-making tool to promote sustainable production practices[1]. There are a number of peer-reviewed studies have been published on using LCA to quantify environmental impacts of leather production at different geographical locations such as China[2], Chile[3], India[4], Bangladesh[5], Spain and Italy[6] with various system boundaries, functional units and impact assessment methods. The impact assessment methods have been used mainly include IMPACT2002+, Ecoindicator 99, and CML 2000.

The definition of life cycle impact assessment (LCIA) is a phase of understanding and assessing the extent and importance of the potential environmental impact of a product system. According to ISO, every LCIA must at least include classification and characterization, while normalization, ranking and weighting are optional. Adopting a unified impact categories or even characterization models in LCIA is an issue of debate in the LCA community in recent years[7]. Developers of the LCIA methods are devoted to develop a new method or to improve existing ones to make the assessment more precise and make it popular.

To further progress LCIA methods beyond the current consensus state of the art, Huijbregts et al.[8] updated the ReCiPe2008

method to its version of 2016. Before that, most characterization models have a continental focus, particularly focusing on Europe. ReCiPe2016 providing characterization factors that are representative for the global scale and make it more suitable for LCA study in non-European regions. CML-IA (3.05 version) is a LCIA methodology developed by the Center of Environmental Science of Leiden University and released in 2016. The first version of this method dates back to the beginnings of the development of LCA, and it has been updated for the validation of the characterization factors[9]. The established CML-IA method is defined for the midpoint approach and it mainly provides an analysis for European context.

When tanneries handle raw hides from different sources, they may adopt different processing techniques so that have different impacts on the environment. We can quantify the impact of different leather-making processes through LCA and its characterization methods. Although there have been not a few studies on the LCIA of the leather-making process, the used characterization methods mostly are superseded or no longer applicable. We collected the inventory analysis data from two tanneries handling different resources of cattle raw hide and used two latest impact assessment methods (ReCiPe2016 and CML-IA) to quantify the environmental impact of the leather-making process in this study. At the same time, the results obtained by the two characterization methods will used appropriately for comparison which are limited to analogous impact categories. We will also analyze the contribution rate of different section and the consumed electricity, water and chemicals in leather-making process to the results of each impact category. Results showed within this study add scientific value by providing inventory data and information for identification of environmental "hotspots" of leather-making process in order to promote cleaner and more sustainable production techniques of leather.

2. Methodology

2.1 Goal

The goal of this LCA study was to collect data on electricity, water, chemicals consumed and wastewater treatment across leather-making process, and to quantify the environmental burden of the production of crush leather with a cradle-to-gate approach. It also need to figure it out if there will be different environmental impacts when dealing with raw hides from different sources, and strive to provide information to intermediate and final consumers. The data produced will help the tanners to reduce environmental pollution and develop more sustainable production process.

2.2 Functional Unit

The primary purpose of a functional unit is to provide a reference for inputs, outputs, and impact assessment results. The mass of raw hides is usually related to the input of water and chemicals, and the mass of crush leather also provide commodity information to downstream consumers. Therefore 1000 kg raw hides and 1 kg crust leather were used as functional unit in our research, respectively.

2.3 System Boundaries

System boundary defines which unit processes, inputs, and outputs were included in this LCA study. Figure 1 shows the system boundary established to determine the environmental impact of the production of crush leather. Upstream processes, such as agriculture, animal husbandry, and slaughtering, due to the lack of agricultural production data from countries with different sources of cattle hides, were not included in these assessments. The production process from raw hide to crush leather can be divided into three main sections: beamhouse, tanning and retanning. From raw hide to limed pelt, it is mainly subjected to soaking, liming and splitting operations. The tanning section mainly includes deliming, pickling, tanning, shaving and trimming, and the retaining section mainly includes retanning, filling, dyeing and draining. These operations require the input of water, electricity and chemicals, while the output to the environment mainly includes exhaust, solid waste and wastewater. The environmental impact of the production of electricity, water and chemicals is within the scope of this study, and the wastewater treatment process is also within the assessment. Exhaust gas emissions, disposal of solid waste, downstream processing of crust leather and final disposal are unfortunately not included in this research.

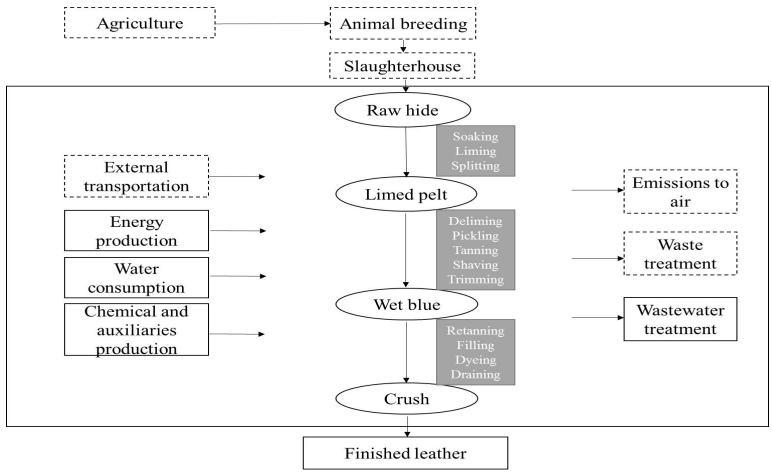

Figure 1. System boundary for LCA study of crush leather

2.4 Collection of Data

We collected the input and output data involved in inventory analysis in the leather-making process in China from Chen's previously reported work[2]. Briefly, two tanneries in Shandong and Anhui province studied in this research all use the traditional chrome tanning process. Raw hides of Shandong Tannery were from Uganda (raw hide A) and Vietnam (raw hide B), and the weight of each hide is 20.8 kg and 11 kg, respectively. The raw hide of Anhui tannery was from China (raw hide C), and the average weight of the hide is 32 kg. The operation of raw hide A and B in a tannery in Shandong is exactly the same and the processing of raw hide C is more in line with the average level of leather-making in China. The main input and output data used to simulate the leather-making process are shown in Table 2. Crush leather A (192 kg), B (300 kg) and C (175 kg) were obtained by processing 1000 kg of raw hide.

Table 1. Input and output analysis for crush leather A, B and C

Section	Input/Output	Crush leather A/kg	Crush leather B/kg	Crush leather C/kg
Beamhouse				
	Electricity	66.68	67.07	96
	Water	5212	5205	20500
	Degreasing agent	5.5	5.5	2
	Soaking agent	31.59	31.54	1
	Sodium sulfide	16.59	16.54	11
	Lime	88	88	30
	Sodium hydrosulfide	11	11	9
	Sodium carbonate			4
	Bactericide			3
	Liming auxiliary			8
Tanning				
	Electricity	31.5	33.2	118
	Water	9413	9090	5954
	Degreasing agent	4.7	4.5	3.7
	Ammonium sulfate	18.8	18.2	5.0

	Enzyme	1.9	1.8	2.48
	Sodium chloride	75	72.7	43.4
	Formic acid	11	11	3.7
	Sulfuric acid	4.7	4.54	6.8
	Chromium powder	56	54.5	40.3
	Sodium bicarbonate	16	15.45	
	Sodium sulfate			3.1
	Sodium formate			6.2
	Magnesium oxide			2.5
	Fungicide			0.6
Retanning				
	Electricity	39	63	77
	Water	4446	7535	6395
	Degreasing agent	0.5	0.8	0.22
	Formic acid	5	8	3.29
	Chromium powder	9.6	15.5	4.38
	Sodium formate	6	9.7	9.86
	Sodium bicarbonate	1.2	1.9	1.53
	Acrylic resin	12	27	8.76
	Dye	2	6	4.38
	Ammonium bicarbonate	3.6	5.8	
	Oil	22	31	
	Filler	23	48	
	Protein	4.8	3.9	
	Cationic resin	3.9	3.9	
	Tanning agent			4.38
	Fatliquoring agent			15.39
	Lanolin			4.38
	Neutralization auxiliary			4.38
	Resin			28.5
Wastewater		18063	20510	31301

The LCA data for electricity, water and chemicals mainly come from database such as Ecovinent 3 and Industry data 2.0 in simapro. Since some auxiliaries used in leather-making process are mixtures, the host material will be analyze instead. It is worth noting that chromium powder was measured by 1/4 of chromic oxide and sodium bicarbonate was replaced by ammonium bicarbonate. Treatment of 1 m^3 tannery wastewater requires 0.97 kWh of electricity, 151.3 g of sulfuric acid, 37.83 g of aluminum sulfate, and 75.65 g of ferrous sulfate to reach the indicators of wastewater discharge, but the treatment data does not include oxidation ditch culture and sludge treatment process[10].

3. Results and Discussion

The characterization process is actually based on the selected life cycle impact category and point type to establish a characterization model, and then characterization factor is derived from the characterization model which converts the life cycle inventory analysis results into general parameter results[11]. In short, characterization helps explain LCA research by

translating emissions and resource extractions into a limited number of environmental impact scores.

3.1 Characterization by ReCiPe2016

ReCiPe is based on the Eco-indicator 99 and CML methods and has a consistent framework to assess the impact of product at the midpoint and endpoint levels[12]. ReCiPe2016 provides characterization factors that represent global scales and provides three different perspectives: individualist, hierarchist, and egalitarian. Because the endpoint (damage oriented) will make the results more uncertain, this study will adopt the midpoint and the hierarchical perspective evaluation model.

3.1.1 1000 kg raw hide as functional unit

The impact assessment of 1000 kg raw hide from different sources in leather-making process was quantified, and the characterization result is listed in Table 2. The characterization factor of climate change is the global warming potential (GWP), and the GWP of carbon dioxide is 1 and the other greenhouse gases is based on IPCC 2013 report. The unit of characterization result can be expressed as kg CO_2 equivalents. When processing 1000 kg of raw hide, the effect of A, B and C on climate change are respectively equivalent to the emission of 873.36, 1088.16 and 1031.26 kg CO_2. The characterization factors of stratospheric ozone (SO) depletion are ozone depleting substances which can destruct the SO by anthropogenic emissions. According to the results in Table 2, it is known that the effect on the SO is negligible in leather-making process. The characterization factor of ionizing radiation is based on the level of exposure for the global population. In leather-making process, A, B and C respectively generated ionizing radiation equivalent to 36.422, 41.371 and 35.025 kBq Co-60 to air. The characterization factor of ozone formation is determined from the change in intake rate of ozone due to change in emission of precursors (NO_x and NMVOC). Ozone pollution from leather-making process causes damage to human health and is roughly the same as damage to terrestrial ecosystems. For the impact category of fine particulate matter formation, the degree of damage of 1000 kg raw hide B is equivalent to the emergence of 1.675 kg PM 2.5. Terrestrial acidification is mainly due to the emission of acid gases and its characterization factor is acidification potential derived using the emission weighted world average fate factor of SO_2. Table 2 shows that raw hide A has the least effect on terrestrial acidification. The emission of P and N containing nutrients can cause freshwater and marine eutrophication. Among the eighteen impact categories, raw hide C only caused the greatest damage to marine eutrophication, while B had the greatest damage to other impact categories. The characterization factor of human toxicity and ecotoxicity accounts for fate, exposure and toxicity of a chemical and its result can expressed as kg 1,4-dichlorobenzeen (1, 4-DCB)$_{equivalents}$ emitted. In these toxic categories, the leather-making process appears to be the most harmful to human carcinogenic. The characterization factor of land use accounts for the amount of land transformed or occupied for a certain time and its result can expressed as m^2a (year) crop equivalents. Interestingly, the land use of both A and B is about twice that of C. Mineral and fossil resources scarcity can also be expressed in the consumption of mineral and fossil resources. In the result of water consumption, the amount of wastewater is subtracted (due to the wastewater treatment), therefore the water consumption of the hide A, B and C are 28.292, 32.635 and 40.584 m^3, respectively.

Table 2. Characterization of 1000 kg raw hide in leather-making process by ReCiPe2016

Impact category	Unit	Raw hide A	Raw hide B	Raw hide C
Global warming	kg CO_2 eq	873.357	1088.152	1031.240
Stratospheric ozone depletion	kg CFC11 eq	3.314E-4	3.519E-4	2.223E-4
Ionizing radiation	kBq Co-60 eq	36.422	41.371	35.025
Ozone formation, Human health	kg NO_x eq	1.731	2.209	2.202
Fine particulate matter formation	kg PM2.5 eq	1.342	1.675	1.629
Ozone formation, Terrestrial ecos.	kg NO_x eq	1.785	2.293	2.282
Terrestrial acidification	kg SO_2 eq	3.559	4.496	4.303
Freshwater eutrophication	kg P eq	0.209	0.238	0.196

Marine eutrophication	kg N eq	0.129	0.142	0.170
Terrestrial ecotoxicity	kg 1,4-DCB eq	1845.241	2034.485	1305.870
Freshwater ecotoxicity	kg 1,4-DCB eq	44.770	48.630	34.120
Marine ecotoxicity	kg 1,4-DCB eq	65.678	71.276	49.609
Human carcinogenic toxicity	kg 1,4-DCB eq	2253.452	2407.649	1575.415
Human non-carcinogenic toxicity	kg 1,4-DCB eq	572.685	627.663	431.867
Land use	m^2a crop eq	24.357	24.969	12.137
Mineral resource scarcity	kg Cu eq	3.232	3.474	2.276
Fossil resource scarcity	kg oil eq	277.522	360.124	304.754
Water consumption	m^3	10.229	12.125	9.283

3.1.2 1 kg crush leather as functional unit

When 1 kg crust leather is used as the functional unit, we find that crush leather B has less damage in all impact categories than A because of its higher leather yield. It's interested that A and C both occupies half the first place in the eighteen impact categories. Hence, we reorganize the comparison result between the three crush leather and divide into figure 2 and 3. Because the unit of different impact categories is different, we convert the Y-axis to a percentage, with the highest degree of damage in each impact category being 100%.

Figure 2 shows the characterization result of the LCA study of crust leather A, B and C by ReCiPe2016 which includes only the impact categories of C bigger than A. For climate change, the electricity, chromium powder and resin used in leather-making process are major contributors (data are not showed). According to Table 1 and the C1 column in Figure 2, it is found that the consumption of electricity in beamhouse and tanning section and the resin in retanning section of crush leather C are greater than that of A and B, so the carbon emission are greater than A and B. The reason why the retanning section of A and B contribute more to carbon emission than the other two sections is that the consumption of electricity and resin is bigger. The maximum amount of ionizing radiation generated by crust leather C during the entire leather-making process is attributed to the large amount of water consumed, and the largest water consumption in the beamhouse section accounts for the largest proportion of ionizing radiation. Why the tanning section of A and B cause most of the ionizing radiation is the excessive consumption of formic acid and water. Excessive concentrations of ozone in the air can not only directly invade the human respiratory system, but even damage the nervous and reproductive system. The electricity, resin coating and surfactants consumed in leather-making process are the major contributors to ozone pollution. Ozone formation can also cause damage to terrestrial ecosystems, and the reasons and consequences of damage to human health and terrestrial ecosystems during the production of crust are roughly the same. For fine particulate matter formation, the electricity consumption contribution rate are 22.3%(A), 19.5%(B) and 36.5%(C), respectively. Other major contributors include chromium powder, resin, surfactants and sodium sulfide. When 1 kg of crust leather A, B and C were obtained, 1.85E-2, 1.50E-2 and 2.46E-2 kg SO_2 equivalents are respectively emitted, thereby causing damage to terrestrial acidification. For freshwater eutrophication, the production of chromium powder and electricity is the main factor that causes damage to it. The contribution rates of chromium powder for A, B and C were 16.2%, 15.3% and 11.8%, and the electricity were 12.1%, 12.6% and 26.8%, respectively. Since a certain amount of ammonia nitrogen compounds still exist after the wastewater treatment, which aggravate the marine eutrophication. The large water consumption of crust leather C in beamhouse section resulted in a large amount of wastewater, which led to the contribution of this section to marine eutrophication was greater than that of other sections. The use of electricity, resins and surfactants in leather-making process will accelerate the scarcity of fossil resource.Production of 1 kg crust leather A, B and C are equivalent to oil consumption of 1.45, 1.20 and 1.74 kg for fossil resource scarcity, respectively.The causes and results of marine ecotoxicity are roughly the same as freshwater ecotoxicity.

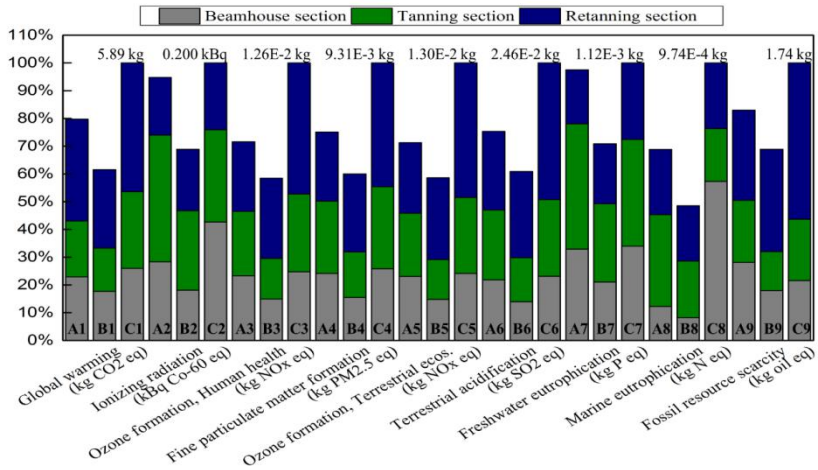

Figure 2. Characterization result of 1 kg crush leather by ReCiPe2016 (Impact categories included: C>A).

The second part of the characterization result of the LCA study of crust leather is shown in Figure 3, which includes only the impact categories of A bigger than C. For SO depletion, the production of crust seems to have less impact on it. The result of A is greater than C mainly due to the excessive demand for formic acid during pickling process. From the results of the human toxicity and ecotoxicity categories in Figure 3, it can be seen that the tanning section causes more damage in all this category than the other two sections. For terrestrial ecotoxicity of A, it is mainly originated from the chromium powder consumed in tanning section and the surfactant and sodium sulfide consumed in beamhouse section. The freshwater ecotoxicity produced by 1 kg crush leather A, B and C in leather-making process is equivalent to 0.233, 0.162 and 0.195 kg 1,4-DCB, respectively. And the contribution of chromium powder used in tanning and retanning processes to this impact category is between 60.0% to 67.4%. It is suggested from the result that the consumption of chromium powder seems to cause the greatest damage to human carcinogenic toxicity, and its contribution rate exceeds 96% in all three crusts. The production of chromium powder, electricity, sodium sulfide and surfactants can also cause non-carcinogenic toxicity to human. It can be concluded from the result that obtaining 1kg crust leather A, B and C need to occupy crop land 0.127, 0.0832, and 0.0694 m^2/year, respectively.For mineral resource scarcity, the consumption of chromium powder contributes the most, and its contribution rate is around 50% in all crust leather. Figure 3 suggested that the water consumption of A and C was similar.

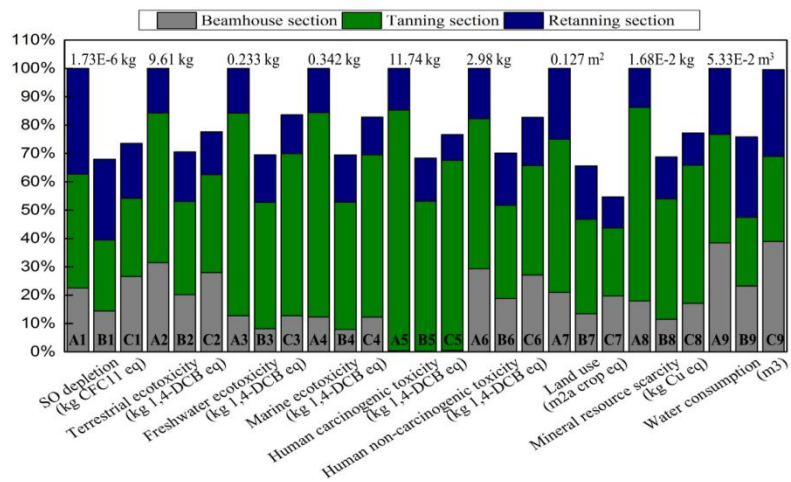

Figure 3. Characterization result of 1 kg crush leather by ReCiPe2016 (Impact categories included: A>C).

3.2 Characterization by CML-IA baseline (version 3.05)

3.2.1 1000 kg raw hide as functional unit

The characterization result of 1000 kg raw hide by CML-IA baseline is listed in Table 3. 1000 kg raw hide B has more impact on all impact categories than A and C, the same as the result by ReCiPe2016.Abiotic depletion is similar with resource scarcity in ReCiPe2016, but their characterization models and units are different, so it is difficult to compare them. This impact category indicator is related to extraction of minerals and fossil fuels due to inputs in the system. The abiotic depletion of fossil fuels is related to the low calorific value (LHV) expressed in MJ per kilogram of fossil fuel. For global warming, its result was close to the first method, but the result of global warming by ReCiPe2016 is slightly bigger than CML-IA because climate-carbon feedbacks are included for non-CO_2 GHGs in the Hierarchist perspective. For ozone layer depletion and SO depletion, they all use characterization model and unit developed by World Meteorological Organization, but their results have slightly different due to the different time span. It can be seem from the results of the human toxicity categories and ecotoxicity in Table 2 and Table 3 are quite different, and the difference may be originate from the version of characterization model, the conditions of use, the time span etc.Photochemical oxidation and Ozone formation both can be used to evaluate ozone pollution, but their characterization model and unit are different. Although the two methods adopt different characterization model, acidification and terrestrial acidification can expressed in same unit and their results are roughly similar. The three kinds of crust leather have roughly the same degree of impact on eutrophication.

Table 3. Characterization of 1000 kg raw hide in leather-making process by CML-IA baseline

Impact category	Unit	Raw hide A	Raw hide B	Raw hide C
Abiotic depletion (elements)	kg Sb eq	9.995E-3	1.075E-2	7.156E-3
Abiotic depletion (fossil fuels)	MJ	11879.970	15393.645	13046.325
Global warming (GWP100a)	kg CO_2 eq	851.590	1059.578	1000.619
Ozone layer depletion (ODP)	kg CFC11 eq	6.397E-5	7.569E-5	6.220E-5
Human toxicity	kg 1,4-DCB eq	374.308	425.152	324.822
Fresh water aquatic ecotox.	kg 1,4-DCB eq	292.285	330.220	270.840
Marine aquatic ecotoxicity	kg 1,4-DCB eq	943060.156	1095314.774	1040858.570
Terrestrial ecotoxicity	kg 1,4-DCB eq	1.906	2.016	1.519
Photochemical oxidation	kg C_2H_4 eq	0.213	0.273	0.240
Acidification	kg SO_2 eq	4.212	5.339	5.207
Eutrophication	kg PO_4^{3-} eq	1.138	1.308	1.202

3.2.2 1 kg crush leather as functional unit

When 1 kg crust was used as functional unit, the impact result of B is the smallest, and the most of the impact categories of C is bigger than A (besides abiotic depletion of elements, human toxicity and terrestrial ecotoxicity). Figure 4 shows the characterization result of the LCA study of crust leather A, B and C by CML-IA which includes only the impact categories of C bigger than A. For abiotic depletion of fossil fuels, the proportion of retanning section is the largest in its result which originated from the use of resin. The impact indicator of A, B and C can expressed as 4.44, 3.53 and 5.72 kg CO_2 equivalents for global warming, respectively. The cause of climate change is similar to the assessment by ReCiPe2016 method. For ozone layer depletion, formic acid, sodium hydrosulfide, and sodium formate are the main chemicals that cause damage to it. The results of Fresh water aquatic ecotoxicity of A and C are very close, and the use of chromium powder and electricity accounts for the largest contribution.For marine aquatic ecotoxicity, the result shows considerable and the consumed electricity become the largest contributor. The contribution of electricity of A and B is about 25.0%, while C is 46.7%. The reason for the considerable result may be originated from that the consumed Chinese electricity of medium voltage is not quite suitable for the European assessment method. The impact indicator of A, B and C can expressed as 1.11E-3, 0.91E-3

and 1.37E-3 kg C_2H_4 equivalents for photochemical oxidation, respectively. Acidification comes mainly from the consumption of electricity, chromium powder and resin. The impact indicator of A, B and C can expressed as 5.93E-3, 4.36E-3 and 6.87E-3 kg PO_4^{3-} equivalents for eutrophication, respectively.

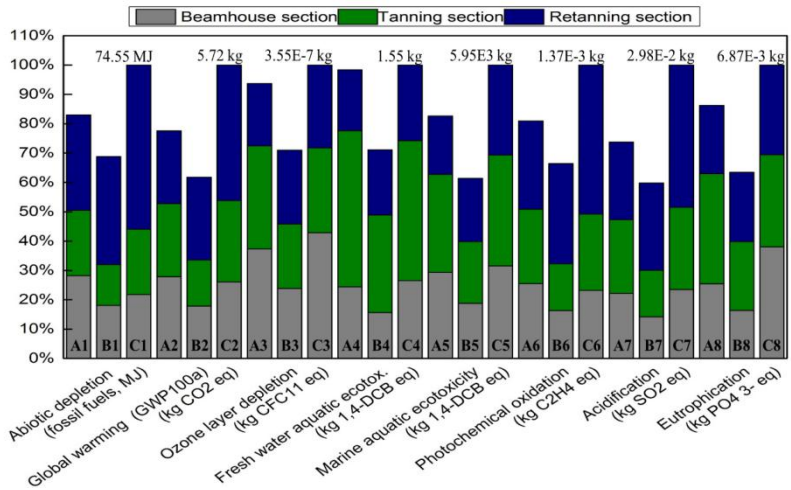

Figure 4. Characterization result of 1 kg crush leather by CML-IA (Impact categories included: C>A).

The second part of the characterization result of crust leather by CML-IA is shown in Figure 5. It can be seen from Figure 5 that tanning section is the main contribution for abiotic depletion of elements, and the used chromium powder is the main contributor. The impact result of A, B and C can equivalent to 1.95, 1.42 and 1.86 kg 1,4-DCB for human toxicity, respectively. For terrestrial ecotoxicity, the used electricity, surfactants and water have the major impact on it.

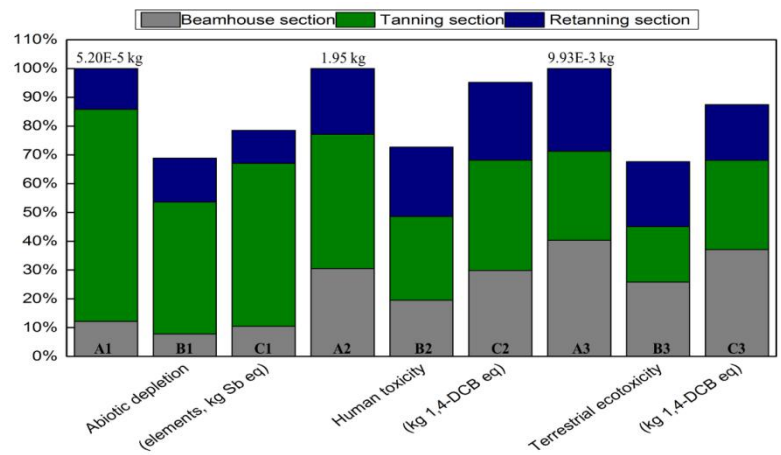

Figure 5. Characterization result of 1 kg crush leather by CML-IA (Impact categories included: A>C).

4. Conclusions

The environmental impact of cattle raw hide A, B and C from different sources in leather-making process was characterized by two different impact assessment methods ReCiPe2016 and CML-IA. When 1000 kg raw hide was used as functional unit, although the processing of raw hide A and B is roughly the same, the characterization results of raw hide B in all impact categories are greater than A, mainly due to the excessive consumption of chemicals in the leather-making process. All impact indicators of raw hide B are bigger than C except for marine eutrophication because raw hide C consumed a large amount of water during the soaking process and produced more wastewater. Results presented within this study suggested that reducing the consumption of electricity, water and chemicals during leather-making process is a key to reduce environmental impact.

When 1 kg crust leather was used as functional unit, the characterization results of crust leather B in all impact categories are

smaller than A due to the high leather yield of B. With ReCiPe2016, crush leather A has 9 impact categories results bigger than C including all human toxicity and ecotoxicity which derived from the consumption of more chromium powder by A during the tanning process. In order to reduce environmental impact of the production of crush leather, tanners should attach importance to how to improve the yield of leather and improve the economic value of by-products. Besides electricity and water, the used chemicals such as chromium powder, resins, surfactants, sodium sulfide, and formic acid are major contributors to damage to human and environment. By comparing the characterization results of analogue impact categories in the two assessment methods, it can be found that some results are very close, but there are also significant gap in results.

The development of a leather-making process that saves water and electricity, and the exploitation for cleaner and more sustainable clean materials has become imminent. During the exploration process, LCA study will help to compare different processes and raw materials through inventory analysis and impact assessment. At the same time, the establishment of life cycle database of leather chemicals needs to be put on the agenda as soon as possible, which can be beneficial for LCA research.

Reference

Kılıç, E; Puig R; Zengin, G; et al. Corporate carbon footprint for country Climate Change mitigation: A case study of a tannery in Turkey. *Sci. Total Environ.***635**, 60-69, 2018.

Chen, P. Life cycle assessment in cattlehide tannery. Shaanxi University of Science & Technology, 2009.

Rivela, B; Moreira, M. T; Bornhardt, C; et al. Life cycle assessment as a tool for the environmental improvement of the tannery industry in developing countries. *Environ. Sci. Technol.***38**(6), 1901–1909, 2004.

Joseph, K; N. Nithya. Material flows in the life cycle of leather. *J Clean. Prod.***17**(7), 676–682, 2009.

Chowdhury, ZUM; Ahmed, T; Hashem, MA. Materials and energy flow in the life cycle of leather: a case study of Bangladesh. *Matériaux & Techniques***105**(5-6), 502, 2018.

Notarnicola, B; Rita, P; Andrea, R; et al. Life cycle assessment of Italian and Spanish bovine leather production systems. *Afinidad***68**(553), 167–180, 2011.

Bach, V; Finkbeiner, M. Approach to qualify decision support maturity of new versus established impact assessment methods—demonstrated for the categories acidification and eutrophication. *Int. J. Life Cycle Assess.***22**(3), 1-11, 2016.

Huijbregts, MAJ; Steinmann, ZJN; Elshout, PMF; et al. ReCiPe2016: a harmonised life cycle impact assessment method at midpoint and endpoint level. *Int. J. Life Cycle Assess.***22**(2), 1-10, 2017.

Souza, HHDS; Ângela, MFL; Esquerre, KO; et al. Life cycle assessment of the environmental influence of wooden and concrete utility poles based on service lifetime. *Int. J. Life Cycle Assess.***22**, 2030–2041, 2017.

Wu, HD. Wastewater treatment technology and engineering example of tannery industry. Beijing: Chemical Industry Press, 2010.

Wang, SB; Zhang, WQ; Yang, TX; et al. Characterization factor and its changes of abiotic resources depletion in LCA. *J Fudan University (Nature Science)***51**(1), 125-130, 2012.

Sampaio, APC; Men, SMSF; Castro, ALA; et al. Life cycle assessment from early development stages: the case of gelatin extracted from tilapia residues. *Int. J. Life Cycle Assess.***22**(5), 1-17, 2016.

P25

Fibering and Papermaking Technology of Finished Leather Cutting Waste

Shengdong Mu[1,2], Li Zhang[1,2], Qiangjun Ling[1,2], Yanru Long[1], Xiong Liu[1,2], Yue Liu[1,2], Guirong Qiu[1], Fangfei Liu[1,2], Haibin Gu[1,2,]*

[1]Key Laboratory of Leather Chemistry and Engineering of Ministry of Education, Sichuan University, Chengdu 610065, China.

[2]National Engineering Laboratory for Clean Technology of Leather Manufacture, Sichuan University, Chengdu 610065, China.

[*]Corresponding author: Haibin Gu, E-mail address: guhaibinkong@126.com

Abstract:

The cutting waste of finished leather, a special kind of leather solid waste, was fully fibered by a pretreatment process and pulping followed, and the obtained leather fibers were then mixed with a certain proportion of paper pulp to prepare leather-paper composite cardboard.Firstly, the fibrous dispersion degree was used as the index to optimize the pretreatment procedure for the finished leather waste, and the optimum fibrosis condition is as follows: temperature of 50-55 °C, acid dosage of 5 %, stirring speed of 1000 r min^{-1} and reaction time of 1 h. Then,by using talcum powder, polyacrylamide and rosin as additives, the papermaking process was then investigated, and theproperties of the obtained cardboards were well characterized by the automatic tensile testing machine, scanning electron microscope (SEM), thermogravimetric analysis (TG) and differential scanning calorimeter (DSC). Results show that, compared to the cardboard prepared by only leather fibers, the composite leather-paper cardboard exhibited much better mechanical properties, namely, the better weaving situation, higher thermal stability and transformation temperature. Based on these results, a feasible procedure of fibering and papermaking was established in this paper for the re-utilization of the cutting waste of finished leather, and the composite board prepared can be used as potential raw material for the manufacture of consumer goods such as light handbags and shoe boxes.

Keywords: Finished leather waste; fibering; papermaking; cardboard; thermal-mechanical properties

1. Introduction

The recycling of solid leather waste is one of the key problems that must be solved for the sustainable development of leather industry, and also a major focus of chemists and technologists of leather. According to its source and composition, the solid waste of leather industry can be broadly divided into four parts, namely, (1) solid leather waste without chromium, including raw material skins and limed hide wastes; (2) solid leather waste containing chromium such as chrome shavings; (3) solid leather waste contain dyes such as cutting and trimming of crust leather and grinding ash etc. (4) finished leather waste from the cutting and trimming of finished leather and waste leather products (leather garbage) etc.[1-4]

As a special kind of leather solid waste, finished leather waste is very difficult to be adequately re-used because of its complex composition such as chromium salts, dyes, fatliquor, retanning agents, polyurethane resins, and acrylic resin etc.[5] Currently, the methods of incineration or landfill were applied to dispose finished leather waste,[6]but this is obviously not a long-term solution and requires a lot of processing costs. At the same time finished leather waste containing a variety of harmful substances may cause serious pollution to the environment and affect the human condition. Therefore, it is significant to study the recycling and utilization of finished leather waste.

Although collagen and chromium are main and valuable components of finished leather waste, it is infeasible to separate and recycle them through chemical or biological treatments that are difficult to be achieved in technology and easily produce secondary pollution.[6] Therefore, mechanical methods or chemical-mechanical methods could be the feasible research directions to deal with finished leather waste.[7-18] For example, Senthil et al.[9] have reported a novel method of prepare regenerated leather composites based on fiberized leather waste and plant fibers (coconut, sugarcane, banana and corn silk etc.) and the obtained composites possessed fairly good mechanical properties, high specific strength, non-abrasive,

eco-friendly and bio-degradability characteristics. And these composites are probably used to prepare leather goods and footwear materials in addition to their cost-effectiveness and environmental pollution abatement.[9]Teklay et al.[10] described value-added composite boards fabricated by finished leather waste and various plant fibers (jute, hibiscus, sisal, palm and enset) as raw materials andnatural rubber latex as adhesive in Ethiopia. The final products may be used as raw material for the preparation of consumer products such as insoles, chapel-uppers, wallets, light hand bags, mouse pads, roofing, wall partitioning, and components of furniture.[10]Ruiz et al.[12] prepared a new and innovative composite material based on vulcanized natural rubber, carbon black, and leather solid waste by thermal compression method, and the composite material has potential to be applied as an antistatic flooring.

In addition, based on the good compatibility of collagen fibers and plant fibers, the finished leather waste (mainly chrome shavings) used as raw material for paper making has been the topic research direction of scientists and technicians in leather and papermaking fields.[19-37] In order to further develop the method for the recycling and utilization of finished leather waste, in this work, the cutting waste of finished leather was fully fibered by a chemical-mechanical pretreatment process and the obtained leather fibers were then mixed with a certain proportion of paper pulp to prepare leather-paper composite cardboard. The physicochemical properties of composite cardboard were well characterized by universal testing machine, SEM, TG and DSC, etc.

2. Experimental

2.1. Materials

The finished leather cutting waste was obtained from Red Dragonfly. Paper pulp was prepared by waste paper of A4 with the help the pulverizing machine. Talcum powder, polyacrylamide, rosinsulfuric acid (H_2SO_4), potassium permanganate ($KMnO_4$) and sodium thiosulfate ($Na_2S_2O_3$)were purchased from Energy Chemical and used directly. All the other chemicals used were analytic grade, commercially purchased and used as received.

2.2. Instruments

UV-visible absorption spectra were measured with a Perkin-Elmer Lambda 19 UV-visible spectrometer. Scanning electron microscopy (SEM) observations were conducted with a SM-7500F field emission SEM instrument (JEOL). TG/DTG analyses were performed with a TGA/DSC Mettler Toledo (Switzerland), in nitrogen flow (99.99 %; 50 ml min^{-1}), 30-800 °C, at a rate of 10 °C min^{-1}. DSC measurement of the sample (1-3 mg) was performed in a sealed aluminum pan with nitrogen flow (99.99 %; 50 mL min^{-1}), at 30-250 °C with a rate of 10 °C min^{-1} using a DSC 1/700 Mettler Toledo (Switzerland). Composite cardboards were tested for tensile properties using the Al-7000 SN Universal Testing Machine under a gauge length of 10 mm at a strain rate of 30 mm min^{-1}. Chemical oxygen demand (COD) was measured with a 5B-1mould quick determining instrument.

2.3. Preparation of leather fiber

The cutting waste of finished leather (50 g) was added into water (500 ml), followed by the dropwise addition of acid solution (5-10 %). The reaction mixture was stirred for 1-2 h at 30-80 °C at the speed of 300-1500 r min^{-1}. The obtained mixture was then converted into leather fiber with the help of a pulverizing machine and the generated leather fiber was separated by filtration, and the leather fiber and wastewater were collected for further experiments.

2.4. Preparation of leather-paper composite cardboard

The leather fibers were mixed with a certain proportion of paper pulp in Juicer with 500 ml water. A certain amount additive (talcum powder, polyacrylamide or rosin) was added into the obtained reaction mixture and were stirred for 1 min. The prepared paste was then poured into Pattern shaper of paper (ZT7-Φ200, china) to prepare wet cardboard and next pressed, using both carpet and steel plate to make leveling, and covered by another both carpet and steel plate, by hydraulic press (ZQYCⅡ,China) at a pressure of 5 Mpa for 1 min. The pressed sheet was dried in vacuum dryer for 10 min at 70 °C under the vacuum of 0.06 Mpa.

2.5. Chemical analysis of finished leather cutting waste

The content of Cr^{6+}, Cr_2O_3, water and its volatiles of finished leathercutting waste were detected by Diphenylcarbazide spectrophotometric method, potassium chlorate method and gravimetric method, respectively. [38]

2.6. Observation of leather fibers

The dispersion of leather fibers were measured by an optical microscope (SZX12, Japan).

2.7. Wastewater analysis

The content of Cr^{6+}, total chromium, suspended substance and COD of waste water were detected by Diphenylcarbazide spectrophotometric method,[39]potassium permanganate- Diphenylcarbazide spectrophotometric method,[40] gravimetric method[41] and 5B-1 mould quick determining instrument, respectively.

2.8. Characterization of cardboard

Composition analysis of paperboard is similar to the finished leathercutting waste. The physicochemical properties of composite cardboard were characterized by Universal Testing Machine, SEM, TG and DSC, respectively.

3. Results and discussion

3.1. Analysis of finished leathercutting waste

Tab. 1 Chemical compositions of finished leather cutting waste

Parameters	Cr^{6+} (mg kg^{-1})	Cr_2O_3 (%)	H_2O and volatiles (%)
Content	1.89	3.3	12.12

As shown in Table 1, the finished leather cutting waste was analyzed to obtain information about Cr^{6+}, Cr_2O_3 and water and other volatiles, and the corresponding contents are 1.89 mg l^{-1}, 3.3 % and 12.12 %, respectively.Obviously, the value of Cr^{6+} is lower than the Cr^{6+} limit of 5 mg l^{-1} and 10 mg l^{-1} of national environmental protection standards of the people's republic of china HJ 507-2009 (Technical requirement for environmental labeling products Leather and synthetic leather) and HJ/T 305-2006 (The Technical requirement for environmental labeling products–footwears), respectively. The value of Cr_2O_3 is between 3 % and 5 %, and thus conforms to the requirement of chrome content in general finished leather.[38]

3.2. Optimization of fibering condition

In the process of fibering pre-experiment, the finished leather was fibered in the case of acid dosage of 5-10 % at the speed of 300-1500 r min^{-1} for 1-2 h, and then mechanical pulverization was conducted. Most of the obtained products are skin fibers, and we believe that the acid dosage, stirring speed and reaction time have little effect on the fibering treatment, while temperature is a key factor of fibrosis treatment. Therefore, under the condition of acid dosage of 5 %, stirring speed of 1000 r min^{-1} and reaction time of 1 h, the fibrous dispersion degree was used as the index to optimize the pretreatment procedure for the finished leather waste.

Tab. 2 Dispersion of leather fibers under different temperatures

Temperatures (°C)	30	40	45	50	55	60	80
Fiber effect	bulk	bulk	bulk	fibers	fibers	solution	solution

As shown in Table 2, the finished leather cutting waste was fibered at 30-45 °C by chemical-mechanical treatment, and the products obtained were still the original cutting waste (Figure 1a).When the temperature was raised to 50-55°C, most of the obtained products are leather fibers (Figure 1b), and no cutting waste is observed. The leather fibers obtained were observed by an optical microscope at magnification of 10 and 20 times, respectively, and the results were shown in Figures 1c and 1d. In these pictures, the leather fibers were clearly seen and the average size ranges between 0.3-1.2 cm in length and 0.3-0.8 mm in width. So, the fibering treatment is successful at 50-55°C. With the further increase of temperature to 60-80 °C, the finished leather cutting waste was completely dissolved in the solution. Therefore, the temperature of 50-55°C was chosen as the best chemical treatment temperature for further experiment.

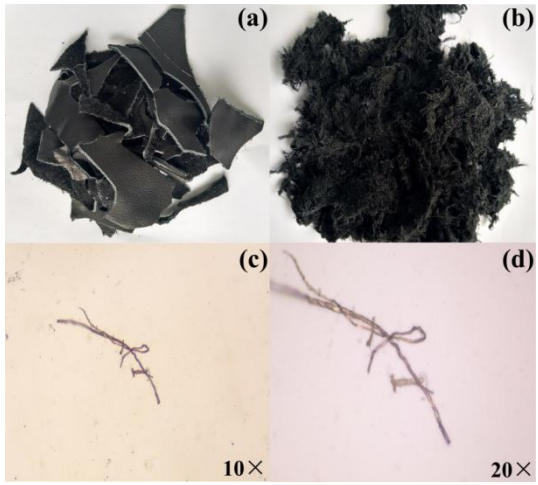

Fig. 1 Pictures of finished leather cutting waste (a) and leather fibers (b) and their micrographs (c, d).

In addition, the wastewater from the fibering treatment process was analyzed and the values of Cr^{6+}, total chromium, suspended solids and COD were 0.111 mg l^{-1}, 1.57 mg l^{-1}, 111 mg l^{-1} and 1480 mg l^{-1}, respectively (Table 3). These indexes of wastewater are far less than those of common tannery wastewater, and can be treated by conventional method used to treat tannery wastewater.

Tab. 3 Component analysis of wastewater

Indexes	Cr^{6+}	Total chromium	Suspended solids	COD
Content (mg l^{-1})	0.111	1.57	111	1480

3.3. Papermaking properties of leather fibers

As shown in Figure 2a, the pure leather cardboard, prepared by using only leather fibers, has a flat surface with the appearance of a common plant fiber sheet and shows the black color of its raw material. Figure 3a shows the SEM image of pure leather cardboard. In this picture, the distribution and intermingling of leather fiber was clearly seen. Compared to the pure vegetable fibers (Figure 3b), the diameter of the leather fiber is slightly smaller than, and exhibit round rope. In addition, the weight of pure leather sheet is slightly lighter than pure paperboard. However, compared to the paper, the pure leather board exhibit bad mechanical property. Its tensile strength was only 0.039 N/mm^2, and the leather board is easily torn apart by hand. Hence, it is infeasible to use the leather fiber alone as raw material for the manufacture of consumer goods such as light handbags and shoe boxes.

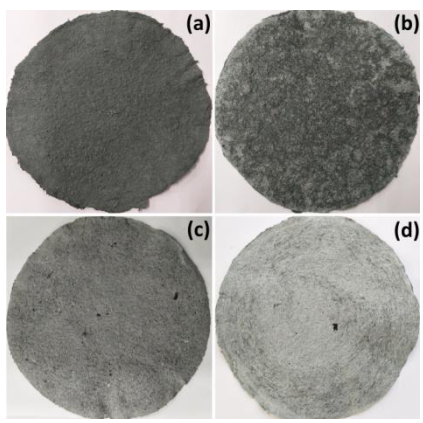

Fig. 2 Photos of cardboards fabricated at the feed molar ratios of leather pulp to vegetable pulp of 1:0 (a), 3:2 (b), 1:1 (c) and 2:3 (d)

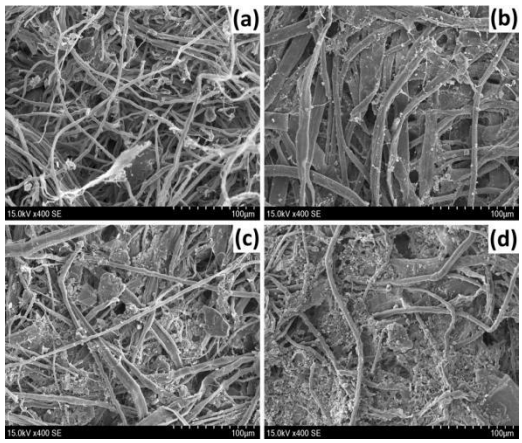

Fig. 3 SEM images of cardboard with different treatment methods. (a) pure leather board; (b) pure paper board; (c) composite cardboard containing fillers; (d) composite cardboard aftersizing treatment.

Tab. 5 Tensile strength of cardboards with different treatment methods (N/mm^2)

Treatment Methods	leather:paper=1:0	leather:paper =3:2	leather:paper =1:1	leather:paper =2:3
No	0.039	0.310	0.368	0.741
Fillers	0.053	0.284	0.345	0.731
Internal sizing	0.121	0.334	0.899	1.170
External sizing	0.684	1.286	1.375	1.673

In order to improve the tensile strength of the "leather board", the obtained leather fiber was mixed in different proportions with the plant fiber (paper fiber) recovered from the A4 waste paper, and the obtained cardboards are shown in Figures 2b-2d. With the increasing of paper fiber, the color of cardboard becomes lighter and the smoothness of paperboard was gradually increased. When the blending ratio of leather fiber and paper fiber is changed from 3:2 to 1:1 and 2:3, the tensile strength of cardboard increases from 0.310 N/mm^2 to 0.368 N/mm^2 and 0.741 N/mm^2, respectively (Table 4). Namely, the tensile strength increase 7, 8 and 18 times, respectively, compared to that of "leather board". These results indicate that the tensile strength of the composite cardboard can be enhanced by the addition of paper pulp, as a result of the high concentration of lignin in the waste paper pulp.[42] Herein, considering the color, flatness, tensile strength and cost of the obtained cardboard, we selected the cardboard with the feed ratio of 1:1 were further investigated. Its tensile strength was further improved by adding reinforcing agent, and the obtained final product was well characterized in tensile strength, fiber interweaving, thermal stability and chemical composition.

3.4. Mechanical properties of cardboard

In this paper, talcum powder, polyacrylamide and rosin were used in the process of paper-making as filler and sizing agent, respectively.

As shown in Table 4, the tensile strength of cardboard was easily influenced by different additives. Cardboard after external sizing treatment exhibited better tensile strength, whereas the addition of filler has no obvious effect on the tensile strength of the cardboard when compared to the control board of pure leather board. Concretely, the tensile strength of the pure leather board treated by external sizing reaches 0.684N/mm^2, which is close to the tensile strength value, 0.741 N/mm^2, of cardboard prepared by a mixture of leather fibers and paper fibers at 3:2. The increase in the tensile strength of the cardboard treated by the sizing agent is probably taken into account by the fact that the rosin of saponification as thickening resin increases the adhesion between the fibers and improves the composite strength of fibers, thereby causing an increase in the tensile strength of the cardboard. Based on the above results, the cardboards treated by surface sizing of rosin can be used as potential raw material for the manufacture of higher strength goods such as light handbags, shoe boxes and so on.

3.5. SEM of cardboard

As shown in Figures 2c and 2d, with the addition of fillers and sizing agent, the distribution of leather fibers and paper fibers was still clearly and orderly visible, and the diameter of paper fibers was slightly wider than that of leather fibers. At the same time, the fibers along with the fillers or adhesive are seen and the binding degree increases, which indicates the excellent compatibility between leather and paper fibers. And this is also the reason for the increase in the tensile strength of cardboard.

3.6. Thermal analyses of cardboard

In order to investigate the effect of different additives on the thermal stability of cardboard, DSC and TG were recorded as shown in Figure 4and Figure 5.

The DSC curve of control pure leather board provides the glass transition temperature (T_g) of 79.74 ºC and enthalpy changes (△H) of 226.03 J g^{-1}, respectively (Figure 4a). Compared to the control sample, the cardboards treated by fillers and sizing agent indicate higher values of T_g and △H, but show similar transitions characteristic. Concretely, the T_g of the cardboard treated by fillers increases by 4.63 °C to 84.37 °C and its △H increases by 23.69 J g^{-1} to 249.72 J g^{-1}(Figure 5b). The T_g of the cardboard treated by internal sizing agent increases by 9.18 °C to 88.92 °C and its △H increases by 37.34 J g^{-1} to 263.37 J g^{-1} (Figure 5c). The T_g of the cardboard treated by external sizing agent increases by 13.09 °C to 92.83 °C and its △H increases by 47.43 J g^{-1} to 273.46 J g^{-1}(Figure 5d). The results of DSC indicate that the fiber interlacing degree can be highly promoted by the treatment of filler and sizing agent, thereby the improved thermal stability is observed. Moreover, the sizing treatment, especially the rosin surface sizing treatment, is more effective.

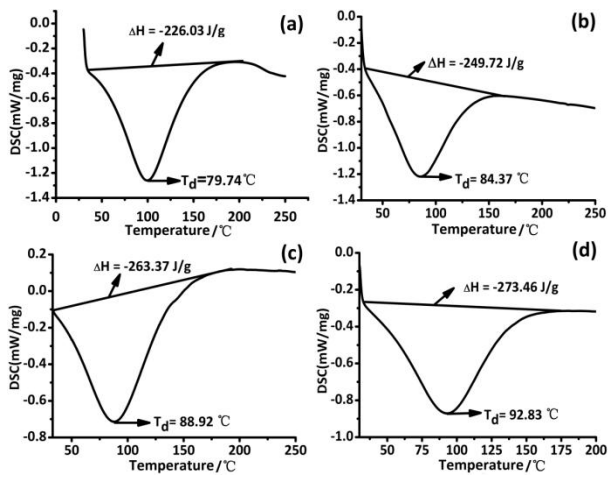

Fig. 4 DSC curves of cardboards with different treatment methods (a: pure leather board; b: filler; c: internal sizing; d: external sizing)

The TG analysis reveals the weight loss of cardboard with the increase in temperature and further indicates thermal stability of paperboard. As shown in Figure 5, the control cardboard (Figure 5a) and composite boards were subjected to TGA from 50 to 800 °C, and a three-step weight loss was observed in the cardboards that were treated with fillers and sizing agent. The first weight loss occurs up to 150 °C, which is due to the loss of water molecules and other volatile substances with small molecular weights in the paperboard. The second loss occurs between 150-600 °C and this weight loss is attributed to the collagen degradation and carbonization process. The last loss occurs above 600 °C, and this may be due to the continued loss of partial organic matter in carbon residue.

The control sample (Figure 5a) has the decomposition temperature of 321.31 °C, and for the cardboards treated with fillers, this temperature is 358.73 °C, and 356.31 and 379.48 °C are observed for the cardboards treated with sizing agent. Obviously, the thermal stability of cardboard is improved by the treatment of fillers and sizing agent. This point was in

agreement with the results of DSC. However, a residue of 31.38 % was observed in Figure 5b. This may be due to the melting point of talcum powder as high as 800 °C, which is not easy to be decomposed. Hence, the results of TG further demonstrate that the existence of fillers or sizing agent can promote fiber intermingling of leather fiber along with paper fiber and improve the thermal stability of cardboard. Obviously, the rosin surface sizing is the most effective.

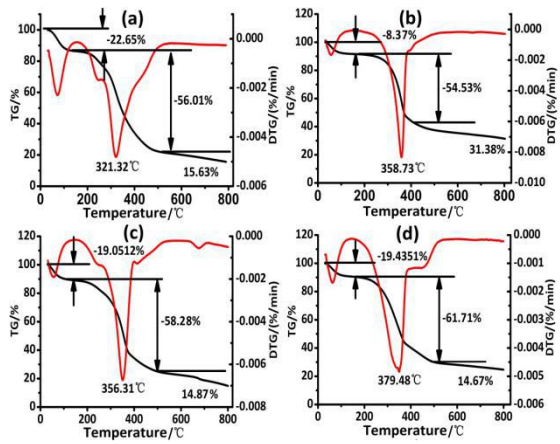

Fig. 5 TG curves of cardboard with different treatment methods (a: pure leather board; b fillers; c: internal sizing; d: external sizing)

3.7. Chromium content of cardboard

Because the raw material of cardboards is finished leather cutting waste, the chromium contents of the fabricated cardboards by different treatment methods are analyzed. As shown in Table 5, the content of Cr^{6+} in cardboards treated with fillers and sizing agent were 2.29, 2.02 and 2.14 mg kg^{-1}, respectively. Compared to the Cr^{6+} content of finished leather cutting waste, the valued of Cr^{6+} in cardboard generally increases, which may be due to the unstable Cr^{3+} be oxidized to Cr^{6+} at 70°C in the drying process. However, the value of Cr^{6+} in cardboard conforms to the requirement of national environmental protection standards of the people's republic of China HJ 507-2009 and HJ/T 305-2006.

Tab. 5 Chromium compositions of cardboard

	Fillers	Internal sizing	External sizing
Cr^{6+} (mg kg^{-1})	2.29	2.02	2.14
Cr_2O_3 (%)	1.0	1.2	0.9

The content of Cr_2O_3 in cardboards treated with fillers and sizing agent were 1.0 %, 1.2 % and 0.9 %, respectively. All the values were lower than that in the finished leather cutting waste, which is attributed to the addition of paper pulp that leads to the decreased proportion of leather fiber cardboard.

4. Conclusion

In conclusion, a feasible procedure of fibering and paper-making of finished leather cutting waste is successfully established in this work. Firstly, a method of combining chemical pretreatment with mechanical pulverization is used, and the optimum fibering condition as following: temperature of 50-55 °C, acid dosage of 5-10 %, stirring speed of 1000 r min^{-1} and reaction time of 4 h. The obtained leather fibers have good dispersion property. Then the leather fibers were mixed with a certain proportion of plant fiber (waste pulp) to prepare paperboard. By using talcum powder, polyacrylamide as fillers or rosin as sizing agent, the tensile strength, fiber structure and thermal stability of the obtained paperboard were studied. Results indicate that the cardboard with the optimum comprehensive property can be obtained at 1:1 feed ratio of leather fibers to waste pulp by using surface sizing of rosin.This work provides a feasible re-utilization method for the finished leather waste and the prepared paperboards could be used as potential raw material for the manufacture of consumer goods such as light

handbags, shoe boxes and non-woven fabrics.

Acknowledgements

Financial support from Science & Technology Department of Sichuan Province (No. 2018HH0038) is gratefully acknowledged.

References

Wang R, Xiang X, Huang B, Zhang, T K. Research progress of waste recycling in footwear industry[J]. China Leather, 2017, 46(4): 52-54.

Jiang H Y, Liu J S, Han W. The status and developments of leather solid waste treatment: A mini-review [J]. Waste Management & Research, 2016, 34(5): 399-408.

Luan J, Diao S, Chen P H, Wang Q J. The Review of leather wastes recycling[J]. Leather Science and Engineering, 2016, 26(5): 28-34.

Scopel B S, Baldasso C, Dettmer A, Santana R M C. Hydrolysis of chromium tanned leather waste: Turning waste into valuable materials - A Review [J]. Journal of the American Leather Chemists Association, 2018, 113(4): 122-129.

Rosu C, Popita G E, Manciula D, Popovici A, Corbu O, Cozma A. Tanned leather waste: A hazardous waste or not? [J]. Journal of Environmental Protection and Ecology, 2015, 16(3): 899-907.

Assamoi B, Lawryshyn Y. The environmental comparison of landfilling vs. incineration of MSW accounting for waste diversion[J]. Waste Management, 2012, 32(5): 1019-1030.

Han X M, Tang M M. Research Progresses on the Application of collage fiber in papermaking industry[J]. West Leather, 2014, 36(8): 29-31.

Zhang Y X, Yu S H, Shao H, Shao S X. Advances on the composites based on collagen fiber and polymers[J]. Leather Science and Engineering, 2013, 23(3): 36-39.

Senthil R, Hemalatha T, Kumar B S, Uma T S, Das B N, Sastry T P. Recycling of finished leather wastes: a novel approach [J]. Clean Technologies and Environmental Policy, 2015, 17(1): 187-197.

Teklay A, Gebeyehu G, Getachew T, Yaynshet T, Sastry T P. Preparation of value added composite boards using finished leather waste and plant fibers—a waste utilization effort in Ethiopia [J]. Clean Technologies and Environmental Policy, 2017, 19(5): 1285-1296.

Santos R J, Agostini D L S, Cabrera F C, Budemberg E R, Job A E. Recycling leather waste: Preparing and studying on the microstructure, mechanical, and rheological properties of leather waste/rubber composite [J]. Polymer Composites, 2015, 36(12): 2275-2281.

Ruiz M R, Budemberg E R, da Cunha G P, Bellucci F S, da Cunha H N, Job A E. An innovative material based on natural rubber and leather tannery waste to be applied as antistatic flooring [J]. Journal of Applied Polymer Science, 2015, 132(3): 41297.

Senthil R, Inbasekaran S, Gobi N, Das B N, Sastry T P. Utilisation of finished leather wastes for the production of blended fabrics [J]. Clean Technologies and Environmental Policy, 2015, 17(6): 1535-1546.

Cardona N, Velasquez S, Giraldo D. Characterization of Leather Wastes from Chrome Tanning and its Effect as Filler on the Rheometric Properties of Natural Rubber Compounds [J]. Journal of Polymers and the Environment, 2017, 25(4): 1190-1197.

Sivaprakash K, Maharaja P, Pavithra S, Boopathy R, Sekaren G. Preparation of light weight constructional materials from chrome containing buffing dust solid waste generated in leather industry [J]. Journal of Material Cycles and Waste Management, 2017, 19(2): 928-938.

Sheng X Y, Chen Z R, Liao X P. Synthesis of Carbon Nanofiber Bundle Using Chrome Shavings as Templates and Investigations to their Properties as Anode Materials of Lithium Ion Batteries[J]. Leather Science and Engineering, 2017,

27(2):16-21.

Konikkara N, Kennedy L J. Electrochemical properties of solid leather wastes based supercapacitor electrodes using H_2SO_4 electrolyte [J]. Materials Letters, 2017, 205: 56-61.

Onukak I E, Mohammed-Dabo I A, Ameh A O, Okoduwa S I R, Fasanya O O. Production and characterization of biomass Briquettes from tannery solid waste [J]. Recycling, 2017, 2(4): 17.

Tan Y, Qiu H Y, Ren J. The isolation of collagen fiber and its effects on pulp and paper[J]. China Leather, 2005, 34(5): 48-52.

Zhang M Y, Liu L. Application of collage Fiber on Papermaking[J]. Paper and Paper Making, 2005, 24(6) :70-72.

Fu L H, Zhang M R. The prospect of composite material from regenerate cellulose and collagen[J]. China Leather, 2001, 30(7); 15-17.

Dang Y H, Li H K, Hu X B, Zhang P N. The application of leather shavings in the production of high porosity shading paper[J]. China Pulp & Paper Industry, 2012, 33(18): 18-21.

Bufalo G, Florio C, Cinelli G, Lopez F, Cuomo F, Ambrosone L. Principles of minimal wrecking and maximum separation of solid waste to innovate tanning industries and reduce their environmental impact: The case of paperboard manufacture [J]. Journal of Cleaner Production, 2018, 174: 324-332.

Wang Q, Zhang S F, Wang X C, Qiang T T. Synthesis of sizing agent with collagen from leather waste[J]. China Pulp & Paper Industry, 2015, 36(2): 50-54.

Wang X L, Wang Z J. Manufacture of Corrugating medium with Paper Mill Sludge and Leather Waste as Raw Material[J]. China Pulp & Paper, 2011, 30(11): 22-25.

Dai D S, Chen X R, Huang B, Chen L. Development of High porosity fruit cultivating bag paper with leather waste[J]. China Pulp & Paper, 2008, 27(1): 17-20.

Peng L X, Wang Z J. Tannery solid waste resource oriented disposal and application in paper making industry[J]. China Leather, 2007, 36(13): 60-63.

Peng L X, Wang Z J. Preparation of collagen and its application in papermaking industry[J]. China Leather, 2007, 36(5): 49-51.

Liu Z W, Zhang M Y, Sun L H. Research on the pulping property of chrome shavings[J]. West Leather, 2007, 29(12): 31-35.

Tan Y, Qiu H Y, Wu S B. Modified leather waste used as strength agent in paper making[J]. Paper and Paper Making, 2007, 26(3): 45-48.

Sun Y C, Zhao C S, Zhang K. Structure and performance of animal and plant fiber mixed paper[J]. China Leather, 2007, 36(17): 33-35, 47.

Li J, Chen G, Wu Z G, Lu Y. Study on preparation of collagen fiber from the leather waste and its sheet characteristics[J], Leather Science and Engineering, 2006, 16(4): 18-23.

Wang Z J, Peng L X. Extracting of collagen and the physical performance of paper mixed with collagen[J]. Paper and Paper Making, 2006, 25(5): 35-36.

Chi D M, Xu Y J, An J J. Study on the compatibility of waste scurf collagen fibers [J]. Southwest Pulp and Paper, 2004, 33(3): 15-18.

Wang Z J, Wang J, Zhang C B, Hou X D. Application of the solid waste of leather for pulp and paper–making[J]. Journal of Northwest University of Light Industry, 2002, 20(6): 28-31.

Fu L H, Zhang M R, Qi Y Q, Qiu H Y. Bonding Mechanism of collagen protein and cellulose fibers[J]. Transactions of China Pulp and Paper, 2002, 17(1): 68-71.

Fu L H, Qi Y Q. The study of the compound structure of collagenous fiber and plant fiber[J]. Leather Science and Engineering, 1999, 9(4): 13-17.

Luo X M, Ding S L, Zhou Q F. Leather and Fur Physical and Chemical Analysis[M]. BeiJing: China Light Industry Press, 2013.

GB 7467-87, Water Quality-Determination of chromium (VI) –Diphenylcarbohydrazid e - spectrophotometric method[S]. 1987.

GB 7466-87, Water Quality-Determination of total chromium[S]. 1987.

GB 11901-89, Water Quality-Determination of suspended substance-Gravimetric method[S]. 1989.

Sun J X, Sun X F, Zhao H, Sun R C. Isolation and characterization of cellulose from sugarcane bagasse[J]. Polymer Degradation and Stability, 2004, 84(2): 331-339.

P26

Controlling Translocation of Trivalent Chromium around Adsorbents with Light: One Step Closer to Sustainability

Xiaoyu Guan[a], Haojun Fan[a,b,*], Sunxian Yan[a]

[a] *Key Laboratory of Leather Chemistry and Engineering (Sichuan University), Ministry of Education, , Chengdu, 610065, P.R. China*

[b] *National Engineering Laboratory for Clean Technology of Leather Manufacture, Sichuan University, Chengdu, 610065, P.R. China*

** Corresponding author. Tel.: +86 28 85401068; fax: +86 28 85405237.*

E-mail address:fanhaojun@scu.edu.cn (H. Fan)

ABSTRACT: Escalating worldwide use of functional adsorbents in disposing trivalent chromium-contaminated water is considered to be an important advance. However, previous adsorbents have long been plagued by the necessity of using chemical desorbents, such as acid or alkaline substance, in regenerating the adsorbents. Here, we demonstrate that light-induced, reversible isomerization of surface-bound spiropyran can be exploited to regulate adsorption, and more importantly, desorption of trivalent chromium in water, avoiding the use of any chemical desorbent to restore the adsorption capacity of the exhausted adsorbents. According to these results, we aim to provide a solution to an otherwise ignored problem that compromises the environmental sustainability of adsorption technology in remediating trivalent chromium-contaminated water.

Keywords: Trivalent Chromium; Spiropyran; Regenerating; Environmental sustainability

P27

Investigation on the influence factors of enzyme mass transfer in bating process

JinZhi Song, XueSong Li, YanChun Li*

College of Leather Chemistry and Engineering, Qilu University of Technology (Shandong Academy of Sciences), No. 3501 Daxue Rd, Changqing District, 250353, Jinan, Shandong Province, China

Abstract

Enzyme possesses irreplaceable role in the bating process of leather making, but the mass transfer mechanism of enzymes in the bating process is not yet thoroughly studied. Fluorescent labeling, a detection mean, is widely used in molecular biology, medicine and other fields. In this study, the fluorescent labeling was used to trace and visualize the enzymes in the skin matrix. The fluorescence detection coupled with frozen section was applied to explore the effect of concentration, process time of enzyme and different part of skin on the mass transfer during bating. Furthermore, the mass transfer mechanism of enzymes of different molecular weights was also investigated by double labeling.

The experimental results indicated that the mass transfer rate of enzymes on the flesh surface was faster than that of the grain surface. The mass transfer difference of flesh and grain surface decreased with the increase of the enzyme concentration and the reaction time. And the mass transfer rate of low molecular weight was faster than that of the higher molecular mass. Moreover, the mass transfer rate of the enzyme was slower in back part than that in belly part.This demonstrated that the fluorescent tracer technique is feasible for studying the enzymatic mass transfer in the skin matrix. Hence, it is of theoretical significance to study the transfer regularity and mechanisms of enzymatic activities during the process of leather making.

Keywords**:** Enzyme; bating; mass transfer; fluorescent tracing; double labeling

1. Introduction

In leather industry, the enzyme has been used in unhairing[1]and bating[2]. With the development of enzyme preparation industry, the using of enzymes has far exceeded this range, and enzymes have been widely used in various processes such as preparation stage and tanning[3]. Because the enzyme has the characteristics of high-efficiency, specificity and the mild reaction conditions, we can use different lipase, protease and carbohydrase to dispose the non-collagenous components of the skin according to the requirements of different process. In addition, some processes such as unhairing and liming will generate large amounts of waste water containing sodium sulfide, lime and other substances. These substances will make the BOD, COD and other indicators of waste water far beyond the national tannery effluent discharge standards. But the use of enzyme preparations can greatly reduce the generation and emission of these pollutants and contribute to the clean production of the leather industry.

Bating is an indispensable process in leather making process. In the traditional leather industry, enzyme preparations were initially used in bating. In order to remove the scud and mesenchyme to disperse fibers, the pancreatic enzyme is generally used during the bating. Nowadays, researchers have studied the enzyme preparations that suitable for bating. And there are more and more new enzyme preparations are being invested in leather industry, which can improve the quality of leather, increasing the benefits of production and promoting the development of the leather industry.

With the development of biotechnology, the requirements for proteins, nucleic acids and cell markers are getting higher. The traditional isotope labeling methods can no longer be adapt to current development. Fluorescent probetechnology[4], with high sensitivity and a wide dynamic response time, has broad application prospects in protein, nucleic acid, cell detection and immunoassay. Therefore, researchers can use fluorescent probe to detect complex biomolecules, including specific components of living cells. In particular, fluorescent chemical sensors and molecular signal systems developed in recent years have greatly expanded the application of fluorescent probe technology. At present, this technology has been applied in many fields, such as pharmacology, physiology, environmental science and information science. With the rapid development of life sciences, the demand for new types of fluorescent probes is becoming more and more urgent. The fluorescent probes used for labeling or derivatization are mainly fluorescein, rhodamine, o-phthalaldehyde and other compounds. Among them,

fluorescein and its derivatives play a very important role in the field of biological research. As a common fluorescent dye, fluorescein isothiocyanate (FITC) [5]is always used for the research of enzymes and proteins. Quantification or visualization of enzymes are mainly carried out by fluorescence labeling of enzymes and detection techniques such as fluorescence spectroscopy and fluorescence microscopy. Cavaco-Paulo A. et al. used protease labeled by FITC to research the effect of protease on wool when processing wool after reconstitution[6]. The results indicated that the protease had a larger molecular weight after recombination than before, and it was difficult to penetrate into the wool. While the uncombined protease was able to enter the middle of the wool, which reduced the strength of the wool and other properties.

In summary, the fluorescent labeling can be used for the labeling of enzyme in solution to study their properties. Moreover, fluorescent labeled enzymes can be used to research the visual detection of the infiltration of enzymes in insoluble matrices such as wool. The principle of enzymatic treatment of animal skins is similar to that of enzyme-treated wool. Therefore, fluorescent labeling technology can be applied to the research of enzymes in leather. In this paper, fluorescent labeling technology was used to research the mass transfer behavior of enzyme during the bating process.

2. Materials and method

2.1 Materials

Salted goatskin was obtained from Tianjin Kaixinmin International Trade Co., Ltd. Fluorescein isothiocyanate (FITC), rhodamine b isothiocyanate (RBITC), and trypsin (bovine pancreas, 1000 U/mg，23 KDa) were purchased from Shanghai Aladdin Biotechnology Co., Ltd. Bovine serum albumin (BSA)[7] was obtained from Hefei Bomei Biological Technology Co., Ltd.

The chemicals used for leather processing were commercial grade. Other chemical reagents used in this study were of analytical grade. The deionized water used during the experiment is produced with a UP Water Purification System.

2.2 Preparation of goatskin

The salted skin was washed to remove salt. Then, 0.2% fungicide MT, 0.1% Na_2S and 0.5% degreaser were added in the drum for soaking. After 3 h, soaked skin was fleshed by meat cleaver. In unhairing process, paste which contained 15 g lime, 10g Na_2S and kaolin was performed on the surface of fleshed skin evenly. Then skin was folded along the back line and placed on the table for 5 h. Moreover, the removal of hair was completed by knife and washed after unhairing. For deliming, 1% degreaser and 2% $(NH_4)_2SO_4$ were utilized.

2.3 Preparation of labeling enzymes

2.3.1 FITC-Trypsin

1.5 g trypsin and 15 mg FITC were dissolved in 30 mL carbonate buffer solution (0.1 mol / L, pH 9.16). And the sample was sealed in 50 mL beaker in dark, and stirred with a magnetic stirrer for 14 h. The stirring speed was based on no bubbles. Then, the labeling solution was centrifuged. Moreover, the labeled trypsin was obtained by chromatographic column and freeze-dried on the freeze dryer for 12 h. The final sample was collected in brown bottle and placed in the refrigerator.

2.3.2 RBITC-BSA

300 mg BSA was dissolved in a part of mixed solution, containing 3 mL carbonate buffer solution and 27 mL physiological saline. 12 mg RBITC was dissolved by the remaining part and magnetic stirred at 4 ℃for 4 h. Then the two solutions were mixed and stirred at 4 ℃ for 16 h by the magnetic stirrer. And repeated the operations for preparing FITC-Trypsin.

2.4 Assay of influencing factors of enzyme mass transfer

2.4.1 Concentration

Different amounts of trypsin were added to FITC-Trypsin[8] solution (40 U/mL) to prepare four solutions which have different concentrations. Four sample skins of 4 × 4 cm, which were along the back line, were used in the bating with the enzyme solutions, when the liquid ratio was 1.2, the rotational speed was 30 r / min, and the time of bathing was 5 and 30

min. Then, the skin was quickly removed from the drum, frozen on the loading table, and sliced to detect the change of fluorescence intensity finally.

2.4.2 Molecular weight

FITC-Trypsin and RBITC-BSA were diluted to the same fluorescence intensity, and the diluents were mixed at 1:1 to be used in bating. The sample skin of 4 × 4 cm was used in bating with mixed solution, when the liquid ratio was 1.2, the rotational speed was 30 r / min, and the time of bating was 15 min. Then, the skin was quickly removed from the drum, frozen on the loading table, sliced vertically, and dried. After immobilized with 4% neutral formaldehyde, the fluorescence microscope was observed.

2) The sample skins of 4 × 4 cm were used in bating with the mixed solution which was mixed by diluents at 1:1, when the liquid ratio was 1.2, the rotational speed was 30 r / min, and the time of bathing was 5 min. The skin was quickly removed from the drum, frozen on the loading table, and sliced to detect the change of intradermal fluorescence intensity.

2.6 Skin part

The sample skins of 4 × 4 cm cutting from belly and back part were used in bating with the FITC-Trypsin of 150 U / mL. Liquid ratio was 1.2, rotational speed was 30 r / min and bathing for 5 min. Then, the skin was quickly removed from drum, frozen on the loading table, and sliced to detect the change of fluorescence intensity.

2.7 Process time

Two sample skins which were symmetrical along the back line were used in bating with FITC-Trypsin of 150 U/mL.Liquid ratio was 1.2, rotational speed was 30 r / min and bathing for 5 and 30 min. Then the skin was quickly removed from the drum, frozen on the loading table, and sliced to detect the change of fluorescence intensity.

Results and discussion

3.1 The effect of enzyme concentration on mass transfer

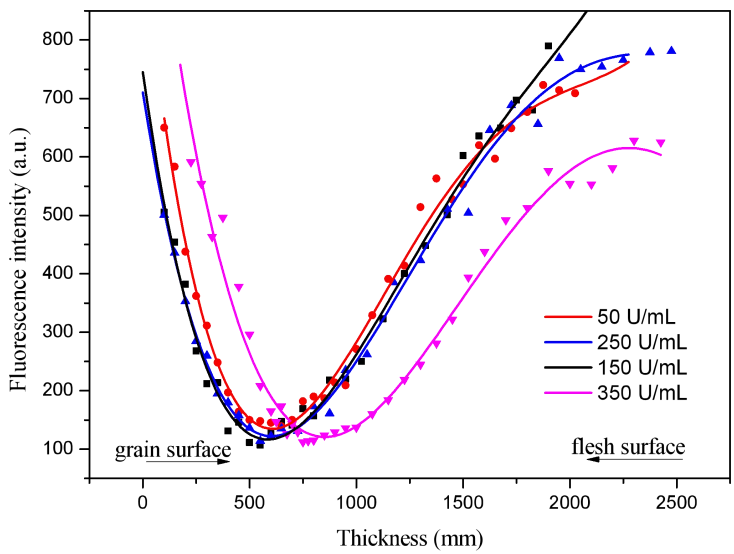

Figure 1. Mass transfer difference of FITC-Trypsin for 5 min at different concentrations

It can be seen from Figure 1 that the change of concentration had minimal effect on mass transfer in a short time. At the same time, there are large differences of mass transfer between the flesh and grain surface. And the mass transfer rate of enzymes on the flesh surface was faster. The changes of fluorescence intensity were similar in the enzyme concentration of 50 - 250 U / mL at 5 min, which indicated that the changes of enzyme concentration had little effect on the mass transfer rate in 5 min.

But the change of fluorescence intensity was obviously different. On the grain surface, the fluorescence intensity was higher than others, and the lowest point offset along x-axis. This may be due to the enzyme concentration of 50-250 U / mL can't destroy the special dense tissue structure of the grain surface in a short time, so the changes of fluorescence intensity were close to each other. However, the concentration of 350 U / mL could destroy the tissue structure of the grain surface in a short time. This accelerated the mass transfer rate of enzyme on grain surface, and decreased the difference of the mass transfer between the grain and flesh surface.

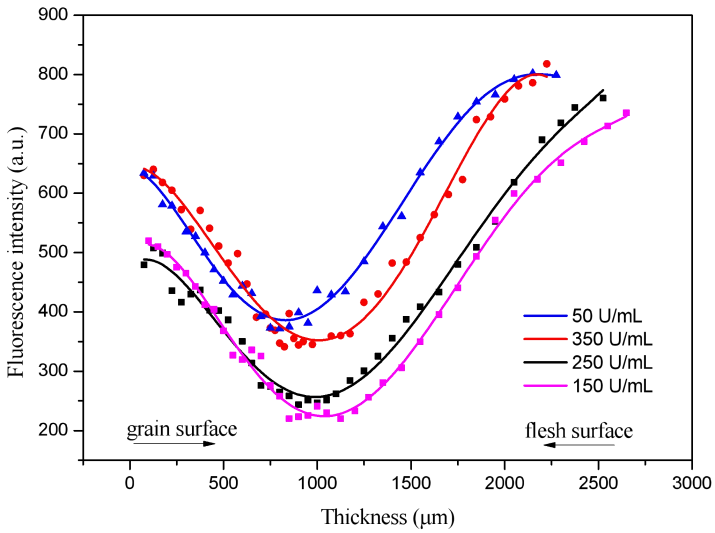

Figure 2. Mass transfer difference of FITC-Trypsin for 30 min at different concentrations

It can be seen from the Figure 2 that the fluorescence intensity of sample with the lowest enzyme concentration was extremely high. It was because that low enzyme concentration had poor effect. Thus, the fiber gap of the skin had not been greatly damaged. So much so that the mass transfer of enzyme was fast. The fluorescence intensity decreased from 50 to 150 U / mL, because the enzyme concentration hindered the mass transfer of the enzyme. With the increase of enzyme concentration, the ability of enzyme to remove inter-fibrillary substance was strengthened, the fiber gap decreased and the mass transfer slowed down. The mass transfer of the enzyme may be driven by a concentration gradient, so the mass transfer rate of the enzyme increased with the increasing of the enzyme concentration.

On the other hand, from 50 to 350 U / mL, the lowest point of fluorescence intensity shifted to the right. This suggested that, from 50 to 350 U / mL, increased enzyme concentration accelerated the mass transfer rate of enzyme.

3.2 Effect of molecular weight of enzyme on mass transfer

Observed by fluorescence microscopy[9], the effects of molecular weight on mass transfer are as follows:

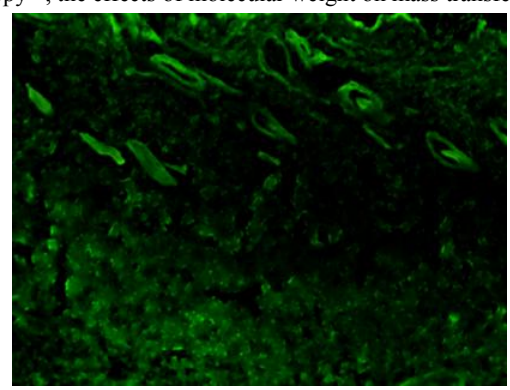

FITC-Trypsin

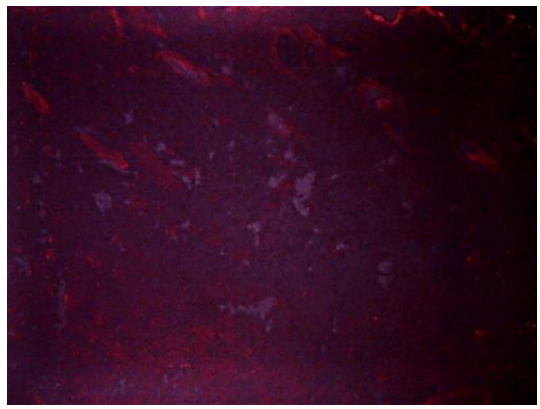

RBITC-BSA

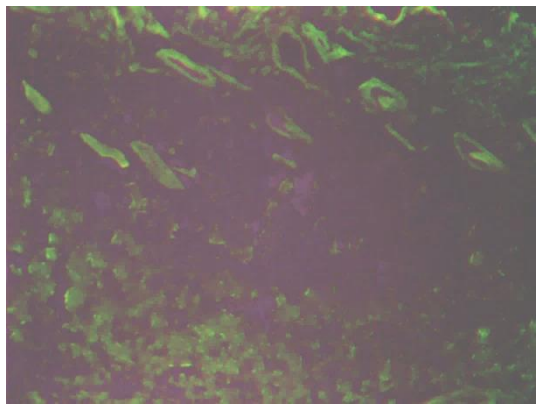

Merge

Figure 3. Fluorescent microscope image

As can be seen from Figure 3, green was more distributed than red in the same time. From this experiment, it could be concluded that the mass transfer of RBITC-BSA, which had higher molecular weight, was slower than that of FITC-Trypsin.

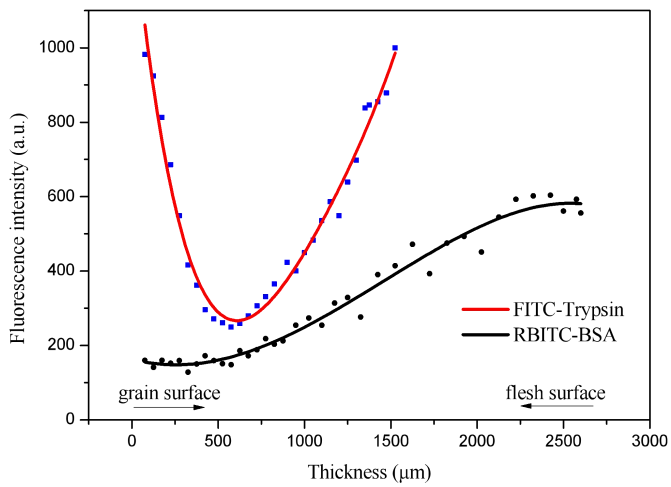

Figure 4. Mass transfer of FITC-Trypsin and RBITC-BSA

As can be seen from the Figure 4, the fluorescence intensity of FITC-Trypsin was higher than that of RBITC-BSA, and the mass transfer symmetry of FITC-Trypsin was better. It indicated that the mass transfer rate of FITC-Trypsin with a low molecular weight was faster than that of RBITC-BSA with a higher molecular weight, and the mass transfer in the skin was more self.

The results were in agreement with the research results of Song Ying and so on.

3.3 Effect of different part of skin on mass transfer

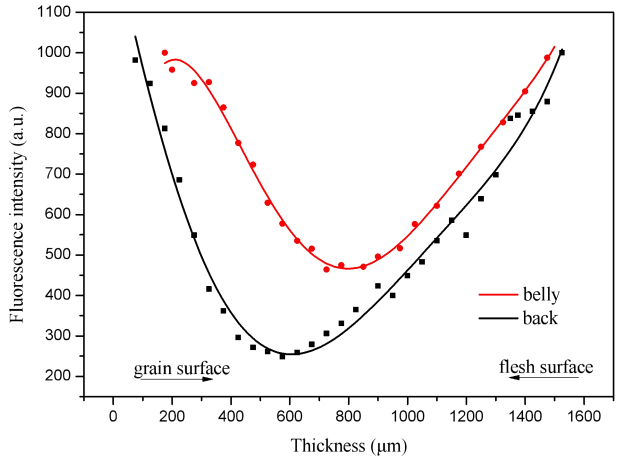

Figure 5. Mass transfer of FITC-Trypsin at belly and back

The belly skin is thin, and the fibers are loose; while the back skin is thicker, and the fibers are dense[10]. Therefore, the difference of position in skin also influences the mass transfer of enzyme.

As can be seen from Figure 5, the fluorescence intensity of the enzyme in the belly was higher which indicated that the mass transfer rate of FITC-Trypsin was faster at the same time. While the fluorescence intensity of the enzyme in the back was lower which indicated that the mass transfer rate of FITC-Trypsin was slower and quantity of mass transfer was less at the same time. At the moment, there was a smaller difference in mass transfer between the grain and flesh surface in the belly, and it was more uniform of the mass transfer than that in the back.

3.4 Effect of process time of enzyme on mass transfer

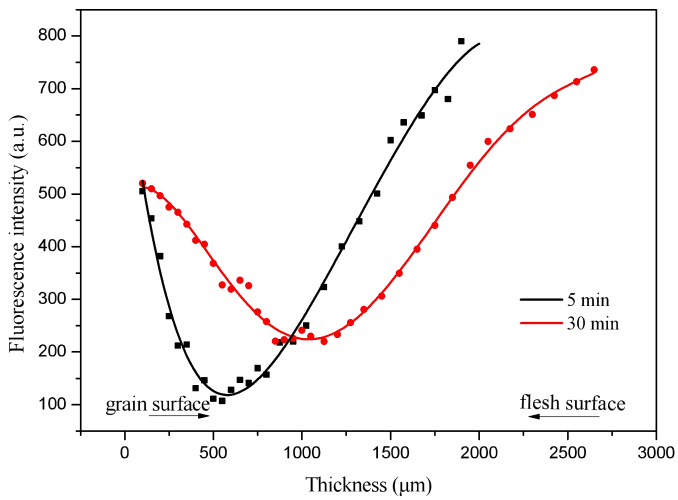

Figure 6. Mass transfer of FITC-Trypsin at 5 and 30 min

As can be seen from Figure 6, at 5 min, the mass transfer of enzyme on grain surface was shallow, and the lowest point of fluorescence intensity was near the grain surface. However, at 30 min, the fluorescence intensity increased obviously, and the lowest point of fluorescence intensity shifted to the flesh surface. It indicated that with the lengthening of time, the symmetry of the fluorescence intensity change was improved, and the difference of mass transfer between the flesh and grain surface decreased. At the same time, the mass transfer of enzyme was more uniform.

Conclusions

In this study, the mass transfer of enzyme in skin under different conditions was studied by the combination of fluorescence tracing and fluorescence detection technique. The conclusions are as follows:

The mass transfer rate of enzyme in flesh surface is faster than that of grain surface.

Enzyme concentration and action time have effects on the mass transfer rate. And these factors have a greater effect on grain surface that that on the flesh surface. But with the increase of enzyme concentration and action time, the difference of mass transfer between the grain and flesh surface was decreased.

The mass transfer rate of low molecular weight was faster than that of the higher molecular mass.

The mass transfer rate of the enzyme was slower in back part than that in belly part

Acknowledgements

This study was financially supported by the National Key Research and Development Program of China under contract No. 2017YFB0308402.

References

[1] A. Dettmer, É. Cavalli, M.A.Z. Ayub, M. Gutterres. Environmentally friendly hide unhairing: enzymatic hide processing for the replacement of sodium sulfide and delimig. J CLEAN PROD. 47 (2013), 11-18.

[2] Z. Li, H. Cheng, L. Liao, X. Sun, M. Chen. Study on the bating properties of EB-1 enzyme and its hydrolytic action to collagen. China Leather (2002).

[3] S.V. Kanth, P.R. Kannan, N. Usharani, G.C. Jayakumar, A. Yasothai, B. Chandrasekaran. Studies on the Use of Enzymes in Tanning Process: Part I. High Exhaust Vegetable Tanning. Journal- American Leather Chemists Association. 104 (2009), 405-415.

[4] G.Y. Wiederschain. The Molecular Probes handbook. A guide to fluorescent probes and labeling technologies. BIOCHEMISTRY-US. 76 (2011), 1276.

[5] B.N.G. Giepmans. The Fluorescent Toolbox for Assessing Protein Location and Function. SCIENCE. 312 (2006), 217-224.

[6] R. Araújo, C. Silva, R. Machado, M. Casal, A.M. Cunha, J.C. Rodriguezcabello, A. Cavacopaulo, A. Cavacopaulo. Proteolytic enzyme engineering: a tool for wool. BIOMACROMOLECULES. 10 (2009), 1655.

[7] T. Murakami, H. Okamoto, H. Kim. Structural and functional changes in high-density lipoprotein induced by chemical modification. Biomater Sci. 3 (2015), 712-715.

[8] C.Q. Liu, X.F. Liao, H.L. Tao, C. Sun, X.U. Jie. A Novel Fluorescent Assay for Detection of Trypsin Based on Fluorescein Isothiocyanate-Bovine Serum Albumin-Pb~(2+) Probe. Journal of Analytical Science (2016).

[9] M. Tang, P. Teng, Y. Long, X. Wang, L. Liang, D. Shen, J. Wang, H. Zheng. Hollow carbon dots labeled with FITC or TRITC for use in fluorescent cellular imaging. MICROCHIM ACTA. 185 (2018).

[10] T. Covington. Tanning chemistry : the science of leather. (2009).

P28

Modelling the kinetics of enzyme infusion in skin matrix

XueSong Li, YanChun Li*, DeYi Zhu

College of Leather Chemistry and Engineering, Qilu University of Technology (Shandong Academy of Sciences), No. 3501 Daxue Rd, Changqing District, 250353, Jinan, Shandong Province, China

Abstract

The application of enzyme preparations is currently being explored with relative success for many areas of leather making. Whatever these processes are, enzymes come into contact with the skin components and perform a variety of functions all do depend on the diffusion process in skin matrix. Obviously, the knowledge of kinetics of enzyme infusion as well as the enzymatic reaction with skin matrix is beneficial to use enzymes in leather industry.

Unlike conventional enzymatic reactions, in the case of leather processing, the substrate, skin, is a complicated three-dimensional matrix of collagen fibers. The mass transfer mechanism of enzyme into skin matrix is thus complex and unpredictable. Fick's second law is commonly used to predict how diffusion causes the solute concentration to change with time in one dimension. In this paper, based on the Fick's second law and the Spiro's "slab" model, a novel kinetics equation model suitable for the enzyme mass transfer in the skin matrix was developed, which is $\ln\left(\frac{c_0}{c-f(t)}\right) = \ln\left(\frac{\pi^2}{8}\right) + \frac{\pi^2}{4L^2}\kappa l$. In order to verify the kinetics equation, a novel technology developed from fluorescent tracer coupled with slices fluorescence detection was employed. The experimental data fit well the equation, and the obtained R^2 values are all larger than 0.900. Moreover, this inferred equation successfully predicted the trend of the mass transfer curve over time. In general, the kinetics equation can provide theoretical guidance for the subsequent study of the mass transfer mechanism of enzyme in the skin matrix and the future application of enzymes in leather industry.

Key words: Skin matrix; modeling; kinetics; diffusion equation

P29

Effects of Enzymatic Unhairing by Combinations of Several Proteases

Yiming Shen, Deyi Zhu, Shan Cao, Yuanmeng Zhou,Yanchun Li*

(College of Leather Chemistry and Engineering, Qilu University of Technology (Shandong Academy of of Sciences) 250323, Shandong, China)

Abstract: To gain effects of combination of several proteases when used in unhairing. Amylase, keratinase and collagenase with high purity were mixed at different ratio to put into practice on unhairing which achieved supreme consequences. The released total protein and digested collagen in the waste solution revealed that more amylase and keratinase enhanced effectivity of hair removal, collagenase was essential for unhairing. Further, the histological observation indicated that plethoric collagenase destroyed collagen fibers in the dermis which are the most important for the leather. In addition, the collagenase activity of mixed enzyme is 5 times than the industrial enzyme used in the unhairing, the leather was very soft and its shrinkage temperature achieved 124.3°C with softness，the tensile strength was 40.4 N/mm^2 and tear strength was 110 N/mm. These findings had fantastic implications for alternative and improvement of enzyme.

Keywords: Enzyme; Unhairing; Hydroxyproline; Protein; Structure of skin

Introduction

Leather making is one of the supportive manufactures around the world, however, it is facing the threat of closure because of environmental pollution problems it possesses. The pressure in environment is mainly caused by some chemicals used during the leather processing, and thence it is necessary to design and adopt cleaner technologies for reducing the heavy pollution from leather industry. Traditionally, unhairing is an essential process meanwhile it generates fundamental pollution in leather making. The significant goals of unhairing are separations of hair from skin and the unfolding up of collagen fibrous structure[1]. However, it is a serious pollution operation. The conventional unhairing process takes the usage of lime and sulfide, which has excellent effects of hair removal, low cost and simple manipulation at the expense of sulfide and alkaline sludge in wastewater. In addition, these wastes in the effluent which were hard to degrade increased the concentration of COD, BOD and TTS[2]. When referring to this aspect, the usage of clean technology in unhairing process is becoming more and more significant for the leather industry.

The hair preserving unhairing process was gradually adopted instead of destructive unhairing process to decrease the pollution. Although other regents like hydrogen peroxide, amines were used to take place of toxic sulfide. Enzymatic unhairing is the most promising approach to eliminate the toxic sulfide from unhairing process. The enzyme accelerated the reaction rate by reducing the activation energy of the chemical reaction, and it characterized specificity, efficiency, variety and mild action. Large amounts of enzymes used in unhairing are protease. As an available choice to lime-sulfide process, enzymatic unhairing gained much attention in recent years. The biggest obstacle for the promotion of enzymes in unhairing was activity and category of protease. Further, the inappropriate utilization of protease is harmful to collagen, thus declining the properties of leather[3].

Obviously, the knowledge of selection and improvement of protease is fundamental for using protease in enzymatic unhairing. In this study, amylase, collagenase and keratinase were compounded at different ratios used in the enzymatic dehairing, which based on the enzymatic activity ratios of different proteases in common industrial enzyme. The analysis of protein and collagen concentration in the liquor, properties of leather and histological section staining are the main methods to explore the changes of different components in leather. These results had good guidances for the selection and promotion in enzymatic unhairing.

2 Materials and methods

2.1 Materials

Wet-salted goatskins were chosen as the raw material for this study. Enzymes including PELTEC X-Zyme UF EXP 4072 was purchased from LANXESS (Changzhou, China), collagenase I (Preparation from Clostridium histolyticum) was

purchased from Life Technologies (Shanghai, China), keratin and Amylase were purchased from Drummer Biotechnology(Shanghai,China). The chemicals used for leather processing were of commercial grade. The chemicals used for analytical techniques were of laboratory grade.

2.2Determination of keratinase activity

Keratinase activity was measured by using modified method of Gradisar[4]. Wool powder used as the substrate was grinded before the experiment. Insoluble residues were removed by centrifugation through TGC-16G high speed benchtop centrifuge (Shanghai, China). Assay mixture containing 10 mg of substrate and 2 mL of appropriately diluted aliquot of enzyme was incubated at 40℃ for 1 h, and the reaction was stopped using 10% TCA. One unit of protease was considered as the increase of 0.1 at 280 nm.

2.3 Determination of collagenase activity

Collagenase activity was estimated using type I collagen as substrates prepared in 0.1 mol/L Tris-HCL buffer pH 7.5. Reaction systems comprised of 10 mg substrate and 1 mL of appropriately diluted enzyme. Reaction mixtures were incubated at 37 °C for 40 min, stopped using 10% chilled TCA[5]. The amount of released free amino acid was measured by the Chloramine T method. One unit of collagenase activity was defined as the amount of hydroxyproline enzyme that liberated 1 μg per minute under the conditions used.

2.4 Determination of carbohydrase activity

Carbohydrase activity was estimated with starch as substrate at 40 °C， pH 7.4 by the improved method described by Amoozegar[6]. The reaction mixture contained 1 mL diluted enzyme solution plus 1 mL 0.5% (w/v) starch dissolved in 0.1 M Tris buffer containing 5% (w/v) NaCl (pH7.8). The reaction took place at 40 °C for 5 min. One unit of the activity was defined as the amount of enzyme that hydrolyses 1 mg starch to dextrin 5 min under optimum conditions.

2.5 Goat hide dehairing assays

Prior to dehairing, hides were soaked with water containing fungicide and degreaser (300 % v/w of salted skin) until they are free from dirt, dung, and blood stains. Soaked goat hide was cut into pieces of approximately 6×6 cm and weighed. Dehairing was performed in the Erlenmeyer for 14 h. The amounts of enzymes and chemicals used in the experiments was showed in table 1. Group A was set as the control, and group B keep other protease activity like group A with no collagenase. In addition, group C and D are twice α-amylase and keratin activity than group A respectively. What's more, group E was also set as another control, while the collagenase activity of group F, G and H are five, ten and fifty times than group E. Further, other protease activities were kept the same. The status of hide was checked among the whole experiment. Hair removal was performed by blunt knife.

Table.1 The amounts of chemicals in different experiments

Group / Materials	A(Cont-rol)	B(expe-riment)	C(expe-riment)	D(expe-riment)	E(Cont-rol)	F(expe-riment)	G(expe-riment)	H(expe-riment)
NaCO3(%)	0.25%	0.25%	0.25%	0.25%	0.25%	0.25%	0.25%	0.25%
PELTEC X-Zyme UF EXP 4072(%)	0.3%	——	——	——	0.3%	——	——	——
α-amylase (%)	——	0.34%	0.68%	0.34%		0.34%	0.34%	0.34%
Keratin (%)	——	0.17%	0.17%	0.34%	——	0.17%	0.17%	0.17%
Collagen-ase (%)	——	——	0.0009%	0.0009%	——	0.0045%	0.009%	0.045%

2.6 Analysis of protein and hydroxyproline concentration

The liquid during whole hair removal was collected as the sample. The hydroxyproline concentration of samples was measured by using modified method of N. Yu. Ignat'eva[7].The oxidation of hydroxyproline was performed on the addition of 2 mL of Chloramine-T to each test tube; the mixture was stood at room temperature for 20 min. After the addition of P-dimethylaminobenzaldehyde solution, the test tubes were placed in a water bath heated to 60 °C for 20 min and then cooled with cold water for 5 min. Absorbance was measured at λ=558 nm to calculate the hydroxyproline concentration of the samples. On the other hand, the concentration of samples was estimated using BSA as the standard by the method of Bradford. The samples were incubated with G-250 dyeing at room temperature for 5min. Absorbance was measured at λ=595 nm to calculate the protein concentration of the samples.

2.7 Histological analysis

A small piece (2×2 cm) of dehaired hide was cut and washed with water and fixed in 10 % formaldehyde solution. Sections of twenty-five-micron thickness of the prepared samples were cut using cryostat and stained with hematoxylin and eosin to examine the histological features. These sections were examined under light microscope and photomicrographs were taken.

2.8 Physical properties of leather

Dehaired hide was tanned by conventional operation into leather as Saravanabhavan described[8]. Then samples for various physical tests were conditioned at Humidity Chamber over a period of 48 h. Physical properties such as tensile strength, tear strength, softness and shrink temperature were examined as per the standard procedures.

3 Results and discussion

3.1 Various enzyme activities in protease used in the experiments

Crude protease exhibited various enzyme activities (Table 2), it had collagenase, keratin, carbohydrase activities. However, collagenase activity seemed to be a little, which was very important for its application in leather processing because collagen forms the chief constituent of leather and its destruction has adverse impact on the leather quality. The enzyme activities of all protease were basis for following dehairing experiments.

Table.2 Different protease activities

Enzyme	Collagenase	Keratin	α-amylase	PELTEC X-Zyme UF EXP 4072（mg）
Collagenase activity(U/g)	46.92	——	——	0.143
Keratin activity(U/g)	——	85.71	——	97.92
Carbohydrase activity(U/g)	——	——	22008.5	13023.8

3.2 Hair efficiency of different groups

Table.3 Effects of enzymatic dehairing

Group / Time(h)	A	B	C	D
3	+	+	++	++
6	++	+	+++	+++
9	+++	++	+++	+++
12	+++	++	++++	++++
14	++++	+++	++++	++++

The effects of enzymatic dehairing were examined during whole dehairing process as shown in table 3. The symbol of "+" represents the difficulty of hair removal, the more "+", the hair were easy to be removed. For the efficiency of dehairing, group C and D were higher than group A, while hair in group B was hard to remove. This unusual phenomenon may because

that certain concentration of collagenase was beneficial of dehairing, keratin and carbohydrase can accelerate the effects of dehairing.

3.3 Protein analysis during the dehairing

The amount of protein dissolved in the waste liquid could reflect the strength of the enzymatic dehairing. To confirm the dehairing efficiency, released protein was examined during dehairing process in Fig 1. As we can see from it, protein concentration increased with the time goes. When compared to group A, the protein concentration in group B was lower which was contributed to little collagenase, it could loosen collagen fibers properly then benefit the promotion of another protease. Large amounts of protein released in group C and D represented that keratin and carbohydrase could enhance dehairing effects.

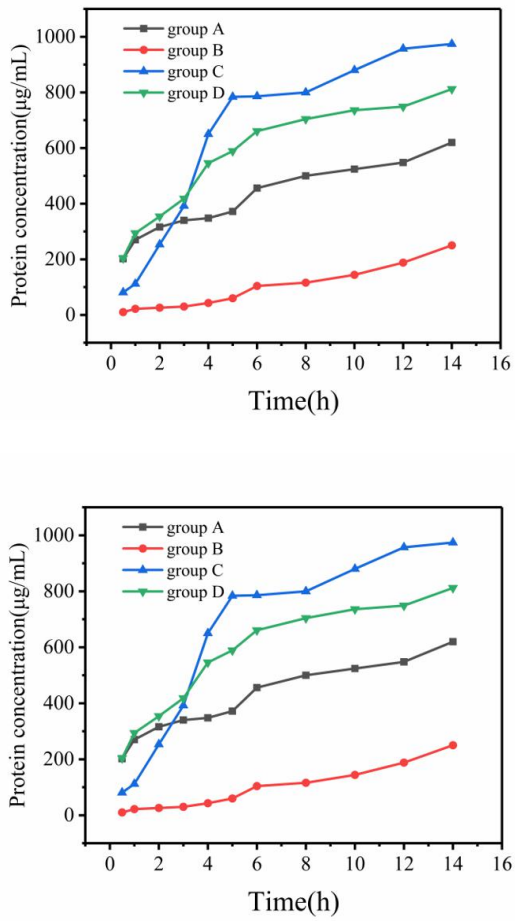

Fig.1 Released protein concentration in dehairing process

3.4 Destructive collagen during the dehairing

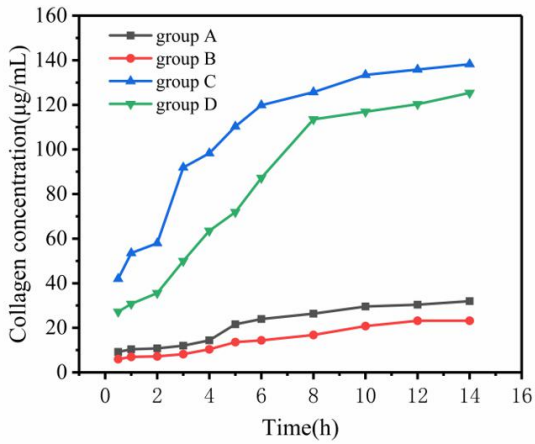

Fig.2 Destructive collagen in dehairing process

Hydroxyproline is a characteristic amino acid of collagen, accounting for about 13% of collagen[9]. Thus, the concentration of hydroxyproline could be transformed into collagen concentration destoryed during dehairing process. Fig.2 showed that the loss of collagen increased with rising time appeal to dehairing effects. It was obvious that the damage to collagen was serious in group C and D. Further, collagen concentration in group A and B was low with ineffective dehairing. It indicated that high-efficiency hair removal accomplished with a large loss of collagen which is important for leather properties.

3.5 Analysis of liquid in different collagenase activities

Certain concentration of collagenase was beneficial for dehairing, excess concentration could damage the collagen then influence leather properties. Different collagenase activities of enzymatic dehairing (Fig.3) were examined to confirm it. From Fig.3a, it found released protein and destructive collagen concentration increased with higher collagenase activity. High collagenase activity enhanced dehairing efficiency at the expense of collagen breaking. Fig.3b could be more intuitive to show the rising of collagenase activity damaged collagen. Therefore, excessive collagenase should avoid in daily leather manufacture.

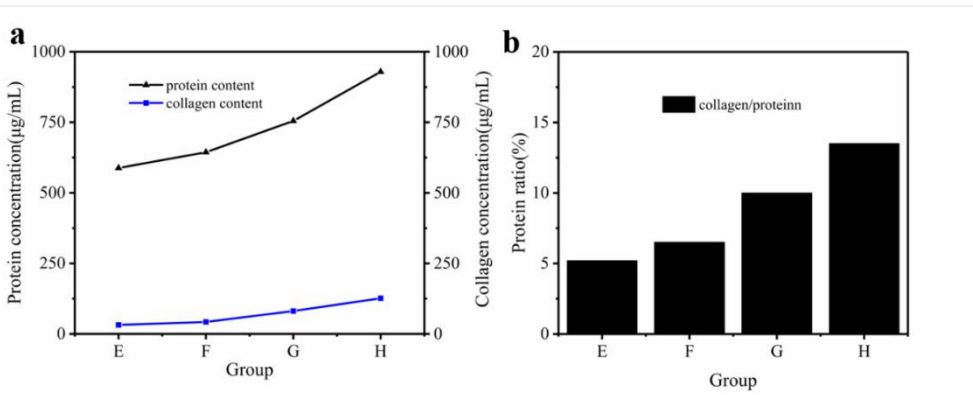

Fig.3 Protein and collagen concentration(a) and protein ratio(b) with different collagenase activities

3.6 Histology of dehaired pelts

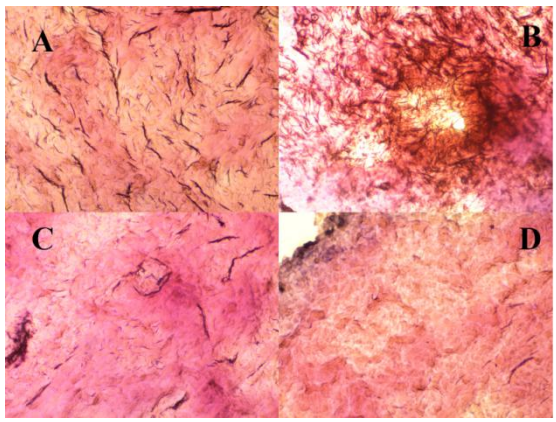

Fig.4 Histology of longitudinal sections of goat skins after dehairing (Group A、B、C、D，×100)

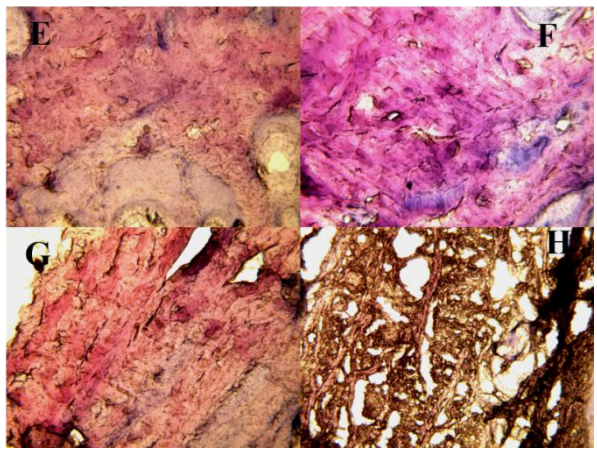

Fig.5 Histology of longitudinal sections of goat skins after dehairing with different collagenase activity(Group E、F、G、H, ×100)

Complete removal of epidermal layer from skin and hide was observed when dehairing was performed using enzymes. The optical micrograph of the stained vertical section of goat skin confirmed the above visible assessment. In Fig.4, collagen fibers in group B were the tightest and group C, D were dispersed. When referred to Fig.5, collagen fibers were damaged seriously within increased collagenase activities. All images made a complement for the results discussed before, keratin and carbohydrase could enhance dehairing efficiency, collagenase was essential for dehairing while excessive collagenase would influence leather properties.

3.7 Physical properties of leather

Table.4 Physical testing data of leather (Group of different collagenase activity)

Group	E	F	G	H
Softness(mm)	6.7	6.7	6.9	7
Tensile strength(N/mm^2)	35.5	40.4	38	34
Tear strength(N/mm)	89.6	110	97	80.4
Shrink temperature(℃)	121.6	124.3	120.6	115.5

Tensile and tear strength tests were carried out for all the leather dehaired by different activities of collagenase. The softness and shrink temperature for all leather were measured. The average values were given in Table.4. It was seen that experiments with higher collagenase activity exhibited tensile, tear strength and shrink temperature lower than experiments with lower

collagenase activity. This could mainly due to excessive collagenase destoryed collagen fibers decrease leather properties[10].

4. Conclusions

Compared to industrial enzymes, the combination of collagenase, keratin and carbohydrase exhibited high dehairing efficiency with proper ratio. Released protein and collagen in the waste water indicated collagenase was essential for hair removal while keratin and carbohydrase enhance dehairing efficiency. However, excessive collagenase may cause permanent damage in collagen influenced quality of leather. Histological examination of enzymatically dehaired pelt also substantiated above findings, wherein proper enzymes could open fiber well. Further, physical tests of dehaired pelts directly explained the relationship between enzyme and quality of leather. These results may give a guidance in selection and promotion for enzymes used in deairing.

5. Acknowledgements

The authors would like to gratefully thank the support from the National Key Research and Development Program of China(No.2017YFB0308402), China.

6.References

[1] Pillai P, Archana G. Hide depilation and feather disintegration studies with keratinolytic serine protease from a novel Bacillus subtilis isolate[J]. Applied Microbiology & Biotechnology. 2008, 78(4): 643-650.

[2] Nazer D W, Al-Sa'Ed R M, Siebel M A. Reducing the environmental impact of the unhairing–liming process in the leather tanning industry[J]. Journal of Cleaner Production. 2006, 14(1): 65-74.

[3] Khandelwal H B, More S V, Kalal K M, et al. Eco-friendly enzymatic dehairing of skins and hides by C. brefeldianus protease[J]. Clean Technologies & Environmental Policy. 2015, 17(2): 393-405.

[4] Gradišar H, Kern S, Friedrich J. Keratinase of Doratomyces microsporus[J]. Applied Microbiology & Biotechnology. 2000, 53(2): 196-200.

[5] Suphatharaprateep W, Cheirsilp B, Jongjareonrak A. Production and properties of two collagenases from bacteria and their application for collagen extraction[J]. New Biotechnology. 2011, 28(6): 649-655.

[6] Amoozegar M A, Malekzadeh F, Malik K A. Production of amylase by newly isolated moderate halophile, Halobacillus sp. strain MA-2[J]. Journal of Microbiological Methods. 2003, 52(3): 353-359.

[7] Eva N Y I, Danilov N A, Averkiev S V, et al. Determination of hydroxyproline in tissues and the evaluation of the collagen content of the tissues[J]. Journal of Analytical Chemistry. 2007, 62(1): 51-57.

[8] Saravanabhavan S, Aravindhan R, Thanikaivelan P, et al. Green solution for tannery pollution: Effect of enzyme based lime-free unhairing and fibre opening in combination with pickle-free chrome tanning[J]. Green Chemistry. 2003, 5(6): 707-714.

[9] Jian S, Tao W, Chen W. Kinetics of enzymatic unhairing by protease in leather industry[J]. Journal of Cleaner Production. 2011, 19(4): 325-331.

[10] Thanikaivelan P, Bharath C K, Saravanabhavan S, et al. Integrated hair removal and fiber opening process using mixed enzymes[J]. Clean Technologies & Environmental Policy. 2007, 9(1): 61-68.

P30

A Potentially Biodegradable and Biocompatible Tissue Scaffold Material: Composites of Dialdehyde Bacterial Cellulose and Gelatin

Ruijun Guo[1], Yaqi Dong, Yanchun Li, Mao Yang*

(College of Leather Chemistry and Engineering, Qilu University of Technology (Shandong Academy of Sciences) 250323, Shandong , China)

Abstract: The composites (marked DB-G) were prepared by crosslinking of gelatin molecules and dialdehyde bacterial cellulose (DHBC) used as 3D network frame. The DHBC was prepared as a potential functional crosslinkers by periodate oxidation in the electric field keeping in dark at 40°C and pH 2.0. By the results of degradation measurement, the DHBC and DB-G composites showed ideal biodegradability. FT-IR spectroscopy demonstrated that at 1600–1680 cm^{-1} the band became wider and shifted to higher wave numbers indicating that with the increase of gelatin content the C=O stretching pick for amide I gradually occupied the dominance substituted for the C=N band. By the analysis of specific surface area and porosity measurement and SEM images, a lower concentration of Gel contributed to the maintainance of porous structure. Suggested that the 0.1 % and 0.2 % gelatin solution was suitable dosage of the reactants. From TG/DTG data, the increase in decomposition temperatures indicated the formation of chemical bond between DHBC and gelatin molecules. Confirmed that the DB-G is a potentially biodegradable and biocompatible tissue scaffold material.

Keywords: Bacterial cellulose; Gelatin; Periodate; Tissue scaffold material.

1. Introduce

By the analysis of the micro assembly, biological function and formation mechanism of natural tissue, designing and fabricating a scaffold suitable with a good biological compatibility, biodegradation and intricate porous structure for tissue engineering applications has been a important research direction for scientists[1]. Recently, more and more evidence demonstrated that the three-dimensional (3D) scaffold materials similar to natural extracellular matrix, not only can provide mechanical support structure for cell adhesion, growth and proliferation, but also effectively regulate the cellular physiological activities [2, 3]. Bacterial cellulose (BC) is a glucose linear supramolecular polymer with the form of 3D nanofibers network, and owns numerous advantages for tissue engineering, including wettability, high crystallinity, tensile strength, biocompatibility and adaptability [4, 5]. However, BC has a similar chemical structure to other celluloses, it can not be degraded in the body internal environment by enzyme, which has become an essential limiting factor for BC's applications as a scaffold material in tissue engineering[6, 7]. For this reason, Li et al. prepared a 2,3-dialdehyde bacterial cellulose by periodate oxidation procedure, which laid a foundation for making a better bioabsorbable biomaterial for tissue engineering scaffold.

In addition, the surface properties and structure of biological tissue material together determine the adsorbed protein layer in which the structure performance also determines whether can provide the suitable extracellular matrix for cell adhesion, migration, breeding and tissue regeneration and repairs or not. The glycoproteins and polysaccharide proteins (all kinds of integrins) on the surface of the cell membrane are directly involved in the cell specificity of recognition and adhesion [8]. Molecular biology studies have shown that integrin molecules and ones which have a specific space conformation of short peptide sequence RGD (Arg-Gly-Asp) mediate connections between cells and substrate material[9-11]. And in the extracellular matrix collagen and adhesion proteins have more repetitive RGD fragments, so fixing these peptides on materials can significantly improve cell adhesion, spreading and breeding. Gelatin as a denatured collagen protein has relatively low antigenicity owing to its animal origin, and doesn't produce harmful byproducts after enzymatic degration[12]. And because of intrinsic protein structure, gelatin has multitudinous accessible functional groups which provide multiple modification opportunities by cross-linking. Furthermore, gelatin molecular chains also contain repetitive motifs of RGD sequences which is in favour of deposition of extracellular matrix (EMX) and integrins and also can modulate adhesion and physiological activities of cells, growth factor spreading, natural permeation, and blood vessels growth to improve the final

biological behavior for scaffold materials[13-15]. Therefore, in this study, a dialdehyde bacterial cellulose (DHBC) was prepared by periodate oxidation under the desired current density, by which oxidation efficiency of the periodate was improved. The DB-G (an **c**omposite of DHBC and gelatin) was prepared by the reaction of DHBC and certain concentration gelatin solution at appropriate pH and temperature. The degradation, microstructure, morphology, BET surface area, pore size and thermostability properties of DB-G were tested by FT-IR, SAP, SEM, and TG. And aimed at preparing a 3D tissue scaffold material with moisture retention, biodegradation, good protein adsorption capacity, excellent biocompatibility and suitable extracellular matrix environment.

2. Materials and methods

2.1 Materials

Bacterial cellulose membranes were supplied from Hainan YiDe Food Co., Ltd.. Sulfuric acid (98%), acetic acid (99.5%), ethylene glycol (99.5%), sucrose (99.5%), hydroxyl lammonium chloride (98.5%) were obtained from Chengdu Kelong Chemical Co., Ltd.. Sodium periodate (99.5%), sodium sulfate (99.5%) were purchased from Tianjin Ke Mi Ou the chemical reagent co., Ltd.. for oxidation of BC by constant current electrolysis. And sodium phosphate (99.5%) was purchased from Tianjin Bo Di Chemical Co., Ltd. for degradation testing.

2.2 Preparation of dialdehyde bacterial cellulose

A certain quality of BC pellicles and distilled water contained 10 g/L Na_2SO_4 (as electrolyte) were added into an electrolytic cell equipped with magnetic force stirring and water-bath heating device. The work condition as below: the pH adjusted to 2.0 with H_2SO_4, the current density adjusted by electrochemical analysis system (LK98BⅡ， LanLiKe, TianJing, China), with titanium plate as cathode, graphite plate as anode, and saturated calomel electrode as reference, 80 % weight of sodium periodate (compare to BC) was added, and the reactants maintained at 40 ºC under continuous stirring in the dark. The reaction process is shown in the Fig. 1. When electrooxidation finished in 4 h, the excess periodate was removed by ethylene glycol, and then DHBC pellicles were washed by distilled water. In addition, the aldehyde content of the DHBC was determined by Schiff base reaction with hydroxyl ammonium chloride[16, 17] .

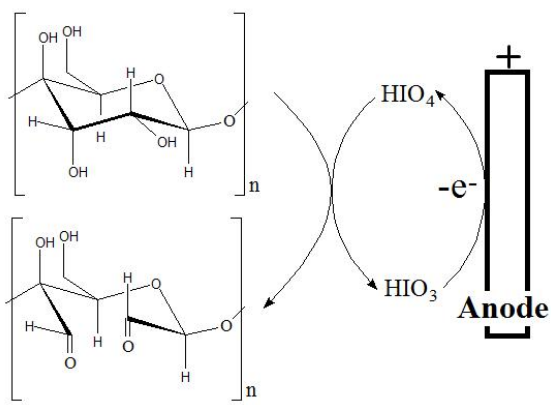

Fig. 1 The oxidation process of BC by periodate under constant current density.

2.2 Preparation of DB-G composite

The purified DHBC samples with distilled water was added in erlenmeyer flask loaded with 0.1 %, 0.2 %, and 0.3 % gelatin solution (based on DHBC weight) and pH was 5.5 ± 0.1. Temperature was kept 40°C for 5 h in oscillation incubator at 100 r/min and the amplitude of 20 mm. After the reaction, the sample, call DB-G, was washed with distilled water to remove the superficial gelatin, then dried by lyophilizer (FD-14, SIM, USA). The resulted composites were marked DB-G0.1, DB-G0.2, DB-G0.3. And the condensation reaction route is shown in the Fig. 2.

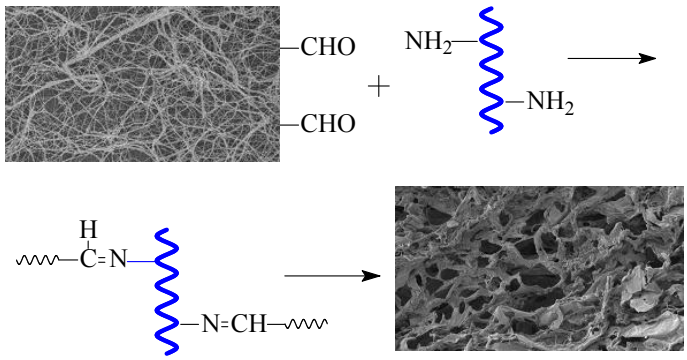

Fig. 2 the condensationroute of DHBC and gelatin.

2.3 Degradation testing

BC, DHBC and DB-G pellicles (15 mm × 15 mm) were immersed in simulated body fluid (SBF) (Oyane et al., 2003) at 37°C. After 1 d, 3d, 7 d, 14 d, 21 d, 30 d, 60 d and 90 d, the all samples were washed with distilled water, then freeze dried and weighed. The rate of weightlessness and standard deviations, three of all BC, DHBC and DB-G pellicles, were calculated by the following equation:

$$ML\ (\%) = \frac{M_0 - M_d}{M_0} \times 100\%$$

M_0 is the initial dry weight of the samples and M_d is the dry weight of samples after degradation at each time point.

2.4 FT-IR measurement

FT-IR spectra of freeze dried BC, DHBC, DB-G0.1, DB-G0.2 and DB-G0.3 were recorded on a Fourier transform infrared spectrometer (FI-1R, PE, USA) in a range of wave numbers from 4000 to 500 cm^{-1}. The resolution was 8 cm^{-1} and the scan number was 32.

2.5 Specific surface area and porosity measurement

Suitable porosity and large BET surface area in the 3D network structure is well for cell adhesion, spreading, breeding and metabolites exchange. More than 100 mg of samples were analyzed by specific surface area and porosity analyzer (Tristar 3000, HOSIC, UK). To eliminate the effect of residual water, before testing, the samples were dried at 45°C for 24 h by sample degas system. The analysis adsorption, analysis bath temperature and equilibration interval in the test were N2 , -195.8°C and 10 s, respectively.

2.6 SEM measurement

The morphology of freeze dried samples were examined with SEM (JSM-7500F, JEOL, Tokyo, Japan). Before testing, the samples were fixed onto metallic sample holders with conducting silver glue and then sputtered with a layer of gold. The voltage was 5 kV.

2.7 TG analysis

Thermogravimetric analysis of samples (3-5 mg) were carried out by using a TG209F1 thermal analyzer (NETZSCH-Gertebau GmbH, Germany) under nitrogen atmosphere at a heating rate of 10°C /min. The range of scanning temperature was from 50°C to 600°C. TG and DTG curves and the initial decomposition temperature (T_i) and temperature of maximum weight loss rate (T_{max}) were drawn up and recorded.

3. Results and discussion

3.1 Degradation

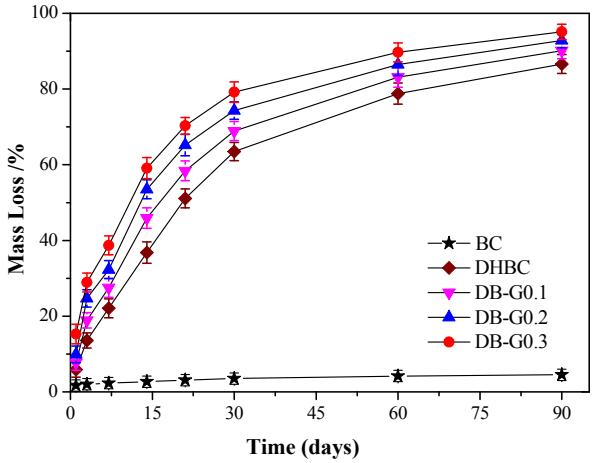

Fig. 3 BC, DHBC and DB-G mass loss cave in SBF.

Biodegradable tissue engineering scaffold materials require proper degradation period. On the one hand, when the organization has not been formed, and would not be enough for mechanical load, make ensure that the scaffold materials can bear the main support effect which is advantageous to the cell amplification, the formation of the organization. On the other hand, after organization forming, the materials should be fully biodegradable to achieve the final repairment and replacement[18, 19] . The principle of cellulose degradability by oxidation has been reported[7, 20, 21] . The degradation performance and test results of the BC, DHBC and DB-G samples in simulated body fluid are shown in Fig. 3. As expected in simulated body fluid environment the BC shown undegradable or degradation-resistant characteristics. By periodate oxidation, DHBC and DB-G composite scaffold materials are showed certain degradability. After 60-90 d, the composite scaffold materials basically achieved full biodegradation. After 90 d, DHBC mass loss rate reached 86.6 % ± 2.5 %, and DB-G0.1, DB-G0.2 and DB-G0.3 are 90.1 % ± 2.1 %, 92.8 % ± 1.9 % and 95.1 % ± 2.0 %, respectively. Degradation performance completely can satisfy the demands of general tissue engineering scaffold materials degradation period. As a result, the DB-G is a potential biodegradable tissue engineering scaffold material.

3.2 FT-IR spectroscopy

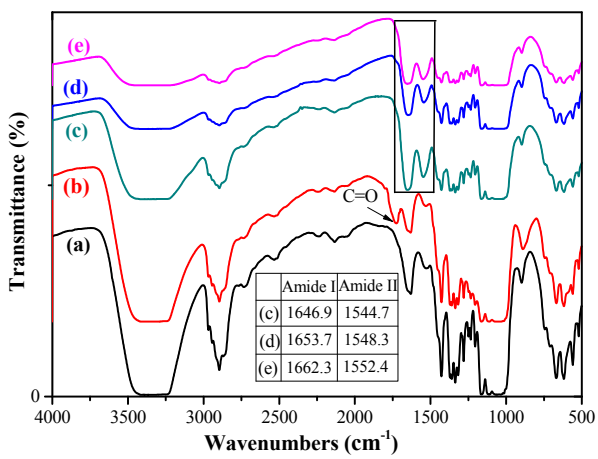

Fig. 4FT-IR spectra of different materials. (a) BC; (b) DHBC; (c) DB-G0.1; (d) DB-G0.2; (e) DB-G0.3.

FT-IR spectra contrasted the structure changes of BC, DHBC, DB-G0.1, DB-G0.2 and DB-G0.3 are shown in Fig. 4. The aldehyde content (42.6 % ± 0.5 %) of DHBC was measured by the method of Schiff base reaction with hydroxylamine. By comparing with BC (curve (a)), the C=O stretching vibration characteristic peak appeared obviously at 1740 cm^{-1} (see arrow mark) in the infrared spectra of DHBC (curve (b))[7, 16] . At 3200 cm^{-1}-3500 cm^{-1} and 1000 cm^{-1}-1150 cm^{-1} the wide association absorption peaks are stretching vibration characteristic absorption peak of OH and C–O[22-24]. Also by contrast to BC and DHBC the C=O stretching vibration absorption peak disappeared, but a set of new characteristic peak (marked with box) occured in the infrared spectra of DB-G. The two peaks are the typical bands as to C=O stretching at 1600-1680 cm^{-1} for amide I (at the same time the –C=N (Fig. 2) stretching vibration absorption peak is also in the wave number region), N–H bending at 1500-1550 cm^{-1} for the amide II[25-27] . It indicated that the crosslinkings (Fig. 2) of –CHO and $–NH_2$ has occurred. In addition, it can be observed that with the increasement of gelatin content the intensity of characteristic absorption peaks and width have become weaker and wider, and the red shift also occurred (Fig. 4). This may be because, with the increase of crosslinking degree, the interaction of hydrogen bonding increased between protein molecules[25, 27] .

3.3 Specific surface area and porosity

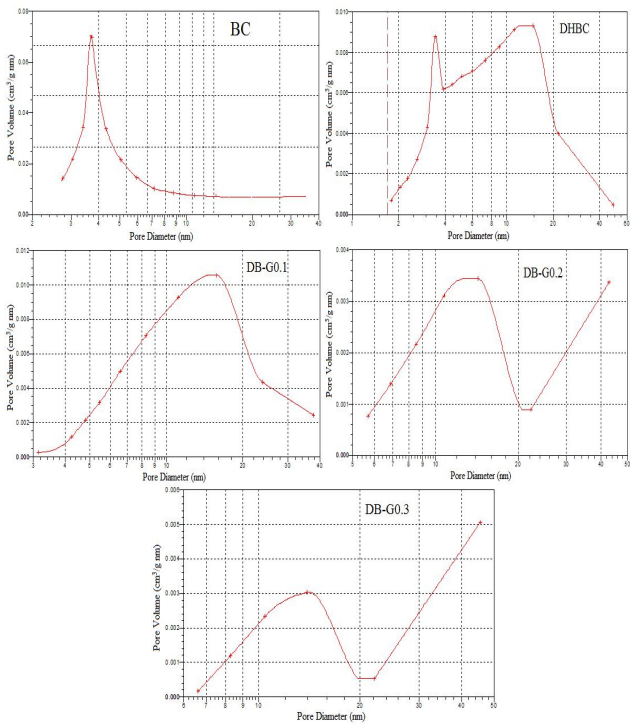

Fig. 6 The porosity distribution of different materials.

Tissue engineering scaffold materials require with three-dimensional porous structure, high porosity and specific surface area in order to meet the exchange of materials, enough space for cell regeneration, inner growth of blood vessels and nerves and exchange channels of metabolites and gas [28]. The changes of BET surface area are shown in Fig. 5. The BET surface area of DB-G0.1, DB-G0.2 and DB-G0.3 (65.1968 ± 0.5565, 53.1310 ± 0.4324, 39.2449 ± 0.7630) were presented declining. This means that as the amount of gelatin increased, aperture of material was decreased, porosity was reduced, but the density of base frame was raised. These features are extremely adverse to scaffold materials. At the same time, from the pore size distribution of material samples (Fig. 6) we also can observe the decreasing pore diameter and pore volume. So according to the comprehensive analysis about specific surface area and pore size distribution, the DB-G0.1 and DB-G0.2 are ideal tissue engineering scaffold materials.

3.4 Scanning electron microscopy

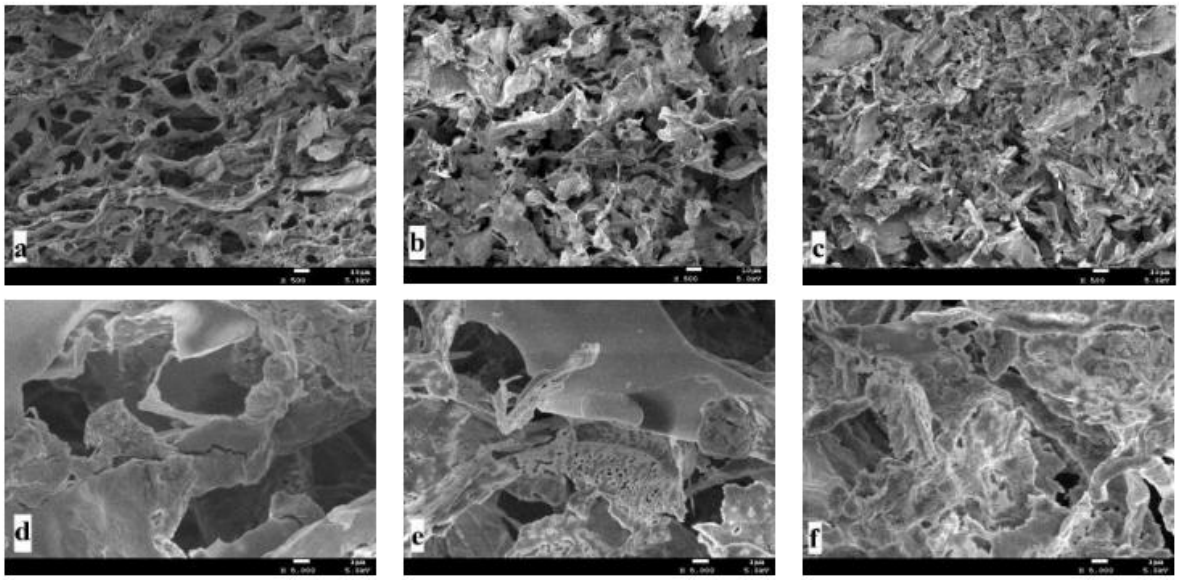

Fig. 7 SEM images of different materials. (a) BD-G0.1 (500 ×); (b) BD-G0.2 (500 ×); (c) BD-G0.3 (500 ×); (d) BD-G0.1 (5000 ×); (e) BD-G0.2 (5000 ×); (f) BD-G0.3 (5000 ×).

The 3D morphology changes of DB-G0.1, DB-G0.2 and DB-G0.3 are shown in Fig. 7. With the increase of gelatin dosage, the aperture and porosity of composite are reduced, on the contrary, the density was increased. The 3D porous structure of DB-G0.1 (Fig. 7(a) and 7(d)) can be clearly observed, and the gelatin molecules formed a regular grid structure. One obvious change in morphology was that more gelatin molecules crosslinked and adhered on the surface of material in the DB-G0.2 (Fig. 7(b) and 7(e)), but the 3D spatial structure was also presented. What's more, from DB-G0.3 space morphology structure (Fig. 7(c) and 7(f)) we can observe that the gelatin molecules were densely covered on the surface of composite, which are extremely unfavorable for the tissue engineering scaffold material required to owe three-dimensional porous structure. It also demonstrated the analysis results of specific surface area and porosity. So the DB-G0.1 and DB-G0.2 composites are potential tissue engineering scaffold materials owing to retainning the 3D network structure and suitable gelatin coating.

3.5 Thermogravimetric analysis

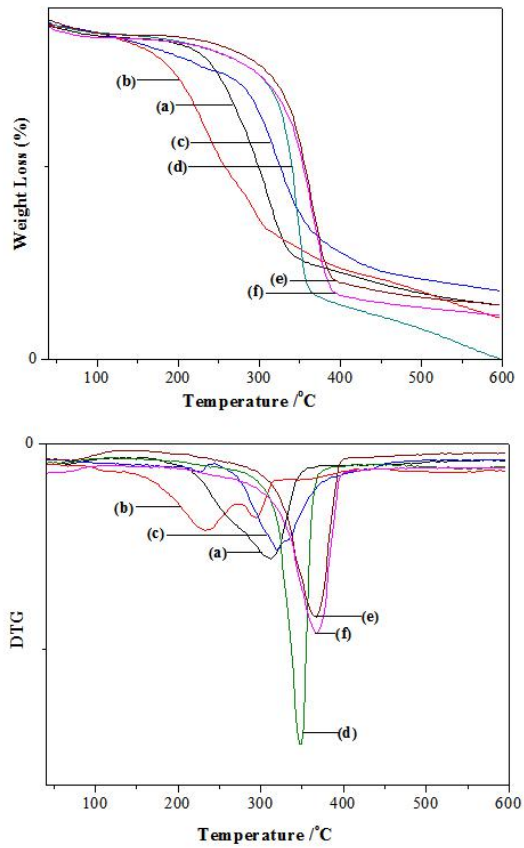

Fig. 8 TG and DTG scan results of different materials. (a) BC; (b) DHBC; (c) gelatin; (d) DB-G0.1; (e) DB-G0.2; (f) DB-G0.3.

The thermal stability test results of materials are shown in Fig. 8. From the data of T_i, we can learn that because of antioxidant oxidation erosion, a mountain of intermolecular and intramolecular hydrogen bondings were broken, and aggregation degree or crystallinity of molecules were droped, which made the heat stability and initial weight-loss temperature of DHBC (187.3°C) were lower than BC (252.5°C). However, due to crosslinkings of DHBC and gelatin, the thermal stability of materials has obviously improved, and the initial weight loss temperature of DB-G0.1, DB-G0.2 and DB-G0.3 (317.3°C, 326.7°C, 328.4°C, respectively) was far higher than gelatin (293.6°C) and DHBC. Similarly according to the peak value of DTG curve from different materials, the biggest weightlessness temperature of DHBC (231.9°C) was lower than BC (312.0°C), decreasing 80.1°C. But the DB-G0.1, DB-G0.2 and DB-G0.3 were reflected the high thermal stability (348.1°C, 365.3°C, and 367.1°C, respectively). In addition, the difference of biggest weightlessness temperature between DB-G0.2 and DB-G0.3 was less than 2°C, which means when the dosage of gelatin reached 0.2 %, the active group of DHBC (–CHO) and gelatin ($–NH_2$) has almost achieved the biggest crosslinking, and adding excessive gelatin dosage just formed surface adhesion by hydrogen bond, hydrophobic bonding, and as on, which was without too much help for the thermal stability of composite. At the same time, illustrated that the thermal stability of DHBC and gelatin crosslinked composites can completely meet the requirements of thermal stability for tissue engineering scaffold material.

4. Conclusions

According to the test results of the degradation DB-G had a good biodegradable properties, and completely could satisfy the demands of general tissue engineering scaffold materials degradation period. By FT-IR spectra analysis, after crosslinking the C=O stretching vibration absorption peak (1740 cm^{-1}) of DHBC disappeared, on the contrary, in 1600-1680 cm^{-1} and

1500-1550 cm-1 the typical amide I (C=O) and amide II (N–H) of infrared absorption peak appeared, and the red shift occured with the increasement of concentration of gelatin solution. Through the comprehensive analysis of the specific surface and porosity and SEM, 0.2 wt% of gelatin solution is appropriate dosage, not only can reach a certain degree of crosslinking, but also can keep the larger specific surface area and appropriate porosity, which is good for materials used in tissue engineering. Through the TG/DTG data analysis, we can observe the composites of DB-GEL owed excellent thermal stability, and the thermal stability of composites were greatly improved along with chemical crosslinking with gelatin molecules. Finally confirmed that the DB-GEL composite is a potentially biodegradable and biocompatible tissue scaffold material.

5. Acknowledgements

The authors wish to acknowledge the financial support of the National Science Fund for Distinguished Young Scholars (51243006).

6. References

[1] Lynch I. Are there generic mechanisms governing interactions between nanoparticles and cells? Epitope mapping the outer layer of the protein–material interface[J]. Physica A Statistical Mechanics & Its Applications. 2007, 373(36): 511-520.

[2] Srouji S, Kizhner T, Suss-Tobi E, et al. 3-D Nanofibrous electrospun multilayered construct is an alternative ECM mimicking scaffold[J]. Journal of Materials Science Materials in Medicine. 2008, 19(3): 1249-1255.

[3] Stevens M M, George J H. Exploring and engineering the cell surface interface[J]. Science. 2005, 310(5751): 1135-1138.

[4] Barud H S, Marques R F C, Lustri W R, et al. Antimicrobial bacterial cellulose-silver nanoparticles composite membranes[J]. Journal of Nanomaterials. 2011, 2011(6): 10.

[5] Hu W, Chen S, Yang J, et al. Functionalized bacterial cellulose derivatives and nanocomposites[J]. Carbohydr Polym. 2014, 101(1): 1043-1060.

[6] Hoffman A S. Applications of radiation processing in biomedical engineering—A review of the preparation and properties of novel biomaterials[J]. Radiation Physics and Chemistry (1977). 1977, 9(1-3): 207-219.

[7] Li J, Wan Y, Li L, et al. Preparation and characterization of 2, 3-dialdehyde bacterial cellulose for potential biodegradable tissue engineering scaffolds[J]. Materials Science and Engineering: C. 2009, 29(5): 1635-1642.

[8] Singh P, Carraher C, Schwarzbauer J E. Assembly of Fibronectin Extracellular Matrix[J]. Annual Review of Cell & Developmental Biology. 2010, 26(26): 397.

[9] Hirschi S D, Gray S D, Thibeault S L. Fibronectin: an interesting vocal fold protein[J]. Journal of Voice. 2002, 16(3): 310-316.

[10] Bradshaw M J, Smith M L. Multiscale relationships between fibronectin structure and functional properties[J]. Acta biomaterialia. 2014, 10(4): 1524-1531.

[11] Copie V, Tomita Y, Akiyama S K, et al. Solution structure and dynamics of linked cell attachment modules of mouse fibronectin containing the RGD and synergy regions: comparison with the human fibronectin crystal structure.[J]. Journal of molecular biology. 1998, 277(3): 663-682.

[12] Elzoghby A O. Gelatin-based nanoparticles as drug and gene delivery systems: reviewing three decades of research[J]. Journal of Controlled Release. 2013, 172(3): 1075-1091.

[13] Wang H, Boerman O C, Sariibrahimoglu K, et al. Comparison of micro-vs. nanostructured colloidal gelatin gels for sustained delivery of osteogenic proteins: Bone morphogenetic protein-2 and alkaline phosphatase[J]. Biomaterials. 2012, 33(33): 8695-8703.

[14] Gómez-Guillén M C, Giménez B, López-Caballero M A, et al. Functional and bioactive properties of collagen and gelatin from alternative sources: A review[J]. Food hydrocolloids. 2011, 25(8): 1813-1827.

[15] Pickford A R, Potts J R, Bright J R, et al. Solution structure of a type 2 module from fibronectin: implications for the structure and function of the gelatin-binding domain[J]. Structure. 1997, 5(3): 359-370.

[16] Luo H, Xiong G, Hu D, et al. Characterization of TEMPO-oxidized bacterial cellulose scaffolds for tissue engineering applications[J]. Materials Chemistry & Physics. 2013, 143(1): 373-379.

[17] Kim U J, Kuga S, Wada M, et al. Periodate oxidation of crystalline cellulose[J]. Biomacromolecules. 2000, 1(3): 488-492.

[18] Nam Y S, Yoon J J, Park T G. A novel fabrication method of macroporous biodegradable polymer scaffolds using gas foaming salt as a porogen additive.[J]. J Biomed Mater Res. 2015, 53(1): 1-7.

[19] Hutmacher D W. Scaffolds in tissue engineering bone and cartilage[J]. Biomaterials. 2000, 21(24): 2529-2543.

[20] Singh M, Ray A R, Vasudevan P. Biodegradation studies on periodate oxidized cellulose[J]. Biomaterials. 1982, 3(1): 16-20.

[21] Devi K S, Sinha T J M, Vasudevan P. Biosoluble surgical material from 2,3-diadehyde cellulose[J]. Biomaterials. 1986, 7(3): 193-196.

[22] Saska S, Barud H S, Gaspar A M, et al. Bacterial cellulose-hydroxyapatite nanocomposites for bone regeneration[J]. International Journal of Biomaterials,2011,(2011-09-27). 2011, 2011(2011): 175362.

[23] Barud H S, Assunção R M N, Martines M A U, et al. Bacterial cellulose–silica organic–inorganic hybrids[J]. Journal of Sol-Gel Science and Technology. 2008, 46(3): 363-367.

[24] Fan Q G, Lewis D M, Tapley K N. Characterization of cellulose aldehyde using Fourier transform infrared spectroscopy[J]. Journal of Applied Polymer Science. 2010, 82(5): 1195-1202.

[25] Chang M C, Ko C C, Douglas W H. Conformational change of hydroxyapatite/gelatin nanocomposite by glutaraldehyde[J]. Biomaterials. 2003, 24(18): 3087.

[26] Payne K J, Veis A. Fourier transform ir spectroscopy of collagen and gelatin solutions: Deconvolution of the amide I band for conformational studies[J]. Biopolymers. 1988, 27(11): 1749.

[27] Chang M C, Ko C C, Douglas W H. Preparation of hydroxyapatite-gelatin nanocomposite.[J]. Biomaterials. 2003, 24(17): 2853-2862.

[28] Wu L, Ding J. In vitro degradation of three-dimensional porous poly(D,L-lactide-co-glycolide) scaffolds for tissue engineering[J]. Biomaterials. 2004, 25(27): 5821-5830.

P31

Research on the fashion of leather products

Yufeng Hou

Zhejiang fashion institute of technology Fenghua road 495 ningbo china 13221922011 542755055@qq.com

Abstract

Thefashion of leather products is an improve factor to enhance the core competitiveness of products and the added value of products. The innovation of style and modeling ,the content and from of patterns ,the rational collocation of color, the re creation the application of new technology, the cross boundary of design and the development of culture are all important ways for the fashion of leather products

Keywords: Leather products; fashion; design; creation

P32

Fundamental studies using synchrotron SAXS highlighting pathways towards sustainable leather processing

Yi Zhang[1], Sujay Prabakar[1]

[1]*Leather and Shoe Research Association of New Zealand, P. O. Box 8094, Palmerston North 4472, New Zealand*

E-mail: sujay.prabakar@lasra.co.nz Tel: +64 6 355 9028

Abstract

Synchrotron small-angle X-ray scattering (SAXS) were applied to leather research to understand the changes in collagen structure during tanning and denaturation (shrinkage) and to reduce the environmental impact of extensive chrome usage. Based on SAXS results from real-time denaturation experiments on leather samples, we will present a mechanistic model of chrome tanning. It suggests that only a low level of chromium species is effectively involved in the cross-linking with collagen, highlighting the excessive use of chrome during conventional tanning processes. Additionally, results from our *in situ* SAXS tanning experiments showing the different mechanisms of chrome-free alternative tannages will also be presented. Overall, synchrotron SAXS provides valuable information about collagen structure changes that could lead to more efficient use of chrome (or other tanning agents) in the global leather processing industry.

Keywords: real-time SAXS, collagen structure, denaturation, chrome tanning, sustainable leather processing.

P33

Establishment of Environmental Risk Assessment and Management System of Leather Chemicals

Chao Zhu[1], Hongrui Ma[2], Huiqin Wang[3], Yongyong Hao[4], Qing Wang[5]

[1] *School of Environmental Science & Technology, Shaanxi University of Science andTechnology, Xi'an 710021, China, 0086-13891858706, 304545693@qq.com*

[2] *School of Environmental Science & Technology, Shaanxi University of Science andTechnology, Xi'an 710021, China, 0086-13991376232, mahr@sust.edu.cn*

[3] *School of Environmental Science & Technology, Shaanxi University of Science andTechnology, Xi'an 710021, China, 0086-15802945809, 635514485@qq.com*

[4] *School of Environmental Science & Technology, Shaanxi University of Science andTechnology, Xi'an 710021, China, 0086-18629058830, 869233262@qq.com*

[5] *School of Environmental Science & Technology, Shaanxi University of Science andTechnology, Xi'an 710021, China, 0086-18729359446, 1193757151@qq.com*

Abstract

The environmental risk assessment of chemicals is described and analyzed on the basis of their objective properties and available data. Typical chemicals of leather industry involve surfactant, auxiliary agents, tanning agent, coating agent, fatliquoring agent and dye for leather. There are now more than 2,000 companies engaged in the production of leather chemicals, about 2,000 kinds of chemicals including 127 substances of very high concern (SVHC) and over 1 million tons of production. At present, China has become a world recognized leather producing country, and also has the largest leather chemical market in the world, which, considering the waste water releases of 1.8×10^9 tons from leather production, requestsa sound risk assessment system and management system for the sustainable development of leather industry. Limited by the scope of the existing legal regulation, management has not yet been fully covered a wide range of chemicals and potentially harmful chemicals, especially being weak in chemical space control , total amount control and access control. This study discussed the existing environmental risk assessment method of the poisonous and harmful chemicals， the standards and details on ecological and healthy risk assessment of leather chemicals. The problems of leather chemicals in production， application and management were analyzed and the feasible countermeasures were put forward in order to establish the environmental risk assessment methods and environmental management system of leather chemical.

Keywords: Leather chemicals; Environmental risk assessment; Management system

P34

Evaluation of the Biostability of Chrome Tanning Waste Liquid in Closed Recycling Process

Chao Zhu[1], Wenxin Li[2], Xihuai Qiang[3], Chuanbo Zhang[4], Zhuangdou Zhang[5]

[1] School of Environmental Science & Technology, Shaanxi University of Science andTechnology, Xi'an 710021, China, 0086-13891858706, 304545693@qq.com

[2] College of Bioresources Chemical & Materials Engineering, Shaanxi University of Science and Technology, Xi'an 710021, China, 0086-13891858706, liwx@sust.edu.cn

[3] College of Bioresources Chemical & Materials Engineering, Shaanxi University of Science and Technology, Xi'an 710021, China, 0086-13992097526, qiangxihuai@163.com

[4] College of Bioresources Chemical & Materials Engineering, Shaanxi University of Science and Technology, Xi'an 710021, China, 0086-13992027810, zhangcb0630@163.com

[5] BIOSK Chemicals Co., Ltd., Shangqiu 476000, China, 0086-13937009899, 2153209283@qq.com

Abstract

End-of-pipe-treatment is generally adopted by leather enterprises to control leather-making wastewater, which wastes a large number of unused chemical materials considering as pollutants and increases the pressure of wastewater control. The recycling of chrome tanning waste shows great potential in the promotion of clean production of leather. In this study the biostability of chrome tanning waste liquid as an critical characteristic to evaluate this process was studied by determination and comparison of the biological oxide demand of 5 days (BOD_5), biodegradable dissolved organic carbon (BDOC) and assimilable organic carbon (AOC) concentration of chrome tanning waste liquid of different recycling periods as well as their influence to microbial metabolism. Results showed that the BOD_5 concentration stayed stable around 25mg/L from recycling times of 2 to 10 which was obviously lower than the 1st recycling and the 60th recycling. BDOC and AOC concentrations were both stable during the recycling period of 60 times and with lower values. Comparing to the control, the recycling tanning liquid, even at a serial dilution from 10 to 1000 times, all represented significantly higher inhibitory effect to microbial metabolism. The biostability of the tested tanning waste liquid in closed recycling process was high and stable, indicating great practical potential.

Keywords: Biostability, Chrome tanning, Microbial metabolism, BOD_5, BDOC, AOC

P35

A Novel Approach for Lightfast Wet-white Leather Manufacture Based on Sulfone Syntan-aluminium Tanning Agent Combination Tannage

Long Zhang[1], Chunhua Wang [1],and Wei Lin[2]

Department of Biomass and Leather Engineering,Collegeof Light Industry , Textile and Food Engineering, Sichuan University, Chengdu, China, 610065

Key Laboratory of Leather Chemistry and Engineering of Ministry of Education, Sichuan University, Chengdu,China, 610065

Abstract

Wet-white tanning as an eco-friendly leather-making process has been attracting considerable attention. Herein, we have investigated a novel combination tannage for lightfast wet-white leather based on sulfone syntan and aluminium tanning agent. By optimizing the technology, 10% sulfone syntan and 3% aluminium tanning agent at final pH 4.0 - 4.5 can raise the shrinkage temperature (T_s) of the wet-white leather to ~81 °C. The synergistic tanning mechanism of the two has been illustrated. As verified by Zeta potential measurements, the introduction of Al^{3+} into the sulfone syntan system ledto the increase in the isoelectric point (IEP) of wet-white leather, which is favorable for the subsequent post-tanning process. Scanning electron microscope-Energy dispersive X-ray spectroscopy (SEM-EDX) results reveal that sulfone syntan and aluminium tanning agent can be evenly bound within the leather matrix, and promote the formation of tightly woven networks of collagen fibres. The novel combination tanning approach not only improves light fastness and lighter shade, but also confers high physical and mechanical properties to the wet-white leather.

Keywords: wet-white leather, sulfone syntan, aluminium tanning agent, combination tannage, light fastness

P36

Hydrolysis of Abandoned Cowhair and Preparation of Protein-Based Liquid Membrane

Wenxin Li(Shaanxi University of Science & Technology) China liwx@sust.edu.cn
Yurou Chen(Shaanxi University of Science & Technology) China 2622157536@qq.com
Sufeng Zhang(Shaanxi University of Science & Technology) China zhangsufeng@sust.sdu.cn

ABSTRACT

In our country,film mulching is one of the main techniques for agricultural cultivation,traditional plastic agricultural mulch will cause white pollution to the environment after use. Abandoned bovine hair produced during the leather tanning process is a keratin resource. Because of its good thermal stability, high biodegradability and mechanical properties, bovine hair keratin also contains large amount of sulfur and nitrogen. Sulfur and nitrogen fertilizers supplement the nutrition of crops. The new liquid mulch film which made of keratin-based waste cattle wool not only has the properties of heat preservation, entropy increase, and promotion of crop growth, but also saves resources and reduces environmental pollution.

In this study, a liquid mulch was prepared from discarded bovine keratin and its physicochemical properties were characterized. Firstly, the cow hair was hydrolyzed by alkali oxidation method, and the hydrolysis conditions such as NaOH concentration, H_2O_2 concentration, hydrolyzate ratio, hydrolysis time and temperature were investigated.Second-ly, the blended membrane was prepared by using bovine hair hydrolysate and PVA, glutaraldehyde and glycerin. The non-volatile content, tensile strength, elongation at break and swellability in water were used as indicators to analyze the single factor method. The effects of the mass ratio of hydrolysate to PVA, the amount of glutaraldehyde, the amount of glycerin, the blending temperature and the blending time on the properties of the blended membrane were investigated. Finally, the structure and properties of the blend membrane were characterized by XRD, FT-IR, SEM and DSC. The experimental results show that the optimal hydrolysis process is: hydrolysis of 5g bovine hair, alkali dosage 1.2g, hydrogen peroxide 15mL, water dosage 45mL, temperature 90°C, time 4h; optimal membrane preparation process: hydrolysate and PVA mass 8:1, glycerol 0.3 g, glutaraldehyde 0.2 g, temperature is 100°C, time 40 min. The blend membrane has the keratin structure, good thermal stability, and has certain characteristics of moisturizing, heat preservation and promoting crop growth and development.

key words：Bovine hair keratin,Alkali oxidation,hydrolysis,Polyvinyl alcohol,Liquid mulch

P37

Preparation of functionalized graphene nanosheet/waterborne organosilicon nanocomposites and their application in leather finishing

Wen Huitao[1,2], YAO Qingda[2,3] , WANG Xiaozhuo[2,3],

YANG Yiqing[2,3] , LIANG Yongxian[2,3], Dan Weihua[1,2*]

[1]*National Engineering Laboratory for Clean Technology of Leather Manufacture, Sichuan Univerisity, Chengdu 610065, China；028-85408988；dwh5607@263.net；*

[2]*Fujian Key Laboratory of Green Design and Manufacture of Leather,Xingye Leather Technology Co., Ltd., Jinjiang 362261, China；0595-68583172；lyx@xingyeleather.com；*

[3]*Xingye Leather Technology Co.,Ltd., Jinjiang, Fujian 362261, China；0595-68583175；wht@xingyeleather.com；*

Abstract

In order to improve the surface properties of the finished leather, functionalized graphene nanosheet/waterborne organosilicon nanocomposites were prepared by the sol-gel method. The formulation and finishing process of the leather top coating agent, which consists of waterborne membrane-forming agents such as waterborne polyurethane, waterborne acrylic resin, assistants and water, was designed and optimized by orthogonal test. The nanocomposites can also be diluted directly by water and used as an effective coating. The results showed that the waterproof performance, dry / wet rubbing resistance and friction resistance were improved, and the sensory performance was good, and the physical and chemical indexes met the leather standard (QB/T 1873-2010).

Keywords: Leather；Finishing；Surface properties；Functionalized graphene；Waterborne organosilicon

P38

Removal of acid dye from aqueous solution by using amphoteric polyvinylamine immobilized on ferroferric oxide

Hao Lan, Yu-lu Wang*, Liqiang Jin, Hong Yang, Shaodi Xiu, Jinxu Xu

School of Leather Chemistry and Engineering, Qilu University of Technology (Shandong Academy of Sciences), 250353, China

** Correspondence: wangyulu@qlu.edu.cn; Tel.: +86-0531-8963-1786*

Abstract

The amphoteric polyvinylamine was immobilized on ferroferric oxide particles to prepare a novel absorbent for the removal of acid dye from aqueous solution. It was proved the amphoteric polyvinylamine was successfully loaded on the ferroferric oxide particles according to the FTIR and TG analysis. The absorption of the acid yellow G was influenced notably by the initial pH of the solution and the removing rate of the dye decreased as the pH increased from 3 to 7. The maximum adsorption capacity to acid yellow G was 1267mg/g at 40 ºC and pH 3, while the adsorption equilibrium data and kinetics could be described by Langmuir model and a pseudo-second-order rate model, respectively.

Key words: amphoteric polyvinylamine; ferroferric oxide; adsorption; dye

1. Introduction

With the rapid development of textile, leather, plastic, paper-making, cosmetics and other manufacturing, water contamination caused by synthetic dyes has become a serious global problem [1, 2]. Most dyes are synthetic in nature and usually composed of aromatic rings, which are inert, non-biodegradable and cause serious pollution on the ecological system as well as tremendous pressure on wastewater treatment systems. Additionally, it has been proved that ingestion of excessive dyes would cause direct damage to liver, digestive system and central nervous system of human beings [3]. Therefore they are considered as the first contaminant of wastewater, which are highly desirable to be eliminated prior to discharging [4-6].

Up to now, many techniques such as flocculation, membrane separation, filtration, oxidation, photocatalysis, electrolysis and ion-exchange are used for the purification of wastewater [7, 8]. However, their extensive applications are restricted by the high capital investment and operating costs [10]. Compared with the methods mentioned above, adsorption has received many attentions and become the major technique for removal of dyes from wastewater due to its low cost, high efficiencies and flexibility in designing and operating [11]. Especially, abundant of interests have been paid on the development of magnetic absorbents with various functionalities [12-14].

It is proved that the introduction of ferroferric oxide (Fe_3O_4) into powdery adsorbents can generate excellent separation efficiency from solution by external magnetic field after absorption, which is in favor of the recovery and reuse of the absorbents [12-17]. And many researches have been focus on developing new kinds of magnetic absorbents and improving their adsorption capacities. In this paper, amphoteric polyvinylamine was immobilized on Fe_3O_4 to prepare a novel magnetic absorbent (APFe) with high adsorption capacities to dyes, and the chemical structures as well as its adsorption performance were studied in details.

2. Experimental

2.1 Materials

$FeSO_4 \cdot 7H_2O$, $Fe_2(SO_4)_3$ anhydrous, $NH_3 \cdot H_2O$ (25%), $Al_2(SO_4)_3$, HCl, NaOH and ethanol absolute used were of analytical grade and purchased from Sinopharm Chemical (Shanghai, China). Amphoteric polyvinylamine (20%, w/w) with carboxyl as the anionic groups and a molecular weight of 150 kDa was provided by BASF (China) Co. Ltd.. The acid light yellow G (C.I. Acid Yellow 11; CAS: 6359-82-6, λ_{max}=418nm), commercial anionic dye, was supplied by Jinan Yongxing Chemical Co. Ltd.

2.2 The preparation of magnetic absorbent

Fe_3O_4 particles were synthesized by coprecipitating Fe (II) and Fe (III) sulfate in aqueous solution with the existence of

$NH_3 \cdot H_2O$ according to a literature elsewhere [18]. Briefly, 11.72 g of iron (II) sulfate and 17.07 g of iron (III) sulfate were dissolved in 200 mL of water at 25 ºC and stirred for 30 min. The pH value of obtained solution was adjusted to 10 by the addition of 25% ammonia solution at 50 ºC. The black precipitates were washed with ethanol and deionized water sequentially until the pH was about 7.0 and collected from the solution by magnetic separation. The precipitates were dried under vacuum at 50 ºC for 12 h.

2.0 g Fe_3O_4 particles was placed in 20 mL deionized water and treated with ultrasonic for 30 min. Then, this black suspension solution was mixed with 10 g amphoteric polyvinylamine solution for 30 min with ultrasonic. After that, about 30 mL ethanol absolute was dropped into the system above with stirring for the precipitation of amphoteric polyvinylamine. 60 min later, 2.0g $Al_2(SO_4)_3$ solution (10%, w/w) was added drop by drop and reacted for 1h at room temperature to immobilize the polymer on the surface of ferroferric oxide. The final products were separated from the supernatant by using a magnetic force and dried under freezing vacuum. Finally, the absorbents (APFe) were pressed for tableting and then sieved at 40–60 mesh.

2.3 Characterization of the absorbents

The FT-IR spectra of Fe_3O_4 particles and APFe were made in powder form by mean of a obtained by TENSOR-27 (Bruker, Ettlingen, Germany) spectrophotometer over the wave number range from 4000–400 cm^{-1} in KBr disks. The thermogravimetric (TG) characteristics of samples were investigated by a Q500 thermogravimetric analyzer (TA Instruments, Milford, MA, USA) from room temperature to 600 ºC at a heating rate of 10◦C/min in a nitrogen atmosphere.

2.4 Batch adsorption experiments

2.4.1 The effect of initial pH on adsorption capacities

50mg APFe was suspended in 100 mL of 300 mg/L acid light yellow G solution. The pH values were adjusted from 3 to 7 by using 1 mol/L HCl and 1 mol/L NaOH solution. The adsorption experiments were conducted with constant shaking at 40 ºC for 5h. After adsorption, the concentration of the residual acid light G was analyzed by UV-Vis Spectrophotometer (UV-Vis 3600, Shimadzu, Japan) on the basis of λ_{max} and the adsorption capacity was calculated by mass equilibrium.

2.4.2 The effect of adsorbent offer on extent of removal dye

10, 50, 100, 150 and 200 mg APFe were suspended in 100 mL of 500 mg/L dye solutions at pH 3 and 40 ºC for 5 h. The adsorption procedures were the same as section 2.4.1.

2.4.3 Adsorption isotherms

Adsorption isotherm tests were conducted by adding 50 mg adsorbent into dye solutions with specific initial concentrations ranging from 100 to 500 mg/L at pH 3 for 5 h at 30, 40 and 50 ºC, respectively. Langmuir and Freundlich models were applied to analysis the adsorption experiments data. The Langmuir model is based on the assumption that monolayer adsorption occurs on the surface of adsorbents and all adsorption sites are identical, which can be expressed as equation 1[19].

$$\frac{C_e}{q_e} = \frac{1}{q_{max} K_L} + \frac{C_e}{q_{max}} \qquad (1)$$

where q_{max} and q_e are the maximum adsorption capacity and the adsorption capacity (mg/g) at equilibrium of the adsorbent (mg/g) respectively, while the C_e (mg/L) is the concentration of the dye at equilibrium. And K_L is the Langmuir constant related to the energy of the adsorption process (L/mg). The q_{max} and K_L were calculated from the intercept and slope of lines obtained from plots between *Ce/qe* versus *Ce*.

The Freundlich model is based on the assumption that multilayer adsorption occurs on the surface of adsorbents with unequally available sites of different adsorption energies. Freundlich equation is expressed as equation 2 [20].

$$\ln q_e = ln K_F + \frac{1}{n} ln C_e \qquad (2)$$

where K_F is the Freundlich constant ((mg/g) $(L/mg)^{1/n}$), n is the heterogeneity factor. The K_F and n are calculated from the

intercept and slope of the Freundlich plots.

2.4.4 Adsorption kinetic

To evaluate the adsorption behavior of the samples, 50 mg adsorbent was respectively added into 100 mL dye solution with fixed concentrations of 300 mg/L. The mixtures were standing in a conical flask (250 mL) at pH 3 and 30, 40, and 50 ºC, respectively. The concentrations of dye in solutions were measured at an interval of 20min during the adsorption processes. In order to analyze the adsorption kinetics for the adsorption of dye onto APFe, pseudo-first-order kinetic model (equation 3) [21] and pseudo-second-order kinetic model (equation 4) [19] were used to fit the experimental data.

$$\frac{1}{q_t} = \frac{k_1}{tq_e} + \frac{1}{q_e} \qquad (3)$$

where q_e and q_t are the adsorption capacity (mg/g) at equilibrium and at time t (h), respectively, and k_1 is the equilibrium rate constant of pseudo-first-order equation (g/mg·h).

$$\frac{t}{q_t} = \frac{1}{k_2 q_e^2} + \frac{t}{q_e} \qquad (4)$$

where k_2 is the equilibrium rate constant of pseudo-second-order equation (g/mg·h).

3. Results and discussion

3.1 Characterization of APFe

The FTIR spectra of Fe_3O_4 particles and the absorbents APFe were shown in Figure 1. As shown in Figure 1, the adsorption peaks at 603 and 3425 cm^{-1} were attributed to the stretching vibration of Fe-O and O-H respectively, which proved that Fe_3O_4 was prepared successfully [22]. Compare with the FTIR spectrum of Fe_3O_4, new adsorption peaks of APFe appeared at 1003 and 1658 cm^{-1}, which were ascribed to the stretching vibration of C-N and C=O, respectively. Especially, the peaks at 3429 and 1573 cm^{-1} corresponded to the two characteristic bands of N-H of primary amine of amphoteric polyvinylamine [23]. The FTIR results indicated that the amphoteric polyvinylamine had been immobilized on the Fe_3O_4 tightly.

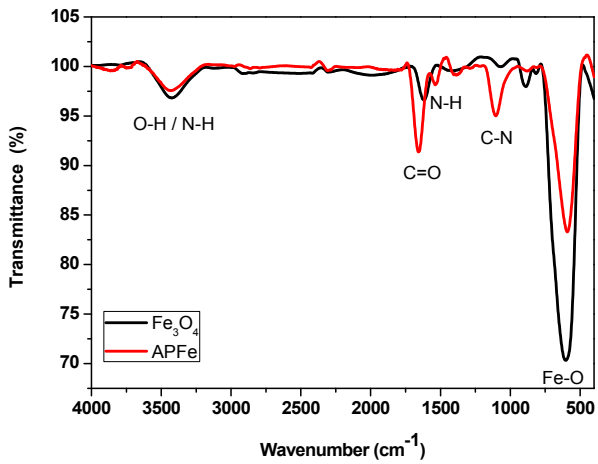

Figure 1. The FTIR spectra of Fe_3O_4 and APFe

Furthermore, the thermal stability of Fe_3O_4 and APFe was investigated by a thermogravimetric (TG) analyzer, while their TG curves were shown in Figure 2. In the case of Fe_3O_4, there was no obvious weight loss from room temperature to 600 ºC. However, about 25% weight loss for APFe was at 120 ºC, which was due to the removal of water adsorbed on APFe. From 120 ºC to 600 ºC, the weight loss of APFe was about 13% which depended on the decomposition of amphoteric polyvinylamine. The analysis of TG agreed well with the results of FTIR.

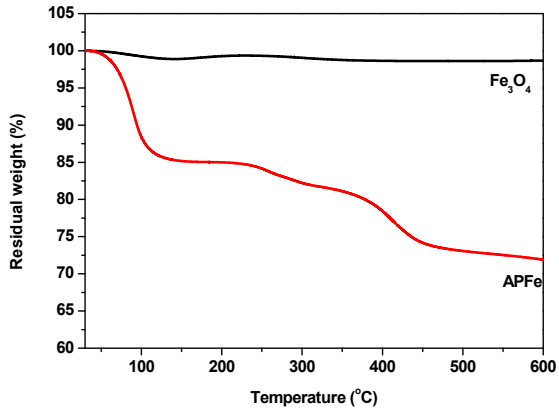

Figure 2. Thermogravimetric (TG) curves of Fe_3O_4 and APFe

3.2 The effect of initial pH on adsorption capacities

Generally, the capacities of most absorbents were greatly influenced by initial pH of the solution as the surface charges were changed. While the effect of initial pH on adsorption capacities of APFe was shown in Figure 3. The adsorption capacities of APFe decreased obviously as the increase of initial pH. The adsorption capacity of APFe to acid light yellow G at equilibrium (q_e) at pH 3 was 577mg/g, however it decreased to about 203mg/g at pH 7. This was because the surfaces of the absorbents are amino groups derived from amphoteric polyvinylamine, which were positive charged at lower pH values. As the increased of pH the electro-positivity of APFe as well as the electrostatic interaction against acid dyes decreased. On the other hand, the electronegativity of APFe increased at high pH and the electrostatic repulsion of the absorbent to acid dye was enhanced [24]. Therefore, the adsorption experiments below were carried out at pH 3.

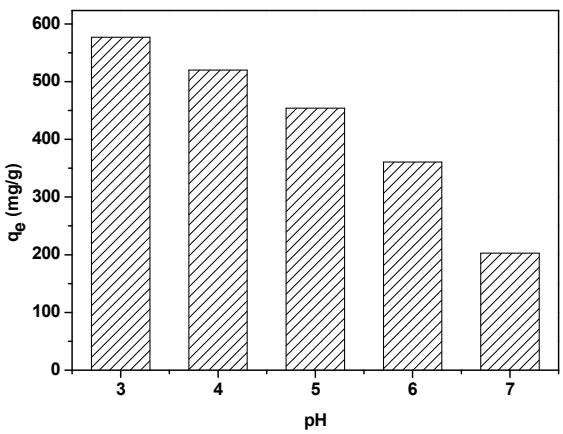

Figure 3. The effect of initial pH on the adsorption capacities of APFe.

3.3 The effect of adsorbent offer on extent of removal dye

The dosage of the APFe has a significant influence on the removal of dyes from aqueous solution. The removal extent of acid light yellow G was 25.34% when 0.01 g of adsorbent was used, while it was greatly increased to 95.96% when 0.20 g of adsorbent was used. However, the higher adsorbent dosage resulted in lower q_e value at a fixed dyes concentration (500mg/L), namely it decreased from 1267 to 240mg/g, as shown in Fig.4b. It was attributed to that the surface sites of the adsorbent are heterogeneous [25]. According to the surface site heterogeneity model, the surface is composed of the site with

a spectrum of binding energies. At low adsorbent offers, all types of sites are entirely exposed and the adsorption on the surface is saturated faster, showing a higher q_e value. But at higher adsorbent dosages, the availability of higher energy sites decreases as a larger fraction of sites with lower energy were occupied, which resulted in the lower q_e value [25, 26].

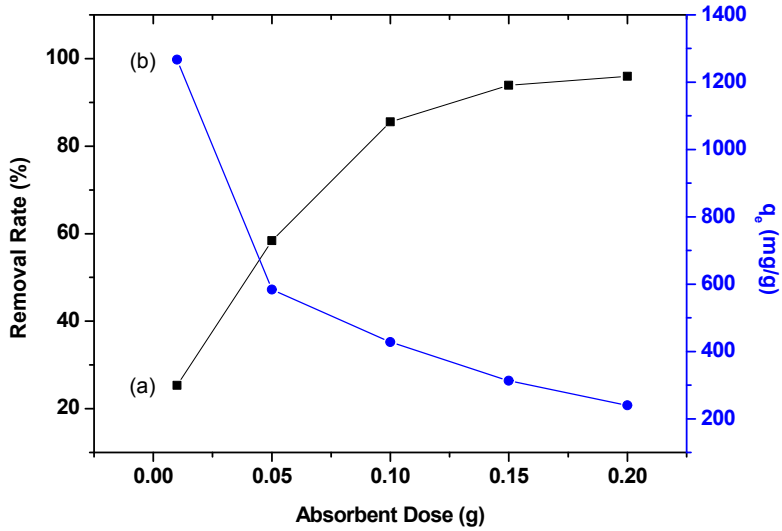

Figure 4. The effect of adsorbent dose on extent of removal of dyes: (a) removal rate and (b) q_e

3.4 Adsorption isotherms

The adsorption isotherms of acid light yellow G adsorbed on APFe at different temperatures were presented in Figure 5. The adsorption capacity of the dye on APFe from 30 to 50 ºC increased firstly and then decreased. It was probably that the energy at 30 ºC was lower and difficult to overcome the steric hindrance derived from the aromatic rings of dye molecules. However, at higher temperature (50 ºC) the dye molecules were easier to escape from the surface of absorbents [27, 28]. Therefore, the adsorption capacities were highest at 40 ºC.

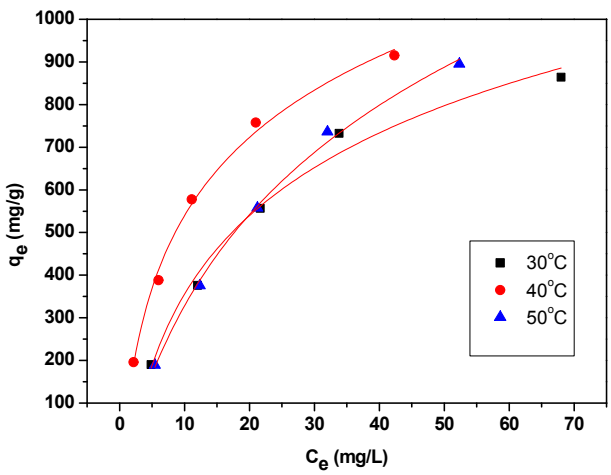

Figure 5. Adsorption isotherms of acid light yellow G on APFe at pH 3.

Moreover, the Langmuir and Freundlich equations were used to analyze adsorption isotherm data, and the parameters of fitting were summarized in table 1. It was found that the Langmuir equation gave a satisfactory fitting to the adsorption isotherms. The nature of dye adsorbed on APFe were the electrostatic interaction of positive charged amino groups on APFe

with the negative charged sulfonic acid groups on dye molecules, which belonged to chemisorption. Therefore, it can be concluded that the adsorption of acid light yellow G on APFe was monolayer chemisorption, which was fitted well by Langmuir model.

Table 1. The Langmuir and Freundlich parameters of dyes on APFe at different temperatures

Model	Parameters	30(ºC)	40(ºC)	50(ºC)
Langmuir	q_{max}(mg.g^{-1})	1250	1250	1667
	$b\times10^5$(L.mg^{-1})	1.672	1.106	1.458
	R^2	0.9934	0.9965	0.9943
Freundlich	ln k (L.g^{-1})	4.410	4.716	4.122
	n	1.691	1.677	1.428
	R^2	0.9644	0.9644	0.9855

3.5 Adsorption kinetic

The adsorption rate curves of acid light yellow G on APFe at different temperatures were illustrated in Figure 6. Its adsorption rate and adsorption capacity were decreased slightly as the increase of temperature. Probably, it was because the electrostatic interaction of APFe with dye was weaker thus higher temperature was in favor of the escaping of dye molecules from the surfaces of APFe.

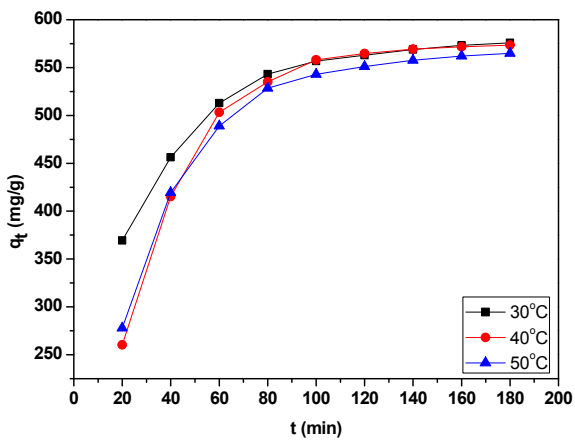

Figure 6. Adsorption rate curves of acid light yellow G on APFe at different temperatures.

Furthermore, in order to further investigate the adsorption mechanism of dyes on APFe, the pseudo-first-order rate model and the pseudo-second-order rate model were used to test the adsorption kinetics data, while the parameters were listed in Table 2. The first-order kinetic model could not give satisfactory fitting to the adsorption kinetic data. However, the description of adsorption rate by the second-order rate equation was considerable and the R^2 are more than 0.99, which indicated that the chemisorption is the rate limiting step [29]. These facts further suggested that the electrostatic interaction of acid dye with APFe could be considered as chemisorption. Similar phenomena were also observed in the adsorption RR189 on cross-linked chitosan beads [30].

Table 2. Adsorption kinetic model parameters of dyes on APFe

Model	Parameters	30(ºC)	40(ºC)	50(ºC)
First-order	$k_1\times10^2$(min^{-1})	2.787	2.718	1.934
model	R^2	0.9934	0.9794	0.9553

	$q_{e,cal}$(mg.g^{-1})	377.6	420.6	309.4
	$q_{e,exp}$(mg.g^{-1})	556.4	577.8	557.5
Second-order	$k_2\times 10^4$(g.mg^{-1}.min^{-1})	0.6484	1.231	0.7975
model	R^2	0.9996	0.9939	0.9971
	$q_{e,cal}$(mg.g^{-1})	625.0	666.7	625.0
	$q_{e,exp}$(mg.g^{-1})	556.4	577.8	557.5

4. Conclusions

A novel absorbent (APFe) was prepared successfully by using amphoteric polyvinylamine immobilized on ferroferric oxide, which was proved by FTIR and TG analysis. It can be used effectively for the removal of anions dyes from aqueous solutions. The adsorption capacities of APFe was influenced greatly by initial pH of the dye solution, while the maximum adsorption capacity of APFe to acid light yellow G at pH 3 and 40 ºC was up to 1267mg/g. Furthermore, the adsorption isotherm analysis indicated that the adsorption process could be fitted well by Langmuir equation, which manifested that the adsorption of acid dye on APFe was monolayer chemisorption. In addition, the satisfactory description of adsorption rate by the second-order rate equation indicated that the chemisorption was the rate limiting step.

Acknowledgement: This paper was supported by the National Key Research and Development Program of China (2017YFB0308503) and the Shandong Provincial Key Research and Development Program, China (2017GGX80103).

References

Xinyi Wan, Yingqing Zhan, Zhihang Long, Guangyong Zeng, Yi He. Core@double-shell structured magnetic halloysite nanotube nano-hybrid as efficient recyclable adsorbent for methylene blue removal. **Chem. Eng. J.** 2017, 330:491-504.

Q. Li, Y. Li, X. Ma, Q. Du, K. Sui, D. Wang, C. Wang, H. Li, Y. Xia, Filtration and adsorption properties of porous calcium alginate membrane for methylene blue removal from water. **Chem. Eng. J.** 2017, 316:623-630.

M.M. El-Zawahry, F. Abdelghaffar, R.A. Abdelghaffar, A.G. Hassabo. Equilibrium and kinetic models on the adsorption of Reactive Black 5 from aqueous solution using Eichhornia crassipes/chitosan composite. **Carbohyd.Polym.** 2016, 136:507-515.

Lixuan Zeng, Meijia Xie, Qiuyun Zhang, Yuan Kang, Xingmei Guo, Huijuan Xiao,Yanni Peng, Jiwen Luo. Chitosan/organic rectorite composite for the magnetic uptake of methylene blue and methyl orange. **Carbohyd.Polym.** 2015, 123:89-98.

Lu Lu, Jia Li, Jing Yu, Peng Song, Dickon H.L. Ng. A hierarchically porous $MgFe_2O_4$/γ-Fe_2O_3 magnetic microspheres for efficient removals of dye and pharmaceutical from water. **Chem. Eng. J.** 2016, 283:524-534.

Chen, Y. F., He, F. B., Ren, Y., Peng, H., Huang, K. X. Fabrication of chitosan/PAA multilayer onto magnetic microspheres by LbL method for removal of dyes. **Chem. Eng. J.** 2014, 249:79-92.

Yang, B. C., Liu, Q., Huo, J., & Huang, R. H. Adsorption of methyl orange from aqueous solutions onto protonated cross-linked chitosan. **J. Funct. Mate.** 2013, 44:376-379.

Yang, Z., Yang, H., Jiang, Z. W., Cai, T., Li, H. J., Li, H. B., et al. Flocculation of both anionic and cationic dyes in aqueous solutions by the amphoteric grafting flocculant carboxymethyl chitosan-graft-polyacrylamide. **J. Hazard. Mater.** 2013, 254–255:36-45.

E. Bulut, M. Ozacar, I.A. Sengil, Equilibrium and kinetic data and process design for adsorption of Congo red onto bentonite, **J. Hazard. Mater.** 2008, 154:613-622.

H. Mittal, S.S. Ray. A study on the adsorption of methylene blue onto gum ghatti/TiO_2 nanoparticles-based hydrogel nanocomposite. **Int. J. Biol. Macromol.** 2016, 88:66-80.

F. Tan, M. Liu, K. Li, Y. Wang, J. Wang, X. Guo, G. Zhang, C. Song. Facile synthesis of size-controlled MIL-100 (Fe) with excellent adsorption capacity for methylene blue. **Chem. Eng. J.** 2015, 281:360-367.

J.L. Gong, B. Wang, G.M. Zeng, C.P. Yang, C.G. Niu, Q.Y. Niu, W.J. Zhou, Y. Liang. Removal cationic dyes from aqueous solution using magnetic multi-wall carbon nanotube nanocomposite as a adsorbent. **J. Hazard. Mater.** 2009, 164:1517-1522.

X.J. Peng, Z.K. Luan, Z.C. Di, Z.G. Zhang, C.L. Zhu. Carbon nanotubes-iron oxides magnetic composites as adsorbent for removal of Pb(II) and Cu(II) from water. **Carbon** 2005, 43:855-894.

C.L. Chen, J. Hu, D.D. Shao, J.X. Li, X.K. Wang. Adsorption behavior of multiwall carbon nanotube/iron oxide magnetic composites for Ni(II) and Sr(II). **J. Hazard. Mater.** 2009, 164:923-928.

Y.-C. Chang, D.-H. Chen. Preparation and adsorption properties of monodisperse chitosan-bound Fe_3O_4 magnetic nanoparticles for removal of Cu (II) ions. **J. Colloid Interface Sci.** 2005, 283:446-451.

X. Tian, W. Wang, N. Tian, C. Zhou, C. Yang, S. Komarneni. Cr (VI) reduction and immobilization by novel carbonaceous modified magnetic Fe_3O_4/halloysite nanohybrid. **J. Hazard. Mater.** 2016, 309:151-156.

Y. Xie, D. Qian, D. Wu, X. Ma. Magnetic halloysite nanotubes/iron oxide composites for the adsorption of dyes. **Chem. Eng. J.** 2011, 168:959 -963.

A. Al-Saadi, C.H. Yu, V.V. Khutoryanskiy, S.J. Shih, A. Crossley, S.C. Tsang. Layerby-Layer electrostatic entrapment of protein molecules on superparamagnetic nanoparticle: a new strategy to enhance adsorption capacity and maintain biological activity. **J. Phys. Chem. C** 2009, 113 (34):15260-15265.

Y.S. Ho, G. McKay, Pseudo-second order for sorption processes. **Process Biochem.** 1999, 34:451-465.

G. Crini, H.N. Peindy, F. Gimbert, C. Robert. Removal of C. I. basic green 4 (malachite green) from aqueous solutions by adsorption using cyclodextrinbased adsorbent: kinetic and equilibrium studies. **Sep. Purif. Technol.** 2007, 53:97-110.

S. Lagergren. About the theory of so-called adsorption of soluble substances, Kungliga Svenska Vetenskapsakademiens Handlingar, General Books LLC., New York, 1898, pp. 1–39. Band 24, No. 4.

L. Han, X. Zhou, L. Wan, Y. Deng, S. Zhan. Synthesis of $ZnFe_2O_4$ nanoplates by succinic acid-assisted hydrothermal route and their photocatalytic degradation of rhodamine B under visible light. **J. Environ. Chem. Eng.** 2014, 2:123-130.

Liqiang Jin, Qiucun Sun, Qinghua Xu, Yongjian Xu. Adsorptive removal of anionic dyes from aqueous solutions using microgel based on nanocellulose and polyvinylamine. **Bioresource Technol.** 2015, 197:348-355.

Malik, P.K.. Use of Activated carbons prepared from sawdust and rice-husk for adsorption of acid dyes: a case study of Acid Yellow 36. **Dyes Pigments** 2003, 56:239-249.

Das, D.P., Das, J. and Parida, K.. Physicochemical characterization and adsorption behaviour of calcined Zn/Al hydrotalcite-like compound (HTlc) towards removal of fluoride from aqueous solution. **J. Colloid Interface Sci.** 2003, 261:213-220.

Liao, X.P. and Shi, B. Adsorption of fluoride on zirconium(Ⅳ)-impregnated collagen fibre. **Environ. Sci. Technol.** 2005, 39:4628-4632.

Netpradit, S. Thiravetyan, P. and Towprayoon, S. Adsorption of three azo reactive dyes by metal hydroxide sludge: effect of temperature, pH and electrolytes. **J. Colloid Interface Sci.** 2004, 270:255-261.

Netpradit, S. Thiravetyan, P. and Towprayoon, S. Application of 'waste' metal hydroxide sludge for adsorption of azo reactive dyes. **Water Res.** 2003, 37:763-772.

Özacar, M. and Şengil, İ.A. Adsorption of reactive dyes on calcined alunite from aqueous solutions. **J. Hazard. Mater.** 2003, 98:211-224.

Chiou, M.S. and Li, H.Y. Equilibrium and kinetic modeling of adsorption of reactive dye on cross-linked chitosan beads. **J. Hazard. Mater.** 2002, 93:233-248.

P39

The elimination of effluent fromthe unhairing-liming process by a novel recycling technology

JIN Liqiang[1], LI Yanchun[1], ZHANG Feifei[1], ZHANG Zhuangdou[2], ZHANG Chuanbo[3]

1. College of Leather Chemical and Engineering, Qilu University of Technology (Shandong Academy Of Sciences), Jinan 250353, China, Phone: 86-531-89631168, E-mail: jin-liqiang@163.com

2. BIOSK chemicals Co., Ltd, Shangqiu 476000, China, Phone: 86-370-3861600, E-mail: support@biosk.cn

3. College of Light Chemical Science & Engineering, Shaanxi University of Science & Technology, Xian 710021, China, Phone: 86-29-86168026, E-mail: zhangcb0630@163.com

Abstract

It is acknowledged that the unhairing-liming process is the main contributor of pollutants in leather manufacturing. The recycling technology is one of the effective solutions to reduce the environmental impact of waste water at source. In this paper, a close recycling technology of unhairing and liming float is introduced which has been verified by five years high-volume leather manufacture. The characteristics of unhairing and liming float and the resultant pelts were analyzed. The results show that total organic carbon, Ca content and other indexes in the float tend to become cumulative balance with the increase of recycling times. The appearance of the limed hides showed normal swelling with necks well extended. Compared with conventional unhairing and liming technology, water, sulfide and other chemicals in unhairing-liming process are saved in this process, and the zero emission of wastewater is realized. The cleaner production technology exhibits promising application prospect for its economic and environmental benefits.

Keywords:liming float; hair-saving unhairing method; close recycling technology; sulphide; lime

Unhairing-liming is one of the most important production processes in leather making.In this process. hair and non-structural components of skin such as glycosaminoglycans (GAGs)、 hyaluronic acid and fat are removed. On the other hand, the collagen fibers are split at the level of the fibril bundles, which allows better penetration of reagents and more effective reaction. In reviewing the totality of the beamhouse processes it will be clear that the properties desired in the final product are largely conferred by the unhairing-liming process in particular[1].

At present, the unhairing-liming method based on sulfide and lime is widely used in leather making industry, which falls into either “hair burning” method or “hair saving” method. Unhairing-liming is traditionally one of the dirtier aspects of leather processing and create considerable pollution load that has been addressed within wastewater treatment. The effluent stream is high in biological load, sulfide, nitrogen and suspended solids from the dehairing-liming process. High volume sludges are also created for disposal.

In recent years, more attention has been paid to the recycling of the liming float in order to decrease the pollution of unhairing-liming process [2-5]. Qu huidong [6] reported a liming wastewater recycling technology based on “hair burning” method. The results showed that the recycling of liming float was helpful to solve loose-grain problem and improve the physical machinery performance of resultant leather. The pollution load of wastewater was also decreased. Zhang jinwei et al.[7] investigated the methods of paint unhairing and unhairing-liming effluent recycle during yak leather making processes. showed that 62.8% sodium sulfide, 84.80% lime, 64.90%water could be saved during the recycle. In addition, no adverse effects on yak hide swelling using this effluent recycle technology were observed when the cycle times was within 10 times and the pollutant was reduced obviously. In order to solve the problem s of conventional unhairing processes, Ding shaolan et al.[8]investigated the hide alkali immuno-unhairing process and effluent recycling. The results showed that more than 90 percent hair was recovered and the COD and viscosity of the effluent were decreased dramatically. Howerer, all previously reported works were done at a laboratory scale, whereas the application at industrial level was not deeply investigated yet.

In order to minimize the impacts of unhairing-liming process on the environment, Biosk company created a novel closed recycle technology- known as BIO-cycle, which resulted in no wastewaters be discharged from unhairing and liming process.

This technology is based on the reusing the lime float recovered from precious processes, and has been introduced to industrialized production in 2011 for full scale manufacture. The aim of this research is to explore the technical points of the recycling technology of liming effluent. The liming wastewater of different recycling times was sampled from a tannery and the characteristics of unhairing and liming float were determined. Finally, the economic benefit of this recycle process was analyzed.

Experimental

2.1 Materials and Instruments

Disodium ethylenediamine tetraacetic acid, sodium hydroxide, calcium hydroxide and chrome blue black R (calcium indicator) are purchased from Tianjin Damao chemical reagent factory. Zinc acetate, sodium thiosulphate, potassium dichromate, silver sulfate, phenanthroline and ammonium ferrous sulfate are supplied by Shandong Baihong new material co. LTD. Sulfuric acid, nitric acid, hydrochloric acid, iodine and potassium iodide are provided by Tianjin Fuyu fine chemical co. LTD.

All the chemical reagents used above are analytical pure.

2. 2 Sampling method

The effluent of liming recycle process (recycle 1,5,10,15,20,25,30 times) was provided by Hebei Huanghua tannery.

2.3 The chemical analysis of liming wastewater

The sample of liming wastewater was precipitated firstly. After natural sedimentation, 500 mL of the wastewater of different recycling times was filtered by double layer gauze for two times. The filter liquor was used to analysis.

2.3.1 The determination of S^{2-} content

The content of sulfide in the wastewater was determined by filtration and iodimetry.

2.3.2 The determination of Ca^{2+} content

TheCa^{2+} content of liming wastewater was determined by EDTA complexometry method.

2.3.3 The detection of Total Organic Carbon (TOC)

The TOC in float was detected by a TOC analyzer (TOC-L CPH CN20, SHIMADZU). The liming liquid waste was diluted 500 times and filtered through filter membrane (0.45 μm) before analysis.

2.3.4 The determination of chemical oxygen demand (COD)

The COD of liming wastewater was determined by HJ828—2017.

2.3.5 The determination of total nitrogen (TN) content

The TN of liming wastewater was determined according to the method of HJ 636—2012.

2.3.6 The detection of buffer capacity of effluent

The buffer capacity of the liming effluent was detected by an automatic potentiometric titrator (ZDJ-4A, Rex Electric Chemical).

3. Results and discussion

3.1 The application of unhairing-liming recycling technology

This recycling technology is based on the hair persevering process. The application formulation is shown in Table I.

When the liming process was completed, the float was re-filtered and collected. Then the float was reused in the next production batch. An addition of fresh water was replenished in every recycling process. This is because only 80% of the liming wastewater was usually collected. The recycling route of the liming wastewater was shown in Figure 1. A certain amount of sodium sulphide as well as the lime was supplemented in each recycling.

Table I

Hair-saving Liming process based on Bio-cycle technology

process	%	chemical	Time
Immunization stage	80	Recovered used lime float at 20℃	
	0.8	DO-PRO*	
	0.2	Sodium hydrosuifide	
	0.8	Calcium hydroxide	Run30min/lay20min
Hair removal		Hair screening/filtration	Run30-60min
Liming stage	0.4	DO-PRO	
	1.0	Calcium hydroxide	
	1	Sodium sulfide	Run 30 min
			Run10min/lay25min×6times/total 4h
Add float	50	Recovered used lime float	
	0.5	Calcium hydroxide	Run 30 min/h, overnight

* Biosk liming assist product.

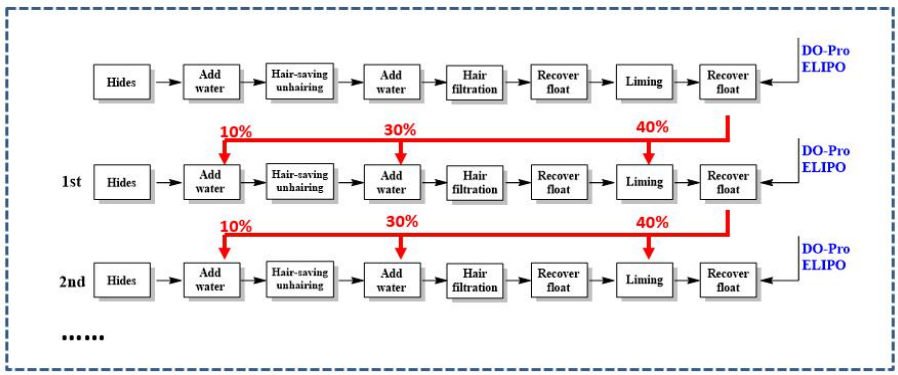

Figure 1. Recycling route of unhairing-liming wastewater

3.2 The S^{2-} content analysis of liming wastewater

The S^{2-} content of liming wastewater in different recycling time was shown in Figure 2. The S^{2-}content in different time of recycling process was in the range of 1.5~2.0 g/L. It looked like that the S^{2-}content appears to reach stability after approximately ten cycles.

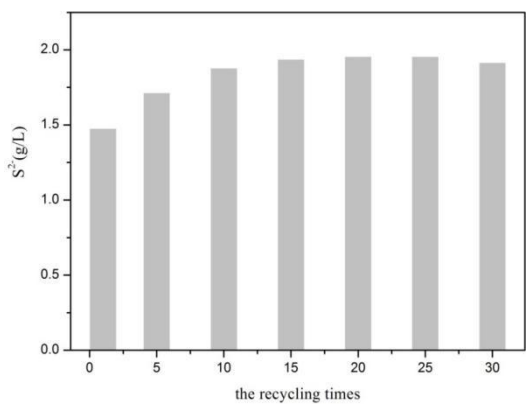

Figure2. The S^{2-} content of liming wastewater in different recycling time

3.3 The TOC and COD analysis of liming wastewater

In order to analysis the content of organic material in the wastewater, the TOC and COD was determined to characterize the pollution of organic material in the wastewater. The results were shown in Figure 3 and Figure 4. The TOC and COD of the effluent increase with the recycling process. This was due to the dissolution of interfibrillar substance in liming process. In the liming process, the interfibrillar substance as well as part of collagen fiber would dissolve in the liming wastewater. Therefore, the content of organic material in wastewater would increase. At the same time, the collagen fiber was dispersed sufficiently. However, the TOC and COD of wastewater tended to be constant after 20 times recycling. Furthermore, the viscosity of liming wastewater did not tend to thicken and the solution was not saturated. These might attribute to the hair persevering technology. In addition, part of the organic material would be absorbed into to the shedding hair and then filtered out the recycling system in the hair filter process. Furthermore, a continuous build-up of soluble materials soluble material was avoided because some water and soluble solubles were absorbed by the liming pelts at the end of each recycle. These solubles were eventually released from the hides in the deliming process as the hides de-swell. Therefore, the recycling process could keep going.

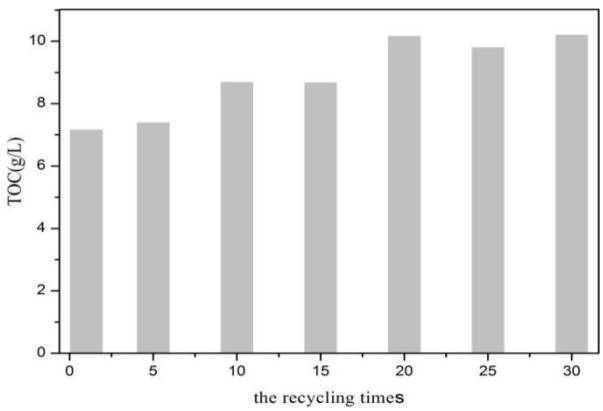

Figure 3. The TOC content of liming wastewater

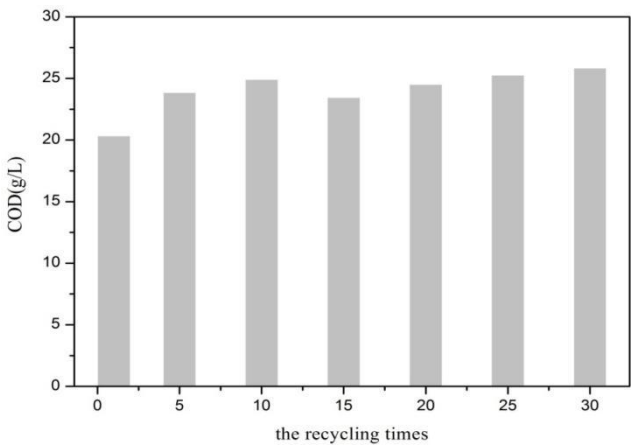

Figure 4. The COD content of liming wastewater

3.4 The Ca^{2+} content analysis of liming recycling wastewater

The variation of Ca^{2+} content in different liming recycling wastewater was shown in Figure 5. According to the results, the Ca^{2+} content in wastewater was in the range of 1.4~1.8 g/L. The Ca^{2+} content in wastewater increases with the recycling times. The variation of Ca^{2+} content in different recycling process indicated that a greater organic solubles in wastewater which are derived from the degradation of the collagen could help the dissolve of lime. The increase was beneficial to the separation of collagen fibers.

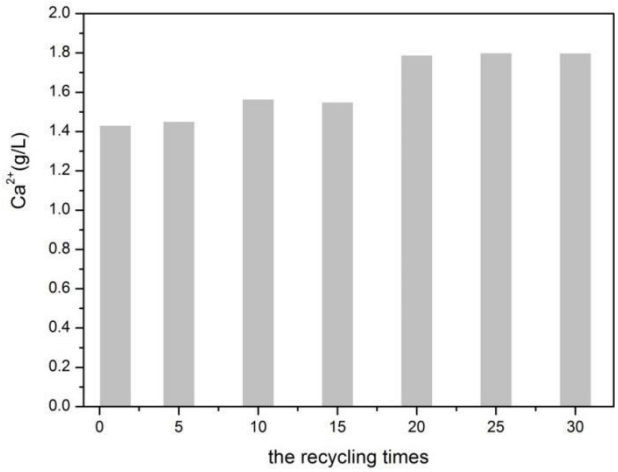

Figure 5. The content of Ca in liming waste liquor

3.5 The total nitrogen (TN) content in liming wastewater

The total nitrogen (TN) content in liming wastewater was shown in Figure 6. The TN content in wastewater increases with the recycling times. The TN content appears to reach stability after approximately fifteen cycles. The total nitrogen (TN) content in liming wastewater come mainly from the dissolution of interfibrillar substance and the degradation of collagen in liming process. It was worth noting that a certain amount of NH_3 was produced when the side groups of collagen were removed in the liming process as shown in Figure 7. which was helpful to unhairing in the recycling process.

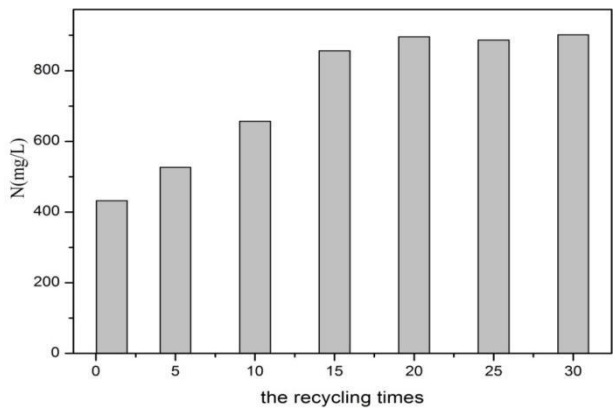

Figure 6. The content of TN in liming wastewater

$$\text{P-(CH}_2\text{)nCONH}_2 + \text{H}_2\text{O} + \text{OH}^- \longrightarrow \text{P-(CH}_2\text{)nCOO}^- + \text{NH}_3$$

Figure 7. The hydrolysis of amide sidechains

3.6 The buffer ability of liming wastewater

The solubility of lime is limited, so the pH of saturated lime solution is in the range of 12~13. The mild liming condition makes the alkaline swelling slowly and uniformly. The operable and safety of lime swelling are attributed to the chemical property of lime. The potentiometric titration results of liming wastewater of different recycling time were shown in Figure 8. According to Figure 8, the titration curves of $Ca(OH)_2$ solution had an obvious pH abrupt points. On contrary, no obvious abrupt point appeared in the titration curves of liming wastewater. So the liming wastewater displayed the outstanding buffering ability. This might be attributed to the existence of degradation products of interfibrillar substance in wastewater. Polysaccharose substance and protein showed a good buffering property, so the pH of the liming wastewater changed slowly when the acid was added. In the liming recycling system, the buffering properties of the liming wastewater would slow

down the swelling rate of the raw hide. Furthermore, the occurrence of liming wrinkle in the liming pelt decreased. Then the obtained pelt became smoother and the yield of crust increased.

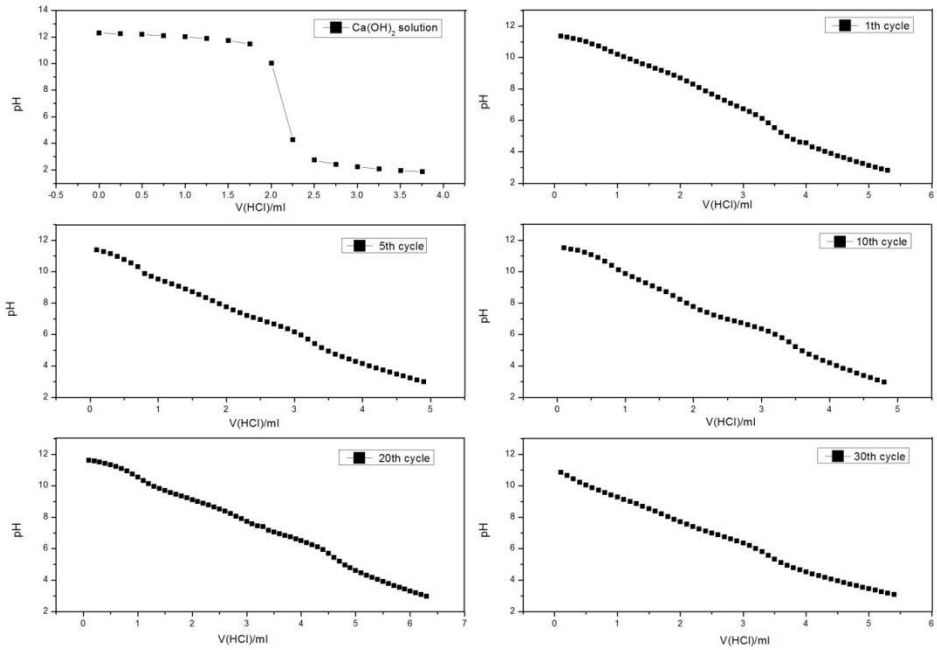

Figure 8. The potentiometric titration curve of liming wastewater at varied cycles

3.7 Economic benefit analysis of liming wastewater recycling technology

The economic benefit analysis of the recycling technology was evaluated by the consumption of used water and chemicals as shown in Table II. In the recycling process, the dosage of water, sodium sulphide and lime for the production output of 30 days were counted according to actual production consumption. While in conventional unhairing-liming process, the dosage of water, sodium sulphide and lime for the production output of 30 days were estimated. The saving rates of water, sodium sulphide and lime were 80.50%, 33.38% and 23.11%, respectively. The results proved that not only the production cost had been decreased by the implementation of the recycling technology but also the zero discharge of liming process was realized.

Table II. The saving rate of water and chemicals in liming recycling process*

Method	Water (T)	sulphide (T)	lime (T)
Conventional process	333.78	7.37	11.68
Recycling process	65.08	4.91	8.98
Saving rate(%)	80.50	33.38	23.11

* The calculation is based on the production output of 30 days.

4. Conclusion

A novel closed recycling of wastewater technology was applied and the zero discharge of liming wastewater was realized. Compared with the conventional process, the novel recycling technology could save more than 80.5% water, 33.38% of sodium sulfide and 23.11% lime in liming process. In the liming wastewater recycling process, the reduction of the dosage of lime and sulfide didn't affect the removing efficiency of hair.

Reference

Anthony D Covington. Tanning Chemistry: The science of leather[M]. The royal society of chemistry, 2009

Thanikaivelan P, Rao J R, Nair B U, et al. Recent trends in leather making: processes, problems, and pathways[J]. Critical

Reviews in Environmental Science and Technology, 2005, 35(1): 37-79.

Saravanabhavan S, Thanikaivelan P, Rao J R, et al. Natural leathers from natural materials: progressing toward a new arena in leather processing[J]. Environmental science & technology, 2004, 38(3): 871-879.

Rao J R, Chandrababu N K, Muralidharan C, et al. Recouping the wastewater: a way forward for cleaner leather processing[J]. Journal of Cleaner Production, 2003, 11(5): 591-599.

Hu J, Xiao Z, Zhou R, et al. Ecological utilization of leather tannery waste with circular economy model[J]. Journal of Cleaner Production, 2011, 19(2): 221-228.

Qu H D. Research on the recycling process of liming effluent. China leather,1994,23(11)：40-44.

Zhang JW, Kong LL, Ma CY, et al. Recycling utilization of unhairing-liming effluent liquid for yak hide[J].West leather, 2015, 34(17)：15-19.

Ding SL, Zhang CB, Gao XZ, et al. Study on the Technology and Effluent Recycling of the Alkali Immuno- unhairing Process[J]. China leather，1997,26(9):7-9.

P40

Preparation and application of a novel cationic fatliquoring agent

Hong Yang [1], Jinlong Wang[1], Xuemei Li[2], Liqiang Jin[1]*, Yulu Wang[1]

College of Leather Chemical and Engineering, Qilu University of Technology (Shandong Academy Of Sciences), Jinan 250353, China; 2 .Shandong Juye Fine Chemical co. Ltd, Ji nan 250021,China)

** Correspondence: jlq@qlu.edu.cn; Tel.: +86-0531-8963-1786*

Abstract: A cationic emulsifier YW based on fatty acid triethanolamine ester was firstly prepared by using stearic acid, triethanolamine and benzyl chloride. Then, a novel cationic fatliquoring agent YH was prepared by mixing a certain amount of YW, non-ionic surfactant and neutral oil. The structure of the cationic emulsifier YW was characterized by infrared spectroscopy and H-NMR and the surface tension of YW aqueous solution was determined by surface tension meter. In addition, the stability of YH was studied, and the particle size and zeta potential of YH emulsion were determined by Nano-ZS90 nanometer. The composition of YH was optimized by its application behavior in cow wet blue as a fatliquor. The results show that YH exhibits good centrifugal stability and electrolyte resistance with an average particle size of 22.4 nm and zeta potential of 60.8 mV. The leather treated by YH shows high softness, tensile strength and tear strength. When YH was also used as a dye-fixing agent, it could promote the absorption and fixation of dyestuff, and improve the dry/wet fastness of leather and the color fastness of washing.

Keywords: Fatty acid triethanolamine ester; Cationic fatliquoring agent; Fatliquoring; Color fixation; Leather

1 Introduction

Fatliquoring agent is the largest used chemical in leather making industry[1, 2]. The properties of fatliquoring agent have important influence on the appearance and inner quality of leather. According to the ionization in aqueous solution, it is divided into anionic, cationic, amphoteric and non-ionic fatliquoring agent[3]. Cationic fatliquoring agents usually contain quaternary ammonium group, which impart the leather unique application properties, such as softening properties, antistatic and antibacterial properties[4]. The cationic fatliquoring agent can used for pre-tanning before chrome tanning to improve the penetration and distribution of chrome tanning agent. It can also be used for secondary fatliquoring, which plays the role of fixing oil and color of leather and adjusting leather handle[5].

In recent years, the development and application of cationic fatliquoring agents have attracted more and more attention as the dosage and application range of cationic fatliquoring agents expand constantly. Zhao et al.[6] prepared a cationic fatliquoring agent by two steps. Firstly, a cationic castor oil having quaternary ammonium structure was obtained by etherification reaction between castor oil and cationic etherifying agent ETA. Then a cationic fatliquoring agent was prepared by mixing the cationic castor oil with chlorinated paraffin wax and Tween-20. Shen et al. [7] prepared a cationic lanolin fatliquoring agent by the reaction between lanolin and etherifying agent, and this cationic fatliquoring agent was applied to the fatliquoring process of goat garment leather. The application results show that the fullness and softness of the leather were improved obviously after fatiliquoring, and the obtained leather sample exhibited the sense of moisture and waxy feel. A waterproof cationic fatliquoring agent (SMF) was prepared by emulsifying alkylenone dimer (AKD) with cationic emulsifier [8]. It was found that the SMF show better waterproof effect when it was applied on the leather making. At a dosage of 4%, the 2 h static water absorption ratio of obtained leather was less than 31.6%. Meanwhile, SMF can also improve the absorption ratio of the crust leather to anionic dyes and fatliquoring agents.

The properties of cationic fatliquoring agent depend not only on the composition of the surface-active substances, but also the types of neutral oil and the ratio between the neutral oil and surface-active substances. Esterquat is one of the varieties of cationic surfactants used as textile softening agents. They are quaternary ammonium compounds, having two long (C16–C18) fatty acid chains with 2 weak ester linkages. In recent years, esterquat cationic surfactant gains superiority due to its environmental friendly, nontoxic and biodegradable properties [9, 10]. However, there are few reports on the cationic fatliquoring agents prepared using esterquat cationic surfactant. In this work, an esterquat cationic emulsifier YW based on

fatty acid triethanolamine ester was firstly prepared by the condensation reaction of stearic acid and triethanolamine and the followed quaternization by using benzyl chloride as the quaternizing agent. Then, a novel cationic fatliquoring agent YH was obtained by mixing a certain amount of YW, non-ionic surfactant and neutral oil. The composition of YH was optimized according to its fatliquor behavior on cow wet blue.The application performance of cationic fatliquoring agent YH was also discussed.

2 Experimental

2.1 Materials

Stearic acid, triethanolamine, Hypophosphorous acid, benzyl chloride and isopropyl alcohol were analytical grade and purchased from Aladdin Company. Span80, White oil, chlorinated neatsfoot oil and chrome tanning agent were kindly provided by Shandong Lining technology Co. TO-15 was supplied by Basf Company.

2.2 Preparation process of cationic fatliquoring agent YH

2.2.1 Synthesis of cationic emulsifier YW

A certain amount of stearic acid was added into a four-necked flask and heated to 70℃ at N_2 atmosphere. After melting, the triethanolamine and hypophosphorous acid were added in certain ratio. Then the flask was heated to 160℃ for 5 hours and cooled down to 60-80℃.

The prepared diester was treated with benzyl chloride for its quaternization. The quaternization was carried out at 60-70ºC for 5 hours in isopropyl alcohol. Finally, the YW was obtained after isopropyl alcohol was removed by vacuum distillation.

The synthesis route of YW was shown in Fig. 1

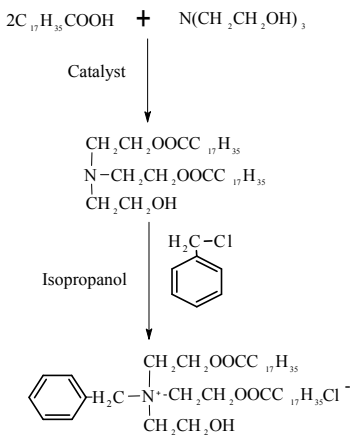

Fig.1. Synthesis route of cationic emulsifier YW

2.2.2 Preparation of YH

A certain amount of non-ionic surfactant and neutral oil were added into a four-necked flask equipped with a mechanical stirrer, a thermometer and a reflux condenser. Then the flask was heated to 60 ℃ and the mixture of cationic emulsifier YW, non-ionic surfactant and a certain amount of water was dripped into the flask after the oil phase was mixed completely. Then the pH was adjusted to about 4 with 10% acetic acid solution. Finally, the mixture was sheared for 120 min by using a high-speed disperser at 10,000r /min and the product YH was obtained.

2.3 Characterization

2.3.1 Fourier Translation Infrared Spectra

FTIR spectra of samples were recorded on Alpha FTIR spectrometer produced by BRUKER at ambient temperature in the range of 500 to 4000 cm^{-1}[11].

2.3.2 H-NMR

H-NMR of samples were operated on AVANCE II 400 NMR spectrometer which produced by BRUKER company. The solvent of samples is Chloroform-d.

2.3.3 Surface tension determination

The surface tensions of samples aqueous solution with different concentration were determined by BZY-48 surface tension meter at 25℃[12].

2.3.4 Physical and chemical *index* of YH

The physical and chemical index of cationic fatliquoring agent YH was determined according to QB/T 2414-1998.

2.3.5 Particle size and Zeta potential of YH

The particle size and Zeta potential of YH latex was determined by Malvern Nano-ZS90 Nanometer size and Zeta potentiometer at 25℃[13].

2.4 Application formulations

The cow wet blue with 1.2 to 1.5mm thickness was used to test the performance of fatliquor agent. The fatliquor application formulation is tabulated in Table I .

Table I

The application formulation of cationic fatliquoring agent YH

Process	Product	Quantity[a]%	Time(min)	T(℃)	pH
Washing	Water	250		40	
	Formic acid	0.5			
	Detergent	0.3	90		pH 3.2
					Drain
Retanning	Water	100		40	
	Chromate	1	120		
	sodium formate	1.5			
	Sodium bicarbonate	0.6	30		pH 4.0
Neutralizing	Water	200		35	
	sodium formate	2	60		
	Sodium bicarbonate	0.5			pH 6
Washing					Drain
Filling	Water	150		35	
	RV	2	30		
	dispersed tannins	2	40		Drain
Dyeing	Water	150	30		
	Dyestuff	2.5		50	
Fatliquoring	Formic acid	2	20×2		pH 3.4
	YH[b]	10	90		
Washing and drain					

a: all percentages are based on wet-blue weight b:omitted in the control test

2.5. Determination of leather properties

2.5.1 Softness measurement

After air conditioning, the softness of leather sample was measured by the Gt-7071-dw leather softness tester according to TUP 36 Standard[14].

2.5.2 Determination of chromatic aberration of leather

The chromatic aberration parameters L, a and b of leather surface were determined under Daylight65 light source by using Gretage Macbeth Color-Eyz 7000A colorimeter[15]. L indicates the lightness. A represents red and green axis. B represents yellow and blue axis. The ΔE betweensample and standard whiteboard is calculated according to the following formula.

$$\Delta E=\sqrt{(\Delta a)^2 + (\Delta b)^2 + (\Delta L)^2}$$

2.5.3 Determination of color fastness of leather

The water-resistant color fastness test of leather is carried out according to international standard ISO 11642. The size of leather sample is 100mm× 40mm, and the washing test is done at 40℃for 30min. After that, the sample was washed bydeionized water. The chromatic aberration of sample was measured after drying.The color fastness to dry and wet rubbing were measured and graded according to GB/ t3290-2008[16].

2.5.4 Mechanical properties measurement

The tensile strength, tearing strength, breaking elongation and breaking strength of leather samples were tested according to QB/ t2710-2005[17].

2.5.5 Determination of dye absorption ratio

The wastewater was collected after dyeing and the dye absorption ratio was calculated according to the following formula[18]:

$$\mathbf{W(\%)} = \frac{m-cV}{m} \times 100$$

Where **W** is the dye absorption ratio, **m** is the offer of dyestuff, **c** is the dye concentration of wastewater and **V** is the volume of wastewater.

3. Results and Discussion

3.1 Synthesis of cationic emulsifier YW

Triethanolamine stearate quaternary ammonium salt is prepared via a two-step process including esterification reaction between stearic acid and triethanolamine followed by quaternary ammonium reaction. Because stearic acid is along chain fatty acid and it's hard to be esterified directly because of low reactivity. It is necessary to choose appropriate catalyst to promote the esterification between stearic acid and triethanolamine. The hypophosphorous acid was used as the catalyst in this work, and its dosage was 0.2% of the reactant.In the esterification of stearic acid and triethanolamine, the resultant product may contain monoester, diester and trimester because of the randomness of the reaction. As we know, the diesterquaternary ammonium salt has better softening effect on fiber. In order to improve the content of diester in the final product,the molar ratio of stearic acid and triethanolamine was controlled as 2:1.In this research, benzyl chloride was selected as quaternization reagent and the quaternization was carried out in isopropyl alcohol. The ratio of diester and benzyl chloride was 1:1.05. The FTIR of triethanolamine stearate and its quaternary ammonium salts are shown in Fig.2.

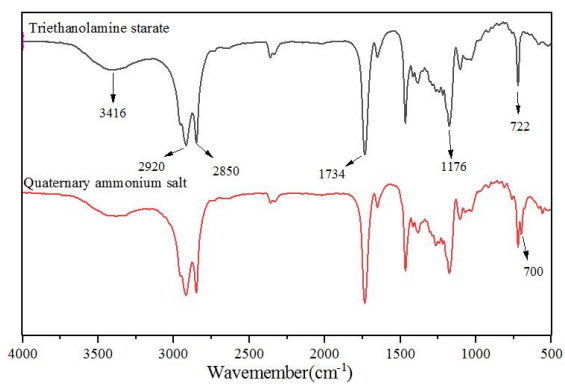

Fig.2 FTIR of triethanolamine stearate and its quaternary ammonium salts

In the spectra of triethanolamine stearate, the bands at 3416cm^{-1} is from –OH stretching vibrations, which is the

conformation of free OH of diester of fatty acid and triethanolamine. The bands at 2920 and 2850cm^{-1} are attributed to $-CH_3$ and $-CH_2$ stretching vibrations. The band at 1737cm^{-1} is due to C=O stretching vibrations, and the band at 1176cm^{-1} is attributed to the -C-O-C- stretching vibration. The peaks indicate the formation of ester bonding. The band at 722cm^{-1} is assigned to the bending vibration of the hydrocarbon chain, which suggests the long-chain alkyl exists [19]. In the spectra of esterquat, the band at 700cm^{-1} is attributed to the C-H curved vibration absorption of benzene ring which confirms the quaternization reaction.

3.2 Surface tension of YW aqueous solution

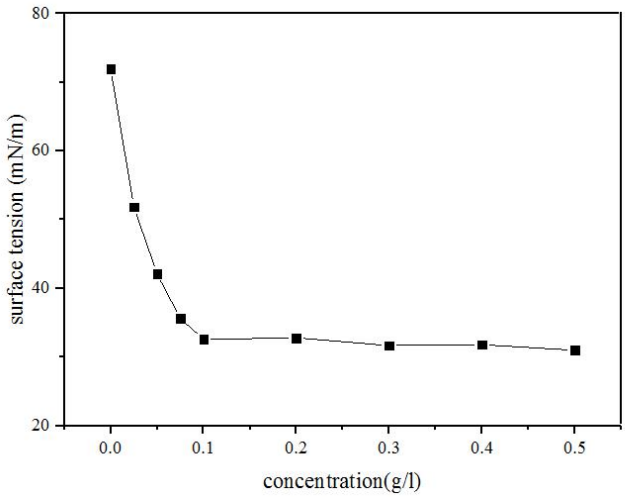

Fig.3 The relationship between the concentration of YW and the surface tension

Surface tension is an important physicochemical property index to reflect the surface activity of a surfactant. The lower the surface tension of the solution, the stronger the surface activity of the substance. The surface tension curve of YW aqueous solution at pH 4.0 is shown in Fig.3. It could be obviously seen that when the concentration of triethanolamine stearate quaternary ammonium salt increased from 0 to 0.1 g/l, its surface tension decreased rapidly from 71.97 mN/m to 32.57 mN/m. The surface tension reached a plateau with the increase of the concentration of the esterquat, which was close to 30 mN/m. The results indicated that the prepared triethanolamine stearate quaternary ammonium salt YW exhibited higher surface activity and could be used to emulsify the neutral oil in the preparation process of fatliquor.

3.3 Optimization of preparation conditions of YH

The Cationic fatliquoring agent YH was prepared by mixing the emulsifier and neutral oil in this research. The dosages of YW and non-ionic emulsifier and type of neutral oil were optimized respectively according to the application results.

3.3.1 Dosage of emulsifier

The stability of YH was investigated at varied dosages of the emulsifier while the mass ratio of YW and non-ionic was fixed at 1:1. The results are shown in Table 2. The stability of YH was improved as the dosage of emulsifier increased. When the dosage of emulsifier was no less than 20% of the final product, YH exhibited better dilution stability (1:9) and centrifugal stability.

Table II

The effect of dosage of YW and nonionic emulsifier on the stability of the product

Sample	emulsifier	1:9dilution stability	centrifugal stability*
1	5%	unstable	unstable
2	15%	unstable	unstable
3	20%	stable	stable
4	30%	stable	stable

* at a speed of 3000rpm

3.3.2 Type of neutral oil

The effect of type of neutral oil on leather properties was studied at a fixed emulsifier dosage of 20%. Three types of neutral oil, white oil, heavy alkyl benzene and chlorinated neatsfoot oil, were selected and compared respectively. The results are shown in Table III. As can be seen from Table III, the variety of neutral oil had a great influence on the properties of the fatiliquored leather. The maximum softness of leather sample (4.64), was obtained by using the fatliquoring agent whose neutral oil was heavy alkyl benzene. The leather sample fatiliquored based on chlorinated neatsfoot oil show the highest tensile and tear strength, 22.07 N/mm^2 and 71.59 N/mm, respectively. This could be due to the strong polarity of chlorinated neatsfoot oil, which could bind strongly with collagen fibers and thus increase the strength of leather. At present, the style of leather products is developing towards the direction of thin and light. During the leather making process, some specific agents are necessary to increase the mechanical properties of obtained leather. The fatliquoring agents which can impart the leather high tensile and tear strength are attracting more and more attention. Therefore, chlorinated neatsfoot oil was selected as the neutral oil component of YH fatliquoring agent.

Table III

The effect of type of neutral oil on the properties of fatliquoring agent

Sample	Neutral oil	softness	Tensile strength (N/mm^2)	Tear strength (N/mm)
5	white oil	4.62	18.03	59.82
6	heavy alkyl benzene	4.64	18.56	65.72
7	chlorinated neatsfoot oil	4.52	22.07	71.59

3.4 Physical and chemical index of YH

The physical and chemical index of YH was listed in Table IV. YH shows the acid and salt resistance ability.

Table IV

The physical and chemical indexes of cationic fatliquoring agent YH

Test item	YH
Appearance	White emulsion
Solid content	25.00%
pH	4.2
1:9 dilution stability（24h）	stable
3000 r/mcentrifugal stability（30min）	stable
Stability to 1 mol/L HCl solution(4h)	stable
Stability to 8% NaCl solution(4h)	stable

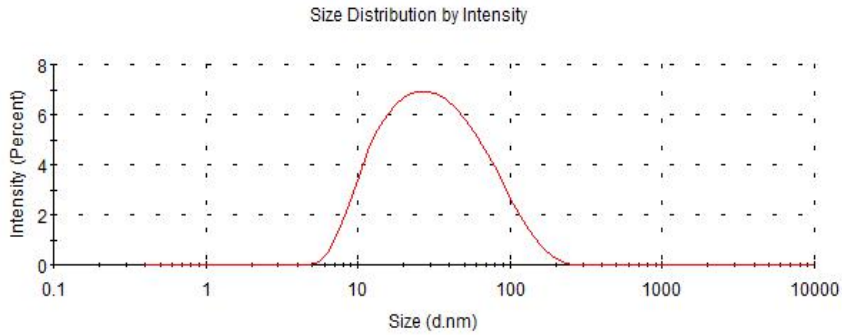

Fig.4 The particle size distribution of cationic fatliquoring agent YH emulsion

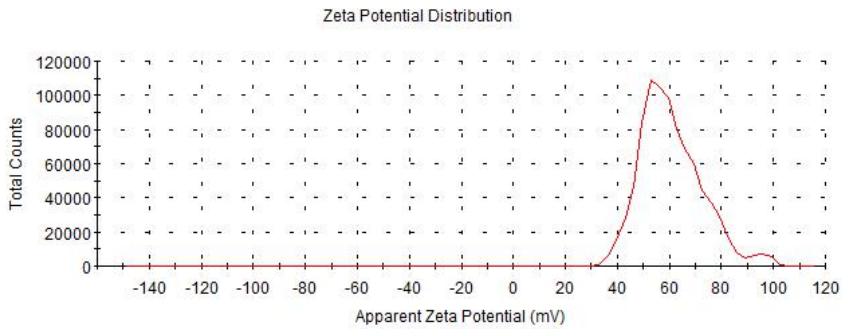

Fig.5 The Zeta potential of cationic fatliquoring agent YH emulsion

The particle size and zeta potential of YH emulsion were shown inFig.4 and Fig.5. The average particle size of cationic fatliquoring agent YH was 24.44 nm and the PDI was 0.324. The size distribution of YH emulsion was homogeneous. The particle size of YH latex is much smaller than the gap between collagen fibers, which makes it easier for particles to infiltrate into the inner part of collagen fibers and play a role of deep fatliquoring. The particles of YH emulsion were positively charged with a zeta potential of +60.8mv, which could keep stable due to the relative high positive surface charges.

3.5 The application results of YH

The cationic fatliquoring agent YH was used in the dyeing and fatliquoring process of the wet cow leather to investigate its effect on the dyeing and physicochemical properties of crust. The influence of YH on the absorption ratio of dyes and the dry and wet rubbing fastness of crust was shown in Fig.6. Compared with the blank sample, the absorption ratio to acid dyes increased from 92.56% to 98.01% after the crust was fatliquored by YH. At the same time, the dry and wet rubbing fastness of the crust increased from grade 3 to grade 3.5 and grade 4, respectively. The chromatic aberration ΔE of the treated leather before and after washing was shown in Table V.It could be seen from Table V that after treated with YH, the change rate of ΔE of the leather after washing was 2.28%, while the change rate of ΔE of the blank sample after washing was 26.83%.It suggested that the cationic fatliquoring agent YH has a good color fixation effect, which could help to fix dyestuff and so that improve the color fastness of the dyed leather and the fastness to be washed.

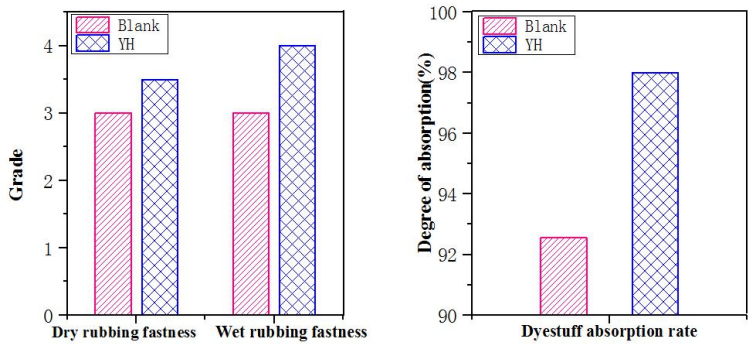

Fig. 7 The influence of YH on dyestuff absorption ratio and the dry and wet rubbing fastness of leather

Table V

The influence of YH onwater-resistant color fastness of leather

Process	Sample	L	a	b	△E	Change rate of △E
	White board	100	0	0	0	/
Before	YH	77.4	-5.4	49.17	54.38	/
washing	Blank	76.5	-5.8	47.03	52.89	/
After	YH	77.13	-5.93	47.6	53.14	2.28
washing	Blank	78.3	-7.72	31.1	38.7	26.83

The effect of YH on physicochemical properties of leather was shown in Table VI. It can be seen from Table VI that the physical and mechanical properties of leather treated by YH were higher than those of blank. The tensile and tear strength of fatliquored crust increased by 20.54% and 37.9%, respectively. The collagen fibers of crust leather were deeply lubricated after YH fatiliquoring, so that they were more likely to be oriented under external forces, which resulted in the increase of leather's mechanical properties.The YH also had a certain filling capacity, which made the leather plump and soft, and the surface of the leather feels moist.

Table VI

The effect of YH on the physical properties of leather

	YH	Blank
Thickness increment ratio(%)	2.41	1.262
Softness	4.65	4.4
Tensile strength(N/mm^2)	18.12	13.14
Tear strength(N/mm)	67.36	55.88
Break elongation ratio(%)	12.27	9.32
Bursting strength(N/mm)	305.1	239.72

4 Conclusions

In this study, a cationic emulsifier YW based on fatty acid triethanolamine ester was firstly prepared. A novel cationic fatliquoring agent YH was then obtained by mixing a certain amount of YW, non-ionic surfactant and neutral oil.The mean particle size of YH was about 22.4 nm, and the zeta potential was 60.8mV.It exhibited high resistance to dilution, acid and salt.The leather treated with YH was soft and plump, and the physical and mechanical properties were improved.The cationic fatliquoring agent YH also shows a good color fixation effect. After the fatiliquoring, the absorption ratio to anionic dyes can be increased, and the color fastness of leather and the ability to resist washing can be improved.

Acknowledgement: This paper was supported by the National Key Research and Development Program of China (2017YFB0308503) and the Shandong Provincial Key Research and Development Program, China (2017GGX80103).

References

Wang Q J,Zhao F Y, Gao L.Research progress on cationic fatliquor for leather[J]. Leather and Chemicals.2011, 28(02): 26-28.

Liu L,Shao S X.Synthesis and application of cationic fatliquoring agents[J]. China Leather. 2001, 30(11): 12-15.

Cui Y C, Zhao Y L, Lin G R.Preparation and application of cationic leather fat-liquoring agents[J]. Chemical Research. 2003, 14(03): 64-67.

Lv B,Wang H D,Ma J J,et al.The application of cationic surfactant in leather industry[J]. Leather Science and Engineering. 2014, 24(06): 22-28.

Feng G T,Shan Z H.The application of fatliquor in leather-making[J]. West Leather. 2005, 28(6):20-26.

Zhao Y L.Ding X Y,Cui Y C.Synthesis and characterization of a novel cationic castor oil fatliquor[J]. Leather Chemicals.2005, 24(04): 11-13.

Shen Y D,Li X H.Preparation and application of cationic lanolin fatliquor[J]. China Leather. 2002, 31(03): 1-3.

Yin Z X,Shen Y D,Li P Z,et al.Study on the application of special macromolecule waterproof fatliquoring agent[J]. Leather Science and Engineering. 2010, 20(06): 40-42.

Yang X P,Jiang W W.Synthetic methods and applications of stearic acid triethanolamine ester quaternary[J].Wool Textile Journal. 2009, 37(02): 32-35.

Geng T,Li Q X, Li Y L.Study of synthesis and properties of stearic acid triethanolamine quaternary[J]. Wool Textile Journal. 2004, 32(09): 24-27.

Wen P P,Sun Y Q,Shi X Q,et al.Synthesis of stearic acid triethanolamine triester[J]. China Surfactant Detergent & Cosmetics. 2012, 42(06): 424-427.

Zhang W B,Qiu L S S,Zhou C S,et,al.Synthesis and characterization of quaternary ammonium salt surfactant with ester group[J]. Leather and Chemicals. 2016, 33(02): 15-20.

Wang X C,Hao X L,Luo X,et al.Study on the combination of anionic leather fatliquor and cationic polymer[J]. Leather Science and Engineering. 2011,21(04): 11-16.

Lv B,Li P F,Gao D G,et al.Application of waterborne epoxy resin in leather retanning[J]. China Leather. 2018, 47(02): 15-21.

R. Aravindhan, B. Madhan, J. Ragh ava Rao.Studies on tara-phosphonium combination tannage: Approach towards a metal free eco-benign tanning[J].Journal of American Leather Chemists Association.2015, 110(3):80-87.

Guo Z N,Qiang X H,Xu W,et al.Preparation and application of amphoteric fatliquor based on FTE[J]. China Leather. 2018, 47(5): 1-8.

Chen M M,Qiang X H,Chen W,et al.Combination tannage of chrome-free tanning agent F-90 and chrome tanning agent[J]. China Leather. 2016, 45(02): 32-36.

Lin F,Dai J L,Zhang T Y.Study of testing method of dye amount in leather dyeing and fat-liquoring wastewater[J]. Leather science and engineering. 2003, 13(06): 23-25.

Wang M Q,Chen H L.Synthesis and analysis of triethanolamine esters of stearic acid[J].Textile Auxiliaries. 2013, 30(01): 13-17.

P41

Research progress in gelatin-based biohydrogels

Shaodi Xiu, Xuefeng Li, Liqiang Jin*, Yulu Wang

College of Leather Chemical and Engineering, Qilu University of Technology (Shandong Academy of Sciences), Jinan 250353, China,

** Correspondence: jlq@qlu.edu.cn*

Abstract: Gelatin-based biohydrogels have attracted increasing attentions due to its unique properties such as high adsorption capability, environmental friendliness, good biocompatibility and chemical accessibility. In this paper, the preparation methods for gelatin-based biohydrogels, including physical, chemical, and enzymatic cross-linking, were reviewed and compared. The applications of gelatin-based biohydrogels in tissue engineering, drug delivery system and water treatment were summarized.

Keywords: gelatin-based biohydrogels; tissue engineering; drug delivery system; water treatment; preparation method

Introduction

Hydrogel is a kind of polymer network with three-dimensional structure, which can swell in water without being dissolved[1]. Because the hydrogel molecular structure contains a large number of hydrophilic groups, the hydrogel can absorb hundreds or even thousands times of its own weight of water, and it also has good water retention capacity.

There are several ways to classify hydrogels.Depending on the bonding and forces of the hydrogel network, they can be divided into physical gels (also called pseudo gels or thermally reversible gels) and chemical gels (also called true gels).Physical gels are formed by physical forces such as electrostatic interactions, hydrogen bonding, chain twisting, and the like.Chemical gels are three-dimensional network polymers formed by chemical cross-linking.Physical gels are much worse than chemical gels in their ability to withstand tension, pressure, and shear forces.

According to the response of hydrogels to external stimuli, it can be divided into traditional hydrogels and intelligent hydrogels. Traditional hydrogels are insensitive to environmental changes (such as temperature, pH, etc.), while intelligent hydrogels are hydrogels that exhibit different responses to external environmental stimuli[2].Intelligent hydrogels depending on the external environment is divided into temperature-sensitive hydrogels, pH-sensitive hydrogels, photosensitive hydrogel, pressure-sensitive hydrogels, biomolecule-sensitive hydrogels and the electric field sensitive hydrogels, etc. [3, 4].

According to different synthetic materials, hydrogels can be divided into natural polymer hydrogels, synthetic polymer hydrogels and natural-synthetic polymer hydrogels.Natural polymers such as collagen, chitosan, alginate, hyaluronic acid, fibrin and gelatin are often used to prepare natural hydrogels.Polyethylene glycol, polyvinyl alcohol, polyacrylamide and other synthetic polymers materials are commonly used as raw materials for synthetic hydrogels[5].Collagen-polyethylene glycol[6], collagen-polyvinyl alcohol-hydroxyapatite[7], collagen-polyvinylpyrrolidone[8] and the like can be used to prepare natural-synthetic hydrogels.

Gelatin is a chemical product of collagen that undergoes chemical changes, such as acid, alkali, enzymes, etc., or a denatured product under the influence of light, ultraviolet, heat, and other physical conditions. Collagen refers to the extraction of connective tissue which was from animals (such as bone, skin, toughening, cartilage, etc.), therefore, amino acid of gelatin and collagen is similar in chemical composition. However, gelatin has lost its biological activity and the triple helix structure has partially collapsed.

As a natural biological resource, gelatin has excellent physical and chemical properties such as hydrophilicity, low immunity, biocompatibility, biodegradability, hemostasis, and promotion of cell growth.Gelatin was the first widely used commercial protein. Gelatin is widely used in the photographic industry, paper industry, food industry, pharmaceutical preparation, and medicine[9].

2.Gelatin-based biohydrogel preparation method

Gelatin is gelatinous. Collagen molecules can spontaneously form collagen fibers.hydrogels are formed in the presence of aqueous solvents[10-13].Gelatin-based hydrogels are mainly prepared from gelatin, mainly using the method of physical cross-linking, chemical cross-linking and enzyme cross-linking.

2.1 Physical crosslinked hydrogels

Physical crosslinked hydrogels are formed by intermolecular forces such as electrostatic force, van der Waals force, hydrogen bond force, coulomb force or physical entanglement. The structure of physical crosslinked hydrogels can be damaged by changing their physical environment (pH, temperature and ion strength), so that the hydrogel can be transformed into sol and vice versa [14].

During the preparing of physical crosslinked hydrogels, new toxic substances are not introduced without involving chemical reactions and chemical agents. It is a relatively safe cross-linking method. This is also the biggest advantage of physical cross-linking. However, the physical cross-linking hydrogels may be easy to disintegrate in physiological fluid, and it is difficult to obtain uniform and ideal cross-linking degree using physical cross-linking[15, 16].

One of the common methods of physical crosslinking is freezeing-thawing.The principle is to use phase separation technology. Polymer side chain containing a reactive group such as a hydroxyl group or a carboxyl group forms a rigid three-dimensional network structure in a locally enriched phase. The hydrogels prepared by this method is insoluble in water and has high mechanical strength, good elasticity and room temperature stability. Liuet al.[17]prepared polyvinyl alcohol (PVA)/gelatin composite hydrogels by freeze-thaw physical cross-linking, and the solvent sensitivity of the hydrogels transparency was studied. It was found that when the composite hydrogels are periodically immersed in distilled water and dimethyl sulfoxide (DMSO) aqueous solution, the light transmittances of the hydrogels periodically changed in the solvent-exchanging process. With the increase of DMSO concentration, the response rate of light transmittances of the hydrogels increased.

He et al.[18]prepared a tough gelatin hydrogel by immersing the untreated gelatin gel in ammonium sulfate solution. The polymer chains in the covalent, crosslink-free network can freely move to homogeneously distribute stress, and more importantly, the highly kosmotropic ammonium sulfate ions greatly enhanced the hydrophobic interactions and chain bundling within the gelatin gels. As a result, the treated hydrogels have an extraordinary ultimate strength (compressive and tensile strains of over 99% and 500%, respectively, and stresses of 12 and 3 MPa) superior to that of common protein gels. The possible strengthening mechanism was discussed and the mechanism is shown in Fig.1.

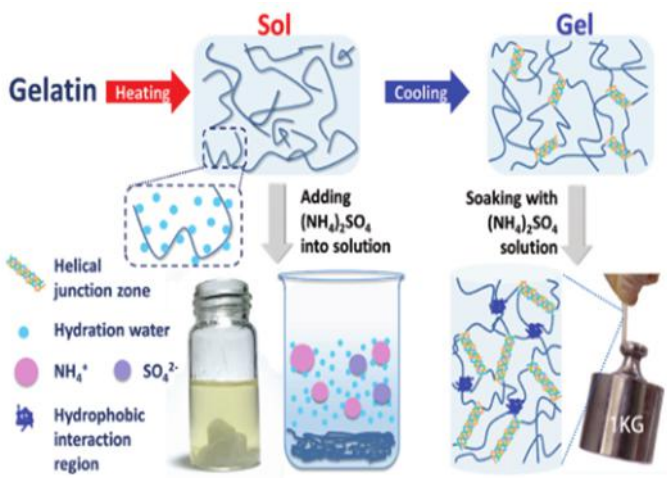

Fig.1 Strengthening mechanisms of gelatin–ammonium sulfate hydrogels.

2.2 Chemical crosslinked hydrogels

Chemical cross-linking refers to the cross-linking of high molecular segments with covalent bonds. It occurs between the compounds by adding a cross-linking agent or initiator to obtain a firm hydrogel network. Its formation process is irreversible. However, hydrogels prepared by chemical cross-linking have potential toxicity to human. So there are limits in biomedical science [19].

2.2.1 Preparation of hydrogels from gelatin and natural polymer materials

The vast majority of plants and animals contain natural polymer gels. These include chitosan, sodium alginate, fibrin, hyaluronic acid, etc. These natural macromolecular materials can be used to prepare hydrogels with gelatin. The resultant composite hydrogels are good biocompatible, sensitive to the environment, rich in source and biodegradable.

Selestina et al.[20] used chitosan (GHT) and gelatin (GEL) as the matrix, N-(3-dimethylaminopropyl)-N′-ethylcarbodiimide hydrochloride (EDC) and N-hydroxysuccinimide (NHS) as a cross-linker to prepare a chitosan-gelatin hydrogel scaffold. The preparation route is shown in Fig. 2. Alterations in the physico-chemical properties of hydrogels were characterized and their biostability was studied within a simulated body-fluid solution (PBS of pH 7.4) at 37°C for 24 h by evaluating the degree of swelling, followed by topography and morphology characterization using scanning electron microscopy (SEM).

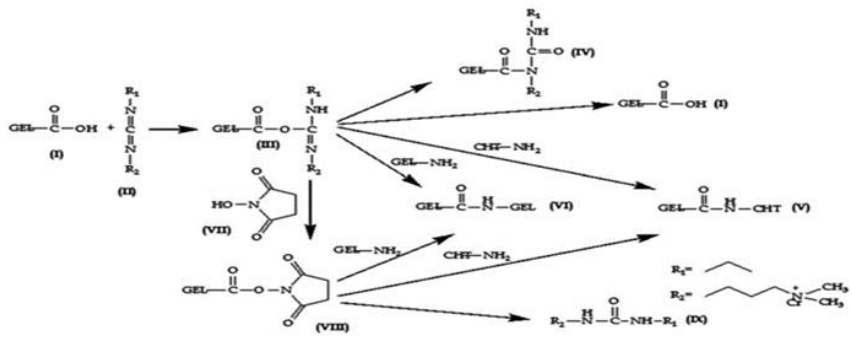

Fig.2 Proposed reaction mechanisms between GEL and EDC with EDC and NHS(Ⅰ) GEL, (Ⅱ)EDC, (Ⅲ)O-acylurea intermediate, (Ⅳ)N-acylurea intermediate, amide bond formation between, (Ⅴ)GEL and CHT or (Ⅵ) two GEL molecules, (Ⅶ)NES, (Ⅷ) NHS-activated carboxylic group in GEL and (Ⅸ) substituted urea.

Shu et al.[21] developed a new method for preparing hyaluronic acid (HA)-gelatin hydrogels using a disulfide cross-linking method. The HA and gelatin were chemically modified using 3,3′-dithiobis (propionic hydrazide) (DTP). After reduction with dithiothreitol (DTT), the thiol derivatives of HA (HA-DTPH) and gelatin (gelatin-) were obtained and characterized. The synthetic route is shown in Fig. 3. Disulfide crosslinked HA-DTPH, gelatin-DTPH, and blends thereof, were degradable enzymatically by collagenase and by hyaluronidase (HAse). The rapid digestion of the crosslinked 100% gelatin-DTPH film by collagenase was significantly retarded by the presence of 20% or 40% HA-DTPH.

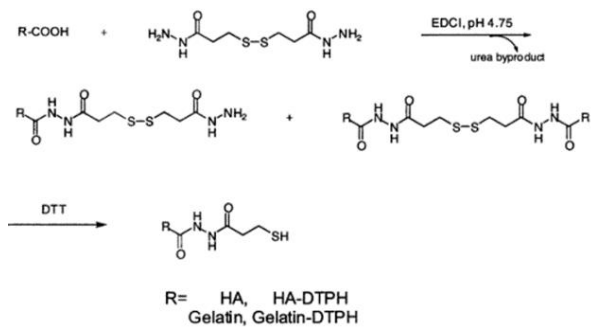

Fig.3 Synthesis of thiolated HA and gelatin.

Xiao et al.[22] designed a new type of photocrosslinked interpenetrating polymer network (IPN) hydrogel based on gelatin methacrylate (GelMA) and sequential polymerization of silk fibroin (SF). It has adjustable structure and biological properties. The preparation process is shown in Fig. 4. Experimental results revealed that IPNs, where both the GelMA and SF were independently crosslinked in interpenetrating networks, demonstrated a lower swelling ratio, higher compressive modulus and lower degradation rate as compared to the GelMA and semi-IPN hydrogels, where only GelMA was crosslinked.

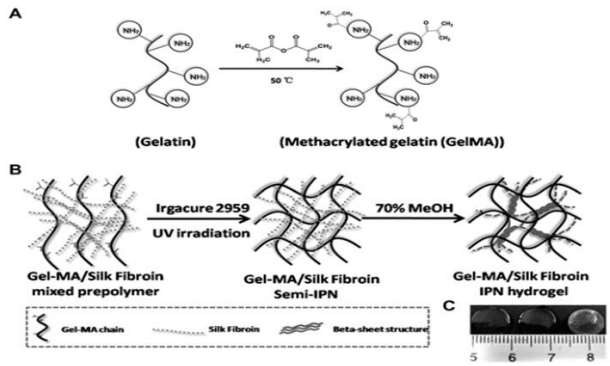

Fig.4 Schematic for synthesizing gelatin methacrylate (GelMA). GelMA-SF composite semi-IPN and IPN hydrogels .Gelatin macromers containing primary amine groups were reacted with methacrylic anhydride (MA) to graft methacrylate pendant groups (A).To create the GelMA-SF IPN hydrogel, the gelatin methacrylate was mixed with SF solution and crosslinked using UA irradiation in the presence of a photoinitiator ,following treatment with 70% methanol to induce SF crystallization (B).Representative optical images of GelMA. G-S-I semi-IPN hydrogel (from left to right) (C).

2.2.2 Hydrogels were prepared from gelatin and synthetic polymer materials

Gelatin based hydrogels can be prepared together with a variety of synthetic polymer materials, such as polyacrylic acid, polyvinyl alcohol, polyurethane, polyethylene glycol, etc. The prepared hydrogels are easy commercialized, and chemical modified, and their properties are tailorable. However, compared with natural polymer hydrogels, biosafety and biodegradability are poor.

Kai et al.[23]used low-temperature (-20°C) deposition techniques to prepare tubular polyurethane (PU) sandwich tubes, ADSC/gelatin/alginate/fibrin constructs. The ADSCs in survived the fabrication and cryopreservation stages by incorporating a cryoprotectant (glycerol or dimethyl sulfoxide (DMSO)) in the cell/hydrogel system. With 5% DMSO or 10% glycerol alone in the hydrogel, the cell viabilities were retained (73% and 62%, respectively). The three-dimensional construct was effectively preserved below -80°C for more than 1 week. After the freeze/thaw processes, cell viability and proliferation ability were regained. This strategy has the potential to be widely used in complex organ manufacturing techniques.

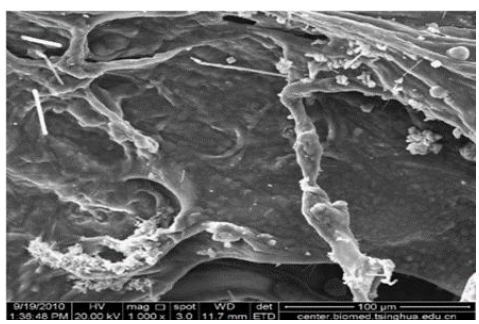

Fig.6 A SEM image of the cell states in the PU sandwich-like gelatin/alginate/fibrin construct after 2 weeks of in vitro culture.

Jason et al.[24]used gelatin methacrylate (GelMA) as a cellular response hydrogel platform for the creation of cell-filled microtissues and microfluidic devices. The synthesis route is shown in Fig. 6. Cells can easily bind, proliferate, elongate, and migrate when inoculated on micropatterned GelMA substrates and encased in micro-manufactured GelMA hydrogels. By varying the methacrylic acid concentration and the gel concentration, it was demonstrated that the hydration and mechanical properties of GelMA were tunable for various applications. Experimental results have shown that GelMA hydrogels can be used to create complex cell-responsive micro-organizations, such as endothelial microvascular systems, or other applications requiring cell-responsive micro-engineered hydrogels.

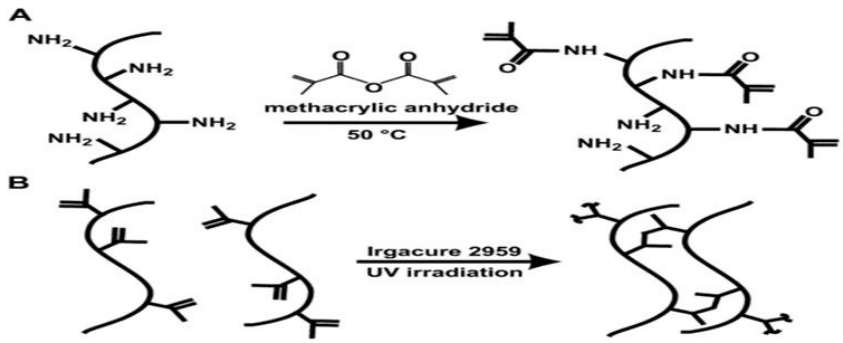

Fig.7 Synthesis of methacrylated gelatin. Gelatin macromers containing primary amine groups were reacted with methacrylic anhydride (MA) to add methacrylate pendant groups(A). To create a hydrogel network, the methacrylated gelatin was crosslinked using UV irradiation in the presence of a photoinitiator (B).

2.2.3 Preparation of hydrogels using gelatin and small molecule cross-linkers

Small molecular crosslinking agents can react with gelatin to prepare a three-dimensional hydrogel. Small molecule cross-linking agents include formaldehyde, glutaraldehyde, epoxy compounds, water-soluble carbodiimides, genipin, and dextran, etc.

Sung et al.[25]analyzed the feasibility of epoxy compound (GRE glue), water-soluble carbodiimide (GAC glue) or genipin (GG glue) as bio-crosslinkers of gels. The preparation mechanism is shown in Fig. 8. GRF glue and GRG glue were used as controls. The results of the cytotoxicity study suggested that the cellular compatibility of the GAC and GG glues was superior to the GRF, GRG, and GRE glues. The GRF and GRG glues had the greatest bonding strengths to tissue among all test adhesives, while the bonding strengths of the GAC and GG glues were comparable. In contrast, there was almost no bonding strength to tissue for the GRE glue. However, the GRF and GRG glues were less flexible than the GAC and GG glues. Subsequent to the bonding strength measurement, each adhesive test was found to adhere firmly to the tissue surface and underwent cohesive failure during the bond breaking.

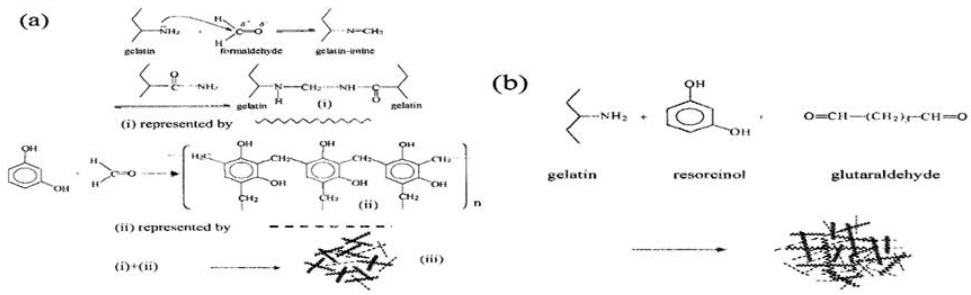

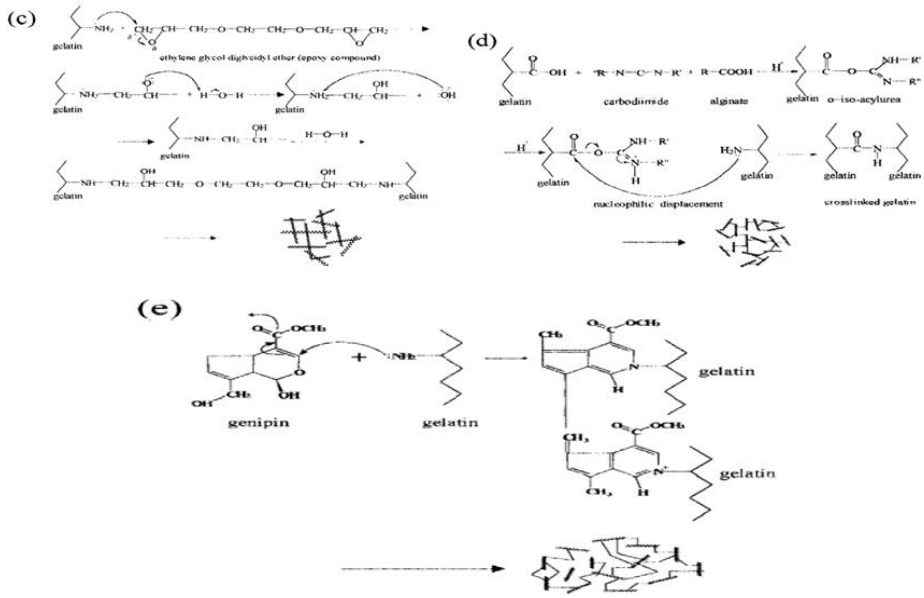

Fig.8 Presumable reaction mechanism for each test adhesive evaluated in the study: (a) the GRF glue, (b) the GRG glue, (c) the GRE glue, (d) the GAC glue, and (e) the GG glue.

Draye et al.[26] prepared hydrogel films by cross-linking of gelatin with dextran dialdehydes (weight ratio of 2:1), containing either fluorescein isothiocyanate-dextran (M8 70000) or polypeptides. The films were evaluated in terms of their release characteristics and mechanical properties upon increasing storage time at 4°C. Significant changes in release kinetics and mechanical properties of the cross-linked gelatin films were observed, especially during the first week after the hydrogel production. Rheological and NMR measurements showed that the mechanical properties of the gelatin hydrogel films were improved with increasing storage time.

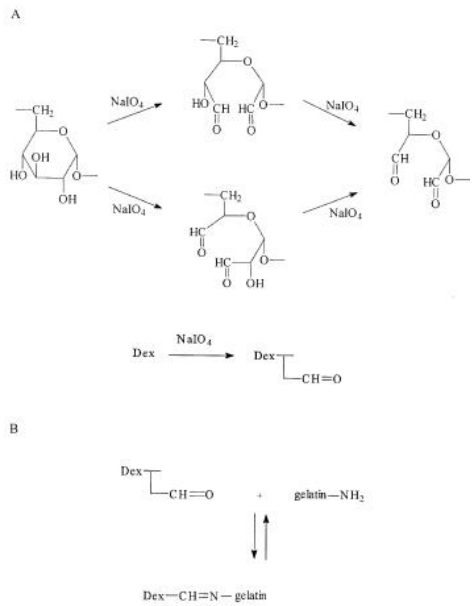

Fig.10 Hydrogel preparation. (A) Partial oxidation of dextran: periodate oxidation of dextran (dex) is a convenient way for the preparation of polyaldehyde derivatives. Since in dextran, the structural units contain three vicinal hydroxyl groups, the oxidation can lead to different types of aldehydes. (B) Cross-linking of gelatin: the cross-linking predominantly due to schiff base formation between the e-amino groups of lysine and hydroxylysine residues of gelatin and the available aldehyde.

2.3 Enzymatic cross-linking method

Enzymes can usually effectively catalyze biochemical reactions. Previous studies have reported that the enzymes used to synthesize hydrogels include transglutaminase, tyrosinase, etc. The amino acid residues contained in gelatin can be catalyzed by transferases to form a network of peptide bond cross-linking. Since the enzyme cross-linking method uses a biocompatible enzyme without involving chemical cross-linking agents, the obtained hydrogels have excellent biocompatibility.

Zhu et al.[27]prepared a new gelatin-based hydrogel in the presence of transglutaminase (mTG). The swelling behavior of the hydrogels obtained with different Bloom value gelatins was measured. Subsequently, the swelling kinetics was investigated. The swelling ratios in various salt solutions (NaCl, $CaCl_2$, $FeCl_3$, $CrCl_3$) and at different temperatures were also determined. Additionally, the swelling of hydrogels was measured in solutions with pH ranged 1-12. Finally, the morphology of the samples was examined by scanning electron microscopy (SEM).

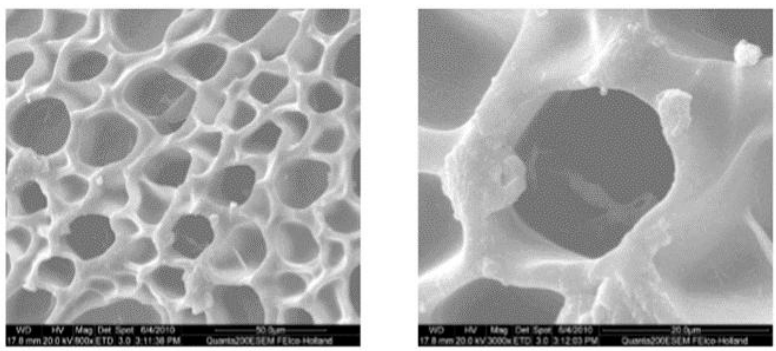

Fig.11 Scanning electron microscope images of transversal sections of swollen hydrogel dehydrated with freeze drying method. left: 800×; right: 3000×

Li et al.[28]first introduced tyramine into the gelatin chains to provide an enzyme cross-linking point for gel formation after injection. Then, heparin, a polysaccharide with binding domains to many growth factors, was covalently linked to the tyramine-modified gelatin. Finally, vascular endothelial growth factor (VEGF) was incorporated into the gelatin derivative by binding with the heparin in the gelatin derivative, and an injectable gel with controlled VEGF release was formed by an enzymatic catalytic reaction with hydrogen peroxide and horseradish peroxidase (HRP). The synthetic route is shown in Fig. 11. The results suggest that the gelatin derivative/VEGF is an excellent injectable delivery system for induced angiogenesis of soft tissue regeneration.

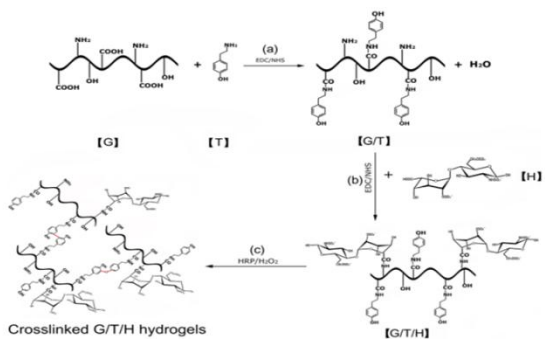

Fig.11 Illustration of the synthesis G/T/H hydrogels. (a) Synthesis of G/T by the coupling of the –COOH in the gelatin chains with the $–NH_2$ in the tyramine. (b) Synthesis of G/T/H conjugates by the condensation of the –COOH in the heparin and the $–NH_2$ in the gelatin. (c) Addition of HRP and H_2O_2 to form injectable G/T/H hydrogels.

3 Application of gelation-based hydrogels

Due to the special responsiveness, low immunity, biocompatibility, biodegradability and high water absorption of the 3D network hydrogels, in recent years, gelatin-based hydrogels have been widely used in water treatment, tissue engineering, drug carrier, regenerative medicine and intelligent materials.

3.1 Applications in water treatment

In China's industrial wastewater, printing and dyeing wastewater account for a large proportion. Biodegradation, photocatalytic degradation, coagulation and adsorption are the main methods to treat these wastewater.The hydrogel adsorption has been paid more attention because it does not introduce new pollutant and realize the recycling of waste resource.

Xiong et al.[29]prepared interpenetrating network hydrogels with chitosan and gelatin as raw materials and genipin as crosslinking agent. The adsorption performance on acid orange II dye was studied. The experimental results show that when the concentration of genipin is 0.5 mmol/L and the pH is 3, the acid orange II dye can be efficiently adsorbed, and the higher the temperature, the greater the adsorption capacity. The chitosan/gelatin interpenetrating network hydrogels can be regerated recycled.

3.2 Application in organizational engineering

The damage and loss of human tissue are one of the most important hazards to human health and the main cause of human diseases and death. Autologous tissue transplantation is a common clinical repair method. Although satisfactory results can be achieved, it is at the expense of self-health organizations. It will lead to many complications and auto-injury. Synthetic tissue substitutes have been widely used in recent years.However, it has the risk of foreign body reaction, infection and other risks, or is eventually expelled from the body. Therefore, gelatin hydrogels have been widely used in tissue engineering due to their low immunity, biocompatibility, biodegradability, anti-bleeding and promoting cell growth.

Feng et al.[30]prepared a novel biodegradable hydroxyapatite/chitosan-gelatin network (HA/CS-Gel) complex by phase separation of bone tissue engineering. The HA granules were dispersed uniformly in the organic network with intimate interface contact via pulverizing and ultrasonically treating commercial available HA particles. Results indicated that the osteoblasts attached to and proliferated on the scaffolds.

Fan et al.[31]prepared a gelatin/silk fibroin composite scaffold material by means of silk protein fiber reinforcement. The results demonstrated that silk cable-reinforced gelatin/silk fibroin scaffold possesses the appropriate mechanical properties and had enlarged surface area. It was also capable of supporting cell proliferation and differentiation for ligament tissue engineering.

3.3 Applications as intelligent materials

Hydrogels can be used as carriers for drug release due to the network with a large number of pores, which provides a pathway for storage and delivery of the drug. At the same time, by adjusting the stimulating factors, the carrier polymer or the polymer hydrogel undergoes volume phase transformation, thereby realizing the targeted administration in vivo, that is, the drug carrier undergoes phase change and local release of the drug when local stimulation is performed around the target organ.

Spizzirri et al.[32]synthesized a novel spherical hybrid hydrogel composed of gelatin and multi-walled carbon nanotubes by emulsion polymerization in the presence of sodium methacrylate and N,N'-ethylenebisacrylamide. The microspheres are used for the electrical response release of diclofenac sodium salt. Different amounts of nanotubes (up to 35% by weight) were covalently inserted into the polymeric network in order to determine the percentage conferring the highest electric sensitivity to the composite microspheres. The obtained gelatin/CNT hybrid hydrogels were able to modulate the release of Diclofenac sodium salt in response to an electric stimulation has been successfully demonstrated.

4 Conclusions and outlook

Although there have been quite a lot of research on the preparation and application of gelatin-based hydrogels, they are not mature enough as an emerging biomaterial and need to be further improved. In the future, the research on gelatin-based bio-gels can be carried out in the following aspects: (1) Improving cross-linking are preparation technology, and reducing the preparation cost of gelatin-based hydrogels; (2) Selecting and developing new crosslinking agents to enhance the mechanical strength and biocompatibility of gelatin-based hydrogels; (3) Strengthening the development of specific functional gelatin-based hydrogels with selective adsorption functions and specific sensitivity to the environment.

Acknowledgement: This paper was supported by the National Key Research and Development Program of China (2017YFB0308503) .

References

[1] Zhang X, Yang Y, Yao J, et al. Strong Collagen Hydrogels by Oxidized Dextran Modification[J]. ACS Sustainable Chem. Eng. 2014, 2(5): 1318-1324.

[2] Yin D W，Zhou Y，Liu Y T，et al. The latest research progress of hydrogel [J]. New Chemical Materials. 2012, 40(2): 21-23, 71.

[3] Qi R，He Z G. Research progress of "smart" hydrogel and its application in medicine and bioengineering [J]. Journal of Shenyang Pharmaceutical University. 2001(06): 447-451.

[4] Wang B，Zhang Y C，Zhang F L, et al. Research progress on intelligent hydrogel modification [J]. Journal of Gansu Lianhe University (Natural Science Edition). 2006(01): 47-51.

[5] Antoine E E, Vlachos P P, Rylander M N. Review of Collagen I Hydrogels for Bioengineered Tissue Microenvironments: Characterization of Mechanics, Structure, and Transport[J]. Tissue Engineering Part B: Reviews. 2014, 20(6): 683-696.

[6] Sargeant T D, Desai A P, Banerjee S, et al. An in situ forming collagen-PEG hydrogel for tissue regeneration[J]. Acta Biomaterialia. 2012, 8(1): 124-132.

[7] Song W, Markel D C, Jin X, et al. Poly(vinyl alcohol)/collagen/hydroxyapatite hydrogel: properties and in vitro cellular response[J]. J Biomed Mater Res A. 2012, 100(11): 3071-3079.

[8] Ren K, He C, Cheng Y, et al. Injectable enzymatically crosslinked hydrogels based on a poly(l -glutamic acid) graft copolymer[J]. Polym. Chem. 2014, 5(17): 5069-5076.

[9] Bai H Y，Ke L F，Zhu W H，et al. Progress in collagen application [J]. Journal of Jilin Medical College. 2013, 34(2): 133-135.

[10] Wallace D G, Rosenblatt J. Collagen gel systems for sustained delivery and tissue engineering.[J]. Advanced Drug Delivery Reviews. 2003, 55(12): 1631-1649.

[11] Parenteaubareil R, Gauvin R, Berthod F. Collagen-Based Biomaterials for Tissue Engineering Applications[J]. 2010, 3(3): 1863-1887.

[12] Raub C B, Unruh J, Suresh V, et al. Image Correlation Spectroscopy of Multiphoton Images Correlates with Collagen Mechanical Properties[J]. Biophysical Journal. 2008, 94(6): 2361-2373.

[13] Achilli M, Mantovani D. Tailoring Mechanical Properties of Collagen-Based Scaffolds for Vascular Tissue Engineering: The Effects of pH, Temperature and Ionic Strength on Gelation[J]. Polymers. 2010, 2(4): 664-680.

[14] Ryu J H, Lee Y, Do M J, et al. Chitosan-g-hematin: Enzyme-mimicking polymeric catalyst for adhesive hydrogels[J]. Acta Biomaterialia. 2014, 10(1): 224-233.

[15] Jin R, Linb C, Cao A. Enzyme-mediated fast injectable hydrogels based on chitosan-glycolic acid/tyrosine: Preparation, characterization, and ch[J]. 2014, 5(2): 391-398.

[16] Joung Y K, You S S, Park K M, et al. In situ forming, metal-adhesive heparin hydrogel surfaces for blood-compatible

coating[J]. Colloids and Surfaces B: Biointerfaces. 2012, 99: 102-107.

[17] Liu J，Yang X Y，Tang K Y，et al. Solvent sensitivity of physical cross-linked polyvinyl alcohol/gelatin composite hydrogel transparency [J]. Polymer Materials science & Engineering. 2012, 28(09): 69-71.

[18] He Q, Huang Y, Wang S. Hofmeister Effect-Assisted One Step Fabrication of Ductile and Strong Gelatin Hydrogels[J]. Advanced Functional Materials. 2018, 28(5): 1705069.

[19] Tran N Q, Joung Y K, Lih E, et al. In Situ Forming and Rutin-Releasing Chitosan Hydrogels As Injectable Dressings for Dermal Wound Healing[J]. Biomacromolecules. 2011, 12(8): 2872-2880.

[20] Gorgieva S, Kokol V. Preparation, characterization, and in vitro enzymatic degradation of chitosan-gelatine hydrogel scaffolds as potential biomaterials[J]. Journal of Biomedical Materials Research Part A. 2012, 100A(7): 1655-1667.

[21] Shu X Z, Liu Y, Palumbo F, et al. Disulfide-crosslinked hyaluronan-gelatin hydrogel films: a covalent mimic of the extracellular matrix for in vitro cell growth[J]. Biomaterials. 2003, 24(21): 3825-3834.

[22] Xiao W, He J, Nichol J W, et al. Synthesis and characterization of photocrosslinkable gelatin and silk fibroin interpenetrating polymer network hydrogels[J]. Acta Biomaterialia. 2011, 7(6): 2384-2393.

[23] He K, Wang X. Rapid prototyping of tubular polyurethane and cell/hydrogel constructs[J]. Bioactive and Compatible Polymers. 2011, 26(4): 363-374.

[24] Nichol J W, Koshy S T, Bae H, et al. Cell-laden microengineered gelatin methacrylate hydrogels[J]. Biomaterials. 2010, 31(21): 5536-5544.

[25] Sung H W, Huang D M, Chang W H, et al. Evaluation of gelatin hydrogel crosslinked with various crosslinking agents as bioadhesives: in vitro study[J]. J Biomed Mater Res. 1999, 46(4): 520-530.

[26] Draye J, Delaey B, Van de Voorde A, et al. In vitro release characteristics of bioactive molecules from dextran dialdehyde cross-linked gelatin hydrogel films[J]. Biomaterials. 1998, 19(1): 99-107.

[27] Zhu D, Jin L, Wang Y, et al. Swelling behavior of gelatin-based hydrogel cross-linked with microbial transglutaminase[J]. journal of aqeic. 2012, 2(63): 11-19.

[28] Li Z, Qu T, Ding C, et al. Injectable gelatin derivative hydrogels with sustained vascular endothelial growth factor release for induced angiogenesis[J]. Acta Biomaterialia. 2015, 13: 88-100.

[29] Xiong Z H，Cui L，Wang J，et al. Adsorption of Acid Orange II by Chitosan/Gelatin Interpenetrating Network Hydrogel [J]. Dyeing &Finishing. 2015, 41(05): 10-14.

[30] Zhao F, Yin Y, Lu W W, et al. Preparation and histological evaluation of biomimetic three-dimensional hydroxyapatite/chitosan-gelatin network composite scaffolds[J]. Biomaterials. 2002, 23(15): 3227-3234.

[31] Fan H, Liu H, Wang Y, et al. Development of a silk cable-reinforced gelatin/silk fibroin hybrid scaffold for ligament tissue engineering[J]. Cell Transplant. 2008, 17(12): 1389-1401.

[32]Spizzirri U G, Hampel S, Cirillo G, et al. Spherical gelatin/CNTs hybrid microgels as electro-responsive drug delivery systems[J]. International Journal of Pharmaceutics. 2003(3): 398-402.

P42

Optimization of Hydrolysis Conditions of Chromium-containing Leather Shavings by Orthogonal Test

Ding Fan[1],Wang Quanjie[1],Peng Han[1]

(1.College of Chemistry and Chemical Engineering, Yantai University, Yantai 264005, China)

Abstract: Chrome-containing shavings hydrolyzed solution is a polydisperse polymer system, in order to make reasonable use of it, it is necessary to first determine the molecular weight of the hydrolyzate obtained under different hydrolysis conditions.In this study, the Ubbelohde viscosity method was used to measure the intrinsic viscosity of the hydrolysate to characterize its viscosity average molecular weight,the intrinsic viscosity of the hydrolyzate is proportional to the size of its viscosity average molecular weight.the minimum Intrinsic viscosity is optimal.The effects of alkali dosage, hydrolysis temperature, liquid-solid ratio and hydrolysis time, on the intrinsic viscosity of the hydrolysate were investigated, the optimal parameter combination of the hydrolysis conditions of chrome shavings was obtained by orthogonal test.The optimal combination of parameters is:the alkali dosage is 17%, the hydrolysis temperature is 100 ℃, the liquid-solid ratio is 6:1 (g: g), and the hydrolysis time is 9 h.

Keywords: Chrome shavings; Ubbelohde viscosity method; Intrinsic viscosity; Viscosity average molecular weight; orthogonal test

Introduction

Chromium containing leather, as a solid waste, will cause serious harm to the environment, which contains valuable protein resources in these solid wastes. It can be hydrolyzed into polypeptide under certain conditions. The polypeptide liquid in the range of different molecular weight has different uses. Therefore, the waste chrome leather is used in the waste. In the process, it is very important to control the molecular weight of the hydrolysate.

Viscosity method is a relative method to determine the molecular weight of polymers. This method is simple in equipment, and easy to operate and has good accuracy. Therefore, it has been widely used in the production and research of polymers.[1] Li Lin et al. determined the relative viscosity of polyvinyl alcohol aqueous solution by Ubbelohde viscosity method and obtained good experimental results[2]. Zhang Wenbin used the Ubbelohde viscosity method to measure the molecular weight of the protein hydrolyzate prepared under the optimal hydrolysis conditions, and the hydrolyzate was compounded by a certain method to prepare a protein type cement foaming agent[3]. Zhang Li measured the molecular weight of three chitosan by Ubbelohde viscosity method and determined the degree of deacetylation. It was found that during the degradation process of chitosan, the value of deacetylation did not change significantly, thus ensuring the stability of chitosan of different molecular weights [4] .

Utilizing the Ubbelohde viscosity method to determine the molecular weight has been applied in many fields. This experiment mainly uses the Ubbelohde viscosity method to determine the intrinsic viscosity of the chrome-containing leather crumb hydrolysate, and to characterize the viscosity average molecular weight by changing the hydrolysis. The conditions were subjected to an orthogonal test to obtain a combination of process parameters capable of obtaining a minimum molecular weight hydrolyzate. The experimental data obtained in this experiment will be a good foundation for future research.

1 Experiment

1.1 Main experimental materials and instruments

Experimental Materials：Chrome-containing shavings，Yantai Wendeng Tannery；Sodium hydroxide，Analytical purity，Tianjin Yongda Chemical Reagent Co., Ltd.；Hydrochloric acid, analytical grade, Yantai Sanhe Chemical Reagent Co., Ltd.

Experimental instruments：DHG-9073 Electric thermostat blast drying oven，Electric thermostat blast drying oven；AR2140 Electronic balance，House Instruments (Shanghai) Co., Ltd.；JJ-1 Precision booster，Guohua Electric Co., Ltd.；HH-SDigital

thermostat oil bath，Jintan Medical Instrument Factory；251 Ubbelohde viscometer，Beijing Xihuayi Technology Co., Ltd.；SYP-DSmart glass thermostatic water bath， Shanghai Weikai Instrument Equipment Co., Ltd.； SHZ-D(III) Circulating water multi-purpose vacuum pump， Gongyi Yuhua Co., Ltd.； Desktop high speed centrifuge， Hunan Hexin Instrument Equipment Co., Ltd.

1.2 Experimental method

1.2.1 Pretreatment of chrome-containing shavings

Weigh a certain amount of chrome-containing black shavings, place them in a tray, then put them into an oven, set the temperature to 50 °C, and weigh them every 5 hours under constant temperature conditions until the difference between the two times is less than 0.2g. It is considered to be dry, taken out, and tested.

1.2.2 Single factor test of the amount of hydrolysis alkali

Weigh 50 g of dry shavings into 500 mL three-necked flask, which hydrolysis temperature is 90 ° C, the liquid-solid ratio is 6, the hydrolysis time is 8 h, and the alkali dosage is changed 8%, 11%, 14%, 17%, 20%. The reaction was carried out under high-speed stirring. After the completion of the hydrolysis, the mixture was allowed to stand, suction-filtered, centrifuged, and neutralized to pH 7 with hydrochloric acid.

1.2.3 Single factor test of hydrolysis temperature

The amount of alkali which can obtain the minimum intrinsic viscosity hydrolyzate is selected, the liquid-solid ratio is 6, and the hydrolysis time is 8 h, and the hydrolysis temperatures are sequentially changed to 60 ° C, 70 ° C, 80 ° C, 90 ° C, and 100 ° C. The processing method is as above.

1.2.4 Single factor test of liquid-solid ratio

The amount of alkali and temperature at which the minimum intrinsic viscosity hydrolyzate was obtained was selected, and the hydrolysis time was 8 h, and the liquid-solid ratio (g: g) was sequentially changed to 4, 4.5, 5, 5.5, and 6. The processing method is as above.

1.2.5 Single factor test of hydrolysis time

The amount of alkali, temperature and liquid-solid ratio which can obtain the minimum intrinsic viscosity hydrolyzate were selected, and the hydrolysis time was changed 6 h, 7 h, 8 h, 9 h, 10 h. The processing method is as above.

1.2.6 Ubbel viscosity method for measuring the viscosity of hydrolyzate

Wash the Ubbelohde viscometer (Figure 1), put it into a dry box for drying, adjust the temperature of the constant temperature water bath at 25±1 °C, and place the dried Ubbelohde viscometer vertically into the water bath. The G ball was completely immersed, and 10 mL of distilled water was pipetted into the A tube, and the B and C tubes were each set with a hose, and the C tube was clamped with a clamp. After the temperature was kept for 10 minutes, the ear tube was used to suck the B tube. The hose draws the distilled water in the A tube to half of the G ball, and then removes the clip of the C tube, so that the distilled water in the B tube slowly falls, and records the time elapsed between the a-scale and the b-scale of the concave surface of the distilled water, parallel Three groups were measured, and the error between the two before and after was less than 0.2 seconds, and the average value was obtained, that is, the outflow time of the distilled water was recorded as t_0. After the distilled water is poured out, the Ubbelohde viscometer is rinsed with the hydrolyzate to be tested, and 10 mL of the hydrolyzate to be tested is injected into the tube A by the same method, and then an appropriate amount of distilled water is added thereto for dilution, and then sequentially measured. The outflow time is recorded as t_1, t_2, t_3, t_4, t_5.

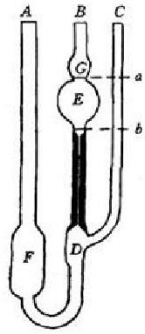

Fig. 1 Ullmann viscometer

1.2.7 Calculation method of intrinsic viscosity of hydrolyzate

Calculation of data obtained by Ubbelohde viscometer：Relative viscosity $\eta_r = t_x/t_0$（x=1,2,3,4,5）, Specific viscosity $\eta_{sp} = \eta_r -1$. Fig. 2，Plot ηsp/C-C and lnηr/C-C, extrapolate to C=0 to obtain intrinsic viscosity [η].

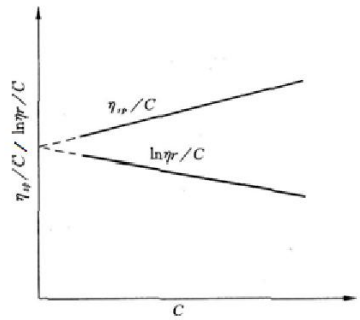

Fig. 2 Calculates [η]

1.2.8 Orthogonal test protocol

Table 1 Orthogonal test plan table

Level	NaOH content %	Hydrolysis temperature / °C	Hydrolysis time / h	Liquid to solid ratio
1	11	80	7	5
2	14	90	8	5.5
3	17	100	9	6

In this study, four factors and three levels of orthogonal experiments were used. Each factor was selected from three levels including the optimal level for L9 (34) orthogonal test. The orthogonal test was used to obtain the best minimum viscosity. The combination of parameters, the three levels selected for each factor are shown in Table 1.

2 Results and discussion

2.1 Single factor test of alkali dosage

As can be seen from Fig 3, With the increase of the amount of alkali, the intrinsic viscosity of the hydrolyzate gradually

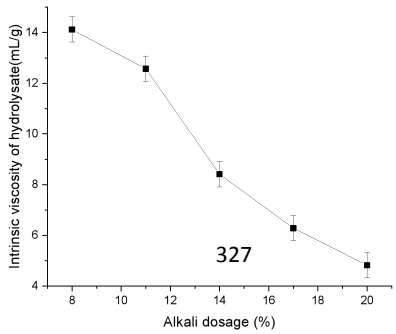

decreased, and the amount of alkali decreased by 11% to 14%.When NaOH hydrolyzes chrome shavings， The free OH- penetrates into the skin collagen to form Cr(OH)3 precipitate, which causes the collagen to degrade and the hydrolyzate characteristic viscosity is reduced. Within a certain range of alkali concentration, as the amount of alkali increases, the OH-concentration increases, thereby promoting the degradation of collagen. However, when the amount of the base exceeds 14%, the degree of intrinsic viscosity decreases, which may be due to the presence of some high alkali-resistance of certain groups of Cr and collagen, so that the continuously increasing OH- cannot react with Cr to form Cr. (OH)3, so that collagen degradation cannot continue. Taking into account the cost problem, 14% is selected as the optimum alkali amount.

Fig. 3 Effect of alkali dosage on the intrinsic viscosity of hydrolysate

2.2 Single factor test of hydrolysis temperature

It can be seen from Fig. 4 that the intrinsic viscosity of the hydrolyzate gradually decreases as the hydrolysis temperature increases, but when the temperature exceeds 90 ° C, the decrease in the intrinsic viscosity is significantly slowed down. At the beginning of heating, the hydrolysis of the skin fiber is accelerated, and the Cr is separated from the collagen. Therefore, as the temperature increases, the intrinsic viscosity of the hydrolyzate decreases, but after the hydrolysis reaches a certain level, the temperature is further increased, and the molecular motion reaches the limit. Therefore, the reduction in the special viscosity number becomes slower. In order to reduce energy consumption, it is optimal to select a heating temperature of 90 °C.

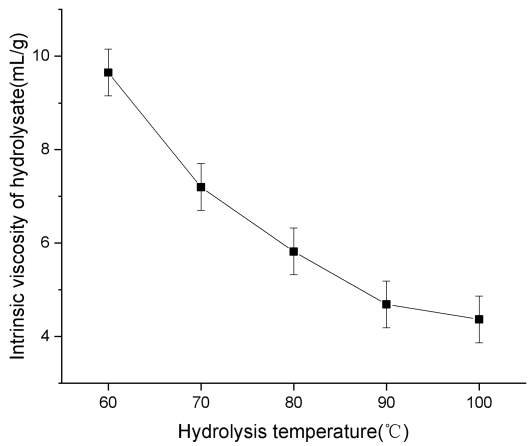

Fig. 4 Effect of hydrolysis temperature on the intrinsic viscosity of hydrolysate

2.3 Single factor test of liquid-solid ratio

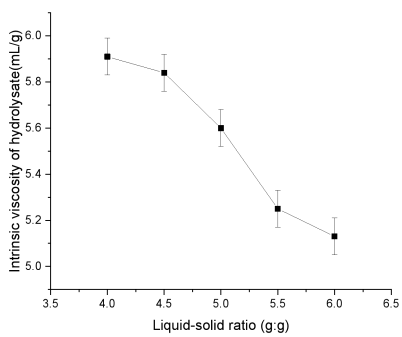

Fig. 5 Effect of liquid-solid ratio on the intrinsic viscosity of hydrolysate

It can be seen from Fig. 5 that as the liquid-solid ratio increases, the intrinsic viscosity of the hydrolyzate gradually decreases. When the liquid-solid ratio is in the range of 4 to 4.5, the increase of the liquid-solid ratio does not significantly contribute to the reduction of the intrinsic viscosity. When the liquid-solid ratio is in the range of 4.5 to 5.5, the intrinsic viscosity of the hydrolyzate is remarkably decreased, but when the liquid-solid ratio exceeds 5.5, the decrease in the intrinsic viscosity is somewhat slowed down. If the amount of water added during hydrolysis is too small, it will cause the shavings to be sufficiently stirred in the three-necked flask, so that it cannot be sufficiently contacted with the alkali solution, and the hydrolysis is incomplete. When the amount of water added is sufficient to allow the shavings to fully contact the lye, continue to add water. Instead, the lye will be diluted. In summary, the optimal liquid-solid ratio was chosen to be 5.5.

2.4 Single factor test of hydrolysis time

It can be seen from Fig. 6 that the intrinsic viscosity of the hydrolyzate gradually decreases with the prolongation of the hydrolysis time, and the decrease of the intrinsic viscosity decreases when the hydrolysis time exceeds 8 h. Within 8 h of the start of the reaction, the collagen fibers of the skin are hydrolyzed, and at the same time, the more OH- which is infiltrated into the collagen and reacts with Cr to form Cr(OH)3 to cause degradation, thereby reducing the intrinsic viscosity of the hydrolyzate, but when After the hydrolysis time exceeds 8 h, the acidic subunit and the basic subunit generated by the cleavage of the peptide bond may be recombined, so that the decrease in the intrinsic viscosity is slowed down. In order to save costs, 8h was chosen as the optimal hydrolysis time.

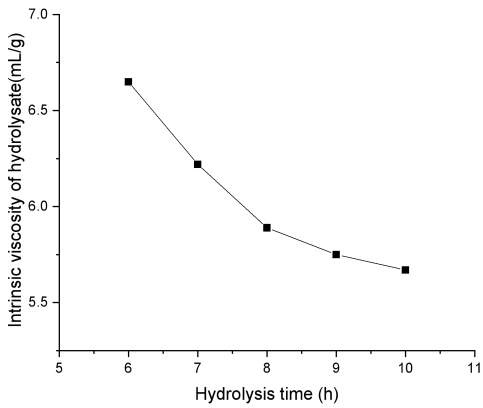

Fig. 6 Effect of hydrolysis time on the intrinsic viscosity of hydrolysate

2.5 Orthogonal test

From Table 2, it can be visually seen that the optimal combination of hydrolysis parameters is: 17% alkali, 100 °C hydrolysis temperature, liquid-solid ratio (g: g): 6:1, hydrolysis time 9 h. This result is different from the single factor test result, which may be the interaction between the four factors.

Table 2 Orthogonal experiment results table

factor	NaOHcontent /%	temperature / °C	time / h	L/S ratio	viscosity	A	B
C	D	（mL/g）					
EXP 1	1	1	1	1	12.62		
EXP 2	1	2	2	2	11.31		
EXP 3	1	3	3	3	10.40		
EXP 4	2	1	2	3	8.80		
EXP 5	2	2	3	1	8.42		
EXP 6	2	3	1	2	8.06		

EXP 7	3	1	3	2	6.23
EXP 8	3	2	1	3	5.79
EXP 9	3	3	2	1	5.32
K_1	34.33	27.65	26.47	26.36	
K_2	5.28	25.52	25.43	25.60	
K_3	17.34	23.78	25.05	24.99	
k_1	11.44	9.22	8.82	8.78	
k_2	8.43	8.51	8.48	8.53	
k_3	5.78	7.93	8.35	8.33	
R	5.66	1.29	0.47	0.45	

factor：A＞B＞C＞D

Better combination：$A_3B_3C_3D_3$

3 Conclusion

In this study, the viscosity-average molecular weight of the hydrolyzate was characterized by the intrinsic viscosity number. The influence of four factors, such as alkali dosage, hydrolysis temperature, liquid-solid ratio and hydrolysis time, on the intrinsic viscosity of chrome shavings hydrolysate was investigated by Ubbelohde viscosity method. The process parameters of the minimum intrinsic viscosity hydrolyzate were obtained by orthogonal test, namely: 17% alkali, 100 °C hydrolysis temperature, liquid-solid ratio (g: g): 6:1, hydrolysis time 9 h. The data obtained from this experiment will provide a good foundation for future research.

References:

(1) Luo, Y. H.; Wang, Q. J.; Chen, P. H. *Leather and chemical industry***2017**, 10.

(2) Li, L.; Tan, G. L.; Su, M. C. *College chemistry***2006**, 53.

(3) Zhang, W. B. M.C.E, Dalian University of Technology, 2016.

(4) Hu, L. M.C.E., Ocean University of China, 2010.

P43

Sunlight-activated color-tunable long persistent luminescent polyurethane leather coatings

Saiqi Tian[1] Haojun Fan[1,2*],Yi Chen[1], Jun Yan[1]

[1] *National Engineering Laboratory for Clean Technology of Leather Manufacture, Sichuan University, Chengdu, 610065, P.R. China*

[2] *State Key Laboratory of Polymer Materials Engineering, Sichuan University, Chengdu 610065, China*

**Corresponding authors' email: fanhaojun@scu.edu.cn*

Abstract As one of the significant steps in leather manufacturing, finishing can endow specific functional properties to the final leather, thus adding the fashion values of creatively designed leather products. Among various coating-forming materials, polyurethane is one of the best candidate for leather finishing in modern leather industry. In this study, some sunlight‐activated color-tunable long persistent luminescent polyurethanes are prepared as leather coatings, via incorporated by amino-functionalized long persistent luminescent phosphors and other functional materials. The luminescent properties and principles of color-tunable effects are investigated. After stoppage of excitation, the polyurethanes emit light in darkness, and the light color can be changed with different conditions.

Key words color-tunable, long persistent luminescent, polyurethane, leather coatings

P44

Optimization of the Process of Preparing Collagen Powder by Experimental Spray Dryer

Zhou Jian,Wang Quanjie*

(School of Chemistry and Chemical Engineering, Yantai University, Yantai 264005, China)

Abstract

Inthis paper, the using of chrome shavings to make collagen powderwasmainly explored. Firstly, collagen hydrolyzate was prepared by alkali dechromization, then the influences such asthe concentration of the feed solution, the inlet and outlet of the experimental spray dryer, the feed volume, the frequency of the fan and other factors on the efficiency of powder spray was explored by orthogonal test in order to find out the best process. The best processrouteisasfollowed: feed liquid solid content is 30%, import temperature 240℃, the outlet temperature is automatically adjusted with the inlet temperature, feeding amount 15r/min,fan frequency 60Hz. The collagen powder obtained under this condition has a good color and the amount of powder sprayed is as high as 2.749g/min.

Keywords: chrome-containing shavings; spray drying; collagen powder;Powdering amount

Introduction

China is one of the leather-making countryin the world, With the output of leatheris about 600 million square meters, and which accounting for about a quarter of the world's total production. On August 1, 2016, the Ministry of Environmental Protection designated chromium-containing waste as hazardous waste. It was not allowed to be burned or buried, and it could only be disposed of by a qualified hazardous waste plant. Thus, The accumulation of waste leather chips is like a mountain, which seriously restricts the development of the leather industry. However,The chrome-containing leather shavings contain valuable protein resources and have high resource utilization value. Some traditional methods for disposal of waste shavings are burying, burning, making recycled leather, vegetable tanned materials, etc.; even some unscrupulous traders use chrome-containing leather shavings to make poison capsules and leather milk, which seriously threaten people's health. Thus, Dechromizing chrome tanning waste to extract collagen powder can not only solve the pollution problem of chrome-containing leather shavings, but also realize the recycling of valuable protein resources. Spray drying to produce collagen powder has the advantages of large evaporation area, short drying time (seconds to tens of seconds), less damage to active ingredients, and is widely used in the chemical industry and food industry[1]. It has been found that the dechromization of chrome-containing leather shavings by alkali method can effectively reduce the chromium content in the collagen hydrolysate. Therefore, the use of chrome-containing leather shavings to produce collagen powder is of great significance for the recycling and utilization of waste.

In this study, the technology of the spray drying is applied to the manufacture of collagen powder, and the solid solution content of the feed liquid, the peristaltic pump speed, the inlet and outlet temperature, and the fan frequency are optimized for the spray volume of the experimental spray dryer, so that the powder is sprayed. The efficiency has been greatly improved.

1. Experiment and Method

1.1. Materials

DHG-9073 electric heating constant temperature air drying oven (Longkou electric furnace manufacturing plant);AR2140 Electronic Balance (House Instruments (Shanghai) Co., Ltd.);JJ-1 precision booster (Guohua Electric Co., Ltd.);HH-S digital display constant temperature oil bath (Jintan Medical Instrument Factory);SHZ-D(III) circulating water multi-purpose vacuum pump (Gongyi City Yuhua Co., Ltd.);Desktop high speed centrifuge (Hunan Hexin Instrument Equipment Co., Ltd.); S212-100L double-layer glass reactor (Changzhou Yawang Instrument Co., Ltd.); L6000Y experimental spray dryer (Shanghai Billion Instrument Co., Ltd.).

1.2. Chemicals

Chrome-containing leather shavings(Yantai Wendeng tannery); CaO, NaOH was provided by Tianjin Yongda Chemical Reagent Co., Ltd.,; HCl was provided byYantai Sanhe Chemical Reagent Co., Ltd..All chemicals were of analytical grade.

1.3. Method

1.3.1. Preparation of Collagen Hydrolysate

The chromium in the leather shavings is mainly coordinated with the carboxyl group of the collagen in the form of a complex. The coordination ability of the hydroxyl group (-OH) with chromium is far greater than the coordination ability of the carboxyl group (-COOH) with chromium. The carboxyl group of collagen can be replaced from the chromium complex to deminelate the chrome collagen. Therefore, the alkali treatment method utilizes this principle to remove chromium from the chrome-containing leather shavings. The free-OH in the alkaline solution enters the chromium complex and is then replaced by the use of collagen carboxyl groups from the chromium complex. The collagen is dechromated while degrading to a certain extent, and then dissolved in water. Chromium combines with -OH to form Cr(OH) precipitate. Separation of collagen hydrolysate from Cr(OH) precipitation by suction filtration or centrifugation. There are many methods for alkali treatment, the main method is to use lime, sodium hydroxide, sodium carbonate, magnesium oxide, etc. This experiment mainly uses the combination of lime and sodium hydroxide, so as to ensure the degree of hydrolysis and achieve a good chromium removal effect. The main component of lime is calcium oxide, which is easy to obtain and inexpensive[2]. The main test methods are as follows:

50 g of chrome-containing black shavings were placed in a three-necked flask, and then 2 g of sodium hydroxide was weighed, 2 g of calcium oxide was added to a three-necked flask, and 400 mL of distilled water was added to the three-necked flask, and finally, the oil bath was used. Heat to about 90 °C. And it is necessary to stir the hydrolyzed leather shavings with a stirring paddle, and the hydrolysis time is generally 6 hours, so that the chrome-containing leather shavings can be completely hydrolyzed.[3]

1.3.2. Filtration of Collagen Hydrolysate

The hydrolyzate after the hydrolysis is completely taken out, since the collagen hydrolyzate after hydrolysis is relatively viscous and is not easily filtered, in order to shorten the time of filtration, the hydrolyzed collagen hydrolyzate can be centrifuged by a bench-top high-speed centrifuge. After the end of the centrifugation, the supernatant is taken, and then the supernatant is subjected to suction filtration using a circulating water type vacuum pump, which can save half of the time. Finally, the hydrolyzate obtained by suction filtration is barreled for use in a subsequent process.

1.3.3. Concentration of collagen hydrolysate

The collagen hydrolyzate after suction filtration is pumped into a double-layer glass kettle by a vacuum pump to be concentrated, and the collagen hydrolyzate is neutralized before concentration, neutralized to a pH of 6.5 to 7, and then neutralized. The collagen hydrolyzate is concentrated, the concentration temperature is adjusted to about 100 ° C, and the collagen hydrolyzate is continuously stirred by a double-layer glass kettle. When the collagen hydrolysate was evaporated and concentrated to four different concentrations of solid content of 20%, 25%, 30%, and 35%, 5 L of collagen hydrolyzate was used for spray drying to investigate the different solid content of the powder. influences.

1.3.4. Spray drying of collagen hydrolysate

The main equipment used for spray drying the concentrated collagen hydrolysate is an experimental spray dryer. The main influencing factors in the dusting process are the solid content of the feed liquid, the inlet temperature, the peristaltic pump speed and the frequency of the fan. The effect of the inlet and outlet temperature of the experimental spray dryer, the peristaltic pump speed and the fan frequency on the dusting was investigated by using a collagen hydrolyzate concentrated to a solid content of 20%.

2. Results and discussion

Table 1. Preparation of collagen powder at different inlet temperatures

Inlet temperature （℃）	Fan frequency （Hz）	Peristaltic pump speed （r/min）	Needle time（s）	Dusting state
120	60	10	5	Collagen powder contains a lot of liquid
140	60	10	5	Collagen powder contains a lot of liquid
160	60	10	5	Collagen powder contains a small amount of liquid
180	60	10	5	Collagen powder is almost dry, but a small amount sticks to the wall of the powder bottle
200	60	10	5	Collagen powder is dry and the color is milky white
220	60	10	5	Collagen powder is dry and the color is milky white
240	60	10	5	Collagen powder is dry and the color is milky white
260	60	10	5	The color of collagen powder is light yellow
280	60	10	5	Collagen powder color is yellow

It can be seen from Table 1 that when the experimental type spray dryer is used for the powder spraying experiment, the inlet temperature is compared differently. The study finds that the collagen powder sprayed out when the inlet temperature reaches 200 ° C or higher has a low moisture content, relatively dry.However, it can be seen from the color of the collagen powder that when the inlet temperature is 200 ° C ~ 240 ° C, it is milky white, which is the upper color of the collagen powder, and the price difference of the collagen powder produced by each factory is very large. The main influencing factors are the content of amino nitrogen, the content of chromium, and the color.Among them, the milky white collagen powder market is better, but it is difficult to sell the yellowish collagen powder. The cause is due to the high temperature. It is found that too high temperature will cause the collagen powder to degenerate. And the loss of nutrients.Therefore, it can be seen from the experimental results that in order to increase the amount of powder sprayed per unit time, the optimum temperature should be controlled at 240 °C.

Table 2. Preparation of collagen powder at different peristaltic pump speeds

Inlet temperature （℃）	Fan frequency （Hz）	Peristaltic pump speed （r/min）	Needle time（s）	Dusting state
240	60	10	5	Collagen powder is dry and the color is milky white
240	60	15	5	Collagen powder is dry and the color is milky white
240	60	20	5	Collagen powder contains a small amount of liquid

According to Table 2, the speed of the peristaltic pump is used to explore the amount of powder sprayed per unit time. It is concluded that when the solid content of collagen hydrolysate is kept at a certain value, the higher the peristaltic pump speed, the more the powder spray per unit time will be. more. The experiment found that the best peristaltic pump speed was 15r/min.

Table 3. Preparation of collagen powder at different fan frequencies

Inlet temperature （℃）	Fan frequency （Hz）	Peristaltic pump speed（r/min）	Needle time（s）	Powder collection(g/min)
240	20	15	5	1.681
240	40	15	5	1.700
240	60	15	5	1.712

Table 3 can be used to find out that the fan frequency has little effect on the amount of powder collected per unit time. For the yield of collagen powder, the amount of collagen is increased, and more collagen powder is pumped to the collection bottle. In the middle, the yield of collagen powder is increased, but when the amount of air is too large, the collagen powder in some collection bottles is taken away and discharged into the air, resulting in a decrease in the yield of collagen powder. Therefore, to ensure the optimization of collagen powder yield, the frequency is set to 60Hz.[4]

The above experiments mainly explore the influence of the inlet temperature of the experimental spray dryer, the speed of the peristaltic pump and the frequency of the fan on the amount of powder sprayed. In order to ensure the rigor of the experimental results, the influence of the feed liquid under different solid contents was further studied.

Table 4. Preparation of collagen powder under different solid content feed liquid

Inlet temperature （℃）	Fan frequency （Hz）	Peristalticpump speed（r/min）	Needle time （s）	Solid content（%）	Powder collection(g/min)
240	60	15	5	20	1.712
240	60	15	5	25	2.327
240	60	15	5	30	2.749
240	60	15	5	35	High solid content

It is concluded from Table 4 that among the factors affecting the amount of powder collected per unit time, the solid content of collagen hydrolyzate accounts for a large proportion. And when the solid content is 30%, the powder collection amount per unit time is the highest, which can reach 2.749g/min.

3. Conclusion

Summarize the above groups of experiments to explore the best process route for the production of collagen powder by using the experimental spray dryer. The first method is to dechromate by alkali method, thereby greatly reducing the chromium content in the collagen hydrolysate; The experimental spray dryer spray-dried the concentrated hydrolyzate to explore the optimal process route for collecting powder per unit time. Through experiment, the best process route can be obtained: the feed liquid solid content is 30%, the inlet temperature is 240 °C, the outlet temperature is automatically adjusted with the inlet temperature, the peristaltic pump speed is 15r/min, and the fan frequency is 60Hz, thus obtaining the powder amount per unit time is 2.749 g/min.

References

(1) Li, S. Y.; Feng, W. H.*Shenyang Chemical***1990**, 24.

(2) He, X. W.; Xie, S. Z.; Huang, Q.*Leather Science and Engineering***2006**, 42.

(3) Zhang, Y.C.; Yang, Y. Z.; Fu, L. H.; Gao, J. J.*Leather and chemical industry***2014**, *31*, 1.

(4) Zhang, Y. C.; Fu, L. H.*Chinese leather***2008**, 6.

P45

Preparation of mussel-like leather finishing materials and strong adhesion, self-healing ability

Baoshuai Wang, Xingchu Liang, Hong Yang, Liqiang Jin, Rong Luo*

School of Leather Chemistry and Engineering, Qilu University of Technology (Shandong Academy of Sciences), Jinan 250353, China, lrcity@qlu.edu.cn

Abstract

Leather finishing plays a pivotal role in tanning process. However, the adhesion force between traditional leather finishing materials and leather substrate is weak relatively, which leads to the coating suffer damaged easily and shortened the functional lifetime of the leather product. Therefore, improving the adhesion of finishing materials, especially in the aqueous, and achieving the self-healing ability of polymer materials after minor damage remain a challenging topic. Inspired by wet self-healing adhesion of mussel, a bionic leather finishing material with strong adhesive characteristics and biological self-healing in dry/water that is surface-functionalized with mussel-inspired dopamine is designed. Here we demonstrate these properties of these synthetic dopamine-functionalized polyacrylate and polymethacrylate materials. Compared with the traditional polyacrylate finishing materials, the adhesion ability, dynamic waterproofing ability, and TABER friction resistance ability coated with bionic leather finishing material are improved significantly. The self-healing properties of these materials also have been tested, and the repaired and pristine samples show similar mechanical properties. Such results directly suggest the importance of dopa. The adhesion properties of mussel-based bionic coating materials also follow the classical polymer viscoelastic principle, that is， the greater the rigidity of the polymer, the weaker its adhesion. In addition, molecular mobility, viscosity and volume have an effect on the strong adhesion and self-healing properties of bionic coating materials. The major studies in this paper also include the mechanism of the catechol-mediated hydrogen bond in this self-healing adhesion process. This study will provide new thoughts and new methods for the investigation of leather finishing material.

Keywords: finishing materials; leather; adhesive; biomimetic; dopaminergic

P46

Preparation of Chrome Tanning Liquor Using the Chrome Sludge from Chrome Shavings and its Application Performance

Wan Xue-chun[1,2], Li Guo-ying[1,2]

[1]*The Key Laboratory of Leather Chemistry and Engineering of Ministry of Education, Sichuan University, Chengdu 610065, PR China, wxc_1130@hotmail.com, 15198028895*

[2]*National Engineering Laboratory for Clean Technology of Leather Manufacture, Sichuan University, Chengdu 610065, PR China,liguoyings@163.com*

Abstact

The chrome sludge was recycled by chrome shavings in presence of CaO and NaOH, the chrome tanning liquor was prepared when dissolved by sulphuric acid, testing showed that it contained high protein content, its tolerance to alkali was so wide that it counted against permeation and combination. Thus enzymatic hydrolysis and water scrubbing were applied to regulate the protein content of chrome sludge, the tolerance to alkali of the recycled chrome tanning liquor was same as a commercial one, application performance of this tanning liquor was investigated. Results showed that when the dosage was 1.44%（based on Cr_2O_3）, the wet-blue leather has excellent appearance such as light color and fine grain. Furthermore the shrinkage temperature was above 100℃, and that the absorbility of Cr_2O_3 was more than 78%. Moreover, the use of the recycled chrome tanning liquor had little affection on the dye absorption, and the leather showed a fine appearance and excellent mechanical properties. Leathers tanned by means of such liquors are comparable to leathers tanned and produced through usual operating procedures. Eventually, the recovery rate of Cr_2O_3 can reach 77.47% by this method. In this way, the purpose of cleaner production and resources recovery can be achieved.

Key words：chrome shavings；chrome tanning liquor；application performance

P47

Modification of Collagen Membrane with Sulphited Quebracho Extract

Hanyu SU [1,2], Yi DENG[1,2], Guoying LI[1,2]

[1]*The Key Laboratory of Leather Chemistry and Engineering of Ministry of Education, Sichuan University, Chengdu 610065, China*

[2]*National Engineering Laboratory for Clean Technology of Leather Manufacture, Sichuan University, Chengdu 610065, China*

Abstract

Collagen membrane was modified by sulphited quebracho extract. The result showed that the color of collagen membrane (CM) would vary with different concentration of tannin or different pH value of reacting solution, while the color levels of CM could be influenced by temperature or time of reaction. The optimum modifying effect was obtained by using 5.0 g/L tannin at pH 5 and 20 °C for 1.0 h. The Fourier transform infrared spectrum demonstrated the generation of hydrogen bonding between tannin and CM, and the triple-helical structure of collagen was remained. After the modification, denaturation temperature of CM raised from 51.9 °C to 57.9 °C. The relative water absorption increased by 16.12%. The tensile strength raised 4.08 MPa while the elongation at break reduced by 3.07%. The enzymatic degradation rate decreased from 64.8% to 15.28%.

Keywords: sulphited quebracho extract, collagen membrane, modification

P48

Microwave irradiation：an effective and innovative routine to promote chrome tanning process

Jinwei Zhang[1], Jiacheng Wu[2], Wuyong Chen[3]

1 National Engineering Laboratory for Clean Technology of Leather Manufacture, SICHUAN UNIVERSITY, CHENGDU 610065, CHINA, +86-13880068495, scutanner@163.com

2 National Engineering Laboratory for Clean Technology of Leather Manufacture, SICHUAN UNIVERSITY, CHENGDU 610065, CHINA, +86-15882474108, 805263831@qq.com

3 National Engineering Laboratory for Clean Technology of Leather Manufacture, SICHUAN UNIVERSITY, CHENGDU 610065, CHINA, +86-13330945940, wuyong.chen@163.com

Abstract

The faster rate, higher yield and milder condition of chemical reactions are obtained under microwave assistant, and better thermal stability of leather is promoted through microwave inducing tanning. In order to study the influence of microwave on chrome tanning process further, the tanning with microwave heating (MW) was regarded as experimental sample and with water bath heating (WB) was control in this work. The chrome tanning processes under different initial pH and ending pH were carried out at first. Then the shrinkage temperature, chrome content and chrome distribution of wet blue were determined to study the influence of microwave on tanning effect. Finally, FT-IR, SEM and XPS were used to illustrate how microwave affect leather structure. The results showed that microwave had positive effect on chrome tanning process representing as higher shrinkage temperature and chrome content as well as more uniform chrome distribution of MV leather. Furthermore, the shrinkage temperature of wet blue exceeded 100℃ when ending pH of tanning at 3.3, indicating tanning could complete under lower pH with microwave assistance which was the unique promotion effect of microwave in chrome tanning. Moreover, the collagen structure and combination between protein and chromium of MV leather were same as WB. In sum, microwave could promote the penetration and combination of chrome during tanning, which might be the evidence of non-thermal effect of microwave in chrome tanning.

Key word: microwave irradiation, chrome tanning, shrinkage temperature, penetration, non-thermal effect

P49

Study on the influence of the crosslinkers on the properties of resin films

Jie Liu*, Feifei Zhang, Weixu Chen, Hao Li, Xuesong Li

College of Leather Chemistry and Engineering, Qilu University of Technology (Shandong Academy of Sciences) , China, Jinan, 250353, ljie1986823@163.com

Abstract

This article focuses on the properties of room-temperature crosslinkers (aziridine, 9090 and polycarbodiimide, EDC) for four commercially available finishing materials (polyurethane, acrylic, casein, and aqueous nitrocellulose). The influence of the type and the amount of cross-linking agent, and the type of resin on the mechanical properties of the resin, solvent resistance, DSC and other comprehensive physical properties was investigated.

The results showed that the addition of two different cross-linking agents increased the tensile strength of the resin film, but the elongation at break gradually decreased. The proper dosage of 9090 to the polyurethane resin was 1.0%, and the amount of EDC was 0.3%. The optimum amount of 9090 for the mechanical property of the acrylic resin was 0.5%, and the amount of EDC used was 0.1%. For the improvement of the mechanical property of casein, the amount of 9090 was 1.5%, and the amount of EDC was 0.2%. The study found that 9090 had better tensile strength than EDC for the four resin films. At the same time, it had the greatest effect on the elongation at break of nitrocellulose, followed by casein and polyurethane, and minimal impact on acrylic acid. The swelling degree of the four resins in the toluene solution, the 0.05 M NaOH solution and the aqueous solution continuously decreased with the increase of the amount of the cross-linking agent. It was found that 9090 has an effect on the yellowing resistance of the resin film. The two crosslinking agents have little effect on the glass transition temperature of the resin.

Key words: Leather finishing agent; crosslinker; property; influencing factors

Introduction

In recent years, the leather industry has grown more demanding for finishing, and it is hoped that the coating has better resistance, wet and dry rubbing, water resistance, solvent resistance and hardness.The cross-linking agent can improve the defects of mechanical properties, water resistance and solvent resistance of the coating material due to insufficient internal crosslinking.The crosslinked resin emulsions increase the molecular weight, block the hydrophilic group and form a network structure, which improves the dry, wet rubbing and solvent resistance remarkably, and the tensile strength of the coating and the inner adhesion of the top layer to the bottom will be enhanced accordingly[1-3]. It can be seen that the excellent properties of crosslinking agents determine the properties of leather products.

The main purpose of this paper is to explore the influence of crosslinking agents on the physical properties of different resins. The changes of the tensile strength, elongation at break, water resistance, alkali resistance, solvent resistance and surface hydrophilicity of the resin film are mainly studied with the variety and dosage of the crosslinker.

2. Experiment

2.1 Materials

Aziridine crosslinkerLINKER 9090, aromatic PU (RU2089, solid content: 17.4%), acrylic resin (RA1105, solid content: 25.2%), casein (CASEIN 5833, solid content: 8.0%) and aqueous nitrocellulose (LW 6182, solid content: 9.7%) were purchased from Sichuan Dawei Technology Co., Ltd. Polycarbodiimide crosslinker EDC was purchased from Maclean Biochemical Technology Co., Ltd (Shanghai, China). Sodium hydroxide (AR grade) were purchased from Sinopharm Chemical Reagent Co., Ltd. Methanol (AR grade)were purchased from Fuyu Fine Chemical Co., Ltd (Tianjin, China). Acetone (AR grade) was obtained from fine chemical plant in Laiyang economic and technological development zone.

2.2 Preparation of crosslinked films

A certain amount of crosslinking agent was added and slowly added to the resin emulsion. After 15 min of crosslinking, it was taken out and poured on the polytetrafluoroethylene plate. After natural flow and no bubble, it was put into a ventilator

and dried 24 h, dried in a oven at 60 °C, and then dried completely after drying to make a resin with a film thickness of about 1 mm and a mass of about 3g.

2.3 Performance testing and characterization

2.3.1 Mechanical properties test[4-6]

The dumbbell shaped sample was cut out from the resin film by the dumbbell mold. According to the standard operation method, the thickness of the sample was measured with a fixed weight gauge. The measuring points were at least three points and the average value was taken. The test method was carried out on the XDL multi-function testing machine. The tensile strength was calculated as follows:

$$\alpha = \frac{F}{bd}$$

Where α is the tensile strength (Mpa); F is the force applied by the sample (N); b is the thickness of the working part of the sample (mm); d is the width (mm) of the working part of the sample.

Elongation at break:

$$\beta = \frac{L - L_0}{L_0} \times 100\%$$

Where β (%) is the elongation at break; L (mm) is the gauge length of specimen when it is breaking; L_0 (mm) is the initial gauge length of sample.

2.3.2 Water resistance test

The circular specimen with a diameter of 1.5 cm was dried in a vacuum oven to constant weight. The sample was soaked in distilled water for 24 h. Then the sample was taken out and quickly dry the surface moisture with filter paper. The calculation formula was as follows:

$$\delta = \frac{m_1 - m_0}{m_0} \times 100\%$$

Where δ is the water absorption of sample, $m_0$and m_1 are the weights of the sample before and after water absorption respectively.

2.3.3 Alkali resistance test

The circular specimen with a diameter of 1.5 cm was dried in a vacuum oven to constant weight. Then it was soaked in 0.5 M NaOH for 24 h. Then the sample was taken out and quickly dry the surface moisture with filter paper. And the swelling of the sample was observed. The calculation formula was as follows:

$$\omega = \frac{m_1 - m_0}{m_0} \times 100\%$$

Where ω is the alkali absorption rate of the sample, $m_0$and m_1 are the weights of the sample before and after alkali absorption respectively.

2.3.4 Organic solvent resistance test

The circular specimen with a diameter of 1.5 cm was dried in a vacuum oven to constant weight. Then it was soaked in toluene for 24 h. Then the sample was taken out and quickly dry the surface moisture with filter paper. The calculation formula was as follows:

$$Z = \frac{m_1 - m_0}{m_0} \times 100\%$$

Where Z is the rate of absorption of toluene, $m_0$and m_1 are the weights of the sample before and after toluene absorption respectively.

2.3.5Contact angle measurement

The resin film was cut into a standard sample of 15 mm x 15 mm. On the test bed, the wettability of water to the surface of

the resin film was measured by the contact angle tester (JC2000C1, China). The contact angle was observed and the wetting effect of water on the resin film with different crosslinkers was compared.

2.3.6 DSC measurement

DSC measurement was conducted on a differential scanning calorimeter (DSC) from NETZSCH Instrument Company (PC200-DSC, German). The lyophilized sample (ca. 4 mg) was sealed in an aluminum pan with an empty aluminum pan as the reference and heated at a constant rate of 5 ^{o}C/min from -30 ^{o}C to 150 ^{o}C under a nitrogen flow.

3. Results and discussion

3.1 Influence of crosslinker on mechanical properties of resin film

The tensile strength and elongation at break are the important indexes to detect the mechanical properties of the resin film. It is important to understand the force and deformation of the resin film under a certain external force, so as to judge the performance and durability of the film.

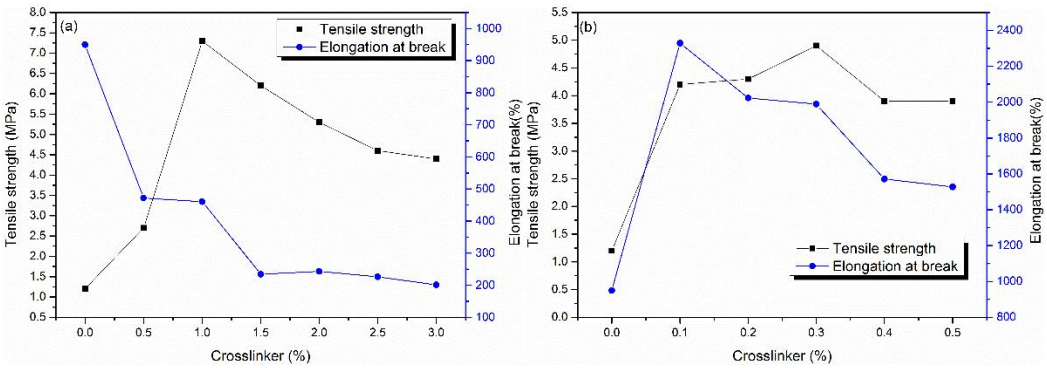

Fig.1 Tensile strength and elongation at break of polyurethane cross-linked with 9090 (a) and EDC (b)

Figure 1 shows that the tensile strength of the resin films crosslinked with 9090 is significantly higher than that of the resin films without crosslinking agent. The trend is to increase at first and then decrease, and there is a tendency to rise obviously within the range of 0-1.0% of the crosslinker. It is gradually decreasing in the range of 1-3%, indicating that it has the best effect on the mechanical properties of the resin film when the amount of crosslinker is about 1%. At the same time, the elongation at break of the resin film shows a trend of decreasing. Because with the increase of the crosslinking agent, the reticular formation is formed inside the resin film, the more difficult it is to be stretched and the elongation at break is lower. After adding the crosslinker EDC, it can be seen that the optimum amount of EDC is 0.3%. After more than 0.3%, the tensile strength has slightly decreased, and the elongation at break has also declined.

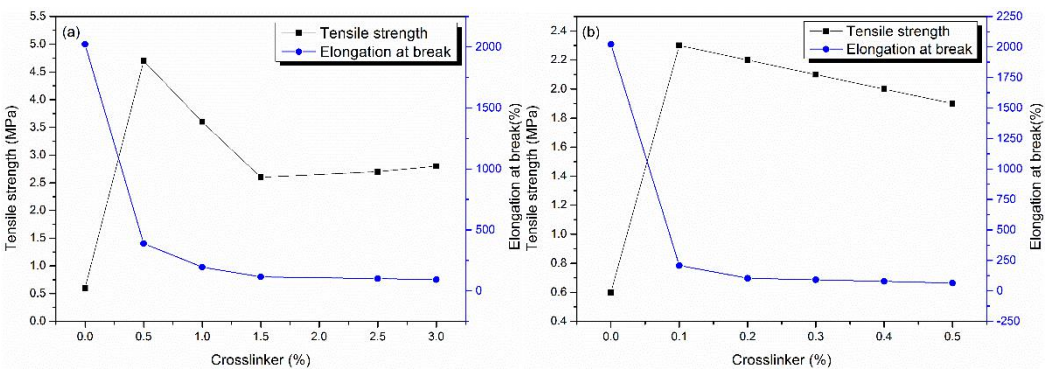

Fig.2 Tensile strength and elongation at break of acrylic resin cross-linked with 9090 (a) and EDC (b)

As shown in Fig. 2, the change of tensile strength and elongation at break of acrylic resin film cross-linked with LINKER 9090 and EDC are similar. In the range of 0-0.5% 9090, the fluctuation trend is very obvious. In the range of 0.5-3%, the tensile strength begins to decrease gradually and the elongation at break decreases. It shows that the resin has the best

mechanical properties when the dosage of 9090 is 0.5%.In contrast, the tensile strength and elongation at break of the resin film cross-linked with 9090 are better than that of EDC.

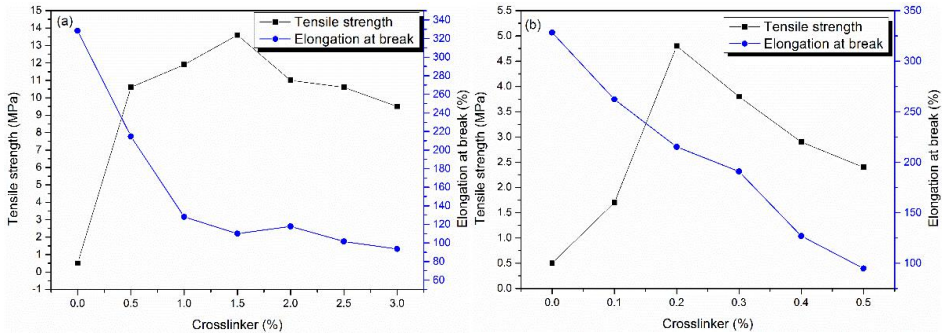

Fig.3 Tensile strength and elongation at break of casein cross-linked with 9090 (a) and EDC (b)

According to Fig. 3, when the amount of crosslinker 9090 is 1.5%, the tensile strength of the film is the largest and then begins to decrease, while the tensile strength is the largest when the amount of crosslinker EDC is 0.2%. Generally speaking, two kinds of crosslinking agents have the same effect on the mechanical properties of casein.

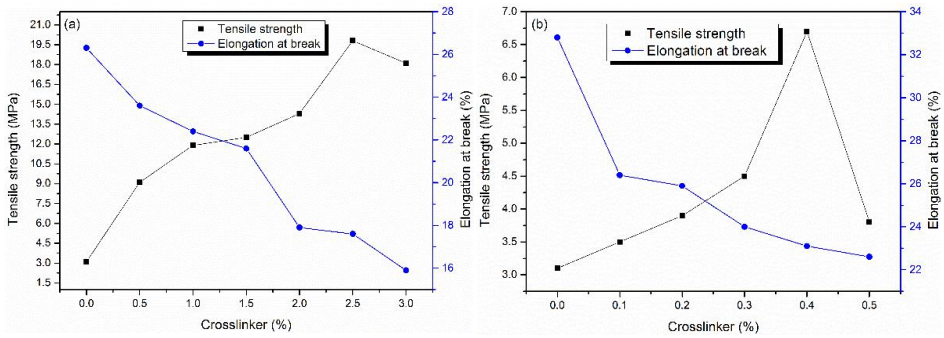

Fig.4 Tensile strength and elongation at break of waterborne nitrocellulose cross-linked with 9090 (a) and EDC (b)

From Fig.4, it can be seen that with the increase of the amount of crosslinker, the tensile strength of the aqueous nitrocellulose first rises and then decreases. When the amount of 9090 is 2.5%, the tensile strength is maximum, and the tensile strength becomes lower more than 2.5%. When the crosslinker EDC dosage is 0.4%, the tensile strength is the largest, but the tensile strength of the resin film cross-linked with 9090 is stronger than that of EDC. Elongation at break decreases as the amount of crosslinking agent increases.

3.2 Water resistance of crosslinked film

Water resistance refers to the ability of resin film to resist water damage. The damage of water to the properties of adhesive film is reflected in different aspects. The most obvious phenomenon is the decrease of mechanical properties of materials. Because the adhesive force is weakened after water is absorbed by the film, it will lead to varying degrees of decreases in the strength of the material.

Table 1. Water absorption rate of resin film before and after crosslinking

Crosslinker (%)		RU2089	RA1105	CASEIN 5833	LW 6182
9090	0	34.48	53.13	Dissolve	34.52
	0.5	22.80	41.28	95.12	22.49
	1.0	9.35	28.26	40.96	20.85
	1.5	4.83	14.31	35.62	16.60
	2.0	4.42	12.89	20.61	16.27
	2.5	4.13	12.22	13.14	11.59
	3.0	4.02	11.77	9.54	10.57

Crosslinker (%)		RU2089	RA1105	CASEIN 5833	LW 6182
EDC	0.1	63.09	207.89	Dissolve	17.02
	0.2	49.48	203.45	Dissolve	15.16
	0.3	39.87	201.89	Dissolve	14.63
	0.4	36.19	183.46	Dissolve	11.44
	0.5	34.77	182.95	Dissolve	11.08

According to Table 1, the water absorption of resin film decreases with the increase of crosslinking agent dosage. Compared with the 9090, the water absorption of the resin film cross-linked with EDC is relatively high, which is related to the smaller amount of EDC. In addition, 9090 may have a better cross-linking effect, which makes the three-dimensional network structure of the crosslinked film more solid and more resistant to hydrolysis.

3.3Alkali resistance of crosslinked film

The test of alkali resistance refers to the ability of resin film to resist the destruction of alkaline medium.

Table 2. Alkali absorption rate of resin film before and after crosslinking

Crosslinker (%)		RU2089	RA1105	CASEIN 5833	LW 6182
9090	0	254.07	163.02	Dissolve	23.39
	0.5	27.65	94.55	Dissolve	19.38
	1.0	7.02	70.73	Dissolve	17.49
	1.5	6.57	30.50	Dissolve	15.43
	2.0	2.84	12.67	Dissolve	13.68
	2.5	2.21	11.12	Dissolve	12.92
	3.0	2.08	10.92	Dissolve	10.31
EDC	0.1	119.36	51.01	Dissolve	18.68
	0.2	88.60	45.38	Dissolve	10.51
	0.3	75.00	36.84	Dissolve	7.04
	0.4	70.58	36.32	Dissolve	6.83
	0.5	69.24	35.37	Dissolve	6.81

As shown in Table 2, the alkali absorption rate of the films after 9090 and EDC crosslinking decreases except casein. The results show that the use of crosslinking agent increases the alkali resistance of the resin. The low alkali resistance of casein (all dissolve) may be due to the hydrolysis of peptide bonds which is easily occurring under alkaline conditions.

3.4 Organic solvent resistant

Solvent resistance refers to the ability of resin film to resist swelling, dissolution, cracking or deformation caused by solvents.

Table 3. Absorption rate of toluene of the film before and after crosslinking

Crosslinker (%)		RU2089	RA1105	CASEIN 5833	LW 6182
9090	0	414.64	Dissolve	173.70	93.49
	0.5	155.13	Dissolve	15.64	74.72
	1.0	131.93	Dissolve	13.43	72.94
	1.5	130.62	Dissolve	13.25	70.74
	2.0	126.90	Dissolve	7.40	65.97
	2.5	123.55	Dissolve	7.24	62.98
	3.0	103.56	Dissolve	1.96	58.68

EDC	0.1	396.26	Dissolve	4.80	68.39
	0.2	328.48	Dissolve	4.75	47.78
	0.3	294.72	Dissolve	4.67	47.57
	0.4	276.96	Dissolve	3.36	45.56
	0.5	257.77	Dissolve	1.10	29.66

As can be seen from Table 3, the solvent resistance of each resin film decrease with the increase of the amount of crosslinker. And solvent resistance of of resin films crosslinked with the two crosslinkers are strengthened. Among them, crosslinking agent 9090 is better than crosslinking agent EDC for solvent resistance of resin. In addition, compared with the other three resins, acrylic resin has the worst toluene resistance.

3.6 The hydrophilic property of the resin film

The contact angle of material surface reflects the hydrophilicity of the material surface and indirectly represents the number of hydrophilic groups of the material.

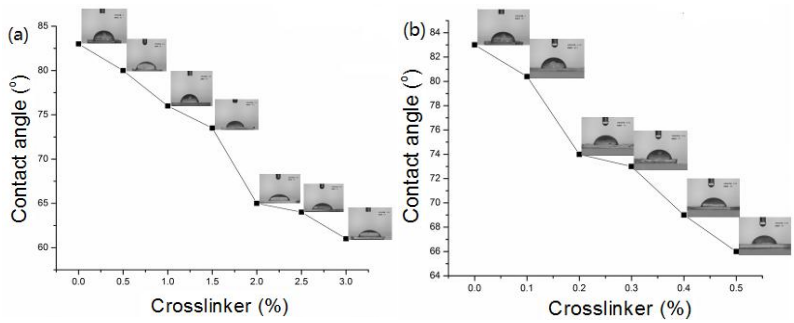

Fig.5 Contact angle of polyurethane cross-linked with 9090 (a) and EDC (b)

Fig.5 is the contact angle of polyurethane resin linked by adding different amounts of 9090 and EDC. As the amount of crosslinking agent increases, the angle of contact angle gradually decreases, and the wetting effect of resin film becomes better. It may be related to the roughness of the surface of the membrane. With the increase of the crosslinking agent, the three-dimensional reticular structure of the crosslinked polymer is further solidified and the surface of the film becomes more and more smooth. The surface hydrophilicity will gradually become larger when the chemical properties of the resin (hydrophilic group) have little change[7,8].

3.7 DSC analysis

With the glass temperature as the boundary, the physical properties of the polymer show a significant change with the change of the degree of freedom of the polymer chain movement[9]. Consequently, the change of heat capacity makes the DSC thermal analysis method an effective mean to determine the glass temperature of polymer materials.

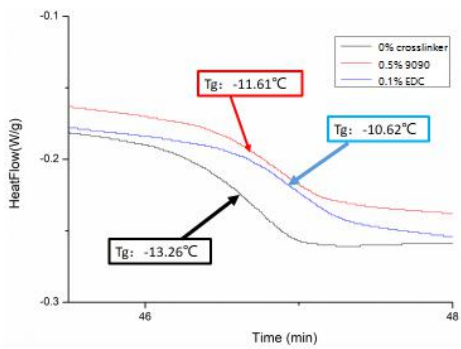

Fig.6 DSC curves of acrylic resin films cross-linked with 0.5% 9090 and 0.1% EDC

It can be seen from Fig. 6 that the glass transition temperature (Tg) of the crosslinked resin film is slightly improved

compared with that of the non-crosslinked resin. And the degree of improvement is within 2-3 °C. Tg refers to the process of resin transition from glass to high elastic state. The chain segment rigidity of the resin increases after crosslinking, and the difficulty of heat movement between the molecules increases slightly, so the glass transition temperature rises. The degree of improvement is small, indicating that crosslinking agent has little effect on the glass transition temperature of the resin.

4. Conclusion

Four main finishing agents were selected as main raw materials, and linkers 9090 and EDC were used to crosslink the resins. The results show that the tensile strength of the crosslinked resin film is obviously enhanced. The optimum amount of 9090 to polyurethane resin, acrylic resin, casein and nitrocellulose is 1%, 0.5%, 1.5% and 2.5%, while the amount of crosslinker EDC is 0.3%, 0.1%, 0.2% and 0.4%. For the tensile strength, 9090 is better than the EDC, and the elongation at break of the resin film after crosslinking has a significant decreasing trend. The elongation at break of acrylic resin is the highest, followed by polyurethane and casein. And nitrocellulose is the worst. With the increase of the crosslinking agent, the water resistance, solvent resistance, alkali resistance and surface hydrophilicity of the resin film are constantly enhanced. The swelling degree of resin film is the largest in the toluene, followed by in the NaOH solution. The swelling degree is the smallest in the water, and the glass transition temperature of the resin film after crosslinking is not high, and the membrane still has a superior low temperature flexibility.

Acknowledgments

The authors wish to acknowledge financial support from the National Key Research and Development Program of China (Project No. 2017YFB0308603).

References

[1] D Wei, Fei Xie, Li Jia, et al. Study on synthesis and properties of crosslinker used to leather finishing [J]. China Leather, 2002, 31(19): 25-30.

[2] J Sun, S Zeng, L Zhu. Application of Crosslinker in the Top Coating of Furniture Leather[J]. China Leather, 2006, 35(3): 3-7.

[3]F Yu, L Cao, ZH Meng, N Lin, XY Liu.Crosslinked waterborne polyurethane with high waterproof performance [J]. Polymer Chemistry,2016 , 7 (23) :3913-3922.

[4]Li J H, Hong R Y, Li M Y, et al. Effects of ZnO nanoparticles on the mechanical and antibacterial properties of polyurethane coatings[J]. Progress in Organic Coatings, 2009, 64(4): 504-509.

[5]Bistričić L, Baranović G, Leskovac M, et al. Hydrogen bonding and mechanical properties of thin films of polyether-based polyurethane–silica nanocomposites[J]. European Polymer Journal, 2010, 46(10): 1975-1987.

[6]Kim B K, Seo J W, Jeong H M. Morphology and properties of waterborne polyurethane/clay nanocomposites[J]. European Polymer Journal, 2003, 39(1): 85-91.

[7]Lee J H, Ju Y M, Kim D M. Platelet adhesion onto segmented polyurethane film surfaces modified by addition and crosslinking of PEO-containing block copolymers[J]. Biomaterials, 2000, 21(7): 683-691.

[8] Alves P, Cardoso R, Correia T R, et al. Surface modification of polyurethane films by plasma and ultraviolet light to improve haemocompatibility for artificial heart valves[J]. Colloids and Surfaces B: Biointerfaces, 2014, 113: 25-32.

[9] Barrioni B R, de Carvalho S M, Oréfice R L, et al. Synthesis and characterization of biodegradable polyurethane films based on HDI with hydrolyzable crosslinked bonds and a homogeneous structure for biomedical applications[J]. Materials Science and Engineering: C, 2015, 52: 22-30.

P50

Preparation and characterization of collagen fibers spun from liquid-crystalline collagen

Osamu Harada

Technical Support Center for Leather Industries, Hyogo Prefectural Institute of Technology, 3 Nozato, Himeji, Hyogo 670-0811, Japan

Abstract

Studies on wet-spun synthetic collagen fibers were mainly performed in the 1980s, and recent research on synthetic collagen fibers is rare because this material is low in strength and alternative synthetic fibers have become common. However, native collagen fiber is known to be very strong; consequently, improvements in the wet-spinning process may lead to the synthesis of strong collagen fibers.

The objective of this study was the fabrication of high-strength collagen fibers by improving the wet-spinning process from liquid-crystalline collagen. Fibers were drawn in air to produce macromolecular unidirectionally oriented collagen fibers that were as strong as polyester. Since high-strength collagen fibers can be machine knitted, they can be used in both medical and apparel applications. Moreover hollow collagen fibers were fabricated from liquid-crystalline collagen by wet spinning with an improved nozzle; these fibers are light, exhibit good heat retention, and can also be used as artificial blood vessels.

Key words: collagen fiber, liquid crystalline, air gap spinning, high strength, hollow fiber

1. Introduction

Collagen is the most important animal protein and the most widely used extracellular matrix protein for cell culturing because it facilitates the attachment, growth, differentiation, migration, and tissue morphogenesis of cells. Synthetic materials are extensively used in medicine, but these materials have limitations and drawbacks. The poor biocompatibilities of synthetic materials are the most serious issues, often resulting in inflammation. Hence, collagen has been heralded as an appropriate replacement implantable material.

This study details the spinning of synthetic collagen fibers using a highly concentrated collagen solution that exhibits liquid-crystalline properties, whereas DuPont self-organized para-aramid molecules into nematic crystalline states in solution, and commercialized the resulting Kevlar fiber, which is a high-strength fiber prepared by air-gap spinning. We hypothesized that a monomeric liquid-crystalline collagen solution could be transformed into fibers by air-gap spinning, such as that used for the preparation of Kevlar. During air-gap spinning, the precursor polymer is in a liquid-crystalline phase in a suitable solvent prior to being spun into a nonsolvent bath. Since the liquid-crystalline phase, which has one- or two-dimensional order, is oriented in the direction of the shear force or flow, the resultant fiber forms a highly oriented structure upon solidification. The solubilized collagen spontaneously assembles into a liquid-crystalline phase at high concentrations, as determined by polarized-light microscopy. As high-performance fibers can be machine-knitted, they can also be used in apparel. This study investigated the production of high-strength collagen fibers by air-gap spinning; moreover hollow collagen fibers were fabricated from liquid-crystalline collagen by wet spinning using an improved nozzle.

2. Experimental and Methods

2.1 Materials

The collagen was sourced from pickled cowhide, which was washed in cold water and Soxhlet extracted to remove fats.

2.2 Preparation of solubilized collagen solutions

Solubilized collagen was extracted according to the method of Shunji Hattori et al.,[1] with some modification. The cowhide was immersed in a solution of 2.0 wt% NaOH and 0.5 wt% monomethylamine at 10 °C for one week. The monomeric collagen was precipitated by adjusting the pH to 4.2 with 3 M HCl. The precipitate was collected by centrifugation at 8,500 rpm for 30 min and then dissolved in water at pH 3.0. This procedure was repeated three times to desalt the material.

The desalted collagen solution was filtered though a GF/B-grade Whatman glass microfiber filter to remove collagen

oligomers. The purified solubilized collagen solution obtained in this manner was then freeze-dried.

2.3 Air-gap wet spinning

Solutions of collagen, with concentrations of 9.3–24.4 wt%, were obtained by adding the required amount of the freeze-dried collagen to 0.1 M lactic acid solution. The solubilized-collagen solution of the required concentration was degassed and injected into a stainless-steel tube. The tube, equipped with a steel needle with an inner diameter of 0.2 mm, was positioned above a coagulation bath containing 20-wt% Na_2SO_4 solution, as shown in Figure 1. The solution was extruded bypressure at a rate of 0.1 mL/min. The collagen solution exhibiting die swelling at the exit of the syringe during ejection, before entering the coagulation bath. A roller was rotated to extend the fiber, which enhanced extensional stress in the 0.5-cm air gap between the spinneret and the coagulation bath, which helped to align the molecules prior to coagulation. After the collagen fibers were guided from the coagulation bath, they were wound directly onto a bobbin, cross-linked with formaldehyde, and then dried under vacuum at 70 °C. The draw ratio of the fiber was determined from the fiber diameter before and after drawing. All procedures described above were performed below 25 °C unless otherwise specified.

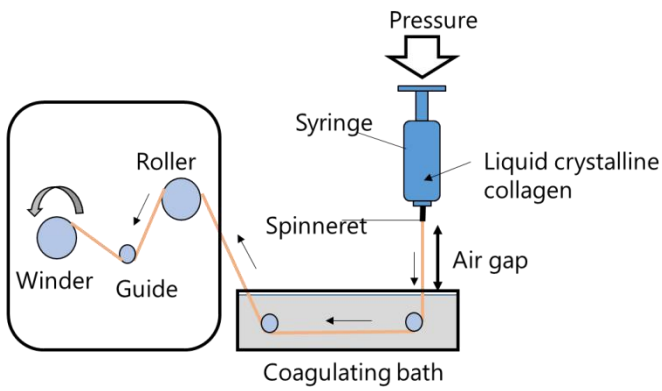

Figure 1. Apparatus for air-gap wet spinning.

2.5 Hollow collagen fibers by wet spinning

The process for the spinning of hollow fibers is shown schematically in Figure 2. The solubilized collagen solution (20.0 wt%) and the coagulant (20 wt% Na_2SO_4) were degassed prior to spinning, and filtered through a 15- m metal filter to remove any particles from the solution during spinning. Hollow collagen fibers were fabricated by pumping the collagen solution through a spinneret using a tube-in-orifice structure, with an inner diameter of 0.4 mm and an outer diameter of 0.8 mm. The solubilized collagen solution was forced through the spinneret and the annular space of the spinneret. The internal coagulant was driven through the central tube by a circulation pump.

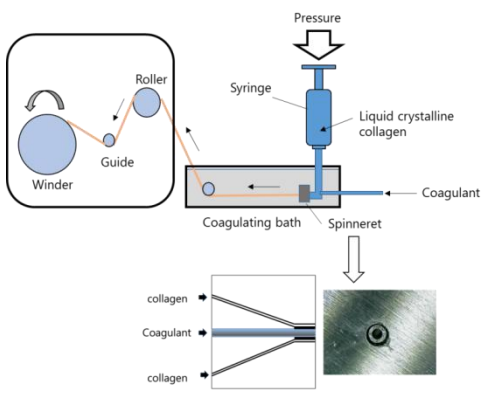

3. Results and discussion

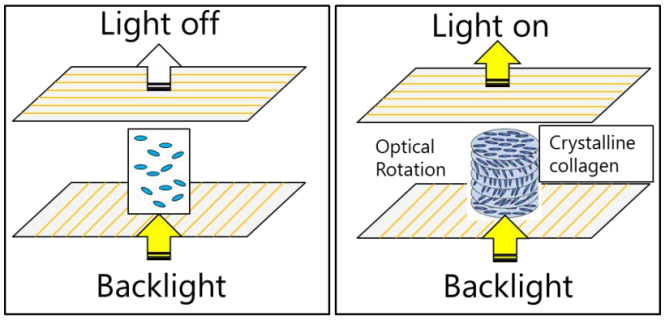

Figure 2. Apparatus for hollow collagen-fiber spinning.

Figure 3. Depicting the fundamentals of cross polarization.

3.1 Liquid-crystallinity

Polarized optical microscopy is typically used to detect the presence of liquid-crystal phases in solution, the principles of which involve polarized light. A polarizer is a filter that only permits light oriented in a specific (polarizing) direction to pass through. A polarizing optical microscope has two polarizing filters that are oriented at right angles to each other in a state that is known as "cross polarization". The fundamentals of cross polarization are illustrated in Figure 3. The polarizing direction of the instrument is aligned with the incident beam, so only that waves that are aligned with the polarizer can pass through. The filtered wave is subsequently blocked by the second polarizer, since this polarizer is oriented orthogonally to the incident wave.

Figure 4 displays images of solubilized collagen solutions at various concentration obtained by polarization microscopy, as described above, which revealed that collagen is liquid crystal It is well known that when shear stress or extension stress is applied to a cholesteric liquid-crystal or nematic liquid-crystal polymer, a band structure with zigzag-oriented molecular chains is formed. As shown in Figure 5, a band structure was observed when a spun collagen fiber was examined by polarizing microscopy, confirming that the collagen solution is liquid crystalline.

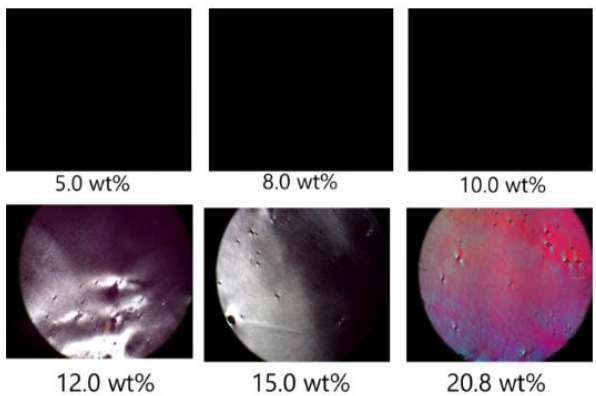

Figure 4. Polarizing optical microscopy images of various collagen solutions.

Figure 5. Polarizing optical microscopy image of a collagen fiber obtain from 20.8 wt% collagen.

3.2 Air-gap wet spinning and collagen-fiber characterization

Novel collagen fibers were fabricated by air-gap wet spinning from liquid-crystalline collagen. As shown in Figure 6, the collagen fibers are shiny and resemble silk. Figure 7 shows scanning electron microscopy (SEM) images of the fibers at different magnification, which reveal cylindrical structures with smooth surfaces.

Figure 6. Photographic image of collagen fibers.

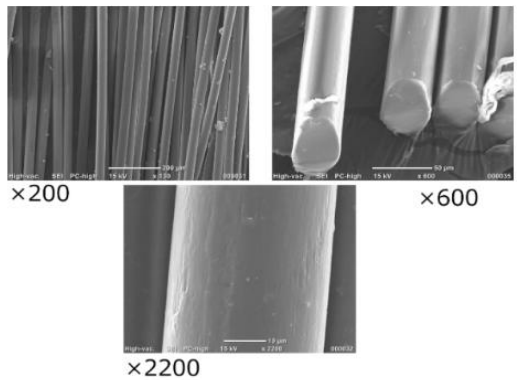

Figure 7 SEM images of collagen fibers.

To determine the effect of the fiber draw ratio on the mechanical properties of the drawn fibers, the formaldehyde cross-linked fibers were subjected to tensile-stress testing. Figure 8 displays the tensile strengths of the collagen fibers obtain from solutions of various concentration, which reveals that tensile strength is significantly affected by the draw ratio and the concentration.

Figure 9 displays the tensile strength of the collagen fiber spun from 24.4 wt% collagen as a function of birefringence, which is a known indicator of collagen-fiber orientation;[2] birefringence increases with increasing draw ratio.

Highly oriented structures were presumably formed by the combined effects of shear flow and drawing in the air gap. The maximum strength obtained was 3.5 cN/dtex, which is equal to or higher than that of silk and cotton.

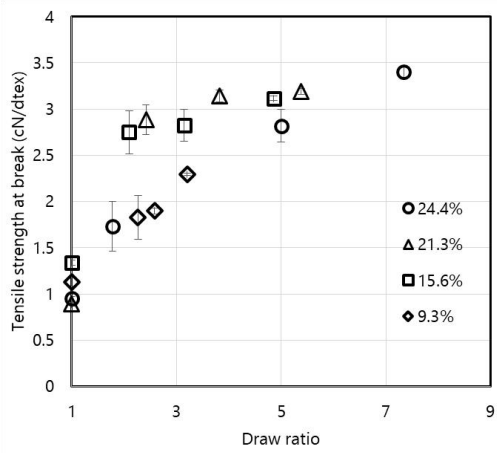

Figure 8. Tensile strength at break as a function of draw ratio.

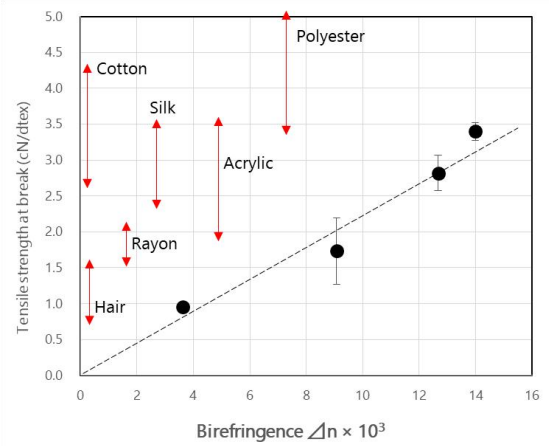

Figure 9. Tensile strength at break as a function of birefringence.

3.3 Hollow collagen fibers

Hollow collagen fibers were fabricated using the apparatus shown in Figure 2. Surface and cross-sectional SEM images of the hollow collagen fibers are presented in Figure 10; these fibers had diameters of about 0.6 mm and fiber-wall thicknesses of about 50 m. The diameters of these hollow fibers can be reduced by drawing.

Although synthetic blood-vessel prostheses have successfully been used for large-diameter vascular reconstructions, until now no functional small-diameter (< 6 mm) artificial vascular grafts are available. Autologous veins and arteries are currently being used as vessel substitutes, but restricted artery supply and compliance mismatches are some of the main drawbacks encountered using this approach. Figure 11 reveals that a liquid, such as blood, can pass through the lumen of the

hollow collagen fiber; consequently, we expect that the fiber can function as an artificial blood vessel.

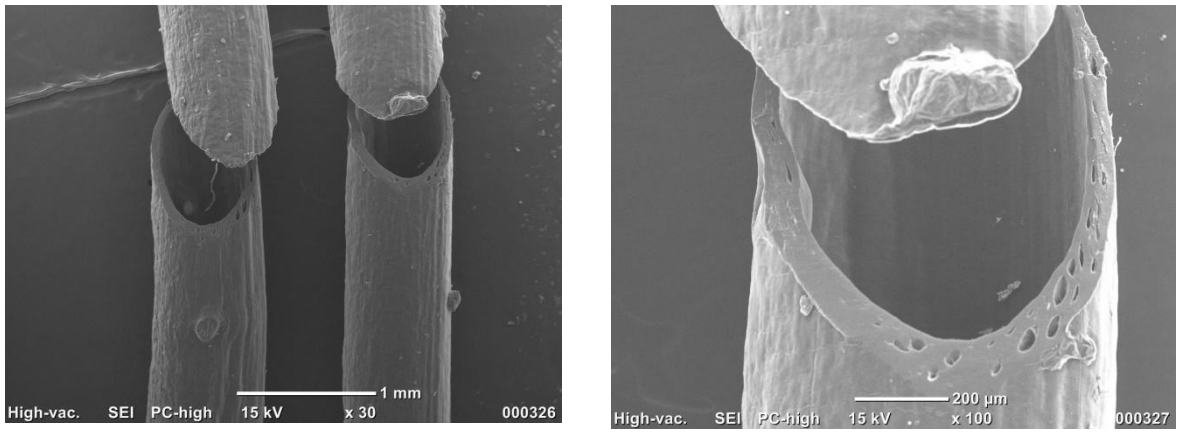

Figure 10. SEM images of the hollow collagen fiber.

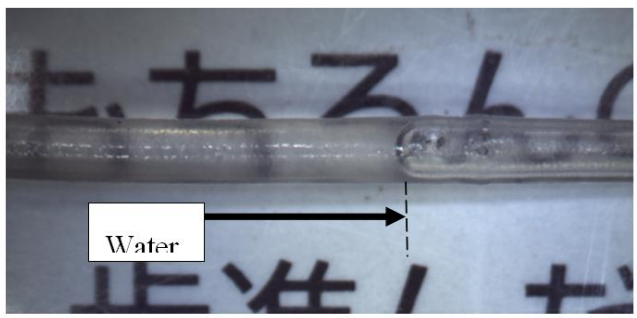

Figure 11. Depicting the flow of water through the lumen of the hollow collagen fiber.

4. References

(1)S. Hattori; E. Adachi; T. Ebihara, et al., J. Biochem., 125, 676-684 (1999).

(2) R.B. Martin, P.V. Mathews, V.A. Gibson, S.M. Stover, J. Biomechanics, 29, 1515-1521 (1996).

P51

Synthesis and characterization of polyurethane-based polymeric surfactant with different length of fluorocarbon chain

Abstract A series of fluorine-containing polyurethane-based polymerJiating Wen[1], Haojun Fan[12]*, Yi Chen[1], Jun Yan[1]

[1]*Key Laboratory of Leather Chemistry and Engineering of Ministry of Education, Sichuan University, Chengdu, 610065, P.R, China*

[2]*State Key Laboratory of Polymer Materials Engineering, Sichuan University, Chengdu, China*

*Corresponding author. Tel.: +86 28 85401068;

E-mail address: fanhaojun@scu.edu.cn (H. Fan);

ic surfactant(FPS) were synthesized successfully by using fluoro alcohol-terminated isocyanate trimer (F-HDIT) prepared from fluorinated monohydric alcohol with different fluorocarbon chain lengths and hexamethylene diisocyanate trimer (HDIT).The chemical structure of FPS were conferred by Fourier-transform infrared spectroscopy(FTIR), ^{1}HNMR and High Performance Liquid Chromatography (HPLC). The surface tensions of FPS in the aqueous solutions were determined using a surface tensionmeter and the particle sizes of FPS at 5 critical micelle concentrations(CMC) were analyzed by dynamic light scattering (DLS). The surface behaviors of FPS at air/water interface were also investigated including the effects of concentration, molecular structure, and electrolytes. The results show that FPS exhibited excellent surface activity: FPS with fluorocarbon chain number of 13(FPS-13) could attain surface tension as low as 28.9 mN m^{-1} while the CMC of FPS-6 were 1.56×10^{-6} mol·L^{-1}. Meanwhile, the critical surface tensions of FPS decreased with increasing the length of hydrophobic chain whilst the CMC increased with the increase of fluorocarbon chain. More interestingly, according to the images of Atomic force Microscope (AFM), FPS could self-assemble vesicle-like aggregates in DMSO comprised of hydrophilic block PEO surrounded by hydrophobic block fluorocarbon chains. Due to the excellent surface activity, FPS could have great potential in cleaning and nano carriers.

Keywords Polymeric surfactant; Surface tension; Self-assemble

P52

Smart Ag/TiO_2 and Ag/N- TiO_2 nanoparticles for leather surface coating and their cytoxicological impact

Carmen Gaidau[1], Manuela Calin[2], Daniela Rebleanu[2], Geanina Voicu[1], Cristina Ana Constantinescu[1] Alina Butu[3]

[1]*LeatherResearch Department, The Research and Development National Institute for Textiles and Leather- Division Leather and Footwear Research Institute, 93, Ion Minulescu Str., Bucharest, 031215, Romania, +403235060, carmen.gaidau@icpi.ro*

[2]*Nanotherapy Laboratory, Institute of Cellular Biology and Pathology "Nicolae Simionescu" of Romanian Academy, 8, P. B. Hasdeu Str., 050568, Bucharest, Romania, +40213194518, manuela.calin@icbp.ro*

[3]*Department of Biotechnology, National Institute of Research and Development for Biological Sciences, Splaiul Independentei, 296, P.O. Box 17-16, 060031, Bucharest, Romania, +4021220 0880,alina_butu@yahoo.com*

Abstract

Smart Ag/TiO_2 and Ag/N-TiO_2nanoparticles were successfully experimented in leather surface coating and showed antimicrobial and self-cleaning properties under visible light exposure. These new multifunctional properties transferred from photocatalyst with activity in visible light domain to leather surface allow improving the comfort and durability of added value leather products and reducing the use of organic solvents.

Nanoparticles are new chemicals for which the toxicity impact is in discussion at different legislative levels. In this context, the present work deals with research on nanoparticle leachability and cytotoxicity evaluation of Ag/TiO_2 and Ag/N-TiO_2nanoparticles. In this sense the results regarding the resistance of leather surface to rub fastness test followed by SEM-EDS analyses or different nanoparticles are presented. The other analyses on the cytotoxicity effects induced by different Ag/TiO_2 and Ag/N-TiO_2nanoparticles and concentrations on human cell lines with conclusions on safe concentration for industrial use are set. The possibility to use *in silico* methods for nanoparticle concentration toxicity alert is presented as a tool for safety use of new and innovative materials.

Keywords: nanoparticles, leather surface, cytotoxicity, smart properties

P53

The application of hyperbranched polymer modified buffing powder filler in PU film

Feifei Zhang *, Jie Liu, Hong Li, Zhendi An, Ya Wang

College of Leather Chemistry and Engineering, Qilu University of Technology (Shandong Academy of Sciences) , China, Jinan, 250353, fei626-918@163.com

Abstract

In this paper, the synthesis and characterization of amino hyperbranched polymer modified buffing powder (BP) were studied. Diethylenetriamine (DETA), methyl acrylate (MA) and methanol were used as raw materials to synthesize the amino hyperbranched polymer. It is used to modify leatherBP, increase the amount of amino groups, and use modified BP (MBP) as filler in synthetic leather polyurethane (PU) film. The optimum coating process was obtained by adjusting the wet solidification process, such as the content and proportion of MBP, DMF concentration, temperature of washing process. Under the same conditions, the properties of modified synthetic leather and common lignin, light calcium as fillers were investigated, too.

Through the characterization of PU film with MBP as filler, it is shown that MBP improve the sanitary performance of synthetic leather, especially its moisture permeability, thus enhancing the hand feeling of PU film.

Key words: hyperbranched polymer,buffing powder, wet solidification, filler, PU film

P54

Application and prospect of microwave assisted technology in protein-related industry

Jiacheng Wu[1], Jinwei Zhang[2], Yue Liu[3], Wuyong Chen[4]

[1]*National Engineering Laboratory for Clean Technology of Leather Manufacture, Sichuan University, Chengdu 610065, China, +8602885464462, 805263831@qq.com;*

[2]*National Engineering Laboratory for Clean Technology of Leather Manufacture, Sichuan University, Chengdu 610065, China, +8602885464462, 827021640@qq.com;*

[3]*National Engineering Laboratory for Clean Technology of Leather Manufacture, Sichuan University, Chengdu 610065, China, +8602885464462, 302740542@qq.com;*

[4]*National Engineering Laboratory for Clean Technology of Leather Manufacture, Sichuan University, Chengdu 610065, China, +8602885464462, wuyong.chen@163.com;*

Abstract：Owing to the advantages of high recovery, rapid heating, easy temperature control, and pollution-free, microwave is a sustainable and environmentally friendly forward-looking green technology. In protein-related industry including food, medicine, leather and bioscience, microwave has been used widely and fruitful. Microwave-assisted extraction of collagen could increase the products yield, shorten the time and improve the production efficiency.As a pretreatment method, using microwave for acid, alkali and enzyme treatment of protein materials could obtain expectant collagenous product. For protein analytical testing process, microwave helped for material hydrolysis and digestion, which simplified the operation and improved inspection efficiency and accuracy. In gelatin-based biomaterials synthesis, faster reaction rate with better product performance such as antibacterial activity and physicochemical property could be obtained under microwave. Collagen/gelatin drying with microwave had advantages of fast drying and reduced the loss of collagen as well as amino acids contents. In addition, microwave-assisted thawing maintained a high nutritional value of meat includes essential and non-essential amino acids. Although, microwave neither destroyed the triple helix structure nor made collagen denaturing below the denaturizing temperature, high power microwave could lead to the decrease and disorder of amino acids in animal brain, as well ascaused surface damage to muscle fiber with separation of some portions and denaturation of collagen. These results showed that microwave gave a potential choice for innovating the materials processing and improving products performance. Therefore, microwave introduced in protein-related industry will promote the development of protein-related industry,providing the possibility of efficient and clean production.

Keywords: Microwave, protein, collagen, amino acid, application.

P55

Self-matting waterborne polyurethane leather finishing agent

Zhe Sun[1], Jiating Wen[1], Haojun Fan[1, 2, *], Yi Chen[1], Jun Yan[1]

[1]*National Engineering Laboratory for Clean Technology of Leather Manufacture, Sichuan University, Chengdu, 610065, P.R. China*

[2] *State Key Laboratory of Polymer Materials Engineering, Sichuan University, Chengdu 610065, China*

** Corresponding author. Tel.: +86 28 85401068; fax: +86 28 85401068.*

E-mail address:fanhaojun@scu.edu.cn (H. Fan)

ABSTRACT:

Leather finishing agents are always used to endow the leather a certain aesthetic effect and particular functional properties. Among various finishing agents, waterborne polyurethane (WPU) is increasingly popular whereas its plenty of outstanding properties. In this study, one kind of environmental friendly self-matting waterborne polyurethane (SMWPU) was successfully prepared as leather finishing agent. The structure and surface morphology of SMWPU film were characterized by Fourier transform infrared spectrometer (FTIR), Scanning electron microscope (SEM) and Atomic force microscope (AFM). Then the effects of R value (nNCO/nOH), trimethylolpropane (TMP) and dimethylolpropionic acid (DMPA) content on optical properties of WPUs were studied to optimize an appropriate formulation for SMWPU.

Keywords: self-matting; waterborne polyurethane; leather finishing agent;

Introduction

After tanning, dyeing and fatliquoring, etc. the leather usually needs to be further finished to meet the needs of different customers. [1-3] Among various leather finishing agents, waterborne polyurethane has been rapidly developed in recent years due to its excellent performance, such as non-toxic, excellent adhesive properties, reasonably high mechanical strength and mar resistance. [4-7] Also, with the improvement of people's living standard as well as growing needs of novelty and artistry, WPU finishing agents with different optical effects have received conspicuous attention, which can give different appearances and aesthetics to the leather and expand its application range. Among them, recently, matt polyurethane has received extensive attention and research because of its ability to endow the leather a strong texture.

The matt effect is closely associated with the smoothness of the coating surface. [8] As shown in Fig. 1, matt effect usually results from the diffuse reflection of light that occurs on a rough surface. However, for an extremely smooth surface, the incident light will be completely reflected at a certain angle, showing a high gloss effect.

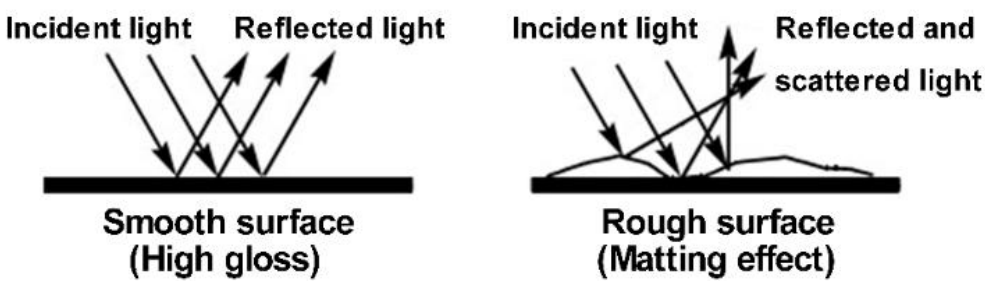

Fig. 1 Relationship between gloss and smooth degree of coating surface

At present, the most economical and commonly used way to obtain the matt finishing agent is by adding a variety of matting agents into the resins. [9-10] Although traditional physical blending is convenient to implement, there are still some obstacles in its application. In such a context, great efforts had been taken into the chemical extinction area and also made an enormous amount of achievements. [11-13] In our previous work, we had studied the effect of structure factors, involving the type of diisocyanates and glycols, crosslinking degree, hard-segment content, as well as crystallinity on optical property of WPU, which provided the theoretical basis for the self-matting WPU preparation. [14] Further, in this work, a single factor

variable method was employed to systematically investigate the effect of reaction condition on the gloss and transmittance, involving R value, TMP content, as well as DMPA content on the optical properties of WPU. This kind of self-matting waterborne polyurethane can be applied inleather finishing.

Experimental

Materials

Isophorone diisocyanate (IPDI), polyester glycol (E220, M_n=2000 g/mol) and *2,2*-Bis(hydroxymethyl) propionic acid (DMPA) were supplied by Dymatic Post Polymer Material*Co*. (Lishui, China). Bismuth acid catalyst, trimethylolpropane (TMP), triethylamine (TEA), and hydrazine hydrate were obtained from Kelong Chemical Engineering Co. Ltd. (Chengdu, China). All the chemicals were used after dehydration.

Synthesis of waterborne polyurethane (WPU)

The synthesis of WPU was outlined in Scheme 1.

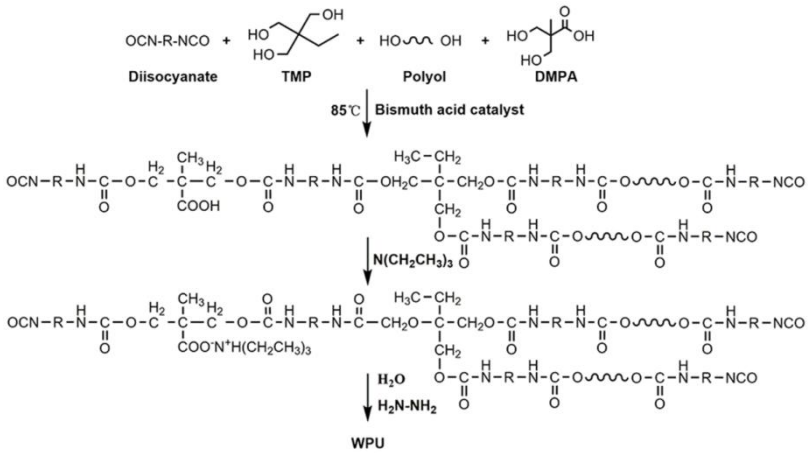

Scheme 1. The synthesis of WPU.

First, bismuth acid catalyst, polyester glycol E220, different amount of IPDI, TMP and DMPA were added to a flask fitted with a mechanical stirrer and a thermometer. The reaction was carried out under a nitrogen atmosphere at 85 °C for 4.5 h. Subsequently, the prepolymer was cooled to 40 ℃ and then neutralized by TEA. Finally, a large amount of deionized water was fed into the vessel to obtain a certain solid content emulsion. The post chain extension was performed with a solution of hydrazine hydrate under vigorous stirring.

Preparation of WPU films

The WPU films with a thickness of about 0.5 mm were obtained by drying WPU dispersions on PTFE plates at ambient temperature for 3 days and then vacuum dried at 60 °C for 24 h. Before characterization, all the films were placed in a desiccator at room temperature.

Measurements

Structural characterization

The chemical structure of SMWPU resin was identified by Fourier transform infrared spectroscopy (FTIR) using a Nicolet IS10 FTIR spectrometer (Thermo Scientific, United States) at ambient temperature in the range from 400 to 4000 cm^{-1} after 32 scans at a spectral resolution of 2 cm^{-1}. As for SMWPU, it was coated directly onto the compressed KBr slices to form the solution cast films.

Optical properties tests of WPU film and coated leather.

The optical properties of the films were measured by WGT-S light transmittance/haze tester (Jingke, Shanghai, China). First, open the instrument and preheat the tester for 30 min. After that, put the films on the light hole and click the test button. The light transmittance of the films was averaged from three measurements.

The gloss of samples was tested based on the leather by using a gloss meter (REFO60, Germany). SMWPU emulsion was coated on the leather surface by using linear rods with firm pressure firstly, and then the coated leathers were put into a drying oven at 60-70 °C for 2 min. All the measurements were carried out with a 60° incidence angle.

Surface microstructural characterization of WPU film

The surface morphologies of WPU films were examined using a Scanning Electron Microscope (JSM-7500F, Japan) and the magnification of films was 1000 times.

3D surface morphology observation of WPU films were performed with atomic force microscope (SPM-9500, Japan). The scanning rate was 1 Hz.

Particle size analysis of WPU

The particle size of WPU dispersions was measured using a Mastersizer 2000 (Malvern Instruments).

Results and discussion

Structure of SMWPU resin

To demonstrate successful synthesis of SMWPU resin, the chemical structure of SMWPU was confirmed by FTIR.

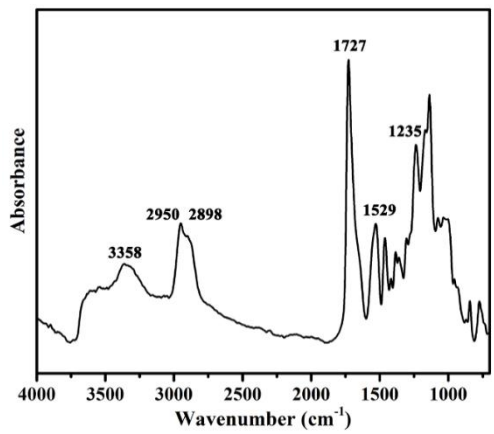

Fig. 2 The FTIR spectra of SMWPU resin.

As shown in Fig. 2, the disappearance of characteristic absorption bands at 2270 cm^{-1} and 3500 cm^{-1} referred to the -N=C=O and -OH groups respectively, indicating that all the isocyanate and hydroxyl groups were completely reacted in this system. As for the SMWPU resin, the broad bands at 3358 cm^{-1} could be attributed to the N-H stretching vibration. The bands at 2950 cm^{-1} and 2898 cm^{-1} were assigned to the C-H stretching vibration. E220 exhibited a strong absorption band at 1727 cm^{-1} belonging to the stretching vibration of C=O. The detailed characteristic FTIR bands were listed in Table 1.

Table 1. The FTIR bands of SMWPU

Wavelengths (cm^{-1})	Assignments
3358	ν N-H
2950, 2898	ν C-H (CH, CH_2 and CH_3)
1727	ν C=O
1529	ν C-N, δ N-H
1235	ν N-CO-O, ν C-O-C

Surface morphology and particle size of SMWPU

SEM is usually used to observe the microscopic morphology of the WPU film surface. The surface morphology of SMWPU film was shown in Fig. 3, and the corresponding particle size distribution was shown in Fig. 4.

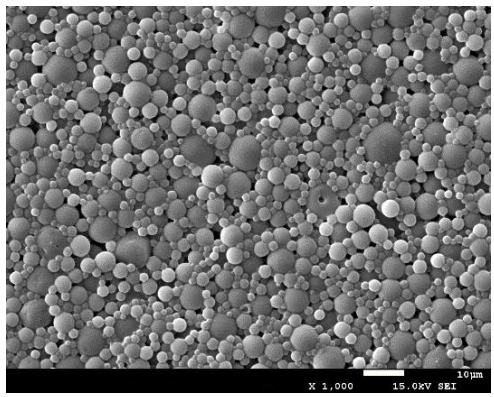

Fig. 3 The SEM image of SMWPU film (1000 times).

As could be seen from the figure, the WPU spherical latex particles were uniformly distributed on the film surface. The formation of spherical latex particles during film formation could be attributed on the one hand to the emulsion particle size D50 = 7.2 μm (Fig. 4), and on the other hand to the special structure of the WPU latex particles. First, when TMP was used as cross-linking agent, it had an auxiliary effect on the formation of spherical latex particles; secondly, with a higher R value, the number of hard segments (urethane and urea bonds) increased and the two adjacent hard segments were closer, which helped the latex particles to maintain their shape without collapsing during the film forming process, so that a certain microscopic roughness could be formed on the film surface. Thus, when the light irradiated on the film surface, a strong diffuse reflection occurred instead of specular reflection, the matt effect was achieved. After 60° angle gloss test, the gloss of SMWPU coating was 0.8°, and the more intuitive matt effect was shown in Fig. 5.

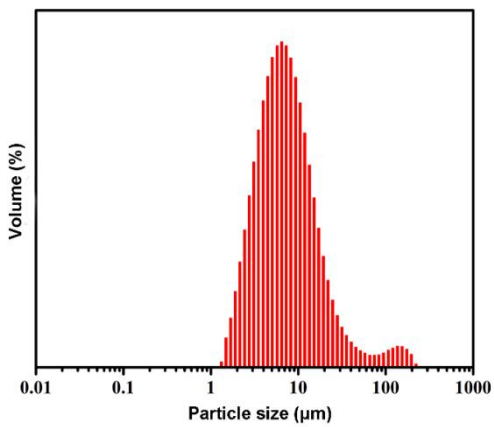

Fig. 4 The particle size distribution of SMWPU emulsion.

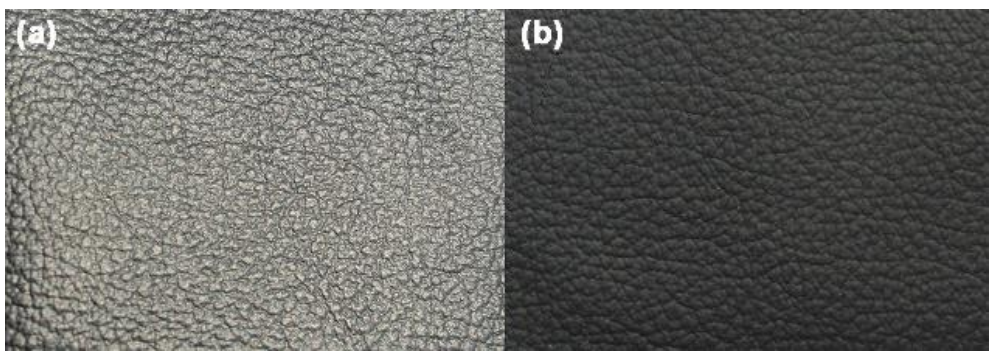

Fig. 5 The matt effect of SMWPU: (a) original leather, (b) leather coated by SMWPU.

The effect of R value on surface morphology and matt effect of WPU

R value is the molar ratio of isocyanato (-NCO) and hydroxyl (-OH) which has an important influence on the properties of waterborne polyurethane emulsions and films. In this section, the variation of surface morphology of WPU films under different R values was studied by single factor variable method.

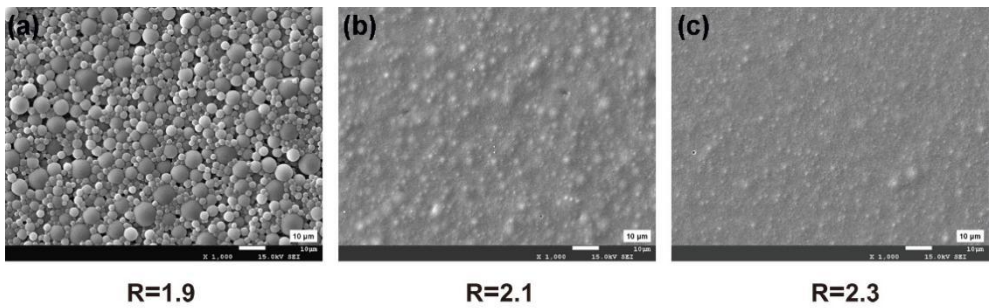

Fig. 6 Effect of R value on the surface morphology of WPU films. (Reaction condition: TMP wt%=2, DMPA wt%=1.75).

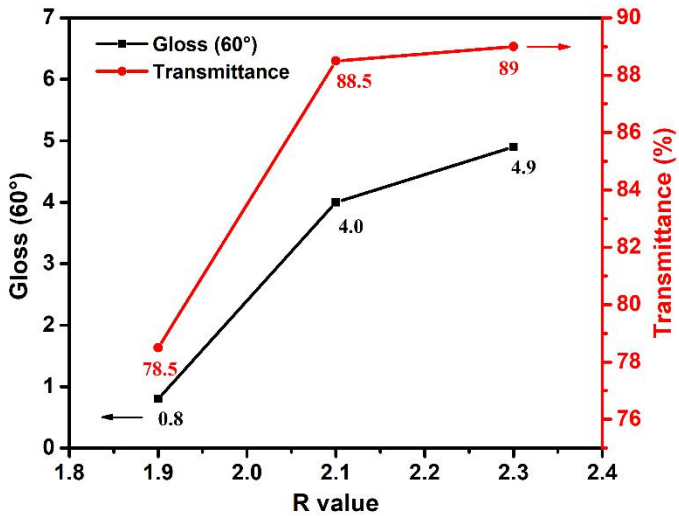

Fig. 7 Effect of R value on the gloss and transmittance of WPU films.

As could be seen from Fig. 6, as the R value increased, the microsphere structure on the film surface gradually disappeared, transitioning from a rougher surface to a relatively smooth surface. Correspondingly, both the film transmittance and the coating gloss showed an increasing tendency (Fig. 7). This was because, as the R value increased, the particle size decreased, which in turn led to a decrease in the surface roughness of the film, a decrease in the intensity of the diffuse reflection of light on the surface of the film, an increase in the luminous flux of reflection and transmission, and an increase in gloss and transparency. Therefore, R=1.8~2.0 was a suitable R value for preparing matting WPU.

The effect of TMP content on surface morphology and matt effect of WPU

Crosslinking generally endows a three-dimensional structure to the polymer. [15] Figure 8 showed the SEM images of the film surface under different cross-linking agent content. It could be seen from the figure that when no cross-linking agent was used, the micro-surface of the film was smooth and the convex structure was not obvious. With the introduction of cross-linking agent, the film surface began to show evident microsphere structure (Fig. 8 (b) ~ (e)), indicating that the use of TMP played an important role in the formation of microspheres.

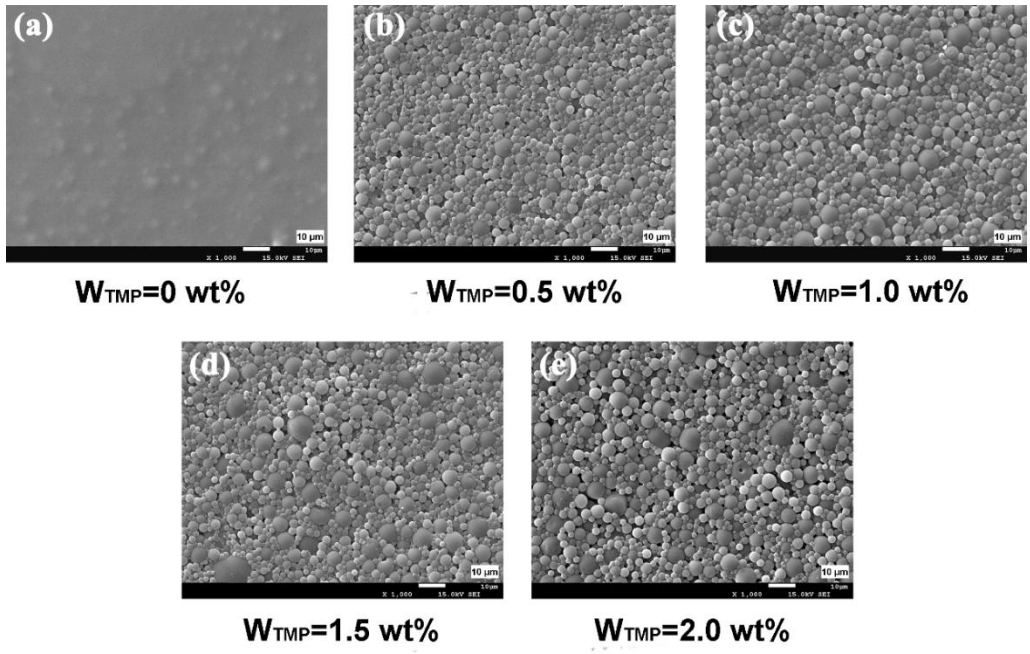

Fig. 8 Effect of TMP content on the surface morphology of WPU films. (Reaction condition: R=1.9, DMPA wt%=1.75).

At the same time, the change in cross-linking degree would cause a difference in the surface roughness of the film, which in turn affected the coating gloss. As shown in Fig. 9 and 10, when no cross-linking agent was added, the surface roughness (Rq) of the WPU film was only 0.109 μm, the coating gloss was higher (5.1°); and when the cross-linking agent was 0.5 wt%, the surface roughness of the WPU film was significantly increased to 0.309, and accordingly, the coating gloss was significantly decreased from 5.1° to 1.1°. With the further increase of TMP content, the surface roughness increased slightly, and the gloss of the coating decreased further. When TMP wt%=2%, the surface roughness of the film was the largest and the coating gloss was the lowest (0.8°). In addition, as the amount of cross-linking agent increased, the transmittance and gloss of the WPU film showed the same change rule. Therefore, the TMP content of 0.5 to 2 wt% was suitable for the preparation of matt WPU.

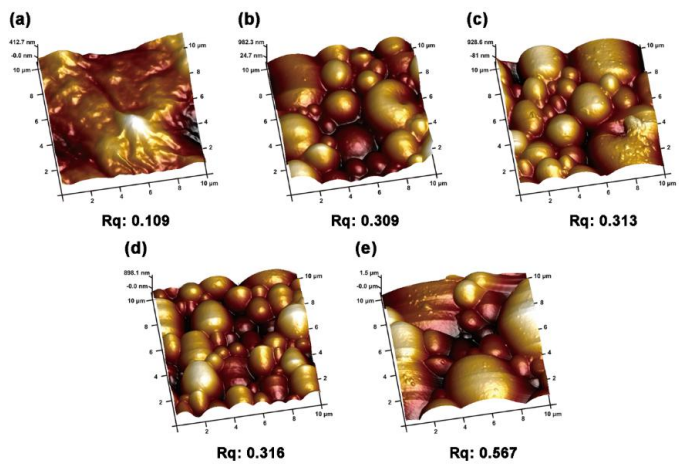

Fig. 9 Three-dimensional AFM images of WPU film surfaces with various TMP content: (a) 0 wt%, (b) 0.5 wt%, (c) 1 wt%, (d) 1.5 wt%, and (e) 2 wt%.

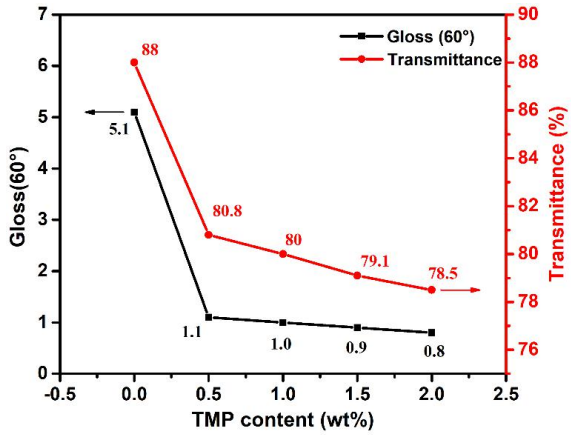

Fig. 10 Effect of TMP content on the gloss and transmittance of WPU films.

The effect of DMPA content on surface morphology and matt effect of WPU

DMPA is the most commonly used hydrophilic chain extender for the preparation of anionic waterborne polyurethanes. The particle size of polyurethane emulsions is closely related to the hydrophilic group content.

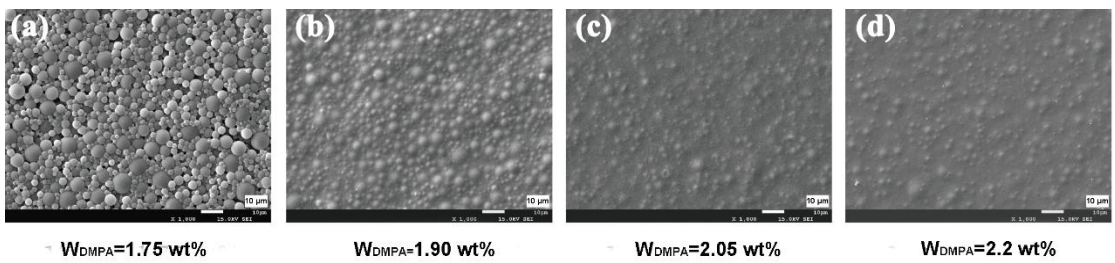

Fig. 11 Effect of DMPA content on the surface morphology of WPU films. (Reaction condition: R=1.9, TMP wt%=2).

The effect of DMPA content on the surface morphology of WPU film was shown in Fig. 11. With the DMPA content increasing from 1.75 wt% to 2.2 wt%, the micro-roughness of the film surface gradually decreased. When DMPA wt%=1.75, the microsphere structure of the film surface was obvious; when DMPA wt%>1.9, it was difficult to observe the microscopic convex structure of the film surface, and the latex particles tend to be fusion in the film forming process. Fig. 12 showed the effect of DMPA content on the gloss and light transmittance of WPU coatings. When DMPA wt%=1.75, its surface microstructure had strong diffuse reflection and scattering ability to incident light, so the gloss and light transmittance were lower, the gloss is 0.8°, and the extinction effect was excellent. When the DMPA content was more than 1.9 wt%, the gloss and the transmittance were sharply increased, and the matte effect was remarkably decreased.

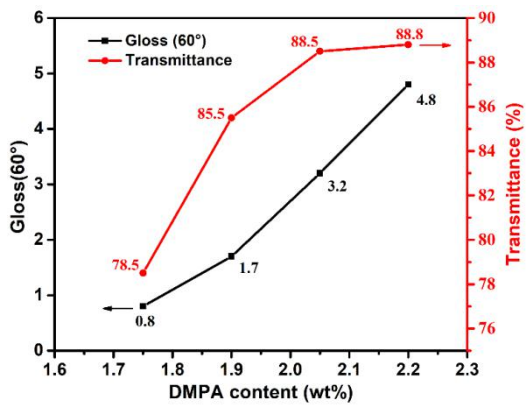

Fig. 12 Effect of DMPA content on the gloss and transmittance of WPU films.

Conclusions

A kind of self-matting waterborne polyurethane leather finishing agent was successfully prepared. The results indicated that the particle size of WPU emulsion determined the surface microstructure of the film and then affected the coating matt effect.When the latex particle size was 7-8 μm, the film surface was composed of a large number of spherical latex particles, which gave a certain microroughness to the coating surface, endowing the coating an excellent matting effect. R value, crosslinking degree and DMPA content affected the film surface roughness. With the R value increased, the film surface roughness decreased, and then the matt effect decreased.The addition of the crosslinking agent contributed to the formation of the WPU microspheres. As crosslinking degree increased, the film surface roughness increased, endowing an excellent matt effect; The DMPA content determined the emulsion particle size and then affected the surface roughness. When DMPA content was 1.75%,evident microsphere structure could be found on the film surface, giving the coating an excellent matting effect. With the increase of DMPA content, when the DMPA wt%>1.9, the microscopic surface protrusion of the film gradually disappeared, and the matt effect decreased distinctly.

Acknowledgement

The authors wish to acknowledge financial support from National Key Research and Development Program of China (Project No: 2017YFB0308600).

The authors would thank Wang Zhonghui (College of Light Industry, Textile and Food Engineering, Sichuan University) for her great help in AFM/FT-IR observation.

References

[1] Ren, Long‐Fang, Geng, Jin, Chen, Ting, et al. Synthesis and application of hyperbranched poly(urethane‐urea) finishing agent with amino groups[J]. Journal of Applied Polymer Science, 2016, 133(43).

[2] Wang Z, Lin. Synthesis and the Durability of Aqueous Acrylate-Styrene-Polyurethane Finishing Agent[J]. Polyurethane Industry, 2011.

[3] Qin W, Qiu-Feng A N, Zhao J, et al. Synthesis of Polyurethane Modified Amino Silicone Fabric Finishing Agent and Its Application[J]. Fine Chemicals, 2014.

[4] Meng L, Liu F, Yu L, et al. Synthesis of stable cationic waterborne polyurethane with a high solid content: insight from simulation to experiment[J]. Rsc Advances, 2017, 7(22):13312-13324.

[5] Zhang P, Fan H, Hu K, et al. Solvent-free two-component polyurethane conjugated with crosslinkable hydroxyl-functionalized ammonium polyphosphate: Curing behaviors, flammability and mechanical properties[J]. Progress in Organic Coatings, 2018, 120:88-99.

[6] Villwock R D. A METHOD FOR RECYCLING POLYURETHANE AND A COMPOSITION COMPRISING RECYCLED POLYURETHANE[J]. 2005.

[7] Zhang Z, Guangming W U, Shen J, et al. Preparation and Characterization of Leather Polyurethane/SiO_2 Nano-composite Materials[J]. Materials Science & Engineering, 2003.

[8] Yong Q, Nian F, Liao B, et al. Synthesis and characterization of solvent-free waterborne polyurethane dispersion with both sulfonic and carboxylic hydrophilic chain-extending agents for matt coatings application[J]. Rsc Advances, 2015, 5(130):107413-107420.

[9] Kumar V, Misra N, Paul J, et al. Organic/inorganic nanocomposite coating of bisphenol A diglycidyl ether diacrylate containing silica nanoparticles via electron beam curing process[J]. Progress in Organic Coatings, 2013, 76(7–8):1119-1126.

[10] Ou J, Zhang M, Liu H, et al. Matting films prepared from waterborne acrylic/micro-SiOblends[J]. Journal of Applied Polymer Science, 2014, 132(13).

[11] Li J, Zheng W, Zeng W, et al. Structure, properties and application of a novel low-glossed waterborne polyurethane[J]. Applied Surface Science, 2014, 307(18):255-262.

[12] Cao X, Ge X, Chen H, et al. Effects of trimethylol propane and AAS salt on properties of waterborne polyurethane with low gloss[J]. Progress in Organic Coatings, 2017, 107:5-13.

[13] Uribe-Padilla J, Graells-Sobré M, Salgado-Valle J. A novel contribution to the modeling of the matting efficiency of aqueous polyurethane dispersions[J]. Progress in Organic Coatings, 2017, 109:179-185.

[14] Sun Z, Fan H, Chen Y, et al. Synthesis of self‐matting waterborne polyurethane coatings with excellent transmittance[J]. Polymer International, 2018, 67(1).

[15] Ward I M, Klein P G. Polymer Physics[M]// eMagRes. John Wiley & Sons, Ltd, 2007.

P56

Characteristics Analysis of Operating Liquid Properties in Liming Waste Liquid Recycling Process

Li Wenxin[1], Chen Chen[1],Qiang Xihuai[1], Zhang Chuanbo[1], Zhang Zhuangdou[2]

[1] College of Bioresources Chemical and Materials Engineering, Shaanxi University of Science and Technology, Xi'an 710021, China;

[2] BIOSK Chemicals Co., Ltd., Shangqiu 476000 , China

ABSTRACT

The liming waste liquid recycling technology has a stable technical operation process and good cycle stability after nearly three years of large-scale production and application. In this study, the liming waste liquid of large-scale production was sampled. And the pH, total solids, suspended solids content, lime content, sulfur element content, ammonia nitrogen content, COD content and TOC content of the liming waste liquid were measured. The results show that during the liming cycle operation, the content and index of each component of its waste liquid have a certain regular change. With the increasing of cycling times, the change of the content and index of the components in the liming bath first accumulated and then stabilized within a certain range. This change reveals the scientific balance of the closed cycle process of the liming waste liquid. The theoretical calculation and evaluation suggest that the technology can significantly reduce the usage of water and the consumption of chemical materials. The economic and environmental benefits are very significant. The technology has good practicability and application prospects for its economic and environmental benefits.

Key words: tanning, liming, liming waste liquid, recycling

P57

Study on hydrolysis of waste shavings by the system of calcium oxide/tetramethylammonium hydroxide

YUAN Yan[1], ZHAO Caide[1], GE Shuhua[1], LUANN JUN[2], ZHAO Dandan[1], DIAO Shen[1*], WANG Quanjie[1,2]

[1]*College of Chemistry and Chemical Engineering, Yantai University,Yantai 264005, China;*

[2]*State Leather Technology Research Development Center, Yantai 264005, China;*

Abstract

In this paper, waste shavings were hydrolysed by the system of calcium oxide/tetramethylammonium. The optimum hydrolysis conditions through orthogonal test. In the first hydrolysis system of CaO, using the chromium content as the standard, it was found that the dechromization rate is the highest under the conditions of the amount of calcium oxide is 9%, the temperature is 90°C, the reaction time is 4 hours, and the solid-liquid ratio is 1:7. The chromium content in the hydrolysate was 149 ppm and the dechromization rate was 97.3%. In the second hydrolysis system of tetramethylammonium, using the content of free amino acids as the standard, it was found that the hydrolysis rate is the highest under the conditions of the amount of tetramethylammonium is 9%, the reaction time is 4 hours, the solid-liquid ratio is 1:10, the temperature is 70°C. The hydrolysis rate is 1.5%.

Keywords: waste shavings; calcium oxide; dechromization rate; tetramethylammonium;hydrolysisrate;

P58

Greener Dyestuff for Leather Industry

Yun-Tai Yeh, Chih-Hung Yu, Hsiu-Fu Liang, Shun-Te Lin

Technical Service for Leather, Everlight Chemical Industrial Corp., No.271, Zhongshan N. Rd., Dayuan Dist., Taoyuan City 337, Taiwan, +886-3-386-8081, yehyuntai@ecic.com.tw

Abstract

The public's awareness of environmental protection has motivated brands and third-party organizations to become more rigorous in supply chain communication and product safety management of the leather industry. Providing greener and more eco-friendly dye chemicals has became must for the leather industry. Leather dyeing often uses metal-complex dyes to achieve high fastness or to broaden the color range. However those dyestuffs are not suitable for chrome-free or heavy metal free leather products. This study investigates the extractable heavy-metals of leather dyed by Everlan MF series, which meets the Oeko-Tex Leather standard regulations. On the other hand, Aniline is one of the raw materials commonly used in leather dyes, especially in reddish and bluish black ones, which might cause the concerns about the end products. For example, ANEC, the European consumer voice in standardisation, proposed an aniline limit of <30 ppm for toys intended for use by children under 36 months, or to be placed in the mouth. To eliminate the concerns, it is required to use dyes that obeys the regulations. This study proves that Everlan AF series complies the regulations without compromising the shades. The importance of compliance to The Candidate List of Substances of Very High Concern (SVHC) is also emphasized.

Keywords: Dyestuff, heavy-metal, aniline

P59

Effects of pH on the Interaction between tannic acid and Collagen in Dilute Acidic Solution

Liyuan Hu, Sichuan university, China 1176265775@qq.com
Wei Lin, Sichuan university , China wlin@scu.edu.cn

Abstract

The interaction between tannin and collagen at the similar pH of the practical tanning process was investigated byUltraviolet Spectrum (UV), Atomic Force Microscopy (AFM), Fourier Transform Infrared Spectroscopy (FTIR) and Ultrasensitive Differential Scanning Calorimetry (US-DSC). The AFM shows the individual collagen fiberin the presence of tannin at pH 2.5 and the tannin can induce the aggregation of collagen fibril at pH 4. Results of UV and FTIR indicate that the introduction of tannin do not alter the triple helix backbone structure of collagen and prove the existence of hydrogen bond between tannin and collagen. US-DSC measurement suggests that the thermal stability of the tannin-collagen dispersion improves slightly in comparison with pure collagen, and the enthalpy change (△H) values of thedispersion increases remarkably with the increasing content of tannin at pH 4, while decreases at pH 2.5. Moreover, the effect of urea in the tannin-collagen system has been investigated and it further proves the presence of hydrogen bonds between the tannin and collagen. It suggests that the reaction mechanism between tannin and collagen mainly involves with electrostatic interaction and hydrogen bonds, the non-covalent interaction can be stronger at pH 4 than pH 2.5.

Keywords：Collagen, Tannic Acid, Interaction, US-DSC, AFM

P60

Preparation of ultrafine leather powder and its application in synthetic leather

Xiaomin Luo[1]*, Wenjie Hu[1], Jianyan Feng[1]

(1.College of Bioresources Chemical and Materials Engineering, Key Laboratory of Leather Cleaner Production, China National Light Industry, Shaanxi University of Science & Technology, Xi'an, Shaanxi,710021, China)

Abstract: The solid wastes of leather are crushed, solidified and ground to obtain ultra-fine leather powder. As a filler for polyurethane, the leather - containing synthetic leather was prepared by wet solidification process. The effects of the amount of leather powder added, wood powder and light calcium carbonate composite ratio are discussed on slurry viscosity, Myogenicity property, microporous structure, mechanical properties, hygienic properties, hydrolysis resistance, etc. And comparison with conventional methods for preparing base performance. The experimental results show that the suitable application conditions of leather powder are: $w_{(leather\ powder)}$: $w_{(wood\ powder)}$: $w_{(light\ calcium\ carbonate)}$= 15:5:25. At the same time, the slurry viscosity is 10400 cps, the myogenicity property is 46.3%, the tensile strength of base is 15.7Mpa, the tearing strength is 126.6N/mm, the peel strength is 102N/3cm, the hydrolytic resistance time is 18h, the water vapor permeability is 2152mg/10cm^2•24h, and the breathability is 376 mL/cm^2•h. Ultrafine leather powder is used as a synthetic leather wet base filler to reduce cost, improve smoothness, feeling, and improve skin comfort.

Key words: Leather powder, Synthetic leather, Filler, Wet coating

0 Introduction

China's natural leather production and consumption are ranked first in the world. The annual production of scraps and solid waste generated by the production enterprises is as high as 1.4 million tons, of which chromium-containing waste leather chips account for 75% [1-3]. If the data add discarded the waste of leather products after use will be multiplied several times. The Ministry of Environmental Protection listed chromium-containing wastes as a list of hazardous wastes in 2016, landfill and incineration are prohibited. Production companies and environmental protection departments are troubled by the treatment of leather solid waste. Therefore, how to establish a circular economy in the leather industry from the aquaculture industry - raw skin - leather making - leather products - market - waste recycling - market [4], has become the focus on current researchers.

A variety of products can be produced by recycling and recycling leather waste and leather products, such as using waste leather chips as a base material to produce organic fertilizer with protein content, which can be used as foliar fertilizer, drip irrigation and flushing fertilizer. It can solve a series of problems such as long-term use of chemical fertilizers, thinning of cultivated fields, decreased organic matter content, and soil acidification [5]. Haudhary R [6] et al. used protein hydrolysate purified from chrome tanned leather waste as feed instead of soy flour to feed broilers. The growth process of broilers was studied. The results showed that the protein hydrolysate could replace up with 75% of soy flour in broiler feed. Without affecting the growth performance of the chicken and the characteristics of the meat. Cavalcante [7] et al. combined natural rubber with solid waste of leather as a filler to develop a new composite for the footwear and textile industries, which releases low concentrations of chromium and releases the main substance trivalent. chromium.

Synthetic leather is a substitute for natural leather, which has developed rapidly in recent years, and its annual output far exceeds that of natural leather. In the production of wet solidification polyurethane synthetic leather, a large amount of filler is used in the polyurethane coating [8]. The filler particles provide a nucleation point of the macromolecular agglomeration of the polyurethane, play the role of "nucleation", accelerate the aggregation speed, and play the role of adjusting the microporous structure to change the mechanical properties, feeling properties and reduce the production cost of the coating. There are lignin, light calcium carbonate, etc. [9,10]. The addition of fillers increases the mechanical properties of the coating, while nanoscale fillers are recognized as the most desirable polyurethane elastomer reinforcements [11]. Therefore, refining the particle size helps to improve the leveling of the slurry and improve the surface of the coating. Flatness reduces the loss

of mechanical properties of the coating due to the filler. Leather powder can replace lignin as a polyurethane synthetic leather filler [12]. Because natural leather fiber is soft and tough, it is difficult to pulverize. It is more difficult to prepare ultrafine powder. At present, the skin fineness of the market is mostly about 300 meshes. In this study, the method of adding curing agent to prepare ultra-fine leather powder can reach 600 meshes. The preparation method is simple and easy to implement. It does not destroy the structure of the skin fiber, does not produce acid-base wastewater, and has short preparation time period and low cost. The prepared leather powder is used as a filler for preparing a synthetic leather coating, and the suitable application conditions of the leather powder are explored to prepare a synthetic leather product having the required performance. The leather powder is derived from solid waste and the cost is lower than that of wood powder. This research is to recycle the leather waste and find a simpler and easier application direction for a large amount of leather waste. It not only solves the pollution problem of leather solid waste, but also reduces wood consumption and reduces the production cost of synthetic leather. It has "multiple values".

1 Experimental Content

1.1 Experimental materials and equipment

The raw materials for preparing the leather powder are waste leather shavings, ethanol, leather degreaser, curing agent, etc.; the raw materials of the coating are polyurethane (PU), antifoaming agent, flatting agent, dimethylformamide (DMF), ultrafine and light. Calcium carbonate, domestic lignin.

The main equipment include adjustable speed mixer EUROSTAR 20, Aika (Guangzhou) Instrument Equipment Co., Ltd.; high-speed centrifuge, Anhui Zhongke Zhongjia Scientific Instrument Co., Ltd.; constant temperature oven DZ-2BC, Shanghai Dasu Experimental Instrument Co., Ltd.; Scanning electron microscope, Tianmei (China) Scientific Instrument Co., Ltd.; leather pull (pressure) force testing machine, Xi'an Dingnuo Measurement and Control Technology Co., Ltd.; YG035 square instrument, NDJ-4 rotary viscometer, Shanghai Jingke Tianmei Scientific Instrument Co., Ltd.

1.2 Preparation of leather powder

The waste shavings are immersed in a mixed solution prepared by mass concentration of 95% ethanol, leather degreaser and deionized water at a volume ratio of 1:1:1 and intermittently stirred for 24 hours (The ratio of waste shavings to mixed solution is 1:1), remove the waste shavings and put them into the oven at 300°C for drying; then add $w_{(dispersant)}$ = 1% curing agent at a mass ratio of 1:1 for 12 h, dry and then carry out strong magnetic treatment. The coarse pulverization was carried out, and the 300-mesh sieve was sieved, and the coarse leather powder was sieved to be finely pulverized, and sieved through a 600-mesh sieve to obtain ultrafine leather powder.

1.3 Preparation of synthetic leather base

The metered DMF and the filler are added to the dispersion kettle, and the filler is uniformly dispersed by stirring, and the PU resin is added, stirred at a high speed for 30 minutes, and then a flatting agent, a defoaming agent, etc. are added, and the mixture is uniformly stirred. The slurry was subjected to vacuum defoaming to test the viscosity and solid content, and after filtration, it was applied to a raised cloth having a moisture content of 30%, coated with a thickness of 2.3 mm, and then placed in a coagulation bath having a DMF concentration of 25% to 28% and a temperature of 36°C. Solidified for 10 min; washed and dried for testing.. The coating slurry formulation is shown in Table 1:

Table 1 Coating slurry formula

Experiment number	PU/part	Filler			DMF /part	Auxiliary /part
		Leather powder / part	Wood powder / part	Calcium carbonate/ part		
1-1	360	0	30	0	85	6.5

1-2	360	30	0	0	85	6.5
2-1	360	0	0	25	85	6.5
2-2	360	5	0	25	85	6.5
2-3	360	10	0	25	85	6.5
2-4	360	15	0	25	85	6.5
2-5	360	20	0	25	85	6.5
2-6	360	25	0	25	85	6.5
3-1	360	5	15	25	85	6.5
3-2	360	10	10	25	85	6.5
3-3	360	15	5	25	85	6.5

1.4 Base structure and performance testing

Viscosity test: tested according to national standard GB/T 22235-2008; SEM observation: the sample was freeze-braked and adhered to conductive adhesive in liquid nitrogen, and sprayed with gold to test the sample with accelerated voltage of 30KV; performance test : According to the literature in [13], the tensile strength, elongation, tear strength, gas permeability, water vapor permeability and peel strength of the synthetic leather coating were tested; the sample was cut into 100×30 mm samples and placed in 10% sodium hydroxide solution, the change of the sample was observed each 1 hour. Myogenicity property testing: Thickness is measured at 5 points in different locations of Base, and the thickness is marked, placed in an oven at 120 °C, and the thickness after drying is measured at the original mark; the ratio of thickness before and after drying is calculated, expressed in % .

Myogenicity=$d_1/d_0 \times 100\%$ (1)

In formula (1):d_1 - thickness of coating after drying, mm;

d_0 - wet thickness of coating, mm.

2 Results and discussion

2.1 Appearance and structure analysis

The results of the slurry and coating prepared by comparing the s powder and wood powder as a filler are shown in Tables 2 and 3 below:

Table 2 Comparison of different filler preparation slurry and coating appearance

Category	Shape	Fineness/mesh	Viscosity /cps	Flatting property	Micropore structure
Wood powder (30 servings)	Lamellar	400	9500	Normal	Large finger hole
Leather powder (30 servings)	Fibrous	600	9800	Normal	Large finger hole

Table 3 Comparison of different filler preparation slurry and coating properties

Category	Wood powder (30 servings)	Leather powder (30 servings)
Myogenicity (%)	44.3	44.6
Hydrolysis resistance (h)	20	16
Water vapor permeability (mg/10cm^2•24h)	2144	1893
Breathability (mL/cm^2•h)	367	313
Tensile Strength (MPa)	16.9	14.7
Tear strength（N/mm）	130.1	90.8
Peel strength (N/3cm)	118	112

It can be seen from Table 2 that the wood powder belongs to the lamellar shape, the leather powder is fibrous, and the viscosity of the leather powder is large, this is because the leather powder has a fibrous structure. If the amount of the powder is small, entanglement of the fiber and the polyurethane molecule has been affected to a certain extent. As the amount of filler increases, the entanglement between the filler and the polyurethane molecule is more obvious, and the viscosity will be improved. Normal flatting and finger-shaped pore structure are obvious. It can be known from Table 3 that the coating prepared by the ultrafine leather powder has better muscularity than the coating prepared by the wood powder, and the hydrolysis resistance is poor, which is caused by a large amount of oxygen-containing functional groups and aromatic rings in the wood powder. Hydrogen bonds are formed into the molecules of the polyurethane, and the intermolecular force enhances the compatibility. In addition to the surface active groups, the ultrafine leather powder is not alkali resistant and is used in synthetic leather products. The alkali resistance is gradually lowered, so that the hydrolysis resistance is deteriorated. Compared with hygienic performance and mechanical properties, the synthetic leather made from the leather powder as a filler has a slightly lower performance than the wood powder as a filler. From the data, it can be found that the mechanical properties and hygienic properties need to be enhanced. However, it does not affect the use of leather powder as a synthetic leather filler.

SEM characterization is shown in Figure 1.

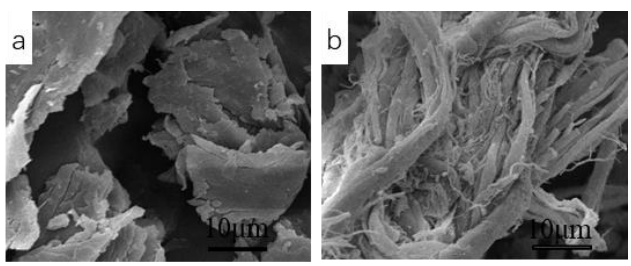

Note: a-wood powder b-leather powder

Figure 1 SEM image of two different fillers

It can be seen from Fig. 1 that there is a clear difference between a and b, a shows a large number of lamellar structures and massive structures; b has a very pronounced fiber structure, and the fibers have quite good strength, elasticity and hygroscopicity, etc., combined with polyurethane can well simulate the grain layer of the dermis, which helps to enhance the softness and macropore structure of the synthetic leather. Therefore, the use of the leather powder as a kind of filler in the synthetic leather has a very excellent effect.

2.2 Effect of the amount of leather powder on the performance of base

Table 4 Effect of the amount of leather powder on the performance of base

Experiment number	1-1	2-2	2-3	2-4	2-5	2-6
Myogenicity (%)	44.3	44.6	45.4	46.1	44.8	43.6
Hydrolysis resistance (h)	20	20	19	18	17	15
Tensile Strength (MPa)	16.9	16.7	17.8	18.5	14.8	14.3
Tear strength（N/mm）	130.1	99.8	114.0	126.9	92.6	90.7
Peel strength (N/3cm)	118	80	96	123	70	64
Water vapor permeability ($mg/10cm^2•24h$)	2144	1991.7	2055.9	2163.4	1799.7	2186.3
Breathability ($mL/cm^2•h$)	367	238.4	290.3	313.0	297.5	241.6

It can be found from Table 4 that with the increase in the amount of the leather powder filler, the amount of calcium carbonate added does not change, and the mechanical properties showed a trend of first increasing and then decreasing. Because the leather powder and the polyurethane molecules are well dispersed uniformly, resulting in a certain internal cross-linking effect. So the mechanical properties increase. At the moment, when the amount of the leather powder is 15 parts, the amount of calcium carbonate is 25 parts. When the amount of the leather powder is more than 25 parts, agglomeration occurs, which destroys the continuity of film formation. The local stress concentration is caused during the stretching process, and the absorption energy and the deformation resistance of the film are decreased, resulting in deterioration of the toughness of the material and a decrease in mechanical properties. The hydrolysis resistance of base gradually decreased from the increase in the amount of leather powder, which reason was partly consistent with the hydrolysis resistance in Table 3. The water vapor permeability and gas permeability also showed a trend of increasing first and then decreasing. The reason was that the dispersion of ultrafine leather powder in polyurethane molecules was better, DMF has a good affinity with the reactive groups such as hydroxyl group and carboxyl group on ultrafine leather powder, so that some DMF combined with the leather powder cannot directly enter the water, water and leather powder react with DMF, which causes competition, slows the dissolution rate of DMF into water, and the concentration gradient of coagulation bath does not change. The finer the leather powder particles, the lower the diffusion rate of DMF into the water, and the low affinity of the leather powder itself and the water molecules.Therefore, the water molecules enter the film at a slower rate, the upper and lower solidification speed of the film tends to Consistently. The polyurethane rapidly precipitates to form a solid and produces a tendency towards de-liquid shrinkage. The stress caused by shrinkage is difficult to transfer onto the flow of the polymer, and can only be eliminated by the creep of the solid of the polymer, so that the film forms more finger shape pores and the through holes improve the water vapor permeability and gas permeability of the membrane. When the amount of the leather powder is too large, the formation of the dense layer on the surface is accelerated during the film formation, the DMF in the film does not diffuse out for a sufficient period of time, it cannot be exchanged with water, which is disadvantageous for the formation of pores, and thus the water vapor permeability and gas permeability are decreased. The myoscularity of base is up to 46.1%. Compared with the parameters of other serial numbers, the performance parameters of the first 1-1 pure wood powder in the table are not much changed into myogenicity. Although the hydrolysis resistance value is small, the hydrolysis resistance of the pure leather powder in Table 3 is overall increased actually, because the addition of calcium carbonate filler, Calcium carbonate granular filler, the space occupied by adding to the high polymer is relatively large, which can improve the order of the polymer, and is effectively and uniformly dispersed in the

matrix. Therefore, the hydrolysis resistance is improved; the tensile strength, the peel strength and the water vapor permeability are poor, indicating that the effect of using the two fillers is not obvious, and the performance of the compounding with the wood powder filler may be increased.

2.3. Leather powder application process optimization

2.3.1.Effect of filler on the appearance of slurry and coating

Table 5 Comparison of the appearance of three kinds of fillers into slurry and coating

Experiment number	Viscosity /cps	Flatting	Micropore structure	Myogenicity (%)
2-1	9000	Normal	Large finger hole	43.4
2-5	9800	Normal	Large finger hole	44.8
3-1	10200	Normal	Large finger hole	45.1
3-2	10500	Normal	Large finger hole	45.6
3-3	10300	Normal	Large finger hole	46.3

It can be found from Table 5 that as the filler type increases, the viscosity gradually increases, the flatting property is normal, and the micropore structure gradually changes from a small finger hole to a large finger hole, and the myogenicity also shows an increasing trend. It is fully stated that the addition of three fillers are more effective than the use of filler alone. When the total amount of the three fillers is constant and the various fillers are added in different proportions, with the amount of wood powder decreasing, the viscosity, flattling and macropore structure show better performance with the increase of the amount of leather powder. The myogenicity has even increased, indicating that the ultra-fine leather powder and a small amount of wood powder has better performance.

2.3.2. Effect of filler on hydrolysis resistance of coating

Through long-term observation, the changes of the leather samples in different time periods are listed as follows:

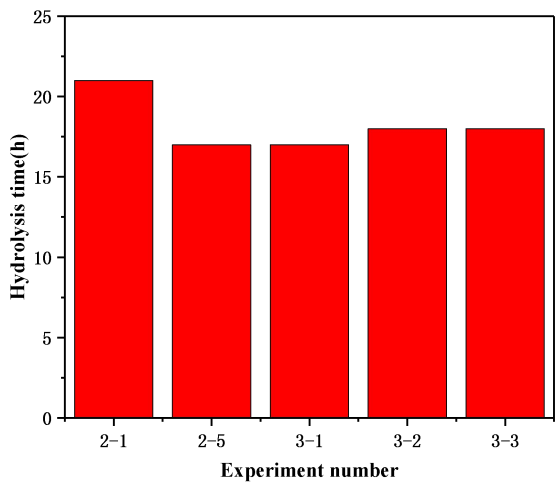

Figure 2 The effect of filler on the hydrolysis resistance of the coating

It can be seen from Fig. 2 that the increase of the filler type and the different compounding ratio will have an effect on the hydrolysis resistance of the synthetic leather product. In the alkaline aqueous solution, the surface is always flat and has a certain strength within 10 hours, there is also no wrinkles or even detachment from the substrate. When the time exceeds 10 hours, the surface of the leather product gradually cracks and wrinkles, and reaches the limit gradually. It can be clearly seen

from the figure that the hydrolysis resistance of the calcium carbonate-containing filler is slightly better than that of combining the leather powder with the calcium carbonate, which is caused by a sharp increase in the amount of the ultrafine leather powder, In addition to containing surface active groups, it is not resistant to alkali and is used in synthetic leather products. With the increase of the amount of leather powder, the alkali resistance will gradually decrease, the hydrolysis resistance is enhanced when the wood powder is added. Because the three kinds of fillers are used in combination to make up for the defects of various fillers used alone in the leather, as a nucleation point, carrying a certain binding capacity.

2.3.3.Effect of filler on mechanical properties of coating

It can be seen from Fig. 3 that when the content of calcium carbonate added is fixed and the content of ultrafine leather powder is increased to 20 parts, the tensile strength and the tear strength tend to decrease. Because the amount of the leather powder increases, the leather powder can not be uniformly dispersed with the calcium carbonate filler, the stress concentration is large, the particle size distribution is wide and the agglomeration is large, so it will decrease. After adding the wood powder, as the content of the wood powder decreases, the amount of the ultra-fine leather powder increases, the total amount remains unchanged, and the tear strength and the peel strength all increase. The reason is that the combination of ultrafine leather powder and wood powder and calcium carbonate enhances the interaction between the filler and the polyurethane molecule, resulting in an increase in mechanical properties. But if the amount of wood powder and ultrafine leather powder is increased, Agglomeration will occur, which is not conducive to the improvement of mechanical properties. Therefore, the total amount of filler is controlled, and the relative proportion is changed. Finally, the amount of leather powder is 15 parts, the amount of wood powder is 5 parts, and the amount of calcium carbonate is 25 parts. The mechanical properties are the best at this time.

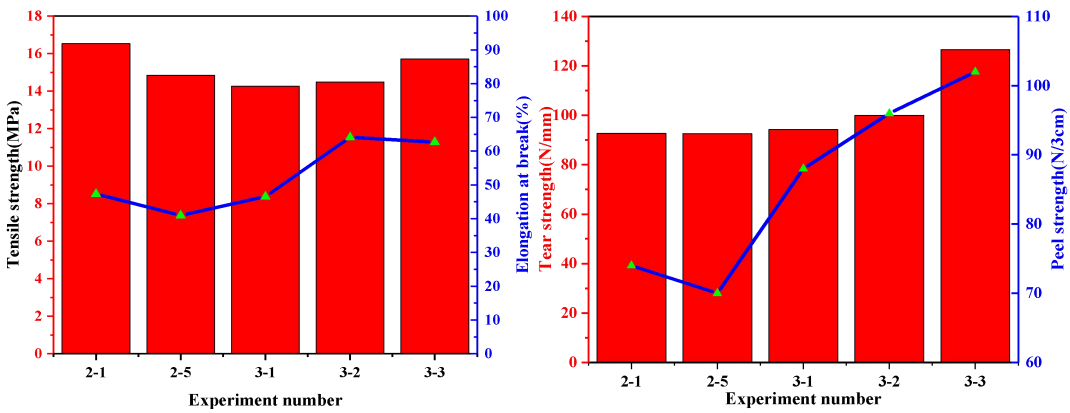

Figure 3 Effect of filler on the mechanical properties of the coating

2.3.4. Effect of filler on the hygienic properties of coatings

Table 6 Water vapor permeability and gas permeability test results

Experiment number	Water vapor permeability (mg/10cm^2•24h)	Breathability (mL/cm^2•h)
2-1	1687.3	232.3
2-5	1799.7	297.5
3-1	1846.2	300.2
3-2	1961.9	339.6
3-3	2152.4	376.1

It can be seen from Table 6 that as the type of filler increases, the hygienic performance shows an increasing trend, which is slightly worse than pure wood powder as a filler. Because calcium carbonate is an ionic compound, which is easily wetted by water, and calcium carbonate particles. The siphon effect of the capillary pores on the surface allows water to easily move from one end to the other, and calcium carbonate acts as a core point during solidification, changing the solidification state

of the polyurethane and reducing the continuous penetrating pores. After the wood powder and the leather powder is added, the hydrophilic groups in the structure are increased, the capillary effect is enhanced, the water vapor permeability and gas permeability are increased. In other words， the hygienic performance is improved, because the polyurethane rapidly precipitates to form a solid during the film formation process, and the tendency of dehydration shrinkage occurs, the stress caused by shrinkage is difficult to transfer through the flow of the polymer, and can only be eliminated by the creep of the solid of the polymer, so that the film forms more finger holes and through holes, the water vapor permeability of the film increased gas permeability. By controlling the total amount of filler and changing the ratio between the fillers, the results showed that the hygienic performance was best when the amount of leather powder was 15 parts, 25 parts of calcium carbonate and 5 parts of wood powder.

2.3.5.Influence of filler on the microstructure and morphology of the coating

In order to clearly observe the dispersion of the filler in the polyurethane and the microporous structure of the film formation, the side of the base was observed by a scanning electron microscope(SEM), as shown in Fig. 4: Fig. a is the group 1-1; Fig. b is the group 1-2; Figure c is group 2-4; Figure d is group 3-3.

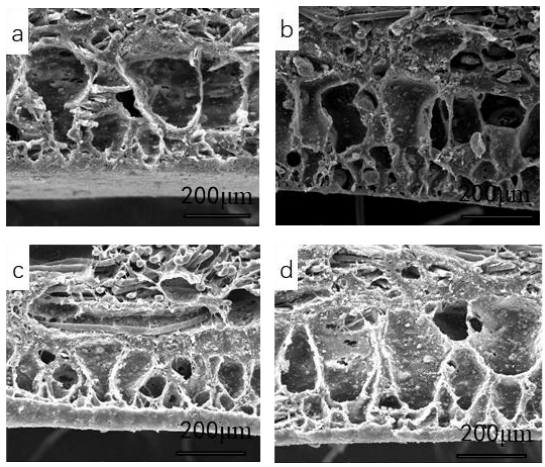

Fig. 4 Microporous structure of two kinds of fillers in polyurethane synthetic leather

It can be seen from Fig. 4 that Fig. a has a large size, a large number, a continuous hole, a deep hole structure, a very thin hole wall, and an excellent sanitary performance. Fig. b has a small hole size and a continuous hole number. More, the wall of the hole is thin, and the structure of the loose hole is obvious. Figure c the structure of the hole is uniform, the number of holes is large, the wall of the hole is relatively complete, and the structure of the hole is dense, which is caused by the exchange rate during the molding process. Figure d the structure of the finger hole is obvious. The finger hole structure is uniform, the hole is large, the micropore wall is relatively complete, and the hole is continuous. The reason for the large pore structure is that the addition of wood powder increases the nucleation point in the coating and increases the probability of forming a large pore structure. The filler can be uniformly dispersed in the polyurethane, and functions as a "skeleton". As a nucleation point in solidification, a finger-type pore structure is formed, which shows that the filler has an important significance of the synthetic leather.

3 Conclusion

(1) In this experiment, the effects of wood powder, leather powder and light calcium carbonate as fillers on the properties of synthetic leather were compared by the preparation of ultrafine leather powder and the application in synthetic leather. The results showed that: Suitable leather powder application conditions are: $w_{(leather\ powder)}$: $w_{(wood\ powder)}$: $w_{(light\ calcium\ carbonate)}$ = 15:5:25, at this time, the slurry viscosity is 10400 cps, the muscle formation is 46.3%, The base has a tear strength of 126.6 N/mm, a peel strength of 102 N/3 cm, a tensile strength of 15.71MPa, a hydrolysis resistance time of 18 h, a water vapor

permeability of 2152.4 mg/10 cm ^{2}•24 h, and a gas permeability of 376.1 mL/cm ^{2}•h.

(2) It can be seen from the scanning electron micrograph that the filler acts as a "skeleton" in the polyurethane coating. As a nucleation point of condensation, the rate of DMF and water exchange changes during the film formation process, and the polyurethane rapidly precipitates solids. The tendency of dehydration shrinkage occurs, and the stress caused by shrinkage is difficult to transfer through the flow of the polymer, and can only be eliminated by solid peristalsis, thereby forming a relatively obvious finger-shaped pore structure, providing excellent conditions for hygienic performance.

(3) Reasonable pulverization treatment of ultra-fine leather powder reduces the bundle-like accumulation, and the reasonable dosage has the reinforcing effect on the flatness, hygienic performance and mechanical properties after film formation, and solves the problem of waste of leather waste. , providing an effective way for resource utilization.

References

[1] Berry F J, Costantini N, Smart L E. Synthesis of chromium-containing pigments from chromium recovered from leather waste[J]. Waste Management, 2002, 22(7): 761-772.

[2] Geng Jun, Diao Shen, Chen Peihai, Wang Quanjie.Research Progress in the Utilization of Leather Chips[J].Leather Science and Engineering,2016,26(05):28-34.

[3] Rao J R, Thanikaivelan P, Sreeram K J, et al. Green route for the utilization of chrome shavings (chromium-containing solid waste) in tanning industry[J]. Environmental science & technology, 2002, 36(6): 1372-1376.

[4]Zhang Shuhua. The leather industry is advancing on the road of exploring circular economy [J]. China Collective Economy, 2010 (1): 26-30.

[5]Chen Peihai, Wang Quanjie, Luo Yanhua, et al. Feasibility of preparing soil organic fertilizer by using waste chrome shavings[J]. Leather and Chemicals, 2017, 34(2): 13-16.

[6] Chaudhary R, Pati A. Poultry feed based on protein hydrolysate derived from chrome-tanned leather solid waste: creating value from waste[J]. Environmental Science and Pollution Research, 2016, 23(8): 8120-8124.

[7] Cavalcante D G S M, Gomes A S, Santos R J, et al. Composites Produced from Natural Rubber and Chrome-Tanned Leather Wastes: Evaluation of their In Vitro Toxicological Effects for Application in Footwear and Textile Industries[J]. Journal of Polymers and the Environment,2017: 1-9.

[8]Feng Jianyan, Qu Jianbo, Luo Xiaomin. The eighteenth lecture on the status and development trend of chemicals for polyurethane synthetic leather[J]. Polyurethane, 2008 (9): 84-88.

[9]Qu Jianbo. Synthetic Leather Technology [M]. 1st ed. Beijing: Chemical Industry Press, 2010

[10]Wei Liling, Liu Yakang, Tang Zhigang, et al. Preparation and preliminary application of lignin reticulated polyurethane foam [D]. , 2007.

[11]Liu Xibin, Li Wanjie, Lin Yinlei. Effect of Different Inorganic Fillers on Properties of Polyurethane Elastomers[J]. Shanxi Chemical Industry, 2011, 31(5): 5-9.

[12] Stewart D. Lignin as a base material for materials applications: Chemistry, application and economics[J]. Industrial crops and products, 2008, 27(2): 202-207.

[13] Ding Shaolan, Luo Xiaomin, Zhou Yue. Analysis and Inspection of Leather Products [M]. 1st ed. Beijing: China Light Industry Press, 2010.

P61

Preparation and properties of Superhydrophobic coating based on modified grapene oxide

Xiaomin Luo[1]*, Qianqian Huo, Jianyan Feng[3]

([1] College of Bioresources Chemical and Materials Engineering, Key Laboratory of Leather Cleaner Production, China National Light Industry, Shaanxi University of Science & Technology, Xi'an, Shaanxi,710021, PR China, Tel:15809282916, E-mail:1070746017@qq.com)

([2] College of Bioresources Chemical and Materials Engineering, Key Laboratory of Leather Cleaner Production, China National Light Industry, Shaanxi University of Science & Technology, Xi'an, Shaanxi,710021, PR China, Tel:18309293729, E-mail:1795131688@qq.com)

([3] College of Bioresources Chemical and Materials Engineering, Key Laboratory of Leather Cleaner Production, China National Light Industry, Shaanxi University of Science & Technology, Xi'an, Shaanxi,710021, PR China, Tel:13992036146, E-mail:80128662@qq.com)

Abstract

The modified graphene was prepared by graphene oxide(GO) as the raw material with hydrophobic modification of octadecylamine. The superhydrophobic copper mesh for oil-water separation was prepared by spraying with copper mesh as substrate. The structure of superhydrophobic copper was characterized by infrared spectrometer, the micro-morphology and wettability of superhydrophobic copper were analyzed by scanning electron microscope and contact angle apparatus respectively. Oil-water separation performance of superhydrophobic copper was also studied. The results showed that octadecylamine modified GO successfully. The surface roughness of superhydrophobic copper was obvious increased. Contact angle of superhydrophobic copper was about 157.8° and sliding angle was about 4.0°. The separation efficiency of superhydrophobic copper was up to 99.80% with efficient separation. Moreover, When separated 35 times, the separation efficiency was 90.30%, and the superhydrophobic copper had good recycling performance. .

Key words: Graphene oxide, Octadecylamine, Modified graphene, Superhydrophobic, Oil-water separation

IMPORTANT: Poster presentation.

1 Introdution

The study of superhydrophobic water is inspired by nature. As early as 1997, German scientists[1] began to study a large number of plant leaves. It was found that the characteristics of plants that produced silt and did not stain were caused by the rough structure of nanometer on the leaf surface and the waxy substance on the surface.In the 1950s, the international research on superhydrophobic coatings began[2]. With the rapid development of surface treatment technology, more attention has been paid to superhydrophobic coatings[3].Graphene is a hot research topic recently, because it has a large specific surface area, which endows graphene with many excellent properties such as high conductivity, high thermal conductivity and good mechanical performance[4]-[6].Graphene research application field is very broad, graphene oxide is the most common graphene derivative. The properties of graphene oxide are similar to graphene, and a large number of active functional groups provide favorable conditions for the functional modification of grapheneits properties similar to graphene.Grafting and modification of graphene oxide can improve the dispersibility of graphene while giving it reactivity, which is conducive to the development of high-performance graphene-based composites[8].

Water pollution caused by organic substances in industrial waste water, such as chemical industry, printing and dyeing industry and leather industry, poses a great threat to human health.At present, the separation efficiency of oil and water is low, and the separation equipment is expensive and complex.Super hydrophobic material is a new functional material with high separation efficiency and good separation effect[9].In 2004, the JiangLei research group of the Chinese academy of sciences first published the application of ptfe coating on stainless steel net to prepare stainless steel net film materials with super hydrophobic and oil-loving properties, and applied to oil-water separation research[10].In this study, hydrophobic modified graphene oxide was prepared, and the oil and water separation material - superhydrophobic copper mesh was

prepared by simple and easy spraying method[11], which has the characteristics of mild modification condition, simple preparation process and easy operation.And the hydrophobic materials are multifunctional. It is of positive significance to the application of new carbon materials in hydrophobic coatings and provides a new idea for the research and application of graphene-based hydrophobic materials.

2 Experiments

2.1 Experimental materials and instruments

Graphene oxide; Anhydrous ethanol; Octadecylamine; Acetone. Ultrasonic cell disruptor (Ningbo xinzhi biotechnology co. LTD.); Magnetic stirrer with concentrated heat and constant temperature heating (Gongyi yuhua instrument co. LTD.); High-speed centrifuge (Anhui zhongke zhongjia scientific instrument co. LTD.); Vacuum desiccant box (Beijing songyuan huaxing technology development co. LTD.); Spray gun (Fujian provincial strength brand air pressure mechanism manufacturing co. LTD.); Analytical balance (Beijing sidoris balance co., LTD.);Fourier transform infrared spectrometer (BRUKER, Germany);Video optical contact Angle measurement instrument (Dataphysics, Germany);Scanning electron microscope (FEI company, USA)

2.2 experimentcontent

2.2.1 Preparation of modified graphene

The dispersible solution was made from 0.5 g of graphene oxide(GO) and 150 mL of anhydrous ethanol, and 2.5 g of octadecylamine (ODA) was added for ultrasonic dispersion for 40 minutes.Magnetic stirring reaction under 80 ℃ for 24 h. After cooling to room temperature, centrifuge with anhydrous ethanol for 6 times and then centrifuge with distilled water for 1 time to remove excess ODA. Finallyr the last product will dry completely made of modified graphene (GO - ODA) under 60 ℃

2.2.2 Preparation of oil - water separation materials

50 mg GO-ODA and 50 ml acetone were used to make dispersible liquid, Spray a small amount of dispersing liquid on the surface of the copper mesh several times with an air spray gun. After Copper mesh dry 30 minutes under 60 ℃, oil water separation materials-super hydrophobic copper mesh was made.

2.3 Structural characterization and performance testing

2.3.1 Structure characterization of modified graphene

(1) Fourier infrared spectroscopy characterization(FTIR)

The powder materials before and after modification were tested by Fourier transform infrared spectroscopy. GO and GO-ODA powder were dry for 24 h, and potassium bromide was dry 4 h in 120 ℃. The powder was mixed with ground potassium bromide powder, and the infrared analysis was carried out after pressing.

(2) Scanning electron microscope testing(SEM)

Morphological observation and microstructure analysis of the samples were carried out using the us FEI Q45 scanning electron microscope. The sample preparation method is as follows: the samples are bonded with conductive adhesive on the carrier platform for gold injection treatment, and then SEM is used for scanning at different amplification multiples. The test acceleration voltage is 30 kV.

2.3.2 Oil and water separation performance test

(1) Water contact Angle test

The CA of superhydrophobic copper net was determined by video optical contact Angle tester. The measurement parameter of CA is: the volume of water drops is set to 5 μL. The average value of water drops is obtained after five points are randomly measured on the ultra-hydrophobic copper network.

(2) SEM

orphological observation and microstructure analysis of the samples were carried out using the us FEI Q45 scanning electron

microscope. The sample preparation method is as follows: the samples are bonded with conductive adhesive on the carrier platform for gold injection treatment, and then SEM is used for scanning at different amplification multiples. The test acceleration voltage is 30 kV.

(3) Oil and water separation test

The oil solvent kerosene was mixed with tap water (the tap water was stained with prismatic aquamarine) and the quality ratio was 1:1. The prepared oil and water separation material is placed on the beaker, and the oil and water mixture is slowly poured into the box superhydrophobic material at a constant speed. The oil phase can easily pass through the pores and into the lower beaker, while the water accumulates in the upper material. The oil and water separation efficiency of the material can be obtained by collecting and comparing the quality of the water phase in the material with that in the mixture.

3.Results and Discussion

3.1 Characterization of structure and hydrophobic properties of modified graphene

3.1.1 FTIR characterization

Figure 1 is the infrared spectrum of GO before and after modification.As can be seen from figure 1, the characteristic absorption peak of -OH appears in GO at 3375 cm^{-1}; the characteristic absorption peak of -COOH appears in GO at 1716 cm^{-1}; the characteristic absorption peak of C=Cappears in GO at 1616 cm^{-1};the characteristic absorption peak of epoxygroupappears in GO at 1095 cm^{-1}.The characteristic absorption peak of -COOH at 3375 cm^{-1} and 1716 cm^{-1} of GO-ODA was significantly weakened. Characteristic absorption peaks of $-CH_3$, $-CH_2$ and -NH-C=O appeared at 2920 cm^{-1}, 2848 cm^{-1} and 1461 cm^{-1} respectively. This indicates that ODA has successfully modified GO, and the appearance of $-CH_3$ and $-CH_2$indicates that the long alkyl chain with hydrophobic water has been successfully grafted to the surface of GO.

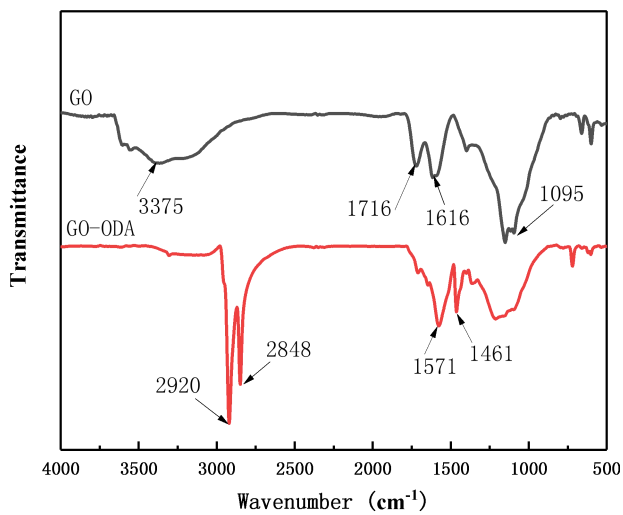

Figure 1. Infrared spectrogram of GO and GO-ODA

3.1.2 Microstructure and hydrophobic property analysis

Figure 2 is the SEM diagram before and after the modification of GO, (a) and (c) are the SEM diagrams of GO and GO-ODA powders at ×1000 magnification respectively, (b) and (d) are the SEM diagrams of GO and GO-ODA powders at ×2000 magnification respectively, and the embedded pictures in (b) and (d) are the water contact angles of GO and GO-ODA coatings respectively. It can be seen from the figure that both GO and GO-ODA powders have obvious lamellar structure. Compared with GO, the surface of GO-ODA is more rough, which is conducive to the construction of super-hydrophobic surface. The CA of GO coatings is about 45.1°, while GO-ODA coating is about 160.0°, these show that the GO after the modification has excellent hydrophobic performance. Contrary to the nature of macroscopic interface [12], the rougher the interface is, the smaller the frictional resistance of water molecules on its surface, the easier it will be for

water molecules to slide and the more hydrophobic the interface will be.

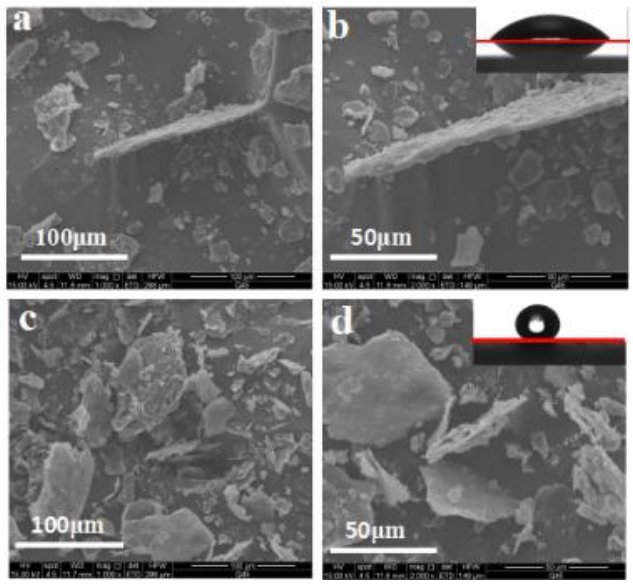

Figure 2. SEM images of (a) and (b) GO at different magnification rates, and SEM images of (c) and (d) GO-ODA at different magnification rates

3.2 Analysis on structure and properties of oil-water separation materials

3.2.1 Microstructure and hydrophobic property analysis

Figure 3 is the SEM diagram of opper mesh and super hydrophobic copper mesh prepared by copper mesh which coated GO-ODA.

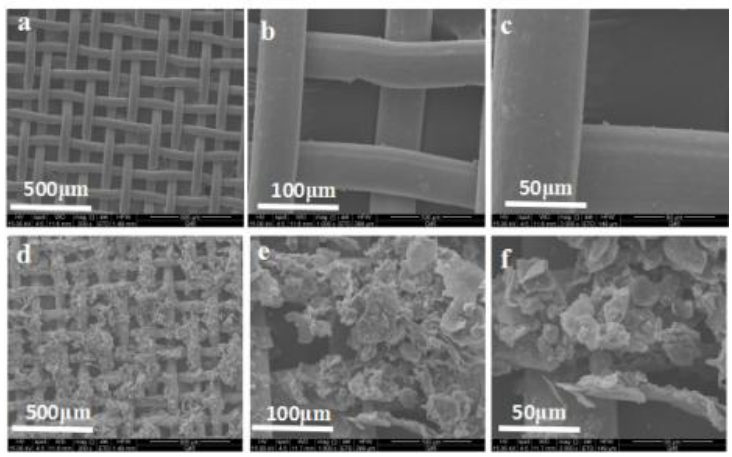

Figure 3. SEM diagram of copper mesh surface at different magnification rates :(a) - (c) copper mesh, (d) - (f) superhydrophobic copper mesh

As can be seen from figure 3 (a)-(c), the surface of copper mesh is relatively smooth. As can be seen from FIG. 3 (d)-(f), after the go-oda treatment, a large number of flake micro-nano rough structures appeared on the surface of the ultra-hydrophobic copper network, and the morphology changed significantly. This phenomenon may be caused by the structure of the go-oda molecule, which is very beneficial to the construction of the superhydrophobic surface, because ODA itself is a low-surface energy substance, and GO itself can form the coarse structure of micro-nanometer scale.

Figure 4 is a picture of water droplets on the surface of a superhydrophobic copper net. The CA of Superhydrophobic copper net is about 157.8°,the SA is about 4.0°.These show that the superhydrophobic copper net has excellent hydrophobic

performance.

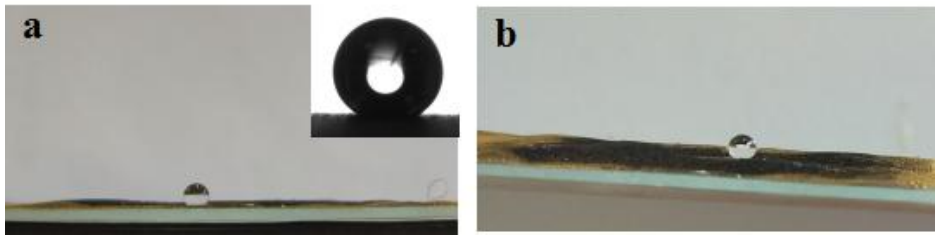

Figure 4. Pictures of water droplets on the surface of a superhydrophobic copper net

3.2.2 Oil and water separation applications

The treated copper net has the opposite infiltration to oil and water, so it can be used for oil and water separation.When a drop of water touches the surface of the copper mesh, it can roll easily due to low adhesion.When the oil drops come into contact with the copper net,they spread out quickly and pass through. However, when oil and water droplets contact the copper net, there is a special case. On the one hand, the oil phase spreads out rapidly and fills in the gap of the micro-nano structure, and the material surface begins to become smooth; on the other hand, the water phase can slide easily on the oil film.

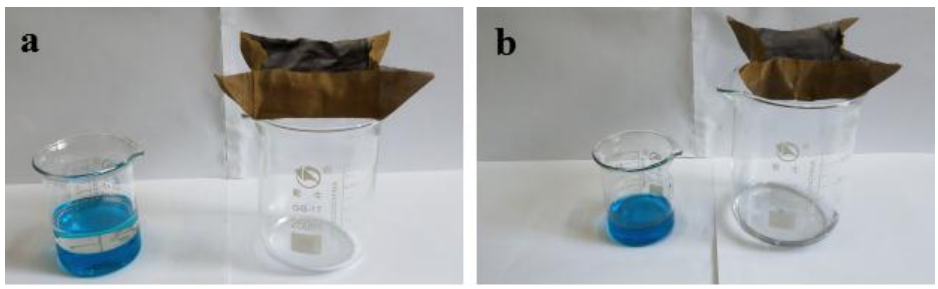

Figure 5. Diagram of separation process of oil and water mixture :(a) device diagram before separation, (b) device diagram after separation

Figure 5 (a-b) is the diagram of oil-water separation device, and Figure. 6 is the result diagram of separation efficiency of ultra-hydrophobic copper network. The copper net was used to separate kerosene/water mixture for 35 times and the data is recorded every time.The separation efficiency of superhydrophobic copper was up to 99.80%. The superhydrophobic copper had good recycling performance. When separated 35 times, the separation efficiency was still 90.30%

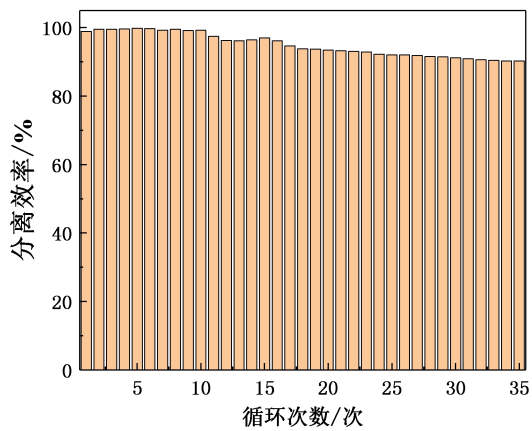

Figure 6. Test results of circulating efficiency of superhydrophobic copper net

4 Conclusion

Go hydrophobic modification: Modified graphene was prepared from GO prepared by modified Hummers method, The

modified condition is that the mass ratio of GO and ODA is 1:5. FTIR test results show that after modification by ODA, most of the oxygen-containing functional groups such as hydroxyl group, carbonyl group and ether bond disappeared, and new hydrophobic groups such as -CH_3, -CH_2 and -NH-C=O emerged. These indicate that ODA has successfully modified GO; Comparing the SEM images of GO and go-oda powders, it is found that both have obvious lamellar structure. After the modification of ODA, the roughness of GO-ODA increased significantly, so its CA increased significantly, making it super hydrophobic

Oil and water separation material: The oil-water separation material-super hydrophobic copper net was prepared by spraying copper net. The SEM diagram shows that the surface roughness of the superhydrophobic copper mesh is obviousSuper hydrophobic surface of the bronze CA is about 157.8°, SA of about 4.0°, The separation efficiency of superhydrophobic copper was up to 99.80% with efficient separation. And the super - hydrophobic copper net has good circulation. When the separation was 35 times, the separation efficiency was still 90.30%.

5 Reference

[1] Ball P. Engineering Shark skin and other solutions[J]. Nature, 1999, 400(6744): 507-509

[2] 徐蕊, 马英子, 肖新颜. 仿生超疏水涂层材料研究新进展[J]. 化工新型材料, 2009, 37(2): 1-4

[3] 黄燕, 涂伟萍. 水性透明隔热涂料的性能研究[J]. 化工新型材料, 2011, 39(11): 115-117.

[4] 许园. 基于改性氧化石墨烯作为低渗透油藏注水开发纳米减阻剂研究[D]. 成都:西南石油大学, 2015.

[5] 唐秀之. 氧化石墨烯表面功能化修饰[D]. 北京: 北京化工大学, 2012.

[6] 邓尧, 黄肖容, 邬晓龄. 氧化石墨烯复合材料的研究进展[J]. 材料导报, 2012, 26(15): 84-87.

[7] Kim Y M, Nagappan S, Jeong J H, et al. Properties of hydrophobically-modified graphene oxide (HG)/butyl rubber (IIR) nanocomposites prepared by shear mixing process[J]. Composite Interfaces, 2016, 23(8): 819-829.

[8] 宋波. PBO 纤维表面耐紫外涂层的制备及其光老化性能研究[D]. 哈尔滨: 哈尔滨工业大学, 2013.

[9] 曹敏. 水性聚氨酯基超疏水涂层的制备及在油水分离中的应用研究[D]. 西安: 陕西科技大学, 2017.

[10] Feng L, Zhang Z, Mai Z, et al. A super‐hydrophobic and super-oleophilic coating mesh film for the separation of oil and water[J]. Angewandte Chemie, 2004, 116(15): 2046-2048.

[11] 高亮娟, 何溥, 李晓禹, 等. 喷涂法构筑二氧化硅纳米粒子涂层及其光学和润湿性质[J]. 影像科学与光化学, 2012, 30(4): 260-268.

[12] 华军利, 文秀芳, 郑大锋, 等. 有机-无机杂化超疏水涂层的制备[J]. 电镀与涂饰, 2009, 28(12): 49-52.

P62

The Study of Preparation and Performance of Solvent-Free Polyurethane Synthetic Leather with Flame Retardant Properties

Xiaomin Luo[1]*, Wen Jiang[2]

([1] College of Bioresources Chemical and Materials Engineering, Key Laboratory of Leather Cleaner Production, China National Light Industry, Shaanxi University of Science & Technology, Xi'an, Shaanxi,710021, PR China, Tel:15809282916, E-mail:1070746017@qq.com)

([2] College of Bioresources Chemical and Materials Engineering, Key Laboratory of Leather Cleaner Production, China National Light Industry, Shaanxi University of Science & Technology, Xi'an, Shaanxi,710021, PR China, Tel:15094055590, E-mail:843930493@qq.com)

ABSTRACT

Fifteen kinds of flame retardants were blended in solvent-free polyurethane systems with polyurea respectively and non-woven fabric was used as the substrate then semi-dry paste process was adopted to prepare the flame retardant solvent-free PU synthetic leather by means off-type paper transfer coating. The effects of different flame retardants on the flame retardant properties of the coatings was studied. Combustion experiment results showed that the synergistic flame-retarding effect of inorganic phosphorus and nitrogen(P-NZRJ) was the optimal and flame retardant rating could reach B_1 level with excellent flame retardant performance. The experimental results of flame retardant dosage optimization showed that with the increase of P-NZRJ content, mechanical and hygienic properties of the coating were decreased slightly, however hydrolysis resistance was unaffected basically. When the addition amount of P-NZRJ was 10%, comprehensive performance was good. The peel strength of synthetic leather coating was 51.2 N which reached the industry standard.

Key words:Solvent-free polyurethane synthetic leather; Synergistic flame-retarding effect of inorganic phosphorus and nitrogen; Mechanical property

1 Introduction

Polyurethane (PU) synthetic leather, as a substitute for natural leather, is a composite material which can simulate the structure and performance of natural leather. PU synthetic leather products are mainly composed of substrates that can simulate the natural leather reticular layer and micro-porous PU coating that can simulate the natural leather grain layer, with many advantages such as softness, light weight, wear-resisting, anti-aging and good air permeability. Therefore, it is widely used in shoe-making, clothing, furniture covering and automobile interior decoration[1]. With the increasing awareness of global environmental protection and health, the research and development of environmentally friendly synthetic leather manufacturing technology has gradually formed a trend. In order to develop a cleaner production method for synthetic leather, besides paying more attention to waterborne PU synthetic leather in recent years, solvent free PU synthetic leather production technology based on rapid reactive molding technology is another important research and development direction[2]. At present, environmental friendly PU synthetic leather has been increasing in the market of shoe leather, garment leather, luggage leather, automobile interior leather and so on, and these products have very high requirements for inflaming retarding performance[3]. However, as an organic polymer synthetic material, polyurethane is easy to burn in the air and releases a lot of toxic gases in the air, which makes the PU synthetic leather products have a huge potential for safety in the process of production and use, and there are few researches on flame-retardant solventless PU synthetic leather. Therefore, the study of polyurethane with flame-retardant effect can meet the needs of the market for the functionalization and diversification of polyurethane synthetic leather products[4].

In many flame retardant systems, reactive flame retardants have the characteristics of stability, non-toxicity and little influence on the comprehensive properties of polymers. However, the preparation process is complex and the cost is high[5]; Organic flame retardants have many safety problems, such as large amount of smoke and gas release; The powder inorganic flame retardant has the advantages of good thermal stability, low toxicity, no corrosive gas and no volatility, and has a wide

range of sources and low price. It can be widely used in polyurethane flame retardant system[6-8]. Therefore, the simplest and most effective way to reduce the combustion performance of polyurethane is to add inorganic flame retardant to polyurethane. In this study, 15 kinds of flame retardants, such as aluminum hydroxide (ATH), were used to produce solvent-free PU synthetic leather with environmental protection and no pollution, and suitable preparation scheme of flame-retardant solvent-free synthetic leather was explored.

2 Experimental

2.1 Materials

Resin BZ-9535, curing agent P-903 were purchased from Baoze Polymer Materials Co., Ltd. Aluminum hydroxide, magnesium hydroxide, microencapsulated red phosphorus, antimony trioxide, ammonium polyphosphate, melamine, pentaerythritol, P-NZRJ, whitening red phosphorus were all purchased from Shenzhen Hongtai Industrial Co., Ltd. Zinc borate, melamine cyanuric acid salt, melamine pyrophosphate were purchased from Jinan Taixing fine chemical co., Ltd. Triphenyl phosphate was purchased from Sichuan Kelon Chemical Reagent Factory. And Sodium hydroxide purchased from Anhui Huai Hua co., Ltd.

2.2 preparation of flame retardant solvent-free polyurethane coating

The different types of flame retardants and resin BZ-9535 were mixed successively, and then the curing agent P-903 was added and stirred evenly, among which the mass ratio of the three was 32.76:100:9.2. Then, the slurry was scraped onto PTFE plate with 0.5 mm coating gap and bake in oven at 160 ℃ for 10 min. The sample was removed and stripped off after natural cooling. It is worth noting that the slurry was used within 8 hours. The operation flow is shown in figure 1,

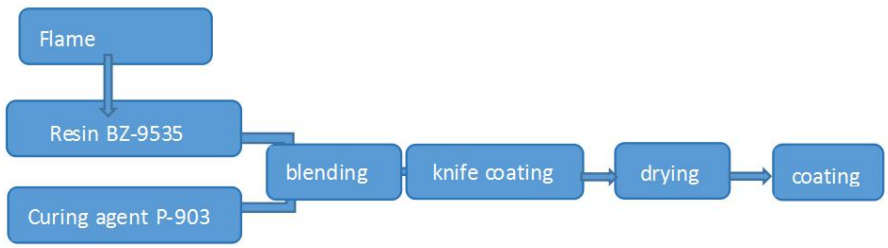

FIG. 1 flowchart of flame retardant PU coating preparation

2.3 preparation of flame retardant solvent-free synthetic leather

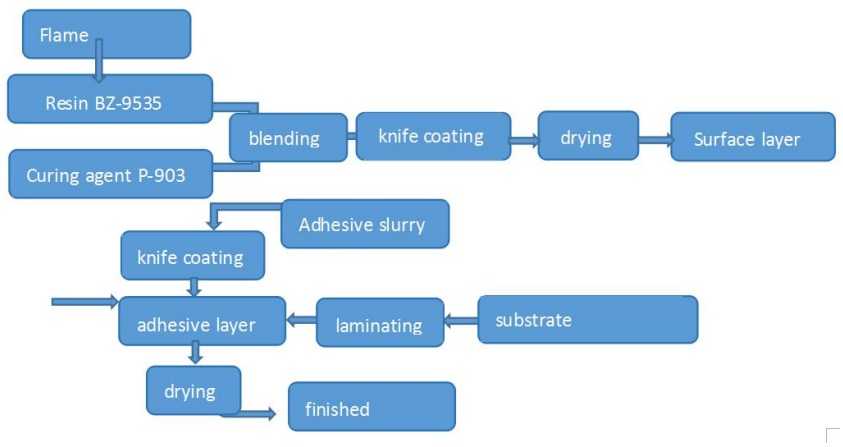

FIG. 2 flowchart of synthetic leather preparation

In this paper, a semi-dry paste process was adopted. The prepared slurry was scraped onto the cured PU coating with a coating gap of 0.2mm. After baking 1min at 160 ℃, the coating roll was rolled repeatedly to make it close to the substrate.

After redrying at 160 ℃ for 10 minutes, taken out the sample and peeled it into leather after natural cooling. The operation flow is shown in figure 2.

2.4 Performance testing

Flame retardancy tests are performed according to vertical combustion tests in accordance with GB/T5455--2014 standards. Mechanical properties were tested by tension machine and tensile speed was 100 mm/min. The sanitary performance test includes the permeability test using static method and the permeability test using H.C. Fedorov synthetic leather apparatus. Hydrolysis resistance is measured by immersing the sample (about 50mm × 50mm) in 10% NaOH aqueous solution. The surface phenomena of PU coating are observed every 0.5 h. Synthetic leather sensory index evaluation is a subjective evaluation method, consisting of 5 teachers and students to form an objective evaluation team, through the hand to the eye evaluation.

3 Results and discussion

3.1 Screening of flame retardant for synthetic leather

Table 1 effects of different flame retardants on the properties of solvent-free polyurethane coatings

Type of flame retardant	Afterflame time/s	Afterglow time/s	Molten drop	Damaged carbon length/cm
no flame retardant	0	0	slightly	7.3
ATH	0	0	slightly	10.2
MH	86.1	0	severly	burn off
CRP	23.2	0	slightly	18.2
Sb_2O_3	0	0	little	8.9
APP	2.9	0	slightly	9.5
MEL	0	0	slightly	6.6
P-NZRJ	0	0	slightly	6.2
FR-BMRP02	0	0	little	6.7
Zinc borate	24.3	0	severly	burn off
MCA	2.8	0	slightly	10.1
MPP	6.0	0	little	11.3
FR-BMRP02/$Al(OH)_3$	60.5	0	slightly	14.1
FR-BMRP02/$Mg(OH)_2$	49.9	0	severly	burn off
APP/PER/MEL	0	0	little	8.7

The influence of various kinds of flame retardants on the inflaming retarding performance of the coating was quite different. In this experiment, several flame retardant systems which had been widely used in industry have been selected, and the effects of different flame retardants on the inflaming retarding performance of solvent-free polyurethane coatings had been investigated. With the vertical combustion performance as the evaluation index, a better flame retardant was screened for further optimization experiment. According to the above requirements, 15 kinds of flame retardant polyurethane coatings prepared by different flame retardants and their combinations were designed in table 1.

The vertical combustion test showed that the PU coating with ATH, Sb_2O_3, MEL, P-NZRJ, FR-BMRP02 and APP/PER/MEL were the same as the blank sample, and there was no open flame combustion, so the inflaming retarding performance of the flame retardant can only be ranked by the size of the spreading distance of the melt droplet: P-NZRJ>MEL>FR-BMRP02>no flame retardant. The other flame retardants, especially FR-BMRP02/$Mg(OH)_2$, MH, zinc

borate, had poor flame retardancy in the system.The reason may be that magnesium hydroxide and zinc borate as inorganic flame retardants have a positive correlation with the amount of flame retardants. The amount of flame retardant added fails to achieve a better flame retardant performance of PU coatings, while too many flame retardants affect the curing and forming of solvent-free coatings. As an intumescent flame retardant of inorganic phosphorus and nitrogen, the flame retardant mechanism of P-NZRJ lies in the comprehensive action of condensed phase flame retardant and gas phase flame retardant. P-NZRJ decomposes endothermic, decomposes to form inorganic acid such as phosphoric acid, polyphosphoric acid and so on, can form a layer of non-volatile protective film on the surface of the flame-retardant substrate, isolating the air; At the same time, it is easy to release ammonia, nitrogen, water vapor and deep nitrogen oxides after heating, which block the supply of oxygen and take away most of the heat along with the flame retardant decomposition and endothermic, so the surface temperature of the flame retardant substrate is greatly reduced; PO• is formed when the base material is burned. It can combine with H• and HO• free radicals in the flame area to inhibit the flame[9].

Therefore, after considering the flame-retardant properties of different flame retardants, P-NZRJ was chosen as the additive of flame retardants to carry out further optimization experiments.

3.2 Effect of flame retardant dosage on performance of solvent-free PU coatings

3.2.1 Effect on flame retardant performance

In the sensory inspection, the appearance of PU coating without flame retardant was yellow and translucent, while the appearance of the flame retardant PU coating was mostly milky white because the flame retardant was mostly white powder. As can be seen from table 2, with the increase of P-NZRJ, the coating was soft handle, smooth and fine appearance, and the coating thickness was consistent. This may be due to the good compatibility between p-nzrj and polyurethane resin, which generates less stress concentration points in PU coatings, so that the addition of P-NZRJ has less impact on the feel of coatings [10].

Table 2 effect of P-NZRJ on inflaming retarding performance of PU coating

sample	P-NZRJ/%	Afterflame time/s	Afterglow time/s	Molten drop	Damaged length/cm	Sensory evaluation
1#	0	0	0	slightly	11.6	Softness and smoothness
2#	10	0	0	little	7.5	Softness and smoothness
3#	15	0	0	little	7.9	Softness and smoothness
4#	20	0	0	little	7.2	Softness and smoothness
5#	25	0	0	little	6.9	Softness and smoothness
6#	30	0	0	little	6.2	Softness and smoothness

As can be seen from table 2, PU coating had good flame retardant performance.When the dosage of P-NZRJ was 10%, the damage length was shortened from 11.6cm to 7.5cm, and the flame retardant effect was significantly improved. When the dosage was over 10%, the damage length was basically unchanged, and some damage lengths even increased, indicating that when the dosage of P-NZRJ exceeded a certain proportion, it had little effect on the flame retardancy of PU coating. The reason may be that the flame retardant is reacted with isocyanate and inserted into the polyurethane molecular structure in hard segment. At the time of combustion, the phosphate ester first decomposes into a liquid film of non flammable phosphoric acid, which covers the surface of the fabric and acts as an isolating agent. With the increase of temperature, phosphoric acid is further polymerized to form polyphosphoric acid. Polyphosphoric acid can easily make the polymer dehydrated and carbonized，forming carbon film on the surface of fabrics, which can insulate oxygen and suppress smoke and prevent droplets from occurring thus playing a stronger role in flame retardation. In addition, nitrogen and phosphorus in the structure promote carbonization reaction, showing a remarkable synergistic effect of phosphorus and nitrogen. Initially,

the flame retardancy of polyurethane increased with the increase of phosphorus content. However, when the phosphorus content is increased to a certain value, the molecular chain of the system is prone to thermal cracking and fracture, which results in the loss of phosphorous element in the polymer without giving full play to the flame-retardant effect and reduces the flame retardant property[11]. Therefore, when 10% P-NZRJ was added, the flame retardant effect of PU coating was good, as shown in figure 3.

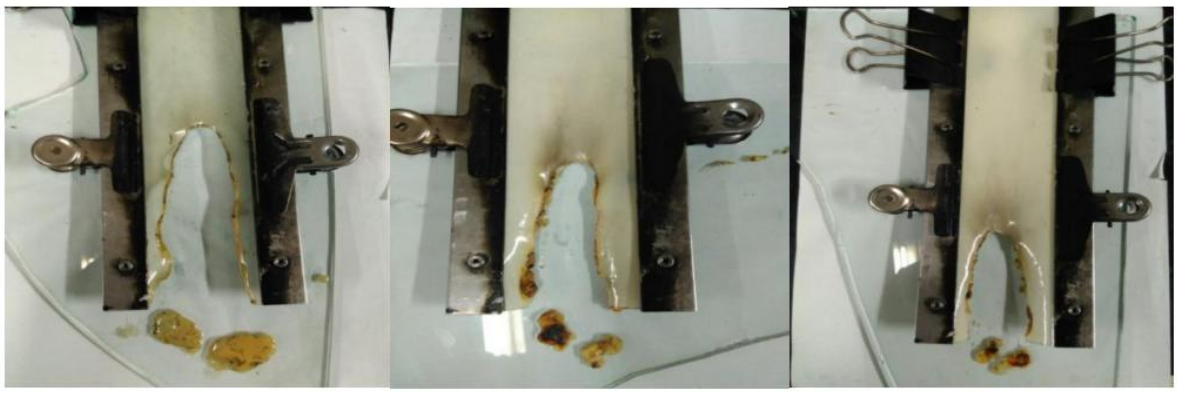

FIG. 3 vertical combustion effect diagram of PU coating mixed with P-NZRJ 0%, 10% and 15% dosage

3.2.2 Effects on mechanical properties

As shown in Figure 4, with the increase of the amount of P-NZRJ, the tensile strength and elongation of the PU coating decreased, and the elongation of the coating decreased obviously when the amount of the flame retardant was 10%, and then decreased slightly. This is due to the fact that P-NZRJ basically does not react with the two components of the system A and B in polyurea polyurethanes. Because when the slurry is mixed, the B component is at the blocking, and the strong reactivity of A component after heating will make it react quickly with the unblocking B component. P-NZRJ mostly exists in the system PU coating in the form of additive flame retardant. At this time, the more powder particles P-NZRJ has, the more physical blocking the formation of PU macromolecular chain, and the faster the mechanical performance of PU coating declines.

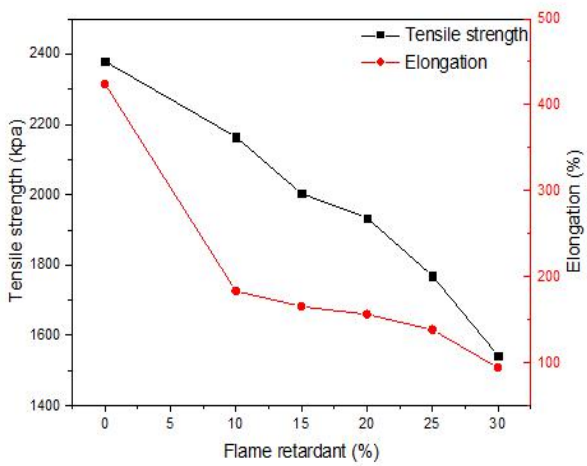

FIG. 4 relationship between the amount of P-NZRJ and the tensile strength and elongation of PU coatings

3.2.3 Effect on hydrolysis resistance

When the PU coating with different dosage of P-NZRJ was soaked in 10% NaOH solution for more than 8 hours, the surface of PU coating was still free of defects and had a good handle, but there was no defect in the blank sample after immersion for 10 hours. This shows that the hydrolysis resistance of PU coating with different dosage of P-NZRJ was lower than that of

the blank sample, but the hydrolysis resistance of PU coating was good on the whole. The influence of P-NZRJ on the hydrolysis resistance of PU coating was mainly due to the influence of flame retardant particles on the formation of PU macromolecular chain.

3.2.4 Effects on hygiene performance

As shown in figure 5, with the increase of P-NZRJ dosage, the moisture permeability and air permeability of PU coating decreased. This is because the PU coating is a solvent-free foaming coating, and the addition of P-NZRJ will destroy the foam hole structure of the solvent free PU coating, leading to the decrease of moisture permeability and air permeability of the PU coating and the decline of hygiene performance.

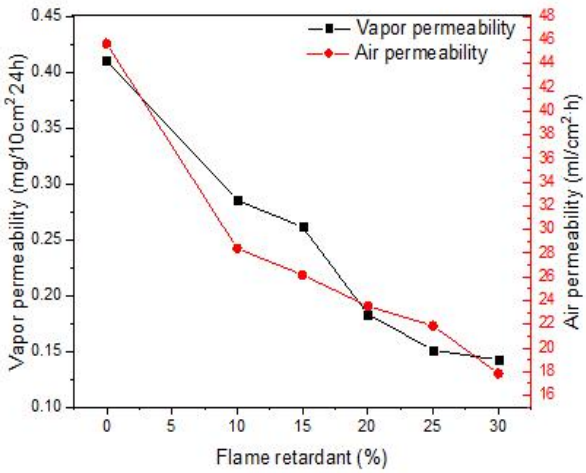

Fig. 5 the relationship between the amount of P-NZRJ and the hygienic properties of PU coating

3.3 Preparation and properties of flame retardant solvent-free PU synthetic leather

After comprehensive consideration, when the dosage of P-NZRJ is 10%, the coating has a good flame retardant effect and will not damage the basic physical and mechanical properties of the coating. The selected P-NZRJ flame retardant was added to the PU slurry with 10% dosage, and the nonwovens were used as the bonding material to prepare the flame retardant solvent free PU synthetic leather, and the peel strength and the flame retardancy of the synthetic leather coating were measured. The test results are shown in table 4.

Table 4 peel strength and vertical combustion test results of flame retardant solventless PU synthetic leather coatings

system	Types of flame retardants	dosage/ %	Peel strength /N	Afterflame time/s	Afterglow time/s	Molten drop	Damaged length/cm
Polyurea polyurethane	P-NZRJ	10	51.2	4.1	0	little	3.2

Table 4 shows that the peeling strength of synthetic leather coating is more than 30N and the adhesion between coating and substrate is strong, which meets the requirement of leather products peeling load in GB/T4194-2011 polyurethane synthetic leather for automotive use. According to the evaluation grade of decorative fabrics in GB/ T17591-2006 "flame retardant fabric", it can be concluded that the flame retardant solvent-free PU synthetic leather has reached class B1 and has excellent flame retardant performance.

4 Conclusion

A series of flame retardant solvent-free polyurethane coatings were prepared by dispersing 15 common flame retardants such as aluminum hydroxide (ATH), magnesium hydroxide (MH), antimony trioxide and a new halogen-free flame retardant (P-NZRJ) in Polyurea polyurethane system. The suitable flame retardant P-NZRJ was selected through combustion test, and the best dosage was 10%. The grade of synthetic leather was B1 grade.

The experimental results of flame retardant dosage optimization showed that with the increase of P-NZRJ content, mechanical and hygienic properties of the coating were decreased slightly, however hydrolysis resistance was unaffected basically. When the addition amount of P-NZRJ was 10%, comprehensive performance was good. The peel strength of synthetic leather coating was 51.2 N which reached the industry standard.

(3) Sensory examination showed that the coating was soft handle, smooth and fine appearance, and the coating thickness was consistent.

Reference

[1] Ma Xingyuan, Feng Jieyan, Zhang Taolin. Synthetic leather chemistry and technology [M]. China light industry press, 2015.

[2] Wu Ze. Preparation technology and properties of solvent-free polyurethane synthetic leather [D]. Shaanxi university of science and technology, 2014.

[3] Chang Suqin, Liu Jianhui, Feng Na. Research status and prospect of leather flame retardant technology [J]. Chinese leather, 2012, 41(15): 50-53.

[4] Peng Huaqiao, Xia Zuxi, Yu Xinhua, et al. Research progress on halogen-free flame retardant of soft polyurethane foam [J]. New chemical materials, 2008, 36(8):25-26.

[5] Ou Yuxiang, Li Jianjun. Flame retardant - performance, manufacture and application [M]. Beijing: chemical industry press, 2008.

[6] Zhang Yulong, Xia Yubin. Formulation design and processing of flame-retardant macromolecular materials [M]. Beijing: China petrochemical press, 2010.

[7] Huang Zan, Li Lixin, Chen Wuyong. The latest development of leather flame retardant and flame retardant technology [J]. Journal of shaanxi university of science and technology (natural science edition), 2004, 22(3):139-142.

[8] Ou yuxiang. Halogen free, low smoke, low toxic flame retardant polyurethane foam plastics [J]. Jiangsu chemical industry, 2000, 28(3):22-24.

[9] Tang Junjie, Tang Anbin, Huang Jie. Research and application progress of phosphor-nitrogen co-effective flame retardants [J]. Materials guide, 2008, 22(8):73-77.

[10] Luo Xiaomin, Cao min, Wei Zhaofan, et al. Study on preparation of flame-retardant synthetic leather wet fabis [J]. Journal of shaanxi university of science and technology, 2016, 34(4):16-20.

[11] Li Fen, Luo Yunjun, Li XiaoTong, et al. Flame retardant finishing of p-nitrogen water-based polyurethane for polyester fabric [J]. Printing and dyeing, 2013, 39(1):13-15.

P63

Preparation and application of graphite based controllable adsorption material

Xiaomin Luo[1*], Chi Zheng[2], Xinhua Liu[3], Wenjie Hu[4]

([1] College of Bioresources Chemical and Materials Engineering, Key Laboratory of Leather Cleaner Production, China National Light Industry, Shaanxi University of Science & Technology, Xi'an, Shaanxi,710021, PR China, Tel:15809282916, E-mail:1070746017@qq.com)

([2] College of Bioresources Chemical and Materials Engineering, Key Laboratory of Leather Cleaner Production, China National Light Industry, Shaanxi University of Science & Technology, Xi'an, Shaanxi,710021, PR China, Tel:18089189393, E-mail:569832834@qq.com)

([3] College of Bioresources Chemical and Materials Engineering, Key Laboratory of Leather Cleaner Production, China National Light Industry, Shaanxi University of Science & Technology, Xi'an, Shaanxi,710021, PR China, Tel:18710981268, E-mail:582964751@qq.com)

([4] College of Bioresources Chemical and Materials Engineering, Key Laboratory of Leather Cleaner Production, China National Light Industry, Shaanxi University of Science & Technology, Xi'an, Shaanxi,710021, PR China, Tel:18700821859, E-mail:1628539335@qq.com)

Abstract

In this paper, graphene oxide was prepared by modified Hummers method. The grapheme@Fe_3O_4 composite particles were prepared by coprecipitation method and hydrothermal method. The composite particles with magnetic properties were used for the adsorption of methyl orange dyes. The results showed that the adsorption properties of the composite particles with two methods were both good, and the equilibrium adsorption capacity was more than 55 mg/g. The adsorption kinetics of the composite particles conformed to the pseudo-first order adsorption kinetics. However, the magnetic properties of GNs@Fe_3O_4 composite particles prepared by hydrothermal method were better, and the maximum magnetic field strength was 63.24 emu/g, which had good controllability.

Keywords: Graphene, adsorption, magnetic, methyl orange

P64

Preparation of Amino Functionalized Carbon Quantum Dots and Its Application in Formaldehyde Detection

Xuechuan Wang[1*], Pengxia Bai[2], Xiaomin Luo[3]

([1] College of Bioresources Chemical and Materials Engineering, Key Laboratory of Leather Cleaner Production, China National Light Industry, Shaanxi University of Science & Technology, Xi'an, Shaanxi, 710021 , China, Tel:029-86168008, E-mail:306472253@qq.com)

([2] College of Chemical Engineering, Shaanxi University of Science & Technology, Xi'an, Shaanxi, 710021 , China, Tel:18291809150, E-mail:1350779128@qq.com)

([3] College of Bioresources Chemical and Materials Engineering, Key Laboratory of Leather Cleaner Production, China National Light Industry, Shaanxi University of Science & Technology, Xi'an, Shaanxi, 710021 , China, Tel:15809282916, E-mail:1070746017@qq.com)

Abstract

This article based on the principle that formaldehyde can quench the fluorescence of amino functionalized carbon quantum dots (NH_2-CQDs), an economical, environmental and facile synthetic method is used to prepare luminescent NH2-CQDs through hydrothermal treatment Citric acid and Urea as carbon source and amino group respectively. The structure and fluorescence properties of NH_2-CQDs were characterized by Fourier transform infrared spectroscopy(FT-IR), transmission electron microscope(TEM), UV-visible spectrometer(UV-Vis), X-ray photoelectron spectroscopy(XPS), X-ray diffraction(XRD), fluorescence spectrometer(PL), the results show that NH_2-CQDs have been successfully prepared, it has rich oxygen-containing functional groups and good photobleaching performance, good fluorescence performance and fluorescence stable, furthermore, the effect of pH on its fluorescence intensity was investigated, the results indicated that the fluorescence was quenched under acidic conditions, and the fluorescence was strong under neutral and alkaline conditions. More interestingly, the prepared NH_2-CQDs can be used as fluorescent probes for detect formaldehyde in aqueous solution, the results showed that $(F_0\text{-}F)/F_0$ had a good linear relationship with formaldehyde at 0~8ug/mL. Selective experiments have demonstrated that a rigid fluorescent probe can be used for the targeted detection of formaldehyde. It can be seen that the method is low in cost, simple in operation, and exhibits high selectivity and accuracy to formaldehyde in the presence of various substances that may interfere, importantly, which can be used for the detection of formaldehyde in leather.

Keywords: NH_2-CQDs, formaldehyde, luminescence

P65

A Novel Non-pickling Combination Tanning for Wet-white Leather Based on Granofin Easy F-90 and Tannic acid

Yuanhang Xiao[1], Chunhua Wang [1], Wei Lin[2]

Department of Biomass and Leather Engineering,Collegeof Light Industry , Textile and Food Engineering, Sichuan University, Chengdu, China, 610065

Key Laboratory of Leather Chemistry and Engineering of Ministry of Education, Sichuan University, Chengdu,China, 610065

Abstract

Herein, a non-pickling combination tanning for the wet-white (chrome-free) leather has been investigated, which is based on Granofin Easy F-90 and Tannic acid. The shrinkage temperature (*T*s) of crust leathers and the uptake of tanning agents were tested to optimize the tanning technology. The results show that the two-bath combination tanning, 10% F-90 and 4% tannic acid at the final pH 3.0-3.5, can raise the shrinkage temperature (*T*s) of the wet-white leather to ~86 °C. Scanning electron microscopy (SEM) results reveal that the wet-white leather exhibits fine grain surface and dispersed collagen fiber networks. The manifested synergistic tanning mechanism of the two has been illustrated. Our results also show that the novel combination tanning approach not only improves lighter shade and light fastness, but also confers high physical and mechanical properties to the wet-white leather. And most importantly, the non-pickling organic combination tanning would be helpful to the development of the clean production technology for leather manufacture.

Keywords: wet-white leather, Granofin Easy F-90, tannic acid, non-pickling, combination tanning

P66

Preparation and properties of protein plastics based on waste collagen

Hailin Tang [1], Wei Lin[1], Chunhua Wang[1]

(1.National Engineering Laboratory for Clean Technology of Leather Manufacture, Sichuan University, Chengdu, Sichuan 610065, China)

Abstract：The collagen plastics were prepared by injection molding method, using glycerol or urea as the plasticizer and limed hide scraps as raw materials. The effects of plasticizer content and type on thermal stability and mechanical properties of the plastic were studied. The changes of collagen molecular structure and the processing temperature were discussed. The results show that the addition of glycerol or urea can reduce the decomposition temperature of the materials. The molding temperature of the collagen plastic with glycerol as the plasticizer is 84 ~ 219℃. The protein plastics are in high elastic state at room temperature after molding and the mechanical properties of the materials can meet the GB requirements of polyethylene for injection molding. The collagen plastics based on leather waste are prepared from blue wet powder with, glycerin as a plasticizer, and oxalic acid as complex bond breaking reagent by injection molding process. The effects of oxalic acid dosage on the thermal stability, rheological properties, mechanical properties and water resistance of the materials during the forming process were investigated. The results show that the addition of oxalic acid significantly improves the processing performance of the blue wet powder. The blue wet powder can be injection-molded when the amount of oxalic acid is more than 4.0 %, When the amount of oxalic acid is less than 5.0 %, the samples has high shrinkage rate. Oxalic acid also reduces the tensile strength, thermal stability, and water resistance of the material while improving processability.

Key words: Collagen plastics; injection molding; glycerin; oxalic acid;the powder of wet blue

P67

Preparation of Aminated Gelatin Nanoparticles Used to Stabilize Pickering Emulsion

Wanbo Xue(Sichuan University) China 1945551944@qq.com
Wei Lin(Sichuan University) China wlin@scu.edu.cn

Abstract： Fairly monodispersed aminated gelatin nanoparticles (AGNPs, PDI ≈ 0.068) have been synthesized from type B gelatin by a two-step desolvation method. The particle is positively charged (ζ ≈ 35 mV), with an average size of 240 nm. The effects of pH on the size and dispersity of AGNPs is investigated in the preparation process. It shows that the optimized reaction condition is pH = 4, which can endow the AGNPs with a smaller particle size (≈ 240 nm) and uniform distribution. The results from atomic force microscopy (AFM), scanning electron microscope (SEM) and transmission electron microscopy (TEM) showed that the AGNPs exhibited spherical

morphology with a narrow particle size distribution. And compared with gelatin nanoparticles (GNPs), the rigid structure and homogeneity of AGNPs is enhanced. Moreover, the higher three-phase contact angle of AGNPs (θ_{ow} = 67° ± 5°) than that of GNPs (θ_{ow} = 31° ± 6°), as evaluated by surface wettability analysis, indicates the increased surface hydrophobicity and capability for the stabilization of O/W Pickering emulsion. Pickering emulsion stabilized by AGNPs can store at 4 ℃ for 9 months without stratification, possessing good storage stability and potential application advantages.

Key words: aminated gelatin; AGNPs; rigid structure; three-phase contact angle; Pickering emulsion

P68

Modification of collagen with a natural cross-linked agent oxidized chondroitin sulfate A

Huilin Tian, Wei Kuang, Lihong Fu, Yujie Zhang, Donglei Liu

School of Leather Chemistry and Engineering ，Qilu University of Technology(Shandong Academy of Sciences), Jinan, Shandong 250353, China

Abstract

Nowadays a promising approach for the development of functional biomaterials is the combination of native extracellular matrix (ECM) components. Both collagen and chondroitin sulfate A (CSA) are the most widely used scaffold materials for tissue engineering because of their many advantages, including lack of antigenicity, abundant availability, bioresorbability and biocompatibility. However the simple system fabricated by single component of ECM might fail to meet the requirements of structure and functional complexity of the in vivo microenvironments.

In this study, aldehyde-based oxidized CSA (OCSA) was first obtained by the oxidation of CSA using sodium periodate and was applied as a natural crosslinker to modify collagen. Infrared (IR) spectroscopy and Ubbelohde viscometer were used to characterize OCSA. The structures and properties of OCSA modified collagen (Col/OCSA) materials were characterized with infrared spectroscopy, water absorption test, differential scanning thermal analyzer(DSC), scanning electron microscopy (SEM).

The results showed that as a result of oxidation, a small peak of 1739cm-1 representing the aldehyde groups appeared in the IR spectroscopy and the relative viscosity of OCSA decreased according to the viscometer method. After crosslinking with OCSA, the three helix structure of collagen retained, and the thermal stability and stability in water of collagen were improved too. Meanwhile the net structure of Col/OCSA materials was more closely than that of the pure collagen material. With the increase of OCSA dosage and oxidation degree, the water stability of modified Col/OCSA materials continues to increase, however the thermal stability increased slightly.

Keywords: collagen, oxidized chondroitin sulfate, modification, stability

P69

Study on adsorption of low concentration chromium (III) by porous organic polymer

Wei Kuang [*a], Lihong Fu[a], Huilin Tian[a], Donglei Liu[a], Lianxiang Feng[b], Qingquan Bai[b]

[a] *Qilu University of Technology (Shandong Academy of Sciences), Jinan 250353, PR China*

[b] *Qihe Leahou chemical industry CO., LTD, Dezhou 251100, PR China*

Abstract

It is difficult to remove Cr (Ⅲ) with the lower concentration from the solution, so the porous organic polymers（POPs）were used on the depth of low concentrationof Cr (Ⅲ) processing. The kinetic data has been tested in the process of adsorptionfor Cr(III), and proved that it follows the pseudo-second-order rate equation. Both Langmuir equations and Freundlich equations were used for explaining the experimental data of adsorption isotherm, which demonstrated a better fit to theFreundlich model. Moreover, the adsorption principle of Cr (Ⅲ) by POPs was alsodiscussed in the paper.

Key words: Trivalent chromiumion, Porous polymer, Chromium pollution, Water treatment, Adsorption

P70

Study on construction and properties of leather waterproof layer based on "lotus leaf effect"

Wei Kuang*[a], Xiaolong Li[b], Lihong Fu[a], Donglei Liu[a], Huilin Tian[a], Lianxiang Feng[c], Qingquan Bai[c]

[a] *Qilu University of Technology (Shandong Academy of Sciences), Jinan 250353, PR China*

[b] *China Leather and Footwear Industry Research Institute, Beijing 100016, PR China*

[c] *Shandong Leahou Light Industrial of New Material Co., Ltd, Jinan 250031, PR China*

Abstract

The waterproof layer of leather was constructed according the bionic principle of "lotus leaf effect". Specifically， Titanium dioxide (TiO2) nanoparticles were modified by fluorine groups by Atom Transfer Radical Polymerization (Atom Transfer Radical Polymerization, ATRP), which were finished on the leather surface to form a permanent waterproof layer. Static waterproof, water vapor permeability, surface contact Angle and coating wear resistance experiments were evaluated the performance of leather, the results show that the surface contact Angle of leather can be increased from 117.56 ° to 141.17 °, static waterproof effect can be kept for a long time. All other tested indexes are in line with the usage requirements of abrasive leather.

Key words: Lotus leaf effect, bionic, leather, coating, waterproof.

P71

Preparation and Properties of Polyacrylate Coating Material Modified by Carbon Nanotubes

Zi-Liang Li, Xin-Qiu Hong

College of Material and Textile Engineering, Jiaxing University (314001, Jiaxing, China, 0573-83643022, 305726789@qq.com)

As a new type of nanomaterials, carbon nanotubes had unique structure and properties, but their applications were seldom studied in leather industry.Polyacrylate emulsions modified by carbon nanotubes were prepared based on in-situ emulsion polymerization method. Polyacrylate emulsions were obtained by copolymerizing carbon nanotubes with acrylic acid, methyl acrylate and ethyl acrylate. The film forming and application properties of the emulsion were investigated. The results show that polyacrylate emulsion film-forming performance was the best, when the usage of carbon nanotubes was 0.09% of the quality of acrylic monomers, reaction temperature was 85℃ and reaction time was 2 h. The tensile strength of the thin film reached 22.1MPa。

Keywords: carbon nanotubes; modification; polyurethane; coating

P72

The Discussion on Design and Market Analysis of Affordable Luxury Leather Brands

YAO Yunhe[1,2,3*] ,LIU Mengyuan[3] ,Ding Wanjing[3] ,Xie Ling[3]

(1.Key Laboratory of Leather Chemistry and Engineering of Ministry of Education, Sichuan University,Chengdu,610065,China;2.National Engineering Laboratory for Clean Technology of Leather Manufacture, Sichuan University,Chengdu,610065,China;3.Biomass and Leather Engineering Department, Sichuan University,Chengdu,610065,China)

Abstract: With the development of economy and the improvement of people's livelihood, the current market of affordable luxury can't meet the diversified demand of consumers for goods, which results in the market decline. Therefore, it is imperative for affordable luxury to remodel their image and strike for innovation in product design. At present, the economy in China has a good momentum for growth, and the rapid growth of the middle class is providing a vast consumer market and space for development of affordable luxury. Taking affordable luxury as the focus of research, the research data, market information and key cases were integrated. Furthermore, relative parameters like the brand development, product positioning, product design and other related factors were summarized. Based on the market positioning and design orientation of the affordable luxury, combining with the current social, economic prospects and consumer trends, the purpose of study was conducting the SWOT analysis about the development of affordable luxury in the Chinese market, and putting up some developing advice of the brand positioning, product planning, design orientation and other aspects.

Keywords: Leather goods; Affordable luxury; Design; Marketing; Position

1Developments of affordable luxury leather brands

"Affordable luxury" is an attitude to pursue high quality life, while affordable luxury product is a position of fashion and consumption view generated by conforming to this life attitude. Affordable luxury leather products have similar design elements and quality with luxury product [1]. However, the brand of affordable luxury leather products does not pursue forward-looking design, but attach great importance to cost performance. Of course, the biggest difference lies in the price. Affordable luxury leather goods are not as expensive as luxury goods, and their price is generally around 2000-10000 yuan, which can be consumed by ordinary small-capital people. Most of the products which are located in the price range can be called light luxury products.

The different birthplace of the brand also creates different cultural and design characteristics. European countries have a long history, and the high demand of the royal led to the development of the design industry, so the concept of brand was formed earlier. Most European brands have a long history, such as Furla, LONGCHAMP, Lancel, and the shorter, like Pinko and MOSCHINO (fig.1). LONGCHAMP and Lancel are French brands which have a long history and whose design are famous for classic and practical, while MOSCHINO is an Italian brand and its design is famous for humorous and weird. In 2005, MCM (Mode Creation Munich), an affordable luxury leather brand originated in Germany, was acquired by a south Korean. However, the brand persists in the use of pure manual production and traditional printing whose design and production always maintain the German's consistent rigorous. SOPHIE HULME and Mulberry are British brands which have been popular in recent years.

The United States is home to the majority of the world's population, and its history is shorter than that of other countries. Besides, there is no royal and noble tradition that has been carrying on in Europe, so there is no "luxury" concept in the traditional sense [2]. As a result, there are many affordable luxury leather brands born here, such as Kate Spade, Marc Jacobs, and 3.1Phillip Lim. In addition to COACH, other designer brands such as MICHAEL KORS, Marc Jacobs, Tory Burch, 3.1Phillip Lim, Kate spade and Rebecca Minkoff are among the newer brands brands.

Fig. 1 The motorcycle bags of "MOSCHINO"

Compared with Europe and the United States, the affordable luxury leather industry in Asia is not developed enough. Although the clothing design in Japan is at the leading level in Asia, there are few affordable luxury leather brands, including the Samantha Thavasa. Charles&Keith is an affordable luxury leather brand in Singapore. Its price is lower than that of ordinary affordable luxury leather products. However, the refresh rate of Charles&Keith is extremely fast. The Chinese affordable luxury leather brands include DISSONA and the YU·JIANG of Hongu.

China is a huge consumer market of affordable luxury goods, and the number of Chinese middle class has increased significantly. Since the affordable luxury entered China, many consumers of affordable luxury leather products have been born in China, which provides a good development for affordable luxury leather brands. However, there are few affordable luxury brands in China, and most of them are in their infancy. Therefore, the development of domestic affordable luxury brands still has a great developing space and potential.

2Research and analysis on the consumer group of affordable luxury leather products

2.1 Comparison between affordable luxury leather brands and other levels of leather brands

Currently, leather brands include luxury brands, affordable luxury brands, ordinary commodities, and fast fashion brands, street fashion brands and so on. In the case of luxury leather brands, most of them have deep historical roots, such as Hermes, Chanel, Dior. Luxury brands like Jimmy Choo which is only 20 years old are rare. Most consumers of luxury products are wealthy people. Such consumers have complex and diversified requirements for brands. When choosing products, they pay more attention to the overall image of the brand and even consider whether the brand conforms to their social status. According to the survey, some young consumers of affordable luxury goods do not pay much attention to whether the product can highlight their social status, but to the product itself. Consumers of all ages have different demands and focuses on ordinary commodities. For example, young consumers attach great importance to appearance, while middle-aged consumers think that the practicality is more important than appearance. Therefore, in order to meet different consumer groups, the design features and styles of ordinary commodities are more diversified and its positioning is more extensive.

From the perspective of design, the design of luxury products is often original and forward-looking. For example, the classic bag of Chanel2.55, which releases women's hands and makes single-shoulder bag popular, or the "new look" collection of Dior, which brought women a new look and rebuilt women's beauty. There is no doubt that luxury is at the top of fashion. Compared with luxury goods, affordable luxury leather goods update quickly, but they are not as refined as luxury goods in design and production. Fashion trend is formed from the top of high order to thel public clothing, so it is a gradual diffusion process. The forward-looking of luxury brands makes its fashion one step ahead, because in the spring they prepare for the fall clothes, and then other levels of brands can follow the fashion trend. That is also the spread of fashion from the wealthy to the general public. However, there will be a similar design element and style which may lead to the lack of original design,

so it is difficult for ordinary brands to form a unique brand culture. Fast fashion brands have a high degree of fashion, and their products are updated very fast. Compared with the product quality, they pay more attention to the avant-garde nature of design. Therefore, for most consumers, they consider the fashion and beauty of the products more when buying fast fashion products. Street fashion brand is a brand for designers to show their thoughts and attitudes, and its design is highly personalized. Therefore, these brands' consumers are almost only young people, so it leads to the consumers of street fashion brands being less than ordinary clothing brands.

2.2 Analysis of consumers' behavior and psychological

To improve the accuracy of the results, author combined the field research and analysis. The survey was conducted in March 2018 at the IFS shopping center on Chunxi road, Chengdu. As the top high-end shopping center in Chengdu, IFS gathers a large number of luxury brands and affordable luxury brands, and has a large passenger flow, which can provide abundant data. The research content mainly includes: comparison of passenger flow per weekday and weekend, average shopping time of consumers, and consumers' purchase rate, etc.

The research took place around 3-5 PM and lasted four days, avoiding holidays. The data recorded in table 1 is the number of people entering the store per unit time, from which it can be seen that the passenger flow in weekday of affordable luxury leather brands is significantly lower than that on weekend, with an average reduction of about 30% per half hour. Therefore, the number of consumers will be affected by the date. Second, there is a significant difference in traffic between brands. Based on previous research about the consumption of affordable luxury goods in Chongqing [3], it can be concluded that as one of the most successful affordable luxury leather brands in the Chinese market, COACH has a high awareness among young and middle-aged consumers, while the designer brand MOSCHINO only has a high awareness among young consumers. During the working day, most of the young consumers are at work, which results in a big impact on the customer flow of MOSCHINO. COACH, which is better known and has a wider consumer base, is less affected.

Table 1 The customers' flow of some affordable luxury brands in the same time

	COACH	Marc Jacobs	Tory Burch	LONGCHAMP	MOSCHINO
weekday（per/30mins）	20	19	12	7	11
weekend（per/30mins）	22	26	15	16	24

According to observation, the average consumers' shopping time is about 10 minutes. 50% of consumers will try on product, and 60% of consumers will seek help, but the purchase rate is low. The purchase flow rate for half an hour is less than 10%. In the research of five affordable luxury leather brands, Tory Burch is the brand with the highest purchase rate, reaching 20%. Thus it can be seen that consumers have been carefully selected in shopping with less impulsive consumption. Besides, in the center of IFS shopping center, COACH is adjacent to Marc Jacobs and LONGCHAMP is adjacent to MOSCHINO. These brands are in different styles, so it makes the observation about the flow rate of consumers between different styles of stores during the research easier. For example, the consumers entering COACH's store and LONGCHAMP's store were rarely entering Marc Jacobs's store or MOCHINO's store, even though they are close to each other. There are also a few consumers who are unfamiliar with the brands and they will come back to the store after passing by several times. At this time, the store image becomes the main attraction for consumers. The above situation shows that consumers mainly buy products according to their own preferences and actual needs, not just for the affordable luxury.

In order to cope with the decrease of passenger flow in weekday, the brands can increase promotion efforts and improve the awareness of consumers, such as increasing the advertising coverage of office buildings or using new media for targeted promotion, as well as adding new products lines to attract more consumer groups. Consumers select carefully based on their own preferences, and impulsive consumption rarely occurs, which proves that rational consumption type occupies the market of affordable luxury consumption. It can be found from the high purchase rate of Tory Burch that consumers are

more inclined to buy fashion clothes with leisure style and applicable to more occasions. Moreover, the brand has a relatively fixed consumer group, and their loyalty is relatively high, which is especially important for brand development. Therefore, when determining the brand positioning, it should not only consider the current consumption demand, but also have a certain difference with the existing brands in the market, especially the strong brands.

3 Design and analysis of affordable luxury leather products

3.1Trend --the trend of rejuvenation and stylization is gradually prominent

Affordable luxury leather products have high cost performances, and this is one of the main reasons for attracting consumers. The leading luxury brands in the beginning started to make products younger, especially women's products. With the changes in the market, the affordable luxury brands of the larger groups such as COACH and MICHAEL KORS are going rebrand and product innovation, so their designs are more creative and unique than before, and the attraction of the products to the young consumers has been significantly improved.

At present, nearly half of the affordable luxury brands on the market are designer brands with short histories, so the products of such brands are full of designers' personal characteristics. Other non-designer brands are more diversified because of the change of design team and different design teams are responsible for different product lines.Therefore, the trend of product stylization is more significant

3.2 Patterns - classics go hand in hand with innovation

Generally speaking, there are two design elements of a brand, and one is a classic one and the other is a new fashion element that changes every quarter. Classic elements can be the design features of the brand, as well as reflecting the brand design style. The Double C of COACH, logo print of MICHAEL KORS, spades of Kate Spade, double T of Tory Burch and daisy of Marc Jacobs (fig. 2) are typical design elements. This type of design elements is relatively simple, and most of them are extended from the logo of the brand. They are highly recognizable, and have strong adaptability and collocation of patterns. Some design elements help to build brand style and image while strengthening consumers' brand memory. But on the choice of other fashionable element, brands do not need to consider the timelines of element overmuch, and they just need to think how to accord with fashionable trend.

3.3 Accessories -- typical application of accessories and explorations of new elements

Accessories as the punch line, they play an important role in the design of shoes and bags. Not only they can influence the design style of products, but also serve as the representative elements of brands. Taking SOPHIE HULME as an example, the metal sheet on the bag surface and the metal sheet hanging with different shapes becomes the unique design elements of the brand. The fasteners of Pinko “swallow bag” (fig.3) are similar to Gucci's Dionysus bags, so they have been named “Small Dionysus bag”, attracting many consumers. “Swallow” fastener is the classic design of Pinko, and due to the popularity of “swallow bag”. Pinko also launched a variety of design elements of "swallow bag". It can be seen that, accessories as a part of the product, have an important influence on the overall style. Once a certain style becomes the classic of the brand, then the brand can extend all kinds of styles around it and attract consumers as much as possible.

3.4 Color -- highly recognisable colors coexist with diversified color designs

Today's consumer market tends to be younger, which makes the color design of products to be more diversified and innovative. The colors’ change is no longer limited to the “three color principle”. The brands often use colors that are more recognizable. For example, COACH's products always use brown, red, yellow and other heavy colors to show the warm tone, while MCM uses claybank mainly.

The colors of classic products are the brand commonly used color, and new products use popular color in the majority. Zou ziye et al. [4] analyzed the bags in the current market, and found that the bags are more colorful, and the collision of various color materials brings freshness to the products. Every year, the professional fashion institute will predict the color of the coming season, which can be fully reflected in the forward-looking luxury brand show. For example, the popular colors of

2018 include "Meadowlark", "Cherry Tomato" and "Little Boy Blue". Accordingly, each brand according to popular color rolls out the classic products with the same style but different colors which already became a way of design

In addition to the colors provided by artificial dyeing, gorgeous animal grain is also an important source of color. The combination of the snake skin and the rubber makes the design of “jelly bag” more layered, and makes the colorful snake skin more slightly (fig.4). The natural patterns make the products’ appearance more unique, such as leopard grain, snakeskin grain, tiger grain and zebra grain.

3.5 The differentiation strategy of products -- the innovation and application of materials and the characteristic of excellent technology

In addition to the above elements, product design elements also include process, material and so on. The selection of materials is also one of the key points of design. Leather is the most commonly used material for bags. The use of some creative materials will make consumers feel refreshing. LONGCHAMP’s bags use the nylon material to make bags light and high folding endurance. The "jelly pack" is made of natural rubber, which has no stitching problems and is more resistant to abrasion.

The craft can not only enhance the artistic value of the product, but also show the individuality of the product as a design highlight. However, the affordable luxury brands focus on sales volume, which means that products will be mass produced. So the affordable luxury leather brands that pursue high sales generally use less complicated technology. Among the affordable luxury leather brands, MCM is one of the few brands that stick to pure handmade production. Chinese brand YU·JIANG not only uses full manual production, but also adds complex leather carving technology in the design, and the brand takes this as the characteristic to promote the product value. In addition to leather carving, weaving hollowing and other processes can also give products unique charm. Currently, there are few brands that use complex craftsmanship as the design highlight of affordable luxury leather products. However, in order to reflect the brand features, certain craftsmanship will be adopted to make the brand more consistent and recognizable.

Fig. 2 The swallow bags of “Pinko”

Fig. 3 The splicing jelly bag of "Furla"

Fig. 4 The signature series of "COACH"[33]

4 SWOT analysis and discussion of development strategies of affordable luxury leather brands

SWOT analysis of affordable luxury leather brand in the face of current and future situation

The current market of affordable luxury leather products has experienced a bottleneck period after rapid development, and the changes of social demand and consumption market have brought challenges to the brand development. The current affordable luxury leather brands have a huge consumer market, but they are also facing the impact of emerging patterns such as fast fashion. In the future when people's material life is increasingly rich, they will be strict with products. According to the experts' analysis, it is still a good time for domestic leather industry to develop before 2020 or longer [5]. Therefore, SWOT analysis of the brands can help clarify the current and future situation and provide certain reference for the brand development.

SWOT analysis is to enumerate the main internal strengths, weaknesses, opportunities and threats that are closely related to the research object, and then analyzing them to draw a series of corresponding conclusions. By using this method, the situation of the research object can be comprehensively and accurately understood, so as to formulate the development and countermeasures of the brands under the current situation according to the research results.

Strength

(1)The high cost-performance ratio of affordable luxury leather goods accords with the rational consumption psychology of consumers.

(2)The affordable luxury positioning of affordable luxury leather goods brand satisfies some consumers' flaunting

psychology.

(3)The current brand positioning of affordable luxury leather goods is accurate, meticulous, and rarely occurs the same positioning, so the competitive pressure between brands is relatively small.

(4)There are more affordable luxury leather goods brands and different brand styles in the market at present, which is very attractive to the young consumers who pursue the individuation and high quality life, but the economic strength is not strong.

At present, there are many affordable luxury leather goods brands in the market with different brand styles, which has great attraction for young consumers who pursue individualization and high-quality life, but are not rich in economic strength.

Weakness

(1)The style of some affordable luxury leather brands is unique but simple, so it is difficult to make a breakthrough in the diversification of consumer groups.

(2)The larger affordable luxury leather group is too much in the pursuit of sales volume, so the quality of product process design cannot be well balanced with the yield.

(3)Take COACH and MICHAEL KORS for example, affordable luxury leather brands have experienced a surge in sales in the past few years, and the overall profit has been weak. Consumer aesthetic fatigue is one of the main reasons for this situation.

(4)Some affordable luxury leather brands can't meet the changing consumer demand.

4.1.3 Opportunity

(1)The rapid development of electronic commerce has greatly expanded the sales channels of products. Nevertheless, factors such as the image of luxury brands and the nature of their products are not suitable for e-commerce sales, which makes e-commerce become an important sales platform for affordable luxury leather brands.

(2) With the rapid development of domestic economy, people's living standards have been improved, and more consumers are pursuing a better quality of life, the current affordable luxury market has great room for development.

(3)China has a large mass of affordable luxury consumers, but currently there are few local affordable luxury leather brands, which can't fully meet the needs of domestic consumers. Therefore, it is the right time for affordable luxury brands to enter the Chinese market and step up efforts to develop the Chinese market.

(4)The luxury market continues to be depressed, which may create opportunities for the development of affordable luxury leather brands to some extent.

(5)Under the trend of globalization, it is easier for foreign affordable luxury leather brands to enter the Chinese market, and consumers can easily understand and purchase affordable luxury leather goods from various countries.

4.1.4 Threat

(1)The continuous growth of national economy enables more and more consumers to make it possible to purchase luxury goods, which may lead to the loss of some consumers of affordable luxury goods.

(2)The rapid development of emerging industries such as fast fashion may have an impact on the affordable luxury leather industry.

(3)Prices of products of affordable luxury brands vary because of national tax rates and other factors, leading most consumers to choose the country of origin as a way of purchasing, which provides a way for the sales of fake products and makes fake products more rampant.

(4) The large influx of foreign affordable luxury leather brands into the domestic market may, to a certain extent, reduce the living space of existing domestic affordable luxury leather brands, and in front of foreign affordable luxury leather brands with relatively perfect development, How to occupy a place has become the domestic brand faces the difficult problem.

Through the SWOT analysis of the affordable luxury leather brands, we can see that the strengths of the brand outweigh the

weaknesses and the opportunities coexist with the crisis. Therefore, the current situation for affordable luxury leather brands, there are stable and upward development prospects, but also need brands to improve weaknesses, expand strengths, seize the existing opportunities, efforts to overcome the crisis under the current situation. In the process of development, the affordable luxury leather brands should pay attention to the present and make positive responses to the development of the future situation.

In the future, in the case of the overall economic level of the consumer market, some of the affordable luxury leather goods consumer group may transfer to the luxurious consumption, but also have the consumer groups of ordinary goods transfer to the affordable luxury consumption, so the affordable luxury consumer group base in the future, in the consumer market overall economic level promotion. Some affordable luxury leather goods consumer group may transfer to the luxurious consumption, but also has the ordinary commodity consumer group to the affordable luxury consumption transfer, therefore the affordable luxury consumer group base will not have the obvious decline the change. In addition, consumers on product design and personalized product needs will be gradually increased with the social development, for the brand, the face of the future trend of change is a gradual process, so the current should start to launch targeted layout and strategic research, to the greatest possible to avoid future crises may occur. There will be no significant decline in the number of changes. In addition, consumers on product design and personalized product needs will be gradually increased with the social development. For the brand, the face of the future trend of change is a gradual process, so the current should start to launch targeted layout and strategic research, to the greatest possible to avoid future crises may occur.

Strategies to address social needs and future development

First of all, the affordable luxury leather brands should pay attention to product and consumer group positioning, on the basis of clear brand positioning for follow-up development. The brand positioning of affordable luxury leather products should be more accurate and have differentiated characteristics, and try to be different from other brands to avoid positive conflict. In order to expand the consumer group, brand positioning can be more flexible. For example, a large positioning direction should be determined first, which is the trunk of the tree. Then, various precise positioning should be made under the big positioning, which is the branches of the tree. Such brand positioning will be more abundant, but also to maximize the benefits of the brand, while as much as possible to attract consumers.

Second, in the design and manufacture, the affordable luxury leather brands can solidify the use of a certain process, which can not only improve the production level of products, but also show the brand personality. Innovative design is an effective strategy for consumers' aesthetic fatigue. The affordable luxury leather brands can seek a breakthrough in design elements, materials, colors and so on, and provide consumers with a new sense of design. Overall, consumer demand has changed from simply satisfying vanity to humanistic concern. In order to meet this transformation, the affordable luxury leather brands should first start from the product itself, make the product design younger and more personalized, and at the same time endow the product with unique brand culture connotation, and promote the brand image remodeling through design innovation.

In addition, the improvement of people's economic strength will inevitably lead to the transfer of some consumer groups of affordable luxury leather goods to luxury goods. The affordable luxury leather brands can expand its product line similar to luxury goods, which can not only reduce the transfer of consumer groups, but also improve the brand image. For example, COACH has launched a high-end product line, “COACH1941”, whose price is close to that of luxury products. The high level of production technology and design has attracted many luxury consumers. Although fast fashion products are fashionable, their service life is short due to their low quality and rapid update speed. Therefore, in the face of the impact brought by the fast fashion industry, the affordable luxury leather brands need to stand out its own advantages, such as personalized design, high quality of products and long service life.

Finally, although foreign brands of affordable luxury leather have been relatively mature, domestic brands of affordable

luxury leather still have certain competitiveness. Attracted by western art and design, most young Chinese designers have gone abroad for further study, which makes them fully feel the cultural differences between the east and the west. Therefore, the traditional Chinese art can be taken as the cultural connotation and inspiration source of the brand, combined with the modern design concept of the west, and pursue the integration of things in design, so as to create an international light luxury brand with Chinese characteristics.

5 Conclusions

The rejuvenation of the consumer market for affordable luxury leather goods and the shift in consumer demand has brought new problems to the development of various brands. In this context, the affordable luxury leather brands need to adjust the strategy and appropriate changes. The current and future social situation has created a good development opportunity for the affordable luxury leather brands. Therefore, these brands will usher with more favorable policies and a better market environment, if they can face the difficulties and solve the problems.

Reference:

[1] Zhong Yi. Fast Moving Consumer Goods Are in Cold and Affordable Luxury Counterattack [J]. CHINA APPAREL, 2013(12): 14-15

[2] Ye Qizheng. Why Did Americans Create “Affordable Luxury” Brands [J]. Public Relations World, 2017(5): 114-115

[3] Liu Mengyuan, Yao Yunhe. Investigation and Analysis on the Consumption Demand of Entry Luxury in Chongqing [J]. Leather Science and Engineering, 2018, 28(01): 67-70, 75

[4] Zou Ziye, Li Xuemei. A New Focus of Contemporary Luggage Design: Analysis and Research of Fabric Patterns [J]. DESIGN, 2016(1): 126-127

[5]Jiang Wenjia, He Jianfeng, Xu Weixin,*et al*. Establishing Brand to Expand Luggage Making Industry [J]. Leather Science and Engineering, 2011, 21(01): 72-75

P73

Preparation of Cationic Polysiloxane Hybrid Emulsion and its Use as Superhydrophobic Leather Finishing Agent

Wei Xu[1*], Jiaojiao Yang[2], Lifen Hao[2], Xuechuan Wang[1**]

(1 College of Bioresources Chemical and Materials Engineering, Shaanxi University of Science and Technology, Xi'an Shaanxi, 710021, China; 2 College of Chemistry and Chemical Engineering, Shaanxi University of Science and Technology, Xi'an Shaanxi, 710021, China)

Abstract

Under the catalyst of tetramethylammonium hydroxide (THMA), the present work performed the anionic ring-opening polymerization of octamethylcyclotetrasiloxane (D_4), 2, 4, 6, 8-tetramethyl-2, 4, 6, 8-tetravinylcyclotetrasiloxane (D_4^{Vi}), and methyltriethoxysilane (MTES) to prepare hydroxyls-terminated polyvinylmethylsiloxane intermediate, which was then reacted with polymethylhydrosiloxane (PHMS) via hydrosilylation to produce the hydrophobic cross-linked polysiloxane (JPDMS). Afterwards, a cationic polysiloxane hybrid emulsion was prepared via reaction of polyaminopropylmethylsilsesquioxane (PAMSQ) and JPDMS and AEO3/AEO9 used as composite emulsifiers. The effects of the PAMSQ particle size and the amount of PAMSQ-JPDMS emulsion on performance properties of the PAMSQ-JPDMS/Lea were investigated. Chemical composition and microstructure of the leather surface were studied by XPS and FESEM, respectively. FT-IR confirmed structures of the resultants. Results showed that PAMSQ-JPDMS/Lea had the best hydrophobicity, and water static contact angle was 163.8° when average particle size of PAMSQ was 128.7 nm, its content was 15% and solid content of the PAMSQ-JPDMS emulsion was 1.2%. Moreover, water vapor transmittance rate could still attain 3074.01 g/(m^2·day). FESEM observation confirmed that construction of superhydrophobic leather surface was mainly rooted from a layer of dense silicon film and many lotus-like nano protuberances. The above results indicate that this as-synthesized PAMSQ-JPDMS emulsion is a promising candidate for superhydrophobic leather finishing agent.

Keywords: Polysilsesquioxane; Hybrid nanocomposite;Superhydrophobic leather

Corresponding author: Wei Xu, xuwei@sust.edu.cn; Xuechuan Wang, Email: wangxc@sust.edu.cn

1 Introduction

Currently, with the ever-increasing development of economy and growth in the living standard, higher requirements have been put forward by the customers on the quality and performance properties of leather products, such as fasion style, necessarily hydrophobic, antifouling, health breathable and durable properties [1]. Therefore, there has been becoming a new research trend to prepare a kind of leather superhydrophobic material with high performance and environmental features. To dates, there have been some documents concerning the superhydrophobic materials for leather which include long-chain fatty acids and their derivatives, waterproof fatliquoring agents, acrylic retanning and water repellent, organo-silicone and fluorine-containing waterproof agents, etc [2-6]. Qing *et al* used ring-opening polymerization at the low temperature to synthesize a sort of amino-polysiloxane and its emulsions; finally, the treated leather had good softness and hydrophobicity [7]. Luo *et al* prepared a kind of fluoropolymer emulsion as the leather waterproof fatliquoring agent [8]. The processed leather owned the excellently soft, durable and hydrophobic properties; moreover, waterproof property of the leather was improved with the increase of fluorine content in the fatliquoring agent. Novel carboxyl and dodecyl modified polysiloxane (RCAS) was synthesized by Xu *et al* [2] and then was emulsified to treat the wet-blue goat. The treated crust leather by 1.92% RCAS active ingredients based on the weight of wet-blue goat had favorable hydrophobicity and water contact angle on its grain side attained 126°.

Polysilsesquioxane (PSQ) nanoparticles are a sort of new inorganic-organic hybrid materials with easily chemically-modified and functionalized surface and interior, which provides convenience for the construction of superhydrophobic leather surface with high performance properties. For this reason, a hydroxyl-terminated cross-linked polysiloxane (JPDMS) with high hydrophobicity was first prepared in this study and next reacted with

polyaminopropylmethylsilsesquioxane (PAMSQ) nanoparticles to acquire the PAMSQ-JPDMS latex. At last, bionic superhydrophobic leather was fabricated via spraying of the PAMSQ-JPDMS latex onto the surface. Properties of the resultant leather such as superhydrophobicity, sanitation and dry rubbing fastness were researched in detail.

2 Experimental

2.1 Reagents

Octamethylcyclotetrasiloxane (D_4), tetramethyltetraethylene cyclosiloxane (D_4^{Vi}), and methyltriethoxysilane (MTES), all industrial grades, were purchased from Tangshan Sanyou Chemical Co., Ltd, Hubei Debang Chemical New Material Co., Ltd, Beijing Huawei Ruike Chemical Co., Ltd, respectively. PHMS was synthesized in our lab with a Si-H content of 0.08% (expressed by the moles of Si-H groups contained in 1 grams silicone) and viscosity of 138 mPa • s. Tetramethylammonium hydroxide, chemical purity, was supplied by Nanjing Zhonghao Chemical Co., Ltd. Polyaminopropylmethylsilsesquioxane (PAMSQ) nanoparticles were prepared by our lab and its structure and synthetic method can be referred to the literature [9]. The cow nubuck leather was kindly provided by Zibo Polygrace Group, China. Isopropanol, fatty alcohol-polyoxyethylene ethers (AEO-3 and AEO-9), all A.R., were from Xi'an Chemicals, all in China.

2.2 Preparation of crosslinked polysiloxane (JPDMS) with hydrophobicity

In a 250 *ml* three-necked flask equipped with a mechanical stirrer, a reflux condenser and a thermometer, appropriate amount of D_4, D_4^{Vi}, and MTES were added, gently stirred and then bubbled by N_2 for 10 minutes. When the mixture was heated to 90 °C, a catalytic amount of tetramethylammonium hydroxide (Me_4NOH) was slowly dropped and the reaction was kept for 30 min. Then, the temperature was elevated to 110 °C and the mixture was kept at this temperature for an additional 6 h. At the end of the reaction, low-boiling residues were removed by vacuum distillation. Finally, a flavescent and viscous fluid, the hydroxyls-terminated polyvinylmethylsiloxane, was obtained.

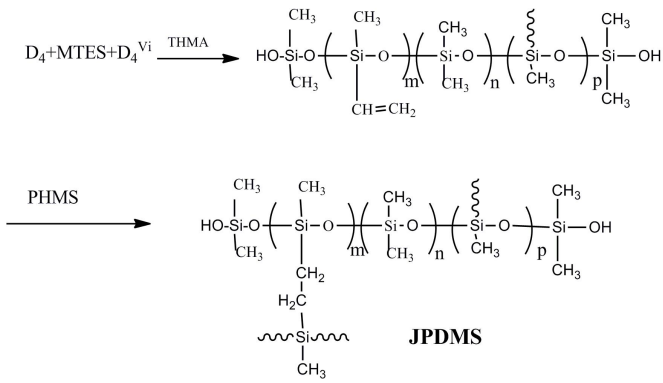

Fig.1 Synthesis procedure of the JPDMS

The above-mentioned reaction system was cooled down to 80-85 °C, PHMS with low viscosity and isopropyl alcohols were added into the mixtures. A catalytic amount of H_2PtCl_6 was dropped. Then, the mixture was maintained at this temperature for an additional 3-4 h. At the end of the reaction, low-boiling residues were removed by vacuum distillation. Finally, a clear and viscous fluid, the crosslinked polysiloxane noted as JPDMS, was acquired. The synthetic route can be seen in Fig.1.

2.3 Preparation of the PAMSQ-JPDMS composite emulsion

An established amount of JPDMS, PAMSQ and AEO-3/AEO-9 mixed emulsifiers were poured into a 250 *ml* three-necked flask at ambient temperature and mixed uniformly. Then, a certain amount of de-ionized water was slowly added into the flask under magnetic stirring. At last, the pH value in system was adjusted to about 6 and the PAMSQ-PJDMS composite emulsion with milk white was obtained. A series of composite emulsions were prepared via adjustment of doses of the combined PAMSQ and its particle sizes so as to investigate their effects on performance properties of the resultant leather. The structure representation of the PAMSQ-JPDMS can be seen in Fig.2.

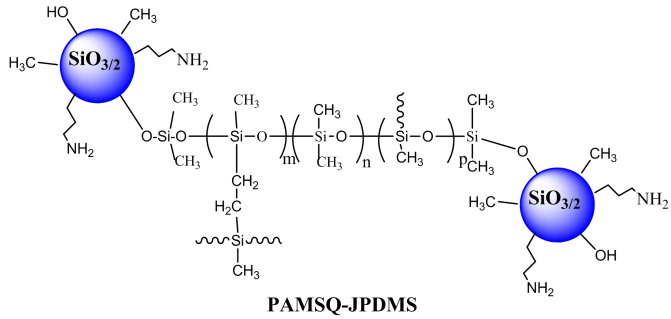

PAMSQ-JPDMS

Fig.2 Structural representation of the PAMSQ-JPDMS

2.4 The treatment process of spraying onto the leather surface

According to the reference [10], the leather surface was cleaned up using the tidy gauze soaked with the cleaning solutions of ammonium hydroxide, absolute ethyl alcohol and water (their volume ratios were 5:10:85) to remove the dirt. Then, the PAMSQ-JPDMS emulsion was diluted to different solid contents, such as 0.3%, 0.6%, 0.9%, 1.2% and 1.5% and next was crosswise sprayed twice onto the leather surface. Afterwards, the treated leather samples were dried at 80 °C to finally acquire the superhydrophobic leather coatings (noted as PAMSQ-JPDMS/Lea). The different superhydrophobic leather coatings treated with JPDMS and different PAMSQ contents were denoted as JPDMS, PAMSQ-JPDMS-1, PAMSQ-JPDMS-2, PAMSQ-JPDMS-3, and PAMSQ-JPDMS-4, other diverse ones treated with different solid contents of PAMSQ-JPDMS were signed as 1#, 2#, 3#, 4#, and 5#, respectively.

2.5 Characterization

FT-IR spectra of samples were recorded between 4000 cm^{-1} and 400 cm^{-1} on a Bruker VECTOR-22 spectrophotometer using KBr pellet technique.

The water contact angles (CA) on crust leather surface were measured using an optical contact angle goniometer (DSA100, KRUSS) and the average of five readings was used as the final contact angle of each sample.

Water vapor transmittance rates of various samples were determined by W3/060 water vapor transmittance tester where the diameter of the testing sample was 74 mm, the testing area was 33 cm^2, the testing temperature was 38 °C and the testing humidity was 85%.

Rub resistance of the superhydrophobic coatings was tested by GT7034 leather rubbing colour fastness tester under 25 cycles of dry rub where the results could be given based on changes of water contact angles on leather surfaces.

The surface morphology of the leather surface treated by PAMSQ-JPDMS were observed by S4800 Hitachi FESEM after the leather samples were coated with gold in vacuum.

3 Results and Discussion

3.1 Structure characterization

FTIR spectra of (1) PAMSQ, (2) JPDMS and (3) PAMSQ-JPDMS were analyzed and are shown in Fig. 3. Obviously, the weak peak at 1594 cm^{-1} in Fig. 3(1) was derived from the N-Hbending vibration of the $–NH_2$ group, which denotes that amido groups are located at the surface of PAMSQ. Furthermore, there were still typical adsorption bands appearing separately at 2971-2886 cm^{-1}, 1413 cm^{-1}, 1277 cm^{-1}, 1129-1027 cm^{-1}, 775 cm^{-1}, which indicates that functional groups such as methylenes, $-Si-CH_2-$, Si-O-Si groups have existed in the PAMSQ molecule. In particular, there was no characteristic absorption peak of Si-OH larger than 3000 cm^{-1}, which further testify that the hydrolytic and condensation reactions proceeded well between $Si-OC_2H_5$ groups. Fig. 3(2) is the spectrum of the JPDMS where those spectra were displayed at 2966 cm^{-1}, 1408 cm^{-1}, and 997-870 cm^{-1}, which should come from the characteristic absorption peaks of the $–CH_3$, $-CH_2-$, and overlapping Si-O-Si and C-O-C bonds, respectively. However, there was no characteristic absorption peaks of C=CH- bonds at 3100-3000 cm^{-1} and 1650 cm^{-1}, which denotes that the hydrosilylation reactions have completely finished. IR

spectrum of PAMSQ-JPDMS is shown in Fig. 3(3). By comparison with the JPDMS, the absorption peaks at 2964 cm^{-1} and 2907 cm^{-1} were clearly intensified due to the combination of PAMSQ. In addition, there was new absorption peak at 1594 cm^{-1} assigned to the bending vibration absorption peak of N-H. Furthermore, double-shoulders peak at 1130-1032 cm^{-1} was broadened and the bending vibration peak at 1261 cm^{-1} of C-H bond from Si-CH_3 was strengthened. In a word, we have successfully prepared the anticipative product.

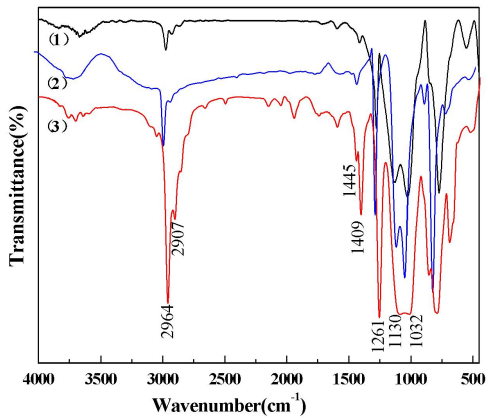

Fig.3 FTIR spectra of (1)PAMSQ，(2) JPDMS 和(3)PAMSQ-JPDMS

3.2 Influencing factors of hydrophobicity of the PAMSQ-JPDMS treated leather

(1) Effect of particle size of the PAMSQ

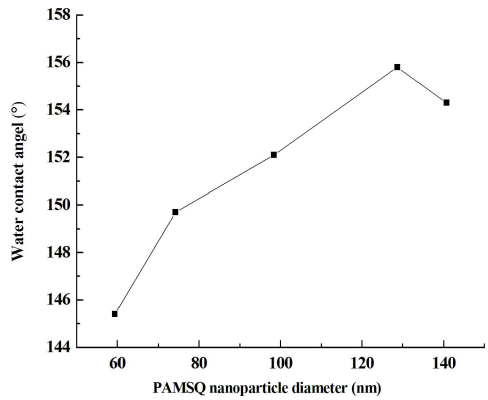

Fig.4 Effect of size of PAMSQ nanoparticle on WCA of PAMSQ-JPDMS/Lea

Microscopic rough structure of one solid surface plays an important role in fabrication of superhydrophobic surface and in our system particle size of the PAMSQ nanoparticles will directly influence the microscopic nano-scaled roughness of the treated leather surface [12]. Therefore, effect of average particle size of the PAMSQ nanospheres was investigated on hydrophobicity of the PAMSQ-JPDMS/Lea while the other terms were fixed and the result is shown in Fig. 4. It can be seen from Fig. 4 that WCA on the treated leather surface continuously increased until average particle size of the PAMSQ nanospheres was increased to 128.7 nm with the smallest PDI. By this time, the biggest WCA attained 155.8 ° and it would slightly decrease while average particle size of the PAMSQ nanospheres was further fortified. Thus, proper choice of the PAMSQ nanospheres with optimal sizes is a key factor to successfully fabricate suerphydrophobic leather surface.

Thus, average particle size of the PAMSQ nanospheres is optimized as 128.7 nm.

(2) Effect of the PAMSQ content

Table 1The effect of PAMSQ dose on hydrophobics of PAMSQ-JPDMS/Lea

No.	Content of PAMSQ/%	Particle size of PAMSQ-JPDMS/nm	PDI	WCAs on PAMSQ-JPDMS/Lea (°)
JPDMS	0	267.4	0.101	141.6
PAMSQ-JPDMS-1	5	280.7	0.165	153.0
PAMSQ-JPDMS-2	10	304.9	0.281	157.1
PAMSQ-JPDMS-3	15	320.6	0.207	161.4
PAMSQ-JPDMS-4	20	522.6	0.422	155.8

In our experiments, we also discovered that the PAMSQ content in PAMSQ-JPDMS would exert a great impact on hydrophobicity of the treated leather. Therefore, this present work kept other parameters unchanged and chose the PAMSQ nanoparticles with average size of 128.7 nm to discuss effec of the PAMSQ content in PAMSQ-JPDMS on hydrophobicity of the PAMSQ-JPDMS/Lea. Those results are presented in Table 1. From Table 1, it is clearly demonstrated that WCA on the JPDMS treated leather surface attained 141.6 °. With increasing amount of the PAMSQ content in PAMSQ-JPDMS, average particle diameters and PDI of the as-prepared PAMSQ-JPDMS composite latexes were gradually augmented, which denotes that their particles size distributions were widened. However, hydrophobicity of the treated PAMSQ-JPDMS/Lea was first rose then declined. Its hydrophobicity reached the best with WCA of 161.4 ° while the PAMSQ content was 15 wt%. Nevertheless, its hydrophobicity would slightly decrease as the PAMSQ dosage continued to increase to 20 wt%. And this should be resulted from the fact that adsorption amount of the PAMSQ nanoparticle in the hybrid coating on the treated leather surface exceeds the saturated one, and it forms multi-layer adsorption, which is not conducive to the construction of the superhydrophobic surface [13]. Hence, PAMSQ-JPDMS-3 sample with the PAMSQ content of 15 wt% was selected in this work.

3.3 Performance properties of the PAMSQ-JPDMS treated leather

Table 2 Effect of the PAMSQ-JPDMS dose on performance properties of PAMSQ-JPDMS/Lea

Leather samples	Solid content of PAMSQ-JPDMS (%)	Static WCA/°	Water vapor permeability g/(m^2.day)	Dry rubbing resistance
Blank	0	71.8	3213.53	2
1#	0.3	158.4	3186.72	2~3
2#	0.6	160.6	3133.93	3
3#	0.9	161.3	3104.82	3~4
4#	1.2	163.8	3074.01	4
5#	1.5	159.8	3025.06	3

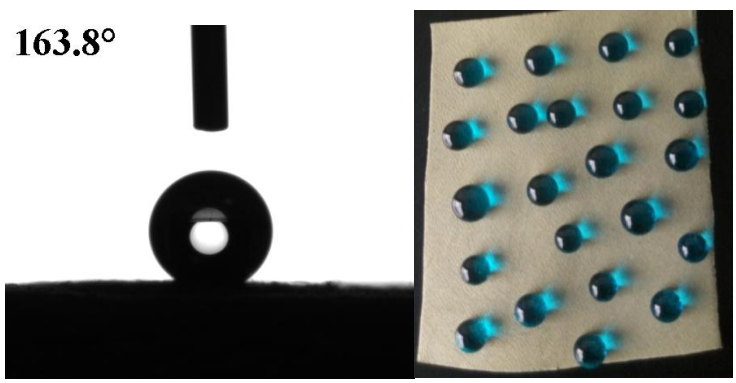

Fig.5 Water contact angle and optical photograph of PAMSQ-JPDMS/Lea

In the process of leather spraying, dosage of the PAMSQ-JPDMS directly affects its adsorption amount on the treated leather

surface, and next their application performances of leather, such as super hydrophobicity and “respiration”. In consideration of this, effect of the PAMSQ-JPDMS dose was investigated on the integrated application performances compared with the untreated leather sample. Their results are displayed in Table 2. It is apparently discovered from Table 2 that the untreated leather sample was hydrophilic and WCA on its surface was only 71.8 ° whereas the PAMSQ-JPDMS treated leathers all acquired the superhydrophobic properties with WCA larger than 150°. Hydrophobicity of the PAMSQ-JPDMS/Lea was increasingly reinforced with increasing amount of the PAMSQ-JPDMS and its best WCA attained 163.8° (seen in Fig. 5) while the PAMSQ-JPDMS dose was 1.2 %. However, its WCA would slightly decrease with further increase of the PAMSQ-JPDMS amount.

In addition, we also investigated effect of the PAMSQ-JPDMS dose on moisture permeability of the treated leather. With reference to water vapor permeability of the untreated leather of 3213.53 g/(m^2·day), the water vapor permeability of PAMSQ-JPDMS/Lea decreased slowly with the increase of its dosage, which may be due to some of the pores in the fibers blocked by the PAMSQ-JPDMS. But in general, PAMSQ-JPDMS coating had little effect on the moisture permeability of leather. According to the test results of color fastness to dry cleaning, PAMSQ-JPDMS/Lea had good dry fastness and grade 4 when the dosage of PAMSQ-JPDMS emulsion was 1.2 wt%.

3.4 FESEM observation

In order to in depth explore the inherent relationship between the micro-morphology of PAMSQ-JPDMS coated leather surface and its application performance, film-forming morphology and micro-morphology of PAMSQ-JPDMS coating on 4# leather surface were observed using FESEM and the results are seen in Fig. 6.

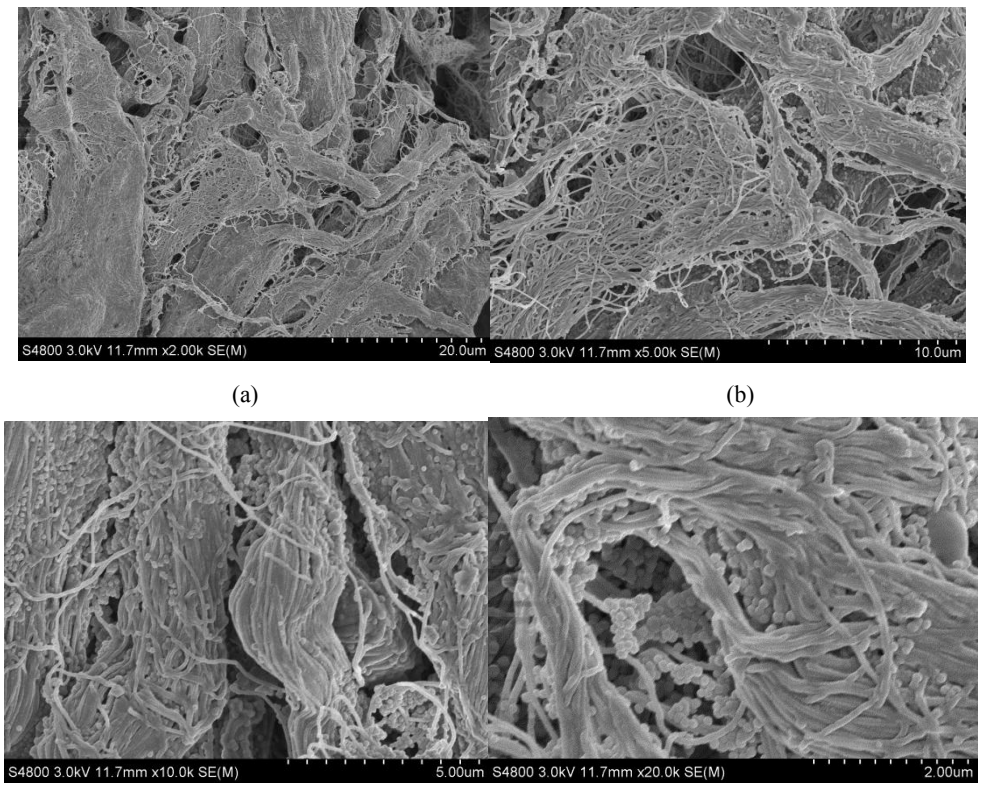

Fig.6 FESEM images of 4# PAMSQ-JPDMS/Lea in different magnifications

As is seen from Fig.6(a) there was clearly a PAMSQ-JPDMS finishing film coated on the leather fibers at a magnification of 2000. While the magnification times were enlarged to between 10000 and 20000, microstructure of PAMSQ in PAMSQ-JPDMS coating was clearly visible, and it is basically single-layer adsorption with uniform dispersion. The particle

size of nanoparticles was mostly between 100 and 150 nm. PAMSQ nanoparticles enhanced the nano-scaled roughness of leather surface, which makes PAMSQ-JPDMS/Lea produce unique micro/nano rough structure and this will play an important role in the construction of ultra-hydrophobic leather surface.

4 Conclusion

Structure of the product was confirmed by IR spectroscopy, and the superhydrophobic leather coating was constructed by spraying method.

PAMSQ-JPDMS/Lea had the best hydrophobicity, and water static contact angle was 163.8° when average particle size of PAMSQ was 128.7 nm, its content was 15% and solid content of the PAMSQ-JPDMS emulsion was 1.2%. Moreover, water vapor transmittance rate could still attain 3074.01 g/(m^2·day).

FESEM observation confirmed that construction of superhydrophobic leather surface was mainly rooted from a layer of dense silicon film and many lotus-like nano protuberances.

Acknowledgements

We are grateful to the National Key R＆D Program of China（2017YFB0308500）for financial supports of our research.

References

[1] Xin E Z, Wang Q J. Functional Leathers: Hydrophobic Leather [J]. China Leather, 2013, 42(3): 58-62.

[2] Xu W, An Q F, Ding Y, et al. Synthesis and application of carboxyl and dodecyl modified polysiloxane in leather water repellency [J]. Journal of Shaanxi University of Science & Technology, 2013, 31(2):9-13.

[3] Yin Z X, Shen Y D, Li P Z, et al. Study on the application of special macromolecule waterproof fatliquoring agent [J]. Leather Science and Engineering, 2010, 20(6): 40-42.

[4] Ma J Z, Zhang X Y, Bao Y, et al. A facile spraying method for fabricating superhydrophobic leather coating[J]. Colloids & Surfaces A Physicochemical & Engineering Aspects, 2015, 472:21-25.

[5] Xu W, An Q F, Hao L F. Synthesis of fluorinated acrylates water-and oil-repellent agent [J]. Leather Science and Engineering, 2010, 20(6): 35-39.

[6] Hao L F, An Q F, Ding Y, et al. Synthesis and application of carboxylated polymethyltrifluoropropylsiloxane [J]. Leather Science and Engineering, 2013, 23(1): 48-51.

[7] Qing N, Zhang X L, Zhou J H, et al. Preparation and application of aminopolysiloxane soft agents [J]. China Leather, 2000, 29(11): 12-16.

[8] Luo Z Y, Fan H J, Lu Y, et al. Synthesis and properties of fluorine-containing polymer-base fatliquoring agent [J]. China Leather, 2007, 36(23): 12-16.

[9] Hao L F, Gao T T, Wang X C, et al. Synthesis and characterization of polyaminopropylmethylsilsesquioxane nanospheres [J]. Fine Chemicals, 2016, 33(7):721-725.

[10] Zhang X Y. Fabrication of superhydrophobic leather coating [D]. Xi'an: Shaanxi University of Science and Technology, 2015.

[11] Li J H, Wang R. Preparation of nano-SiO_2/amino-modified polysiloxane hybrid superhydrophobic coating and thermal-stability characterization[J]. Journal of Wuhan University of Technology(Material Science Education), 2014, 29(1): 35-39.

[12] Nosonovsky M, Bhushan B. Patterned Nonadhesive Surfaces: Superhydrophobicity and Wetting Regime Transitions[J]. Langmuir the Acs Journal of Surfaces & Colloids, 2008, 24(4):1525.

[13] Hao L F, An Q F, Xu W. Synthesis of modified polysiloxane/nano-silica hybrid film and its hydrophobicity [J]. Journal of Function Materials, 2011, 42(s4):662-665.

P74

Preparation and application ofamphoteric polyurethane retanning agent with multi-aldehyde groups

Xiao-yeCHAI[1,2], Wei XU [1], Ji LI [1], Xue-chuan WANG [1]*

[1]*College of Bioresources Chemical and Materials Engineering, Shaanxi University of Science &Technology, Xi'an 710021,China*

[2]*College of Chemistry and Chemical Engineering, Shaanxi University of Science &Technology, Xi'an 710021,China*

Abstract

Amphotericpolyurethane(AAPU)retanning agentwith multi-aldehyde groups wasprepared bypolyaddition reactionusingisophoronediisocyanate (IPDI), polytetrahydrofuran glycol (PTMG), 2,4-dihydroxybenzaldehyde(DDBA), 2,2-dihydroxymethylpropionic acid (DMPA) and N-methyldiethanolamine (N-MDEA) as raw materials.The structure of AAPU was characterized by UV and FT-IR. The size and morphology of latex particles were measured by nano particle size meter and transmission electron microscopy, respectively.The AAPU retanning agent was applied to the retanning experiment of non-metallic tanning system.The results show that the products have the expected structurevia the UV and IR spectratests.The isoelectric point of AAPU is 5.16 anditsaverage particle size is 42.6nm. The applicationexperiments show that the binding ability of the crust leatherto anionic wet finishing materials has been improved while the AAPU retanning agentwas utilized in the retanningprocess of the non-metal tanning system.Finally,the absorptivity of the retanned leather to dyes is up to 99% andthe physical properties of the retanned leather are better than thoseof the treated leather by acrylic retanningagent,which demonstrates thatthe AAPU retanning agent can be as a candidate for retanning agent in the non-metal tanning system.

Keywords: aldehyde group; amphoteric polyurethane; leather retanning agent; preparation and characterization

1. Introduction

Chrom tannage, which increases the environment risk seriously, has a series of problems, such as chromate waste water, chromate waste solid and so on. (Qiang et al. 2018). So it restricts the sustainable development of leather industry. Therefore, many developed countries in the world will develop chromium-free ecological leather manufacturing technology as the most important development direction of the leather industry. Compared with chrome tanned leather, the non-metallic tanned crust leather lacks a large amount of positively charged metal ions on the surface and inside the fiber under wet conditions, and has strong negative electrical properties, so there is a poor reaction with traditional anionic counterstaining materials, resulting in a significant reduction in the counterstaining effect of non-metallic tanned leather. Therefore, it is very important to study the finishing materials, such as high performance retanning agents, which match with non-metallic tanning system.

There are sorts of retanning agents which meet different performance requirements of crust leather in tannery industry. Polyurethane retanning agents are divided into anionic, cationic and amphoteric ones that have excellent comprehensive properties because their molecular chains are similar to those of leather collagen peptides (Bao et al. 2007, Lan et al. 2002, Lan et al. 2002, Brunstedt et al. 1993). The amphoteric polyurethane retanning agent contains active groups such as amino group and carboxyl group, which can obviously improve the physical-mechanical properties of the leather, and didn't bring a light color effect in the dyeing process. In recent years, much attention has been paid by researchers of leather materials (LI et al. 2016, Li et al. 2017, Yin et al. 2009).

In the present study, novel amphoteric polyurethane retanning agent with multi-aldehyde groups was prepared by polyaddition reaction using isophorone diisocyanate (IPDI), polytetrahydrofuran glycol (PTMG), 2,4-dihydroxybenzaldehyde (DDBA), 2,2-dihydroxymethylpropionic acid (DMPA) and

N-methyldiethanolamine (N-MDEA) as raw materials. The combination of the highly reactive aldehyde groups in the AAPU retanning agent with the alkaline amino group of the collagen fibers is expected to improve the bonding strength of the tanning agent and the billet. In addition, the effect of AAPU retanning agent on the anionic finishing material and the physical and mechanical properties of the crust leatherwere investigated in the less-vegetable tanning system.

2. Materials and methods

2.1. Reagents

Isophorone diisocyanate (IPDI), of analytically pure grade, were purchased from Shanghai Dibo Chemical Technology Co., Ltd. polytetrahydrofuran glycol (PTMG), 2,4-dihydroxybenzaldehyde(DDBA), and 2,2-dihydroxymethylpropionic acid (DMPA), of analytically pure grade, were purchased from Shanghai Macklin Biochemical Technology Co., Ltd. N-methyldiethanolamine (N-MDEA), of analytically pure grade, were purchased from Aladdin Reagent Co., Ltd. The less-vegetable tanning leather was prepared in our lab. Acrylic resin retanning agent was purchased from Sichuan T&J New Materials Co., Ltd.

2.2. Preparation of amphoteric polyurethane with multi-aldehyde groups (AAPU) retanning agent

The amphoteric polyurethane with multi-aldehyde groups (AAPU) retanning agent was synthesized by using polyaddition reaction. In the first step, IPDI and PTMG according to the stoichiometric ratio were added into a 250mL three our-necked flask with a mechanical stirrer, catalyzed by DBTDL in the presence of N_2 atmosphere. The mixture was stirred at 40℃ for 30min and then heated at 70℃ for 1h. The NCO-terminated pre-polymer was obtained. Second,DMPA, N-MDEA and DDBA were added as chain extenders to extend the chain reaction for 4h (acetone was added to reduce the viscosity). Then, TEA was added to neutralize the carboxylic groups of the DMPA at 40 °C for 30 min. Dis-tilled water was added drop by drop within 5 min and the stirring rate was kept at 600 rpm. Finally, the amphoteric polyurethane with multi-aldehyde groups retanning agent was obtained after removing acetone at 40 °C for 30 min by rotary evaporation instrument.The synthetic route of AAPU was presented in Scheme 1.

To compare and contrast, the amphoteric polyurethane without aldehyde groups (APU) was prepared using the above method by DMPA and N-MDEA as a chain extender.

2.3. Retanning procedure

Table 1 Retanning Procedure of less-vegetable tanning system

process	materials	dosage/%	temperature/℃	time/min	pH	remarks
rewetting	water	200	25			
	degreasing agent	1.5		40		
washing	water	200	25	10		
neutralizing	water	150	25			
	sodium bicarbonate	0.8		3*20+30		dilution 1:10
	sodium formate	1		3*20+30	6.5	checking incision
washing	water	200	25	10		
retanning	water	150	30			
	retanning agent	3		120		comparative test
washing	water	200	30	10		
fatliquoring	water	100	55			

and dyeing	fatliquor LQ-5	6.0	60	
	black dyestuff	2.5	30	
	formic acid	1.5	3*10+30	3.5-4.0
		drying		

3. Results and Discussion

3.1. UV-Vis analysis

The UV−Vis absorption spectra of APU and AAPU were displayed in Fig 1(a) and 1(b),respectively. As seen in the picture, there is no maximum absorption between 200nm~400nm in the curves of APU (Figure 5a) and the maximum absorption wavelength of AAPU was at 262 nm (Figure 5b),which attributed to the incorporation of 2,4-dihydroxybenzaldehyde to AAPU where the conjugation effect of C=O and benzene ring existed. Thus the UV absorption at 262nm produced owing to the transition of n electrons in C=O to π* on the benzene ring.

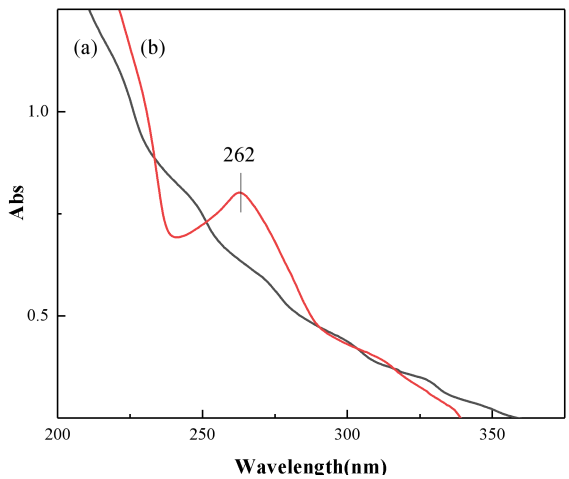

Fig. 1 UV spectra of (a) APU and (b) AAPU

3.2. FT-IR analysis

FT-IR technologies were adopted to characterize the structures of the DDBA, IPDI and the final product. The IR result is shown in Fig. 2.It can be interpreted as follows: a broad peak at 3130 cm^{-1} is due to the stretching vibrations of O-H, (b) 2942cm^{-1} and 2854cm^{-1} are the absorption peaks of methylene asymmetry and symmetric expansion, 2263cm^{-1} was the characteristic absorption peak of -NCO in IPDI, and 1713cm^{-1} is the vibration absorption peak of C=O. From the FT-IR spectrum of AAPU(c), it can be interpreted as follows: The band at 3323 cm^{-1} which was attributed to N-H stretching vibration. The bands at 2942 cm^{-1} and 2854 cm^{-1} are attributed to C-H stretching vibrations of aldehyde group. One peak at 1713 cm^{-1} and 1103cm^{-1} is for C=O stretching vibrations and C-O absorption of vibration peak, a small peak at 2820 cm^{-1} attributed to the C-H stretching vibration. Compared with the curve of (b) in Figure 2, the characteristic absorption peak of -NCO at 2263cm^{-1} almost disappeared.

Therefore, on basis of the above analysis, we have successfully prepared the expected in our study.

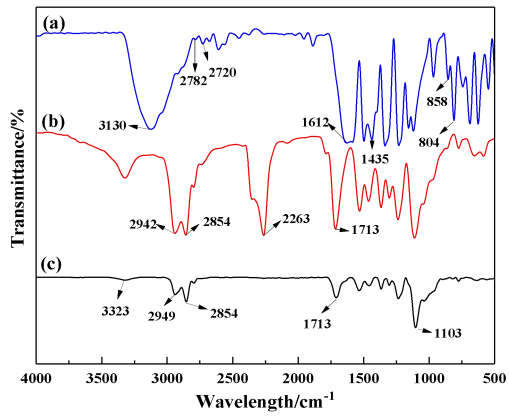

Fig. 2 FT-IR spectrum of (a) DDBA;(b)IPDI;(c)AAPU

3.3. Morphology and its average size of AAPU latex particle

Morphology, average size and its distribution of one latex colloidal particles will play a crucial role in its performance properties and application fields. Therefore, particles morphology and the average size of the AAPU emulsions were researched in our studies and the results are displayed in Figs 3(a) and 3(b). It can be seen from Fig. 3(a) that AAPU latex particles emerged as the regular spherical structure with the average diameters being about 20~130 nm. It can be noted that the average particle sizes of the AAPU latexes were 42.6 nm which was consistent with the TEM results.

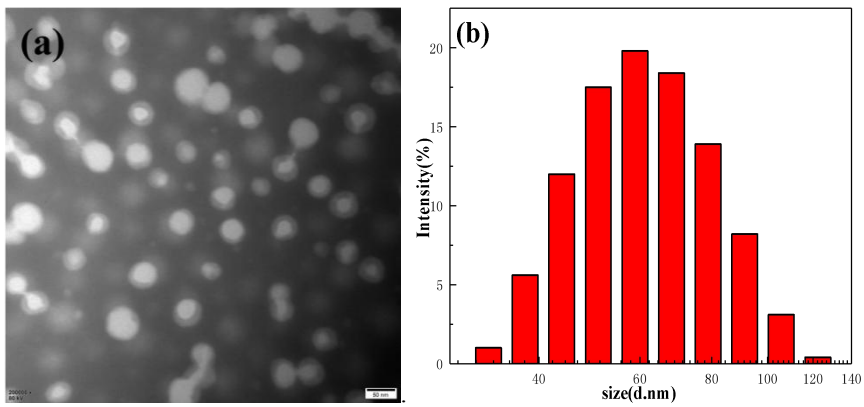

Figure 3 TEM image (a) and size distribution (b) of the AAPU latex particles

3.4. Isoelectric point analysis

The relationship between the Zeta potential and pH of AAPU emulsion was shown in figure 4.As shown in Fig. 4,amphoteric of AAPU emulsion was indicated that the zeta potential was negative and gradually increases and it turns into a positive value and gradually increases when crossing the isoelectric point. When pH was below 5.16, the $-CH_3N(CH_2)_2-$ in AAPU emulsion was changed to $H^+(-CH_3NH^+)$ through the H^+ in the binding system, which was cationic and the Zeta potential is positive. When pH was beyond 5.16, The -COOH in AAPU emulsion lost proton and changed to $-COO^-$, which showed negative electricity and Zeta potential was negative. When pH was 5.16, the AAPU emulsion was electric neutrality due to the equality of positive and negative charge, which is the isoelectric point of AAPU.Therefore, the binding rate of leather and anionic wet-finishing materials and the retanning effect were improved by the amphoteric polyurethane with multi-aldehyde groups in non-metallic tanning system.

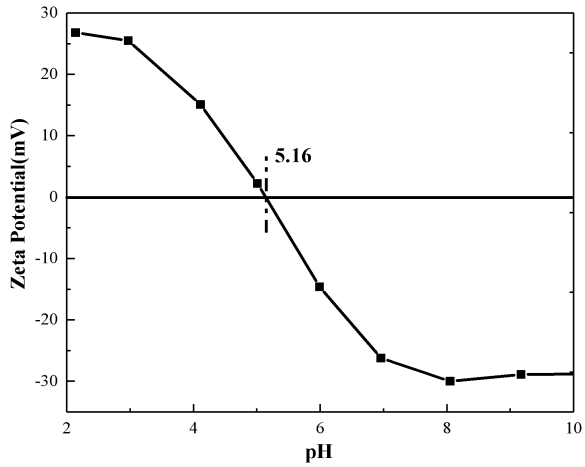

Fig. 4 The relationship between Zeta potential and pH of AAPU

3.5. Effect on dyes binding capacity of the crust leather

3.5.1. Dye absorption rate

The absorptivity of the crust leather to dyes after retanning with acrylic resin retanning agent and AAPU retanning agent respectively was shown in table 2. It was known from table 2 that the absorptivity of the crust leather to dye retanned by acrylic resin retanning agent was 85%, while that of the crust leather retanned by AAPU retanning agent was as high as 99%. So the absorptity of crust leathers to dyes after retanning with AAPU tanning agent is significantly better than that of crust leather retnned by the acrylic retanning agent.

Table2 The dyes absorption rate of crust leather retanned with AAPU and acrylic resin

crust leather	absorption rate of dyes
acrylic resin retanning agent treatment	85%
AAPU retanning agent treatment	99%

3.5.2. Color yields on the surface of crust leather after dyeing

The value of K/S can indicate the color depth of the surface of an object (Xue et al. 2004). The K/S curves on the surface of the crust leather retanned and dyed by AAPU retanning agent and acrylic resin retanning agent were shown in Fig. 5(a) and 5(b), respectively. From the K/S curves in Fig 5, in the wavelength range of 300~750 nm, the value of K/S on the surface of the crust leather after retanning with AAPU retanning agent was significantly larger than that of the crust leather after retanning with acrylic resin retanning agent. Compared with the K/S curve of 5(b), the K/S curve of 5(a) had a clear gentle trend, indicating that the dyeing effect on the surface of the skin after AAPU retanning is higher in level, more pure, and fuller in color.

In a word, the binding ability of the crust leather to anionic wet finishing materials has been improved and the absorption of dyes were promoted while the AAPU retanning agent was utilized in the retanning process of the non-metal tanning system.

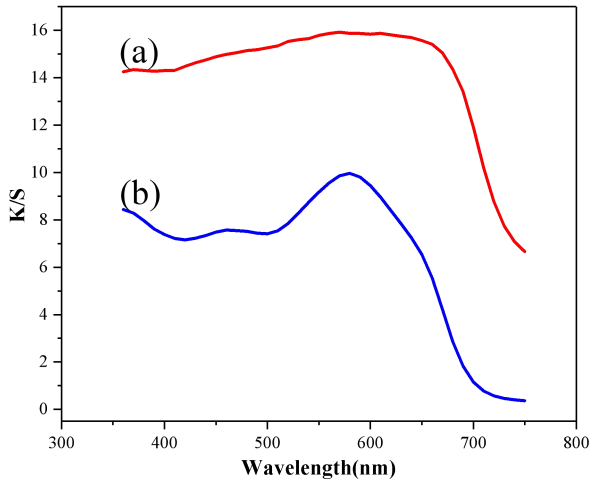

Fig5 The K/S curves of (a) AAPU retanning agent treatment;
(b) Acrylic resin retanning agent treatment

3.5.3. Physical properties characteristics of crust leathers

The physical characteristics of leathers reflect the quality of leather. The test results of the physical properties characteristics of crust leather retanned by acrylic resin retanning agent and AAPU retanning agent were shown in Fig.6. As shown in Fig.6, The results indicate that strength properties such as tensile strength, tear strength and the thickness percentage of crust leather retanned by AAPU retanning agent were better than those of one that retanned with the acrylic resin retanning. AAPU, a kind of retanning agent containing the reactive aldehyde groups that combine with alkaline amino groups in the collagen by the covalent bond (QIANG et al. 2017), was prepared by using polyaddition reaction and has big molecular weight. The combining capacity of anionic wet-finishing materials and crust leather was improved duo to the positive charge increased in crust leather after retanned by AAPU retanning agent and the wet-finishing material was effectively filled and covered on the inner and surface of the fiber, lubricating collagen fibers and preventing the adhesion of collagen fibers (Guo et al. 2018). Thus, the physical properties of the crust leather were raised.

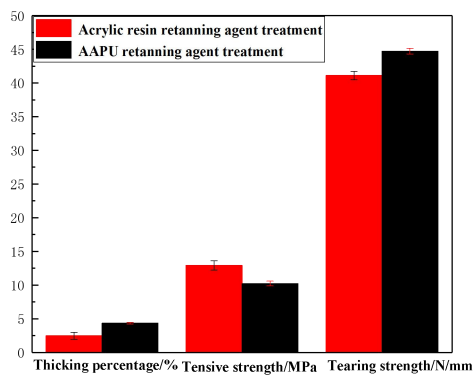

Fig.6 Physical properties characteristics of crust leathers.

4. Conclusions

This paper was prepared a novel amphoteric polyurethane retanning agent with multi-aldehyde groups (AAPU) retanning agent by polyaddition reaction. The isoelectric point of AAPU is 5.16 and its average particle size is 42.6nm. The binding ability of the crust leather to anionic wet finishing materials has been improved while the AAPU retanning agent was utilized in the retanning process of the less-vegetbale tanning system. The

absorptivity of the retanned leather to dyes is up to 99%, the dyed bath liquid is transparent and clear, and the crust leather is evenly dyed and full of color. The value of K/S, the physical-mechanical properties and thickness percentage of the retanned leather are better than those of the treated leather by acrylic retanning agent, which demonstrates that AAPU retanning agent has potential application prospects in non-metallic tanning systems.

Acknowledgements

We are grateful to the National Key R＆D Program of China（2017YFB0308500）for financial supports of our research.

References

Qiang T T, Chen L, Zhang Q, et al. A sustainable and cleaner speedy tanning system based on condensed tannins catalyzed by laccase[J]. Journal of Cleaner Production, 2018, 197(1): 1117-1123.

Bao L H, Lan Y J, Zhang S F. Aliphatic anionic polyurethane microemulsion leather filling-retanning agent[J]. Journal of the Society of Leather Technologists & Chemists, 2007, 91(2):73-80.

Lan Yunjun, Pang Xiaoyan. The synthesis of aliphatic anion waterborne polyurethane as retanning and filling agent[J]. China Leather, 2005, 34(9):1-5.

Lan Yunjun, Chai Yuye, Li Linsheng. Syntheses and configuration of amphoteric polyurethane retanning filling agents PUR- A[J]. China Leather, 2002, 31(13):9-12.

Brunstedt M R, Ziats N P, Schubert M, et al. Protein adsorption and endothelial cell attachment and proliferation on PAPI-based additive modified poly(ether urethane ureas)[J]. Journal of Biomedical Materials Research, 1993, 27(4):499-510.

LI Hanping, JIANG Weilong, FAN Baozhu, et al. Progress of aqueous polyurethane retanning agent[J]. China Leather, 2016, 45(6):40-42.

Li C T, Qiang T T, Li X N, et al. Preparation and application of collagen-based waterborne polyurethane retanning agent[J]. Journal of the Society of Leather Technologists & Chemists, 2017, 101(3):149-154.

Yin Zhaoxia, Shen Yiding, Li Ganghui, et al.等. Applied and Action Mechanism of Imidazole End Capped Water-based Polyurethane Retanning Agent [J]. China Leather, 2009, 38(23):3-6.

XUE Chao—hua, J1A Shun-tian. Application of computer color matching technology in leather dyeing[J]. Journal of Shaanxi University of Science ＆ Technology, 2004, 22(3):129-132.

QIANG Tao-tao, HAN Mi-mi. Study application properties of several new types of retanning agent[J]. Journal of Shaanxi University of Science ＆ Technology, 2017, 35(4):6-10.

Guo Zhuoneng, Qiang Xihuai, Xu Wei, et al. Preparation and application of amphoteric fatliquor based on FTE modification[J]. China Leather, 2018, 47(5):6-13.

P75

Poly(γ-glutamic acid)-NHS ester: a dual-functional modifier to prepare polyanionic collagen with superior thermal stability

Min Zhang[a,*], Qili Yang[a], Junhui Yang[a], Cuicui Ding[b], Yonghao Ni[a], Liulian Huang[a], Lihui Chen[a]

[a]*College of Materials Engineering, Fujian Agriculture and Forestry University, Fuzhou 350002, PR China.*

[b]*College of Ecological Environment and Urban Construction, Fujian University of Technology, Fuzhou 350108, PR China.*

Abstract: γ-PGA-NHS ester, which was prepared using poly(γ-glutamic acid) (γ-PGA) and N-hydroxysuccinimide(NHS) as the raw materials, was synthesized as a novel modifier of collagen. FTIR analysis suggested that the products displayed the characteristic absorption peak of ester. Results from ^{1}H NMR analysis indicated that the esterification degree of γ -PGA-NHS ester was increased with the increase of NHS. The results of CD and FTIR analysis indicated modified collagen retained the triple helix structure of natural collagen. Isoelectric point of the modified collagens shifted continuously to lower values with increasing the γ-PGA-NHS/collagen ratios (w/w). Consequently, the modified collagen can form a clear solution in neutral pH buffer. The denaturation temperature (Td) of the modified collagens reached 44.8-49.9°C, which was higher than that of native collagen. In addition, the modified collagens possessed excellent cytocompatibility. These results indicated that dual-functional modification in regards to both of water solubility and thermal stability on collagen can be achieved using γ-PGA-NHS esters, which was helpful for the utilizing or the processing of water-soluble anionic collagen in aqueous solution in the fields such as cosmetics, health care products, tissue engineering and biomedical materials, etc.

Keywords: Polyanionic collagen; Poly(γ-glutamic acid); N-hydroxysuccinimide; Cross-linking

1.Introduction

Collagen, the major structure component in connective tissues such as tendon, skin and bone, is widely used as a natural biopolymer in different formats including sponges, films, membranes and tubes due to its advantages such as readily availability, biocompatibility, low antigenicity and high mechanical strength [1-3].

Collagen is a typical polyampholyte and has an isoelectric point near physiological pH, which means that it does not swell or dissolve in the neutral pH solution, limiting the potential of collagen in many fields such as cosmetics, injectable biomaterial etc. In order to improve the water-solubility of collagen, several researchers have tried to introduce additional carboxylic groups to make collagen to be polyanionic collagen [4-7]. For instance, Zhang et al. [6] compared part of the physicochemical properties between calfskin pepsin-solubilized collagen (PSC) and succinylated PSC; Sripriya et al.[5] modified collagen with succinic anhydride to make a polyanionic collagen, and the attractive feature of which was its good swelling behavior resulting in dissolution, which offers transparency in neutral pH buffer. The superior water-solubility of polyanionic collagen ensures that a clear solution can be obtained at physiological pH, which makes it as an ideal candidate for injectable biomaterials. Films formed from such solutions have been considered as the replacements of corneal and lenticules for modifying the cornea [8]. Furthermore, the increased net negative charge on polyanionic collagen molecules also bring about the surface antibacterial, minimizing the bacterial adhesion without affecting the animal cell attachment [9]. In addition, considering that the creams or emulsions of cosmetics should be close to physiological pH, the polyanionic collagen can also be used as the bioactive substances in cosmetics. As a whole, acylation modification of collagen will be greatly helpful in designing collagen molecule for applications in many fields such as biomaterials, medicine, ophthalmology as well as cosmetics.

It could be detected from the relevant reports that the water-soluble collagen was prepared through the reaction between native collagen and anhydride, of which succinic anhydride was used on most occasions. However, there are shortcomings of this method. It has been demonstrated that the succinylated collagen possessed a denaturation temperature of 34.7 °C, which was lower than that of the native collagen (38.4 °C), mainly due to the strong electrostatic repulsion amongst the electronegative collagen molecules[6]. As is well known, natural collagen itself possesses a poor thermal stability since it would be denatured if temperature was above ~40 °C. Hence, the instability of collagen triple-helical conformation has been

aggravating due to the acylation modification, which would further restrict the application of collagen as a biopolymer. To reinforce collagen structure for the purpose of fabricating collagenous materials with more suitable physicochemical properties, a mass of chemicals such as glutaraldehyde (GTA)[10], formaldehyde[11], hexamethylenediisocyanate[12], carbodiimide or carbodiimide/N-hydroxysuccinimide (NHS)[13, 14], genipin[15], plant tannins[16], polyepoxy compound[17], acylazide[18], reducing sugars [19] and dialdehyde compound derived from natural biomass[20-22], have been developed to be cross-linkers of collagen.

Nevertheless, there is a direct competition between acylation and cross-linking modification, because succinic anhydride reacts with the Ɛ-amino groups of the lysine or hydroxylysine residues on the side chains of collagen, while most of the chemical cross-linkers also need to react with the same Ɛ-amino sites, which means that the two kinds of modification could not be achieved simultaneously for collagen. Therefore, we designed a novel dual-functional modifying agent γ-PGA-NHS esters, with poly(γ-glutamic acid) (γ-PGA) as the starting material, to produce the water-soluble collagen accompanied with an excellent thermal stability. Like collagen, γ-PGA is also a natural polymer isolated from Bacillus[23]. The outstanding biodegradability and biocompatibility properties displayed by γ-PGA make it as a useful biomaterial which has potential applications in cosmetic, drug delivery systems and tissue engineering [24-27]. The backbone of γ-PGA is formed by linking the γ-COOH group of glutamic acid instead of the α-COOH group, so there are a large number of α-COOH groups on the side chains. After part of α-COOH groups were esterified by N-hydroxysuccinimide (NHS), the activated NHS-ester groups could react with the Ɛ-amino groups of collagens to form a stable amide bond, leading to the cross-linking amongst collagen molecules[28]. Synchronously, the net negative charge of collagen could be increased, owing to the introduction of abundant un-esterified α-COOH groups of γ-PGA molecules, which are favorable for the dissolution of collagen in neutral pH water. In addition, when react with proteins, NHS residues of NHS-activated esters will be split away off and can be removed simply by dialysis, so recently NHS-activated esters have attracted many interests as a new sort of cross-linking agent with good cytocompatibility and biocompatibility [29, 30].

In the present work, we synthesized γ-PGA-NHS esters with γ-PGA and NHS as the raw materials. γ-PGA-NHS ester was then characterized by several methods, including fourier transform infrared spectroscopy (FTIR), nuclear magnetic resonance (NMR). Thereafter, γ-PGA-NHS ester was used to modify collagen solution. The resultant collagen was then systematically characterized by circular dichroism (CD) analysis, the water solubility was assessed by determining of isoelectric point (pI), and the thermal stability was examined with differential scanning calorimetry (DSC). Furthermore, the cytocompatibility and the aggregation behavior were evaluated by fluorescence measurements.

2.1. Materials

Poly(γ-glutamic acid) (γ-PGA) (MW 1000 kDa) was purchased from Nanjing Saitaisi biotechnology Co., Ltd (China). Trypsin (from bovine pancreas, 2500 units/mg), N-hydroxysuccinimide (NHS) and 1-ethyl-3-(3-di-methylaminopropyl) carbodiimide hydrochloride (EDC) were purchased from Aladdin Co., Ltd (China). Protein marker (6.6-200 KDa) was purchased from Sigma-Aldrich Co., Ltd (China). Type I collagen was extracted from bovine split according to the method of Zhang et al.[28]. In brief, the supernatants extracted from the delimed and neutralized bovine split pieces by 0.5 mol/L acetic acid containing 3% pepsin (1:3000) were collected, and thenthe supernatants were salted out by adding NaCl to 0.7 mol/L. The precipitate was dissolved and dialyzed against 0.1 mol/L acetic acid. Finally pepsin-soluble collagen was obtained by lyophilizing and stored until used.

2.2. Synthesis of γ-PGA-NHS ester

20 mL of dimethyl sulfoxide (DMSO) and γ-PGA (1 g) were added into a conical flask. After γ-PGA was dissolved into DMSO completely, NHS was added with the molar ratios of NHS to α-COOH groups of γ-PGA to be 1/20, 1/10, 1/5, 1/2, 1/1, and 5/1. Then EDC was added with the constant EDC/NHS molar ratio of 1/1. The mixed solution was gently stirred at room temperature for 24 h. After that, the mixture was washed for three times with acetone and n-hexane. Finally the residue was lyophilized at -50 °C for 2 days and stored at 4 °C until used.

2.3. FTIR spectra of γ-PGA-NHS esters

FTIR were carried out using Thermo Fisher Scientific instrument (Nicolet IS10, USA) at 25 °C. γ-PGA or γ-PGA-NHS ester power were mixed with potassium bromide power (1:100) and then pressed into a disk. All spectra were obtained with a resolution of 2 cm^{-1} in the wavenumber region from 400 to 4000 cm^{-1} and the spectra polts represented the average of 48 scans.

2.4. ^{1}H-NMR spectra of γ-PGA-NHS esters

The content of NHS groups reacted with γ-PGA was determined by nuclear magnetic resonance (NMR) spectroscopy[31]. The synthesized γ-PGA-NHS ester was dissolved in deuterated DMSO with the concentration of 10 mg/mL, and its NMR spectrum was recorded by a Bruck instrument (ADVANCE III 500, Germany). The esterification extent was determined from the relative peaks area at 2.8 and 4.2 ppm, corresponding to the protons of N-hydroxysuccinimide and those binding to the α-carbon of γ-PGA, respectively. The esterification degrees were calculated from three replicates.

2.5. Modification of collagen solutions

Collagen was dissolved in water acidified to pH 4.0 using dilute HCl to obtain a concentration of 5 mg/mL, and then the pH of solution was adjusted to 9.0 by adding aqueous NaOH (1.0 mol/L). A solution of poly(γ-glutamic acid)-NHS ester in DMSO with concentration of 100 mg/mL was added dropwise to collagen solution and to reach the final weight ratios between γ-PGA-NHS and collagen = 5%, 10%, 20% and 50%, respectively. During addition, pH value was maintained at near 9.0 by adding NaOH solution. The reaction mixture was stirred at room temperature for 30 min, and then the resultant was dialyzed against deionized water for 3 days. Finally the resultant solution was lyophilized at -50 °C and stored at 4 °C until used.

The lyophilized native and modified collagens (γ-PGA-NHS /collagen ratio (w/w) reached 20%) were respectively dissolved in 0.1 mol/L acetic acid and deionized water to stock concentrations of 0.1, 0.3, 0.4, 0.5, 0.6, 0.8 and 1.0 mg/mL. The samples of the native and modified collagen solutions were named COL and MCOL, respectively.

2.6. Circular dichroism (CD) analysis

The lyophilized native and modified collagens were dissolved in 0.1mol/mL acetic acid or deionized water respectively to stock concentration of 0.5 mg/mL. Then the mixtures were equilibrated at 25 °C before testing and scanned in a wavelength range from 180 to 260nm. The molar ellipticity was recorded with aJ-810CD spectropolarimeter (Jasco, J-810, Japan) at a speed of 20 nm/min and each sample was scanned for three times.

2.7. Fourier transform infrared (FTIR) spectroscopy of collagens

FTIR spectra of the collagen samples were examined according to the method of section 2.3.

2.8. Isoelectric potential (pI) of collagens

The native and modified collagens with concentration of 0.5 mg/mL were prepared by dissolving lyophilized samples in 0.1 mol/L acetic acid and deionized water, respectively. The solutions were titrated with 0.25 mol/L NaOH or 0.25 mol/L HCl. Then, the Zeta potential at a given pH value was recorded by a Zeta potential titration apparatus (Malven Zetaweight Nano ZS, UK) with triplicate at 20 °C and the isoelectric point (pI) was determined at the pH value where the Zeta potential was zero.

2.9. Differential scanning calorimetry (DSC) of collagens

The thermal stability of modified collagen was evaluated by DSC (Netzsch DSC 200PC, Germany). The native and modified collagens with concentration of 10 mg/mL were prepared by dissolving lyophilized samples in 0.1 mol/L acetic acid and 0.2 mol/L phosphate buffer (PBS), respectively. Samples (~10 mg) were weighted accurately into aluminium pans and sealed, and scanned over the range from 20 to 60 °C at a heating rate of 3 °C/min in a nitrogen atmosphere. Liquid nitrogen was used as a cooling medium. Pans with 0.1 mol/L acetic acid or 0.2 mol/L PBS were used as the reference, respectively. T_d values were calculated from three replicates.

2.10. Determination of the cross-linking degree

Determination of residual amino groups in collagen was performed according to the previous method with slight modifications [32]. 0.25 mL of collagen samples, 2.00 mL borax buffer (pH 10.0) and 2.0 mL of freshly prepared 0.1% (v/v) trinitro-benzen-sulfonic (TNBS) acid solution were mixed together. After reaction at 30 °C for 60 min, 4.0 ml of 0.1 mol/L HCl was added to the mixtures, and then stayed standing for 30min at 20 °C. The mixed solution was measured at 340 nm using a UV spectrophotometer (PerkinElmer Lambda 25, USA). The degree of cross-linking was calculated as described by the following equation [33]:

$$\text{The degree of cross-linking (\%)} = (1 - \text{absorbance}_c / \text{absorbance}_n) \times 100\% \quad (1)$$

where the subscripts c and n stand for the cross-linked and native collagen, respectively. The values were calculated from three replicates.

2.11. Field-emission scanning electron microscopy (FESEM) of collagens

The morphologies of lyophilized collagen sponges were examined with a field-emission scanning electron microscope (Navo FEI NanoSEM 230, USA), operated at an accelerating voltage of 15 kV.

2.12. In vitro biocompatibility study

HFF-1 cells were purchased from Shanghai Institute for Biological Sciences, Chinese Academy of Sciences (China). Before test, collagen samples were sterilized using gamma rays at 25 KGy. Then the solutions were placed into 24-well cell culture plate seeded with HFF-1 fibroblasts at the density of 1 × 104/mL and cultured for 1, 3 and 5 days. The cell culture medium was changed every 2 days. The viability of fibroblasts was determined by the 3-(4,5-dimethyl-2-thiazolyl)-2,5-diphenyl-2-H-tetrazolium bromide (MTT) assay. The optical density was determined at 490 nm with a microplate reader (Model 550, Bio Rad, USA). Data was calculated from the mean value of 6 parallel samples and the whole test was repeated 3 times [34-36].

2.13. Statistical analysis

Statistical analyses were performed via PASW statistics program package, version 18 (SPSS Inc., Chicago, IL,SA). Compari son of the obtained data for different samples was performed with One-Way ANOVA. The significance level was set at $p < 0.05$.

3. Results and discussion

3.1. The characterization of γ-PGA-NHS esters

The FTIR spectra of γ-PGA-NHS ester can be correlated to γ-PGA-NHS ester backbone conformation. Fig.1 shows the FTIR spectra of pure γ-PGA and γ-PGA-NHS ester. The amide A and B bands at 3299 and 3083 cm^{-1}, respectively, are mainly associated with the stretching vibrations of N-H groups[37]. The amide I band at 1643 cm^{-1} is dominantly attributed to the stretching vibrations of C=O groups, and the amide II absorbance at 1552 cm^{-1} arises from the N-H bending vibrations coupled to C-N stretching vibrations. The amide III centered at 1238 cm^{-1} is assigned to the C-N stretching and N-H bending vibrations from amide linkages, as well as wagging vibrations of CH_2 groups[38]. The positions of these major amide bands do not change with the increasing NHS/COOH ratios. However, with the increase of NHS/COOH, the peak located at 1817 cm^{-1}, which could be assigned to the esterbond [39], became more obvious, especially when NHS/COOH reached 1/2, 1/1 and 5/1. Meanwhile the band between 1035 and 1110 cm^{-1} associated with the C-O stretching vibrations appeared. These peaks indicated that γ-PGA-NHS ester was prepared successfully.

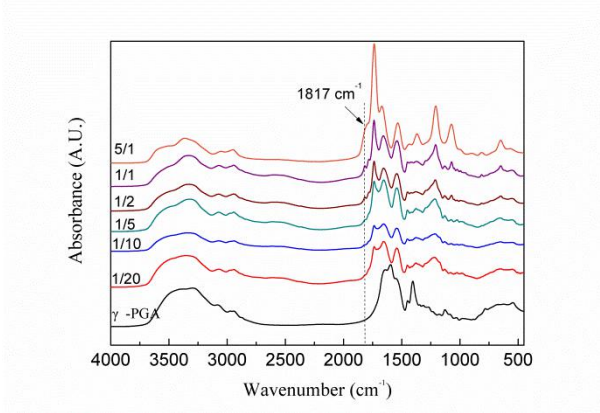

Fig.1 FTIR spectra of γ-PGA and γ-PGA-NHS esters

To determine the esterification degree of γ-PGA-NHS esters, the ^{1}H-NMR spectra of γ-PGA-NHS ester were obtained and are shown in Fig. 2a. The peak intensity at 2.8 ppm corresponding to the protons of N-hydroxysuccinimide[40] increased with the increase of NHS/COOH ratios. The esterification extent could be calculated from the relative area of this peak and the peak at 4.2 ppm corresponding to the α-carbon of γ-PGA. The degree of esterification histogram is displayed in Fig. 2b. As for γ-PGA-NHS esters with NHS/COOH ratios increased from 1/20 to 5/1, the degrees of esterification of γ-PGA-NHS esters were gradually increased in the range from 2.8±0.8 to 89.0±1.6%.

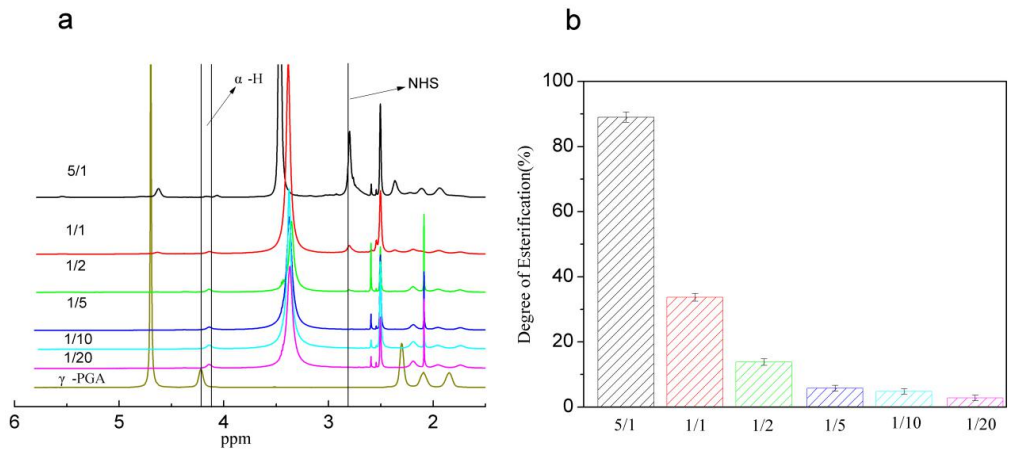

Fig.2 (a) Typical ^{1}H-NMR spectra of γ-PGA-NHS esters, (b) the degree of esterification histogram of γ-PGA-NHS esters.

3.2. CD analysis of collagens

Generally, the CD spectra of the triple helical conformation of collagen includes a rotatory maximum at 210-230nm contributed to the π-π* transition of peptide bonds, a minimum at about 198 nm primarily attributed to the α-helix structure of collagen and a consistent crossover point at about at 213nm[41]. Fig. 3 showed the CD spectra of native collagen and modified collagen. The CD spectra of native collagen and modified collagen exhibited significant positive and negative peaks at ~222 and ~197 nm, which indicated that the structure integrity of the two collagens was still maintained. Besides, the intensity ration of the positive peak to the negative peak, interpreted intensity as Rpn, could directly reflect the triple helical conformation of collagen to some extent[42]. The Rpn value of modified collagen was 0.139±0.005, which was higher than that of native collagen (0.107±0.004), indicating that the modified collagen possessed a higher degree of molecular order and inter- or intra- molecular cross-linking[43].

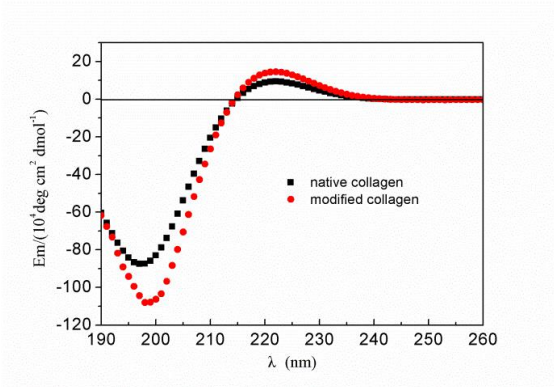

Fig.3 Typical CD spectra of the native and modified collagens.

3.3. FTIR spectra of collagens

It is believed that the integrity of collagen is the foundation for maintaining its superior biological properties[42]. Fig.4 shows the FTIR spectra of the native and collagens modified with γ-PGA-NHS(1/20) and γ-PGA-NHS(1/5). The native collagen displayed bands at 1653, 1553 and 1239 cm^{-1}, respectively, which are characteristics of amide I, II and III bands of collagen [44]. The spectra of modified collagens were similar to that of the native one. In addition, the absorption ratios of amide III to 1450 cm^{-1}, denoted as A_{III}/A_{1450} are also considered as a measurement of preservation of integrity of the modified collagens[42]. The calculated A_{III}/A_{1450} values are 0.86, 0.99 and 0.92 for the native collagen and collagens modified by γ-PGA-NHS(1/20) and γ-PGA-NHS(1/5), respectively. Furthermore, it has been reported that the ratio of gelatin, which is the denatured products of collagen, is just about 0.59 [45]. The results of circular dichroism have indicated the structure integrity of the modified collagens was maintained. So it was further demonstrated by the FTIR results that γ-PGA-NHS esters just acted as a modifier, without destroying the backbone of collagen molecules.

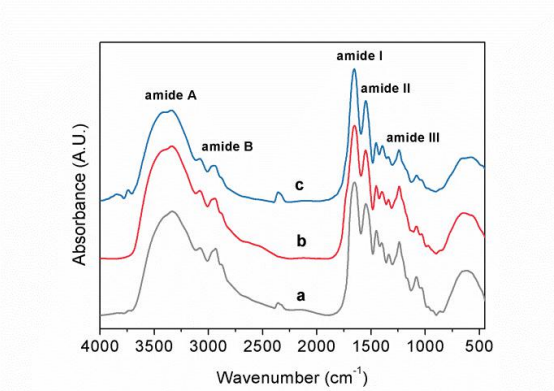

Fig.4 FTIR spectra of the native collagen (a) and collagens modified with γ-PGA-NHS(1/20) (b) and γ-PGA-NHS(1/5) (c). The modifier/collagen ratio (w/w) = 20%.

3.4. Influences of γ-PGA-NHS esters on the pI and T_d values of collagens

Isoelectric point (pI) is an important parameter of proteins, which is related to the proportion of acid amino and basic amino residues in protein. It is well known that a protein usually has the worst solubility when the pH of solution was at the pI [46, 47]. Fig. 5 displayed the zeta potential curves as a function of pH, from which the pI of the native collagen and collagens modified by γ-PGA-NHS esters can be obtained at the point when zeta potential was zero. According to the curves, the pI of the un-modified collagen was recorded to be 6.91, located at the neutral region, which was in accordance with results previously reported [48, 49], suggesting that the prepared collagen kept its side amide residues intact. For collagens modified with γ-PGA-NHS(1/20) or γ-PGA-NHS(1/5), pI values were found to drop rapidly with increasing modifier/collagen from

5% to 50%, indicating that the solubility of collagen in neutral pH buffer would be improved. The decrease in pI values could be ascribed to two reasons: on one hand, the number of Ɛ-amino groups on the side amide residues of collagen were reduced due to the cross-linking reaction between amino groups and γ-PGA-NHS esters; on the other hand, plentiful carboxyl groups derived from the γ-PGA-derivatives would be drawn into the modified collagen molecules since γ-PGA linked with collagen molecules. Hence, as for both of the two NHS-esters, in the range of modifier/collagen applied, pI values were decreased along with the increase of doses of γ-PGA-NHS esters.

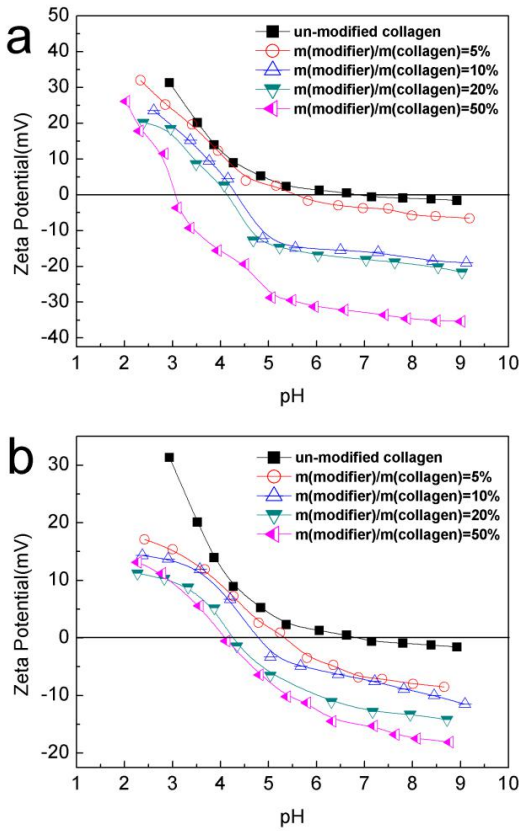

Fig.5 Zeta potential of the native collagen and collagens modified with different γ-PGA-NHS esters (a) γ-PGA-NHS(1/20); (b) γ-PGA-NHS(1/5) with various modifier/collagen ratios (w/w).

DSC thermograms of the native collagen and collagens modified using γ-PGA-NHS(1/20) or γ-PGA-NHS(1/5) with various doses are shown in Fig.6. Endothermal peaks associated with the helix-coil transition due to the thermal disruption of hydrogen bonds, which was thought to stabilize the triple helix of collagen [50, 51], could be detectable from the heat flow curves as a function of temperature. The un-modified collagen had a denaturation temperature (T_d) of 38.8 ±0.3 °C, which was in line with those previously reported [52, 53]. As for the modified collagens, the T_d values were located in the region of 44.8-49.9 °C, which means that the T_d values were 6.0-11.1 °C higher than that of the un-modified one, contrary to the results of succinylation modification [6]. Compared with the results from many other modification methods, the increase of T_d by the use of γ-PGA-NHS esters seemed to be remarkable. For instance, Tian et al. [54] cross-linked collagen solutions using GTA and found that the T_d increased by 2.0 °C at most compared with the uncross-linked collagen solution when GTA/collagen ratio (w/w) = 0.3. Ding et al. [52] prepared collagen/HPMC blended solution and found that the increase of T_d for the modified collagen solution was no more than 1.2 °C.

Compared with either the chemical modification by micromolecule-based modifiers such as GTA or the simple blending modification with other macromolecules such as HPMC, the modification of collagen with γ-PGA-NHS esters seems more

complex. That is, both of the two effects could be found in the γ-PGA-NHS ester/collagen modification blends: one was the chemical cross-linking effect, resulted from the formation of stable amide bonds between NHS-ester groups of γ-PGA and $–NH_2$ groups of collagen; the other was the hydrogen bonding between γ-PGA and collagen macromolecules, since the existence of α-COOH groups from γ-PGA and the $–NH_2$ or –OH groups from collagen makes the hydrogen bonding easy to form. Generally, the thermal stability of collagen in the blends with other biopolymers could be improved by the multipoint hydrogen bonding interactions between the two components, which has been demonstrated in many blending systems, such as collagen/HPMC [52, 55], collagen/cellulose [56], and (succinylated collagen)/CMC [57]. Therefore, the significant improvement in T_d of collagens modified by γ-PGA-NHS esters could be ascribed to both of the cross-linking effect and hydrogen bonding between the two macromolecules.

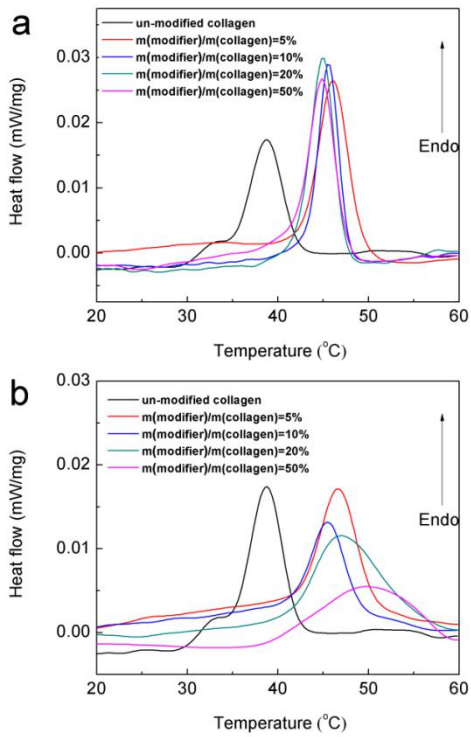

Fig.6 Typical DSC thermograms of the native collagen and collagens modified with different γ-PGA-NHS esters (a) γ-PGA-NHS(1/20); (b) γ-PGA-NHS(1/5) with various modifier/collagen ratios (w/w).

To further reveal the dual-effects of γ-PGA-NHS ester on the pI and T_d values of collagen, the curves of pI and T_d as functions of modifier/collagen were plotted (as shown in Fig. 7a), based on the data of Fig. 5 and Fig. 6. The pI values were reduced with the increase of modifier/collagen. While with respect to the T_d values, as modifier/collagen ≤ 10%, a decrease in T_d could be observed for both of the two γ-PGA-NHS esters; as modifier/collagen ratios were further increased to 20%-50%, the T_d value was continuously declined for collagen modified by γ-PGA-NHS(1/20), however, a jump could be observed for collagen modified by γ-PGA-NHS(1/5).

In addition, as shown in Fig. 7b, for both the two γ-PGA-NHS esters, a higher cross-linking degree could be obtained with increasing the modifier/collagen ratios, suggesting that the NH_2-linking of collagens occurred [19]. Moreover, the cross-linking degrees of γ-PGA-NHS(1/5) were always significantly greater than those of γ-PGA-NHS(1/20) at each modifier/collagen ratio. Thus, it could be speculated that the jump of T_d with a large dose of γ-PGA-NHS(1/5) used was related to the greater cross-linking degrees for collagen.

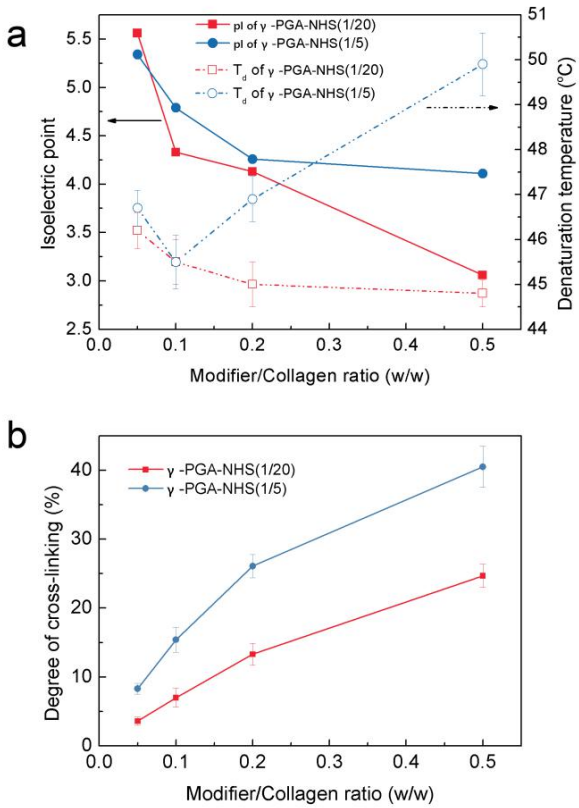

Fig.7(a) The pI and Td curves as a function of the dose of γ-PGA-NHS(1/20) and γ-PGA-NHS(1/5), respectively. (b) The degree of cross-linking of collagens modified with γ-PGA-NHS(1/20) and γ-PGA-NHS(1/5) as a function of γ-PGA-NHS ester/collagen ratios (w/w), expressed as the percentage of primary amine group content lost after cross-linking.

3.5. The microstructure of modified collagens

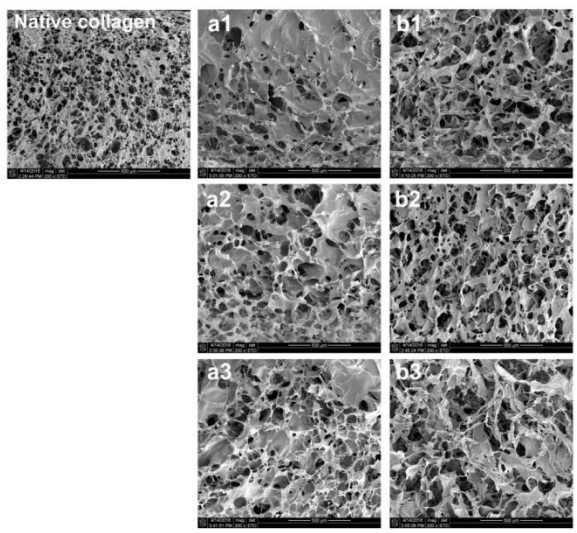

Fig.8 FESEM images (scale bar = 500 μm) of the surface of the native collagen and collagens modified using γ-PGA-NHS esters (a) γ-PGA-NHS(1/20); (b) γ-PGA-NHS(1/5) with different modifier/collagen ratios: (a1, b1), 5%; (a2, b2), 10%; (a3, b3), 50%.

FESEM images as shown in Fig.8 indicate a well-ordered porous structure of native collagen. As for collagens modified by

γ-PGA-NHS(1/20) and γ-PGA-NHS(1/5), when modifier/collagen = 5%, the overall network structure seems to be less homogeneous (Fig.8a1 and b1, respectively) than that of native collagen; when modifier/collagen was increased to 10%, the structures for both of the two samples became homogeneous (Fig.8 a2 and b2, respectively), together with many pores and filaments compared to those modified with modifier/collagen = 5%; as modifier/collagen was up to 50% (Fig.8 a3 and b3, respectively), the microstructure of collagen modified by γ-PGA-NHS(1/20) grew more homogeneous, and more pores and filaments could be observed. On the contrary, collagen modified by γ-PGA-NHS(1/5) exhibited a less regular morphology consisted of a crowd of sheet-like structures compared to that modified with modifier/collagen = 10%. The deterioration of collagen sponge network at this point (γ-PGA-NHS(1/5) with dose of 50%) might reflect the formation of the disorganized aggregates in solution was induced by the excessive cross-linking effect of modifier [58].

3.6. The mechanism of the dual-function effects of γ-PGA-NHS esters on collagen

The multi-impact of modification with γ-PGA-NHS esters as modifiers on the structure of collagen was illustrated by a simplified scheme (Fig.9). Collagen is a kind of polyampholyte, which carry equal positive and negative charges in the neutral pH buffer (visible in Fig.10). Thus, the native collagen does not swell or dissolve in the neutral water. In the present work, γ-PGA-NHS esters were employed as modifiers to reduce the pI of collagen. As illustrated in Fig.9, the activated NHS-ester groups of γ-PGA-NHS esters could react with the Ɛ-amino groups of the lysine or hydroxylysine residues on the side chains of collagen, to form a stable amide bond, leading to the cross-linking between collagen molecules and γ-PGA-NHS esters. The water-soluble collagen was fabricated successfully via this method, as indicated by the formation of clear solution at pH 7.0 (visible in Fig.10).

In details, with respect to γ-PGA-NHS esters with relatively low degree of esterification (γ-PGA-NHS(1/20)), when modifier/collagen = 5%, pI value was decreased slightly, leading to the aggregation of collagen molecules due to the weak electrostatic repulsion between collagen chains when dispersed in neutral water [59]. Therefore, the water solubility and the microstructure of collagen were not undesirable, but the T_d value was significantly higher than that of native collagen; when more modifiers were added (modifier/collagen = 20% or 50%), more electronegative carboxyl groups carried by γ-PGA were introduced to collagens, so the pI value would be further deceased to the level far below the neutral pH, meanwhile the cross-linking degree of collagen were still at a relatively low level. Therefore, the modified collagens could be well dissolved in neutral water to form clear solutions (as shown in Fig.8 a1, a2, a3), bringing about the uniform morphologies of sponges but a slight reduction in T_d value (but the T_d value of this modified collagen was still 6 °C higher than that of the native collagen).

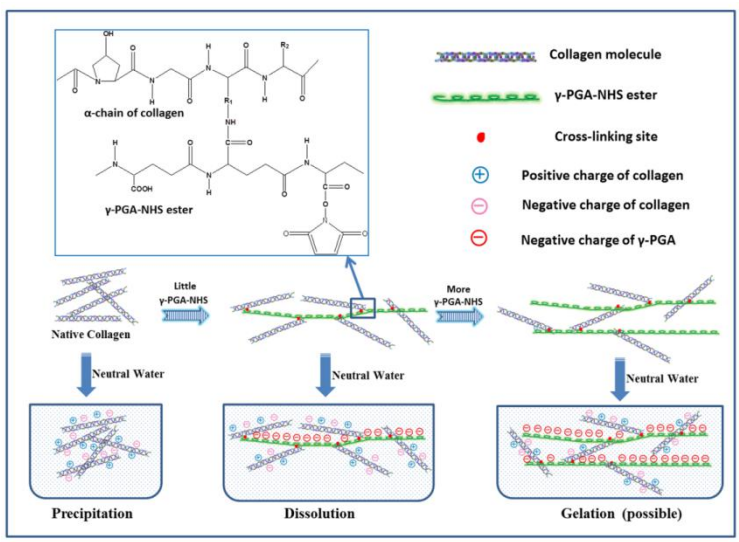

Fig.9 Schematic mechanism illustrating the interactions between γ-PGA-NHS esters and collagen macromolecules.

As for γ-PGA-NHS ester with higher degree of esterification (γ-PGA-NHS(1/5)), in the beginning the trend similar to that of γ-PGA-NHS(1/20) can be observed when a small amount of modifier were added to collagen (modifier/collagen ≤ 10%) (as shown in Fig.8 b1, b2). However, as more doses of γ-PGA-NHS(1/5) were added, the greater cross-linking degree enabled more collagen macromolecules to form multi-point cross-links with γ-PGA, compared to γ-PGA-NHS(1/20) with the same doses. Therefore, although the pI of collagen still decreased continuously, the water solubility would not become better because actually gelation occurred (as shown in Fig.8 b3), and this was the reason for the abrupt rise of T_d values as well as the deterioration of collagen morphology. Kajiyama et al. [60] reported the gelation of collagen using NHS activated poly(a,β-malic acid) with esterification degrees of 22.0-89.1%, which was much higher than those employed in the present work (2.8% and 5.8%, respectively). Thus, for the purpose of preparing a flowable collagen solution but not a gel, neither the excessive esterification degree of γ-PGA nor the excessive cross-linking degree of collagen was desired.

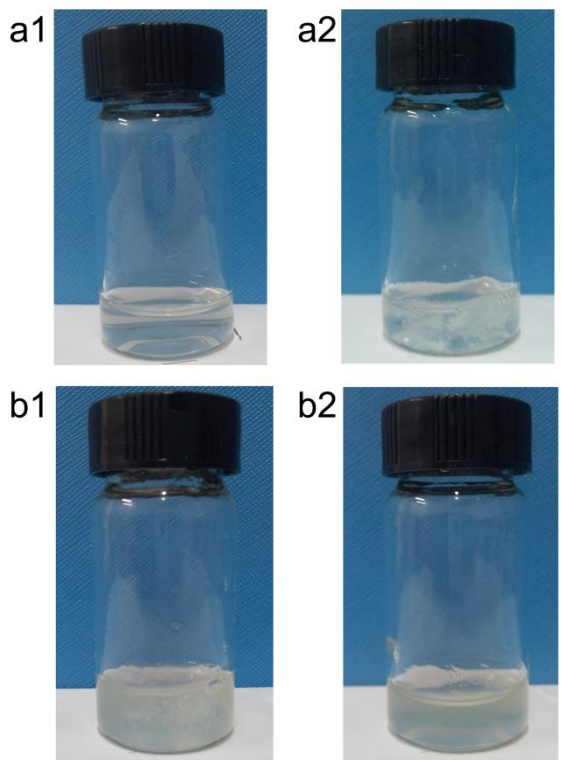

Fig.10 The status of the native collagen and collagen modified by γ-PGA-NHS(1/20) with modifier/collagen ratio (w/w) = 10%, dissolved in 0.1 mol/L acetic acidic solution (pH = 2.8) and 0.2 mol/L PBS (pH = 7.0), respectively. The native collagen was soluble in acetic acidic solution (a1) and could not be dissolved in neutral pH buffer (a2), while the modified collagen was soluble in neutral pH buffer (b2) and could not be dissolved in acetic acidic solution (b1).

3.7. Cytotoxicity of modified collagens

MTT has been widely accepted as a characterization method for the cell attachment and proliferation. The results of the cell viability assay of HFF-1 fibroblasts seeded on collagens modified by different γ-PGA-NHS esters was compared to that of fibroblasts seeded on the native collagen and the neat γ-PGA, as measured by fluorescence optical density (OD) shown in Fig.11. A superior affinity of the cells to the pure γ-PGA compared with the native collagen could be observed. This result was in line with a previous report [61], which indicated that γ-PGA was favorable for the proliferation of L929 fibroblast. So the affinity of the cells to the modified collagens could be improved by the introduction of γ-PGA, as exhibited in the figure.

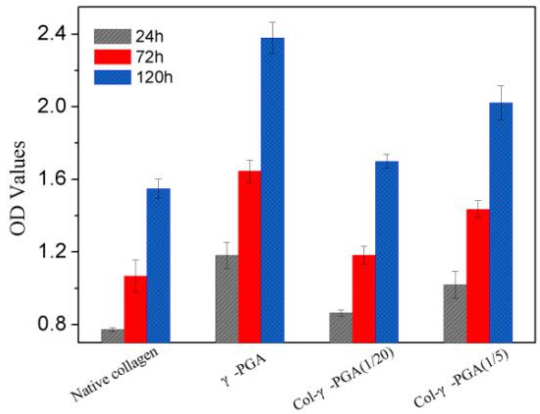

Fig.11 The viability displayed as OD curves of fibroblasts on the native collagen, γ-PGA, and collagens modified by γ-PGA-NHS(1/20) and γ-PGA-NHS(1/5) at different time intervals (1, 3, 5 days), $p < 0.05$. The modifier/collagen ratio (w/w) = 20%.

4. Conclusion

To endow collagen a better thermal stability and to maintain its biocompatibility, in this study collagen was modified by a natural polymer derivative γ-PGA-NHS ester. FTIR and ^{1}H-NMR spectra showed that γ-PGA-NHS ester was successfully synthesized. After cross-linked with γ-PGA-NHS ester, collagen retained the native triple helix structure,the modified collagen can be dissolved in the neutral pH water to form a clear solution due to the decrease of isoelectric point (pI); meanwhile, the modified collagen had a significantly improved denaturation temperature (T_d), which was at least 6.0 °C higher than that of the native collagen; the MTT assay and DAPI method implied that the affinity of the cells to the modified collagens could be improved. The results provide some useful information for the design of collagen structure via multi-functional chemical modification, and are in favour of the application of aqueous collagen in the fields including cosmetics, biomaterials etc.

Acknowledgements

This work was financially supported by the National Natural Science Foundation of China (Grant Nos. 21306024 and 21606046), the Natural Science Foundation of Fujian Province (Grant No. 2016J01208).

References

1. M. G. Patino, M. E. Neiders, S. Andreana, B. Noble and R. E. Cohen, *Implant Dentistry*, 2002, **11**, 280-285.
2. W. Friess and G. Lee, *Biomaterials*, 1996, **17**, 2289-2294.
3. X. Yu, C. Tang, S. Xiong, Q. Yuan, Z. Gu, Z. Li and Y. Hu, *Current Organic Chemistry*, 2016, **20**, 1-1.
4. S. H. Kim, J. H. Lee, S. Y. Yun, J. S. Yoo, C. H. Jun, K. Y. Chung and H. Suh, *Rapid Communications in Mass Spectrometry*, 2000, **14**, 2125-2128.
5. R. Sripriya, R. Kumar, S. Balaji, M. S. Kumar and P. Sehgal, *Reactive and Functional Polymers*, 2011, **71**, 62-69.
6. Z. Zhang, W. Liu, D. Li and G. Li, *Bioscience, Biotechnology, and Biochemistry*, 2007, **71**, 2057-2060.
7. T. Nezu and F. M. Winnik, *Biomaterials*, 2000, **21**, 415-419.
8. D. DeVore, C. Kelman and W. Stark, *Refract Corneal Surg*, 1993, **9**, 208-209.
9. R. Kumar, R. Sripriya, S. Balaji, M. S. Kumar and P. Sehgal, *Journal of Molecular Structure*, 2011, **994**, 117-124.
10. G. P. Huang, S. Shanmugasundaram, P. Masih, D. Pandya, S. Amara, G. Collins and T. L. Arinzeh, *Journal of Biomedical Materials Research Part A*, 2015, **103**, 762-771.
11. C. L. Hawkins and M. J. Davies, *Biochimica Et Biophysica Acta*, 2001, **1504**, 196-219.
12. M. J. van Luyn, P. B. van Wachem, L. O. Damink, P. J. Dijkstra, J. Feijen and P. Nieuwenhuis, *Journal of Biomedical*

Materials Research Part A, 1992, **26**, 1091–1110.

13. J. Kozłowska and A. Sionkowska, *International Journal of Biological Macromolecules*, 2015, **74**, 397-403.

14. R. Usha, K. Sreeram and A. Rajaram, *Colloids and Surfaces B: Biointerfaces*, 2012, **90**, 83-90.

15. A. Satyam, G. S. Subramanian, M. Raghunath, A. Pandit and D. I. Zeugolis, *Journal of Tissue Engineering & Regenerative Medicine*, 2014, **8**, 233–241.

16. C. M. P. Vidal, A. A. Leme, T. R. Aguiar, R. Phansalkar, J. W. Nam, J. Bisson, J. B. Mcalpine, S. N. Chen, G. F. Pauli and A. Bedranrusso, *Langmuir the Acs Journal of Surfaces & Colloids*, 2014, **30**, 14887-14893.

17. R. Tu, S. H. Shen, D. Lin, C. Hata, K. Thyagarajan, Y. Noishiki and R. C. Quijano, *Journal of Biomedical Materials Research Part A*, 1994, **28**, 677-684.

18. H. Petite, I. Rault, A. Huc, P. Menasche and D. Herbage, *Journal of Biomedical Materials Research Part A*, 1990, **24**, 179–187.

19. D. M. C. Vergne, R. A. Batista, M. M. Freitas, O. D. Freitas, N. L. Pereira and J. C. Cardoso, *Journal of Thermal Analysis & Calorimetry*, 2017, 1-9.

20. C. Mu, F. Liu, Q. Cheng, H. Li, B. Wu, G. Zhang and W. Lin, *Macromolecular Materials and Engineering*, 2010, **295**, 100-107.

21. T. Du, Z. Chen, H. Li, X. Tang, Z. Li, J. Guan, C. Liu, Z. Du and J. Wu, *International Journal of Biological Macromolecules*, 2016, **82**, 580-588.

22. B. Kaczmarek, A. Sionkowska and A. M. Osyczka, *International Journal of Biological Macromolecules*, 2017.

23. Z. Luo, G. Yuan, J. Liu, Q. Hua, M. Zhao, Z. Wei and S. Li, *Biotechnology for Biofuels*, 2016, **9**, 134.

24. J. P. D. Garcia, M.-F. Hsieh, B. T. Doma, D. C. Peruelo, I.-H. Chen and H.-M. Lee, *Polymers*, 2013, **6**, 39-58.

25. C.-Y. Hsieh, S.-P. Tsai, D.-M. Wang, Y.-N. Chang and H.-J. Hsieh, *Biomaterials*, 2005, **26**, 5617-5623.

26. S. Yan, X. Zhang, K. Zhang, H. Di, L. Feng, G. Li, J. Fang, L. Cui, X. Chen and J. Yin, *Journal of Materials Chemistry B*, 2016, **4**, 947-961.

27. S.-H. Cho, A. Kim, W. Shin, M. B. Heo, H. J. Noh, K. S. Hong, J.-H. Cho and Y. T. Lim, *International Journal of Nanomedicine*, 2017, **12**, 2607-2620.

28. M. Zhang, K. Wu and G. Li, *Int J Biol Macromol*, 2011, **49**, 847-854.

29. H. Saito, T. Taguchi, H. Kobayashi, K. Kataoka, J. Tanaka, S. Murabayashi and Y. Mitamura, *Materials Science and Engineering: C*, 2004, **24**, 781-785.

30. M. Zhang, J. Li, C. Ding, W. Liu and G. Li, *Food Hydrocolloids*, 2013, **30**, 504-511.

31. H. Iwata, S. Matsuda, K. Mitsuhashi, E. Itoh and Y. Ikada, *Biomaterials*, 1998, **19**, 1869-1876.

32. A. Bigi, G. Cojazzi, S. Panzavolta, K. Rubini and N. Roveri, *Biomaterials*, 2001, **22**, 763-768.

33. N. Nagai, S. Yunoki, T. Suzuki, M. Sakata, K. Tajima and M. Munekata, *Journal of Bioscience and Bioengineering*, 2004, **97**, 389-394.

34. Y.-H. Lee, J.-J. Chang, W.-F. Lai, M.-C. Yang and C.-T. Chien, *Colloids and Surfaces B: Biointerfaces*, 2011, **86**, 409-413.

35. Y. Hu, W. Dan, S. Xiong, Y. Kang, A. Dhinakar, J. Wu and Z. Gu, *Acta Biomaterialia*, 2017, **47**, 135-148.

36. J. Ward, J. Kelly, W. Wang, D. I. Zeugolis and A. Pandit, *Biomacromolecules*, 2010, **11**, 3093-4101.

37. C. T. Tsao, C. H. Chang, Y. Y. Lin, M. F. Wu, J. L. Wang, T. H. Young, J. L. Han and K. H. Hsieh, *Carbohydrate Polymers*, 2011, **84**, 812-819.

38. M. Saeko and N. Aoki, *Biomacromolecules*, 2006, **7**, 2122-2127.

39. X. Liu, H. Cheng, T. Zhao and C. Zhang, *Journal of Colloid and Interface Science*, 2014, **426**, 117-123.

40. R. L. Schnaar and C. L. Yuan, *Biochemistry*, 1975, **14**, 1535-1541.

41. X. Liu, W. Dan, H. Ju, N. Dan and J. Gong, *Rsc Advances*, 2015, **5**, 52079-52087.

42. H. Yang, L. Lan, Z. Gu, W. Dan, N. Dan and X. Yu, *Carbohydr Polym*, 2014, **102**, 324-332.

43. X. Liu, N. Dan and W. Dan, *International Journal of Biological Macromolecules*, 2016, **88**, 179-188.

44. A. Sionkowska, J. Skopinska-Wisniewska, M. Gawron, J. Kozlowska and A. Planecka, *International Journal of Biological Macromolecules*, 2010, **47**, 570-577.

45. G. Goissis, L. Piccirili, J. C. Goes, A. M. De Guzzi Plepis and D. K. Das‐Gupta, *Artificial Organs*, 1998, **22**, 203-209.

46. D. Pelegrine and C. Gasparetto, *LWT-Food Science and Technology*, 2005, **38**, 77-80.

47. H. Dawes, S. Boyes, J. Keene and D. Heatherbell, *American Journal of Enology and Viticulture*, 1994, **45**, 319-326.

48. J. H. Highberger, *Journal of the American Chemical Society*, 1939, **61**, 2302-2303.

49. Z. Zhang, G. Li and B. Shi, *Journal of the Society of Leather Technologists and Chemists*, 2006, **90**, 23.

50. H. Tang, A. Covington and R. Hancock, *Journal of Agricultural and Food Chemistry*, 2003, **51**, 6652-6656.

51. B. Brodsky and A. V. Persikov, *Advances in Protein Chemistry*, 2005, **70**, 301-339.

52. C. Ding, M. Zhang and G. Li, *Journal of Applied Polymer Science*, 2014, **131**.

53. W. Liu and G. Li, *Polymer Degradation and Stability*, 2010, **95**, 2233-2240.

54. Z. Tian, C. Li, L. Duan and G. Li, *Connective tissue research*, 2014, **55**, 239-247.

55. C. Ding, M. Zhang and G. Li, *Carbohydrate Polymers*, 2015, **119**, 194-201.

56. M. Zhang, C. Ding, L. Huang, L. Chen and H. Yang, *Cellulose*, 2014, **21**, 3311-3322.

57. M. Zhang, C. Ding, J. Yang, S. Lin, L. Chen and L. Huang, *Carbohydrate Polymers*, 2016, **137**, 410-417.

58. M. Zhang and G. Li, *Journal of Aquatic Food Product Technology*, 2014, **23**, 44-58.

59. Y. Li, A. Asadi, M. R. Monroe and E. P. Douglas, *Materials Science and Engineering: C*, 2009, **29**, 1643-1649.

60. T. Kajiyama, H. Kobayashi, T. Taguchi, H. Saito, Y. Kamatsu, K. Kataoka and J. Tanaka, *Materials Science and Engineering: C*, 2004, **24**, 815-819.

61. C. T. Tsao, C. H. Chang, Y. Y. Lin, M. F. Wu, J.-L. Wang, J. L. Han and K. H. Hsieh, *Carbohydrate research*, 2010, **345**, 1774-1780.

P76

Clean Tanning Technologies Based On Chrome Free Tanning Agent TWS

Li Jing[1], Shi Bi[2], Li Bin[3], Yan Lan[3], Zhang Jing[3]

[1]*Sichuan Tingjiang New Material, Inc., Shifang, Sichuan, China;*

[2]*National Engineering Laboratory for Clean technology of Leather Manufacture, Sichuan University, Chengdu, China;*

[3]*Foshan Shunde Longting New Material co., LTD, Foshan, Guangdong, China.*

Abstract

Many clean tanning technologies have been proposed owing to chrome pollution problems, but few were widely used. One of the main reasons is that the comprehensive performance of chrome-free tanned leather is not comparable with that of chrome tanned leather. In this study, two kinds of clean tanning technology based on wet white tanned by TWS were investigated. TWS, a novel amphoteric organic tanning agent and synthesized based TWT, posseses smaller molecule weight and can be used to tan bated pelts directly without pickling or salts. So this tannage dose not results in chloride pollution. Moreover, TWS tanning effluent is recycling for water conversation. Two kinds of technology were shown below. The first one, the wet white was directly filled and retanning by using organic materials to produce finished leather without metal salts. By this technology, the comprehensive performance of leather is perfect, but the Ts is only 80～85°C. The second one is named as reversed technology, because in this procedure, retanning, fatliquoring and coloring processes of wet white were carried out before chrome retanning. So in this technology, the chrome contained effluent is only concentrated in the last chrome retanning process and can be treated easily. Moreover, the leather made with this technology has complete conventional chrome-tanned leather quality.

Keywords: tannage, wet white, chrome-free tanning, reversed tannage

P77

Enhancement of Mass Transfer of Protease in Bating Process

Ying Song[1], Qian Yang[1], Yunhang Zeng[1*], Mingrong Cao[2], Bi Shi[1,2]

[1]*National Engineering Laboratory for Clean Technology of Leather Manufacture, Sichuan University, Chengdu 610065, P. R. China, Tel: +86-028-8540-5508, E-mail: zengyunhang@scu.edu.cn*

[2]*Key Laboratory of Leather Chemistry and Engineering (Sichuan University), Ministry of Education, Chengdu 610065, P. R. China*

Abstract

Collagen in surface layers of pelts is liable to be hydrolyzed excessively in bating process due to the low transfer rate and the high reaction rate of protease in pelt, and therefore effects of molecular weight of protease, dosage of protease and auxiliaries on mass transfer of protease as well as collagen damage in bating were investigated to avoid the excessive collagen hydrolysis. It was observed that the protease with lower molecular weight transferred faster in pelt by using fluorescent tracer technique. An increase in the dosage of protease led to a faster transfer of protease but greater damage to grain. Additionally, bating with protease like trypsin and proper auxiliaries (e.g. fatty alcohol-polyoxyethylene and ammonium sulfate) together enhancedthe mass transfer of protease in pelt and reduced the collagen damage. This is mainly because the use of fatty alcohol-polyoxyethylene ether decreased the interfacial tension of trypsin and thus improved its penetrability. The use of ammonium sulfate increased negative charges of trypsin and reduced the electrostatic attraction between trypsin and the pelt (pI 7.0) during bating (pH 8.5),thus promoting the penetration of trypsin in pelt. These results suggested that employing proteases with lower molecular weight and adjusting the interfacial tension and the electrostatic interaction between protease and pelt are effective in enhancement of mass transfer of protease in pelt and reduction in excessive damage to collagen.

Keywords: bating; protease; mass transfer; molecular weight; interfacial tension; electrostatic interaction

P78

Study on Treatment of Leather WastewaterUsingChitosan Composite Flocculant

ZHENG Shun-ji ZHANG Jing-bin JIN Hao

(1. Light industry and weaving department, Qiqihar University，Qiqihar 161006;)

Abstract： The rare earth-chitosan composite flocculant was used to treat tanning wastewater, the treatment process and optimum processing conditions were discussed.The effect of pH value ,the amount of compound floucculant, temperature and stiring time on the removal rate of totle chrome ,chemical oxygen demand (COD)and turbidity were studied with single factor experiment method, the results showed that the optimum treatment conditions were that the amount of chitosancomposite flocculant was 0.25g/L, pH value was 6.5~7, temperature was 35 ～ 45 ℃,stiring time was 10~20min..The rare earth-chitosan composite flocculant shows obvious advantages compared with poly aluminium chloride and polymeric ferric sulfate.

Key words : rare earth; chitosan; flocculant; tanning wastewater； COD; turbidity

Tannery wastewater is one of industrial wasterwater which is difficult to treat, It is characterized by complex composition, high COD value, high chromaticity, and containing a large number of sulfide, chromium and other harmful substances[1]. Flocculation precipitation is a common method in the treatment of leather wastewater. The technical core of the method is to develop new type of flocculant. Chitosan is a kind of natural macromolecular flocculant, which has the advantages of low price, easy availability and non-toxicity. Its application in water treatment has been gradually popularized in recent years. Compared with traditional chemical flocculants, chitosan has the characteristics of fast sedimentation rate, low dosage and high removal efficiency, and has a broad application prospect[2-5] Chitosan molecules have amino and amide groups, which makes it to be natural cationic flocculant .Because of the negative charge of many dirt in tannery wastewater, chitosan can coagulate with dirt and precipitate, which can be used for dyeing, retanning and depilating wastewater with negative charge. Moreover, the amino and hydroxyl groups in chitosan molecules can form stable chelates with heavy metal ions such as Cr^{3+}, Cr^{6+} and $Al^{3+}$and precipitate.Thus, heavy metal ions such as chromium and aluminum in leather wastewater can be effectively treated [6].Some researchers have tried to apply modified chitosan to chrome tanning wastewater, and the removal rate of Cr reaches 94%[7], which has a good application prospect in the treatment of leather wastewater.As a flocculant, rare earth can not only remove suspended matter in water, but also remove COD more effectively. It has a significant synergistic effect as compounded with chitosan. In recent years, studies on the synthesis of rare earth and poly aluminum chloride or rare earth and chitosan, cellulose, etc. into a rare earth-inorganic polymer composite coagulant or a rare earth -organic polymer composite coagulant have started, and have been applied in the treatment of various kinds of wastewater [8]. This study attempted to combine chitosan and rare earth to treat leather wastewate and explored the effect of compound flocculant on leather wastewater treatment to lay a foundation for further application of compound flocculant.

1 materials and methods

Experimental materials

Chitosan, analysis pure, Chlorinated persimmon (rare earth), analysis pure

1.2 The preparation of chitosan - rare earth compound flocculant

0.500 g chitosan (molecular weight: 800,000) was taken to place into a 250ml beaker.then 20 ml glacial acetic acid was added and beaker mouth was sealed with plastic wrap to reduce the volatilization. The chitosan was heated to 40 ~ 50 ℃ and stirred fully with magnetic stirrer until chitosan was dissolved completely (usually mixing time is 2 ~ 4 h); The dissolved chitosan solution was transfered into 500 ml volumetric flask and glacial acetic acid was used to wash beaker and glass rod three times,then transfering washing liquid into volumetric flask to make 500 ml. Finally rare earth and prepared chitosan solution were mixed in a ratio of 3:7 and stirred 24h to be miscible to form 10 g/l rare earth - chitosan composite flocculant.

1.3 Flocculation process of wastewater

400mL tannery wastewater (total chromium: 35mg/L, COD: 2985mg/L, turbidity: 1300FTU) was taken to put into 500mL beaker and 0.1000mol/l halic acid or 0.1000mol/l sodium hydroxide was added to adjust the pH of wastewater. After stirring uniformly with electrical stirrer, the rare earth - chitosan composite flocculant solution was added ,stirring again. After standing for 30min the supernatant was taken to measure total chromium, turbidity and COD and analyze.

1.4 Analysis and test

1.4.1 Determination of total chromium in wastewater

Diphenylcarbonyl dihydrazine colorimetric method was used.

1.4.2 Determination of COD

Potassium dichromate method was used

1.4.3Turbidity

The transmittance of waste water was determined by spectrophotometry to measure the removal of turbidity of waste liquid

Removal rate % = [(A-B)/B] * 100%

Where: A is the transmittance of sewage after treatment; B is the transmittance of sewage before treatment.

2 Results and discussion

2.1 The influence of treatment conditions on treatment effect

2.1.1 The influence of pH value on flocculation effect of chitosan composite flocculant

The flocculation experiment was carried out with changing pH value of waste water to discuss the influence of pH value on treatment effect in 20 ℃, 0.15 g/L dosage of chitosan composite flocculant, The results were shown in figure 1, 2.

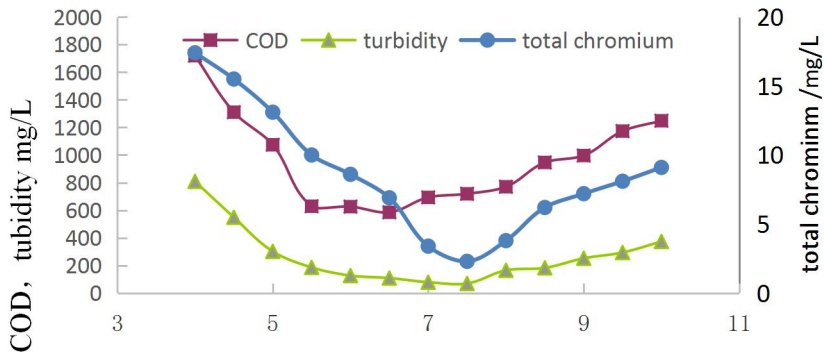

Fig1.The influence of pH on the concentrationt in waste water

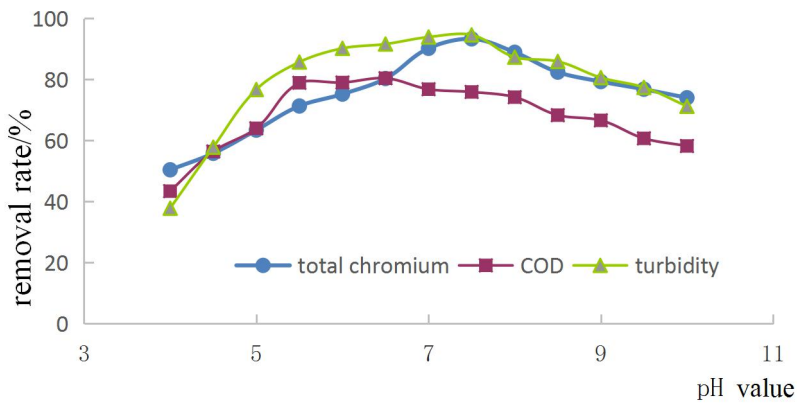

Fig2.The influence of pH on waste water treatment

From figure 1, 2, it can be seen that the removal rate of total chromium , COD and turbidity in wastewater increased with increase of pH value in waste water. The removal rate of COD achieved 80.4% at pH 6 in waste water ,whereas the removal rate of total chromium, , turbidity achieved best at about pH 7.5 ,they were 93.3% and 94.6% respectively. The removal rate of each substance were decreased above optimal pH value.This is because the removal of organic matter in waste water with the rare earth - chitosan composite flocculant is mainly through electrical neutralization and adsorption bridging. In acidic conditions the amino group in chitosan molecular chain can combine with H^+ in the solution to give it positive charge.Introducing rare earth will enhance the electropositivity of flocculant, so as to make it easier to adsorb negatively charged organic substance and inorganic reducing material such as sulfide in solution and neutralize surface charge to form flocculate more easily to sedimentate . But if pH is too low chitosan will combine more H^+ in water and become more positive, at the same time amino group will lose the ability to fix organic matter such as dyestuff because of combinding H^+ by N in amino group. However if pH is too high chitosan cann't combine negatively charged organism because of lack of electropositivity and solubility , which lead to decrease of ability of chitosan to remove COD[9]. The removal of chromium in waste water is mainly through the chelate action of active group such as hydroxyl, amimo .etc.When waste water is acid ,the hydrogen ion will combine with amino group in chitosan to form $-NH_3^+$ to decrease the amount of active group in chitosan. So the ability to absorb metal ion decrease greatly. The amino group in chitosan chain is released to increase ability to absorb metal ion greatlywith increase of pH value, but if pH value is too high the flocculation effect is poor because of causing partial chromium ion to form hydroide[10]. All things considered .pH value of 7 should be chosen.

2.1.2The influence of concentration of composite flocculant on flocculation effect

The flocculation experiment was carried out with changing the amount of flocculant to discuss the influence of concentration of composite flocculant on treatment effect in 20 ℃, pH 7, The result was shown in figure 3

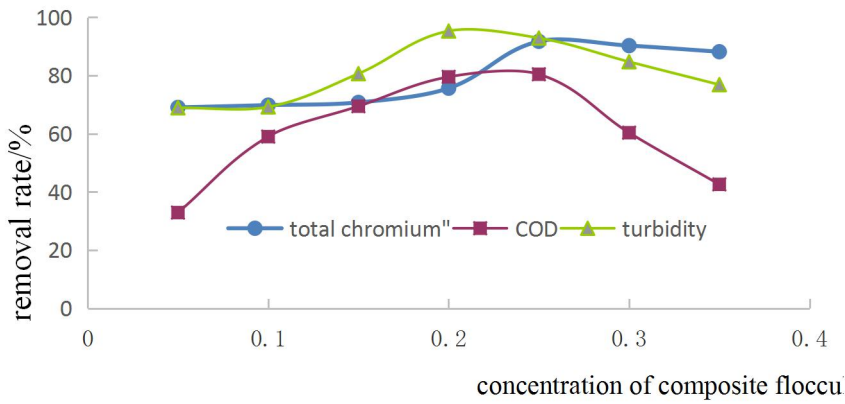

Fig3.The influnce of concentration of composite flocculant on waste water treatment

It can be seen from figure 3 that the amount of compound flocculant had a great influence on the treatment effect of various substances in wastewate . The removal rate of total chromium,COD and turbidity in wastewater increased with increase of the amount of compound flocculant.The removal rate of total chromium achieved maximum-91.7% when the the amount of flocculant was 0.25g/L and COD and turbidity were 80.4% and 95.2% respectively when the amount of flocculant was 0.20g/L. Then, with the continuous increasing of the amount, the removal rate of total chromium, COD and turbidity all showed a downward trend,.Among them COD decreased the fastest..It may be because the addition of too much chitosan will cause secondary adsorption on the surface of colloidal particles and cover the chitosan molecules so that the pollutants can be dispersed again in the solution, and the flocculation effect become worse. In addition, when the dosage of composite flocculants is too large, these flocculants will combine with organic compounds in the wastewater to form floc in wastewater

and more flocculants will be dissolved and dispersed in the treated water. As a result, although the concentration of organics such as dyes in wastewater has decreased, the increase of organics concentration caused by the dissolution of chitosan in water will increase the COD of wastewater[11].

2.1.3 The influence of temperature on flocculation effect.

The flocculation experiment was carried out with changing the temperatue of flocculant to discuss the influence of temperature on treatment effect in 0.15 g/L dosage of chitosan composite flocculant,, pH 7.The results is shown in figure 4.

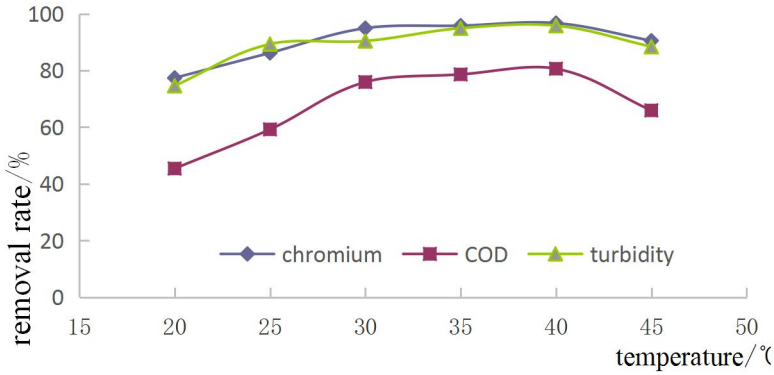

Fig4.The influnce of temperature onwaste water treatment

It can be seen from figure 4 that the temperature has a certain influence on the removal of various substance. In general, with the increase of the temperature, the removal rate of all substances increased. The effec of flocculation was the best in 30~40 ℃. The rate of total chromium can reach 96.7%, the removal rate of COD, , turbidity acheived about 80.6%and 95.6%. But it was found that with the increase of the temperature the removal rate of each material in waste water varied little and tended to be stable in range of 30 ~ 40 ℃. Take total chromium as example although the removal rate of total chromium in wastewater reached the maximum value in 40 ℃,it increased very little compared to 94.8% in 30℃. Inview of the energy cos and equipment cost temperature can be set at 30 ℃.

2.1.4 the influnce t of stirring time on flocculation effect

The effect of mixing time on the removal rate of various substances in wastewater was investigated by adding composite flocculant and stirring for a certain time, the result was shown in figure 5.

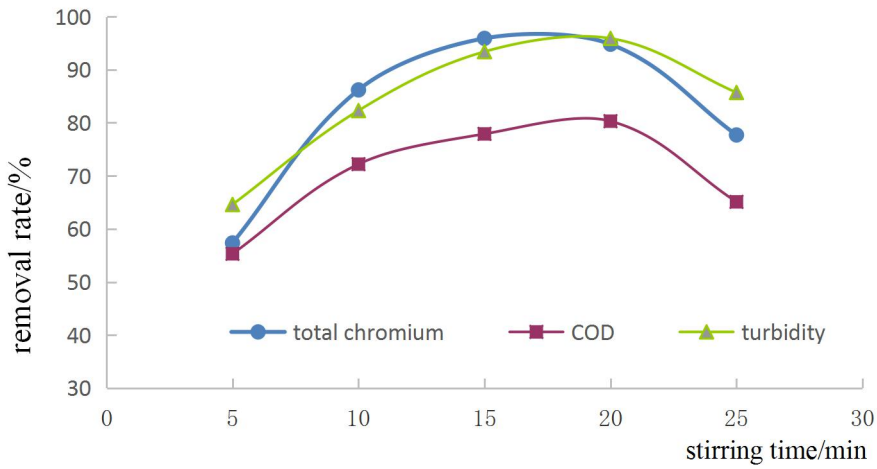

Fig5.The influnce of stirring time on waste water treatment

The purpose of stirring is to make the flocculant contact with the particles in the wastewater fully and form the floc .It can be seen that the effect is the best when the time of stirring is between 10~20min, more than 20min the removal rate of each substance in wastewater all decreased with the increase of stirring time, so it shouldn't be stirred too long . This is because if the stirring time is too long, the deposited particles are broken up and dispersed into small flocs or colloids, which reduce the settling speed and the flocculation effect become worse. However, the mixing time is too short the flocculant cannot fully contact with the colloidal particles, which is not good for flocculant to catch colloidal particles, and the flocculation effect is poor. So the stirring time was chosen 15min.

2.2 Treatment results of different flocculants on leather wastewater

In order to investigate the treatment effect of homemade composite flocculant, the treatment effect of this flocculant was compared with that of traditional flocculant-polyaluminum chloride and polyferric sulfate, the result was shown in table 1.

Tab1 .The treating result in different flocculant

	Removal rate of total chromium/%	Removal rate of COD /%	Removal rate of turbidity /%
chitosan composite flocculants	96.7	80.6	95.6
polyaluminum chloride	85.7	59.6	84.3
polyferric sulfate	88.9	60.3	90.4

It can be seen from table 1 that compared with the other two flocculants, chitosan composite flocculants have obvious advantages in wastewater treatment and the advantages of COD removal rate in waste water were the most obvious. The removal rate of COD is 21% higher than that of poly aluminum chloride, and 20.3% higher than that of poly aluminum sulfate. This is because flocculation of chitosan benefits from its special cationic structure, which can not only compress the diffusion layer of colloidal particle and make the clay colloidal particles condensate and destabilize by the condensation effect of electroneutralization, but also generates flocculation settlement by means of the bonding bridge of the polymer chain to remove organic sunstance in wastewater. In addition, rare earth flocculants can also make the colloidal particles sendimentate in wastewater by electroneutralization. Due to the high charge of rare earth metal ions, the colloidal materials with negative charge in wastewater can be quickly removed by the sedimentation. The combination of the above two substance can make them have synergistic effect and improve the flocculation effect[12], so the effect is better than that of aluminum salt and iron salt. In addition, rare earth-chitosan composite flocculant has a better removal effect on chromium than traditional flocculant. The removal rate of chromium in the experiment was as high as 96.7%, and the total chromium concentration in the wastewater is 1.15mg/L, which meet the waste water discharge standard.

Conclusion

It was found throuh experiment that rare earth - chitosan composite flocculation can be used to treat leather wastewater. The results showed that the amount of rare earth -chitosan composite flocculant ,pH value, temperature and mixing time had certain effects on the flocculation effect. The optimum conditions of treatment was that composite flocculant concentration was 0.25 g/L, pH value of 7, the temperature of 30 ~ 40 ℃, the mixing time was 10 ~ 20 min, under the condition the chromium content in the wastewater was 1.15 mg/L which meet the discharge standards. Compared with the other two flocculants polyaluminum chloride and polyferric sulfate chitosan composite flocculants had obvious advantages in wastewater treatment ,the advantages of COD removal rate in wastewater were the most obvious.

References

[1]Liu MingHua, ZhangXinShen, Jiang XiaoPing. Rreseach about the Adsorption Treatment of Sulphide or Chromiumcontaining Wastewater[J].China Leather, 2000, 29(11): 9- 12.

[2]Gülay Bayramoglu， Meltem Ylmaz， M Yakup Arca.Aity dye -ligand poly (hydroxyethyl

methacrylate)/chi－tosan composite membrane for adsorption lysozyme and kinetic properties[J]. Biochemical Engineering, 2003，7(13): 35-42.

[3] Wang YZ, Zheng JH, Bao DC. Mucoadhesive property of chitosan[J].Jounal of Clinical Rehabilitative Tissue Engineering Research, 2007，19(26): 5140-5143.

[4] Ren Jianmin,Ou Zhongwen. Thermodynamics and Kinertics of p-nitrophenol sorption by Chitosan/PVA Micro-partical from Water [J].Journal of Chongqing Jianzhu University, 2007，

29(3): 95-98.

[5]LiQiong, Xi Danli. Adsorption of Pb from Wastewater by Chitosan [J].Environmental Protection of Chemical Industry, 2005，25(5): 350-352.

[6] WANG Xue-chuan,QIANG Tao-tao,REN Long-fang .Chitosan Accelerates Sustainable Development of Leather Industry[J] FINE CHEMICALS，2006,23（6）：580-582.

[7] LIU Cun-hai, YU Ying, ZHANG Guang-hua . Preparation of Modified Chitosan and Application in Treating Tanning Wastewater [J].Leather and Chemicals,2011 ，28（3）: 1-4.

[8] ZHOUJin. Progress in the application of rare earth elements in wastewater treatment [J]. Environmental Protection of Chemical Industry,2009,29（4）：335-338

[9] Fan Dahe, Cai Zhaosheng. Study on the flocculating properties of composite flocculant of amphoteric chitosan derivative for treating printing and dyeing wastewater[J].Industrial Water Treatment2008 ，28（9）:7-50.

[10].Elwakeel K Z． Environmental application of chitosan resins for the treatment of water and wastewater: A review ［J］． Journal of Dispersion Science and Technology，2010， 31(3) : 273-288．

[11]DING Shi- qiang.Chitosan Treatment of Oily Wastewater by Composite Flocculant [J]. Journal of Filtration & Separatio，2009,19,(4)：13-15.

[12] ZHOUJin. Research on Treatment of Dyeing Wastewater Using Rare Earths-Chitosan Composite Flocculant [J]. Coal and chemicals,2013,26（2）：156-158.

P79

Role of Zinc Ions in Enzymatic Unhairing of Bovine Hides

Chen Mei[1], Chen Junyu[2],Chen Min[3], Cheng Haiming[4]*

[1]*Key Laboratory of Leather Chemistry and Engineering of Ministry of Education, Sichuan University, CHENGDU, 610065, CHINA, +86-28-85405839, 2016223080044@stu.scu.edu.cn*

[2]*Key Laboratory of Leather Chemistry and Engineering of Ministry of Education, Sichuan University, CHENGDU, 610065, CHINA, +86-28-85405839,2015141502004@stu.scu.edu.cn*

[3]*Key Laboratory of Leather Chemistry and Engineering of Ministry of Education, Sichuan University, CHENGDU, 610065, CHINA; National Engineering Laboratory for Clean Technology of Leather Manufacture, Sichuan University, CHENGDU, 610065, CHINA, +86-28-85405839, chenmin_zhou@163.com*

[4]*Key Laboratory of Leather Chemistry and Engineering of Ministry of Education, Sichuan University, CHENGDU, 610065, CHINA; National Engineering Laboratory for Clean Technology of Leather Manufacture, Sichuan University, CHENGDU, 610065, CHINA, +86-28-85405839, ChengHaiming@scu.edu.cn*

Abstract

Traditional hair-burning unhairing technique is the most polluting process in leather manufacturing. Enzymatic unhairing is eco-friendly approach to reducing sulfide pollution, COD and BOD during unhairing process. However, the disadvantages for enzymatic unhairing such as grain damage and excessive hydrolyzing of collagen are existed. In this study, Zn(II) ions have been utilized as inhibitor to AS1.398 protease for efficient and safe enzymatic unhairing. The effect of Zn(II) ions on the activity of collagenase and casease in AS1.398 protease during enzymatic unhairing was determined. The results showed that with the increase of Zn(II) ions' concentration, the activity of collagenase and casease decreased. Then, the effect of Zn(II) ions at different temperatures and enzyme dosages on enzymatic unhairing were investigated. The results illustrated that Zn(II) ions could be beneficial for reducing hydrolysis of hydroxyproline and decrease the grain damage in enzymatic unhairing. This approach could provide a cleaner and efficient method for enzymatic unhairing in leather manufacturing.

Key words: Enzymatic unhairing; AS1.398 protease; Zinc ions; Inhibitors; Bovine hide

P80

The Application of Interaction Design in the Field of Women's Shoes Design

YAO yun-he[123] DING wan-jing[3] LI xin-juan[3]

(Key Laboratory of Leather Chemistry and Engineering of Ministry of Education, Sichuan University ,National Engineering Laboratory fo r Clean Technology of Leather Manufacture, Sichuan University , Biomass and Leather Engineering Department,Sichuan University , Chengdu,610065,China)

Abstract: Interaction design is vital concept in the field of design,which emphasizes the interaction between products and users. With the development of the internet and new technologies,various interactive ways and interactive experience are getting rich. The concept of interaction design also applies to traditional shoe design. The passage analyzes the factors of children's psychological needs,aesthetic tendency and behavior characteristics, then points out the feasibility and advantages of interaction design in women's shoes by taking the design of women's shoes as a starting point.Meanwhile,from the appearance design of shoes,it puts forward three points about the interactive design of women's shoes: function, interest and innovation,then make a detailed analysis.At last,move a further step to forecast the development and trend of Interaction design.

Keywords: Women's shoes,Interaction design,Appearance design,Construction design

P81

Proteolytic activity determination of protease with natural hide powder labeled with low temperature active dyestuff as substrate

ZhangXi[1,3], Zhang Chunxiao[1,3], Li Yanhong[1,2], Hu Menghua[3], Pu Deyi[3] ,Peng Biyu[1,2,3,*]

1. National Engineering Laboratory for Clean Technology of Leather Manufacture, SichuanUniversity, Chengdu 610065, China;

2. Key Laboratory of Leather Chemistry and Engineering of Ministry of Education, SichuanUniversity, Chengdu 610065, China;

3.College of Light Industry, Textile & Food Engineering, Sichuan University, Chengdu, China,

**E-mail of corresponding author:pengbiyu@scu.edu.cn*

Abstract

A proteolytic activity determination method of protease was developed on basis of natural hide powder labeled with low temperature active dyestuff. A kind of hide powder labeled covalently with active yellowish brown (LF), which is was a kind of undamaged collagen because it was labeled at low temperature of 35℃ and there is no crosslinkage forming among collagen fibers during preparing. It was stable and suitable for assaying protease activity in a rather broad pH range. The influences of some key factors, such as reaction time, reaction temperature and concentrations of enzyme, on proteolytic reaction were investigated, and a sensitive method for determining the proteolytic activity of protease was established. Then the proteolytic activities of some commercial proteases frequently used in leather making process were assayed with the established method, and the results were compared with that of denatured hide powder substrate. The results show that the proteolytic activities based on the two different sub substrates are quite different. The nature hide powder is more resistant to enzymatic hydrolysis than that of denatured hide powder.

Key words: stained hide powder; substrate; proteases; enzyme activity

1. Introduction

In recent years, tanners pay more attention to biotechnology of leather-making[1-3]. Proteases are more generally being used in various leather-making processes, such as soaking, dehairing and bating, but the application of proteases still mainly depends on the tanners' experiences. One of the keys to successfully carry out bioprocesses of leather-making is how to control the balance between the desirable effect and the proteolytic degree of structure proteins in skins or hides. Obviously, Collagen is the major structural component of skin proteins, makes up 60-80% of the dry matter in skin[4]. The destruction of collagen has important influence on the leather quality in the leather making process. Excessive degradation of collagen by enzyme action could cause the decline in leather quality, such as the decline of mechanical strength and damaged grain [5-6]. Consequently, properly evaluating the action of proteases on collagen is important for the tanners to rationally use proteases in leather processes.

However, the determination of proteolytic activity still mainly relies on Folin [7] and Lohlein–Volhard (LVU) methods on the basis of the casein substrate in leather processes. Actually, the caseinolytic activity of a protease is not consistent with its effect on collagen. We all know that the characteristic amino acid of collagen is hydroxyproline, and the protease activity can be characterized by the hydroxyproline content.The disadvantages of the method are costly and time consuming. A method determining proteolytic activity of using a stained hide powder-RBB as the substrate was established [8]. During dyeing process with RBB dyestuffs, it underwent boiling treatment, and it was a kind of thermodenatured collagen which is more sensitive to a protease comparing with nature collagen. Therefore, the determination of protease activity using hide powder-RBB as a substrate cannot accurately evaluate the true activity of proteases during leather-making. Hence, it is important to establish a rapid and accurate method for determining protease activity.

In this article, a kind of nature hide powder labeled covalently with a low-temperature reactive dye (LF) in the condition of 35℃ is prepared. It is stable and suitable for assaying protease activity in a rather broad pH range. And, the use of an

natural/denatured second layer of cowhide powder, followed by a determination of protease activity as a substrate, is more indicative of the use of proteases in leather making. The main objective of this paper is to establish a new sensitive method for determining proteolytic activity on the basis of hide powder-LF substrate and compare the proteolytic activities of proteases against hide powder-LF and denatured hide powder-LF substrates.

2. Materials and methods

2.1 Materials

Reactive yellow brown L-F was purchased from Shanghai Anokqi Group Co., Ltd. Natural hide powder (Without special instructions, it is called hide powder) and denatural hide podwer are made in laboratory. Proteases were chosen from commercial leather enzymes, and supplied by Novozymes and Dowell Technology Co., Ltd., etc.

2.2 Methods

2.2.1 Preparation of hide powder-LF

5g hide powder was suspended in 100 ml of 0.9% saline at room temperature in a Erlenmeyer flask and stirred for 1h. Then 50ml 3% (w/v) L-F solution was added to the hide powder suspension. After stirred for another 30 minutes, 50ml 3% (w/v) Sodium carbonate solution was added. After mixing, adjust the pH to 11 with sodium hydroxide .The mixture was stirred for another 120 minutes at 35℃. The product was neutralized to pH 7 and then centrifuged to separate the supernatant solution. The stained hide powder was thoroughly washed with distilled water until the supernatant was quite colorless, and then freeze-dried. The hide powder-LF was ground to a fine powder, and stored under refrigeration and exclusion of moisture.

2.2.2 Performance characterization of hide powder before and after dyeing

2.2.2.1Amino acid full spectrum analysis

Accurately weigh 25mg of hide powder and hide powder-LF, put it into the amperage tube, add 4mL 6mol / L HCl solution, seal the nozzle, hydrolyze at 120 °C for 12 hours, deacidify, dissolve to 25mL, using Hitachi 835 - 50 type An automatic amino acid analyzer was used to analyze the amino acid composition of the hydrolyzed sample by the ninhydrin method, and the injection amount was 20μ*L*.

2.2.2.2Fourier transform infrared spectroscopy

The hide powder hide powder-LF were palletized with potassium bromide respectively, and then tablet compressing. Spectrum GX FT-IR spectrometer (PerkinElmer, US) equipped with a DTGS detector was used to the FT-IR experiment. The spectra were obtained in the range of 4000-400 cm^{-1} and recorded with a resolution of 2 cm^{-1}, a zero filling factor, 32 parallel scans and subtracted the interferences of H_2O and CO_2.

2.2.2.3 Differential thermal scanning test

The instrument was calibrated with metal radium and accurately weighed a certain amount (3 to 5 mg) of the sample (the sample was as dry as possible) in a DSC aluminum crucible. After the lid was sealed, the air was used as a reference, heated from 30 ° C to 200 ° C, the heating rate was 10 ° C / min, and the nitrogen flow rate of the sample chamber was 20 ml / min.

2.2.3 Dye-eluting characteristics of hide powder-LF

Test tubes (2ml) were respectively charged with 6mg of hide powder-LF. 1.5ml of 0.05M Britton-Robinson buffers with pH range from 3.0 to 11.0 were added, individually. The tubes were stirred in an incubator at 35°C for 60 minutes, and then centrifuged to separate the supernatant solution. The optical density of each elution was determined immediately at 416nm.

2.2.4Optical absorption characteristics of reactive yellow brown L-F and hide powder-L-F hydrolysate

Weigh a certain amount of active yellow-brown LF dye, dilute with different pH (3, 4, 5, 6, 7, 8, 9, 10, 11, 12) Britton-Robinson buffers (0.1mol/L), and then perform full band scan in the range of 200-800nm in the UV-Vis spectrophotometer. Weigh a certain amount of hide powder-LF into the test tube, add 5ml Britton-Robinson buffers (0.1mol/L) ofpH9, keep warm at 40°C for 5min, add 35mg/mL SG enzyme solution (have higher collagen hydrolysis activity) 1mL, keep shaking until the substance is completely hydrolyzed. Absorb some of the hydrolysate, dilute with

Britton-Robinson buffers (0.1mol/L) at different pH (3, 4, 5, 6, 7, 8, 9, 10, 11, 12), and then perform full-band scan in the range of 200-800 nm using UV-Vis spectrophotometer.

2.2.5 Determination of hide powder-LF calibration curve

Increasing amounts (5mg to 25mg) of hide powder-LF were incubated in 5ml of 0.1 M Britton–Robinson buffer of pH 9 with excess amount collagenase solutions until completely degraded to clear solutions. Then part of the hydrolysate solution was taken and diluted with Britton–Robinson buffer, respectively. The optical density of each sample was plotted against the respective amount of substrate dissolved. Then the real amount of hydrolyzed hide powder during thecollagenolytic activity analysis was obtained according to the calibration curve.

2.2.6 Collagenolytic activity assaying

Test tubes (2 ml) were charged with 6±0.1 mg of stained substrate and 1.3ml of buffer with differing pH. The tubes were placed in an incubator at 35°C for preheating 5 minutes, and then 0.2 ml of each enzyme solution was added. The tubes were stirred for accurately measured 60 minutes at the rate of 1200 rpm. The tubes were then centrifuged immediately for 2 minutes at the rate of 12000 rpm. The optical density of the supernatant was determined immediately at 416 nm in a spectrophotometer. Blanks were obtained similarly by adding enzyme solutions at the end of the incubation period, immediately before centrifugation. The amount of enzyme digested hide powder was calculated by comparing the OD value with the calibration curve.

One unit of collagenolytic activity was defined as the amount of collagenase capable of digesting 1μg of substrate by incubation at 35°C for 1 minute under standard conditions.

3. Results and discussion

3.1 Optical absorption characteristics of hide powder-LF enzymatic hydrolysate

The hide powder-LF can be completely digested by a collagenase. Fig.1 and Fig.2 show that the maximum absorption peak of prepared hide powder-LF enzymatic hydrolysate and reactive Yellow Brown L-F Hydrolyzate are located at around 416 nm, and the OD curves of the hydrolysate at differing pH from 3 to 11 almost have no move changes.

Proteases are used in different pH processes of leather-making, so the evaluating the impact of proteases on collagen should be undertaken at a broad spectrum of pH, and it needs the dyestuff do not release from the substrate; otherwise, it will affect the accuracy of the determining results. The color-elution characteristics of hider powder-LF is illustrated in Tab.1. Reactive yellow brown L-F is a kind of active dyestuff with vinyl sulfone type active group, which can bind with substrate through covalent bond, so the stained substrate has excellent colorfastness, and the dyestuff cannot be easily released from the substrate even if at extreme pH. The results show that reactive yellow brown L-F can not be eluted and its colour is stable at the broad spectrum of pH, so hide powder-LF is a suitable substrate for assaying collagenolytic activity of proteases used in different processes of leather-making.

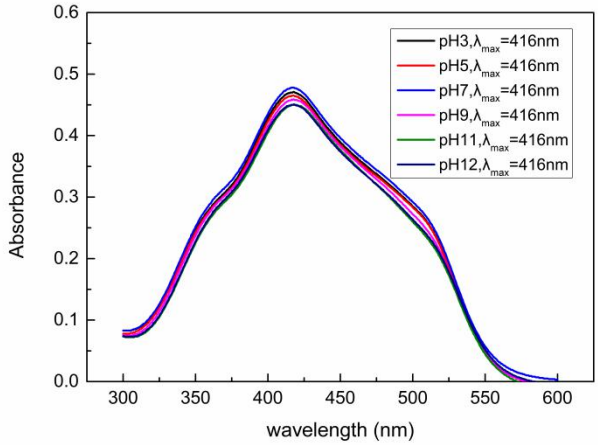

Fig.1 The wavelength scaning of reactive yellow brown L-F

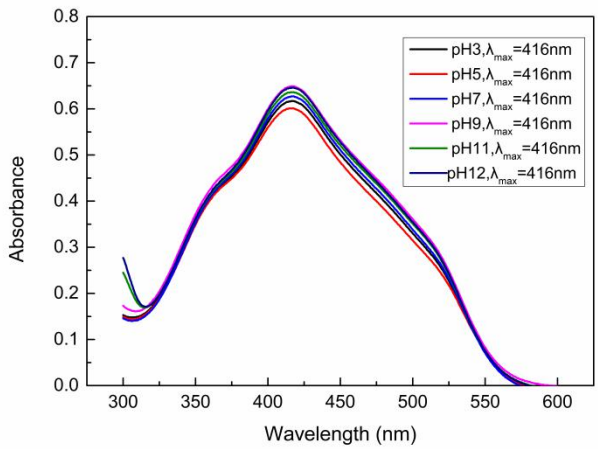

Fig.2 The wavelength scaning of hide powder-LF hydrolysate

Tab.1 The color-elution characteristics of Hide powder-LF

pH	3.0	5.0	7.0	9.0	11.0
The absorbance of the eluate	0.041	0.042	0.050	0.057	0.060

3.2 Performance characterization of hide powder before and after dyeing

3.2.1 Amino acid full spectrum analysis

In order to understand the primary structure of the skin powder before and after dyeing, the amino acid full spectrum analysis was carried out on the hide powder (hide powder and denatural hide powder) before and after dyeing.The ratio of amino acids in the hide powder before and after dyeing shows that the molar percentage of most amino acids increases after dyeing, while methionine and (Met), lysine (Lys) and hydroxylysine (Lylys) and histamine (His) decreases.This may be because the active yellow-brown LF is a divinylsulfone-type dye, and its reactive group, vinylsulfone sulfate, is generally combined with an amino group.Lysine (Lys)，hydroxylysine (Lylys) and histidine (His) have an amino group in the branch,

and the amino group binds to the reactive group of the dye during the dyeing process, resulting in a decrease in the molar percentage.It can also be seen from Table 2 that the total mole percent of alkaline amino acids is reduced after dyeing, which also demonstrates that the dye reactive groups are covalently bound to t the amino group.

At the same time, it can be seen from Table 2 that the molar percentage of glycine (Gly) in the hide powder before and after dyeing is in the range of 34%, which basically conforms to the Gly-X-Y structure of collagen, and glycine accounts for about 1/3.Proline and hydroxyproline are about 22% of the total mole percentage, which is basically consistent with type I collagen, so the basic structure of amino acids before and after basic dyeing does not change.

Tab.2 Amino acid full spectrum analysis of skin powder before and after dyeing

Amino acid	Molar percentage（%）					Ratio(1/2)	Ratio(3/4)
	1.Hide powder	2.Hide powder-LF	3.Denatured hider powder	4.Denatured hider powder-LF	5.Type I collagen		
Non-polar amino acid							
Gly	33.64	34.00	35.54	34.63	32.7	0.99	1.03
Ala	11.02	11.62	10.67	11.04	11.4	0.95	0.97
Val	2.12	2.21	2.01	2.04	2.30	0.96	0.98
Met	0.51	-	0.15	-	0.60	-	-
Ile	1.24	1.33	1.21	1.21	1.20	0.94	1.00
Leu	2.55	2.68	2.51	2.57	2.50	0.95	0.98
Tyr	0.44	0.45	0.36	0.40	0.40	0.98	0.92
Phe	1.30	1.40	1.19	1.26	1.30	0.93	0.94
Thr	1.48	2.33	1.73	1.88	1.60	0.64	0.92
Subtotal：	54.31	56.01	55.37	55.04	54.00		
Alkaline amino acids							
His	0.50	0.45	0.49	0.47	0.50	1.11	1.05
Lys	2.62	1.19	2.52	1.98	2.80	2.19	1.27
Arg	5.19	5.51	4.95	5.10	5.20	0.94	0.97
Subtotal：	8.31	7.16	7.95	7.55	8.50		
Acidic amino acid							
Asp	4.00	4.34	4.12	4.12	4.60	0.92	1.00
Glu	7.32	7.70	7.24	7.29	7.50	0.95	0.99
Subtotal：	11.32	12.03	11.31	11.42	12.10		
Other amino acids							
Ser	3.29	3.72	3.27	3.19	3.10	0.88	1.03
Hylys	0.63	0.44	0.70	0.61	0.70	1.45	1.15
Hypro	10.72	8.92	8.57	10.02	8.60	1.20	0.86
Pro	11.41	11.71	12.77	12.18	13.00	0.97	1.05
Subtotal：	26.06	24.08	25.32	26.00	25.40		

3.2.2 FTIR

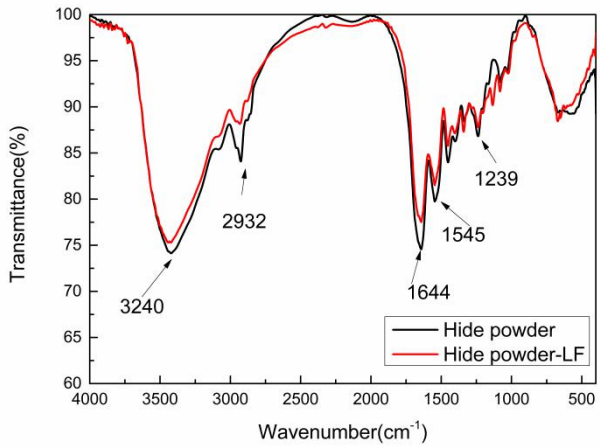

Fig3. FT-IR spectra of hide powder and hide powder-LF

The secondary structure of collagen can be reflected by Fourier transform infrared spectroscopy, and the characteristic amide bands in the spectrum can be used to characterize the integrity of the unique triple helix structure of collagen. The FT-IR spectra of hide powder and hide powder-LF are shown in Fig3. The peak around the 3420cm-1 is the amide A band of collagen, the peak around the 2932cm-1 is the amide B band of collagen. And they are assigned to stretching vibrations of N-H groups. The peak around 1644 is the amide Ⅰ band of collagen, and it is a a stretching vibration of the C=O bond. The amide II band at 1545 cm-1 is caused by N-H bending vibration coupling C-N stretching vibration.The peak around 1239 is the amide Ⅰ band of collagen, it is caused by N-H bending vibration and vibration of the glycine skeleton and proline side chain. As can be seen from the figure, hide powder and hide powder-LF have corresponding absorption peaks at the same wave number. It indicates that the structure of the hide powder before and after dyeing has not changed.

3.2.3 Differential thermal scanning test

In the natural state, collagen is a triple supercoil structure wound by three polypeptide chains. Since the hydrogen bond is broken when the collagen is heated, the collagen molecules are untwisted, the molecular structure changes from an ordered state to a disordered state, and the folded state changes to an irregularly curled state, and the natural conformation is destroyed. Changes in these states are accompanied by changes in energy, so that DSC can be used to measure the thermal stability. Generally, the thermal stability of collagen is expressed by heat shrinkage temperature, and the temperature at which collagen shrinkage is caused is called shrinkage temperature. The operation of collagen is slightly different depending on the animal species and individual. It can be seen from Fig. 4 that the shrinkage temperature before and after dyeing is substantially constant, all at about 78 °C, which is higher than the shrinkage temperature of ordinary calfskin by about 65 °C. The heat-shrinking temperature of collagen is related to hydrogen bonding, which may be caused by mechanically destroying some hydrogen bonds in the preparation process. In general, the structure of the hide powder before and after dyeing did not change substantially.

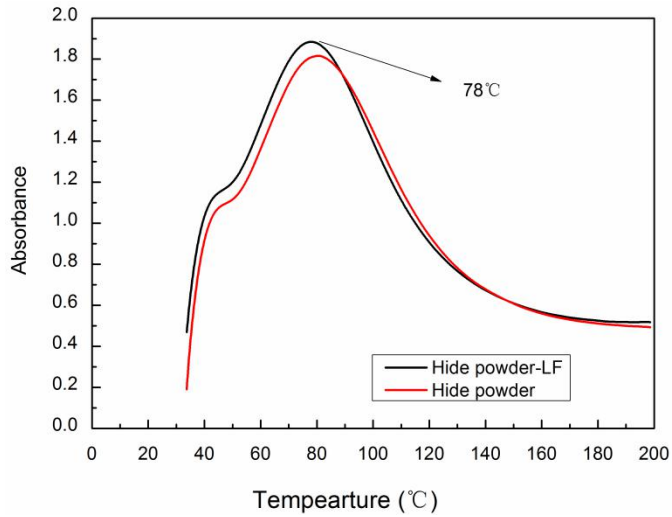

Fig4. Shrinkage temperature of hide powder and hide powder-LF

3.3 Determination of hide powder-LF calibration curve

As mentioned before, one unit of collagenolytic activity was defined as the amount of collagenase capable of digesting 1μg of substrate by incubation at 35°C for 1 min under standard conditions. The relationship between the amount of hide powder-LF and the OD value of its digestion solution should be established. Graded amounts of hide powder-LF were digested to clear solutions with adequate collagenase. The relationship of optical density values of the digested solutions with the amount of substrate is illustrated in Fig.5. It shows the calibration curves of different batches of hide powder-LF are coincident and the linear regression equation is obtained as y=6.390x+0.0384 (R=0.999).

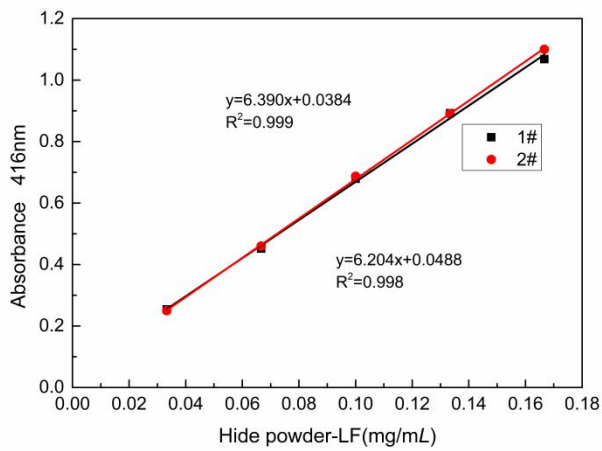

Fig.5 The calibration curves of different batches of hide powder-LF

3.4 Reaction characteristics of collagenase with hide powder-LF

A kind of leather protease from Novozymes Company, named SG and behave relatively high collagenolytic activity, was chosen to study the reaction properties as the representative of leather collagenase.

3.4.1 Effect of reaction time

The effect of reaction time on collagenolytic activity of SG enzyme was studied over a range of reaction time (30-90min) respectively under the condition of 35°C and pH 9.0. The experimental results, presented in Fig.6, demonstrate that under the determination conditions, the relationship between reaction time and the absorbance is linear (R=0.999) within 60 minutes. The enzyme activity is measured by determining the initial velocity of enzymatic reaction, consequently, 60 minutes is reasonably chosen as reaction time for assaying collagenolytic activity in consideration of the shorter reaction time and the lager the experimental error.

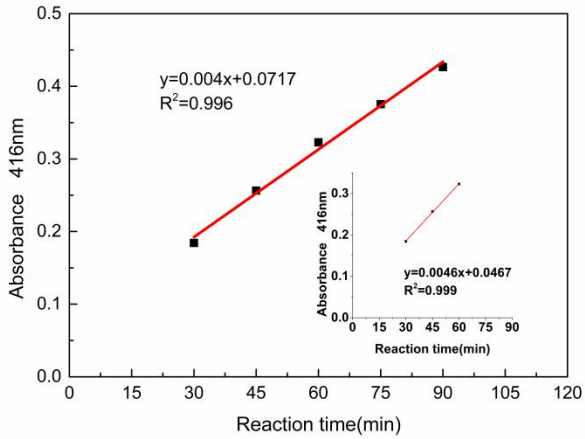

Fig. 6 Effect of time on collagenolytic reaction

3.4.2 Effect of collagenase concentration

The effect of enzyme concentration on collagenolytic activity was studied over a range of enzyme concentration (50-300μg/mL of SG enzyme) respectively under the determination condition of 35°C and pH 9. Fig.7 shows that when the reaction system was charged with a fixed amount of hide powder-LF substrate (6mg) and the enzyme concentration is between 50 and 250μg/mL, the relationship between the enzyme concentration and the absorbance is linear (R=0.999). Consequently, in order to obtain correct value of collagenolytic activity in this reaction system, the absorbance values are more reliable in the range of 0.205-0.463 and the collagenase activity is in the range of 2.08-7.28U/m*L*.

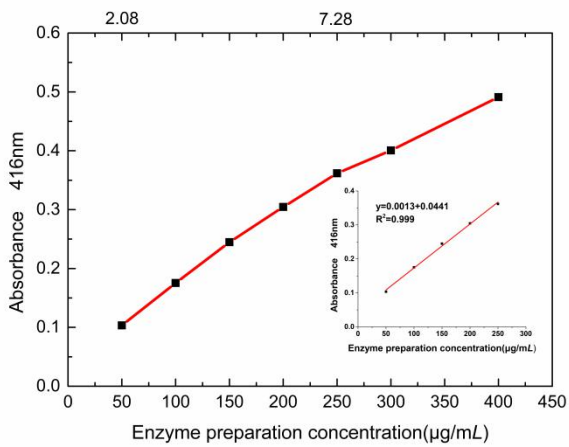

Fig.7 Effect of collagenase concentration on collagenolytic reaction

3.4.3 Effect of pH on collagenolytic reaction of several leather proteases

Several leather proteases, including SG, MP, PY, AX and DY300, were chosen to investigate their impact on collagenase under different pHs. The optimum pHs of these proteases were studied over a broad spectrum of pH (5.0-12.0) with hide powder-LF at the conditions of 35°C and 60 min.Fig.8 shows that the selected five leather proteases are all alkaline enzymes, and the selected three protease have the largest collagenase activity at around pH 10.0,but DY300's optimum pH is about 8.5 and SG's optimum pH is about 9.0. Collagenase activity significantly decreases as pH value falls below 7.0 or above 11.0.

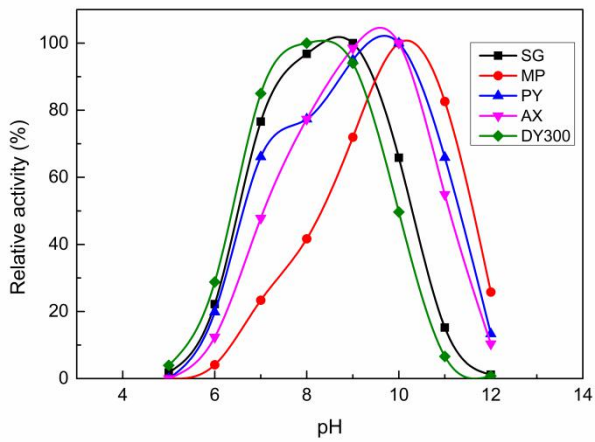

Fig.8 Effect of pH on collagenolytic reaction

3.4.4 Effect of temperature on collagenolytic reaction of several leather proteases

In leather making process, the temperature of the soaking process is room temperature, dehairing process and Softening process are generally not more than 40 ℃. Considering the actual situation, the effect of temperature on collagenase activity was examined at various temperatures (30-45°C) for 60 minutes at pH9.0. collagenase activity linearly increases with temperature raised from 30-45°C. On the five proteases, temperature had the greatest influence on MP's collagenase activity, while PY was the least sensitive to temperature. The experimental result is illustrated in Fig.9.

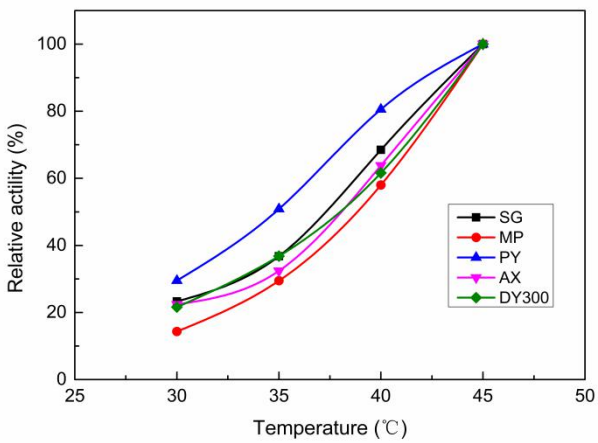

Fig.9 Effect of temperature on collagenolytic reaction

3.5 Reproducibility of collagenolytic activity assay method

For verifying the reproducibility of the proposed method, it was designed to determine the collagenolytic activity at least six times using two batches of hide powder-LF substrate prepared at different time respectively as the substrates. The results are shown in Table 3. It is found that the each result of collagenolytic activity measured is relatively close and the error is within the limit of experiment. The reproducibility of the proposed method for determining the collagenolytic activity based on hide powder-LF substrate was satisfactory.

Tab.3 The reproducibility of the proposed assay method (SG enzyme)

Different batches of hide powder-LF	Collagenolytic activity （ U/g ）						average value	RSD(%)
1#	31985	31364	31683	31314	31314	31381	31507	0.86
2#	35880	34494	34934	34135	34249	34918	34768	1.83
average value	33933	32929	33309	32724	32781	33149	33138	-
relative average deviation	5.74	4.75	4.88	4.31	4.48	5.33	4.92	-

3.6 Investigation of collagenolytic activity of commercial proteases

The main proteases widely used in leather processes were chosen for evaluating their collagenolytic activity.In order to ensure the accuracy of the testing results, all of the selected proteases are in the concentrated form, which are the diluted leather enzyme products' raw materials. The results are show in Table 4. It can be seen that the proteolytic activities of proteases against these two substrates were quite different, and all selected commercial proteases exhibited much lower activity against the natured hide powder-LF comparing with denatured hide powder-LF. Because denatured hide powder-LF is treated with alkali and the triple helix structure of collagen is destroyed. However, hide powder-LF is native and prepared at the low-temperature condition of 35°C. Consequently, the collagenolytic activity measured with natured hide powder-LF can correctly reveal the fact of proteases against skin protein in dehair process. And the collagenolytic activity in softening process was determined by using denatured hide powder-LF as substrate.

Tab.4 The investigation results of commercial proteases

Commercial proteases	The different substrates for assaying enzyme activity		Ratio(2/1)
	1. Hide powder-LF	2. Denatured hide powder-LF	
SG	35365	292261	8.26
DY300	29005	275897	9.51
MP	68260	632152	9.26
PY	24632	159455	6.47
AX	15184	104811	6.90
WB	132	2266	17.17
U	2679	10128	3.78
PTNP110	3121	48034	15.39
Novobate115	1940	10368	5.35

4. Conclusions

A sensitive method for determining collagenolytic activity, based on hide powder-LF substrate, is established. The stained collagen（hide powder-LF）was derived from hide powder labeled covalently with Reactive yellow brown L-F, which is highly stable and is a suitable substrate for assaying collagenolytic activity of leather-using enzymes at the broad spectrum of pH. And, it is known by Fourier transform infrared spectroscopy, amino acid full spectrum analysis and Differential thermal scanning test that there is no change in the structure before and after dyeing. The reproducibility of the proposed method was satisfactory.

The proteolytic activities of proteases used in leather-making pocesses against these two substrates are quit different and all selected commercial proteases exhibited much lower activity against nature hide powder-LF comparing with denatured hide powder-LF. Hide powder was treated with alkali and the triple helix structure of collagen is destroyed. The collagenolytic activity measured with nature hide powder-LF can correctly reveal the fact of proteases against collagen in dehairing process. Meanwhile, denatured hide powder-LF as substrate can accurately determine the collagen activity of protease in softening process .So it should be important for the tanners to get accurate and useful information of protease properties.

5.Acknowledgments

This work was financially supported by National Key R&D Program of China (2017YFB0308402) and College Students Innovation & Entrepreneur Training Plan of Sichuan University (C2018103545).

References

[1] Thanikaivelan P, Rao J R, Nair B U, et al. Progress and recent trends in biotechnological methods for leather processing[J]. Trends in Biotechnology.2004;22(4):181-188.

[2] Foroughi F, Keshavarz T, Evans C S. Specificities of proteases for use in leather manufacture[J]. Journal of Chemical Technology and Biotechnology.2006;81(3):257-61.

[3] Taylor M M, Bailey D G, Feairheller S H. A review of the use of enzymes in the tannery[J]. JALCA.1987;82(6):153-165.

[4] Richard Edmonds. Proteolytic depilation of lambskins[D]. New Zealand: Massey University, 2008

[5] Zhiqiang Li, Nianshu Zhang, Xiaoyu Yin, et al. Study on the actions of different components of enzyme preparations during the enzymatic depilation[J]. China Leather.1995;25(6):10-14.

[6] Biyu Peng, Zhimiao Yu. Action of proteolytical enzymes to the hide components and application of proteases in leather-making process [J].China Leather.2007; 36(7):60-64.

[7]Cupp-Enyard C. Sigma's Non-specific Protease Activity Assay - Casein as a Substrate [J]. Journal of Visualized Experiments, 2008(19).

[8] Chengxia Li, Bingbin Xu, Biyu Peng, et al. Proteolytic activity determination of proteases with denatured hide powder labeled with active dye as substrate[J]. China Leather.2012;41(5):17-23.

P82

The Impact of Proteases on Elastin and Collagen Fibers in Wet Blue Bating

Xu Zhang[1, 2], Shan Li [1, 2], and Biyu Peng[1, 2*]

[1] *National Engineering Laboratory for Clean Technology of Leather Manufacture, Sichuan University, Chengdu, 610065, P.R. China, Phone: +86-28-85401208, E-mail: pengbiyu@scu.edu.cn.*

[2] *Department of Biomass and Leather Engineering, Sichuan University, Chengdu, 610065, P.R. China, Phone: +86-28-85401208, E-mail: pengbiyu@scu.edu.cn.*

** Corresponding author.*

Abstract

During the traditional leather manufacture processes, enzymatic bating operation is usually the first stage of post-tanning process to improve the quality of finished leather. In order to investigate the impact of proteases on elastin and collagen fibers in wet blue bating, the chrome-tanned elastin and collagen fiber activities of four different types of proteases LKT-N, TUST-N, SG and MP were studied, and these proteases were used for bating wet blue under the same conditions. The concentrations of Desmosine (DES) and Hydroxyproline (Hypro) in bating liquors were measured through Amino Acid Analyzer, the degradation of the elastin fiber of bated wet blue were observed through histologic staining method, and the damage of the grain layer were observed through Scanning Electron Microscope (SEM) method. The results showed that different proteases exhibit various caseinolytic activities, chrome-tanned elastin and collagen fibers activities. The application on wet blue bating showed that the four proteases could improve the softness of leather through further opened up the collagen fibers. Elastin fibers could be damaged by the chrome-tanned elastin fiber activity and is helpful to improve the softness of leather. Proteases with higher chrome-tanned elastin fiber activities is suggested to have the best bating effect for wet blue.

Keywords: Wet Blue; Bating; Protease; Elastin Fiber; Collagen Fiber

P83

Comparison of Protein Quantitation Assays in Active Protein Compositions of Typical Proteinase Preparations

GAO Mengchu[1, 3], PENG Biyu[1, 2, 3]

(1.National Engineering Laboratory for Clean Technology of Leather Manufacture, Sichuan University, Chengdu 610065, China; 2.The Key Laboratory of Leather Chemistry and Engineering of Ministry of Education, Sichuan University, Chengdu 610065, China; 3.College of Light Industry, Textile and Food Engineering, Sichuan University, Chengdu 610065, China)

Abstract: Industrial proteinase preparations, containing active enzyme proteins and other impurities, are generally separated and purified with initial steps. The presence of impurities disturbs the quantitative and analysis of active enzyme proteins. There are many kinds of methods for determining protein content, such as Bradford, Lowry, BCA, and Absorbance variation method. However, these methods have different reaction principles, therefore the results maybe different. In order to solve those problems, active protein compositions of AS1.398, LKT-N and WB preparations were obtained from gel filtration chromatography (GFC) and ion exchange chromatography (IEX). Bradford method， Lowry method， BCA method and absorbance variation method were used to quantitate protein of these active protein compositions, respectively， then the data were compared， and the protein qualitative and semi quantitative analysis of SDS-PAGE were used to validate the data． The results indicated that there was significant difference in protein content of these active protein compositions in different industrial proteinase preparations． In compared with these methods， the results of Lowry and BCA method were close, however, the results of Bradford method and absorbance variation method were lower than other methods. Besides, the Lowry and Bradford methods' detection results of active proteins obtained from GFC and IEX were determined, and the specific values of Lowry and Bradford methods' testing results in these two chromatography steps were different, indicating that the presence of the other proteins affected the protein quantification. It is of great significance to choose a relatively accurate, reproducible and convenient method for determining the protein content of active proteins in protease preparations.

Keywords: active protein; gel filtration chromatography; ion exchange chromatography; protein quantitation; Bradford method; Lowry method; BCA method; absorbance variation method; SDS-PAGE electrophoresis

P84

Exploring the Innovative Methods of the Qiang's Yunyun Shoes Used in Modern Footwear Design

LI Xin-juan[3],DING Wan-jing[3],YAO Yun-he*[123]

(Key Laboratory of Leather Chemistry and Engineering of Ministry of Education, Sichuan University,National Engineering Laboratory for Clean Technology of Leather Manufacture, Sichuan University , Biomass and Leather Engineering Department,Sichuan University,Chengdu,610065,China)

Abstract:

With the economic development and improvement of people's living standards, the current footwear market homogenization and plagiarism follow the phenomenon is very serious. Such products have been unable to meet the needs of consumers or the development of the industry itself. At present, the footwear market consumption direction needs to be further developed and refined. A lot of space in the original design area needs to be developed. China's traditional culture is the source of original design inspiration and bright Qiang's clothing culture is one of the important components. Therefore, based on a comprehensive study of the patterns, colors, production techniques and Qiang nationality's cultural connotations, analyzing on the typical cases of the application of Yunyun shoes in the design of modern shoe clothing and sums up the rules of its application. At the same time, according to the characteristics of shoe design method, the paper puts forward the concrete scheme of applying Qiang elements such as Yunyun shoes to modern footwear design, and draws manuscripts or makes physical objects by the corresponding methods. All is to provide a feasible way for the traditional national elements to be used in shoe design, and to develop the original shoe design market.

Keywords: Yunyun Shoes, Footwear, Design, Qiang Culture

1 background

The rapid development of China's modern footwear industry began in the early 1980s, and soon entered a period of constant change and renewal [1]. Since the 1990s, China's footwear design has entered the initial stage and began to realize the importance of brand building. Entering the 21st century, China joined the WTO, and the footwear industry has also joined the competition in the international market. The footwear design of this period is not lacking in vitality, but the phenomenon of homogenization and plagiarism are extremely serious. After the Anti-dumping case and the Global Economic Crisis, China's footwear industry began to realize the importance of originality. At present, China is already a big country in the manufacture and export of footwear, and there are also a number of enterprises or individuals who made original shoes. However, the existing original designs in China are in small scale and the design level is uneven and not understood by consumers. And favor cannot meet the market demand. This incomplete market is a good opportunity we need to grasp.

In today's situation, seeking innovation in footwear design is the first step to establish brand competitiveness and guide the benign development of the market. China's rich national culture can provide a large number of effective design information. Some domestic footwear brands such as SHEME, Tu Huo Luo, Jin Bu, etc. are original brands inspired by traditional ethnic elements. This article will take the Qiang people's Yunyun shoes as the specific foothold, innovatively apply the national elements to the field of footwear product design, and provide new ideas for the product development of China's original brands.

2Cloud shoes overview

Chinese traditional culture has a long history. The use of traditional culture in design and the expression of traditional culture have been recognized and practiced by Chinese designers [2]. The Qiang culture is an important part of the traditional

national cultural treasure house. The Qiang people's costumes are simple in style, exquisite in style and rich in expression, reflecting the superb aesthetic level, skillful craftsmanship and longing for a better life. The Qiang men and women wear a stiletto flat shoes with a cloud pattern - Yunyun shoes.

Yunyun shoes, also known as "spike shoes", the upper is mainly composed of cloud pattern and horn pattern and the combination or deformation of the two (Fig. 1). The name is derived from this. It is the daily wear of the Qiang people. The footwear used is also a ceremonial shoe on a festive or important day, with considerable practical value and artistic value [3]. Yunyun shoes are flat shoes, the tip of the shoe is slightly tilted, and the upper face is mostly two pieces of the front and the middle of the middle to break the outer seam. The overall shape is smooth, and the production process is roughly divided into a clam shell, a shoe upper, a cut pattern, an embroidery machine seam. In the process of line, the sole is made of burlap and stitched with twine, and the colors of blue, white and red are mostly used as the background color. Embroidery is the main decorative technique on the upper surface of Yunyun. The pattern is rigorous and exquisite. The stitching method is varied and the color is bright and colorful. It is known as the “Nan Yi Bei Qiang”, and the pattern of the pattern is not only the common color embroidery. It is also cut and sewn with suede, suede or colored fabric. The motifs of the upper can be divided into three categories: the first category originates from the worship of the totems of the Qiang people, typically the cloud pattern and the horn pattern; the second category originates from the sun, the moon, the stars and the flames that bring the light and warmth to the Qiang people. The worship, the sun pattern and the flame pattern are typical of it; the third category is taken from the animals and plants in the natural environment where the Qiang people live. The most common is the croissant, which is a symbol of love, so this pattern appears more on the pointed shoes worn by women, especially young women [4].

Fig. 1Contrast color matching Yunyun shoes

3Analysis of the Application of the Qiang Elements in Yunyun Shoes in the Design of Modern Shoes and Costumes

The current social and cultural creative industries have gradually become an important part of regional and even national economic development. The profound cultural connotation embodied and carried in the clothing such as Yunyun Shoes is a very valuable creative resource. From appearance to rich patterns, to the cultural and spiritual appeals, we can combine the modern design concept to produce exquisite products. However, as far as the national element products on the market are concerned, there are not many modern design concepts, and most of them are still doing traditional piracy, and all aspects of development need to be improved. The following is an analysis of the excellent design of the Qiang elements in shoes and other apparel products, and the design innovation methods are combined with the characteristics of the products.

It is a very feasible way to modernize the design of the shoes in the modern footwear design. The work in Figure 2 is inspired by Yunyun shoes, which combines traditional ethnic elements with modern design concepts, retaining the traditional

style of Yunyun shoes and adding the modernity and practicality of shoes.

Fig.2 "Auspicious clouds" shoes

The same is the use of elements for the design of the main body, as shown in Figure 3, the scarf design works are more creative. In the arrangement, the designer used the continuous patterns of cloud pattern and fire pattern commonly seen in the embroidery, and made a change of change in the position, size and superposition effect of the arrangement, highlighting a few elements, the contrasting beauty is just right. The effect of superposition adds a sense of layering and deepness, and is extremely expressive and emotional.

Fig.3 “Jiu Gou Huo Di” scarf design[5]

As shown in Fig. 4, it is a handbag with the original brand “one needle and one thread” featuring enamel embroidery, which embodies the idea of deformation, disassembly and reconstruction of elements. The designer disassembles the key parts on the basis of a deep understanding of the cultural connotation and the characteristics of the ornamentation, focusing on extracting the charm and conveying the meaning. Its main image, “Relief”, is the authority and the god of the Qiang people. It has a strong original worship and religious color, while the image is a modern comic technique. The lines are simple and casual, and the Dais are well integrated. Unique cultural heritage and modern aesthetic features.

Fig.4“One stitch & one thread” brand handbag

Through the above case analysis, we can basically summarize and extend the application value and application mode of the Qiang elements such as Yunyun shoes in the design. First of all, as part of the costume culture, it provides a unique and rich pattern, a variety of color matching methods and forms for redesign, as a prototype for direct use, addition and subtraction. Secondly, the deep cultural connotation behind its appearance adds a non-replicable human value to product design, and provides another way of thinking for design. In the process of using it for modern footwear design, we should incorporate modern design ideas on the basis of full interpretation, and then combine shoe design methods to design and create.

4Exploring and practicing the modern footwear design by using the Qiang elements such as Yunyun shoes

Footwear design must first locate the body of the wearer. With a clear target group, they can determine their multifaceted needs for shoes. In general, modern footwear design must grasp the major elements of footwear protection, decoration, practicality, labeling and personalization. In the following, we will explore and try out several important design methods, such as the combination of the genre elements, the collocation method, the detailed method, the deconstruction method, the contrast method, and the interaction method.

4.1Mix and match design

The mashup method is a combination of elements that are different in style, texture, and culture in the traditional sense and that are usually not combined in a natural form, breaking the traditional way to become a new independent individual. The mashup method is a commonly used method in design. Combining the elements of the scorpion and other elements of Yunyun shoes can create innovative solutions for many ethnic elements.

4.1.1 Material mix and match

Cotton linen is the traditional shoe fabric of the Qiang nationality. In the design, cotton burlap can be used to mix and match fabrics with different texture differences. Figure 5 shows a woman's shoes designed by the author, in which the front and back upper faces are made of leather material, the middle upper face is made of transparent PVC material, and the heel is made of wood. This mashup can bring a modern, stylish and rich layering to the shoes.

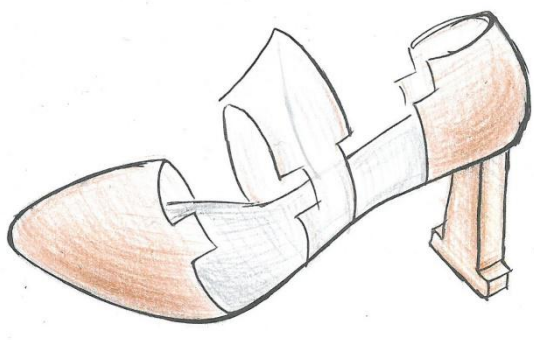

Fig.5Material mix and match design

4.1.2 Mix and match function and style

The mashup on the shape can be roughly classified into two types, one is the functional mix and match. Figure 6 is a functional mix-and-match women's shoes designed by the author. It uses a combination of sandals and boots. The front part has only one strip. The design uses the cloud pattern and fire pattern commonly used on Yunyun shoes. In the back gang, the structure of the boots is used, supplemented by the Qiang pattern lace. Structural innovations have made this shoe a break-through aesthetic.

Fig.6Functional mix and match design

Another type of mashup is a combination of styles and styles in the usual sense. Figure 7 is a mix of shoes designed by the author. The single shoe door line uses the pattern of clouds and fire patterns. The curve is graceful and playful, romantic, and the geometric rock at the heel. The styling reflects the hard texture and combines to form a unique shoe with both characteristics.

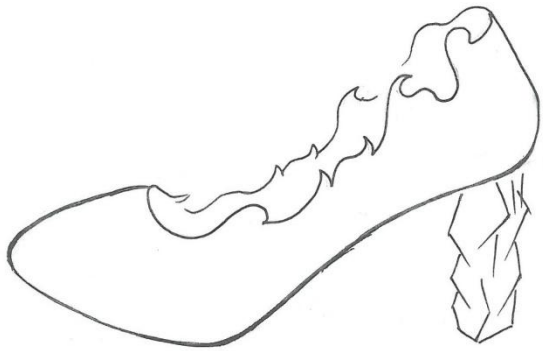

Fig.**7** Style mix and match design

4.2Associative design

4.2.1 The use of bionics and imitation associations

The Associative design method is because two things have certain common characteristics, which makes it easy for people to think of one thing from another. The designer integrates the thinking and finally forms a new method of designing the image.

Bionics is a typical method of association design, one is to give the whole body or gang part of the shoe to the form of animals and plants. The other is to use materials to mimic the natural texture of plants and animals, such as the use of sequins to regularly mimic the effect of fish scales.

The design method of imitation is similar to the bionic design method, except that the object of shape imitation is not limited to animals and plants. Figure 8 is a fashionable and unique bird cage shoe. The whole shoe body is modeled on the structure of the bird cage. It is complemented by tangled vine flowers, romantic and refined.

Fig.8 Bird cage shoes

4.2.2 The use of conceptual association

Conceptual associations are more abstract, and their association bridges are no longer morphologically similar, but rather a concept. The concept of the joint idea must first grasp the cultural connotation of the thing or understand its essence from a certain level and perspective, and then use it with other imaginary and bold and unique visions to make use of it.

4.3Detailed design method

The use of the so-called detailed method refers to the comparison and application of complexity and simplification. There are two main types of structural design used in shoes. One type is based on the function and modeling characteristics

of the upper part, and the design subtraction is applied to the partial structure. Figure 9 is a very simplified design, which uses a smooth strip-shaped surface to rotate and twist to form a fixed foot surface, support the overall heel and the sole part of the force surface, simple and elegant, with a sense of fashion. The other type is the simplification of the partial styling and the simplification of the overall shoe, the significance of which is to form a visual contrast, highlighting the key points to be expressed.

The detailed method is better understood when applied to color. That is, the local color is composed of a plurality of colors, and the other parts are a single color; the pattern is a contrasting design effect of a partial complex pattern and other parts of the simple feeling.

Fig.9Minimalist shoes

4.4Deconstructive design

In the design of footwear, the use of patterns is indispensable. The traditional patterns of the Qiang people in Yunyun shoes are rich and varied, but their expression techniques are often too delicate and complicated. Even the simpler patterns are traditionally used, which is difficult to meet the aesthetic needs of modern clothing. Therefore, the deconstruction of traditional patterns can simplify it, complete the transformation from figuration to abstraction, and focus on retaining the spiritual connotation of the pattern rather than the original shape, which can usually be constructed with a simple shape. Figure 10 shows the design of the cloudpattern of the Yunyun shoes as the center of the design, transforming the traditional cloud pattern, using its smooth curve shape, and expanding the concept of “cloud” as the source. The concept of flying clouds, clouds and wings has been added.

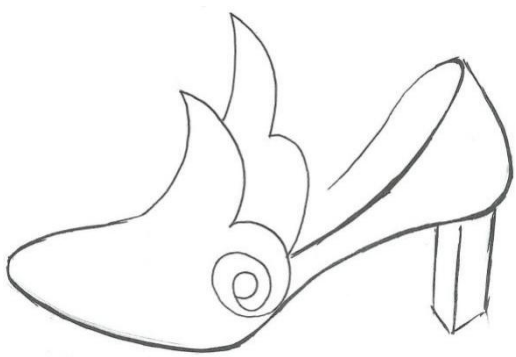

Fig.10Deconstruction design

4.5Contrast design

There are many similarities between the contrast method and the mashup method. The mashup focuses on the overall sense of harmony and collocation, while the contrast focuses on the difference. For example, the velvet suppresses the fluff in different directions, and the direction of reflection of the light is also different. When put together, the visual effect is different. In addition, color can be used for contrast design, which can effectively increase the richness and layering of the product.

4.6 Interactive design thinking

Interaction is a new word in the Internet era. The reference to footwear products here refers to the interaction between the object and the product, the sense of wearing experience, the sense of participation and interest, and the positive feedback and adjustability. In addition, you can develop a design that is interactive. For example, in a shoe using a steroid element, a detachable structure is used to achieve partial replacement, so that a shoe has a variety of different wearing methods, thereby improving the initiative and control of the wearing object.

4.7 Design practice

As a daily clothing item, the practicality is a very important factor. Therefore, when designing an original product, it is necessary to pay attention to the combination of artistry and practicality. The following is a design practice based on the theme of the Qiang people. The style of the work is positioned to have a national style without losing the modern sense, and the overall pursuit of the atmosphere is clear, simple and beautiful. The pattern selects the geometric pattern and the sheep totem that match the concept and aesthetics of modern design, and uses the deconstruction design method to transform the two patterns. The practice works mainly adopt the method of imitation in the modeling. The creation of the Qiang people's Baotou square scarf and the shape of the Qiangzhai tower are based on the prototype. And added elements such as ropes, tassels, etc., to make the overall level rich, and the impression is more cheerful; In terms of color, the blue, red and yellow colors commonly used in Yunyun shoes are selected as the main color tone; the material is mixed and mixed, and the suede and grain skin of the main part form a contrasting effect, which enhances the shoes. Texture (Figure 11).

Fig.11 a series of shoes designed withQiang elements

5 Conclusion

At present, applying Qiang ethnic elements such as Yunyun shoes to modern footwear design is still rare. However, with the development of the times, the consumption level is gradually improving, and the products that can reflect the wearer's aesthetic taste are more and more popular. Therefore, it is necessary to explore the application of traditional and ethnic elements in modern footwear design, which will bring endless inspiration and new foothold to footwear design. It can

also bring good guidance to the market, promote the detailed transformation of the footwear consumption market, and open up new product creative ideas and consumption market. The Yunyun shoes and the Qiang culture behind them are an important part of China's national treasure culture. Through the design and application of Yunyun shoes in modern footwear, the development and progress of China's footwear original design field can be inspired. Meanwhile, the traditional cultural connotation of China can be inherited and developed to enhance China's cultural soft power.

References

[1]Li Yunhe. Investigation and Research on the History of Footwear Professional Development and the Status of Talent Cultivation in China[J].Chinese leather,2009,38(1):55-58.

[2]Fan Yuxin. Preliminary Study on the Application of Dunhuang Mural Elements in Footwear Design[J].Leather Science and Engineering，2018，28(4):66-70

[3]Zhang Wei. Symbolic Semantic Analysis of Decorative Art of Qiang Nationality[J].De- coration,2010(06):114-115.

[4]Wang Xin. Yunyun Shoes—Unique cultural symbols of the Qiang people[J].Local culture research series.2010(00):209.

[5]Wang Wei. Innovative Application of Qiang Traditional Costume Patterns in Modern Scarf Design[J].Silk,2014,51(5):68.

P85

A surfactant-free degreasing method based on lipase multi-insertion in leather making process

Chunxiao Zhang[1,3,4], Fengxiang Luo[3],Shan Li[2,3]; Shencai Pan [3], Yanhong Li[1,2],Biyu Peng[1,2,3,*],Changdao Mu[4]

1. National Engineering Laboratory for Clean Technology of Leather Manufacture, SichuanUniversity, Chengdu 610065, China;

2. Key Laboratory of Leather Chemistry and Engineering of Ministry of Education, SichuanUniversity, Chengdu 610065, China;

3.College of Light Industry, Textile & Food Engineering, Sichuan University, Chengdu 610065, China;

4. School of Chemical Engineering, Sichuan University, Chengdu 610065, China;

**E-mail of corresponding author:pengbiyu@scu.edu.cn*

Degreasing is essential for leather making technology for the grease in hides and skins would cause many product defects. However, large offer of surfactant in common technology will lead to some negative effects on both environmental protection and leather quality. In this research, lipase multi-insertion was investigated to develop a cleaner surfactant-free degreasing method in aqueous condition. A kind of alkaline lipase (LKT) which has excellent integrated performances was selected from a series of lipases by the determination method with natural greasy hide powder as substrate. Then LKT was used alone as pretreating agent at the beginning of degreasing, re-soaking, liming and bating at room temperature. The results showed that, without offering any surfactant, the degreasing rate was up to 84%-90% around when the grease content of skins was degreased to 2.33%-3.33% below, both of which was comparable to conventional technology. The total discharge of COD in the wastewater was reduced by 28.0% around. The offering of water was decreased by 19.0%. And the energy consumption was saved by 252,000-285,600 kJ//t wet-salted skin and the production efficiency was increased at the same time. In addition, the physical and organoleptic properties of crust leather were improved.

Key words: degreasing; lipase; environmental-friendly; cleaner production; leather manufacture

1. Introduction

Degreasing is one of the essential operations in during leather making process, for oil and grease exist and distribute in the all skins hand hides. The existence of oil would cause into many defects on leather including oil cream, odorous smell, Cr(VI), etc.[1] Therefore, to clean the oil and grease from the skins and hides thoroughly is a matter of great concern to tanners.

Organic solvent degreasing is one of the most effective methods that can remove the oil from skin totally. However, the organic solvent, including kerosene, dichloromethane, cyclohexane, etc, is toxic, dangerous and expensive, thereby limiting its application. Saponification with alkali is also a main degreasing method, but it can only get rid of the grease on the surface, for most alkali cannot penetrate effectively in a certain time. The emulsification, i.e. large amounts of surfactants (5%-15% of the wet-salted skins) are used to emulsify the oils, is the most common degreasing approach presently. But surfactant also negative influences on environment and it would increase the difficulty of end-of-pipe treatments. And the recent studies show that surfactant would weaken the waterproofness and atomized value of leather. Hence, cleaner degreasing processing, i.e. minimizing the dosage of surfactant and residual oil content in the skin in aqueous condition, is a matter of great concern to all tanners.

As a green biotechnology, lipase catalytic degreasing is getting more and more attentions with the development of biofermentation technology. It's reported that several kinds of lipase, including YMD,[2] SG-II,[3] Greasex50L,[4] ZG,[5] have been applied in degreasing process. But the degreasing rate of lipase catalytic technology is only 50%-60%, which is far away from the ideal efficiency. The combination of lipase and surfactant can raise the rate to 70% around,[6] but it weakens the advantage of lipase catalytic technology. Therefore, the degreasing technology based on lipase is only used as an assistant technology in leather processing.

In order to improve the lipase degreasing technology, it is essential that the catalytic activity and capacity be increased so as to remove the oil to a maximum degree. For the most part, modification designed to improve degreasing effect is to select the lipase species. However, as mentioned above, the degreasing rate of the every lipase is similar with each other. This is because that, in aqueous condition, the alphatic acid released from the hydrolyzation of oil would re-assemble around, for the alphatic acid is water-insoluble and compatible with oil and grease. It would block the further contact between lipase and grease, then stopping the lipase hydrolyzation of grease. On the other hand, the alphatic acid still keeps in skin and cannot be got rid out. Hence, it is predictable that both the lipase catalytic property and degreasing rate would be improved significantly when the released alphatic acid were removed effectively in time.

Aiming at improve the degreasing effects of lipase technology, a lipase multi-insertion technology was designed according to the characterization of leather making processes in beamhouse. The soaked skins are preprocessed with suitable lipase at the beginning of several operations. Lipase can catalyze oil and grease hydrolysis to the chemical equilibrium. Then the pH will be adjusted to requirement of the technology to remove the alphatic acid and promote oil hydrolyzes further. The oil and grease would be remove more efficiently by the synergistic effect of lipase in different processes.

2. Experimental and methods

2.1 Materials and instruments

Salted-wet pig skins from Sichuan, China, were purchased from a local tannery (Chengdu Xinshi Leather Industry CO., Ltd.). Lipase LKT (Shandong Longkete Enzyme Preparation Co. Ltd.). Greasy pig skin powder (oil content 23%, acid value 52mgKOH/g, saponification value 199mgKOH/g) was made in the Laboratory. Chromosal B (a chromium tanning agent with 33% of basicity and 26% of Cr_2O_3 (0.177% of Cr) content) was purchased from LANXESS Inc. The following applied leather chemicals, including syntans, fatliquors, polymers, filling agents, etc. were of industrial grade and from Sichuan Dowell Science & Technology Co., Ltd China. The other chemicals were of analytic grade.

Stainless Experimental Drum (GSD400-4, Wuxi Xinda Light Industry Machinery Co., Ltd.),

2.2 Methods

2.2.1 Assay of the lipase property

The catalytic property of the selected lipase was evaluated on the basis of greasy hide powder at the pH 3.0-11.0 (CN 107058461 A). The conical flask was charged with 5±0.1g of greasy pig skin powder and 100mL of different pH Buffer, and stirred in an incubator at 40°C for 2h. Then, 10U/mL of the lipase solution was added and stirred for another 90min, 10g NaCl and 5mL HCl solution (6mol/L) were added at the same time to deactivate the lipase. Then the pig skin powder was filtrated and dried in room temperature naturally. Lastly, the oil content of the skin powder as well as the acid value of oil was measured.

2.2.2 Novel surfactant-free degreasing processes

Ten pieces of salted-wet pig skins conducted soaking and fleshing as normal. And then every skin was cut into two half sides along with the backbone line, symmetrically, and they were distributed to different tanning groups for evaluating and comparing degreasing effects. As showed in Table 1, the two groups were carried out a conventional beamhouse processing and a lipase multi-insertion processing.

Table 1 Beamhouse operations of conventional and lipase processing

Conventional processing					**lipase multi-insertion processing**			
Operations	Chemicals	Dosages (%)	Controlling constants		Operations	Chemicals	Dosages (%)	Controlling constants
Degreasing	water	100	38°C		Degreasing	water	100	22°C
	Na_2CO_3	2.0				Lipase LKT	100U/ml	60min
	Degreasing agent	1.5	90min			Na_2CO_3	2.0	60min
Draining					Draining			
Washing	water	100	38°C, 30min		Washing	water	100	22°C,30min
Degreasing	water	100	38°C		Washing	water	100	22°C,30min
	Na_2CO_3	2.0			Resoaking	water	50	22°C
	Degreasing agent	1.5	90min			Lipase LKT	100U/ml	60min
Draining						Na_2CO_3	2.0	30min
Washing	water	100	38°C, 30min			water	200	22°C;the rest operations were conducted as normal without using furfactant
Draining					Dehairing & Liming	water	50	22°C
Washing	water	100	22°C, 30min			Lipase LKT	50U/ml	30min;the rest operations were conducted as normal without using furfactant
Resoaking	water	250	22°C; Conducted as normal processes, the dosage of surfactant was 0.3%		Splitting			Grain layer was 2.0mm

Dehairing & Liming	water	300	22°C; Conducted as normal processes, the dosage of surfactant was 0.3%		Reliming			Conducted as normal processes
Splitting			Grain layer was 2.0mm		Washing			
Reliming			Conducted as normal processes		Deliming			Conducted as normal processes without using furfactant
Washing					Bating	water	50	35°C;
Deliming	water	50	33°C; Conducted as normal processes, the dosage of surfactant was 0.5%			Lipase LKT	50U/ml	30min; the rest operations were conducted as normal without using furfactant
Bating	water	50	35°C; Conducted as normal processes, the dosage of surfactant was 0.5%					

2.2.3 Determination of oil content and the acid value of the oil in skin

The samples of pig skin were pickled in the solutions of 10% NaCl and 10% HCl (w/w) for 24h at 4°C to adjust the pH below 3.0 and were soaked in 10% NaCl solution for 12h twice in 4°C to remove the residual HCl. Have been Then the samples were freeze-dried at -55°C and 20pa vacuum for 24hours. The dried leathers were cut into pieces about 1mm×1mm, the oil contents and the acid values were evaluated as per ISO 4048-2008 and ISO 3657-2002. The saponification value was determined as per ISO 660-1996.

2.2.4 Determination of COD concentration in spent liquors

The spent liquors in the main operations were centrifugal separated at 3500rpm for 6min. The liquid supernatants were appropriately diluted and their COD concentrations were measured as per ISO 15705-2002.

2.2.5 Test of physical and mechanical properties of crust leather

Dried crust leather samples of each tanning group were taken out in the adjacent and symmetrical parts of the same skin testing physical and mechanical properties. Samples were conditioned as per IUP method (IUP 2, 2000). Physical properties,

such as tensile strength, elongation at break, tear strength and bursting strength, were examined as per the standard procedures (IUP 6, 2000; IUP 8, 2000; IUP 9, 1996).

3 Results and discussions

3.1 Catalytic property of lipase in different pH

As mentioned above, pH differs from 3.0 to 13.0 in the beamhouse processing of leather making. This means that the catalytic activity of lipase could keep stable in wide pH range. Therefore, the catalytic property of LKT lipase was evaluated at the pH from 5.0 to 10.5 around on the basis of greasy skin powder, the conditions of which is similar to the leather making processes, and the results are illustrated in Fig. 1. It can be seen that the optimum pH of LKT lipase is 7.0-8.0, and there is another adequate range at pH 9.5-10.0. This is because the alphatic acid would be saponified in to alphatic salt when the pH is raised to 9.5 around, which could promote the hydrolyzation of grease. Therefore, LKT lipase can be used in the pretreating operations of degreasing, re-soaking, liming, bating, etc, where the pH can be adjusted to pH 7.0-8.0 and 9.5-10.0 easily, to promote the removing of oils from skins.

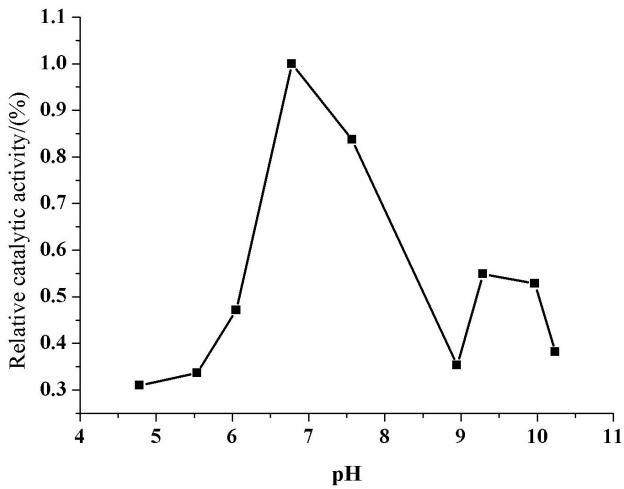

Fig. 1 Effect of pH on lipase catalytic activity

3.2 Degreasing efficiency of lipase catalytic processing

Based on the results above, LKT lipase was applied at the beginning of degreasing, re-soaking, liming, bating as the insertion operation to catalyze oil hydrolyze, then the pHs ware raised to match the requirement of the processes in beamhouse. The oil contents of the skins were tracked following the processing. The results are shown in Fig. 2.

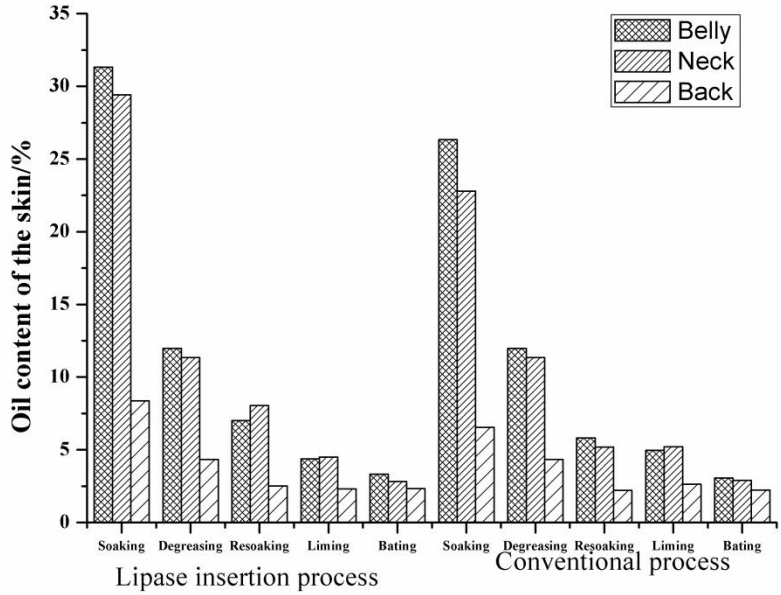

Fig. 2 Change of oil contents of the skins with processing

The reduction of the oil content in skin can evaluate the degreasing efficiency intuitively. Fig. 2 indicates that oil contents of the skins are decreased with the processing in both lipase and conventional processes. The oil contents of the bated pelts are reduced to 2.33-3.33 which differs with the skin bodies, and the negative influence of oil on chrome tanning would be avoided effectively. What's more, the lipase insertion technology can remove the oil more efficiently in degreasing and liming operations, although there is no surfactant used, which would improve the effects of resoaking and liming.

3.3 Comparison of leather properties

One of the main factors affecting the acceptability of a novel technical method by tanners is whether it can improve or at least keep the original properties of crust leather. Hence the main properties of the leathers from the adjacent and symmetrical parts of a same skin degreased with lipase and conventional processes were evaluated.

The leathers made with the two procedures shown in Table 1 were pickled, chrome tanned shaved (thickness 1.0mm), neutralized, retanned, fatliquored, vacuum-dried and staked as per the same standard procedures. The organoleptic properties of these crust leathers were evaluated by 10 professional skilled tanners. They thought there were no visible differences among these leathers in the respects of colour, gain pattern, softness, handle feeling and so on. The main physical and mechanical properties of the crust leathers are illustrated in Table 2. It can be seen that the tear strength, tensile strength, bursting strength and elongation at break of all the leathers produced from lipase process are similar with that of the leather made with conventional degreasing.

Table 2 Physical Properties of the Crust Leathers Produced with different Degreasing Technology

Technology	Tear strength (N/mm)	Tensile strength (N/mm^2)	Elongation at break (%)	Bursting Strength (N/mm)	Bursting height (mm)
Conventional	85	25	76	380	8.9

Lipase insertion	86	27	74	368	8.6

3.4 Sustainability of the lipase insertion technology

The main objective of the study is to reduce the surfactant and COD pollution from the origin of leather processing. The comprehensive efficiency of lipase insertion degreasing technology on reducing effluents and saving energy is summarized in Table 3.

Table 3 indicates that, the total volume of the wastewater, the amount of COD emission and the total dosage of surfactant is decreased by 19.0%, 28.0% and 100% respectively, and the energy consumption is reduced by at least 252,000-285,600 kJ//t salted-wet skin, which are attributed to the lipase catalytic degreasing technology. Though the COD concentration of the effluents is still relatively high, the wastewater is more easily to be treated through aerobic and anaerobic technology. This is because the residual organic chemicals in the sewage are the natural matrixes that derive from the skins, which are biodegradable. Moreover, the precipitation performance of the suspended solid is increased for the dosage of surfactant has been avoided totally. At the same time, the treatment effect of the biological sludge in the sewage disposal system will be improved further for the biotoxicity of surfactant to the microorganism is resolved effectively. Lastly, the technical difficulty is decreased and the technical safety is increased for the whole lipase insertion technology is conducted at the room temperature (22°C around), when the conventional degreasing technology is conducted at 38-40°C around, thereby causing into a do-undo operation between degreasing and resoaking/liming. The novel lipase insertion technology has exhibited remarkable advantages in environmental and energy conservation.

Table 3 Efficiency of the lipase insertion degreasing technology on reducing pollution emission

Operations	Conventional	Novel	Decrease rate (%)
Volume of Wastewater (L/t salted-wet skin) [a]	10,500±250	8,500±250	19.0
Amount of COD emission (kg/t salted-wet skin) [a]	370.8±25	267.0±20	28.0
Dosage of surfactant (kg//t salted-wet skin)	460-500	0	100
Energy consumption (kJ//t salted-wet skin) [b]	252,000-285,600	-	-

a the amounts were calculated in the operations of degreasing, washing, resoaking, liming

b the energy was calculated by the equation: $Q=cm\triangle t$; c-the specific heat capacity of water (4.2×10^3J/(kg·°C)); m-volume of heated water (kg); $\triangle$t-the increased temperature of water (°C).

4 Conclusions

The studies show that multi-inserting lipase at the beginning of degreasing, resoaking, liming, bating would produce a significant synergistic effect. The degreasing rate can be raised to 85%-90% without using any surfactant. The residual oil in the skins is reduced to 2.33-3.33, which is comparable with conventional emulsion degreasing technology. The emission of COD and wastewater are reduced by 28.0% and 19.0%, and the treatability of effluents is improved at the same time. This

investigation provides an improved lipase assistanting method, which is technically and commercially viable, to make cleaner degreasing come true and help to promote leather industry to develop sustainably.

Acknowledgements

This work was financially supported by National Key R&D Program of China (2017YFB0308402), China Postdoctoral Science Foundation (2018M633366), Research & Development Fund for Teaching Post Doctorate of Sichuan University (2017SCU12022) and College Students Innovation & Entrepreneur Training Plan of Sichuan University (C2018101333).

References

[1] Jurgen Christner. The use of lipases in the beamhouse processes [J]. Journal of the American Leather Chemists Association, 1992,87:128-139.

[2] Wei Dong, Guo Jiarong, Yu Kaihua, Wang Guowei. Degreasing effect of lipase enzyme YMD for sheepskin [J]. Leather Science and Engineering, 2014, 24(1):31-34.

[3] Cheng Haiming, Chen Min, Liao Longli, et al.. Application of alkaline lipase on sheepskin degreasing process [J]. Leather Science and Engineering, 2003, 13(4):37-40.

[4] Chen Ping, Chen Min, Liao Longli, et al.. The effects of alkaline lipase Greasex 50L in pigskin degreasing [J]. China Leather, 2000, 29(9):22-24.

[5] Liu Yan, Zhu Ling, Chen Qian, et al.. Application properties of diesel lipase ZG in leather making [J]. China Leather, 2015,44(5):21-24.

[6] Zhang Xueqing, Zeng Yunhang, Zhou Yutao, et al.. Application of lipase in sheepskin degreasing process [J]. China Leather, 2015,44(16):1-5.

P86

Green Hybrid Nanocapsules for Leather Finishes: Fragrance-Controlled Release and Antibacterial Behaviors

Qianqian Fan,Jianzhong Ma*, Qunna Xu*

[a] *College of Bioresources Chemical and Materials Engineering, Shaanxi University of Science & Technology, Xi'an 710021, China*

[b]*Key Laboratory of Leather Cleaner Production, China National Light Industry, Xi'an 710021, China*

**Email: majz@sust.edu.cn (J. Ma),xxqqnn870304@163.com (Q. Xu), *Tel.:86-029-86168002*

ABSTRACT

Nowadays consumers' concern towards hygiene and active lifestyle is creating new challenges for leather industry. As is known, the intimate contact of garment leather with human body often generates unpleasant smells, which are unbearable for consumers. To better resolve this problem, fragrance-encapsulated chitosan-based silica nanocapsules for leather finishes were successfully fabricated via interfacial polymerization method. The capsule structure was confirmed by transmission electron microscope (TEM), atomic force microscope (AFM) and X-ray diffractrometer (XRD). Significantly, chitosan in the outer shell may endow the nanocapsule with intrinsic antimicrobial activity and film-forming capacity, while silica in the inner shell could give a sustained fragrance release. Releasing results indicated that these nanocapsules could ensure a lasting release for nearly 120h. More importantly, it was noted that these nanocapsules showed a good compatibility with the common used film binders during leather finishing process. Compared with pure fragrance treated leather samples, those nanocapsules finished ones demonstrated superior sustained release property, improved hygienic properties, as well as excellent antibacterial properties, which hold much promise in obtaining functional coatings.

Key Words: Chitosan, Nanocapsule, Fragrance release, Antibacterial, Leather finishing

P87

Insight into Accessibility of Clay Nanoparticles in the Transformation of Collagen Fibers to Wet-white Leather Matrix

Jiabo Shi[1,2], Wei Lin[2,*], To Ngai[3,*]

[2]*National Engineering Laboratory for Clean Technology of Leather Processing, Sichuan University, Chengdu 610065, China*

[3]*Department of Chemistry, The Chinese University of Hong Kong, Shatin, N. T., Hong Kong, China*

Abstract

More recently, wet-white (chrome-free) tanning approaches based on non-mental tanning agents have been intensively investigated in order to develop reasonable tanning materials and related technologies with low potential risks to human health in leather processing towards eco-friendly leather manufacture. Our studies reveal that the synthesized nanoclay, Laponite, with non-toxicity and security to human health, confers tannic acid-tanned wet-white leather with suitable physical strength properties and improved environmental benefits. However, there is relatively little knowledge about the accessibility of Laponite within collagen fibers which is an important fundamental issue for the formation of leather matrix. In this study, we have studied the diffusion process of Laponite into the collagen fibers. The results show that Laponite can easily diffuse into the collagen fibers and the diffusion behaviors exhibit the Langmuir adsorption verifying its affinity for collagen. The introduction of Laponite leads to a shift in the isoelectric point of collagen from ~6.8 to ~4.5, implying the ionic bonding between the positively charged amino groups of the collagen and negatively charged Laponite. Atomic force microscopy (AFM), field-emission scanning electron microscopy (FE-SEM) and energy-dispersive X-ray spectroscopy (EDX), X-ray photoelectron spectroscopy (XPS) and wide-angle X-ray diffraction (WAXD) studies indicate that Laponite can penetrate into the collagen microstructure and evenly distributed onto the collagen fibrils without altering native D-periodic banding patterns of the collagen fibrils.

Keywords: Collagen fibers; Clay nanoparticles; Accessibility; Leather matrix

Acknowledgement: This work is supported by National Natural Science Foundation of China (21476148), Scientific Research Program of Shaanxi Provincial Education Department (18JK0611), Natural Science Basic Research Plan in Shaanxi Province of China (2018JQ2060) and Open Project Program of National Demonstration Center for Experimental Light Chemistry Engineering Education (2018QGSJ02-11).

P88

Determination of free formaldehyde in leather chemicals

Yudan Yi[1], Wei Ding[2], Ya-nan Wang[1,2*], Bi Shi[1,2]

[1] *National Engineering Laboratory for Clean Technology of Leather Manufacture, Sichuan University, Chengdu 610065, China, Tel: +86-28-85405508, Email: wangyanan@scu.edu.cn*

[2] *Key Laboratory of Leather Chemistry and Engineering (Sichuan University), Ministry of Education, Chengdu 610065, China*

Abstract

Formaldehyde is widely used in the synthesis of various leather chemicals due to its high reactivity and low cost. Formaldehyde will be introduced into leather when applying these chemicals, and then released during processing, storage and use, which may pose a potential risk for human health. Existing method for determining formaldehyde content in leather is difficult to deal with the complicated chemicals. In this study, a method was developed for accurate determination of free formaldehyde in leather chemicals. No more than 0.5 g solid or 0.2 ml liquid sample with formaldehyde range from 3.9 to 49.2 μg was heated at 90°C in nitrogen atmosphere. The released formaldehyde was purged at a flow rate of 300 ml/min for 30 min, captured and derivatized using a DNPH solution, and then detected by HPLC-DAD. The recovery rate of formaldehyde standard solution was 94%-109% with relative standard deviation (RSD) of 4.7% in seven times repeated trials. Then the formaldehyde content in three aldehyde tanning agents and four amino resin retanning agents were detected, showing the recovery rate higher than 90%. As a result, this method could accurately determine the formaldehyde content in leather chemicals available, and provide support for the development of novel formaldehyde-free tanning agents.

Keywords: formaldehyde; leather chemicals; tanning agent; amino resin

P89

Interaction of Al-Zr tanned leather with retanning agents

Wanli Huang[1], Ya-nan Wang[1,2*], Ying Song[1], Yunhang Zeng[1], Bi Shi[1,2]

[1] *National Engineering Laboratory for Clean Technology of Leather Manufacture, Sichuan University, Chengdu 610065, China, Tel: +86-28-85405508, Email: wangyanan@scu.edu.cn*

[2] *Key Laboratory of Leather Chemistry and Engineering (Sichuan University), Ministry of Education, Chengdu 610065, China*

Abstract

The development of chrome-free tanning technology is a key issue for leather industry. A type of novel Al-Zr tanned leather that we have develped has similar isoelectric point with chrome tanned leather, thus it is likely to perform well in post-tanning processes and result in finished leather with excellent physical and organoleptic properties. This paper aims to elucidate the interaction mechanism of this chrome-free tanned leather with retanning agents. The zeta potential and particle size of four retanning agents, i.e. mimosa extract (ME), melamine-formaldehyde resin (MR), acrylic resin (AR) and amphoteric acrylic resin (AAR) were measured. The effect of the retanning agents on the charge property of Al-Zr tanned leather was investigated, and the penetration and distribution of the retanning agents in leather were explored by fluorescent tracing technique. It was found that the negative charge of ME and AR was stronger than MR and AAR in the post-tanning pH range (pH 3-7). AR had the largest particle size, while the particle size of AAR was the smallest. These results coincided with the charge properties of retanned leather and the distribution of retanning agents in leather. The addition of ME and AR resulted in a significant decrease in the isoelectric point of retanned leather, which was greater than the influence of MR and AAR. AAR could completely penetrate into the Al-Zr tanned leather, while the penetration ability of AR was the worst at the same dosage. Retanning with multiple retanning agents promoted the penetration of the agents in leather. This work could provide theoretical guidance for the efficient interaction of leather with post-tanning chemicals and upgrade of the properties of chrome-free leather.

Keywords: retanning; chrome-free tanning; zeta potential; fluorescent tracing technique

P90

Study the Dyeing Effect of Myrica Extract on Rabbit Fur

YOU TAO(National Engineering Laboratory for Clean Technology of Leather Manufacture，Sichuan University)

Abstract

Ferrous sulfate was selected as a mordant to study the dyeing performance of Bayberry extract for rabbit fur. First, the rabbit fur was pretreated with hydrogen peroxide / formic, and the optimum pretreatment process was selected by orthogonal test. The effect of mordant dosage, temperature, time and pH on the dyeing properties of tannin extract were investigated. Dyeing properties such as leveling property, fiber strength and dry/wet rub fastness were tested. The results shown that the optimal pretreatment condition of rabbit fur dyeing was identified under the following conditions: 30ml/L hydrogen peroxide, 50 ml/L formic acid, 45℃ for 90 min. The dosage of mordant of 45g/L, mordant dyeing temperature of 65℃, mordant dyeing time of 60min, mordant dyeing pH of 3.0-4.0 were found to be the optimal conditions for rabbit fur dyeing with myrica rubra extract, and black color can be obtained. Compared with normal dyeing process, the rabbit fur dyed by pretreatment process has a better leveling property and a higher dry/wet rub fastness and shrinkage temperature, but the fiber strength and glossiness is inferior to the normal dyeing.

P91

Fabrication of Polyacrylate/Nano-Ag Composites Toward Antibacterial and Antistatic Properties Enhancement of Leather

Yan Bao[a,b]*, Lu Gao[a,b], Jianzhong Ma[a,c]*

[a] *College of Bioresources Chemical and Materials Engineering, Shaanxi University of Science and Technology, Xi'an, 710021, PR, China, *E-mail: 2373840247@qq.com, Tel: +86-18729095629*

[b]*National Demonstration Center for Experimental Light Chemistry Engineering Education, Shaanxi University of Science and Technology, Xi'an, 710021, PR, China, *E-mail: baoyan@sust.edu.cn, Tel: +86 029 86168133*

[c]*Shaanxi Research Institute of Agricultural Products Processing Technology, Xi'an, 710021, PR, China, *E-mail: majz@sust.edu.cn, Tel: +86-029-86168006*

Abstract

Considerable attention has been devoted to fabricate antibacterial and antistatic coating on leather matrix, owing to the production of bacteria during storage and use or the special requirements of garment leather. In this paper, nano-Ag were synthesized with the help of ethylene glycol and characterized by X-ray diffraction (XRD) and scanning electron microscope (SEM). Moreover, nano-Ag as antibacterial agent and conductivefiller were introduced into polyacrylate coating to significantly enhance the antibacterial and antistatic properties of leather. The results showed that nano-Ag with high crystallinity was successfully fabricated. Nano-Ag was composed of Ag nanowires (AgNWs) and Ag nanoparticles (AgNPs). Compared with polyacrylate film, the antibacterial properties of composite film with 7% nano-Ag was increased by 61.67%, and the surfaceresistivity was reduced by 3 orders. Besides, the antibacterial properties of leather finished by composite emulsion was increased by 10.33% and the surface resistivity of leather finished by composite emulsion was decreased about 3 orders. The reason for this is that AgNPs were evenly dispersed in composite coating, which effectively prevented the invasion of bacteria. Moreover, the existence of AgNWs was contributed to the reduction of surfaceresistivity because it is more easy to form a conductive network in the matrix. Thus, a promising coating with antibacterial and antistatic properties for leather finishing agent was approved.

Keywords: Polyacrylate/nano-Ag composites; antibacterial; surface resistivity; leather finishing

P92

Study on Physical-chemical Properties of Mink Shavings

Yujie Zhang, Lihong Fu *, Donglei Liu, Huilin Tian, Wei Kuang

College of Leather Chemistry and Engineering, Qilu University of Technology(shandong Academy of Sciences) Jinan, Shandong, China, 250323

Abstract

China has become the largest fur processing center in the world, the amount of finish for about 75%. In production of mink, amounts of collagen waste including scurf and other waste would be produced. It is a research hotspot about utilization of these collagen waste. The physical-chemical properties of mink shavings were studied from amino acid composition chemical, constituent, hygienic property, mechanical behavior and the parametric variation in the process of washing and rewetting. It was found that: ①The protein of mink shavings is composed of 16 kinds amino acids, neutral amino acids accounted for 77.35%, acidic amino acids and basic amino acids were 13.87% and 8.78%, hydroxyproline were 8.53%, free of sulfur amino acid; ②After washing, the mink shavings were increased in volatiles, methylene chloride extract, water absorbency, shrinkage temperature, while total ash, the contents of water soluble substances, water vapor permeability, tear resistance and tensile strength were declined; ③Dehydration is mainly caused by thickness reduction, the area varies little; ④The washing methods of continue stirring, stirring and static soaking can accelerate the exudation of water soluble substance, the state of the solution is balanced with three times of repeated, it needs five times with static soaking method; ⑤The absorbates in the ultraviolet region were washed, besides collagen hydrolysate, other substances need further discussion.

Keywords: mink shavings; chemical constituent;hygienic property; mechanical behavior

Introduction

Tannery and fur processing industry is one of the ancient traditional industries, Parings and other waste which produced in the process of production cause serious pollution in the environment, it is one of the important factors restricting the sustainable development of leather and fur industry. In recent years, researchers have done a lot of research about paring and other waste, achieving remarkable results, for example, leather waste is used for producing methane, preparation of food, biochemical material, leather chemicals and industrial fiber materials[1], however, in the fur industry, especially mink industry, the utilization of solid waste and research technology is relatively few. China is the largest fur raw materials importer, fur garment producer, exporter, consumer in the world, and mink is one of the most important products in the international fur trade market, with “king of fur” name. According to statistics, in 2017, the number of mink in China reached 20.6 million, ranking first among the three fur products: mink skin, fox skin and raw raccoon skin[2]. In production and the treatment of shabby goods exists the problems of resource utilization of protein waste including hide fiber and wool fiber. Therefore, in this paper, the physicochemical properties of mink were analyzed which provided the basis for the utilization of protein waste in mink

1 Experimental Section

1.1 Materials and Instruments

1.1.1 Materials

Shavings of mink, a mink skin company in Hebei; Ultrafilter membrane(Φ0.3μm), Shanghai dense granular membrane separation technology Co. Ltd.

1.1.2 Instruments

Amino acid automatic instrument(L-8900), Hitachi; Ultraviolet spectrophotometer(UV-2000), Unico (Shanghai) instrument Co. Ltd; Digital display conductivity meter(DDS-11A), Shanghai Leici Xinjing instrument Co. Ltd; pH meter(PHS-3C), Shanghai precision scientific instruments Co. Ltd; Rotary evaporator(EYELA, N-1300), Shanghai eron instrument Co. Ltd; Rotary evaporator(RE-52A), Shanghai Ya rong biochemical instrument factory; Circulating water vacuum pump(SHZ-ⅢA),

Gongyi Yuhua instrument Co. Ltd; Electrothermal constant temperature dryness box(DHG-9140A), Shanghai Jinghong experimental equipment Co. Ltd; Low temperature permeation test instrument(GT-7045-EV), Gotech testing machines (Dongguan) Co. Ltd; Environmental stability test instrument(GT-7071-H), Gotech testing machines (Dongguan) Co. Ltd; XWN-20 Microcomputer controlled electronic universal testing machine.

1.2 Experimental Content

1.2.1 Amino acid composition of mink

The sample 0.0401g was accurately weighed after dryingin hydrolysis tube,then adding 6 mol/L hydrochloric acid 15ml, placing hydrolysis tube in electrothermal constant temperature dryness box, hydrolysis of 42h under 110℃. After cooling, the hydrolysate has constant volume of 25ml, filtering the solution and drawing 5ml into a round bottomed flask, steaming to constant weigh in high-vacuum, then it is dissolved with 0.02mol/L hydrochloric acid(5ml), analysis of amino acids.

1.2.2 Chemical constituent of mink

Chemical components of mink are measured before and after washing, using oven method to test water and volatiles content, using soxhlet extractor method to test methylene chloride extract, using vibration method to test water soluble content, using ignition method to test total ash[3].

1.2.3 Hygienic property and mechanical behavior of mink

The samples have to be air-conditioned 24h(20±2℃, 65±5%), using cooper's dish method to test water absorbency, using dynamic method to test water vapor permeability[3], and measuring shrinkage temperature, tear resistance, tensile strength of mink[4].

1.2.4 Relationship between three-dimensional structure of mink and water content

Washed mink is placed in weighing bottle, treating in temperature and humidity box((20±2℃, 65±5%), taking out every 30min, weighing after cooling 30min in desiccator, measuring the length, width and thickness of mink before and after treatment, repeating drying and the above operations until constant weight. 2 skin carry out experiment in parallel.

1.2.5 Relationship between washing parameters and washing method of mink

(1) Washing condition: Liquor ratio 50, Temperature 31℃, Time 30min.

(2) Operation: The skin were washed in three different ways. ①Continue stirring for 5min with glass rods; ②Stirring for 1min with glass rods and Static soaking 4min. ③Static soaking 5min. Washing repeated 6 times, measuring pH and conductivity of the solution after washing every time, and scanning the filtered solution by ultraviolet spectrum.

2 Results and Discussion

2.1 Amino acid composition of mink

Amino acid composition and content of mink hydrolysate is shown in Table 1.

Table 1 Amino acid composition and content of hydrolysate of mink slices

Amino acid name	nmol ratio（%）
Aspartic acid	5.39
Threonine	2.08
Serine	3.99
Glutamic acid	8.48
Glycine	35.26

Alanine	11.01
Cysteine	0
Valine	2.51
Methionine	0
Isoleucine	1.22
Leucine	2.75
Tyrosine	0.07
Phenylalanine	1.58
Lysine	2.70
Histidine	0.83
Arginine	5.25
Proline	8.35
Hydroxyproline	8.53

Note: nmol ratio (%) = (nmol of amino acid/nmol of all amino acids) x 100%

As shown in Table 1 following, mink consists of 16 kinds of amino acids, glycine content (35.26%) is the most in mink hydrolysate, and following is alanine (11.01%), hydroxyproline (8.53%); Neutral amino acids accounted for 77.35%, acidic amino acids were 13.87% and basic amino acids were 8.78%, and free of sulfur amino acid.

2.2 Chemical constituent of mink

Mink is rinsing before processing. The effect of rinsing on mink chemical constituent is shown in Table 2.

Table 2 The content of main chemical constituent in mink slices

All items	Chemical constituent（%）			
	Volatiles	Methylene chloride extract	Total ash	Water soluble substances
Before washing	6.85	35.81	1.86	3.43
After washing	7.88	40.61	0.72	0.825

Note: In addition to volatiles, all other composition were based on samples without volatiles.

As shown in Table 2 following, after washing, the mink shavings increased in volatiles and methylene chloride extract while total ash and the contents of water soluble substances declined. This is because water washes away most of inorganic salts in skin and other soluble substances such as tannins which was not firmly supported on skin. After washing, the content of methylene chloride extract increased, mainly because the salt and water soluble substances between the fibers affected the exudation of oil in the skin. After washing, the gap between the collagen fibers increased and the oil was more easily extracted.

2.3 Hygienic property of mink

Water absorbability and water vapor permeability can characterize the level of Hygienic property of mink. Hygienic properties of skins before and after washing is shown in Table 3.

Table 3 Hygienic property of mink slices

All items	Water absorbability（%）	Water vapor permeability mg/(cm²·h)
Before washing	507.80	5.464
After washing	543.18	3.042
Δ	35.38	-2.422

Note: Δ= Before washing - After washing

As shown in Table 3 following, after washing, water absorbability was increased 35.38% while water vapor permeability was declined 2.4 mg/(cm²·h). The reason is that, before washing, salts, oils and other fillers which on the surface of skin or between the fibers affect the water absorbability of the active groups in the skin fibers, so the water absorbability is relatively low. After washing, the hydrophilic groups on the surface of the skin fiber are exposed, so the water absorbability was increased.

The water vapor permeability of the skin is the ability that water vapor moves from higher humid air to lower humid air. The water vapor permeability is the result that vapor migration in the micropores of the skin under pressure. The higher the porosity of the skin, the more hydrophilic groups, and the better the water vapor permeability[5]. It can be seen that the main reason for the decrease of water vapor permeability after washing may be that the active groups in skin fibers are exposed more, and the hydrophilic groups are greatly reduced by a large number of cross-linking between the fibers after drying, and the water vapor permeability decreases because of the increase of cross-linking effect and the decrease of fiber gap.

2.4 Mechanical behavior of mink

Shrinkage temperature can characterize tanning condition and the stability to wet heat. Tear resistance and tensile strength can reflect the degree of tear resistance and resistance to external forces. Mechanical behavior of skins before and after washing is shown in Table 4.

Table 4 Mechanical behavior of mink slices

All items	Shrinkage temperature（℃）	Tear resistance（N/mm）			Tensile strength（N/mm²）		
		Transverse	Longitudinal	Average	Transverse *	Longitudinal *	Transverse
Before washing	59.45	412.7	84.4	248.6	4.377	13.442	16.36
After washing	62.07	290.39	76.33	183.4	6.199	13.524	11.11

Note: Longitudinal direction of parallel ridges, *indicates that the data of before and after washing do not belong the same mink.

As shown in Table 4 following, tear resistance and tensile strength are declined while shrinkage temperature is increased. The transverse tear resistance is much greater than the longitudinal tear resistance, while the longitudinal tensile strength is greater than the transverse. The reason is that mink skin fibers are mainly arranged along the direction of dorsal ridge (longitudinal) and relatively less transverse, so the longitudinal tear resistance is lower, but the tensile strength is higher. The tear resistance and tensile strength all decreased after washing, because the cross-linking strength of the fiber decreased, and the main cross-linking agent was aluminum tanning agent. The combination of aluminum tanning agent and collagen was

unconsolidated, so tear resistance and tensile strength decreased after washing. In addition, due to individual difference in the structure of mink skin, the transverse tensile strength of mink skin varies greatly.

2.5 Relationship between three-dimensional structure of mink and water content

During the drying process of wet skin, because of continuous water loss in skin, the weight, thickness, area and volume of wet skin will be changed in varying degrees. By the changes of three-dimensional parameters and weight, we can understand the effect of moisture removal in wet skin on the three-dimensional structure. Changes of skin parameters during drying process is shown in Fig. 1.

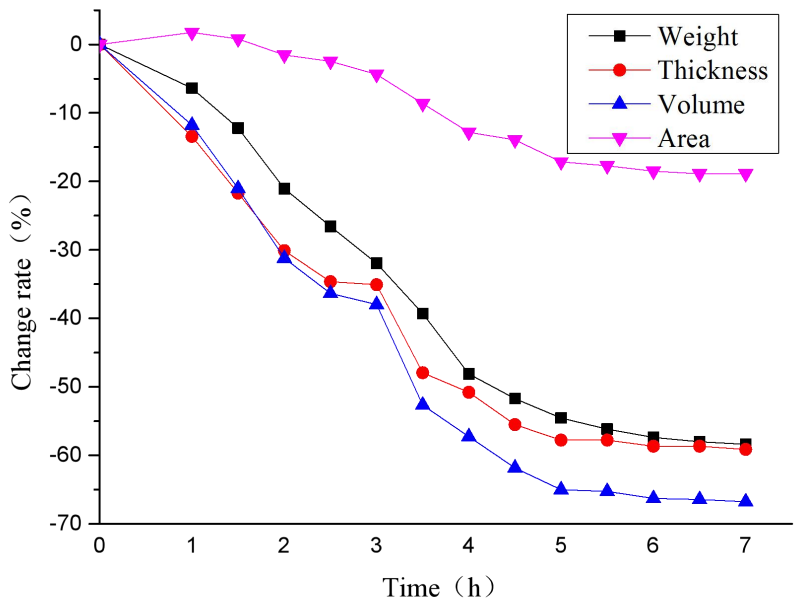

Fig. 1 Relationship between parametric variation and time in drying process of wet leather (20℃，65%)

As is shown Fig. 1 following, the change trend of the weight, volume and thickness of skin slices was similar, all of them were reduced first and then basically unchanged. The reason is that, during the drying process, free water removal which attached to skin surface and between the fiber pores does not cause skin shrinkage. Capillary water removal will make leather fiber bond and volume reduction, thus causing the reduction of leather area and thickness [6]. It can be seen that, within 1 hour of drying, the volume of the skin slice changed, but the area remained basically unchanged, indicating that the free water evaporated at this time; within 1-5.5 hours of drying, the change rate of the skin slice parameters decreased sharply, free water and capillary water evaporated; after 5.5 hours, the change rate of the skin slice parameters remained basically unchanged, indicating bound water existing at this stage.

During the drying process, the change trend of skin volume and thickness was similar, and area change was mild, indicating that the loss of water was mainly related to thickness change.

2.6 Relationship between washing parameters and washing method of mink

(1) The change of pH and conductivity

Mink is rinsing before processing, mainly removing surface contaminants and fillers. The removal degree of them can be characterized by the change of washing solution parameters. The changes of pH and conductivity of the washing solution

can reflect the changes of chemical composition and ions in the process of washing skin in a certain extent, and the washing effect of different washing methods is different. The change of pH and conductivity of water washing fluid during washing process is shown in Fig. 2.

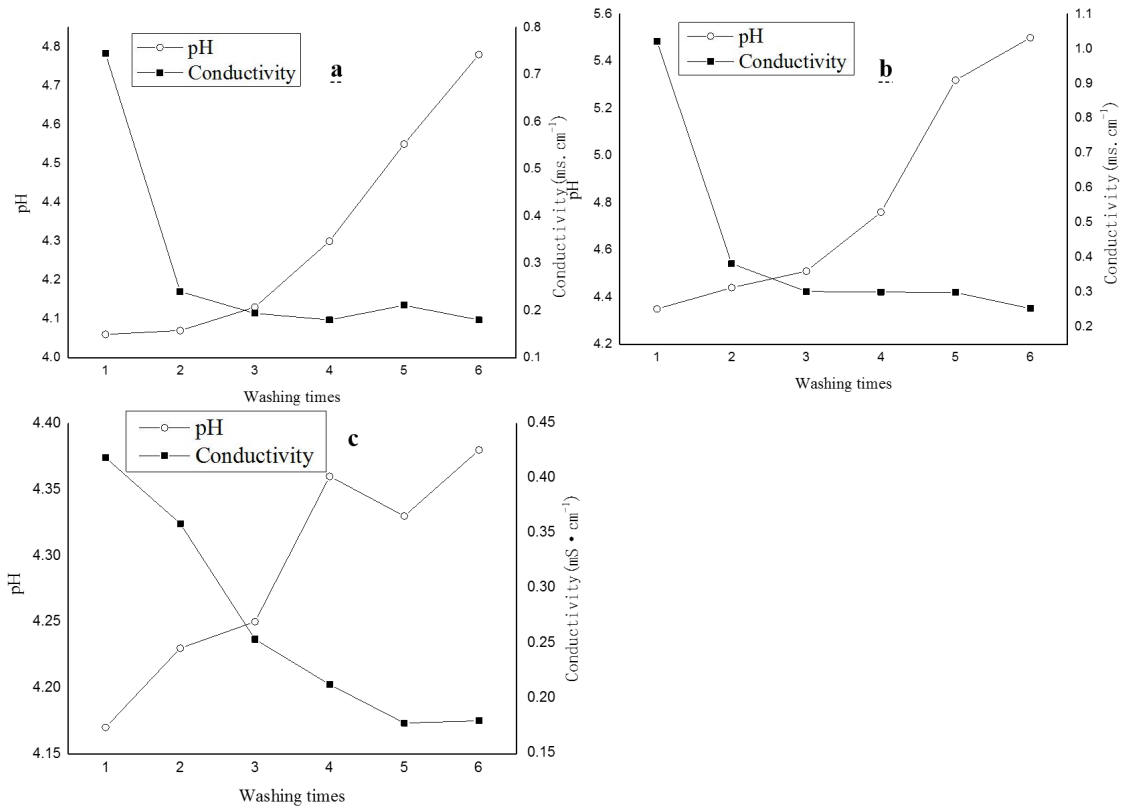

Fig. 2 Relationship between pH and electronic conductivity of water washing solution and water washing methods (31℃, liquor ratio 50)

(a: Continue stirring, B: Stirring and static soaking, c: Static soaking)

As shown in Fig. 2 following, with the increase of washing times, the variation trend of conductivity of washing solution with continuous stirring and stirring-stopping is similar, all of them are decreased sharply first, then decreases slowly and then remains basically unchanged, and the decreases are the largest in the first two washing times, and basically remains unchanged after three washing times. The static soaking slowly drops to the same electrical conductivity during continuous washing for 5 times. However, the conductivity descender of the three washing methods is different, three methods continue stirring, stirring and static soaking, static soaking conductivity descender is 0.57, 0.74 and 0.24 $\mu S \cdot cm^{-1}$ respectively after two washing. This is because mink skin contains acid, alkali, salt, tanning agent and surface treatment agent after preparation and tanning. During washing process, the substances which are not firmly combined with the skin and the skin surface substances will diffuse to the solution, and the stirring action can accelerate the diffusion. Therefore, the conductivity of the second lotion is sharply lower. Because the collagen fibers make up the skin exist in braided form[9], the skin is filled with water when washing, and the number of ions in the skin and on the skin surface is reduced, so the conductivity gradually decreases to unchanged at the later stage of washing. However, the conductivity of the static soaking solution decreases slowly because the static soaking mainly depends on the difference of the concentration of ions inside and outside the skin, which makes the soluble substances inside and outside the skin diffuse uniformly into the solution. Therefore, the rate of conductivity decrease during the five washing processes is basically the same, until the later stage of washing, the

concentration of ions inside and outside the skin is basically balanced, so the conductivity is basically unchanged.

With the increase of washing times, the pH of washing water increased slowly first and then increased sharply by continue stirring or stirring and static soaking. But the pH of washing water has been growing by static soaking. This is because the skin is weak acidic after aluminum tanning, and the combination of Al^{3+} and collagen is the internal rail complexation, the binding ability is relatively lower[7], with the diffusion of intradermal H^+ to the solution during washing, Al^{3+} and OH^- are combined, so H^+ is increased, so the solution pH is in the acidic range. In addition, the water-filling effect of the skin can reduce the concentration of hydrogen ions in the skin, and the breakage of Al^{3+} and COO^- will increase the probability of $Al(OH)_3$precipitation. At the same time, the COO^- on the skin collagen will bind to H^+, and the diffusion rate of H^+ to the solution will decrease, so the pH of the solution will increase slowly in the later washing period, but it is still in the range of weak acidity.

(2)Analysis of ultraviolet absorption spectrum

Because the washing process will not only lead to detanning, but also eluting treatment agent on the skin, it may change the combination of collagen and a small amount of collagen hydrolysis, in addition, the skin is weak acidic, the placement process will also lead to partial collagen hydrolysis, we can understand these changes by UV spectrum. Amino acid analysis shows that mink skin contains a large amount of phenylalanine and a small amount of tyrosine, both of them are absorbed in the ultraviolet region [8], phenylalanine absorption peaks at 222 nm and 259 nm, tyrosine absorption peaks at 231 nm and 272 nm. The ultraviolet absorption spectrum of lotion during washing is shown in Fig. 3.

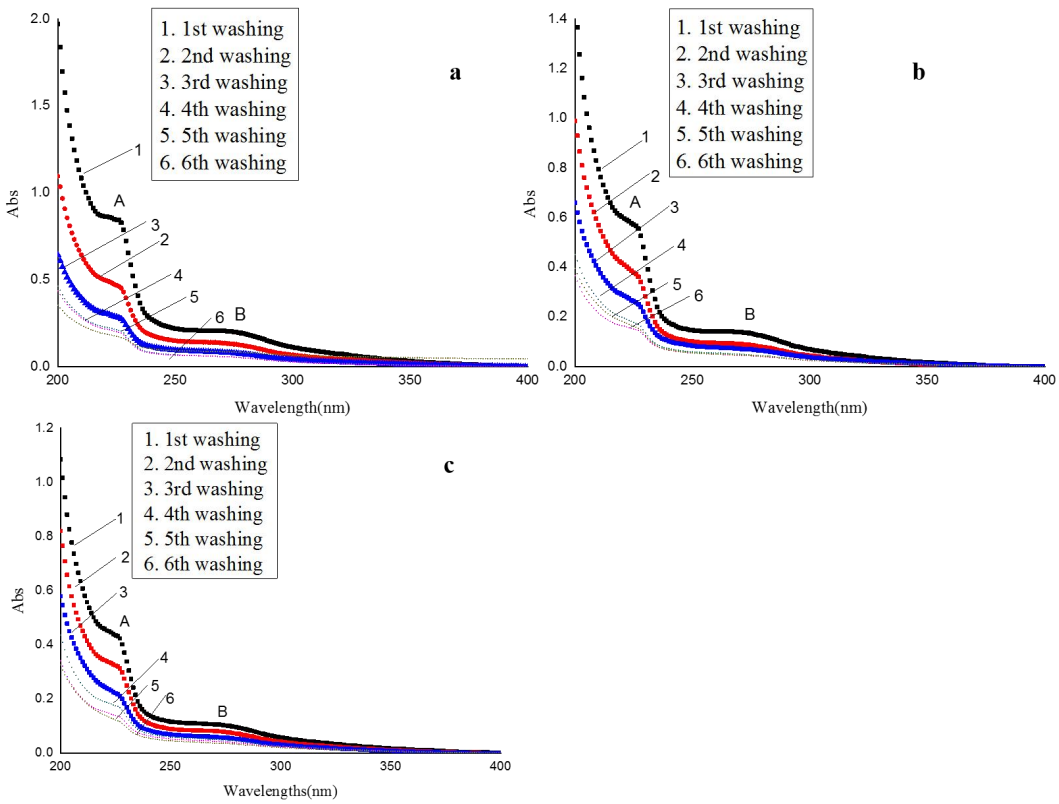

Fig. 3 Ultraviolet absorption spectra of water washing solution (a: Continue stirring, B: Stirring and static soaking, c: Static soaking)

As shown in Fig. 3 following, the ultraviolet absorption spectrums are similar with different washing methods, all of their absorption peaks are at 227nm and 270nm, and absorption strength is reduced with the increase of washing times. The UV

absorption curves of 5th washing and 6th washing were basically coincided, and absorption is extremely low. The results showed that the original hydrolysate and collagen hydrolyzed by the skin itself were gradually washed out, the amount of hydrolyzed collagen decreased with the number of washing times increased. So the more washing times, the lower the absorption.

3 Conclusions

(1) Mink consists of 16 kinds of amino acids, neutral amino acids accounted for 77.35%, acidic amino acids were 13.87% and basic amino acids were 8.78%, hydroxyproline were 8.53%, and free of sulfur amino acid.

(2) After washing, the mink shavings were increased in volatiles and methylene chloride extract while total ash and the contents of water soluble substances were declined.

(3) After washing, the mink shavings were increased in water absorbency while water vapor permeability were declined.

(4) After washing, the mink shavings were increased in shrinkage temperature while tear resistance and tensile strength were declined.

(5) Dehydration is mainly caused by thickness reduction, the area varies little.

(6) The washing method of continue stirring, stirring and static soaking can accelerate the exudation of water soluble substance, the state of the solution is balanced with three times of repeated, it needs five times with static soaking method; The absorbates in the ultraviolet region were washed, besides collagen hydrolysate, other substances need further discussion.

Acknowledgment

This work was financially supported by the National Natural Science Foundation of China (No.21606139).

References

[1] Wang Xiaopeng. Comprehensive Utilization and Prospect of Leather Solid Waste[J]. Western leather, 2017, 39(17): 38-42.

[2] Wang Dianhua. Statistics on Skin Number of Chinese Mink, Fox and Raw Raccoon Skin in 2017[J]. Leather and Chemical Industry, 2018, 35(02): 43-44.

[3] Teaching and Research Section of Northwest Institute of Light Industry. Analysis and Inspection of Leather[M]. Beijing: Light Industry Press, 1979: 528-555, 689-671.

[4] Luo Xiaomin, Ding Shaolan, Zhou Qingfang. Physical and Chemical Analysis of Leather[M]. Beijing: China Light Industry Press, 2013: 265-272.

[5] Tang Keyong, Wang Fang, Liu Jie. Study on the Water Vapor Permeability of Leathers[J]. Chinese Leather, 2002(07): 19-21.

[6] Shan Zhihua. Tanning Chemistry and Technology (The second volume)[M]. Beijing: Science Press, 2005: 188-189.

[7] Liao Longli, Chen Wuyong. Tanning Chemistry and Technology (The first volume)[M]. Beijing: Science Press, 2005: 189, 382-383.

[8] Dong Xin, Wang Liyan. Redetermination of Amino Acids Ultraviolet Spectrum[J]. Dezhou University Newspaper, 2015, 31(2): 44-46.

P93

Effect of Hydrolytic Reagent on Amino Acid Composition of Mink

Yujie Zhang, Lihong Fu *, Huilin Tian, Donglei Liu, Wei Kuang

College of Leather Chemistry and Engineering, Qilu University of Technology (Shandong Academy of Sciences) Jinan 250353, China

Abstract

Mink is the fur material of slap-up fur, in production and the treatment of shabby goods exists the problems of resource utilization of protein waste, including hide fiber and wool fiber. In addition, analysis on amino acids composition also exists the problems that different methods of pre-treatment effects determination result. Sulphuric acid and hydrochloric acid as a hydrolytic reagent onto shavings of mink, the effect of hydrolytic reagent and condition on the hydrolysis products were studied by analysis on amino acids composition. It was found that: When sulphuric acid as the hydrolytic reagent, amino acids can be oxidized, the longer the time, the more complete the oxidation; When hydrochloric acid as the hydrolytic reagent, 16 kinds of amino acids can be obtained, among them, the content of glycine and glutamic acid were 24.36% and 11.47%, hydroxyproline were 10.29%, acidic amino acids were 18.07%, basic amino acids were 13.23% and neutral amino acids were 68.70%, after 9 days being placed, hydrolysates treated with hydrochloric acid, the contents of threonine and tyrosine were increased, other amino acids were decreased, among them, the decline rate of acidic amino acids was higher than that of neutral amino acids and basic amino acids.

Keywords: shavings of mink; sulphuric acid; hydrochloric acid; amino acid composition

Introduction

Mink is one of the most important product in the international fur trade market, with “king of fur” name, in production and the treatment of shabby goods exists the problems of resource utilization of protein waste, including hide fiber and wool fiber. In addition, analysis on amino acids composition also exists the problem that different methods of pre-treatment effects determination result.

Amino acid is the basic unit of enzyme and protein in organism. In nature, there are more than 20 kinds of amino acids involved in protein synthesis, more than 1000 kinds of non-protein amino acids have been found[1]. Amino acids analysis is widely applied into biochemistry, proteomics, clinical medicine, chemical industry, food science fields, analytical methods of amino acids are varied, it is mainly divided into two methods: direct detection of non-derivatization and indirect detection of derivatization, high performance liquid chromatography (HPLC) is the most widely used method[2]. The major error of amino acid analysis comes from sample preparation. Main methods for the preparation of protein hydrolysates are acid hydrolysis, alkali hydrolysis and enzyme hydrolysis[3], acid hydrolysis is widely used in sample pretreatment at present[4], low cost of hydrolysis, complete hydrolysis, and the hydrolysates are not racemic, the most commonly used hydrolysates are sulphuric acid and hydrochloric acid[3]. In this paper, the effect of hydrochloric acid and sulfuric acid on the hydrolysates of mink shavings was studied by amino acid automatic instrument, and the amino acid composition of mink was analyzed, which provided the basis for the utilization of protein waste in mink and the pretreatment of amino acid analysis.

1 Experimental Section

1.2 Materials and Instruments

1.1.1 Materials

Shavings of mink(The content of volatiles is 7.88%), a mink skin company in Hebei; Potassium sulphate(AR), Fine chemical plant of Laiyang economic and technological development zone; Copper sulphate(AR), Jinan chemical reagents factory; Sulphuric acid(AR), Fine chemical plant of Laiyang economic and technological development Zone; Hydrochloric acid(AR), Fine chemical plant of Laiyang economic and technological development zone; Ultrafilter membrane(Φ0.3μm), Shanghai dense granular membrane separation technology Co. Ltd.

1.1.2 Instruments

Amino acid automatic instrument(L-8900), Hitachi; Rotary evaporator(EYELA, N-1300), Shanghai eron instrument Co. Ltd; Rotary evaporator(RE-52A), Shanghai Ya rong biochemical instrument factory; Circulating water vacuum pump(SHZ-ⅢA), Gongyi Yuhua instrument Co. Ltd; Electrothermal constant temperature dryness box(DHG-9140A), Shanghai Jinghong experimental equipment Co. Ltd.

1.3 Experimental Content

1.2.1 Hydrolysis of mink shavings by sulphuric acid

(1)The sample 0.8289g was accurately weighed after drying. It was packed in the quantitative paper and placed in the 150ml kjeldahl flask, and the potassium sulphate 4.9305g, copper sulphate 0.6572g, and concentrated sulfuric acid 30ml were added in turn. A small funnel was inserted at the mouth of the bottle, then the kjeldahl flask was slanted on the electric stove and heated slowly. After a large number of foam was removed, the heating temperature is raised and the bottleneck slope was increased(About 60°). The total digestion time was 29h, which was heated by 19h and stayed overnight 10h[5]. Transferred the cooled hydrolysate to 250ml volumetric flask, constant volume with ultrapure water. Then removed 10ml from it and constant volume to 10ml volumetric flask with ultrapure water,analysis of amino acids in the filtered solution

(2) Analysis of amino acid from the filtered solution which placing 9 days in 250ml volumetric flask.

1.2.2 Hydrolysis of mink shavings by hydrochloric acid

(1)The sample 0.0401g was accurately weighed after dryingin hydrolysis tube,then added 6 mol/L hydrochloric acid 15ml, placing hydrolysis tube in electrothermal constant temperature dryness box, hydrolysis of 42h under 110℃(heating 32h and placing 10h unheated). Transferred the cooled hydrolysate to 25ml volumetric flask, constant volume with ultrapure water, then filtered the solution. Using 5ml solution to a round-bottom flask which filtered, steaming with a rotary evaporator(0.028MPa) 7h20min, stayed overnight 11h20min, steaming to constant weight(50min) in high-vacuum($5x10^{-3}$MPa), then dissolved with 0.02mol/L hydrochloric acid(5ml), analysis of amino acids.

(2) Using 5ml solution to a round-bottom flask which filtered and placing 9 days, steaming to constant weight(30min) in high-vacuum($5x10^{-3}$MPa), then dissolved with 0.02mol/L hydrochloric acid(5ml), analysis of amino acids.

1.2.3 Analysis methods

The Hitachi L-8900amino acid automatic instrument was used for sample analysis, the injection volume was 20μL.

2 Results and Discussion

Mink is mainly composed of protein, and protein is a ampholyte which basic unit is amino acid, it can react with acid or alkali. Amino acids are linked to each other by peptide bonds, and make up protein through hydrogen bond, van der waals force, electrical reaction and other molecular forces, all kinds of amino acids can be dissolved in strong acid or alkali solution.

(1) Amino acid analytical spectrogram of hydrolysates

Amino acid analytical spectrogram of hydrolysates with different hydrolytic reagents is shown in Fig. 1.

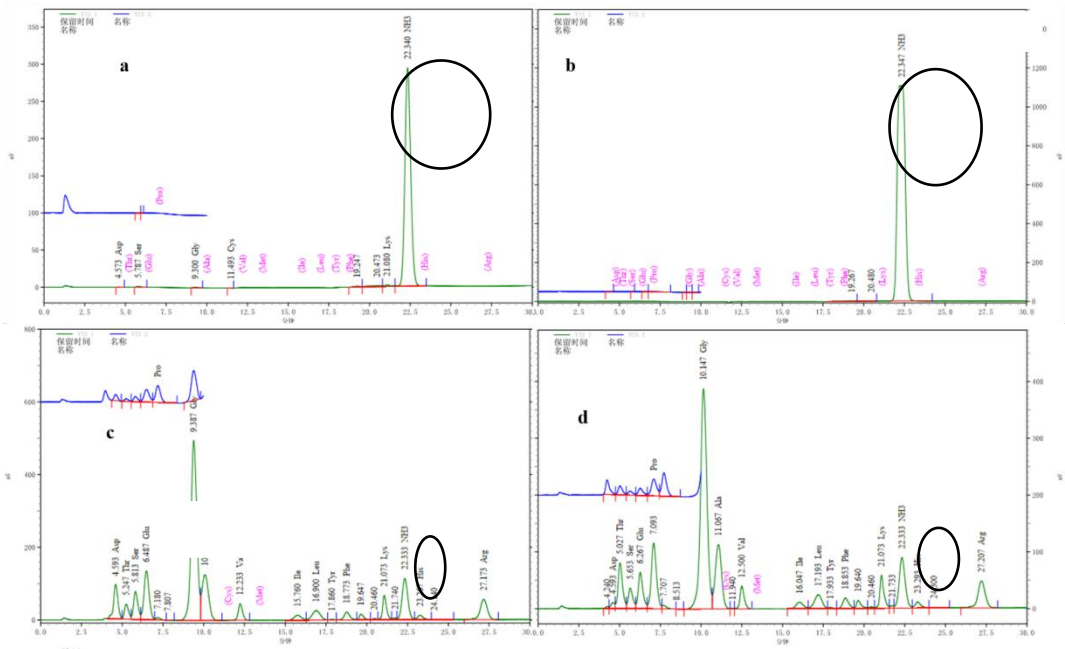

Fig. 1 Amino acid analytical spectrogram of hydrolysates
（a: hydrolysate of H_2SO_4，b: hydrolysate of H_2SO_4 for 9 days，c: hydrolysate of HCl，d: hydrolysate of HCl for 9 days）

As shown in Fig. 1 following, 16 amino acids in Hydrolysate of hydrochloric acid have a good effect on separation; The peak of hydrolysate which treated with sulphuric acid is less, only 5 amino acids, aspartic acid, serine, glycine, cysteine and lysine, there is no amino acid after 9 days.

(2) NH_3 content of hydrolysates

NH_3 content of hydrolysates with different hydrolytic reagents is shown in Table 1.

Table 1 NH_3 content of hydrolysates with different hydrolytic reagents

	H_2SO_4	H_2SO_4（9d）	HCl	HCl (9d)
Peak height	1173705	4423039	455311	356090
Peak area	28949811	149911917	11145474	91440281

As shown in Table 1 following, the content of NH_3 in hydrolysate of sulphuric acid is the highest, and increased greatly after 9 days. However, the content of NH_3 hydrolyzed by hydrochloric acid is far less than sulphuric acid, and also increased greatly after 9 days. It is concluded that sulphuric acid has a strong oxidative effect on hydrolysates, and most of amino acids are oxidized and decomposed, whereas oxygenolysis of hydrochloric acid is much weaker than sulphuric acid.

(3) Amino acid content of hydrolysates

Amino acid content of hydrolysates with different hydrolytic reagents is shown in Table 2.

Table 2 Amino acid content of hydrolysates with different hydrolytic reagents

Amino acid name	Mass ratio（%）			
	H_2SO_4	H_2SO_4（9d）	HCl	HCl（9d）

Aspartic acid	3.19	0	6.60	0.80
Threonine	0	0	2.28	6.23
Serine	13.07	0	3.86	2.47
Glutamic acid	0	0	11.47	6.47
Glycine	6.51	0	24.36	27.47
Alanine	0	0	9.03	10.33
Cysteine	8.40	0	0	0
Valine	0	0	2.71	3.01
Methionine	0	0	0	0
Isoleucine	0	0	1.47	1.67
Leucine	0	0	3.32	3.76
Tyrosine	0	0	0.12	0.26
Phenylalanine	0	0	2.41	2.78
Lysine	68.83	0	3.63	4.20
Histidine	0	0	1.18	1.34
Arginine	0	0	8.41	9.63
Proline	0	0	8.85	8.17
Hydroxyproline	0	0	10.29	11.42

Note: Mass ratio (%) = (quality of amino acid/quality of all amino acids) x 100%

As shown in Table 2 following, only 5 kinds of amino acids in hydrolysate which treated with H_2SO_4, in addition to lysine the content of amino acids is precious few. After 9 days, peak area of NH_3 is 149911917(Table 1) in hydrolysate without any kinds of amino acid. It can be seen that sulfuric acid can completely decompose the protein and have oxidative deamination in hydrolytic process, and the content of NH_3 is increased[6]. Five amino acids are lysine, serine, cysteine, glycine and aspartic acid, all of them are polar amino acids, amino acid content order is as following, alkaline, neutral, acid. Because polar groups in amino acid side chain form hydrogen bonds with water, so, the solubility of amino acids in water is increased[6]. Amino acid is amphoteric ion compound, it is easier to hydrolyze which side-chain groups are alkaline.

(4) Fluctuation of amino acid content after 9 days of hydrochloric acid hydrolysate

Fluctuation of amino acid content after 9 days of mink hydrolysate which treated with hydrochloric acid is shown in Table 3.

Table 3 Fluctuation of amino acid content after 9 days of hydrolysate

Name	Aspartic acid	Glutamic acid	Serine	Proline	Hydroxyproline	Valine	Glycine	Leucine
Variation ratio (%)	-90.69	-56.73	-50.88	-39.06	-14.83	-14.66	-13.50	-13.15
Name	Isoleucine	Histidine	Alanine	Arginine	Phenylalanine	Lysine	Threonine	Tyrosine
Variation ratio (%)	-12.84	-12.76	-12.26	-12.19	-11.60	-11.41	+109.27	+68.35

Note: Variation ratio (%) =（variations in amino acid content /original amino acid content）x 100%

As shown in Table 2 following, glycine content(24.36%) is the most in mink hydrolysate which treated with hydrochloric acid, and following is glutamic acid(11.47%), hydroxyproline(10.29%), alanine(9.03%), proline(8.85%), least is histidine(1.18%) and tyrosine(0.12%), free of sulfur amino acid. Neutral amino acids accounted for 68.79%, acidic amino acids were 18.07% and basic amino acids were 13.23%. Hydroxyproline is a cyclic amino acid, which can form intramolecular hydrogen bonds. It is a necessary condition for the stability of collagen helical chains[6].

After 9 days, 14 kinds of amino acids content is reduced, 2 kinds of amino acid content is increased(Table 3). ①Decline rate of acidic amino acids is greater than basic and neutral. Because amino acid is a ampholyte, it can dissociate amino acid cation of positive charge, and have a reaction with salt to produce amino acid hydrochloride[6]. ②The content of threonine and tyrosine is increased, because they are neutral amino acids with -OH and easier to dissolve in water.

3 Conclusions

(1) The type of acid has great influence on mink amino acid composition in acid hydrolysis

(2) Sulfuric acid as a hydrolysate, amino acids in hydrolysate are lysine, serine, cysteine, glycine and aspartic acid, all of them are polar amino acids, the amino acid content order is as following, alkaline, neutral, acid; And sulphuric acid has a strong oxidative effect on hydrolysates, the longer the time, the more complete the reaction.

(3) Hydrochloric acid as a hydrolysate, glycine content(24.36%) is the most, and following is glutamic acid(11.47%), hydroxyproline(10.29%), free of sulfur amino acid. Neutral amino acids accounted for 68.70%, acidic amino acids were 18.07% and basic amino acids were 13.23%.

(4)Hydrochloric acid as a hydrolysate, the content of threonine and tyrosine is increased and the rest is reduced after 9 days, decline rate of acidic amino acids is greater than basic and neutral.

Acknowledgment

This work was financially supported by the National Natural Science Foundation of China (No.21606139).

References

[1] RODGERS K J. Non-protein Amino Acids and Neurodegeneration; the Enemy within[J]. Anal Bioanal Chem, 2009, 393(2): 445-452.

[2] Ding Song, Huang He, Hu Yi. Research Progress on Amino Acids Analysis[J]. Chinese Journal of Bioprocess Engineering, 2018, 16(3): 12-21.

[3] Zhang Shaobo, Jin Dongwu, Li Mingsheng. Research Progress of Preparation Process of Protein Hydrolysates and Its Application in Biotechnology fields[J/OL]. Natural Product Research and Development: 1-15[2018-07-12].

[4] Li Mei, Wang Guirong. Practice on Pretreatment of Acid hydrolysis of Protein for Amino Acids Analysis[J]. Journal of Anhui Agricultural Sciences, 2014, 42(10): 2846-2847+2862.

[5]Teaching and Research Section of Northwest Institute of Light Industry. Analysis and Inspection of Leather[M]. Beijing: Light Industry Press, 1979: 543-547.

[6] Tang Keyong. Collagen Physics and Chemistry[M]. Beijing: Science Press, 2016: 21-23, 12-13, 110-111, 17-19.

P94

Influence of Sodium Chromate Colorimetry Factors on Chromium Content in Chromium Wastewater

Yujie Zhang, Lihong Fu *, Wei Kuang , Huilin Tian, Donglei Liu

College of Leather Chemistry and Engineering, Qilu University of Technology(shandong Academy of Sciences) Jinan, Shandong, China, 250323

Abstract

Chrome tanning can entrusted to leather excellent performance, but it contaminate the environment. High chrome exhaustion and less chrome tanning not only improve the exhaustion rate of chromium but also reduce the dosage of chromium. In spite of this, chromium wastewater is still produced. Therefore, timely and accurate analysis of chromium content in chromium wastewater is very important. Sodium chromate colorimetry is the usual method of chromium content in chromium wastewater. Due to the different chromium content and the different the amount of sodium peroxide consumed, it caused a large difference in pH value. In order to reduce the pH value, it is necessary to add hydrochloric acid, but the amount of sodium chloride in the solution is increased. The effect of the pH value and the amount of sodium chloride on the chromium content assay was studied. It was found that: Under the acid condition, the maximum absorption wavelength (243nm) can be used as the measuring wavelength. The pH value and the amount of sodium chloride has no effect on the chromium content assay; Under the conditions of neutral and alkaline, the maximum absorption wavelength (371nm) can be used as the measuring wavelength. The pH value and the amount of sodium chloride affects the chromium content assay. The higher the pH, the greater the sodium chloride content, the larger the chromium content assay. 390nm was used as the measuring wavelength, the chromium content is low.

Keywords: chromium content; sodium chromate colorimetry; sodium chloride content; pH

P95

Innovative design practice of local leather goods brands with “Chinese traditional culture gene”

Xuemei Li，Associate professor

Beijing institute of fashion technology

With decades of rapid development, China's leather enterprises have achieved high overall manufacturing level in terms of industrial scale, processing technology and production strength. Products on the domestic are extremely rich and ones of them become well-known brands. However, most of commercially successful domestic famous brands are based on the grafting of European leather goods, and the brand image is also the traditional classic style of European countries. However, with the upgrading of consumption, younger and innovative design has become an international trend. Chinese consumers have turn interest into a new brand innovation trends including Chinese traditional culture. Therefore, domestic brands urgently need to create a local brand with "Chinese cultural genes" instead of the traditional European leather goods. This paper firstly discusses and analyzes the fashion trends and innovation connotations of the leather industry, and proposes the importance and urgency of building Chinese local brands and establishing the Chinese cultural gene. It is a demonstration that domestic brands need to transcend traditional cultural concepts and provide consumers with personalized products with Chinese beauty with an open and confident attitude. Finally, for a practical evidence, we analyze and elaborate our own leather goods brand products in terms of the design concept, innovation inspiration and product development, and hope to provide readers with the experience and methods of combining Chinese aesthetic elements with modern fashion.

Keywords: Fashion leatherwear, design innovation, brand genes, Chinese traditional culture.

P96

Research of Fluorine-containing Acrylate Leather Finishing Agent

Zhihui Sui(School of Light Industry and Textile，Qiqihar University) China szh2736@163.com

Abstract

The fluorinated acrylate copolymers with core-shell structure were prepared with dodecafluoroheptyl methacrylate (G04), ethyl acrylate (EA), methacrylate (MMA) and acrylic acid (AA) as main raw materials through semi-continuous emulsion polymerization method, and it was applied to finishing leather. Structure and properties of product were studied by FTIR, XPS, TEM and TG and so on. The experimental result indicates that this method can be used to prepare bluish fluorinated polyacrylate emulsion. The emulsion has good stability and clear core-shell particles, and its film has a relatively high thermal stability as well. When it was used in leather finishing, the waterproof performance of the leather was improved significantly.

P97

Synthesis and Application of Fluorine Silicon modified Polyacrylate Leather Finishing Agent

Jinglong San(School of Light Industry and Textile，Qiqihar University) China 15944272156@163.com

Zhihui Sui(School of Light Industry and Textile，Qiqihar University) China szh2736@163.com

Abstract

Polypropylene acid ester emulsion finishing agent containing fluorine silicon was synthesized from these materials as follows: dodecafluoroheptyl methacrylate (G04), vinyltrimethoxysilane (A-171), methyl methacrylate (MMA) and ethyl acrylate (EA),using the method of semi-continuous seed emulsions, and applied to the finishing of the leather. The FT-IR, XPS, SEM, contact angle, wear resistance and other test methods were used to characterize the emulsion and its films. The results showed that organic fluorine, silicone and acrylate monomers reacted and fluorine silicone polyacrylate emulsions were successfully prepared. The water repellency and abrasion resistance of leather samples after finishing with fluorine silicone polyacrylate have been greatly improved.

P98

Fabrication of MOFs and Their Application in Polyacrylate Leather Finishing Agents

MA Jianzhong[1]* ,YANG Fan[2], BAO Yan[1], Chen Jie[1]

1 College of Bioresources Chemical and Materials Engineering, Shaanxi University of Science and Technology, Xi'an 710021

2 College of Chemistry and Chemical Engineering, Shaanxi University of Science and Technology, Xi'an 710021;

Polyacrylate emulsions are widely used in leather coating because of their excellent properties such as good film formation, strong adhesion, simple production process and low cost, etc. However, their application is limit due to their poor hygienic properties and not resistant to solvents, etc. MOFs are coordination polymers formed by metal ions and organic coordination, which have the advantages of porous structure and large specific surface area. In this paper, MOFs were introduced into polyacrylate emulsion by physical blending method to improve comprehensive properties of polyacrylate film. Firstly, MOFs were prepared by solvothermal method, and their structure and morphology were characterized by X-ray diffraction and field emission scanning electron microscopy. Then, MOFs were introduced into polyacrylate emulsion to obtain polyacrylate/MOFs composite emulsion. At the same time, the influence of MOFs dosage on the properties of polyacrylate/MOFs composite film were investigated. At last, the composite emulsion was applied to leather finishing. The experimental results showed that MOFs with a distinct octahedral structure and particle size of around 100 nm were successfully prepared by solvothermal method. When the dosage of MOFs was 1.0%, the blending temperature was 80°C, and the blending time was 5 h, the comprehensive performance of the polyacrylate/MOFs composite emulsion was optimal. Compared with those of the leather finished by pure polyacrylate emulsion, the tensile strength, tear strength, breaking strength, water resistance and water vapor permeability of the leather finished by polyacrylate/MOFs composite emulsion were improved by 5.65%, 10.34%, 21.43%, 8.62% and 5.89%, respectively.

Keywords: polyacrylate emulsion;MOFs; leather finishing; solvothermal method;

P99

A METHOD OF GENERATING SEAMLESS REPEAT PATTERN UTILIZING ADOBE ILLUSTRATOR FOR SIMULATING LITCHI GRAIN LEATHER SURFACE

WANG Wei[1], PENG Biyu[2], YANG Luming[3]

[1,2,3]Sichuan University, National Engineering Laboratory for Clean Technology of Leather Manufacture, South Section 1, Yihuan Road, No.24, 610065, Chengdu, China

[2,3] Sichuan University,Key Laboratory of Leather Chemistry and Engineering, 610065, Chengdu, China

Abstract

The purpose of this study was to introduce a method of generating seamless repeat pattern for simulating litchi grain leather surface using Adobe Illustrator CC. This is generic vectorial design software that provides pattern-editing mode, in order to solve the problems that leather products designers cannot simulate the litchi grain surface easily and realistically. For the methods, we referred to a scanning of a litchi grain leather sample image under 10 times the stereo microscope, with the help of different Tile types provided by Pattern Option panel in Adobe Illustrator CC, and on the basis of the rationale of seamless repeat pattern, we generated wrinkles and pores of litchi grain leather without using any complicated algorithm. The results of this study demonstrate that the seamless repeat pattern of litchi grain leather can be generated easily and quickly and present realistic and various effects when designing leather products. Moreover, the exported pattern tile could be widely used in other software. Furthermore, this method provides solutions for generating other different kinds of leather grain surfaces.

Key words: seamless repeat pattern, litchi grain leather, surface simultion, Adobe Illustrator

P100

Improve the Tanning Performance of Graphene Oxide by Thiol-ene Click Chemistry

LV Sheng-hua, LEI Ying, SUN Li, HU Hao-yan

(College of Bioresources Chemical and Materials Engineering,Shaanxi University of Science and Technology,Xi'an 710021, Shaanxi,China)

Abstract: Functionalization of graphene oxide (GO) with mercaptoacetic acid and vinyltrimethoxysilane to obtain fluorenated graphene oxide (GO-HS) and alkenylated graphene oxide (GO-VTMS), and then the GO-click-GO material was prepared by a thiol-ene click chemistry reaction between GO-HS and GO-VTMS. Thereafter, GO-click-GO was compounded with a chrome tanning agent to apply to the sour skin of sheep. The structure and morphology of GO-click-GO were characterized by FT-IR, XRD and SEM. The results showed that the GO layer in GO-click-GO material is fixed by the addition reaction of thiol-ene as a bridge, which increased the interlayer spacing of GO-click-GO and improved the dispersion of GO-click-GO. Tanning test results showed that when 4% chrome tanning agent and 0.3% GO-click-GO compounded leather had the best performance, the thickening rate was 38%, the shrinkage temperature was 99.4 ^{o}C, the tear strength was 58.47 N/mm, the breathability was 1722 mL/(cm^2·h), the tensile strength was 33.02 MPa, and elongation at break was 104.21%.

Key words:graphene oxide;click chemistry;thiol-ene; tanning agent

Foundation item: *National Natural Science Foundation of China (21276152)

P101

Research on the Design of Intelligent Shoes based on the Theory of Value Engineering

WAN Pengbo[1], ZHAO Xumei[2], ZHANG Wenli[3], HUI Pinpin[4]

[1]College of Art and Design, Shaanxi University of Science & Technology, 710021, Xi'an, China, 15249215290，wanpengbo@yeah.net

[2]College of Art and Design, Shaanxi University of Science & Technology, 710021, Xi'an, China,15289479265，1914529816@qq.com

[3]College of Art and Design, Shaanxi University of Science & Technology, 710021, Xi'an, China, 15802997657，1020357875@qq.com

[4]College of Art and Design, Shaanxi University of Science & Technology, 710021, Xi'an, China, 15191818740，1428513236@qq.com

Abstract

Based on the diversification and individuation of consumers' demand and with the development of the continuous progress of science and technology and information technology, intelligent wearable devices have an unstoppable development trend. As shoes are a branch of wearable devices, it will be an important direction for the development of intelligent shoes to combine material science and information technology with traditional shoes making industry organically to develop new intelligent shoes. Based on the exploration of the development of intelligent shoes, this paper analyzed the present situation and the existing problems, and found that the function is not enough to offset the cost and other related problems are the most serious in the process of product design. To resolve these problem, the theory of value engineering was used to optimize the design scheme, and it was applied to every stage of the design of intelligent shoes. Taking the function analysis as the core, the value engineering theory is used to guide the design of the intelligent shoes from the aspects of requirement analysis of customers, analysis of key intelligent technology, analysis of design scheme and so on. The application of the theory of value engineering in designing intelligent shoes is propitious to obtain greater value of shoes and provide guidance for the development and design of shoes, and at the same time to obtain greater economic benefits and market competitiveness for enterprises through reasonable cost control.

Key words: Value Engineering; Intelligent shoes; Design

P102

Application of Chinese traditional Art in Shaped Design of Footwear

WAN Pengbo[1], HUI Pinpin[1], ZHAO Xumei[3]

[1]College of Art and Design, Shaanxi University of Science & Technology, 710021, Xi'an, China, 15249215290，wanpengbo@yeah.net

[2]College of Art and Design, Shaanxi University of Science & Technology, 710021, Xi'an, China, 15191818740，1428513236@qq.com

[3]College of Art and Design, Shaanxi University of Science & Technology, 710021, Xi'an, China,15289479265，1914529816@qq.com

Abstract

This paper discussed the application of facial makeup and paper-cut art in the design of footwear from the viewpoint of the integration of Chinese traditional culture and art into the design, from the perspective of "Chinese Dream" and "Chinese creation". And briefly introduced the origin and development of these 2 kinds of art, and analyzed the color, pattern, culture and artistic characteristics. The combination of facial makeup, paper-cut art and footwear design were discussed in detail, including pattern application, color application and modeling technique. In the use of patterns, considering the angle of surface segmentation, uppers modeling design, fabric reconstruction and pattern application, it was emphasized that the pattern application should embody the shoe style and beautify the shoes, and consider the production technology, to stop beautification from reducing the processability. In the use of color, we should fully understand consumers' preferences and needs, grasp the cultural meanings of different colors, and also draw lessons from points, lines, facial techniques and the design style of color expression of facial makeup and paper-cut to meet the needs of consumers. In the aspect of modeling technique, emphasized the reference of aesthetic principle, attention to the expression of spiritual connotation in the design; and introduced the common craft technique and its requirement to the material, the style characteristic and the consideration factors. Finally, pointed out several requirements of the application of traditional art in current design, so as to better integrate traditional art into design.

Key words: traditional art; shoe design; pattern; shape

P103

Casein-based bifunctional antistatic flame retardant leather finishes

Wen An, Jianzhong Ma*, Qunna Xu*

College of Bioresources Chemical and Materials Engineering, Shaanxi University of Science & Technology, Xi'an 710021, China

**Email: majz@sust.edu.cn, Tel.:86-029-86168002*

ABSTRACT

With the development of science and technology, the functional requirements for leather products are getting higher and higher. This paper mainly introduces a fabrication route of bifunctional antistatic flame retardant leather finishing materials to give functionality of leather in use. In detail, modified Hummers method was used to prepare graphene oxide (GO), and the GO was reduced by $NaBH_4$ to obtain RGO, which was then introduced into the casein matrix by ultrasonic dispersion. The as-obtained casein-based RGO nanocomposite emulsion were applied to leather finishing process. Natural graphite and GO were characterized by XRD and FT-IR, indicating that GO has been successfully prepared. Performance of the as-obtained composite was demonstrated by tests of smoke density and surface resistivity. The results showed that surface resistivity of casein based RGO composite increased from 2.827×10^10 to 1.178×10^9, while smoke density increased from 13.14 to 8.825, which suggested that the as-prepared composite had expected antistatic flame retardant effect.

Key Words:casein, graphene, ultrasonic dispersion, antistatic, flame retardant

P104

Oxidized sodium alginate / layered double hydroxides Nanocomposite prepared by via exfoliation-reassembly: Application as a fatliquorting agent

Bin Lyu[1,2,*], Yue-Feng Wang[1], Dang-ge Gao[1], Jian-zhong Ma[1,2,*], Meng-di Gong[1]

1 College of Bioresources Chemical and Materials Engineering, Shaanxi University of Science and Technology, Xi'an 710021, China

2 Key Laboratory of Leather Cleaner Production, China National Light Industry, National Demonstration Center for Experimental Light Chemistry Engineering Education, Shaanxi University of Science & Technology, Xi'an 710021, P.R. China

**Corresponding Author: xianyanglvbin@163.com;majz@sust.edu.cn*

Abstract

The small molecular substances volatilized during the leather fogging process will pollute the air environment inside the car and will condense on the car window, which will adversely affect the driving line of sight. Therefore, reducing the fogging value of automotive interior leather is a common concern in the leather industry. In this paper, a series of nanocomposite based on different mass ratios of oxidized sodium alginate (OSA) and layered double hydroxide (LDH) were prepared via exfoliation-reassembly and used to inhibit the leather fogging phenomenon. The OSA-LDH were introduced into modified Zanthoxylum Bungeanum Maxim Seed Oil (MZBMSO) to obtained the MZBMSO/OSA-LDH nanocomposites through in solution-blending method. The MZBMSO/OSA-LDH was applied in fatliquoring process of Cr^{3+}-tanning goatskin wet-blue. In contrast to the leather treated with MZBMSO, the leather treated by MZBMSO/OSA-LDH shows a remarkable improvement on fogging characteristic, decreasing of fogging value from 18.53mg to 10.35mg. The softness reached 7.3mm from 7.2 mm. In addition, compared with these of leather treated by MZBMSO, the tear strength and elongation at break of leather treated by MZBMSO/OSA-LDH were reached 35.26N/mm and 40% from 31.21N/mm and 23% respectively. The OSA-LDH could cross-link with leather collagen fibers to block the migration of small molecules substances in leather, as well as could not affect leather's softness and physical and mechanical properties.

Key words: Zanthoxylum bungeanum Maxin Seed Oil, Layered Double Hydroxide, Fogging characteristic.

P105

Preparation of Protein-based Liquid Agricultural Film with Hydrolyzate from Cowhair Waste

LI Wen-xin, CHEN Yu-rou, ZHANG Su-feng

(Shaanxi University of Science & Technology, Xi'an, 710021)

ABSTRACT：In this study, a liquid agricultural film was prepared from discarded cowhair keratin and its physicochemical properties were characterized. The cowhair was hydrolyzed by alkali oxidation method, the blended film was prepared by using cowhair hair hydrolyzate and PVA, glutaraldehyde and glycerin. The effects of the mass ratio of hydrolyzate to PVA, the amount of glutaraldehyde, the amount of glycerol, the blending temperature and time on the properties of the blend membrane were investigated. The effects of the mass ratio of hydrolyzate to PVA, the amount of glutaraldehyde, the amount of glycerin, the blending temperature and the blending time on the properties of the blended film were investigated. The structure and properties of the blend film were characterized by X-ray diffractometer (XRD), Fourier Transform infrared spectroscopy (FT-IR) and Differential Scanning Calorimetry (DSC). The experimental results show that the optimal film preparation process: hydrolyzate and PVA mass 8:1, glycerol 0.3g, glutaraldehyde 0.2g, temperature is 100°C, time 40min. The film has good thermal stability and has certain characteristics of moisturizing, heat preservation and promoting crop growth and development.

Key words: Cowhair keratin, Hydrolysis, Polyvinyl alcohol, Liquid agricultural film

At present, plastic film is one of the main techniques of agricultural cultivation in China. The traditional plastic agricultural film will damage the soil structure, hinder the transportation of water and nutrients, and cause white pollution to the environment [1]. The development of green and environmentally friendly new degradable films, such as liquid agricultural film, photodegradable film, photo-biodegradable film and fully degradable film, bring broad prospects for agricultural production[2-3]. Wasted cowhair produced during the leather tanning process is a rich renewable keratin resource, which is mainly rich in five elements of C, O, N, H and S. Among them, sulfur and nitrogen can be used as sulfur and nitrogen supplements to provide nutrition of crops. Hair removal and hair removal recovery of cattle hair due to the action of calcium hydroxide in the process of hair removal, the formation of a special -S-O-Ca-S- crosslinking bond inside the molecule, so in addition to above five common elements, the calcium content is also high[4]. Cowhair keratin also has good thermal stability, biodegradability and mechanical properties. Therefore, the research and development of wasted cowhair can not only achieve high value-added conversion of tannery waste, but also save resources and reduce environmental pollution. However, cowhair keratin is structurally stable and difficult to dissolve. At present, the hydrolysis methods of cowhair are acid hydrolysis method[5], alkaline hydrolysis method[6], enzymatic hydrolysis method[7], hydrogen peroxide hydrolysis method[8], alkali-enzyme synergistic hydrolysis method [9] and the like. Among them, the alkaline hydrolysis method is the preferred method for large-scale industrial hydrolysis of cowhair because of its simple operation and low cost. In this study, the alkali oxidizing method was used to hydrolyze cowhair keratin, and the hydrolyzed keratin was made into a new keratin-based liquid film. The structure and application properties of the solution film formation were studied. The results showed that the liquid mulch film has heat preservation, entropy increase and promote the crop growth.

1. Experimental part

1.1 Materials and Instruments

cowhair (Processed cowhair), Hebei Huangqi Defu Leather Company; sodium hydroxide, Xi'an Chemical Glass Station Chemical Factory; hydrogen peroxide 30%, Tianjin Fuyu Fine Chemical Company; polyvinyl alcohol (degree of polymerization 1750±50), Tianjin Chemical Reagent Wholesale Company; glycerin, Tianjin Fuyu Fine Chemical Company; glutaraldehyde (content ≥50%), Tianjin Fuchen Chemical Reagent Factory; all the above reagents are of analytical grade.

313-A Thickness Gauge, High Speed Rail Technology Company; TH-8203S Servo Computerized Table Tensile Testing

Machine, Suzhou Tuobo Machinery Equipment Company; Vertex70 Infrared Spectrum, Bruker, Germany;D8 Advance X-ray Diffractometer,Germany Bruker;DSC200PC differential scanning calorimeter, Netzsch, Germany.

1.2 Preparation of keratin hydrolyzate

Cowhair pretreatment: wash the cowhair by washing powder for 20 minutes, and wash the cowhair naturally and air dry under ventilation conditions.

Hydrolysis of cowhair by alkali oxidation: mixing cowhair, sodium hydroxide (in a ratio of 1:0.24), adding deionized water and hydrogen peroxide (3:1 parts) in a water bath at 90 ° C, stirring and hydrolyzing for 4 h, cooling and suctioning .The filtrate is ready for use.

1.3 Preparation of blend film

Add a certain amount of PVA to the cowhair hydrolyzate, heat it in a water bath, and then completely dissolve the PVA. Add appropriate plasticizer glycerin or cross-linking agent glutaraldehyde. After stirring thoroughly, pour the mixed solution onto the glass plate and push the film,dry down, peel off the film.

1.4 Performance testing of blended films

⑴ Thickness of film: The thickness of any three points on the film was measured with a thickness gauge, and the average value was calculated.

⑵ Tensile strength of the film: according to GB13022 (Test method for tensile properties of plastic film).

⑶ Elongation at break: According to GB13022 (Test method for tensile properties of plastic film).

⑷ Swelling rate of film formation in water: according to GB1034-70 (plastic water absorption test method).

⑸ The method for determining the nonvolatile content of the liquid mulch film is carried out in accordance with GB-T1725-2007 (measurement of the nonvolatile content of paints, varnishes and plastics).

1.5 Structural Characterization of Blend film

⑴ Infrared spectroscopy (FT-IR)

The film with a thickness of less than 0.025 mm was uniformly mixed with KBr and compressed, and the blend film was tested by a Brooke Bruker VERTEX 70 Fourier infrared spectrometer.

⑵ X-ray diffraction analysis (XRD)

Using a Bruker D8 Advance X-ray diffractometer from Bruker, Germany, the X-ray of the Cu target was 11°·min-1, the tube voltage was 40 kV, the tube current was 40 mA, and the blend film was scanned 5°to 50°.

⑶ Differential Scanning Calorimetry (DSC)

Under the protection of nitrogen, the endothermic curve of the sample was measured directly on a DSC200PC integrated thermal analyzer (Netzsch, Germany) at a heating rate of 10 °C/min and a scanning range of 20℃ to 500 °C.

1.6 Application experiment of liquid agricultural film

(1) Moisturizing degree

Sand and water were added to the two surface plates to control other conditions. The No. 1 was blank, and the No. 2 surface was sprayed with liquid agricultural film. The quality of the watch glass was measured at the same time every day. The difference in mass was compared to compare the evaporation of water to investigate the film.

(2) Seed germination rate

The 100 processed green cabbage seeds were planted in two pots, and the other conditions were controlled. No. 1 was blank, and No. 2 was sprayed into the liquid mulch to investigate the germination of the seeds in a certain period.

2. Results and analysis

2.1 Optimization of preparation conditions of blend film

2.1.1 Effect of keratin hydrolyzate and PVA mass ratio

The effect of the mass ratio of the hydrolyzate to the PVA on the film formation swelling ratio, elongation at break, tensile strength, and nonvolatile content is shown in Fig. 1 (a) and (b).

The pure cowhair hydrolyzate is not continuous in film formation. After drying at room temperature, the film is hard and brittle, and the mechanical properties are not good, and the film cannot be peeled off. However, PVA has good film-forming properties and adhesive properties, and it still has good film-forming properties after blending with keratin.It can be seen from the figure (a) that the tensile strength and elongation at break of the film at the mass ratio of the hydrolyzate to the PVA are 8:1, and then the tensile strength and the elongation at break show a decreasing trend as the mass ratio increases. Because PVA is easy to form a film, the physical and mechanical properties of the blended film are better. However, as the mass of the hydrolyzate increases, the PVA content per unit volume decreases. Therefore, as the mass ratio increases, the physical and mechanical properties decrease.

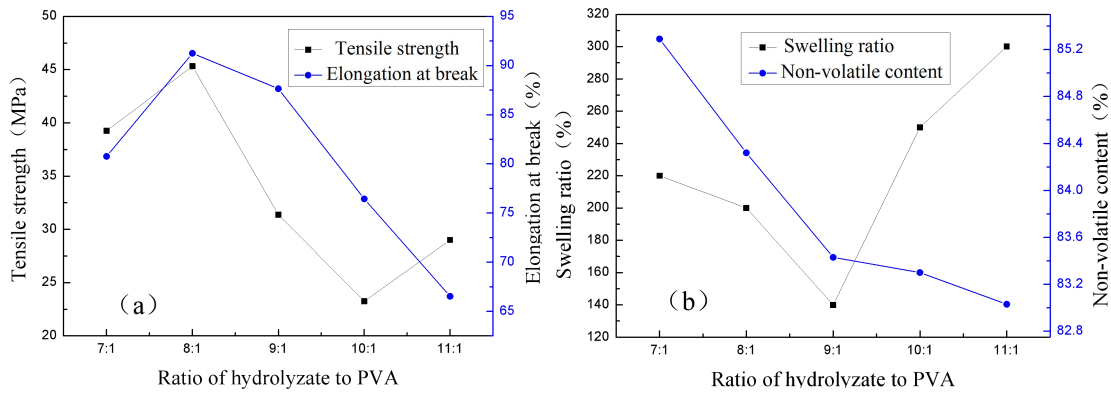

Fig.1 Effect of ratio of hydrolyzate to PVA on liquid film performance：

(a) tensile strength,andelongation at break;(b) swelling ratio and non-volatile content

The pure cowhair hydrolyzate is not continuous in film formation. After drying at room temperature, the film is hard and brittle, and the mechanical properties are not good, and the film cannot be peeled off. However, PVA has good film-forming properties and adhesive properties, and it still has good film-forming properties after blending with keratin.It can be seen from Fig.1(a) that the tensile strength and elongation at break of the film are the highest when the mass ratio of hydrolyzate to PVA is 8:1, and then the tensile strength and elongation at break are decreasing with the increase of the mass ratio. The trend is that PVA is easy to form a film, which makes the physical and mechanical properties of the blend film better. However, as the mass of the hydrolyzate increases, the PVA content per unit volume decreases, so the physical and mechanical properties decrease with the increase of the mass ratio.

It can be seen from Fig. 1 (b) that when the mass ratio of the hydrolyzate to the PVA is 9:1, the swelling ratio is the lowest, and when the mass ratio is less than 9:1, the swelling ratio decreases as the mass ratio increases, because as the mass ratio increases, the polyvinyl alcohol content per unit volume decreases, and the polyvinyl alcohol contains a network structure of a hydrophilic group.As the mass ratio increases, the non-volatile content of the product decreases continuously because the protein and PVA in the hydrolyzate are both solid substances, and the increase or decrease of the amount have a certain influence on the non-volatile content. When the mass ratio is increased, the content of protein in the hydrolyzate is unchanged, but the content of PVA is continuously reduced, so the non-volatile content is continuously reduced.

During the experiment, it was found that when the blending quality of the hydrolyzate and PVA was relatively large, the blend film was discontinuous and could not be uncovered, and it needs to be modified. It can be seen from the analysis that when the mass ratio of the hydrolyzate to the PVA is 8:1, the performance is great, so the mass ratio of the selected hydrolyzate to the PVA is 8:1.

2.1.2 Effect of glutaraldehyde dosage

The effect of the amount of glutaraldehyde on the film formation swelling ratio, elongation at break, tensile strength

and non-volatile content is shown in Fig. 2 (a) and (b).

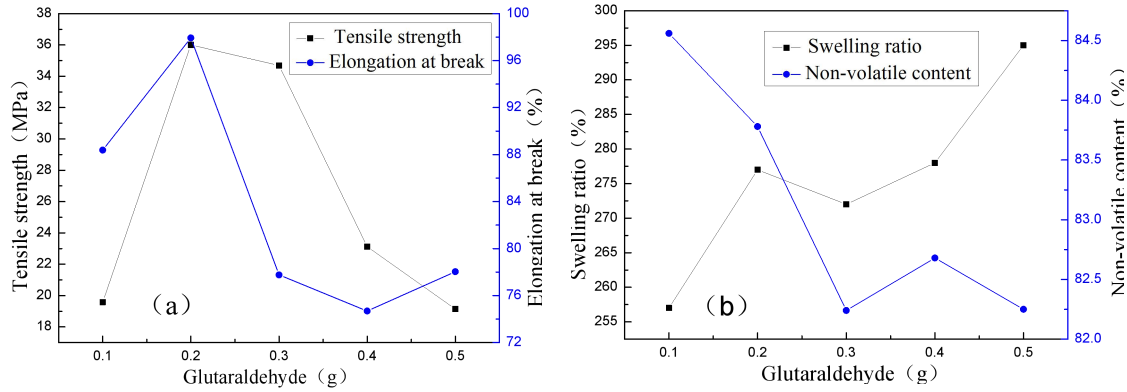

Fig.2-2 Effect of glutaraldehyde content on liquid film performance：

(a) tensile strength,andelongation at break;(b) swelling ratio and non-volatile content

In the process of blending the film, glutaraldehyde can also act as a cross-linking agent, and under certain conditions, the linear polymer, monomer or prepolymer can be converted into a three-dimensional network structure material.It can be seen from Fig. 2 (a) that when the mass of glutaraldehyde is 0.2 g/g, the tensile strength and elongation at break of the film are the largest, and then decrease as the mass of glutaraldehyde increases.The elongation at break is lower because of glutaraldehyde crosslinks keratin and PVA. This cross-linking mainly reacts with the amino group on the peptide chain. When both the aldehyde groups of the amino group and glutaraldehyde react, Crosslinking occurs, and as the amount of glutaraldehyde increases, the cross-linking effect increases, it will increase the compactness of the film.The reaction principle is shown in Fig. 3[10].

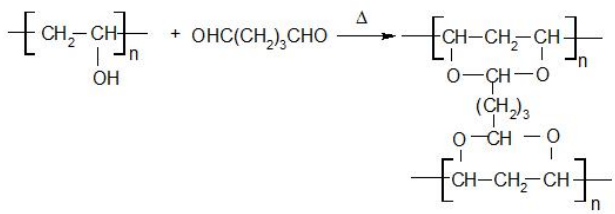

Fig. 3 Reaction mechanism of glutaraldehyde with amino group

It can be seen from Fig. 2 (b) that the swelling ratio increases with the increase of the amount of glutaraldehyde. Because the hydrophilicity of glutaraldehyde is great, the more the amount of glutaraldehyde, the swelling ratio of the liquid film is also relatively growth trend.Because glutaraldehyde is a colorless, transparent oily liquid with a pungent odor, it has a low melting point and volatile, so the non-volatile content is substantially reduced as the amount of glutaraldehyde is increased.Therefore, the suitable amount of glutaraldehyde is 0.2 g/g.

2.1.3 Effect of glycerol consumption

The effects of the amount of glycerin on the tensile strength, elongation at break, swelling ratio, and non-volatile content of the film are shown in Figures 2-4 (a) and (b).

It can be seen from Fig. 4 (a) that as the amount of glycerin increases, the tensile strength and elongation at break of the film increase. When the amount of glycerin reaches 0.3 g, the tensile strength and elongation at break of the film begin to decrease. Since glycerin has good plasticizing properties, when the amount of glycerin is increased, the plasticity of the film is also increased, and the tensile strength is enhanced.Since glycerin has a lubricating action, this action promotes the movement between molecules in the film, so the elongation at break increases as the amount of glycerin increases.

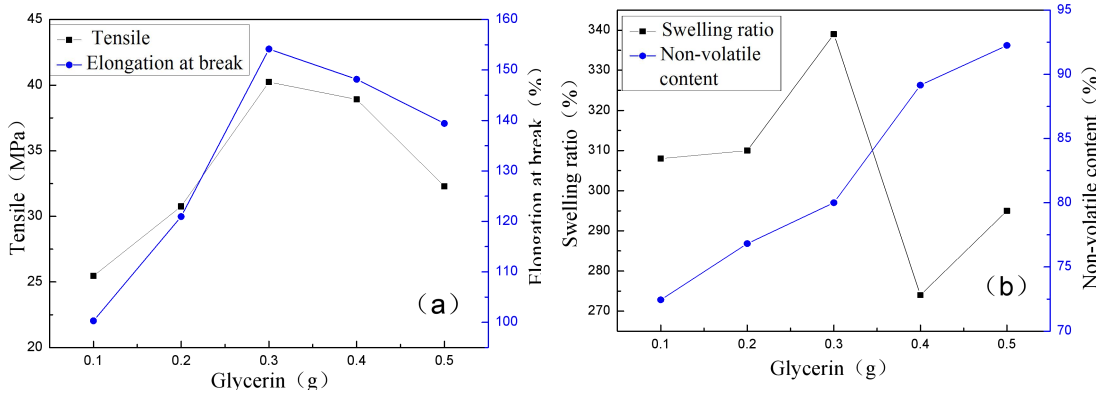

Fig.4 Effect of glycerol dosage on liquid film performance：

（a）tensile strength,andelongation at break;（b）swelling ratio and non-volatile content

It is known from Fig. 4 (b) that as the amount of glycerin increases, the swelling ratio and non-volatile content of the film gradually increase, and the maximum is reached when the amount of glycerin is 0.3 g, and then reduced.The increase in the swelling ratio is due to the fact that the glycerin has three reactive hydroxyl groups per molecule, making the film dense and highly absorbent.Since the amount of the plasticizer is too large, the spacing between the molecules of the film-forming material becomes large, so that the strength of the film is lowered, and because the amount of glycerin is too large, the film is not easily dried at room temperature, and the viscosity of the film is increased, so glycerin is The dosage should be moderate, so the amount of glycerin is 0.3 g/g.

2.1.4 Effect of blending temperature

The effects of blending temperature on film tensile strength, elongation at break, swelling ratio, and non-volatile content are shown in Fig. 5 (a) and (b).

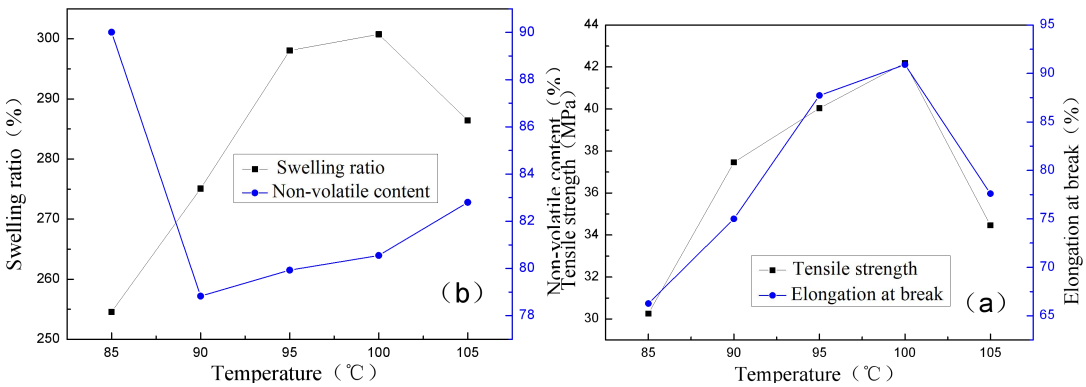

Fig. 5 Effect of temperature on liquid film performance

（a）tensile strength,andelongation at break;（b）swelling ratio and non-volatile content

It can be seen from Fig. 5 (a) that the tensile strength and the elongation at break of the film increase as the temperature increases, but when the temperature reaches 100°C, the tensile strength and the elongation at break begin to decrease. This is because the increase in temperature accelerates the condensation of the aldol and the esterification reaction, and it is advantageous for the film reaction, and the more complete the reaction, the better the performance of the film.However, if the temperature is too high, the water in the solvent will evaporate quickly, which will affect the uniformity of the blended film to a certain extent. It is difficult to push the film and accelerate the further degradation of the hydrolyzed product, so the

tensile strength and elongation at break has declined.

It can be seen from Fig. 5 (b) that as the temperature increases, the swelling ratio of the film increases, the swelling ratio reaches a maximum at 100°C, and begin to decrease after 100°C. The non-volatile content is the largest at 85 °C, the smallest at 90 °C, and the upward trend after 90 °C, and the non-volatile content fluctuates from 77% to 90%, because when the temperature rises to a certain extent, the solid content tends to stable, so the trend of non-volatile content is relatively flat.The increase in temperature can improve the efficiency of the reaction, so that the physical properties of the blended film are better, but the excessive temperature causes the cross-linked product to decompose, so the blending temperature is preferably 100 °C.

2.1.5 Effect of blending time

The effects of blending time on film tensile strength, elongation at break, swelling ratio, and non-volatile content are shown in Fig. 6 (a) and (b).

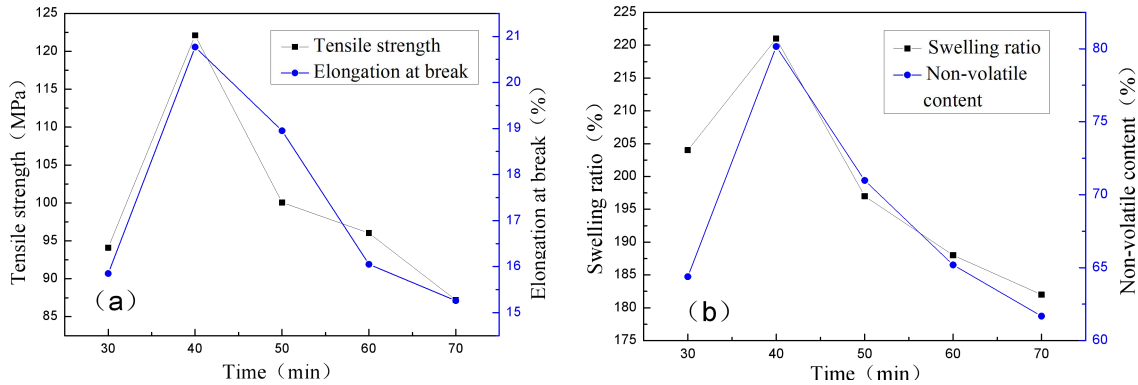

Fig. 6 Effect of time on liquid film performance:

（a）tensile strength,andelongation at break;（b）swelling ratio and non-volatile content

It is known from Fig. 6 (a) that the tensile strength and the elongation at break are maximum at a film forming time of 40 min, and then the tensile strength and elongation at break of the liquid film are decreased with time. In a certain period of time, the longer the film formation time, the better the degree of crosslinking with PVA, the better the tensile strength of the film. When the time is too long, the film forming performance is poor, and it is difficult to form a film.

It is known from Fig. 6 (b) that the swelling ratio and the non-volatile content are the largest when the film forming time is 40 min, and then decrease with time, because the film forming process increases with the film forming time. The water in the evaporation is more, and when the non-volatile content is measured, the quality of the film after drying is lowered.Because it is necessary to completely dissolve the polyvinyl alcohol at the time of film formation, it can be obtained through many experiments that the polyvinyl alcohol can be completely dissolved at 30 minutes. If the time is too long, the film will eventually become a viscous substance and cannot be formed into a film. According to the above obtained performance at 40 min, the performance of the film is in a superior state.

2.2 Blending film characterization

2.2.1 Infrared Spectroscopy Analysis of Blend Films (FT-IR)

Infrared spectroscopy and functional group characterization of hydrolyzate and blend films (see Figure 7) can reflect the characteristics of the molecular groups of the two.

It can be seen from Fig. 7 that the strong absorption peak at 1660.08 cm^{-1} and b at 1690.45 cm^{-1} is the amide I spectrum, so it can be inferred that the amide bond will be present in the hydrolyzate of the cowhair and the blend film. There is also a polypeptide structure, and the structure of the molecule can be changed from ordered to disordered.A peak at 3342.42 cm^{-1} is wide because of the high vibration frequency. The strong absorption peak at 1397.42 cm^{-1} is due to the fact that more side chain carboxyl groups are produced during the hydrolysis of keratin during the alkali reaction[11-13]. The peak at b at 3596.93

cm^{-1} may be due to the influence of external moisture, or may be caused by free-OH in the material; the peak at 2179.50 cm^{-1} is due to the expansion and contraction of double bonds in polyvinyl alcohol. Vibration; there is a peak at 1270.62 cm^{-1} because of the amide III band.

Through the comparison of the two, the blend film still has the characteristic peak of the protein, indicating that the keratin structure is not completely destroyed. After the keratin and PVA are blended, although there is no new chemical bond between the two, strong hydrogen bonding It cannot be ignored that these hydrogen bonding effects increase the interaction between the molecules of the blend and improve the compatibility of keratin with PVA [14].

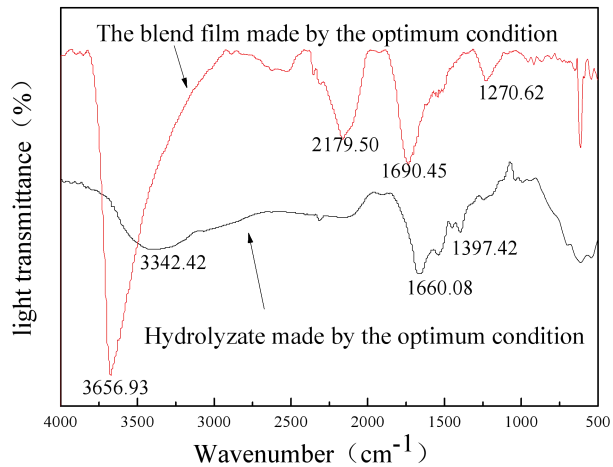

Fig.7. FTIR spectra of the blend film and hydrolyzate made by optimum condition

2.2.2 Blended film differential scanning calorimetry (DSC)

Differential Scanning Calorimetry (DSC) is a thermal analysis method that analyzes the composition of a substance by studying the relationship between the thermal properties of the substance and the temperature.The relationship between the blended film and the temperature can be reflected by measuring the film formed under the optimum conditions.

It can be seen from Fig.8 that there is a peak at each of the temperatures of 115℃, 206℃, and 249℃, indicating that the blend film contains three components, and the temperature is 115℃because of the escape of free water in the bound water. It contains a certain amount of water, which evaporates due to gradual heat absorption during the temperature rise [13], and two peaks appear at high temperature, while at 249 °C, the peak is narrower, which indicates a melting peak. The melting peak is caused by the melting of α-crystal, so the peak reflects the melting property of α-crystal, and the temperature at which PVA is completely dissolved is low. When PVA is blended with keratin, the thermal properties of the blended film can be changed.

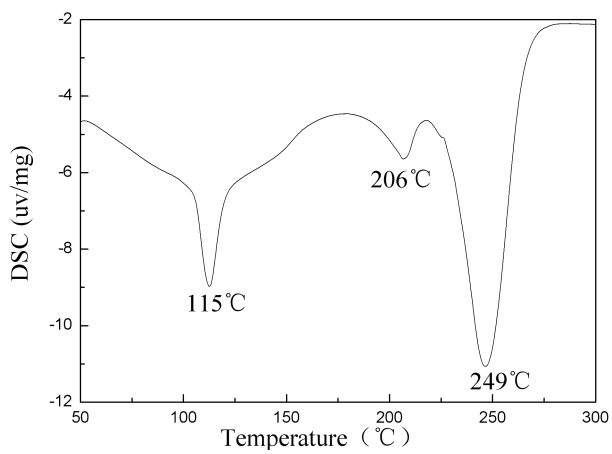

Fig. 8. DSC of the blend film made by optimum condition

2.2.3 Blend film X-ray diffraction analysis (XRD)

X-ray diffraction is a method of crystal detection. X-rays are generated on the crystals arranged in the atomic cycle to produce a diffraction pattern. The diffraction pattern reflects the arrangement of atoms in the crystal. The crystallization of the blend film can be characterized by XRD.It is known from Fig. 9 that the hydrolyzate is an amorphous phase structure, so its crystallinity is zero; pure PVA has a certain degree of crystallinity; and the blend film exhibits diffraction peaks at 2θ=19.60, 21.50, 23.90, which is similar with pure PVA. The peak position is the same, indicating that the blend film has the same crystal as the PVA.The narrow and sharp diffraction peak appearing at 2θ=28.46 is due to the precipitation of a new crystal phase in the blend film, indicating that the performance and structure of the film are changed after the hydrolyzate and PVA are blended.

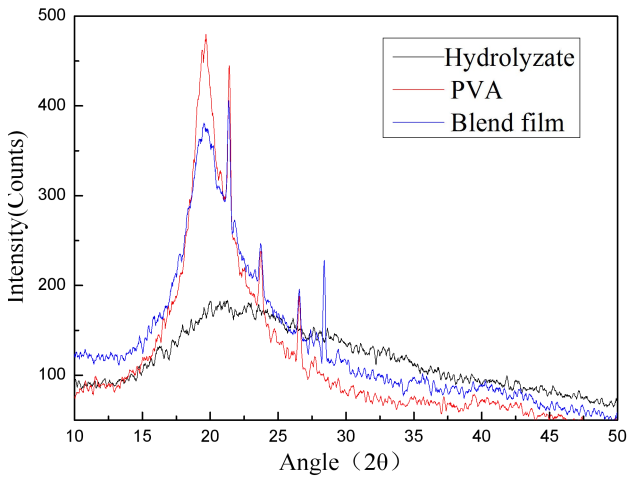

Fig.9. X-ray diffractograms of hydrolyzate,PVA and the blend film

2.3 Application effect of liquid film

2.3.1 Land moisturizing effect

After the sand was added to the two watch glasses, the mass was 86.322 g, and 15 mL of water was added to the two watch glasses to make the humidity uniform. One sprayed uniformly into the 5 mL liquid film and the other was used as a control. Finally, the quality of the control group was 101.322g, the mass of the liquid film sprayed into the liquid was 106.322g.

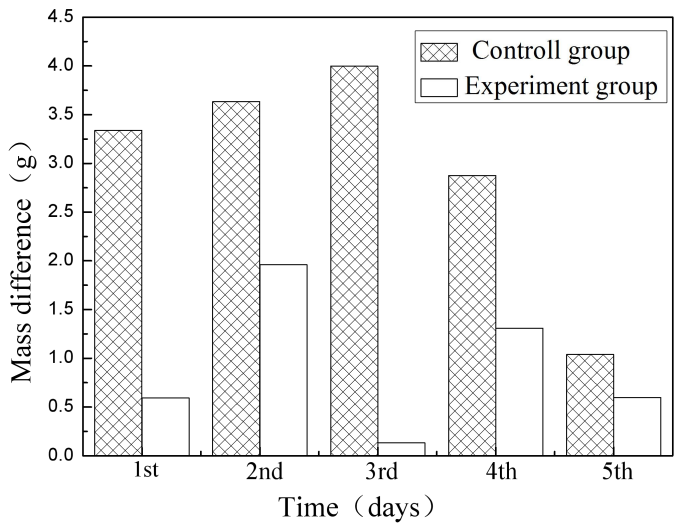

Fig. 10. Comparison of Moisturizing properties between the liquid film on the soil surface and the uncovered

The difference in mass indicates the volatilization of water. As can be seen from Fig. 10, the amount of volatile water in

the film without liquid spray is significantly higher than that of the film sprayed with liquid, so the moisturizing effect of the liquid film is better.The reason for the moisturizing of the liquid mulch can be understood as: when any kind of material is laid on the soil, a physical barrier layer can be formed to effectively resist the evaporation of water on the surface, but the liquid mulch is different from ordinary materials due to its own functional molecules. The large molecular weight of the soil particles is similar, and the functional groups and the active sites in the soil can be effectively combined, which can reduce the amount to a certain extent, making it feasible in cost.

The liquid mulch combines with the surface particles of the soil and acts only on the surface of the soil. It is essentially a profile-controlled evaporation of a very low level of water flux defined by an organic-inorganic barrier layer. The water vapor molecules slowly penetrate the liquid mulch. The closed layer formed after covering the ground is then lost to the atmosphere [15].

2.3.2 Germination rate of seeds

Two discs were planted with 100 seeds, one sprayed with liquid mulch and one without spray. The germination of the two disc seeds was observed in a cycle of 7 days. The germination rate of the seeds is shown in Table 1 below:

Table 1 Comparison of germination percentage

Sample	germination percentage
Experiment group	30%
Controll group	13%

According to the above Table 1, the germination rate of the seeds sprayed with the liquid mulch was significantly higher than that of the blank group. Within 7 days, about 30 germinations were sprayed with liquid mulch, while only 13 germinated without spraying, so the liquid mulch had the property of promoting seed germination.This is because the liquid mulch has a certain role of moisture retention, warming and moisturizing, and it can also be used as a fertilizer to transport nutrients for crops and promote the growth of crops, so it can promote seed germination. Therefore, the liquid mulch film can also promote the growth and development of crops while appropriately reducing the pollution to the environment.

3. Conclusion

(1) The optimal process for film formation is that the mass ratio of hydrolyzate to PVA is 8:1, water bath is heated at 100°C, glutaraldehyde is 0.2 g/g, glycerol is 0.3 g/g, film is formed for 40 min, and dried at room temperature. The film formation effect is great.

(2) Characterization of the film formed under the optimal conditions showed that the blend film had the characteristics of protein, good thermal stability and improved crystallinity.

(3) The liquid film developed in this experiment has good application effect and performance, and has certain advantages of moisturizing and improving seed germination rate.

Reference:

[1] Chao Song. Effects of polyethylene film mulch residue on crop yield/soil quality and soil microbial community composition [D]. Lanzhou University, 2014.

[2] Immirzi B, Santagataa G, Vox G, et al. Preparation, characterization and field-testing of a biodegradable sodium alginspray mulch[J]. Biosystems Engineering, 2009, 102(4) : 461-472.

[3] Tan Z, Yi Y, Wang H, et al. Physical and degradable properties of mulching films prepared from natural fibers and biodegradable polymers[J]. Applied Sciences, 2016, 6(5): 147.

[4] Pei Mao. Study on the preparation of leather filling materials by hair removal and hair removal [D]. Wenzhou University,

2014.

[5] Guolian Cui, Xiaolong Wang, Nianhua Dan, etal. Optimization of cowhair hydrolysis method and product performance characterization[J]Leather Science and Engineering, 2013, 23(6): 19-25.

[6] Xiaojun TAN, Beirong CAO, Quanjie WANG. Optimization of hydrolysis conditions of discarded cow's hair base for tannery[J]. Western Leather, 2010, 32(13): 8-11.

[7] Villa A L V, Arago MRS, dos Santos E P, etal. Feather keratin hydrolyzates obtained from microbial keratinases: effect on hair fiber[J]. BMC Biotechnology, 2013, 13(1): 1.

[8] Meng Liu, Haiming Cheng. Analysis of Hydrolysis and Performance of hydrolyzate in Cattle[J].China Leather, 2012, 41(17): 27-31.

[9] Xiaojun Tan, Beirong Cao, Quanjie Wang. Study on the hydrolysis process of abandoned cow's hair alkali from tannery[J]. Western Leather, 2010, 32(13): 8-11.

[10]Daxin Geng, Ying Chen, Li Xu. Preparation of Membrane and Study on Its Gas Separation Performance[J]. Membrane Science and Technology, 2005(5): 45-48.

[11]Guolian Cui, Xiaolong Wang, Nianhua Dan, etal. Optimization of cowhair hydrolysis method and product performance characterization[J]Leather Science and Engineering, 2013, 23(6): 19-25.

[12] Meng Liu, Haiming Cheng. Analysis of Hydrolysis and Performance of hydrolyzate in Cattle[J].China Leather, 2012, 41(17): 27-31.

[13] Zu-chun Yuan, Shui-wang Huang, Hong-xi Wu, etal. Preparation and Thermal Properties Analysis of Wool Keratin Films[J]. Progress in Textile Science and Technology, 2012(2): 36-38.

[14] Zongliang Chen. Development of keratin-based biodegradable mulch film [D]. Shaanxi University of Science and Technology, 2009.

[15] Liang Hao. Development of liquid film and its water retention effect [D]. University of Chinese Academy of Sciences, 2013

P106

Determination of short chain chlorinated paraffins in leather based on hydro-dechlorination technique

Ma He-Wei* and Tu Xiao-Juan

(College of Material and Textile Engineering，Jiaxing University，Jiaxing 314001,China)

Abstract: Short Chain Chlorinated Paraffins (SCCPs) were analyzed based on the hydro- dechlorination technique combined with Gas Chromatography - Flame Ionization Detection (GC-FID). SCCPs were successfully dechlorinated and hydrogenated to the corresponding alkanes (C_{10}-C_{13}) in the GC injector which is filled with Pd-catalyst. The relationship between the amounts of given SCCPs and the contents of yielded C_{10}-C_{13} could be well fitted by linear regression. The analytical procedure was applied for the determination of SCCPs in leather and presented 96-103% recovery and satisfactory precision (RSD＜6%) with detection limits 40 mg/kg. The real sample tests indicated the pollution significance of leather by SCCPs

Keywords: Leather, Short chain chlorinated paraffins, Gas Chromatography, Determination

P107

Study on The Technology of Preparing Peptide Calcium Chelate from Leather Waste

GE Shuhua[1], DIAO Shen[1], LUANN JUN[2] YUAN Yan[1], DAI Xuefeng[1], JIANG Shishun[1], WANG Quanjie[1,2*]

(1.College of Chemistry and Chemical Engineering, Yantai University,Yantai 264005, China;

2. State Leather Technology Research Development Center, Yantai 264005, China;)

Abstract: In this paper, mainly through the hydrolysis of waste scraps, and hydrolysis of calcium chloride and chelation reaction peptide - calcium metal chelate. The performance of the hydrolyzate was characterized and its concentration of free amino group was determined. Single-factor experiment and orthogonal experiment were designed to study the influence of pH, temperature, time, peptide-calcium ratio on the chelation reaction. The optimal conditions of chelating calcium chloride with peptides were determined. The study found that the impact of various factors on the chelation rate size: temperature> time> peptide / calcium ratio> pH; the extent of the impact on the yield: pH> temperature> peptide calcium> time. The best chelating conditions were as follows: the reaction time was 90 min, the ratio of peptide / calcium was 4:1, the reaction temperature was 70 ℃, the pH was 7 and the chelating rate was 86.55% under optimal conditions. Finally, FTIR analysis showed that the calcium ions chelated to the peptide successfully, resulting in calcium peptide chelates.

Key words: leather waste; peptide calcium chelate; chelate; chelating rate

Preface：

Leather industry accounts for an important proportion in light industry. At the same time, China is also a big country producing and consuming leather in the world.However, a large number of leather wastes are produced in the leather industry, which seriously affect the environment and human health.In the traditional tannery process, only 20% of the raw material is converted into of finished leather through a series of processing[1]. The rest of the leather is discarded as solid waste. This behavior has caused great waste of resources. At the same time, it also brought great challenge and pressure to the treatment of solid waste in tannery industry.With the increasing severity of global problems such as natural resources and social environment, the disposal of tannery waste has become a major issue related to the success or failure of the tannery industry.As early as the 1990s, some experts proposed that [2]:On the issue of tannery pollution, the tannery industry is faced with two choices, on the one hand, from the source to minimize waste emissions;On the other hand, it maximizes the disposal and recovery of by-products.How to minimize environmental pollution and make full use of solid waste has become a hot and important issue in the study of high value conversion of tannery wastes.

The study of trace element polypeptide chelates began in the 1960s. In the late 70s, the chelate of protein iron was synthesized from the animal and plant proteins and iron elements for the first time in the Albion Laboratory of the United States. The research and development of protein or polypeptide chelates began with the development of [3-5].It was not until the early 1990s that trace element polypeptide chelates were studied in China. For the rapid development of trace elements, a lot of industrialization has been realized, such as "3D" complex polypeptide chelating Fe (III), Cu (II), Co (II), Mn (II), etc. produced by Chengdu Aili company.Many domestic scholars have studied the chelate of trace element polypeptide. For example, Yang Wenbo [6] uses the hydrolysis of casein to explore the chelating process of Ca. Taking chelation rate as a study index, it is found that the chelation rate is related to the variety of protein and the length of peptide chain in protein hydrolysates except the mass ratio of peptide /Ca, pH, reaction temperature and reaction time. The shorter the peptide chain, the easier it is to be separated from Ca. Chelate. Zhao Wei, Li Tao and others used soybean meal as a source of complex peptides, and prepared complex polypeptide zinc chelate by deep hydrolysis[7].The results showed that the chelating rate of zinc was 66.16% and the yield of zinc chelate of polypeptide could reach 42.41% under the optimum conditions of the mass ratio of polypeptide to zinc 2:1, reaction temperature 60, PH=7 and reaction time 120 min.Zhao Haijun et al. [8] used soybean and metal zinc to prepare polypeptide chelates, to explore the effect and mechanism of soybean polypeptide chelating zinc on natural aging mice model, and to detect the content of MDA, SOD, lipofuscin (LPO) and total antioxidant capacity

(T-AOC) in liver homogenate by enzyme chemical method. Results the aging model of mice was successfully established.The results showed that soybean polypeptide zinc chelate could inhibit senescence through antioxidant mechanism.Fan Hongbing et al. [9] Polypeptide Ca chelate was synthesized from collagen of silver carp bone and acid hydrolyzed bone powder as Ca source.Maintaining the activity of some important enzymes is the normal development of plants.Regulate the PH value in the cell, prevent the accumulation and poisoning of organic acids in the plants, promote the absorption of nitrate in plants, improve the physical and chemical properties of the soil and reduce the barren soil.Polypeptide Ca chelates have good application prospects in fertilizers because of their high stability, high bioavailability and easy absorption by passive plants.The important significance of this paper is to realize the recovery and utilization of chrome shavings, solve the pollution problem of waste chrome shavings, and realize its resource utilization. Secondly, synthetic polypeptide Ca chelate organic fertilizer can be used in agriculture.

1.Materials and methods

1.1 Reagents and instruments

Leather shavings: Hebei Xinji Dongming Leather Factory; Phthalaldehyde: Shanghai Yuanye Biotechnology Co., Ltd; Other chemical reagents are analytical pure.Ultraviolet visible spectrophotometer: Shanghai Jinghua Science and Technology Instrument Co., Ltd.; Automatic nitrogen fixing instrument: Shanghai Sheng Sheng automatic analysis instrument Co., Ltd.; Nicolet 80 FTIR Fourier infrared spectrometer: United States; rotary evaporator: Shanghai Ya Rong biochemical instrument factory;Constant temperature water bath pot: Shanghai Ya Rong biochemical instrument factory; constant temperature and constant humidity box: Shanghai Bo Xun Industrial Co., Ltd. medical equipment factory; graphite digestion instrument: Shanghai true Analysis Instrument Co., Ltd.; Taiwan type high-speed centrifuge: Hunan Hersey instrument and Equipment Co., Ltd.; circulation water vacuum pump: Gongyi City to China Limited Liability Limited Company;Type JJ224BC electronic balance: Changshou City double Jay test instrument factory; gel permeation chromatography: Dalian Yi et analytical instruments Co., Ltd.; Viscotek TDA305max multi detector gel permeation chromatography: British Malvern Instrument Co.

1.2 Experimental method

1.2.1Preparation of polypeptide liquid

400 g of leather shavings were weighed into a 5 L three-necked flask. The liquid ratio is 5:1 and the amount of NaOH is 8%.The reaction temperature was 80°C (internal temperature), and the reaction time was 6 h. After the completion of the reaction, the hydrolyzate was centrifuged and suction-filtered to obtain a polypeptide solution, and the molecular weight thereof was measured.

1.2.2 Preparation of polypeptide chelated Ca

In this investigation, the alkaline hydrolysis of the polypeptide solution and CaCl2 chelation reaction, the experimental process is shown in Figure 1:The obtained hydrolyzate was concentrated to have a solid content of about 30%. CaCl2 was added to the obtained concentrate, and the peptide Ca was chelated at a certain temperature, pH, and time. The chelating solution was subjected to precipitation treatment with absolute ethanol and washed several times to remove Ca ions. The resulting precipitate was dried and ground to a powder.

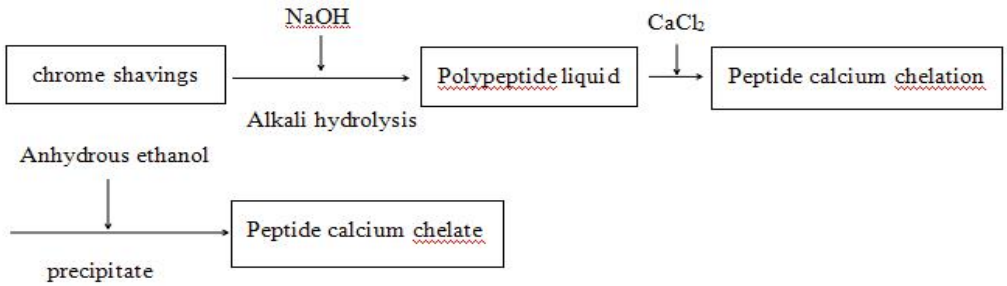

Figure 1 Peptide-Ca chelation process flow chart

1.2.3 Determination of chelation rate and yield

Titration was carried out using a standard concentration of 0.02 mol/L EDTA solution, and the chelation rate was calculated as follows:

$$\text{Chelation rate (\%)} = \frac{C_0 \times V_0 \times m \times 111}{0.1 \times 1000 \times m_{CaCl_2}} \times 100\%$$

C_0 is the concentration of EDTA (mol/L);

V_0 is the volume of the consumed EDTA (mL);

m is the total mass of the chelate (g);

$m_{CaCl2}$is the mass of anhydrous $CaCl_2$ added (determined by EDTA titration) (g).

10 mL of chelating solution was measured to determine the yield:

$$\text{Yield (\%)} = \frac{m \times V}{m_s \times 10} \times 100\%$$

m is the total mass of the chelate (g);

V isthetotal volume of hydrolyzate after chelation (mL);

m_s is the mass of solid after drying (g);

The premise of this method is that there is almost no soluble solid matter in the hydrolyzate except for the polypeptide.

1.2.4 Content determination of chelating calcium and chromium

a Establishment of a standard curve

A standard working solution with a concentration gradient of 0, 0.004, 0.008, 0.012, 0.016, and 0.020 mg/L is accurately prepared by taking a certain amount of chromium standard solution. The standard working solution of each concentration was placed in a sample tube of a graphite furnace atomic absorption spectrometer (AAS), the absorbance was measured, and a standard curve was drawn[10].

b Preparation and determination of samples

Accurately weigh 0.1 g of absolute dry chelated calcium (accurate to 0.0001 g), place it in a dry and clean hard digestive tube, accurately add 5 mL of concentrated sulfuric acid to it, shake gently, and place a small necked funnel on the tube. Put the hard digestive tube into the graphite digestion furnace, keep the temperature of the digestion furnace at 250 °C, remove it after heating for 10 min, add 2 mL H_2O_2 dropwise after cooling for a while, shake it and put it back into the digestion furnace to continue. Keep heating at 250 °C for 10 min, remove the digestive tube and then add 2 mL of H_2O_2 again. Repeat this operation for 3~4 times. After the color of the sample in the digestive tube becomes clear, continue heating for 10 min to decompose excess H_2O_2 in the tube. Remove the digestive tract, and then completely transfer the liquid to the 100 mL volumetric flask after cooling, and dilute to volume with ultrapure water, then dilute 10000 times with 1 mL of solution to

prepare the solution to be tested. The test solution is placed in a sample tube of an atomic absorption spectrophotometer, and the absorbance is measured to calculate the chromium concentration[11,12].

1.2.5 Determination of molecular weight of peptide hydrolysate by GPC method

1.2.5.1Preparation of solvent and sample

The ultrapure water was selected as the solvent.

Solvent treatment: filtration and degassing of the chromatographically pure solvent using a solvent filtration system (vacuum filtration);

Sample preparation: Take a certain amount of sample, dissolve it with ultrapure water, and stir overnight.

Sample Filtration: After the sample was dissolved, the sample solution was filtered using a microporous membrane (pore size 0.22 μm), and the filtrate was stored for use.

1.2.5.2Determination of molecular weight

Chromatographic conditions: column AGuard+1 x A6000M; mobile phase 0.1 mol/L $NaNO_3$ solution, pH 6.0; flow rate 0.7 mL/min; column temperature 35 °C; injection volume 100 μL. The polypeptide hydrolyzate was mixed into a standard sample solution having a mass concentration of 1.0 mg/mL using a mobile phase, and the injection amount was 100 μL, and the molecular weight was measured.

2 Experimental design of peptide Ca chelation

2.1The effect of reaction time

$CaCl_2$ was added to the concentrate obtained above, the pH was 7.0, the peptide Ca ratio was 3:1, the reaction temperature was 60 ° C, and the reaction time was 30 min, 60 min, 90 min, 120 min, 150 min, respectively. The chelating solution was precipitated with absolute ethanol and washed several times to remove Ca ions which were not subjected to the chelation reaction. The resulting precipitate was dried and grounded to a powder.

2.2 The effect of peptide Ca ratio

$CaCl_2$ was added to the concentrate obtained above, the pH was 7.0, the reaction temperature was 60 ° C, the reaction time was 60 min, the peptide Ca chelation reaction was carried out at the peptide Ca ratio was 0.5:1, 1:1, 2:1, 3:1, 4:1, 6:1, 9:13, respectively. The chelating solution was precipitated with absolute ethanol and washed several times to remove Ca ions. The resulting precipitate was dried and grounded to a powder.

2.3 The effect of reaction temperature

$CaCl_2$ was added to the concentrate obtained above, the pH was 7.0, the reaction time was 60 min, the peptide Ca ratio was 3:1, and the reaction temperature was 40 ° C, 50 ° C, 60 ° C, 70 ° C, 80 ° C, respectively. The chelating solution was precipitated with absolute ethanol and washed several times to remove Ca ions. The resulting precipitate was dried and grounded to a powder.

2.4 The effect of pH

$CaCl_2$ was added to the obtained concentrate, the reaction temperature was 60 ° C, the reaction time was 60 min, the peptide Ca ratio was 3:1, and the pH of Ca chelation reaction was carried out at pH 5.0, 6.0, 7.0, 8.0, 9.0, and 10.0, respectively. The chelating solution was precipitated with absolute ethanol and washed several times to remove Ca ions. The resulting precipitate was dried and grounded to a powder.

2.5 Experimental design of anhydrous ethanol dosage

Since the polypeptide Ca-chelate is a water-soluble chelate, we chose to precipitate it with absolute ethanol. The amount of anhydrous ethanol affects the yield of the chelate. If the amount of absolute ethanol is too small, the water will dilute the anhydrous ethanol, and a part of the polypeptide chelate Ca will be dissolved by the mixed phase of water and absolute ethanol, which will lower the yield of the polypeptide-Ca chelate. If there is an excess of absolute ethanol, it will cause waste of anhydrous ethanol, so it is necessary to find a suitable amount of anhydrous ethanol. The polypeptide Ca chelating

solution under any of the above conditions was divided into 10 groups of 20 mL each, and the ratio of absolute ethanol to chelate was: 2:1, 3:1, 4:1, 5:1, 6 : 1, 7: 1, 8: 1, 9: 1, 10: 1, 11:1, the amount of absolute ethanol is corresponding to 40, 60, 80, 100, 120, 140, 160, 180, 200, 220 mL. The yield of the polypeptide Ca chelate under each group was calculated.

2.6 Infrared spectroscopy of Chelated Ca

The complex polypeptide hydrolyzate is dried, ground into a powder, and mixed with potassium bromide to be a tablet for Fourier transform infrared spectroscopy (FTIR). The test is performed by PerkinElmer Fourier infrared spectrometer with a scan range of 500 cm^{-1} to 4000 $cm.^{-1,}$ resolution is 0.5 cm-1, and the number of scans is 32.

3Results and discussion

3.1Standard content curve of chromium

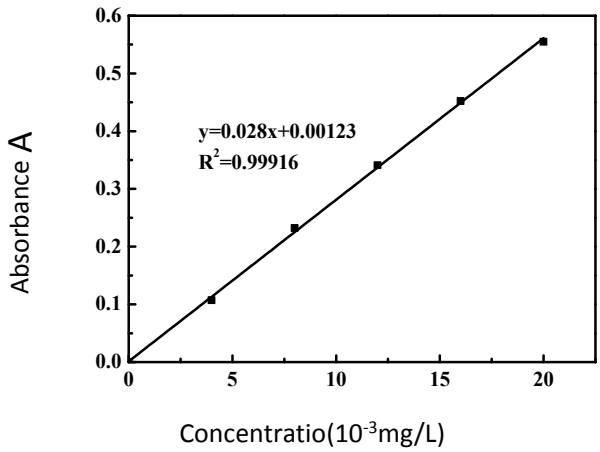

Fig. 2 Chromium content and absorbance curve

It can be seen from Fig. 2 that the chromium content has a good linear relationship with the absorbance. The linear regression equation of the standard curve of chromium content is y=0.028x+0.00123, and the correlation modulus R^2=0.99916.

The results show that the chromium content in the chelated calcium is

A=21.8 mg/kg

3.2 The molecular weight of hydrolyzate molecular

The molecular weight of the hydrolyzate was measured to be 6048 Da.

3.3 The result of chelate

3.3.1 Effect of the Amount of Anhydrous Ethanol on the Yield of Chelate

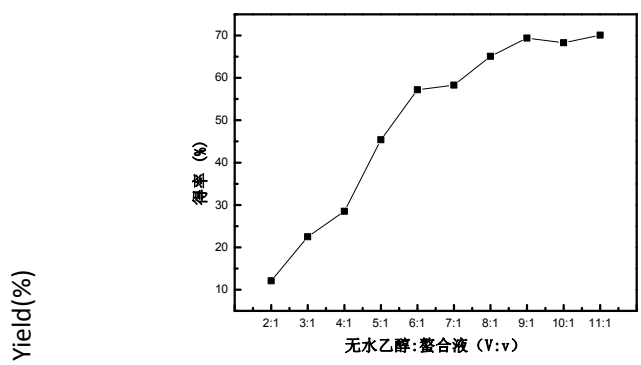

Fig 3 Effect of the amount of anhydrous ethanol on the yield

It can be seen from Fig. 3 that the yield of the polypeptide-Ca chelate is relatively low when the amount of anhydrous ethanol is small, and the yield of the chelate is also increased as the amount of anhydrous ethanol is increased. When the amount of absolute ethanol is reached, that is, the volume ratio of absolute ethanol to the chelating solution is 9:1, the yield of the chelate compound is increased without increasing the amount of anhydrous ethanol. At this point, the yield of the chelate can be maximized and no waste of anhydrous ethanol is caused.

3.3.2 Effect of reaction time on chelation reaction

The reaction conditions were as follows: pH was 7, reaction temperature was 60 ° C, and the mass ratio of polypeptide to Ca was 3:1. The effect of reaction time on the chelation reaction is shown in Figure 4:

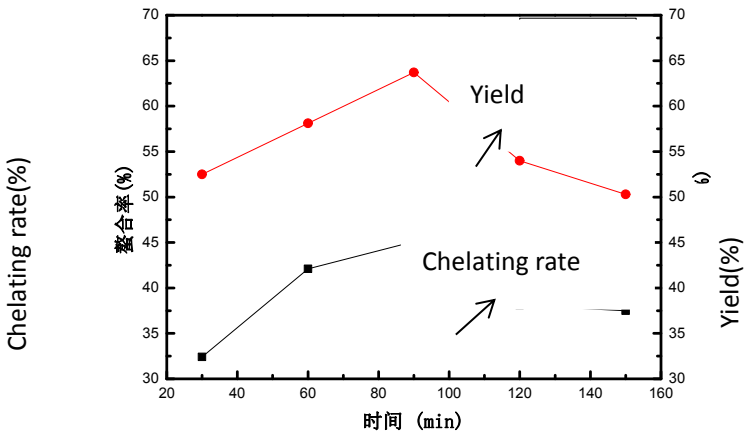

Fig 4 Effect of Time(min) elation reaction

It can be seen from Fig. 4 that the yield and chelation rate of the reaction increase with the increase of the reaction time, and the increase of the reaction yield and the chelation rate is not obvious with time. When the reaction time is 60 min, the chelation rate of the reaction is already large. The reaction time reached 90 min and the reaction is almost complete. The chelation rate of the reaction is 66.97%, so the optimal time for determining the chelation reaction is 90 min.

3.3.3 Effect of peptide Ca ratio on chelation reaction

The reaction conditions were as follows: pH was 7, reaction temperature was 60 ° C, and reaction time was 60 min. The effect of reaction time on the chelation reaction is shown in Figure 5:

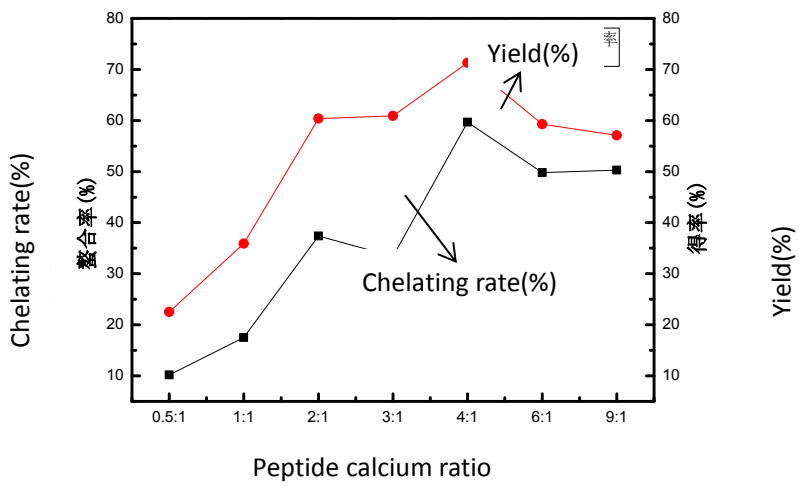

Fig 5 Effect of peptide Ca ratio on chelation

It can be analyzed from Fig. 5 that the yield and the chelation rate of the reaction increase as the amount of Ca chloride

decreases, and when it is reduced to a certain amount, there is a tendency to decrease. When the molar ratio of polypeptide to Ca ion is 0.5:1, the chelation rate of Ca ion is low, indicating that the Ca ion is excessive at this time, and a large amount of Ca ions are not involved in chelation; when the ratio of the two is increased, the chelation of Ca .The rate rises in a straight line. When the ratio exceeds 4:1, the chelation rate of Ca no longer rises, indicating that the amount of peptide added is saturated at this time. The addition has a little effect on the chelation rate, and the chelation rate of the reaction is 75.36%.

3.3.4 Effect of pH on chelation reaction

The reaction conditions were as follows: reaction temperature 60 ° C, reaction time 60 min, and peptide Ca ratio of 3:1. The effect of pH on the chelation reaction is shown in Figure 6:

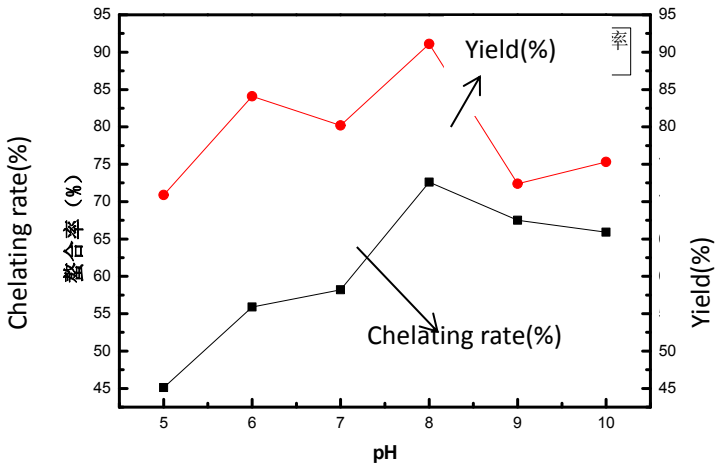

Fig 6 Effect of pH on the chelation reaction

It can be seen from Fig. 6 that pH has a great influence on the chelation rate and yield of the chelating reaction of the polypeptide with Ca chloride. The pH is in the range of 5-8, and the reaction chelation rate increases with the pH of the reaction system. Increasing, when pH>8, the chelation rate decreases as the pH increases, but the tendency to decrease is not too great. The reason may be that in a weak acid environment, H+ binds to the surface of the polypeptide molecule, causing some groups to be positively charged, thereby forming a repulsive effect on Ca ions, which is not conducive to the formation of chelate; under weak alkaline conditions, COOH ionization Loss of H+ with negative charge, -NH2 can also attract positively charged ions, which are beneficial to the chelation reaction, so that the chelation rate is increased; if the pH is too high, the system is too alkaline, OH- and peptide The electron donating group competes for Ca ions, and a Ca hydroxide precipitate is formed, and the chelation rate is lowered. Therefore, the pH of the condensation reaction is too high or too low to be detrimental to the main reaction. It has been proved by experiments that the reaction system is controlled at pH=8, and the chelation rate and yield are maximized [13].

3.3.5 Effect of temperature on chelation reaction

The reaction conditions were: pH 7, reaction time 60 min, and peptide Ca ratio of 3:1. The effect of temperature on the chelation reaction is shown in Figure 7:

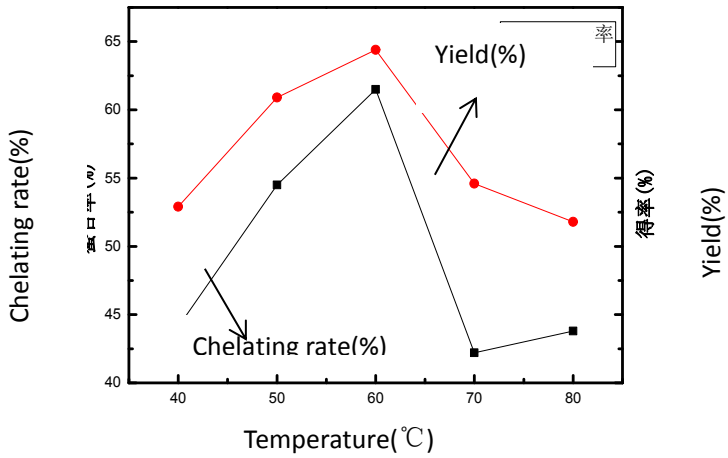

Fig 7 Effect of temperature on the chelation reaction

It can be seen from Fig. 7 that the yield and chelation rate of the chelation reaction increase with increasing temperature within a certain range, and the yield and chelation rate reach the maximum when the temperature reaches 60 °C, and the yield at 70 °C. The chelation rate is significantly reduced. When the chemical reaction is at a low temperature, the reaction rate is slow, the yield and the chelation rate are low, and when the temperature is raised, the speed of the chelation reaction is accelerated, and the yield and the chelation rate are improved. This is because an appropriate increase in the reaction temperature is advantageous in increasing the number of collisions of the polypeptide with the Ca ion, so that the chelation reaction proceeds smoothly. However, when the temperature is too high, the polypeptide is prone to carbonylation [14], which reduces the chelation site of Ca ions, and the chelation of amino acids or small peptides with metal ions is an exothermic reaction [15], too high temperature. It is not conducive to chelation. A suitable temperature range is 50 to 70 °C. Considering the chemical reaction equilibrium constant, the temperature is too high, the reverse reaction rate is greater than the positive reaction rate, and the chemical equilibrium shifts in the opposite direction, so the yield and chelation rate will decrease. At the same time, the temperature rise will accelerate the side reaction of Ca ions, resulting in a decrease in yield. Therefore, the chelation temperature should not be too high or too low. When the temperature of the reaction system is controlled at 60 ° C, the yield and chelation rate of the chelation reaction are the largest.

3.4 Optimization of chelation reaction orthogonal test

According to the results of single factor experiment, the L9 (3^4) orthogonal test was carried out on the factors of pH, peptide to Ca mass ratio, reaction time and reaction temperature. The test results are shown in Table 1 below.

Table 1 Factor of orthogonal experment

Level	factor							
	A	pH	B	Peptide to calcium mass ratio	C	Time/min	D	T/℃
1	7		2:1		30		50	
2	8		3:1		60		60	
3	9		4:1		90		70	

Table 2 Result of chelation rate orthogonal experment

number	factor				Yield/%
	A	B	C	D	
1	1	1	1	1	70.7639
2	1	2	2	2	64.2865
3	1	3	3	3	86.5502
4	2	1	2	3	79.2579
5	2	2	3	1	62.0900
6	2	3	1	2	66.2448
7	3	1	3	2	73.6265
8	3	2	1	3	82.8216
9	3	3	2	1	56.5156
K1	73.8669	74.5494	73.2768	68.8255	
K2	69.2109	69.7327	66.6867	68.0526	
K3	70.9879	69.7702	74.0889	87.8763	
R	4.656	4.8167	7.4022	19.8373	
	因素主次			D>C>B>A	

Table 3 Result of yield orthogonal experment

number	factor				Yield/%
	A	B	C	D	
1	1	1	1	1	85.63
2	1	2	2	2	73.83
3	1	3	3	3	93.65
4	2	1	2	3	77.00
5	2	2	3	1	63.08
6	2	3	1	2	72.86
7	3	1	3	2	74.81
8	3	2	1	3	77.09
9	3	3	2	1	69.52
K_1	84.37	79.16	78.53	72.74	
K_2	70.98	71.33	73.45	73.83	
K_3	73.81	78.68	77.18	82.58	
R	13.39	7.83	5.08	9.84	
Primary and secondary factors			A>D>B>C		

As can be seen from the data in Table 2, the degree of influence on the chelation rate can be arranged in order of magnitude > temperature > reaction time > peptide Ca ratio > pH. The degree of influence on the yield can be arranged in order of pH > temperature > peptide Ca ratio > time. The best chelating conditions were obtained with a reaction time of 90 min, a peptide Ca ratio of 4:1, a pH of 7, and a reaction temperature of 70 °C.

3.5 Characterization and Analysis of Infrared Spectra of Polypeptide and Polypeptide-Ca Chelate

The NaOH hydrolyzed waste leather chip liquid was characterized by Fourier transform infrared spectroscopy. The analysis results are shown in Figure 8:

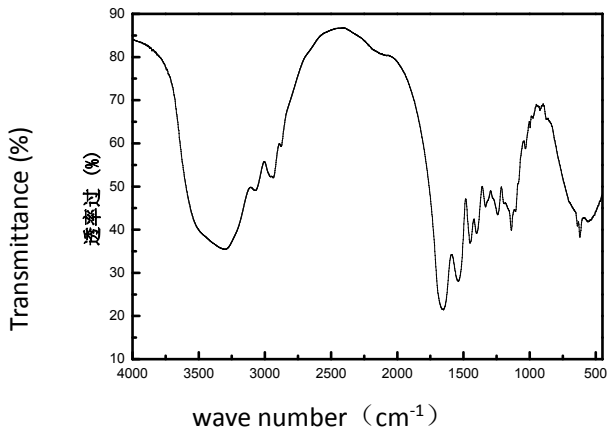

Fig 8 IR spectrum of the polypeptide

The peptide-Ca chelate was characterized by Fourier transform infrared spectroscopy. The results are shown in Figure 9:

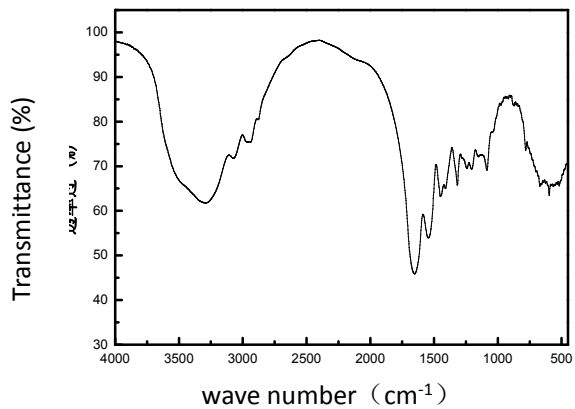

Fig.9 IR spectrum of polypeptide Ca.

The infrared spectrum of the polypeptide and polypeptide-Ca is shown in Figures 8 and 9. It can be seen that the characteristic absorption of 3302.58 cm-1 caused by the stretching vibration of the amino group (-NH2) in the polypeptide and the characteristic absorption of the 1651.12 cm-1 caused by the stretching vibration of the carbonyl group (-C=O) are very obvious. When the peptide is chelated with Ca, the infrared spectrum of the chelate shows that the characteristic absorption peak of the polypeptide still exists, but the blue shift to 3292.12 cm-1 [7]. At the same time, the characteristic absorption of the carbonyl group shifts blue to 1650.96 cm-1. This is due to the fact that the amino group and the carbonyl group of the polypeptide participate in the coordination to form a chelate, demonstrating the formation of the polypeptide chelate Ca.

Conclusion

In this paper, chrome shavings are alkali hydrolyzed using NaOH, and then the hydrolyzate is concentrated, and the

concentrate and CaCl2 are chelated under different conditions. According to the different conditions, the single factor experiment was designed first, and the orthogonal experiment was carried out under the appropriate conditions of the single factor experiment to obtain the following conclusions.

When the volume ratio of absolute ethanol to the chelating solution is 9:1, the yield of the chelate compound is increased without increasing the amount of anhydrous ethanol. At this point, the yield of the chelate can be maximized and no waste of anhydrous ethanol is caused. According to the results of the orthogonal test, the degree of influence on the chelation rate can be arranged in order of temperature>reaction time>peptide Ca ratio>pH. The degree of influence on the yield can be arranged in order of pH > temperature > peptide Ca ratio > time. The optimal chelating conditions were obtained for a reaction time of 90 min, a peptide Ca ratio of 4:1, a pH of 7, and a reaction temperature of 70 °C.

The chelation of the polypeptide with Ca not only promotes the bioavailability of the organism to Ca, but also better recycles the solid waste of leather. The experimental conditions and results have certain reference value for the preparation of chelate compounds of other trace elements and peptides.

Reference

[1] Alexander K. T. W., Corning D. R., Cory N. J., et al., Environmental and safety issues-clean technology and environmental auditing, Journal of the society of leather technologists and chemists, 1991, 76(1): 15-23.

[2] Zhang Y. X., Zhang D. J., Comprehensive Utilization of Tannery Waste, Journal of Gansu Science and Technology, 2009, 25(6): 74-76.

[3] Zhu D. Y., Li Y. C., Pei L. Q., et al., Study on the binding properties of collagen peptide and Ca, China Leather, 2005, 34 (3): 26-29.

[4] Yang W. B., Yao F. Y., Study on Iron Synthesis and Coupling Reaction of Compound Amino Acids, Chemical Bulletin, 1991, 1:46-47.

[5] Zhou G. L.. Progress in the research and application of amino acid chelating iron. Ci Poetry, 1998, 10(6): 10-12.

[6] Yang W. B., Research on the Process of Peptide Ca Chelate, Food Research and Development, 2016, 37(15): 149-151.

[7] Zhao W., Li T., Preparation of Hydrolyzed Peptides from Soybean Meal and Zinc Chelate, Food Research and Development, 2013, 34(19):133-136.

[8] Zhao H. J., Wang G. G., Zhang G. Y., et al. Effects of soy peptide chelated zinc on natural aging mice, Chinese Journal of Gerontology, 2009, 6(29):1501-1502.

[9] Fan H. B., Wang Z. Y., Preparation of Chelated Ca of Collagen Polypeptide from Carp, South China Fisheries Science, 2014, 10(2): 72-78.

[10] Tao J., Jiang Y. L., Wang H. Methodology for Determination of Lead in Tea by Graphite Furnace Atomic Absorption Spectrometry, Journal of Chinese Institute of Food Science and Technology, 2010, 10(6): 208-212.

[11] Yu X., Zhang S. X., Wang L. M., Determination of total chromium in soil by diphenylcarbazide spectrophotometry, Zhejiang Agricultural Sciences, 2014(3): 406-407.

[12] Quan M. P. Determination and Analysis of Heavy Metal Content in Livestock and Poultry Meat Products, Cereals and Oils Food Science and Technology, 2013, 21(3): 88-89.

[13] Xiao S., Huang L. X., Zhao Y. Q. Preparation and Structural Characterization of Chelate Polypeptide Chelated Ca, Food Science and Technology, 2013, 34(24): 253-257.

[14] Liu X., Liu L. Z., Li X. N., et al. Optimization of Chelation of Ca by White Catfish Collagen Polypeptide, Food Science, 2014, 35(10): 76-81.

[15] Cui W., Jiang H. R., Liu X. L., et al. Optimization of process conditions for tilapia skin collagen peptide chelated magnesium by response surface methodology, Food Industry Science and Technology. 2013, 34(15): 238-241.

P108

Study on hydrolysis of waste shavings by the system of calcium oxide/tetramethylammonium hydroxide

YUAN Yan[1], ZHAO Caide[1], GE Shuhua[1], LUAN JUN[2], ZHAO Dandan[1], DIAO Shen[1*], WANG Quanjie[1,2]

(1.College of Chemistry and Chemical Engineering, Yantai University,Yantai 264005, China;

2. State Leather Technology Research Development Center, Yantai 264005, China;)

Abstract: In this paper, waste shavings were hydrolysed by the system of calcium oxide/tetramethylammonium. The optimum hydrolysis conditions through orthogonal test. In the first hydrolysis system of CaO, using the chromium content as the standard, it was found that the dechromization rate is the highest under the conditions of the amount of calcium oxide is 9%, the temperature is 90°C, the reaction time is 4 hours, and the solid-liquid ratio is 1:7. The chromium content in the hydrolysate was 149 ppm and the dechromization rate was 97.3%. In the second hydrolysis system of tetramethylammonium, using the content of free amino acids as the standard, it was found that the hydrolysis rate is the highest under the conditions of the amount of tetramethylammonium is 9%, the reaction time is 4 hours, the solid-liquid ratio is 1:10, the temperature is 70°C. The hydrolysis rate is1.5%.

Key words: waste shavings; calcium oxide; dechromization rate; tetramethylammonium; hydrolysis rate

Introduction

The tanning industry is a pillar industry in China's light industry. However, the tremendous pressure on the environmental and ecological balance of wastewater, waste gas and solid waste generated during the tanning process has become an important factor hindering the development of the tanning industry. China's extensive tanning characteristics lead to the generation of about 1 million tons of solid waste every year. The main component of these solid waste is protein, which is used for recycling and resource utilization, which is conducive to the sustainable and healthy development of the leather industry and in line with the basic national policy of environmental protection in China[1]. Therefore, more and more researchers are devoted to the resource utilization of tannery waste, and these wastes are processed into various products for use in leather, agriculture, medicine, oil field, papermaking, etc., and have achieved considerable economic and environmental benefits[2]. Among tanning solid wastes, chromium-containing solid waste is the most hazardous and difficult to handle. According to statistics, the world produces more than 600,000 tons of chromium-containing waste every year. The annual production in China is more than 300,000 tons. The main hazards are: encroachment on land; pollution of soil, water and air; affecting environmental sanitation; explosion, contact poisoning, corrosion and other special hazards[3]. The chrome containing leather shavings are mainly composed of collagen and trivalent chromium. If measured on a dry basis, the content of chromium trioxide in the chrome shavings is about 3% to 6%, and the collagen content is about 90%[4]. Recycling chrome containing leather shavings is an effective way to reduce environmental pollution and turn waste into treasure. It has become one of the important topics of resource recycling and environmental protection.

At present, the treatment methods of chrome shavings can be divided into incineration method, oxidation method and hydrolysis[5]. Among them, the hydrolysis method is the most studied at present. It mainly includes acid hydrolysis method, enzymatic hydrolysis method and alkali hydrolysis method. Acid Dechromium principle of chrome shavings is processed using relatively concentrated acid. The combination of H+ and collagen carboxyl ions forms a competitive reaction with the combination of chromium and collagen carboxyl groups, so as to achieve removal of chromium. At this time, the cross-linking bonds and hydrogen bonds between the collagen molecules and the peptide chains are opened. As the temperature increases and the time prolongs, the collagen main peptide chains degrade to form small-molecule polypeptides and amino acids [6]. When using acid hydrolyzed leather shavings, the general system pH is <2. In this case, the degree of degradation of collagen is large, and the product is a small molecule, but since trivalent chromium and collagen are in a dissolved state, the yield of collagen and Chromium recovery is low and strong acids can also corrode equipment. Due to

these factors, it is generally less preferred to use an acid alone for hydrolysis, and most of them are combined with an acid method and other methods. The principle of enzymatic dechromation is the application of a complex and special mechanism of action. In the hydrolysis process, the enzyme is used to catalyze the breakdown of collagen peptide bonds into small molecular peptide chains and amino acids, and the collagen is separated from chromium to finally obtain chromium salts and The partially hydrolyzed collagen is used to achieve the purpose of dechromation. The enzymatic hydrolysis method has mild reaction conditions, strong specificity and no corrosion equipment. The product obtained by hydrolysis has small molecular weight and narrow molecular weight distribution, and the product also has biological activity, which makes it have good industrial application prospects[7-9]. However, the low enzymatic dechromation rate and high cost limit its promotion and industrialization. The principle of alkaline dechromization is that under alkaline hydrolysis conditions, OH^- will hydrolyze the amide bond of the protein to degrade the collagen, and at the same time replace the collagen carboxyl group with Cr^{3+} to form $Cr(OH)_3$ precipitate. The most commonly used bases for alkali hydrolysis are NaOH, CaO and MgO. Among them, NaOH has high hydrolysis strength and high hydrolysis rate, and post-treatment of leather residue after hydrolysis is convenient. When CaO is used as a hydrolyzing agent, raw materials are easy to obtain and cheap. The rate is high, but the CaO is low in alkali, the degree of hydrolysis and the hydrolysis rate are not as high as NaOH; the condition of MgO is mild, and a high variety of gelatin can be obtained, but a large amount of chrome mud is produced, which also produces a waste of chromium resources. Secondary pollution. The alkaline hydrolysis method is relatively simple, and can control the reaction conditions of different molecular sizes to obtain reaction products of different molecular sizes. The yield of collagen and the high chromium removal rate are the most effective methods for recycling waste chrome shavings [10-12].

Based on the original research of alkali hydrolysis in the research group [13-19], this paper proposes a new ash-alkali hydrolysis system using calcium oxide-tetramethylammonium hydroxide to hydrolyze waste chrome shavings, and studied the optimal process conditions of two-step alkali hydrolysis.

1 Experimental part

1.1 Experimental materials and instruments

Leather scraps were purchased from Yantai Wendeng tannery. Tetramethylammonium hydroxide was purchased from Nanjing Reagent Chemical Co., Ltd. Phthalaldehyde (OPA) was purchased from Tianjin Guangfu Fine Chemical Research Institute. And other chemical reagents were purchased from China Pharmaceutical Group Chemical Reagent Co., Ltd.

The semi-automatic Kjeldahl nitrogen-fixing instrument was used to determine the nitrogen content of the hydrolysate.The absorbance of hydrolysate was determined by UV-vis spectrophotometer. The content of chromium in hydrolysate was determined by atomic absorption spectrometer.

1.2 Determination of physical and chemical properties of waste leather waste

In the process of leather making, there are differences in the leather itself due to different process conditions, and there are almost no two pieces of leather with the same properties. Therefore, there are great differences in the different chrome-containing leather shavings. The physical and chemical properties of the chips are known, and the control of the test process is facilitated. The physical and chemical properties of the used shavings need to be determined before the test begins.

1.2.1 Determination of moisture content

The moisture content of the chrome-containing shavings used was determined by the oven method (ie, the National Standard Method)[20]. Calculated as follows:

$$\text{Water Content}(\%) = \frac{m_1 - m_2}{m_1} \times 100$$

in formula:

m_1 - pre-bake weight, g.

m_2 - weight after baking, g.

1.2.2 Ash content determination

Take a certain amount of dried chrome-containing leather shavings in a muffle furnace for burning and ashing, and then weigh and measure[21]. Calculated as follows:

$$\text{Ash content (\%)} = \frac{m_1 - m_2}{m_3} \times 100$$

in formula:

m_1-crucible and ash weight, g.

m_2- crucible weight, g.

m_3- sample weight, g.

1.2.3 Determination of chromium content

The instrument used to determine the chromium content is an atomic absorption spectrometer. Weigh 0.1 g of waste chromium residue that had been dried to constant weight and placed it in the digestive tract. Add 5 mL of concentrated sulfuric acid or the like to the digestive tube, shake well, and place the glass funnel over the nozzle. Set the temperature of the digestion furnace to 250 °C, the heating time is 5 min, remove the cooling film, add hydrogen peroxide dropwise thereto, shake it and put it into the digestion furnace. During the heating process, the color become darker, and the hydrogen peroxide was added again. Until the color was clear, continue heating until no bubbles were produced. The liquid was transferred to a 100 mL volumetric flask and made up to volume with deionized water. The final dilution was 10,000 times. A 1 ppb chromium standard solution was prepared and a standard curve was drawn. The test solution was transferred to a sample tube and the chromium concentration was determined.

1.2.4 Determination of nitrogen content

The semi-micro-Kjeldahl method can measure the nitrogen content in the leather shavings [22]. The steps were as follows: Accurately weigh about 0.5 g of the cut chrome-containing leather shavings, put them into the crucible, add 4 g of potassium sulfate, 0.3 g Anhydrous copper sulfate, 15 mL of concentrated sulfuric acid and a small amount of zeolite were placed on an electric furnace for 2 h, completely digested, and taken out to cool to room temperature. Transfer the digestion solution to a volumetric flask, dilute to 100 mL, and shake well. Then the 25 mL solution was removed to the distillation bottle, put into the nitrogen-fixing instrument, the conical bottle was placed under the condenser, the boric acid solution of 50 mL was added, the indicator was added in the solution, and the quantitative NaOH solution was added to the distillation bottle. And then start distilling. After no nitrogen is produced, the instrument was turned off and titrated with hydrochloric acid. When the color of the solution in the triangle flask changes, the data are recorded. The formula is as follows:

$$w_N(\%) = \frac{c_{NaOH} \times (V_2 - V_1) \times 10^{-3} M_N}{m} \times 100$$

in formula:

C_{NaOH}-The concentration of NaOH standard solution, mol / L.

V_2-The volume of NaOH standard solution was consumed in titration, mol / L.

V_1-The volume of NaOH standard solution was consumed in the titration of blank sample, mL.

m-Sample quality,g.

1.3 Primary hydrolysis of waste leather shavings with calcium oxide

The processed chrome shavings, calcium oxide and water were put into a three-necked bottle in a certain proportion, then refluxed and hydrolyzed in the oil bath for a certain time. After centrifugation and filtration, a hydrolysate was obtained,

and the chromium content was determined after drying (reference 1.2.3 method).The specific experimental scheme is as follows:

Table 1 The first hydrolysis experiment scheme

Factor	alkali content /% A	hydrolysistemperature / ℃ B	hydrolysis time /h C	solid-liquid ratio D
1	8	4	80	1:5
2	8	6	90	1:7
3	8	8	100	1:10
4	9	4	90	1:10
5	9	6	100	1:5
6	9	8	80	1:7
7	10	4	100	1:7
8	10	6	80	1:10
9	10	8	90	1:5

1.4 Secondary hydrolysis of tetramethyl ammonium hydroxide

A mixture of primary hydrolysate and tetramethylammonium hydroxide at a given solid-liquid ratio was hydrolyzed at different temperature and time. After hydrolysis, tetramethylammonium hydroxide was destroyed at high temperature and the secondary hydrolysis product was obtained. The specific schemes of the secondary hydrolysis are as follows:

Table 2 The second hydrolysis experiment scheme

Factor	alkali content /% A	hydrolysis temperature / ℃ B	hydrolysis time /h C	solid-liquid ratio D
1	3	50	4	1:5
2	3	70	6	1:7
3	3	90	8	1:10
4	6	50	6	1:10
5	6	70	8	1:5
6	6	90	4	1:7
7	9	50	8	1:7
8	9	70	4	1:10
9	9	90	6	1:5

1.5 Determination of free amino content of hydrolysates

The OPA method is a fast, convenient and time-consuming method for measuring the degree of protein hydrolysis. The principle is that phthalaldehyde reacts with free amino in alkaline condition to produce isoindole derivatives with fluorescence. The absorbance can be measured by spectrophotometer under 340 nm UV irradiation.

In this experiment, the method of measuring the degree of hydrolysis of cottonseed protein hydrolysate by the OPA method[23,24] is referred to, and which is improved to make the measurement more convenient and accurate. The methods are as follows:

(1) The preparation of standard solution: accurately weighing 0.32795 g / L leucine with electronic balance into 1000 mL volumetric bottle and then removing 0.2, 0.4, 0.6, 0.8, 1 ml solution to 25ml colorimetric tubes with constant volume to 25mL, and numbering 0, 1, 2, 3, 4, 5 according to the concentration level respectively.

(2) The configuration of OPA solution: Firstly, taking 80 mg OPA to use 2 mL anhydrous ethanol in darkness to avoid light and dissolve, then taking 1.9068 g sodium tetraborate, 0.1 g SDS (dodecyl sodium sulfate), 88 mg DTT (dithiothrelito) to dissolve in water. Finally, they were transferred to 100 mL brown volume bottle and fixed volume.

(3) The measurement of the absorbance of standard solution: the specific methods are as follows: firstly, the wavelength of UV-Vis spectrophotometer was adjusted to 340nm, 0.4 mL of the solution to be tested and 3 mL of OPA solution was removed to the colorimetric dish, and the time was started with a stopwatch. In the blank control group, the absorbance was 0 when the stopwatch was timed to 2 min, and then the absorbance of the remaining 5 groups of solutions at 2 min was determined by this method, and the standard curve was draw.

(4) The determination of free amino concentration in leather hydrolysate: the absorbance of the prepared residue hydrolysate was measured after dilution and brought into the standard curve equation, the free amino concentration could be obtained.

1.6 Determination of hydrolysis degree of hydrolysates

The degree of hydrolysis of a protein (DH) is based on the number of peptide bonds that are cracked during the catalytic hydrolysis to indicate the hydrolysis of the protein.It is defined as the ratio of peptide bonds broken by hydrolysis to total peptide bonds in protein molecules[25]. The formula is expressed as:

$$DH = \frac{h}{h_{tot}} \times 100\%$$

in formula：

h-The number of peptide bonds cleaved per gram of protein after hydrolysis(mmol / g).

h_{tot}*-The number of peptide bonds per gram of protein (mmol/g).*

Generally speaking, a free amino group and a carboxyl group can be produced at the same time with each break of a peptide bond, so the H value can be obtained by quantitatively measuring the amount of free amino group. Htot is a constant for a particular protein and can be determined by the amino acid content (nitrogen content) of the protein.Therefore, for the leather hydrolysate, we can replace the h with the free amino concentration of the hydrolysate and replace the Htot with the hydrolytic liquid nitrogen content, and the formula is as follows[26]:

$$DH = \frac{C_1}{C_2} \times 100\%$$

in formula：

C_1 *- The concentration of free amino group of hydrolysate (mol/L).*

C_2 *- The nitrogen content of hydrolytic liquid (mol/L).*

2 Results and Discussion

2.1 Physical and Chemical Properties of Leather Shavings

The physical and chemical properties of the leather shavings used in this paper are shown in Table 3. All the hydrolyzed raw materials in this experiment were tested using the same batch of waste shavings.

Table 3 The physical and chemical properties of chrome leather scraps

	Moisture /%	Chromium /%	Ash/%	Nitrogen /%
Content	32.1	0.55	15.2	14.71

2.2 Study on One Hydrolysis Condition

Alkaline hydrolysis of waste shavings has been reported in the paper. The commonly used bases are sodium hydroxide, calcium oxide and magnesium oxide. The main purpose of this experiment is to dechromate, so calcium oxide was used for one hydrolysis, and four-factor and three-level orthogonal experiments were designed. The optimal reaction conditions were studied by using the chromium content in the hydrolyzate as the standard. The main experimental results are shown in Table 4.Table 4 The orthogonal experimental results of first hydrolysis

Test number	Factor				Chromium content /ppm
	A	B	C	D	
1	8	4	80	1:5	289
2	8	6	90	1:7	213
3	8	8	100	1:10	700
4	9	4	90	1:10	183
5	9	6	100	1:5	167
6	9	8	80	1:7	152
7	10	4	100	1:7	228
8	10	6	80	1:10	715
9	10	8	90	1:5	198
Mean 1	400	233	385	218	
Mean 2	167	365	198	197	
Mean 3	380	350	365	533	
Range	233	131	188	335	
Primary and secondary factors			D>A>C>B		

It can be known from the data in Table 4 that the degree of influence on the dechromation rate of the hydrolyzate can be arranged in order of magnitude to solid-liquid ratio > calcium oxide dosage > hydrolysis temperature > hydrolysis time. The optimum conditions for the primary hydrolysis of the obtained calcium oxide are a solid-liquid ratio of 1:7, a calcium oxide content of 9% of the leather shavings, a reaction temperature of 90 ° C, a reaction time of 4 h, and a chromium content of 149 ppm.

2.3 Study on Secondary Hydrolysis Conditions

Since the hydrolysis of calcium oxide is weak and the hydrolysis rate is not high, the hydrolyzate is hydrolyzed twice. At present, the common hydrolysis system is a ash-acid, ash-enzyme hydrolysis system, and the ash-base hydrolysis system is rarely used. The main reason is that the gray-alkali hydrolysis system introduces new metal ions, and these metal ions are difficult to remove. In this experiment, the organic base of tetramethylammonium hydroxide is used for secondary

hydrolysis. After the hydrolysis, the alkali will decompose at high temperature, and there will be no residual metal ions. Therefore, four-factor and three-level orthogonal experiments were designed to determine the free amino and nitrogen contents of the hydrolyzate of each group. As shown in Table 5, studies have shown that the free amino group content in the hydrolyzate varies with the hydrolysis conditions. The change, while the nitrogen content does not change much, indicating that the hydrolysis process only hydrolyzes the long peptide chain of the protein into a short peptide chain, which has little effect on the element content of the protein.

Table 5 The free amino content and nitrogen content of second hydrolysis

Test number	Free amino acid content/10mol·mL^{-1}	Nitrogen content/%
1	1.13	13.61
2	1.17	14.26
3	1.09	13.41
4	1.46	14.32
5	1.04	14.43
6	1.07	14.4
7	1.18	14.00
8	1.28	12.95
9	1.38	14.29

The degree of hydrolysis of the hydrolyzate was calculated by calculation, and the optimum hydrolysis conditions were studied using the degree of hydrolysis as a standard. The main experimental results are shown in Table 6.

Table 6 results of one-time hydrolysis orthogonal experiment

Test number	Factor				Degree of hydrolysis /%
	A	B	C	D	
1	3	50	4	1:5	1.16
2	3	70	6	1:7	1.15
3	3	90	8	1:10	1.14
4	6	50	6	1:10	1.43
5	6	70	8	1:5	1.01
6	6	90	4	1:7	1.04
7	9	50	8	1:7	1.18
8	9	70	4	1:10	1.38
9	9	90	6	1:5	1.35
Mean 1	1.15	1.26	1.19	1.17	
Mean 2	1.16	1.18	1.31	1.12	
Mean 3	1.30	1.17	1.11	1.32	
Range	0.153	0.08	0.20	0.19	
Primary and secondary factors			A>C>D>B		

It can be known from the data in Table 6 that the degree of influence on the hydrolysis rate of the secondary hydrolyzate can be arranged in order of magnitude of tetramethylammonium hydroxide>hydrolysis time>solid-liquid ratio>hydrolysis temperature. The optimum conditions for the primary hydrolysis of the obtained tetramethylammonium hydroxide are 9% of tetramethylammonium hydroxide, reaction time of 6h, solid-liquid ratio of 1:10, reaction temperature of 50℃, the hydrolysis rate is 1.5%.

Conclusion and Outlook

In this paper, a new ash-base hydrolysis system using calcium oxide-tetramethylammonium hydroxide was used to treat chromium-containing swarf, and the optimal reaction conditions for two-step hydrolysis were obtained by orthogonal test.Among them, the main purpose of the primary hydrolysis of calcium oxide is to dechromate. It is found that the degree of influence on the dechromation rate of the hydrolyzate can be arranged in order of magnitude to solid-liquid ratio > calcium oxide dosage > hydrolysis temperature > hydrolysis time.The optimum conditions for the primary hydrolysis of the obtained calcium oxide are a solid-liquid ratio of 1:7, a calcium oxide content of 9% of the leather shavings, a reaction temperature of 90 ℃, a reaction time of 4 h, and a chromium content of 149 ppm. The second hydrolysis uses organic base tetramethylammonium hydroxide. At the end of the hydrolysis, tetramethylammonium hydroxide can be directly decomposed to achieve the effect of not introducing metal ions. It is found that the order of influence of the reaction conditions on the hydrolysis rate of the hydrolyzate is that the amount of methylammonium hydroxide>hydrolysis time>solid-liquid ratio>hydrolysis temperature.The optimal condition for the secondary hydrolysis of the tetramethylammonium hydroxide is that the amount of tetramethylammonium hydroxide is 9% of the black shavings, the reaction time is 6 h, the solid-liquid ratio is 1:10, and the reaction temperature is 50℃,the hydrolysis rate was 1.5%. The use of a new hydrolysis system avoids the desalting process in the current alkaline hydrolysis process of proteins, which simplifies the hydrolysis process and is particularly suitable for applications requiring severe metal ion content.

Reference

[1] Qiang, T.T.; Ren, L.F. Development of Efficiently Reusing Chrome Shavings. Leather Chemicals, 2004(2): 5-8.

[2] Zhou, W.; Dan, W.H. Recycle Route of Chrome-contained Shavings Produced by Leather Manufacturing. Western Leather Journal, 2011, 33(18): 50-56.

[3] Li, W.X. Treatment of tannery pollution and utilization of waste resources. Beijing: Chemical Industry Press, 2005: 165-166.

[4] Wang, H.R.; Wei, X.L. The method of extracting collagen products from chrome leather. Leather Chemicals, 2001, 18(3): 6-9.

[5] He, X.W.; Xie, S.H.; Huang, Q. Advances in the Extraction of Collagen from Chrome Leather Shavings. Leather science and Engineering, 2006, 16(1): 42-45.

[6] Jiang, T.D. Collagen protein. Beijing: Chemical Industry Press, 2001, 25-33.

[7] Zhou, W.; Dan, W.H. Study on Extraction of Collagen Hydrolysate from Chromium-Containing Leather Shavings by Enzyme Preparation. Chinese leather, 2012, 41(13): 25-29.

[8] Chen, W.Y.; Gu, H.B.; Q, T.; etc. Study on the hydrolysis of chrome leather by neutral protease. Chinese leather, 2001, 30(21); 2-5.

[9] Du, S.S.; Zhu, X.L.; Du, B.B. Study on the technological conditions for enzymatic hydrolysis of chrome leather. Western leather, 2013, 35(24): 29-32.

[10] Yang, X.F.; Li, M.N. Hydrolysis and application of chrome shavings. Inner mongolia science technology and economy, 2003, 4(13); 97-98.

[11] Su, D.Q.; Wang, K.Y.;et al. Study on the extraction of hydrolyzed collagen from chrome shavings hydrolyzed by sodium hydroxide. Leather science and Engineering, 2008, 18(5): 8-11.

[12] Cao, J.; Chen, X.J.; Zeng, S.; et al. Study on Preparation of collagen hydrolysate from dechromed leather shavings by alkaline hydrolysis. Chinese leather, 2003, 32(21): 12-14.

[13] Tan, X.J.; Cao, B.R.;, Wang, Q.J. Study on alkali hydrolysis process of discarded leather from tannery. Western leather, 2010(13): 8-11.

[14] Wang, C.X.; Xu, C.T.; Wang, X.; Wang, Q.J. Study on alkali hydrolysis conditions of waste chips. Western leather, 2012(14); 14-17.

[15] Wang, H.Q.; Wang, Q.J.; Zhao, J.L.; Qu H.X.;Zhao, H.Y. Preparation of a new leather degreasing agent by using waste leather. Leather and chemical industry, 2014, 31(2): 4-9.

[16] Wang, J.X.; Wang, Q.J.; Qu, J.L.; Duan, B.R.; etc. Synthesis and properties of protein based surfactants. Chinese leather, 2015, 44(3): 6-11.

[17] Luan, J.; Wang, Q.J.; Wang, S.S.; Diao, S. Preparation and application of Dodecylbenzene sulfonyl degreaser from chrome-containing leather shavings. Leather and chemical industry, 2015, 32(6): 12-16.

[18] Luan，J;Wuang，Q，J；Chen，P，H；CaO、NaOH effects of sodium hydroxide on chrome Leather chips.J.Leather and chemicals.2017,34(3)1-12.

[19] Ge, S.H.; Zhao, D.D.;Zhao, J.Y.; etc. The Liquid flush and fertilization precursor was prepared by using chrome leather chips.J. Leather and chemicals. 2017,34(5): 15-20

[20] Yu, C.Z.;Ding, S.L.; Sun，G.X. Leather analysis and inspection technology. Chemical Industry press. 2005: 246-248.

[21] Yu, C.Z.; Ding, S.L.; Sun, G.X. Leather analysis and inspection technology. Chemical Industry press. 2005: 251-252.

[22] Li, D.Q.; Mao, J.X.; Le, Y.G.; Method for determination of protein content by type KDY-9820 kjeldahl apparatus. Heilongjiang grain. 2002(6):45-46.

[23] Lin, Q.; Huan, W.; Son, Y.K. Comparison of three methods for determination of hydrolysis degree of cottonseed protein hydrolysate.J.Journal of Fujian agriculture. 2011, 26(6):1076-1078.

[24] Luo, Y.H.Preparation and properties of surfactants with different peptide chain lengths.D.Xian:Shaanxi university of science and technology. 2017.

[25] Xu, Y.C.; Liu, C.H. Methods for determination of proteolysis degree.J.Food research and development. 2007, 28(7): 173-175.

[26] Xu, Q.; Ge, X.Y.; Liu, J.F. Improvement of formaldehyde method for determination of hydrolysis degree of soybean protein. Feed industry. 2008, 29(5): 46-47.

P109

Kinetic analysis of the thermal degradation of shorn sheep skin wastes

Lan Luo, Jie Liu, Keyong Tang

School of Materials Science and Engineering, Zhengzhou University, Zhengzhou, Henan 450001, China

Abstract

Large amount of shorn sheep skin wastes is generated from the tanneries every year, and it causes a waste of natural resources and environment pollution. Compare to the traditional combustion method, the method of pyrolysis is easy to operate, green and environmentally friendly, which can better recycle this kind of waste. In this work, the activation energy (E), pre-expotential factor (A), and $f(\alpha)$ were accurately calculated, and the fitting of pyrolysis process was realized. Thermogravimetric analysis (TG) was used to investigate the thermal degradation behavior of the shorn sheep skin wastes at 5, 10, 20, 30 °C·min^{-1} in a N_2 atmosphere. Through the data from different heating rates, the E value obtained by the method of KAS was 307.3 KJ·mol^{-1}. Considering that complexity of the components in shorn sheep skin, the experimental DTG curve of the sample was fitted to three peaks using deconvolution treatment carried out by Lorentz model, which corresponding to three pseudo-components in the waste. Nonlinear model-fitting methods were carried to simulate the three pseudo-components respectively, and finally integrate them into one model. The model was successfully applied to experimental data, and the thermal decomposition reaction of kinetics can be accurately described by the three kinetic factors.

Keywords: thermal degradation, shorn sheep skin, nonlinear fitting

P110

Attapulgite Modified Polyacrylate Emulsion and its Flame Retardancy

Yan Bao[a,b]*, Xinqian Li [a,c], Jianzhong Ma [a,b]*

[a] College of Bioresources Chemical and Materials Engineering, Shaanxi University of Science and Technology, Xi'an, 710021, PR, China.

[b]Shaanxi Research Institute of Agricultural Products Processing Technology, Xi'an, 710021, PR, China.

[c]National Demonstration Center for Experimental Light Chemistry Engineering Education, Shaanxi University of Science and Technology, Xi'an, 710021, PR, China.]

ABSTRACT

Polyacrylate emulsions are widely used in leather finishing and other fields due to their advantages of low cost, availability, no pollution, easy production and application.However, it threats life safety and causes a huge loss of economic and property due to poor flame retardants. Attapulgite is a hydrated magnesium aluminum silicate natural mineral with one-dimensional nanorod structure, and has the characteristics of the large specific surface area, high stability, and excellent environmental protection.Adding attapulgite to the polymer matrix can improve the flame retardant properties of the materials.Take into account this, we incorporated attapulgite into the polyacrylate emulsion by in-situ polymerization to improve the flame retardants of polyacrylate coating. First, attapulgite was activated by HCl after ball milling and its internal -OH content was determined by acid-base titration.After that, KH570 was grafted onto the surface of the acidified attapulgite. The graft rate of KH570 was measured by gravimetric method. Finally, the modified attapulgite was introduced into the polyacrylate emulsion by in-situ polymerization and the flame retardant properties of thecomposite film was tested.The results showed that with the increase of the amount of attapulgite, the flame retardants of the composite film were gradually improved, and the vertical combustion level reached UL94V-1.

Keywords: attapulgite; polyacrylate emulsion; leather; flame retardant

P111

Research of Characteristics on Wool Electrochemical Degradation

Yuzeng Wang[1], Min Gu[1], Hui Chen[1], Jie Yi[2], Shuqing Li[2], Zhihua Shan[1*]

(1.National Engin. Lab. for Clean Tech. Leather Manuf., Sichuan University, Cheng Du, Sichuan, 610065, P.R.China; 2. College of Material and Textile Engineering, Jiaxing College, Jiaxing 314001, China)

Abstract:

Wool is a valuable resource rich in keratin, but structural stability limits the use of wool resources. The dissolution of wool is the basis for the utilization of wool keratin. The degradation of wool treated with electrochemical indirect oxidation method was explored in this paper. Through the optimization of experimental process and the analysis of the degradation product, it can be concluded that temperature, sodium chloride concentration and current density were important factors affecting the degradation of wool in electrochemical indirect oxidation. The optimal condition assembly of degrading wool into a solution was 150mA of current, 1.71mol/L of NaCl, 0.83mol/L of H_2O_2, 30°C. The analysis results of degradation products showed that electrochemical indirect oxidation can greatly increase efficiency to degrade wool keratin. Observed by scanning electron microscopy, it was shown that the wool scale layer degradation process was from the outside to the inside. Completely degraded product dispersed in solution in a translucence microemulsion form which showed the mean particle size was 458.8nm. According to the results of gel chromatography the largest molecular weight Mn was 388Da which belonged to low molecular electrochemical degradation. Elemental analysis of degradation product revealed that the S element content decreased to 1.12% and the N content dropped to 4.56%, which meant the structure of some amino acids were destroyed. Amino acid composition analysis also showed that some amino acids has been missing. It is the features that both advantages and disadvantages are simultaneous existence in the electrochemical indirect oxidation treatment of wool.

Keyword: Electrochemisty; Degradation; Wool; Keratin

P112

Degradation of Artificially Aged Vegetable-Tanned Leather using RP-HPLC and FTIR-ATR

Yadi Hu[1, a], Eleni Tziamourani[2, b],S C Boyatyzis[2, c], Jingru Wang[1, d], Lvyang Wang[1, e], Keyong Tang[1, f, *]

(2. School of Materials Science and Engineering ,Zhengzhou university ,Zhengzhou, Henan, 450001; 2.University of West Attica, Department of Conservation of Antiquities & Works of Art, Egaleo 12210, Greece)

[a]hyd2017@gs.zzu.edu.cn[b]eltzia@gmail.com[c]sboyatzis@teiath.gr

[d]18380125534@163.com [e]wanglvyang123@126.com

**Corresponding author: kytang@126.com, Tel. +8613938526389*

Abstract

As a collagen-based material, leather is susceptible to such environmental factors as temperature, relative humidity,microbes, light, and so on, especially to the sudden and great changes of these parameters.The amino acids of collagen in leather are mainly glycine, repeated on Gly-X-Y in tripeptides, where the X and Y are generally proline and hydroxyproline respectively. It is well known that degradation occurs in leather, usually accompanying the deterioration of collagen structure.In this paper, Reversed Phase-High Performance Liquid Chromatography (RP-HPLC) and Fourier Transform Infrared-Attenuated Total Reflection (FTIR-ATR) were employed to investigate the effects of temperature and relative humidity on the degradation of modern commercial vegetable-tanned leather and the deterioration of collagen structure by degradation were discussed. The samples were artificial aged at 50°C， 40% RH for 0 day, 3 days and 8 days respectively. Results of RP-HPLC indicated that relative concentrations of proline and hydroxyproline decreases after the artificially aging treatment. FTIR-ATR analysis showed that the amide I band of C=O at 1660 cm^{-1} increases whereas the amide II band at 1539 cm^{-1} decreases, which was possibly attributed to the new free amino acids or peptides by ageing. Meanwhile, the triple helix structure of collagen was destroyed by artificial aging. Therefore, the intensity of peak at 1634 cm^{-1} which is related to random coil content gradually increases with increasing the aging time.

Key words: Artificially aged leather; Degradation; Amino acid concentration; Amide I; Amide II

1. Introduction

Leather has been used for centuries for clothing. It is a complex natural collagen-based biological martial constituent of many precious artifacts including armor,boots, etc. However, leather may easily degrade by the effect of temperature, humidity, light, microorganism and pollutants. Therefore, their conservation is determined by the storage conditions. These environmental factors alone or synergistically will lead to different degradation of leather. According to previous researches, partial denaturation (gelatinization), hydrolysis and oxidation are the main degradation processes occurring in leather [1-3].

Due to the historical value of objects of leather, it is significant to study the degradation of leather and its mechanism. To make clear the natural degradation mechanism of leather, a large number of researchers focused on the artificially aging treatment by exposure leathers to the environment factors for different times and then investigated the changes through various techniques. Thermal analysis methods (TG, DTA, DSC or MHT) are commonly used techniques. The shrinkage temperature (T_S) obtained by DSC or MHT is considered as a crucial index to evaluate the hydrothermal stability of leather. It is defined as the temperature at which collagen fibers shrinks under excess water condition [4-6].P. Budrugeac et al. [7] reported that T_S of some collagen-based materials ranked as follows: old leathers ≈ new and old parchments < new vegetable-tanned leathers < new combined tanned (vegetable with Cr) leathers. They also pointed out that the first degradation stage of leather was the breaking of cross-linking bonds, followed by splitting of collagen macromolecules during natural degradation process [8].K. M. Axelssonet al. [9] stated that the samples heated at 120°C for 24, 48, and 96 hours caused a decrease in hydrothermal stability, as well as changes in the amino acid composition. E. Badea et al. [10] investigated the synergistic effects of temperature and relative humidity (RH) on deterioration of parchment and indicated that ageing temperature resulted in a significant variation of DSC parameters, whereas RH is less influential.Furthermore, P.

Budrugeac et al. [11] studied the effects of pollutants (SO_2 and NO_X) in the air on the thermal characters of leather and parchment exposed in atmospheres containing SO_2, NO_2 or SO_2 + NO_2. They proposed that chemical pollutants could accelerate the degradation of collagen matrix, thereby leading to the decrease of T_d (denaturation temperature).

Although thermal techniques have been reported to be suitable for indicating the level of deterioration of leather or parchment, it is still not clear about the changes of collagen structure during the degradation process. Therefore, it is urgent to employ other techniques to monitor the conformation, secondary structure, and amino acid composition changes of collagen after artificially aging. Since FTIR-ATR is a nondestructive method and RP-HPLC method is suitable for the analysis of the extremely small samples from historical leather, both of them have been widely applied in theheritage conservation field in the past years. The aim of the present study was to analysis the degradation of collagen in molecular level due to aging. RP-HPLC and FTIR-ATR were used toidentify the bond loss or generation and amino acids changes of the artificially aged leather samples.

2. Materials and methods

2.1 Samples

The new vegetable-tanned leather samples used in this study is commercial calf leather bought from a store in the center of Athens. The samples were artificially aged at 50°C, 40%RH for 0 day, 3 days and 8 days in a climate chamber (Rumed®, Rubarth apparate GmbH, Laatzen, Germany).

2.2 Analysis methods

2.2.1 RP- HPLC

A GBC system equipped with an LC 1150 HPLC Pump and a GBC LC 1250 fluorescence detector was used for the separation and quantification of the fluorescent amino acid derivatives in reference and authentic samples. The results of chromatograms were processed by YL-Clarity software. A Hypersil C_{18} (ODS) column with dimensions 250×4.6 mm, 3 μm was used in a 54 minutes gradient program. The solvent gradient used in this paper is shown in **Table 1**. The column temperature was set at 38°C with the solvent flow rate at 0.8 mL/min. The excitation wavelength of the fluorescence detector was at 270 nm and the emission at 316 nm.

Table 1 Solvent gradient procedure for HPLC analysis of amino acids

Time (min)	Flow rate (mL/min)	Eluents (%)		
		Solvent A	Solvent B	Solvent C
Initial	0.8	17.0	68.0	15.0
0.5	0.8	17.0	68.0	15.0
32.0	0.8	10.8	43.2	46.0
34.0	0.8	10.8	43.2	46.0
35.0	0.8	0.0	0.0	100.0
47.0	0.8	0.0	0.0	100.0
49.0	0.8	17.0	68.0	15.0
54.0	0.8	17.0	68.0	15.0

Solvent A: 20mM ammonium dihydrogenphosphate (pH 6.5) in 15% methanol 85% water

Solvent B: 15% methanol in water

Solvent C: 10% water in acetonitrile

Leather samples about 10 mg were inserted in a screw cup Pyrex micro-vial containing 1mL 6N HCl. Hydrolysis follows at 110°C for 24 h. The hydrolysate is completely dried in an oven at about 40°C. The dried residue is cooled,

dissolved in 1 mL H_2O (HPLC) and dried again. Washing is repeated until pH 7 is achieved. The dried residue is redissolved in a 5 mL of the derivatization buffer to prepare a stock solution which should be stored at 4°C. Amino acids were derivatized with 9-fluorenylmethyl chloroformate (FMOC-Cl) using a method developed by Haynes et al [12]. The derivatization procedure and used regents are showed in the **Figure 1.** In this experiment, 2.5 mM amino acids standard solution from Sigma Aldrich was used as a reference. The authentic sample amino acid profiles were compared with the amino acid patterns obtained by analyzing, with the same procedure, pure proteinaceous materials such as collagen from calf skin. Separation of FMOC-AA derivatives was carried out using a ternary gradient elution based on the aminomate method [13]. It is worth to note that all the reagents and water used for HPLC test were of HPLC grade. Moreover, each sample was tested three times with the same injection volume to ensure the repeatability of the resulting amino acids concentration.

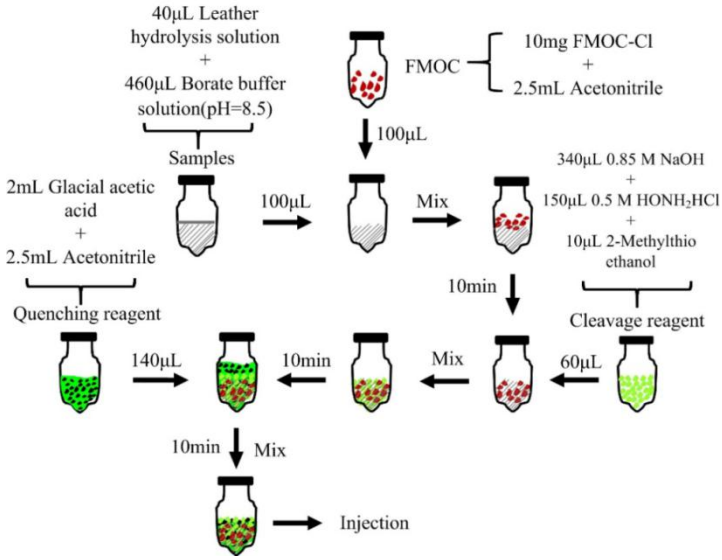

Figure 1 Schematic of FMOC derivatization procedure of amino acids

2.2.2 FTIR-ATR

FTIR analysis was carried out using a Bruker Vertex 70v spectrometer equipped with a DTGS detector. All the measurements employed an A225/Q Platinum attenuated total reflection (ATR) setup coupled with single reflection diamond crystal. FTIR spectra were scanned in the mid-IR region from 4000 to 520 cm^{-1} at a resolution of 1 cm^{-1}. Moreover, the resulting FTIR peaks at range of 1700–1500 cm^{-1} were deconvoluted by PeakFit v4.12 software.

3. Results and discussion

3.1 HPLC results of amino acids analysis

Amino acids species in leather were identified by chromatography of amino acids standard mixture, as presented in **Figure 2.** There were 15 major amino acids observed in leather and the full names of abbreviated amino acids are listed in **Figure 2.** Generally, hydrolysis and oxidation are the main degradation mechanism of leather or parchment under the synergistic effect of temperature and relative humidity. Larsen et al [14] found that the effects of oxidation on the distribution of amino acids were more significant than that of hydrolysis. They also concluded that oxidative degradation induced cleavage of collagen macromolecular chain into small fragments, intramolecular and intermolecular crosslinking bonds and changes of amino acids content.

As previously mentioned in this paper, collagen contains three polypeptide chains repeating on tripeptides of Gly-X-Y.

Moreover, it has been widely accepted that the typical character of collagen that distinguish it from other proteins is the high content of proline and hydroxyproline (around 30%), which contributes significantly to stable triple helix structure of the collagen [15]. Since the ageing treatment time in our experiment is short, the small or random variation of amino acids content may partly be due to the individual differences in samples. However, it still can conclude from **Figure 3a** that relative concentrations of hydroxyproline and proline decrease after aging, suggesting that oxidative degradation by artificially aging treatment attacks the site of X, Y in Gly-X-Ytripeptides, which in turn decreases the stability of triple helix structure in collagen. Nevertheless, the decrease of phenylalanine content with the increase of aging time is probably ascribed to its transformation to tyrosine [9]. Additionally, results of **Figure 3b** showed the significant increases of serine and alanine. The reason for this phenomenon is uncertain and further studies are needed. However, an explanation for this maybe is the loss of other amino acids caused by degradation.

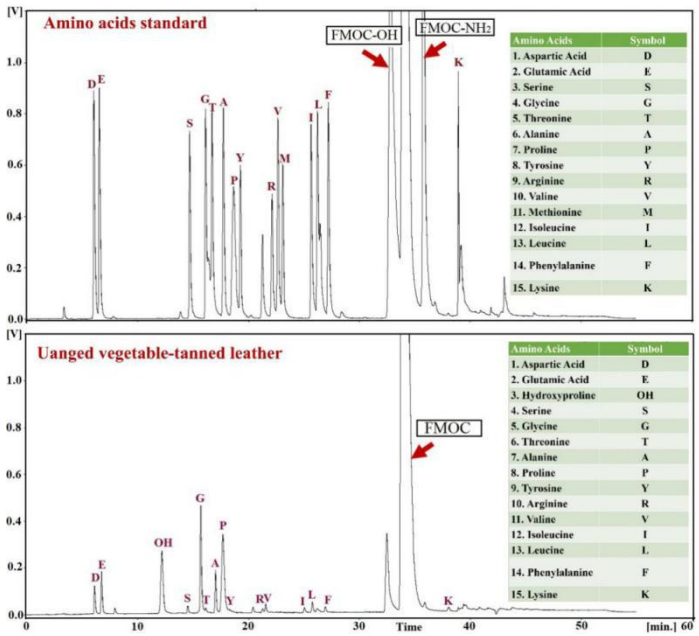

Figure 2 Chromatography of (a) standard amino acids mixture and (b) vegetable-tanned leather sample obtained by RP-HPLC: the injection volume of sample was 20 μL

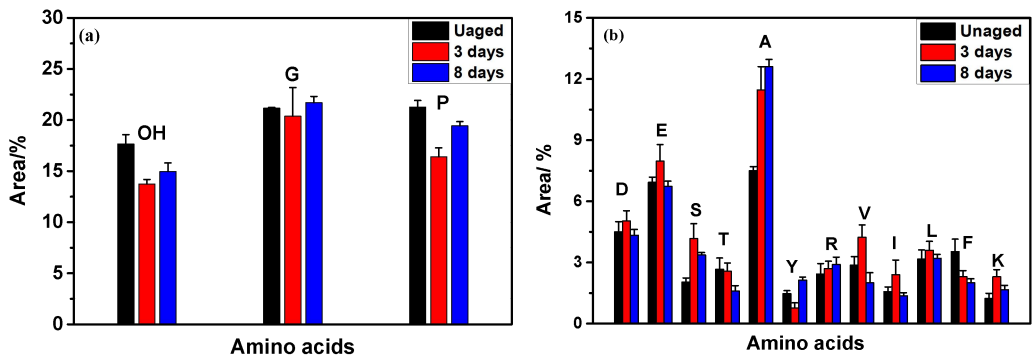

Figure 3 Relative amino acids concentrations of (a)Glycine, proline and hydroxyproline and (b) relative concentrations of other amino acids in vegetable-tanned leather samples artificially aged for different time: the injection volume of sample was 5 μL

3.2 FTIR-ATR results of artificially aged samples

FTIR analysis is an effective method to study the structure of biopolymers or polypeptide chains [16, 17]. **Table 3** showed the main FTIR peaks of the leather samples and their assignment. It was indicated that there is no significant difference of peak distribution between unaged and artificially aged leathers, which was also confirmed by **Figure 4a**. The small absorption bands at 1281 cm^{-1}, 1204 cm^{-1}, 1160 $cm^{-1}$and 1112 cm^{-1} in **Figure 4b** might be attributed to the existence of tannins in leather [18-20]. It is noteworthy that the relative intensity of FITR peaks at 1455 cm^{-1} corresponding to the δCH_2 of Pro^- graduallydecreased, which illustrated the proline or hydroxyproline in samples degraded by aging and it is consistent with the results of HPLC.

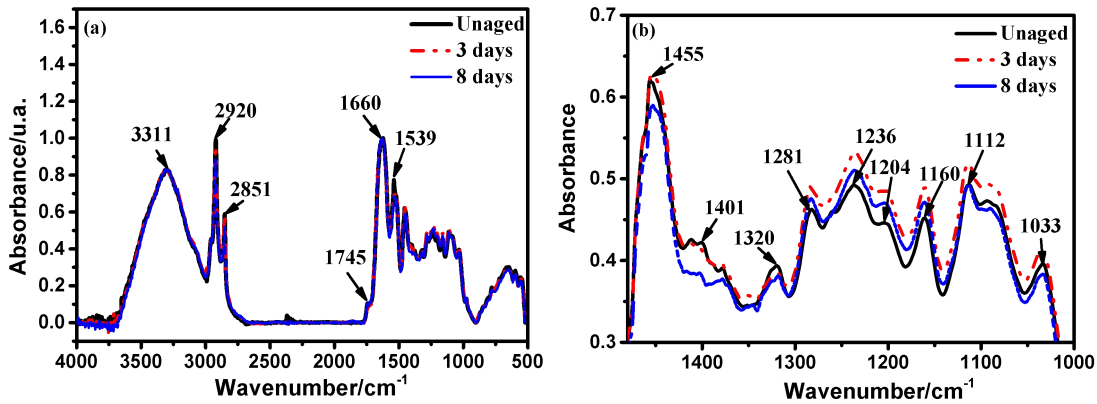

Figure 4 FTIR spectra of leather samples: (a) Full spectrum; (b) Zoomed-in spectrum of selected region

Table 3 Main FTIR peaks of collagen-based leather samples and their assignment

Absorption maximum(cm^{-1})			Assignment [21-23]
Unaged leather	Aged for 3 days	Aged for 8 days	
3311	3312	3312	Amide A: first component of νN-H in Femi resonance with the amide II overtone
2920	2921	2921	νC-N
1660	1665	1663	Amide I: νC=O with small contributions from νC-N and δN-H
1539	1539	1538	Amide II: (νC-N with contributions from δ_{ip}N-H
1455	1452	1453	δCH_2 of Pro^-
1401	1401	1403	δ_{ip}C-O-H (carboxylic side chains) and
1320	1318	1318	wCH_2/δC-H (methine)
1236	1236	1235	Amide III: (νC-N+ δN-H with contributions from νC-C and δ_{ip}C=O)
1033	1034	1033	Breathing of proline ring with carbohydrate νC-O and νC-O-C (glycosylation sites)

ν-stretching; δ-bending; d-deformation; ip- in-plane

Numerous researches have shown that the conformational changes of the collagen macromolecule induced by deterioration affect the relative positions and intensities of the amide I and amide II bands[24]. Accordingly, the structural changes caused by artificial aging can be revealed by analyzing the amide I and II bands in FTIR spectroscopy. However, the peaks reflecting structural changes upon ageing are always hidden under amide I and amide II peak envelopes [25]. In this paper, deconvolution of amide I and amide II was realized with Gauss PeakFit v4.12 software, as shown in **Figure 5**. The spectra of amide I and II regions for all the samples and the corresponding peak positionare presented in **Figure 5a**. **Figure 5b, c and d** show the deconvolution results of amide I and amide II bands observed on the samples artificially aged for 0 day, 3 days and 8 days, respectively. The peak intensity in the range of 1634 -1639 cm^{-1}, related to the random coil content of collagen in leather samples, slightly increased with the increase of aging time. Moreover, amide II of samples after short time of aging showed more small peaks. This can be explained that cross-linking by tannins in leather with the amide group of the collagen through hydrogen bond, which then affects the stretching of C-N and bending of N-H.

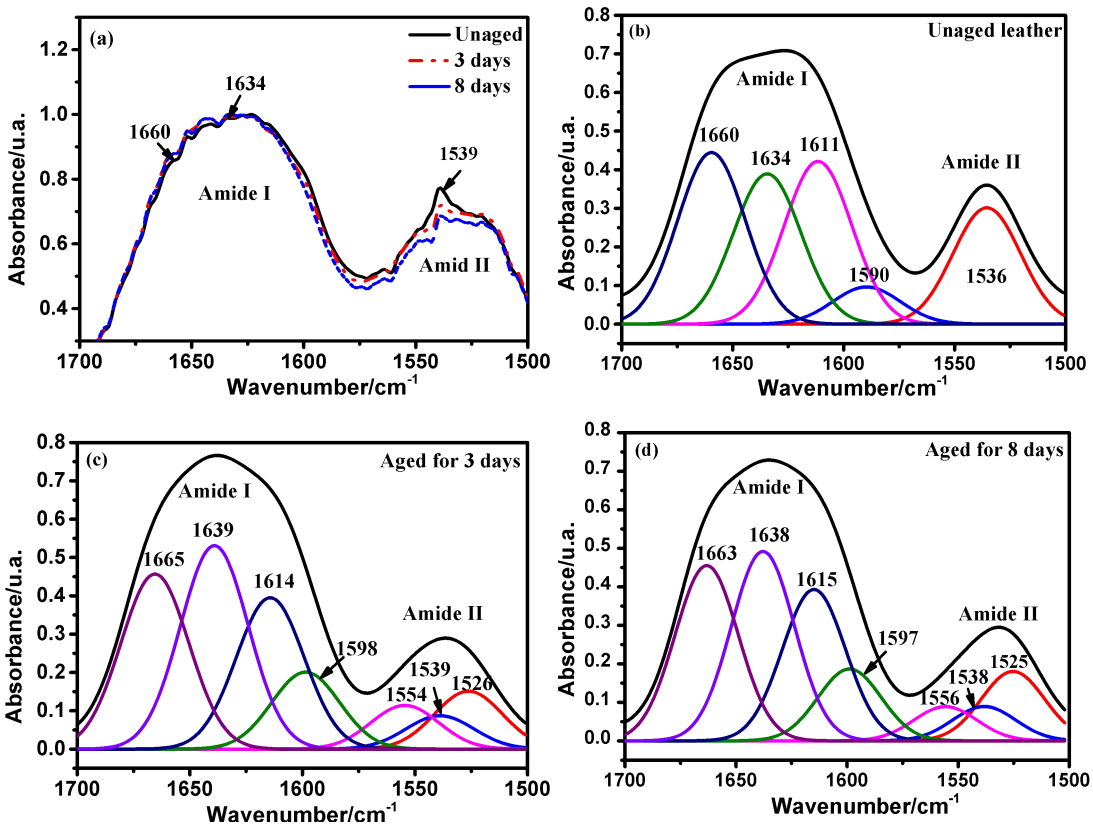

Figure 5FTIR spectra of amide I and amide II bands observed on vegetable-tanned leather: (a) Amide I and II regions for all the samples (b) deconvolution of amide I and II regions in unaged sample (c) deconvolution of amide I and II regions in sample aged for 3 days (d) deconvolution of amide I and II regions in sample aged for 8 days

4. Conclusions

Artificially aging treatment for different times affects the structure and conformation of collagen in leather, resulting in the degradation of leather. Proline and hydroxyproline are attacked during aging process. More free amino acids are released from the collagen macromolecular chain due to aging. A close examination of amide I and amide II bands showed an increasing content of random coil, suggesting a decreasing in the triple helix structural stability of collagen in leather. However, the present results merely provide an early sign for degradation of leather. Long time aging cycles are necessary to further investigate the deterioration mechanism.

Acknowledgements

This work was supported by the National Key R & D Program of China（No.2017YFB0308500）and the National Natural Science Foundation of China (Grant No. 51373158).

References

[1] Budrugeac P, Carşote C, Miu L. Application of thermal analysis methods for damage assessment of leather in an old military coat belonging to the History Museum of Braşov—Romania[J]. Journal of Thermal Analysis & Calorimetry, 2017, 127(1):1-8.

[2] Cucos A, Budrugeac P, Miu L. DMA and DSC studies of accelerated aged parchment and vegetable-tanned leather samples[J]. Thermochimica Acta, 2014, 583(14):86-93.

[3] Hansen E F, Lee S N, Sobel H. THE EFFECTS OF RELATIVE HUMIDITY ON SOME PHYSICAL PROPERTIES OF MODERN VELLUM: [J]. 1992.

[4] Larsen R, Vest M, Nielsen K. Determination of hydrothermal stability (shrinkage temperature) of historical leather by the micro hot table technique[J]. Journal- Society of Leather Technologists and Chemists, 1995, 77:151-156.

[5] Cohen N S, Odlyha M, Foster G M. Measurement of shrinkage behaviour in leather and parchment by dynamic mechanical thermal analysis[J]. Thermochimica Acta, 2000, 365(1–2):111-117.

[6] Wang Y J, Guo J, Chen H, et al. Influence of containing moisture on hydrothermal stability of modified collagen thermal characteristics analysis by DSC[J]. Journal of Thermal Analysis & Calorimetry, 2010, 99(1):295-300.

[7] Budrugeac P, Miu L. The suitability of DSC method for damage assessment and certification of historical leathers and parchments[J]. Journal of Cultural Heritage, 2008, 9(2):146-153.

[8] Budrugeac P, Cucos A, Miu L. The use of thermal analysis methods for authentication and conservation state determination of historical and/or cultural objects manufactured from leather[J]. Journal of Thermal Analysis & Calorimetry, 2011, 104(2):439-450.

[9] Axelsson K M, Larsen R, Sommer D V P, et al. Degradation of collagen in parchment under the influence of heat-induced oxidation: Preliminary study of changes at macroscopic, microscopic, and molecular levels[J]. Studies in Conservation, 2014, In press (1):165-172.

[10] Badea E, Gatta G D, Usacheva T. Effects of temperature and relative humidity on fibrillar collagen in parchment: Amicro differential scanning calorimetry (micro DSC) study[J]. Polymer Degradation & Stability, 2012, 97(3):346-353.

[11] Budrugeac P, Badea E, Gatta G D, et al. A DSC study of deterioration caused by environmental chemical pollutants to parchment, a collagen-based material ☆[J]. Thermochimica Acta, 2010, 500(1):51-62.

[12] Haynes P A, Sheumack D, Kibby J, et al. Amino acid analysis using derivatisation with 9-fluorenylmethyl chloroformate and reversed-phase high-performance liquid chromatography[J]. Journal of Chromatography A, 1991, 540(1-2):177.

[13] Amino Acid Analysis by Precolumn Derivatisation using a New FMOC Procedure, Application Note 013, http://www.gbcscientific.com/appnotes/HPLC_app_note_013.pdf

[14] Larsen R, Sommer D V P, Vest M, et al. Amino acid analysis of new and historical parchments[J]. 2002: 9-93.

[15] Ramachandran G N. Stereochemistry of collagen[J]. Chemical Biology & Drug Design, 1988, 31(1):1.

[16] Krimm S, Bandekar J. Vibrational spectroscopy and conformation of peptides, polypeptides, and proteins[J]. Adv Protein Chem, 1986, 38(C):181-364.

[17] Mantsch H H. New insight into protein secondary structure from resolution-enhanced infrared spectra[J]. Biochimica Et Biophysica Acta, 1988, 952(2):115-130.

[18] Falcão L, Araújo M E M. Application of ATR–FTIR spectroscopy to the analysis of tannins in historic leathers: The

case study of the upholstery from the 19th century Portuguese Royal Train[J]. Vibrational Spectroscopy, 2014, 74(5):98-103.

[19] Falcão L, Araújo M E M. Tannins characterization in historic leathers by complementary analytical techniques ATR-FTIR, UV-Vis and chemical tests[J]. Journal of Cultural Heritage, 2013, 14(6):499-508.

[20] Falcão L, Araújo M. Vegetable Tannins Used in the Manufacture of Historic Leathers[J]. Molecules, 2018, 23(5):1081.

[21] Bi X, Li G, Doty S B, et al. A novel method for determination of collagen orientation in cartilage by Fourier transform infrared imaging spectroscopy (FT-IRIS)[J]. Osteoarthritis & Cartilage, 2005, 13(12):1050-1058.

[22] Boyatzis S C, Velivasaki G, Malea E. A study of the deterioration of aged parchment marked with laboratory iron gall inks using FTIR-ATR spectroscopy and micro hot table[J]. Heritage Science, 2016, 4(1):13.

[23] Barth A. Infrared spectroscopy of proteins[J]. Biochimica Et Biophysica Acta, 2007, 1767(9):1073.

[24] C Sendrea, C Carsote, E Badea. NON-INVASIVE CHARACTERISATION OF COLLAGENBASED MATERIALS BY NMR-MOUSE AND ATR-FTIR[J]. U.P.B. Sci. Bull., Series B, 2016(78):27-38.

[25] Srour B, Bruechert S, Sla A, et al. Secondary Structure Determination by Means of ATR-FTIR Spectroscopy[J]. Methods in Molecular Biology, 2017, 1635:195.

P113

Chromium (Cr(III)) basic point - alkali (OH^-) capturing: the mechanism of high exhaustion chrome tanning

Chunxiao Zhang,[abc] Jieming Hu,[c] Cong Xia,[c] Yanhong Li,[ac] Biyu Peng [abc] *

a National Engineering Laboratory for Clean Technology of Leather Manufacture, Sichuan University, Chengdu 610065, P. R. China

b Key Lab. of Leather Chemistry and Engineering of Ministry of Education, Sichuan University, Chengdu, Sichuan 610065, P. R. China

c College of Light Industry, Textile & Food Engineering, Sichuan University, Chengdu, China

ABSTRACT

High exhaustion chrome tanning technology is deemed to be one of the most effective methods to reduce chromium emission during chrome tanning, which is the major stumbling block for the leather industry. However, the majority of the present technologies are difficult to be accepted in tanyard due to the improvement is limited. To break through the technical bottleneck, this study researches a mechanism of chromium penetration and combination, and the key factors to hinder chromium absorption during tanning is explored. The main effect of carboxylic masking agent was to prevent chromium forming over-crosslinkage among collagen fibers and increase the buffer performance of the tanning liquors. Not only cannot the carboxylic chemicals promote chromium penetration, but it was the key factor that decreases chromium absorption. Tanning at high initial pH appropriately would not cause into chromium overload on the grain layer of leather, but it could improve the chromium absorption and the evenness of Cr distribution in leather significantly. At least 50% of the combined Cr in leather was attributed to the hydrolyzation of Cr(III) during basification. It suggested that chromium exhaustion was primarily depended on the quantity and the hydrolytic polymerization capacity of the Cr(III) coordinated with the carboxylic on the side chain of collagen. Therefore, the new mechanism of chromium penetration and combination, the model of "Chromium (Cr(III)) basic point and alkali (OH^-) capturing", is finally established to guide the research of high exhaustion chrome tanning technology.

KEYWORDS: *High exhaustion chrome tanning, Masking agent, Chromium hydrolyzation, Tanning cross-linking mechanism, Collagen fiber*

* Corresponding Author E-mail: pengbiyu@scu.edu.cn; Tel.+86-28-85401208.

P114

Effects of Salt-enzyme Solution on the Opening of Collagen Fiber Bundles

Yafei Zhang, Hui Liu, Yadi Hu, Keyong Tang*

(School of Materials Science and Engineering, Zhengzhou University, Henan, Zhengzhou, 450001, P. R. China)

**Corresponding author: kytang@126.com, Tel. +8613938526389*

Abstract:

Liming is a crucial process in leather-making. Many chemical reagents are used in liming, and the physical and chemical interaction between reagents and hides is complex. Different reagents lead to different results. The purpose of liming is to open the collagen fiber bundles, ready for the penetration and reaction of subsequent reagents with hides. Sulphur sulfide and lime are generally used in conventional liming, causing remarkable pollutants and harmful gas, H_2S. Therefore, sulfur-free and lime-free liming methods have attracted increasingly attention.

In this paper, the control variable method, comparative experiments and various testing methods were used to explore the influence of salt-enzyme solution system on the opening of collagen fiber bundles in cow hides.

The unhairing rate and effect of traditional unhairing, enzyme unhairing and salt-enzyme unhairing were compared and the results showed that the unhairing of enzyme is fast, with a good hair root removal. Less than 0.4 wt% KCl in the enzyme unhairing system may further increase the unhairing rate. If KCl is more than 0.4 wt%, however, no significant contribution to the unhairing rate was found, but obvious shrink took place in the grain layer.

Four liming methods were used and their opening effect on collagen fiber bundles were compared and discussed. The results showed that liming with enzyme opens the collagen fiber bundles better than the traditional liming. The addition of KCl in liming may promote the opening of collagen fiber bundles, resulting in abetter tanning with increased softness and the mechanical properties of resultang leathers.

Keywords Leather; fiber dispersion; liming; salt-enzyme; KCl

1 Introduction

Since the beginning of the 21st century, more and more people pay their attention to environmental pollution. In order to protect the environment from the pollution, people are increasingly appeal for the cleaner production[1]. The leather industry is not only a long-established industry but also an industry with considerable pollutant emissions. The chemicals employed in the leather-making process are the source of the huge large of pollution in the leather industry[2]. Liming and reliming processes result in about 60%-70% of total pollution in the tanning industry[3]. Conventionally, fiber opening process is carried out using calcium hydroxide and sodium sulfide[4]. With the deepening of the application of sustainable development, researchers[4-9] devoted themselves to open the collagen fiber bundles by enzymes instead of lime and sodium sulfide due to the toxicity of S^{2-}. There are several fiber opening operations such as enzyme-only or enzyme assisted process have been reported and developed [5-8; 10-17].

As a cleaner, more efficient and specific biological material, enzyme is widely applied to various fields. In the leather industry, by the use of enzyme, a great amount of water resources may be saved, and harmful chemical reagents may be avoided. Ajitha Pandi *et al*[18] reported to remove fibrous interstitial and to open fiber bundles with α-amylase, and obtained a good effect. Enzyme and ionic liquid were reported to open the collagen fiber bundles[4; 19; 20]. In this study, salt-enzyme system for fiber opening was used, including potassium chloride, protease, and DMC liming assistant reagent. Four such liming methods as potassium chloride-protease, potassium chloride-DMC, DMC and sodium sulfide-calcium hydroxide were used and their opening effect on collagen fiber bundles were compared and discussed.

2 Materials and Methods

2.1 Materials

Dry salted cowhide from Xinxiang. ERHAVIT® DMC Liming Reagent, TFL Leather Chemicals. Neutral protease was produced by Bacillus subtilis with its CAS of 9068-59-1. All other chemicals were of analytical grade, purchased by

Aladdin.

2.2 Enzyme Activity

In order to estimate the activity of enzyme with little salt, the Folin-reagent method was employed in this study. The single activity unit defined as the numbers of tyrosine (μg) that 1 g of enzyme hydrolyzed the casein to tyrosine every minute under the experimental condition. Six parts of protease solution with a concentration of 0.8wt% were prepared, and 0, 0.2 wt%, 0.4 wt%, 0.6 wt%, 0.8 wt% and 1.0 wt% potassium chloride were added, respectively. Estimated the number of micrograms of hydrolyzed tyrosine according to the standard curve under standard assay conditions and calculate the activity of enzyme.

2.3 Optimization of Unhairing

Experiments were carried out to optimize the quantity of salt-enzyme for unhairing, compared to that of the conventional method. Protease solution, protease-potassium chloride solution and sodium sulfide solution were prepared at a concentration of 0.4 wt%, 0.8 wt%, and 1.2 wt%. The hides were put in these solutions for dehairing a temperature of 34 ℃ with stirring. A digital photograph of the hair removal status was recorded every two hours.

2.4 Fiber Opening

Experiments for fiber opening was carried out under the optimum concentration of unhairing. The hide after unhairing were divided into four parts, all in the size of about 4×8 cm. The liming solutions were 1.0 wt% protease-potassium chloride, 1.0 wt% DMC-potassium chloride, 1.0 wt% DMC and 1.0 wt% Sodium sulphide-calcium hydroxide, respectively. Hides were put into liming solutions for liminng with the temperature of 34℃ and drummedat 60 r/min, liquid ratio 5:1, for 24 hours.

2.5 Tanning

After liming, the hides were transferred into leathers by tannin tanning agent. 5 wt% of hide weight tannin solution was used with the liquor of 2:1 and tanned for 90 min in a rotating drum for the first tanning. The next step was prepared 20% of hide weight tannin solution at a control solution ratio of 2:1 and tanned for 20 h in a rotating drum, which stopped the drum for 10 min every 2 h.

2.6 Scanning Electron Microscope

All hides were cut into 4×10 cm and placed in GT2-Type-8 vacuum freeze-drying machine, LOYTECH Germany at -50℃ for 24 h, and then lyophilized. The freeze dried samples were made into scanning electron microscope samples. All SEM samples were gold coated and the surface and the cross section were observed by using JSM-F scanning electron microscope, Japan Electronics Co., Ltd.

2.7 Estimation of Absorption of Tannin

Subsequent to fiber opening, the samples were tanned using tannin tanning reagent. Ultraviolet-visible spectrophotometry was carried out to estimate the amount of adsorption of tannin. The characteristic absorption of tannin at 275 nm. Tannin solution was diluted to 10000 times and the absorbance of solution at 275 nm was measured by standard curve, and the absorption amount of leather to tannin tanning reagent was calculated.

2.8 Physical Properties of Leather and Sensory Characteristics

The physical characteristics of leather such as tensile strength (MPa), elongation at break (%) and tear strength (N/mm) were measured by a SMSTA. XTPlus texture analyzer, Lotun Science Co Ltd. Britain. All the samples were cut to pieces sized 30×4×3 mm.

The sensory characteristics of leather involves in fullness, smoothness, softness and visual feel, all of which were identified by five leather experts and graded from 1 to 5.

3 Results and Discussion

3.1 Protease Activity

The activity of protease are presented in Figure 1. It can be concluded from Figure 1 that when the potassium chloride was mixed with protease, an increased activity of protease was found with increasing the potassium chloride concentration, at the potassium chloride content less than 0.4%. However, it will decrease the protease activity when the concentration of potassium chloride is more than 0.4%.

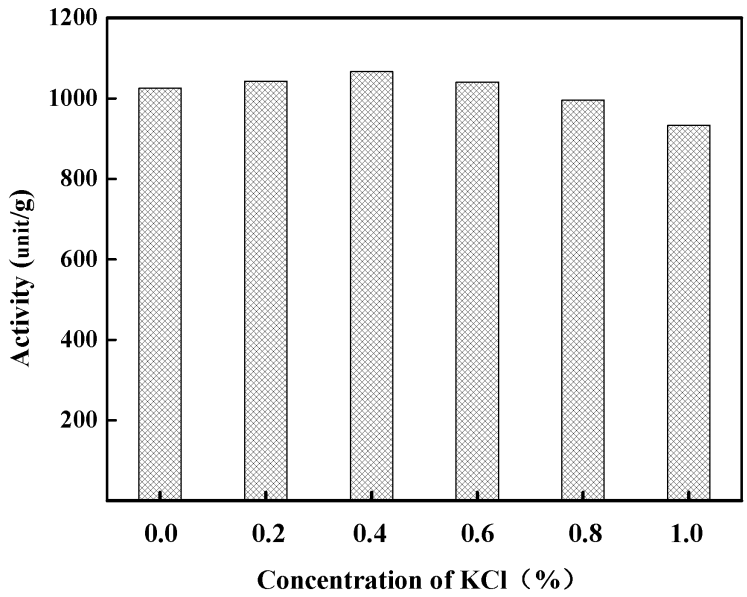

Figure 1 Protease activities at different KCL concentrations

In general, the activity of protease in present study was obviously low, compared to the reported[21; 22] and the potassium chloride had little effect on the activity of protease. In other words, it was reported that K+ and Cl- acted as the activator of protease[21]. When using protease, the enzymatic effects can be improved by using little potassium chloride. More than 0.4% of potassium chloride, however, will lead to dehydration.

Figure 1 Protease activities at different KCL concentrations

In general, the activity of protease in present study was obviously low, compared to the reported[21; 22] and the potassium chloride had little effect on the activity of protease. In other words, it was reported that K^+ and Cl^- acted as the activator of protease[21]. When using protease, the enzymatic effects can be improved by using little potassium chloride. More than 0.4% of potassium chloride, however, will lead to dehydration.

Table 1 Digital photos of hides at different liming times

Time	Concentrations								
	0.4 wt%			0.8 wt%			1.2 wt%		
	Protease	Protease +KCl	Na_2S	Protease	Protease +KCl	Na_2S	Protease	Protease +KCl	Na_2S
0 h									
2 h	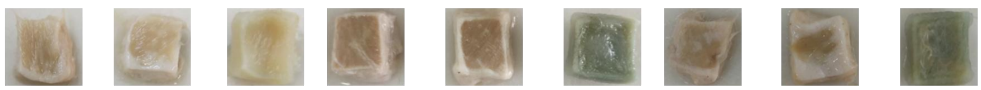								
4 h									
6 h									
	↓	↓	↓	↓	↓	↓	↓	↓	↓
	12 h	8 h	14 h	10 h	7 h	10 h	6 h	6 h	8 h
Finish time									

3.2 Optimization of Unhairing

Initially, trials were performed to optimize the condition of unhairing matching the requirements of the cleaner production. Trials with different condition of enzyme unhairing, salt-enzyme unhairing and sodium sulfide unhairing with different concentration of 0.4 wt%, 0.8 wt%, 1.2 wt% were carried out in this study. The assessment of digital photos of hides for different times are presented in Table 1. From Table 1, it can be obviously inferred that the enzymatic unhairing is faster, compared with sodium sulfide unhairing and the addition of potassium chloride could further promote the unhairing rate. From the detailed investigation of microstructure, the surface topography can be clearly seen, as shown in Figure 2. When the concentration of potassium chloride was exceed 0.4 wt%, the surface of the hides may be observed, Figure 2(A, B, C). It is probably because of the dehydration induced shrink of hides by the excessive concentration of potassium chloride. .

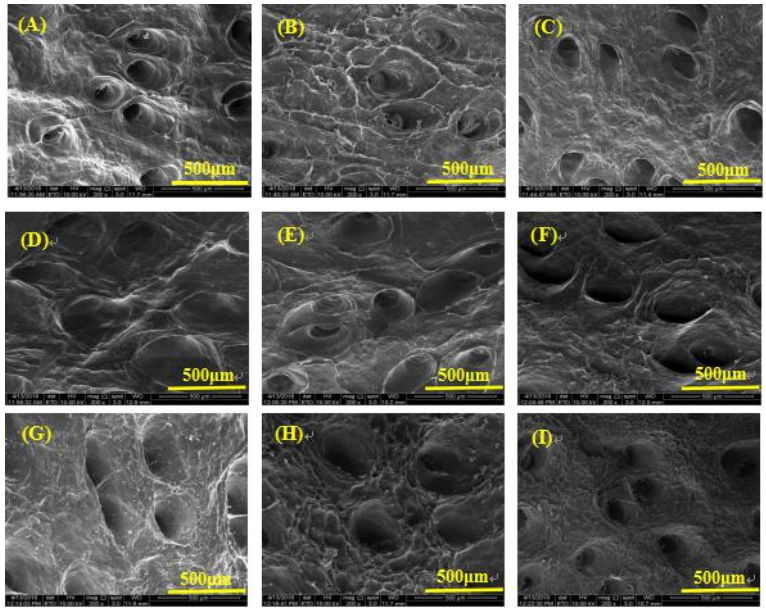

Figure 2 SEM images hides after unhairing. Simples: A~C, protease-potassium chloride unhairing, 0.4 wt%, 0.8 wt%, 1.2 wt%. D~F, protease uhairing, 0.4 wt%, 0.8 wt%, 1.2 wt%. G~I, sodium sulfide unhairing, 0.4 wt%, 0.8 wt%, 1.2 wt%.

In the case of pure enzyme unhairing, however, no shrink occurred on the surface, with big and shallow pores of unhaired hides, Figure 2(D, E, F). It had a slight dehydration when the enzyme concentration reached 1.2 wt%. For the conventional sodium sulfide unhairing in Figure 2(G, H, I), the damaged of unhairing hides were observed at all of experimental concentration and the higher concentration, the greater damage.

The traditional sodium sulfide unhairing substance is damaging rather than keeping, not only couldn't unhairing completely but also could cause a certain degree of harm to the environment due to the presence of sulfur. Compared to the enzymatic unhairing, many short plates were shown in the conventional unhairing. At the same time, it also highlights the advantages of enzymatic unhairing, which is environmental-friendly, clean and no harmfully.

3.3 Scanning Electron Microscopic Evaluation

Scanning electron micrographs showing the fiber dispersion state of the cross section of all the experimental hides are presented in Figure 2. Compared to the Sodium sulfide-calcium

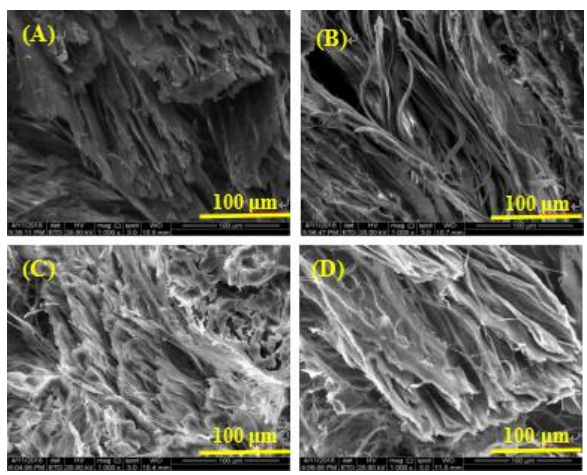

Figure 3 Images of SEM after fiber opening. Simples: A, protease+ potassium chloride. B, DMC+ potassium chloride. C, DMC. D, Sodium sulfide-calcium hydroxide.

hydroxide liming system (Figure 3 D), the enzymatic liming showed the better fiber opening with formation of a clearer fiber microstructure in Figure 3(A, B, C). Figure (B, C) showed the dispersion of fiber with DMC-potassium chloride and DMC liming system, from which it can be obviously indicated that potassium chloride had a positive effect on fiber opening. Collagen fiber processing by protease was extruded into a lamellar rather than fibers compared to Figure 3(B, C). Conventional liming method using Sodium sulfide and calcium hydroxide was showed in Figure 3 D, which was not as good as Figure 3(B, C). This is can be explicitly inferred that enzyme liming is capable of opening up the collagenous matrix and assists loosening of the fiber structure and at the same time potassium chloride takes a promotion on fiber opening.

3.4 Tannin Absorption

The uptake of tanning reagents is depended on the extent of opening up of collagen fiber bundles. So the absorption of the tanning reagent by leathers may act as an indirect judgment of fiber opening. The amount of tannin absorbed by leather using the protease- potassium chloride liming system was the highest in this study, above 203 mg/g. On the contrary, the amount of absorption of DMC-potassium chloride with good liming effect was only 184 mg/g, close to that by conventional liming method.

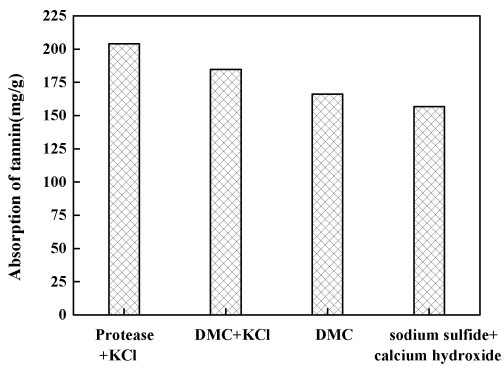

Figure 4 The absorption of tannin

3.5 Physical Properties of Leather and Sensory Characteristics

Leather is a widely used product and the mechanical properties of leathers determines their application and value. So it is necessary to study the influence of liming method on the mechanical properties. The physical characteristics results of leather such as tensile strength (MPa), elongation at break (%) and tear strength (N/mm) are presented in Table 2. The physical properties of leathers were quite different for different liming methods. Compare with that by traditional sodium sulfide-calcium hydroxide limed leathers, the enzymatic lime leather is better in physical properties. The addition of potassium chloride not only helps open the collagen fiber bundles, but also facilates to improve the properties of leather. The tensile strength and tear strength of the leather treated with DMC-potassium chloride was 8.82 MPa, 35.10 N/mm, respectively, the best properties one in all. So salt-enzymatic limed leathers exhibited a better physics properties. On the contrary, the elongation at break of the leather treated with DMC-potassium chloride was 24.10%, not as good as the leather treated with Protease-KCl and Na2S-Ca(OH)2.

The sensory characteristics of leather graded from 1 to 5 are presented in Table 3. It can be inferred that leather by enzyme limingleads to good organoleptic properties such as softness, smoothness and fullness, compared to those of traditional limed leathers. The addition of potassium chloride significantly improves the softness of the leather, while the leather without potassium chloride is not soft. Potassium chloride in liming system might promote the opening of collagen fiber. So tanning agents could get into the interior of leather, and thereby improve the softness of the leather, with the fullness and smoothness improved to some extent.

Table 2 Physical testing data of leather

Sample	Tensile strength (MPa)	Elongation at break (%)	Tear strength (N/ mm)
Protease-KCl	7.92±1.13	26.67±6.84	31.73±4.54
DMC-KCl	8.82±0.85	24.10±3.54	35.10±3.05
DMC	5.70±0.48	18.31±0.72	24.03±2.60
Na_2S-$Ca(OH)_2$	4.64±0.91	27.72±2.93	19.96±5.08

Table 3 Sensory characteristics of leather

Experiments	Protease-KCl	DMC-KCl	DMC	Na_2S +$Ca(OH)_2$
fullness	3	4	4	3
smoothness	4	4	3	3
softness	5	4	2	4

Scale of 1–5; 1—poor; 5—best

4 Conclusions

Enzymatic unhairing is efficient, environmentally friendly and clean. The addition of potassium chloride during unhairing could shorten the hair removal time. However, the epidermis will be dehydrated and shrunk when the amount of KCl is 0.4 % (w/v). The use of enzymes for fiber opening is comparable or better than traditional liming, which further promotes the opening of fiber bundles. The mechanical properties leathers with enzyme are better than those by traditional liming. With KCl in protease liming, the tensile strength and tearing strength of the leather can be obviously improved.

Acknowledgement

The financial supports from the National Natural Science Foundation Commission of China (No. 51673177) and National Key R & D Program of China（No.2017YFB0308500）are greatly appreciated.

References

[1] Jia S T, Wang J. Performing Cleaner Production in Leather Industry[J]. Environmental Science & Technology, 2001, 6(98): 45-47.

[2] Durga J, Ranjithkumar A, Ramesh R, et al. Replacement of lime with carbohydrases – a successful cleaner process for leather making[J]. Journal of Cleaner Production, 2016, 112: 1122-1127.

[3] Capello C, Fischer U, Hungerbühler K. What is a green solvent? A comprehensive framework for the environmental assessment of solvents[J]. Green Chemistry, 2007, 9(9): 927-934.

[4] Alla J P, Rao J R, Fathima N N. Integrated Depilation and Fiber Opening Using Aqueous Solution of Ionic Liquid for Leather Processing[J]. ACS Sustainable Chemistry & Engineering, 2017, 5(10): 8610-8618.

[5] Sivasubramanian S, Manohar B M, Rajaram A, et al. Ecofriendly lime and sulfide free enzymatic dehairing of skins and hides using a bacterial alkaline protease[J]. Chemosphere, 2008, 70(6): 1015-24.

[6] Sivasubramanian S, Manohar B M, Puvanakrishnan R. Mechanism of enzymatic dehairing of skins using a bacterial alkaline protease[J]. Chemosphere, 2008, 70(6): 1025-34.

[7] Murugappan G, Zakir M J A, Jayakumar G C, et al. A Novel Approach to Enzymatic Unhairing and Fiber Opening of Skin Using Enzymes Immobilized on Magnetite Nanoparticles[J]. ACS Sustainable Chemistry & Engineering, 2016, 4(3): 828-834.

[8] Thanikaivelan P, Rao J R, Nair B U, et al. Progress and recent trends in biotechnological methods for leather processing[J]. Trends Biotechnol, 2004, 22(4): 181-8.

[9] Punitha V, Kannan P, Saravanabhavan S, et al. Chemical degradation of melanin in enzyme based dehairing and fiber opening of buff calfskins[J]. Clean Technologies and Environmental Policy, 2008, 11(3): 299-306.

[10] Ranjithkumar A, Durga J, Ramesh R, et al. Cleaner processing: a sulphide-free approach for depilation of skins[J]. Environ Sci Pollut Res Int, 2017, 24(1): 180-188.

[11] Kanth S V, Venba R, Madhan B, et al. Cleaner tanning practices for tannery pollution abatement: Role of enzymes in eco-friendly vegetable tanning[J]. Journal of Cleaner Production, 2009, 17(5): 507-515.

[12] Saravanabhavan S, Aravindhan R, Thanikaivelan P, et al. Green solution for tannery pollution: effect of enzyme based lime-free unhairing and fibre opening in combination with pickle-free chrome tanning[J]. Green Chemistry, 2003, 5(6): 707.

[13] Ma J, Hou X, Gao D, et al. Greener approach to efficient leather soaking process: role of enzymes and their synergistic effect[J]. Journal of Cleaner Production, 2014, 78: 226-232.

[14] Cho S, Choi Y, Lee J, et al. Optimization of enzyme extractions for total folate in cereals using response surface methodology[J]. J Agric Food Chem, 2010, 58(19): 10781-6.

[15] Ganesh Kumar A, Swarnalatha S, Sairam B, et al. Production of alkaline protease by Pseudomonas aeruginosa using proteinaceous solid waste generated from leather manufacturing industries[J]. Bioresour Technol, 2008, 99(6): 1939-44.

[16] Liu Y, Li Y, Chang R, et al. Species identification of ancient leather objects by the use of the enzyme-linked immunosorbent assay[J]. Analytical Methods, 2016, 8(42): 7689-7695.

[17] Sivakumar V, Swaminathan G, Rao P G, et al. Use of ultrasound in leather processing industry: effect of sonication on substrate and substances--new insights[J]. Ultrason Sonochem, 2010, 17(6): 1054-9.

[18] Pandi A, Ramalingam S, Rao J R, et al. Inexpensive α-amylase production and application for fiber splitting in leather processing[J]. RSC Advances, 2016, 6(39): 33170-33176.

[19] Vijayaraghavan R, Vedaraman N, Muralidharan C, et al. Aqueous ionic liquid solutions as alternatives for sulphide-free leather processing[J]. Green Chemistry, 2015, 17(2): 1001-1007.

[20] Jayakumar G C, Mehta A, Rao J R, et al. Ionic liquids: new age materials for eco-friendly leather processing[J]. RSC Advances, 2015, 5(40): 31998-32005.

[21] 张丽平, 李桂菊. 皮革加工技术[M]. 中国纺织出版社, 2006.

[22] 马建中, 卿宁, 吕生华. 皮革化学品[M]. 化学工业出版社, 2008.

P115

Proceedings of the 11th Asian leather conference-Xi'an, China
Effect of salt-lime solution on hide swelling and solution properties

Qian Zhang[1], Hui Liu[2], Yadi Hu[3], Jie Liu[4], Keyong Tang*

(College of Materials Science and Engineering, Zhengzhou University, Henan Zhengzhou, 450001 China)

[1]1576166442@qq.com, Tel. +8613633812520; [2]853489841@qq.com, Tel. +8615981902409;

[3]1741569964@qq.com, Tel +18838221602 ; [4]15001558@qq.com, Tel +13838001503

**Corresponding author: kytang@126.com, Tel. +8613938526389*

Abstract

Liming is a very important process in leather making, which directly affects the structure and properties of collagen and leathers. The quality of leathers is determined by liming to some extent. The composition of liming system is complex, and interaction between liming agents and hides varies a lot. In this study, four such salts as Na_2SO_4, Na_2HPO_4, $CaCl_2$ and $MgCl_2$ were added in the $CO(NH_2)_2/Ca(OH)_2$ solution for liming. The pH and conductivity of the mixture solution and swelling of the hide was measured. Then vegetable-tanned leather was characterized by scanning electron microscopy(SEM). The interaction between Na_2SO_4, Na_2HPO_4, $CaCl_2$, $MgCl_2$ and $CO(NH_2)_2/Ca(OH)_2$ solution and the effect of salt/ $CO(NH_2)_2/Ca(OH)_2$ solution on swelling of hides were explored. Salts slightly affect the pH of the $CO(NH_2)_2/Ca(OH)_2$ solution. The conductivity of solution with Na_2SO_4 and $CaCl_2$ increases with the increase of salt concentration, while the conductivity of solution with Na_2HPO_4 and $MgCl_2$ decreases with the increase of concentration. The conductivity of solution increases slightly with the increase of liming time, then nearly unchanged, indicating less ion exchange in liming solution. The swelling of hidesprocessed by the solution with 1% $CaCl_2$ and $MgCl_2$ was decreased. The result of SEM showed that liming solution with 1% $CaCl_2$ had better opening up effect on collagen fibers.

Key words: liming, salt solution, discipline of interaction, swelling

P116

Fragrance Lasting/ Antibacterial Casein-based Microcapsule Leather Finishes via Interface Template Method

Qunna Xu[1,2],Ruijie Qiu[1,2],Jianzhong Ma[1,2],Teng Zhao[1,2]

1 College of Bioresources Chemical and Materials Engineering, Shaanxi University of Science & Technology, Xi'an 710021, China

b Key Laboratory of Leather Cleaner Production, China National Light Industry, Xi'an 710021, China

Abstract

Casein-based titanium dioxide microcapsules with fragrance controlled release property and antibacterial function for leather finishes were prepared by interface template method. The amount of precursor and fragrance were optimized by single factor experiment when stability, antibacterial and slow release properties were taken as the main indexes. The morphology and size distribution of the capsules were characterized by dynamic laser light scattering (DLS) and atomic force microscopy (AFM). The release behavior was tested by UV spectrophotometry. Antibacterial properties of the microcapsules were tested by the inhibition zone method. The results showed that performance of microcapsule emulsion was best when the dosage of TBOT was 50μL, the dosage of flavor was 60mg and the dosage of casein was 50mg. AFM and DLS result showed that particle had a clear capsule structure with the size of about 60nmm. Antimicrobial test showed that the as-prepared capsule emulsion had obvious antibacterial property.Through application, it's noted that the as-obtained microcapsule could gave leather samples expected fragrance lasting behaviors and antibacterial properties, which had great potential use in leather industry.

Keywords: casein, titanium dioxide, microcapsules, interface polymerization, sustained release, antibacterial

P117

Application of Soluble Soybean Polysaccharide in Leather Finishing

Zhenye Tang[a], Yadi Hu, Hui Liu, Jie Liu, Keyong Tang*,

(College of Materials Science and Engineering, Zhengzhou University, Zhengzhou 450001, P. R. China)

*([a]15737938329@163.com *Corresponding author: kytang@zzu.edu.cn)*

Abstract:

Soluble soybean polysaccharide (SSPS) from soybean dregs is an acidic polysaccharide, which is rich in raw materials and low in cost with good film-forming ability. Waterborne polyurethane (WPU) emulsion with water as medium exhibits low organic solvent content, which is environmentally friendly with good compatibility, safety and reliability. Therefore, they two have attracted increasing attention. In this paper, anionic WPU emulsion and SSPS solution were used as raw materials in leather finishing. Physically blending method was employed to modify polyurethane emulsion with SSPS. The effects of soybean polysaccharide amount and pH of the mixed emulsion on the polyurethane emulsion and its film-forming properties were studied. The results showed that the stability of the mixed emulsion gradually deteriorated with increasing the SSPS amount. With the pH decreases, demulsification and coagulation of emulsion might take place, resulting in the loss of its application value. In alkaline condition, however, no significant change was found. With the increase of SSPS amount, both the water absorption rate and the tensile strength of the resultant film gradually increased, while the elongation at break gradually decreased. The effect of SSPS on the performance of waterborne polyurethane leather finishing agent was explored as well.

Keywords: Waterborne polyurethane; SSPS; Blending modification; Leather finishing

1.Introduction

Finishing agent is a general term for leather auxiliaries used to protect leather surface and improve hand feeling. It is composed of film-forming materials, pigments, solvents and auxiliaries with some proportion, among which film-forming materials are the basis [1]. Waterborne polyurethane finishing agent has good film-forming properties, and the products have good hand feeling. So it is very commonly used for leather finishing. However, due to the poor solvent resistance and hardness, its application and development are limited [2].

Soluble soybean polysaccharide (SSPS) is an acidic polysaccharide whose backbone consists of long-chain rhamnogalacturonan, short-chain homogalacturonan and neutral sugar of galactose and arabinose as side chains [3]. In addition, SSPS is characterized by a compact, globular structure [4]. Properties are determined by structure, so SSPS has high water solubility, resistance to acid, alkali and temperature, as well as film forming ability, and emulsification. Therefore, SSPS can be used to modify waterborne polyurethane by these good performances to improve the properties of waterborne polyurethane finishing agent.

In the paper, the physically blending method was used to modify anionic waterborne polyurethane by SSPS. Such influencing factors as amount of SSPS solution, acidity and alkalinity of modified emulsion on film formation ability were explored, in terms of the mechanical property and water absorption in water, acid, alkali, salt solutions. The results in the present study might be used in the application of modified anionic polyurethane leather finishing agent.

2.Materials and Methods

2.1 Materials

SSPS was kindly provided by Pingdingshan Jinjing Biotechnology Co., Ltd. Anionic waterborne polyurethane was obtained from Zhengzhou Gaoxin Leather Technology Co., Ltd. All other chemicals were of analytical grade and made in China.

2.2 Preparation of SSPS solution and modified emulsion

2.2.1 Preparation of SSPS solution

The 10 wt% SSPS solution was obtained by dissolving the SSPS in deionized water with stirring at 50℃ for 40 minutes.

The solution was deformed for 10 minutes under ultrasonic to get homogeneous solution for subsequent use.

2.2.2 Modified emulsion Preparation

The SSPS solution was slowly added into the anionic waterborne polyurethane emulsion with stirring for 10 minutes at room temperature. Then the SSPS/WPU mixture with different proportions was ultrasound dispersed for 20 minutes to obtain homogenous emulsions.

Table 1. The amount of two components in latex films

number	SSPS solution (10%wt)/ml	Anionic WPU/ml
1	0	12
2	1	12
3	1	14
4	1	16

2.2.3 Preparation of latex film

The final mixture were poured in a rectangular teflon mould (8 cm×2 cm) and dried at 25℃ for 48 h. According to the proportion of SSPS/WPU, the prepared SSPS/WPU composite films were named as pure latex film (anionic WPU), 1-12 (1:12, SSPS:WPU), 1-14 (1:14, SSPS:WPU), and 1-16 (1:16, SSPS:WPU), respectively.

2.3 Methods

2.3.1 Stability of the modified emulsion

The different proportions of mixed emulsions were prepared and their appearance after 24 h at 25℃, -10℃ and 60℃ was observed to know their stability.

2.3.2 Solid content of emulsion

The anionic WPU emulsion was weighed, note as m_2, and dried at 60℃ for 24 hours to reach constant weight, m_1. The solid content of anionic WPU-emulsion was calculated according Equation (1).

$$\mathrm{w} = \frac{m_1}{m_2} \times 100\% \quad (1)$$

Where W is the solid content (%), m_1 is the weight after drying (g), and m_2 is the original weight of emulsion (g);

2.4 Water absorption of latex film

The obtained latex film was cut into a sample with the size of 2.0 × 2.0 cm. After being weighed, noted as m_1, the sample was placed in such solutions as deionized water, acetic acid solution, aqueous ammonia solution, and sodium chloride solution, respectively for 24h. After being taken out, the surface water was quickly removed by filter paper and weighed again, m_2. Three parallel experiments were done for one sample with the average reported. The water absorption rate was calculated according to Equation (2).

$$\mathrm{Z}(\%) = \frac{m_2 - m_1}{m_1} \times 100\% \quad (2)$$

Where Z is the water absorption rate (%), m_1 is the latex film weight (g), and m_2 is the latex film weight after absorbing water (g).

2.5 Mechanical properties of latex film

The latex film was cut into a dumbbell-shaped sample as shown in Figure 1, and then its mechanical properties were tested with the texture analyzer, Lotun Science Co Ltd. Britain.

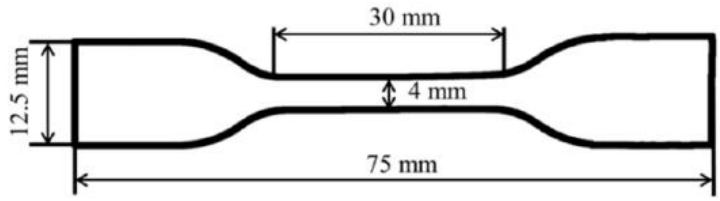

Figure.1 Schematic diagram of dumbbell-shaped sample

3.Results and discussion

3.1 Stability of modified emulsion

When the ratio of anionic WPU to SSPS solution was above 12, after being kept for 24h at 25℃, -10℃ and 60℃, no obvious change was found. Macroscopically, it was still a homogeneous emulsion. When the ratio of anionic WPU to SSPS solution was below 12, however, obvious stratification was found at all the temperatures of 25℃, -10℃ and 60℃. When the ratio dropped to 10, the stratification was apparent and the lower layer appeared precipitation. Compared with the amount of SSPS solution, the effect of acidity and alkalinity of the modified emulsion was more special. Firstly, the ratio of anionic WPU to SSPS solution was 12, with the acidity of the modified emulsion increasing, precipitation appears, resulting in the loss of its application value. However, with the increase of alkalinity, no significant changes was found in the appearance of the mixed emulsion. The WPU emulsion is anionic, and the surface of the SSPS molecule is also negatively charged. It will neutralize and remove negative charge in acidic environment, causing the demulsification of latex particles to form precipitation.

3.2 Solid content.

Solid content is the proportion of solid components in the WPU emulsion, which directly affects the fullness and brightness of leather surface. The solid content of the anionic waterborne polyurethane used in this experiment was calculated as 34.55%.

3.3 Film-forming mechanism

With the evaporation of water, the concentration of latex particles gradually increased and got closer to each other. When the concentration of latex particles increases to a critical value, latex particles could get close enough to form a compact accumulation. At the same time, due to the effect of the electric double layer on the surface of latex particles, a small gap is formed between latex particles, which is equivalent to a "capillary" filled by water, thus further producing capillary force. Further volatilization of water makes the latex particles more closely packed, and the "capillary" force increases until the latex particles were sufficiently deformed to overcome the electric double layer force, and the latex particles formed a continuous film [5]. The mechanism is shown in the Figure 2.

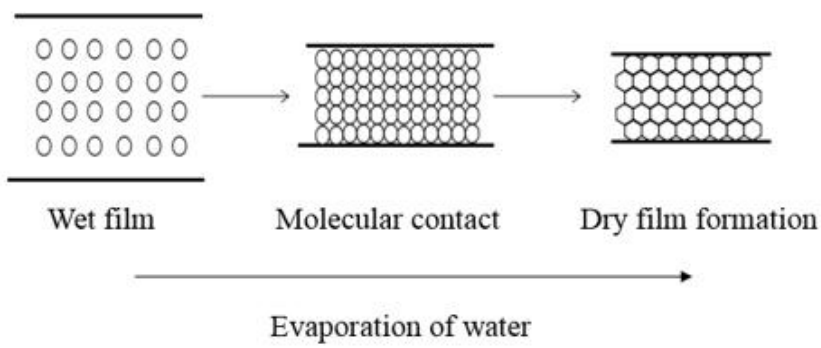

Figure 2 Schematic diagram of film forming process

3.4 Water absorption

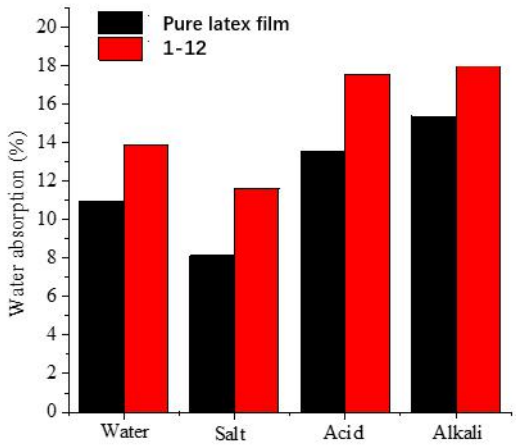

Figure 3 Water absorption of the film in four different solutions

In Figure 3, when no SSPS was added in the anionic WPU emulsion, the water absorption rate of the film in water, salt, acid and alkali solution were respectively 10.95%, 8.13%, 13.56%, 15.37%. When the ratio of anionic WPU to SSPS solution was 12, the water absorption rate of the film in water, salt, acid and alkali solution were all increase to 13.86%, 11.61%, 17.57%, 19.44%, respectively. So the water absorption rate of anionic WPU film is increased with the addition of SSPS in these four different solutions. As to the water absorption rate of the latex films in the four solutions, the water absorption rate in alkali solution is the largest, followed by the one in the acid solution, and then the one in the salt solution, with the one in water the smallest. Meanwhile,the water absorption of the latex film also rises with the increase of SSPS amount.

Based on the above results, it can be concluded that the water resistance of the latex film modified by SSPS is decreased. SSPS belongs to sugars, and there are a large number of hydrophilic groups such as hydroxyl groups in the molecular chain. The introduction of these groups further deteriorates water resistance of the latex film [6].

3.5 Analysis of mechanical properties

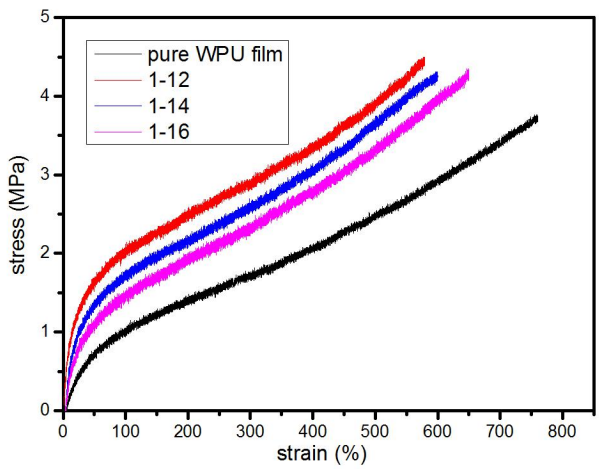

Figure 4 Stress and strain diagram of latex film

Tensile strength and elongation at break are important mechanical properties for leather finishing agents, which determine the final use of the finishing agents. Softness is one of the quality requirements too. A quantitative evaluation method of softness is to use the slope of stress-strain curve at the elastic deformation stage. In Figure 4, the tensile strength was increased, and the elongation at break were decreased by the SSPS modification of the WPU. The SSPS molecule contact the WPU molecule to form an interface, called a phase interface. Due to hydrogen bonding, the phase interface has high interface bonding strength, to enhance the mechanical properties. However, when the latex film was deformed, the force at the phase interface was larger, and stress concentration occurred, resulting in an increased tensile strength and decreased elongation at break. It was expected that the leather finishing agent with ideal mechanical properties could be obtained by controlling the ratio of anionic WPU to SSPS.

4.Conclusion

Physically blending method was employed to modify polyurethane emulsion with SSPS in the present study. The addition of SSPS will reduce the water resistance of the latex film. The tensile strength of latex film gradually increases, while the elongation at break gradually decreases. With the sustainable development and higher requirements for leather finishing agents, the modified waterborne polyurethane finishing agents have a wider development prospect.

Acknowledgement

This project is financially supported by National Key R & D Program of (ChinaNo.2017YFB0308500) and the National Natural Science Foundation Commission (NO.51673177) are greatly appreciated.

References

[1] Wei J, Wang L N, Gang-Qiang L I. Latest Research Progress on Leather Finishing Agents[J]. Fine & Specialty Chemicals, 2006, 19, 8.

[2] Wu XH, Ding SL, Yang CJ. Research progress of waterborne polyurethane leather finishing agent [J]. China Leather, 2004(2): 47-50.

[3] Maeda H, Phillips G O, Williams P A. Soluble soybean polysaccharide. [M] Handbook of Hydrocolloids. 2000.

[4] Wang Q, Huang X, Nakamura A, et al. Molecular characterisation of soybean polysaccharides: an approach by size exclusion chromatography, dynamic and static light scattering methods. [J]. Carbohydr Res, 2005, 340(17): 2637-2644.

[5] Hong XW, Feng HB. Coating Chemistry [M]. Beijing: Science Press 2005: 22-24.

[6] Wang GQ. Principle and application of polymer blending modification[M]. Beijing，China Light Industry Press. 2007, 7, 87.

P118

Unhairing of Cowhides with KCl Assisted Neutral Protease for Leather Making

Liu Hui, Zhang Qian, Zhang Yafei, Tang Keyong *, Liu Jie, Zheng Xuejing, Pei Ying, Li Xiumin
School of Materials Science and Engineering, Zhengzhou University, Zhengzhou 450001, P. R. China
**Corresponding author: kytang@126.com, Tel. +8613938526389*

Abstract

Nowadays, tannery pollution is of great concern worldwide. The unhairing process contributes the majority of the pollution because of the use of sodium sulfide and calcium hydroxide, which were replaced by neutral protease and potassium chloride (KCl) in the present work. Moderate amount of potassium chloride can speed up the unhairing rate with the papillary layer not destroyed in neutral protease solution. The effect of potassium chloride concentration and temperature on the activity of neutral protease was systematically studied by central composite design (CCD) of response surface methodology (RSM). The results indicate that the potassium chloride concentration is insignificant, but the temperature is very significant. The effect of potassium chloride content on the turbidity and light transmittance of neutral protease solution was investigated. The turbidity and light transmittance of neutral protease solution was reduced and increased respectively after adding potassium chloride. Potassium chloride was added into neutral protease solution to increase the dissolution of carbohydrates, but less impact on protein hydrolysis. The results of COD value shown the wastewater of conventional unhairing method is the highest.

Keywords: potassium chloride (KCl), unhairing, leather, neutral protease,response surface methodology

1. Introduction

The beamhouse processing of leather production involves soaking, unhairing, liming, reliming, deliming, bating, pickling with much water solution unit processes [1-5]. Many biochemical and chemical reagents are used in beamhouse with the objective to remove dust, hair, epidermislayer, non-collagenous proteins (proteoglycan) and fat from rawhide as well as to open up collagen fiber bundles, ready for the subsequent tanning process. During this process, the conventional unhairing process uses calcium hydroxide and sodium sulfide. The low solubility of calcium hydroxide leads to the formation of lime sludge and the liberation of toxic hydrogen sulfide through the use of sodium sulfide [6]. What's more, the mechanism of unhairing using calcium hydroxide and sodium sulfide is to destroy hair, resulting in suspended solids, and carbon and nitrogen pollution are caused. To address these problem, various approaches have been tried to reduce or avoid calcium hydroxide and sodium sulfide in leather making [4].

In unhairing, enzyme is used to hydrolyze the protein in the hair-hide junction in the hide and to destroy the bond between the hair and the hide *via* catalytic action on the enzyme, with hair not destroyed, by which the environmental pollution may be reduced and unhairing is faster and cleaner [7]. However, protease is usually used in enzymatic unhairing. The protease is high molecular weight protein, which is hard to be dissolved or dispersed in aqueous solution. So it is difficult to for the active center of protease to contact the hairy proteoglycan to take the catalytic action. Besides, the collagen of hides soaked in protease solution for a long-time may be partly hydrolyzed, especially in the two sides of the hides, resulting in a damaged papillary layer and grain.

Proper inorganic salts may be used to improve the solubility and dispersibility of protease in aqueous solution. By inorganic salt, the osmotic pressure of the solution is improved to accelerate the penetration of solution in hides.

Unhairing with KCl/neutral protease system was used in the present paper. Two such comparison groups as only neutral protease solution and calcium hydroxide/sodium sulfide solution systems were used. Hair removal rate, neutral protease activity, turbidity and transmittance of the solution, the content of protein, carbohydrate and COD of the solution wastewater were compared.

2.Materials and methods

2.1 Materials

Salted cowhides were kindly provided from Xinxiang Huixian Leather CO. LTD, Henan, China. Neutral protease (BR, 50u/mg), sodium sulfide nonahydrate (ACS), calcium hydroxide(ACS, ≥95.0%) and silver nitrate (AR, 99.8%) were purchased from Aladdin reagent co. LTD. Sulfuric acid (AR, 98%) was from Luoyang Haohua Chemical Reagent Co., Ltd. Anthrone (AR) was provided by Tianjin Komiou Chemical Reagent Co., Ltd. Potassium chloride (KCl, AR, 99.5%) was provided Tianjin Sailboat Chemical Reagent Technology Co., Ltd. Distilled water. The enhanced BCA protein assay reagent kit was purchased from Beyotime Institute of Biotechnology, China.

2.2 The treatment of cowhides

Dried salted cowhides with uniform thickness from the same part was immersed in quintuple distilled water in volume, and then transited and rolled in the rollers of leather tanning machine (DJD⌀ 350, Xishan, Beitang Mine Leather Machinery Factory, Jiangsu, China). The soaking liquor was substituted every hour until no precipitation was found when dropping silver nitrate solution. The cowhides were washed by distilled water.Next, the bovine hides were cut into square pieces weighed 2g and stored at 4 ℃.

Table 1 Unhairing Process.

Process	Materials	Percentages (%)			Temperature (℃)	Time (h)	Remarks
		C	1#	2#			
Unhairing	Cowhides [a]	100	100	100	30	13	Stirring at about 200r/min
	Distilled water [b]	1000	1000	1000			
	Neutral protease	-	8	8			
	Potassium chloride	-	-	8			
	Sodium sulfide nonahydrate	8	-	-			
	Calcium hydroxide	50	-	-		19	

[a] At the weight of 2g.

[b] The units of distilled water is mL.

Unhairing of cowhides using KCl assisted neutral protease for leather making was denoted as C, 1#, and 2#. C was the conventional unhairing and fiber-opening method. 1# was the unhairing using the solution of neutral protease, and 2# was carried out using the solution of KCl/neutral protease. As a detailed description of the unhairing process was provided in **Table 1**.The percentages reported in the table are based on cowhides weight.

2.3Neutral protease activity

For the measurement of the activity of the neutral protease, the universal protease activity assay with casein as the substrate and tyrosine was used as the standard. 0.8g of neutral protease was dissolved in 100 mL of phosphate buffer solution (pH 7.2). 1 mL enzyme solution was picked up and 10 times diluted. Next, 1mL of the diluted solution was measured and added with 1 mL of casein solution (0.02g/mL), and the mixture was kept 40 ℃ for 10 min.After the activity had been inhibited using trichloroacetic acid, the solution was filtered and used for colorimetric analysis. The optical density was measured at 680 nm after the addition of sodium carbonate and Folin's phenol reagent. Detailed experimental steps were referred to the national standard of China SB/T10317-1999.

In addition, the neutral protease activity was analyzed in the presence of the KCl at different concentrations and temperature using the central composite design (CCD) of response surface methodology (RSM). The selection of CCD was made based on preliminary experiments in order to identify the minimum number of experimental runs and fitting surface model based on the second order polynomial equation [8, 9]. At last, the regularization of neutral protease activity at different KCl content and temperature was achieved. The independent variables were the contents of KCl (x_1) and temperature (x_2), which varied

at the real levels and coded levels as shown in **Table 2**. The activity of neutral protease (y) was selected as dependent variables.The data was analyzed withstatistical and graphical analysis software [10] (Design Expert software 8.0.6). Design Expert software was used for regression analysis of the data obtained and to estimate regression equation coefficient. 13 runs of experiments were conducted concluding the analysis of variance (ANOVA) applied to analyze the results and the following second order polynomial model was used to fit the observations：

$$y = \alpha_0 + \sum_{i=1}^{2} \alpha_i x_i + \sum_{i=1}^{2} \alpha_{ii} x_i^2 + \sum_{i=0}^{1} \sum_{j=i+1}^{2} \alpha_{ij} x_i x_j \qquad (1)$$

where y is the predicted response i.e. the activity of the neutral protease, α_0 is the constant coefficient, α_i is the ith linear coefficient of the input factor x_i, α_{ii} is the ith quadratic coefficient of the input factor of x_{ii}, and α_{ij} is the different interaction coefficient between the input factors x_i and x_j.

The interactions between the process variables and response were obtained from ANOVA. The correlation coefficient (R^2) demonstrated the goodness-of-fit of the second order polynomial model and an F-test was performed to determine the statistical significance of the model.The ANOVA of the model was analyzed using the 95% confidence level ($P < 0.05$).

Table 2 Real and coded levels of variables(α=1.5).

Variable	Symbol	Coded levels				
		-α	-1	0	+1	+α
KCl content (%)	x_1	0	0.2	0.6	1	1.2
Temperature (℃)	x_2	20	26	38	50	56

2.4 Turbidity and transmittance of neutral protease solution

The turbidity and transmittance of neutral protease solution were determined using turbidity meter and ultraviolet spectrophotometer (UVS), respectively. 0.8% (w/v) neutral protease and 0.0% (w/v) potassium chloride solution 20mL, 0.8% (w/v) neutral protease and 0.2% (w/v) potassium chloride solution 20mL, 0.8% (w/v) neutral protease and 0.6% (w/v) potassium chloride solution 20mL, 0.8% (w/v) neutral protease and 0.8% (w/v) potassium chloride solution 20mL, and 0.8%(w/v) neutral protease and 1.0%(w/v) potassium chloride solution 20mL were prepared respectively and used to research the turbidity of neutral protease solution. Besides, 0.8% (w/v) neutral protease and 0.0% (w/v) potassium chloride solution 20mL, 0.8% (w/v) neutral protease and 0.2% (w/v) potassium chloride solution 20mL, 0.8% (w/v) neutral protease and 0.6% (w/v) potassium chloride solution 20mL, 0.8% (w/v) neutral protease and 0.8% (w/v) potassium chloride solution 20mL, and 0.8% (w/v) neutral protease and 1.0%(w/v) potassium chloride solution 20mL were prepared respectively, in order to investigate the transmittance of neutral protease solution.

2.5Protein and carbohydrate analysis

To know the protein content of the solution after unhairing and fiber-opening, the method of bicinchoninic acid (BCA) was used at 562 nm. The concentration of carbohydrate was measured using the anthrone colorimetry with glucose as the standard. 2 mL of solution after unhairing and fiber-opening was measure and added with 4mL of anthrone solution (2 g/L, concentrated sulfuric acid as solvent). After being boiled for 10 minutes, the mixture was cooled down to room temperature, and then measured at 652 nm.

2.6 Wastewater analysis

Concentration of COD was measured using multi-parameter water quality analyzer (5B-3B (V8), Beijing Lianhua Yongxing Technology Development Co., Ltd.). A wide range and 30 mm glass cuvette colorimetry was used.

3. Results and discussion

3.1 KCl Assisted Neutral Protease for unhairing process

The conventional calcium hydroxide sulfide method was employed for unhairing as sown in **Figure 1** C. Many hairs were found left on the hide surface after 19 h, and osmotic swelling occurred in the conventional process. Neutral protease method was used in unhairing as shown in **Figure 2** 1#, and it was found although some hairs were removed from the hide surface after 13h, there did exist many hairs. There were some short hairs on the hide surface had after 9h. The hairs were completely removed after 13h. After unhairing, no swelling was observed, and the hide was lighter in color, compared to the control. The results shown the hair removal rate was better using KCl assisted neutral protease solution (**Figure 1** 2#).

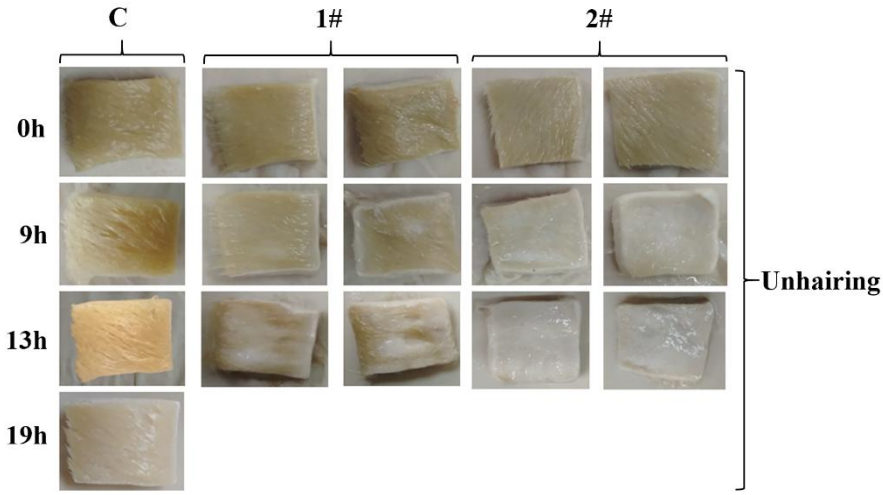

Figure 1. The digital images of samples of cowhides during unhairing process.

3.2. Optimization of operational parameters by the central composite design

Proper KCl added can speed up the unhairing rate. Therefore, the effect of KCl and temperature on neutral protease activity was studied using CCD. The results of the CCD experiments about the two independent variables together with the predicted and actual responses are shown in **Table 3**. In this study, the experimental data fits well with the empirical second order polynomial models. Final equation in terms of actual factors:

$$y = -17.72701 - 25.61260x_1 + 2.16475x_2 + 0.14709x_1x_2 + 16.13318x_1^2 + 2.32390\text{E} - 003x_2^2 \quad (2)$$

Analysis of variance (ANOVA) was conducted to test the significance of fit of the second order polynomial equation for the experimental data as shown in **Table 4**. ANOVA for neutral protease activity indicated that the F-value was 371.06, implying that the model was significant. The model terms with the values of 'Prob>F' less than 0.05 are considered to be significant [11], while the values higher than 0.1 are not significant [12]. Therefore, the variables of x_2 and x_1^2 are significant in neutral protease activity, but x_1, x_1x_2, $x_1x_2$and x_2^2 are not significant.

Furthermore, the correlation coefficient R^2 (**Table 5**) of 0.9962 indicated that only 0.38% of the total variation could not be explained by the empirical model. The value of Adeq. Precision higher than 4 was desirable [13]. Adeq. precision measures the signal to noise ratio, which in this case the value of 64.980 was obtained, indicating an adequate ratio. Besides, low coefficient of variation (C.V. % is 3.12 less than 10%) and the standard deviation (Std. Dev. is 1.98) values proved that this model is efficient for navigating the design space [14], implying a good model.

Table 3 Experimental results of CCD and predicted responses.

Run	Variable				Actual value(U/mg)	Predicted value(U/mg)
	x_1	*Coded*	x_2	*Coded*		
1	0.60	0	56.00	1.5	103.88	102.24
2	1.20	1.5	38.00	0	66.66	65.31
3	1.00	1	26.00	-1	32.89	34.47

4	0.20	-1	26.00	-1	33.93	40.65
5	0.20	-1	50.00	1	94.52	90.86
6	0.60	0	38.00	0	61.7	61.68
7	0.60	0	38.00	0	61.7	64.14
8	1.00	1	50.00	1	96.3	91.74
9	0.60	0	38.00	0	61.7	59.26
10	0.60	0	20.00	-1.5	21.33	21.13
11	0.60	0	38.00	0	61.7	61.68
12	0.60	0	38.00	0	61.7	61.68
13	0.00	-1.5	38.00	0	68.66	64.53

Table 4 ANOVA results for response surface quadratic model for neutral protease activities.

Source	Sum of Squares	df	Mean Square	F Value	p-value Prob > F	Status
Model	7283.27	5	1456.65	371.06	< 0.0001	significant
x_1	0.60	1	0.60	0.15	0.7078	Not significant
x_2	7225.32	1	7225.32	1840.54	< 0.0001	significant
x_1x_2	1.99	1	1.99	0.51	0.4991	Not significant
x_1^2	55.20	1	55.20	14.06	0.0072	significant
x_2^2	0.93	1	0.93	0.24	0.6417	Not significant
Residual	27.48	7	3.93			
Lack of Fit	27.48	3	9.16			
Pure Error	0.000	4	0.000			
Cor Total	7310.75	12				

Table 5 Statistical parameters of ANOVA of the neutral protease activities predicted model

Statistics	Value	Statistics	Value
Std. Dev.	1.98	R-Squared	0.9962
Mean	63.59	Adj R-Squared	0.9936
C.V. %	3.12	Pred R-Squared	0.9729
PRESS	197.91	Adeq Precision	64.980

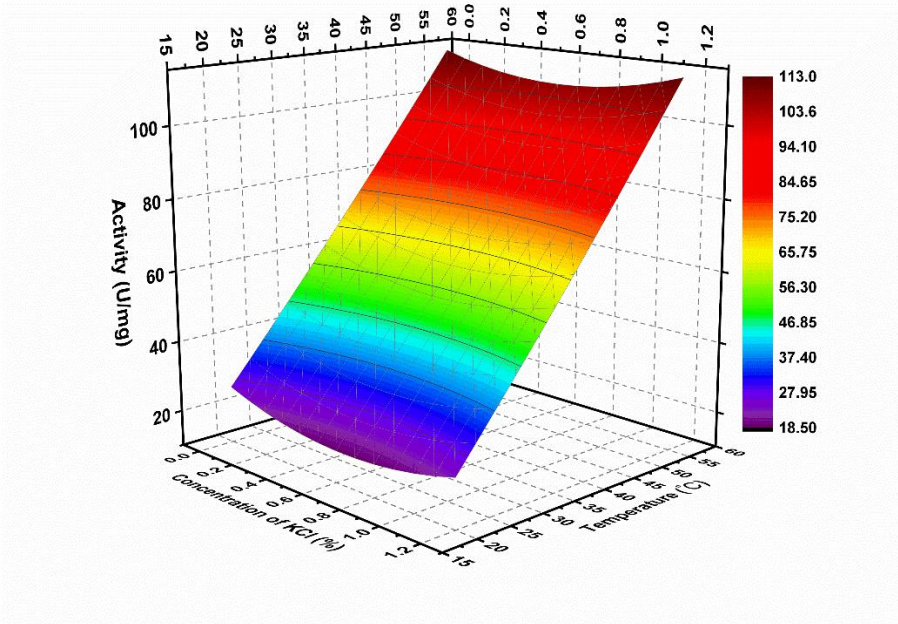

Figure 2.Three-dimensional response plots of neutral protease activities at different KCl concentrations and temperature.

Figure 2 shown the relationship among KCl content (insignificant, independent variables), temperature (significant, independent variables) and the activity of neutral protease (dependent variable). The activity of neutral protease showed a slightly concave trend with the increase of KCl content from 0% to 1.2%. The content of KCl was not significant on the activity of neutral protease, which has been demonstrated in 3.2. At a proper temperature, it does not affect the depilatory activity of the neutral protease. In contrast, the variable of temperature is very significant to affect the neutral protease activity. As the **Figure 2** shows, the activity of neutral protease increases with increasing the temperature in the range of 20-56℃, and there is a linear relationship between the activity of neutral protease and temperature in same content of KCl.

3.3 Turbidity and transmittance of neutral protease solution

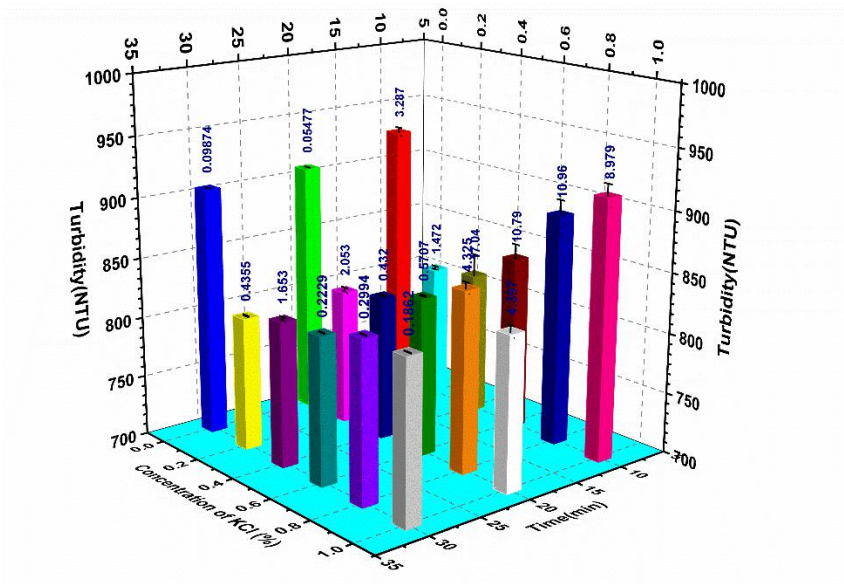

Figure 3. Effect of KCl content on turbidity of neutral protease solution.

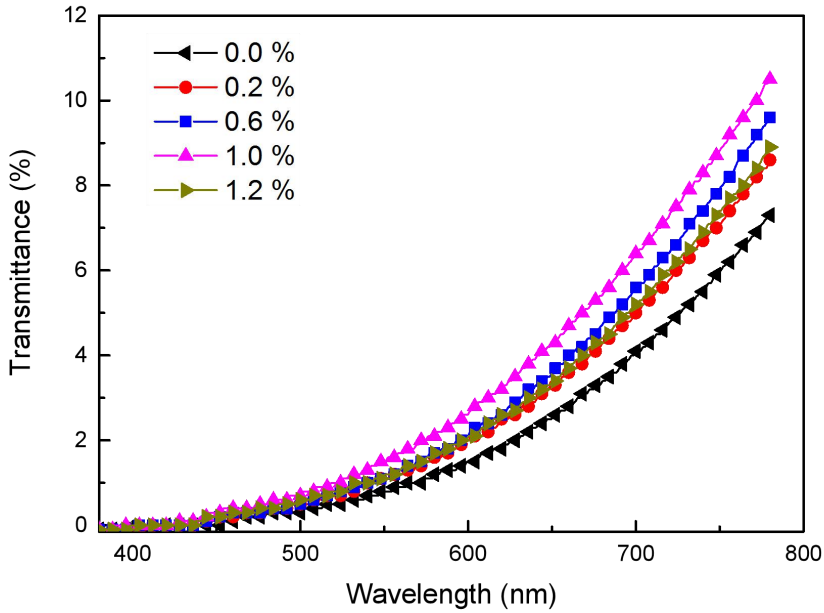

Figure 4. Effect of KCl content on transmittance of neutral protease solution.

The turbidity of neutral protease was lowered when proper amount of KCl was added, which can be seen in **Figure 3**. At the beginning, the turbidity is increased with the increase of KCl content (0-1%), which is lower compared to the one without KCl in the neutral protease solution. The turbidity is decreased after 20 min, much lower than the solution of neutral protease without KCl. The turbidity is tended to be stable and identical when different amount of KCl was added to the neutral protease solution for 30 min. However, the turbidity is still high, just like that at the beginning. Therefore, proper amount of KCl may help to improve the solubility and dispersibility of neutral protease.

The transmittance of neutral protease solution with different amounts of KCl was studied using ultraviolet spectrograph (UVS). The transmittance of neutral protease solution increases firstly and the decreases with increasing the KCl amount, with the highest at the KCl amount of 1%, as shown in **Figure 4**. So proper amount of KCl is good to improve the solubility of protease.

3.4 Protein and carbohydrate analysis

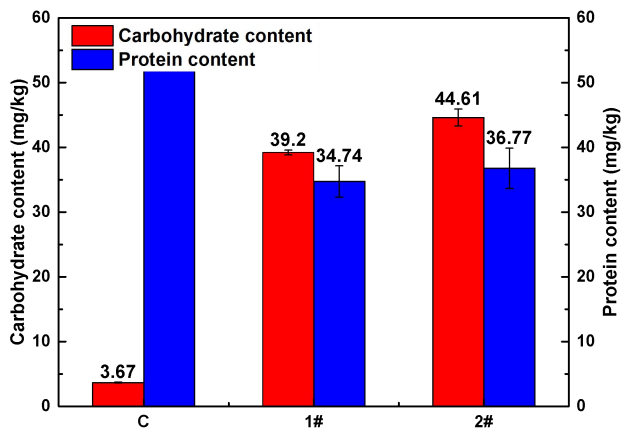

Figure 5. Comparison of protein and polysaccharide content in wastewater of method C, method 1# and method 2#.

The unhairing mechanism of neutral protease is to hydrolyze the protein of the hair-hide junction in the hide to destroy the bond between the hair and the hide *via* catalytic action on the enzyme. The protein of hair-hide junction is mostly composed of proteoglycan and glycoprotein. Proteoglycans is mostly proteins and glycoproteins are mostly polysaccharides, which are all combinations of carbohydrates. The carbohydrate content is higher with the addition of KCl, compared with that of neutral protease, as **Figure 5** (1# and 2#) shown. For both methods of 1# and 2#, the carbohydrate contents are much higher than conventional method (**Figure 5** C). Therefore, the addition of proper amount of KCl in neutral protease solution is conducive to the dissolution of carbohydrates. The solubility of neutral protease and osmotic pressure of the solution were improved by the addition of KCl, which accelerates the penetration of the enzyme into the interior of the epidermis and inside the pores. So, the contact time between the enzyme and the hairy proteoglycan is shorten and more chance for enzyme to reach the proteoglycan and the contact area is provided. The proteoglycan in hides may be hydrolyzed quickly to facility the unhairing process. The conventional unhairing is to destroy the hair using $Na_2S/Ca(OH)_2$ system. The carbohydrate dissolution process is complicated, and it only small molecule of polysaccharide may be dissolved under the action of osmotic pressure. So, the carbohydrate content in the wastewater of conventional method is the least, Figure 5 C.

Free amino acids and peptides were produced by the neutral protease hydrolysis of proteoglycan and glycoprotein. At the same time, a small amount of collagen and elastin are also hydrolyzed by neutral proteases into free amino acids and peptides. Therefore, higher protein contents in the wastewater of method 1# and 2# and almost the same (**Figure 5** 1#, 2#). The protein of solution of conventional method is the highest (**Figure 5** C), which is mainly because the destroy effect of hair. Sodium sulfide may destroy the keratin constituting hair and cuticle and hydrolyze them into amino acid and polypeptide. Some collagen is also hydrolyed into small-molecule amino acid and polypeptide in the sodium sulfide solution too.

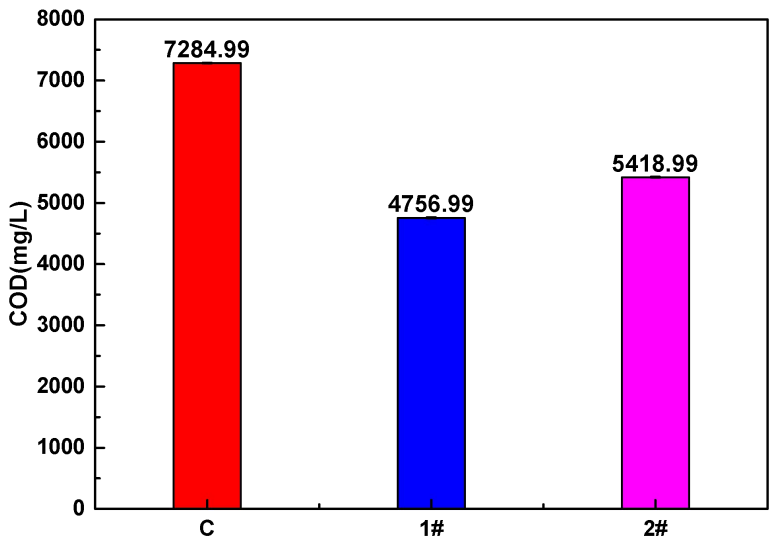

Figure 6.COD content in wastewater of method C, method 1# and method 2#.

Tannery wastewater has the characteristics of large water volume, complicated composition and high pollutant concentration. It is also a major problem faced the development of the tanning industry. COD is very important targeted on study the organic pollution parameter of tannery wastewater. The larger the value of COD, the more serious the contamination of the water. COD of method 1# is smaller, method 2# is higher and method C is the highest, Figure 6. Method C is to destroy hairs in unhairing and produce a large amount of organic pollutants. Both methods of 1# and 2# use the way of save hairs in unhairing and produced lower organic pollutants. Method 2# assisted by KCl may accelerate the dissolution of the

polysaccharide, so the COD is higher than method 1#. Therefore, the way to destroy hairs in unhairing by method C produced higher pollution.

4. Conclusions

Proper amount of KCl in neutral protease solution can speed up the rate of hair removal by improve the solubility and dispersibility, not increase the activity of neutral protease.The way of destroy hairs to unhairing produced pollution is higher.

Acknowledgement

The financial supports from the National Key R & D Program of China（No.2017YFB0308500）and National Natural Science Foundation Commission of China (No. 51673177) are greatly appreciated.

References

[1] Kanth S V, Venba R, Madhan B, et al. Cleaner tanning practices for tannery pollution abatement: role of enzymes in eco-friendly vegetable tanning [J]. Journal of Cleaner Production, 2009, 17(5): 507-515.

[2] Sannino D, Vaiano V, Ciambell P. Mathematical modelling of a vegetable tanning process [J]. Journal- Society of Leather Technologists and Chemists, 2013, 97 (4):139-144.

[3] Saravanabhavan S, Thanikaivelan P, Rao J R, et al. Reversing the conventional leather processing sequence for cleaner leather production [J]. Environmental Science & Technology, 2006, 40 (3): 1069-1075.

[4] Durga J, Ranjithkumar A, Ramesh R, et al. Replacement of lime with carbohydrases-a successful cleaner process for leather making [J]. Journal of Cleaner Production, 2016, 112: 1122-1127.

[5] Wang Y, Zeng Y, Zhou J, et al. An integrated cleaner beamhouse process for minimization of nitrogen pollution in leather manufacture[J]. Journal of Cleaner Production, 2016, 112: 2-8.

[6] Alla J P, Rao J R, Fathima N N. Integrated depilation and fiber opening using aqueous solution of ionic liquid for leather processing[J]. ACS Sustainable Chemistry & Engineering, 2017, 5(10): 8610-8618.

[7] Ma J, Hou X, Gao D, et al. Greener approach to efficient leather soaking process: role of enzymes and their synergistic effect[J]. Journal of cleaner production, 2014, 78: 226-232.

[8]Deshmukh R K, Naik J B. Aceclofenac microspheres: Quality by design approach[J]. Materials Science and Engineering: C, 2014, 36: 320-328.

[9]Cheng S W, Wu C F J. Factor screening and response surface exploration[J]. Statistica Sinica, 2001: 553-580.

[10]Othman A M, Elsayed M A, Elshafei A M, et al. Application of response surface methodology to optimize the extracellular fungal mediated nanosilver green synthesis[J]. Journal of Genetic Engineering and Biotechnology, 2017, 15(2): 497-504.

[11]Pinho C, Melo A, Mansilha C, et al. Optimization of conditions for anthocyanin hydrolysis from red wine using response surface methodology(RSM)[J]. Journal of agricultural and food chemistry, 2010, 59(1): 50-55.

[12]Ali A A, Eltabey M M, Farouk W M, et al. Electrospun precursor carbon nanofibers optimization by using response surface methodology[J]. Journal of Electrostatics, 2014, 72(6): 462-469.

[13]Talib N A A, Salam F, Yusof N A, et al. Optimization of peak current of poly (3, 4-ethylenedioxythiophene)/multi-walled carbon nanotube using response surface methodology/central composite design [J]. RSC Advances, 2017, 7(18): 11101-11110.

[14]García-Gómez C, Drogui P, Zaviska F, et al. Experimental design methodology applied to electrochemical oxidation of carbamazepine using Ti/PbO2 and Ti/BDD electrodes[J]. Journal of Electroanalytical Chemistry, 2014, 732: 1-10.

P119

Exploring Ionic liquids for Collagen Stabilization: A New Paradigm

Aafiya Tarannum, J Raghava Rao, N Nishad Fathima*

Inorganic and Physical Chemistry Laboratory, Central Leather Research Institute, Council of Scientific and Industrial Research, Adyar, Chennai 600020, India

** Email: nishad.naveed@gmail.com; nishad@clri.res.in*

Abstract

Ionic liquids (ILs), have been in spotlight as "task specific" and "designer solvents", as they can be tuned depending on the nature of cation and anion for the desired interest. Herein, we report the investigations carried out on collagen at different hierarchical orderings using various ILs. The conformational stability of collagen at the molecular level, thermal and dimensional stability at the inter-fibrillar level and fibre structure at skin matrix level using different types of ILs viz., imidazolium and choline as cations with different anions have been explored. Imidazolium based ILs have altered the secondary structure of collagen at molecular level with huge distortions in rat tail tendon collagen fibres at fibrillar level as well. Choline based ILs stabilized collagen at both molecular and fibrillar level by exerting an electrostatic force between cations and anions of IL and functional groups of collagen for tissue engineering applications. They have been explored as unhairing cum fibre opening agent by eliminating the use of lime and sodium sulphide during leather making. Thus, the interaction of collagen with ionic liquids unfolds the propensity of ILs to stabilize or destabilize collagen and their properties can be customized and fine-tuned for applications ranging from biomedical to tanning.

Keywords: Collagen; Ionic liquids; Conformational stability; Unhairing; Fiber opening

P120
Application and Development of Interactive Design concept in Women's shoes

YAO yun-he[123] DING wan-jing[3] LI xin-juan[3]

(Key Laboratory of Leather Chemistry and Engineering of Ministry of Education, Sichuan University ,National Engineering Laboratory for Clean Technology of Leather Manufacture, Sichuan University , Biomass and Leather Engineering Department, Sichuan University , Chengdu,610065,China)

Abstract: Interaction design is vital concept in the field of design, which emphasizes the interaction between products and users. With the development of the internet and new technologies, various interactive ways and interactive experience are getting rich. The concept of interaction design also applies to traditional shoe design. The passage analyzes the factors of children's psychological needs, aesthetic tendency and behavior characteristics, then points out the feasibility and advantages of interaction design in women's shoes by taking the design of women's shoes as a starting point. Meanwhile, from the appearance design of shoes, it puts forward three points about the interactive design of women's shoes: function, interest and innovation, then make a detailed analysis. At last, move a further step to forecast the development and trend of Interaction design.

Keywords: Women's shoes, Interaction design, Appearance design, Construction design

1 Introduction

Interactive design refers to the interaction between the product and the user, which is intended to enhance consumer autonomy and Selection space of product appearance in the process of product use, thus forming a better user experience. Nowadays, people's standard of living is improving, and the choice of products is becoming wider and wider. Users pay more attention to the use experience outside of paying attention to the products. In foreign countries, interactive design has formed a subject field closely related to visual design, product design, environmental design and so on. [1] Therefore, we should focus on the design of interactive products. Not only requiring the appearance of products in the form of beauty, at the same time, we should pour attention into the diversification of functions. The communication and interaction between products and users is realized, which brings more rich experience.

As a basic daily wearing product, shoes are closely related to people's life. Therefore, the user's needs and experience are extremely essential. From this point of view, the concept of interactive design and footwear design have a perfect fit. By analyzing the application of interactive design in the field of footwear, this paper discusses the feasibility and application method of interactive design of women's shoes, and then looks forward to the development in interactive design in the footwear industry application.

2 The requirement and feasibility analysis of interactive design in the field of women's shoes

In the Internet era, customer needs and feedback can be more effectively received and processed. The interactive design based on customer feedback can better meet the needs of the market, but in the women's shoes industry, especially in the Chinese market, the research on consumers' psychological needs, aesthetic needs and consumption habits needs to be further improved. And there are relatively few examples that can mature and apply the idea of interactive design. It is necessary to conduct relevant analysis and research for the reason that the most direct factor influencing the development of the market is Consumer demand.

2.1.1 Psychological needs

Female psychological need is a special psychological satisfaction emotion based on female physiological and psychological characteristics. The psychological needs of women are more obvious for the reason that women's psychological activities are more emotional than men's.

With the development of the times, women's self-consciousness is becoming more and more intense, and the definition of themselves is becoming more and more diverse. First of all, interactive products can meet Women's various psychological

needs. And all kinds of chic, exquisite shoes can reflect the appearance of different women. For example, Burberry's side-strap Martin boots (fig. 1), with the outer side laces as its design focus, form a maverick and stylish look that attract women with unique insights and meet the psychological needs of showing their personal style.

Figure 1 Burberry side strap Martin boots

2.1.2 Aesthetic needs

The aesthetic demand of women is formed with the development of human culture. It is not only a social historical process, but also an individual emotional process, from instinctive desire to aesthetic demand.

Beauty is the nature of women, so the interactive products and women's aesthetic needs are inseparable. Modern women have changed from aesthetic objects to aesthetic subjects. Instead of focusing on "what kind of women conform to the aesthetic standards of the times", they put up their own flags calmly and their own individual clothing styles confidently. Objectively speaking, shoes account for a small proportion of a person's overall dress, but indispensable. Fashion has been changing, different styles of clothing need to match the right shoes. A pair of well-matched shoes is the finishing touch of clothing. Therefore, only variety, rich characteristics and strong collocation women's shoes products can meet the changing aesthetic needs of contemporary women.

2.1.3 Consumption demand

Since the reform and opening up, China's shoe industry has accelerated the pace of development. people's awareness of the consumption of shoes is getting stronger, especially female consumers. The interaction between women's shoes and Characteristics of consumer behavior mainly manifest two aspects. First is the fashion of women's consumption. Women like novel and unique items, pay attention to the "newness" and "uniqueness" of clothing, and keep up with the "trends". Second is the flaunting characteristics of female consumption. Shoes have been a symbol of identity since ancient times, and a pair of shoes that are different and can attract the attention of others can reflect the identity and status of the wearer. Women's shoes for women's psychological, physical and consumer needs can better meet the needs of women's individuation, fashion and novelty. It can satisfy women's pursuit of consumer goods beyond their practicality and use value.

2.2 Analysis of the Feasibility of using Interactive Design in Women's shoes

The focus of interaction design is the two-way interaction between users and products. From the analysis of women's psychological needs, aesthetic needs and consumer demand, with the diversification of modern women's lifestyles, female consumers pay more attention to whether the style of products fits, whether the form is novel, and whether the functions are perfect. Their demands for the collocation, innovation and functionality of women's shoes is increasing.

Users have a demand for products, and products can achieve a certain performance in the structure and appearance. This interactive design product with fashion appearance and can meet the diverse needs is the vane of women's shoes industry in the future.

3 Analysis of the application of interactive design in women's shoes

3.1 Improving the collocation of women's shoes

The women's shoes on the market are basically batch-produced products, and there are many styles, but they are all very similar. Therefore, the space for consumers to choose products is not really large. Based on the needs of female consumers, through a variety of interactive forms such as online and offline customization of consumers, late DIY products can improve the diversification and collocation of products, and provide consumers with a richer emotional experience.

Personalized products are products that customers really want from the fundamental needs of users. In the personalization of women's shoes, you can choose from the shape of the skull to the shoe parts, accessories design, etc., so that users can customize one or more links from the online and offline according to their own situation. NIKEiD is an online and offline customization service launched by NIKE. Users can select the color and materials of each part of the shoes after selecting the shoes on the official website. In addition, Nike also provides comfortable customized shoes that can change the width of the shoe cavity. It is worth mentioning that as a personalized customization service, NIKEiD provides users with a very rich range of shoes, and the price is relatively close to the people.

In addition, products that can achieve DIY during wear can also enhance the fun and collocation of the product. In the past two years, Nike has launched a series of interchangeable Swoosh (meaning "a bang", which is Nike's most famous mark) sneakers based on the Air Force 1 basic model (Fig. 2). In addition to its own color matching Swoosh, each pair of shoes comes with five pairs of different colors of Swoosh Velcro, users can mix and match, and even stack multiple Swoosh at the same time, a variety of matching and design effects on a pair of shoes.

Figure 2 Nike Air Force 1[Swoosh Pack]

I Suddenly Sneezed is a footwear brand co-founded by illustrator Mo Houche and graphic designer Nemo Chan. The brand launched a series of loafer shoes with detachable pearl tassels in 2017 (Fig. 3). The tassel on the shoes can be changed color and material at will, or they can be disassembled directly. In this design, a variety of shoe ornaments can be used to bring users a variety of visual feelings, improve the overall matching of shoes, very interesting.

Figure 3 ISS Achilles loafer shoes with detachable pearl tassels

In the process of wearing women's shoes, interaction design can help the user to replace each part according to their own requirements, including accessories, side parts, sole and heels. This is very helpful to enhance the taste of the product and user experience. At the same time, it is also in line with the younger generation of users to follow the green, low-carbon

concept of life. KI Ecobe's environmentally friendly assembly shoes (Fig. 4) are designed to reduce waste of resources and environmental pollution caused by fast fashion. Unlike traditional shoes, KI ecobe is a non-adhesive construction where all parts can be replaced, reused or recycled, reducing manufacturing costs. After analyzing the ergonomic data, the designer designed three custom insoles of different heights in order to support the arch of the foot. They can be used as daily shoes or household shoes, better around the user's intended use to express personality.

Figure 4 Environmentally-friendly assembly shoes KI ecobe

3.2 Combining new materials with new technologies

In the mid-1950s, with the innovative use of steel materials by shoe manufacturers, stilettos with lightweight, long shape and high weight were born. They were recognized by women because they could highlight the graceful body. The heavy chunky heel shoes gradually withdrew from the market. It can be seen that the innovation of the shape, structure and materials of the shoes (including the upper surface, the sole, the decorative materials, etc.) gives the product a new development direction, which can effectively improve the design space of the women's shoes.

Adidas Futurecraft 4D (Fig. 5) is the world's first high-performance running shoe developed by Adidas using digital light synthesis. The manufacturing of the insole is different from the 3D printing technology in the general sense (The way in which resin is extruded by a material nozzle and then stacked layer by layer). It is to slowly stretch the photosensitive resin material from a special container. The ultraviolet light projection at the bottom of the container allows the photosensitive resin to cure, while the oxygen inhibits solidification, and the liquid resin at the bottom of the sink maintains a stable liquid region due to contact with oxygen, thereby ensuring the continuity of curing. The midsole of running shoes is printed by nearly 20,000 small brackets of different sizes. It is designed for the different forces on the soles of the feet during exercise, so the feel of each area is different. The application completes an innovative interaction design by changing the material of the midsole and the structure of each part.

In the interaction design of women's shoes products, the softness and resilience of the midsole of women's shoes can also be improved by similar techniques.For example, the material and structure of the midsole of the shoes can be improved according to Pressure distribution of various parts of the sole during continuous wearing of high heels (the toe area > the heel part > the toe part > the lumbar part)[2] to improve the comfort of the women's shoes.

Figure 5 Adidas Futurecraft 4D running shoes

3.3 Integrating smart wearable technology

A wearable device is a portable device that is worn directly on the human body or integrated into the user's clothing. It implements powerful interactive functions through software support, data interaction, and cloud interaction. At present, wearable device applications are mostly used in sports shoes and casual shoes. If it can be introduced into the women's shoes market, it will bring about tremendous changes in the fashion of women's clothing.

Figure 6 Li Ning 2018 Women's Smart Wearable Lightweight Running Shoes

Li Ning smart running shoes (fig. 6) can monitor the data by placing intelligent chips in the middle, and send data to the mobile phone using Bluetooth technology, so that the wearer can understand their own motion data and improve their performance.

Similarly, similar techniques can be applied to women's shoes, especially high heels. Studies have shown that wearing high heels can cause damage to bones, muscles, ligaments and soft tissues of the lower extremities [3]. Through the real-time monitoring of the smart chip, the user can always understand the health of the foot, scientifically monitor and protect the foot, and reduce the foot injury caused by the high heel.

Apparel products are direct interpreters of interaction design. If the wearable device, footwear and new manufacturing technology are deeply integrated, the deep interaction between the user and the product can be realized, and the external form of the female shoe product, especially the intrinsic function and the user experience, can be revolutionized.

4 The development trend of the interactive products of women's shoes in the future

In the future, the application of interactive design in women's shoes products will extend to a wider range of areas, such as smart materials, health care and so on.

4.1 Smart material

Nowadays, smart materials have been paid more and more attention to by researchers all over the world because of their unique applications. For example, intelligent fiber clothing made of smart materials can sense and respond to environmental stimuli, such as light, heat, electricity, humidity, machinery and chemicals, it can respond to external stimuli through changes in color, vibration, electrical properties, energy storage, etc. Boulder and Co lorado-based microencapsulated the phase change materials into fibers and woven them into fabrics to make garments. In the same way, when the smart material is used in the design of women's shoes, its products can automatically adjust and feedback when stimulated by environmental factors, so as to regulate the health of the feet and increase the wearing experience.

4.2 Health care

It is not difficult to find from the previous examples that the interaction between sports shoes and medical technology has gradually matured, but there are few interactive products related to disease and disease prevention in the area of women’s shoes. If women's shoes products can be designed for different diseases or groups of women, or apply smart detection equipment in sneakers to women's shoes, it will be possible to measure the health of the feet to improve or prevent

foot disease.

4.3 Cutting edge science and technology

With the rapid development of science and technology, many advanced technologies have been gradually integrated into our life, the combination of high-tech and women's shoes products are also a hot spot in the future interactive design of women's shoes products. The following figure is the conceptual design of fashionable women's shoes (fig. 7) by the author, the sole of which is completed by 3D printing technology. Pressure sensors were designed in the soles, the pressure sensor device can not only feedback the pressure of the foot, but also feed back the pressure data to the processor. The shoes control the brightness of the sole photosensitive material through pressure change, and the visual effect of the photosensitive material simulates the flash of fireflies. Moreover, the appearance of the product has a strong sense of technology. Such a design can not only protect the health of the feet, but also meet the needs of users for fashion.

Fig 7 Shoes based on interaction design concept

5 Conclusion

Since ancient times, shoes are the symbol of noble status, a pair of fancy, beautiful shoes can enhance the overall grade, showing unique temperament. With the enhancement of self-consciousness and consumption consciousness of modern women, the importance of shoes has almost been raised to the same important position as clothing, and their psychological needs, aesthetic needs and consumer needs for footwear are becoming more and more diverse.

The concept of interactive design attach great importance to the two-way interaction between the user and the product, setting up a good connection between the product and the user, and the interactive design is applied in the field of women's shoes, which can provide more thinking and development direction for the designer. The design and innovation space of sublimated women's shoes can meet the diversified demand of modern female consumers for shoes to a greater extent.

References

[1]Tang Lei. Current situation and trend of Interactive Design [J]. Journal of Changchun Institute of Education, 2012, (4): 56-57

[2][3]Yang Luming. Effects of continuous wearing of high heels on plantar pressure in young women [J]. Leather Science and Engineering, 2015,25 (5): 57-60

[4]Chen Zhilin. Current situation of Intelligent Garment Development and Application [J]. Advances in Textile Science and Technology, 2010, (2): 88-90

P121

A cleaner chrome-free tanning process:tetrakis(hydroxymethyl)phosphonium sulfate and cage-likeocta(aminosilsesquioxane)

Dangge Gao[1,2], Pingping Wang[1,2], Jiabo Shi[1,2],Bin Lyu[1,2], Jianzhong Ma[1,2]

[1] *College of Bioresources Chemical and Materials Engineering, Shaanxi University of Science & Technology, Xi'an 710021, China;*

[2] *National Demonstration Center for Experimental Light Chemistry Engineering Education (Shaanxi University of Science & Technology), Xi'an 710021, Shaanxi, China;)*

Abstract

Tetrakis(hydroxymethyl)phosphonium sulfate （THPS） is a chrome-free tanning agent, which produces leathers with soft, white and T_s about 78.6℃ and it is also benefit to the following process like fatliquoring and dyeing. However, there will be free formaldehyde in the THPS tanned leather due to the preparation process of THPS and the tanning process. In the present study, a novel combination tanning system based on THPS with cage-like octa(aminosilsesquioxane) (POSS-NH_2) for leather production has been established. The tanning process is optimized as 6wt% POSS-NH_2 combination with 2.5% THPS, giving the leather with shrinkage temperature (T_s) above 83.0℃ and thickening 44.6% due to the presence of POSS-NH_2 enhancing crosslinking effect with collagen fiber. Scanning electron microscopy and energy dispersive X-ray (SEM-EDX) measurements indicate that POSS-NH_2 can be evenly and tightly bound within the leather matrix. The resultant leathers have reasonable good physical properties that can meet the standard requirements for furniture leather without containing hazardous Cr(VI). Also, the formaldehyde content in the tanning system notably decreased from 1.934ug/mL to 1.415ug/mL compared with THPS tanning, because POSS-NH_2 as a scavenger of free formaldehyde present in THPS tanned leather.

Keywords: THPS; POSS-NH_2; combination tanning; formaldehyde

Acknowledgement: The authors are grateful for the financial support of National Natural Science Foundation Project (No. 21878182) and Open Project Program of National Demonstration Center for Experimental Light Chemistry Engineering Education (2018QGSJ02-14).

P122

SYNTHESIS OF AN AMPHOTERIC POLYMER AUXILIARY AGENT AND ITS APPLICATION ON THE CHROME-FREE LEATHER

Luo Jianxun, Feng Yanjuan

Materials & Textile Engineering College, Jiaxing University, Jiaxing 314000,P.R.China

ABSTRACT

In order to reduce the disadvantages of the chrome tannage, the chrome-free tannage was developed by many technologists and tanneries. But because of the structures and charge of the tanning materials in the chrome-free tannge, the absorption rate of the chrome-free leather for anionic dyestuff, re-tanning agents and fat-liquors is lower than that of the chrome-tanned leather. Therefore in order to improve the absorptivity of the chrome-free leather for dyestuffs, re-tanning agents and fat-liquors, etc, an amphoteric polymer auxiliary agent was synthesized with methy-acrylic acid, sodium methylallyl sulfonate and dimethyl diallyl ammonium chloride (DMDAAC) by free radical copolymerization using ammonium persulfate at 80°C for 3 hours. The mol ratio of methy-acrylic acid, sodium methylallyl Sulfonate and dimethyl diallyl ammonium chloride was confirmed to be 1.0, 0.3, 1.0. The structure of the amphoteric polymer auxiliary agent was characterized by FTIR, ^{1}H-NMR, ^{13}C-NMR. The charge and properties of the solution of the amphoteric polymer auxiliary agent were charaterized. Applied results of the amphoteric polymer auxiliary on the absorption of chrome-free leather for dyestuff, and fat-liquor show that it has strong auxiliary absorptive capacity and the absorptive rate of dyestuff and fat-liquor is more than 96%.

Keywords: An amphoteric polymer auxiliary agent; pI； uptake; absorption rate; chrome-free tannage

INTRODUCTION

Chrome tanning has been used for more than 100 years. Now about 90% of all the tanneries in the world have adopted chrome tannage. Though chromium is considered as the best mineral tanning agent which leads to high hydrothermal stability, i.e. shrinkage temperature (Ts) over 100°C, it has its own negative image such as low absorptive rate of chromium, oxidation to Cr(VI) by light, heat, sweat, some chemical materials, etc, which is a proven carcinogen, etc[1-2]. So there is a requirement for eco-friendly tanning process. Chrome free tannage is one of eco-friendly tannages. Nowadays, the chrome-free leather is more and more favorable for the customers.

However, each of other tanning agents such as vegetable tannins, oxazolidine, aluminium, titanium, zirconium has their own disadvantages[3]. Combination tannages is thus considered to be a suitable alternative for chrome free tanning system. Amongst the innumerable combination tannages that are currently exploited, Combination tannages with vegetable tannins and oxazolidines,Combination tannages with vegetable tannins and aluminium tanning agent are the most promising process[4-5]. But during the process of the combination tannages, there are some problems such as the low shrinkage temperature, softness of the finished leather, the low absorption rate for dyestuff, re-tanning agents, fat-liquor, etc.

The present work focus on preparing an amphoteric polymer auxiliary agent by the copolymerization of methy-acrylic acid, sodium methylallyl sulfonate and dimethyl diallyl ammonium chloride (DMDAAC), which can effectively improve the absorptivity for dyestuff, re-tanning agents, fat-liquors, etc. The synthesis, co-monomer ratio, the molecular weight, structure and pI of the amphoteric polymer auxiliary agent have been studied and the application properties are discussed.

EXPERIMENTAL

Materials

Methy-acrylic acid (MAc), Sodium methylallyl sulfonate (SMAS), Dimethyl diallyl ammonium chloride (DEMAAc), ammonium persulfate (APS), sodium hydroxide were of chemical pure grade. SPR, CHROMOPOL UFB/W were purchased from Hongguang Chemicals s.p.a, Taiwan, TFL(China) Ltd,respectively.

The goatskin crust tanned by combination tannage with vegetable tannins and oxazolidine, Combination tannage with vegetable tannins and aluminium tanning agent were made by ourselves respectively.

Preparation of the amphoteric polymer auxiliary agents

The co-polymer was synthesized by free radical co-polymerization under the conditions listed in TABLE I and TABLE II[9-10]. Firstly, the relevant methy-acrylic acid, water and sodium methylallyl sulfonate were weighted and the mixture solution was neutralized with 30wt% sodium hydroxide solution, and then dimethyl diallyl ammonium chloride solution was added into the neutralized solution to form mixed monomers solution. Secondly, the relevant ammonium persulfate solution was prepared. Thirdly, the co-polymerization was performed in a stirred 500mL four mouth flask with two feed funnels and a thermometer. At the beginning, the relevant water was added into the flask and heated to 76°C, then part of ammonium persulfate solution and mixed monomers solution were added into the flask and stirred for 30min. The surplus ammonium persulfate solution and the monomer mixture were drip fed in. The rate of addition was controlled in order to be complete within 90min. Then the temperature was regulated to 80-82°C and was kept constant for 240min. At last the flask was cooled to 50°C and form the amphoteric polymer auxiliary agent. The scheme of the reaction is described in Fig.1.

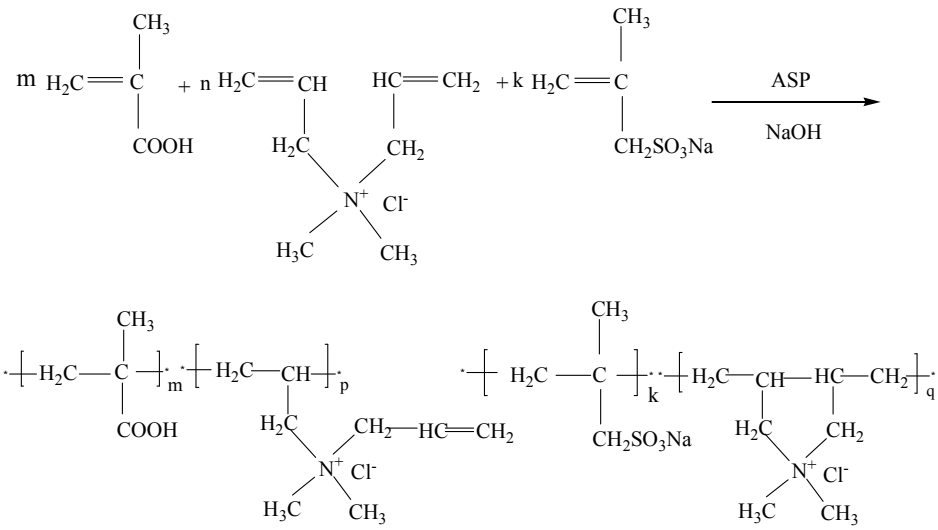

Fig.1 The synthesis of the amphoteric polymer auxiliary agent

TABLE I

Parameters of orthogonal experiment

Factor	Level 1	Level 2	Level 3
A/MAc/mol	0.5	1.0	1.5
B/DEMAAC/mol	0.5	1.0	1.5
C/ SMAS/mol	0.1	0.2	0.3
APS/wt%	1.0	1.5	2.0

TABLE II

Formulation of $L_9(3^4)$ copolymer reaction among methyacrylic acid, dimethyl diallyl ammonium chloride ,sodium methylallyl sulfonate

No	A/MAc/mol	B/DEMAAC/mol	C/SMAS/mol	D/APS/wt%
1	0.5	0.5	0.1	1.0
2	0.5	1.0	0.2	1.5
3	0.5	1.5	0.3	2.0
4	1.0	0.5	0.2	2.0

5	1.0	1.0	0.3	1.0
6	1.0	1.5	0.1	1.5
7	1.5	0.5	0.3	1.0
8	1.5	1.0	0.1	1.5
9	1.5	1.5	0.2	2.0

Application of series of the copolymers and the selection of the synthetic recipe

Series of these co-polymers were applied respectively in the dyeing and fat-liquoring process of the goatskin crust tanned by Combination tannages with vegetable tannins and oxazolidine. The dyeing and fat-liquoring process is shown as TABLE III, and the uptake of dyestuff, the absorption rate of fat-liquor were examined. The uptake of dyestuff was investigated using a spectrometer to measure dye absorption in the initial and the last stage. Exactly 1ml of dyeing liquor was diluted to 100ml for these measurements. The dye was a common commercially available black dyestuff, usage at 3% based on the weight of the leather. A nephelometer was used to measure the absorptivity of the fat-liquor during the fat-liquoring process. The initial turbidity of the fat-liquoring bath was measured on a dilution of 1ml fat-liquor bath in 100ml or 50ml. The fat-liquoring agent is CHROMOPOL UFB/W (TFL company), added at 18% on the weight of the leather. The experiments are also described in TABLE III[11]. According to data-processing method of the orthogonal experiment, the optimized synthetic recipe was confirmed. According to the best synthetic recipe, the amphoteric polymer auxiliary agent (APAA) was synthesized.

Molecular Weight of the amphoteric polymer auxiliary agent and its Structure determination

The molecular weight of the amphoteric polymer auxiliary agent (APAA)was investigated by gel permeation chromatograph (Sephadex G-25, using tetrahydrofuran as mobile phase, the flowing speed 1.0mL/min, using Polyethylene Glycol as Reference Standard). Then the amphoteric polymer auxiliary agent was precipitated with acetone and dried for 6hrs at 80ºC in vacuo. The infrared (IR) spectrum was determined with Nicolet Nexus 470 FTIR spectrophotometer, and ^{13}C-NMR, ^{1}H-NMRwere determined with a Bruker Avance 600 spectrometer.

TABLE III

The process of dyestuff or fat-liquor of the goatskin leather tanned by Combination tannages with vegetable tannins and oxazolidine

Process	Chemicals	%	T/ºC	Time	Remarks
Re-wet	water	150	35		
	Degreasing agent	0.3			
	Formic acid	0.3		60 min	pH 4.5
Washing	water	200			drain
Neutralization	water	150-200	30		
	PAK-N-c	2			
	sodium formate	1.2		90min	pH 6.0
Washing	water	200			drain
Dyeing or fat-liquoring	water	200	50		
	Dyestuff/fat-liquor	3/18		60min	Sample of emulsion
	APAA	3/X*		30min	
Fixation	Fromic acid	0.5		15min	
	Fromic acid	0.5		15min	
	Fromic acid	0.5		15min	pH3.6-3.7;sample of liquor

Washing	water	200	20min	drain

*Note: X=0, 1%, 2%, 3%

Test of isoelectric point (pI) of the amphoteric polymer auxiliary agent

A 0.4g/L polymer auxiliary agent (APAA) solution was prepared and the pH value of this solution was changed by adding 0.1mol/L HCl or 0.1mol/L NaOH solution. The pH of this solution is adjusted to 3.5, 4.0, 4.2, 4.5, 4.8, 5.0, 5.5 respectively and its Zeta potential is examined using Acoustic and Electroacoustic spectrometer[12]. When its Zeta potential is equal to zero, the pH was considered to be isoelectric point (pI).

Application and the optimum amount of the amphoteric polymer auxiliary agent on goatskin crust tanned by combination tannages

The amphoteric polymer auxiliary agent (APAA) was respectively applied in the dyeing and fat-liquoring process of the goatskin leather tanned by Combination tannages with vegetable tannins and oxazolidine, Combination tannages with vegetable tannins and aluminium tanning agent. The process is the same as TABLE III. The amount of the amphoteric polymer auxiliary agent (APAA) is 0, 1%, 2%, 3% respectively. The method of the uptake of dyestuff and absorptive rate of fat-liquor is consistent with the former. Compared with the uptake and the absorptive rate under the condition of different amount of the amphoteric polymer auxiliary agent (APAA), the optimal amount of APAA is determined.

RESULTS AND DISCUSSION

Analysis of the optimized formulation of the copolymer

TABLE IV shows the uptakes of dyestuff and the absorptive rates of the fat-liquor in the dyeing and fat-liquoring process of the goatskin leather tanned by Combination tannages with vegetable tannins and oxazolidine with the different copolymer synthesized by the relevant recipe. Different co-polymer may have different isoelectric point so as to show different results for dyestuff and fatliquor. Based on the uptake of dyestuff and absorptive rates of the fatliquor, the mol ratio of monomers has been optimized. The optimized mole ratio is $A_1B_2C_2D_1$. That is, MAc 0.5mol, SMAS 0.2mol, DMDAAC 1.0mol, APS 1wt%.

TABLE IV

Results of $L_9(3^4)$ copolymer reaction and application

No	A/MAc/mol	B/DEMAAC/mol	C/SMAS /mol	D/APS/wt%	Uptake/%	Absorptive rate/%
1	0.5	0.5	0.1	1.0	99.0	99.3
2	0.5	1.0	0.2	1.5	99.9	99.6
3	0.5	1.5	0.3	2.0	99.9	99.8
4	1.0	0.5	0.2	2.0	99.4	80.5
5	1.0	1.0	0.3	1.0	99.8	99.5
6	1.0	1.5	0.1	1.5	99.9	99.8
7	1.5	0.5	0.3	1.0	95.2	-14.9
8	1.5	1.0	0.1	1.5	99.9	99.8
9	1.5	1.5	0.2	2.0	99.8	99.8

Analysis of the molecular weight and the structure optimized formulation of the copolymer and its characteristics

As shown in Figure 2, the molecular weight and the distribution index (M_w/M_n) of the amphoteric polymer auxiliary agent (APAA) are 3606 and 1.72 respectively, which indicates that the APAA is easily permeated into the chrome-free leather.

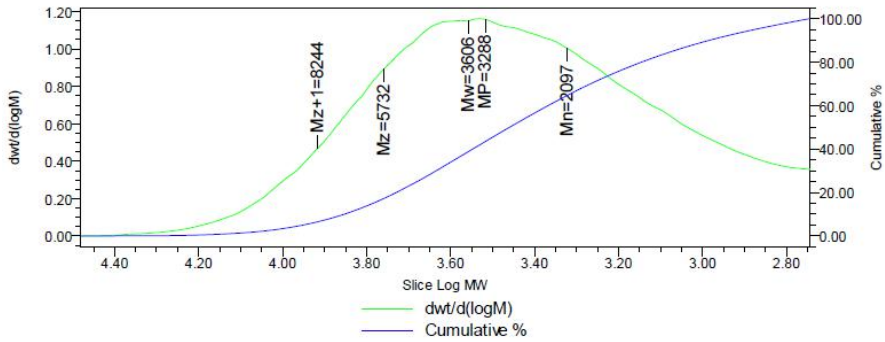

Fig. 2 Curve of GPC of APAA

Fig.3, Fig.4, Fig.5 shows the FTIR spectra, ^{1}H-NMR, ^{13}C-NMR of the amphoteric polymer auxiliary agent (APAA) respectively. The relation between the bands or Chemical shifts and its relevant groups was shown as Table V, Table VI and Table VII. So the chemical structure is confirmed by FTIR, ^{1}H-NMR and ^{13}C-NMR[13].

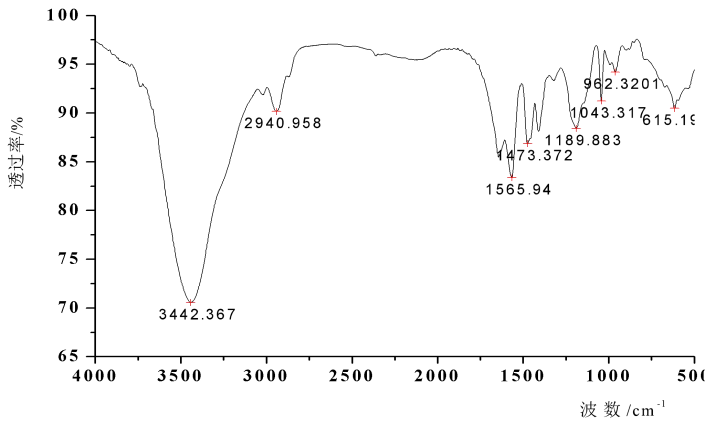

Fig.3. IR Spectrum of APAA

TABLE V

Relation between the band and the relevant group of APAA

No	Band/cm^{-1}	Group
1	3442	O-H (-COOH)
2	3016	C-H(=CH_2)
3	2994	C-H (-CH_3)
4	1556,1473	-COO^-
5	1189,1120	C-N
6	1043	-SO_3^-
7	962	-$N^+(CH_3)_2Cl^-$

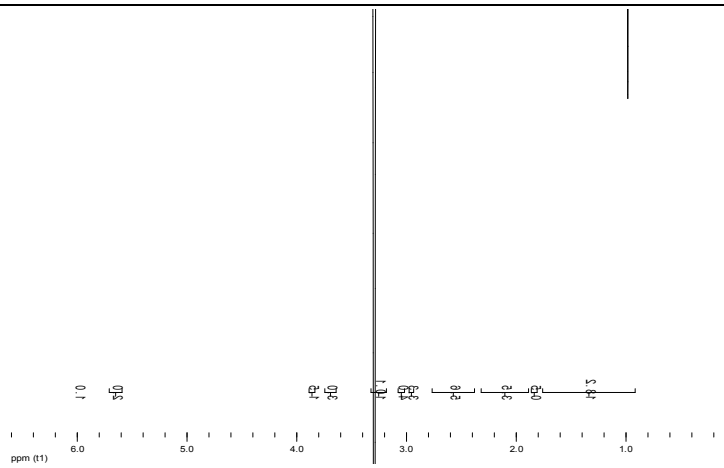

Fig.4. ^{1}H-NMR of APAA

TABLE VI

Relation between the band and the relevant group of APAA

No	Chemical shift/ppm	Group
1	5.7	-CH=CH_2
2	3.7-3.8	-CH_2SO_3Na
3	2.6-3.2	-CH_2 (-$N^+(CH_2)_2(CH_3)_2Cl^-$)
4	1.3-1.8	-CH_3 (MAC,SMAS)

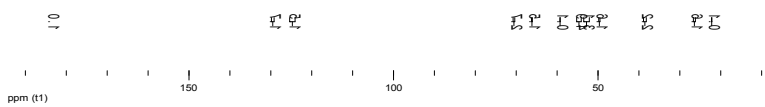

Fig.5. ^{13}C-NMR of APAA

TABLE VII

Relation between the band and the relevant group of APAA

No	Chemical shift/ppm	Group
1	183	-COOH(MAC)
2	119	-CH=CH_2(DMAAC)
3	59.3	-CH_2SO_3Na(SMAS)
4	49.7-54.5	-CH_2, -CH_3(DMAAC)
5	22.2-26.5	-C-(SMAS)

Isoelectric point (pI) of the copolymer solution

Fig.6 shows the relation between zeta potential and pH of the amphoteric polymer auxiliary agent (APAA) solution. When the pH of the solution is higher than 4.2, the zeta potential is negative and the solution becomes negative charge. However, when the pH of the solution is lower than 4.2, the zeta potential is positive and the solution becomes positive charge. When the pH of the solution is at range of 4.1 to 4.2, the zeta potential is zero, and the pH range is isoelectric point (pI) of the APAA. So based on the relation between zeta potential and pH of the APAA solution, the copolymer shows positive or negative charge when the pH of the copolymer solution deviates from the isoelectric point (pI). Thus the charge of the bath of dyeing and fat-liquioring can be changed by adding formic acid.

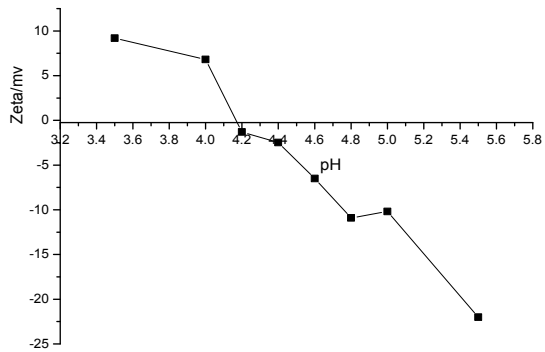

Fig.6. Relation between zeta potential and pH of APAA

Results of application on goatskin crust tanned by combination tannages

Fig.7 and Fig.8 shows individually the relation between the consumption of the amphoteric polymer auxiliary agent (APAA) and the uptake of dyestuff and absorptive rate of fat-liquor in the goatskin crust tanned by Combination tannages with vegetable tannins and aluminium tanning agent, Combination tannage with vegetable tannins and oxazolidine. With the consumption of the APAA increasing, the uptake of dyestuff and absorptive rate of fat-liquor during the dying and fat-liquoring of the two different Chrome-free goatskin crust rise. For the goatskin crust tanned by Combination tannages with vegetable tannins and aluminium tanning agent, when the dosage of the APAA copolymer is 2%, the uptake of dyestuff and absorptive rate of fat-liquor is over 96%. For the goatskin crust tanned by Combination tannage with vegetable tannins and oxazolidine, when the dosage of the APAA copolymer is 3%, the uptake of dyestuff and absorptive rate of fat-liquor is over 96%. So for the two different Chrome-free goatskin crust, the best dosage of the APAA is between 2% and 3%.

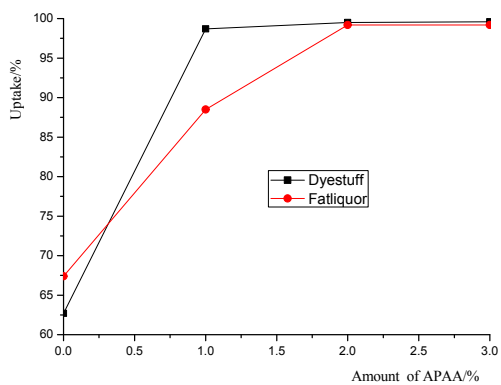

Fig.7. Relationship of the uptake of dyestuff and absorptive rate of fat-liquor during the dying and fat-liquoring of the goatskin crust tanned by Combination tannage with vegetable tannins and aluminium tanning agent and the

dosage of APAA

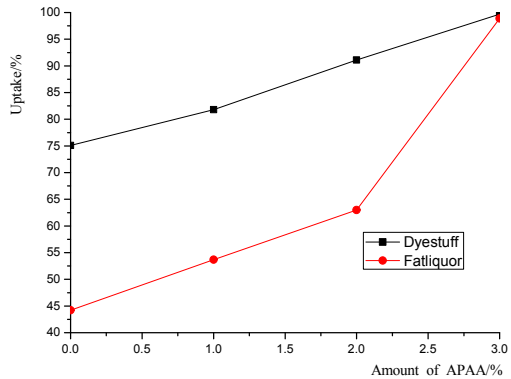

Fig.8. Relationship of the uptake of dyestuff and absorptive rate of fat-liquor during the dying and fat-liquoring of the goatskin crust tanned by Combination tannage with vegetable tannins and oxazolidine and the dosage of APAA

CONCLUSION

Based on the results of preparation and application of the noval amphoteric polymer auxiliary agent, it shows that methy-acrylic acid, sodium methylallyl sulfonate and dimethyl diallyl ammonium chloride (DMDAAC) have been synthesized by free radical copolymerization using ammonium persulfate at 80°C for 3 hours, the optimal mole ratio of methyacrylic acid, sodium methylallyl Sulfonate and dimethyl diallyl ammonium chloride is 1.0,0.3,1.0. The structure of the amphoteric polymer auxiliary agent was characterized by FTIR, ^{1}H-NMR, and ^{13}C-NMR. The properties of charge of the solution of the amphoteric polymer auxiliary agent was charaterized. Applied results of the amphoteric polymer auxiliary on the absorption of chrome-free crust for dyestuff, and fat-liquor show that it has strong auxiliary absorption capacity and the absorptive rate of dyestuff and fat-liquor can reach over 96%.

ACKNOWLEDGMENT

The author would like to acknowledge the support and guidance of Professor Bi Shi, Sichuan University, Sichuan Province and the help of Zhejiang Mingxin Leather, co.,Ltd, Zhejiang Province.

REFERENCES

1.Covington, A.D., Modern tanning chemistry. Chem. Soc. Rev., 1997, 26(2), 111-126.

2.Luo Jianxun, Feng Yanjuan, Shan Zhihua. Complex Combination Tannage among Phosphoniumcompounds, Vegetable tannins and Aluminium tanning agent. Journal of the Society of Leather Technologists and Chemists 95, 215-220.

3.Luo Jianxun, Feng Yanjuan. CLEANER PROCESSING OF BOVINE WET WHITE: SYNTHESIS AND APPLICATION OF A NOVEL CHROME-FREE TANNING AGENT BASED ON AN AMPHOTERIC ORGANIC COMPOUND. *J.*Soc.*Leather. Technol. Chem.,*2015, 99(4), 190-196.

4.Hernandez J.F., Kallenberger W.E., Combination tannage with vegetable tanning and aluminium,*J. Amer. Leather Chem. Ass*., 1984, 79(2), 182-206.

5.D·Aquino, A., Barbani, N, D·Elia, G., et al., Combined organic tanning based on mimosa and Oxazolidine development of a semi-industrial scale process for high-quality bovine upper leather. *J.*Soc.*Leather. Technol. Chem.,*2004, 88(2), 47-55.

6.Dang Hongxin, Pan hui, Zhang Zhijun, etc. Synthesis and study of new Amphoteric copolymer re-tanning agent ADV . China Leather, 2003, 20(5): 29-32.

7.Pan Hui, Zhang Juxian, Zhang Zhijun, etc. Synthesis and study of new Amphoteric copolymer re-tanning agent DR . Leather Chemicals, 2003, 20(5): 29-32.

8.Jin Liqiang, Yu jing, Zhang Jing. Preparation and application of poly(MAA-AN-DM) Amphoteric polymer as re-tanning agent. Fine Chemicals, 2008, 25(4): 380-383.

9. George Odian，John Wiley ＆Sons，Inc. Principles of polymerization. 2004.

10.Yang De. Design of experiments and analysis[M]. Beijing: Chemical industry Press, 1999.

11.LuoJianxun, Li Jing,Liao Xuepin, Zhang Wenhua, Shi Bi. Cleaner Chrome Tanning – A Non-Pickling Process Using an Aliphatic Aldehyde as Pre-tanning Agent. J. Soc. Leather. Technol.Chem. 2012,96 (1):21-26.

12.Wang Yinghong, Chen Wuyong, Gu Haibin,etc. Zeta potential of Gelatin and Cr（III）complex compound. China Leather, 2007, 36(21): 34-37.

13.Ning Yongcheng. Structure identification of Organic compounds and organic spectroscopy[M]. Beijing:Science Press, 2002.

P123

Effect of Food to Algal biomass ratio on the assimilation of ammonical nitrogen from the secondary tannery effluent coupled with bioenergy generation using grown algal biomass

V.Nagabalaji, T.Muthukumar, J.R.Juhna, S.V. Srinivasan*, R.Suthantharajan

Environmental Science and Engineering Division, CSIR-Central Leather Research Institute, Chennai – 600 020, India

**Corresponding author: srinivasansv@yahoo.com*

Abstract

The conventional treatment plants are designed mainly for removal of suspended solids and organic matter such as Biochemical Oxygen Demand (BOD) to meet the discharge standards to protect ecosystem and human health. However, the secondary treated effluents from the wastewater treatment plants contain nutrients such as nitrogen and phosphorus (in the form of ammonium, nitrates and phosphates) were considered to be the major cause for the eutrophication in the natural water bodies. Conventional treatment using biological treatment nitrification and denitrification for the removal of nutrients from the wastewater ends up in high sludge content and lacks economic feasibility. Hence, this bottle neck requires new technology which is cost and energy efficient. Microalgae is receiving a great attention towards the biofuel as well as removal of nutrients from the wastewater as an alternative biological treatment. In the current study, five different Food to Algal biomass ratios (0.25, 0.5, 1.0, 1.5 and 1.75) were experimented with *Chlorella vulgaris* and ratio of 1 was found to be optimum and further studies were carried out in lab scale tubular photo bioreactor. The removal efficiency of ammonical nitrogen, Total Kjeldahl Nitrogen (TKN) and total organic carbon were found to be 66.6 %, 62.5 % and 69.09 % respectively. Grown microalgal biomass was subjected to biomethanation for recovery of bioenergy in the form of methane. The specific methane yield obtained was 233 ml/g VS using standard Biomethane Test using AMPTS=II. This results of the study is a promising option, as it was observed that the coupling of both process i.e algal treatment integrated with anaerobic digestion for grown algal biomass will benefits wastewater treatment for nutrient removal and energy production rather than waste generation

Key words: *Chlorella vulgaris*, Tannery wastewater, Nutrient removal, Sustainability, AMPTS II.

1. Introduction

Developing countries are the leading producer of finished leather and leather products due to the availability of raw materials and industrialization. Over the decades there is improvement in leather production using cleaner production methods like application of enzymes for leather processing. Despite the development in leather sector, the discharge of wastewater from tanning processes poses environmental pollution if it is not properly collected, treated and disposed. Biological treatment has more economic benefits when compared to chemical oxidation for the treatment of industrial effluent in reduction of organic content.The conventionally designed treatment plants i.e. activated sludge process treatment treats only the organics such as COD and BOD only but the nutrients (nitrogen) in form of ammonia (NH_3^+) and nitrates (NO_3^{-}) are left untreated. As ammonia nitrogen (NH_3-N)is one of the major pollutants in tannery effluent due to the high protein content in the effluent eluted from the collagen, amino acids from the skin, fatty aldehydes and quinones from the tannins which lead to the ammonia-N concentration up to 300 - 400 PPM in the effluents (Wang et al 2012). However, the treated effluents from conventional treatment plants contain nutrients such as ammonium, nitrates and phosphates (NH_4^+, NO_3^-, PO_4^{3-}) were considered to be the major cause for eutrophication in the natural water bodies. Ammonia-N from the tannery effluents which is highly toxic to aquatic organisms which may leads to death due to the toxic buildup in their blood and internal tissues. Another major problem is eutrophication of fresh and marine water ecosystem due to the discharge of effluents without the removal of nutrients which ends in the formation of algal blooms in the water habitats that has the

several negative impacts on human health and ecosystem such as production of toxins in water bodies and hypoxic conditions also affects the nature of aquatic system. (Wiesmann et al 1994; Cerda and estela 2006).

The Conventional treatment methods for removal of ammonical nitrogen such as air stripping, chemical precipitation, adsorption ends up in high sludge content and use of constructed wetland system require complicated operation to achieve nitrogen removal and requires larger land area. Other electrochemical treatment methods like electro coagulation, fenton and electro oxidation are chemical and energy consuming (Lin et al 2002; kabdasli et al 2003; Di Iaconi et al 2002; Anglada et al 2009; Szpyrkowicz et al 2005;) which lacks economic viability. In addition to this, the excess sludge content generated from these treatments require further treatment and disposal which in turn increase the operational and maintenance cost. So this high operational and maintenance cost and the stringent environmental regulations and standards for ammoniacal nitrogen (NH_3-N) (Kabdasli et al 2002; MoEF&CC 2016) necessitate the research for the development of cost effective treatment technologies in this area.

Biological treatment using Microalgae is receiving a great attention towards the removal of nutrients from the wastewater. They have capacity to consume simple organic compounds directly and assimilate them as carbohydrates and amino acid (Liu et al 2015). As a result of photosynthesis microalgae can able to assimilate inorganic carbon, there by reduction in energy requirement for the treatment of effluent when compared to the conventional aerobic treatment technologies which needs the presence of oxygen. Advantages of using microalgae in wastewater treatment are economical, less energy, reduced sludge formation, reduction in emission of greenhouse and potential for utilization of algal biomass. Microalgal technology was developed not only for wastewater treatment, but also the biomass produced could be a source of raw material for pharmaceutical and other industries. The biomass can also be used to produce biofuels (Richmond et al., 2008).

In most of the nutrient removal studies using micro algae, it was not clear about total nitrogen (TN) to microalgae ratio i.e. food to microbe ratio (F/M) which plays a major role in nutrient removal efficiency. So the current study mainly focused on the effect of the food to microalgae ratio in order to improve the treatment efficiency and to investigate the bio-methane potential of grown algal biomass for bioenergy production.

2. Materials and Methods

2.1 Screening of Micro algae

Pure cultures of *Chlorella vulgaris, Chlamydomonas sp., Chlorococcum sp. and Scenedesmus dimorphus* were collected from Centre for Advanced Studies in Botany, Madras University, Chennai, India was screened to evaluate the efficiency for nutrient removal based on their performance in nutrient removal in synthetic wastewater (Nagabalaji et al 2017). Based on their nutrient removal efficiency, fresh water microalgae *C.vulgaris* was selected for the current study.

2.2 Media and Cultivation conditions

Bold- Basal Modified (BBM) medium was used to develop the culture where the initial pH of the media was adjusted to 7.0 – 7.2, prepared with distilled water and sterilized at 121°C for 20 min, and maintained at 28°C (Nichols and Bold, 1965).

2.3 Stock culture for nutrient removal studies

Stock culture of *C.vulgaris* was cultivated in tubular photo bioreactor with the capacity of 7 litre and the working volume of 5 litre of BBM at 27 ± 2°C completly aerated (0.5 vvm) with light and dark cycle of 16h:8h at the light intensity of 5000 – 6000 lux (Ballestero et al 2016; He et al 2013). The growth of *C.vulgaris* were frequently monitored by measuring the optical density at 675 nm in UV- Spectrophotometer. The values were plotted to obtain the growth curve of *C.vulgaris*.

2.4 Tannery wastewater

The secondary treated tannery wastewater was collected from a Common Effluent Treatment Plant (CETP) located in Tamilnadu, India and the parameters were analyzed as per APHA 2000. The concentrations of NH_3-N, TKN, NO_3-N in secondary treated effluent were found to be in the range of 400 – 460 PPM, 600 – 650 PPM, 2.5-5.0 PPM respectively.

2.5 Batch studies in shake flask

The initial batch studies were conducted with different the Food to Microalgae ratio (F/M Ratio), i.e, $TN_{Food}/TSS_{Microalgae}$ and the culture used for over all treatment studies has the biomass ranging from 945 – 1000 mg/L in terms of dry weight. During the batch operation, five different F/M ratios were performed (0.25, 0.5, 1, 1.5, 1.75). The batch cultivations were done in 250 ml Erlenmeyer flasks with the volume of 100 -120 ml (Fig 1). All experiments were conducted in duplicates with the constant mixing of 120 rpm in a rotatory shaker illuminated with 5000 – 6000 lux at 27 ± 2°C for a period of 15 days. The samples were withdrawn at regular intervals and analyzed for nutrient removal efficiency

Figure.1 Batch studies in shake flask

Figure.2 Batch studies in Tubular Photo - Bioreactor

2.6 Batch studies in tubular Photo BioReactor (PBR)

Batch studies were carried out in tubular photo bioreactor of 7 L capacity with the working volume of 5 L. The reactor was aerated with 0.5 vvm (gas volume flow per unit of liquid volume per minute) of air through air pump. The PBR was illuminated with 5000 – 6000 lux with the light and dark cycle of 16 h:8 h (Fig 2). The pH inside the reactor was adjusted using 1N HCl and 1N NaOH to maintain in the range of 7.0 – 7.5. Among the five different F/M ratios studied in batch experiments, the optimized ratio was taken to PBR for the scale up study for the period of 7 days. The treated samples were withdrawn at the specific intervals for the analysis.

2.7 Analytical parameters and Biochemical Characterization

The treated wastewater samples were withdrawn at specific intervals for a period of 15 days and the concentration of ammoniacal nitrogen (NH_3-N), Total Kjeldhal Nitrogen (TKN), Nitrate Nitrogen (NO_3-N), were analysed according to standard methods (APHA 2000).The treated wastewater containing grown algal biomass was centrifuged at 3000 g, for 10min and the pellet was subjected to analysis of biochemical composition. Carbohydrate content, Total lipid content and the total protein were estimated by Phenol-sulphuric acid method, gravimetric method and Lowry's method (Dubois et al., 1956;Blighand Dyer 1959;Lowry et al 1951) respectively.

2.8 Biomethanation of harvested micro algal biomass for bio-energy production

The sludge from anaerobic digester was used as inoculum for Bio-methane potential (BMP) sludge from anaerobic digester. The physiochemical parameters of the inoculums andbiochemical composition of *C.vulgaris*were shown in table 1. BMP of *C.vulgaris* was performed as per VDI standard 4630 (German method) for determination of Specific methane (CH_4) yield and Substrate degradation was performed by Automatic Methane Potential Test System (AMPTS) II (Bioprocess, Sweden) with online monitoring system supported by software AMPTS v5.0 (Badshah et al., 2012). The substrate to inoculum ratio

(S:I) was set based on the Volatile solids (VS). The S: I ratio was maintained at 0.5. All the experiments were run in triplicates.

Table 1.Characterization for anaerobic sludge and *C. vulgaris*

Analytical parameter	Anaerobic sludge	*C.vulgaris*
pH	6.8	7.5
TS (mg/g)	39.66	73.9
VS (mg/g)	22.21	55.2
%VS in TS	55.9	74.6
Moisture (%)	96	92.6
Carbohydrates (% W/W)	Nd	30.8
Lipids(% W/W)	Nd	28.4
Proteins(% W/W)	Nd	14.5
Nd – Not determined		

Figure.3 Automated methane potential test system II (AMPTS II) experimental set up

3.Results and Discussion

3.1 Batch studies on biological nutrient removal in secondary treated tannery wastewater

The profile of pollutant concentration in wastewater are shown in Fig 4 (a) NH_3-N, 4 (b) TKN, 4 (c). Among different F/M ratios studied, the degradation of ammoniacal nitrogen (NH_3-N), Nitrate nitrogen (NO_3-N) and Total Kjeldhal Nitrogen (TKN) were found to be similar in F/M Ratios of 0.5, 1, 1.5 in which the removal efficiency in NH_3-N was 56.17 %, 55.48 %, 57.76 % whereas NO_3-N was 77.94 %, 70.39 %,78 % and TKN 50 %, 50 %, 60 %. Among these three ratios there is no significant difference on removal efficiency. Hence, further studies were extended with ratio of 0.25 and 1.75. During the further set of experiments, ratio of 0.25 has resulted in maximum removal efficiency of NH_3-N (60.57 %) and 1.75 has lesser amount of nutrient removal efficiency (37.5 %). In all three ratios (0.5, 1, 1.5) there is a gradual decrease in the pollutant concentration as shown in Fig 4. Based on the results in this batch studies and considering Hydraulic Retention Time (HRT) in the continuous reactor, F/M ratio of 1 was selected and the further studies were to be carried out in Tubular photo bioreactor.

3.2 Batch studies in Tubular Photo Bioreactor

The nutrient removal studies performed in the PBR is shown in Fig 5. The performance of *C.vulgaris* in PBR showed better results when compared with the shake flask experiments which might be due to the complete mixing with the help of aeration, availability of CO_2 and surface area of the reactor. From the Fig 5 (a), it was found that *C. vulgaris* has a very clear

growth pattern in the composite secondary treated tannery wastewater. The removal efficiencies of NH_3-N and TKN were found to be 66.6 % and 62.5 % with the initial concentration of 252 mg/L and 448 mg/L respectively as shown in fig 5 (b). The degradation profile of NO_3-N and PO_4-P were shown in Fig 5 (C) and their respective removal efficiencies were found to be 70.02 % and 62.62%. *C.vulgaris,* a mixotrophic species has ability to consume carbon source from the wastewater which was also evidently seen in Fig 5 (d) showing removal efficiency of TOC 69.09% with the initial concentration in the reactor was 275.45 mg/L.

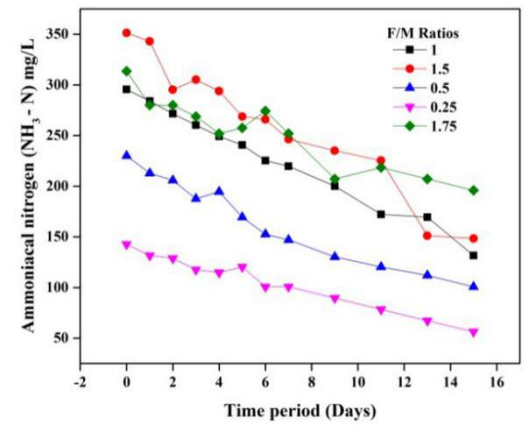

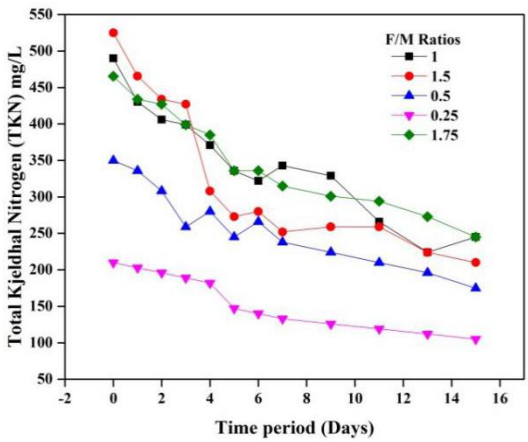

Parameters / F/M ratios	0.25	0.5	1	1.5	1.75
NH_3-N	60.57	56.17	55.48	57.76	37.5
TKN	50	50	50	60	47.36
NO_3-N	72.80	77.94	70.39	78	55.23

Fig 4 (b) TKN

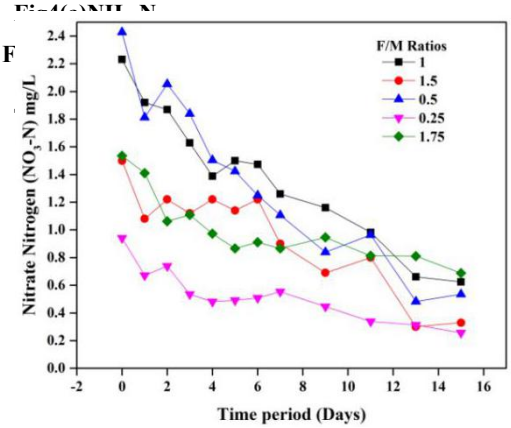

Fig 4 Pollutant removal Efficiency using *Chlorella vulgaris* in batch studies with different F/M ratios

3.3 Bio-methane Potential of *C.vulgaris* in AMPTS II

Fig 6 shows the specific methane yield with respective time period from the anaerobic digestion of *C.vulgaris* (harvested algal biomass). The methane production from the inoculum was deducted from the methane produced in reactor which has substrate and inoculum in order to get the true methane production from the substrate. The specific methane yield produced from micro algal biomass was found to be 233 ml/g VS with the standard deviation of ±27 ml. The substrate reduction was estimated from initial and final samples of the anaerobic reactor in which the VS reduction was 80.22 % which is shown in Fig 7 clearly indicates the biodegradability of *C.vulgaris*.

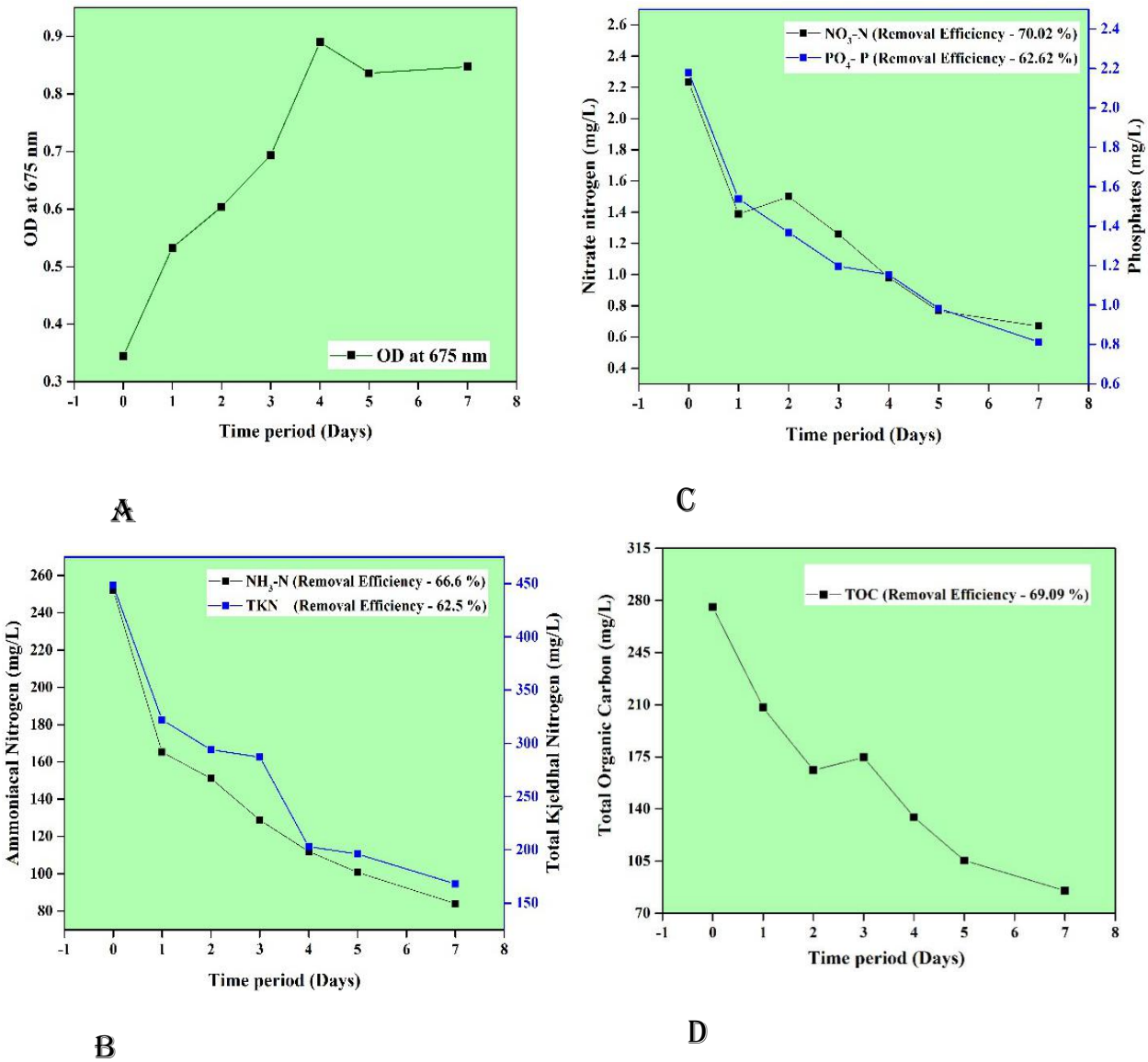

Fig 5 Pollutant removal eefficiency using *Chlorella vulgaris* in tubular PBR

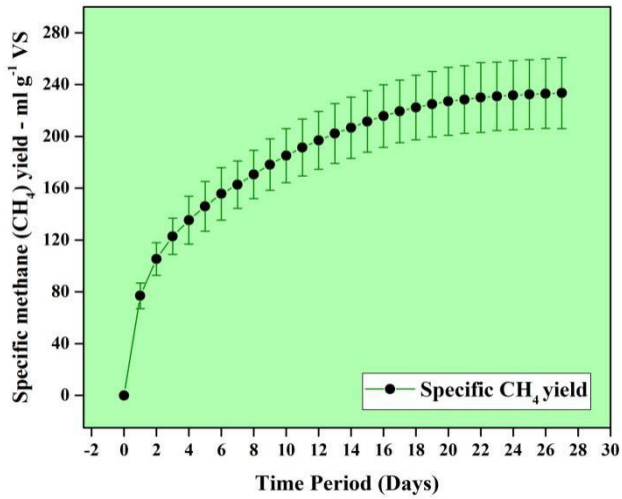

Figure.6 Specific CH_4 production during anaerobic digestion of *C.vulgaris* in AMPTS II

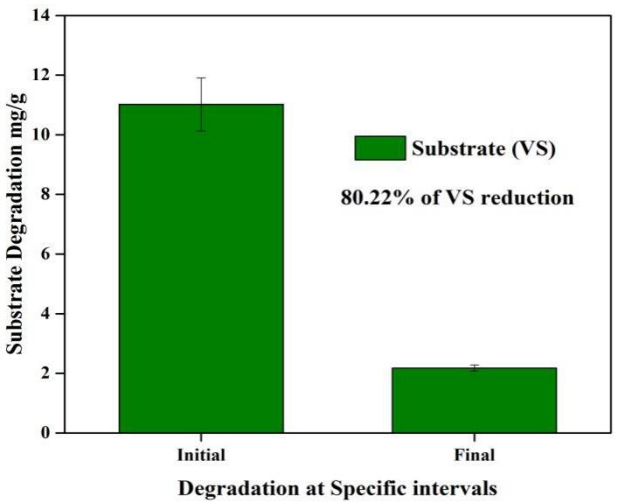

Figure.7 Substrate degradation during the anaerobic digestion of *C.vulgaris* in AMPTS II

4. Conclusion

The current study deals with the nutrient removal in secondary treated composite tannery wastewater and biomethanation of grown algal biomass. Among the five different F/M ratio (0.25, 0.5, 1, 1.5, 1.75) studied, F/M ratio of 1 was found to have effective removal of nutrients from secondary treated composite tannery wastewater. Removal efficiency of ammoniacal nitrogen - 66.6 %, TKN - 62.5 %, nitrate nitrogen - 70.02%, phosphate - 62.62% and Total organic carbon - 69.09 % which confirmed that *C.vulgaris* has capability on not only removing the nutrients but also can degrade the organic carbon present in the wastewater. Further, it gives the clear evidence that *C.vulgaris*, a mixotrophic species which has the potential to grow in both autotrophic and heterotrophic conditions. In addition, harvested *C.vulgaris* biomass showed specific methane yield of 233 ml/g VS. Based on the experimental results, *C.vulgaris* has the ability to grow in ammoniacal nitrogen rich wastewater streams with high TDS and saline conditions. It is concluded that *C.vulgaris* (phycoremediation) is a potential alternative technology to remove nutrients from the secondary treated tannery effluents and the microalgae grown in effluent can be used as an energy source.

References

1. American Public Health Association (APHA). Standard methods for examination of water and wastewater. 22th ed. Washington (DC): APHA; 2000.
2. American Public Health Association, & American Water Works Association. (2000). *Standard methods for the examination of water and wastewater*. American public health association.

3. Anglada, A., Urtiaga, A., & Ortiz, I. (2009). Contributions of electrochemical oxidation to waste‐water treatment: fundamentals and review of applications. Journal of Chemical Technology & Biotechnology, 84(12), 1747-1755.
4. Ballestero M, Philippe J, Cristina S. Comparison of Chlorella vulgaris and cyanobacterial biomass: cultivation in urban wastewater and methane production. Bioprocess Biosyst Eng. 2016;39(5):703–712
5. Bligh, E. G., & Dyer, W. J. (1959). A rapid method of total lipid extraction and purification. Canadian journal of biochemistry and physiology, 37(8), 911-917.
6. Cerdá, V., & Estela, J. M. (2006). Nutrient Control. Wastewater Quality Monitoring and Treatment, 219-245.
7. Di Iaconi, C., Lopez, A., Ramadori, R., Di Pinto, A. C., &Passino, R. (2002). Combined chemical and biological degradation of tannery wastewater by a periodic submerged filter (SBBR). Water research, 36(9), 2205-2214
8. Dubois, M., Gilles, K. A., Hamilton, J. K., Rebers, P. T., & Smith, F. (1956). Colorimetric method for determination of sugars and related substances. Analytical chemistry, 28(3), 350-356.
9. He, H., Zhou, M., Yang, J., Hu, Y., & Zhao, Y. (2014). Simultaneous wastewater treatment, electricity generation and biomass production by an immobilized photosynthetic algal microbial fuel cell. Bioprocess and biosystems engineering, 37(5), 873-880.
10. Kabdaşli, I., Ölmez, T., &Tünay, O. (2003). Nitrogen removal from tannery wastewater by protein recovery. Water science and technology, 48(1), 215-223.
11. Kabdaşli, I., Tünay, O., Çetin, M. Ş., &Ölmez, T. (2002). Assessment of magnesium ammonium phosphate precipitation for the treatment of leather tanning industry wastewaters. Water science and technology, 46(4-5), 231-239.
12. Lin, Y. F., Jing, S. R., Lee, D. Y., & Wang, T. W. (2002). Nutrient removal from aquaculture wastewater using a constructed wetlands system. Aquaculture, 209(1-4), 169-184.
13. Liu, N., Li, F., Ge, F., Tao, N., Zhou, Q., & Wong, M. (2015). Mechanisms of ammonium assimilation by Chlorella vulgaris F1068: isotope fractionation and proteomic approaches. Bioresource technology, 190, 307-314.
14. Lowry, O. H., Rosebrough, N. J., Farr, A. L., & Randall, R. J. (1951). Protein measurement with the Folin phenol reagent. Journal of biological chemistry, 193(1), 265-275.
15. Ministry of Environment, Forest and Climate Change(MoEF&CC).Environmental Standards for Common Effluent Treatment Plants (CETP).S.O. 4 (E) [01-01-2016] 2016.
16. Nagabalaji, V., Sivasankari, G., Srinivasan, S. V., Suthanthararajan, R., &Ravindranath, E. (2017). Nutrient removal from synthetic and secondary treated sewage and tannery wastewater through phycoremediation. Environmental technology, 1-9.
17. Richmond, A. (Ed.). (2004). Handbook of microalgal culture: biotechnology and applied phycology (Vol. 577). Oxford: Blackwell Science.
18. Wang, Y., Zeng, Y., Chai, X., Liao, X., He, Q., & Shi, B. (2012). Ammonia nitrogen in tannery wastewater: distribution, origin and prevention. Journal of the American Leather Chemists Association, 107(2), 40.

P124

New hybrid nanocomposite applied to the leather finishing process, with favourable environmental impact

Simion Demetra[1], Gaidau Carmen[1], Jianzhong Ma[2], Zhang Wenbo[2], Qunna Xu[2]

[1]*The Research Development National Institute for Textiles and Leather, Division Leather and Footwear Research Institute, 93 Street Ion Minulescu, 031215, Bucharest, Romania, E-Mail:icpi@icpi.ro*

[2]*Shaanxi University of Science and Technology Division Shaanxi Collaborative Innovation Center of Industrial Auxiliary Chemistry and Technology, Xi'an 710021, China*

Abstract

The paper is focused on creating new hybrid nanocomposites based on cellulose/silica/surfactants (bolaform and gemini) applied to the smart leather finishing process to provide outstanding properties (waterproofing, fire retardance, abrasion resistance) with favourable environmental impact, reducing pollution by replacing the toxic, classical chemicals. Innovation consists in technologies for obtaining hybrid nanocomposites, solubilisation/compatibilisation of their component substances for the conditioning of leather processed with the created nanocomposites. Cellulose/silica nanocomposites have been stabilized with bolaform and gemini surfactants. The results showed that the presence of the coupling agent/surfactants increased the uniformity of the silica-shell nanocomposites. The existence of the silane coupling agent and the presence of surfactants could provide the hybrid film with increased mechanical resistance to water and heat. Leather processing with the composite thus prepared can yield finished leather with wet/dry friction resistance, water resistance and tensile strength. Environmentally-friendly leather with smart multifunctional features are obtained for various applications. By using the new composites, color intensification or dermal filling effects can be pursued with the possibility of reducing synthetic materials (dyeing auxiliaries, syntans, classical tensides).

Keywords: new hybrid nanocomposites based on cellulose/silica/surfactants (bolaform and gemini), smart leather finishing process, environmental impact

Acknowledgements: This works were supported by Romanian Ministry of Research and Innovation, CCCDI–UEFISCDI, Project number PN-III-P1-1.2-PCCDI-2017-0743/44PCCDI/2018, and bilateral cooperation project proposal Romania-China_HNAN, within PNCD III.

P125

The Properties of Collagen Extracted from Pickled Skin

Zhenhua Tian[1, 2]

[1]*College of Bioresources Chemical and Materials Engineering, Shaanxi University of Science and Technology, Xi'an 710021, Shaanxi, China (Email: tianzhenhua@sust.edu.cn)*

[2]*National Demonstration Center for Experimental Light Chemistry Engineering Education, Shaanxi University of Science & Technology, Xi'an 710021, Shaanxi, China*

Abstract

Two kinds of collagens were extracted from fresh skin and pickled skin, respectively, and the physicochemical properties of the obtained collagens were characterized. Both the two kinds of collagens possessed integral triple-helical structure with high purity, which were investigated by Fourier transform infrared spectroscopy, ultraviolet spectroscopy and sodium dodecyl sulfonate-polyacrylamide gel electrophoresis. The isoelectric point test showed that the isoelectric point of pickled skin collagen (PS) (6.92) was similar to that of fresh skin collagen (FS) (6.90). Differential scanning calorimetry showed that the denaturation temperature of PS sponge and FS sponge was 62.4 °C and 59.0 °C, respectively, indicating that both of two collages had good thermal stability. The apparent viscosities of the collagen solutions were similar and the collagen solutions exhibited shear-thinning behavior. Additionally, the flow index n and m obtained from Ostwald-de waele and Carreau models reflected the collagen solutions belonged to peseudoplastic fluid. Furthermore, The turbidity curves displayed that the fibril formation rate of PS was slightly lower than that of FS, which was confirmed by the fact that the mean diameter of PS fibrils (44.56 ± 8.55 nm) was slightly smaller than that of FS fibril (51.5 ± 6.45 nm). Consequently, the tripe helix of collagen was not obviously affected during the pickling process, and pickled skin was a promising raw material for extraction of collagen.

Key words:pickled skin; collagen; extraction; structure; properties

Acknowledgements: This work is supported by National Natural Science Foundation of China (21706151), Research start-up funding of Shaanxi University of Science and Technology (2016BJ-85) and Open Project Program of National Demonstration Center for Experimental Light Chemistry Engineering Education (2018QGSJ02-16).

[1] Seligsberger L. Leather research and technology in the age of chrome [J]. Journal of the American Leather Chemists Association, 1991, 86: 246-258.

[2] Sundar V J, Rao J R, Muralidharan C. Cleaner chrome tanning—emerging options [J]. Journal of Cleaner Production, 2002, 10(1): 69-74.

[3] Bieńkiewicz K. Physical chemistry of leather making [M]. Krieger Pub. Co, 1983.

[4] Zeng X T, Yuan C H, Hong X U, et al. Industrial situation and strategy of China's chrome resource [J]. Resources & Industries, 2015, 17(3): 39-44.

[5] Bacardit A, Morera J M, Ollé L, et al. High chrome exhaustion in a non-float tanning process using a sulphonic aromatic acid [J]. Chemosphere, 2008, 73(5):820-4.

[6] Cao S, Wang K, Zhou S, et al. Mechanism and effect of high-basicity chromium agent acting on Cr-wastewater-reuse system of leather industry [J]. ACS Sustainable Chemistry & Engineering, 2018, 6(3): 3957-3963.

[7] Nair B U, Thanikailevan P, Saravanabhavan S, et al. Integration of chrome tanning and wet finishing processes for making garment leathers [J]. Journal of the American Leather Chemists association, 2005, 100(6): 225-232.

[8] Chao W, Zhang W, Liao X, et al. Transposition of chrome tanning in leather making [J]. Journal of the American Leather Chemists association, 2014, 109(6): 176-183.

[9] Saravanabhavan S, Thanikaivelan P, Rao J R, et al. Reversing the conventional leather processing sequence for cleaner leather production [J]. Environmental Science & Technology, 2006, 40(3): 1069-1075.

[10] Sivakumar V, Rao P G. Application of power ultrasound in leather processing: an eco-friendly approach [J]. Journal of Cleaner Production, 2001, 9(1): 25-33.

[11] Zhang J, Wang Y, Bo T, et al. New chrome tanning method assisted by wringing and ultrasound [J]. Journal of the American Leather Chemists association, 2013, 108(12): 445-448.

[12] Sivakumar V, Swaminathan G, Rao P G, et al. Use of ultrasound in leather processing industry: effect of sonication on substrate and substances-new insights [J]. Ultrasonics Sonochemistry, 2010, 17(6): 1054-1059.

[13] Yu Y, Wang Y N, Ding W, et al. Preparation of highly-oxidized starch using hydrogen peroxide and its application as a novel ligand for zirconium tanning of leather [J]. Carbohydrate Polymers, 2017, 174: 823-829.

[14] Ding W, Zhou J, Zeng Y, et al. Preparation of oxidized sodium alginate with different molecular weights and its application for crosslinking collagen fiber [J]. Carbohydrate Polymers, 2017, 157: 1650-1656.

[15] Krishnamoorthy G, Sadulla S, Sehgal P K, et al. Greener approach to leather tanning process: d -Lysine aldehyde as novel tanning agent for chrome-free tanning [J]. Journal of Cleaner Production, 2015, 42(3):277-286.

[16] Ramasami T, Rajamani S, Rao J R. Pollution control in leather industry: emerging technological options [C]. Proceedings of the International Symposium on Surface and Colloidal Science and Its Relevance to Soil Pollution. 1994.

[17] RamonPalop. The effect of basification and temperature on chrome tanning [J]. Beijing leather: 2001(8): 45-48.

[18] Covington A D. Chrome tanning: exploding the perceived myths, preconceptions and received wisdom [J]. Journal of the American Leather Chemists Association, 2001, 96(12): 467-480.

[19] Han W, Zeng Y, Zhang W. A further investigation on collagen-Cr(III) interaction at molecular level [J]. Journal-American Leather Chemists Association, 2016, 111(3): 101-106.

[20] Cheng J. The Effects of chromium-olation length on crosslinking effects investigated by molecular dynamics simulation [J]. Soft Materials, 2015, 13(1): 24-31.

[21] Onem E, Yorgancioglu A, Yilmaz O, et al. Evaluation of the analysis conditions for DSC instrument to realize the thermal behaviors of leathers [C]. IV International Leather Engineering Congress. 2017.

[22] Covington A D. Tanning chemistry: the science of leather [M]. Royal Society of Chemistry, 2009.

[23] Musa A E. Semi-chrome upper leather from rural goat vegetable tanned crust [J]. Journal of Applied and Industrial Sciences, 2013, 1(1):43-48.

[24] Xu W X. The reinforcement of leather split by in-situ polymerization and recombination [D]. Chengdu: Sichuan university. 2017.

P126

Study on the RapidSoaking Clean Manufacturing Technique on Twinface Sheepskin

ZHONG Jide[a]， WANG Xuechuan[b]，YANG Jin[a] ，LIU Xinhua[b]，

ZHANG Xiaoqing[a]，LI Hailin[a]

(a：Henan Prosper Skins&Leather Enterprise Co.Ltd., Mengzhou454750, China

b：Shaanxi University of Science and Technology，Xian710000，China)

Abstract: Salt-wet sheepskin is usually used as raw material for processing Twinface Sheepskin products.

In order to refresh salt-wet sheepskin to the fresh leather state, benefitting for the subsequent leather processing, soaking progress is of great importance.Nowadays, the traditional soaking method is so-called salt immersion method. Repeated reports has confirmed that it have the superiorityof low cost and stable quality, but after soaking progress, there is high chloride ion content in the waste water that would be difficult to be treated. Further the cycle of traditional soaking method presents more than 10 h, and these do not conform to the requirements of the present policy for energy conservation and emissions reduction. Therefore, this paper studies the technology of clean and rapid soaking method for Twinface sheepskin producing. In soaking process, alkyl sulfonic acid salts additives (FELIDERM MS POWDER), compound enzymes (DESOBATE DB), poly phosphate ester wet agent (FELIDERM SWP POWDER) and surface active agent (BORRON SE) were introduced synthetically to clear natural oils and soluble protein of sheepskin, and open the leather fiber, so that it can accelerate soaking effects and promote the rawhide quickly back to the fresh state. Finally, the soaking effect was evaluated by measuring the water filling degree. It is found that the soaking process cycle is about 4 h, which is more than half shorter than the traditional process, and have a uniform refreshed effect. Meanwhile, the content of chlorine ion in waste water was reduced by 50% at the same time, it achieves the goal of the clean rapidly soaking.

Key words：Twinface sheepskin；rapid soaking；Water filling degree

Foreword

As a raw material for processing Twinface Sheepskin, Australian lamb skin is mainly preserved by salting method. After being salted, the skin can lose more than 70% of the water , so as to prevent the skin rot. But in the leather making process, all the operations (except mechanical operations) in the preparation process are basically carried out in the bath liquid. The purpose of soaking process is that the raw material skin absorbs moisture evenly and returns to fresh skin state. Only when the moisture content of raw leather is restored to the fresh skin state can the following process steps of leather making be carried out[1,2].

The traditional method of soaking is normal temperature immersion, adding some surfactant auxiliaries, preservatives and a small amount of acid or alkali to the soaking liquid. Long time of immersion and slow action can only remove dirt, part of blood stain, simple soluble protein and a small amount of oil, and the degree of loose action on skin fiber is small[5].Therefore, salt immersion which also named salinity is used by most tannery. Salt immersion was carried out at room temperature, but a small amount of sulfuric acid and a large amount of sodium chloride (40g/L or more) were added to the soaking solution. Salt soaking has a certain function of loose fibers, and the skin pelt is soft and fast, safe and reliable, which will not cause quality problems such as hair slip. However, due to large consumption of sodium chloride, the treatment technology of submerged wastewater is difficult, and the treatment cost is high, which has adverse effects on the environment.

Base on the above problems, this paper selects some kinds of new type of soaking auxiliary and studies the application performance. All kinds of materials are organically combined to play a synergistic role to create a rapidly soaking process, which is back to wet fast, have a uniform water absorption, and have not hair slip, effectively guarantee the all kinds of

chemical materials effect on collagen evenly, to lay a good foundation for the chemicals penetration and combination with leather fiber in the following processes.

1 Materials and methods

1.1Main materials and equipments

(1)Main materials

Australian wet- salted lamb skin

Soaking auxiliary: Feliderm MS Powder, STAHL ;

Soaking auxiliary: Feliderm SWP Powder，STAHL；

Enzyme for soaking :DESOBATE DB，DECISION；

Wetting agent: Borron SE，TFL；

Other materials used in the process are industrial grade, and the reagents used for the analysis are all analytical pure grade.

（2）Main equipments

Stainless steel paddle, 450LZ90140, Jiangsu wuxi hongyuan mechanical leather factory.

Dryer, LFS-HGX-008, Suzhou industrial park gaopeng printing equipment co., LTD.

Analysis balance, AUX220, shimadzu, Japan.

1.2 Experimental methods and testing

1.2.1Sampling

Take an Australian wet-salted lamb skin, sampling symmetrically along the dorsal ridge.

1.2.2 Conventional salt soaking process

Soak the leather sample according to the process method in table 1.

1.2.3Rapid soaking process

Soak the leather sample according to the process method in table 2.

1.2.4 Water filling degree test

Take a representative sample of 2 ~ 6 g and shred the sample with scissors to homogenize the sample and mix it thoroughly.2 h of natural drying, and then under the temperature of 105 ℃ drying to constant weight, measure the loss of quality.

Water filling degree（%）

$$=\frac{\text{The weight of the skin after filling with water}-\text{The weight of the skin before it is filled with water}}{\text{The weight of the skin after filling with wate}}\times 100\%$$

1.2.5 Determination of BOD, COD and chloride ion content in wastewater

The wastewater samples after conventional salt soaking and rapid soaking were taken respectively according to the wastewater testing standards HJ505-2009, HJ828-2017, and GB11896-89 for the determination of BOD, COD and chloride ion content.

1.2.6 Evaluation of sample appearance

Samples were taken after conventional and rapid soaking respectively. Evaluate and describe the sample appearance and hand feeling through the technology supervisor.

Table 1 Conventional salt soaking technology

Process	Materials	Dosag（g/L）	Time（min）	Temp（℃）	pH	Remark

Soaking	Water			25℃		liquor ration 1:15
	Salt	40	30			
	Borron SE	1				
	Bactericide	0.5	30			
			120		6.5	take sample
			120			take sample
			120			take sample
			120			take sample
	Bactericide	0.5	120			take sample
			120			take sample
			120			take sample
			120			take sample

Table 2 Rapid soaking technology

Process	Materials	Dosag（g/L）	Time（min）	Temp（℃）	Remark
Soaking	Water			25/30/35/40	Liquor ration 1:15
	Feliderm MS Powder	0.5			
	DESOBATE DB	0.5/0.7/0.9/1.1			
	Feliderm SWP Powder	0.5			
	Borron SE	0.5			
	Bactericide	0.5			
			30		take sample
			30		take sample
			30		take sample
			30		take sample
			30		take sample
			30		take sample
			30		take sample
			30		take sample

Table 3 The content of BOD, COD, Cl^- of wastewater

Sample No.	BOD（mg/L）	COD（mg/L）	Cl^-（mg/L）	Remark
1#	6370	14156	28700	Wastewater from salt soaking

2#	7280	17200	12700	Wastewater from rapid soaking

Table 4 The appearance and sensory evaluation of the soaked leather sample

Sample No.	Fullness	White degree of pelt	Incision inspect	Remark
1#	Medium fullness	Medium white	No yellow	Salt soaking
2#	Very fullness	Pure white	No yellow	Rapid soaking

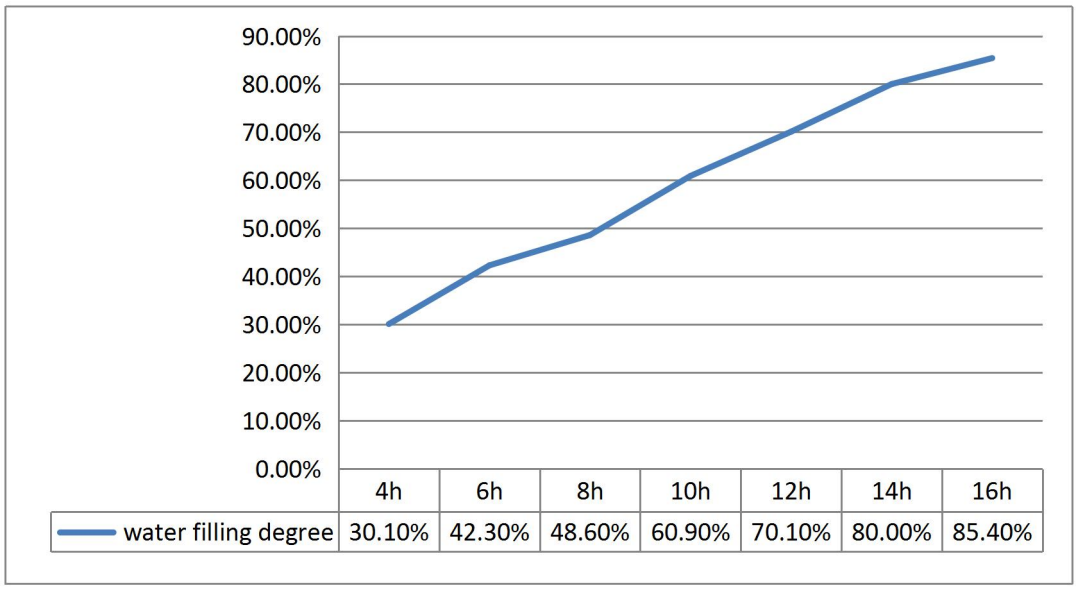

Figure 1 The Water filling degree of the leather with the time of salt soaking

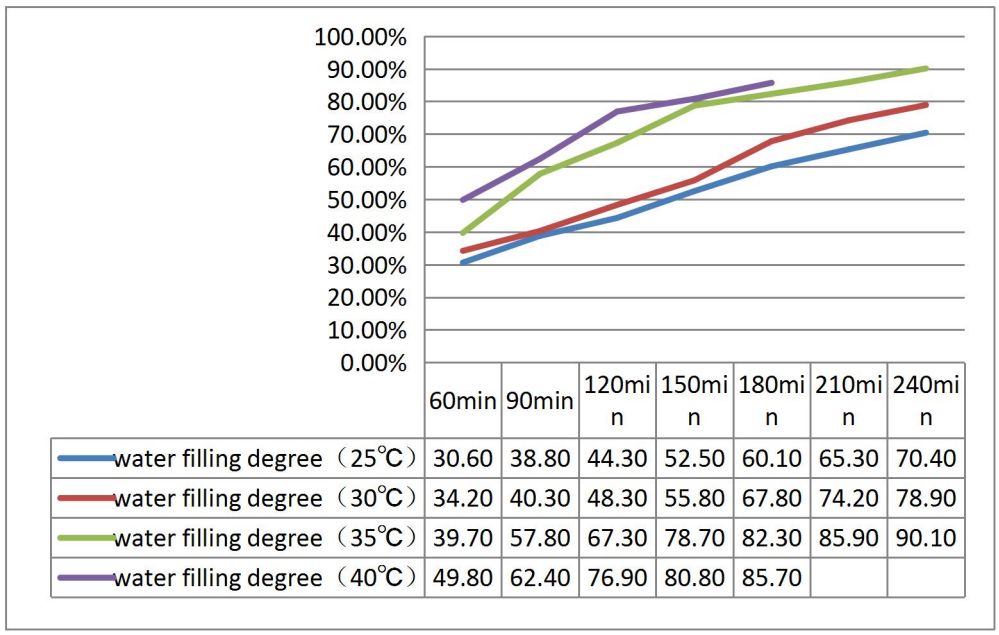

	60min	90min	120min	150min	180min	210min	240min
water filling degree（25℃）	30.60	38.80	44.30	52.50	60.10	65.30	70.40
water filling degree（30℃）	34.20	40.30	48.30	55.80	67.80	74.20	78.90
water filling degree（35℃）	39.70	57.80	67.30	78.70	82.30	85.90	90.10
water filling degree（40℃）	49.80	62.40	76.90	80.80	85.70		

Figure 2 The water filling degree of the rapid soaking process at different soaking temperatures

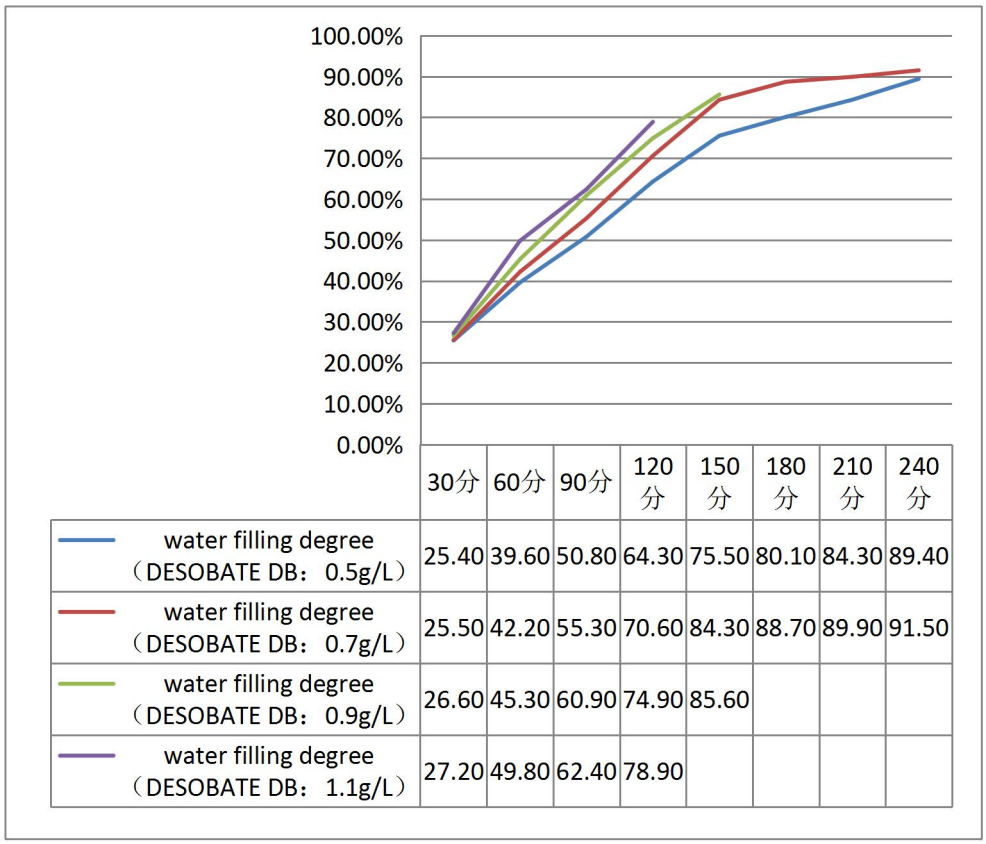

	30分	60分	90分	120分	150分	180分	210分	240分
water filling degree（DESOBATE DB：0.5g/L）	25.40	39.60	50.80	64.30	75.50	80.10	84.30	89.40
water filling degree（DESOBATE DB：0.7g/L）	25.50	42.20	55.30	70.60	84.30	88.70	89.90	91.50
water filling degree（DESOBATE DB：0.9g/L）	26.60	45.30	60.90	74.90	85.60			
water filling degree（DESOBATE DB：1.1g/L）	27.20	49.80	62.40	78.90				

Figure 3 Results of water filling test for DESOBATE DB under different dosage and soaking time

2 Results and discussion

2.1 The effect of soaking temperature on water filling degree

Raising the soaking temperature will promote better penetration of the chemicals into the skin, and thus increase the rate of soaking. However, in the case of higher temperature, the presence of enzymes and bacteria in the soakage will strengthen the function of hair roots, and the severity will cause the phenomenon of hair slip [3,4]. This paper studies the water filling degree of the skin at the DESOBATE DB dosage in 0.5 g/L with the soaking temperature set for 25/30/35/40℃ respectively, the results are shown in figure 2.

As can be seen from the data in figure 2, with the rising of temperature, water filling degree increase obviously, especially under the condition of 35℃, the skin absorbs the water rapidly, and ultimately the water filling degree of high value. But when the temperature reaches 40℃ at the soaking time of the 210 minutes, the problem of loose and wool slip appeared in the skin. Therefore, to set the soaking temperature in 35℃ to 38℃ range is more appropriate.

Secondly, compared with the results in figure 1 and figure 2, it can be clearly seen that under the condition of the presence of the soaking auxiliaries and the soaking enzyme, the soaking rate is significantly improved. The soaking time of the rapid soaking process can be reduced by more than 10 hours compared with the conventional salt immersion process.

2.2 The effect of soaking enzyme on water filling

DESOBATE DB is a kind of compound enzyme preparation, and its various enzyme preparation components play an important role in the process of soaking. This paper studies when the soaking temperature of 35℃, dosage of DESOBATE DB were 0.5g/L, 0.7g/L, 0.9g/L, 1.1g/L, the water filling degree of the skin at different soaking time. It can see form figure 3 that when the dosage of DESOBATE DB > 0.7g/L, the water filling degree of the results can be stable at more than 84.3% after 150 minutes, and as the dosage of soaking enzymes increase to 0.9g/L and 1.1g/L, although the water filling degree increase quickly, but there is a serious problem of wool slip in skin, which affects the quality of product, therefore, DESOBATE DB dosage is 0.7g/L to 0.8g/L is relatively reasonable, which can achieve rapid soaking effect, also can get a better quality of the product.

2.3 The effect of different soaking method on wastewater indexes

It can be seen from the test results of table 3 that the BOD, COD content in wastewater from the rapidly soaking process were slightly higher than from the regular salt soaking process, but the content of chlorine ion in waste water was significantly reduced. Thus the rapid soaking method can solve the problem of the treatment of wastewater containing chlorine from fountainhead. And the higher BOD, COD value is mainly due to the high efficiency of enzyme preparation, making more organic impurities from the skin to the process of soaking dissolution, achieved the purpose of efficient rapid soaking.

2.4 The leather appearance and hand feeling of different soaking process

It can be seen from table 4 that the appearance whiteness, hand feelling fullness and elasticity of the leather after the rapid water soaking process are better than the traditional salt soaking process, which indicates that the rapid water soaking process has the characteristics of full and even return of the leather and fully open the leather fiber.

3 Conclusion

（1）After the application of the Soaking auxiliary and the soaking enzyme in the process of soaking, the soaked skin has the characteristics of rapid return to the fresh, high cleanness, high water filling and good loose fiber. But the dosage of soaking enzyme preparation must be appropriate to prevent the problem of wool slip.

（2）The soaking temperature has a great influence on the effect of soaking process. When the soaking temperature of 35℃, the skin absorbs water rapidly, but when the temperature is higher than 40℃, there are wool slip problems. The best soaking temperature is between 35 to 38℃.

（3）The rapid soaking process studied in this paper reduces the soaking time from the traditional 10-16 hours to 4 hours, and reduces the content of chloride ion in the wastewater by about 16000mg/L. It Improves the efficiency of

production and reduce the difficulty of effluent treatment of leather industry, and also opens up a new idea for clean leather making technology.

References

[1] Lu Xingfang, Li Jingmei. The effects of soaking auxiliary on leather properties [J]. Journal of northwest institute of light industry, 1998, 19 (1): 46-50.

[2] Yang Xiaoyang, Ma Jianzhong, Gao Dangge, Lv Bin. The research status and prospects of leather soaking auxiliary [J]. Leather science and engineering, 2007, 17(5): 43-45.

[3] Cheng Fengxia, Wang Xuechuan, He Youjie, Fu Lihong, Zhou Yongxiang, Qiang Taotao. Modern fur technology [M]. Beijing: China light industry press, 2013.9.

[4] Cheng Fengxia, Zhang Daimin, Wang Xuechuan. Fur processing principle and technology [M]. Beijing: chemical industry press, 2005.

[5] Wei Shilin, Liu Zhenhua, Wang Hongru. Tannery technology [M]. Beijing: China light industry press, 2007.9.

.

Diamond Sponsors:

Gold Sponsors:

Silver Sponsors:

Media Partners

Room of Committee affairs group: Room 701，Xi’ an Xianglong Grand Hotel
会务组房间：西安翔龙大酒店 701 房间
Room of Medical care group: Room 703，Xi’ an Xianglong Grand Hotel
医疗保障组房间：西安翔龙大酒店 703 房间

Contact persons:
联系人及电话:
Qunna Xu (徐群娜)　TEL：+86-029-86132559;+86-15291486817
Bin Lyu (吕　斌)　TEL：+86-029-86168235;+86-13991372196
Cheng Zhou (周　诚)　TEL：+86-010-85113971;+86-13436304886

www.2018AICLST.org